Stony Brook University

Design, Synthesis, Biological Evaluation and Molecular Modeling of Novel

Taxane-Based Anticancer Agents and Paclitaxel Mimics

A Dissertation Presented

by

Liang Sun

to

The Graduate School

in Partial Fulfillment of the Requirements

for the Degree of

Doctor of Philosophy

in

Chemistry

Stony Brook University

May 2008

STONY BROOK UNIVERSITY

THE GRADUATE SCHOOL

LIANG SUN

We, the dissertation committee for the above candidate

for the Doctor of Philosophy degree, hereby recommend

acceptance of this dissertation.

Professor Iwao Ojima – Dissertation Advisor
Distinguished Professor, Department of Chemistry

Professor Kathlyn A. Parker – Chairperson of Defense
Professor, Department of Chemistry

Professor Robert C. Kerber – Third Member
Professor, Department of Chemistry

Dr. George A. Ellestad – Outside Member
Senior Research Scientist, Department of Chemistry
Columbia University

This dissertation is accepted by the Graduate School

Lawrence Martin
Dean of the Graduate School

Abstract of the Dissertation

Design, Synthesis, Biological Evaluation and Molecular Modeling of Novel Taxane-Based Anticancer Agents and Paclitaxel Mimics

by

Liang Sun

Doctor of Philosophy

in

Chemistry

Stony Brook University

2008

Paclitaxel (Taxol$^®$) is one of the most important anticancer drugs currently used in cancer chemotherapy. Paclitaxel binds to the β-tubulin portion of the α,β-tubulin dimer, promotes the polymerization of tubulins, stabilizes microtubules, and blocks microtubular dynamics, which eventually leads to apoptosis. However, paclitaxel has a number of undesirable side effects as well as multidrug resistance

(MDR). The development of new-generation taxoids with higher potency, and better pharmacological properties could overcome the problems.

Second-generation taxoids were designed and synthesized with modifications at the C-10, C-3' and C-2 positions. These taxoids exhibit one to three orders of magnitude higher potency than paclitaxel against various cancer cell lines, including multidrug resistant cell lines. A series of C-seco taxoids with different functional groups at the C2 and C3' positions were synthesized, which exhibited much higher activity than paclitaxel against various drug-resistant cell-lines, overexpressing specific tubulin isotypes.

Based on the REDOR-NMR experiment as well as molecular modeling and molecular dynamics studies, we proposed a new biologically active conformation of paclitaxel-"REDOR-Taxol". Based on the "REDOR-Taxol" structure, conformationally restricted macrocyclic taxoids bearing various linkers connecting different positions of the taxoid framework were synthesized and their biological activities evaluated. One of the macrocyclic taxoids, SB-T-2054, showed similar or slightly better activity in cytotoxicity and tubulin polymerization assay to that of paclitaxel, which strongly supports that the "REDOR-Taxol" structure is a valid binding structure, i.e., bioactive conformation, in tubulin/microtubule.

Novel baccatin-free anticancer agents, mimicking paclitaxel, with a tricyclic scaffold were designed and synthesized based on the "REDOR-Taxol" structure. The fused 5-6-6/5-7-6 tricyclic scaffolds were synthesized from a hydroxyproline derivative. These paclitaxel mimics exhibited moderate cytotoxicity.

Docosahexanoic acid (DHA), linolenic acid (LNA) and linoleic acid (LA) were linked to the C2'-position of the second-generation taxoids. The new conjugates, assayed *in vivo*, exhibited highly promising antitumor activity against drug-resistant colon cancer xenograft (DLD-1) as well as drug-sensitive ovarian cancer xenograft (A121) in nude mice.

Dedicated to my parents

Table of Contents

Chapter I
Cancer, Taxol and New-Generation Taxoids

Chapter II
Synthesis and Evaluation of Novel Fatty Acid-2nd-generation Taxoid Conjugates as Promising Anticancer Agents

Chapter III
Design, Synthesis and Biological Evaluation of Macrocyclic Taxoids

Chapter IV
Computational Study of the Binding Conformation of Paclitaxel in Tubulin

Chapter V
Design and Synthesis of *De Novo* Taxol-Mimicking Anticancer Agents

Chapter VI
Synthesis and Molecular Modeling Studies of C-seco-Taxoids

Appendices

List of Figures

Chapter III

Chapter IV

Chapter V

Chapter VI

List of Schemes

Scheme   **Page**

Chapter I

Chapter II

Chapter III

Chapter V

Chapter VI

List of Tables

Chapter V

Chapter VI

List of Abbreviations

Å	angstrom
Ab	antibody
Ac	acetyl
AcOH	acetic acid
Anal	analysis
atm	atmosphere
ATP	adenosine triphosphate
b	broad
bd	broad doublet
Bn	benzyl
bp	boiling point
bs	broad singlet
Boc	*tert*-butoxycarbonyl
t-Bu	*tert*-butyl
n-BuLi	*n*-butyllithium
Bz	benzoyl
Calcd	calculated
CAN	cerium(IV) ammonium nitrate
COSY	homonuclear (^{1}H-^{1}H) correlated spectroscopy
CsA	cyclosporine A
d	doublet
DAB	10-deacetylbaccatin III
DCC	*N,N'*-dicyclohexylcarbodiimide
dd	doublet of doublet
de	diastereomeric excess
DHA	docosahexaenoic acid
DIBALH	diisobutylalluminum hydride
DIC	*N,N*-diisopropylcarbodiimide
DMAP	4-*N,N'*-dimethylaminopyridine
DMF	*N,N'*-dimethylformamide
DMS	dimethyl sulfide
DMSO	dimethylsulfoxide
EDC.HCl	1-ethyl-3-(3-dimethylaminopropyl)carbodiimide hydrochloride
ee	enantiomeric excess
EE	ethoxyethyl
eq	equivalent
Et	ethyl
EtOAc	ethyl acetate
EVE	ethyl vinyl ether

FDA	Food and Drug Administration
g	gram
GBSA	Generalized Born surface area
GI	gastrointestinal
GTP	guanosine 5'-triphosphate
h	hour
HMDS	1,1,1,3,3,3-hexamethyldisilazane
HOBT	1-hydrobenzotriazole hydrate
HPLC	high performance liquid chromatography
HRMS	high resolution mass spectrometry
Hz	hertz
IC_{50}	concentration for 50 % inhibition
*i*Pr	isopropyl
IR	infrared spectroscopy
J	coupling constant
kDa	kilodalton
kg	kilogram
KHMDS	potassium 1,1,1,3,3,3-hexamethyldisilazide
L	liter
LDA	lithium diisopropylamide
LiHMDS	lithium 1,1,1,3,3,3-hexamethyldisilazide
m	multiplet
MAPs	microtubule associated proteins
MDR	multi-drug resistance
MDS	methyldisulfanyl
Me	methyl
mg	milligram
MHz	megahertz
min	minute
mL	milliliter
mmol	millimole
mol	mole
mp	melting point
MD	molecular dynamics
MM-GBSA	molecular mechanics Generalized Born surface area
MM-PBSA	molecular mechanics Poisson-Boltzmann surface area
MPA	methylpyridinium acetate
MS	mass spectrometry
NaHMDS	sodium 1,1,1,3,3,3-hexamethyldisilazide
NCI	National Cancer Institute
nM	nanomolar

NMO	*N*-methylmorpholine-*N*-oxide
NMR	nuclear magnetic resonance
Pgp	P-glycoprotein
Ph	phenyl
PLAP	pig liver acetone powder
PMP	*para*-methoxyphenyl
ppm	parts per million
p-TSA	*para*-toluenesulfonic acid
q	quartet
RCM	ring closing metathesis
Red-Al	bis(methoxyethoxy)aluminum hydride
rt	room temperature
s	singlet
SAR	structure-activity relationship
t	triplet
TAP	tumor activated prodrug
TBDMS	*tert*-butyldimethylsilyl
TEA	triethylamine
tert	tertiary
TES	triethylsilyl
Tf	triflouromethanesulfonate
TFA	trifluoroacetic acid
THF	tetrahydrofuran
TIPS	triisopropylsilyl
TLC	thin layer chromatography
TMS	trimethylsilyl
TPAP	tetrapropylammonium perruthenate
tRA	taxane reversal agent
wt	weight
[α]	specific optical rotation
δ	chemical shift
μM	micromolar

Acknowledgments

Chapter I

Cancer, Taxol and New-Generation Taxoids

§ 1.1 Introduction

§ 1.1.1 Cancer

Cancer is the collective name referring to a group of complex diseases characterized by abnormal cells that grow and divide in a disorderly fashion. Cancer cells are not able to control their own growth, and they are inconsistent in size and shape. Cancer could be caused by both external (chemicals, radiation, and viruses) and internal (hormones, immune conditions, and inherited genetic mutations) factors. The accelerated, uncontrolled growth of cancer cells results in a mass, which is called a tumor or neoplasm. Some cancers, like leukemia, involve the blood and blood-forming organs and circulate through other tissues where they grow.[1]

Cancer is a growing public health problem, whose estimated worldwide new incidences are more than six million cases per year. Cancer is the second leading cause of death in the US, exceeded only by heart disease and is the first leading cause of death among the people younger than 85 years old.[1] Half of all men and one third of all women in the United States will develop cancer during their lifetimes.[2] The four major types of treatment for cancer are surgery, radiation, chemotherapy, and biological therapies.[2]

Chemotherapy is the treatment of cancer with cytotoxic drugs. Depending on the type and developmental stage of cancer, chemotherapy can be used to cure cancer, to slow the growth of cancer, to prevent the cancer from spreading, to kill cancer cells spreading to other parts of the body, or to relieve symptoms caused by cancer.

§ 1.1.2 Paclitaxel and Docetaxel

Among a variety of chemotherapeutic drugs, paclitaxel (Taxol®) and docetaxel (Taxotère®) are currently two of the most successful drugs extensively used in the fight against cancer. Paclitaxel was first extracted from the bark of the pacific yew tree (*Taxus brevifolia* Nutt) by the Wall group in 1962, and the cytotoxic activity of the pure compound against KB cells was also proved.[3] The structure of paclitaxel was reported in 1971, which is a complex diterpene with an intricate system of four fused rings, including a highly rigid oxetane ring, with an *N*-benzoylphenylisoserine side chain at the C13 position. It has eleven chiral centers and various oxygen functionalities.[4]
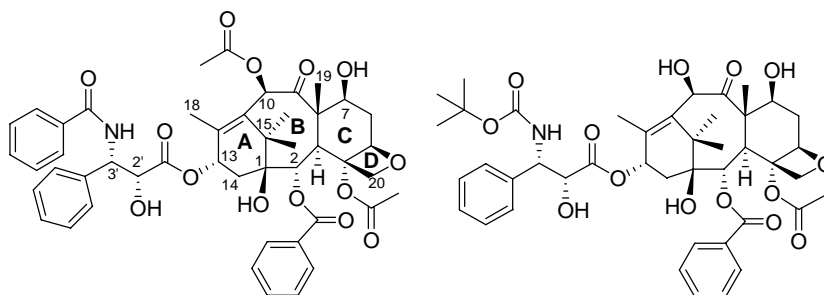
Figure 1-1. Paclitaxel (Taxol®) and Docetaxel (Taxotére®)

In 1979, Susan Horwitz and coworkers discovered that Taxol is a promoter of microtubule assembly.[5, 6] Instead of inhibiting the tubulin polymerization, which is the mechanism of a series of naturally occurring spindle poisons, paclitaxel promotes the polymerization, stabilizes the resulting microtubules and prevents depolymerization, thereby inhibiting the normal dynamic reorganization of microtubular network required for mitosis, which eventually induces apoptosis.[6] The discovery of paclitaxel's unique mechanism of action triggered intense interest and efforts to fully understand the function of paclitaxel at the molecular level.

Cells have a characteristic life cycle that could be divided into two major phases based on cellular activity: interphase, the period of time between successive cell divisions, and mitosis, in which the actual division occurs. Mitosis is further divided into several small phases: prophase, metaphase, anaphase and telophase. In anaphase, the sister chromatids of each chromosome split apart and begin their poleward movement. The migration of each chromosome toward a pole is facilitated by the shortening of the microtubules to which they are attached. It is between metaphase and anaphase that microtubule-targeting agents such as paclitaxel or vinblastine disrupt the regular dynamics required for mitosis. As a result of this mitotic block, apoptosis or programmed cell death is eventually induced.[7, 8]
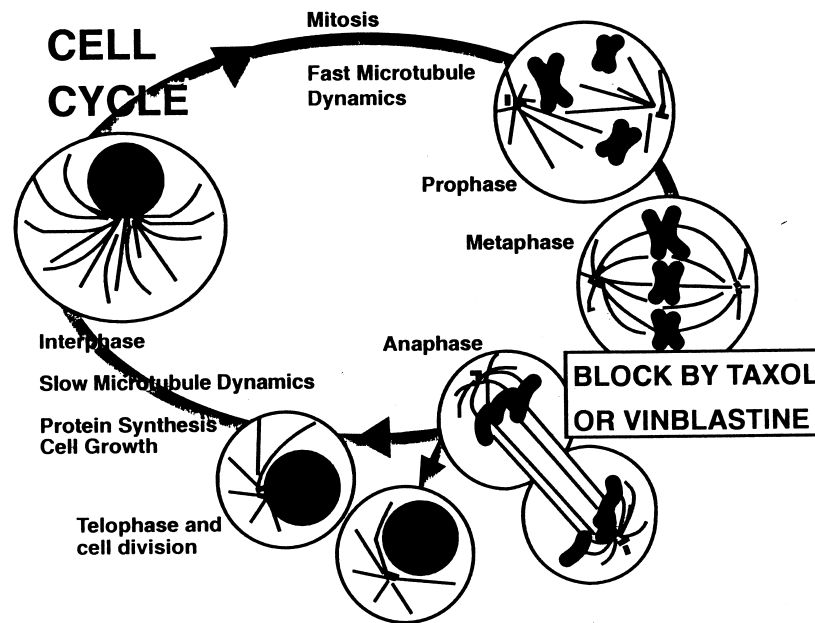
Figure 1-2. The cell cycle and microtubule-targeting anticancer agent
[Adpted from ref. 8]

Microtubules are major structural component of the cell and perform vital functions in cellular division, such as the positioning and transport of smaller organelles within the cell, and the formation of the cytoskeleton, which helps to shape the cell. The process of microtubule formation and the mechanism of action of paclitaxel are summarized in **Figure 1-3**. Microtubules are primarily formed by the dimerization of two protein subunits, α- and β-tubulin, which are structurally similar proteins of approximately 440

amino acid residues with a molecular weight of about 50 kD each. In the presence of magnesium ions, guanosine 5'-triphosphate (GTP), and microtubule-associated proteins (MAPs), the α- and β-tubulins form dumbbell-shaped heterodimers. The heterodimer could grow both along and perpendicular to the axis until the two edges join to form a microtubule which is composed of 13 protofilaments with an average diameter of about 24 nm. Paclitaxel binds to the α,β-tubulin heterodimer aggregate in a 1:1 ratio to promote the polymerization and stabilize the resulting microtubules in an irreversible manner, even in the absence of GTP, MAPs and magnesium. The microtubules thus formed are different from the ones produced by MAP induction in that only 12 protofilaments are present with an average diameter of about 22 nm, and are stabilized to regular microtubule depolymerization conditions, thereby inhibiting their depolymerization. This results in the arrest of the cell division cycle mainly at the G2/M stage, leading to apoptosis through the cell-signaling cascade.
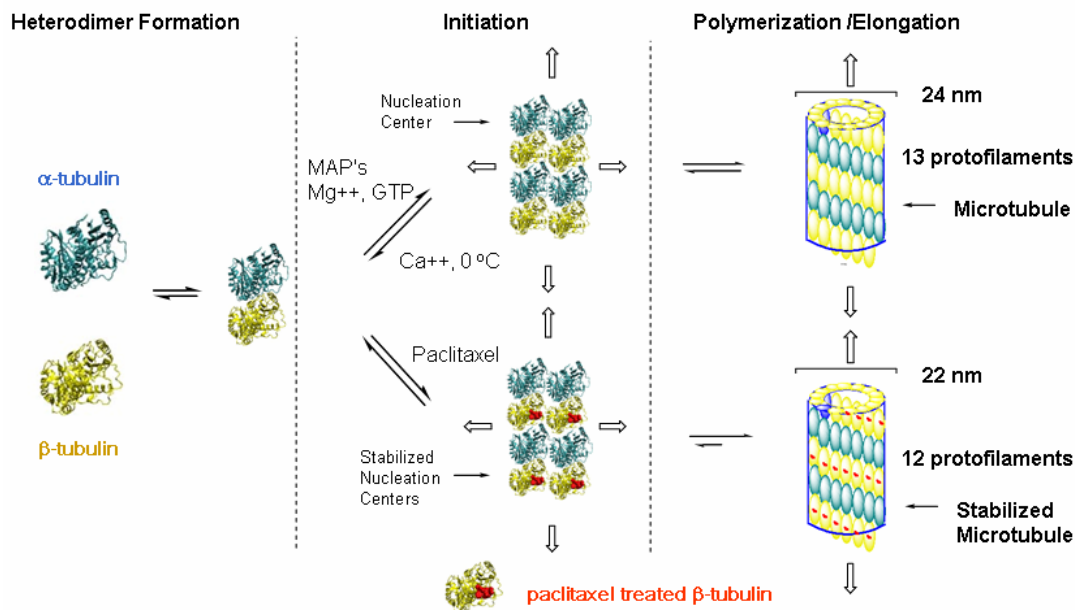
Figure 1-3. Microtubule formation and mechanism of action of paclitaxel[5]

Paclitaxel was approved by the U.S. Food and Drug Administration (FDA) for the treatment of refractory ovarian cancer (December 1992), breast cancer (April, 1994), Kaposi's sarcoma (1997), and lung cancer (1998). Phase II and III clinical trials for the treatment of other cancers, such as colon and prostate cancers, in addition to combination therapy with other chemotherapeutics, are also currently in progress.

However, the only known source of the drug was the isolation from the extracts of the bark of the pacific yew tree (*Taxus brevifolia*), a slow-growing coniferous tree growing in the forest of the American Pacific Northwest.[9] The stripping of the bark is fatal to the tree, making it a limited and non-renewable source. Approximately 3,000 yew trees have to be sacrificed to supply the 10,000 kg of bark, which is necessary to obtain 1 kg of paclitaxel (0.01% yield) to treat approximately 500 patients.

Fortunately, 10-deacetylbaccatin III (DAB, **Figure 1-4**), a diterpenoid that comprises the complex tetracyclic core of paclitaxel, was isolated from the leaves of the European

yew, *Taxus baccata*, in good yield (1 g/1 kg of fresh leaves).[10, 11] This was an important discovery since the yew leaves are readily renewable sources.
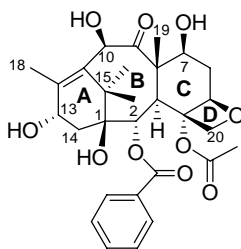
Figure 1-4. 10-Deacetylbaccatin III (10-DAB III)

In 1988, the first semi-synthesis of paclitaxel utilizing 10-DAB III was accomplished by Greene and Potier, as shown in **Scheme 1-1**.[10] However, significant epimerization occurred at the C-2' position on the side chain under the high reaction temperature and long reaction time.
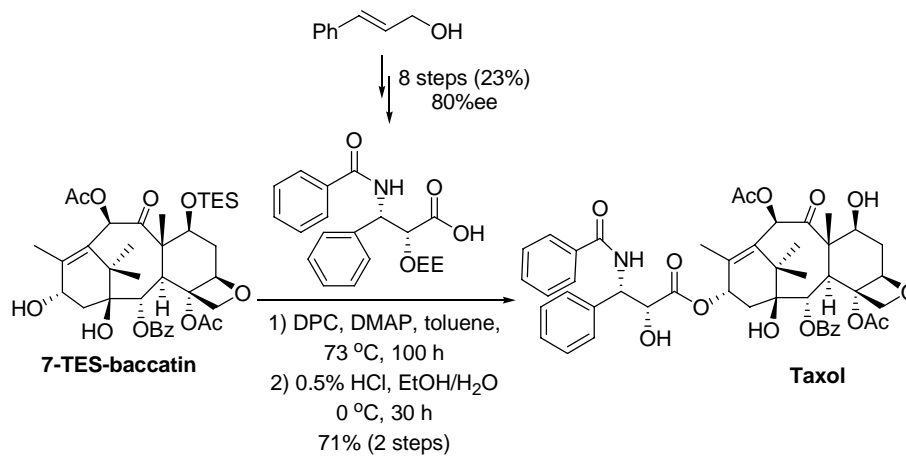
Scheme 1-1. Greene's semi-synthesis of paclitaxel

In 1984, Rhone-Poulenc Rorer (currently Sanofi-Aventis), a French pharmaceutical company, developed Taxotére® (docetaxel), a semi-synthetic analog of paclitaxel (**Figure 1-1**).[11-13] This analog contains a C3'*N-tert*-butoxycarbonyl moiety and a free hydroxyl group at C10, as opposed to the benzoyl and acetyl groups of paclitaxel respectively. Docetaxel was found to share the same mechanism of action as paclitaxel and was twice as potent as paclitaxel. The FDA approved docetaxel for the treatment of breast cancer (May 1996) and non-small cell lung cancer (December 1999).[14]

§ 1.1.3 β-Lactam Synthon Method

A more practical and efficient semi-synthesis of paclitaxel was introduced by Ojima *et al.* using the *β-Lactam Synthon Method*.[15-17] The optically pure β-lactam (*3R,4S*)-4-phenylazetidin-2-one was prepared *via* a highly efficient lithium chiral ester enolate-imine cyclocondensation in high yield and with high enantioselectivity (> 96% ee).[16, 18] The β-lactam was then coupled with 13-*O*-metalated derivatives of 7-TES- baccatin III. A variety of bases such as *n*-BuLi, LDA, LiHMDS, NaHMDS, KHMDS and suspensions of NaH in THF solutions were examined, and NaHMDS was found to be the best base for these ring-opening coupling of *N*-acyl-β-lactams with baccatins. The ring-opening coupling proceeded smoothly at -30 ^{o}C ~ 0 ^{o}C using only a slight excess of β-lactam (1.2 equivalent to a baccatin) to give the coupling product within 30 min in excellent yield (**Scheme 1-2**). The subsequent deprotection afforded paclitaxel in high overall yield. This method solved the limitations of Holton's protocol using 4-dimethylaminopyridine (DMAP) as the base, in which 5 equivalent of β-lactam was need.[15]
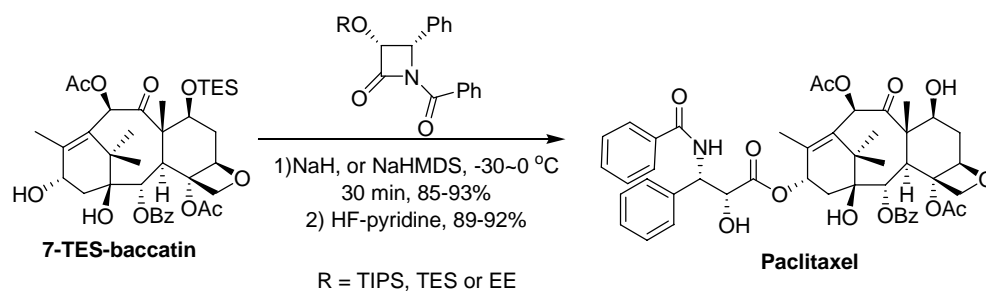
Scheme 1-2 Semi-synthesis of paclitaxel by *β-Lactam Synthon Method*

The Ojima-Holton β-lactam coupling has been the most frequently used method for the total and semi-syntheses of paclitaxel, the SAR studies of taxoids, and for the commercial production of paclitaxel.[19-23] Currently, all paclitaxel production for Bristol-Myers Squibb (BMS) uses plant cell fermentation (PCF) technology, which eliminates the need for many hazardous chemicals and saves a considerable amount of energy, comparing to the semisynthesis.[24]

§ 1.1.4 Second-Generation Taxoids

Although paclitaxel and docetaxel have exhibited excellent anti-tumor activity against various cancer cell lines, it has been shown that treatments with these drugs often result in various undesired side effects as well as multi-drug resistance (MDR),[25, 26] and the low water solubility without a proper vehicle into the organism. Thus, it is very important to develop new taxane-based anticancer agents with fewer side effects, superior pharmacological properties, and improved activities against various classes of tumors, especially against drug-resistant human cancers. Extensive structure-activity relationship (SAR) studies of paclitaxel, docetaxel, and their analogues have been conducted. Several excellent reviews on this topic have been published.[3, 27-29] The SAR studies of different positions of the paclitaxel are summarized in **Figure 1-5**.[30] The upper part of the taxane skeleton appears to be much more flexible for various modifications as compared to the

lower part of the molecule, according to the SAR studies performed on paclitaxel.
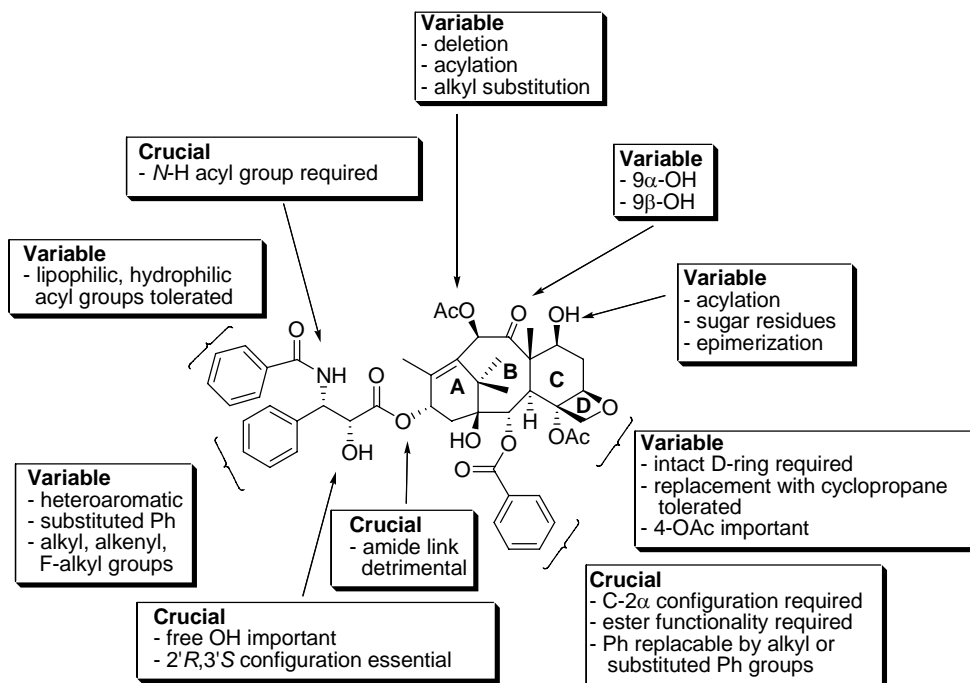
Figure 1-5. Summary of SAR studies of paclitaxel[30]

The Ojima group has developed a series of highly active second-generation taxoids through SAR studies.[31-36] Most of these taxoids exhibited one order of magnitude higher potency than those of paclitaxel and docetaxel against drug-sensitive cancer cell lines, and two to three orders of magnitude higher potency than those of paclitaxel and docetaxel against drug-resistant cell lines expressing MDR phenotypes. There are four key factors responsible for the strong anticancer activity of these new taxoids: (1) the presence of a *tert*-butoxycarbonyl group at C3'-*N* instead of benzoyl group; (2) the replacement of C3 phenyl with an alkenyl or alkyl group; (3) proper modification at C10 position; and (4) modifications at the *meta* position of the C2 benzoate of paclitaxel.[31-36]

R¹ = (structures) (R' = F, Cl, MeO, N₃)

R² = R'CO, R'OCO, R'2NCO, R' (R' = alkyl or alkenyl)

R³ = (structures) CF_3 CF_2H

R⁴ = O^{t}Bu, Ph, R', OR' (R' -= alkyl or alkenyl)
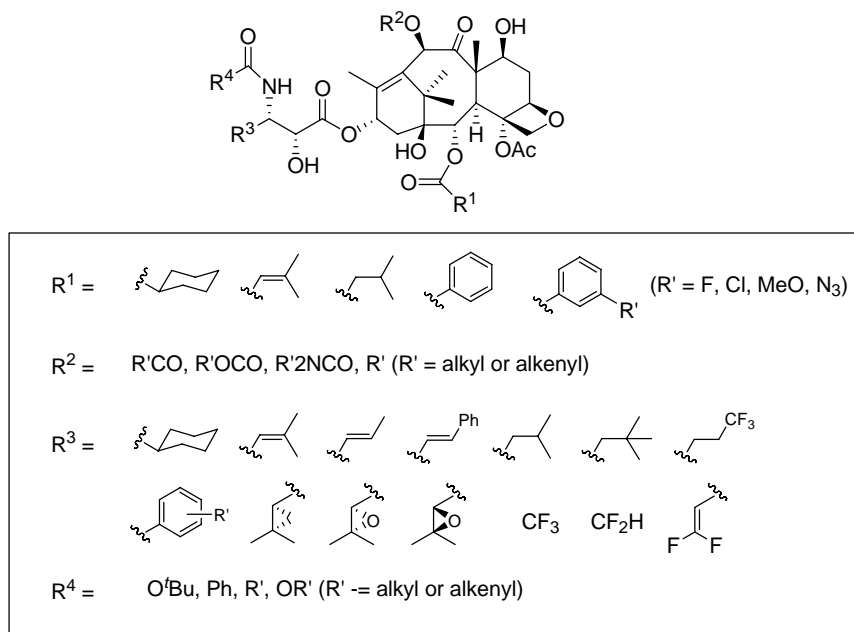
Figure 1-6. Second-generation taxoids synthesized from 10-DAB

One second-generation taxoid, **SB-T-110131 (IDN5109; BAY59-8862; Ortataxel)** has shown promising pharmacological profiles in preclinical studies and has been the focus of extensive biological studies. It is currently undergoing phase II human clinical trials sponsored by Spectrum Pharmaceuticals, Ins..[37, 38]
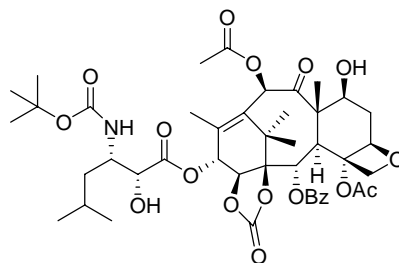
Figure 1-7. SB-T-110131 (IDN5109; BAY59-8862 ; Ortataxel)

In this chapter, the synthesis of enantiopure β-lactams and new-generation taxoids will be discussed.

§ 1.2 Synthesis of β-Lactam

§ 1.2.1 Chiral TIPS-Ester Enolate-Imine Cyclocondensation

The β-lactam synthon method has been successfully utilized for the preparation of C13 side chain precursors in the semi-synthesis of paclitaxel,[16] docetaxel[39] and a great number of taxoids possessing extremely high antitumor activity.[28, 29] Extensive studies and investigations in Ojima's laboratory showed that through an efficient chiral TIPS-ester enolate-imine cyclocondensation reaction, β-lactams can be synthesized in good yields and high enantiomeric purity.[16] (-)-*trans*-2-Phenyl-cyclohexanol (Whitesell's chiral auxiliary, **1-1**)[40] was used as the chiral auxiliary employed in the method to prepare highly optically pure β-lactams (**Scheme 1-3**).[16] Paclitaxel and numerous novel taxoids could be obtained by the efficient coupling of β-lactams with properly modified baccatins and deprotections.[31-36]
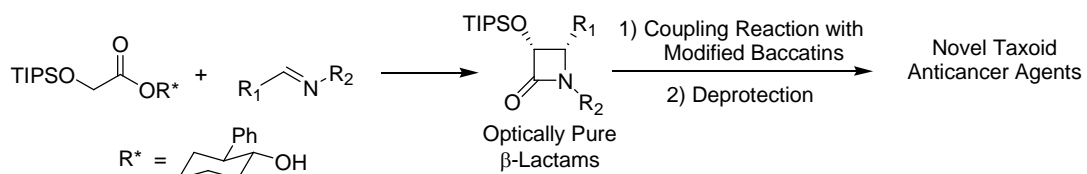
Scheme 1-3. β-lactam as the C13 side chain precursors of taxoids

§ 1.2.2 Results and Discussion

The synthesis of Whitesell's chiral auxiliary (**1-1**) is shown in **Scheme 1-4**.[40] CuI-catalyzed ring opening of cyclohexene oxide with phenylmagnesium bromide provided racemic *trans*-2-phenylcyclohexanol (**1-1**). After acetylation of the alcohol, enzymatic kinetic resolution of the racemic acetate **1-2** using pig liver acetone powder afforded chiral auxiliary **1-1** with >99.9% ee in good yield.
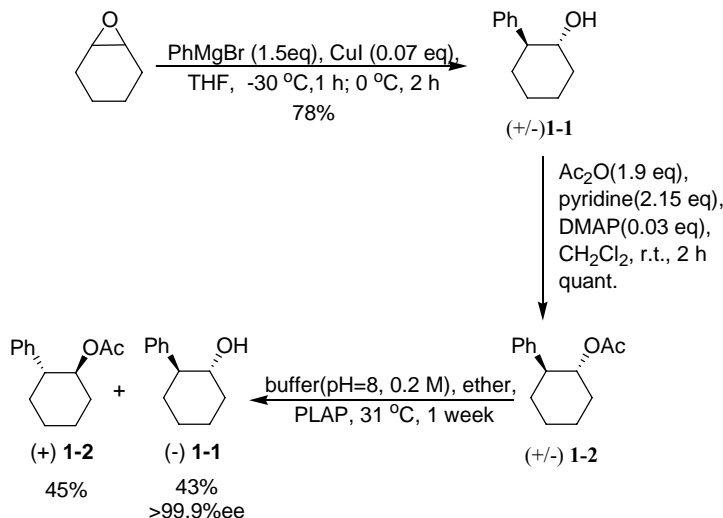
Scheme 1-4. Synthesis of Whitesell's chiral auxiliary (1-1)

The reaction of bromoacetic acid with the sodium alkoxide of benzyl alcohol afforded benzyloxyacetic acid (**1-3**), which was then reacted with chiral alcohol **1-1** to give ester **1-4** in good yield. Hydrogenolysis of **1-4**, followed by TIPS protection of the resulting alcohol afforded the chiral TIPS-ester **1-6** in good yield (**Scheme 1-5**).
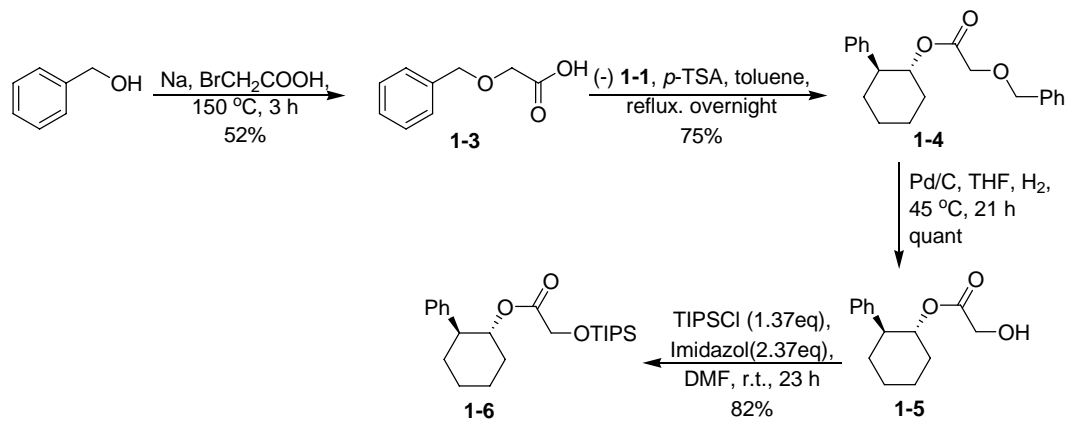
Scheme 1-5. **Synthesis of TIPS-Ester 1-6**

The synthesis of the β-lactam **1-10** is shown in **Scheme 1-6**. 3-Methylbut-2-enal was first reacted with *p*-anisidine in methylene chloride to generate *N-p*-methoxyphenyl(isobutenyl)aldimine (**1-7**). TIPS ester **1-6** in THF was slowly added to LDA. The resulting enolate was then reacted with **1-7** to yield β-lactam (**1-8**) in good yield. The *para*-methoxyphenyl group was then removed by ammonium cerium (IV) nitrate (CAN) oxidation in aqueous acetonitrile. The enantiomeric excess of **1-9** (> 97%) was measure by chiral HPLC. Subsequent standard acylation with di-*tert*-butyldicarbonate gave the desired β-lactam **1-10** in high yield.[32]
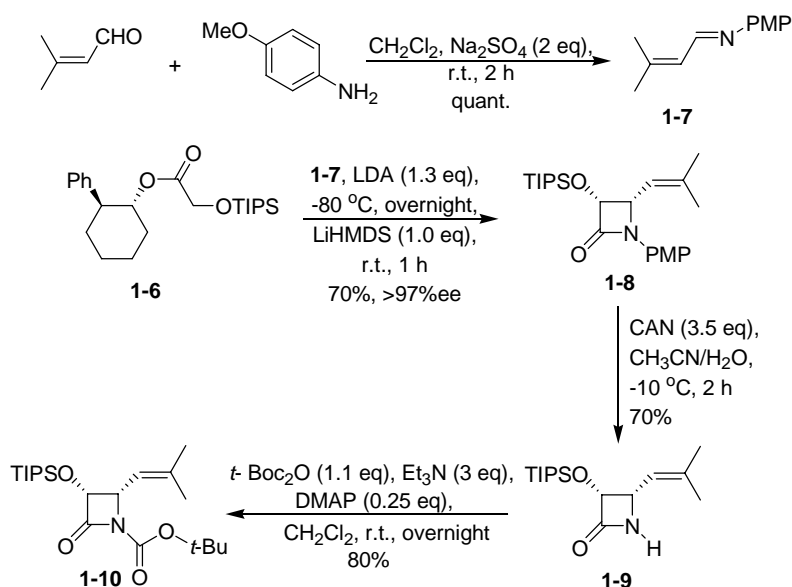
Scheme 1-6. Synthesis of 1-10

The selective formation of *cis*-β-lactam with high enatiomeric purity could be explained by the 6-member-ring transition state proposed in **Scheme 1-7**.[16] At low temperature, (*E*)-enolate is predominantly formed and the initial enolate addition to imine would occur from the less hindered face (back), thus forming the β-amino ester intermediate, which could be isolated upon quenching the reaction at low temperature. When warmed up to room temperature, this intermediate cyclizes to afford the chiral β-lactam and release the chiral auxiliary.

Molecular modeling study (Spartan program; MM2) of conformation of
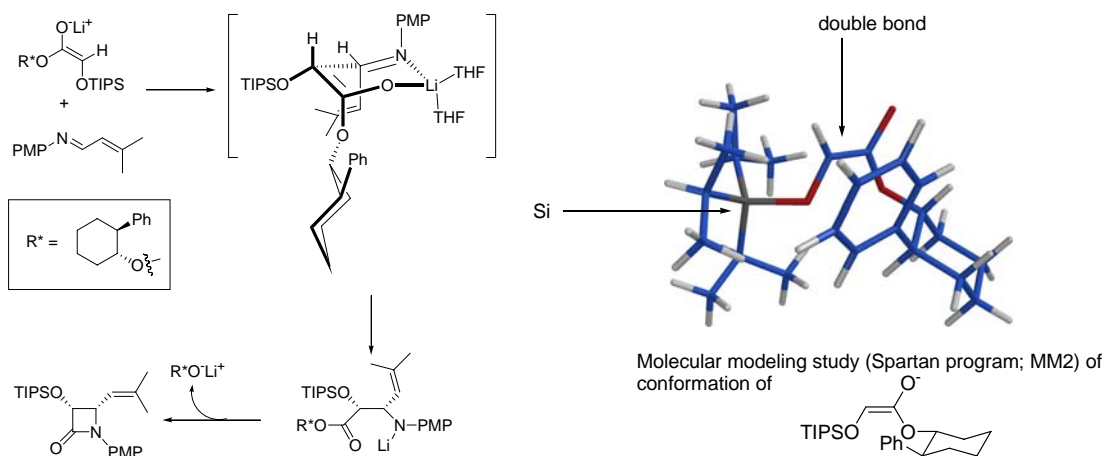
Scheme 1-7. A proposed mechanism of chiral TIPS-ester enolate-imine condensation

§ 1.2.3 [2+2] Cycloaddition Reaction followed by Enzymatic Kinetic Resolution

The reaction between acid chlorides and imines (Staudinger reaction) is assumed to proceed through *in situ* formation of a ketene,[41] followed by reaction with an imine to form a zwitterionic intermediate, which undergoes an electrocyclic conrotatory ring closure to give the β-lactam ring. In general, (*E*)-imines lead preferentially to the more hindered *cis*-β-lactams, while (*Z*)-imines give predominantly the corresponding *trans* isomers (**Scheme 1-8**).[42-44] The theoretical studies undertaken to establish the origin of the *cis/trans* stereoselection have revealed that the relative energies of the rate-determining transition states, led from the zwitterions to β-lactams, are dictated not necessarily by steric effects, but by electronic torquoselectivity.[45-47]

11
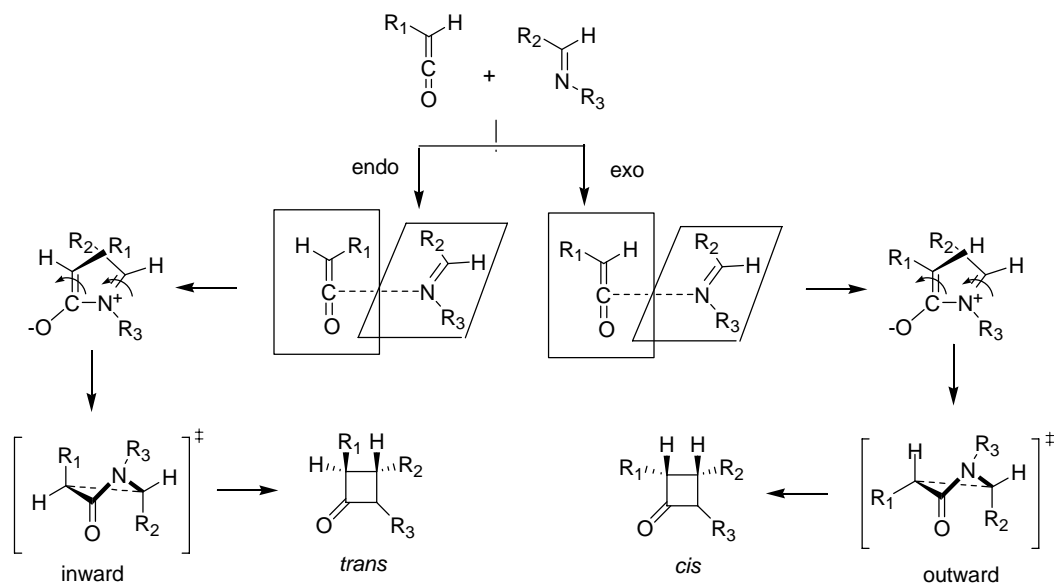
Scheme 1-8. Synthesis of *β*-lactams by Staudinger reaction[48]

Lipases have been widely used for the kinetic resolution of racemic alcohols and carboxylic esters.[49] The resolved enantiopure *β*-lactams are important intermediates in the synthesis of the C13 side chain of taxoids. The commercial availability and relative stability of the lipases make them an attractive class of catalysts for effecting industrial-scale kinetic resolution process.

§ 1.2.4 Results and Discussion

In the presence of triethylamine, acetoxyacetylchloride was reacted with imine **1-11** to give the corresponding racemic *β*-lactam **1-12**. PS-Amano lipase preferentially hydrolyzed acetate moiety at C3 of the (*3S,4R*) enantiomer of **1-12** to afford **(+)-1-12** in 42% yield with 97%ee.[49] The *p*-methoxyphenyl group in **(+)-1-12** was removed through the CAN oxidation, and the acetoxy group was hydrolyzed to give **1-15**. The hydroxyl group was protected with EE (1-ethoxyethyl) group to afford the desired *β*-lactam **1-16** in good overall yield (**Scheme1-9**).

The same [2+2] reaction was performed with imine **1-7** to give the corresponding racemic *β*-lactam **1-17**. The enzymatic resolution afforded **(+)-1-17** with 97%ee in 46% yield.[49] The acetoxy group was hydrolyzed and the resulting 3-hydroxyl group was protected with TIPS group to give **1-8**. The *p*-methoxyphenyl group was removed through oxidation with CAN and the acylation with di-*tert*-butyldicarbonate anhydride gave the desired *β*-lactam **1-10** in good overall yield (**Scheme 1-10**).

MeO—⬡—NH₂ + ⬡—CHO →(CH₂Cl₂, Na₂SO₄ (2 eq), r.t., 2 h, 95%)→ Ph—CH=N—⬡—OMe **1-11**

AcOCH₂COCl (1.5 eq), Et₃N (2 eq), CH₂Cl₂, -78 °C to r.t., 1 day, 100%

AcO⟍ /Ph ... O=⟍N—PMP **(+/-)-1-12**

PS-AMANO, 10% CH₃CN, buffer (0.2 M, pH=7.5), 50 °C, 48 h,

AcO⟍ /Ph O=⟍N—PMP **(+)-1-12** 42%, 97%ee + HO⟍ /Ph O=⟍N—PMP **(-)-1-13** 49%

CAN (4.0 eq), CH₃CN/H₂O, -10 °C, 2 h, 88%

AcO⟍ /Ph O=⟍N—H **1-14** →(1M KOH (10 eq), THF, 0 °C, 1.5 h, 90%)→ HO⟍ /Ph O=⟍N—H **1-15** →(C₂H₅OCH=CH₂ (3 eq), p-TSA (5%), THF, 0 °C, 2 h, 75%)→ EEO⟍ /Ph O=⟍N—H **1-16**

Scheme 1-9. Synthesis of β-lactam 1-16

⟍N—PMP **1-7** →(AcOCH₂COCl (1.5 eq), Et₃N (2 eq), CH₂Cl₂, -78 °C to r.t., overnight, 74%)→ AcO⟍ ⟍ O=⟍N—PMP **(+/-)-1-17**

PS-AMANO, 10% CH₃CN, buffer (0.2 M, pH=7.5), 50 °C, 26 h

HO⟍ ⟍ O=⟍N—PMP **(+)-1-18** ←(1N KOH (10 eq), THF, 0 °C, 1h)— AcO⟍ ⟍ O=⟍N—PMP **(+)-1-17** 46%, 97%ee + HO⟍ ⟍ O=⟍N—PMP **(-)-1-18** 48%

TIPSCl (1.5 eq), Et₃N (4.5 eq), DMAP (0.2 eq), CH₂Cl₂, r.t., overnight, 99% in 2 steps

TIPSO⟍ ⟍ O=⟍N—PMP **1-8** →(CAN (3.5 eq), CH₃CN/H₂O, -10 °C, 2 h, 86%)→ TIPSO⟍ ⟍ O=⟍N—H **1-9** →(t-Boc₂O (1.1 eq), Et₃N (3 eq), DMAP (0.25 eq), CH₂Cl₂, r.t., overnight, 99%)→ TIPSO⟍ ⟍ O=⟍N—C(=O)O—t-Bu **1-10**

Scheme 1-10: Synthesis of β-lactam 1-10

§ 1.3 Synthesis and Biological Evaluation of New-Generation Taxoids

§ 1.3.1 Introduction

A series of novel second-generation taxoids with systematic modifications at the C2, C10, and C3'N positions were developed by Ojima's laboratory. These taxoids exhibited exceptional potencies against drug-sensitive and drug-resistant cell lines.[31, 32, 36] Several taxoids exhibited virtually no difference in potency against the drug-sensitive and drug-resistant cell lines, hence circumvented the multi-drug resistance observed for paclitaxel. These exceptionally potent taxoids were termed "third-generation taxoids".[50]

In this section, four second-generation taxoids: **SB-T-1213**, **SB-T-1214**, **SB-T-1216**, **SB-T-1217** and three third-generation taxoids: **SB-T-121303**, **SB-T-12130301**, **SB-T-121303021** were synthesized. All of these taxoids were re-synthesized for further biological evaluation or for the synthesis of the fatty acid-second-generation taxoid conjugates (See **Chapter II**).
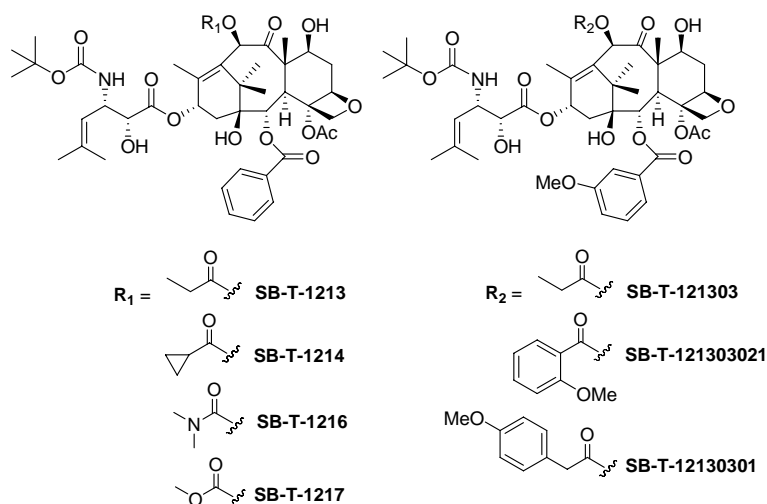
Figure 1-8. Structure of second- and third-generation taxoids

§ 1.3.2 Results and Discussion

§ 1.3.2.1 Synthesis of SB-T-1213

Synthesis of the new second-generation taxoid using the β-lactam ring-opening coupling protocol with a modified baccatin started from the natural product 10-DAB. The acid anhydride was selectively reacted with the C10 hydroxyl group in excellent yield in the presence of cerium chloride.[51] Then, a selective protection of the C7-OH using 2.5 equivalents of triethylsilyl chloride (TESCl) and an excess amount of imidazole in dimethylformamide (DMF) solution gave desired 7-TES-10-propanoyl-10-DAB **(1-21)** in excellent yield.[36] β-Lactam **1-11** was coupled with the modified baccatin **1-21** to afford protected taxoid **1-22** in 91% yield. Global silyl group deprotection using HF-pyridine conditions afforded **1-23** (**SB-T-1213**) in 95% yield.
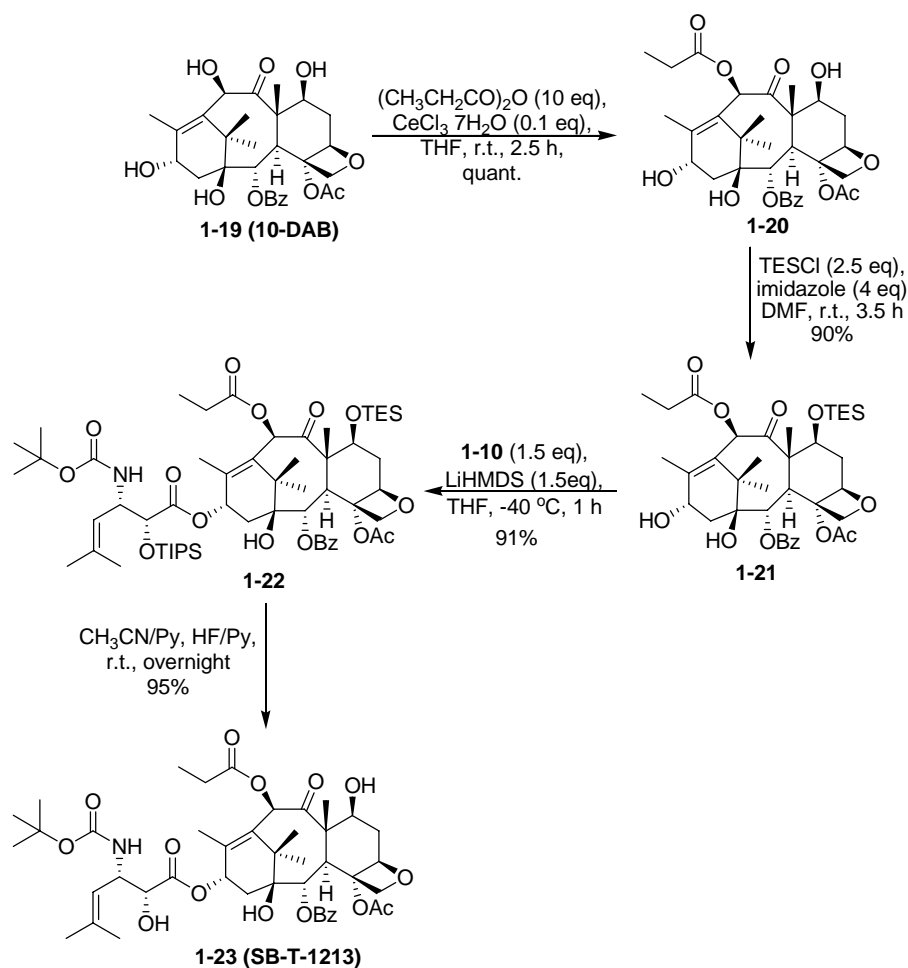
Scheme 1-11. Synthesis of SB-T-1213

§ 1.3.2.2 Synthesis of SB-T-1214, SB-T-1216 and SB-T-1217

A selective protection of the C7-OH of 10-DAB using 3 equivalents of triethylsilyl chloride (TESCl) and an excess of imidazole in DMF solution gave the desired 7-TES-10-DAB (**1-24**) in 95% yield.[36] Then **1-24** was treated with lithium bis(trimethylsilyl)-amide (LiHMDS) at -40 °C, followed by the addition of a proper acid chloride to afford C10-modified baccatins **1-25** selectively in high yield.[36] The *β*-lactam **1-11** was coupled with modified baccatins **1-25** to afford protected taxoids **1-26** in the presence of LiHMDS. The global silyl group deprotection using HF-pyridine conditions gave second-generation taxoids **1-27** (**SB-T-1214**, **SB-T-1216** and **SB-T-1217**) in high yields, as shown in **Scheme 1-12**.
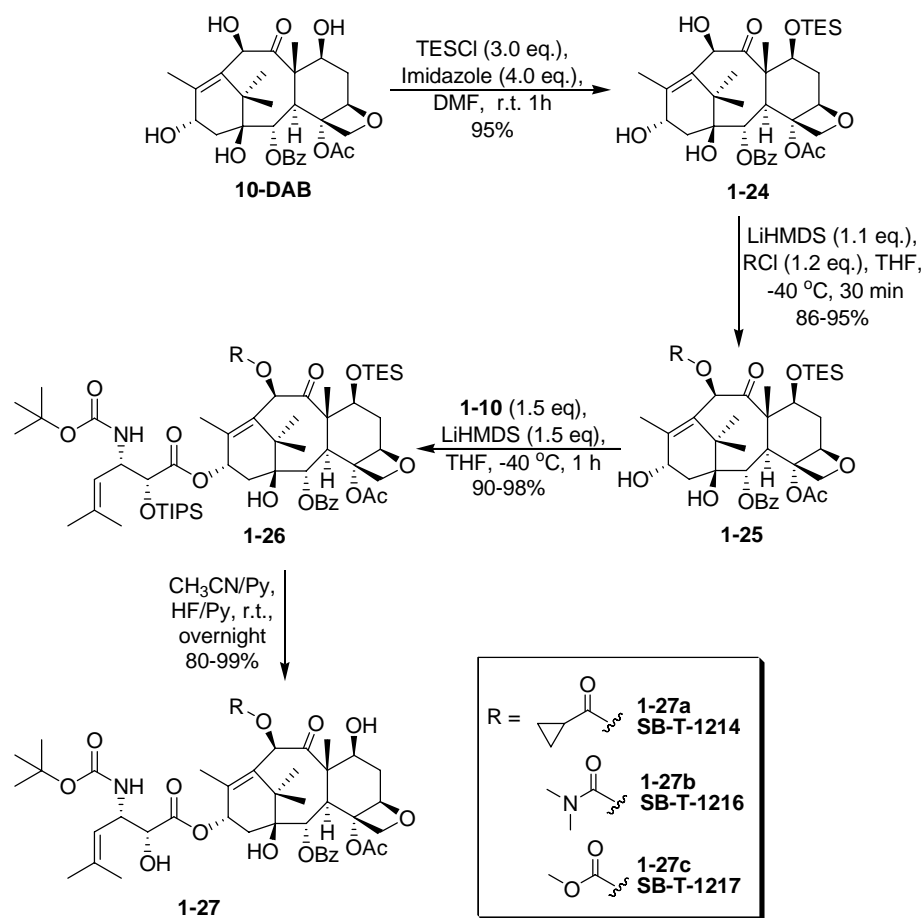
Scheme 1-12. Synthesis of SB-T-1214, SB-T-1216 and SB-T-1217

§ 1.3.2.3 Synthesis of SB-T-121303

TES-protection of 10-DAB using an excess amount of triethylsilyl chloride (TESCl) and imidazole in DMF solution afforded 7,10,13-tri-TES-baccatin **1-28** in high yield. Reductive cleavage of the C2-benzoyl group using Red-Al gave 7,10,13-tri-TES-baccatin diol **1-29** in quantitive yield. Then, this diol was mixed with a large excess of *m*-anisic acid, 1,3-diisopropylcarbodiimide (DIC) and *N,N*-dimethylaminopyridine (DMAP), and refluxed in a concentrated dichloromethane solution overnight to afford the desired C2-modified tri-TES-baccatin **1-30** in 80% yield. A global removal of the TES groups using HF-pyridine gave baccatin **1-31**. Propanoic anhydride was selectively reacted with the C10-hydroxyl group in excellent yield in the presence of cerium chloride.[51] Then a selective protection of the C7-OH using TESCl and imidazole afforded modified-baccatin **1-33** in excellent yield. **1-33** was coupled with *β*-lactam **1-11** to afford the protected taxoid **1-34**. Finally, deprotection of the silyl groups using HF-pyridine gave taxoid **1-35** (**SB-T-121303**) in good overall yield.

16
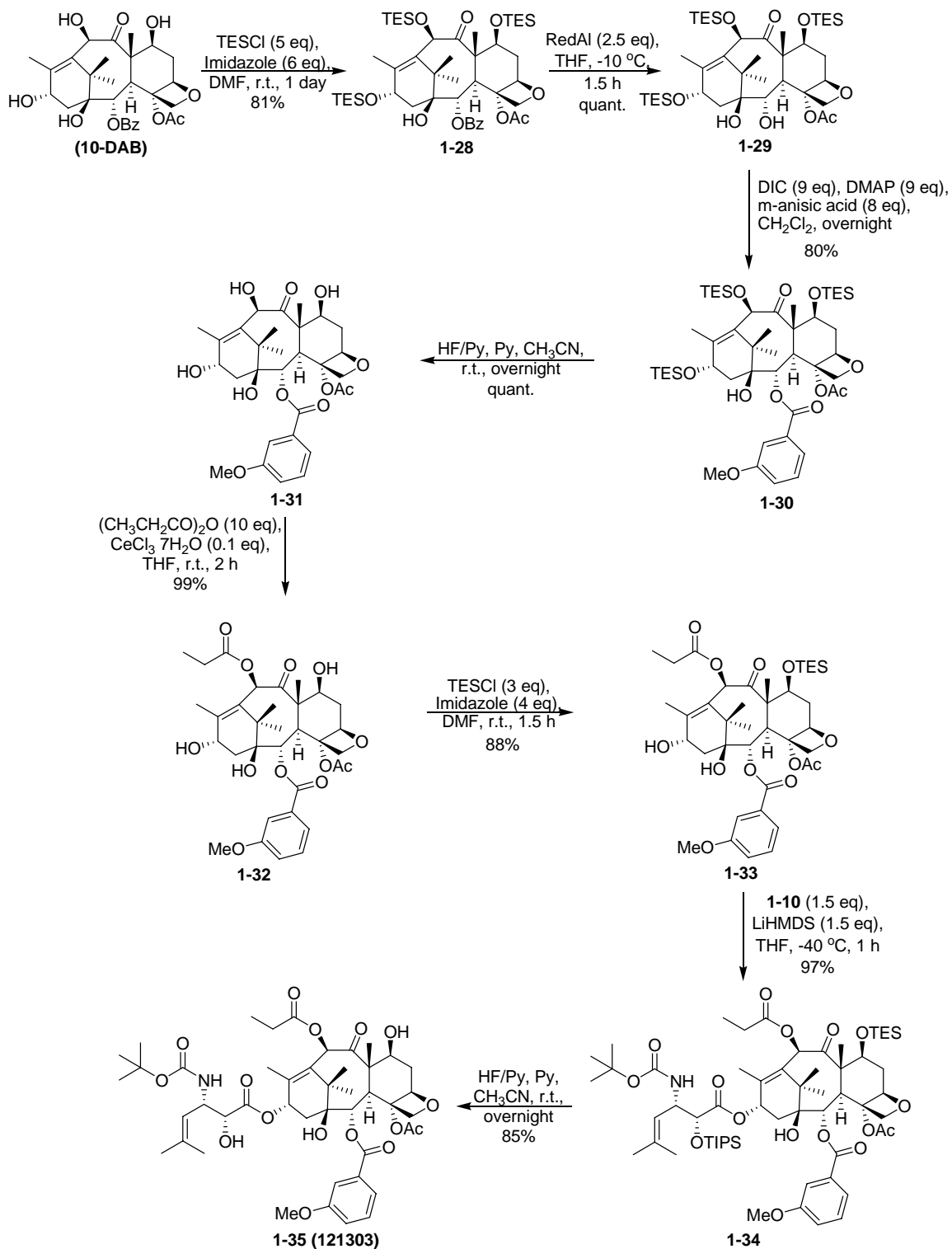
Scheme 1-13. Synthesis of SB-T-121303

§ 1.3.2.4 Synthesis of SB-T-12130301

The selective protection of the C7-OH of the C2-modified 10-DAB **1-31** using 3 equivalents of triethylsilyl chloride (TESCl) and an excess of imidazole in DMF solution gave the desired 7-TES-baccatin **1-36** in 93% yield. Then, **1-36** was treated with LiHMDS at -40 °C, followed by the addition of an acid chloride to afford C10-modified baccatin **1-37** selectively in high yield.[36] The *β*-lactam **1-11** was coupled with modified baccatin **1-37** to afford protected taxoid **1-38** in the presence of LiHMDS. The silyl group deprotection using HF-pyridine conditions gave **SB-T-12130301** in high yield.
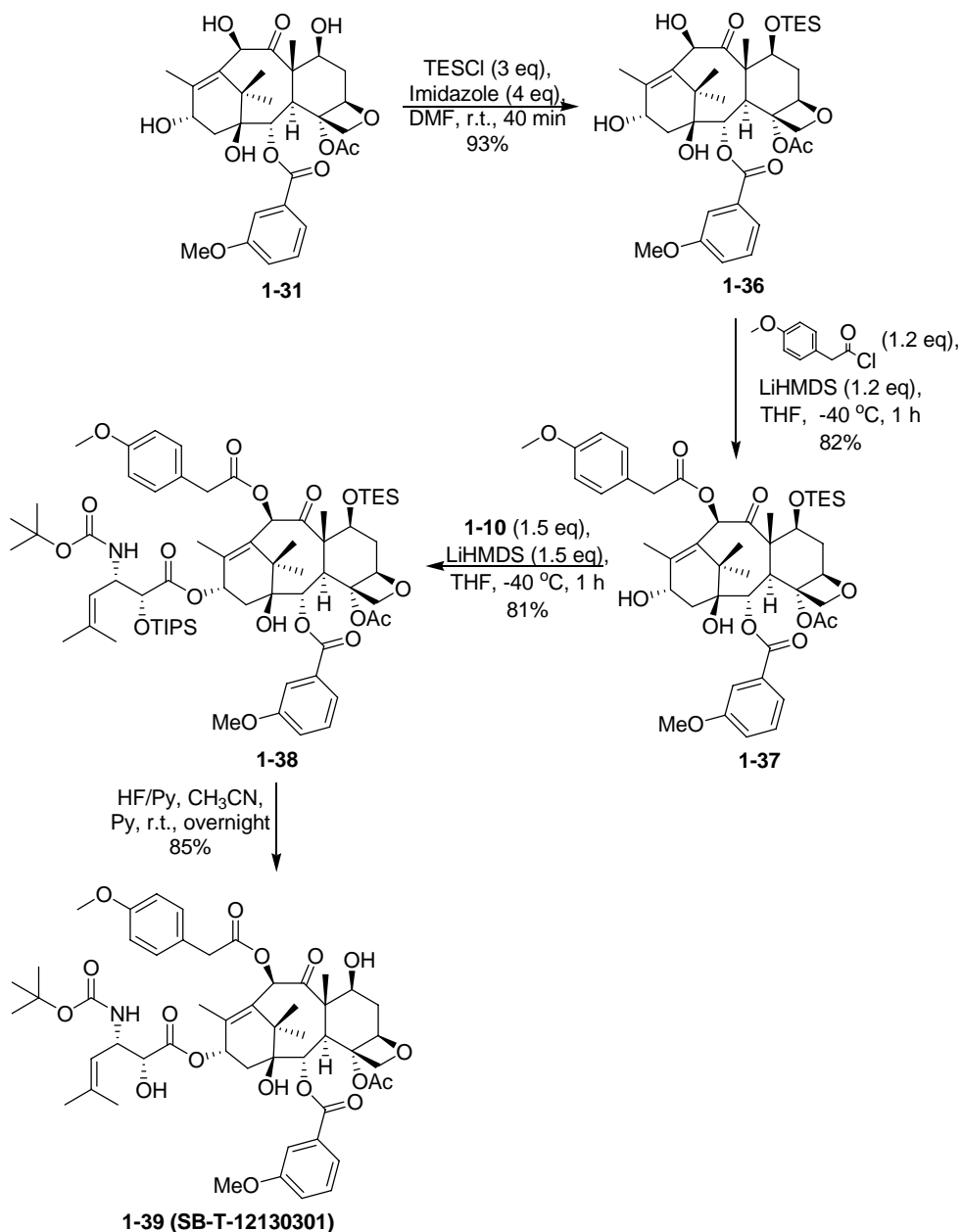
Scheme 1-14. Synthesis of SB-T-12130301

§ 1.3.2.5 Synthesis of SB-T-121303021

Selective introduction of the *o*-anisoyl group to the C10 position was not possible by the methods described above. However, selective oxidation of the C13 position of **1-36** using tetrapropylammonium perruthenate (TPAP) and *N*-methylmorpholine-*N*-oxide (NMO) provided 13-oxo baccatin **1-40** in good yield. The C10 position was then acylated with *o*-anisoyl chloride in the presence of DMAP to afford the C10-modified compound **1-41**. Reduction of the C13 ketone with NaBH₄ gave the desired C10-modified baccatin **1-42** in reasonable yield. The *β*-lactam was coupled with modified baccatin **1-42** to afford protected taxoid **1-43** in the presence of LiHMDS. Following global silyl group deprotection using HF-pyridine conditions gave **SB-T-121303021** in high yield.
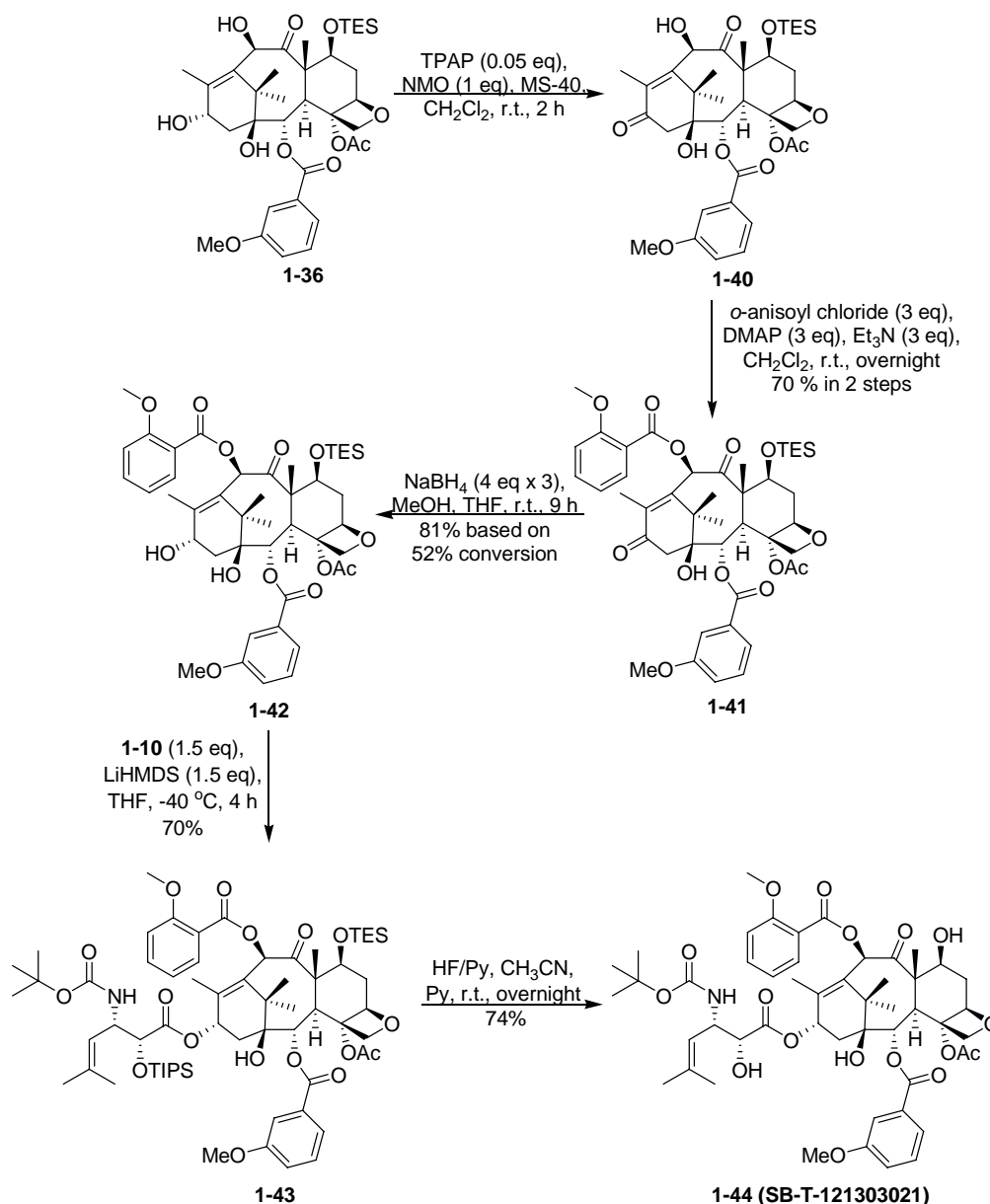
Scheme 1-15. Synthesis of SB-T-121303021

§ 1.3.3 Biological Evaluation of New-Generation Taxoids

§ 1.3.3.1 Cytotoxicity of New-Generation Taxoids against Human Breast and Ovarian Cancer Cell Lines

The second- and third-generation taxoids thus synthesized, were evaluated for their cytotoxicity against human breast cancer cell line MCF7 (P-glycoprotein negative, Pgp-), human ovarian cancer cell line NCI/ADR (P-glycoprotein positive, Pgp+) and selected taxoids were also assayed for their potency against drug-sensitive (LCC6-WT, Pgp-) and drug-resistant (LCC6-MDR, Pgp+) human breast cancer cell lines at the Roswell Park Cancer Institute. Results are summarized in **Table 1-1** with the values of paclitaxel shown for comparison purpose. As **Table 1-1** shows, the taxoids are exceptionally potent, especially against drug-resistant cell lines. All of the taxoids show one order of magnitude higher potency than paclitaxel against drug-sensitive cancer cell lines, MCF7 and LCC6-WT, and two-three orders of magnitude higher potency than paclitaxel against drug-resistant cancer cell lines, NCI/ADR and LCC6-MDR.

Table 1-1. Cytotoxicity of second and third-generation taxoids (IC_{50} nM)[a]

Taxoid	LCC6-WT[b]	LCC6-MDR[c]	R/S[d]	MCF7[e]	NCI/ADR[f]	R/S[d]
Paclitaxel	3.1	346	112	1.7	300	176
Docetaxel	1.0	120	120	1.0	235	235
SB-T-1213	/	/	/	0.18	4.0	22
SB-T-1214	/	/	/	0.20	3.9	20
SB-T-1216	/	/	/	0.13	4.9	6.3
SB-T-1217	/	/	/	0.14	5.3	2.9
SB-T-121303	/	/	/	0.36	0.33	7.5
SB-T-121303021	0.4	0.9	2.3	1.1	3.3	3.0
SB-T-12130301	0.4	0.4	1.0	0.6	1.8	3.0

[a]Concentration of compound which inhibits 50% (IC_{50}, nM) of the growth of human tumor cell line after 72 h drug exposure. [b]LCC6-WT: human breast carcinoma cell line (Pgp-). [c]LCC6-MDR: *mdr1* transduced cell line (Pgp+). [d]Resistance factor = (IC_{50} for drug resistant cell line, R) / (IC_{50} for drug-sensitive cell line, S). [e]MCF7: human breast carcinoma cell line. [f]NCI/ADR: multi-drug resistant human ovarian carcinoma cell line.

§ 1.3.3.2 Cytotoxicity of New-Generation Taxoids against Paclitaxel-Resistant Cancer Cells with Point Mutations in Tubulin

Multidrug-resistance (MDR) to paclitaxel mainly arises from the overexpression of ATP-binding cassette (ABC) transporters,[52] but other drug-resistance mechanisms are also involved in paclitaxel resistance.[53] One of the significant mechanisms is associated with alterations of its cellular target, tubulin/microtubule.[54-59] In this regard, two paclitaxel-resistant sublines, 1A9PTX10 and 1A9PTX22 derived from 1A9 cell line, have been reported.[58] The parental 1A9 is a clone of the human ovarian carcinoma cell line A-2780. Point mutations in class I β-tubulin in both 1A9PTX10 and 1A9PTX22 have been identified by sequence analysis.[58] Thus, the cytotoxicity of new-generation taxoids against these two paclitaxel-resistant cell lines would provide critical information about their ability to deal with drug resistance other than ABC transporters.

Selected new-generation taxoids, **SB-T-1214**, **SB-T-121303** and **SB-T-11033** (the C3'-hydrogenated analog of **SB-T-121303**), were assayed against both drug-resistant cell lines and the parental cell line, according to the reported procedure.[60, 61] As **Table 1-2** shows, all three taxoids exhibit extremely potent activity, against drug-resistant cell lines 1A9PTX10 and 1A9PTX22, with two orders of magnitude higher potency than paclitaxel. The results clearly demonstrate that these second- and third-generation taxoids are capable of effectively circumventing the paclitaxel drug-resistance arising from point mutations in tubulins/microtubules besides MDR. This makes the new-generation taxoids even more attractive.

Table 1-2. Cytotoxicity of new-generation taxoids against 1A9PTX10 and 1A9PTX22 cell lines (IC$_{50}$ nM)^a

Taxoids	1A9	1A9PTX10	R/S^b	1A9PTX22	R/S^b
Paclitaxel	1.38±0.05	532.95±3.18	386	160.70±14.70	116
SB-T-1214	0.44±0.04	9.00±0.77	20.4	3.94±0.03	9.0
SB-T-121303	0.76±0.01	3.65±0.21	4.8	3.88±0.54	5.1
SB-T-11033	0.25±0.01	4.91±0.53	19.6	2.10±0.13	8.4

^{a}Concentration of compound which inhibits 50% (IC$_{50}$, nM) of the growth of human tumor cell line after 72 h drug exposure.
^{b}Resistance factor = (IC$_{50}$ for drug resistant cell line, R) / (IC$_{50}$ for drug-sensitive cell line, S).

§ 1.3.3.3 Tubulin Polymerization Assay

The activities of **SB-T-1214** and **SB-T-121303** were evaluated in the *in vitro* tubulin polymerization assay at the Albert Einstein College of Medicine. Paclitaxel was also used as the standard for comparison. Changes in absorbance in this spectrophotometric assay provide a direct measure of turbidity, hence indicating the extent of tubulin polymerization. Taxoids, **SB-T-1214** and **SB-T-121303**, induced tubulin polymerization in the absence of GTP in a manner similar to paclitaxel. The microtubules formed with these new-generation taxoids as well as paclitaxel were stable against Ca^{2+}-induced depolymerization. As **Figures 1-14** shows, taxoids **SB-T-1214** and **SB-T-121303** promote rapid polymerization of tubulin at a faster rate than that of paclitaxel. The

turbidity of the tubulin solution treated by **SB-T-1214** or **SB-T-121303** reaches plateau quickly and does not change with time. This observation may imply that there is a difference in structure between microtubules formed with the new-generation taxoids and those with paclitaxel. Third-generation taxoid **SB-T-121303** causes spontaneous tubulin polymerization, reaching >90% of a plateau within 5 min from onset, while it takes about 12 min for second-generation taxoid **SB-T-1214** to reach the same point.
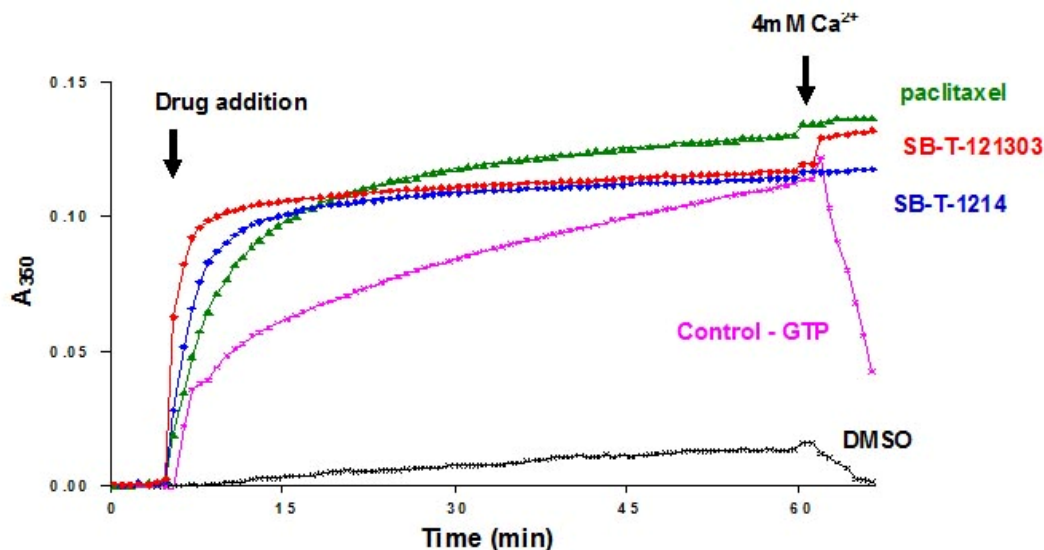
Figure 1-9. Tubulin polymerization with SB-T-1214, SB-T-121303 and paclitaxel: microtubule protein 1 mg/mL, 37 ^{o}C, GTP 1 mM, Drug 10 μM

§ 1.3.3.4 Electron Microscopy Analysis

The microtubules formed with new-generation taxoids (**SB-T-1214** and **SB-T-121303**) were analyzed further by electron microscopy for their morphology and structure in comparison with those formed by using GTP and paclitaxel. The electron micrographs of microtubules formed with the two taxoids, paclitaxel and GTP are summarized in **Figures 1-15**. As **Figures 1-15a** and **1-15b** show, GTP and paclitaxel form long and straight microtubules. The microtubules formed with a second-generation taxoid **SB-T-1214** (**Figures 1-15c**) are shorter than those with GTP or paclitaxel. In contrast, the morphology of the microtubules formed by the action of third-generation taxoid **SB-T-121303** is very unique in that those microtubules are very short and numerous (**Figures 1-15d**).
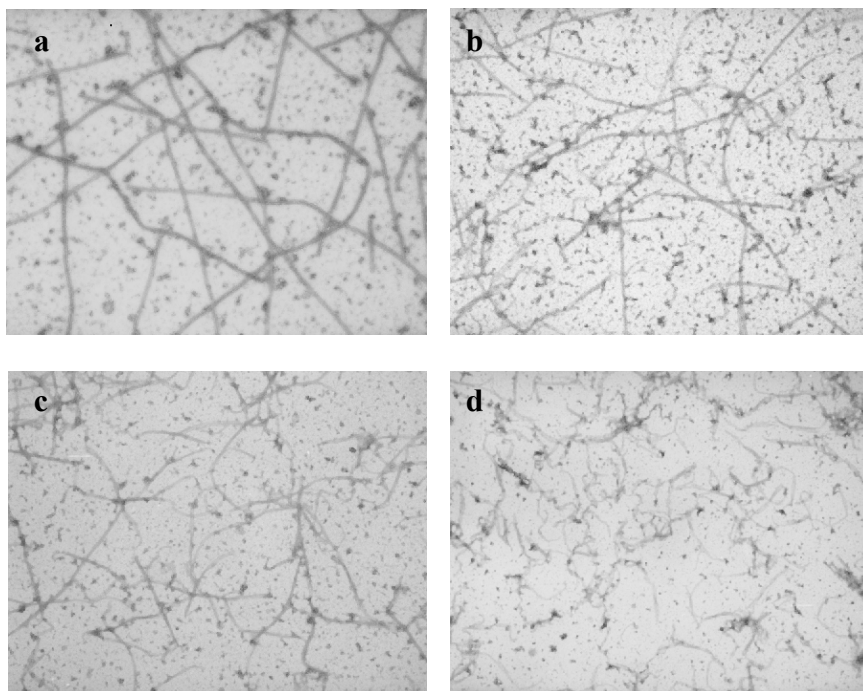
Figure 1-10. Electromicrographs of microtubules: (a) GTP; (b) paclitaxel; (c) SB-T-1214; (d) SB-T- 121303

§ 1.3.4 Synthesis and Biological Evaluation of C3'-Difluorovinyl-Taxoids

§ 1.3.4.1 Introduction

Fluorine is one of the smallest atoms with the highest electronegativity. Thus, the introduction of fluorine to a bioactive molecule causes minimal steric alteration, while significantly affects the physico-chemical properties of the molecule.[62] The replacement of an oxidizable C-H group by a C-F group increases the metabolic stability of the molecule. The presence of fluorine(s) enhances lipophilicity of drugs and thus increases hydrophobic interactions and membrane permeability.[62] New and effective biochemical tools as well as medicinal and therapeutic agents have been successfully developed through rational design exploiting these special properties of fluorine.[62, 63] Fluorinated analogues of biologically active molecules can also serve as excellent probes for the investigation of biochemical mechanisms. ^{19}F-NMR can provide unique and powerful tools for the mechanistic investigations in chemical biology. [28, 62, 64-67]

In recent years, a series of fluoro-containing taxoids were synthesized and evaluated in Ojima's laboratory.[65, 68-70] The introduction of the CF_2H and CF_3 groups to the C3'-position of taxoids, creates a class of fluorinated taxoids with improved biological activity compared with paclitaxel and docetaxel, especially against multi-drug resistant cell lines.[70] Recent metabolism studies conducted on C3'-isobutyl- and C3'-isobutenyl-taxoids, in collaboration with Dr. Gut, disclosed that the metabolism of second-generation taxoids (**SB-T-1214**, **SB-T-1216**, and **SB-T-1103**) is markedly different from that of docetaxel and paclitaxel.[71] It was found, in fact, that these taxoids are oxidized by

the cytochrome P450 3A4 at the two allylic methyl groups of the C3'-isobutenyl group and the methyne moiety of the C3'-isobutyl group as primary metabolic sites (**Figure 1-11**). On the contrary, docetaxel has the *tert*-butyl group on the C3'nitrogen as the single metabolic site.[2] Based on these considerations, we have designed and synthesized C3'-difluorovinyl taxoids, in order to block the allylic oxidation by CYP 3A4 mentioned above to increase the metabolic stability.
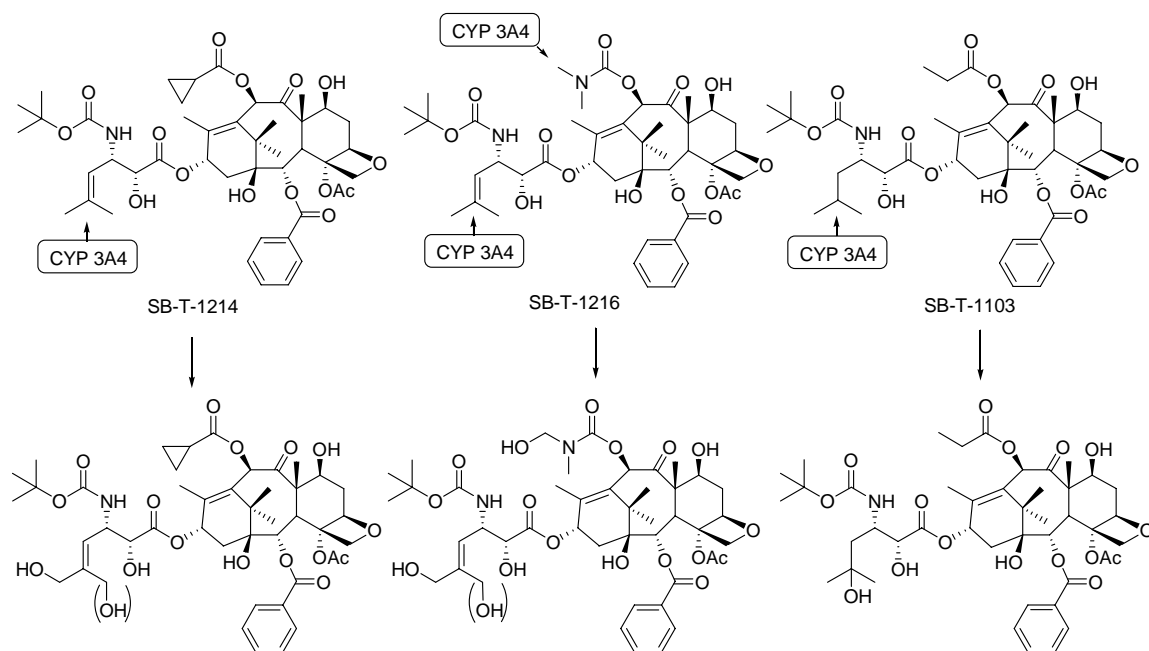
Figure 1-11. **Primary sites of hydroxylation on the second-generation taxoids by P450 family enzymes**

Based on the metabolism studies, a series of C3'-difluorovinyl taxoids with different substitution at C10 and C2 positions were synthesized and evaluated in Ojima's laboratory.[70] These novel taxoids exhibit exceptional potency against MCF7 cell line, i.e., most of these taxoids possess less than 100 pM IC_{50} values, exceeding the potency of the highly potent second-generation taxoids previously developed in the laboratory. Cytotoxicities against NCI/ADR cell line are almost all subnanomolar level IC_{50}'s, which are three orders of magnitude more potent than paclitaxel.
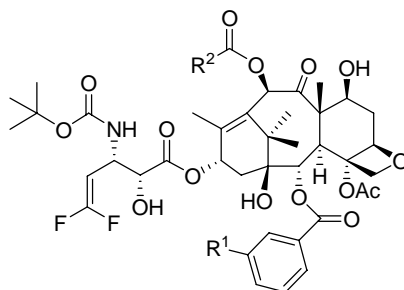
Figure 1-12. C3'-Difluorovinyl-taxoids

In this section, enantiopure 4-difluorovinyl-β-lactam **1-48** and difluorovinyl-taxoid, **SB-T-12853**, were synthesized in a large scale. Four C3'-difluorovinyl-taxoids (**Figure 1-18**) were evaluated for the potency in cytotoxicity assay and tubulin polymerization assay.
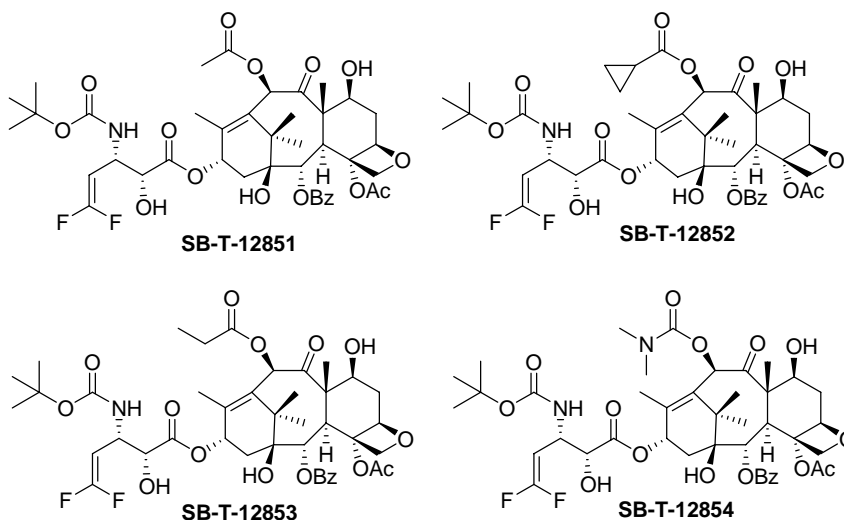
Figure 1-13. **Structure of C3'-difluorovinyl-taxoids**

§ 1.3.4.2 Results and Discussion

Enantiopure β-lactam **1-8** was subjected to ozonolysis, affording **1-45** in 92% yield[69], which was transformed to **1-46** by using CBr_2F_2, hexamethylphosphoroustriamide (HMPT), and Zn in THF (**Scheme 1-16**).[72, 73] The yield of this step (80%) was greatly improved from the previous study (20-60%)[74] by using a larger amount of HMPA and Zn. The PMP group was removed using CAN to give enantiopure β-lactam **1-47**, followed by acylation with Boc_2O to afford the desired (3R,4S)-N-Boc-3-TIPSO-4-difluorovinylazetidin-2-one (**1-48**) in excellent yield. The ring-opening coupling of β-lactam **1-48** with modified baccatin **1-21** was carried out at -40°C in THF using LiHMDS. The subsequent removal of the silyl protecting groups using HF/pyridine gave the corresponding difluorovinyl taxoid **SB-T-12853** in excellent yield (**Scheme 1-16**).
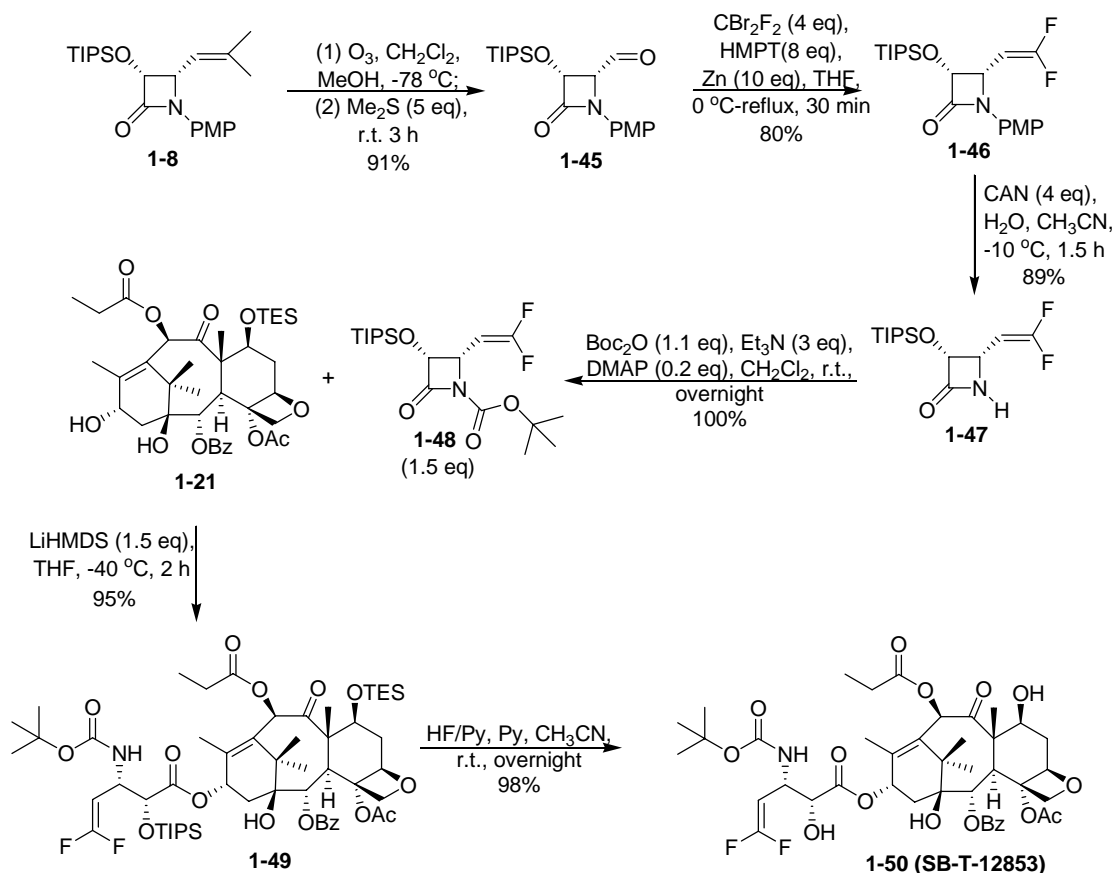
Scheme 1-16. Synthesis of SB-T-12853

§ 1.3.4.3 Biological Evaluation of Difluorovinyl-Taxoids

§ 1.3.4.3.1 Cytotoxicity of Difluorovinyl-Taxoids against Human Breast and Ovarian Cancer Cell Lines

The cytotoxicity of the novel difluorovinyl-taxoids **SB-T-12851**, **SB-T-12852**, **SB-T-12853**, and **SB-T-12854** was evaluated *in vitro* against human breast cancer cell line MCF7 (Pgp-) and human ovarian cancer cell line NCI/ADR (Pgp+) respectively at the Roswell Park Cancer Institute. The IC$_{50}$ values were determined through 72 h exposure of the fluoro-taxoids to the cancer cells according to the protocol developed by Skehan et al[75]. The received data are summarized in **Table 1-3**.

Table 1-3. *In vitro* cytotoxicity (IC$_{50}$ nM) of C3'-difluorovinyl-taxoids[a]

Taxoid	MCF7[b]	NCI/ ADR[c]	R/S[d]
Paclitaxel	1.7	300	176
SB-T-1213	0.18	2.2	12
SB-T-12851	0.14	0.95	6.7
SB-T-12852	0.17	6.03	35.5
SB-T-12853	0.17	1.2	7.06
SB-T-12854	0.19	4.27	22.5

[a]Concentration of compound which inhibits 50% (IC$_{50}$, nM) of the growth of human tumor cell line after 72 h drug exposure. [b]MCF7: human breast carcinoma cell line. [c]NCI/ADR: multi-drug resistant human ovarian carcinoma cell line. [d]Resistance factor = (IC$_{50}$ for drug resistant cell line, R) / (IC$_{50}$ for drug-sensitive cell line, S).

As shown in **Table 1-3**, the C3'-difluorovinyl-taxoids possess one order of magnitude higher potency than paclitaxel against the drug-sensitive cell line MCF7, two-three orders of magnitude higher potency than paclitaxel against drug-resistant cell line NCI/ADR, and comparable cytotoxicity with second-generation taxoid **SB-T-1213** against these two cell lines.

§ 1.3.4.3.2 Cytotoxicity of Difluorovinyl-Taxoids against Human Pancreatic and Colon Cancer Cell Lines

The four difluorovinyl-taxoids were also tested against drug-resistent pancreatic cancer cell line, PANC-1 and colon cancer cell line, HT-29, using standard MTT assay. The results are summarized in **Table 1-4**.

Table 1-4. *In vitro* cytotoxicity (IC$_{50}$ nM ± SE)[a] of C3'-difluorovinyl-taxoids

Taxoid	PANC-1[b]	HT-29[c]
Paclitaxel	25.68 ± 3.05	4.26 ± 0.44
SB-T-12851	1.19 ± 0.14	0.49 ± 0.04
SB-T-12852	5.85 ± 0.73	1.01 ± 0.12
SB-T-12853	0.65 ± 0.07	0.40 ± 0.06
SB-T-12854	1.58 ± 0.15	0.54 ± 0.06

[a]Concentration of compound which inhibits 50% (IC$_{50}$, nM) of the growth of human tumor cell line after 72 h drug exposure. [b]PANC-1: human pancreatic carcinoma cell line. [c]HT-29: human colon carcinoma cell line.

The difluorovinyl-taxoids show 4-10 times higher potency than paclitaxel against colon cancer cell line, HT-29 and 5-40 times higher potency than paclitaxel against pancreatic cancer cell line PANC-1. The efficacy of the compounds did not appear to be affected by the expression of multidrug resistance proteins in the PANC-1 cell line.

§ 1.3.4.3.3 Tubulin Polymerization Assay

The activities of three C3'-difluorovinyl-taxoids **SB-T-12851**, **SB-T-12852** and **SB-T-12854** were evaluated in the *in vitro* tubulin polymerization assays at the Albert Einstein College of Medicine. Paclitaxel was used as the standard for comparison purpose. Changes in absorbance in this spectrophotometric assay provide a direct measure of turbidity, hence indicating the extent of tubulin polymerization. All three difluorovinyl-taxoids induced tubulin polymerization in the absence of GTP in a manner similar to that of paclitaxel (**Figures 1-17**). The microtubules formed with these new generation taxoids as well as paclitaxel were stable against Ca^{2+}-induced depolymerization. As **Figure 1-14** shows, all three difluorovinyl-taxoids promote rapid polymerization of tubulin at a faster rate than that of paclitaxel. The microtubules formed with the new fluoro-taxoids are similar to those with second-generation taxoid **SB-T-1214** (**Figure 1-9**).
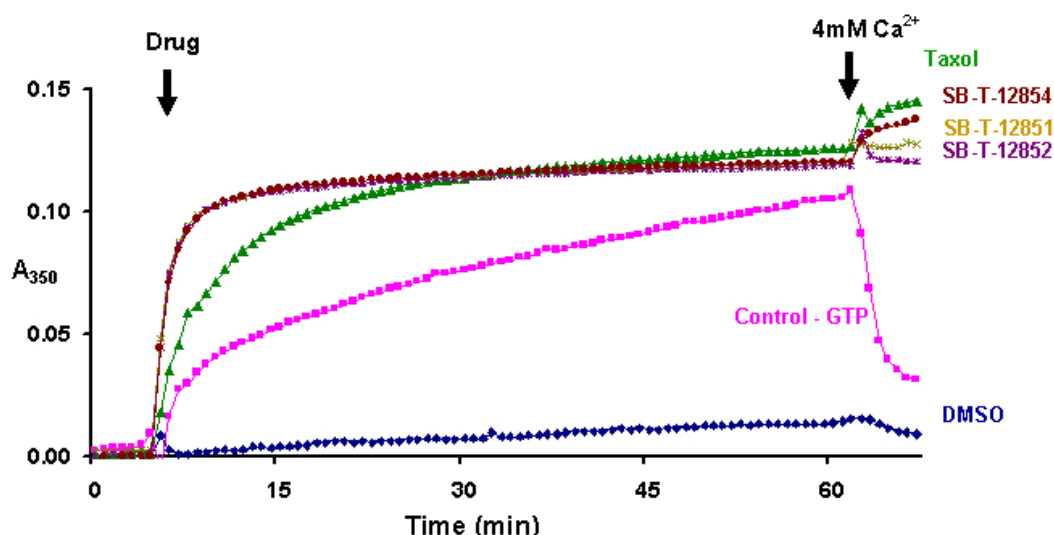
Figure 1-14. Tubulin polymerization with SB-T-12851, SB-T-12852, SB-T-12854 and paclitaxel: microtubule protein 1 mg/mL, 37 ^{o}C, GTP 1 mM, Drug 10 μM

§ 1.3.3.4.4 Electron Microscopy Analysis

The microtubules formed with the fluoro-taxoids were also analyzed further by electron microscopy for their morphology and structure in comparison with those formed by using GTP and paclitaxel. The electron micrographs of microtubules formed with the three fluoro-taxoids are summarized in **Figures 1-15**. The morphology of the microtubules formed by the action of C3'-difluorovinyl-taxoids is very similar to those formed by second-generation taxoid **SB-T-1214** (**Figures 1-15c**).
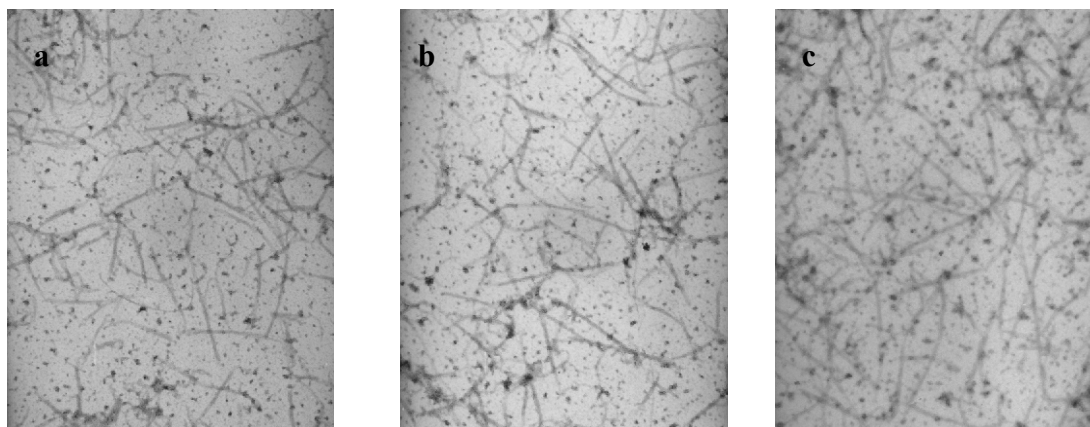
Figure 1-15. Electromicrographs of microtubules: (a) SB-T-12851; (b) SB-T-12852; (c) SB-T-12854

§ 1.3.4.4 Proposed Binding Conformation of Fluoro-Taxoids

Recently, Ojima group proposed a new bioactive conformation of paclitaxel, "REDOR-Taxol"[76], based on the ^{19}F-^{13}C distances obtained by the REDOR experiment[66], the photoaffinity labeling of microtubules[77], the crystal structure of α,β-tubulin dimer model determined by cryo-electron microscopy (cryo-EM)[78, 79], and molecular modeling. The REDOR-Taxol structure is fully consistent with the recent solid state REDOR-NMR experiment.[67]

To investigate the microtubule-bound structures of the 3'-CF2H-, 3'-CF3-, and 3' CF2C=CH-taxoids, using the updated REDOR-Taxol-1JFF structure (see **Chapter 4**) as the starting structure. Three fluoro-taxoids, **SB-T-1284, SB-T-1282** (**Figure 1-16**) and **SB-T-12853** were docked into the binding pocket of paclitaxel in the β-tubulin subunit by superimposing the baccatin moiety with that of the REDOR-Taxol, and their energies minimized (InsightII 2000, CVFF). The resulting computer-generated binding structures of three fluorotaxoids are shown in **Figure 1-17** (a, b and c).
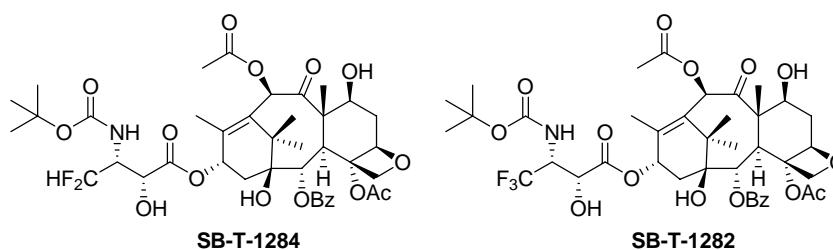
Figure 1-16. Structure of fluoro-taxoids

As **Figure 1-20** (**a-c**) shows, the baccatin moiety occupies virtually the same space in all cases, as expected. Each fluoro-taxoid fits comfortably in the binding pocket without any high-energy contacts with the protein. There is a very strong hydrogen bond between the C2'-OH of the fluoro-taxoids and His227 of β-tubulin in all three cases, which shares the same key feature with the REDOR-Taxol structure[76]. The CF$_2$H and CF$_3$ moieties fill essentially the same space, as anticipated. However, the CF$_2$C=CH moiety occupies more extended hydrophobic space than the CF$_2$H and CF$_3$ moieties. It is likely that this

additional hydrophobic interaction is substantially contributing to the exceptional cytotoxicity of difluorovinyl-taxoids. The overlay of **SB-T-12853** with a representative second-generation taxoid, **SB-T-1213** shows excellent fit, which may prove that difluorovinyl group mimics the isobutenyl group (**Figure 17d**). However, the difluorovinyl group is in between vinyl and isobutenyl groups in size, and two fluorine atoms may mimic two hydroxyl groups rather than two methyl groups electronically. Accordingly, the difluorovinyl group can be regarded as "magic vinyl", like "magic methyl" for the trifluoromethyl group, in drug design, including its anticipated metabolic stability against P-450 family enzymes.
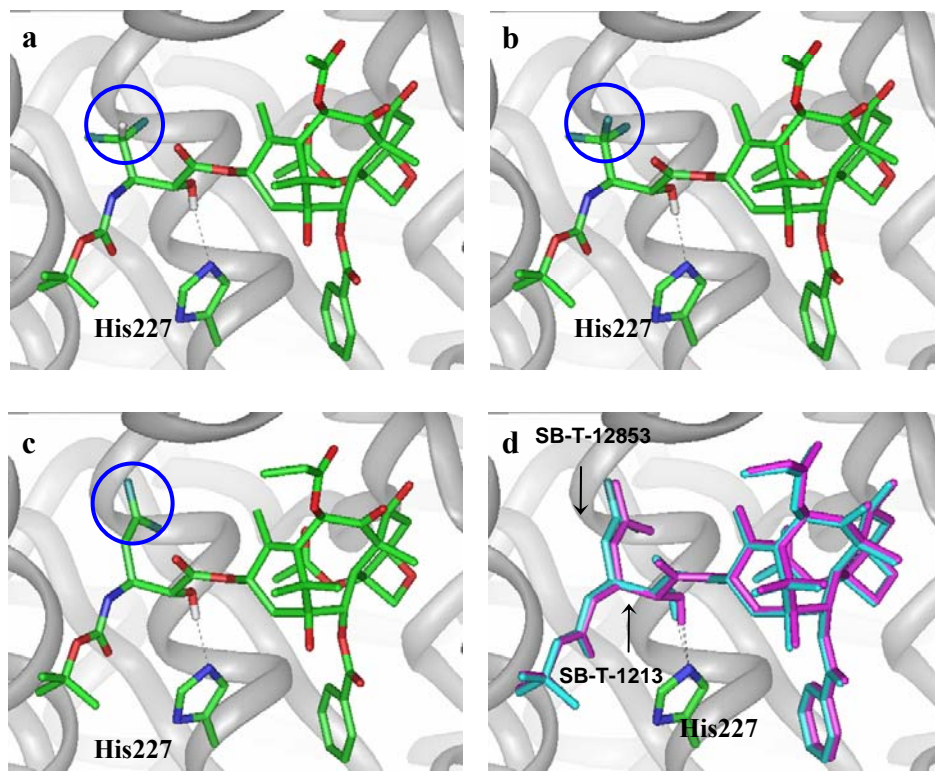
Figure 1-17. Computer-generated binding structures of fluoro-taxoids to β-tubulin: (a) SB-T-1284 (C3'-CF$_2$H) ; (b) SB-T-1282 (C3'-CF$_3$) ; (c) SB-T-12853 (C3'-CF$_2$=CH); (d) Overlay of SB-T-12853 (cyan) and SB-T-1213 (magenta)

§ 1.3.5 Synthesis of ¹³C-Labeled Paclitaxel

In collaboration with Synta Pharmaceuticals, 100 mg ¹³C-labeled paclitaxel was synthesized. The synthesis began with ¹³C-labeled benzoic acid, which was converted to an acid chloride **(1-51)** by using oxalyl chloride. Then β-lactam **(1-17)** was reacted directly with **1-51** in the presence of triethylamine and DMAP to give the desired β-lactam **1-53** in 62% yield. The modified baccatin **1-54** was coupled with the β-lactam **1-53** in 75% yield. The deprotection of TES and EE group by using hydrochloric acid in ethanol gave the labeled paclitaxel in good yield.[16]
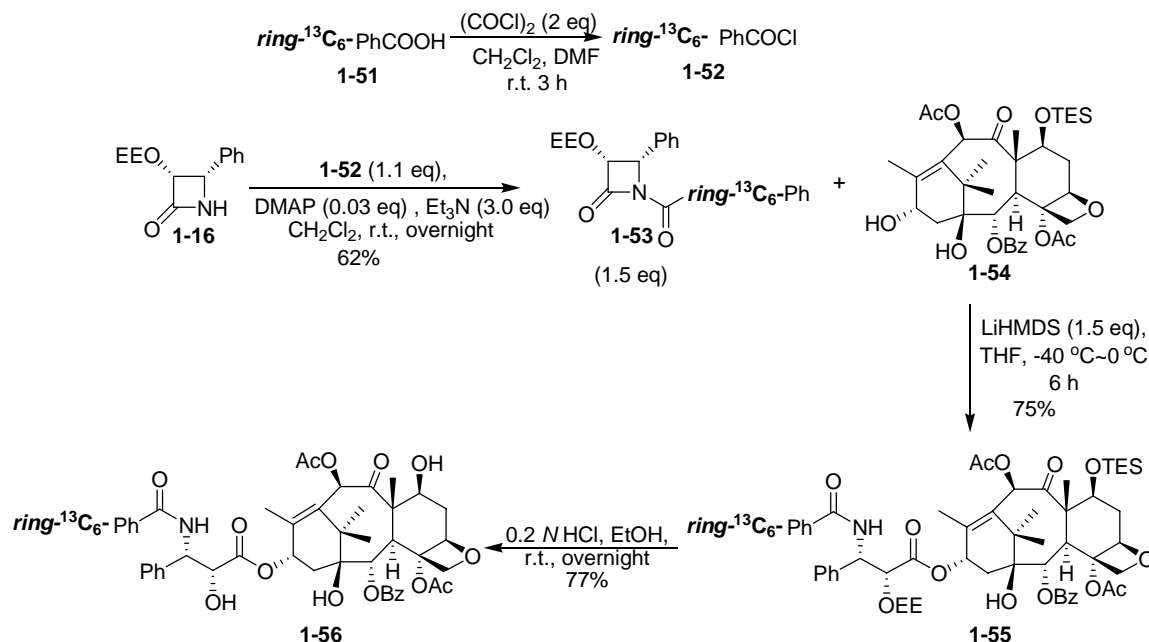
Scheme 1-17. Synthesis of ¹³C-labeled paclitaxel

§ 1.3.6 Synthesis and Biological Evaluation of Taxane-based Potential Antimalarial Agents

§ 1.3.6.1 Introduction

Malaria is a tropical disease transmitted to humans by the bite of a female *Anopheles* mosquito infected with parasites of the genus *Plasmodium*. Today more than 40% of the world's population is at risk, counting over 300-500 million people infected and about 2 million deaths per year (primarily children). The main reason for the epidemic is that the development of *Plasmodium* is highly resistant to the classical antimalarial drugs (**Figure 1-21**).
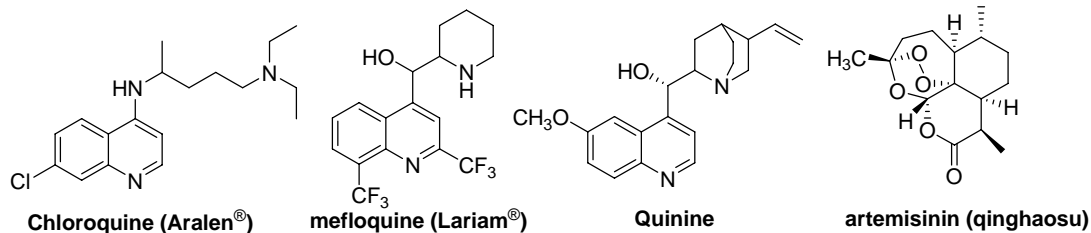
Figure 1-18. Classical antimalarial drugs

Paclitaxel and docetaxel were reported to have antimalarial activity. Paclitaxel can block the replication of *Trypanosomacruzi* and *Trypanosoma brucei* parasites, selectively inhibit proliferation of *Leishmania dovani* promastigotes, and have a significant inhibitory effect on *P. falciparum* growth. Docetaxel can inhibit *P. falciparum* erythrocytic development *in vitro* at nanomolar concentrations, in both chloroquine-sensitive (F32/Tanzania) and chloroquine-resistant (FcB1/Colombia, FcR3/Gambia) strains. However, there are clear differences in the drug susceptibility of mammalian tubulin and those of parasites. Based on the systematic SAR studies of taxane-based anticancer agents, it is suggested that *para*-substituted C2-benzoyl analogues would to reduce the apparent interactions with tubulin which are responsible for cytotoxicity to mammalian cells. In this section, 3 new C2-modified **SB-T-1213** analogues were synthesized and their antimalarial activity evaluated to examined this hypothesis.

§ 1.3.6.2 Result and Discussion

As shown in **Scheme 1-18**, the synthesis started with the C2 modification of 10-DAB. Diol **1-29** was mixed with a large excess of acid, DIC and DMAP, and refluxed overnight to 3 days to give the desired C2-modified tri-TES-baccatins **1-57** in good yield. Then, a global removal of the TES groups using HF-pyridine, followed by C10-modification with propanoic anhydride and cerium chloride afforded baccatins **1-59**. The selective protection of the C7-OH using TESCl and imidazole gave modified 10-DABs **1-60** (**a-c**) in excellent yield. Baccatins **1-60** (**a-c**) were coupled with β-lactam **1-10** to afford the protected taxoids **1-61**. Finally, deprotection of the silyl groups using HF-pyridine gave taxoids **1-62** (**a-c**) in good overall yield.

TESO O OTES

TESO''' OH OH
HO H OAc
1-29

R$_1$—COOH (8 eq)
R$_2$

DIC (10 eq), DMAP (10 eq),
DMF, toluene, 60 °C,
overnight - 3 days
60% - 75%

TESO O OTES

TESO''' OH H OAc
HO O
O
R$_1$ R$_2$
1-57

HF/Py, Py, CH$_3$CN,
r.t., overnight
73%

HO O OH

HO''' OH H OAc
HO O
O
R$_1$ R$_2$
1-58

(CH$_3$CH$_2$CO)$_2$O (10 eq),
CeCl$_3$·7H$_2$O (0.1 eq),
THF, r.t., 2 h

O O OH

HO''' OH H OAc
HO O
O
R$_1$ R$_2$
1-59

TESCl (3 eq),
Imidazole (4 eq),
DMF, r.t., 1.5 h
68% - 90%

O O OTES

HO''' OH H OAc
HO O
O
R$_1$ R$_2$
1-60

1-10 (1.5 eq),
LiHMDS (1.5 eq),
THF, -40 °C, 1 h
81% - 84%

O O OTES
BocNH
O OTIPS
HO H OAc
HO O
O
R$_1$ R$_2$
1-61

HF/Py, Py, CH$_3$CN,
r.t., overnight
72% - 88%

1-62a (SB-T-1213P05): R$_1$ = CH$_3$, R$_2$ = H
1-62b (SB-T-1213P07): R$_1$ = CH$_3$, R$_2$ = CH$_3$
1-62c (SB-T-1213P08): R$_1$ = OCH$_3$, R$_2$ = OCH$_3$

O O OH
BocNH
O OH
HO H OAc
HO O
O
R$_1$ R$_2$
1-62

Scheme 1-18. Synthesis of C2-modified SB-T-1213 analogues

§ 1.3.6.3 Biological Evaluation

These three compounds as well as other five conpounds (synthesized by Dr. Jin Chen and Xianrui Zhao) were sent to Dr. Simon Croft's laboratory (Department of Infectious Diseases and Tropical Diseases, London School of Hygiene and Tropical Medicine) to assay the antimalarial activities and the cytotoxicities against K1 strain of *P. falciparum* and MRC-5 cells. Unfortunately, most of them only exhibited modest antimalarial activity. Two of them, **SB-T-1213P01** and **SB-T-1213P07** showed similar antimalarial activities as chloroquine against K1 strain of *P. falciparum*.

Table 1-5. Antimalarial activities and cytotoxicities of taxoids against K1 strain of *Plasmodium falciparum* and MRC-5 cells

Compound	IC_{50} (µg/mL)		Selectivity
	K1 strain*	MRC-5 cells**	MRC-5/K1
SB-T-1213P01	0.45	0.23	0.5
SB-T-1213P02	6.7	0.35	0.05
SB-T-1213P03	5.8	0.25	0.04
SB-T-1213P04	6.6	0.98	0.1
SB-T-1213P05	**6.0**	**0.25**	**0.04**
SB-T-1213P06	6.5	1.45	0.2
SB-T-1213P07	**0.65**	**0.13**	**0.2**
SB-T-1213P08	**6.8**	**0.26**	**0.04**
Artemisinin***	0.0096	ND****	-
Chloroquine***	0.3	ND****	-

* drug resistant strain, **human diploid embryonic cells
*** standard antimalarial drug ****not determined

§ **1.4 Summary**

Paclitaxel is one of the most important drugs in current clinical treatment of cancer. The *β-Lactam synthon method* was proven to be an efficient method to synthesize paclitaxel, docetaxel or various new-generation taxoids.

Enantiopure *β*-lactam was synthesized by imine-ester cyclocondensation and [2+2] cycloaddition-enzymatic kinetic resolution in large scales. The synthesized *β*-lactams were used in the synthesis of a series of new-generation taxoids.

Several second/third-generation taxoids with different substitution on C2, C10 and C3' positions were resynthesized. The new-generation taxoids showed one order of magnitude better anticancer activity against drug sensitive cell lines and more than two orders of magnitude better activity against drug-resistant cell lines. Three new-generation taxoids exhibited excellent activity against paclitaxel-resistant 1A9PTX10 and 1A9PTX22 ovarian cancer cell lines, wherein the drug-resistance was mediated by *β*-tubulin mutation.

One C3'-difluorovinyl-taxoid, **SB-T-12853**, was successfully synthesized in a large scale. The C3'-difluorovinyl-taxoids showed one order of magnitude better anticancer activity against drug sensitive MCF7 cell line and more than two orders of magnitude better activity against drug-resistant NCI/ADR cell line. Also these analogues were tested against PANC-1 (pancreatic) and HT-29 (colon) cancer cell lines, exhibiting much higher cytotoxicity than paclitaxel. These results showed that C3'-difluorovinyl taxoids are very promising preclinical candidates for further development.

Three C2-modified second-generation taxoids as potential antimalarial agent were synthesized and evaluated, which exhibited only modest antimalarial activity.

§ 1.5 Experimental Section

General Methods: ^{1}H and ^{13}C NMR spectra were measured on a Varian 300, 400 or 500 NMR spectrometer. Melting points were measured on a Thomas Hoover Capillary melting point apparatus and are uncorrected. Optical rotations were measured on a Perkin-Elmer Model 241 polarimeter. TLC was performed on Merck DC-alufolien with Kieselgel 60F-254 and column chromatography was carried out on silica gel 60 (Merck; 230-400 mesh ASTM). Chemical purity was determined with a Waters HPLC assembly consisting of dual Waters 515 HPLC pumps, a PC workstation running Millennium 32, and a Waters 996 PDA detector, using a Phenomenex Curosil-B column, employing CH$_3$CN/water (2/3) as the solvent system with a flow rate of 1 mL/min.

Materials: The chemicals were purchased from Aldrich Co. and Sigma and purified before use by standard methods. Tetrahydrofuran was freshly distilled from sodium metal and benzophenone. Dichloromethane was also distilled immediately prior to use under nitrogen from calcium hydride. 10-Deacetyl baccatin III (DAB) was donated by Indena, SpA, Italy.

(±)-*trans*-2-Phenylcyclohexanol [(±)-1-1]:[40]
A solution of phenylmagnesium bromide in THF (150 mL) was prepared from magnesium (7.07 g, 0.291 mol) and bromobenzene (31 mL. 0.294 mol) using standard conditions. After cooling the solution to -30 °C, 2.52 g (13.2 mmol) of CuI was added. The resulting solution was stirred for approximately 10 min, and a solution of cyclohexene oxide (20 mL, 0.2 mol) in THF (200 mL) was added dropwise over a period of 1 h. The reaction mixture was then allowed to warm to 0 °C and was stirred for an additional 2 h. The reaction was quenched at 0 °C with a saturated aqueous NH$_4$Cl solution (50 mL) and extracted with ethyl acetate (100 mL x 3). The organic layer was washed with a saturated aqueous NH$_4$Cl solution until there was no longer any colour change in the aqueous layer. The combined aqueous layers were extracted with ether and the combined organic layers dried over anhydrous MgSO$_4$, filtered and concentrated *in vacuo*. Recrystallization from hexane gave **1-1** (27.6 gm 78%) as a white solid: mp 57-58 °C; ^{1}H NMR (300 MHz, CDCl$_3$) δ 1.25-1.53 (bm, 4 H), 1.62 (s, 1 H), 1.76 (m, 1 H), 1.84 (m, 2 H), 2.11 (m, 1 H), 2.42 (ddd, *J* = 16.6 Hz, 10.8 Hz, 5.4 Hz, 1 H), 3.64 (ddd, *J* = 16.6 Hz, 10.8 Hz, 5.4 Hz, 1 H), 7.17-7.35 (m, 5 H); ^{13}C NMR (75 Hz, CDCl$_3$) δ 25.1, 26.1, 33.4, 34.6, 53.3, 74.3, 126.7, 127.9, 128.7, 143.4. IR: 3592, 3461, 2941, 2863, 1604, 1497, 1451 cm^{-1}; MS (EI): 176 (*M*$^+$), 158, 143, 130, 117, 104, 91 (base). All data are in agreement with literature values.[40]

(±) *trans*-2-Phenylcyclohexyl acetate [(±)-(1-2)]:[40]
To a solution of 4-dimethylaminopyridine (DMAP, 0.415 g, 4.71 mmol), pyridine (16.8 mL) and racemic alcohol **1-1** (27.6 g, 157 mmol) in CH$_2$Cl$_2$ (22.9 mL), was added dropwise a solution of acetic anhydride (17.26 mL) in CH$_2$Cl$_2$ (27.7 mL) over a period of 2 h. The reaction mixture was then poured into a solution of 6 *N* HCl (48 mL), ice (73 g) and ether (149 mL). The organic layer was washed with 2 *N* HCl aqueous solution (50 mL) and the combined aqueous layers were extracted with ether (100 mL x 3). The combined organic layers were washed with a saturated aqueous NaHCO$_3$ solution and

dried over anhydrous MgSO$_4$, filtered and concentrated *in vacuo* to afford **1-2** (41.707 g, 100%) as a pale yellow oil: ^{1}H NMR (300 MHz, CDCl$_3$) δ 1.35 (m, 1 H), 1.41 (m, 1 H), 1.46 (m, 1 H), 1.56 (m, 1 H), 1.74 (s, 3 H), 1.78 (m, 1 H), 1.84 (m, 1 H), 1.93 (m, 1 H), 2.65 (ddd, *J* = 16.6 Hz, 11.0Hz, 5.4 Hz, 1 H), 4.98 (ddd, *J* = 11.0, 11.0, 5.4 Hz, 1 H), 7.17-7.35 (m, 5 H); ^{13}C NMR (75 Hz, CDCl$_3$) δ 20.7, 24.8, 25.9, 32.4, 33.9, 49.8, 75.7, 126.4, 127.5, 128.2, 143.1, 169.9; IR: 3070, 2940, 2860, 1730, 1604, 1497 cm^{-1}; MS (EI): 175, 158 (base), 130, 91. All data are in agreement with literature values.[40]

(+)-*trans*-2-Phenylcyclohexyl acetate [(+)-1-3] and (-)-*trans*-2-phenylcyclohexanol [(-)-1-1]:[40]

To 0.5 M aqueous buffer at pH = 8 (KH$_2$PO$_4$/K$_2$HPO$_4$, 1.2 L) was added racemic acetate **1-2** (41.71 g, 0.157 mol) in ether (160 mL) at 31 ºC. After stirring for 30 min, pig liver acetone powder (PLAP) (9.1 g) was added. The mixture was stirred for 7 days at 31 ºC, until ^{1}H NMR of the crude organic layer showed <50/50 ratio of alcohol **(-)-1-1** and acetate **(+)-1-2**. The reaction mixture was quenched by acidifying to pH = 4 with 2 *N* HCl solution. To the resulting mixture was added ether (200 mL) with stirring for 1 h. After the PLAP was allowed to settle, the supernatant organic layer was removed (Addition of ether and removal of the organic layer were repeated 3 times). The organic and aqueous layers were filtered and the aqueous layer was extracted with ether. The combined organic layers were dried over anhydrous MgSO$_4$, filtered and concentrated *in vacuo*. The remainder of the crude product was purified *via* column chromatography on silica gel using Hexane/ethyl acetate (15/1) as the eluant to afford acetate **(+)-1-2** (18.7 g, 45%) as a slightly yellow oil and pure **(-)-1-1** (11.9 g, 43%) as a white solid: mp: 63-64 ºC; ^{1}H NMR (300 MHz, CDCl$_3$) δ 1.25-1.53 (bm, 4 H), 1.62 (s, 1 H), 1.76 (m, 1 H), 1.84 (m, 2 H), 2.11 (m, 1 H), 2.42 (ddd, *J* = 16.6 Hz, 10.8 Hz, 5.4 Hz, 1 H), 3.64 (ddd, *J* = 16.6 Hz, 10.8 Hz, 5.4 Hz, 1 H), 7.17-7.35 (m, 5 H); ^{13}C NMR (75 Hz, CDCl$_3$) δ 25.1, 26.1, 33.4, 34.6, 53.3, 74.3, 126.7, 127.9, 128.7, 143.4. IR: 3592, 3461, 2941, 2863, 1604, 1497, 1451 cm^{-1}; MS (EI): 176 (M^+), 158, 143, 130, 117, 104, 91 (base). All data are in agreement with literature values. [40]

Benzyloxyacetic acid (1-3):[16]

At room temperature, sodium metal (13.5 g, 0.589 mol) was added gradually to benzyl alcohol (220 mL, 2.12 mol) with stirring. After most of the sodium had reacted, the reaction mixture was heated to 150 ºC and complete reaction of the sodium was observed. Then bromoacetic acid (35.5 g, 0.257 mol) in THF (50 mL) was added dropwise. The reaction mixture was stirred at 150 ºC for 3 h and then cooled to room temperature. Cold water (50 mL) was added and the two layers separated. The aqueous layer was carefully extracted with dichloromethane (30 mL x 3) to remove any remaining benzyl alcohol. The water layer was acidified with 10% HCl until a pH of 2-3 and extracted with ether (100 mL x 3). The organic layer was then dried over magnesium sulfate, filtered and concentrated *in vacuo*. The oil residue was distilled under reduced pressure to afford **1-3** (21.9 g, 52%) as a colorless oil: bp 138-140 ºC (0.3 mm Hg); ^{1}H NMR (CDCl$_3$, 300 MHz) δ 4.17 (s, 2 H), 4.67 (s, 2 H), 7.38 (m, 5 H); ^{13}C NMR (75 Hz, CDCl$_3$) δ 66.5, 73.4, 128.1, 128.2, 128.6, 136.5, 175.6. All data are in agreement with literature values.[16]

(*1R,2S*)-(-)-2-Phenylcyclohexyl benzyloxyacetate (1-4):[16]

A solution of (-)-*trans*-2-phenylcyclohexanol (**1-1**) (9.190 g, 0.051 mol), of benzyloxyacetic acid (**1-3**) (9.422 g, 0.051 mol), and a catalytic amount of *p*-toluenesulfonic acid (*p*-TSA) in toluene (120 mL) was refluxed overnight. The toluene was evaporated off *in vacuo* and the reaction mixture was diluted with ether and washed with saturated aqueous solution of NaHCO$_3$. The organic layer was dried over MgSO$_4$, filtered and concentrated *in vacuo* to afford **1-4** (12.4 g, 75%) as a white solid: mp 52-53 °C; ^{1}H NMR (CDCl$_3$, 400 MHz) δ 1.26-1.63 (m, 4 H), 1.76-1.99 (m, 3 H), 2.10-2.20 (m, 2 H), 2.70 (dt, *J* = 11.0, 4.1 Hz, 1 H), 3.73 (d, *J* = 16.5 Hz, 1 H), 3.84 (d, *J* = 16.5 Hz, 1 H), 4.25 (s, 2 H), 5.13 (td, *J* = 11.0Hz, 4.1 Hz, 1 H), 7.16-7.39 (m, 10 H). All data are in agreement with literature values.[16]

(*1R,2S*)-(-)-2-Phenylcyclohexyl hydroxyacetate (1-5):[16]

A mixture of 10% palladium on carbon (Pd-C) (1.76 g) and (-)-benzyloxyacetate (**1-4**) (6.98 g, 21.5 mmol) in THF (65 mL) was stirred overnight at 45 °C under hydrogen. The reaction mixture was filtered through celite and concentrated *in vacuo* to afford **1-5** (5.01 g, 100%) as a white solid: mp 59-60 °C; 1H NMR (CDCl3, 300 MHz) δ 1.30-1.66 (m, 4 H), 1.78-2.00 (m, 3 H), 2.10-2.20 (m, 2 H), 2.67 (dt, *J* = 11.0, 4.2 Hz, 1 H), 3.72 (d, *J* = 17.0 Hz, 1 H), 3.93 (d, *J* = 17.0 Hz, 1 H), 5.07 (td, *J* = 11.0 Hz, 4.2 Hz, 1 H), 7.16-7.32 (m, 5 H); ^{13}C NMR (75 Hz, CDCl$_3$) δ 24.2, 25.2, 31.7, 33.2, 49.1, 59.7, 76.4, 126.0, 126.9, 127.8, 142.2, 172.0. All data are in agreement with literature values.[80]

(*1R,2S*)-(-)-2-Phenylcyclohexyl triisopropylsilyloxyacetate (1-6):[16]

To a solution of imidazole (3.48 g, 0.05 mol) and hydroxy- acetate (**1-5**) (4.98 g, 0.0213 mol) in DMF (10.8 mL) was added chlorotriisopropylsilane (TIPSCl) (6.4 mL, 0.029 mol). The reaction was stirred under nitrogen for 24 h, quenched with water, and extracted with ether. The organic layer was washed several times with water and brine, dried over magnesium sulfate, filtered and concentrated *in vacuo*. The oil residue was distilled under reduced pressure to afford **1-6** (6.80 g, 82%) as a colorless oil: bp 195-205 °C (0.8 mm Hg); [α]$_D$[20] -17.1° (c 3.15, CHCl$_3$); ^{1}H NMR (CDCl3, 300 MHz) δ 0.94-1.25 (m, 21 H), 1.35-1.70 (m, 4 H), 1.80-2.05 (m, 3 H), 2.10-2.20 (m, 1 H), 2.70 (dt, *J* = 11.0 Hz, 4.2 Hz, 1 H), 3.91 (d, *J* = 16.5 Hz, 1 H), 4.08 (d, *J* = 16.5 Hz, 1 H), 5.07 (td, *J* = 11.0 Hz, 4.2 Hz, 1 H), 7.16-7.30 (m, 5 H); ^{13}C NMR (75 Hz, CDCl$_3$) δ 11.7, 17.6, 24.6, 25.7, 32.2, 49.6, 61.6, 75.0, 126.3, 127.3, 128.2, 142.8, 170.8; IR (neat) 1759, 1730 cm^{-1}; Anal Calcd for C$_{23}$H$_{38}$O$_3$Si: C, 70.72; H, 9.81. Found: C, 70.79; H, 9.85. All data are in agreement with literature values.[16]

_N_-(4-Methoxyphenyl)-3-methyl-2-butenaldimine (1-7):[36]

To a solution of *p*-anisidine (0.370 g, 2.98 mmol, recrystalized once from methanol) and anhydrous Na$_2$SO$_4$ (1.0 g) in CH$_2$Cl$_2$ (15 mL) was added 3-methylbut-2-enal (0.35 mL, 3.72 mmol) dropwise, and then the reaction mixture was stirred at room temperature for 2 h. The solution was filtered and the solvent was removed *in vacuo* to afford the imine (**1-7**) as a viscous yellow oil, which was immediately used for the synthesis of β-lactam without further purification: ^{1}H NMR (CDCl$_3$, 300MHz) δ 1.95 (s, 3 H), 2.01 (s, 3 H), 3.80 (s, 3 H), 6.20 (d, J = 9.5 Hz, 1 H), 6.89 (d, J = 7.0 Hz, 2 H), 7.11 (d, J = 7.0 Hz, 2 H),

8.38 (d, J = 9.5 Hz, 1 H); ^{13}C NMR (CDCl$_3$) δ 19.0, 26.9, 55.5, 114.3, 122.0, 126.3, 146.0, 149.5, 157.1, 158.5. All data are in agreement with litera- ture values.[16]

1-*p*-Methoxyphenyl-3-triisopropylsilyloxy-4-(2-methylpropen-2-yl)azetidin-2-one (1-8):[36]

To a solution of diisopropylamine (0.34 mL, 2.42 mmol) in THF (8 mL) was added 2.5 M *n*-butyllithium in hexanes (0.977 mL, 2.42 mmol) at -15 °C. After stirring for 60 min, the reaction solution was cooled to -85 °C. A solution of the **1-6** (0.726 g 1.86 mmol) in THF (8 mL) was slowly added via cannula over a period of 1 h. After stirring for an additional hour, a solution of imine **1-7** (2.97 mmol in 10 mL THF) was carefully added via cannula over a period of 2 h. The reaction mixture was stirred at -85 °C overnight. Then 1 M LiHMDS in THF (1.86 mL, 1.86 mmol) was added and the reaction mixture allowed to warm up to -15 °C after 1 h. The reaction was then quenched with a saturated aqueous NH$_4$Cl solution (30 mL). The aqueous layer was extracted with ethyl acetate (50 mL x 3) and the combined organic layers were washed with brine (30 mL). The organic layer was then dried over MgSO$_4$ and concentrated under reduced pressure. The crude product was then purified by column chromatography on silica gel (hexane:EtOAc = 25/1) to afford 1-*p*-methoxy-phenyl-3-triisopropylsiloxy-4-(2-methylpropen-2-yl)azetidin-2-one (**1-8**) (630 mg) with >97 % ee in 70% yield: mp 78-89 °C; ^{1}H NMR δ (CDCl$_3$, 300 MHz) 0.97-1.24 (m, 21 H), 1.88 (d, J = 2.3 Hz, 3 H), 1.84 (d, J = 2.3 Hz, 3 H), 3.77 (s, 3 H), 4.82 (dd, J = 9.9, 5.1 Hz, 1 H), 5.04 (d, J = 5.1 Hz, 1 H), 5.33 (d, J = 9.9 Hz, 1 H), 6.84 (d, J = 8.7 Hz, 2 H), 7.32 (d, J = 8.7 Hz, 2 H). All data are in agreement with literature values.[36]

3-Triisopropylsilyloxy-4-(2-methylpropen-2-yl)azetidin-2-one (1-9):[36]

To a solution of 1-*p*-methoxyphenyl-3-triisopropylsiloxy-4-(2-methylpropen-2-yl)azetidin-2-one (**1-8**) (0.567 g, 1.4 mmol) in 55 mL of acetonitrile, water (11 mL) at -10 °C was added cerium ammonium nitrate (CAN) (2.68 g, 49 mmol) in H$_2$O (44 mL) dropwise via addition funnel. The reaction mixture was allowed to stir for 2 h and then quenched with saturated aqueous NaHSO$_3$. The aqueous layer was extracted with ethyl acetate (50 mL x 3) and the combined organic layers were washed with brine. After drying over MgSO$_4$ and concentrating under reduced pressure, the crude product was purified by column chromatography on silica gel (hexane/EtOAc = 6/1) affording 3-triisopropylsiloxy-4-(2-methylpropen-2-yl)azetidin-2-one (**1-10**) (257 mg, 70 %) as a white solid: mp 85-86 °C; ^{1}H NMR (CDCl$_3$, 400 MHz) δ 0.97-1.21 (m, 21 H), 1.68 (d, J = 2.3 Hz, 3 H), 1.19 (d, J = 2.3 Hz, 3 H), 4.43 (dd, J = 9.5, 4.7 Hz, 1 H), 4.98 (dd, J = 4.7, 2.3 Hz, 1 H), 5.31 (d, J = 9.5 Hz, 1 H), 6.28 (bs, 1 H); ^{13}C NMR (CDCl$_3$, 75 MHz) δ 11.9, 17.6, 18.2, 25.9, 53.5, 79.4, 121.5, 137.8, 169.9. Anal. Calcd for C$_{16}$H$_{31}$NO$_2$Si: C, 64.59; H, 10.50; N, 4.71. Found: C, 64.45; H, 10.25; N, 4.58. All data are in agreement with literature values.[36]

1-(*tert*-Butoxycarbonyl)-3-triisopropylsiloxy-4-(2-methylpropen-2-yl)azetidin-2-one (1-10):[36]

To a solution of 3-triisopropylsiloxy-4-(2-methylprop-2-enyl) azetidin-2-one (**1-9**) (257 mg, 0.865 mmol), triethylamine (0.449 mL, 2.6 mmol), and a catalytic amount of DMAP in CH_2Cl_2 (5 mL), was added di-*tert*-butyl dicarbonate (0.207 g, 0.952 mmol) in CH_2Cl_2 (5 mL). The reaction mixture was stirred overnight, quenched by saturated NH_4Cl (30 mL), and extracted with ethyl acetate (30 mL x 3). The organic layer was washed with brine, dried over $MgSO_4$, and concentrated under reduced pressure. The crude product was purified via column chromatography on silica gel (hexane/EtOAc = 25/1) to yield pure 1-(*tert*-butoxycarbonyl)-3-triisopropylsiloxy-4-(2-methyl-prop-2-enyl)-azetidin-2-one (**1-10**) (270 mg, 80%) as a clear oil: ^{1}H NMR ($CDCl_3$, 300 MHz) δ 1.02-1.2 (m, 21 H), 1.48 (s, 9 H), 1.77 (d, *J* = 1.0 Hz, 3 H), 1.79 (d, *J* = 1.0 Hz, 3 H), 4.75 (dd, *J* = 9.8, 5.6, 1 H), 4.98 (d, *J* = 5.6 Hz, 1 H) (H on C4), 5.28 (dd, *J* = 9.8, 1.0 Hz, 1 H); ^{13}C NMR ($CDCl_3$) δ 11.8, 17.5, 18.2, 26.0, 28.0, 56.8, 77.2, 82.8, 128.4, 139.6, 148.1, 166.3. All data are in agreement with literature values.[36]

N-(4-Methoxyphenyl)benzaldimine (1-11):[16]

To a solution of *p*-anisidine (3.16 g, 26 mmol; recrystalized once from methanol) and anhydrous Na_2SO_4 (5.0 g) in CH_2Cl_2 (60 mL) was added benzaldehyde (2.93 mL, 29 mmol) dropwise, and then the reaction mixture was stirred at room temperature for 2 h. The solution was filtered and concentrated under reduced pressure. After recrystallization, *N*-(4-methoxyphenyl)benzaldimine was obtained as white solid (5.98 g, 95% yield): mp 70-71 °C; ^{1}H NMR (300 MHz, CDCl3) δ 3.77 (s, 3H), 6.88-6.85 (m, 2H), 7.17-7.15 (m, 2H), 7.39-7.37 (m, 3H), 7.82-7.80 (m, 2H), 8.41 (br s, 1H); ^{13}C NMR (75 MHz, CDCl3) δ 55.6, 114.5, 122.3, 128.7, 128.9, 131.2, 136.5, 145.0, 158.4, 158.6; IR (KBr): 2955, 1622, 1505, 1249 cm-1. MS (EI) *m/z* 211 (M+, 78), 196 (M+-CH3, 100). All data are consistant with literature data.[16]

(±)-1-(4-Methoxyphenyl)-3-acetoxy-4-phenylazetidin-2-one (1-12):[16]

To a solution of **1-11** (2.19 g, 10 mmol), and triethylamine (2.2 mL, 15.4 mmol) in CH_2Cl_2 (45 mL) at -78 °C was added dropwise a solution of α-acetoxyacetyl chloride (1.96 g, 12 mmol) in CH_2Cl_2 (15 mL). The reaction mixture was allowed to warm to 25°C over 18 h, then diluted with CH_2Cl_2 (50 mL). The organic layer was washed with water (30 mL) and saturated aqueous sodium bicarbonate (30 mL), dried over $MgSO_4$, and concentrated to afford the product as a white crystal (3.61 g, 100% yield): ^{1}H NMR (300 MHz, $CDCl_3$.) δ 1.68 (s, 3 H), 3.75 (s, 3 H), 5.34 (d, *J* = 4.9 Hz, 1 H), 5.81(d, *J* = 9.0 Hz, 1 H), 6.81 (d, *J* = 9.0 Hz, 2 H), 7.35-7,26 (m, 7 H). ^{13}C NMR (100.5 MHz): δ 19.8, 55.5, 61.5, 76.4, 114.4, 118.8, 127.9, 128.5, 128.8, 130.1, 132.3, 156.0, 161.3 172.0. MS (*m/z*): 311, 212, 167, 162, 149, 120. Anal. Calcd for $C_{18}H_{17}NO_4$: C, 69.44; H, 5.50; N, 4.50. Found: C, 69.30; H, 5.47; N, 4.51. All data are consistant with literature data.[16]

Enzymatic resolution of β-lactam (1-12):[49]

To **1-12** (3.59 g) suspended in 0.2 M sodium phosphate buffer (pH =7.5, 480 mL) and acetonitrile (45 mL) was added PS-Amano lipase (1.5 g), and the mixture was vigorously stirred at 50 °C. After 35 h, the reaction was terminated by extraction of the mixture with ethyl acetate three times (3 x 50 mL). The residue was dissolved in CH_2Cl_2 and the product mixture was separated using column chromatography on silica gel (hexane/EtOAc = 3/1 and 1/1) to give (*3R,4S*)-l-(*p*-methoxyhenyl)-3-acetoxy-4-phenylazetidin-2-one (**1-12**) (1.45 g, 41% yield) (97.5% ee by chiral HPLC) and (*3S,4R*)-l-(*p*-methoxyhenyl)-3-hydroxy-4-phenylazetidin-2-one (**1-13**) (1.495 g, 41% yield). This reaction was monitored by NMR.

(*3R,4S*)-3-Acetoxy-4-phenylazetidin-2-one (1-14):[49]

To a solution of **1-12** (1.26 g) in acetonitrile (120 mL) and water (20 mL) at -10°C was slowly added a solution of ceric ammonium nitrate (1.0 g) in water (120 mL) over a 30-min period. The mixture was stirred for 30 min at -10°C and quenched by saturated sodium bisulfate (80 mL). The aqueous layer was extracted with ethyl acetate (100 mL x 3), and the combined organic layer was washed with brine, to afford *(3R,4S)*-3-acetoxy-4-phenylazetidin-2-one (**1-14**) (0.741 g, 88%) as a white solid: ^{1}H NMR (300 MHz, CDCl$_3$): δ 1.67 (s, 3 H), 5.05(d, *J* = 4.7 Hz, 1 H), 5.87 (dd, *J* = 4.7, 2.7 Hz, 1 H), 6.54 (s, 1 H), 7.30-7.38 (m, 5 H). All data are consistent with literature data.[16]

(*3R,4S*)-3-Hydroxy–4-phenylazetidin-2-one (1-15):[49]

To a solution of THF (38 mL) and 1 M KOH aqueous solution (54 mL) at 0 °C was added a solution of **1-14** (0.929 g, 4.53 mmol) in THF (54 mL). The solution was stirred at 0 °C for 1 h and saturated sodium bicarbonate (40 mL) was added. The mixture was extracted with ethyl acetate (30 mL x 3) and the combined organic layers were dried over sodium sulfate and concentrated to give **1-15** (676 mg, 90%) as white solid. ^{1}H NMR (300 MHz, CDCl$_3$) δ 2.10 (s, 1 H), 4.94 (d, *J* = 4.7 Hz, 1 H), 5.04 (d, *J* = 4.7 Hz, 1H), 6.20 (s, 1 H), 7.25-7.35 (m, 5 H); IR (KBr) ν 3373, 3252, 1732, 1494, 1453. Anal. Calcd for $C_9H_9NO_2$: C, 66.25; H, 5.56; N, 8.58. Found: C, 66.42; H, 5.74; N, 8..All data are consistent with literature data.[16]

(*3R,4S*)-3-Ethoxyethoxy-4-phenylazetidin-2-one (1-16):[16]

To a solution of (*3R,4S*)-3-hydroxy-4-phenylazetidin-2-one (**1-16**) (831 mg, 5.1 mmol) in THF (25 mL) at 0 °C was added ethyl vinyl ether (2.2 mL, 15.3 mmol) and a catalytic amount of *p*-tolunensulfonic acid (25 mg, 0.2 mmol). The mixture was stirred at room temperature for 2 h, quenched with saturated ammonium chloride (30 mL) and extracted with dichloromethane (60 mL x 3). The combined organic layers were dried over magnesium sulfate and the product was separated using column chromatography on silica gel (hexane/EtOAc = 3/1 and 1/1) to afford (*3R,4S*)-3-ethoxyethoxy-4-phenylazetidin-2-one (**1-16**) as white solid (958 mg, 80% yield): mp 78-80 °C; ^{1}H NMR (CDCl$_3$, 300MHz) [0.98 (d, *J* = 5.4 Hz), 1.05 (d, *J* = 5.4 Hz), 3H], [1.11 (t, *J* = 7.1 Hz), 1.12 (t, *J* = 7.1 Hz), 3H], [3.16-3.26 (m), 3.31-3.42 (m), 3.59-3.69 (m), 2H], [4.47 (q, *J* = 5.4 Hz), 4.68 (q, *J* = 5.4 Hz), 1H], [4.82 (d, *J* = 4.7 Hz), 4.85 (dd, *J* = 4.7 Hz), 1H], 5.17-5.21 (m, 1 H), 6.42 (bs, 1 H), 7.35 (m, 5 H); IR (KBr) ν 3214, 2983, 2933, 1753, 1718, 1456 cm^{-1}. Anal.

Calcd for $C_{13}H_{17}NO_3$: C, 66.36; H, 7.28; N, 5.95. Found: C, 66.46; H, 7.11; N, 5.88. All data are consistent with literature data.[16]

(±)-1-(4-Methoxyphenyl)-3-acetoxyl-4-(2-methylprop-1-enyl)azetidin-2-one (1-17):[31]
To a solution of **1-7** (crude, 0.035 mol), triethylamine (7.3 mL, 0.70 mol) in CH_2Cl_2 (140 mL) was added acetoxyacetyl chloride (8.0 g, 0.052 mol) at -78 ˚C. The reaction mixture was warmed up to room temperature overnight. The reaction was quenched with saturated aquous ammonium chloride 100 mL and the water layer was extracted with CH_2Cl_2 (100 mL x 3). The organic layer was washed with water, brine, dried over anhydrous $MgSO_4$, and concentrated *in vacuo*. The residue was purified by column chromatography on silica gel (hexanes/EtOAc = 3/1) to afford **1-17** (7.40 g, 74 %) as a white solid: mp 107-109 ˚C; ^{1}H NMR (300 MHz, CDCl$_3$) 1.70 (s, 3 H), 1.72 (s, 3 H), 2.01 (s, 3 H), 3.67 (s, 3 H), 4.83 (dd, J = 9.9Hz, 4.8 Hz, 1 H), 5.02 (d, J = 9.3 Hz, 1 H), 5.67 (d, J = 4.8 Hz, 1 H), 6.74 (d, J = 8.9 Hz, 2 H), 7.20 (d, J = 8.9 Hz, 2 H); ^{13}C NMR (300MHz, CDCl$_3$) 18.3, 20.2, 27.0, 76.1, 114.3, 117.5, 118.4, 130.7, 141.8, 156.4, 161.3, 169.3. Anal. Calcd for $C_{16}H_{19}O_4N$: C, 66.42; H, 6.62; N, 4.84. Found: C, 66.56; H, 6.54; N, 4.86. All data are in agreement with literature values.[81]

Enzymatic resolution of β-lactam (1-17):[49]
To racemic β-lactam **1-17** (6.35 g) suspended in 0.2 M sodium phosphate buffer (pH = 7.5, 750 mL) and acetonitrile (75 mL) was added PS Amano lipase (2.56 g), and the mixture was vigorously stirred at 50 ˚C. After 26 h, the ^{1}HNMR showed the conversion of the reaction was 50%. The reaction was terminated by adding ethyl ether (400 mL) and the mixture was extracted of the mixture with ethyl ether (3 x 100 mL). The residue was separated using flash column chromatography on silica gel (hexanes/EtOAc = 3/1 and then 1/1) to give (*3R,4S*)-l-(4-methoxyhenyl)-3-acetoxy-4-(2-methylprop-1-enyl)-2-one (**1-17**) (2.99 g, 47% yield, 97% ee) and (*3S,4R*)-l-(4-methoxyhenyl)-3-hydroxy-4-(2-methylprop-1-enyl)- 2-one (**1-18**) (2.573 g) in 48% yield.

(*3R,4S*)-1-(4-Methoxyphenyl)-3-hydroxy-4-(2-methylprop-1-enyl)azetidin-2-one (1-18):[36]
To a solution of THF (120 mL) and 1 M KOH aqueous solution (103 mL) at 0 °C was added a solution of **1-17** (2.98 g, 10.3 mmol) in THF (175 mL). The solution was stirred at 0 °C for 1 h and saturated NH_4Cl (200 mL) was added. The mixture was extracted with CH_2Cl_2 (100 mL x 4). The combined organic layers were dried over $MgSO_4$ and concentrated to give **1-18** (2.71 g, 100%) as a white solid: ^{1}H NMR (CDCl$_3$) δ 1.85 (s, 6 H), 3.75 (s, 3 H), 4.63 (d, J = 7.5 Hz, 1 H), 4.86 (dd, J = 9.2, 5.2 Hz, 1 H), 5.04 (dd, J = 7.0, 5.2 Hz, 1 H), 5.33 (d, J = 9.2 Hz, 1 H), 6.79 (d, J = 9.0 Hz, 2 H), 7.27 (d, J = 9.0 Hz, 2 H); ^{13}C NMR (62.5 MHz, CDCl3) δ 18.6, 26.2, 55.4, 57.3, 76.3, 114.3, 118.1, 118.6, 130.8, 141.2, 156.3, 166.6. All data are in agreement with literature values.[81]

1-(4-Methoxyphenyl)-3-triisopropylsiloxy-4-(2-methylpropen-2-yl)azetidin-2-one (1-8):[36]
To a solution of **1-18** (2.70 g, 10.3 mmol), DMAP (0.250 g, 2.06 mmol) and triethylamine (5.8 mL, 41.1 mmol) in CH_2Cl_2 (37 mL) was added chlorotriisopropyl-silane (2.9 mL, 13.3 mmol). The reaction mixture was stirred for overnight and quenched

with saturated NH_4Cl (100 mL). The mixture was extracted with ethyl ether (100 mL x 3). The residue was separated using flash column chromatography on silica gel (hexanes/EtOAc = 15/1) to give 1-*p*-methoxyphenyl-3-triisopropylsiloxy-4-(2-methylpropen-2-yl)azetidin-2-one (**1-8**) (4.30 g, 100%) as a white solid: ^{1}H NMR δ (CDCl₃, 300 MHz) 0.97-1.24 (m, 21 H), 1.88 (d, *J* = 2.3 Hz, 3 H), 1.84 (d, *J* = 2.3 Hz, 3 H), 3.77 (s, 3 H), 4.82 (dd, *J* = 9.9, 5.1 Hz, 1 H), 5.04 (d, *J* = 5.1 Hz, 1 H), 5.33 (d, *J* = 9.9 Hz, 1 H), 6.84 (d, *J* = 8.7 Hz, 2 H), 7.32 (d, *J* = 8.7 Hz, 2 H). All data are in agreement with literature values.[36]

10-Deacetyl-10-propanoylbaccatin III (1-20):[51]

To the solution of **10-DAB** (**1-19**) (300 mg, 0.549 mmol) in THF (16.9 mL) was added cerium chloride heptahydrate (0.021 g, 0.055 mmol) and propanoic anhydride (0.7 mL, 5.49 mmol). The reaction mixture was stirred at room temperature for 2 h. The solution was quenched with H_2O (50 mL), extracted with CH_2Cl_2 (50 mL x 3). The organic layers were washed with brine, dried over $MgSO_4$, and concentrated *in vacuo*. The product **1-20** was obtained as white solid (340 mg, 100%): ^{1}H NMR (400 MHz, CDCl₃) δ 1.09 (s, 6 H), 1.19 (m, 3 H), 1.66 (s, 3 H), 1.85 (m, 1 H), 2.04 (s, 3 H), 2.27 (s, 3 H), 2.29 (m, 1 H), 2.45 (m, 1 H), 2.53 (m, 3 H), 3.87 (d, *J* = 6.8 Hz, 1 H), 4.14 (d, *J* = 8.7 Hz, 1 H), 4.29 (d, *J* = 8.7 Hz, 1 H), 4.46 (m, 1 H), 4.87 (m, 1 H), 4.97 (d, *J* = 9.6 Hz, 1 H), 5.61 (d, *J* = 6.8 Hz, 1 H), 6.32 (s, 1 H), 7.47 (m, 2 H), 7.60 (m, 1 H), 8.08 (m, 2 H); ^{13}C NMR (100.5 MHz, CDCl₃) δ 9.11, 9.51, 15.6, 21.0, 22.6, 27.0, 27.7, 28.8, 35.6, 38.7, 42.7, 46.2, 58.7, 67.9, 72.3, 74.9, 76.0, 76.4, 76.0, 76.4, 79.1, 80.8, 84.4, 128.5, 129.2, 130.0, 131.8, 133.5, 146.2, 166.9, 170.1, 170.5, 174.5, 204.0. All data are consistent with the reported values.[32]

7-Triethylsilyl-10-deacetyl-10-propanoylbaccatin III (1-21):[32]

To a solution of **1-20** (340 mg, 0.549 mmol) and imidazole (0.149 g, 2.19 mmol) in DMF (10 mL) was added chlorotriethylsilane (0.28 mL, 1.64 mmol) dropwise *via* syringe at 0 °C, and the reaction mixture was stirred for 3 h at room temperature and quenched with saturated NH_4Cl solution (30 mL). The mixture was extracted by ethyl acetate (30 mL x 3), and then washed with H_2O (30 mL x 2), brine (30 mL), dried over anhydrous $MgSO_4$ and concentrated. The crude product was purified on a silica gel column using hexanes/ethyl acetate (2/1) as eluant to give **1-21** as a white solid (0.351 g, 90% yield): ^{1}H NMR (300 MHz, CDCl₃) 0.56 (m, 6 H), 0.89 (t, *J* = 7.8 Hz, 9 H), 1.15 (s, 3 H), 1.26 (s, 6 H), 1.53 (s, 6 H), 1.68 (s, 3 H), 1.77 (s, 6 H), 1.90 (s, 4 H), 2.25 (s, 3 H), 2.36 (s, 3 H), 2.43 (m, 2 H), 3.82 (d, *J* = 7.0 Hz, 1 H), 4.20 (d, *J* = 8.5 Hz, 1 H), 4.31 (d, *J* = 8.5 Hz, 1 H), 4.43 (m, 1 H), 4.78 (m, 1 H), 4.96 (d, *J* = 8.1 Hz, 1 H), 5.32 (d, *J* = 8.3 Hz, 1 H), 5.67 (d, *J* = 7.0 Hz, 1 H), 6.17 (t, *J* = 8.6 Hz, 1 H), 6.51 (s, 1 H), 7.45 (m, 2 H), 7.59 (m, 1 H), 8.10 (m, 2 H); ^{13}C NMR (75.0 MHz, CDCl₃) 5.2, 6.7, 9.2, 9.9, 14.9, 20.1, 22.6, 26.7, 27.6, 37.2, 38.3, 42.7, 58.6, 67.8, 72.3, 74.7, 78.7, 80.0, 84.2, 128.5, 129.4, 130.0, 132.6, 133.5, 143.9, 167.8, 170.7, 174.5, 202.3. All data are consistent with the reported values.[36]

7-Triethylsilyl-2'-triisopropylsilyl-3'-dephenyl-3'-(2-methylprop-1-enyl)-10-propanoyldocetaxel (1-22):[36]

To a solution of a baccatin **1-21** (0.351 g in 45 ml THF) and 1.5 equiv of β-lactam **1-11** in dry THF was added dropwise 1.5 equiv of LiHMDS (1.0 M in THF) at -40 °C. The reaction mixture was stirred for 1 h. Then, the reaction was quenched with saturated NH_4Cl. The mixture was extracted with ethyl acetate and the organic layers were washed with saturated NH_4Cl and brine, dried over $MgSO_4$, and concentrated *in vacuo*. Purification of the crude product by silica gel chromatography (hexane/ethyl acetate = 4/1) afforded the corresponding taxoid with protecting groups **1-22** as a white solid (0.495 g 91% yield): ^{1}HNMR (400 MHz, $CDCl_3$) δ 0.55 (m, 6 H), 0.91 (m, 9 H), 1.11 (m, 21 H), 1.17 (s, 3 H), 1.20 (s, 3 H), 1.22 (m, 3 H), 1.22 (s, 3 H), 1.33 (s, 9 H), 1.69 (s, 3 H), 1.75 (s, 3 H), 1.79(s, 3 H), 1.87 (m, 1 H), 2.01 (s, 3 H), 2.36 (s, 3 H), 2.46 (m, 3 H), 3.84 (d, *J* = 7.0 Hz, 1 H), 4.18 (d, *J* = 8.3 Hz, 1 H), 4.29 (d, *J* = 8.4 Hz, 1 H), 4.42 (d, *J* = 2.2 Hz, 1 H), 4.47 (dd, *J* = 10.4, 6.6 Hz, 1 H), 4.80 (m, 2 H), 4.93 (d, *J* = 8.8 Hz, 1 H), 5.32 (d, *J* = 8.2 Hz, 1 H), 5.68 (d, *J* = 7.0 Hz, 1 H), 6.08 (t, *J* = 8.8 Hz, 1 H), 6.48 (s, 1 H), 7.45 (t, *J* = 7.5 Hz, 2 H), 7.59 (t, *J* = 7.3 Hz, 1 H), 8.09 (d, *J* = 7.5 Hz, 2 H). All data are consistent with the reported values.[36]

3'-Dephenyl-3'-(2-methylprop-1-enyl)-10-propanoyldocetaxel(1-23, SB-T-1213):[32]

To a solution of **1-22** (0.478 g, 0.43 mmol) in a 1:1 mixture of pyridine (9.65 mL) and acetonitrile (9.65 mL) was added HF/pyridine (70:30) (4.78 ml) at 0 °C. The reaction mixture was stirred at room temperature overnight and the reaction mixture was diluted with ethyl acetate. The organic layer was washed with aqueous $NaHCO_3$ solution (20 mL x 2), $CuSO_4$ solution (20 mL x 3) and brine (20 mL x 2), dried over $MgSO_4$, and concentrated *in vacuo*. Purification of the crude product by silica gel chromatography (hexanes/EtOAc = 1/1) afforded the corresponding taxoid **1-23** as a white solid (0.346 g, 95% yield): $[α]^D$ -40.0° (*c* 1.00, $CHCl_3$); ^{1}H NMR (300 MHz, $CDCl_3$) δ 1.08 (s, 3 H), 1.13-1.18 (m, 6 H), 1.28 (s, 9 H), 1.60 (s, 3 H), 1.69 (br s, 6 H), 1.72 (m, 1 H), 1.83 (s, 3 H), 2.29 (s, 3 H), 2.31 (s, 2 H), 2.44 (m, 3 H), 3.38 (br s, 1 H), 3.74 (d, *J* = 6.9 Hz, 1 H), 4.10 (d, *J* = 8.1 Hz, 1 H), 4.13 (bs, 1 H), 4.22 (d, *J* = 8.1 Hz, 1 H), 4.33 (dd, *J* = 10.1, 7.5 Hz, 1 H), 4.67 (m, 2 H), 4.88 (d, *J* = 9.3 Hz, 1 H), 5.23 (d, *J* = 8.4 Hz, 1 H), 5.59 (d, *J* = 6.9 Hz, 1 H), 6.06 (m, 1 H), 6.24 (s, 1 H), 7.37 (t, *J* = 7.6 Hz, 2 H), 7.51 (t, *J* = 8.0 Hz, 1 H), 8.01 (d, *J* = 8.0 Hz, 2 H); ^{13}C NMR (63 MHz, $CDCl_3$) δ 9.0, 9.5, 14.9, 18.5, 21.8, 22.3, 25.7, 26.6, 27.5, 28.2, 35.5, 43.1, 45.6, 51.6, 55.5, 58.5, 72.1, 72.3, 73.7, 75.0, 75.4, 76.4, 76.5, 77.0, 77.5, 79.1, 79.9, 81.0, 84.3, 120.6, 128.6, 129.2, 130.1, 132.9, 133.6, 137.8, 142.4, 155.4, 166.9, 170.1, 173.0, 174.6, 203.8; HRMS (FAB, DCM/NBA) *m/z* calcd for $C_{44}H_{59}O_{15}NH^+$ 842.3962, found 842.4007. All data are consistent with the reported values.[32]

7-Triethylsilyl-10-deacetylbaccatin III (1-24):[32]

To a solution of 10-deacetylbaccatin III (344 mg, 0.629 mmol) and imidazole (171 mg, 2.516 mmol) in DMF (5.8 mL) was added chlorotriethylsilane (0.32 mL, 1.89 mmol) dropwise *via* syringe at 0 °C, and the reaction mixture was stirred for 25 min at room temperature and diluted with saturated NH_4Cl (15 mL). The mixture was extrated with EtOAc (30 mL x 3), dried over anhydrous $MgSO_4$ and concentrated. The crude product was purified on a silica gel column using hexanes/EtOAc 2/1) as eluent to give **1-24** as a

white solid (398 mg, 96%): ^{1}H NMR (400 MHz, CDCl$_3$) δ 0.56 (m, 6 H), 0.94 (m, 9 H), 1.08 (s, 6 H), 1.59 (d, J = 2.5 Hz, 1H), 1.73 (s, 3H), 1.90 (m, 1 H), 2.05 (d, J = 4.8 Hz, 1H), 2.08 (s, 3 H), 2.24 (s, 1 H), 2.28 (s, 3 H), 2.48 (m, 1 H), 3.95 (d, J = 7.1 Hz, 1 H), 4.16 (d, J = 8.3 Hz, 1 H), 4.25 (s, 1 H), 4.31 (d, J = 8.3 Hz, 1 H), 4.40 (dd, J = 6.4, 10.5 Hz, 1 H), 4.85 (t, 1 H), 4.95 (d, J = 8.0 Hz, 1 H), 5.17 (s, 1 H), 5.60 (d, J = 7.0 Hz, 1 H), 7.47 (t, J = 7.5 Hz, 2 H), 7.60 (t, J = 7.5 Hz, 1 H), 8.10 (d, J = 7.3 Hz, 2 H); ^{13}C NMR (CDCl$_3$, 75.0 MHz) 5.1, 6.7, 9.9, 15.1, 19.5, 22.6, 26.8, 37.2, 38.6, 42.7, 47.0, 57.9, 67.9, 72.9, 74.6, 74.8, 76.5, 78.8, 80.7, 84.2, 87.6, 128.6, 129.4, 130.0, 133.6, 135.1, 141.8, 167.0, 170.7, 210.3. All data are consistent with the reported values.[32]

General procedure for the synthesis of a C10-modified 7-(triethylsilyl)-10-deacetylbaccatin III (1-25):[32]

To a solution of 7-TES-DAB in THF (0.055 M) was added 1.1-1.2 equiv of LiHMDS at -40 °C. After the reaction mixture was stirred for 10 min, 1.1-1.2 equiv of an alkanoyl chloride, an *N,N*-dialkylcarbamoyl chloride was added dropwise at -40 °C. The mixture was warmed to 0 °C over a period of 1 h and then concentrated *in vacuo*. Purification of the crude product by silica gel chromatography (hexanes/EtOAc = 3/1 to 2/1) afforded the 10-modified 7-TES-baccatin III **1-25** as a white solid.

7-Triethylsilyl-10-cyclopropanecarbonyl-10-deacetylbaccatin III (1-25a):[32]

95 % yield; ^{1}H NMR (CDCl$_3$) 0.55 (m, 6 H), 0.90 (m, 9 H), 1.00 (s, 3 H), 1.16 (s, 3 H), 1.64 (s, 3 H), 1.73 (m. 1 H), 1.82 (m, 1 H), 2.14 (s, 3 H), 2.23 (m, 2 H), 2.24 (s, 3 H), 2.49 (m, 1 H), 3.84 (d, J = 6.9 Hz, 1 H), 4.11 (d, J = 8.0 Hz, 1 H), 4.26 (d, J = 8.2 Hz, 1 H), 4.45 (dd, J = 6.7, 10.3 Hz, 1 H), 4.77 (t, J = 7.8 Hz, 1 H), 4.92 (d, J = 8.6 Hz, 1 H), 5.59 (d, J = 7.0 Hz, 1 H), 6.43 (s, 1H), 7.43 (t, J = 7.4 Hz, 2 H), 7.56 (t, J = 7.6 Hz, 1 H), 8.05 (d, J = 7.3 Hz, 2 H). All data are consistent with the reported values. [32]

7-Triethylsilyl-10-deacetyl-10-(*N,N*-dimethylcarbamoyl)-baccatin III (1-25b):[32]

95% yield; ^{1}H NMR (400 MHz, CDCl$_3$) δ 0.57 (m, 6 H), 0.90 (m, 9 H), 1.04 (s, 3 H), 1.16 (s, 3 H), 1.67 (s, 3 H), 1.83 (m, 1 H), 2.02 (s, 3 H), 2.18 (m, 3 H), 2.33 (s, 3 H), 2.27 (s, 3 H), 2.51 (m, 1 H), 2.93 (s, 3 H), 3.07 (s, 3 H), 3.89 (d, J = 7.6 Hz, 1 H), 4.14 (d, J = 8.2 Hz, 1 H), 4.29 (d, J = 8.0 Hz, 1 H), 4.48 (dd, J = 10.2, 6.7 Hz, 1 H), 4.82 (t, J = 7.6 Hz, 1 H), 4.95 (d, J = 8.8 Hz, 1 H), 5.63 (d, J = 6.8 Hz, 1 H), 6.37 (s, 1 H), 7.46 (t, J = 8.0 Hz, 2 H), 7.59 (t, J = 7.2 Hz, 1 H), 8.10 (d, J = 7.2 Hz, 1 H). All data were in agreement with literature values.[32]

7-Triethylsilyl-10-deacetyl-10-methoxycarbonylbaccatin III (1-25c):[32]

86% yield; ^{1}H NMR (400 MHz, CDCl$_3$) δ 0.54 (q, J = 7.8 Hz, 6 H), 0.90 (t, J = 7.8 Hz, 9 H), 1.04 (s, 3 H), 1.16 (s, 3 H), 1.64 (s, 3 H), 1.83 (m, 1 H), 2.02 (s, 3 H), 2.18 (m, 3 H), 2.26 (m, 4 H), 2.49 (m, 1 H), 3.80 (m, 4 H), 4.09 (d, J = 8.2 Hz, 1 H), 4.28 (d, J = 8.2 Hz, 1 H), 4.47 (dd, J = 10.2, 6.7 Hz, 1 H), 4.84 (t, J = 7.5 Hz, 1 H), 4.92 (d, J = 8.5 Hz, 1 H), 5.60 (d, J = 7.0 Hz, 1 H), 6.27 (s, 1 H), 7.44 (t, J = 7.7 Hz, 2 H), 7.60 (t, J = 7.3 Hz, 1 H), 8.09 (d, J = 7.3 Hz, 1 H); ^{13}C NMR (75.0 MHz, CDCl$_3$) δ 5.3, 6.8, 9.9, 15.0, 20.0, 22.7, 26.7, 37.2, 38.3, 42.7, 47.2, 55.0, 58.5, 67.9, 72.4, 74.7, 75.5, 78.7, 79.2, 80.8, 84.2, 128.6,

129.4, 130.1, 132.3, 133.6, 144.8, 154.8, 167.1, 170.7, 201.7. All data were in agreement with literature values.[32]

General procedure for the syntheses of taxoids 1-27:[32]

To a solution of a baccatin **1-25** (0.02 M in THF) and 1.5 equiv of **1-10** in dry THF was added dropwise 1.5 equiv of LiHMDS (1.0 M in THF) at -40 °C. The reaction mixture was stirred for 1h. Then, the reaction was quenched with saturated NH₄Cl. The mixture was extracted with EtOAc and the organic layers were washed with saturated NH₄Cl and brine, dried over MgSO₄, and concentrated *in vacuo*. Purification of the crude product by silica gel chromatography (hexanes/EtOAc = 5/1) afforded the corresponding taxoid with protecting groups **1-26** as a white solid.

To a solution of **1-26** (0.015 M) in a 1:1 mixture of pyridine and acetonitrile was added HF/pyridine (70:30) (0.1 mL/10 mg of the starting material) at 0 °C. After the reaction mixture was warmed to room temperature overnight, the reaction mixture was diluted with EtOAc. The organic layer was washed with aqueous NaHCO₃, CuSO₄ solution and brine twice each, dried over MgSO₄, and concentrated *in vacuo*. Purification of the crude product by chromatography on silica gel (hexanes/EtOAc = 1/1) afforded the corresponding taxoid **1-27** as a white solid.

7-Triethylsilyl-2'-triisopropylsilyl-3'-dephenyl-10-(cyclopropanecarbonyl)-3'-(2-methyl-2-propenyl)docetaxel (1-26a):

96% yield; ¹HNMR (500 MHz, CDCl₃) δ 0.55 (m, 6 H), 0.93 (m, 9 H), 1.05 (m, 1 H), 1.11 (m, 21 H), 1.17 (s, 3 H), 1.20 (s, 3 H), 1.22 (m, 3 H), 1.26 (s, 3 H), 1.33 (s, 9 H), 1.69 (s, 3 H), 1.75 (s, 3 H), 1.79(s, 3 H), 1.87 (m, 1 H), 2.01 (s, 3 H), 2.36 (s, 3 H), 2.51 (m, 1 H), 3.84 (d, J = 7.0 Hz, 1 H), 4.19 (d, J = 8.3 Hz, 1 H), 4.30 (d, J = 9.0 Hz, 1 H), 4.44 (d, J = 2.2 Hz, 1 H), 4.47 (dd, J = 10.4 , 6.6 Hz, 1 H), 4.81 (m, 2 H), 4.94 (d, J = 9.0 Hz, 1 H), 5.34 (d, J = 8.5 Hz, 1 H), 5.69 (d, J = 6.5 Hz, 1 H), 6.09 (t, J = 9.0 Hz, 1 H), 6.48 (s, 1 H), 7.47 (t, J = 7.5 Hz, 2 H), 7.60 (t, J = 6.0 Hz, 1 H), 8.11 (d, J = 6.8 Hz, 2 H). All data are consistent with the reported values.[36]

7-Triethylsilyl-2'-triisopropylsilyl-3'-dephenyl-10-(*N,N*-dimethylcarbamoyl)-3'-(2-methyl-2-propenyl)docetaxel (1-26b):

90% yield; ¹HNMR (400 MHz, CDCl₃) δ 0.55 (m, 6 H), 0.91 (m, 9 H), 1.11 (m, 21 H), 1.17 (s, 3 H), 1.20 (s, 3 H), 1.22 (m, 3 H), 1.22 (s, 3 H), 1.33 (s, 9 H), 1.69 (s, 3 H), 1.75 (s, 3 H), 1.79(s, 3 H), 1.87 (m, 1 H), 2.01 (s, 3 H), 2.36 (s, 3 H), 2.46 (m, 3 H), 3.84 (d, J = 7.0 Hz, 1 H), 4.18 (d, J = 8.3 Hz, 1 H), 4.29 (d, J = 8.4 Hz, 1 H), 4.42 (d, J = 2.2 Hz, 1 H), 4.47 (dd, J = 10.4 , 6.6 Hz, 1 H), 4.80 (m, 2 H), 4.93 (d, J = 8.8 Hz, 1 H), 5.32 (d, J = 8.2 Hz, 1 H), 5.68 (d, J = 7.0 Hz, 1 H), 6.08 (t, J = 8.8 Hz, 1 H), 6.48 (s, 1 H), 7.45 (t, J = 7.5 Hz, 2 H), 7.59 (t, J = 7.3 Hz, 1 H), 8.09 (d, J = 7.5 Hz, 2 H). All data are consistent with the reported values.[36]

7-Triethylsilyl-2'-triisopropylsilyl-3'-dephenyl-10-(methoxycarbonyl)-3'-(2-methyl-2-propenyl)docetaxel (1-26c):

90% yield; ¹HNMR (400 MHz, CDCl₃) δ 0.55 (m, 6 H), 0.91 (m, 11 H), 1.11 (m, 23 H), 1.17 (s, 3 H), 1.20 (s, 3 H), 1.22 (m, 3 H), 1.22 (s, 3 H), 1.33 (s, 9 H), 1.69 (s, 3 H), 1.75 (s, 3 H), 1.79(s, 3 H), 1.87 (m, 1 H), 2.01 (s, 3 H), 2.36 (s, 3 H), 2.46 (m, 3 H), 3.84 (d, J

= 7.0 Hz, 1 H), 4.18 (d, *J* = 8.3 Hz, 1 H), 4.29 (d, *J* = 8.4 Hz, 1 H), 4.42 (d, *J* = 2.2 Hz, 1 H), 4.47 (dd, *J* = 10.4 , 6.6 Hz, 1 H), 4.80 (m, 2 H), 4.93 (d, *J* = 8.8 Hz, 1 H), 5.32 (d, *J* = 8.2 Hz, 1 H), 5.68 (d, *J* = 7.0 Hz, 1 H), 6.08 (t, *J* = 8.8 Hz, 1 H), 6.48 (s, 1 H), 7.45 (t, *J* = 7.5 Hz, 2 H), 7.59 (t, *J* = 7.3 Hz, 1 H), 8.09 (d, *J* = 7.5 Hz, 2 H). All data are consistent with the reported values.[36]

3'-Dephenyl-10-(cyclopropanecarbonyl)-3'-(2-methyl-2-propenyl)docetaxel (1-27a, SB-T-1214):[32]

99% yield; [α]^D -160° (*c* 1.00, CHCl3); ^{1}H NMR (250 MHz, CDCl3) δ 1.10 (m, 2 H), 1.14 (s, 3 H), 1.25 (s, 3 H), 1.34 (s, 9 H), 1.65 (s, 3 H), 1.71 (s, 2 H), 1.75 (br s, 6 H), 1.84 (m, 1 H), 1.88 (s, 3 H), 2.34 (s, 3 H), 2.37 (s, 2 H), 2.46 (m, 1 H), 2.56 (d, *J* = 3.3 Hz, 1 H), 3.36 (m, 1 H), 3.78 (d, *J* = 6.9 Hz, 1 H), 4.13 (d, *J* = 8.4 Hz, 1 H), 4.18 (br s, 1 H), 4.27 (d, *J* = 8.4 Hz, 1 H), 4.40 (m, 1 H), 4.72 (m, 2 H), 4.93 (d, *J* = 8.6 Hz, 1 H), 5.28 (d, *J* = 7.6 Hz, 1 H), 5.64 (d, *J* = 6.9 Hz, 1 H), 6.16 (m, 1 H), 6.28 (s, 1 H), 7.43 (t, 2 H), 7.56 (t, 1 H), 8.07 (d, 2 H); ^{13}C NMR (63 MHz, CDCl3) δ 9.1, 9.4, 9.5, 13.0, 14.9, 18.5, 21.9, 22.4, 25.7, 26.7, 28.2, 35.5, 35.6, 43.2, 45.6, 51.6, 58.5, 72.2, 72.3, 73.7, 75.0, 75.4, 76.5, 77.0, 77.5, 79.2, 79.7, 81.0, 84.4, 120.6, 128.6, 129.2, 130.1, 132.9, 133.6, 137.9, 142.6, 155.4, 166.9, 170.1, 175.1, 203.9; IR (neat, cm-1) *v* 3368, 2989, 2915, 1786, 1754, 1725, 1709, 1641, 1630, 1355, 1315, 1109; HRMS (FAB, DCM/NBA/NaCl) *m/z* calcd for $C_{45}H_{59}O_{15}$ NNa$^+$ 876.3784, found 876.3782. All data are consistent with the reported values. [36]

3'-Dephenyl-10-(*N,N*-dimethylcarbamoyl)-3'-(2-methyl-2-propenyl)docetaxel (1-28b, SB-T-1216):[32]

80% yield; [α]$_D^{20}$ -50.0 (*c* 2.00, CHCl$_3$); ^{1}H NMR (250 MHz, CDCl$_3$) δ 1.13 (s, 3 H), 1.23 (s, 3 H), 1.33 (s, 9 H), 1.64 (s, 3 H), 1.74 (br s, 6 H), 1.85 (m, 1 H), 1.89 (s, 3 H), 2.33 (s, 3 H), 2.36 (s, 2 H), 2.45 (m, 1 H), 2.93 (s, 3 H), 3.02 (s, 3 H), 3.20 (br s, 1 H), 3.45 (m, 1 H), 3.78 (d, *J* = 6.9 Hz, 1 H), 4.14 (d, *J* = 8.4 Hz, 1 H), 4.18 (br s, 1 H), 4.26 (d, *J* = 8.4 Hz, 1 H), 4.40 (dd, *J* = 10.2, 6.7 Hz, 1 H), 4.69 (m, 1 H), 4.80 (s, 1 H), 4.93 (d, *J* = 8.6 Hz, 1 H), 5.27 (d, *J* = 7.6 Hz, 1 H), 5.62 (d, *J* = 6.9 Hz, 1 H), 6.12 (m, 1 H), 6.23 (s, 1 H), 7.41 (t, 2 H), 7.55 (t, 1 H), 8.06 (d, 2 H); ^{13}C NMR (63 MHz, CDCl$_3$) δ 9.3, 15.0, 18.5, 22.2, 22.3, 25.7, 26.8, 28.2, 35.3, 35.6, 36.0, 36.6, 43.1, 45.6, 51.6, 58.4, 72.3, 72.4, 73.7, 75.2, 76.2, 76.4, 76.5, 77.0, 77.5, 79.2, 81.0, 84.6, 128.6, 129.2, 130.1, 133.1, 133.6, 137.8, 142.9, 155.4, 156.1, 166.9, 170.0, 173.0, 205.6; HRMS (FAB, DCM/NBA) *m/z* calcd for $C_{44}H_{60}O_{15}N_2Na^+$ 879.3891, found 879.3870. All data are consistent with the reported values. [36]

3'-Dephenyl-10-(methoxycarbonyl)-3'-(2-methyl-2-propenyl)docetaxel (1-27-c, SB-T-1217):[32]

84% yield; [α]$_D^{20}$ -15.0 (*c* 2.00, CHCl$_3$); ^{1}H NMR (400 MHz, CDCl$_3$) δ 1.14 (s, 3 H), 1.23 (s, 3 H), 1.33 (s, 9 H), 1.68 (s, 3 H), 1.71 (br s, 6 H), 1.87 (m, 1 H), 1.92 (s, 3 H), 2.34 (s, 3 H), 2.47 (m, 2 H), 2.55 (m, 1 H), 3.40 (br s, 1 H), 3.76 (d, *J* = 6.9 Hz, 1 H), 3.85 (s, 3 H), 4.15 (d, *J* = 8.3 Hz, 1 H), 4.19 (br s, 1 H), 4.28 (d, *J* = 8.3 Hz, 1 H), 4.38 (m, 1 H), 4.72 (m, 2 H), 4.93 (d, *J* = 8.6 Hz, 1 H), 5.29 (d, *J* = 7.8 Hz, 1 H), 5.64 (d, *J* = 6.9 Hz, 1 H), 6.11 (s, 1 H), 6.15 (s, 1 H), 7.43 (t, *J* = 7.5 Hz, 2 H), 7.56 (t, 1 H), 8.07 (d, *J* = 7.5 Hz, 2 H); ^{13}C NMR (75 MHz, CDCl$_3$) δ 9.4, 15.0, 18.5, 21.7, 22.3, 25.7, 26.5, 28.2,

35.5, 43.1, 45.6, 51.6, 55.5, 58.6, 72.0, 72.2, 73.7, 75.0, 76.4, 76.5, 77.0, 77.2, 77.4, 78.3, 79.1, 79.9, 81.0, 84.3, 120.6, 128.6, 129.2, 130.1, 132.5, 133.6, 137.9, 143.4, 155.4, 155.7, 166.9, 170.1, 172.9, 203.9; HRMS (FAB, DCM/NBA/PPG) *m/z* calcd for $C_{43}H_{57}O_{16}NH^+$ 844.3710, found 844.3755. All data are consistent with the reported values.[36]

7,10,13-Tris(triethylsilyl)-10-deacetylbaccatin III (1-28):[82]

To a solution of **10-DAB** (350 mg, 0.643 mmol) and imidazole (263 mg, 3.86 mmol) in dry DMF (1.17 mL) was added chlorotriethylsilane (0.54 mL, 3.215 mmol) dropwise *via* syringe at room temperature. The reaction mixture was stirred overnight at room temperature and quenched with saturated NH_4Cl solution (20 mL) and extracted with ethyl acetate (30 mL x 3). The mixture was then washed with water (10 mL x 2), brine (10 mL), dried over anhydrous $MgSO_4$ and concentrated. The crude product was purified on a silica gel column (hexane/EtOAc = 20/1) to afford **1-28** as a white solid (0.561 g, 95%): mp: 187-189 $^\circ$C; $[\alpha]_D^{20}$ -38.8 (*c* 0.28, CHCl$_3$); ^{1}H NMR (250 MHz, CDCl$_3$) δ 0.65 (m, 18 H), 0.99 (m, 27 H), 1.11 (s, 3 H), 1.18 (s, 3 H), 1.64 (s, 3 H), 1.87 (m, 1 H), 1.97 (s, 3 H), 2.08 (dd, *J* = 15.2, 8.8 Hz, 1 H), 2.21 (dd, *J* = 15.1, 8.2 Hz, 1 H), 2.27 (s, 3 H), 2.51 (m, 1 H), 3.84 (d, *J* = 7.0 Hz, 1 H), 4.13 (d, *J* = 8.3 Hz, 1 H), 4.27 (d, *J* = 8.3 Hz, 1 H), 4.40 (dd, *J* = 10.5, 6.6 Hz, 1 H), 4.92 (m, 2 H), 5.18 (s, 1 H), 5.61 (d, *J* = 7.1 Hz, 1 H), 7.44 (t, *J* = 7.3 Hz, 2 H), 7.57 (t, *J* = 7.3 Hz, 1 H), 8.07 (d, *J* = 7.4 Hz, 1 H); ^{13}C NMR (62.9 MHz, CDCl$_3$,) δ 4.7, 5.2, 5.9, 6.9, 10.4, 14.8, 20.5, 22.4, 26.3, 37.3, 19.8, 42.4, 46.8, 58.2, 68.3, 72.6, 75.4, 75.7, 76.6, 79.5, 80.7, 83.9, 128.5, 129.6, 130.0, 133.4, 135.7, 139.3, 167.1, 169.7, 205.6. HRMS (FAB/DCM/NaCl) m/z calcd. for $C_{47}H_{78}O_{10}Si_3Na^+$: 909.4801 found: 909.4833 (Δ = 3.5 ppm). All data are in agreement with literature values.[82]

7,10,13-Tris(triethylsilyl)-2-debenzoyl-10-deacetylbaccatin III (1-29):[82]

To a solution of **1-28** (657 mg, 0.74 mmol) in dry THF (11 mL) at -10 $^\circ$C was added dropwise a solution of Red-Al in toluene (70% wt, 0.57 mL, 1.85 mmol), and the reaction mixture was stirred for 1 h at -10 $^\circ$C. The reaction was quenched with aqueous saturated NH_4Cl solution (40 mL), and the aqueous layer was extracted with ethyl acetate (30 mL x 3). The combined extracts were then dried over anhydrous $MgSO_4$ and concentrated *in vacuo*. The residue was purified on a silica gel column (hexane/ethyl acetate = 10/1 followed by 4/1) to afford **1-29** as a white solid (612 mg, 100%): mp 68-70 $^\circ$C; $[\alpha]_D^{20}$ -35.6 (*c* 0.87, CHCl$_3$); ^{1}H NMR (250 MHz, CDCl$_3$) δ 0.57 (m, 18 H), 0.94 (m, 27 H), 1.11 (s, 3 H), 1.55 (s, 3 H), 1.87 (m, 1 H), 1.88 (s, 3 H), 1.94 (m, 1 H), 2.00 (m, 1 H), 2.12 (s, 3 H), 2.47 (m, 1 H), 3.42 (d, *J* = 6.6 Hz, 1 H), 3.80 (d, *J* = 6.6 Hz, 1 H), 4.31 (dd, *J* = 10.4, 6.5 Hz, 1 H), 4.50 (d, *J* = 9.0 Hz, 1 H), 4.57 (d, *J* = 9.1 Hz, 1 H), 4.63 (s, 1 H), 4.89 (d, *J* = 8.3 Hz, 1 H), 4.91 (m, 1 H), 5.08 (s, 1 H); ^{13}C NMR (62.9 MHz, CDCl$_3$) δ 4.7, 5.1, 5.8, 6.7, 6.8, 10.5, 14.4, 20.5, 22.3, 37.3, 40.3, 42.5, 58.1, 65.0, 66.3, 72.6, 74.6, 75.7, 77.9, 78.5, 81.9, 83.7, 126.8, 127.4, 128.4, 135.9, 138.9, 169.6, 206.3. All data are in agreement with literature values.[82]

7,10,13-Tri(triethylsilyl)-2-debenzoyl-2-(3-methoxybenzoyl)-10-deacetylbaccatin III (1-30):[82]

To a solution of **1-29** (275 mg, 0.351 mmol), *m*-anisic acid (426 mg, 2.81 mmol) and DMAP (3.86 mg, 3.16 mmol) in CH_2Cl_2 (2.4 mL) was added DIC (0.496 mL, 3.16 mmol) and the reaction mixture was refluxed overnight. The reaction mixture was diluted with ethyl acetate (150 mL) and washed with saturated aqueous $NaHCO_3$ solution (15 mL), H_2O (15 mL) and brine (15 mL). The organic lawyer was dried over anhydrous $MgSO_4$. The solvent was removed under reduced pressure and the residue was purified on a silica gel column (hexane/EtOAc = 12/1) to afford **1-30** as a white solid (221 mg, 70%): mp 201-202 °C; ^{1}H NMR (400 MHz, $CDCl_3$) δ 0.60 (m, 18 H), 0.98 (m, 27 H), 1.11 (s, 3 H), 1.18 (s, 3 H), 1.57 (bs, 1 H), 1.62 (s, 3 H), 1.85 (m, 1 H), 1.96 (s, 3 H), 2.14 (m, 2 H), 2.26 (s, 3 H), 2.50 (m, 1 H), 3.83 (m, 4 H), 4.13 (d, J = 7.9 Hz, 1 H), 4.30 (d, J = 8.1 Hz, 1 H), 4.39 (dd, J = 10.4 Hz, 6.9 Hz, 1 H), 4.92 (m, 2 H), 5.17 (s, 1 H), 5.59 (d, J = 6.9 Hz, 1 H), 7.10 (m, 1 H), 7.35 (t, J = 7.9 Hz, 1 H), 7.61 (s, 1 H), 7.66 (d, J = 7.7 Hz, 2 H); ^{13}C NMR (62.9 MHz, $CDCl_3$) δ 4.9, 5.2, 6.0, 6.9, 10.4, 14.6, 20.6, 22.4, 26.3, 37.3, 39.9, 43.0, 46.9, 55.3, 58.3, 68.3, 72.6, 75.5, 75.8, 76.6, 79.5, 80.9, 84.0, 114.3, 120.2, 122.5, 129.5, 130.9, 135.8, 139.4, 159.6, 167.0, 169.9, 205.7. HRMS: *m/e* calcd for $C_{48}H_{80}O_{11}Si_3 \cdot H^+$: 917.5087. Found: 917.5084 (Δ = 0.3 ppm). All data are in agreement with literature values.[82]

2-Debenzoyl-2-(3-methoxybenzoyl)-10-deacetylbaccatin III (1-31):[82]

To a solution of **1-30** (184 mg, 0.20 mmol) in 7.2 mL of pyridine/acetonitrile (1:1) was added dropwise HF/pyridine (70:30, 1.8 mL) at 0 °C, and the mixture was stirred overnight at room temperature. The reaction was quenched with saturated aqueous $NaHCO_3$ solution (30 mL). The mixture was then diluted with ethyl acetate (150 mL), washed with saturated aqueous $CuSO_4$ solution (20 mL x 2) and H_2O (20 mL), dried over anhydrous $MgSO_4$ and concentrated *in vacuo* to afford 2-debenzoyl-2-(3-methoxybenzoyl)-10-deacetylbaccatin III (**1-31**) as a white solid. The crude compound was used in the next step without further purification.

2-Debenzoyl-2-(3-methoxybenzoyl)-10-deacetyl-10-propanoylbaccatin III (1-32):[82]

To the solution of **1-31** (141 mg, 0.2 mmol) in THF (6.1 mL) was added cerium chloride heptahydrate (7 mg, 0.02 mmol) and propanoic anhydride (0.26 mL, 2 mmol). The reaction mixture was stirred at room temperature for 2 h. The solution was added 50 mL of H_2O. This mixture was extracted with CH_2Cl_2 (50 mL x 3). The organic layers were washed with brine, dried over $MgSO_4$, and concentrated *in vacuo*. The product **1-32** was obtained as white solid (125 mg, 99%): ^{1}H NMR (400 MHz, $CDCl_3$) δ 1.11 (s, 6 H), 1.18 (d, 1 H), 1.25(t, 6H), 1.67 (s, 3 H), 1.85 (t, 1 H), 2.06 (s, 3 H), 2.28 (m, 5 H), 2.48 (m, 5H), 3.88 (ss, 4 H), 4.15 (d, J = 10.8Hz, 1 H), 4.34 (d, J = 10.8 Hz, 1 H), 4.43 (dd, J = 10.4, 6.9 Hz, 1 H), 4.89 (t, 1 H), 4.99 (d, 1 H), 5.61 (d, J = 7.6 Hz, 1 H), 6.34(s, 1H), 7.14 (d, 1 H), 7.39 (t, J = 8 Hz, 1 H), 7.64 (s, 1 H), 7.70 (d, J = 7.76 Hz, 1 H). All data are in agreement with literature values.[82]

7-Triethylsilyl-2-debenzoyl-2-(3-methoxybenzoyl)-10-deacetyl-10-propanoylbaccatin III (1-33):[82]

To a solution of **1-32** (124 mg, 0.197 mmol) and imidazole (54 mg, 0.786 mmol) in DMF (2 mL) was added chlorotriethylsilane (0.13 mL, 0.59 mmol) dropwise *via* syringe at 0 $^{\circ}$C. The reaction mixture was stirred for 1 h at room temperature and quenched with saturated NH$_4$Cl solution (30 mL). The mixture was extracted by ethyl acetate (30 mL x 3), and then washed with H$_2$O (30 mL x 2), brine (30 mL), dried over anhydrous MgSO$_4$ and concentrated *in vacuo*. The crude product was purified on a silica gel column using hexane/ethyl acetate (2/1) as eluant to give **1-33** as a white solid (0.126 g, 86% yield): mp 105-107 $^{\circ}$C; ^{1}H NMR (400 MHz, CDCl$_3$) δ 0.56 (q, *J* = 7.8 Hz, 6 H), 0.85 (t, *J* = 7.8 Hz, 9 H), 0.99 (s, 3 H), 1.20 (m, 7 H), 1.64 (s, 3 H), 1.83 (m, 1 H), 2.00 (s, 3 H), 2.16 (s, 3 H), 2.23 (m, 3 H), 2.40 (m, 3 H), 3.85 (m, 4 H), 4.09 (m, 2 H), 4.29 (d, *J* = 8.3 Hz, 1 H), 4.45 (dd, *J* = 10.2, 6.7 Hz, 1 H), 4.79 (t, *J* = 7.9 Hz, 1 H), 4.94 (d, *J* = 8.9 Hz, 1 H), 5.57 (d, *J* = 6.9 Hz, 1 H), 6.45 (s, 1 H), 7.09 (dd, *J* = 8.3, 2.2 Hz, 1 H), 7.33 (t, *J* = 8.1 Hz, 1 H), 7.60 (s, 1 H), 7.66 (d, *J* = 7.7 Hz, 1 H); ^{13}C NMR (62.9 MHz, CDCl$_3$) δ 5.3, 6.7, 9.2, 9.9, 14.2, 14.9, 20.1, 22.5, 26.8, 27.7, 37.2, 38.3, 42.7, 47.2, 55.3, 58.6, 60.4, 67.8, 72.3, 74.8, 75.6, 76.4, 78.7, 80.8, 84.2, 1114.7, 119.9, 122.5, 129.6, 130.6, 132.6, 144.1, 159.6, 166.9, 170.6, 172.7, 202.4. HRMS: *m/e* calcd for C$_{39}$H$_{56}$O$_{12}$Si·H$^+$: 745.3619. Found: 745.3617 (Δ = 0.3 ppm). All data are in agreement with literature values.[82]

3'-Dephenyl-3'-(2-methyl-2-propenyl)-2-debenzoyl-2-(3-methoxybenzoyl)-10-propanoyldocetaxel (1-35, SB-T-121303): [82]

To a solution of baccatin **1-33** (142 mg, 0.191 mmol) and *β*-lactam **1-11** (114 mg, 0.287 mmol) in dry THF (17.5 mL) was added 1.0 M LiHMDS in THF (0.287 mL, 0.287 mmol) dropwise at -40 $^{\circ}$C, and the solution was stirred at -40 $^{\circ}$C for 1 h. The reaction was quenched with saturated aqueous NH$_4$Cl solution (30 mL), and the aqueous layer was extracted with ethyl acetate (30 mL x 3). The combined extracts were dried over anhydrous MgSO$_4$ and concentrated *in vacuo*. The residue was purified on a silica gel column using hexane/ethyl acetate (4/1) as the eluant to afford the coupling product **1-34** as a white solid (212 mg, 97%).

To a solution of **1-34** thus obtained (210 mg, 0.18 mmol) in pyridine /acetonitrile (1:1, 8 mL) was added dropwise HF/pyridine (70:30, 2 mL) at 0 $^{\circ}$C, and the mixture was stirred overnight at room temperature. The reaction was quenched with saturated aqueous NaHCO$_3$ solution (30 mL). The mixture was then diluted with ethyl acetate (150 mL), washed with saturated aqueous CuSO$_4$ solution (20 mL x 3) and H$_2$O (20 mL), dried over anhydrous MgSO$_4$ and concentrated *in vacuo*. The residue was purified on a silica gel column using hexanes/EtOAc (1/1) as the eluant to afford **SB-T-121303 (1-35)** as a white solid (135 mg, 85%): mp 130-132 $^{\circ}$C; ^{1}H NMR (400 MHz, CDCl$_3$) 1.13 (s, 3 H), 1.28 (m, 8 H), 1.33 (s, 9 H), 1.66 (m, 3 H), 1.73 (s, 3 H), 1.75 (s, 3 H), 1.89 (m, 5 H), 2.37 (m, 6 H), 2.52 (m, 3 H), 3.80 (d, *J* = 6.9 Hz, 1 H), 3.86 (s, 3 H), 4.12 (m, 2 H), 4.32 (d, *J* = 8.5 Hz, 1 H), 4.40 (dd, *J* = 10.6, 6.8 Hz, 1 H), 4.72 (m, 2 H), 4.96 (d, *J* = 8.3 Hz, 1 H), 5.30 (d, *J* = 7.6 Hz, 1 H), 5.64 (d, *J* = 7.0 Hz, 1 H), 6.16 (t, *J* = 8.6 Hz, 1 H), 6.30 (s, 1 H), 7.13 (d, *J* = 7.9 Hz, 1 H), 7.33 (t, *J* = 8.0 Hz, 1 H), 7.62 (s, 1 H), 7.68 (d, *J* = 7.6 Hz, 1 H); ^{13}C NMR (75.0 MHz, CDCl$_3$) 9.0, 9.5, 14.9, 18.5, 21.8, 22.4, 25.7, 26.6, 27.5, 28.2, 35.5, 43.2, 45.6, 51.5, 55.3, 58.5, 72.2, 72.3, 73.7, 75.1, 75.4, 76.2, 79.1, 79.9, 81.1, 84.4, 114.6, 120.1, 120.6, 122.5, 129.6, 130.4, δ132.9, 137.8, 142.5, 155.4, 159.6, 166.8, 170.0, 174.0,

174.6, 203.8. HRMS: *m/e* calcd for $C_{45}H_{61}O_{16}N \cdot H^+$: 872.4069. Found: 872.4072 (Δ = - 0.4 ppm). All data are in agreement with literature values.[82]

2-Debenzoyl-2-(3-methoxybenzoyl)-7-triethylsilyl-10-deacetylbaccatin III (1-36):[82]
To a solution of **1-31** (244 mg, 0.425 mmol) and imidazole (112 mg, 1.70 mmol) in DMF (4.3 mL) was added chlorotriethylsilane (0.30 mL, 1.28 mmol) dropwise *via* syringe at 0 $^{\circ}$C. The reaction mixture was stirred for 40 min at room temperature and diluted with saturated NH_4Cl (20 mL). The mixture was extrated with EtOAc (40 mL x 3), dried over anhydrous $MgSO_4$ and concentrated *in vacuo*. The crude product was purified on a silica gel column using hexanes/EtOAc (2/1) as eluant to give **1-36** as a white solid (273 mg, 93% for 2 steps): mp 103-109 $^{\circ}$C; ^{1}H NMR (300 MHz, $CDCl_3$) δ 0.60 (m, 6 H), 0.98 (m, 9 H), 1.11 (s, 3 H), 1.18 (s, 3 H), 1.57 (bs, 1 H), 1.62 (s, 3 H), 1.85 (m, 1 H), 1.96 (s, 3 H), 2.14 (m, 2 H), 2.26 (s, 3 H), 2.50 (m, 1 H), 3.83 (m, 4 H), 4.13 (d, *J* = 7.9 Hz, 1 H), 4.30 (d, *J* = 8.1 Hz, 1 H), 4.39 (dd, *J* = 10.4, 6.9 Hz, 1 H), 4.92 (m, 2 H), 5.17 (s, 1 H), 5.59 (d, *J* = 6.9 Hz, 1 H), 7.10 (m, 1 H), 7.35 (t, *J* = 7.9 Hz, 1 H), 7.61 (s, 1 H), 7.66 (d, *J* = 7.7 Hz, 2 H). All data are consistent with the reported values.[82]

2-Debenzoyl-2-(3-methoxybenzoyl)-7-(triethylsilyl)-10-deacetyl-10-(4-methoxy-phenylacetyl)baccatin III (1-37):
To a solution of 7-TES-DAB **1-36** (20 mg, 0.029 mmol) in THF (0.7 mL) was added 1.2 equiv of LiHMDS at -40 $^{\circ}$C. After the reaction mixture was stirred for 10 min, 1.2 equiv of 4-methoxyphenylacetyl chloride was added dropwise at -40 $^{\circ}$C. The reaction was quenched by saturated NH_4Cl (15 mL) after 1h and extracted with dichloromethane (20 mL x 3). The organic layer was concentrated *in vacuo*. Purification of the crude product chromatography on silica gel (hexanes/EtOAc = 3/1 to 2/1) afforded the C10-modified 7-TES-baccatin III **1-37** as a white solid (20 mg, 82%): ^{1}H NMR (400 MHz, $CDCl_3$) δ 0.55 (m, 6 H), 0.89 (m, 9 H), 0.92 (s, 3 H), 1.09 (s, 3 H), 1.27 (s, 3 H), 1.68 (s, 3 H), 1.87 (m, 1 H), 2.17 (s, 3 H), 2.24 (m, 2 H), 2.25 (s, 3 H), 2.50 (m, 1 H), 3.69 (d, *J* = 3.6 Hz, 1 H), 3.78 (s, 1 H), 3.85 (dd, *J* = 7.2, 1.6 Hz, 1 H), 3.86 (s, 3 H), 4.14 (d, *J* = 8.4 Hz, 1 H), 4.33 (d, *J* = 8.0 Hz, 1 H), 4.47 (dd, *J* = 10.8, 6.8 Hz, 1 H), 4.78 (t, *J* = 7.9 Hz, 1 H), 4.95 (d, *J* = 9.6 Hz, 1 H), 5.60 (d, *J* = 6.8 Hz, 1 H), 6.85 (dt, *J* = 6.8, 2.8 Hz, 2 H), 7.13 (dt, *J* = 8.4, 0.8 Hz, 1 H), 7.24 (d, *J* = 8.8 Hz, 2 H), 7.37 (t, *J* = 8.0 Hz, 1 H), 7.64 (t, *J* = 1.2 Hz, 1 H), 7.70 (dd, *J* = 6.4, 0.8 Hz, 1 H). All data are consistent with the reported values.[36]

3'-Dephenyl-3'-(2-methyl-1-propenyl)-2-debenzoyl-2-(3-methoxybenzoyl)-10-(4-methoxyphenyl)acetyldocetaxel (1-39, 12130301):[82]
To a solution of baccatin **1-37** (20 mg, 0.028 mmol) and 1.5 equiv of 4-isobutenyl-1-(*tert*-butoxycarbonyl)-3-(triisopropylsilyloxy)azetidin-2-one (**1-11**) in dry THF (3 ml) was added dropwise LiHMDS (0.042 mL, 1.0 M in THF) at -40 $^{\circ}$C. The reaction mixture was stirred for 1.5 h. Then, the reaction was quenched with saturated NH_4Cl (30 mL). The mixture was extracted with EtOAc (30 mL x 3) and the organic layers were washed with saturated NH_4Cl (20 mL) and brine (20 mL), dried over $MgSO_4$, and concentrated *in vacuo*. Purification of the crude product by silica gel chromatography on silica gel (hexanes/EtOAc = 5/1) afforded the taxoid **1-38** with protecting groups as a white solid (24 mg, 81%).

To a solution of **1-38** (21 mg, 0.017 mmol) in a 1:1 mixture of pyridine and acetonitrile (0.80 mL) was added HF/pyridine (70:30) (0.2 mL) at 0 °C. After the reaction mixture was warmed to room temperature for overnight, the reaction mixture was diluted with EtOAc. The organic layer was washed with aqueous $NaHCO_3$, $CuSO_4$ solution and brine twice each, dried over $MgSO_4$, and concentrated *in vacuo*. Purification of the crude product by silica gel chromatography on silica gel (hexanes/EtOAc = 1/1) afforded the corresponding taxoid **SB-T-12130301** as a white solid (14 mg, 70% for 2 steps): mp 152-154 °C; ^{1}H NMR (300 MHz, $CDCl_3$) δ 1.07 (s, 3 H), 1.18 (s, 3 H), 1.34 (s, 9 H), 1.59 (s, 3 H), 1.67 (s, 3 H), 1.73 (s, 3 H), 1.76 (s, 3 H) 1.86 (s, 3 H), 1.86 (m, 1 H), 2.17 (m, 4 H), 2.37 (s, 3 H), 2.39 (m, 2 H), 2.55 (m, 1 H), 3.34 (bs, 1 H), 3.79 (m, 4 H), 3.68 (s, 3 H), 4.19 (m, 1 H), 4.32 (d, $J = 8.4$ Hz, 1 H), 4.39 (m, 1 H), 4.73 (m, 2 H), 4.94 (d, $J = 8.1$ Hz, 1 H), 5.30 (m, 1 H), 5.64 (d, $J = 6.9$ Hz, 1 H), 6.15 (t, $J = 8.1$ Hz, 1 H), 6.30 (s, 1 H), 6.86 (d, $J = 8.4$ Hz, 2 H), 7.12 (dd, $J = 7.8$ Hz, 2.1 Hz, 1 H), 7.24 (m, 2 H), 7.37 (t, $J = 7.5$ Hz, 1 H), 7.63 (s, 1 H), 7.68 (d, $J = 7.8$ Hz, 1 H); ^{13}C NMR (63 MHz, $CDCl_3$) δ 9.53, 14.2, 14.9, 18.5, 21.6, 22.4, 25.7, 26.4, 28.2, 30.9, 35.6, 40.1, 43.1, 45.6, 51.5, 55.2, 55.3, 58.5, 72.1, 72.3, 73.7, 75.0, 75.8, 79.0, 79.9, 81.0, 84.4, 87.5, 114.0, 114.6, 120.1, 120.6, 122.5, 129.6, 130.4, 130.5, 132.7, 142.5, 159.6, 166., 170.0, 172.0, 203.4, 206.9. HRMS (FAB): *m/e* calcd for $C_{51}H_{65}O_{17}N \cdot H^+$: 964.4331. Found: 964.4366 (Δ = 3.7 ppm).[36] All data are consistent with the reported values.[36]

2-Debenzoyl-2-(3-methoxybenzoyl)-7-triethylsilyl-10-deacetyl-13-oxo-baccatin III (1-40):

To a solution of 2-debenzoyl-2-(3-methoxybenzoyl)-7-triethylsilyl-10-deacetylbaccatin III (**1-36**) (24 mg, 0.035 mmol) in CH_2Cl_2 (0.5 mL) was added NMO (4.6 mg, 0.035 mmol) and 4 Å mol sieves (4.4 mg). After the solution was stirred for 10 min, TPAP (8.2 mg, 0.002 mmol) was added and the solution was allowed to stir for 1.5 hrs. The mixture was then filtered and concentrated *in vacuo* to give 24 mg (crude) of 2-debenzoyl-2-(3-methoxybenzoyl)-7-triethylsilyl-10-deacetyl-13-oxo-baccatin III (**1-40**) as a white solid: [1]H (300 MHz, $CDCl_3$) δ 0.49 (m, 6 H), 0.95 (m, 9 H), 1.15 (s, 3 H), 1.22 (s, 3 H), 1.24 (m, 1H), 1.71 (s, 3 H), 1.84 (m, 2 H), 2.10 (s, 3 H), 2.17 (s, 3 H), 2.47 (m, 1 H), 2.60 (d, $J = 19.8$ Hz, 1 H), 2.89 (d, $J = 19.8$ Hz, 1H), 3.85 (m, 6 H), 4.11 (d, $J = 8.7$ Hz, 1 H), 4.35 (m, 4 H), 4.90 (d, $J = 8.1$ Hz, 1 H), 5.31 (d, $J = 1.8$ Hz, 1 H), 5.62 (d, $J = 6.6$ Hz, 1 H), 7.13 (dd, $J = 8.4$ Hz, 2.7 Hz, 1 H), 7.38 (t, $J = 5.4$ Hz, 1 H), 7.58 (s, 3 H), 7.64 (d, $J = 7.5$ Hz, 1 H). HRMS calcd. for $C_{44}H_{56}O_{13}SiH^+$: 821.3568, found 821.3561 (Δ= -0.9 ppm). All data are consistent with the reported values.[36]

2-Debenzoyl-2-(3-methoxybenzoyl)-7-triethylsilyl-10-deacetyl-10-(2-methoxy-benzoyl)-13-oxo-baccatin III (1-41):[83]

To a solution of 2-debenzoyl-2-(3-methoxybenzoyl)-7-triethylsilyl-10-deacetyl-13-oxo-baccatin III (**1-40**) (24 mg, 0.035 mmol), DMAP (13 mg, 0.105 mmol), and triethylamine (10.6 mg, 0.105 mmol) in CH_2Cl_2 (0.44 mL) was added *o*-anisoyl chloride (17.8 mg, 0.105 mmol). The mixture was allowed to stir for overnight, quenched with saturated aqueous $NaHCO_3$, and the reaction mixture was extracted with EtOAc. The combined organic layers were washed with water and brine, dried over $MgSO_4$, filtered, and concentrated. The resulting solid was purified by column chromatography on silica gel (hexanes:EtOAc = 8:1) to give 16 mg (70% in 2 steps) of 2-debenzoyl-2-(3-

methoxybenzoyl)-7-triethylsilyl-10-deacetyl-10-(2-methoxybenzoyl)-13-oxo-baccatin III (**1-41**) as a white solid: ^{1}H (300 MHz, CDCl$_3$) δ 0.58 (m, 6 H), 0.91 (q, J = 7.8 Hz, 9 H), 1.10 (s, 3 H), 1.12 (s, 3 H), 1.37 (s, 3 H), 1.92 (m, 1 H), 1.97 (bs, 1 H), 2.19 (s, 3 H), 2.30 (s, 3 H), 2.55 (m, 1 H), 2.64 (d, J = 19.8 Hz, 1 H), 2.93 (s, J = 19.8 Hz, 1 H), 3.54 (m, 3 H), 3.85 (m, 8 H), 3.97 (d, J = 6.6 Hz, 1 H), 4.13 (d, J = 8.1 Hz, 1 H), 4.35 (d, J = 8.7 Hz, 1 H), 4.54 (dd, J = 6.6 Hz, 3.9 Hz, 1 H), 4.93 (d, J = 8.1 Hz, 1 H), 5.73 (d, J = 6.6 Hz, 1 H), 6.82 (s, 1 H), 6.66-7.07 (m, 3 H), 7.14-7.19 (m, 2 H), 7.28-7.42 (m, 1 H), 7.48-7.68 (m, 1 H), 8.01 (m, 1 H). All data are consistent with the reported values.[83]

2-Debenzoyl-2-(3-methoxybenzoyl)-7-triethylsilyl-10-deacetyl-10-(2-methoxy-benzoyl)-baccatin III (1-42):[83]

To a solution of 2-debenzoyl-2-(3-methoxybenzoyl)-7- triethylsilyl-10-deacetyl-10-(2-methoxybenzoyl)-13-oxo baccatin III (**1-41**) (32 mg, 0.039 mmol) in MeOH (1.5 mL) and THF (1 mL) at 0 °C was added NaBH$_4$ (25 mg, 0.156 mmol) and the solution was allowed to stir for 9 h. Then the reaction was quenched with saturated NH$_4$Cl (20 mL), and extracted with CH$_2$Cl$_2$ (30 mL x 3). The organic layer was then dried over MgSO$_4$, filtered, and concentrated *in vacuo*. The resulting solid was purified by column chromatography on silica gel (hexanes:EtOAc = 3:1) to give **1-42** (15 mg, 42% based on 50% conversion) of as a white solid: ^{1}H (300 MHz, CDCl$_3$) δ 0.58 (m, 6 H), 0.91 (q, J = 7.8 Hz, 9 H), 1.10 (s, 3 H), 1.12 (s, 3 H), 1.37 (s, 3 H), 1.92 (m, 2 H), 1.97 (bs, 1 H), 2.19 (s, 3 H), 2.30 (s, 3 H), 2.55 (m, 1 H), 3.54 (m, 1 H), 3.85 (m, 7 H), 3.94 (d, J = 6.9 Hz, 1 H), 4.15 (d, J = 7.8 Hz, 1 H), 4.34 (d, J = 7.8 Hz, 1 H), 4.53 (dd, J = 6.6 Hz, 3.6 Hz, 1 H), 4.84 (m, 1H), 4.97 (d, J = 7.8 Hz, 1 H), 5.66 (d, J = 6.9 Hz, 1 H), 6.69 (s, 1 H), 6.95-7.07 (m, 2 H), 7.14-7.19 (m, 1 H), 7.28-7.42 (m, 2 H), 7.65-7.73 (m, 2 H), 8.01 (m, 1 H). HRMS calcd. for C$_{44}$H$_{58}$O$_{13}$SiH$^+$: 823.3725, found 823.3723 (Δ= -0.2 ppm). All data are consistent with the reported values.[83]

3'-Dephenyl-3'-(2-methyl-1-propenyl)-2-debenzoyl-2-(3-methoxybenzoyl)-10-(2-methoxybenzoyl)acetyldocetaxel (1-44, 121303012):[83]

To a solution of baccatin **1-42** (12 mg, 0.014mmol) and 1.5 equiv of 4-isobutenyl-1-(*tert*-butoxycarbonyl)-3-(triisopropylsilyoxy)azetidin-2-one (**1-11**) in dry THF (3 ml) was added dropwise LiHMDS (0.021 mL, 1.0 M in THF) at -40 °C. The reaction mixture was stirred for 5 h. Then, the reaction was quenched with saturated NH$_4$Cl (20 mL). The mixture was extracted with EtOAc (30 mL x 3) and the organic layers were washed with saturated NH$_4$Cl and brine, dried over MgSO$_4$, and concentrated *in vacuo*. Purification of the crude product by silica gel chromatography on silica gel (hexanes/EtOAc = 5/1) afforded taxoid **1-43** with protecting groups as a white solid (12 mg, 70%).

To a solution of **1-43** (12 mg, 0.001 mmol) in a 1:1 mixture of pyridine and acetonitrile (0.5 mL) was added HF/pyridine (70:30) (0.15 mL) at 0 °C. After the reaction mixture was warmed to room temperature overnight, the reaction was diluted with EtOAc (30 mL). The organic layer was washed with aqueous NaHCO$_3$ solution (10 mL x 2), CuSO$_4$ solution (10 mL x 2) and brine (10 mL x 2), dried over MgSO$_4$, and concentrated *in vacuo*. Purification of the crude product by silica gel chromatography on silica gel (hexanes/EtOAc = 1/1) afforded taxoid **SB-T-121303012** as a white solid (7 mg, 74%): mp 143-145 °C; ^{1}H NMR (300 MHz, CDCl$_{13}$) δ 1.28 (s, 3 H), 1.31 (s, 3 H), 1.34 (s, 9 H), 1.60 (m, 1 H), 1.71 (s, 3 H), 1.75 (s, 3 H), 1.77 (s, 3 H), 1.91 (m, 1 H), 1.96 (s, 3 H), 2.37

(s, 3 H), 2.59 (m, 2 H), 3.35 (bs, 1 H), 3.88 (s, 3 H), 3.91 (s, 3 H), 4.22 (m, 2 H), 4.35 (d, J = 8.4 Hz, 1 H), 4.51 (m, 1 H), 4.76 (m, 2 H), 4.98 (d, J = 8.1 Hz,1 H), 5.32 (m, 1 H), 5.71 (d, J = 6.9 Hz, 1 H), 6.21 (m, 1 H), 6.57 (s, 1 H), 6.99 (m, 2 H), 7.13 (dd, J = 8.4 Hz, 1.8 Hz, 1 H), 7.36 (t, J = 7.5 Hz, 1 H), 7.50 (m, 1 H), 7.65 (s, 1 H), 7.70 (d, J = 7.5 Hz, 1 H), 7.99 (dd, J = 7.8 Hz, 2.1 Hz, 1 H); ^{13}C NMR (63 MHz, CDCl$_3$) δ 9.56, 15.0, 18.5, 22.4, 25.7, 26.6, 28.2, 35.6, 43.3, 45.7, 55.4, 55.9, 58.7, 72.2, 72.4, 73.7, 75.2, 75.6, 79.2, 81.2, 84.5, 87.6, 105.0, 105.1, 112.1, 120.2, 120.3, 122.6, 129.7, 130.5, 132.7, 134.6, 159.7, 160.0, 165.9, 166.9, 170.1, 203.8. HRMS calcd. for C$_{50}$H$_{63}$NO$_{17}$SiH$^+$: 950.4174, found 950.4149 (Δ= -2.7 ppm). All data are consistent with the reported values.[83]

1-(4-Methoxylphenyl)-3-triisopropylsiloxy-4-formylazetidin-2-one (1-45):[69]

Nitrogen gas was bubbled into a solution of β-lactam **1-9** (237 mg, 0.59 mmol) in MeOH/CH$_2$Cl$_2$ (1/2, 27 mL) at -78 ˚C for 3 min. Then, O$_3$ gas was bubbled into the solution till the color of the solution turned blue (5 min), and N$_2$ was bubbled into the solution for another 3 min until the blue color disappeared. Dimethyl sulfide (0.184 mL, 2.5 mmol) was added to the solution and the reaction mixture was allowed to warm to room temperature. The reaction mixture was stirred at room temperature for 3 h. The solvents were removed *in vacuo* and the residue was purified on a neutral alumina column using hexanes/EtOAc (4/1 followed by 2/1) as the eluant to afford **1-45** as a white solid (199 mg, 91%): mp 78-80 ˚C; [α]$_D^{20}$ +158.0 (*c* 0.50, CHCl$_3$); ^{1}H NMR (250 MHz, CDCl$_3$) δ 1.06 (m, 21 H), 3.74 (s, 3 H), 4.43 (dd, J = 5.1, 3.8 Hz, 1 H), 5.25 (d, J = 5.4 Hz, 1 H), 6.81 (d, J = 8.8 Hz, 1 H), 7.22 (d, J = 8.8 Hz, 1 H), 9.72 (d, J = 3.8 Hz, 1 H); ^{13}C NMR (62.9 MHz, CDCl$_3$) δ 11.6, 17.4, 55.3, 64.2, 78.6, 114.4, 117.8, 130.7, 156.7, 164.2, 199.6. Anal. Calcd for C$_{20}$H$_{31}$NO$_4$Si: C, 63.63; H, 8.28; N, 3.71. Found: C, 63.80; H, 8.05; N, 3.72. All data were in agreement with literature values.[69]

1-(4-Methoxyphenyl)-3-triisopropylsiloxy-4-(2,2-difluorovinyl)azetidin-2-one (1-46):[73]

Dibromodifluoromethane (0.28 mL, 1.8 mmol) was added by pre-cooled syringe to the solution of hexamethylphosphorous triamide (HMPT) (0.68 mL, 3.6 mmol) in THF (4.7 mL) at 0 °C and the suspension was transferred to the mixture of β-lactam **1-45** (172 mg, 0.45 mmol) and zinc dust (294 mg, 4.5 mmol) in THF (4.7 mL) at room temperature. The mixture was heated to reflux for 30 min, and the reaction was quenched by water (20 mL). The water layer was extracted by dichloromethane (30 mL x 3). The organic layer was washed by brine (20 mL) and dried over MgSO$_4$. The filtrate was concentrated under reduced pressure to give yellow oil. Crude material was purified by flash chromatography on silica gel (hexanes/EtOAc = 20/1) to yield **1-46** (148 mg, 80%): ^{1}H NMR (CDCl$_3$, 300 MHz) δ 1.08-1.15 (m, 21 H), 3.79 (s, 3 H), 4.54 (ddd, J = 16.5, 6.3, 1.5 Hz, 1 H), 4.83 (m, 1 H), 5.14 (d, J = 5.1 Hz, 1 H), 6.87 (d, J = 9.0 Hz, 2 H), 7.32 (d, J = 9.0 Hz, 2 H); ^{13}C NMR (CDCl$_3$, 75.5 MHz) δ 12.1, 17.9, 54.1 (d, J = 8.5 Hz), 55.8, 75.8 (dd, J = 22.1, 5.0 Hz), 76.9, 77.4, 114.8, 118.6, 130.9, 156.7, 164.9; ^{19}F NMR (282 MHz, CDCl$_3$) δ -80.80 (d, J = 32.7 Hz, 1 F), -86.34 (dd, J = 28.2, 2.8 Hz, 1 F). HRMS (FAB$^+$, m/z): Calcd. for C$_{21}$H$_{31}$F$_2$NO$_3$Si·H$^+$, 412.2114; Found, 412.2127. All data were in agreement with literature values.[74]

3-Triisopropylsiloxy-4-(2,2-difluorovinyl)azetidin-2-one (1-47):[36]

To a solution of *N*-PMP-*β*-lactam **1-46** (1.322 g, 3.2 mmol) in acetonitrile (96 mL) and H_2O (20 mL), was added dropwise a solution of ceric ammonium nitrate (7.2 g, 12.8 mmol) in water (80 mL). The reaction mixture was stirred for 2 h, and worked up with saturated Na_2SO_3 solution (40 mL). After filtration, the aqueous layer was extracted with EtOAc (50 mL x 3), and the combined organic layer was washed with H_2O (10 mL x 3), dried over $MgSO_4$ and concentrated. The product mixture was purified on a silica gel column (hexanes/EtOAc = 10/1) to yield **1-47** as a colorless oil (867 mg, 89%): ^{1}H NMR (CDCl$_3$, 400 MHz) δ 1.03-1.18 (m, 21 H), 4.44-4.54 (m, 2 H), 5.04 (dd, *J* = 2.4, 1.6 Hz, 1 H), 6.59 (bs, 1 H); ^{13}C NMR (CDCl$_3$, 100 MHz): 12.1, 17.8 (d, *J* = 4.6 Hz), 50.4 (d, *J* = 7.6 Hz), 77.1 (dd, *J* = 15.9, 23.5 Hz), 79.3, 157.6 (t, *J* = 289.9 Hz), 169.4; ^{19}F NMR (282 MHz, CDCl$_3$) δ -82.33 (d, *J* = 34.7 Hz, 1 F), -87.50 (dd, *J* = 25.7, 9.3 Hz, 1 F). HRMS (FAB$^+$, m/z): Calcd. for $C_{14}H_{25}F_2NO_2Si\cdot H^+$, 306.1701; Found, 306.1706 (Δ= 1.7 ppm). All data were in agreement with literature values.[74]

1-(*tert*-Butoxycarbonyl)-3-triisopropylsiloxy-4-(2,2-difluorovinyl)azetidin-2-one (1-48): [36]

To a solution of *N*-H-4-(2,2-difluorovinyl)-*β*-lactam (865 mg, 2.8 mmol), triethylamine (1.4 mL, 8.5 mmol), and DMAP (68 mg, 0.56 mmol) in CH_2Cl_2 (16.5 mL), was added Boc$_2$O (700 mg, 3.1 mmol) at room temperature. The reaction mixture was stirred overnight and quenched with saturated NH_4Cl solution (20 mL). The organic layer was extracted with dichloromethane (40 mL x 3). The organic layer was washed with brine, dried over $MgSO_4$, and concentrated under reduced pressure. Crude material was purified by flash chromatography to afford **1-48** as a colorless oil (1.15 g, 100%): $[\alpha]_D^{20}$ +24.17 (c 14.4, CHCl$_3$); ^{1}H NMR (CDCl$_3$, 300 MHz) δ 1.04-1.17 (m, 21 H), 1.49 (s, 9 H), 4.49 (ddd, *J* = 23.7, 13.8, 1.6 Hz, 1 H,), 4.75 (dddd, *J* = 9.0, 5.1, 2.4, 0.9 Hz, 1 H), 5.04 (d, *J* = 5.7 Hz, 1 H), 6.59 (bs, 1 H); ^{13}C NMR (CDCl$_3$, 100.5 MHz) δ 12.0, 17.8 (d, *J* = 5.3 Hz), 28.2, 53.6 (d, *J* = 8.4 Hz), 74.5 (dd, *J* = 26.5, 10.6 Hz), 77.2, 83.9, 147.9, 158.5 (t, *J* = 292.2 Hz), 165.3; ^{19}F NMR (282 MHz, CDCl$_3$) δ -81.20 (d, *J* = 31.0 Hz, 1 F), -85.83 (dd, *J* = 29.3, 5.6 Hz, 1 F). HRMS (FAB$^+$, m/z): Calcd. for $C_{19}H_{33}F_2NO_4Si\cdot Na^+$, 428.2039; Found, 428.2050. All data were in agreement with literature values.[74]

3'-Dephenyl-3'-(2,2-difluorovinyl)-10-propanoyldocetaxel (SB-T-12853):[74]

10-Deacetyl-10-propanoyl-7-TES-baccatin **1** (1.14 g, 1.59 mmol) and difluorovinyl-*β*-lactam **1-21** (916 mg, 2.25 mmol) were dissolved in THF (160 mL). The mixture was cooled to -40 ºC, and 1 M LiHMDS (2.4 mL, 2.4 mmol) was added. The reaction mixture was stirred for 2 h and quenched with 60 mL of NH_4Cl. The aqueous layer was extracted with dichloromethane (100 mL x 3), and the combined organic phases were dried with brine and $MgSO_4$. The crude product was purified on silica gel column using hexane/ethyl acetate (8/1-6/1) to yield the desired coupling product 7-TES-2'-TIPS-fluorinated taxoid (**1-49**) (1.69 g) in 95% yield.

To a solution of **1-49** (1.68 g, 1.5 mmol) in a 1:1 mixture of pyridine and CH_3CN (70 mL) cooled to 0 °C was added HF-pyridine (16 mL). The reaction mixture was allowed to warm to room temperature and stirred overnight. The reaction was then quenched with with ethyl acetate and the organic layer was washed with NaHCO$_3$ (30 mL x 4), CuSO$_4$ (30 mL x 4) and brine, dried with $MgSO_4$ and concentrate. The residue was purified by

chromatography on silica gel using hexane/ethyl acetate (1/1) as eluant to afford **1-50** (**SB-T-12853**) (1.251 g, 98%) as a white solid: mp 175-181 °C; $[\alpha]_D^{20}$-82.83 (c 5.01, CHCl$_3$); ^{1}H NMR (CDCl$_3$, 400 MHz) δ 1.14 (s, 3 H), 1.24 (m, 6 H), 1.30 (s, 9 H), 1.67 (s, 3 H), 1.78 (m, 1 H), 1.87 (m, 4 H), 2.31 (m, 2 H), 2.38 (s, 3 H), 2.53 (m, 4 H), 3.55 (bs, 1 H), 3.81 (d, J= 6.8 Hz, 1 H), 4.17 (d, J= 8.4 Hz, 1 H), 4.29 (m, 2 H), 4.39 (m, 1 H), 4.56 (ddd, J= 24.8, 9.6, 1.6 Hz, 1 H), 4.86 (t, J= 8.8 Hz, 1 H), 4.96 (m, 2 H), 5.66 (d, J= 7.2 Hz, 1 H), 6.25 (t, J= 8.4 Hz, 1 H), 6.30 (s, 1 H), 7.49 (t, J= 7.6 Hz, 2 H), 7.60 (t, J= 7.2 Hz, 1 H), 8.11 (d, J= 7.2 Hz, 2 H); ^{13}C NMR (CDCl3, 75.5 MHz) δ 9.2, 9.8, 15.1, 22.1, 22.5, 26.9, 27.8, 28.4, 35.7 (d, J= 12.9 Hz), 43.5, 45.9, 48.2, 58.8, 72.2, 72.4, 72.9, 73.3, 75.3, 75.6, 76.6, 77.4, 79.3, 80.7, 81.3, 84.6, 128.9, 129.3, 130.4, 133.5, 133.9, 142.2, 155.1, 156.7, 167.3, 170.5, 172.6, 174.8, 203.9; ^{19}F NMR, (CDCl$_3$, 282 MHz) δ − 84.31 (dd, J= 34.7, 23.7 Hz, 1 F), −86.23 (dd, J= 36.4 Hz, 1 F); HRMS (FAB$^+$, m/z): Calcd. for $C_{42}H_{53}F_2NO_{15}$·H$^+$, 850.3456; Found 850.3450. All data were in agreement with literature values.[74]

ring-^{13}C$_6$-Benzoyl chloride (1-52):[76]

To a solution of *ring*-^{13}C$_6$-benzoic acid (50 mg, 0.39 mmol) in CH$_2$Cl$_2$ (1.7 mL) was added oxalyl chloride (0.07 mL, 0.78 mmol) and 2 drops of DMF. The reaction mixture was stirred for 3 h and the solvent was removed under vacuum to afford **1-52** as a white solid. This crude product was used directly for next step without further purification.

(*3R,4S*)-1-(*ring*-^{13}C$_6$-Benzoyl)-3-ethoxyethoxy-4-phenylazetidin-2-one (1-53):[76]

To a solution of *β*-lactam **1-17** (84 mg, 0.356 mmol), triethylamine (0.14 mL, 0.980 mmol) and DMAP (8 mg, 0.073 mmol) in CH$_2$Cl$_2$ (1 mL), was addeda solution of *ring*-^{13}C$_6$-benzoyl chloride, prepared as described above, in CH$_2$Cl$_2$ (2 mL) dropwise at 0 °C. The mixture was stirred overnight at room temperature and the reaction was quenched with saturated aqueous NH$_4$Cl solution (10 mL). The mixture was then extracted with CH$_2$Cl$_2$ (20 mL x 3). The combined extracts were dried over anhydrous MgSO$_4$ and concentrated *in vacuo*. The crude product was purified on a silica gel column using hexanes/EtOAc (8/1) as the eluant to afford **1-53** as a colorless oil (70 mg, 62% yield): ^{1}H NMR (400 MHz, CDCl$_3$) δ 0.92 (d, J = 5.2 Hz, 2 H), 1.03 (m, 4 H), 3.15-3.32 (m, 1.5 H), 3.58 (m, 0.5 H), 4.45 (q, J = 5.6 Hz, 0.5 H), 4.64 (q, J = 5.6 Hz, 0.5 H), 5.16 (dd, J = 6.4, 1.6 Hz, 1 H), 5.33 (dd, J = 12.4, 6.0 Hz, 1 H), 7.14-7.28 (m, 6.5 H), 7.56(mb, 1 H), 7.69 (mb, 1.5 H), 8.10 (mb, 1 H). ^{13}C NMR (100.5 MHz, CDCl$_3$) δ [14.9, 15.1, 15.2], [19.9, 20.1], 28.8 (m), [59.9, 60.7], [60.9, 62.4], [74.7, 75.9], [99.3, 99.6], [127.4-127.6], [127.9-128.2], [128.3-128.7], [129.2-129.3], [129.7-129.9], [130.3-130.4], [131.3-131.4], [131.8-132.0], [132.8-133.0], [133.3-133.6], [133.9-134.0], 164.6, 165.0.

3'*N*-debenzoyl-3'*N*-(*ring*-^{13}C$_6$-benzoyl)-paclitaxel (1-56):[16]

To a solution of **1-54** (33 mg, 0.058 mmol) and *β*-lactam **1-53** (60 mg, 0.174 mmol) in THF (4.5 mL) was added LiHMDS (0.09 ml, 0.09 mmol) at -40 °C. The reaction mixture was warmed up to 0 °C over 3 h and then quenched with saturated aqueous NH$_4$Cl solution and extracted with EtOAc. The organic layers were combined and solvent was removed under reduced pressure. The residue was purified by chromatography on silica gel (eluent: hexanes/EtOAc, 8/1-3/1) to afford **1-55** as a white solid. (50 mg, 71%); HRMS calcd. for ^{12}C$_{51}$^{13}C$_6$H$_{73}$NO$_{15}$SiH$^+$: 1046.5029, found 1046.5020 (Δ= -0.9 ppm).

To a solution of the protected paclitaxel **(1-55)** thus obtained in ethanol (1.2 mL) was added 0.2 *N* HCl in ethanol (1.4 mL) and the reaction mixture was stirred overnight. The reaction mixture was quenched with 20 mL saturated aqueous $NaHCO_3$ and extracted with dichloromethane (30 mL x 3) and washed with brine (10 mL). The organic layer was dried over anhydrous $MgSO_4$ and solvent was removed under reduced pressure. The residue was purified by a chromatography on silica gel (hexanes:EtOAc =2/1) to afford **1-56** as white solid (32 mg, 77%): mp 186-188 ^{o}C; ^{1}H NMR (400 MHz, $CDCl_3$) δ 1.15 (s, 3 H), 1.24 (s, 3 H), 1.69 (s, 3 H), 1.79 (s, 3 H), 1.88 (m, 1 H), 2.24. (s, 3 H), 2.29 (dd, $J =$ 15.4, 8.9 Hz, 1 H), 2.35 (dd, $J =$ 15.4, 8.9 Hz, 1 H), 2.39 (s, 3 H), 2.43 (bs, 1 H), 2.55 (ddd, $J =$ 15.5, 9.6, 6.0 Hz, 1 H), 3.55 (bs, 1 H), 3.80 (d, $J =$ 7.0 Hz, 1 H), 4.19 (d, $J =$ 8.4 Hz, 1H), 4.31 (d, $J =$ 8.4 Hz, 1 H), 4.40 (dd, $J =$ 10.8, 6.4 Hz, 1 H), 4.79 (d, $J =$ 2.8 Hz), 4.94 (dd, $J =$ 9.2, 2.0 Hz, 1 H), 5.67 (d, $J =$ 7.2 Hz, 1 H), 5.79 (dd, $J =$ 8.8, 2.4 Hz, 1 H), 6.23 (td, $J =$ 9.2, 1.2 Hz, 1 H), 6.27 (s, 1 H), 6.98 (d, $J =$ 8.4 Hz, 1 H), 7.19 (mb, 1 H), 7.27-7.70 (m, 11 H), 7.93 (mb, 1 H), 8.14 (dd, $J =$ 6.4, 1.6 Hz, 2 H); ^{13}C NMR (100.5 MHz, $CDCl_3$, diluted) δ [126.3-126.5], [126.9-127.0], [127.4-127.6], [128.1-128.2], [128.6-128.7], [129.2-129.3], [131.4, 131.5], [131.9-132.0], [132.5, 132.6], [133.0, 133.1], [133.6, 133.7], [134.1, 134.2]. HRMS calcd. for $^{12}C_{41}$$^{13}C_6H_{51}NO_{14}SiH^+$: 860.3589, found 860.3611 (Δ= 2.5 ppm).

7,10,13-Tris(triethylsilyl)-2-debenzoyl-2-(4-methylbenzoyl)-10-deacetyl-baccatin III (1-57a):[82]

To a solution of **1-29** (50 mg, 0.064 mmol), 4-methylbenzoic acid (70 mg, 0.51 mmol) and DMAP (89 mg, 0.58 mmol) in toluene (0.4 mL) was added DIC (0.09 mL, 0.58 mmol) and the reaction mixture was refluxed overnight. The reaction mixture was diluted with ethyl acetate (20 mL) and washed with saturated aqueous $NaHCO_3$ solution (20 mL), H_2O (20 mL) and brine (10 mL). The organic lawyer was dried with anhydrous $MgSO_4$. The solvent was removed under reduced pressure and the residue was purified on a silica gel column (hexanes/EtOAc = 15/1) to afford **1-57a** as a white solid (43 mg, 75% yield): ^{1}H NMR (400 MHz, $CDCl_3$) δ 0.63 (m, 18 H), 0.97 (m, 27 H), 1.13 (s, 3 H), 1.19 (s, 3 H), 1.25 (m, 1 H), 1.65 (s, 3 H), 1.85 (m, 1 H), 1.96 (s, 3 H), 2.14 (m, 2 H), 2.27 (s, 3 H), 2.42 (m, 4 H), 3.83 (d, 1 H), 4.13 (d, $J =$ 7.9 Hz, 1 H), 4.30 (d, $J =$ 8.1 Hz, 1 H), 4.39 (dd, $J =$ 10.4, 6.9 Hz, 1 H), 4.92 (m, 2 H), 5.10 (s, 1 H), 5.60 (d, $J =$ 6.9 Hz, 1 H), 7.26 (d, 2 H), 7.98 (d, $J =$ 7.7 Hz, 2 H); ^{13}C NMR (400 MHz, $CDCl_3$) δ 5.1, 5.4, 6.2, 6.6, 7.0, 10.7, 14.8, 20.9, 21.9, 22.6, 26.6, 29.9, 37.5, 40.1, 43.2, 47.2, 58.5, 68.6, 72.9, 75.5, 76.0, 79.8, 84.2, 127.1, 128.9, 129.5, 130.3, 136.0, 139.6, 144.5, 167.5, 170.2, 205.9. HRMS calcd. for $C_{48}H_{80}O_{10}Si_3Na^+$: 923.4957, found 923.4933 (Δ= -2.6 ppm).

2-Debenzoyl-2-(4-methylbenzoyl)-10-deacetylbaccatin III (1-58a):[82]

To a solution of **1-57a** (43 mg) in 1.8 mL of pyridine/acetonitrile (1:1) was added dropwise HF/pyridine (70:30, 0.4 mL) at 0 ^{o}C, and the mixture was stirred overnight at room temperature. The reaction was quenched with saturated aqueous $NaHCO_3$ solution (20 mL). The mixture was then diluted with ethyl acetate (50 mL), washed with saturated aqueous $CuSO_4$ solution (20mL x 2) and H_2O (20mL), dried over anhydrous $MgSO_4$ and concentrated *in vacuo* to afford 2-debenzoyl-2-(4-methylbenzoyl)-10-deacetylbaccatin III (**1-58a**) as a white solid (44mg, crude). The crude compound was used in the next step without further purification.

2-Debenzoyl-2-(4-methylbenzoyl)-10-deacetyl-10-propanoylbaccatin III (1-59a):[51]
To the solution of **1-58a** (44 mg, crude) in THF (2.4 mL) was added cerium chloride heptahydrate (4 mg, 0.005 mmol) and propanoic anhydride (0.075 mL, 0.47 mmol). The reaction mixture was stirred at room temperature for 1.5 h. To the solution was added 40 mL of H_2O. This mixture was extracted with CH_2Cl_2 (30 mL x 3). The organic layers were washed with brine, dried over $MgSO_4$, and concentrated *in vacuo*. The residue was purified on a silica gel column using hexane/ethyl acetate (1/1) as the eluant to afford **1-59a** as a white solid (19 mg, 76% for 2 steps): ^{1}H NMR (500 MHz, CDCl$_3$) δ 1.10 (s, 6 H), 1.25(m, 7 H), 1.66 (s, 3 H), 1.85 (m, 1 H), 2.05 (d, J = 3Hz 3 H), 2.09 (s, 1H), 2.28 (m, 5 H), 2.43 (s, 3 H), 2.54(m, 4 H), 3.88 (d, J = 6.5, 1 H), 4.14 (m, 1 H), 4.30 (d, J = 8 Hz, 1 H), 4.47 (m, 1 H), 4.88 (t, 1 H), 4.99 (d, J = 6 Hz, 1 H), 5.61 (d, J = 7Hz, 1 H), 6.33(s, 1H), 7.24 (d, J = 8Hz, 2 H), 7.98 (d, J = 3.5Hz, 2 H). HRMS calcd. for $C_{33}H_{42}O_{11}H^+$: 615.2805, found 615.2792 (Δ= -2.1 ppm).

7-Triethylsilyl-2-debenzoyl-2-(4-methylbenzoyl)-10-deacetyl-10-propanoylbaccatin III (1-60a):[36]
To a solution of **1-59a** (19 mg, 0.0309 mmol) and imidazole (9 mg, 0.13 mmol) in DMF (0.3 mL) was added chlorotriethylsilane (0.017 mL, 0.093 mmol) dropwise *via* syringe at 0 ^{o}C. The reaction mixture was stirred for 45 min at room temperature and quenched with saturated NH_4Cl solution (10 mL). The mixture was extracted by ethyl acetate (30 mL x 3), and then washed with H_2O (20 mL x 2), brine (20 mL), dried over anhydrous $MgSO_4$ and concentrated. The crude product was purified on a silica gel column using hexanes/ethyl acetate (2/1) as eluant to afford **1-60a** as a white solid (15 mg, 66% yield): ^{1}H NMR (500 MHz, CDCl$_3$) δ 0.57 (m, 6 H), 0.95 (m, 9 H), 1.02 (s, 3 H), 1.22 (m, 9 H), 1.69 (s, 3 H), 1.87 (m, 1 H), 2.19 (m, 3 H), 2.25 (m, 3 H), 2.46 (ms, 6 H), 3.87 (d, J = 8.5 Hz, 1 H), 4.13 (d, J = 10 Hz, 1 H), 4.29 (d, J = 10 Hz, 1 H), 4.48 (m, 2 H), 4.82 (t, J = 7.9 Hz, 1 H), 4.95 (d, J = 10 Hz, 1 H), 5.62 (d, J = 9.5 Hz, 1 H), 6.46 (s, 1 H), 7.26 (d, J = 9.5 Hz, 1 H), 7.98 (d, J = 10 Hz, 1 H). HRMS calcd. for $C_{39}H_{56}O_{11}SiH^+$: 729.3670, found 729.3691 (Δ= 2.9 ppm).

7-Triethylsilyl-2'-triisopropylsilyl-2-debenzoyl-2-(4-methylbenzoyl)-3'-dephenyl-3'-(2-methylprop-1-enyl)-10-propanoyldocetaxel (1-61a):[36]
To a solution of baccatin **1-60a** (29 mg, 0.04 mmol) and *β*-lactam **1-11** (24 mg, 0.06 mmol) in dry THF (3.7 mL) was added 1.0 M LiHMDS in THF (0.06 mL, 0.06 mmol) dropwise at -40 ^{o}C, and the solution was stirred at -40 ^{o}C for 1 h. The reaction was quenched with saturated aqueous NH_4Cl solution (10 mL), and the aqueous layer was extracted with ethyl acetate (20 mL x 3). The combined extracts were then dried over anhydrous $MgSO_4$ and concentrated *in vacuo*. The residue was purified on a silica gel column using hexanes/ethyl acetate = 4/1 as the eluant to afford the coupling product **1-61a** as a white solid (37mg, 82%): ^{1}HNMR (400 MHz, CDCl$_3$) δ 0.56 (m, 6 H), 0.97 (m, 9 H), 1.09 (m, 21 H), 1.17 (s, 3 H), 1.20 (s, 3 H), 1.30 (m, 3 H), 1.33 (s, 9 H), 1.44 (m, 3 H), 1.61(s, 3 H), 1.75(s, 3 H), 2.00 (s, 3 H), 2.34 (s, 3 H), 2.46 (m, 6 H), 3.82 (d, J = 6.8 Hz, 1 H) (H$_3$), 4.17 (d, J = 8.4 Hz, 1 H), 4.29 (d, J = 8.4 Hz, 1 H), 4.45 (m, 2 H), 4.75 (t, J = 8.4 Hz, 2 H), 4.94 (d, J = 10 Hz, 1 H), 5.32 (d, J = 8.4 Hz, 1 H), 5.66 (d, J = 7.2 Hz, 1 H) (H$_2$), 6.07 (t, J = 8.4 Hz, 1 H), 6.48 (s, 1 H), 7.24 (d, J = 7.8 Hz, 2 H), 7.98 (t, J = 8.0

Hz, 2 H). HRMS calcd. for $C_{60}H_{95}O_{15}NSi_2H^+$: 1126.6319, found 1126.6267 (Δ= -4.6 ppm).

3'-Dephenyl-3'-(2-methylprop-1-enyl)-2-debenzoyl-2-(4-methylbenzoyl)-10-propanoyldocetaxel (1-62a):[36]

To a solution of **1-61a** (36 mg, 0.032 mmol) in 1.5 mL of pyridine /acetonitrile (1:1) was added dropwise HF/pyridine (70:30), (0.4 mL) at 0 ^{o}C, and the mixture was stirred overnight at room temperature. The reaction was quenched with saturated aqueous NaHCO$_3$ solution (30 mL). The mixture was then diluted with ethyl acetate (60 mL), washed with saturated aqueous CuSO$_4$ solution (20 mL x 2) and H$_2$O (20 mL), dried over anhydrous MgSO$_4$ and concentrated *in vacuo*. The residue was purified on a silica gel column using hexane/ethyl acetate (1/1) as the eluant to afford **1-62a** as a white solid (23 mg, 84%): ^{1}H NMR (400 MHz, CDCl$_3$) 1.15 (s, 3 H), 1.25 (m, 8 H), 1.36 (s, 9 H), 1.67 (s, 3 H), 1.75 (m, 3 H), 1.90 (m, 4 H), 2.08(s, 6 H), 2.35 (m, 7 H), 2.55 (m, 4 H), 3.81 (d, *J* = 7.2 Hz, 1 H), 4.20 (m, 2 H), 4.30 (d, *J* = 8.8 Hz, 1 H), 4.36 (m, 1 H), 4.75 (m, 2 H), 4.97 (d, *J* = 8.8 Hz, 1 H), 5.32 (d, *J* = 8.0 Hz, 1 H), 5.65 (d, *J* = 8.0 Hz, 1 H), 6.17 (t, *J* = 8.8 Hz, 1 H), 6.31 (s, 1 H), 7.27 (d, *J* = 7.6 Hz, 2 H), 7.99 (d, *J* = 8.0 Hz, 2 H); ^{13}C NMR (400 MHz, CDCl$_3$) δ 9.2, 9.8, 15.2, 18.8, 20.7, 22.0, 22.1, 22.6, 25.9, 26.9, 27.8, 28.4, 29.9, 35.8, 43.4, 45.9, 58.8, 72.5, 72.7, 74.0, 75.0, 75.7, 76.8, 79.4, 81.3, 84.7, 120.9, 126.7, 129.6, 130.4, 142.6, 144.8, 155.7 167.3, 170.3, 174.9, 176.1, 204.1. HRMS calcd. for $C_{45}H_{61}O_{15}NH^+$: 856.4119, found 856.4107 (Δ= -1.5 ppm).

7,10,13-Tris(triethylsilyl)-2-debenzoyl-2-(3,4-dimethylbenzoyl)-10-deacetyl-baccatin III (1-57b):[82]

To a solution of **1-29** (100 mg, 0.128 mmol), 3,4-dimethylbenzoic acid (153 mg, 1.02 mmol) and DMAP (78 mg, 1.27 mmol) in DMF (0.5 mL) and toluene (0.3 mL) was added DIC (0.198 mL, 1.27 mmol) and the reaction mixture was refluxed 34 h. The reaction mixture was diluted with ethyl acetate (30 mL) and washed with saturated aqueous NaHCO$_3$ solution (20 mL), H$_2$O (20 mL) and brine (10 mL). The organic lawyer was dried over anhydrous MgSO$_4$. The solvent was removed under reduced pressure and the residue was purified on a silica gel column to afford **1-57b** as a white solid (~50 mg, with impurity), the crude compound was used in the next step without further purification.

2-Debenzoyl-2-(3,4-dimethylbenzoyl)-10-deacetylbaccatin III (1-58b):[82]

To a solution of **1-57b** (~50 mg) in 2 mL of pyridine/acetonitrile (1:1) was added dropwise HF/pyridine (70:30, 0.5 mL) at 0 ^{o}C, and the mixture was stirred overnight at room temperature. The reaction was quenched with saturated aqueous NaHCO$_3$ solution (20 mL). The mixture was then diluted with ethyl acetate (50 mL), washed with saturated aqueous CuSO$_4$ solution (20 mL x 2) and H$_2$O (20 mL), dried over anhydrous MgSO$_4$ and concentrated *in vacuo* to afford 2-debenzoyl-2-(3,4-dimethylbenzoyl)-10-deacetyl-baccatin III (**1-58b**) as a white solid (34 mg, 47% yield for 2 steps). The crude compound was used in the next step without further purification.

2-Debenzoyl-2-(3,4-dimethylbenzoyl)-10-deacetyl-10-propanoylbaccatin III (1-59b):[51]

To the solution of **1-58b** (34 mg, 0.054 mmol) in THF (2.4 mL) was added cerium chloride heptahydrate (4 mg, 0.005 mmol) and propanoic anhydride (0.1 mL, 0.54 mmol). The reaction mixture was stirred at room temperature for 2 h. The solution was added 30 mL of H_2O. This mixture was extracted with CH_2Cl_2 (30 mL x 3). The organic layers were washed with brine, dried over $MgSO_4$, and concentrated *in vacuo*. The residue was purified on a silica gel column using hexanes/ethyl acetate=1/1 as the eluant to afford **1-59b** as a white solid (18 mg, 51%): ^{1}H NMR (500 MHz, CDCl$_3$) δ 1.13 (s, 6 H), 1.18 (d, 1 H), 1.25(t, 6H), 1.67 (s, 3 H), 1.85 (m, 2 H), 2.06 (d, 3 H), 2.17 (s, 1H), 2.28 (m, 3 H), 2.48 (m, 6H), 3.88 (m, 1 H), 4.15 (m, 2 H), 4.33 (d, *J* = 9 Hz, 1 H), 4.47 (m, 2 H), 4.88 (t, 1 H), 4.99 (d, *J*=9.5 Hz, 1 H), 5.61 (d, *J* = 6.5Hz, 1 H), 6.34(s, 1H), 7.24 (d, *J*=7.5Hz, 1 H), 7.39 (t, *J* = 8 Hz, 1 H), 7.84 (d, *J*=7.5Hz, 1 H), 7.90 (s, 1 H). HRMS calcd. for $C_{34}H_{44}O_{11}H^+$: 629.2962, found 629.2933 (Δ= -4.6 ppm).

7-Triethylsilyl-2-debenzoyl-2-(3,4-dimethylbenzoyl)-10-deacetyl-10-propanoyl-baccatin III (1-60b):[36]

To a solution of **1-59b** (17 mg, 0.027 mmol) and imidazole (8 mg, 0.1 mmol) in DMF (0.3 mL) was added chlorotriethylsilane (0.015 mL, 0.07 mmol) dropwise *via* syringe at 0 °C, and the reaction mixture was stirred for 1.5 h at room temperature and quenched with saturated NH_4Cl solution (20 mL). The mixture was extracted by ethyl acetate (20 mL x 3), and then washed with H_2O (20 mL x 2), brine (20 mL), dried over anhydrous $MgSO_4$ and concentrated *in vacuo*. The crude product was purified on a silica gel column using hexanes/EtOAc (2/1) as eluant to afford **1-60b** as a white solid (18 mg, 90% yield): ^{1}H NMR (500 MHz, CDCl$_3$) δ 0.56 (m, 6 H), 0.92(m, 9 H), 1.05 (s, 3 H), 1.24 (m, 11 H), 1.69 (s, 3 H), 1.75 (m, 1 H), 2.00 (m, 3 H), 2.20 (s, 3 H), 2.27 (m, 3 H), 2.47 (m, 5 H), 3.85 (d, *J* = 0.65 Hz, 1 H), 4.15 (d, *J* = 8 Hz, 1 H), 4.32 (d, *J* = 9 Hz, 1 H), 4.50 (m, 2 H), 4.85 (t, *J* = 7.9 Hz, 1 H), 4.94 (d, *J* = 7.5 Hz, 1 H), 5.62 (d, *J* = 7 Hz, 1 H), 6.49 (s, 1 H), 7.24 (d, *J* = 8 Hz, 1 H), 7.85 (d, *J* = 6 Hz, 1 H), 7.91(s, 1 H). HRMS calcd. for $C_{40}H_{58}O_{11}SiH^+$: 743.3827, found 743.3814 (Δ= -1.7 ppm).

7-Triethylsilyl-2'-triisopropylsilyl-2-debenzoyl-2-(3,4-dimethylbenzoyl)-3'-dephenyl-3'-(2-methylprop-1-enyl)-10- propanoyldocetaxel (1-61b):[36]

To a solution of baccatin **1-60b** (17 mg, 0.023 mmol) and *β*-lactam **1-11** (14 mg, 0.034 mmol) in 2.3 mL dry THF was added 1.0 M LiHMDS in THF (0.04 mL, 0.04 mmol) dropwise at -40 °C, and the solution was stirred for 1.5 h. The reaction was quenched with saturated aqueous NH_4Cl solution (10 mL), and the aqueous layer was extracted with ethyl acetate (20 mL x 3). The combined extracts were then dried over anhydrous $MgSO_4$ and concentrated *in vacuo*. The residue was purified on a silica gel column using hexanes/EtOAc (4/1) as the eluant to afford the coupling product **1-61b** as a white solid (21 mg, 81%): ^{1}HNMR (400 MHz, CDCl$_3$) δ 0.57 (m, 6 H), 0.90 (m, 9 H), 1.05 (m, 21 H), 1.17 (s, 3 H), 1.20 (s, 3 H), 1.25 (m, 3 H), 1.45 (s, 9 H), 1.35 (m, 3 H), 1.73 (s, 3 H), 1.79(s, 3 H), 2.01 (s, 3 H), 2.36 (m, 9 H), 2.46 (m, 3 H), 3.83 (d, *J* = 7.2 Hz, 1 H) (H$_3$), 4.18 (d, *J* = 4.4 Hz, 1 H), 4.31 (d, *J* = 8.4 Hz, 1 H), 4.43 (d, *J* = 2.8 Hz, 1 H), 4.47 (dd, *J* = 10.4 , 6.6 Hz, 1 H) (H$_7$), 4.94 (d, *J* = 9.5 Hz, 2 H), 5.33 (d, *J* = 8.8 Hz, 1 H), 5.68 (d, *J* = 7.0 Hz, 1 H) (H$_2$), 6.48 (s, 1 H) (H$_{10}$), 7.25 (d, *J* = 8.0 Hz, 1 H), 7.82 (t, *J* = 8.0 Hz, 1 H),

7.89 (s, 1 H). HRMS calcd. for $C_{61}H_{97}O_{15}NSi_2H^+$: 1140.6475, found 1140.6448 (Δ= -2.4 ppm).

3'-Dephenyl-3'-(2-methylprop-1-enyl)-2-debenzoyl-2-(3,4-dimethylbenzoyl)-10-propanoyldocetaxel (1-62b):[36]

To a solution of **1-61b** (20 mg, 0.018 mmol) in pyridine /acetonitrile (1:1) (0.8 mL) was added dropwise HF/pyridine (70:30), (0.2 mL) at 0 °C, and the mixture was stirred overnight at room temperature. The reaction was quenched with saturated aqueous NaHCO$_3$ solution (20 mL). The mixture was then diluted with ethyl acetate (80 mL), washed with saturated aqueous CuSO$_4$ solution (10 mL x 2) and H$_2$O (20 mL), dried over anhydrous MgSO$_4$ and concentrated *in vacuo*. The residue was purified on a silica gel column using hexane/ethyl acetate (1/1) as the eluant to afford **1-62b** as a white solid (13 mg, 85%): ^{1}H NMR (400 MHz, CDCl$_3$) 1.15 (s, 3 H), 1.260 (m, 8 H), 1.35 (s, 9 H), 1.60 (m, 3 H), 1.76 (m, 3 H), 1.91 (m, 5 H), 2.33 (m, 10 H), 2.54 (m, 4 H), 3.38 (s, 1 H), 3.81 (d, J = 6.8 Hz, 1 H), 4.20 (m, 1 H), 4.32 (d, J = 8.4 Hz, 1 H), 4.42 (d, J = 6.8 Hz, 1 H), 4.75 (m, 2 H), 4.96 (d, J = 8.0 Hz, 1 H), 5.32 (d, J = 7.2 Hz, 1 H), 5.64 (d, J = 4.8 Hz, 1 H), 6.23 (t, J = 6 Hz, 1 H), 6.31 (s, 1 H), 7.22 (d, J = 8 Hz, 1 H), 7.83 (t, J = 8.0 Hz, 1 H), 7.89 (s, 1 H); ^{13}C NMR (400 MHz, CDCl$_3$) δ 9.2, 9.8, 14.3, 14.4, 15.2, 18.8, 20.1, 20.3, 22.1, 22.6, 25.9, 26.9, 27.8, 28.4, 29.9, 35.8, 43.4, 45.9, 58.8, 60.6, 72.5, 72.7, 74.0, 75.0, 75.7, 76.8, 79.4, 80.2, 81.4, 84.6, 120.9, 126.9, 128.0, 130.1, 131.5, 133.2, 137.1, 143.5, 167.4, 170.2, 174.9, 204.1. HRMS calcd. for $C_{46}H_{63}O_{15}NSi_2Na^+$: 892.4095, found 892.4125 (Δ= 3.3 ppm).

7,10,13-Tri(triethylsilyl)-2-debenzoyl-2-(3,4-dimethoxybenzoyl)-10-deacetyl-baccatin III (1-57c):[82]

To a solution of **1-29** (50 mg, 0.064 mmol), 3,4-dimethoxybenzoic acid (93 mg, 0.51 mmol) and DMAP (70 mg, 0.58 mmol) in toluene (0.4 mL) was added DIC (0.09 mL, 0.58 mmol) and the reaction mixture was refluxed for 37 h. The reaction mixture was diluted with ethyl acetate (30 mL) and washed with saturated aqueous NaHCO$_3$ solution (20 mL), H$_2$O (20 mL) and brine (20 mL). The organic lawyer was dried over anhydrous MgSO$_4$. The solvent was removed under reduced pressure and the residue was purified on a silica gel column (hexane/ethyl acetate =6/1) to afford **1-57c** as a white solid (37 mg, 60% yield, at 66% conversion): ^{1}H NMR (500 MHz, CDCl$_3$) δ 0.63 (m, 18 H), 0.97 (m, 27 H), 1.13 (s, 3 H), 1.19 (s, 3 H), 1.25 (m, 1 H), 1.65 (s, 3 H), 1.88 (m, 1 H), 1.98 (s, 3 H), 2.11 (m, 1 H), 2.25 (s, 3 H), 2.42 (m, 1 H), 3.85 (d, J = 7.0 Hz, 1 H), 3.93 (m, 6 H), 4.14 (d, J = 8.5 Hz, 1 H), 4.31 (d, J = 8.5 Hz, 1 H), 4.41 (dd, J = 10, 6.9 Hz, 1 H), 4.94 (m, 2 H), 5.20 (s, 1 H), 5.61 (d, J = 7.5 Hz, 1 H), 6.91 (d, J = 8.5 Hz, 1 H), 7.60 (d, J = 2.0 Hz, 2 H), 7.74 (dd, J = 8.0 Hz, 2.0 Hz, 1 H).

2-Debenzoyl-2-(3,4-methoxybenzoyl)-10-deacetylbaccatin III (1-58c):[82]

To a solution of **1-57c** (37 mg) in pyridine/acetonitrile (1:1) (1.5 mL) was added dropwise HF/pyridine (70:30) (0.4 mL) at 0 °C, and the mixture was stirred overnight at room temperature. The reaction was quenched with saturated aqueous NaHCO$_3$ solution (20 mL). The mixture was then diluted with ethyl acetate (50 mL), washed with saturated aqueous CuSO$_4$ solution (20 mL x 2) and H$_2$O (20 mL), dried over anhydrous MgSO$_4$ and concentrated *in vacuo* to afford 2-debenzoyl-2-(3,4-dimethoxy-benzoyl)-10-deacetyl-

baccatin III (**1-58c**) as a white solid (17mg, 73% yield). The crude compound was used in the next step without further purification.

2-Debenzoyl-2-(4-methylbenzoyl)-10-deacetyl-10-propanoylbaccatin III (1-59c):[51]
To the solution of **1-58c** (17 mg, crude) in THF (1.2 mL) was added cerium chloride heptahydrate (2 mg, 0.003 mmol) and propanoic anhydride (0.05 mL, 0.3 mmol). The reaction mixture was stirred at room temperature for 2 h. The reaction mixture was quenched with H_2O (30 mL), extracted with CH_2Cl_2 (30 mL x 3). The organic layers were washed with brine, dried over $MgSO_4$, and concentrated *in vacuo* to get crude product as a white solid (25 mg): ^{1}H NMR (400 MHz, CDCl$_3$) δ 1.10 (s, 6 H), 1.21(m, 11H), 1.67 (s, 5 H), 1.85 (m, 2 H), 2.04 (d, *J* = 2.4 Hz, 3 H), 2.24 (s, 2 H), 2.28 (d, *J* = 8 Hz, 3 H), 2.48 (m, 6H), 3.88 (d, *J* = 6.8 Hz, 1 H), 3.93 (m, 6 H), 4.13 (m, 1 H), 4.35 (d, *J* = 8.4 Hz, 1 H), 4.47 (m, 1 H), 4.87 (d, *J* = 8 Hz, 1 H), 4.99 (d, *J* = 9.5 Hz, 1 H), 5.60 (d, *J* = 7.2 Hz, 1 H), 6.36(s, 1 H), 6.93 (d, *J* = 4.8 Hz, 1 H), 7.61 (d, *J* = 1.6 Hz, 1 H), 7.76 (dd, *J* = 8.4 Hz, 1 H). The crude compound was used in the next step without further purification.

7-Triethylsilyl-2-debenzoyl-2-(3,4-dimethoxylbenzoyl)-10-deacetyl-10-propanoyl-baccatin III (1-60c):[36]
To a solution of **1-59c** (23 mg, 0.038 mmol) and imidazole (10 mg, 0.15 mmol) in DMF (0.35 mL) was added chlorotriethylsilane (0.02 mL, 0.114 mmol) dropwise *via* syringe at 0 °C, and the reaction mixture was stirred for 1 h at room temperature. The reaction mixture was quenched with saturated NH_4Cl solution (10 mL). The mixture was extracted by ethyl acetate (30 mL x 3), and then washed with H_2O (20 mL x 2), brine (20 mL), dried over anhydrous $MgSO_4$ and concentrated. The crude product was purified on a silica gel column using hexanes/EtOAc (2/1) as eluent to give **1-60c** as a white solid (16 mg, 74% yield for 2 steps): ^{1}H NMR (400 MHz, CDCl$_3$) δ 0.56 (m, 6 H), 0.92(m, 9 H), 1.03 (s, 3 H), 1.20 (m, 7 H), 1.67 (s, 3 H), 1.85 (m, 1 H), 2.05 (m, 3 H), 2.20 (s, 5 H), 2.25 (m, 3 H), 2.47 (m, 3 H), 3.85 (d, *J* = 0.65 Hz, 1 H), 3.95 (s, 6 H), 4.15 (d, *J* = 8 Hz, 1 H), 4.32 (d, *J* = 9 Hz, 1 H), 4.50 (m, 2 H), 4.82 (t, *J* = 7.9 Hz, 1 H), 4.96 (d, *J* = 7.5 Hz, 1 H), 5.62 (d, *J* = 7 Hz, 1 H), 6.93 (d, *J* = 7 Hz ,1 H), 7.62 (d, *J* = 2 Hz, 1 H), 7.88 (dd, 1 H) ; ^{13}C NMR (400 MHz, CDCl$_3$) δ 5.5, 7.0, 9.4, 10.1, 15.2, 20.3, 22.9, 27.1, 27.9, 37.5, 38.5, 43.0, 47.5, 56.1, 56.3, 58.9, 68.3, 72.6, 74.7, 75.8, 78.9, 81.3, 84.5, 94.6, 110.7, 112.6, 112.9, 124.6, 133.1, 144.0, 148.9, 153.8, 167.2, 170.8, 173.0, 185.8, 202.5. HRMS calcd. for $C_{40}H_{58}O_{13}SiH^+$: 775.3725, found 775.3737 (Δ= 1.5 ppm).

7-Triethylsilyl-2'-triisopropylsilyl-2-debenzoyl-2-(3,4-dimethoxybenzoyl)-3'-dephenyl-3'-(2-methylprop-1-enyl)-10- propanoyldocetaxel (1-61c):[36]
To a solution of baccatin **1-60c** (15 mg, 0.019 mmol) and *β*-lactam **1-11** (12 mg, 0.029 mmol) in dry THF (1.9 mL) was added 1.0 M LiHMDS in THF (0.029 mL, 0.029 mmol) dropwise at -40 °C, and the solution was stirred for 1.5 h. The reaction was quenched with saturated aqueous NH_4Cl solution (10 mL), and the aqueous layer was extracted with ethyl acetate (20mL x 3). The combined extracts were then dried over anhydrous $MgSO_4$ and concentrated *in vacuo*. The residue was purified on a silica gel column using hexanes/EtOAc (4/1) as the eluant to afford the coupling product **1-61c** as a white solid (19 mg, 84%): ^{1}HNMR (400 MHz, CDCl$_3$) δ 0.57 (m, 6 H), 0.92 (m, 9 H), 1.05 (m, 21 H),

1.17 (s, 3 H), 1.20 (s, 3 H), 1.25 (m, 3 H), 1.45 (s, 9 H), 1.35 (m, 3 H), 1.73 (s, 3 H), 1.79(s, 3 H), 2.01 (s, 3 H), 2.36 (m, 9 H), 2.46 (m, 3 H), 3.83 (d, J = 7.2 Hz, 1 H), 4.18 (d, J = 8.4 Hz, 1 H), 4.31 (d, J = 8.4 Hz, 1 H), 4.43 (d, J = 2.8 Hz, 1 H), 4.47 (dd, J = 10.4 , 6.6 Hz, 1 H), 4.82 (m, 2 H), 4.98 (d, J = 3.6 Hz, 2 H), 5.33 (d, J = 8.4 Hz, 1 H), 5.68 (d, J = 7.0 Hz, 1 H), 6.08 (t, 1 H), 6.48 (s, 1 H), 7.20 (d, J = 8.0 Hz, 1 H), 7.83 (d, J = 8.0 Hz, 1 H), 7.89 (m, 1 H). HRMS calcd. for $C_{61}H_{97}O_{17}NSi_2H^+$: 1172.6373, found 1172.6368 (Δ= -0.4 ppm).

3'-Dephenyl-3'-(2-methylprop-1-enyl)-2-debenzoyl-2-(3,4-dimethoxybenzoyl)-10-propanoyldocetaxel (1-62c):[36]

To a solution of **1-61c** (18 mg, 0.015 mmol) in pyridine /acetonitrile (1:1) (0.7 mL) was added dropwise HF/pyridine (70:30) (0.2 mL) at 0 $^{\circ}$C, and the mixture was stirred overnight at room temperature. The reaction was quenched with saturated aqueous NaHCO$_3$ solution (20 mL). The mixture was then diluted with ethyl acetate (80 mL), washed with saturated aqueous CuSO$_4$ solution (20 mL x 2) and H$_2$O (20 mL), dried over anhydrous MgSO$_4$ and concentrated *in vacuo*. The residue was purified on a silica gel column using hexanes/EtOAc (1/1) as the eluent to afford **1-62c** as a white solid (10 mg, 72%): mp 134-136 $^{\circ}$C, ^{1}H NMR (400 MHz, CDCl$_3$) δ 1.15 (s, 3 H), 1.260 (m, 8 H), 1.35 (s, 9 H), 1.62 (m, 3 H), 1.72 (m, 3 H), 1.91 (m, 4 H), 2.35 (s, 4 H), 2.54 (m, 4 H), 3.38 (s, 1 H), 3.81 (d, J = 6.8 Hz, 1 H), 3.96 (s, 6 H), 4.21 (ss, 2 H), 4.36 (d, J = 6.8 Hz, 1 H), 4.42 (m, 1 H), 4.73 (m, 2 H), 4.97 (d, J = 9.6 Hz, 1H), 5.32 (d, J = 6.4 Hz, 1 H), 5.66 (d, J = 6.8 Hz, 1 H), 6.20 (t, J = 6 Hz, 1 H), 6.31 (s, 1 H), 6.93 (d, J = 8.8 Hz, 1 H), 7.62 (s, J = 0.8 Hz, 1 H), 7.76 (dd, J = 8.4 Hz, 2.0 Hz, 1 H); ^{13}C NMR (400 MHz, CDCl$_3$) δ 9.2, 15.1, 18.8, 22.7, 25.9, 26.9, 27.8, 28.4, 29.9, 35.8, 43.5, 45.8, 56.1, 56.3, 58.8, 72.4, 73.9, 75.7, 79.3, 84.7, 110.7, 149.0, 167.1, 170.2, 174.9, 214.8. HRMS calcd. for $C_{46}H_{63}O_{17}NNa^+$: 924.3994, found 924.4034 (Δ= 4.4 ppm).

In vitro cell growth inhibition assay:

(a) Tumor cell growth inhibition was determined according to the method established by Skehan et al.[84] Human cancer cells LCC6-WT (Pgp-), MCF-7 (Pgp-), LCC6-MDR (Pgp+) and NCI/ADR (Pgp+), were plated at a density of 400-2,000 cells/well in 96-well plates and allowed to attach overnight. These cell lines were maintained in RPMI-1640 medium (Roswell Park Memorial Institute growth medium) supplemented with 5% fetal bovine serum and 5% Nu serum (Collaborative Biomedical Product, MA). Taxoids were dissolved in DMSO and further diluted with RPMI-1640 medium. Triplicate wells were exposed to various treatments. After 72 h incubation, 100 μL of ice-cold 50% trichloroacetic acid (TCA) was added to each well, and the samples were incubated for 1 h at 4 °C. Plates were then washed five times with water to remove TCA and serum proteins, and 50 μL of 0.4% sulforhodamine B (SRB) was added to each well. Following a 5-min incubation, plates were rinsed five times with 0.1% acetic acid and air-dried. The dye was then solubilized with 10 mM Tris-base (pH 10.5) for 5 min on a gyratory shaker. Optical density was measured at 570 nm. The IC$_{50}$ values were then calculated by fitting the concentration-effect curve data with the sigmoid-E_{max} model using nonlinear regression, weighted by the reciprocal of the square of the predicted effect.[85]

(b) Human ovarian cancer cell lines cells A2780, 1A9PTX10 and 1A9PTX22, were cultured as specified by ATCC (Manassas, Virginia). For cytotoxicity assays the cells

were plated at a density of 10,000 cells/well in 96-well plates and allowed to adhere overnight. The media was changed the following morning and replaced with media containing taxane derivatives or vehicle control. Taxoids were dissolved in DMSO to 10 mM concentration and were further diluted in appropriate media prior to addition to cells. Each dose of drug or vehicle was tested in triplicate, and the experiment is representative of at least 3 independent trials. After 72 hours of treatment the media was aspirated and the cells were washed in warm PBS. MTT reagent (Sigma) was diluted in RPMI-1640 media without phenol red (Invitrogen), and added to the cells at a concentration of 0.5 mg/mL. After 3 hours of incubation, the reagent was aspirated, the plate was washed with PBS and MTT formazan crystals were dissolved in 50 μL acidified isopropanol (0.1N hydrochloric acid). Absorbance at 570 nM was measured on a thermomax plate reader (Molecular Devices). The IC$_{50}$ values were obtained by using the same method as that described for (a).

Tubulin polymerization assay
(Professor Susan B. Horwitz's laboratory at the Albert Einstein College of Medicine):
Assembly and disassembly of calf brain microtubule protein (MTP) was monitored spectrophotometrically (Beckman Coulter DU 640, Fullerton, CA) by recording changes in turbidity at 350 nm at 37 °C.[86, 87] MTP was diluted to 1mg/mL in MES buffer containing 3 M glycerol. The concentration of tubulin in MTP is 85% and that is taken into consideration when the ratios of tubulin to drug are presented in **Figures 1-9** and **Figure 1-14**. Microtubule assembly was carried out with 10 μM new-generation taxoids. Paclitaxel (10 μM) was also used for comparison purpose. Calcium chloride (6 mM) was added to the assembly reaction after 50 min to follow the calcium-induced microtubule depolymerization.

Electron microscopy
(Professor Susan B. Horwitz's laboratory at the Albert Einstein College of Medicine):
Aliquots (50 μL) were taken from *in vitro* polymerization assays at the end of the reaction and placed onto 300-mesh carbon-coated, formavar-treated copper grids. Samples were then stained with 20 μL of 2% uranyl acetate and viewed with a JEOL model 100CX electron microscope.

Molecular modeling studies of fluoro-taxoids:

The structures fluoro-taxoids **SB-T-1282**, **SB-T-1284** and **SB-T-12853** as well as second-generation taxoid **SB-T-1213** in the 1JFF were produced by directly changing the subsitiutions at the C3' and C10 positions of the REDOR-Taxol in the 1JFF complex using the Builder module in the InsightII 2000 program (CVFF). Then, these structures were energy-minimized in 5000 steps or till the maximum derivative being < 0.001 kcal/A by means of the conjugate gradients method using the CVFF force field and the distance-dependent dielectric. The backbone of the protein was fixed throughout the energy minimization. After the energy minimization, the snapshots were overlaid by superimposing the backbones of the proteins. The conformationss are shown in **Figure 1-20**. **SB-T-1213** and **SB-T-12853** exhibit very good overlay. During the energy minimizations of taxoids derived from the REDOR-Taxol structure, the C'2-OH--N(His227) H-bond was very stable.

§ 1.6 References

1.   http://www.cancer.org
2.   Vuilhorgne, M.; Gaillard, C.; Sanderlink, G. J.; Royer, I.; Monsarrat, B.; Dubois, J.; Wright, M. Metabolism of Taxoid Drugs. In *Taxane Anticancer Agents: Basic Science and Current Status, ACS Symp. Ser. 583*, Georg, G. I.; Chen, T. T.; Ojima, I.; Vyas, D. M., Eds. American Chemical Society: Washington, D. C., 1995; pp 98-110.
3.   Georg, G. I.; Chen, T. T.; Ojima, I.; Vyas, D. M. *Taxane Anticancer Agents: Basic Science and Current Status*. American Chemical Society: Washington D.C., 1995.
4.   Wani, M. C.; Taylor, H. L.; Wall, M. E.; Coggon, P.; McPhail, A. T. Plant antitumor agents. VI. The isolation and structure of taxol, a novel antileukemic and antitumor agent from Taxus brevifolia. *J. Am. Chem. Soc.* **1971,** 93, 2325-7.
5.   Schiff, P. B.; Fant, J.; Horwitz, S. B. Promotion of Microbubule Assembly *in vitro* by Taxol. *Nature* **1979,** 277, 665-667.
6.   Schiff, P. B.; Horwitz, S. B. Taxol stabilizes microtubules in mouse fibroblast cells. *Proc. Natl. Acad. Sci. USA* **1980,** 77, 1561-5.
7.   Lin, S. Design, synthesis and medicinal chemistry of novel taxane-based anticancer agents. Ph.D. Dissertation, State University of New York, Stony Brook, **1999**.
8.   Georg, G. I.; Chen, T. T.; Ojima, I.; Vyas, D. M. In *Taxane Anticancer Agents: Basic Science and Current Status*, ACS Symp. Ser. 583, American Chemical Society, Washington D.C., 1995.
9.   Nicolaou, K. C.; Dai, W.-M.; Guy, R. K. Chemistry and Biology of Taxol. *Angew. Chem. Int. Ed. Engl.* **1994,** 33, 15-44.
10.   Denis, J.-N.; Greene, A. E.; Guénard, D.; Guéritte-Voegelein, F.; Mangatal, L.; Potier, P. A. Highly Efficient, Practical Approach to Natural Taxol. *J. Am. Chem. Soc.* **1988,** 110, 5917-5919.
11.   Guénard, D.; Guéritte-Vogelein, F.; Potier, P. Taxol and Taxotere: Discovery, Chemistry, and Structure-Activity Relationships. *Acc. Chem. Res.* **1993,** 26, 160-167.
12.   Colin, M.; Guénard, D.; Guéritte-Voegelein, F.; Potier, P. Taxotere, European Patent Application. *Eur. Pat. Appl.* **1988**, EP 253,738: *Chem. Abstr.* **1988**, *109*, 22762w.
13.   Guéritte-Voegelein, F.; Mangatal, L.; Guénard, D.; Potier, P.; Guilhem, J.; Cesario, M.; Pascard, C. Structure of a Synthetic Taxol Precursor: *N-tert*-Butoxycarbonyl-10-deacetyl-*N*-debenzoyltaxol. *Acta Crstallogr.* **1990,** C46, 781-784.
14.   Bissery, M. C.; Guéritte-Vogelein, F.; Guénard, D.; Lavelle, F. Experimental Antitumor Activity of Taxotere (RP 56976, NSC 628503), a Taxol Analog. *Cancer Res.* **1991,** 51, 4845-4852.
15.   Holton, R. A. Method for Preparation of Taxol. *Eur. Pat. Appl.* **1990**, US Patent, **1992**, 5,175,315; EP 400,971, 1990: *Chem. Abstr.* **1990**, *114*, 164568q.
16.   Ojima, I.; Habus, I.; Zhao, M.; Zucco, M.; Park, Y. H.; Sun, C. M.; Brigaud, T. New and Efficient Approaches to the Semisynthesis of Taxol and Its C-13 Side-

Chain Analogs by Means of β-Lactam Synthon Method. *Tetrahedron* **1992,** 48, 6985-7012.

17.	Ojima, I. Recent Advances in the β-Lactam Synthon Method. *Acc. Chem. Res.* **1995,** 28, 383-389.

18.	Ojima, I.; Habus, I.; Zhao, M.; Georg, G. I.; Jayasinghe, R. Efficient and Practical Asymmetric Synthesis of the Taxol C-13 Side Chain, *N*-Benzoyl-(2*R*,3*S*)-3-phenylisoserine, and Its Analogs via Chiral 3-Hydroxyl-4-aryl-β-lactams Through Chiral Ester Enolate − Imine Cyclocondensation. *J. Org. Chem.* **1991,** 56, 1681-1684.

19.	Holton, R. A.; Somoza, C.; Kim, H.-B.; Liang, F.; Biediger, R. J.; Boatman, P. D.; Shindo, M.; Smith, C. C.; Kim, S.; Nadizadeh, H.; Suzuki, Y.; Tao, C.; Vu, P.; Tang, S.; Zhang, P.; Murthi, K. K.; Gentile, L. N.; Liu, J. H. First Total Synthesis of Taxol. 1. Functionalization of the B Ring. *J. Am. Chem. Soc.* **1994,** 116, 1597-1598.

20.	Holton, R. A.; Kim, H.-B.; Somoza, C.; Liang, F.; Biediger, R. J.; Boatman, P. D.; Shindo, M.; Smith, C. C.; Kim, S.; Nadizadeh, H.; Suzuki, Y.; Tao, C.; Vu, P.; Tang, S.; Zhang, P.; Murthi, K. K.; Gentile, L. N.; Liu, J. H. First Total Synthesis of Taxol. 2. Completion of the C and D Rings. *J. Am. Chem. Soc.* **1994,** 116, 1599-1600.

21.	Nicolaou, K. C.; Yang, Z.; Liu, J. J.; Ueno, H.; Nantermet, P. G.; Guy, R. K.; Claiborne, C. F.; Renaud, J.; Couladouros, E. A.; Paulvannan, K.; Sorensen, E. J. Total Synthesis of Taxol. *Nature* **1994,** 367, 630-634.

22.	Danishefsky, S.; Masters, J.; Young, W.; Link, J.; Snyder, L.; Magee, T.; Jung, D.; Isaacs, R.; Bornmann, W.; Alaimo, C.; Coburn, C.; Di Grandi, M. Total Synthesis of Baccatin III and Taxol. *J. Am. Chem. Soc.* **1996,** 118, 2843-2859.

23.	Wender, P. A.; Badham, N. F.; Conway, S. P.; Floreancig, P. E.; Glass, T. E.; Houze, J. B.; Krauss, N. E.; Lee, D.; Marquess, D. G.; McGrane, P. L.; Meng, W.; Natchus, M. G.; Shuker, A. J.; Sutton, J. C.; Taylor, R. E. The Pinene Path to Taxanes. 6. A Concise Stereocontrolled Synthesis of Taxol. *J. Am. Chem. Soc.* **1997,** 119, 2757-2758.

24.	Ritter, S. K. Green innovations. *Chem. Eng. News* **2004,** 82, 25-30.

25.	Arbuck, S. G.; Blaylock, B. A. Taxol: Clinical Results and Current Issues in Development. In *Taxol®: Science and Applications*, Suffness, M., Ed. CRC Press: Boca Raton, 1995; pp 379-415.

26.	Verweij, J.; Clavel, M.; Chevalier, B. Paclitaxel (Taxol) and Docetaxel (Taxotere): Not Simply Two of a Kind. *Ann. Oncol.* **1994,** 5, 495-505.

27.	Kingston, D. G. I. Recent Advances in the Chemistry and Structure-Activity Relationships of Paclitaxel. In *Taxane Anticancer Agents: Basic Science and Current Status; ACS Symp. Ser. 583*, Georg, G. I.; Chen, T. T.; Ojima, I.; Vyas, D. M., Eds. American Chemical Society: Washington, D. C., 1995; pp 203-216.

28.	Ojima, I.; Kuduk, S. D.; Chakravarty, S. Recent Advances in the Medicinal Chemistry of Taxoid Anticancer Agents. In *Adv. Med. Chem.*, Maryanoff, B. E.; Reitz, A. B., Eds. JAI Press: Greenwich, CT, 1998; Vol. 4, pp 69-124.

29.	Ojima, I.; Lin, S.; Wang, T. The Recent Advances in the Medicinal Chemistry of Taxoids with Novel b-Amino Acid Side Chains." In "The Chemistry and Biology of b-Amino Acids." Hoekstra, W. J. Ed;. *Curr. Med. Chem.* **1999,** 6, 927-954.

30. Kingston, D. G. I. Recent Advances in the Chemistry of Taxol. *J. Nat. Prod.* **2000,** 63, 726-734.

31. Ojima, I.; Kuduk, S. D.; Pera, P.; Veith, J. M.; Bernacki, R. J. Synthesis of and Structure-Activity Relationships of Non-Aromatic Taxoids. Effects of Alkyl and Alkenyl Ester Groups on Cytotoxicity. *J. Med. Chem.* **1997,** 40, 279-285.

32. Ojima, I.; Slater, J. C.; Michaud, E.; Kuduk, S. D.; Bounaud, P.-Y.; Vrignaud, P.; Bissery, M.-C.; Veith, J.; Pera, P.; Bernacki, R. J. Syntheses and Structure-Activity Relationships of the Second Generation Antitumor Taxoids. Exceptional Activity against Drug-Resistant Cancer Cells. *J. Med. Chem.* **1996,** 39, 3889-3896.

33. Ojima, I.; Lin, S. Efficient Asymmetric Syntheses of β-Lactams Bearing a Cyclopropane or an Epoxide Moiety and Their Application to the Syntheses of Novel Isoserines and Taxoids. *J. Org. Chem.* **1998,** 63, 224-225.

34. Ojima, I.; Kuduk, S. D.; Slater, J. C.; Gimi, R. H.; Sun, C. M. Syntheses of New Fluorine-Containing Taxoids by Means of β-Lactam Synthon Method. *Tetrahedron* **1996,** 52, 209-224.

35. Ojima, I.; Duclos, O.; Zucco, M.; Bissery, M.-C.; Combeau, C.; Vrignaud, P.; Riou, J. F.; Lavelle, F. Synthesis and Structure-Activity Relationships of New Antitumor Taxoids. Effects of Cyclohexyl Substitution at the C-3' and/or C-2 of Taxotère (Docetaxel). *J. Med. Chem.* **1994,** 37, 2602-2608.

36. Ojima, I.; Slater, J. S.; Kuduk, S. D.; Takeuchi, C. S.; Gimi, R. H.; Sun, C.-M.; Park, Y. H.; Pera, P.; Veith, J. M.; Bernacki, R. J. Syntheses and Structure-Activity Relationships of Taxoids Derived from 14β-Hydroxy-10-deacetylbaccatin III. *J. Med. Chem.* **1997,** 40, 267-278.

37. Nicoletti, M. I.; Colombo, T.; Rossi, C.; Monardo, C.; Stura, S.; Zucchetti, M.; Riva, A.; Morazzoni, P.; Donati, M. B.; Bombardelli, E.; D'Incalci, M.; Giavazzi, R. IDN5109, a taxane with oral bioavailability and potent antitumor activity. *Cancer Res.* **2000,** 60, 842-846.

38. Polizzi, D.; Pratesi, G.; Monestiroli, S.; Tortoreto, M.; Zunino, F.; Bombardelli, E.; Riva, A.; Morazzoni, P.; Colombo, T.; D'Incalici, M.; Zucchetti, M. Oral Efficacy and Bioavailability of a Novel Taxane. *Clin. Cancer Res.* **2000,** 6, 2070-2074.

39. Ojima, I.; Sun, C. M.; Zucco, M.; Park, Y. H.; Duclos, O.; Kuduk, S. D. A Highly Efficient Route to Taxotère by the β-Lactam Synthon Method. *Tetrahedron Lett.* **1993,** 34, 4149-4152.

40. Whitesell, J. K.; Lawrence, R. M. Practical Enzymatic Resolution of Chiral Auxiliaries--Enantiomerically Pure *trans*-2-Phenylcyclohexanol and *trans*-2-(α-Cumyl)cyclohexanol. *Chimia* **1986,** 40, 318-321.

41. Lynch, J. E.; Riseman, S. M.; Laswell, W. L.; Volante, R. P.; Smith, G. B.; Shinkai, I.; Tschaen, D. M. Mechanism of an acid chloride-imine reaction by low-temperature FT-IR: β-lactam formation occurs exclusively through a ketene intermediate. *J. Org. Chem.* **1989,** 54, 3792-6.

42. Georg, G. I.; Ravikumar, V. T. Stereocontrolled ketene-imine cycloaddition reactions. In *Organic Chemistry β-Lactams*, Georg, G. I., Ed. VCH: New York, 1993; pp 295-368.

43. Hegedus, L. S.; Montgomery, J.; Narukawa, Y.; Snustad, D. C. A contribution to the confusion surrounding the reaction of ketenes with imines to produce β-

lactams. A comparison of stereoselectivity dependence on the method of ketene generation: acid chloride/triethylamine vs photolysis of chromium carbene complexes. *J. Am. Chem. Soc.* **1991,** 113, 5784-5791.

44.   Dumas, S.; Hegedus, L. S. Electronic Effects on the Stereochemical Outcome of the Photochemical Reaction of Chromium Carbene Complexes with Imines to Form *β*-Lactams. *J. Org. Chem.* **1994,** 59, 4967-4971.

45.   Cossio, F. P.; Ugalde, J. M.; Lopez, X.; Lecea, B.; Palomo, C. A semiempirical theoretical study on the formation of β-lactams from ketenes and imines. *J. Am. Chem. Soc.* **1993,** 115, 995-1004.

46.   Lopez, R.; Sordo, T. L.; Sordo, J. A.; Gonzalez, J. Torquoelectronic effect in the control of the stereoselectivity of ketene-imine cycloaddition reactions. *J. Org. Chem.* **1993,** 58, 7036-7037.

47.   Cossio, F. P.; Arrieta, A.; Lecea, B.; Ugalde, J. M. Chiral Control in the Staudinger Reaction between Ketenes and Imines. A Theoretical SCF-MO Study on Asymmetric Torquoselectivity. *J. Am. Chem. Soc.* **1994,** 116, 2085-2093.

48.   Palomo, C.; Aizpurua, J. M.; Ganboa, I.; Oiarbide, M. Asymmetric synthesis of *β*-lactams by Staudinger ketene-imine cycloaddition reaction. *Eur. J. Org. Chem.* **1999**, 3223-3235.

49.   Brieva, R.; Crich, J. Z.; Sih, C. J. Chemoenzymic synthesis of the C-13 side chain of Taxol: optically active 3-hydroxy-4-phenyl b-lactam derivatives. *J. Org. Chem.* **1993,** 58, 1068-75.

50.   Ojima, I.; Chen, J.; Sun, L.; Borella, C. P.; Wang, T.; Miller, M. L.; Lin, S.; Geng, X.; Kuznetsova, L.; Qu, C.; Gallager, D.; Zhao, X.; Zanardi, I.; Xia, S.; Horwitz, S. B.; Clair, J. M.; Guerriero, J. L.; Bar-Sagi, D.; Veith, J. M.; Pera, P.; Bernacki, R. J. Design, Synthesis and Biological Evaluation of New-Generation Taxoids. *J. Med. Chem.* **2008**, In press.

51.   Holton, R. A.; Zhuming, Z.; Clarke, P. A.; Nadizadeh, H.; Procter, D. J. Selective Protection of the C(7) and C(10) Hydroxyl Groups in 10-Deacetyl Baccatin III. *Tetrahedron Lett.* **1998,** 39, 2883-2886.

52.   Gottesman Michael, M.; Fojo, T.; Bates Susan, E. Multidrug resistance in cancer: role of ATP-dependent transporters. *Nat Rev Cancer* **2002,** 2, 48-58.

53.   Dumontet, C.; Sikic, B. I. Mechanisms of action of and resistance to antitubulin agents: Microtubule dynamics, drug transport, and cell death. *J. Clin. Oncol.* **1999,** 17, 1061-1070.

54.   Cabral, F.; Wible, L.; Brenner, S.; Brinkley, B. R. Taxol-requiring mutant of Chinese hamster ovary cells with impaired mitotic spindle assembly. *J. Cell Biol* **1983,** 97, 30-9.

55.   Schibler, M. J.; Cabral, F. Taxol-dependent mutants of Chinese hamster ovary cells with alterations in alpha- and beta-tubulin. *J. Cell Biol* **1986,** 102, 1522-31.

56.   Lu, Q.; Luduena, R. F. Removal of beta III isotype enhances taxol induced microtubule assembly. *Cell Struct. Funct.* **1993,** 18, 173-82.

57.   Haber, M.; Burkhart, C. A.; Regl, D. L.; Madafiglio, J.; Norris, M. D.; Horwitz, S. B. Altered expression of Mbeta 2, the class II beta -tubulin isotype, in a murine J774.2 cell line with a high level of taxol resistance. *J. Biol. Chem.* **1995,** 270, 31269-75.

58.   Giannakakou, P.; Sackett, D. L.; Kang, Y.-K.; Zhan, Z.; Buters, J. T. M.; Fojo, T.; Poruchynsky, M. S. Paclitaxel-resistant human ovarian cancer cells have mutant beta -tubulins that exhibit impaired paclitaxel-driven polymerization. *J. Biol. Chem.* **1997,** 272, 17118-17125.

59.   Kavallaris, M.; Kuo, D. Y. S.; Burkhart, C. A.; Regl, D. L.; Norris, M. D.; Haber, M.; Horwitz, S. B. Taxol-resistant epithelial ovarian tumors are associated with altered expression of specific beta -tubulin isotypes. *J. Clin. Invest.* **1997,** 100, 1282-1293.

60.   Giannakakou, P.; Sackett, D. L.; Kang, Y.-K.; Zhan, Z.; Buters, J. T. M.; Fojo, T.; Poruchynsky, M. S. Paclitaxel-resistant human ovarian cancer cells have mutant b-tubulins that exhibit impaired paclitaxel-driven polymerization. *J. Biol. Chem.* **1997,** 272, 17118-17125.

61.   Yang, C.-G.; Barasoain, I.; Li, X.; Matesanz, R.; Liu, R.; Sharom, F. J.; Yin, D.-L.; Diaz, J. F.; Fang, W.-S. Overcoming tumor drug resistance with high-affinity taxanes: a SAR study of C2-modified 7-acyl-10-deacetyl cephalomannines. *ChemMedChem* **2007,** 2, 691-701.

62.   Bohm, H.-J.; Banner, D.; Bendels, S.; Kansy, M.; Kuhn, B.; Muller, K.; Obst-Sander, U.; Stahl, M. Fluorine in medicinal chemistry. *ChemBioChem* **2004,** 5, 637-43.

63.   Ojima, I.; McCarthy, J. R.; Welch, J. T.; Editors. *Biomedical Frontiers of Fluorine Chemistry.* 1996; p 356 pp.

64.   Ojima, I.; Kuduk, S. D.; Slater, J. C.; Gimi, R. H.; Sun, C. M.; Chakravarty, S.; Ourevitch, M.; Abouabdellah, A.; Bonnet-Delpon, D.; Begue, J.-P.; Veith, J. M.; Pera, P.; Bernacki Ralph, J. Syntheses, biological activity, and conformational analysis of fluorine-containing taxoids. *ACS Symposium Series* **1996,** 639, 228-243.

65.   Ojima, I.; Kuduk, S. D.; Chakravarty, S.; Ourevitch, M.; Begue, J. P. A Novel Approach to the Study of Solution Structures and Dynamic Behavior of Paclitaxel and Docetaxel using Fluorine-Containing Analogs as Probes. *J. Am. Chem. Soc.* **1997,** 119, 5519-5527.

66.   Li, Y.; Poliks, B.; Cegelski, L.; Poliks, M.; Cryczynski, A.; Piszcek, G.; Jagtap, P. G.; Studelska, D. R.; Kingston, D. G. I.; Schaefer, J.; Bane, S. Conformation of Microtubule-Bound Paclitaxel Determined by Fluorescence Spectroscopy and REDOR NMR. *Biochemistry* **2000,** 39, 281-291.

67.   Paik, Y.; Yang, C.; Metaferia, B.; Tang, S.; Bane, S.; Ravindra, R.; Shanker, N.; Alcaraz, A. A.; Johnson, S. A.; Schaefer, J.; O'Connor, R. D.; Cegelski, L.; Snyder, J. P.; Kingston, D. G. I. Rotational-Echo Double-Resonance NMR Distance Measurements for the Tubulin-Bound Paclitaxel Conformation. *J. Am. Chem. Soc.* **2007,** 129, 361-370.

68.   Ojima, I.; Lin, S.; Slater, J. C.; Wang, T.; Pera, P.; Bernacki, R. J.; Ferlini, C.; Scambia, G. Syntheses and biological activity of C-3'-difluoromethyl-taxoids. *Bioorg. Med. Chem.* **2000,** 8, 1619-1628.

69.   Ojima, I.; Inoue, T.; Slater, J. C.; Lin, S.; Kuduk, S. C.; Chakravarty, S.; Walsh, J. J.; Gilchrist, L.; McDermott, A. E.; Cresteil, T.; Monsarrat, B.; Pera, P.; Bernacki, R. J. Synthesis of Enatiopure F-Containing Taxoids and Their Use as Anticancer Agents as well as Probes for Biomedical Problems. In *"Asymmetric*

Fluoroorganic Chemistry: Synthesis, Application, and Future Directions"; ACS Symposium Series 746, Ramachandran, P. V., Ed. American Chemical Society: Washington, D. C., 1999; pp 158-181.

70. Ojima, I.; Kuznetsova, L. V.; Sun, L. Organofluorine chemistry at the biomedical interface: a case study on fluoro-taxoid anticancer agents. *ACS Symposium Series* **2007,** 949, 288-304.

71. Ehrlichova, M.; Vaclavikova, R.; Ojima, I.; Pepe, A.; Kuznetsova, L. V.; Chen, J.; Truksa, J.; Kovar, J.; Gut, I. Transport and cytotoxicity of paclitaxel, docetaxel, and novel taxanes in human breast cancer cells. *Naunyn-Schmiedeberg's Arch. Pharmacol.* **2005,** 372, 95-105.

72. Yamazaki, T.; Hiraoka, S.; Sakamoto, J.; Kitazume, T. Mesyloxy-group migration as the stereoselective preparation method of various functionalized olefins and its reaction mechanism. *Org. Lett.* **2001,** 3, 743-746.

73. Lim, M. H.; Kim, H. O.; Moon, H. R.; Chun, M. W.; Jeong, L. S. Synthesis of Novel D-2'-Deoxy-2'-C-difluoromethylene-4'-thiocytidine as a Potential Antitumor Agent. *Org. Lett.* **2002,** 4, 529-531.

74. Kuznetsova, L. Design, synthesis and biological evaluation of novel taxane-based anticancer agents and their tumor delivery. Ph.D. Dissertation, State University of New York, Stony Brook, **2005**.

75. Skehan, P.; Storeng, R.; Scudiero, D.; Monks, A.; McMahon, J.; Vistica, D.; Warren, J. T.; Bokesch, H.; Kenney, S.; Boyd, M. R. New colorimetric cytotoxicity assay for anticancer-drug screening. *J. Natl. Cancer Inst.* **1990,** 82, 1107-12.

76. Geney, R.; Sun, L.; Pera, P.; Bernacki Ralph, J.; Xia, S.; Horwitz Susan, B.; Simmerling Carlos, L.; Ojima, I. Use of the tubulin bound paclitaxel conformation for structure-based rational drug design. *Chem. Biol.* **2005,** 12, 339-48.

77. Rao, S.; He, L.; Chakravarty, S.; Ojima, I.; Orr, G. A.; Horwitz, S. B. Characterization of the Taxol Binding Site on the Microtubule. . *J. Biol. Chem.* **1999,** 274, 37990-37994.

78. Nogales, E.; Wolf, S. G.; Downing, K. H. Structure of the α,β Tubulin Dimer by Electron Crystallography. *Nature* **1998,** 391, 199-203.

79. Lowe, J.; Li, H.; Downing, K. H.; Nogales, E. Refined structure of alpha beta-tubulin at 3.5 A resolution. *J. Mol. Bol.* **2001,** 313, 1045-1057.

80. Georg, G. I.; Cheruvallath, Z. S.; Himes, R. H.; Mejillano, M. R.; Burke, C. T. Synthesis of biologically active taxol analogs with modified phenylisoserine side chains. *J. Med. Chem.* **1992,** 35, 4230-7.

81. Lin, S.; Geng, X.; Qu, C.; Tynebor, R.; Gallagher, D. J.; Pollina, E.; Rutter, J.; Ojima, I. Synthesis of highly potent second-generation taxoids through effective kinetic resolution coupling of racemic .beta.-lactams with baccatins. *Chirality* **2000,** 12, 431-441.

82. Ojima, I.; Wang, T.; Miller, M. L.; Lin, S.; Borella, C. P.; Geng, X.; Pera, P.; Bernacki, R. J. Syntheses and Structure-Activity Relationships of New Second-Generation Taxoids. *Bioorg. Med. Chem. Lett.* **1999,** 9, 3423-3428.

83. Borella, C. P. Design, synthesis, and structure-activity relationship (SAR) of novel taxane anticancer agents. Ph.D. Dissertation, State University of New York, Stony Brook, **2001**.

84. Skehan, P.; Storeng, R.; Scudiero, D.; Monks, A.; McMahon, J.; Vistica, D.; Warren, J. T.; Bokesch, H.; Kenney, S.; Boyd, M. R. New colorimetric cytotoxicity assay for anticancer-drug screening. *J. Natl. Cancer Inst.* **1990,** 82, 1107-12.

85. Motulsky, H. J.; Ransnas, L. A. Fitting curves to data using nonlinear regression: a practical and nonmathematical review. *FASEB J.* **1987,** 1, 365-74.

86. Weisenberg, R. C. Microtubule formation in vitro in solutions containing low calcium concentrations. *Science* **1972,** 177, 1104-5.

87. Shelanski, M. L.; Gaskin, F.; Cantor, C. R. Microtubule assembly in the absence of added nucleotides. *Proc. Natl. Acad. Sci. USA* **1973,** 70, 765-8.

Chapter II

Synthesis and Evaluation of Novel Fatty Acid-2nd-Generation Taxoid Conjugates as Promising Anticancer Agents

§ 2.1 Introduction

A serious drawback in conventional anticancer drugs is the lack of tumor-specificity, which causes undesirable side effects. The development of 'tumor-targeting prodrugs', based on a conjugate of a cytotoxic drug to a tumor-specific molecule, is a promising approach to solve this problem. The prodrugs are premised to be inactive until it is delivered to the targeted tumor cells by the tumor-specific molecule and the drug could be released from the carrier to restore its original activity after internalization.[1]

Polyunsaturated fatty acids (PUFAs) are ideal candidates as tumor-targeting molecules. Representative naturally occurring PUFAs possess 18, 20, and 22 carbons, and 2-6 unconjugated *cis*-double bonds separated by one methylene, such as linolenic acid (LNA), linoleic acid (LA), arachidonic acid (AA), and docosahexaenoic acid (DHA).[2-4] These PUFAs are found in vegetable oils, cold-water fish, and meat. DHA is classified as a nutritional additive by the FDA in the US. Thus, DHA and its metabolites are considered to be safe to humans.[5-7] Perfusion studies of tissue isolated from hepatomas with a single arterial inflow and a single venous outflow demonstrated that some PUFAs are taken up more rapidly by tumor cells than by normal cells, presumably as biochemical precursors and energy sources.[8] In addition, PUFAs are readily incorporated into the lipid bilayer of cells, which results in disruption of membrane structure and fluidity.[9] This has been suggested to influence the chemosensitivity of tumor cells. These findings strongly suggest the benefit in the use of PUFAs for tumor-targeting drug delivery.
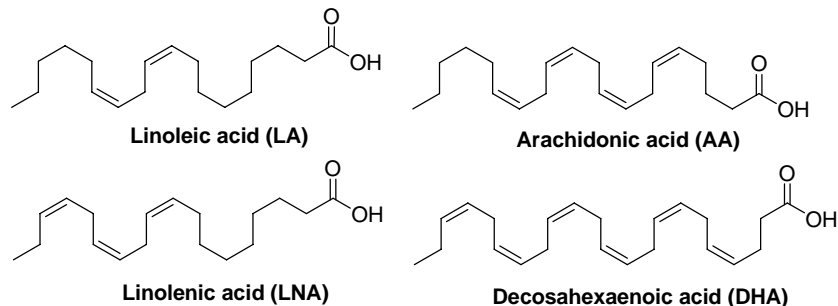
Figure 2-1. Polyunsaturated fatty acids (PUFAs)

Bradely *et al.* developed the conjugation of DHA and paclitaxel, which could target tumors and reduce toxicity to normal tissues.[10] The data showed that the conjugate possesses remarkably increased antitumor activity in animal models. In 2001, a phase II trial program started for the treatment of eight different types of cancer: breast, colon/rectum, kidney, lung, pancreas, prostate, skin and stomach. In 2002, the FDA allowed two separate phase III studies in metastatic melanoma and pancreatic cancer. The drug seems to be much less active as a cytotoxic agent until metabolized by cells to an active form, so 4.4-fold higher molar doses than paclitaxel can be delivered to mice. DHA-paclitaxel is primarily confined to the plasma compartment, and high concentrations are maintained in mouse plasma for long period of time. The pharmacokinetic studies in M109 tumor-bearing mice indicated that the concentration of DHA-paclitaxel in tumors is 8-fold higher than paclitaxel at equimolar doses and 57-fold higher at equitoxic doses. It is believed that DHA-paclitaxel may kill the slowly cycling

or residual tumor cells that eventually come into cycle, because DHA-paclitaxel remains in tumors for long times at high concentrations and is slowly converted to paclitaxel.[10] The results showed that DHA-paclitaxel eliminated all measurable tumor masses against M109 mouse lung carcinoma, while paclitaxel did not.[10]
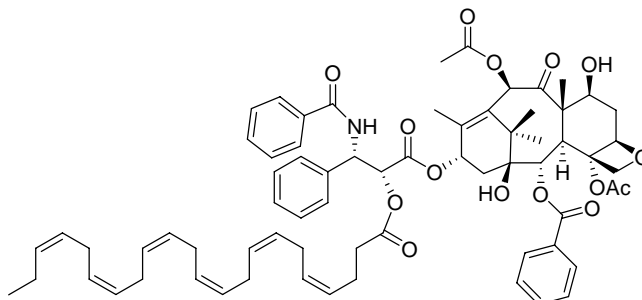
Figure 2-2. Taxoprexin® (DHA-paclitaxel)

Paclitaxel is efficient against breast, ovary, and lung cancers, but it does not show any efficacy against colon, pancreatic, melanoma, and renal cancers. Human colon carcinoma is multidrug-resistant due to the overexpression of P-glycoprotein (Pgp), which is an ATP-dependent drug-efflux pump that can transport a diverse range of hydrophobic compounds across the plasma membrane including paclitaxel and docetaxel.[10] In contrast with paclitaxel, several second-generation taxoids, such as **SB-T-101131**, **SB-T-1213**, **SB-T-1214** and **SB-T121303**, show excellent activity against drug resistant cancer cells. Although DHA-paclitaxel was found to be a weak substrate of Pgp as compared to paclitaxel, paclitaxel molecules released slowly was still caught by the Pgp efflux pump and eliminated from the cancer cells. Therefore, it would be beneficial to develop DHA conjugates of the second-generation taxoids.

Previous studies by our group indicate that one of the new DHA-taxoid conjugates exhibited even better activity against the drug-sensitive tumor A121 xenograft, compared to DHA-paclitaxel.[11] **DHA-SB-T-1213** (30 mg/Kg×3) delayed the tumor growth for more than 186 days and caused complete regression of tumor in all surviving (4 of 5) mice even at the non-optimized dose (**Figure 2-3**). **DHA-SB-T-1216** also delayed the growth of the tumor xenograft for >186 days, but 4 of 5 mice died at the same dose. DHA-paclitaxel also cured 2 of 5 mice, but the tumor recurred after 150 days in 3 of 5 mice.

In this chapter, a series of PUFA conjugates of the second-generation and advanced second-generation (third-generation) taxoids were synthesized, and they were evaluated against drug-resistant human colon tumor xenograft (Pgp+) DLD-1 in SCID mice.
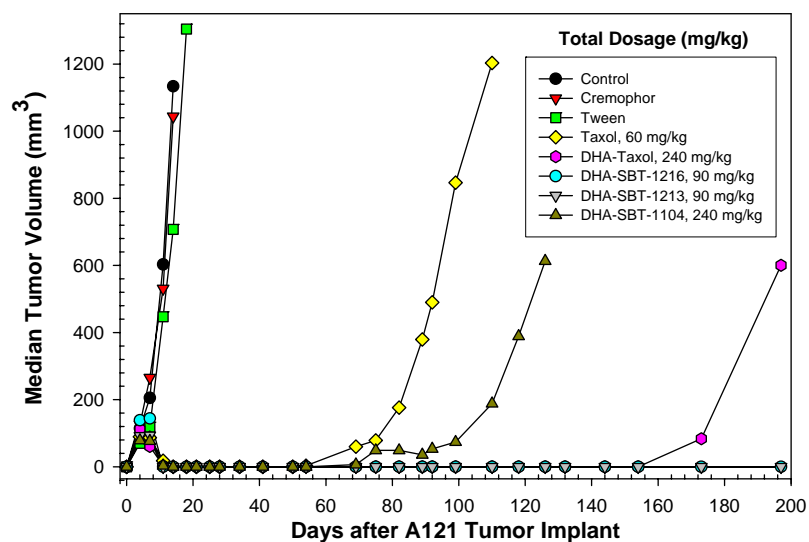
Figure 2-3. Effect of DHA-Taxoid conjugates on human ovarian tumor xenograft (Pgp-) A121[11]

§ 2.2 Results and Discussion

§ 2.2.1 Preparation of DHA-2nd-Generation-Taxoid Conjugates

The synthesis of the DHA-taxoid conjugates is straightforward. Because the C2'-OH is less sterically hindered than the corresponding C7-OH group,[11] direct coupling of DHA with a taxoid in the presence of DIC and DMAP gave the DHA-taxoid conjugates in high yields.

Scheme shows compound **2-1** plus R_3COOH, reacting with:

DIC (2.0 eq), DMAP(1.0 eq)
CH_2Cl_2, r.t., 1h

to give compound **2-2**.
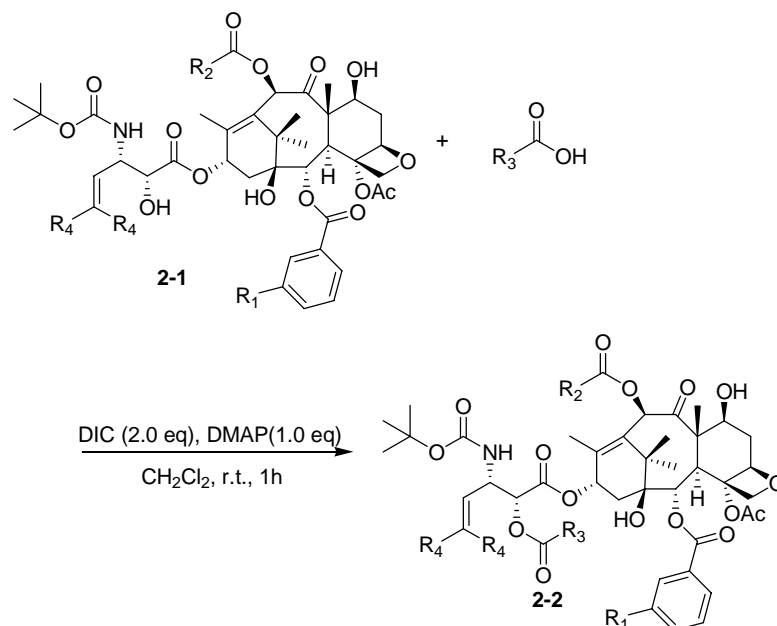
Conjugates	R_1	R_2	R_3COOH	R_4	Yield
a. LA-SB-T-1213	H	CH_3CH_2-	LA	CH_3	76%
b. LNA-SB-T-1213	H	CH_3CH_2-	LNA	CH_3	63%
c. DHA-SB-T-121303	MeO	CH_3CH_2-	DHA	CH_3	76%
d. LNA-SB-T-121303	MeO	CH_3CH_2-	LNA	CH_3	78%
e. LA-SB-T-1214	H	▷—	LA	CH_3	67%
f. LNA-SB-T-1214	H	▷—	LNA	CH_3	71%
g. DHA-SB-T-1214	**H**	▷—	**DHA**	**CH_3**	**87%**
h. DHA-SB-T-12851	H	CH_3-	DHA	F	90%
i. DHA-SB-T-12853	H	CH_3CH_2-	DHA	F	78%
j. DHA-SB-T-12854	H	⟩N—	DHA	F	76%

Scheme 2-1. Synthesis of PUFA second-generation taxoid conjugates

It is well known that the methylene groups between the double bonds are readily oxidized. DHA-taxoid conjugates are more stable in ethanol than in dichloromethane, while they are extremely unstable in the solid state. To increase the stability of DHA-taxoid conjugates, a small amount of antioxidants, vitamin E and vitamin C,[12] were added to the Tween 80 solution (or Cremophor solution only for DHA-paclitaxel) of the conjugates.

§ 2.2.2 Biological Evaluation of PUFA-2nd-Generation Taxoid Conjugates

The PUFA-taxoid conjugates were assayed for their efficacy against a drug-resistant human colon tumor xenograft (Pgp+) DLD-1 in SCID mice (**Tables 2-1**). As expected, paclitaxel and DHA-paclitaxel were totally ineffective against the drug-resistant (Pgp+) DLD-1 tumor xenograft (**Figure 2-4**). In contrast, **DHA-SB-T-1214** achieved complete regression of the DLD-1 tumor in 5 of 5 mice at 80 mg/kg dose administered on days 5, 8

and 11 (total dose 240 mg/Kg; tumor growth delay>187 days). This is a very promising result, which promotes this compound as a lead candidate for further preclinical studies. The activities of DHA-difluorovinyl-taxoid conjugates are still under investigation.[13]
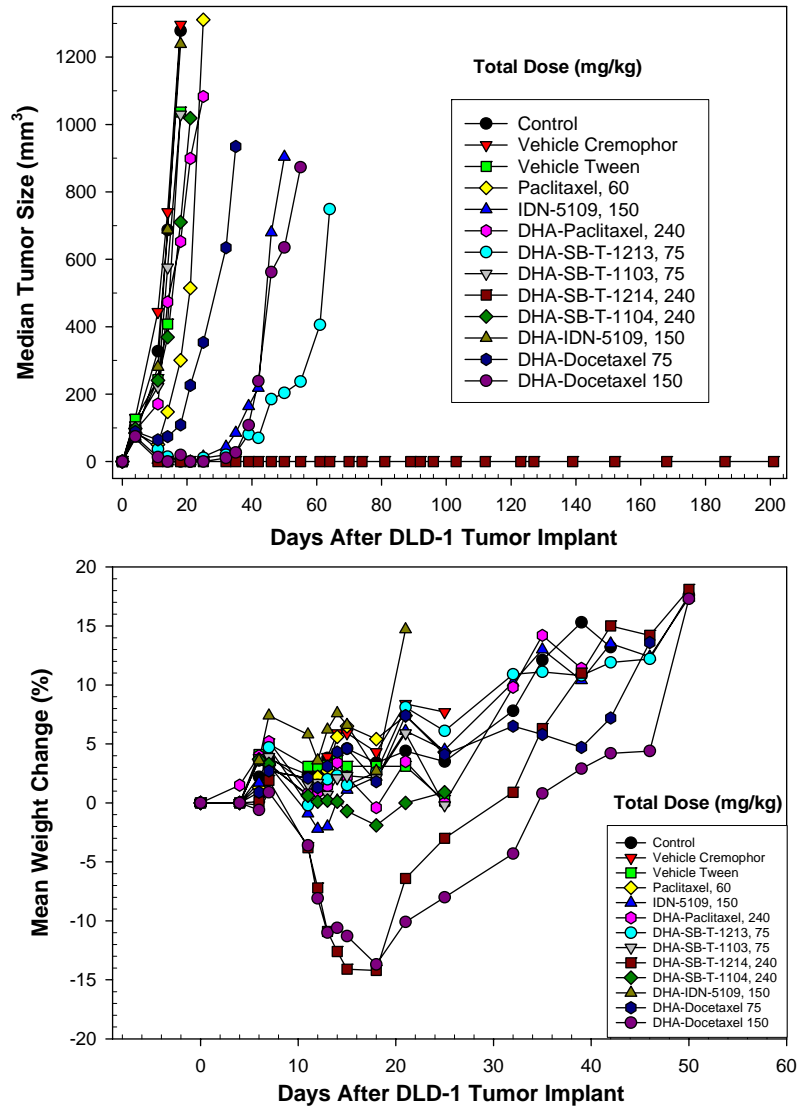
Figure 2-4. Effect of DHA-taxoid conjugates on human colon tumor xenograft (Pgp+) DLD-1[11]

Table 2-1. Antitumor effect of DHA-taxoid conjugates delivered *i.v.* to SCID mice bearing a Pgp+ human colon tumor xenograft, DLD-1

Treatment[a] (*i.v.*)	Total Dose (mg/kg)	Growth Delay (days)	Toxicity[b]	Cured mice[3]/ group
Control	0	---	0	0 / 7
Vehicle-Crem	0	--	0	0 / 3
Vehicle-Tween	0	--	0	0 / 3
Paclitaxel	60	8	0	0 / 3
DHA-Paclitaxel	240	4	0	0 / 5
DHA-SB-T-1213	75	54	0	0 / 5
DHA-SB-T-1103	75	4	0	0 / 5
DHA-SB-T-1214	240	>187	0	5 / 5
DHA-SB-T-1104	240	4	0	0 / 5
DHA-Docetaxel	75	17	0	0 / 4
DHA-Docetaxel	150	34	0	0 / 4

[a]Treatment given *i.v.* to SCID mice on days 5, 8 and 11 tumor implant, paclitaxel and DHA-paclitaxel formulated in Cremophor:EtOH; DHA-taxoid conjugates formulated in Tween:EtOH. [b]Number of animals that either died or lost greater than 20% body weight. [c]SCID mice with tumors less than 600 mm^3 after 201 days.

The impressive results obtained with DHA-taxoids prompted us to investigate the use of different PUFAs and their efficacy. The results are shown in **Table 2-2** and **Figure 2-5**. The conjugates of **SB-T-1213** with DHA, LNA and LA were synthesized and their efficacy against **DLD-1** colon tumor xenograft (Pgp+) was examined. **LA-SB-T-1213** and **LNA-SB-T-1213** exhibited strong antitumor activity, while paclitaxel was ineffective. **LNA-SB-T-1213** exhibited the complete regression in 2 of 5 mice tested against drug-resistant human colon tumor xenografts (Pgp+) **DLD-1** (tumor growth delay>109 days). Although the toxicity of **LNA-SB-T-1213** to the animals was higher than **DHA-SB-T-1213**, **LNA-SB-T-1213** exhibited better overall activity than **DHA-SB-T-1213** at the dose (not optimized) examined. **LA-SB-T-1213** did not show meaningful efficacy in the same assay, which revealed the marked difference between n-3 PUFA (LNA, DHA) and n-6 PUFA (LA). These results suggest that DHA is not the only PUFA that can be used for the PUFA-taxoid conjugates. The conjugates of advanced second-generation (third-generation) taxoid **SB-T-121303** with DHA and LNA are extremely toxic and all the mice died at the dose (not optimized) examined.

Table 2-2. Antitumor effect of PUFA-Taxoid conjugates delivered i.v. to SCID mice bearing a Pgp+ human colon tumor xenograft.[11]

Treatment[a] (*i.v.*)	Total Dose (mg/kg)	Growth Delay (days)	Toxicity[b]	Cured mice[c]/ group
Control	0	---	0	0 / 7
Vehicle-Crem	0	---	0	0 / 4
Vehicle-Tween	0	---	0	0 / 4
Paclitaxel	75	9	0	1 / 5
DHA-SB-T-1213	75	54	0	0 / 5
LNA-SB-T-1213	75	>109	2	2 / 5
LA-SB-T-1213	75	21	1	0 / 5

[a]Treatment given *i.v.* to SCID mice on days 5, 8 and 11 after DLD-1 human colon tumor implant. Paclitaxel formulated in Cremophor: EtOH; DHA-taxoid conjugate, LNA-taxoid conjugate and LA-taxoid conjugate formulated in Tween:EtOH.
[b]Number of animals who either died or lost greater than 20% body weight.
[c]SCID mice with no palpable tumor on day 120, end of experiment.
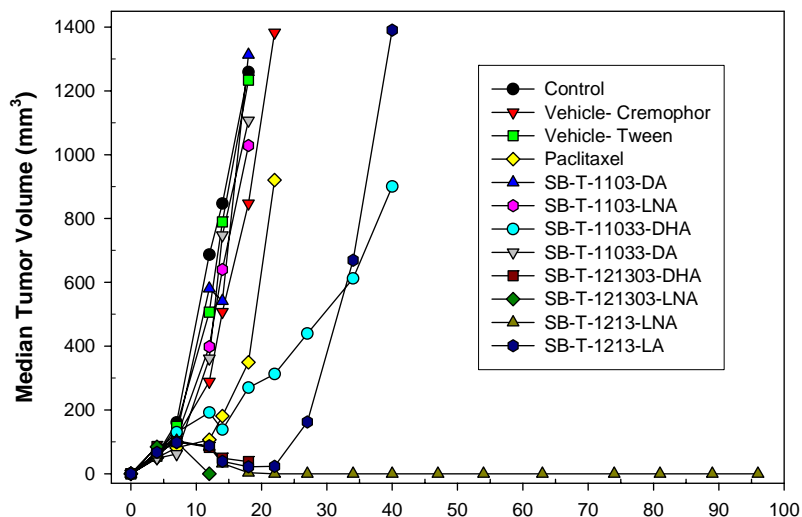
**Figure 2-5. Antitumor effect of PUFA–taxoid conjugates delivered iv
to SCID mice bearing a Pgp+ human colon tumor xenograft, DLD-1**[11]

§ 2.2.3 Docking Studies of DHA-SB-T-1214 in Human Serum Albumin (HSA)

Human serum albumin (HSA) is the most abundant human plasma protein, which contains a single polypeptide chain of 585 amino acids. HSA is composed of three structurally homologous domains (I, II,III).[14] Each domain contains 10 helices: helices 1–6 form subdomains A and helices 7–10 form subdomains B. Albumin is an important transport protein known to bind a wide variety of endogenous and exogenous compounds. Solution of the X-ray crystallographic structure of HSA facilitated the location of the two major drug binding sites, site I and site II, in subdomains IIA and IIIA of the protein, respectively.[15, 16]

Long-chain fatty acids (LCFAs) are among the main physiological ligands of HSA. They are able to bind in at least seven different sites on the protein and the binding to the five highest-affinity sites was proposed to be cooperative. LCFA binding to albumin induces considerable conformational changes and influences drug binding properties of the protein through direct competition and allosteric interactions.[17]

Due to its hydrophobic nature, paclitaxel binds to plasma proteins extensively.[18] Its interaction with human serum albumin was originally concluded to be non-specific with moderate affinity, and other evidence indicates high affinity binding to the site I.[18-21] Detailed knowledge of the paclitaxel-albumin interaction is important for the thorough understanding of the pharmacokinetic behavior of the drug and facilitates the design of analogues with more favorable pharmacological properties.

Very recently, Paal and coworkers performed docking experiments to search for potential high-affinity paclitaxel binding sites in two conformations of HSA: the fatty acid-free (HSA, 1UOR, **Figure 2-6a**) and the fatty acid-induced (FA-HSA, 1E7H, **Figure 2-6b**) conformations.[22, 23] Although different binding conformations were obtained using different conformations of the protein, the results provided further evidence for the high-affinity binding of paclitaxel to human serum albumin. The

predicted primary binding site was found to overlap with the drug binding site I of HSA, whereas the secondary site is near the heme binding site (**Figure 2-7**).
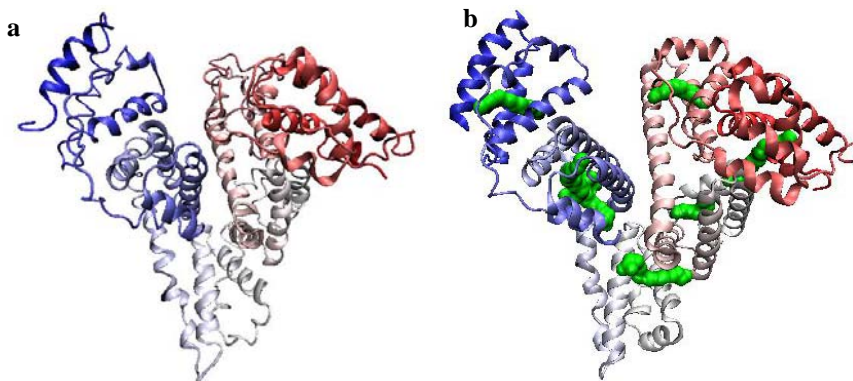
Figure 2-6. 1UOR (a) and 1E7H (b, with 7 palmitic acids in green)
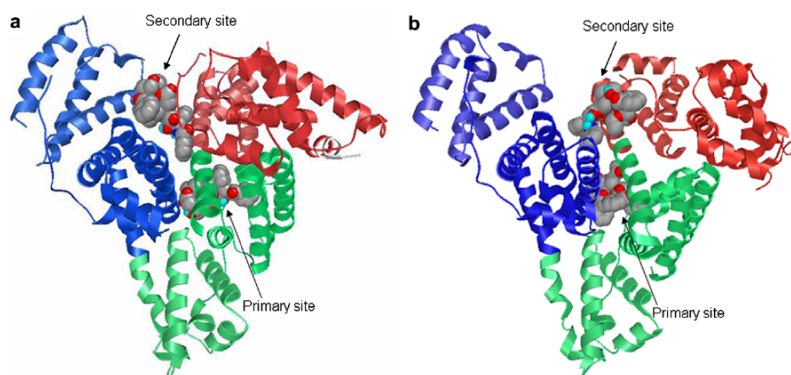
Figure 2-7. Docking results of paclitaxel in 1UOR and 1E7H

Because the DHA-taxoid conjugates are far more hydrophobic than paclitaxel or second-generation taxoids, they should bind to HSA in plasma. **SB-T-1214** and **DHA-SB-T-1214** were flexibly docked into the fatty acid-induced (FA-HSA, 1E7H) protein (the palmitic acids were removed before docking) using Dock 6® program.[24] However, because the two molecules are too flexible (containing too many rotatable bonds), the detailed binding conformations may not be reliable. Nevertheless, both molecules could bind to the primary and secondary binding sites of HSA, and the binding affinities to the primary binding site are higher than the ones to the secondary binding site.
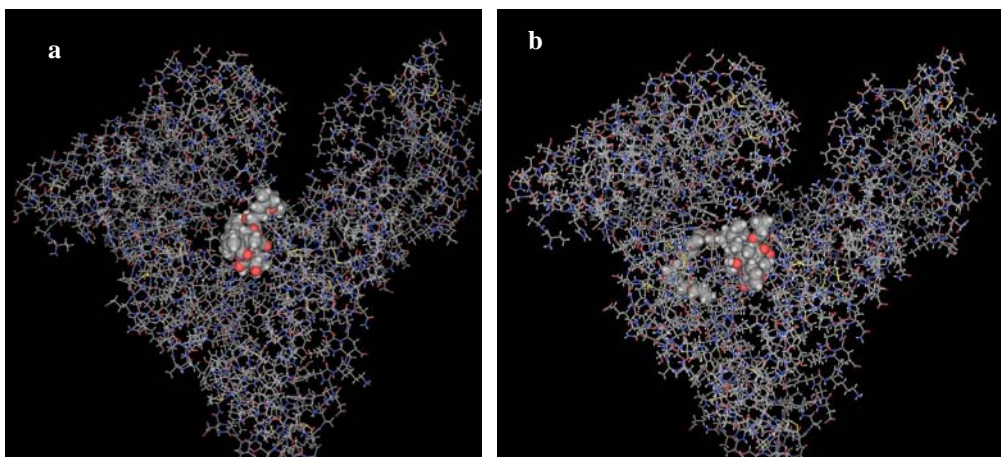
Figure 2-8. Docking results of SB-T-1214 (a) and DHA-SB-T-1214 (b) at the primary binding site of 1E7H

The taxoid part of **DHA-SB-T-1214** could bind to the primary binding site, and the DHA part could insert into one of the fatty acid binding sites. The binding affinity of **DHA-SB-T-1214** (**Figure 2-10**, -163.97 kcal/mol) is much higher than the one of **SB-T-1214** (**Figure 2-9**, -95.72 kcal/mol), which is mainly ascribed to the hydrophobic interaction between DHA and HSA. This docking study indicates that PUFA-2nd-generation taxoid conjugates will bind to HSA in plasma with high binding affinity.
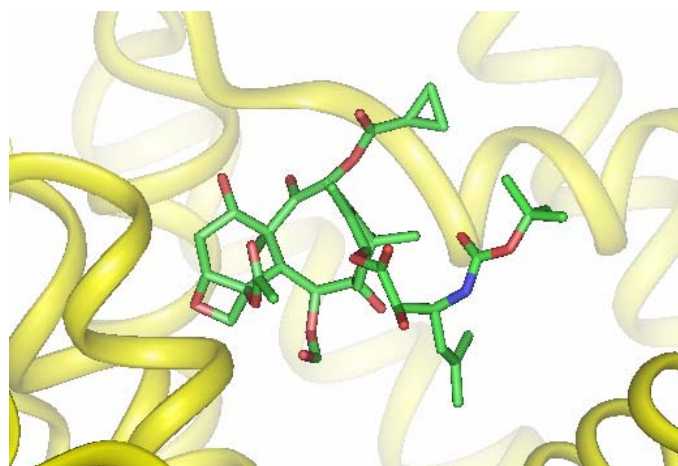
Figure 2-9. SB-T-1214 in HSA binding site (1E7H)
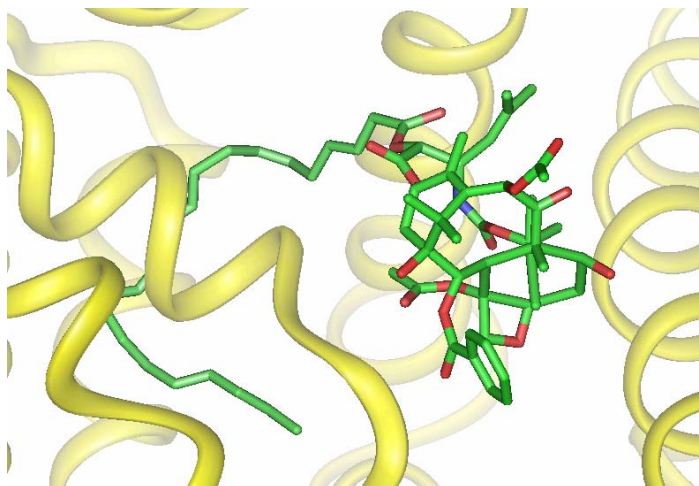
Figure 2-10. DHA-SB-T-1214 in HSA binding site (1E7H)

§ 2.3 Summary

PUFA-2nd-generation taxoid conjugates were synthesized through coupling of PUFAs, such as DHA, LNA and LA, with taxoids at the C2'-OH position and were evaluated against drug-sensitive and drug-resistant human tumor xenografts in SCID mice. **DHA-SB-T-1213** showed outstanding efficacy against the drug-sensitive A121 ovarian tumor xenograft. **DHA-SB-T-1214** caused complete regression of the tumor for the duration of experiment (201 days) in all treated animals bearing the drug-resistant DLD-1 human colon tumor xenograft. **LNA-SB-T-1213** also exhibited excellent efficacy against the DLD-1 tumor xenograft although the systemic toxicity of this conjugate was higher than that of **DHA-SB-T-1214**. These results demonstrate the exceptional efficacy of PUFA-2nd-generation taxoid conjugates against drug-sensitive and drug-resistant human tumor xenografts.

The docking studies indicated that **DHA-SB-T-1214** could bind to human serum albumin (HSA) with much higher binding affinity than **SB-T-1214**, although the exact binding conformation may be difficult to identify due to the high-flexibility of the compounds.

§ 2.4 Experimental Section

General Methods: ^{1}H, ^{13}C and ^{19}F NMR spectra were measured on a Varian 300, 400, 500, or 600 MHz NMR spectrometer. The melting points were measured on a "Uni-melt" capillary melting point apparatus from Arthur H. Thomas Company, Inc.. Optical rotations were measured on a Perkin-Elmer Model 241 polarimeter. High-resolution mass spectrametric analyses were conducted at the Mass Spectrometry Laboratory, University of Illinois at Urbana-Champaign, Urbana, IL. TLC analyses were performed on Merck DC-alufolien with Kieselgel 60F-254 and were visualized with UV light, iodine chamber, 10 % sulfuric acid and 10% PMA solution. Column chromatography was carried out on silica gel 60 (Merck; 230-400 mesh ASTM). Chemical purity was determined with a Waters HPLC assembly consisting of dual Waters 515 HPLC pumps, a PC workstation running Millennium 32, and a Waters 996 PDA detector, using a Phenomenex Curosil-B column, employing CH_3CN/water as the solvent system with a flow rate of 1 mL/min, or shimazu HPLC.

Materials: The chemicals were purchased from Aldrich Co. and Sigma and purified before use by standard methods. Dichloromethane was also distilled immediately prior to use under nitrogen from calcium hydride. The second-generation taxoids were synthesized from 10-DAB, as described in **Chapter I**.

General Procedure for synthesis of DHA-taxoid:
To a solution of **SB-T-1213** (70 mg, 0.083 mmol), DMAP (10 mg, 0.083 mol) and DIC (21 mg, 0.166 mol) in dichloromethane (5 ml) under nitrogen was added LA (26 mg, 0.091 mol). The reaction mixture was stirred at room temperature for 1 h. The reaction mixture was concentrated *in vacuo* and the residue was purified by column chromatography on silica gel (hexanes/EtOAc = 2:1) to afford 2'-Linoleyl-3'-dephenyl-3'-(2-methyl-1-propenyl)-10- propanoyldocetaxel (**2-2a**) as a white solid (78 mg, 76%).

2'-Linoleyl-3'-dephenyl-3'-(2-methyl-1-propenyl)-10-propanoyldocetaxel (LA-SB-T-1213, 2-2a):
76% yield; white solid; mp 55-57 $^{\circ}$C; ^{1}H NMR (400 MHz, CDCl$_3$) δ 0.89 (m, 5 H), 1.15 (s, 3 H), 1.23 (s, 3 H), 1.25 (s, 3 H), 1.25-1.35 (m, 14 H), 1.34 (s, 9 H), 1.67 (s, 3 H), 1.76 (s, 6 H), 1.85 (m, 1 H), 1.93 (s, 3 H), 2.04 (q, *J* = 6.4 Hz, 4 H), 2.36 (s, 3 H), 2.45 (m, 8 H) 2.53 (m, 3 H), 2.77 (t, *J* = 6.4 Hz, 2 H), 3.83 (d, *J* = 6.8 Hz, 1 H), 4.17 (d, *J* = 8.4 Hz, 1 H), 4.31 (d, *J* = 8.4 Hz, 1 H), 4.46 (dd, *J* = 10.6, 6.6 Hz, 1 H), 4.77 (d, *J* = 8.8 Hz, 1 H), 4.98 (m, 3 H), 5.19 (d, *J* = 8.0 Hz, 1 H), 5.36 (m, 4 H), 5.68 (d, *J* = 6.8 Hz, 1 H), 6.19 (t, *J* = 8.5 Hz, 1 H), 6.31 (s, 1 H), 7.48 (t, *J* = 7.6 Hz, 2 H), 7.60 (t, *J* = 7.6 Hz, 1 H), 8.12 (d, *J* = 7.6 Hz, 2 H); ^{13}C NMR (CDCl$_3$) δ 9.2, 9.7, 14.2, 14.3, 14.9, 18.7, 22.3, 22.6, 22.7, 22.8, 23.7, 24.9, 25.8, 26.8, 27.4, 27.4, 27.7, 28.4, 29.2, 29.3, 29.4, 29.5, 29.8, 29.9, 31.7, 34.0, 35.6, 35.7, 43.4, 45.8, 49.1, 58.7, 71.8, 72.3, 74.6, 75.4, 75.6, 76.6, 76.9, 79.5, 80.0, 81.2, 84.7, 120.2, 128.1, 128.3, 128.8, 129.5, 130.2, 130.4, 130.4, 132.6, 133.8, 138.1, 143.6, 155.0, 167.2, 168.6, 169.8, 173.1, 174.8, 204.2.

2'-Linolenoyl-3'-dephenyl-3'-(2-methyl-1-propenyl)-10-propanoyldocetaxel (LNA-SB-T-1213, 2-2b):

63% yield; white solid; mp 55-57 °C; $[\alpha]_D^{22}$ -54 (c 1.7, CHCl$_3$); ^{1}H NMR (400 MHz, CDCl$_3$) δ 0.99 (t, J = 7.65 Hz, 3 H), 1.15 (s, 3 H), 1.23 (s, 3 H), 1.25 (s, 3 H), 1.25-1.35 (m, 12 H), 1.34 (s, 9 H), 1.67 (s, 3 H), 1.76 (s, 6 H), 1.85 (m, 1 H), 1.93 (s, 3 H), 2.04 (q, J = 6.4 Hz, 4 H), 2.36 (s, 3 H), 2.45 (m, 8 H) 2.53 (m, 3 H), 2.77 (t, J = 6.4 Hz, 2 H), 3.82 (m, 3 H), 4.17 (d, J = 8.4 Hz, 1 H), 4.31 (d, J = 8.4 Hz, 1 H), 4.46 (dd, J = 10.6, 6.6 Hz, 1 H), 4.77 (d, J = 8.8 Hz 1 H), 4.98 (m, 3 H), 5.18 (d, J = 8.0 Hz, 1 H), 5.36 (m, 6 H), 5.68 (d, J = 6.8 Hz, 1 H), 6.19 (t, J = 8.5 Hz, 1 H), 6.31 (s, 1 H), 7.48 (t, J = 7.6 Hz, 2 H), 7.60 (t, J = 7.6 Hz, 1 H), 8.12 (d, J = 7.6 Hz, 2 H); ^{13}C NMR (CDCl$_3$, 400 MHz) δ 9.0, 9.5, 14.2, 14.7, 18.5, 20.5, 22.1, 22.4, 23.4, 24.7, 25.5, 25.6, 25.7, 26.6, 27.1, 27.5, 28.1, 29.0, 29.0, 29.1, 29.5, 29.6, 33.7, 35.4, 42.2, 43.1, 45.6, 58.4, 71.6, 72.1, 74.3, 75.2, 25.4, 76.3, 79.3, 80.9, 84.4, 120.0, 127.1, 127.7, 128.2, 128.3, 128.6, 129.3, 130.1, 130.2, 131.9, 132.4, 133.6, 137.9, 143.3, 154.8, 167.0, 168.3, 169.6, 172.9, 174.6, 204.0.

2'-Docosahexaenoyl-3'-dephenyl-3'-(2-methyl-2-propenyl)-2-debenzoyl-2-(3-methoxybenzoyl)-10-propanoyldocetaxel (DHA-SB-T-121303, 2-2c):

76% yield; white solid; mp 62-64 °C; $[\alpha]_D^{22}$ -53 (c 2.4, CHCl$_3$); ^{1}H NMR (CDCl$_3$, 400MHz) δ 0.97 (t, J =8.0, 3 H), 1.14 (s, 3 H), 1.28 (m, 8 H), 1.33 (s, 9 H), 1.66 (m, 3 H), 1.73 (s, 3 H), 1.75 (s, 3 H), 1.89 (m, 5 H), 2.04 (m, 2 H), 2.43 (m, 6 H), 2.55 (m, 7 H), 2.84 (m, 10 H), 3.83 (d, J = 6.9 Hz, 1 H), 3.87 (s, 3 H), 4.18 (d, J = 8.5 Hz, 1 H), 4.34 (d, J = 8.5 Hz, 1 H), 4.45 (dd, J = 10.6, 6.8 Hz, 1 H), 4.76 (m, 2 H), 4.99 (m, 2 H), 5.18 (d, J = 7.6 Hz, 1 H), 5.36 (m, 12 H), 5.66 (d, J = 7.0 Hz, 1 H), 6.19 (t, J = 8.6 Hz, 1 H), 6.30 (s, 1 H), 7.14 (d, J = 7.9 Hz, 1 H), 7.37 (t, J = 8.0 Hz, 1 H), 7.64 (s, 1 H), 7.70 (d, J = 7.6 Hz, 1 H); ^{13}C NMR (CDCl$_3$, 400 MHz) δ 9.0, 9.5, 14.7, 18.4, 20.5, 22.1, 22.4, 22.5, 23.4, 25.6, 25.6, 25.6, 26.6, 27.5, 28.1, 29.6, 33.6, 35.4, 42.2, 43.1, 45.5, 48.8, 55.3, 58.4, 71.6, 72.1, 74.5, 75.2, 75.4, 76.3, 79.2, 79.8, 81.0, 84.4, 114.4, 119.9, 120.2, 122.5, 126.9, 127.5, 127.8, 127.9, 128.0, 128.3, 128.4, 128.5, 129.6, 129.6, 130.5, 132.0, 132.4, 137.9, 143.3, 154.8, 159.6, 166.8, 168.2, 169.5, 172.3, 174.6, 204.0.

2'-Linolenoyl-3'-dephenyl-3'-(2-methyl-2-propenyl)-2-debenzoyl-2-(3-methoxybenzoyl)-10-propanoyldocetaxel (LNA-SB-T-121303, 2-2d):

78% yield; white solid; mp 58-59 °C; $[\alpha]_D^{22}$ -65 (c 1.7, CHCl$_3$); ^{1}H NMR (400 MHz, CDCl$_3$) δ 0.99 (t, J = 7.65 Hz, 3 H), 1.13 (s, 3 H), 1.16 (s, 3 H), 1.25 (s, 3 H), 1.25-1.35 (m, 8 H), 1.33 (s, 9 H), 1.66 (m, 3 H), 1.73 (s, 3 H), 1.75 (s, 3 H), 1.89 (m, 5 H), 2.10 (m, 4 H), 2.37 (m, 6 H), 2.52 (m, 4 H), 2.81 (m, 4 H), 3.80 (m, 3 H), 3.86 (s, 3 H), 4.19 (d, J = 8.8 Hz, 1 H), 4.35 (d, J = 8.8 Hz, 1 H), 4.40 (dd, J = 10.6, 6.8 Hz, 1 H), 4.75 (d, J = 8.8 Hz, 1 H), 4.96 (d, J = 8.3 Hz, 3 H), 5.19 (d, J = 8.4 Hz, 1 H), 5.36 (m, 6 H), 5.67 (d, J = 6.8 Hz, 1 H), 6.19 (t, J = 8.8 Hz, 1 H), 6.31 (s, 1 H), 7.14 (d, J = 6.0 Hz, 1 H), 7.38 (t, J = 7.6 Hz, 1 H), 7.67 (s, 1 H), 7.71 (d, J = 7.6 Hz, 1 H); ^{13}C NMR (CDCl$_3$, 400 MHz) δ 9.0, 9.5, 14.2, 14.7, 18.4, 20.5, 22.1, 22.3, 23.4, 24.7, 25.5, 25.6, 25.7, 26.6, 27.1, 27.5, 28.1, 29.0, 29.0, 29.1, 29.5, 29.6, 33.7, 35.4, 35.4, 42.2, 43.1, 45.5, 55.3, 58.4, 71.6, 72.1, 74.4, 75.2, 75.4, 76.3, 79.2, 81.0, 84.4, 114.4, 120.0, 120.2, 122.5, 127.0, 127.7, 128.2, 128.3, 129.6, 130.2, 130.5, 131.9, 132.4, 137.9, 143.3, 154.8, 159.6, 166.9, 168.3, 169.5, 172,9, 174.6, 204.0.

2'-Linoleyl-3'-dephenyl-3'-(2-methyl-1-propenyl)-10-cyclopropanecarbonyldocetaxel (LA-SB-T-1214, 2-2e):

67% yield; white solid; mp 73-75°C; [α]$_D^{22}$ −54 (c 1.0, CHCl$_3$); ^{1}H NMR (400 MHz, CDCl$_3$) δ 0.89 (t, J = 6.8 Hz, 3 H), 1.13 (m, 4 H), 1.16 (s, 3 H), 1.26 (s, 3 H), 1.25-1.35 (m, 14 H), 1.34 (s, 9 H), 1.64 (m, 2 H), 1.66 (s, 3 H), 1.76 (s, 1 H), 1.87 (m, 1 H), 1.92 (s, 3 H), 2.04 (q, J = 6.8 Hz, 4 H), 2.38 (s, 3 H), 2.45 (m, 2 H), 2.53 (m, 2 H), 2.77 (t, J = 6.8 Hz, 2 H), 3.81 (d, J = 6.8 Hz, 1 H), 4.17 (d, J = 8.4 Hz, 1 H), 4.31 (d, J = 8.4 Hz, 1 H), 4.44 (t, J = 7.2 Hz, 1 H), 4.76 (d, J = 9.2 Hz, 1 H), 4.98 (m, 3 H), 5.19 (d, J = 8.8 Hz, 1 H), 5.36 (m, 4 H), 5.68 (d, J = 7.2 Hz, 1 H), 6.19 (t, J = 8.4 Hz, 1 H), 6.30 (s, 1 H), 7.48 (t, J = 7.6 Hz, 2 H), 7.61 (t, J = 7.6 Hz, 1 H), 8.11 (d, J = 7.2 Hz, 2 H); ^{13}C NMR (100.5 Hz, CDCl$_3$) δ 9.1, 9.3, 9.5, 12.9, 14.0, 14.7, 18.5, 22.4, 22.5, 23.4, 24.7, 25.6, 25.7, 26.7, 27.1, 27.2, 27.7, 28.2, 29.0, 29.1, 29.1, 29.3, 29.6, 29.6, 31.5, 33.7, 35.4, 35.5, 43.1, 45.6, 58.5, 71.6, 72.1, 74.3, 75.2, 75.4, 79.3, 79.8, 80.9, 84.5, 120.0, 127.8, 128.0, 129.2, 129.9, 130.1, 130.2, 132.4, 133.6, 137.9, 143.5, 154.8, 167.3, 168.3, 169.6, 172.9, 175.1, 204.2.

2'-Linolenoyl-3'-dephenyl-3'-(2-methyl-1-propenyl)-10-cyclopropanecarbonyldocetaxel (LNA-SB-T-1214, 2-2f):

71% yield; white solid; mp 71-73 °C; [α]$_D^{22}$ -57 (c 0.94, CHCl$_3$); ^{1}H NMR (400 MHz, CDCl$_3$) δ 0.98 (t, J = 6.8 Hz, 3 H), 1.14 (m, 4 H), 1.26 (s, 6 H), 1.25-1.35 (m, 8 H), 1.34 (s, 9 H), 1.64 (m, 2 H), 1.66 (s, 3 H), 1.78 (s, 1 H), 1.87 (m, 1 H), 1.93 (s, 3 H), 2.04 (q, J = 6.8 Hz, 4 H), 2.38 (s, 3 H), 2.45 (m, 4 H), 2.59 (m, 2 H), 2.81 (t, J = 6.8 Hz, 4 H), 3.81 (d, J = 6.8 Hz, 1 H), 4.18 (d, J = 8.0 Hz, 1 H), 4.31 (d, J = 8.0 Hz, 1 H), 4.44 (t, J = 7.2 Hz, 1 H), 4.76 (d, J = 9.2 Hz, 1 H), 4.98 (m, 3 H), 5.19 (d, J = 8.8 Hz, 1 H), 5.36 (m, 6 H), 5.68 (d, J = 7.2 Hz, 1 H), 6.19 (t, J = 8.4 Hz, 1 H), 6.30 (s, 1 H), 7.48 (t, J = 7.6 Hz, 2 H), 7.61 (t, J = 7.6 Hz, 1 H), 8.11 (d, J = 7.2 Hz, 2 H); ^{13}C NMR (100.5 Hz, CDCl$_3$) δ 9.1, 9.3, 9.5, 12.9, 14.2, 14.7, 18.5, 20.5, 22.3, 24.7, 25.5, 25.6, 25.7, 26.7, 27.1, 28.1, 29.0, 29.0, 29.1, 29.5, 29.6, 33.7, 35.4, 35.5, 43.1, 45.6, 58.4, 71.6, 72.1, 74.3, 75.2, 75.4, 76.3, 79.3, 80.9, 84.5, 120.0, 127.0, 127.7, 128.2, 128.3, 128.6, 129.2, 130.1, 130.2, 131.9, 132.4, 133.6, 137.9, 143.5, 154.8, 167.0, 168.3, 169.6, 172.9, 175.1, 204.1.

2'-Docosahexaenoyl-3'-dephenyl-3'-(2-methyl-1-propenyl)-10-cyclopropanecarbonyl-docetaxel (DHA-SB-T-1214, 2-2g):

87 % yield; white solid; mp 64-67 °C, [α]$_D^{22}$ -52.2 (c 1.8, CHCl$_3$); ^{1}H NMR (CDCl$_3$) δ 0.99 (t, J = 7.5 Hz, 3 H), 1.15 (m, 4 H), 1.28 (s, 3 H), 1.36 (s, 9 H), 1.68 (s, 3 H), 1.75 (m, 1 H), 1.78 (s, 6 H), 1.93 (m, 1 H), 1.95 (s, 3 H), 2.09 (q, J = 7.5, 15.0 Hz, 2 H), 2.39 (s, 3 H), 2.48 (m, 2 H), 2.56 (m, 2 H), 2.65 (d, J = 3.9 Hz, 1 H), 2.87 (m, 10 H), 3.83 (d, J = 6.9 Hz, 1 H), 4.20 (d, J = 8.7 Hz, 1 H), 4.33 (d, J = 8.1 Hz, 1 H), 4.46 (m, 1 H), 4.82 (d, J = 8.8 Hz, 1 H), 4.95 (s, 1 H), 4.99 (d, J = 9.3 Hz, 1 H), 5.21 (d, J = 7.8 Hz, 1 H), 5.41 (m, 12 H), 5.69 (d, J = 7.2 Hz, 1 H), 6.21 (t, J = 8.8 Hz, 1 H), 6.32 (s, 1 H), 7.50 (t, J = 8.1 Hz, 2 H), 7.63 (t, J = 7.5 Hz, 1 H), 8.13 (d, J = 7.2 Hz, 2 H); ^{13}C NMR (CDCl3) δ 9.1, 9.3, 9.4, 9.5, 12.9, 14.2, 14.7, 14.8, 18.4, 18.5, 20.5, 22.2, 22.3, 22.4, 25.5, 25.7, 26.6, 28.1, 28.1, 29.6, 33.6, 35.4, 43.1, 45.5, 45.5, 48.8, 58.4, 71.7, 72.1, 74.4, 74.5, 75.1, 75.3, 75.4, 76.3, 79.2, 79.8, 80.9, 84.4, 84.5, 119.9, 127.5, 127.8, 128.0, 128.2, 128.6, 129.2, 129.5, 130.1, 132.4, 133.5, 137.9, 143.4, 154.9, 166.9, 168.3, 169.6, 172.2, 175.1, 204.1.

10-Acetyl-2'-docosahexaenoyl-3'-dephenyl-3'-(2,2-difluorovinyl)docetaxel (DHA-SB-T-12851, 2-2h):

90% yield; as white solid; mp 60-62 °C; $[\alpha]_D^{21}$ -56.0 (c 1.2, CHCl$_3$); ^{1}H NMR (CDCl$_3$, 400 MHz) δ 0.97 (t, *J* = 7.6 Hz, 3 H), 1.14 (s, 3 H, 1.25 (s, 3 H), 1.32 (s, 9 H), 1.62 (s, 1 H), 1.67 (s, 3 H), 1.88 (m, 1 H), 1.93 (s, 3 H), 2.07 (t, *J* = 7.6 Hz, 2 H), 2.23 (s, 3 H), 2.23 (m, 1 H), 2.44 (s, 4 H), 2.45 (2, 1 H), , 2.48 (m, 3 H), 2.55 (m, 2 H), 2.85 (m, 10 H), 3.82 (d, *J* = 6.8 Hz, 1 H), 4.18 (d, *J* = 8.4 Hz, 1 H), 4.32 (d, *J* = 8.4 Hz, 1 H), 4.40 (m, 1 H), 4.44 (m, 1 H), 4.98 (m, 4 H), 5.40 (m, 12 H), 5.68 (d, J = 6.8 Hz, 1 H), 6.26 (t, J = 9.2 Hz, 1 H), 6.29 (s, 1 H), 7.50 (t, J = 7.6 Hz, 2 H), 7.61 (t, J = 7.6 Hz, 1 H), 8.13 (d, J = 7.6 Hz, 2 H); ^{13}C NMR (CDCl$_3$, 75.5 MHz) δ 9.8, 14.6, 15.1, 20.8, 21.1, 21.1, 22.4, 22.5, 22.7, 25.8, 25.9, 27.0, 28.4, 30.0, 33.8, 35.7, 35.8, 43.5, 45.9, 58.8, 72.0, 72.4, 74.3, 75.4, 75.9, 76.7, 79.5, 80.9, 81.2, 84.7, 127.3, 127.6, 128.1, 128.3, 128.6, 128.7, 128.9, 129.0, 129.4, 130.1, 130.5, 132.3, 133.0, 133.9, 143.3, 154.0, 154.9, 156.9, 159.8, 167.4, 167.6, 170.1, 171.5, 172.2, 204.1; ^{19}F NMR, (CDCl$_3$, 282 MHz) δ -85.3 (d, J = 36.7 Hz, 1 F), -83.6 (dd, J = 33.6, 24.5 Hz, 1 F); MALDI-TOF/MS (*m/z*): 1168.756 ([M+Na]$^+$, calcd 1168.54); C$_{63}$H$_{81}$F$_2$NO$_{16}$ (1145.55).

2'-Docosahexaenoyl-3'-dephenyl-3'-difluorovinyl-10-propanoyldocetaxel (DHA-SB-T-12853, 2-2i):

78% yield; white solid; mp 57-58 °C; $[\alpha]_D^{22}$ -57.6 (*c* 2.5, CHCl$_3$); ^{1}H NMR (500 MHz, CDCl$_3$) δ 0.97 (t, *J*= 7.5 Hz, 3 H), 1.14 (s, 3 H), 1.24 (m, 6 H), 1.32 (s, 9 H), 1.67 (s, 3 H), 1.88 (m, 1 H), 1.93 (s, 3 H), 2.11 (m, 2 H), 2.22-2.40 (m, 2 H), 2.39 (s, 3 H), 2.41-2.61 (m, 5 H), 2.85 (m, 10 H), 3.82 (d, *J* = 7.0 Hz, 1 H), 4.18 (d, *J* = 8.0 Hz, 1 H), 4.31 (d, *J* = 8.0 Hz, 1 H), 4.38-4.47 (m, 2 H), 4.93-5.07 (m, 4 H), 5.30-5.46 (m, 12 H), 5.67 (d, *J* = 7.5 Hz, 1 H), 6.26 (t, *J* = 8.0 Hz, 1 H), 6.31 (s, 1 H), 7.50 (t, *J* = 7.0 Hz, 2 H), 7.61 (t, *J* = 7.0 Hz, 1 H), 8.12 (d, *J* = 7.0 Hz, 2 H); ^{13}C NMR (75.45 MHz, CDCl$_3$) δ 9.0, 9.6, 14.3, 14.7, 20.8, 22.1, 22.2, 22.4, 25.5, 25.6, 25.7, 26.7, 27.5, 28.1, 33.6, 35.3, 35.4, 35.5, 43.2, 45.6, 58.5, 71.7, 72.2, 74.0, 75.1, 75.4, 76.8, 77.2, 79.3, 80.6, 80.9, 84.4, 126.9, 127.3, 127.8, 128.0, 128.3, 128.5, 128.6, 128.7, 129.1, 129.8, 130.2, 132.0, 132.7, 133.6, 142.8, 154.6, 167.1, 167.3, 169.8, 171.9, 174.6, 203.9; ^{19}F NMR, (CDCl$_3$, 282 MHz) δ −83.55 (1 F, dd, *J*= 24.0, 34.9 Hz), −85.34 (1 F, d, *J*= 34.7 Hz). LRMS (ESI) *m/z* calcd for C$_{64}$H$_{83}$F$_2$NO$_{16}$H$^+$ 1160.6, found 1160.6; (MALDI) *m/z* calcd for C$_{64}$H$_{83}$F$_2$NO$_{16}$Na$^+$ 1182.557, found 1182.767.

2'-Docosahexaenoyl-3'-dephenyl-3'-difluorovinyl-10-(*N,N*-dimethylcarbamoyl) docetaxel (DHA-SB-T-12854, 2-2j):

77% yield; white solid; mp 53-55 °C; $[\alpha]_D^{22}$ -57.6 (*c* 2.5, CHCl$_3$); ^{1}H NMR (500 MHz, CDCl$_3$) δ 0.97 (t, *J*= 7.5 Hz, 3 H), 1.14 (s, 3 H), 1.24 (m, 6 H), 1.31 (s, 9 H), 1.67 (s, 3 H), 1.88 (m, 1 H), 1.95 (s, 3 H), 2.07 (m, 2 H), 2.22-2.40 (m, 2 H), 2.39 (s, 3 H), 2.41-2.61 (m, 3 H), 2.85 (m, 10 H), 2.95 (s, 3 H), 3.02 (s, 3 H), 3.23 (d, *J* = 2.4 Hz, 1 H), 3.81 (d, *J* = 7.6 Hz, 1 H), 4.18 (d, *J* = 8.4 Hz, 1 H), 4.31 (d, *J* = 8.4 Hz, 1 H), 4.37-4.50 (m, 2 H), 4.93-5.07 (m, 4 H), 5.30-5.46 (m, 12 H), 5.67 (d, *J* = 7.5 Hz, 1 H), 6.25 (s, 1 H), 6.28 (t, *J* = 9.2 Hz, 1 H), 7.50 (t, *J* = 7.6 Hz, 2 H), 7.61 (t, *J* = 7.2 Hz, 1 H), 8.12 (d, *J* = 7.2 Hz, 2 H); ^{13}C NMR (75.45 MHz, CDCl$_3$) δ 9.4, 14.2, 14.8, 20.5, 22.2, 22.4, 22.5, 22.6, 23.4, 25.5, 25.6, 25.7, 26.9, 28.1, 29.7, 33.6, 35.3, 35.4, 35.9, 36.6, 43.2, 45.6, 58.4, 71.8, 72.4,

74.0, 75.3, 76.1, 76.4, 77.2, 79.4, 80.6, 81.0, 84.7, 126.9, 127.3, 127.7, 127.8, 128.0, 128.1, 128.2, 128.3, 128.4, 128.6, 128.7, 129.2, 129.4, 129.8, 130.2, 132.0, 133.0, 133.6, 143.3, 156.1, 167.2, 167.3, 169.8, 171.8, 205.8; ^{19}F NMR (CDCl$_3$, 376 MHz) δ −83.55 (1 F, dd, $J=$ 24.0, 34.9 Hz), −85.34 (1 F, d, $J=$ 34.7 Hz). LRMS (ESI) m/z calcd for C$_{64}$H$_{84}$F$_2$N$_2$O$_{16}$H$^+$ 1175.6, found 1175.6; (MALDI) m/z calcd for C$_{64}$H$_{84}$F$_2$N$_2$O$_{16}$Na$^+$ 1197.568, found 1197.662.

Drug preparation for *in vivo* experiments
(Dr. Ralph J. Bernacki's Laboratory, Roswell Park Cancer Institute):
Paclitaxel and DHA-Paclitaxel was prepared as a 7.5 mg/mL stock solution in equal parts of Cremophor ELP (BASF, Ludwigshafen, Germany) and absolute ethanol. These were used for comparison purposes. DHA-taxoids and other omega-3 fatty acid-taxoids were prepared as a 30 mg/mL stock solution in equal parts of Tween 80 (polyoxyethylene-sorbitan monooleate; purchased from Sigma Chemical Company) and absolute ethanol. To stabilize the formulation of the DHA-taxoids and other omega-3 fatty acid-taxoids, antioxidants, L-ascorbic acid (3.9 mM) and α-tocopherol (2.0 mM), were added. Each stock solution was further diluted before use in 0.9% NaCl (saline) so that the appropriate concentration of each drug could be injected iv via the tail vein, in a volume of approximately 0.4 mL for a 20 g mouse. Each drug was administered once a day on day 5, 8, and 11.

Animals and tumor xenografts
(Dr. Ralph J. Bernacki's Laboratory, Roswell Park Cancer Institute):
Female severe combined immune deficient, (SCID) mice aged six to eight weeks were obtained from either the in-house breeding facility at Roswell Park Cancer Institute or Taconic (Germantown, NY), all aspects of animal care complied with the Institutional Animal Care and Use Committee guidelines. Either the human ovarian tumor A121, which does not express the mdr protein pgp, or the human colon tumor DLD-1 which does express pgp, were used. Tumors were initiated by implantation of approximately 50 mg of non-necrotic tumor fragments on the right flank using a 12-guage trocar needle. Chemotherapy was started when the tumor was established as a palpable mass, (approximately 50-100 mm3 size). Therapy consisted of *i.v.* injections through the tail vein, given four times, three days apart. Each drug treatment group or drug free vehicle consisted of 4-5 mice per group, untreated controls contained 10 mice per group.

Drug preparation for *in vivo* experiments
(Dr. Ralph J. Bernacki's Laboratory, Roswell Park Cancer Institute):
Taxoids and DHA-Taxoids were prepared as a 30 mg/mL stock solution in equal parts of Tween 80 (polyoxyethylene-sorbitan monooleate; purchased from Sigma Chemical Company) and absolute ethanol. To stabilize the formulation of the DHA-taxoids, antioxidants, L-ascorbic acid (3.9 mM) and α-tocopherol (2.0 mM), were added. Each stock solution was further diluted before use in 0.9% NaCl (saline) so that the appropriate concentration of each drug could be injected *iv* via the tail vein, in a volume of approximately 0.4 mL for a 20 g mouse.

In vivo tumor growth assay
(Dr. Ralph J. Bernacki's Laboratory, Roswell Park Cancer Institute):
For each animal, the tumor length (l) and width (w), each in mm, were measured using electronic calipers and recorded every 3-4 days. Tumor volume (v), in mm^3, was calculated using the formula: $v = 0.4(l \times w2)$. The time in days to the pre-determined target tumor volume of 600 mm^3 was linearly interpolated from a plot of log(volume) versus time. Statistically significant differences in tumor volumes between control and drug-treated mice were determined by the Cox-Mantel test. For the Cox-Mantel test, the time-to-event data for animals that did not reach the target tumor volume, either because of long-term cure (defined as those animals that were still alive at the conclusion of the experiment whose tumors either completely regressed or did not reach the pre-set target volume) or early death due to drug toxicity, were treated as censored data. All statistical tests were two-sided.

Docking method:
Dock6® program was used for docking studies. **SB-T-1214** and **DHA-SB-T-1214** were created by the Build module of the InsightII2000® program and minimized by Macromodel 9.1 using MMFFs force field (GBSA). HSA X-ray crystal structure 1E7H was utilized for the docking experiments. All water and palmitic acid molecules were removed and the MOE® program was used to repair the PDB file (AMBER force field). The maps were centered on His242 (HE2) for the primary and the secondary binding sites of the ligands. Five hundred Genetic Algorithm (GA) runs were performed. Cluster analysis of the resulting conformations was performed by MOE® program. Clusters were ranked in order of increasing binding energy of the lowest binding energy conformation in each cluster. The most populated of the first five clusters was selected for further analysis and the lowest binding energy conformation of this cluster is referred to as the preferred conformation. The results are shown in **Table 2-3** and **Table 2-4**. After the "binding conformations" were obtained, the complexes were minimized by the Discover module of the InsightII2000 program with the backbone of the protein fixed (CVFF force field).

Table 2-3 Docking result of SB-T-1214 in 1E7H

Conformation	Gride Score (kcal/mol)	Cluster Size
1	-95.72	18
2	-95.31	1
3	-93.61	1
4	-93.60	1
5	-89.72	2
6	-88.86	2
7	-88.78	3
8	-88.61	3
9	-88.51	4
10	-88.50	1
11	-88.02	1
12	-87.32	4
13	-85.90	1
14	-85.25	1
15	-85.21	1
16	-84.61	1
17	-84.08	3
18	-83.63	1
19	-83.45	1

Table 2-4 Docking result of DHA-SB-T-1214 in 1E7H

Conformation	Gride Score (kcal/mol)	Cluster Size
1	-163.969467	33
2	-136.236313	1
3	-110.059265	1
4	-108.160019	1
5	-107.045341	1
6	-103.155701	1
7	-101.883072	1
8	-96.966202	1
9	-96.756226	1
10	-94.531914	1
11	-91.556854	1
12	-90.689056	1
13	-78.675949	1
14	-71.000969	1
15	-60.024208	1
16	-43.005062	1

§ 2.5 References

1. Ojima, I. Guided molecular missiles for tumor-targeting chemotherapy-case studies using the second-generation taxoids as warheads. *Acc. Chem. Res.* **2008,** 41, 108-119.
2. Hardman, W. E. Omega-3 fatty acids to augment cancer therapy. *J. Nutr.* **2002,** 132, 3508S-3512S.
3. Tapiero, H.; Nguyen Ba, G.; Couvreur, P.; Tew, K. D. Polyunsaturated fatty acids (PUFA) and eicosanoids in human health and pathologies. *Biomed. Pharmacother.* **2002,** 56, 215-222.
4. Morimoto, K. C.; Van Eenennaam, A. L.; DePeters, E. J.; Medrano, J. F. Hot topic: endogenous production of n-3 and n-6 fatty acids in mammalian cells. *J. Dairy Sci.* **2005,** 88, 1142-1146.
5. Moser, U. N-3 and N-6 PUFAS in healthy and diseased skin. *J. Appl. Cosmetol.* **2002,** 20, 137-142.
6. Heird, W. C.; Lapillonne, A. The role of essential fatty acids in development. *Annu. Rev. Nutr.* **2005,** 25, 549-571.
7. Harris, W. S. Omega-3 fatty acids. *Encycl. Diet. Suppl.* **2005**, 493-504.
8. Sauer, L. A.; Dauchy, R. T. The effect of omega-6 and omega-3 fatty acids on 3H-thymidine incorporation in hepatoma 7288CTC perfused in situ. *Br. J. Cancer* **1992,** 66, 297-303.
9. Takahashi, M.; Przetakiewicz, M.; Ong, A.; Borek, C.; Lowenstein, J. M. Effect of ω-3 and w-6 fatty acids on transformation of cultured cells by irradiation and transfection. *Cancer Res.* **1992,** 52, 154-62.
10. Bradley, M. O.; Webb, N. L.; Anthony, F. H.; Devanesan, P.; Witman, P. A.; Hemamalini, S.; Chander, M. C.; Baker, S. D.; He, L.; Horwitz, S. B.; Swindell, C. S. Tumor Targeting by Covalent Conjugation of a Natural Fatty Acid to Paclitaxel. *Clin Cancer Res.* **2001,** 7, 3229-3238.
11. Kuznetsova, L.; Chen, J.; Sun, L.; Wu, X.; Pepe, A.; Veith, J. M.; Pera, P.; Bernacki, R. J.; Ojima, I. Syntheses and evaluation of novel fatty acid-second-generation taxoid conjugates as promising anticancer agents. *Bioorg. Med. Chem. Lett.* **2006,** 16, 974-977.
12. Bradley, M. O.; Shashoua, V. E.; Webb, N. L.; Swindell, C. S. Compositions comprising conjugates of cis-docosahexaenoic acid and Taxotere. 9744026, **1997**.
13. Ojima, I. Preparation of fluorotaxoid-fatty acid conjugates for the treatment of cancer. 2007-US17806. 2008021242, 20070810., **2008**.
14. Peters, J. t. *All About Albumin: Biochemistry, Genetics, and Medical Applications.* **1995**; p 414 pp.
15. He, X. M.; Carter, D. C. Atomic structure and chemistry of human serum albumin. *Nature* **1992,** 358, 209-15.
16. Sudlow, G.; Birkett, D. J.; Wade, D. N. Further characterization of specific drug binding sites on human serum albumin. *Mol. Pharmacol.* **1976,** 12, 1052-61.
17. Bhattacharya, A. A.; Grune, T.; Curry, S. Crystallographic Analysis Reveals Common Modes of Binding of Medium and Long-chain Fatty Acids to Human Serum Albumin. *J. Mol. Biol.* **2000,** 303, 721-732.

18. Kumar, G. N.; Walle, U. K.; Bhalla, K. N.; Walle, T. Binding of taxol to human plasma, albumin and alpha 1-acid glycoprotein. *Res. Commun. Chem. Pathol. Pharmacol.* **1993,** 80, 337-4.

19. Purcell, M.; Neault, J. F.; Tajmir-Riahi, H. A. Interaction of taxol with human serum albumin. *Biochim. Biophys. Acta, Protein Struct. Mol. Enzymol.* **2000,** 1478, 61-68.

20. Paal, K.; Muller, J.; Hegedus, L. High affinity binding of paclitaxel to human serum albumin. *Eur. J. Biochem.* **2001,** 268, 2187-2191.

21. Trynda-Lemiesz, L. Paclitaxel-HSA interaction. Binding sites on HSA molecule. *Bioorg. Med. Chem.* **2004,** 12, 3269-3275.

22. Paal, K.; Shkarupin, A.; Beckford, L. Paclitaxel binding to human serum albumin - automated docking studies. *Bioorg. Med. Chem.* **2007,** 15, 1323-1329.

23. Paal, K.; Shkarupin, A. Paclitaxel binding to the fatty acid-induced conformation of human serum albumin - Automated docking studies. *Bioorg. Med. Chem.* **2007,** 15, 7568-7575.

24. http://dock.compbio.ucsf.edu/DOCK_6/index.htm.

Chapter III

Design, Synthesis and Biological
Evaluation of Macrocyclic Taxoids

§ 3.1 Introduction

Paclitaxel binds to the *β*-tubulin portion of the *α,β*-tubulin dimer, promotes the polymerization of tubulins, stabilizes the microtubules, and thus disrupts the cell mitosis cycle.[1] This mechanism of action, when it was revealed, was different from any traditional microtubule targeting anticancer drugs such as vinblastine or colchicines.[2] The novel mechanism of action of paclitaxel was later found to be shared by several other natural products. Epothilones A and B,[3] eleutherobin,[4] discodermolide,[5] laulimalide[6] and FR181277[7] showed activities comparable to that of paclitaxel in cytotoxicity assays and inhibition of microtubules disassembly in purified tubulin assembly assays (**Figure 3-1**).[8-10] Those compounds also competitively inhibit [³H]-paclitaxel binding to microtubules, which strongly suggests the existence of a common, or closely overlapping, binding site.[11, 12] The recognition of a pharmacophore common to all those microtubule-stabilizing agents (MSA) based on their binding conformations in tubulin could provide rationale and guidance for the design of the next-generation microtubule-stabilizing anticancer agents.
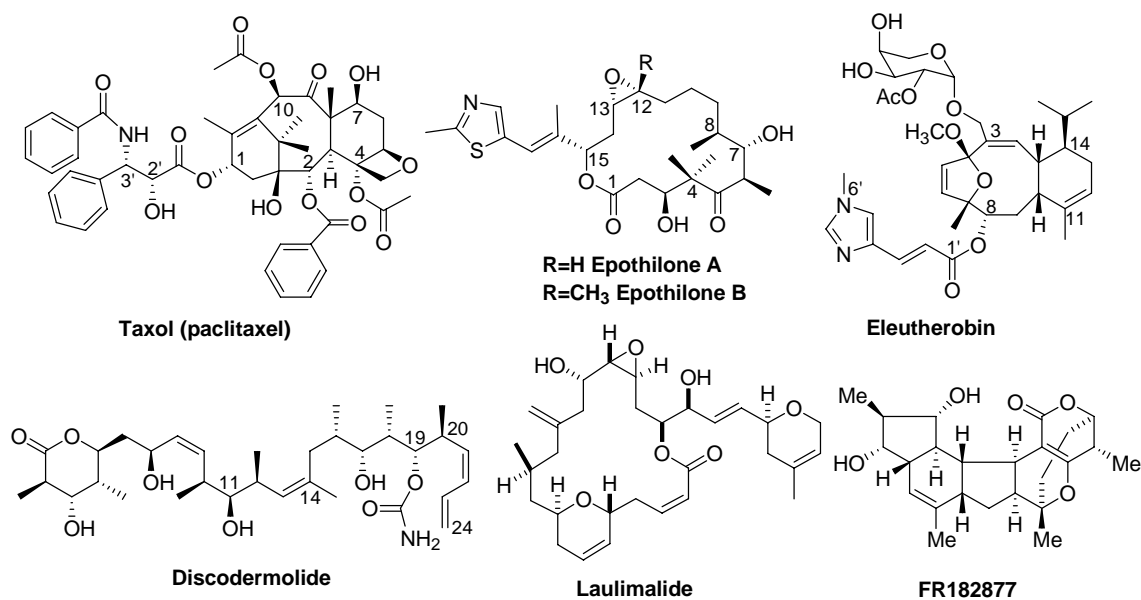
Figure 3-1. Naturally occurring microtubule-stabilizing agents

Although the mechanism of paclitaxel was well studied, the tubulin binding conformation of paclitaxel was not completely known. The major conformations of paclitaxel identified in solution or crystals so far can be divided into two categories: the polar conformation and the nonpolar conformation.

As shown in **Figure 3-2a**, the polar conformation features a hydrophobic clustering among the 3'-Ph, the 2-benzoate, and the 4-acetoxy groups. In this conformation, the C13 side-chain takes a gauche conformation in which the H2'-C2'-C3'-H3' torsion angle is approximately 180°. This conformation was first recognized based on 2D NMR experiments in DMSO-d_6/D$_2$O[13-15] and was found in the X-ray crystal structure of paclitaxel.[16] A similar conformation was used in Ojima's common pharmacophore proposal.[17]
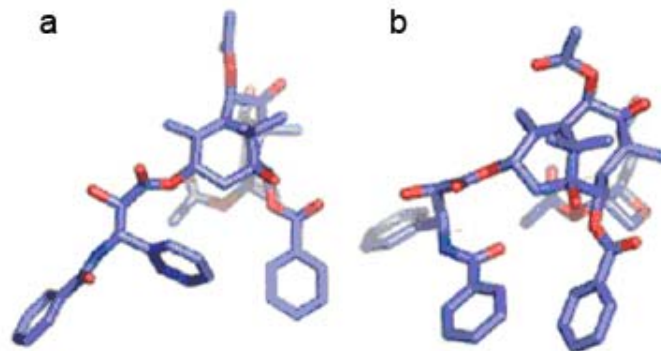
Figure 3-2. Polar conformation (a) and nonpolar conformation (b)
[Adapted from ref. 38]

The nonpolar conformation is represented by the one found in the X-ray crystal structure of docetaxel (**Figure 3-2b**).[18] The conformation features a clustering of 3'-benzoyl, 2-benzoate, and 4-acetoxy and has a gauche conformation with a H2'-C2'-C3'-H3' torsion angle of ~60°. This conformation is commonly observed in aprotic solvents such as $CDCl_3$ and CD_2Cl_2.[19-21] This conformation was proposed to be the likely bioactive conformation based on the assumption that the paclitaxel-binding site on microtubules is hydrophobic.[22]

During our structure-activity relationship (SAR) studies of paclitaxel analogues,[23, 24] we became interested in the investigation of bioactive conformation of paclitaxel and its congeners. Various approaches have been proposed and attempted to search for the "bioactive conformation", with which taxoids bind to the α,β-tubulin dimer. These studies have provided us with valuable information regarding the binding conformation of taxoids in the pocket of α,β-tubulin dimer as well as rationale in the design of future-generation paclitaxel-like novel anticancer agents.

Synthesis of conformationally restricted macrocyclic analogues is one of the widely used approaches in the investigation of bioactive conformation of organic compounds in their interaction with proteins.[25] The incorporation of different types of macrocycles into taxoid molecules will generate constraints and force the taxoid molecules to take certain conformations. By evaluating and comparing the biological activities of different types of macrocyclic taxoids, we could learn substantially about the binding interactions between the taxoids and the tubulins.

The ring-closing metathesis (RCM) reaction,[26] which was first used by Ojima's laboratory in this study, was proven to be the most effective method to create the constrained taxoids, compared to other methods, such as Heck reaction[27], disulfide (sulfide) formation[28], macrocyclic lactone formation[29] and peptide formation[30, 31]. The method was used later by our group as well as other groups to synthesize various macrocyclic taxoids.[17, 32-40] We have designed and synthesized a series of C2-C3'-linked macrocyclic conformationally constrained taxoids,[17, 32] which mimics the polar conformation.[13] Also a series of C2-C3'N linked macrocyclic taxoids have been designed and synthesized[33] to mimic the nonpolar conformation[19] (**Figure 3-3**). The resulting macrocyclic taxoids showed IC_{50} values ranging from micromolar to double-digit nanomolar.[17, 32 33]
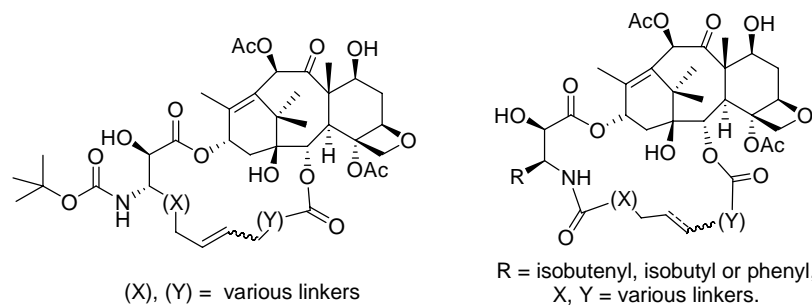
Figure 3-3. C2-C3'-linked and C2-C3'*N*-linked macrocyclic taxoids

14-Hydroxy-10-deacetylbaccatin[41] possesses an extra hydroxyl group at the C14 position and offers a new potential position for modification. Accordingly, a series of macrocyclic taxoids were designed bearing tethers connecting the C14 and the C3' position or the C3'*N* postion to mimic the polar conformation or the nonpolar conformation. The taxoids (**Figure 3-4**) are around 25 times less active than the parent compound paclitaxel.[42]
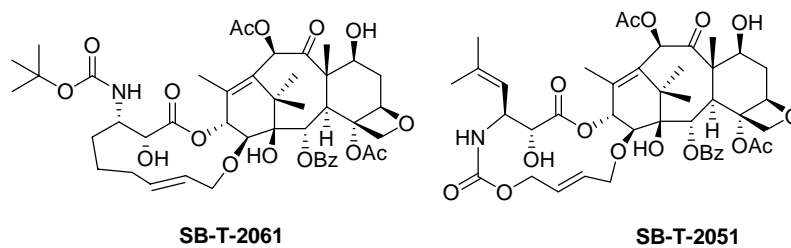
Figure 3-4. C14-C3'- and C14-C3'*N*-linked macrocyclic taxoids

In 1998, the electron crystallographic structure of paclitaxel-bound Zn$^+$-stabilized α,β-tubulin dimer was reported by Nogales *et al.* with 3.7 Å resolution (1TUB structure),[43] and later the resolution was refined to 3.5 Å resolution (1JFF structure).[44] In the 1TUB structure, the drug binding site was identified, which was consistent with the photolabeling studies,[45-47] but the resolution was not high enough to elucidate the binding conformation, so a docetaxel molecule taking nonpolar conformation was placed to show the binding site. In the 1JFF structure (**Figure 3-5**), paclitaxel molecule was actually placed in the binding site. However, the structure of the crucial *N*-benzoylphenylisoserine moiety at C13 was still difficult to determine with confidence due to the low diffraction level in the electron density map for this moiety, especially the C2-phenyl and C3'*N*-phenyl groups.[44]
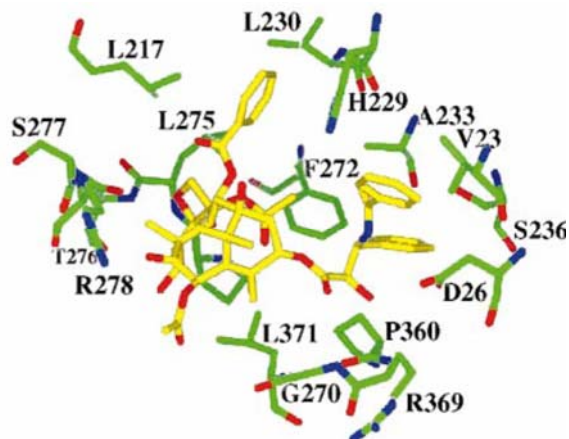
Figure 3-5. Tubulin-bound conformation of paclitaxel (1JFF)
[Adapted from ref. 44]

Based on the electron density map of the crystallographic structure of α,β-tubulin dimer (1TUB),[43] "T-shape" conformer of paclitaxel was reported by Snyder *et al* as the bioactive form in tubulin by molecular modeling study.[48] As shown in **Figure 3-6**, this conformation is much less compact than the nonpolar conformation[19] in that the C3'*N*-benzoylamino moiety is further away from the C2 benzoate. In this model, an amino acid residue in the binding pocket of β-tubulin, His227, is located between the C2 benzoate and the C3'*N*-phenyl group of taxoids. Accordingly, macrocycles connecting the C2 and the C3' or C3'*N* positions might bump into this His227 upon binding with β-tubulin. If this unfavorable interaction indeed exists, it might account for the lower activities of those macrocyclic taxoids.
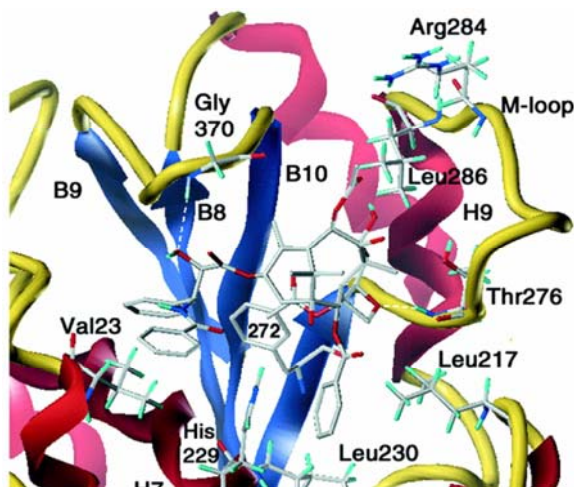
Figure 3-6. "**T-shape" paclitaxel binding conformation**
[Adapted from ref. 48]

To mimic the "T-Taxol" conformation, two conformationally restricted analogues of paclitaxel with linkers connecting the C4- and C3'- phenyl groups were designed and synthesized by the Kingston group. The synthesized analogues possess cytotoxicities ~ 10 times less potent than paclitaxel.[34]
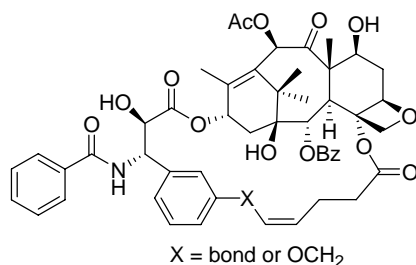
Figure 3-7. Kingston's C4-C3*m*'-linked macrocyclic paclitaxel analogues

In 2004, the Kingston group reported *ortho*-linked C3'-C4-bridged taxoids with 5-6 atoms in the bridge, which are more cytotoxic and have stronger binding with tubulin than paclitaxel (**Table 3-1**).[37] Later the C2-modified **K1a** analogues were synthesized, but they are not as active as **K1a**.[40] The resynthesis of **K1a** and **K2a** and comparison with our macrocyclic taxoids will be discussed in this chapter.
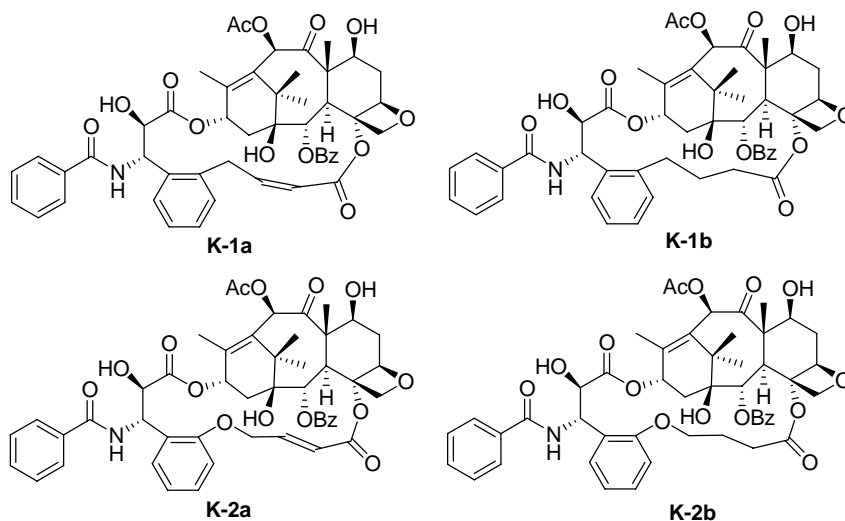
Figure 3-8. Kingston's C4-C3*o*'-linked macrocyclic paclitaxel analogues

Table 3-1. *In vitro* cytotoxicities and tubulin-binding assays of Kingston's macrocyclic taxoids[37]

Compound	IC_{50}/IC_{50}(Taxol) A2780	IC_{50}/IC_{50}(Taxol) PC3	ED50, Tb Polymerizatiom, [a] (µM)	Critical Tb concentration, [b] (µM)	Inhibit binding F-Taxol %
Paclitaxel	---[c]	---[d]	0.50+0.14	1.8+0.30	26
K-1a	0.045	0.69	0.30+0.09	0.53+0.07	72
K-1b	0.97	1	0.28+0.11	1.2+0.24	30
K-2a	0.08	0.67	0.21+0.09	0.35+0.06	79
K-2b	1.2	3.3	0.83+0.19	1.3+0.3	7

[a] Tublin concention, 5 µM ; [b] Taxoid concentration, 10 µM; [c] Taxol has IC_{50} values of 6–15 nM in this assay; [d] Taxol has an average IC_{50} value of 4 nM in this assay

The Dubois group also synthesized a series of C2-C3'*N*-linked macrocyclic taxoids to mimic the docetaxel with nonpolar conformation, and later to mimic the T-Taxol strcuture.[28, 35, 36] These compounds showed much less potency than paclitaxel, although one compound was claimed to have the same activity as paclitaxel in the microtubule

disassembly inhibitory experiment.[36] The biological evaluations of these taxoids are shown in **Table 3-2**.

1a: X=S, n=n'=4
1b: X=S-S, n=n'=3

2a: n=n'=2
2b: n=n'=3
2c: n=4, n'=3
2d: n=n'=4

3a: n=3, *para*
3b: n=4, *para*
3c: n=4, *meta*
3d: n=4, *ortho*
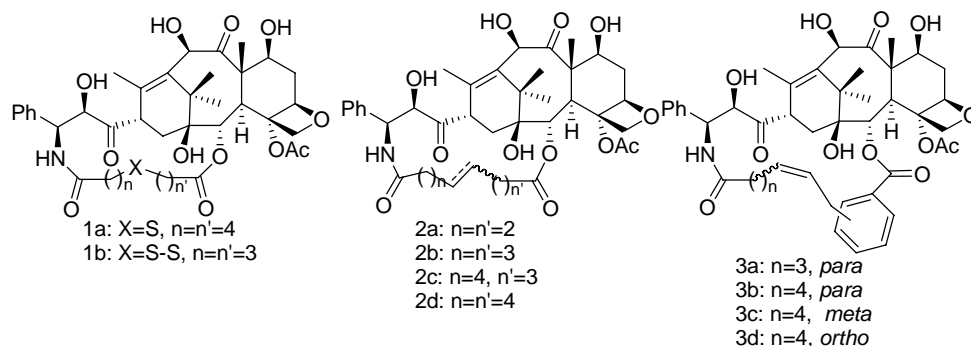
Figure 3-9. Dubois's C2-C3'*N*-linked macrocyclic taxoids

Table 3-2. *In vitro* cytotoxicities and microtubule disassembly inhibitory assays of the C2-C3*N*'-linked macrocyclic taxoids

Compound	Ring size	Microtubule disassembly inhibitory activity IC_{50}/IC_{50} (paclitaxel)[a]	Cytotoxicity against KB cell line[b] (μM)
paclitaxel	-	-	0.0006
docetaxel	-	0.5	0.0003
1a	21	42	45
1b	20	23	15
2a-*Z*	18	Inactive	>100
2a-*E*	18	Inactive	>100
2b-*Z*	20	Inactive	>100
2b-*E*	20	Inactive	45
2c	21	>100	14
2d	22	7	14
2(H)a	18	Inactive	>100
2(H)b	20	Inactive	55
2(H)c	21	30	13
2(H)d	22	45	23
3a	22	Inactive	1.6
3b	23	Inactive	0.28
3c-*E*	22	1	0.07
3c-*Z*	22	1.4	0.2
3d	21	6	0.7

[a]IC_{50} is the concentration that inhibits 50% of the rate of microtubule disassembly. The ratio IC_{50}/IC_{50}(paclitaxel) gives the activity with respect to paclitaxel. [b]IC_{50} measures the drug concentration required for the inhibition of 50% cell proliferation after 72 h of incubation. [c]**3c** showed a dose-response curve, but the 50% inhibition of microtubule disassembly was only achieved at high concentration (>100 μM).

Very recently, the same group synthesized a series of novel docetaxel analogues possessing a peptide side chain at the C2 position as well as peptide-bridged macrocyclic taxoids to mimic a region of the *α*-tubulin loop equivalent to the paclitaxel binding pocket of *β*-tubulin.[30, 31] One of the open chain taxoids possessed similar activity as paclitaxel, while none of the macrocyclic taxoids was as active as paclitaxel in cytotoxicity assay.
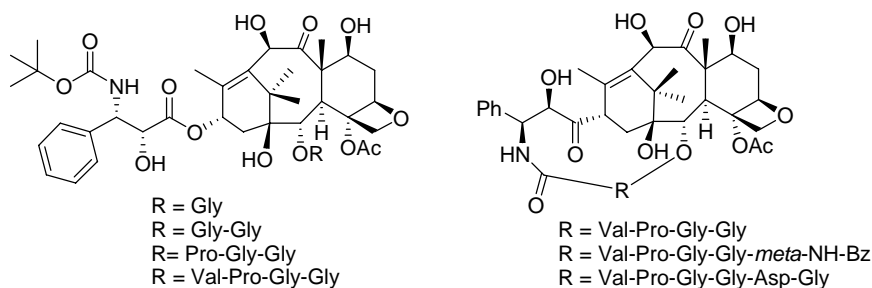
Figure 3-10. Dubois' C2-peptide and C2-C3'*N*-linked macrocyclic taxoids

In our efforts to study the bioactive conformation of taxoids and to design future-generation paclitaxel-like anticancer agents, Ojima's laboratory has proposed a binding conformation of paclitaxel based on docking studies of paclitaxel with α,β-tubulin dimer (**Figure 3-11**).[49] The "*Open-Gauche*" conformation is close to the one proposed by Snyder *et al*.[48]
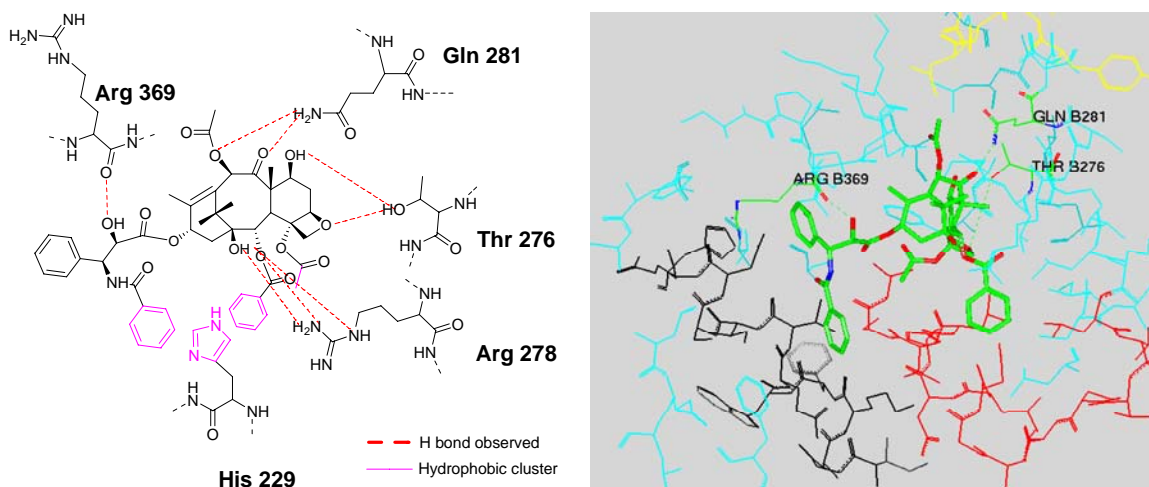
Figure 3-11. The "*Open-Gauche*" conformation[49]

Several conformationally restricted taxoids were synthesized to mimic this conformation. Upon examining the conformation described above, we found that the C4 acetyl group and the C2' position were spatially in close vicinity. Accordingly, we designed the C4-C2'-linked taxoids to mimic this conformation.[49] The structures of those taxoids are shown in **Figure 3-12**.
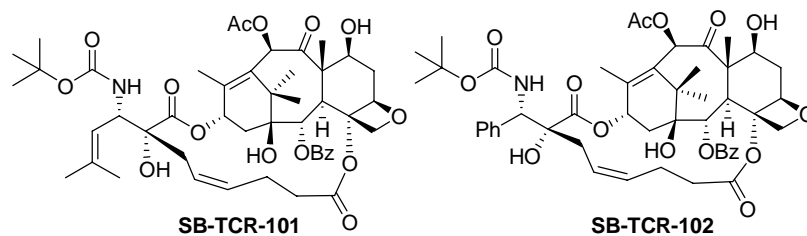
Figure 3-12. C4-C2'-linked macrocyclic taxoids

The synthesis, biological evaluation and molecular modeling studies of **SB-TCR-102** and other macrocyclic taxoids will be discussed in this chapter.

§ 3.2 Results and Discussion

§ 3.2.1 Synthesis and Biological Evaluation of C4-C2'-Linked Macrocyclic Taxoids

§ 3.2.1.1 Synthesis of SB-TCR-102

The synthesis of **SB-TCR-102** requires a β-lactam with a quaternary carbon center that posts certain difficulty in the synthesis. The retro-synthetic analysis of **SB-TCR-102** is shown in **Scheme 3-1**. Using the ring-closing metathesis (RCM) protocol,[26] macrocyclic taxoid could be obtained from diene **3-1**, which could be prepared through ring-opening coupling of β-lactam **3-3** with modified baccatin **3-2**. Baccatin **3-2** could be obtained from **10-DAB**.
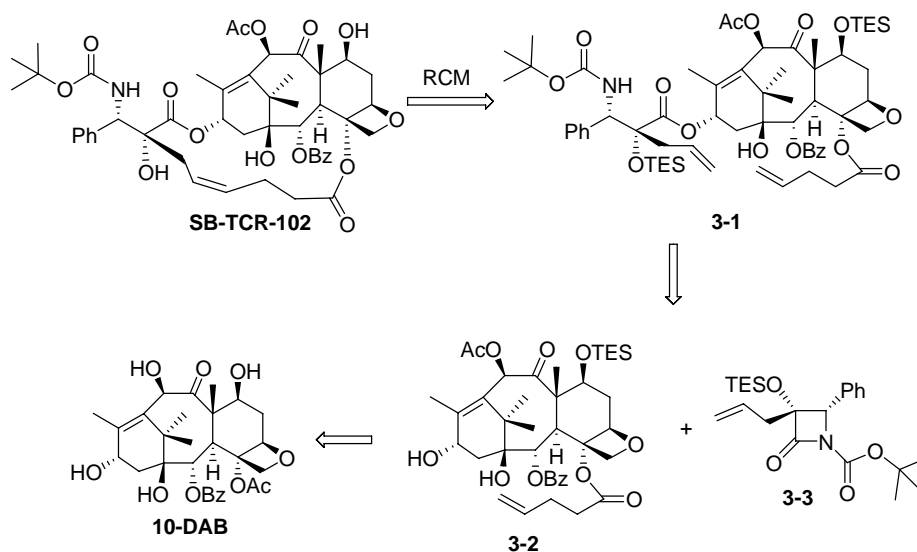
Scheme 3-1. Retro-synthesis of C4-C2'-linked macrocyclic taxoid SB-TCR-102

The C4 modification was carried out using a reported protocol with modifications.[50] The removal of the C4-acetyl group utilizes a Red-Al reductive removal protocol. However, in the Red-Al reduction conditions, the coordination of Red-Al with the C1-hydroxyl group leads to the chemoselective removal of C2-benzoate (**3-4**). To prevent concomitant C2-reduction, the coordination of Red-Al with the C1-hydroxyl group had to be blocked. As a result, the specific coordination of Red-Al to the oxetane ring oxygen would facilitate the selective reduction of the very hindered C4-acetate (**3-5**).[50]
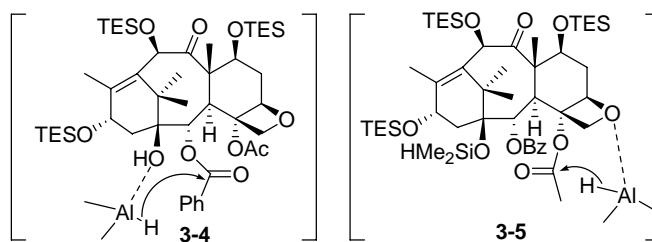
Scheme 3-2. The modification at C2 and C4 positions

Accordingly, as shown in **Scheme 3-3**, 7,10,13-tri-TES-10-DAB (**1-28**) was reacted with chlorodimethylsilane in the presence of imidazole in a DMF solution to protect the hydroxyl group at the C1 position as a dimethylsilyl ether. Baccatin **3-6** was treated with excess amount of Red-Al in a THF solution around 0 ^{o}C to 4 ^{o}C for 1.5 h to afford C4-hydroxyl baccatin **3-7** in good yield. The resulting hydroxyl group was then reacted with LiHMDS and 4-pentenoyl chloride to afford C4-modified baccatin **3-8** in high yield. Then the silyl groups of **3-8** were removed under HF-pyridine conditions, followed by C10 modification with acetic anhydride directly in the presence of cerium chloride heptahyrate.[51] Selective TES protection of the C7-OH using TESCl and imidazole gave modified baccatin **3-2** in good yield.
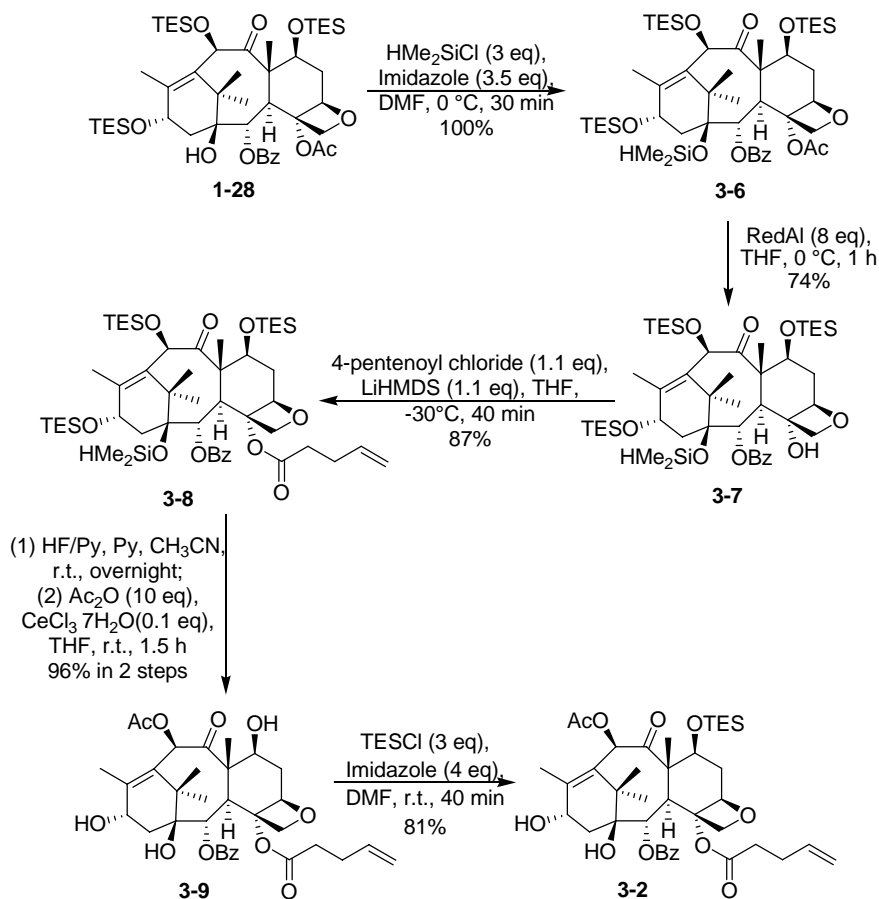
Scheme 3-3. Preparation of C4-modified baccatin 3-2

The synthesis of 3-allyl-β-lactam **3-3** is shown in **Scheme 3-4**, following a reported protocol developed in Ojima's laboratory.[52] First, the acetyl group in β-lactam **1-12** was hydrolyzed under basic conditions and the resulting hydroxyl group was protected as a TES ether to afford **1-13** in good yield. Then, the treatment of **3-10** with LDA followed by allyl bromide at low temperature gave the desired allylated β-lactam **3-11** as single isomer in 75% yield.[52] Standard oxidative removal of *para*-methoxyphenyl (PMP) group by using ammonium cerium (IV) nitrate (CAN) followed by Boc protection afforded β-lactam **3-3** in good overall yield.
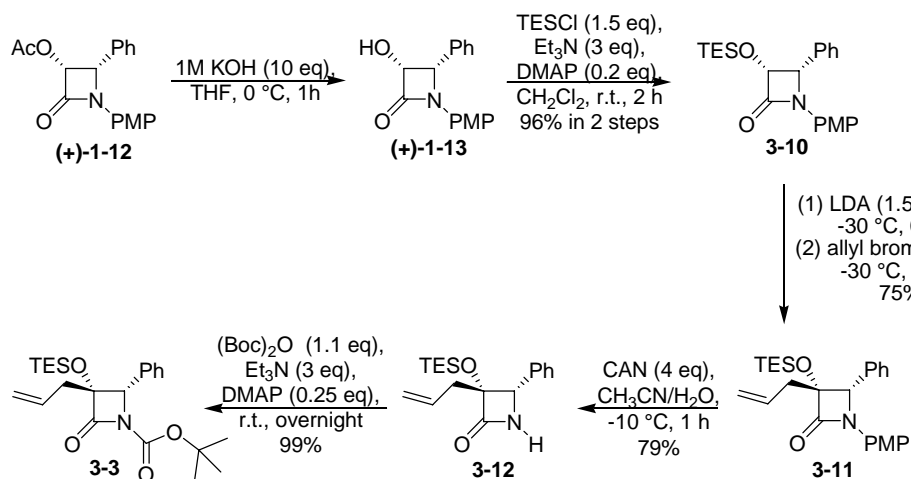
Scheme 3-4. Synthesis of β-lactam 3-3

The allyl group at the C3 position of β-lactam **3-3** introduced extra steric hindrance to the coupling reaction. Accordingly, sodium bis(trimethylsilyl)amide (NaHMDS) was used as the base and 5 equivalents of β-lactam **3-3** were used. Desired diene **3-1** was obtained in 85% yield and it was then subjected to RCM reaction to afford macrocyclic taxoid **3-13** in 82% yield. Desilylation using HF-pyridine conditions was slow due to the steric hinderance, giving **SB-TCR-102** in 70% yield, where *Z*-isomer was exclusively formed.
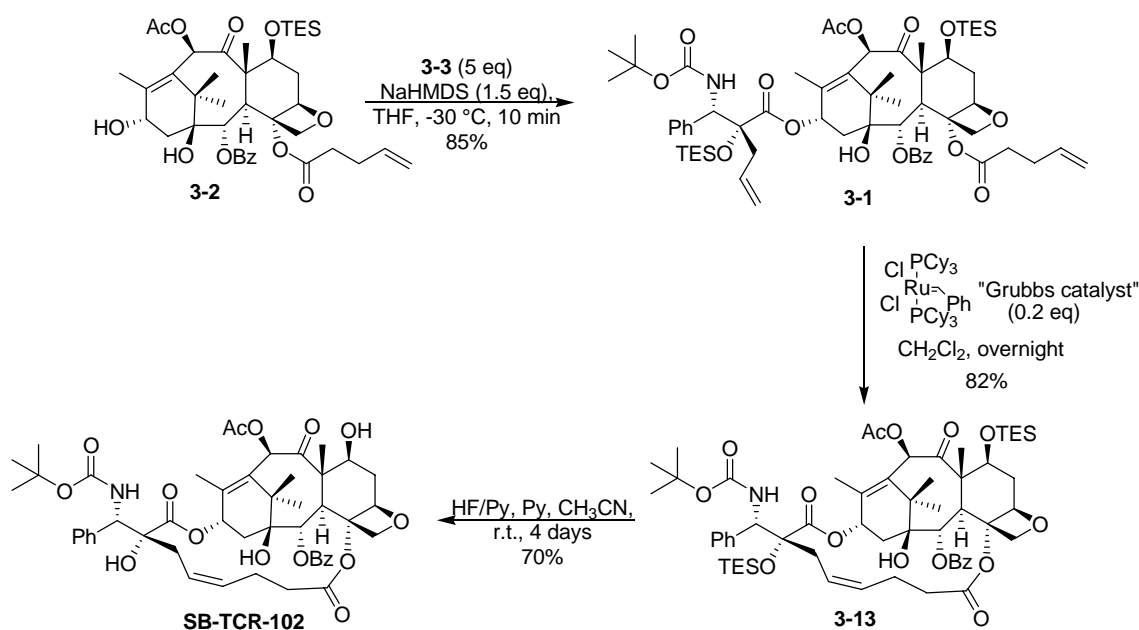
Scheme 3-5. Synthesis of SB-TCR-102

§ 3.2.1.2 Biological Evaluation of C4-C2'-Linked Macrocyclic Taxoids

SB-TCR-101 (synthesized by Yuan Li and Dr. Xudong Geng) and **SB-TCR-102** were evaluated for their cytotoxicity against human breast, ovarian, colon and NSCLC cancer cell lines at Roswell Park Cancer Institute and the results are shown in **Table 3-3**. Both compounds possess very low activities against all cell lines.[53]

Table 3-3. *In vitro* cytotoxicities (IC$_{50}$, μM[a]) of
the C4-C2' linked macrocyclic taxoids

Compound	MCF7[b]	NCI/ADR[c]	LCC6-WT[d]	LCC6-MDR[e]	H460[f]	HT-29[g]
Paclitaxel	0.003	0.518	0.005	0.323	0.005	0.004
SB-TCR-101	34	29.5				
SB-TCR-102	5.63	>10 (20%)*	>10 (25%)*	>10 (34%)*	9.19	7.66

[a]*The concentration of compound which inhibits 50% of the growth of human tumor cell line;*
[b]*MCF7: human breast carcinoma;* [c]*NCI/ADR: MDR phenotype human ovarian carcinoma;*
[d]*LCC6-WT-human breast carcinoma;* [e]*LCC6-MDR - MDR1 transfected line;*
[f]*H460 - NSCLC;* [g]*HT-29 human colon carcinoma*
**Numbers in parentheses are the % GROWTH INHIBITION SEEN AT 10000 nM (the highest conc.tested)*

SB-TCR-101 and **SB-TCR-102** were also sent to the Albert Einstein College of Medicine for tubulin-polymerization assays. As shown in **Figure 3-13**, both compounds can not induce polymerization of the tubulins, while paclitaxel and GTP can. The results are consistent with the *in vitro* cytotoxicity assay (**Table 3-3**), indicating the C4-C2'-linked macrocyclic taxoids do not have the correct conformation on the C13 side-chain.
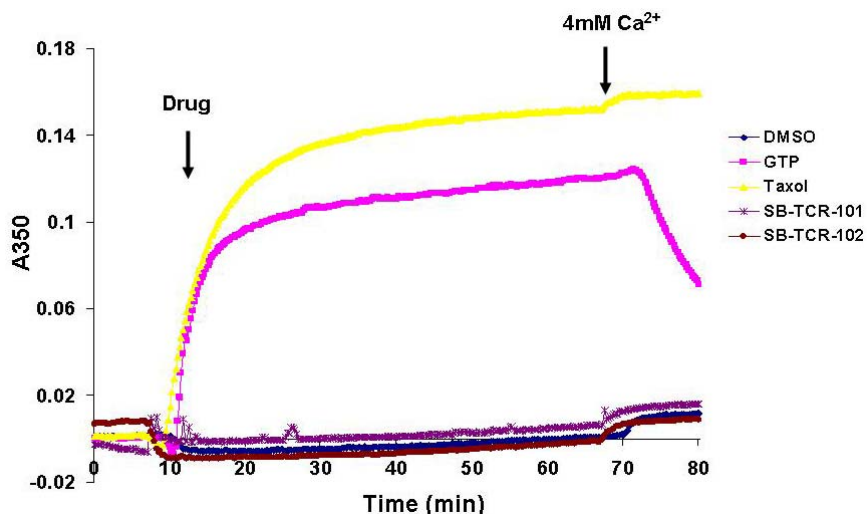
Figure 3-13. Tubulin-polymerization with SB-TCR-101, SB-TCR-102 and paclitaxel: microtubule protein 1 mg/mL, 37 °C, GTP 1 mM, Drug 10 µM

SB-TCR-101 and **SB-TCR-102** were designed based on the conformation similar to the T-Taxol conformation. As shown in **Figure 3-14**, the C4-C2'-linker forced the C2'-OH to point to Arg369 (1TUB), similar to the T-Taxol conformation.[53] Further molecular modeling studies of **SB-TCR-102** in the higher-resolution 1JFF tubulin will be discussed in **Chapter 4**.
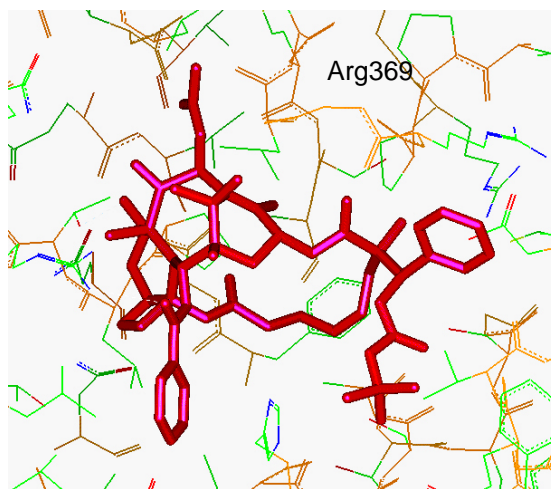
Figure 3-14. SB-TCR-102 in the binding pocket of β-tubulin

§ 3.2.2 REDOR-Taxol conformation

Because of the low activity of the C4-C2'-linked macrocyclic taxoids, we concluded that the "*Open-Gauche*" conformation was not the correct binding conformation. Dr. Raphael Geney proposed a new binding conformation based on the REDOR-NMR experiment.[54]

In 2000, a fluorinated taxoid, 2-(*p*-fluorobenzoyl)paclitaxel (2-FB-PT), was used bound to microtubules in solid state ^{13}C[^{15}N or ^{19}F]-double-REDOR-NMR experiments.[55] After three months of data acquisition, Schaefer and his coworkers were able to determine two ^{13}C-^{19}F intramolecular distances for 2-FB-PT in the bound state.
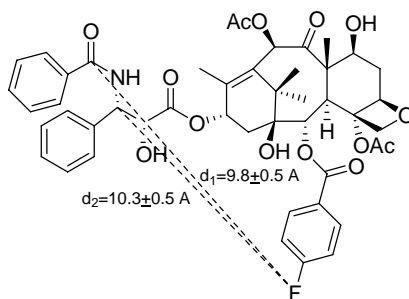
Figure 3-15: Structure of 2-FB-PT with intramolecular REDOR-NMR distances indicated

Molecular Dynamics (MD) simulations were initially conducted on 2-FB-PT in *vacuo* at increasing temperatures from 300K to 500K (InsightII 2000, Accelrys, CVFF force field). Unfortunately, some side chain bonds (e.g. C2'-C3') of the molecule present a high-energy barrier to rotation, impeding adequate sampling. For this reason, we switched to a Monte Carlo (MC) conformational search[56]. The two intramolecular distances determined were then used as constraints in an extensive MC conformational search on 2-FB-PT in *vacuo* (Macromodel 6.5, Schrödinger, Inc., MM3* forcefield). Conformational diversity in a set of resultant minimized structures was assessed by performing a cluster analysis on the 1371 retained conformations with energies in 50 kJ/mol of the global minimum (Xcluster, Schrödinger, Inc.). Sixteen clusters were formed according to the values of 10 dihedral angles of the C13 and C2 side chains. A representative structure for each cluster is shown in **Figure 3-16**. Remarkably, most of these structures have their C3'-benzamido moiety pointing in the same direction as the C2-fluorobenzoate group, as seen for docetaxel in its X-ray structure[19]. Also, to accommodate the REDOR-NMR geometric requirements, the entire C13 side-chain has to move away from the C2-fluorobenzoate, unlike in the polar conformation observed for the free drug.[13, 20, 21]
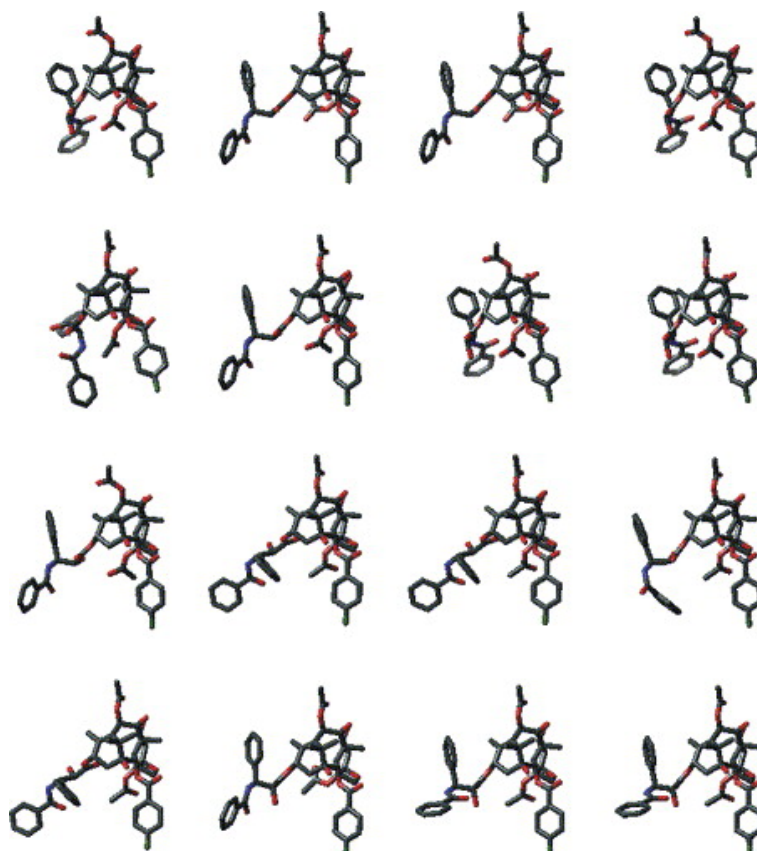
Figure 3-16: REDOR-NMR constrained Monte Carlo conformational search on 2-FB-PT: representative structures of the 16 conformational clusters

A C7-benzodihydrocinnamoyl (C7-BzDC) derivative of paclitaxel **(Figure 3-17)** labeled exclusively the Arg282 residue in the M loop of *β*-tubulin.[47] This specificity prompted us to model the covalent complex, thus formed, as a single molecule. This way, translational and rotational motions of the ligand are hampered, while the ligand evolves in its most likely position. A two-step procedure was then adopted in order to get a refined binding site model. First, the complex formed by *β*-tubulin and the bound C7-BzDc paclitaxel in the possible bioactive conformation inferred from the Monte Carlo conformational search were modeled and minimized. The carbonyl carbon of the benzophenone moiety was connected to the α-carbon of Arg282, since the excited state of the benzophenone moiety would selectively abstract hydrogen from the α-position of an amino acid residue because of the captodative stabilization of the resulting radical species[57]. The peptide backbone atoms of the protein were kept fixed at all times during the energy-minimization, while side chain atoms were free to move, allowing the reorganization of side-chains upon binding of modified taxoids. After cleavage of the BzDc linker, a free ligand-binding site complex, comprising only residues within 10 Å of any ligand or linker atom was minimized again under the same conditions.
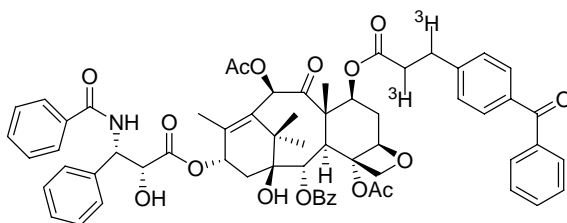
Figure 3-17. Structures of photoaffinity probe [³H]7-BzDc-paclitaxel

The procedure was applied to paclitaxel, starting from all 16 conformations retained from the Monte Carlo conformational search of 2-FB-PT. The REDOR-NMR distances were verified after docking and used as a filter to determine the tubulin-bound paclitaxel conformation. However, none of the representative structures could strictly maintain both distances in the allowed REDOR-NMR ranges after docking. Two factors could contribute to that: (1) the availability of large empty spaces in the binding site, and (2) the fact that the REDOR distances were derived from microtubules while the EC structure corresponds to the Zn-sheet form of tubulin, which might present some structural differences to the microtubule form. The structure deviating the least from the two REDOR-NMR restraints ($d_1 = 9.97$ Å, $d_2 = 9.38$ Å) was selected as our tubulin-bound paclitaxel structure, "REDOR-taxol" **(Figure 3-18)**.
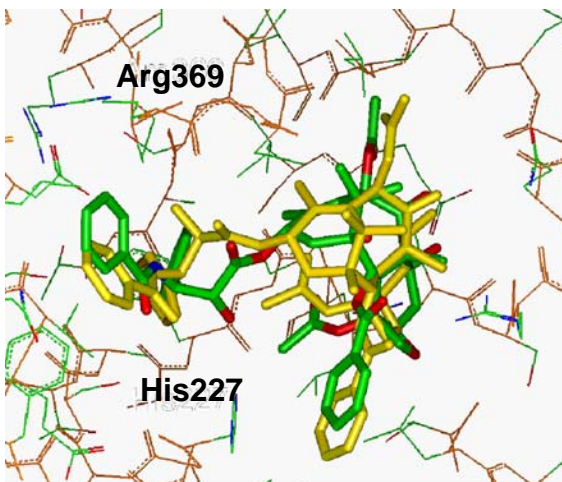
Figure 3-18. Overlay of the REDOR-Taxol (green) and T-Taxol (yellow) structures

The C2'-hydroxyl group which usually forms an intramolecular H-bond with the C1'-carbonyl oxygen in the free drug is pointed towards His227 in the "REDOR-Taxol" structure, forming a very buried H-bond of increased strength. The H-bond between the C2'-hydroxyl and the backbone carbonyl oxygen of Arg369 in the "T-Taxol" binding pose is more solvent exposed.

Very recently, another three intramolecular distances were determined by Schaefer and his coworkers. The comparison of the distances measured in the REDOR-Taxol structure, the T-Taxol structure and experimental value was shown in **Table 3-3**.[58] The data indicated both the T-Taxol structure and the REDOR-Taxol structure are fully consistent with the experimental results.

Table 3-4. Intramolecular atom distances of paclitaxel[58]
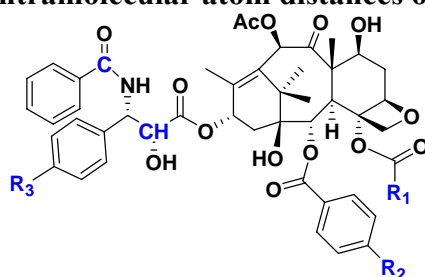
	Distances (Å)		
Separations	REDOR-NMR distances	REDOR-Taxol	T-Taxol
R₁-R₂	7.8	7.3	7.9
R₁-R₃	6.3	6.4	6.6
R₂-R₃	> 8	13.1	12.2
R₂-CH	10.3	9.4	9.9
R₂-C	9.8	10.0	9.1

§ 3.2.3 Design, Synthesis and Biological Evaluation of C14-C3'N Linked Macrocyclic Taxoids

§ 3.2.3.1 Design of the C14-C3'N Linked Macrocyclic Taxoids

The REDOR-Taxol structure was searched for the possible installation of the intramolecular linkers. As shown in **Figure 3-19**, the distance between C14 position and the *ortho* position of C3'*N*-benzoyl group is 7.5 Å and a short linker (~ 4-6 atoms) between these two positions could be used to fix the C13 side-chain. Inserting a linker between the C14 and C3'*N* positions also presents only a small risk of disrupting the original binding of the drug since the linker moiety lies towards the solvent-exposed surface of the binding site, hence should not generate unfavorable contacts with the protein.
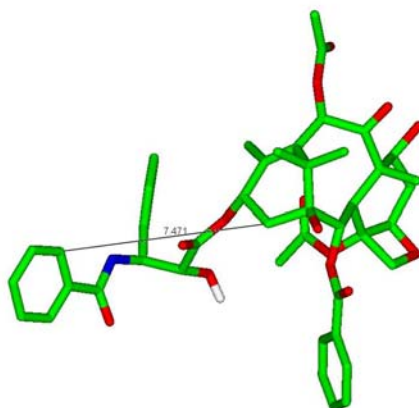
Figure 3-19. Intramolecular distance in the REDOR-Taxol structure

SB-T-2053, bearing a 5-atom linker, was first designed, which showed a very good overlay with REDOR-Taxol (**Figure 3-20**). **SB-T-2054** and **SB-T-2055**, which have linkers of different lengths, were designed to examine the effect of the lengths of linkers. The overlay of the three macrocyclic compounds and REDOR-Taxol is shown in **Figure 3-21**. **SB-T-2052** and **SB-T-2152** with different C3'-substitution were also designed.
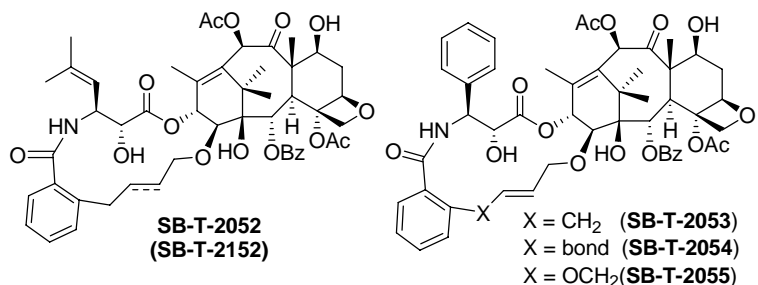
Figure 3-20: C14-C3'*N*-linked macrocyclic taxoids
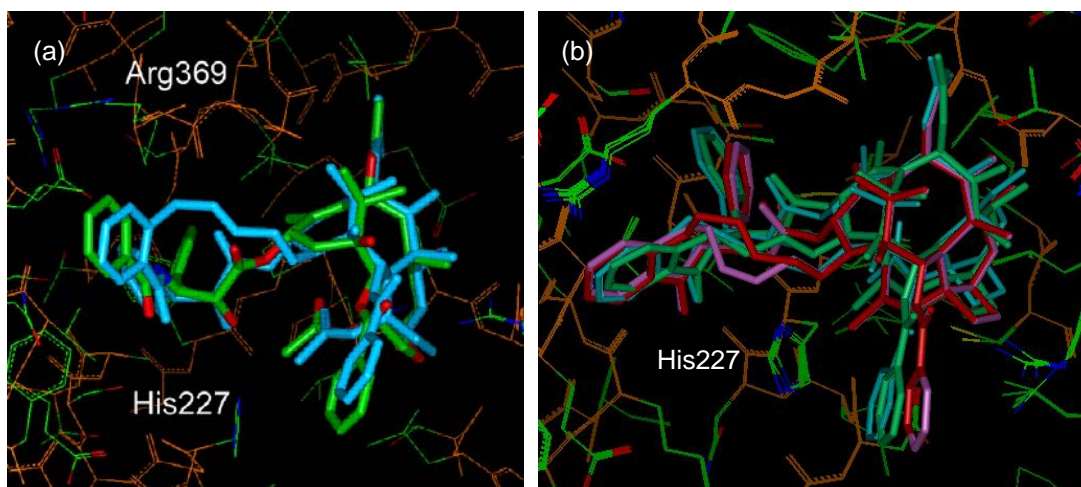
Figure 3-21. Overlay of SB-T-2053 (cyan, a&b), SB-T-2054 (magenta, b), SB-T-2055 (red, b) and REDOR-Taxol (green, a&b)

§ 3.2.3.2 Synthesis of SB-T-2053

As shown in **Scheme 3-6**, ring-closing metathesis (RCM) was utilized as the key reaction in constructing the C14-C3'-linked macrocyclic taxoids. The diene precursor **3-14** was synthesized using the Ojima-Holton coupling[59] between modified baccatin **3-15** and *β*-lactam **3-16**. The *β*-lactams was prepared by modification of *β*-lactam **1-12** and the modified baccatin **3-15** was synthesized from naturally occurring **14-OH-10-DAB**.
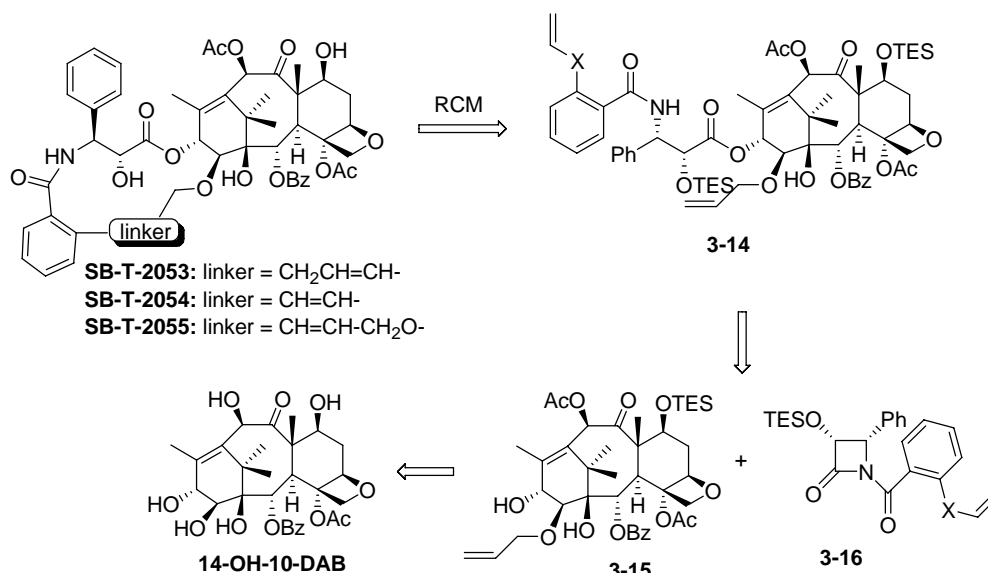
Scheme 3-6. Retro-synthesis of C14-C3' linked macrocyclic taxoids

The synthesis of modified baccatin **3-15** is shown in **Scheme 3-7**. The synthesis required the introduction of an allyl ether moiety at the C14 position of baccatin. The C10-OH of **14-OH-10-DAB** was first reacted with acetic anhydride in the presence of cerium chloride heptahydrate to afford **3-17** in high selectivity.[51] Selective TES protection of the C7-OH using TESCl and imidazole gave 7-TES-14-OH-baccatin **3-18** in good yield. Finally, **3-18** was treated with allyl iodide in the presence of NaHMDS to afford **3-15** bearing an allyl ether moiety attached to the C-14 position in 82% yield.
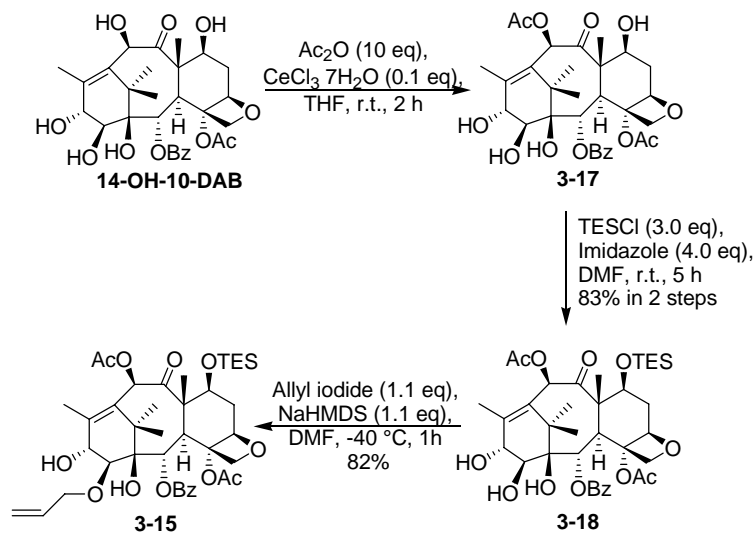
Scheme 3-7. Preparation of modified baccatin 3-15

Since the TES group could not survive in the CAN oxidation, the *p*-methoxyphenyl group was first removed, and the acetoxy group of **1-14** was hydrolyzed to afford **1-15**. The TES protection of the hydroxyl group in **1-15** was performed at 0 °C to give the TES-protected *N*-H *β*-lactam (**3-19**) in good yield.
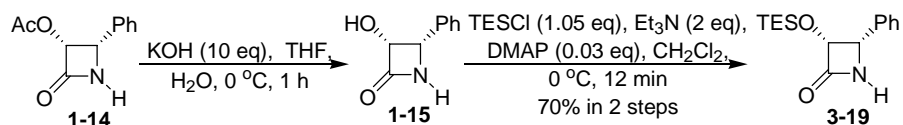
Scheme 3-8. Preparation of 3-19

The synthesis of β-lactam **3-23** is shown in **Scheme 3-9**. The acid chloride **3-22** was first prepared, following the reported procedure.[60] The Stille coupling reaction of methyl 2-bromobenzoate was carried out with allyltributyltin in the presence of Pd(PPh$_3$)$_4$ to afford methyl 2-allylbenzoate (**3-20**), which was then subjected to hydrolysis to give 2-allylbenzoic acid (**3-21**) in 60% yield for two steps. Treatment of acid **3-21** with oxalyl chloride afforded the corresponding acyl chloride **3-22**, which was reacted with *N*-H β-lactam **3-19** in the presence of triethylamine and DMAP to give the desired β-lactam **3-23** in 90% yield.
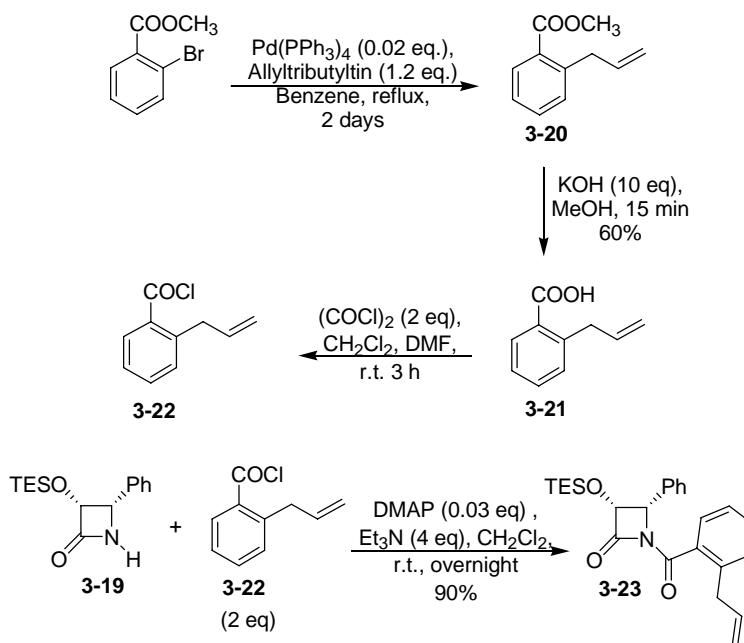
Scheme 3-9. Synthesis of β-lactam 3-23

As shown in **Scheme 3-10**, the coupling reaction of modified baccatin **3-15** at the C13 position and β-lactam **3-23** proceeded smoothly, affording diene **3-24** in 72% yield. RCM reaction using the "first-generation Grubbs catalyst"[26] gave the desired macrocyclic taxoid **3-25** in 85% yield. Then, the silyl groups were removed using HF-pyridine to afford **SB-T-2053** in 93% yield and only the *E*-isomer was obtained.
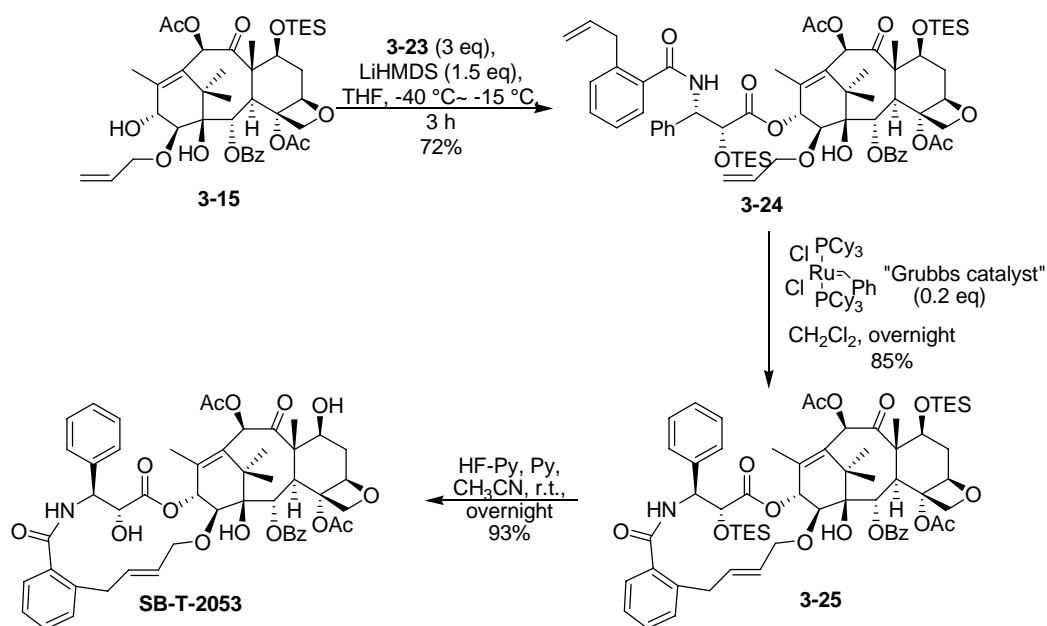
Scheme 3-10. Synthesis of SB-T-2053

§ 3.2.3.3 Synthesis of SB-T-2054

The synthesis of β-lactam **3-28** is shown in **Scheme 3-11**. The Wittig reaction of 2-formyl-benzoic acid with methyltriphenylphosphonium ylide gave methyl 2-vinylbenzoyl acid (**3-26**) in good yield.[61] Treatment of the acid **3-26** with thionyl chloride afforded the corresponding acid chloride **3-27** in 65% yield for two steps after distillation under reduced pressure. Optically pure TES-*N*-H β-lactam **3-19** was reacted with acid chloride **3-27** in the presence of triethylamine and DMAP to give the desired β-lactam **3-28** in 98% yield.
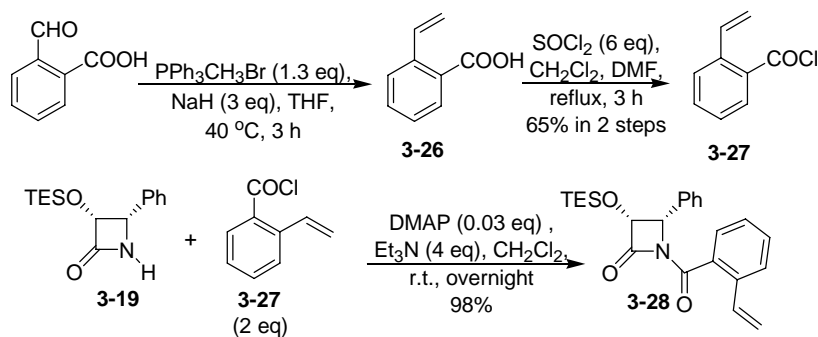
Scheme 3-11. Synthesis of β-lactam 3-28

The diene **3-29** was obtained by using the Ojima-Holton coupling reaction in 82% yield. However, the RCM reaction became problematic. By using the "first-generation Grubbs catalyst" (25% x 3), 25% of the starting material still remained after reflux for 5 days. Di-TES macrocyclic taxoid **3-30** was obtained in 70% yield, which had one more CH$_2$, instead of the designed structure. The final structure was determined by 2-D NMR and X-ray crystallography (**Figure 3-22**). The final deprotection by using HF/Py afforded

SB-T-2054 in good yield. The "second-generation Grubbs catalyst" (25% x 2) was also used, affording no desired product or one-more-carbon product after refluxing for 3 days, although the starting material disappeared completely.
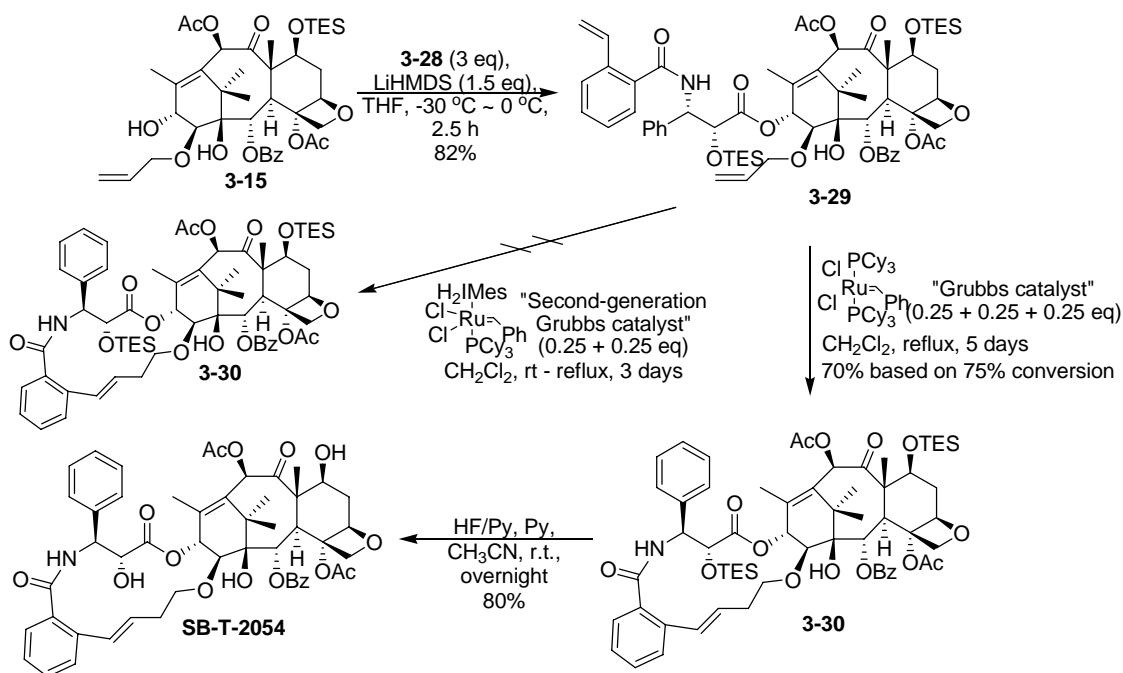
Scheme 3-12. Synthesis of SB-T-2054
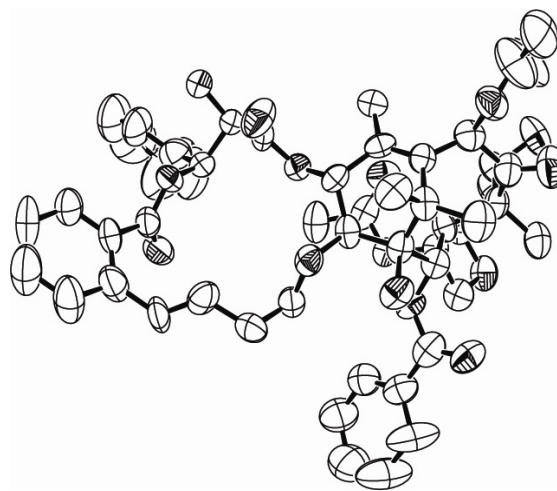
Figure 3-22. X-ray structure of SB-T-2054

A possible mechanism for the formation of the one-more-carbon compound **3-30** is shown in **Scheme 3-13**. In normal RCM mechanism, the "first-generation Grubbs catalyst" **M-1** first reacts with diene **M-2** to give active intermediate **M-3** after the first metathesis. In the second metathesis cycle, four-member ring intermediate **M-4** is formed, and then gives the cyclic compound **M-5** and regenerate catalyst **M-6**.

However, in **3-29**, the two olefins are far from each other, because the linker is too short. Thus, the intermediate **M-7** is formed, instead of **M-4.** The "mismatched" **M-7** can not give the desired product **M-5**. The one-more-carbon product **M-9** can be obtained from **M-7** in two possible pathways. In the first possible mechanism, cyclopropane product **M-8** is formed after reductive elimination, followed by isomerization to give **M-9**. In the second possible mechanism, β-hydride elimination occurs to give π-allylic Ru-complex **M-10**, followed by reductive elimination to afford **M-9**. The β-hydride elimination and reductive elimination can be assisted by the *ortho* amide carbonyl group. In both mechanisms, one equivalent of Ru metal is needed to complete the reaction, which may account for the big catalyst loading.
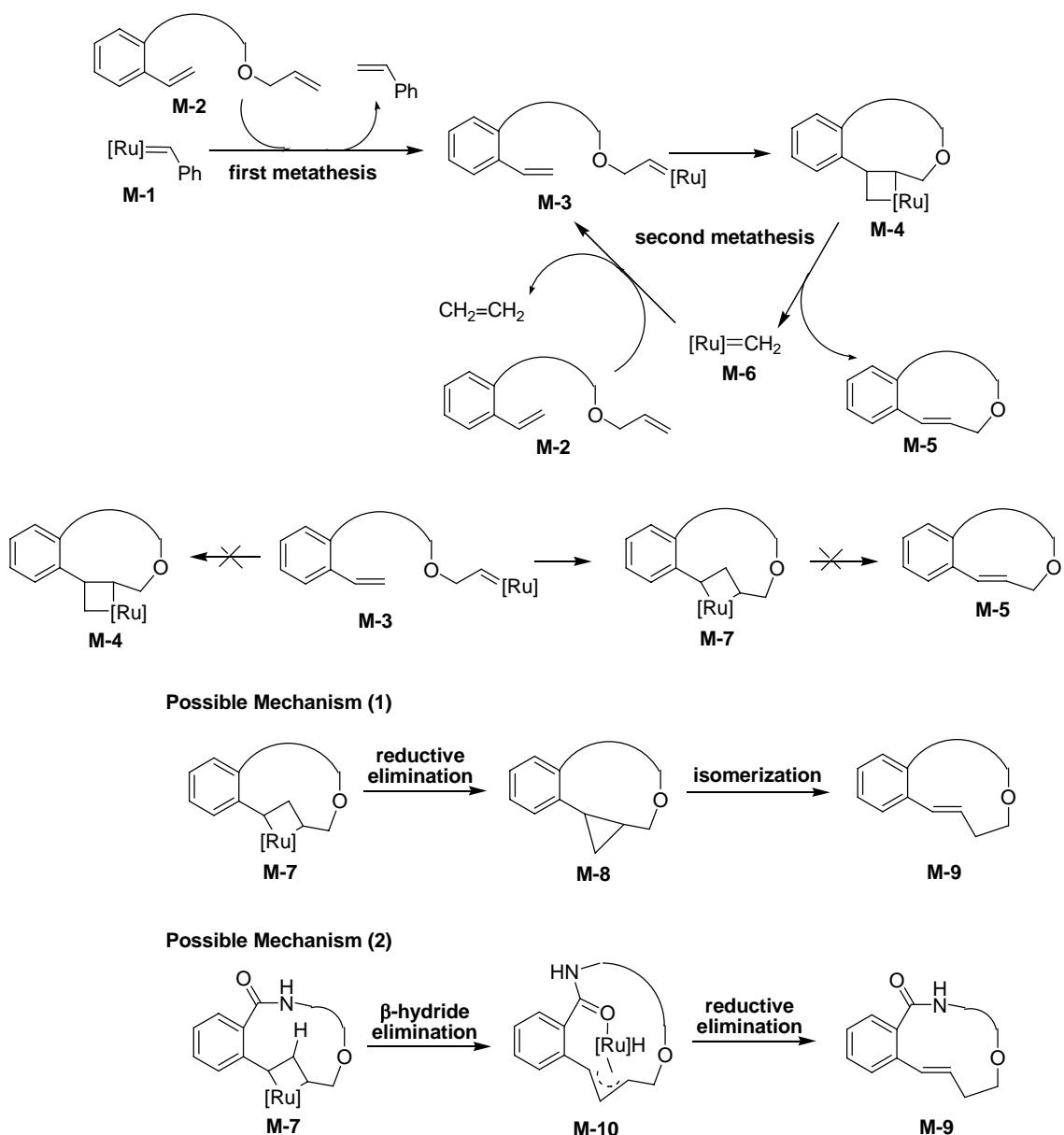
Scheme 3-13. **Possible mechanisms to produce SB-T-2054 (M-9)**

§ 3.2.3.4 Synthesis of SB-T-2055

As shown in **Scheme 3-14**, *β*-lactam **3-19** was reacted with acid chloride **3-30** in the presence of triethylamine and DMAP to afford the desired *β*-lactam **3-31** in high yield. The C13-coupling reaction of **3-15** with **3-31** afforded **3-32** in 77% yield. By using the "second-generation Grubbs catalyst", the macrocyclic compounds **3-33** (*E*) and **3-34** (*Z*) were obtained in 81% total yield. The ratio of **3-33** and **3-34** products was 1:1.3, and a similar result (1:1) was obtained by using the "first-generation Grubbs catalyst". Then, the silyl groups were removed under HF-pyridine conditions to afford **SB-T-2055Z** and **SB-T-2055E** in good yields.
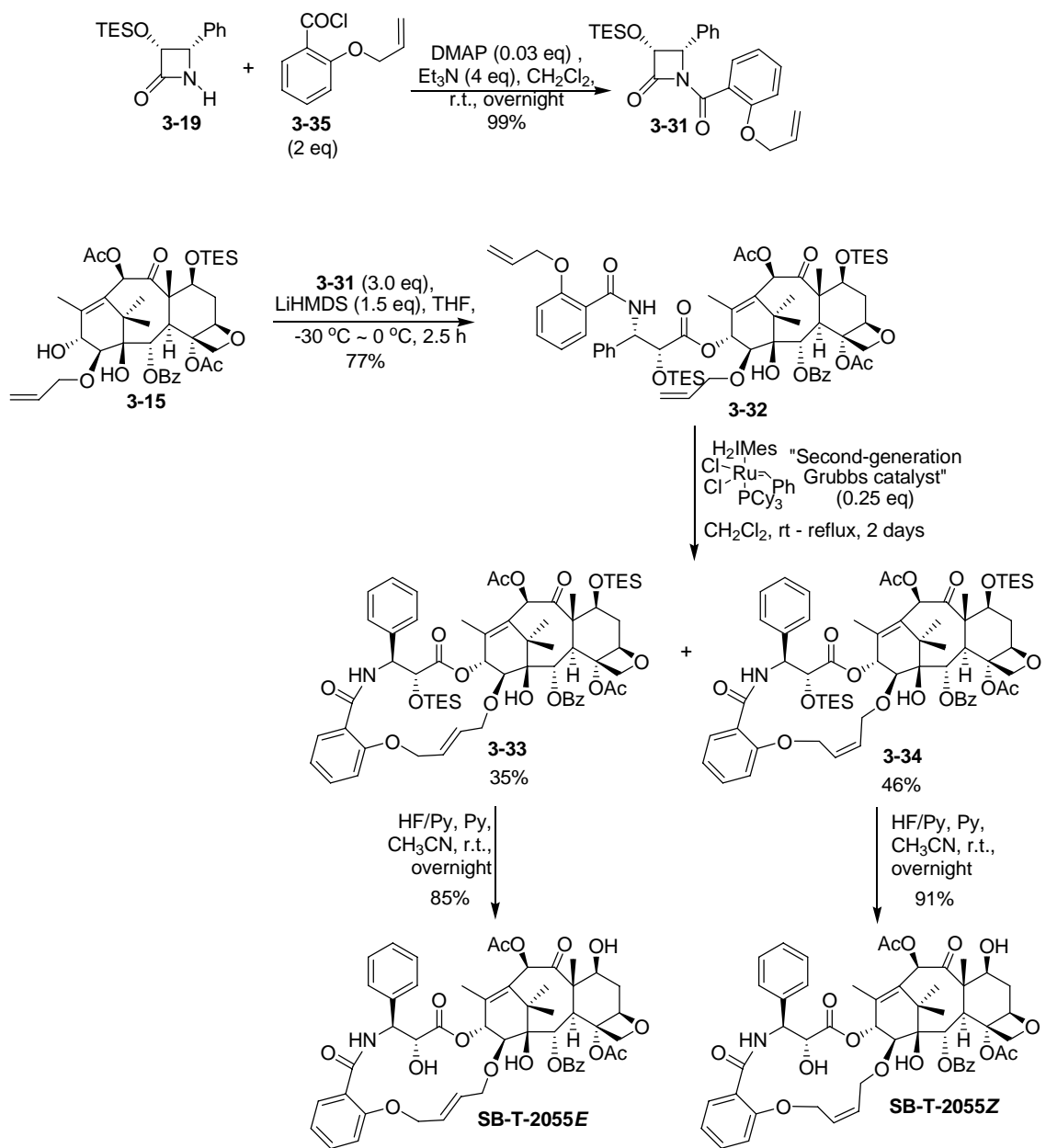
Scheme 3-14. Syntheses of SB-T-2055Z and SB-T-2055E

§ 3.2.3.5 Biological Evaluation of C14-C3'N Linked Macrocyclic Taxoids

§ 3.2.3.5.1 Cytotoxicity of C14-C3'N-Linked Macrocyclic Taxoids

The preliminary *in vitro* cytotoxicity assay was performed at the Roswell Park Cancer Institute. Macrocyclic taxoid **SB-T-2053** exhibits strong potency against LCC6-WT and MCF7 human breast cancer cell lines with IC_{50} values of 15 and 42 nM, respectively (**Table 3-5**). The former IC_{50} value is only 3.3 times less potent than paclitaxel against the same cell line. Considering that **SB-T-2053** is equipotent to or slightly more potent than paclitaxel for tubulin polymerization, the small differences observed in IC_{50} values between paclitaxel and **SB-T-2053** could be ascribed to the cell permeability and solubility factors of two distinct molecules. Also, **SB-T-2053** exhibits the same level of potency as paclitaxel against multidrug-resistant human breast and ovarian cancer cell lines (LCC6-MDR and NCI-ADR), overexpressing P-glycoprotein.[62, 63] **SB-T-2054** showed even higher activity in the assay against MCF7 and NCI-ADR cell lines than **SB-T-2053**. **SB-T-2054** is twice less potent than paclitaxel and seven times more potent than **SB-T-2053** against MCF7 cell line, and twice more active than paclitaxel against NCI-ADR cell line. **SB-T-2055Z** and **SB-T-2055E** show only micromolar activities against the same cell lines, and the Z isomer is more active than the E isomer. **SB-T-2052** as well as its saturated analog, **SB-T-2152** (synthesized by Dr. Xudong Geng), however, are much less potent than paclitaxel, although they have the same linker as **SB-T-2053**.

Table 3-5. *In vitro* cytotoxicities assay
of the C14-C3'N linked macrocyclic taxoids

Compound	MCF7[b]	NCI/ADR[c]	LCC6-WT[d]	LCC6-MDR[e]	H460[f]	HT-29[g]
	IC50 nM (±S.E.)[a]					
Paclitaxel	3.0 ±0.3	518 ±71	4.5 ±0.8	323 ±23	4.7 ±0.7	4.2 ±0.3
SB-T-2053	42 ±2.3	1066 ±59	15 ±1.6	455 ±38	25 ±3.4	23 ±2.1
SB-T-2054	5.96 ± 0.83	240±68				
	IC50 μM (±S.E.)[a]					
SB-T-2055E	1.88 ± 0.21	5.6 ± 1.0				
SB-T-2055Z	0.27 ± 0.03	2.4 ± 0.21				
SB-T-2052	0.46 ± 0.03	> 3.0	0.21 ± 0.02	2.1 ± 0.10		
SB-T-2152	0.76 ± 0.05	2.8 ± 0.14	0.46 ± 0.04	1.9 ± 0.16		

[a]*The concentration of compound which inhibits 50% of the growth of human tumor cell line;*
[b]*MCF7: human breast carcinoma;* [c]*NCI-ADR: MDR phenotype human ovarian carcinoma;*
[d]*LCC6-WT-human breast carcinoma;* [e]*LCC6-MDR - MDR1 transfected line;*
[f]*H460 - NSCLC;* [g]*HT-29 human colon carcinoma*

§ 3.2.3.5.2 Tubulin Polymerization Assay of SB-T-2053 and SB-T-2054

SB-T-2053 and **SB-T-2054** were also sent to the Albert Einstein College of Medicine for tubulin polymerization assay and the results are shown in **Figure 3-23** and **Figure 3-24**. The results indicate that both compounds induce polymerization of tubulins in the same manner as paclitaxel and GTP. After the addition of Ca^{2+}, however, the microtubule formed with GTP depolymerized immediately, while the ones formed with paclitaxel, **SB-T-2053** and **SB-T-2054** did not.
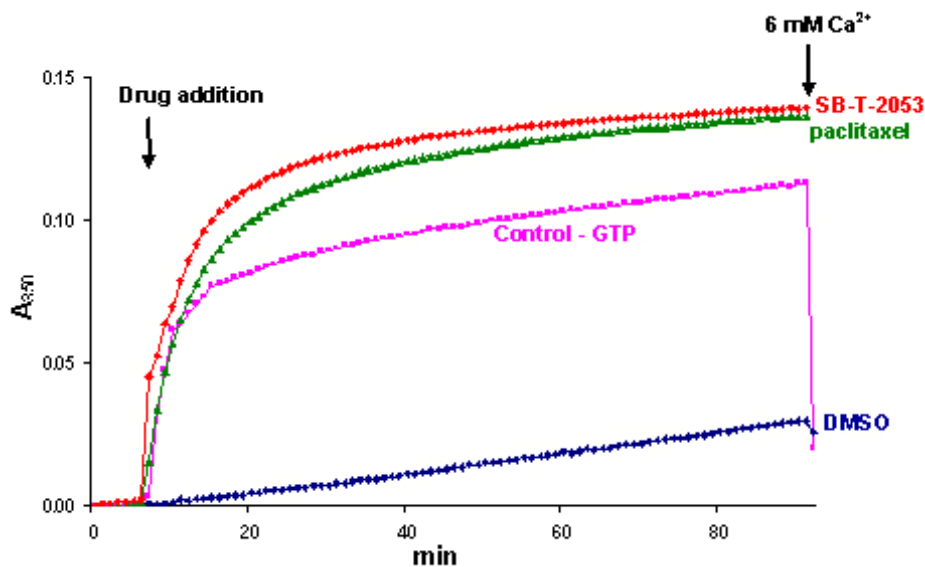
Figure 3-23. Tubulin polymerization with SB-T-2053 and paclitaxel: microtubule protein 1 mg/mL, 37 ^{o}C, GTP 1 mM, Drug 10 μM
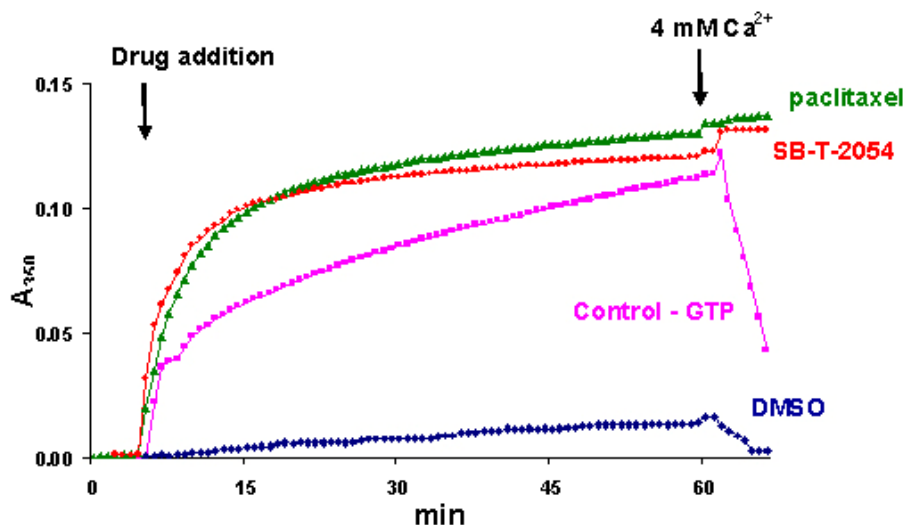
Figure 3-24. Tubulin polymerization with SB-T-2054 and paclitaxel: microtubule protein 1 mg/mL, 37 ^{o}C, GTP 1 mM, Drug 10 μM

§ 3.2.3.5.3 Electron Microscopy Analysis

The microtubules formed with **SB-T-2054** were analyzed further by electron microscopy for their morphology and structure in comparison with those formed by using GTP and paclitaxel. The electron micrographs of microtubules are summarized in **Figure 3-25**. The microtubules formed with **SB-T-2054** (**Figure 3-25c**) are thicker than those with GTP or paclitaxel.
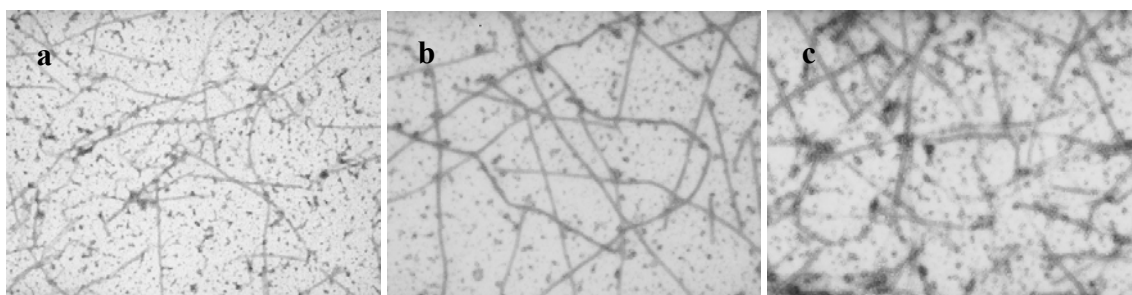
Figure 3-25. Electromicrographs of microtubules formed with GTP (a), paclitaxel (b) and SB-T-2054 (c)

The higher activity of **SB-T-2054** than **SB-T-2053** could be explained by their conformations in β-tubulin. Although they are isomers, the double bond connected to benzene ring (in **SB-T-2054**) make the macrocyclic ring more rigid than the one in **SB-T-2053**, hence **SB-T-2054** has a better overlay with the REDOR-Taxol structure in tubulin (1TUB) (**Figure 3-26**). Further molecular modeling studies of the C14-C3'*N*-linked macrocyclic taxoids (in 1JFF) will be discussed in **Chapter IV**.
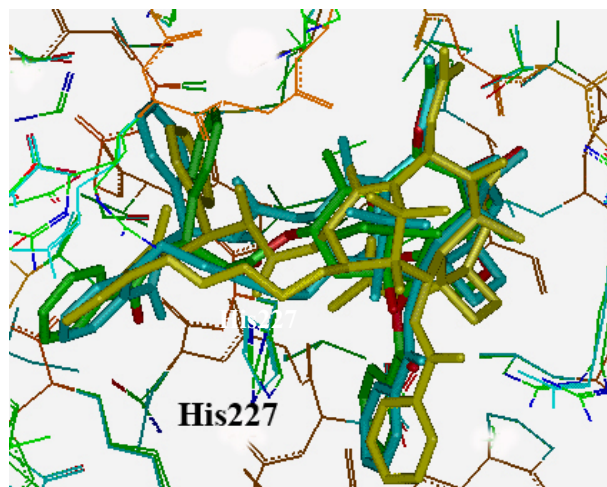
Figure 3-26. Overlay of SB-T-2053 (cyan), SB-T-2054 (yellow) and REDOR-Taxol (green) in binding site (1TUB)

§ 3.2.4 Synthesis of C4-C2'*O*-Linked Macrocyclic Taxoid SB-TCR-501

During the modeling studies, it was found that in the REDOR-Taxol comformation, the C4-acetyl group was close to the C2'-hydroxyl group, instead of the C2' hydrogen as in **SB-TCR-102**, which could explain the low activity of the C4-C2'-linked marcrocyclic taxoids. Some new C4-C2'*O*-linked macrocyclic taxoids were designed, which had very good overlays with the REDOR-Taxol structure in tubulin (1TUB), as shown in **Figure 3-27**.
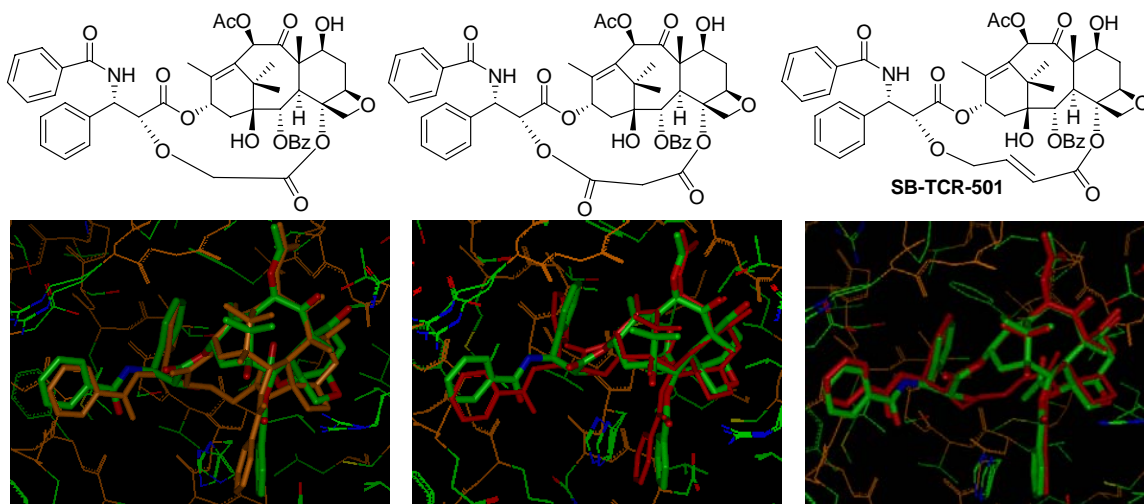
Figure 3-27. Overlays of the designed C4-C2'*O*-linked macrocyclic taxoids (red) and REDOR-Taxol (green)

It is well known that the blockage of the C2'-OH will cause several hundred time loss in potency (**Table 3-6**).[64] However, if the macrocyclic taxoid has some activity, it would be a direct evidence to support the REDOR-Taxol structure, because C2' position is far from C4 position in the T-Taxol structure. **SB-TCR-501** was selected to examine the hypothesis. The detailed molecular modeling studies of **SB-TCR-501** will be shown in **Chapter IV**.

Table 3-6. *In vitro* cytotoxicities of 2'-OH blocked paclitaxel

	HCT116 IC$_{50}$ (µM)
Taxol	0.004
2'-Methoxytaxol	0.866
2'-Desoxytaxol	0.297
2'-Fluorotaxol	0.475

The macrocyclic taxoid can be obtained through RCM reaction of diene **3-35**, which can be synthesized using the *β*-lactam synthon method[59] from modified baccatin **3-36** and *β*-lactam **3-37**. The *β*-lactam **3-37** can be prepared from intermediate **1-13**, and the modified baccatin **3-36** can be synthesized from **10-DAB**.
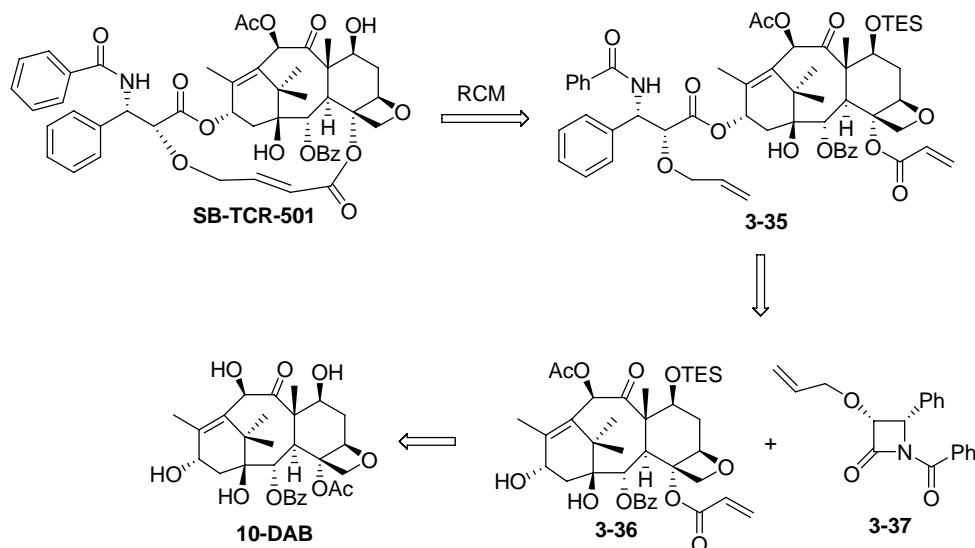
Scheme 3-15. Retro-synthesis of C4-C2'*O*-linked macrocyclic taxoid SB-TCR-501
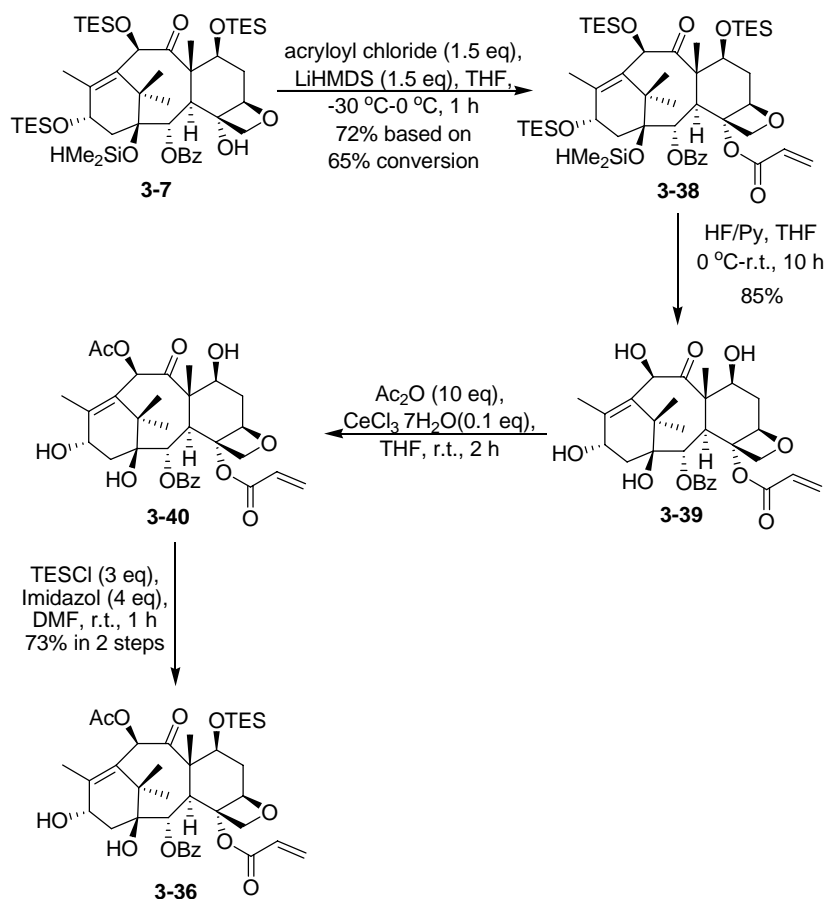
Scheme 3-16. Synthesis of C4 modified baccatin 3-36

The C4 modification of C4-hydroxyl baccatin **3-7** with LiHMDS and acryloyl chloride afforded C4-modified baccatin **3-38** in 47% yield with 35% starting material recovered. The low conversion was caused by the unstable acryloyl group. Previous

studies indicated that the acryloyl group was not stable under the standard HF-pyridine conditions. Accordingly, the milder HF-pyridine/THF conditions was used and the desired C4-modified baccatin **3-39** was obtained in 85% yield. Baccatin **3-39** was reacted with acetic anhydride in the presence of cerium chloride heptahyrate,[65] followed by selective TES protection of the C7-OH using TESCl and imidazole to afford the modified baccatin **3-36** in good yield.

As shown in **Scheme 3-17**, β-lactam **1-13** was allylated to give **3-41** in good yield in the presence of either NaH or NaHMDS, because the PMP-protected β-lactam **1-13** is stable to strong bases. The PMP deprotection gave **3-42** in 84% yield and **3-37** was obtained after *N*-benzoylation.
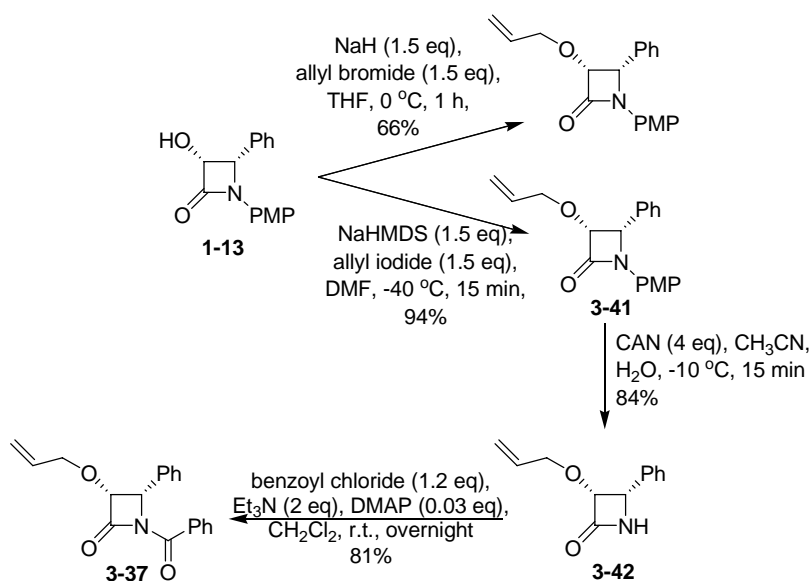
Scheme 3-17. Synthesis of β-lactam 3-37

As shown in **Scheme 3-18**, coupling reaction of **3-36** with **3-37** proceeded smoothly, affording diene **3-35** in 58% yield. RCM reaction using the "first-generation Grubbs catalyst" gave the macrocyclic compound **3-43** in 75% yield (*E*-isomer only). The desired C4-C2'*O*-linked paclitaxel analog **SB-TCR-501** was obtained after deprotection with HF-pyridine.
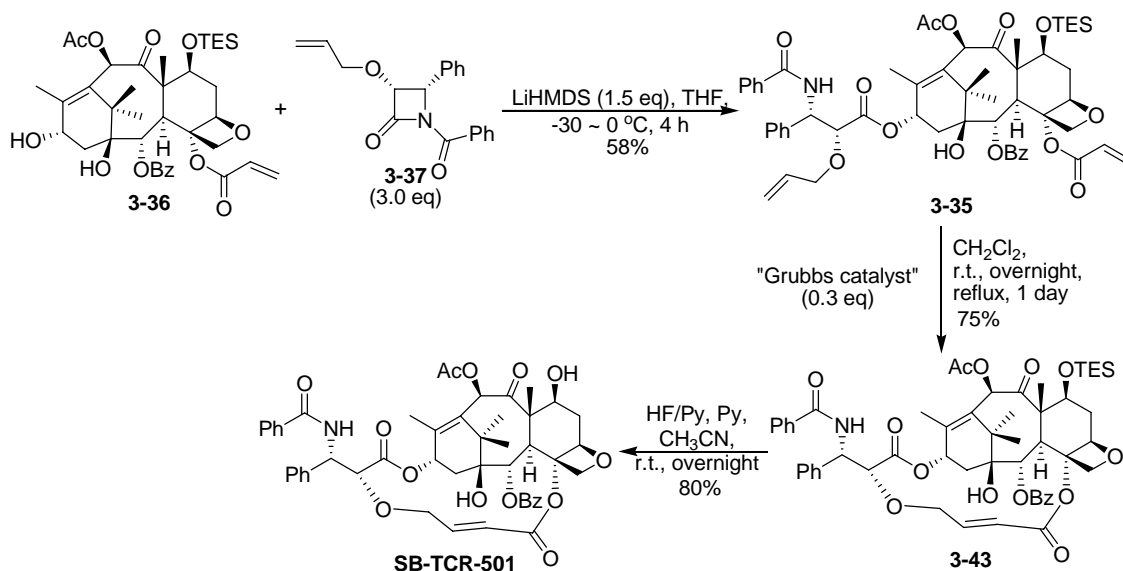
Scheme 3-18. Synthesis of SB-TCR-501

§ 3.2.5 Synthesis of Kingston's C4-C3'-Linked Macrocyclic Taxoids

Four C4-C3'-linked macrocyclic taxoids (**Figure 3-8**), with higher activity than paclitaxel, were reported by the Kingston group.[37] **K1a** is the most active one in this series, which is 2-30 times more potent than paclitaxel.[40] Two of the taxoids, **K1a** and **K2a**, were resynthesized to compare their potency with our active C14-C3'*N*-linked macrocyclic taxoids.

As shown in **Scheme 3-19**, RCM reaction was utilized as the key reaction in constructing the macrocyclic taxoids from diene **3-44**, which was synthesized using the C13 coupling[59] of modified baccatin **3-36** with β-lactam **3-45**. The β-Lactam **3-45** was prepared through [2+2] ketene-imine cycloaddition followed by enzymatic kinetic resolution.
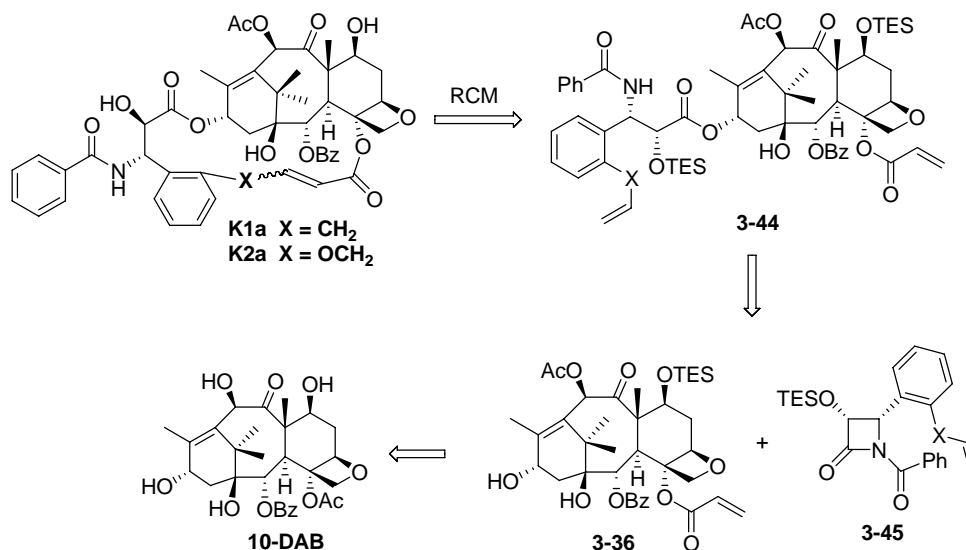
Scheme 3-19. Retro-synthesis of C4-C3'-linked macrocyclic taxoids

The synthesis of 3-allyl-β-lactam **3-53** is shown in **Scheme 3-20**, following a reported protocol developed in our laboratory.[59] First, *O*-allylation of salicylaldehyde with allyl bromide was performed with K$_2$CO$_3$ in acetone, affording **3-46** in quantitative yield after reflux for 2 h.[66] Aldehyde **3-46** was reacted with *p*-anisidine in dichloromethane to generate *N-p*-methoxyphenyl-*o*-allyloxybenzaldimine **3-47**.[67] Imine **3-47** was cyclocondensed with acetoxyacetyl chloride, in the presence of triethylamine, affording the corresponding racemic β-lactam **3-48** in 98% yield for two steps. Enzymatic resolution of **3-48** was performed to **3-48** to give enantiopure β-lactam **(+)-3-48** with 40% yield after 6 days. Then, the *para*-methoxyphenyl (PMP) group in optically pure β-lactam **(+)-3-48** was removed by using ammonium cerium nitrate (CAN), followed by hydrolysis of the acetic group. The resulting hydroxyl group was protected as a TES ether to afford **3-52** in good yield. The benzoylation of **3-52** afforded β-lactam **3-53** in 99% yield.

Scheme 3-20. Synthesis of β-lactam 3-52
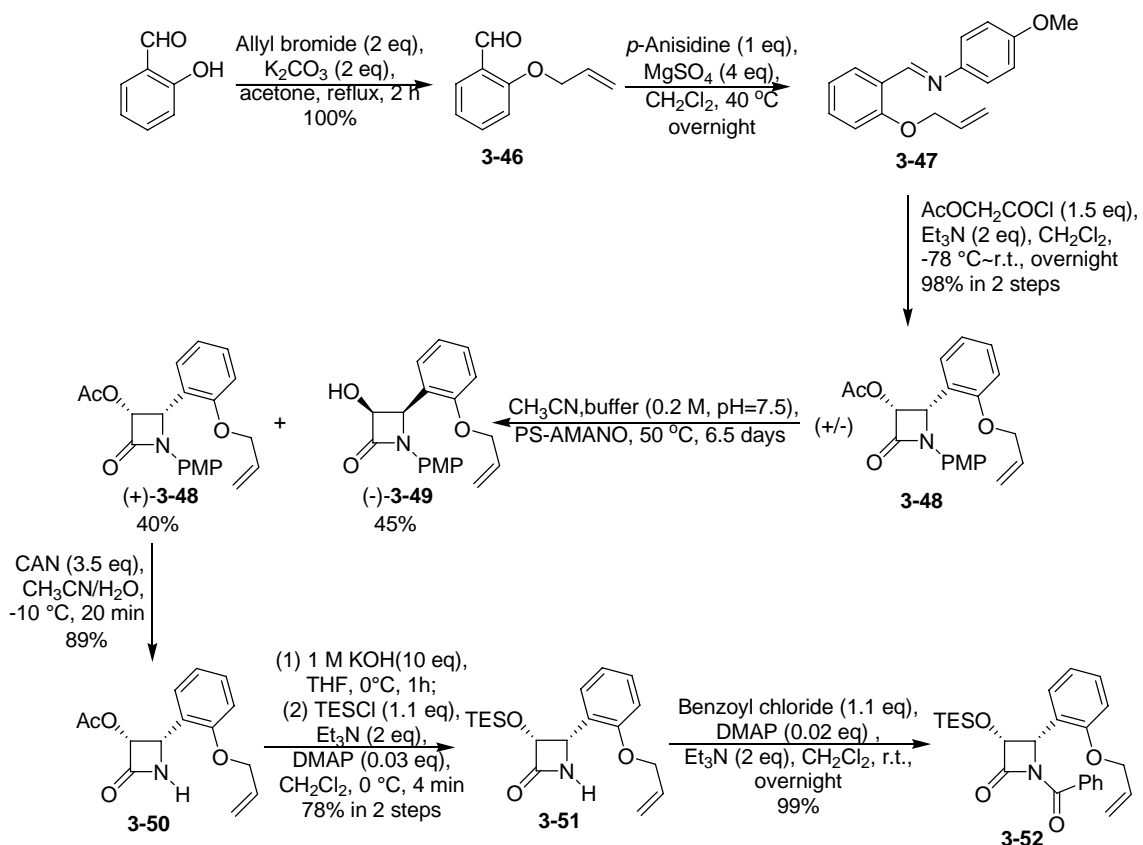
The synthesis of β-lactam **3-61** is shown in **Scheme 3-21**. The reduction of **3-21** by LiAlH$_4$ in refluxing THF afforded the desired alcohol **3-53** in 95% yield.[68] Since the oxidation of **3-53** was not complete by SO$_3$-Py, PCC was used to give complete conversion after 2.5 h.[69] The resulting aldehyde **3-54** was reacted with *p*-anisidine to give the crude imine **3-55**, which underwent cycloaddition with acetoxyacetylchloride to afford the desired β-lactam **3-56** in 79% yield in 3 steps.[67] Enzymatic kinetic resolution afforded enantiopure **(+)-3-56** in 43% yield and alcohol **(-)-3-57** in 46% yield.

Deprotection of the PMP group by CAN, hydrolysisof the acetyl group, TES protection of the resulting hydroxyl group and benzoylation of the N1 position gave the desired β-lactam **3-61** in good overall yield.
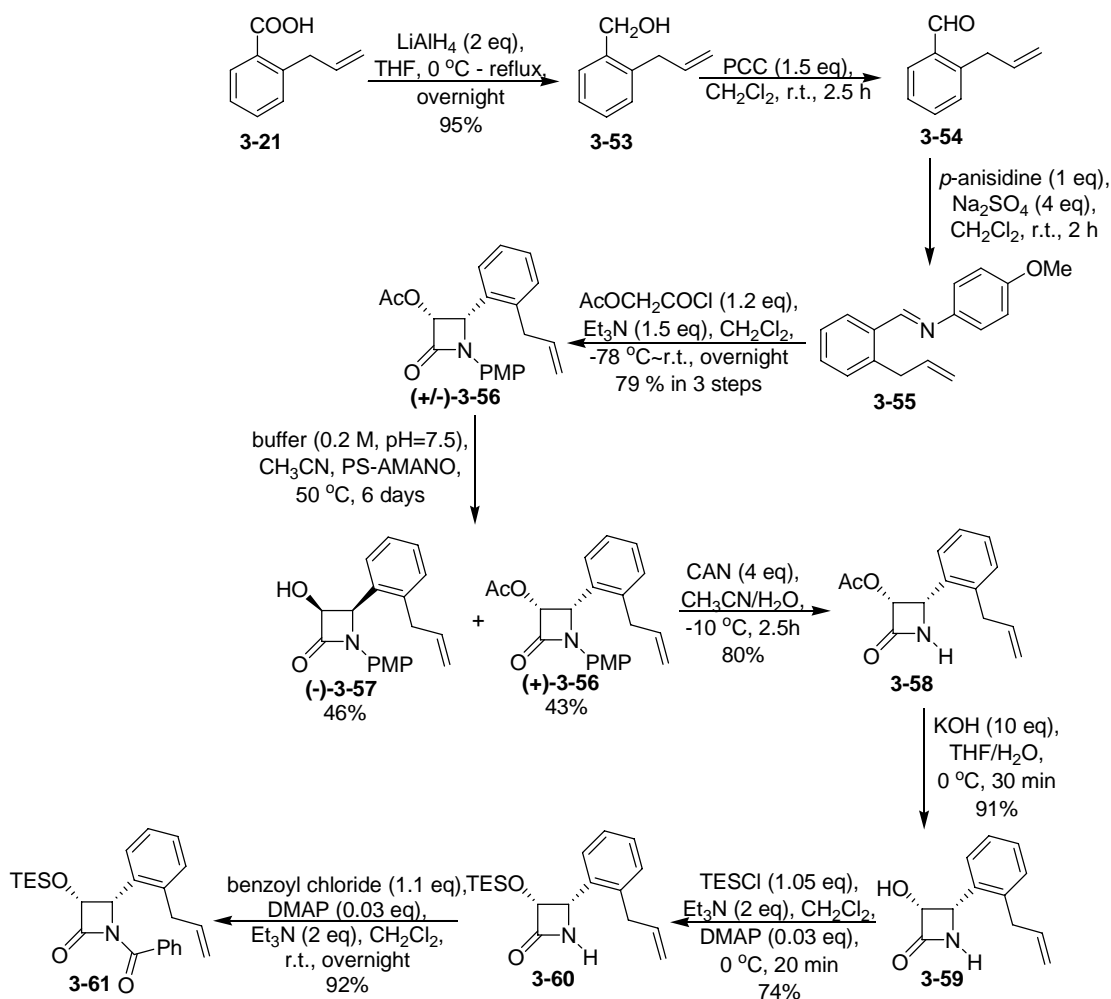
Scheme 3-21. Synthesis of β-lactam 3-61

As shown in **Scheme 3-22**, the Ojima-Holton coupling reaction of **3-36** with **3-52** proceeded smoothly. However, when the reaction was quenched by dilute sodium bicarbonate solution, one of the TES groups was lost under the basic conditions, giving diene **3-62** in 60% yield. The desired macrocycle taxoid **3-63** was obtained, after refluxing **3-62** for two days, using 40% the "first-generation Grubbs catalyst"[26] in a concentrated solution. Then the silyl group was removed using HF-pyridine to afford **K2a** in good yield (*E*-isomer only).
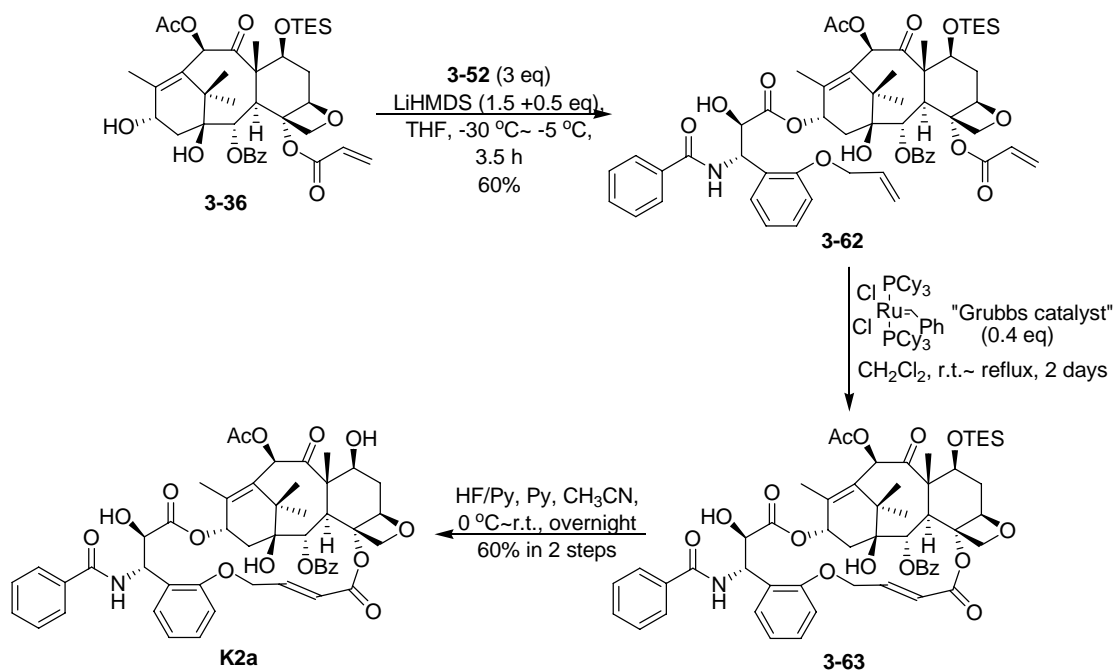
Scheme 3-22. Synthesis of K2a

The synthesis of **K1a** is shown in **Scheme 3-23**. The Ojima-Holton coupling of the modified bacctin **3-36** with β-lactam **3-61** gave diene **3-64** in 75% yield. RCM reaction using the "first-generation Grubbs catalyst" gave a mixture of macrocyclic compounds **3-65 (**Z-isomer) in 60% yield and the E-isomer in 24% yield. **K1a** was obtained after the final deprotection in high yield.
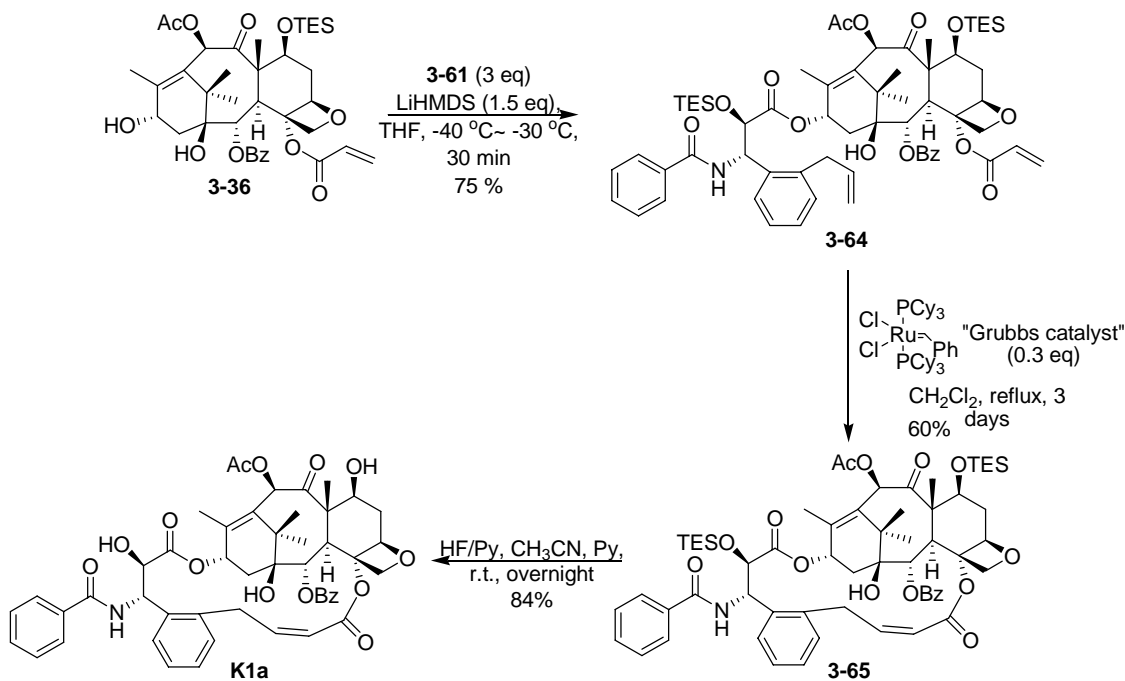
Scheme 3-23. Synthesis of K1a

§ 3.2.6 *In vitro* Cytotoxicity Assay of Macrocyclic Taxoids

Paclitaxel, **SB-T-2053**, **SB-T-2054**, **SB-T-2055Z/E**, **SB-TCR-501**, **K1a**, **K2a** and one second-generation taxoid **SB-T-1214** were evaluated for their cytotoxicity against six cancer cell lines by standard MTT assay.

MTT [3-(4,5-dimethylthiazol-2-yl)-2,5-diphenyltetrazolium bromide] assay is a standard colorimetric assay for measuring cellular proliferation (cell growth). It can also be used to determine cytotoxicity of potential medicinal agents and other toxic materials. The mechanism of the MTT assay is shown in **Scheme 3-24.** The yellow salt can dissolve in water solution and is reduced by mitochondrial reductase in live cell. The product of the reaction is a blue crystal that can only dissolves in acidic organic solvent.[70]
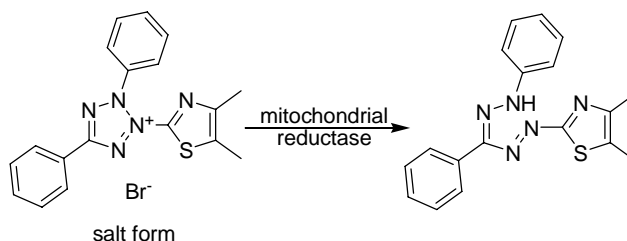
Scheme 3-24 MTT assay

All cell lines were obtained from the Roswell Park Cancer Institute and were cultured by the standard procedure. All experiments were performed in 96-well plates and repeated three times in parallel. The standard deviations were usually less than 10%.

As shown in **Table 3-7**, **SB-T-2053** is 3-10 times less active than paclitaxel in the drug-sensitive cell lines and 2-3 times less active in the drug-resistent cell lines. Similar results were obtained in the previous studies. **SB-T-2054** shows a slightly higher activity compared to paclitaxel, similar to **K2a**, against all cell lines. **SB-T-2055Z** and **SB-T-2055E** are much less active than paclitaxel, while the *Z* isomer is ~ 10 times more active than the *E* isomer. **SB-TCR-501** only shows micromolar activities, similar to **SB-T-2055E**, due to the blockage of the important C2'-OH. Kingston's most active compound **K1a** is at least 10 times more active than paclitaxel. **K1a** also shows similar activity to **SB-T-1214** against the drug-sensitive cell lines, but is less active than **SB-T-1214** against the drug-resistant cell lines.

Table 3-7. Cytotoxicity assay of macrocyclic taxoids

Compounds	A2780[b]	MCF7[c]	NCI-ADR[d]	LCC6-WT[e]	LCC6-MDR[f]	HT-29[g]
			IC50 (nM)[a]			
Paclitaxel	36.10	1.85	394.6	2.45	110.2	7.28
SB-T-2053	114.0	12.27	591.7	12.20	300.3	29.23
SB-T-2054	31.00	3.49	425.3	2.09	129.4	16.97
K2a	25.27	2.97	100.9	4.86	298.6	3.10
K1a	2.78	0.19	8.19	0.28	7.97	0.06
SB-T-1214	2.83	0.33	5.73	0.39	2.36	0.29
SB-T-2055E	1475	1650	10013	2066	2285	522.9
SB-T-2055Z	198.0	196.4	1134	348.0	1923	62
SB-TCR-501	1839	2286	-	1789	3211	2115

[a]Concentration of compound which inhibits 50% (IC$_{50}$, nM) of the growth of human tumor cell line after 72 h drug exposure. [b]A2780 human ovarian carcinoma (Pgp-). [c]MCF7: human breast carcinoma cell line (Pgp-). [d]NCI/ADR: multi-drug resistant human ovarian carcinoma cell line (Pgp+). [e]LCC6-WT: human breast carcinoma cell line (Pgp-). [f]LCC6-MDR: *mdr1* transduced cell line (Pgp+). [g]HT-29 human colon carcinoma (Pgp-).

§ 3.3 Summary

Several macrocyclic paclitaxel analogues were designed and synthesized based on the binding conformations of paclitaxel in β-tubulin. **SB-TCR-102**, designed based on the old model, did not show any activity in both cytotoxicty assay and tubulin polymerization assay.

The REDOR-Taxol conformation was proposed as the bioactive conformation based on the REDOR-NMR, photoaffinity labeling and molecular modeling studies. A series of C3'*N*-C14-linked macrocyclic taxoids were synthesized. **SB-T-2053** showed 2-15 times less activity than paclitaxel in cytotoxicity assay, but similar or slightly higher activity in tubulin polymerization assay. **SB-T-2054**, obtained from a unique ring-closing reaction, possessed the same-size but more rigid ring than that of **SB-T-2053** and showed similar or slightly higher activity than paclitaxel. **SB-T-2055*Z*** and **SB-T-2055*E*,** with more flexible structures, possessed much less activity than paclitaxel. **SB-TCR-501** showed only micromolar activity because of the lack of the important C2'-OH. Kingston's two macrocyclic taxoids were also synthesized and compared to our taxoids. **K1a** was very acitive as reported, similar to the second-generation taxoid, **SB-T-1214**, while **K1b** showed similar activity to **SB-T-2054** or paclitaxel.

§ 3.4 Experimental Section

General Methods: ^{1}H and ^{13}C NMR spectra were measured on a Varian 300, 400, 500 or 600 NMR spectrometer. Melting points were measured on a Thomas Hoover Capillary melting point apparatus and are uncorrected. Optical rotations were measured on a Perkin-Elmer Model 241 polarimeter. IR spectra were recorded on a Perkin-Elmer Model 1600 FT-IR spectrophotometer. TLC was performed on Merck DC-alufolien with Kieselgel 60F-254 and column chromatography was carried out on silica gel 60 (Merck; 230-400 mesh ASTM). Purity was determined with a Waters HPLC assembly consisting of dual Waters 515 HPLC pumps, a PC workstation running Millennium 32, and a Waters 996 PDA detector, using a Phenomenex Curosil-B column, employing CH_3CN/water (2/3) as the solvent system with a flow rate of 1 mL/min. High-resolution mass spectra were obtained from Mass Spectrometry Laboratory, University of Illinois at Urbana-Champaign, Urbana, IL.

Materials: The chemicals were purchased from Aldrich Co. and Sigma and purified before use by standard methods. Tetrahydrofuran was freshly distilled from sodium metal and benzophenone. Dichloromethane was also distilled immediately prior to use under nitrogen from calcium hydride. 10-Deacetylbaccatin III (DAB) and 14-*β*-hydroxy-10-deacetyl baccatin III (14-OH-DAB) were obtained from Indena, SpA, Italy.

1-Dimethylhydrosilyl-7,10,13-tris(triethylsilyl)-10-deacetylbaccatin (3-6):[42]
To a solution of 7,10,13-tris-TES-10-DAB **1-28** (250 mg, 0.281 mmol) and imidazole (77 mg, 1.972 mmol) in DMF (1.25 mL) was added chlorodimethylsilane (0.094 mL, 0.844 mmol) at 0 ^{o}C. The reaction mixture was stirred at 0 ^{o}C for 20 min and quenched with saturated aqueous NH_4Cl solution (5 mL) and extracted with EtOAc (30 mL x 3). The organic layer was washed with H_2O (10 mL x 2) and brine (10 mL) and dried over anhydrous $MgSO_4$. The solvent was removed under reduced pressure and the residue was purified on a silica gel column using hexanes:EtOAc (15/1) as the eluent to afford **3-6** as a white solid (278 mg, 100%): mp 85-87 ^{o}C; ^{1}H NMR (400 MHz, CDCl$_3$) δ -0.30 (d, J = 2.8 Hz, 3 H), 0.06 (d, J = 2.8 Hz, 1 H), 0.55-0.72 (m, 18 H), 0.94-1.05 (m, 27 H), 1.10 (s, 3 H), 1.18 (s, 3 H), 1.65 (s, 3 H), 1.88 (m, 1 H), 1.98 (s, 3 H), 2.28 (s, 3 H), 2.34 (m, 2 H), 2.51 (m, 1 H), 3.84 (d, J = 6.8 Hz, 1 H), 4.23 (dd, J = 13.2, 8.4 Hz, 2 H), 4.38 (dd, J = 10.4, 6.0, 1 H), 4.53 (m, 1 H), 4.95 (m, 2 H), 5.16 (s, 1 H), 5.71 (d, J = 6.8 Hz, 1 H), 7.46 (t, J = 8.0 Hz, 2 H), 7.57 (t, J = 7.6 Hz, 1 H), 8.10 (d, J = 6.8 Hz, 2 H); ^{13}C NMR (62.9 MHz, CDCl$_3$) δ -0.3, 0.1, 4.1, 4.6, 5.0, 5.2, 5.5, 5.8, 6.2, 6.6, 6.7, 10.1, 13.9, 14.2, 20.6, 21.1, 22.1, 27.0, 37.2, 39.1, 43.8, 46.4, 58.0, 60.0, 68.2, 72.5, 75.5, 75.6, 76.3, 80.8, 81.8, 83.8, 128.1, 129.8, 130.3, 132.9, 135.7, 138.4, 165.1, 167.3, 168.1, 169.6, 205.2. All data are consistent with the reported values.[42]

1-Dimethylhydrosilyl-4-deacetyl-7,10,13-tris(triethylsilyl)-10-deacetylbaccatin (3-7): [42]

To a solution of **3-6** (278 mg, 0.286 mmol) in THF (6 mL) was added Red-Al (65% in toluene, 0.7 mL, 2.29 mmol) at 0 $^{\circ}$C and was warmed up to 4 $^{\circ}$C over 2 h. The reaction was quenched with saturated aqueous NH_4Cl solution (30 mL) and extracted with EtOAc (30 mL x 3). The organic layer was washed with H_2O (10 mL) and brine (10 mL) and dried over anhydrous $MgSO_4$. The solvent was removed under reduced pressure and the residue was purified on a silica gel column using hexanes:EtOAc (30/1) as the eluent to afford **3-7** as a white solid (183 mg, 74%): mp 86-88 $^{\circ}$C; ^{1}H NMR (400 MHz, CDCl$_3$) δ - 0.31 (d, J = 2.8 Hz, 3 H), 0.04 (d, J = 2.8 Hz, 1 H), 0.51-0.80 (m, 18 H), 0.81-1.09 (m, 27 H), 1.09 (s, 3 H), 1.18 (s, 3 H), 1.55 (s, 3 H), 1.94 (s, 3 H), 1.99 (m, 1 H), 2.44 (m, 1 H), 2.55 (m, 1 H), 2.80 (dd, J = 15.2, 2.4 Hz, 1 H), 3.60 (d, J = 5.6 Hz, 1 H), 3.76 (s, 1 H), 4.02 (dd, J = 12.0, 6.0 Hz, 1 H), 4.20 (d, J = 7.6 Hz, 1 H), 4.30 (d, J = 7.6 Hz, 1 H), 4.57 (m, 1 H), 4.67 (m, 2 H), 5.22 (s, 1 H), 5.59 (d, J = 7.5 Hz, 1 H), 7.42 (t, J = 8.0 Hz, 2 H), 7.62 (tt, J = 9.2, 1.2 Hz, 1 H), 8.12 (d, J = 6.8 Hz, 2 H); ^{13}C NMR (62.9 MHz, CDCl$_3$) δ 0.2, 0.6, 4.6, 5.1, 5.9, 6.7, 6.8, 6.9, 9.9, 17.0, 18.3, 29.9, 37.6, 38.3, 42.9, 51.5, 59.2, 69.9, 73.0, 73.5, 74.7, 76.4, 79.5, 80.2, 88.3, 128.2, 130.2, 132.9, 135.6, 140.3, 165.0, 205.5. HRMS (FAB/DCM/NaCl) m/z calcd. for $C_{47}H_{82}O_9Si_4H^+$: 903.5114 found: 903.5087 (Δ = -3.0 ppm). All data are consistent with the reported values.[42]

1-Dimethylhydrosilyl-4-deacetyl-4-(pent-4-enoyl)-7,10,13-tris(triethylsilyl)-10-deacetylbaccatin (3-8):[42]

To a solution of **3-7** (179 mg, 0.198 mmol) in THF (1.8 mL) was added LiHMDS (1 N in THF, 0.23 mL, 0.23 mmol) at -30 $^{\circ}$C. The reaction mixture was stirred for 5 min and pent-4-enoyl chloride (0.025 mL, 0.23 mmol) was added at -30 $^{\circ}$C. The reaction mixture was warmed up to -10 $^{\circ}$C over 20 min, quenched with saturated aqueous NH_4Cl solution (20 mL) and extracted with EtOAc (30 mL x 3). The organic layer was washed with brine (10 mL) and dried over anhydrous $MgSO_4$. The solvent was removed under reduced pressure and the residue was purified on a silica gel column using hexanes:EtOAc (40/1) as the eluent to afford **3-8** as a white solid (170 mg, 87%): mp 132-134 $^{\circ}$C; ^{1}H NMR (300 MHz, CDCl$_3$) δ -0.30 (d, J = 2.7 Hz, 3 H), 0.05 (d, J = 2.7 Hz, 1 H), 0.53-0.73 (m, 18 H) (m, 18 H), 0.85-1.02 (m, 27 H) (m, 27 H), 1.10 (s, 3 H), 1.18 (s, 3 H), 1.65 (s, 3 H), 1.86 (m, 1 H), 1.96 (s, 3 H), 2.29 (m, 2 H), 2.52 (m, 3 H), 2.64 (m, 2 H), 3.82 (d, J = 6.9 Hz, 1 H), 4.22 (m, 2 H), 4.36 (dd, J = 10.5, 6.6 Hz, 1 H), 4.53 (m, 1 H), 4.87 (d, J = 6.3, 1 H), 4.95 (d, J = 9.9, 1 H), 5.13 (m, 3 H), 5.71 (d, J = 6.9 Hz, 1 H), 5.89 (m, 1 H), 7.45 (t, J = 7.5 Hz, 2 H), 7.57 (t, J = 7.5 Hz, 1 H), 8.10 (d, J = 7.5 Hz, 2 H); ^{13}C NMR (62.9 MHz, CDCl$_3$) δ 0.0, 0.3, 4.8, 4.9, 5.2, 6.0, 6.8, 6.9, 10.4, 14.3, 21.5, 27.3, 29.0, 34.5, 37.3, 39.3, 44.0, 46.6, 58.2, 68.3, 72.6, 75.6, 75.9, 76.5, 76.6, 81.1, 82.0, 84.2, 116.0, 128.3, 130.1, 130.5, 133.1, 135.9, 136.2, 138.5, 165.3, 171.6, 205.5. All data are consistent with literature data.[42]

4-Deacetyl-4-(pent-4-enoyl)baccatin (3-9):[42]

To a solution of **3-8** (171 mg, 0.184 mmol) in pyridine/acetonitrile (1:1, 6.8 mL) was added dropwise HF/pyridine (70:30, 1.7 mL) at 0 °C, then the mixture was stirred for overnight at room temperature. The reaction was quenched with saturated aqueous $NaHCO_3$ solution (5.0 mL). The mixture was then diluted with EtOAc (60 mL), washed with saturated aqueous $CuSO_4$ solution (10 mL x 3) and H_2O (10 mL), dried over anhydrous $MgSO_4$ and concentrated *in vacuo* to afford 4-deacetyl-4-(pent-4-enoyl)-10-deacetyl-baccatin as a white solid (125 mg). The crude product was used in the next step without further purification.

To a solution of product (125 mg, crude), thus obtained, in THF (6.5 mL) were added $CeCl_3.7H_2O$ (8 mg, 0.02 mmol) and acetic anhydride (0.25 ml, 1.84 mmol). Then, the mixture was stirred for 2 h at room temperature and quenched with H_2O (20 mL). The mixture was extracted with EtOAc (30 mL x 3), washed with brine (15 mL), dried over anhydrous $MgSO_4$ and concentrated *in vacuo*. The residue was purified on a silica gel column using hexanes:EtOAc (1/1) as the eluent to afford **3-9** as a white solid (106 mg, 98% for 2 steps): ^{1}H NMR (500 MHz, $CDCl_3$) δ 1.08 (s, 3 H), 1.09 (s, 3 H), 1.65 (s, 3 H), 1.73 (s, 1 H), 1.83 (m, 1 H), 2.03 (s, 3 H), 2.20 (s, 3 H), 2.25 (m, 2 H), 2.35 (s, 1 H), 2.48 (q, J = 12.0 Hz, 2 H), 2.55 (m, 2 H), 2.69 (m, 2 H), 3.87 (d, J = 7.0 Hz, 1 H), 4.14 (d, J = 8.5 Hz, 1 H), 4.29 (d, J = 8.5 Hz, 1 H), 4.48 (m, 1 H), 4.85 (d, J = 6.5 Hz, 1 H), 4.93 (d, J = 9.0 Hz, 1 H), 5.10 (m, 2 H), 5.61 (d, J = 6.9 Hz, 1 H), 5.89 (m, 1 H), 6.31 (s, 1 H), 7.47 (t, J = 7.5 Hz, 2 H), 7.60 (t, J = 7.5 Hz, 1 H), 8.09 (d, J = 7.0 Hz, 2 H). All data are consistent with literature data.[42]

7-Triethylsilyl-4-deacetyl-4-(pent-4-enoyl)baccatin (3-2):[42]

To a solution of **3-9** (99 mg, 0.158 mmol) and imidazole (43.0 mg, 0.632 mmol) in dry DMF (1.6 mL) was added chlorotriethylsilane (0.11 μL, 0. 474 mmol) dropwise *via* syringe at 0 °C. The reaction mixture was stirred for 1 h at room temperature and quenched with saturated aqueous NH_4Cl solution (20 mL). The mixture was extracted with EtOAc (300 mL x 3), washed with water (10 mL x 2), and brine (10 mL), dried over $MgSO_4$, and concentrated *in vacuo*. The crude product was purified on a silica gel column using hexanes:EtOAc (4/1 followed by 2/1) as the eluent to give **3-2** as a white solid (95 mg, 81%): mp 114-116 °C; ^{1}H NMR (300 MHz, $CDCl_3$) δ 0.58 (m, 6 H), 0.92 (m, 9 H), 1.04 (s, 3 H), 1.19 (s, 3 H), 1.68 (s, 3 H), 1.87 (m, 1 H), 1.96 (d, J = 5.4 Hz, 1 H), 2.18 (s, 6 H), 2.27 (d, J = 8.1 Hz, 2 H), 2.52 (m, 4 H), 2.69 (m, 2 H), 3.87 (d, J = 6.9 Hz, 1 H), 4.15 (d, J = 8.4 Hz, 1 H), 4.31 (d, J = 8.7 Hz, 1 H), 4.49 (m, 1 H), 4.84 (m, 1 H), 4.91 (d, J = 7.8 Hz, 1 H), 5.11(m, 2 H), 5.63 (d, J = 6.6, 1 H), 5.91 (m, 1 H), 6.46 (s, 2 H), 7.48 (t, J = 7.5 Hz, 2 H), 7.61 (t, J = 6.9 Hz, 1 H), 8.12 (d, J = 7.2 Hz, 2 H); ^{13}C NMR (62.9 MHz, $CDCl_3$) δ 5.5, 7.0, 10.2, 15.1, 20.3, 21.2, 27.0, 29.0, 34.9, 37.5, 38.5, 43.0, 47.6, 58.9, 68.2, 72.6, 75.0, 76.0, 76.8, 79.0, 81.1, 84.5, 116.1, 128.8, 129.6, 130.3, 132.9, 133.9, 136.9, 144.1, 167.3, 169.6, 172.7, 202.4. HRMS (FAB/DCM/NaCl) m/z calcd. for $C_{40}H_{56}O_{11}Si_3H^+$: 741.3670 found: 741.3668 (Δ = 0.2 ppm). All data are consistent with literature data.[42]

(*3R,4S*)-1-(4-Methoxyphenyl)-3-triethylsilyloxy-4-phenylazetidin-2-one (3-10):[42]

To a mixture of THF (21 mL) and 1 N KOH (18 mL) at 0 °C was added a solution of **1-12** (565 mg, 1.81 mmol) in THF (31 mL). The solution was stirred at 0 °C for 1 h and saturated NH_4Cl solution (30 mL) was added. The mixture was extracted with ethyl acetate (30 mL x 3), dried over $MgSO_4$ and concentrated to give (*3R,4S*)-1-(4-methoxyphenyl)-3-hydroxyl– 4-phenyl-azetidin-2-one (**1-13**) as white solid (468 mg, crude).

To a solution of **1-13**, thus obtained, and DMAP (42 mg, 0.34 mmol) in CH_2Cl_2 (7.5 mL) was added triethylamine (0.75 mL, 5.13 mmol) and TESCl (0.43 mL, 2.57 mmol). The reaction mixture was stirred for 1.5 h and quenched with saturated aqueous NH_4Cl solution (30 mL), extracted with ether (50 mL x 3), and washed with brine (10 mL). The organic layers were combined, dried over anhydrous $MgSO_4$, and the solvent was removed under reduced pressure. The crude product was purified on a silica gel column using hexanes/EtOAc (15:1) as the eluent to afford **3-10** as a white solid (681 mg, 96 % yield for two steps): mp 108-109°C; ^{1}H NMR (300 MHz, $CDCl_3$) δ 0.45 (m, 6 H), 0.78 (t, $J = 8.1$ Hz, 9 H), 3.74 (s, 3 H), 5.11 (d, $J = 5.1$ Hz, 1 H), 5.14 (d, $J = 5.1$ Hz, 1 H), 6.78 (d, $J = 9.0$ Hz, 2 H), 7.35 (m, 7 H). HRMS (FAB/DCM/NaCl) m/z calcd. for $C_{22}H_{29}NO_3SiH^+$: 384.1995 found: 384.1996 (Δ = 0.3 ppm). All data are consistant with literature data.[52]

(*3R,4S*)-1-(4-Methoxyphenyl)-3-allyl-3-triethylsilyloxy-4-phenylazetidin-2-one (3-11):

To a solution of diisopropylamine (0.133 mL, 0.934 mmol) in THF (4.5 mL) was added 2.5 M *n*-butyllithium in hexane (0.375 mL, 0.934 mmol) at -15 °C and the reaction mixture was stirred for 30 min at -20 °C. Then, the reaction mixture was cooled down to -30 °C and a solution of β-lactam **3-10** (239 mg, 0.623 mmol) in THF (3.1 mL) was added slowly *via* cannula. The reaction mixture was stirred at -30 °C for 30 min and allyl bromide (0.165 mL, 1.87 mmol) was added. The reaction mixture was warmed up to -10 °C over 1 h, quenched with saturated aqueous NH_4Cl solution (20 mL), and extracted with EtOAc (30 mL x 3). The organic layers were combined and dried over anhydrous $MgSO_4$. The solvent was removed under reduced pressure and the crude product was purified on a silica gel column using hexanes:EtOAc (50/1) as the eluent to afford β-lactam **3-11** as a colorless oil (192 mg, 75%): ^{1}H NMR (400 MHz, $CDCl_3$) δ 0.50 (m, 6 H), 0.73 (m, 9 H), 2.62 (dd, $J = 14.0, 7.6$ Hz, 1 H), 2.76 (dd, $J = 14.0, 7.6$ Hz, 1 H), 3.76 (s, 3 H), 4.97 (s, 1 H), 5.26 (m, 2 H), 5.96 (m, 1 H), 6.82 (m, 2 H), 7.19 (m, 2 H), 7.31 (m, 5 H); ^{13}C NMR (100.5 MHz, $CDCl_3$), δ 5.6, 6.6, 41.3, 55.5, 66.4, 87.1, 114.3, 118.8, 119.3, 127.5, 127.7, 128.1, 131.0, 132.4, 134.8, 156.2, 166.9. HRMS (FAB/DCM/NaCl) m/z calcd. for $C_{25}H_{33}NO_3SiH^+$: 424.2308 found: 424.2298 (Δ = -2.4 ppm).

(*3R,4S*)- 3-Allyl-3-triethylsilyloxy-4-phenylazetidin-2-one (3-12):

To a solution of **3-11** (382 mg, 0.88 mmol) in acetonitrile (24 mL) and H_2O (4 mL) at -10 °C was added cerium ammonium nitrate (CAN) (1.4 g, 2.65 mmol) in H_2O (24 mL) dropwise *via* addition funnel. The reaction mixture was allowed to stir for 0.5 h and quenched with saturated aqueous Na_2SO_3 solution (40 mL). The aqueous layer was extracted with EtOAc (50 mL x 3) and the combined organic layers were washed with brine (10 mL x 2), dried over anhydrous $MgSO_4$ and concentrated under reduced pressure. The crude product was purified on a silica gel column using hexanes:EtOAc (8:1) to yield **3-12** as a colorless oil (221 mg, 79%): ^{1}H NMR (500 MHz, $CDCl_3$) δ 0.43 (m, 6 H), 0.77

(m, 9 H), 4.80 (d, J = 4.5 Hz, 1 H), 5.09 (dd, J = 4.5, 2.5 Hz, 1 H), 6.04 (s, 1 H), 7.34 (m, 5 H); ^{13}C NMR (100.5 MHz, CDCl$_3$) δ 5.5, 6.5, 41.2, 62.7, 89.0, 118.9, 126.9, 127.3, 127.8, 132.5, 136.9, 171.4. HRMS (FAB/DCM/NaCl) m/z calcd. for C$_{18}$H$_{27}$NO$_2$SiH$^+$: 318.1889 found: 318.1890 (Δ = 0.2 ppm).

(3R,4S)-1-tert-Butoxycarbonyl-3-triethylsilyloxy-3-allyl-4-phenylazetidin-2-one (3-3):
To a solution of **3-12** (102 mg, 0.315 mmol), DMAP (12 mg, 0.089 mmol) and triethylamine (0.17 mL, 0.95 mmol) in CH$_2$Cl$_2$ (2.9 mL) was added di-*tert*-butyl dicarbonate (77 mg, 0.35 mmol) in CH$_2$Cl$_2$ (1 mL). The reaction mixture was stirred overnight and quenched with saturated aqueous NH$_4$Cl solution (20 mL). The reaction mixture was extracted with EtOAc (30 mL x 3). The organic layer was washed with brine (10 mL), dried over MgSO$_4$, and concentrated under reduced pressure. The crude product was purified by column chromatography on silica gel using hexanes:EtOAc (30:1) as the eluent to yield **3-3** as a colorless oil (136 mg, 99%): ^{1}H NMR (400 MHz, CDCl$_3$) δ 0.43 (m, 6 H), 0.70 (m, 9 H), 1.43 (s, 9 H), 2.58 (dd, J = 14.0, 7.6 Hz, 1 H), 2.69 (dd, J = 14.0, 6.0 Hz, 1 H), 4.89 (s, 1 H), 5.28 (m, 3 H), 5.94 (m, 1 H), 7.13 (d, J = 8.4 Hz, 2 H), 7.30 (m, 3 H); ^{13}C NMR δ (100.5 MHz, CDCl$_3$) δ 5.5, 6.7, 27.8, 41.0, 65.6, 83.4, 87.1, 119.9, 126.9, 127.6, 127.9, 131.4, 134.6, 148.2, 167.6. HRMS (FAB/DCM/NaCl) m/z calcd. for C$_{23}$H$_{35}$NO$_4$SiH$^+$: 418.2414 found: 418.2412 (Δ = -0.4 ppm).

10-Acetyl-4-deacetyl-4-(pent-4-enoyl)-7-triethylsilyl-2'-allyl-2'-triethylsilyloxy-docetaxel (3-1):
To a solution of **3-2** (40 mg, 0.054 mmol) and β-lactam **3-3** (113 mg, 0.27 mmol) in THF (6 mL) was added NaHMDS (1 N in THF, 0.08 ml, 0.08 mmol) at -30 ^{o}C. The reaction mixture was stirred for 20 min, quenched with saturated aqueous NH$_4$Cl solution, and extracted with EtOAc. The organic layers were combined, dried over MgSO$_4$, and solvent was removed under reduced pressure. The residue was purified by column chromatography on silica gel using hexanes:EtOAc (14:1) to afford **3-1** as a white solid (53 mg, 85%): mp 103-105 ^{o}C; ^{1}H NMR (600 MHz, CDCl$_3$) δ 0.58 (m, 6 H), 0.78 (m, 6 H), 0.92 (m, 18 H), 1.17 (s, 9 H), 1.25 (s, 6 H), 1.30 (s, 3 H), 1.87 (m, 1 H), 2.00 (s, 3 H), 2.18 (s, 3 H), 2.22 (m 2 H), 2.35 (m, 1 H), 2.53 (m, 2 H), 2.72 (m, 3 H), 3.29 (m, 1 H), 3.81 (d, J = 7.2 Hz, 1 H), 4.19 (d, J = 8.4 Hz, 1 H), 4.31 (d, J = 8.4 Hz, 1 H), 4.47 (m, 1 H), 4.88 (d, J = 9.6 Hz, 1 H), 5.10 (m, 3 H), 5.22 (d, J = 10.8 Hz, 1 H), 5.33 (d, J = 9.6 Hz, 1 H), 5.71 (d, J = 6.6, 1 H), 5.97 (m, 1 H), 6.31 (t, J = 9.0 Hz, 1 H), 6.46 (s, 1 H), 7.32 (s, 5 H), 7.48 (t, J = 7.2 Hz, 2 H), 7.59 (t, J = 6.6 Hz, 1 H), 8.18 (d, J = 7.2 Hz, 2 H); ^{13}C NMR (100.5 MHz, CDCl$_3$) δ 5.3, 6.7, 7.1, 7.4, 10.2, 14.7, 20.9, 26.9, 28.1, 30.1, 31.6, 35.6, 37.2, 41.9, 43.5, 46.7, 58.4, 60.1, 72.3, 72.4, 74.9, 75.1, 79.2, 79.5, 81.7, 83.4, 84.4, 116.7, 119.9, 128.0, 128.6, 128.8, 129.3, 130.4, 131.8, 132.9, 133.5, 136.0, 137.8, 140.9, 154.5, 167.1, 169.2, 172.1, 174.3, 201.8; HRMS (FAB/DCM/NaCl) m/z calcd. for C$_{63}$H$_{91}$NO$_{15}$Si$_2$H$^+$: 1158.6006 found: 1158.5989 (Δ = -1.4 ppm).

7,2'-Bistriethylsilyl-SB-TCR-102 (3-13):

To a solution of **3-1** (50 mg, 0.043 mmol) in CH_2Cl_2 (24 mL) was added the "first-generation Grubbs catalyst" (10 mg, 0.01 mmol) in CH_2Cl_2 (0.2 mL). The reaction was stirred overnight and solvent was removed under reduced pressure. The crude product was passed through a short silica gel column using hexanes:EtOAc (8:1) to remove the catalyst to afford **3-13** as a yellow solid (40 mg, 82%): mp 143-146°C; ^1H NMR (600 MHz, $CDCl_3$) δ 0.58 (m, 6 H), 0.83 (m, 6 H)), 0.93 (m, 9 H), 0.99 (m, 9 H), 1.22 (s, 3 H), 1.26 (s, 3 H), 1.32 (s, 9 H), 1.67 (s, 3 H), 1.88 (m, 1 H), 1.91 (s, 3 H), 2.19 (s, 3 H), 2.22 (m 2 H), 2.36 (m, 1 H), 2.53 (m, 2 H), 2.66 (m, 2 H), 2.82 (m, 2 H), 3.59 (d, J = 6.6 Hz, 1 H), 4.16 (d, J = 7.8 Hz, 1 H), 4.33 (d, J = 8.4 Hz, 1 H), 4.45 (dd, J = 10.8, 7.2 Hz, 1 H), 4.80 (d, J = 8.4 Hz, 1 H), 5.01 (d, J = 9.0 Hz, 1 H), 5.23 (d, J = 9.0, 1 H), 5.47 (t, J = 8.5 Hz, 1 H), 5.72 (d, J = 7.8, 1 H) (H2), 5.89 (t, J = 9.6 Hz, 1 H), 5.98 (dd, J = 15.0, 11.2 Hz, 1 H), 6.47 (s, 1 H), 7.36 (m, 5 H), 7.53 (t, J = 7.8 Hz, 2 H), 7.65 (t, J = 7.8 Hz, 1 H), 8.13 (d, J = 7.2 Hz, 2 H); ^{13}C NMR (100.5 MHz, $CDCl_3$) δ 5.3, 6.7), 6.7, 7.3, 10.2, 14.6, 20.9, 21.2, 26.7, 28.2, 29.7, 32.9, 35.5, 37.0, 43.4, 47.1, 57.9, 72.1, 74.7, 75.3, 76.3, 79.5, 79.7, 80.5, 82.8, 84.0, 125.8, 128.1, 128.3, 128.6, 128.6, 129.4, 130.2, 132.9, 133.6, 137.5, 141.5, 154.9, 167.0, 169.1, 171.9, 174.3, 201.9; HRMS (FAB/DCM/NaCl) m/z calcd. for $C_{61}H_{89}NO_{15}Si_2H^+$: 1130.5693 found: 1130.5634 (Δ = -5.2 ppm).

SB-TCR-102:

To the solution of **3-13** (39 mg, 0.345 mmol) in CH_3CN (0.8 mL) and pyridine (0.8 mL) was added HF-pyridine (70:30, 0.4 mL) and the reaction mixture was stirred overnight. The reaction mixture was diluted with EtOAc (100 mL) and washed with saturated aqueous $NaHCO_3$ solution (10 mL), $CuSO_4$ solution (5 mL x 3), water (10 mL) and brine (10 mL). The organic layer was dried over anhydrous $MgSO_4$ and solvent was removed under reduced pressure. The residue was purified by column chromatography on silica gel using hexanes:EtOAc (2:1) as the eluent to afford **SB-TCR-102** as a white solid (20 mg, 70%): mp 190-192 °C; $[\alpha]_D^{22}$ −86 (c 0.34, $CHCl_3$); ^1H NMR (500 MHz, $CDCl_3$) δ 1.16 (s, 3 H), 1.25 (s, 3 H), 1.30 (s, 9 H), 1.67 (s, 3 H), 1.85 (m, 1 H), 1.87 (s, 3 H), 2.18 (m 2 H), 2.24 (s, 3 H), 2.48 (m, 4 H), 2.59 (m, 1 H), 2.85 (dt, J = 14.4, 2.8 Hz, 1 H), 3.07 (m, 1 H), 3.61 (d, J = 6.0 Hz, 1 H), 3.89 (s, 1H), 4.16 (d, J = 6.8 Hz, 1 H), 4.36 (d, J = 7.2 Hz, 1 H), 4.43 (dd, J = 8.8, 5.2 Hz, 1 H), 4.81 (d, J = 7.2 Hz, 1 H), 5.05 (d, J = 6.0 Hz, 1 H), 5.15 (d, J = 9.0, 1 H), 5.46 (t, J = 9.0 Hz, 1 H), 5.72 (d, J = 5.6, 1 H), 5.98 (m, 1 H), 6.30 (s, 1 H), 7.38 (m, 5 H), 7.54 (t, J = 8.0 Hz, 2 H), 7.66 (t, J = 6.0 Hz, 1 H), 8.14 (d, J = 6.0 Hz, 2 H); ^{13}C NMR (100.5 MHz, $CDCl_3$) δ 9.7, 15.4, 20.8, 21.2, 26.7, 28.2, 29.7, 33.2, 33.6, 35.2, 35.6, 43.4, 46.1, 58.2, 72.1, 75.3, 75.6, 76.3, 79.3, 79.8, 80.1, 80.7, 84.3, 125.9, 128.7, 128.9, 128.9, 129.0, 129.5, 129.7, 130.5, 132.4, 133.9, 137.2, 143.9, 155.3, 167.3, 171.6, 172.4, 176.8, 204.1. HRMS (FAB/DCM/NaCl) m/z calcd. for $C_{49}H_{59}NO_{15}H^+$: 902.3963, found: 902.3981 (Δ = 2.0 ppm).

14β-Hydroxybaccatin III (3-17):

To a solution of 14β-OH-baccatin III (200 mg, 0.37 mmol) in THF (13 mL) was added CeCl$_3$.7H$_2$O (16 mg, 0.037 mmol) and acetic anhydride (0.5 ml, 3.7 mmol). The mixture was stirred 2 h at room temperature and quenched with saturated aqueous NaHCO$_3$ solution (10 mL). The mixture was then extracted with EtOAc (30 mL x 3), washed with brine (15 mL), dried over anhydrous MgSO$_4$ and concentrated *in vacuo.* The crude product **3-17** was used directly for next step without further purification as a white solid (256 mg): mp 230-234 $^{\circ}$C; [α]$_D^{20}$ -48 (*c* 0.42, CH$_2$Cl$_2$); IR (KBr): ν= 3475, 1740, 1717, 1401, 1240, 1049, 716 cm^{-1}; ^{1}H NMR (500 MHz, CDCl3) δ 1.13 (s, 3 H), 1.16 (s, 3 H), 1.54 (s, 3 H), 1.69 (s, 3 H), 1.87 (m, 1 H), 2.06 (s, 3 H), 2.22 (s, 3 H), 2.24(s, 2 H), 2.43 (d, *J* = 4.0 Hz, 1 H), 2.55 (m, 1 H), 2.90 (d, *J* = 6.0 Hz, 1 H), 3.20 (s, 1 H), 3.81 (d, *J* = 7.5 Hz, 1 H), 4.02 (dd, *J* = 6.5, 4.0 Hz, 1 H), 4.20 (d, *J* = 8.5 Hz, 1 H), 4.29 (d, *J* = 8.0 Hz, 1 H), 4.45 (m, 1 H), 4.78 (t, *J* = 5.0 Hz, 1 H), 4.98 (d, *J* = 8.0 Hz, 1 H), 5.81 (d, *J* = 7.0 Hz, 1 H), 6.31 (s, 1 H), 7.50 (t, *J* = 8.0 Hz, 2 H), 7.62 (t, *J* = 7.0 Hz, 1 H), 8.09 (d, *J* = 6.0 Hz, 2 H); ^{13}C NMR (75.0 MHz, DMSO-d_6) δ 9.6, 14.1, 15.0, 20.8, 21.9, 22.3, 26.4, 36.7, 42.3, 46.2, 57.7, 59.8, 70.6, 72.1, 73.7, 74.7, 75.2, 75.3, 75.5, 80.0, 83.5, 128.7, 129.7, 129.8, 131.8, 133.3, 143.2, 165.4, 168.8, 169.9, 202.9. HRMS (FAB/DCM/NaCl) m/z calcd. for C$_{31}$H$_{38}$O$_{12}$H$^+$: 603.2441 found: 603.2467 (Δ = - 4.2 ppm). All data are consistent with the reported values.[42]

7-Triethylsilyl-14β-hydroxybaccatin III (3-18):[42]

To a solution of 14β-hydroxybaccatin III (**3-17**) (222 mg, 0.37 mmol) and imidazole (98 mg, 1.08 mmol) in DMF (5 mL) was added chlorotriethylsilane (0.18 mL, 1.08 mmol) dropwise *via* syringe at room temperature. The reaction mixture was stirred for 5 h at room temperature, quenched by saturated NH$_4$Cl, and extracted with EtOAc (30 mL x 3). The mixture was washed with H$_2$O (10 mL x 2), brine (10 mL), dried over anhydrous MgSO$_4$, and concentrated. The crude product was purified on a silica gel column using hexanes/EtOAc (2/1 followed by 1/1) as the eluent to give **3-18** as a white solid (219 mg, 83% for 2 steps): mp 164-166 $^{\circ}$C; ^{1}H NMR (300 MHz, CDCl$_3$) δ 0.58 (m, 6 H), 0.91 (m, 9 H), 1.02 (s, 3 H), 1.22 (s, 3 H), 1.68 (s, 3 H), 1.86 (m, 1 H) (H6a), 2.14 (s, 3 H), 2.17 (s, 3 H) (OAc), 2.28 (s, 3 H) (OAc), 2.50 (m, 1 H) (H6b), 3.26 (br s, 1 H), 3.61 (s, 1 H), 3.79 (br s, 1 H), 3.80 (d, *J* = 7.2 Hz, 1 H) (H3), 4.01 (d, *J* = 6.3 Hz, 1 H) (H14), 4.16 (d, *J* = 8.3 Hz, 1 H) (H20a), 4.24 (d, *J* = 8.3 Hz, 1 H) (H20b), 4.46 (dd, *J* = 6.5, 10.3 Hz, 1 H) (H7), 4.67 (d, *J* = 5.5 Hz, 1 H), 4.93 (d, *J* = 8.7 Hz, 1 H) (H5), 5.78 (d, *J* = 7.2 Hz, 1 H) (H2), 6.43 (s, 1 H) (H10), 7.41 (t, *J* = 7.5 Hz, 2 H), 7.55 (t, *J* = 7.5 Hz, 1 H), 8.02 (d, *J* = 7.4 Hz, 2 H); ^{13}C NMR (62.9 MHz, CDCl$_3$) δ 5.2, 6.7, 10.0, 14.6, 20.8, 21.8, 22.3, 26.2, 37.1, 42.8, 46.5, 58.6, 72.2, 74.1, 74.3, 75.5, 76.3, 76.7, 80.7, 84.1, 128.6, 129.3, 133.5, 141.3, 165.4, 169.3, 170.3, 202.3. HRMS (FAB/DCM/NaCl) m/z calcd. for C$_{37}$H$_{52}$O$_{12}$SiH$^+$: 717.3306 found: 717.3276 (Δ = 4.2 ppm). All data are consistent with the reported values.[42]

14-Allyl-7-triethylsilyl-14β-hydroxybaccatin III (3-15):[42]
To a solution of **3-18** (63 mg, 0.09 mmol) in DMF (3 mL) was added NaHMDS (1 N in THF, 0.1 mL, 1 mmol) at -40 °C. The reaction mixture was stirred for 5 min and then allyl iodide (0.012 mL, 0.1 mmol) was added. The reaction was quenched after 1 h with saturated aqueous NH_4Cl solution (20 mL), extracted with EtOAc (30 mL x 3), and washed with H_2O (10 mL x 2) and brine (10 mL). The organic layer was dried over anhydrous $MgSO_4$, filtered and the solvent was removed under reduced pressure. The residue was purified on a silica gel column using hexanes/EtOAc (5/1) as the eluent to afford **3-15** as a white solid (74 mg, 82%): mp 133-135 °C; ^{1}H NMR (300 MHz, CDCl$_3$) δ 0.55 (m, 6 H), 0.90 (m, 9 H), 1.19 (s, 3 H), 1.60 (m, 2 H), 1.66 (s, 3 H), 1.84 (m, 1 H), 2.00 (m, 3 H), 2.12 (s, 3 H), 2.29 (s, 3 H), 2.50 (m, 1 H), 3.22 (d, J = 4.2 Hz, 1 H), 3.69 (d, J = 5.7 Hz, 1 H), 3.77 (m, 2 H), 4.06 (m, 1 H), 4.18 (m, 1 H), 4.29-4.47 (m, 3 H), 4.69 (bs, 1 H), 4.87-4.98 (m, 3 H), 5.61-5.72 (m, 1 H), 5.83 (d, J = 6.9 Hz, 1 H), 7.42 (m, 2 H), 7.55 (m, 1 H), 8.06 (m, 2 H); ^{13}C NMR (62.9 MHz, CDCl$_3$) δ 5.1, 5.4, 6.6, 6.7, 9.7, 10.0, 14.7, 20.8, 21.4, 22.4, 26.2, 37.1, 42.7, 46.4, 58.7, 72.1, 73.0, 74.5, 75.6, 75.7, 76.2, 76.4, 80.9, 81.5, 82.0, 84.0, 117.4, 128.4, 129.7, 129.8, 133.3, 133.6, 133.7, 141.2, 165.6, 169.3, 170.1, 201.9. HRMS (FAB/DCM/NaCl) m/z calcd. for $C_{40}H_{56}O_{12}SiH^+$: 757.3619 found: 757.3643 (Δ = -3.1 ppm). All data are consistent with the reported values.[42]

(*3R,4S*)-3-Triethylsilyloxy-4-phenylazetidin-2-one (3-19):
To a mixture of THF (6 mL) and 1 M KOH aqueous solution (18 mL) at 0 °C was added a solution of **1-14** (236 mg, 1.15 mmol) in THF (6 mL). The solution was stirred at 0 °C for 1 h and saturated NH_4Cl solution (30 mL) was added. The mixture was extracted with dichloromethane (30 mL x 3). The combined organic layers were dried over $MgSO_4$ and concentrated to give **1-15** as crude white solid.
To a solution of the crude **1-15**, DMAP (2 mg, 0.02 mmol) and triethylamine (0.25 mL, 1.6 mmol)in CH_2Cl_2 (40 mL) was added chlorotriethylsilane (0.14 mL, 1.20 mmol). The solution was stirred at 0 °C for 12 min and quenched by saturated NH_4Cl solution (20 mL). The mixture was extracted with CH_2Cl_2 (30 mL x 3) and the combined organic layers were dried over $MgSO_4$. The organic layer was separated using column chromatography on silica gel (hexanes/EtOAc = 8/1 and 4/1) to give (*3R,4S*)-3-triethylsilyloxy-4-phenylazetidin- 2-one **3-19** as white solid (219 mg, 70% for 2 steps): ^{1}H NMR (500 MHz, CDCl$_3$) δ 0.42 (m, 6 H), 0.77 (m, 9 H), 4.79 (d, J = 4.5 Hz, 1 H), 5.09 (dd, J = 4.5, 2.5 Hz, 1 H), 6.04 (s, 1 H), 7.35 (m, 5 H); ^{13}C NMR (62.9 MHz, CDCl$_3$) δ 4.4, 6.2, 59.3, 79.3, 127.8, 127.9, 136.2, 170.1. HRMS (FAB/DCM/NaCl) m/z calcd. for $C_{15}H_{23}NO_2SiH^+$: 278.1576 found: 278.1583 (Δ = 2.4 ppm).

2-Allylbenzoic acid (3-21):[42]

To a degassed solution of methyl 2-bromobenzoate (0.25 mL, 1.8 mmol), and tributylallyltin (0.68 mL, 2.16 mmol) in benzene (11 mL) was added Pd(PPh$_3$)$_4$ (52 mg, 0.045 mmol), and the mixture was refluxed for 2 days. The reaction mixture was concentrated under reduced pressure to afford **3-20** as a yellow oil.

To a solution of the yellow oil, thus obtained, in methanol (3 mL) was added potassium hydroxide (1.01 g, 18 mmol) and the mixture stirred for 15 min. Then, the organic layer was washed with 7 M NaOH solution (10 mL x 3). The aqueous layers were combined and acidified until the pH value reached 2 using 7 M HCl solution. The aqueous layer was extracted with EtOAc (30 mL x 3). The organic layers were combined and dried over anhydrous MgSO$_4$. The organic layer was filtered and concentrated under reduced pressure. The residue was purified on a silica gel column using hexanes/EtOAc (15/1) as the eluent to afford acid **3-21** as a white solid (176 mg, 60% for two steps): ^{1}H NMR (500 MHz, CDCl$_3$) δ 3.83 (d, J = 6.0 Hz, 2 H), 5.02-5.06 (m, 2 H), 6.00-6.08 (m, 1 H), 7.30-7.33 (m, 2 H), 7.50 (t, J = 7.5 Hz, 1 H), 8.03 (d, J = 7.5 Hz, 1 H), 11.00-12.00 (broad peak, 1 H). HRMS (FAB/DCM/NaCl) m/z calcd. for C$_{10}$H$_{10}$O$_2$SiH$^+$: 163.0759 found: 163.0761 (Δ = 1.2 ppm). All data are consistent with the reported values.[42]

2-Allylbenzoyl chloride (3-22):[42]

To a solution of 2-allylbenzoic acid (92 mg, 0.57 mmol) in CH$_2$Cl$_2$ (2.5 mL) was added oxalyl chloride (0.1 mL, 1.14 mmol) and 2 drops of DMF. The reaction mixture was stirred for 3 h and then the solvent was removed under vacuum to afford **3-22** as a white solid. This crude product was used directly for next step without further purification.

(3R,4S)-1-(2-Allylbenzoyl)-3-triethylsilyloxy-4-phenyl-azetidin-2-one (3-23):

To a solution of *N*-H-β-lactam **3-22** (60 mg, 0.216 mmol), triethylamine (0.13 mL, 0.912 mmol) and DMAP (7 mg, 0.06 mmol) in CH$_2$Cl$_2$ (2.4 mL), was added 2-allylbenzoyl chloride in CH$_2$Cl$_2$ (2 mL) dropwise at room temperature. The mixture was stirred overnight at room temperature and the reaction was quenched with saturated aqueous NH$_4$Cl solution (20 mL). The mixture was then extracted with ethyl acetate (30 mL x 3). The combined extracts were dried over anhydrous MgSO$_4$ and concentrated *in vacuo*. The crude product was purified on a silica gel column using hexanes/EtOAc (25/1) as the eluent to afford **3-23** as a colorless oil (97 mg, 91% yield): ^{1}H NMR (400 MHz, CDCl$_3$) δ 0.42 (m, 6 H), 0.77 (m, 9 H), 3.48 (dd, J = 15.6, 6.0 Hz, 1 H), 3.58 (dd, J = 15.6, 6.4 Hz, 1 H, 5.01 (m, 2 H), 5.14 (d, J = 6.4 Hz, 1 H), 5.33 (d, J = 17.5, 6.4 Hz, 1 H), 5.93 (m, 1 H), 7.30 (m, 7 H), 7.4 (dd, J = 8.8, 6.8 Hz, 1 H), 7.57 (d, J = 6.8 Hz, 1 H); ^{13}C NMR (100.5 MHz, CDCl$_3$) δ 4.3, 6.2, 37.2, 61.3, 76.7, 115.9, 125.9, 128.0, 128.1, 128.3, 128.8, 130.2, 131.4, 133.1, 133.6, 136.9, 138.9, 165.4, 166.6. HRMS (FAB/DCM/NaCl) m/z calcd. for C$_{25}$H$_{31}$NO$_3$SiH$^+$: 422.2151 found: 422.2153 (Δ = 0.4 ppm).

14β-Allyloxy-3'N-debenzoyl-3'N-(2-allylbenzoyl)-7,2'-triethylsilylpaclitaxel (3-24):

To a solution of **3-15** (20 mg, 0.026 mmol) and β-lactam **3-23** (33 mg, 0.079 mmol) in THF (2.8 mL) was added LiHMDS (1 N in THF, 0.04 ml, 0.04 mmol) at -40 $^{\circ}$C. The reaction mixture was warmed up to -20 $^{\circ}$C over 3 h, quenched with saturated aqueous NH$_4$Cl solution (20 mL), and extracted with EtOAc (20 mL x 3). The organic layers were combined and solvent was removed under reduced pressure. The residue was purified by column chromatography on silica gel (hexanes/EtOAc = 7/1) to afford **3-24** as a white solid (22 mg, 72%): mp 99-102 $^{\circ}$C; ^{1}H NMR (500 MHz, CDCl$_3$) δ 0.35-0.47 (m, 6 H), 0.55-0.63 (m, 6 H), 0.79 (m, 9 H), 0.93 (m, 9 H), 1.15 (s, 3 H), 1.26 (s, 3 H), 1.74 (s, 3 H), 1.91 (m, 1 H), 2.03 (s, 3 H), 2.19 (s, 3 H), 2.57 (m, 1 H), 2.58 (s, 3 H), 3.43 (dd, J = 16.0, 5.5 Hz, 1 H), 3.53 (dd, J = 16.0, 5.5 Hz, 1 H), 3.66 (s, 1 H), 3.82 (d, J = 7.5 Hz, 1 H), 3.84 (d, J = 8.0 Hz, 2 H), 3.91 (dd, J = 10.5, 6.5 Hz, 1 H), 4.28 (d, J = 9.0 Hz, 1 H), 4.32 (dd, J = 10.5, 4.0 Hz, 1 H), 4.47 (m, 3 H), 4.62 (d, J = 10.5 Hz, 1 H), 4.71 (d, J = 1.5Hz, 1 H), 4.90 (dd, J = 17.0, 2.0 Hz, 1 H), 4.99 (m, 2 H), 5.44 (m, 1 H), 5.57 (d, J = 8.4 Hz, 1 H), 5.99 (m, 2 H), 6.20 (d, J = 7.0 Hz, 1 H), 6.47 (s, 1 H), 6.99 (d, J = 8.5 Hz, 1 H), 7.24 (m, 2 H), 7.40 (m, 8 H), 7.57 (t, J = 8.0 Hz, 1 H), 8.10 (d, J = 7.5 Hz, 2 H); ^{13}C NMR (100.5 MHz, CDCl$_3$) δ 4.6, 5.5, 6.7, 6.9, 10.1, 14.6, 21.1, 23.6, 26.3, 37.5, 43.7, 46.1, 56.2, 59.0, 72.5, 72.8, 75.0, 75.2, 76.7, 76.8, 78.8, 78.9, 81.9, 84.4, 113.8, 116.3, 118.1, 126.6, 126.7, 127.9, 128.2, 128.9, 129.2, 129.8, 130.2, 130.6, 130.8, 133.0, 133.7, 134.5, 135.6, 135.9, 136.5, 137.8, 138.6, 138.8, 138.9, 165.8, 169.1, 169.6, 169.9, 171.7, 201.2. HRMS calcd. for C$_{65}$H$_{87}$NO$_{15}$Si$_2$H$^+$: 1178.5693, found 1178.5703 (Δ= 0.9 ppm).

7,2'-Bistriethylsilyl-SB-T-2053 (3-25):

To a solution of **3-24** (47 mg, 0.041 mmol) in CH$_2$Cl$_2$ (23 mL) was added the "first-generation Grubbs catalyst" (8 mg, 0.01 mmol) in CH$_2$Cl$_2$ (0.2 mL). The reaction was stirred overnight and the solvent was removed under reduced pressure. The residue mixture was passed through a short silica gel column (hexanes/EtOAc = 5/1) to remove the catalyst to afford **3-25** as a crude yellow solid (39 mg, 85%): mp 138-141°C; ^{1}H NMR (500 MHz, CDCl$_3$) δ 0.31-0.43 (m, 6 H), 0.54-0.62 (m, 6 H), 0.79 (m, 9 H), 0.93 (m, 9 H), 1.13 (s, 3 H), 1.30 (s, 3 H), 1.72 (s, 3 H), 1.93 (m, 1 H), 1.99 (s, 3 H), 2.18 (s, 3 H), 2.53 (m, 1 H), 2.61 (s, 3 H), 3.18 (d, J = 16.0 Hz, 1 H), 3.32 (s, 1 H), 3.81 (d, J = 9.5 Hz, 1 H), 3.84 (m, 2 H), 3.95 (d, J = 14.0 Hz, 1 H), 4.12 (d, J = 14.0 Hz, 1 H), 4.26 (d, J = 8.0 Hz, 1 H), 4.46 (m, 2 H), 4.56 (s, 1 H), 4.98 (m, 2 H), 5.34 (d, J = 15.0 Hz, 1 H), 5.47 (m, 1 H), 5.99 (d, J = 7.5 Hz, 1 H), 6.25 (d, J = 8.0 Hz, 1 H), 6.44 (s, 1 H), 6.77 (d, J = 4.5 Hz, 1 H), 7.16 (d, J = 6.5 Hz, 1 H), 7.34 (m, 4 H), 7.40 (m, 2 H), 7.49 (m, 3 H), 7.62 (t, J = 7.0 Hz, 1 H), 8.10 (d, J = 7.5 Hz, 2 H); ^{13}C NMR (100.5 MHz, CDCl$_3$) δ 4.2, 5.3, 6.5, 6.7, 9.9, 14.2, 20.8, 23.4, 29.7, 38.2, 43.6, 45.9, 57.8, 58.6, 72.1, 72.5, 74.4, 74.7, 76.3, 76.7, 78.1, 80.0, 81.8, 84.1, 124.2, 126.5, 127.0, 127.1, 128.1, 128.5, 128.8, 128.9, 130.2, 130.6, 133.9, 135.8, 136.1, 138.6, 138.8, 165.6, 169.5, 169.6, 169.7, 171.8, 201.1. HRMS calcd. for C$_{63}$H$_{83}$NO$_{15}$Si$_2$H$^+$: 1150.5380, found 1150.5404 (Δ= 2.1 ppm).

SB-T-2053:

To a solution of **3-25** (50 mg) in CH_3CN (1.0 mL) and pyridine (1.0 mL) was added HF-pyridine (70:30, 0.5 mL) and the reaction mixture was stirred overnight. The reaction mixture was diluted with EtOAc (120 mL) and washed with saturated aqueous $NaHCO_3$ solution (10 mL x 2), $CuSO_4$ solution (10 mL x 3), water (10 mL x 3) and brine (10 mL x 3). The organic layer was dried over anhydrous $MgSO_4$ and solvent was removed under reduced pressure. The residue was purified by column chromatography on silica gel using hexanes:EtOAc (1/1) as the eluent to afford **SB-T-2053** as white solid (37 mg, 93%): mp 208-210 $^{\circ}$C; $[\alpha]_D^{22}$ –49 (c 0.92, $CHCl_3$); ^{1}H NMR (500 MHz, $CDCl_3$) δ 1.19 (s, 3 H), 1.23 (s, 3 H), 1.71 (s, 3 H), 1.86 (s, 3 H), 1.91 (m, 1 H), 2.23 (s, 3 H), 2.37 (s, 1 H), 2.55 (s, 3 H), 2.59 (m, 1 H), 2.98 (s, 1 H), 3.23 (d, J = 16.0 Hz, 1 H), 3.35 (s, 1 H), 3.81 (d, J = 6.6 Hz, 1 H), 3.84 (m, 2 H), 3.88 (d, J =8.4 Hz, 1 H), 3.96 (m, 1 H), 4.11 (m, 1 H), 4.25 (d, J = 9.0 Hz, 1 H), 4.40 (m, 1 H), 4.45 (d, J = 8.4 Hz, 1 H), 4.67 (d, J = 1.8 Hz, 1 H), 5.00 (d, J =1.2 Hz, 1 H), 5.22 (d, J = 5.4 Hz, 1 H), 5.35 (d, J = 16.2 Hz, 1 H), 5.56 (m, 1 H), 6.24 (d, J = 7.8 Hz, 1 H), 6.29 (s, 1 H), 6.71 (d, J = 6.0 Hz, 1 H), 7.17 (d, J = 7.2 Hz, 1 H), 7.28-7.53 (m, 9 H), 7.62 (t, J = 7.2 Hz, 1 H), 8.09 (d, J = 7.2 Hz, 2 H); ^{13}C NMR (100.5 MHz, $CDCl_3$) δ 9.4, 14.8, 20.8, 23.1, 26.2, 35.7, 37.7, 43.5, 44.9, 55.2, 58.9, 72.0, 72.5, 73.2, 74.6, 75.1, 76.2, 79.3, 79.8, 81.7, 84.3, 125.9, 126.5, 126.9, 127.3, 127.6, 128.2, 128.7, 128.9, 129.3, 129.8, 130.5, 131.4, 133.8, 135.0, 135.5, 137.5, 137.7, 138.1, 165.3, 169.2, 169.6, 171.1, 172.9, 203.0. HRMS calcd. for $C_{51}H_{56}NO_{15}H^+$: 922.3650, found 922.3659 (Δ= 1.0 ppm).

2-Vinylbenzoyl chloride (3-27):[61]

To the suspension of sodium hydride (60% suspension in mineral oil, 1.60 g, 39.9 mmol) in anhydrous THF (17 mL) was added PPh_3CH_3Br (5.70 g, 16.0 mmol) slowly at 0 °C. Then the reaction mixture was stirred at ambient temperature for 1 h and 2-formylbenzoic acid (2.00 g, 13.3 mmol) was added at once. After the mixture was stirred for 3 h at 40 °C, the reaction was quenched with addition of H_2O and the mixture extracted with Et_2O (30 mL x 3). The aqueous phase was acidified (pH=2) and extracted with EtOAc (30 mL x 3). Combined ethyl acetate layers were washed with brine (50 mL), dried over $MgSO_4$ and concentrated to give 2-vinylbenzoic acid **3-26 (**1.938 g 100% yield) as a crude product: ^{1}H NMR (300 MHz) δ 5.2 (dd, J = 12.0, 1.0 Hz, 1 H), 5.5 (dd, J = 18.0, 1.0 Hz, 1 H), 7.7-7.1 (m, 4 H), 8.1 (d, J = 9.0 Hz, 1 H). All data are consistent with the reported values.[61]

To a solution of **3-26** (1.938 mg, ~13.3 mmol) in CH_2Cl_2 (26 mL) was added thionyl chloride (5.8 mL, 80 mmol) and 5 drops of DMF. The reaction mixture was refluxed for 3 h and then the solvent was removed under vacuum to afford crude 2-vinylbenzoyl chloride. The crude oil was distilled under reduced pressure to give pure **3-27** in 65% for 2 steps: bp 100-105°C (2.2 mmHg); ^{1}H NMR (400 MHz, $CDCl_3$) δ 5.44 (dd, J = 11.2, 1.2 Hz, 1 H), 5.72 (dd, J = 17.2, 0.8 Hz, 1 H), 7.27 (dd, J = 17.6, 11.2 Hz, 1 H), 7.44 (m, 1 H), 7.60 (m, 1 H), 8.17 (dt, J = 8.0, 0.8 Hz, 1 H); ^{13}C NMR (100.5 MHz, $CDCl_3$) δ 118.6, 127.7, 127.8, 131.5, 133.1, 134.2, 134.9, 140.2, 167.6.

(3*R*,4*S*)-1-(2-Vinylbenzoyl)-3-triethylsilyloxy-4-phenyl-azetidin-2-one (3-28):[54]

To a solution of *N*-H-β-lactam **3-19** (96 mg, 0.35 mmol), triethylamine (0.2 mL, 1.4 mmol) and DMAP (10 mg, 0.01 mmol) in CH_2Cl_2 (3.5 mL), was added 2-vinylbenzoyl chloride (**3-27**, 0.1 mL) dropwise at 0 °C. The mixture was stirred overnight at room temperature and the reaction was quenched with saturated aqueous NH_4Cl solution (20 mL). The mixture was then extracted with ethyl acetate (30 mL x 3). The combined extracts were dried over anhydrous $MgSO_4$ and concentrated *in vacuo*. The crude product was purified on a silica gel column using hexanes/EtOAc (20/1-10/1) as the eluent to afford **3-28** as a colorless oil (128 mg, 90% yield): ^{1}H NMR (600 MHz, CDCl$_3$) δ 0.44 (m, 6 H), 0.77 (m, 9 H), 5.15 (d, *J* = 6.6 Hz, 1 H), 5.33 (m, 2 H), 5.69 (d, *J* = 17.4 Hz, 1 H), 6.94 (dd, *J* = 17.4, 10.8 Hz, 1 H), 7.33 (m, 6 H), 7.47 (m, 1 H), 7.52 (m, 1 H), 7.59 (d, *J* = 6.8 Hz, 1 H); ^{13}C NMR (100.5 MHz, CDCl$_3$) δ 4.3, 6.16, 61.4, 76.9, 117.3, 126.1, 127.2, 128.1, 128.1, 128.3, 128.5, 131.3, 132.1, 133.5, 133.8, 136.9, 165.3, 166.4. HRMS (FAB/DCM/NaCl) m/z calcd. for $C_{24}H_{29}NO_3SiH^+$: 408.1995 found: 408.1995 (Δ = 0 ppm).

14β-Allyloxy-3'*N*-debenzoyl-3'*N*-(2-vinylbenzoyl)-7,2'-triethylsilylpaclitaxel (3-29):[39]

To a solution of **3-15** (71 mg, 0.09 mmol) and β-lactam **3-28** (115 mg, 0.28 mmol) in THF (10 mL) was added 1 M LiHMDS in THF (0.14 ml, 0.14 mmol) at -40 °C. The reaction mixture was warmed up to 0 °C and stired for 2.5 h, quenched with saturated aqueous NH_4Cl solution, and extracted with EtOAc. The organic layers were combined, dried over anhydrous $MgSO_4$ and the solvent was removed under reduced pressure. The residue was purified by column chromatography on silica gel (hexanes/EtOAc = 8/1~4/1) to afford **3-29** as a white solid (86 mg, 82%): mp 99-102 °C; $[\alpha]_D^{20}$ -42 (c 0.6, CHCl$_3$); ^{1}H NMR (600 MHz, CDCl$_3$) δ 0.34-0.47 (m, 6 H), 0.55-0.63 (m, 6 H), 0.78 (m, 9 H), 0.93 (m, 9 H), 1.15 (s, 3 H), 1.31 (s, 3 H), 1.74 (s, 3 H), 1.95 (m, 1 H), 2.03 (s, 3 H), 2.19 (s, 3 H), 2.56 (m, 1 H), 2.60 (s, 3 H), 3.67 (s, 1 H), 3.82 (d, *J* = 7.2 Hz, 1 H), 3.84 (d, *J* = 8.0 Hz, 1 H), 3.93 (dd, *J* = 10.8, 4.2 Hz, 1 H), 4.28 (d, *J* = 9.0 Hz, 1 H), 4.32 (dd, *J* = 10.5, 4.0 Hz, 1 H), 4.47 (m, 3 H), 4.62 (d, *J* = 10.5 Hz, 1 H), 4.71 (d, *J* = 1.2 Hz, 1 H), 5.00 (d, *J* = 9.0 Hz, 1 H), 5.32 (d, *J* = 7.6 Hz, 1 H), 5.36 (m, 1 H), 5.61 (d, *J* = 8.4 Hz, 1 H), 5.70 (d, *J* = 11.4 Hz, 1 H), 5.99 (d, *J* = 7.8 Hz, 1 H), 6.21 (d, *J* = 7.0 Hz, 1 H), 6.47 (s, 1 H), 6.99 (m, 2 H), 7.26-7.48 (m, 8 H), 7.50-7.58 (m, 3 H), 8.10 (d, *J* = 8.4 Hz, 2 H); ^{13}C NMR (75.5 MHz, CDCl$_3$) δ 4.3, 5.3, 6.4, 6.7, 9.9, 14.4, 20.8, 23.3, 26.1, 37.3, 43.5, 45.9, 56.1, 58.8, 72.3, 72.5, 74.8, 74.9, 76.5, 76.6, 78.6, 78.6, 81.7, 84.1, 117.2, 117.8, 126.3, 126.5, 127.7, 128.0, 128.7, 129.5, 129.9, 130.6, 132.7, 133.5, 134.2, 134.8, 135.6, 136.2, 136.5, 138.6, 165.6, 168.3, 169.4, 169.7, 171.4, 201.0. HRMS (FAB/DCM/NaCl) m/z calcd. for $C_{64}H_{85}NO_{15}Si_2H^+$: 1164.5536 found: 1164.5535 (Δ = 0.1 ppm).

SB-T-2054:[39]

To a sulotion of **3-29** (43 mg, 0.036 mmol) in CH_2Cl_2 (22 mL) was added the "first-generation Grubbs'catalyst" (8 mg x 3, 0.027 mmol) in CH_2Cl_2 (0.08 mL). The reaction was refluxed for 5 days and the solvent was removed under reduced pressure. The residue was passed through a short silica gel column (eluent: hexanes/EtOAc, 3/1) to remove the catalyst to afford **3-30** as a crude yellow solid (20 mg, 50%) with diene **3-29** (11 mg, 25%) recovered.

To a solution of **3-30** (20 mg) in CH_3CN (0.4 mL) and pyridine (0.4 mL) was added HF-pyridine (70:30, 0.2 ml) and the reaction mixture was stirred overnight. The reaction mixture was diluted with EtOAc (50 mL) and washed with saturated aqueous $NaHCO_3$ solution (10 mL x 2), $CuSO_4$ solution (10 mL x 3), water (10 mL x 3) and brine (3 mL). The organic layer was dried over anhydrous $MgSO_4$ and solvent was removed under reduced pressure. The residue was purified by column chromatography on siloca gel using hexanes:EtOAc (1/1) as the eluent to afford **SB-T-2054** as white solid (13 mg, 80% for 2 steps): mp 203-205 ^{o}C; $[\alpha]_D^{22}$ -28 (c 0.92, CHCl$_3$); ^{1}H NMR (600 MHz, CDCl$_3$) δ 1.19 (s, 3 H), 1.23 (s, 3 H), 1.72 (s, 3 H), 1.73 (s, 3 H), 1.91 (m, 1 H), 1.94 (m, 1 H), 2.23 (s, 3 H), 2.24 (m, 1 H), 2.57 (m, 1 H), 2.63 (s, 3 H), 3.35 (s, 1 H), 3.49 (t, J = 9.6 Hz, 1 H), 3.82 (m, 3 H), 4.26 (d, J = 8.4 Hz, 1 H), 4.38 (m, 1 H), 4.40 (d, J = 8.4 Hz, 1 H), 4.78 (m, 1 H), 5.00 (d, J = 6.8 Hz, 1 H), 5.62 (d, J = 7.8 Hz, 1 H), 5.92 (ddd, J = 16.8, 8.4, 2.8 Hz, 1 H), 6.02 (d, J = 7.2 Hz, 1 H), 6.31 (s, 1 H), 6.36 (d, J = 7.8 Hz, 1 H), 6.52 (d, J = 16.2 Hz, 1 H), 6.90 (d, J = 8.4 Hz, 1 H), 7.22 (d, J = 7.2 Hz, 1 H), 7.34-7.63 (m, 10 H), 8.10 (d, J = 7.8 Hz, 2 H); ^{13}C NMR (75.5 MHz, CDCl$_3$) δ 9.1, 15.1, 20.8, 23.0, 23.3, 26.2, 29.7, 32.7, 35.7, 43.6, 44.9, 54.6, 58.9, 72.1, 72.7, 73.3, 75.2, 76.4, 77.2, 77.9, 79.0, 81.6, 84.3, 126.5, 126.7, 126.8, 128.3, 128.4, 128.8, 128.9, 129.0, 129.2, 129.9, 130.0, 131.1, 133.7, 134.9, 135.0, 136.6, 137.9, 138.4, 165.4, 169.4, 170.1, 171.1, 173.2, 202.9. HRMS (FAB/DCM/NaCl) m/z calcd. for $C_{51}H_{55}NO_{15}H^+$: 922.3650 found: 922.3643 (Δ = -0.8 ppm).

X-ray Single Crystal Diffraction Analysis of SB-T-2054 (by Mr. Zhong Li)**:**
A colorless single crystal (0.2×0.3×0.5 mm^3) of **SB-2054** grown in a NMR tube by slow diffusion of hexanes (0.5 mL) into a solution of **SB-2054** (5 mg) in a mixture of dichloromethane (0.1 mL) and ethyl actate (0.05 mL) was selected for X-Ray diffraction analysis. Since the crystals obtained in this way are sensitive to air, the test single crystal was sealed along with some mother liquid in a capillary tube. Intensity data collection was carried out with a Bruker AXS SMART diffractometer equipped with a CCD detector using a Siemens graphite-monochromated Mo radiation tube (λ = 0.71073 Å) at room temperature. The unit cells were determined by a least-squares analysis using the SMART software package. The raw frame data were integrated into SHELX-format reflection files and corrected for Lorentz and polarization effects using SAINT. Corrections for incident and diffracted beam absorption effects were applied using SADABS. The structure was solved by direct method and refined by full-matrix least-squares method on F_2 using the SHELXTL 97 software package. The quality of the structures is due to the quality of the available single crystals. All non-hydrogen atoms were refined anisotropically. The hydrogen atoms were placed in calculated positions and added as fixed contributions.

2054.cif:

```
data_2054bm
_symmetry_cell_setting           orthorhombic
_symmetry_space_group_name_H-M   'P 21 21 21'
_symmetry_Int_Tables_number      19
loop_
_symmetry_equiv_pos_site_id
_symmetry_equiv_pos_as_xyz
1 x,y,z
2 1/2-x,-y,1/2+z
3 -x,1/2+y,1/2-z
4 1/2+x,1/2-y,-z
_cell_length_a                14.575(2)
_cell_length_b                15.572(3)
_cell_length_c                31.027(5)
_cell_angle_alpha              90.00
_cell_angle_beta               90.00
_cell_angle_gamma              90.00
_cell_volume                 7041.95
```

```
loop_
_atom_site_label
_atom_site_type_symbol
_atom_site_fract_x
_atom_site_fract_y
_atom_site_fract_z
C38 C 0.5782(13) 1.0035(12) -0.0416(7)
H38 H 0.5939 1.0539 -0.0558
O10 O 0.4021(3) 0.6840(3) 0.09264(16)
O14 O 0.5206(4) 0.5591(3) 0.13853(16)
O1 O 0.4735(3) 0.4954(3) 0.21310(16)
H1A H 0.4790 0.4605 0.1935
O4 O 0.4666(3) 0.8103(3) 0.21390(16)
C4 C 0.4050(5) 0.7896(4) 0.2494(2)
O5 O 0.4027(4) 0.8608(3) 0.30942(17)
O2 O 0.5042(3) 0.6484(3) 0.24600(15)
O8 O 0.0927(5) 0.5552(4) 0.19575(18)
C12 C 0.2772(5) 0.6349(5) 0.1405(2)
O13 O 0.6926(4) 0.7348(4) 0.02992(19)
O3 O 0.5149(4) 0.5623(4) 0.3048(2)
N1 N 0.5548(4) 0.6962(4) 0.00247(19)
H1 H 0.5232 0.6598 -0.0122
C5 C 0.3541(6) 0.8711(5) 0.2670(3)
H5 H 0.374(5) 0.923(4) 0.252(2)
C13 C 0.3729(5) 0.6147(5) 0.1216(2)
H13 H 0.370(4) 0.560(4) 0.106(2)
C3 C 0.3493(5) 0.7068(4) 0.2373(3)
H3 H 0.332(4) 0.713(4) 0.207(2)
C9 C 0.1832(6) 0.6345(5) 0.2492(3)
C1 C 0.4089(5) 0.5613(4) 0.2005(2)
O12 O 0.3761(3) 0.7400(4) -0.01988(16)
H12 H 0.3544 0.6917 -0.0227
O11 O 0.3541(5) 0.6064(5) 0.03617(19)
O7 O 0.1329(4) 0.5982(4) 0.2756(2)
C7 C 0.2039(6) 0.7911(6) 0.2533(3)
H7 H 0.202(5) 0.798(5) 0.222(3)
C34 C 0.5094(5) 0.7701(5) 0.0222(3)
H34 H 0.531(4) 0.775(4) 0.052(2)
C18 C 0.2230(5) 0.7074(5) 0.1190(2)
H18A H 0.1599 0.7043 0.1278
H18B H 0.2268 0.7016 0.0883
H18C H 0.2483 0.7618 0.1275
C8 C 0.2547(5) 0.7041(5) 0.2645(2)
C14 C 0.4444(5) 0.6081(5) 0.1579(2)
H14 H 0.466(4) 0.666(5) 0.165(2)
C2 C 0.4070(6) 0.6224(5) 0.2398(3)
```

H2 H 0.387(5) 0.590(4) 0.265(2)
C6 C 0.2496(5) 0.8698(5) 0.2725(3)
H6A H 0.2241 0.9207 0.2591
H6B H 0.2354 0.8723 0.3030
C35 C 0.5332(7) 0.8543(7) -0.0008(3)
O15 O 0.3474(5) 0.8658(3) 0.17690(18)
C22 C 0.4602(6) 0.7930(5) 0.2916(2)
H22A H 0.4572 0.7399 0.3080
H22B H 0.5235 0.8104 0.2875
C11 C 0.2514(5) 0.5894(4) 0.1756(3)
C44 C 0.7381(9) 0.5509(8) -0.0843(3)
H44 H 0.7330 0.5486 -0.1142
C49 C 0.6803(6) 0.5418(5) 0.0785(3)
H49 H 0.6234 0.5412 0.0649
C10 C 0.1675(5) 0.6185(5) 0.2008(3)
H10 H 0.147(5) 0.673(5) 0.188(2)
C15 C 0.3126(5) 0.5163(4) 0.1928(2)
O6 O 0.1092(4) 0.7906(4) 0.2694(2)
H6 H 0.0818 0.7491 0.2593
C29 C 0.8374(9) 0.6731(10) 0.2818(5)
H29 H 0.9000 0.6847 0.2821
C51 C 0.6103(6) 0.5942(6) 0.1491(3)
H51A H 0.6197 0.5946 0.1800
H51B H 0.6160 0.6525 0.1384
C25 C 0.5494(7) 0.6095(6) 0.2777(3)
C27 C 0.6851(7) 0.6976(6) 0.2529(3)
H27 H 0.6459 0.7258 0.2340
C43 C 0.6839(6) 0.6077(6) -0.0614(3)
H43 H 0.6421 0.6429 -0.0756
C41 C 0.6472(6) 0.6846(6) 0.0072(3)
C36 C 0.5303(7) 0.8631(8) -0.0454(4)
H36 H 0.5118 0.8166 -0.0621
C42 C 0.6928(6) 0.6114(5) -0.0169(3)
C16 C 0.3159(6) 0.4423(5) 0.1581(3)
H16A H 0.2553 0.4320 0.1472
H16B H 0.3392 0.3908 0.1711
H16C H 0.3554 0.4591 0.1348
C24 C 0.4993(7) 0.8755(6) 0.1463(3)
H24A H 0.4746 0.8662 0.1180
H24B H 0.5536 0.8413 0.1499
H24C H 0.5145 0.9351 0.1497
C33 C 0.4061(5) 0.7514(7) 0.0235(3)
H33 H 0.374(5) 0.801(5) 0.036(2)
C47 C 0.7531(7) 0.5538(6) 0.0066(3)
C32 C 0.3845(6) 0.6724(6) 0.0501(3)
C31 C 0.7071(9) 0.5878(7) 0.3069(4)

H31 H 0.6839 0.5441 0.3242
C17 C 0.2797(6) 0.4709(5) 0.2350(3)
H17A H 0.2773 0.5119 0.2580
H17B H 0.3219 0.4258 0.2423
H17C H 0.2198 0.4469 0.2305
C26 C 0.6500(7) 0.6333(6) 0.2795(3)
C28 C 0.7782(9) 0.7210(7) 0.2541(3)
H28 H 0.8005 0.7660 0.2374
C23 C 0.4290(7) 0.8502(5) 0.1797(3)
C48 C 0.7525(7) 0.5490(6) 0.0541(3)
H48 H 0.8091 0.5514 0.0680
C21 C 0.2688(6) 0.6917(6) 0.3133(3)
H21A H 0.2103 0.6919 0.3275
H21B H 0.3059 0.7376 0.3243
H21C H 0.2990 0.6379 0.3184
C45 C 0.7986(10) 0.4982(9) -0.0640(5)
H45 H 0.8350 0.4617 -0.0805
C46 C 0.8076(7) 0.4975(7) -0.0199(4)
H46 H 0.8493 0.4602 -0.0070
C50 C 0.6814(6) 0.5345(6) 0.1267(3)
H50A H 0.7423 0.5486 0.1372
H50B H 0.6686 0.4754 0.1347
C30 C 0.8021(11) 0.6094(10) 0.3082(6)
H30 H 0.8408 0.5804 0.3271
C39 C 0.5826(14) 1.0046(10) 0.0036(6)
H39 H 0.5982 1.0532 0.0194
C40 C 0.5603(10) 0.9213(8) 0.0237(5)
H40 H 0.5649 0.9149 0.0534
O9 O -0.0014(5) 0.6582(8) 0.2119(4)
C37 C 0.5540(11) 0.9384(12) -0.0654(5)
H37 H 0.5528 0.9430 -0.0952
C19 C 0.0044(12) 0.5891(13) 0.1909(8)
C20 C -0.0608(7) 0.5177(9) 0.1949(4)
H20A H -0.0394 0.4783 0.2164
H20B H -0.0658 0.4885 0.1677
H20C H -0.1198 0.5397 0.2031

#END

(*3R, 4S*)-1-(2-Allyloxybenzoyl)-4-phenyl-3-triethylsilanyloxy-azetidin-2-one (3-31):[39]

To a solution of *β*-lactam **3-19** (104 mg, 0.37 mmol), triethylamine (0.21 mL, 1.5 mmol) and DMAP (11 mg, 0.04 mmol) in CH_2Cl_2 (4 mL), was added 2-allylbenzoyl chloride (0.1 mL, 0.74 mmol) dropwise at 0 °C. The mixture was stirred overnight at room temperature, and quenched with saturated NH_4Cl aqueous solution (20 mL). The mixture was then extracted with ethyl acetate (30 ml × 3). The combined organic layer was washed with brine (10 ml), dried over anhydrous $MgSO_4$, and concentrated *in vacuo*. Flash chromatography on silica gel (hexanes/EtOAc=15/1) gave **3-30** as a colorless oil (161 mg, 99%): ^{1}H NMR (300 MHz, CDCl3) δ 0.40-0.50 (m, 6H), 0.75-0.81 (m, 9H), 4.62 (dd, J = 1.2, 5.7 Hz, 2H), 5.10 (d, J = 6.0 Hz, 1H), 5.22 (dd, J= 0.9, 10.5 Hz, 1H), 5.36 (d, J= 6.0 Hz, 1H), 5.45 (dd, J=1.8, 17.4 Hz, 1H), 6.04-6.20 (m, 1H), 6.96-7.03 (m, 2H), 7.32-7.45 (m, 7H); ^{13}C NMR (75 Hz, CDCl3) δ 4.34, 6.15, 61.5, 69.7, 70.1, 112.2, 118.3, 120.5, 124.2, 127.8, 127.9, 128.0, 129.4, 132.8, 132.9, 133.6, 156.9, 164.6 and 165.0; HRMS (FAB/DCM/NaCl) m/z calcd for $C_{25}H_{31}NO_4SiH^+$: 438.2100, found: 438.2088 (Δ = -2.7 ppm).

14*β*-Allyloxy-3'*N*-debenzoyl-3'*N*-(2-allyloxybenzoyl)-7,2'-triethylsilylpaclitaxel (3-32):[39]

To a solution of **3-15** (91 mg, 0.12 mmol) and *β*-lactam **3-31** (160 mg, 0.36 mmol) in of dry THF (12 mL) was added 1.3 M LiHMDS in THF (0.14 ml, 0.18 mmol) at -40 °C under nitrogen atmosphere. The temperature was gradually increased to 0 °C and the mixture was stirred for 2.5 h before quenched with a saturated aqueous NH_4Cl solution (20 mL) and extracted with dichloromethane (30 mL × 3). The organic layer was washed with brine (10 mL), dried over anhydrous $MgSO_4$ and concentrated *in vacuo*. Flash chromatography on silica gel (hexanes/EtOAc=10/1 followed by 5/1) afforded **3-32** as a white solid (110 mg, 77 %): mp 205-207°C; ^{1}H NMR (400 MHz, CDCl3) δ 0.28-0.48 (m, 6H), 0.52-0.66 (m, 6H), 0.76-0.86 (m, 9H), 0.88-0.98 (m, 9H), 1.11 (s, 3H), 1.25 (s, 3H), 1.73 (s, 3H), 1.88-1.98 (m, 1H), 2.01 (s, 3H), 2.17 (s, 3H), 2.50-2.60 (m, 1H), 2.66 (s, 3H), 3.74 (s, 1H), 3.76-3.88 (m, 3H), 4.20 (dd, J = 4.4, 10.8 Hz, 1H), 4.28 (d, J = 8.4 Hz, 1H), 4.42-4.55 (m, 4H), 4.70 (d, J = 1.6 Hz, 1H), 4.74-4.83 (dd, J= 5.2, 13.2 Hz, 1H), 4.83-4.89 (dd, J= 5.6, 12.8 Hz, 1H), 5.0 (d, J = 8.4 Hz, 1H), 5.20-5.30 (m, 1H), 5.34 (d, J = 10.4 Hz, 1H), 5.44 (d, J = 16.4 Hz, 1H), 5.64 (d, J = 6.4 Hz, 1 H), 5.96 (d, J = 7.2 Hz, 1H), 6.16-6.30 (m, 2H), 6.45 (s, 1H), 6.92-7.0 (m, 2H), 7.26-7.42 (m, 6H), 7.48 (t, J = 7.2 Hz, 2H), 7.59 (t, J= 7.6 Hz, 1H), 8.02 (dd, J = 1.6, 8 Hz, 1H), 8.10 (d, J= 7.2 Hz, 2H), 9.09 (d, J = 7.6 Hz, 1H); ^{13}C NMR (100 MHz, CDCl3) δ 4.3, 5.3, 6,5, 6.7, 9.90, 14.3, 20.9, 22.4, 23.4, 26.0, 29.7, 37.3, 43.4, 45.9, 56.6, 58.8, 70.3, 72.2, 72.7, 74.7, 74.9, 75.1, 76.6, 78.2, 78.5, 81.6, 84.2, 113.0, 117.2, 118.6, 121.1, 126.6, 127.6, 128.5, 128.6, 129.6, 129.9, 132.5, 132.8, 132.9, 133.4, 135.4, 136.4, 139.0, 157.1, 164.6, 165.6, 169.4, 170.0, 171.2 and 201.0; HRMS (FAB/DCM/NaCl) m/z calcd for $C_{65}H_{87}NO_{16}Si_2H^+$: 1194.5462, found: 1194.5509 (Δ = 3.9 ppm).

SB-T-2055 (*Z&E*):[39]

To a solution of **3-32** (108 mg, 0.09 mmol) in dry CH_2Cl_2 (25 mL) was added the "second-generation Grubbs's catalyst" (17 mg, 0.022 mmol) in dry CH_2Cl_2 (1 mL) under nitrogen atmosphere. The reaction mixture was stirred for 1 day at room temperature and 1 day at reflux to convert all of the starting materials. Solvent was removed *in vacuo*. Products were separated on flash chromatography on silica gel (hexanes/EtOAc = 4/1 ~ 3/1) to afford **3-33** as a crude yellow solid (36 mg, 35%) and **3-34** as a crude yellow solid (48 mg, 46%).

Under nitrogen atmosphere, HF-pyridine (70:30, 0.35 mL) was added to a solution of **3-33** (35 mg) in CH_3CN (0.7 mL) and pyridine (0.7 mL) at 0 °C and the reaction mixture was stirred overnight. The reaction mixture was diluted with EtOAc (60 mL) and washed with a saturated aqueous $NaHCO_3$ solution (10 mL × 2), $CuSO_4$ solution (8 mL × 3), water (10 mL × 3), and brine (5 mL). The organic layer was dried over anhydrous $MgSO_4$ and solvent was removed *in vacuo*. Flash chromatography on silica gel (hexanes/EtOAc=1/2) afforded **SB-T-2055*E*** as a white solid (24 mg, 85 %): mp 194-196°C; $[\alpha]_D^{20}$ - 107 (c 12.7, $CHCl_3$); ^{1}H NMR (400 MHz, $CDCl_3$) δ 1.08 (s, 3H), 1.12 (s, 3H), 1.60 (s, 3H), 1.64 (s, 3H), 1.78-1.86 (m, 1H), 2.13 (s, 3H), 2.34 (s, 1H), 2.36 (s, 3H), 2.44-2.56 (m, 1H), 3.27 (s, 1H), 3.69-3.77 (m, 3H), 4.08-4.19 (m, 3H), 4.30-4.33 (m, 3H), 4.60-4.68 (m, 2H), 4.92 (d, *J* = 8.4 Hz, 1H), 5.57 (d, *J* = 15.6 Hz, 1H), 5.82 (dd, *J* = 3.2, 9.2 Hz, 1H), 5.86 (d, *J* = 7.2 Hz, 1H), 5.94 (m, 1H), 6.16 (s, 1H), 6.25 (d, *J* = 6.0 Hz, 1H), 6.89 (d, *J* = 8.4 Hz, 1 H), 7.04 (t, *J* = 7.6 Hz, 1H), 7.17-7.24 (m, 3H), 7.40 (t, *J* = 7.6 Hz, 3H), 7.47 (d, *J* = 7.2 Hz, 2H), 7.53 (t, *J* = 7.2 Hz, 1H), 7.92 (dd, *J* = 1.2, 7.6 Hz, 1H), 8.02 (d, *J* = 7.6 Hz, 2H), 8.52 (d, J = 9.2 Hz, 1H); ^{13}C NMR (100.5 MHz, $CDCl_3$) δ 9.4, 15.3, 20.7, 22.2, 22.5, 26.2, 29.7, 35.6, 43.2, 45.1, 54.8, 58.9, 69.1, 72.1, 72.9, 74.5, 75.3, 76.3, 77.1, 81.5, 83.5, 84.3, 112.3, 121.5, 122.7, 123.9, 127.5, 127.6, 128.1, 128.6, 129.6, 129.9, 131.7, 132.0, 132.9, 133.6, 134.4, 136.9, 138.7, 156.4, 165.2, 165.7, 170.3, 171.0, 202.9; HRMS *m/z* calcd for $C_{51}H_{55}NO_{16}H^+$, 938.3599; found, 938.3590 (Δ = -0.9 ppm).

HF-pyridine (70:30, 0.5 mL) was added to a solution of **3-34** (48 mg) in CH_3CN (1.0 mL) and pyridine (1.0 mL) at 0 °C and the reaction mixture was stirred overnight. The reaction mixture was diluted with EtOAc (60 mL) and washed with a saturated aqueous $NaHCO_3$ solution (10 mL × 2), $CuSO_4$ solution (8 mL × 3), water (10 mL × 3), and brine (5 mL). The organic layer was dried over anhydrous $MgSO_4$ and solvent was removed *in vacuo*. Flash chromatography on silica gel (hexanes/EtOAc=1/2) afforded **SB-T-2055*Z*** as a white solid (35 mg, 91%): mp 166-168 °C; $[\alpha]_D^{20}$ -73 (c 3.7, $CHCl_3$); ^{1}H NMR (500 MHz, $CDCl_3$) δ 1.22 (s, 3H), 1.24 (s, 3H), 1.69 (s, 3 H), 1.84 (s, 3 H), 1.87 (m, 1 H), 2.04 (s, 3 H), 2.24 (s, 3 H), 2.40 (d, *J* = 4.0 Hz, 1 H), 2.50-2.51 (m, 1 H), 2.97 (d, *J* = 8.5 Hz, 1 H), 3.44 (s, 1 H), 3.74 (d, *J* = 7.5 Hz, 1 H), 3.85 (d, *J* = 8.0 Hz, 1H), 4.14 (d, *J* = 11.0 Hz, 1H), 4.19 (d, *J* = 8.0 Hz, 1H), 4.20 (d, *J* = 8.5 Hz, 1H), 4.34-4.44 (m, 3H), 4.60 (dd, *J* = 8.5, 12.5 Hz, 1H), 4.91 (d, *J* = 9.0 Hz, 1H), 5.03 (dd, *J* = 3.5, 8.5 Hz, 1H), 5.49 (dd, *J* = 4.0, 5.5 Hz, 1H), 5.70-5.77 (m, 1H), 5.82 (t, *J* = 9 Hz, 1H), 5.92 (d, *J* = 7.5 Hz, 1H), 6.20 (d, *J* = 6.5 Hz, 1H), 6.28 (s, 1H), 7.00 (d, *J* = 8 Hz, 1H), 7.24-7.26 (m, 1H), 7.34-7.44 (m, 7H), 7.60-7.66 (m, 2H), 8.03 (d, *J* = 7.5 Hz, 2H), 8.35 (dd, *J* = 1, 7.5 Hz, 1H), 8.49 (d, *J* = 6 Hz, 1H); ^{13}C NMR (100.5 MHz, $CDCl_3$) δ 9.4, 14.7, 20.8, 22.2, 23.4, 26.2, 35.4, 43.4, 44.9, 58.6, 59.5, 63.3, 71.1, 71.9, 72.8, 72.9, 75.2, 75.9, 77.2, 78.0, 78.6, 78.8, 81.0, 84.3, 111.8, 122.2, 123.2, 128.1, 128.6, 128.7, 129.7, 129.9, 132.8, 133.5, 133.6, 134.6, 134.7,

135.4, 138.2, 156.3, 165.1, 165.6, 169.9, 171.1, 174.1, 202.9; HRMS *m/z* calcd for $C_{51}H_{55}NO_{16}H^+$, 938.3599; found, 938.3589 (Δ = -1.0 ppm).

1-Dimethylhydrosilyl-4-deacetyl-4-acryloyl-7,10,13-tris(triethylsilyl)-10-deacetyl-baccatin (3-38):

To a solution of **3-7** (252 mg, 0.28 mmol) in THF (3.0 mL) was added LiHMDS (0.36 mL, 0.36 mmol) at -30 °C. The reaction mixture was stirred for 5 min and acryloyl chloride (0.029 mL, 0.33 mmol) was added at -30 °C. The reaction mixture was warmed up to 0 °C over 40 min and quenched with saturated aqueous NH_4Cl solution (20 mL) and extracted with EtOAc (30 mL x 3). The organic layer was washed with brine (10 mL) and dried with anhydrous $MgSO_4$. The solvent was removed under reduced pressure and the residue was purified on a silica gel column using hexanes/EtOAc (35/1) as the eluent to afford **3-38** as a white solid (103 mg, 47%) and unreacted starting material **3-7** (75 mg, 30%) recovered: mp 52-55 °C; ^{1}H NMR (500 MHz, CDCl₃) δ -0.31 (d, *J* = 2.5 Hz, 3 H), 0.04 (d, *J* = 2.5 Hz, 1 H), 0.56-0.70 (m, 18 H), 0.93-1.01 (m, 27 H), 1.09 (s, 3 H), 1.18 (s, 3 H), 1.67 (s, 3 H), 1.90 (m, 1 H), 1.97 (s, 3 H), 2.25 (m, 2 H), 2.53 (m, 1 H), 3.92 (d, *J* = 7.0 Hz, 1 H), 4.28 (m, 2 H), 4.43 (dd, *J* = 10.5, 6.5 Hz, 1 H), 4.53 (m, 1 H), 4.90 (d, *J* = 10.5, 1 H), 5.18 (s, 1 H), 5.72 (d, *J* = 6.5 Hz, 1 H), 5.99 (d, *J* = 11.0 Hz, 1 H), 6.21 (dd, *J* = 16.5, 10.5 Hz, 1 H), 6.52 (dd, *J* = 17.5, 1.0 Hz, 1 H), 7.45 (t, *J* = 7.5 Hz, 2 H), 7.57 (t, *J* = 7.5 Hz, 1 H), 8.10 (d, *J* = 7.5 Hz, 2 H); ^{13}C NMR (100.5 MHz, CDCl₃) δ 0.2, 0.4, 4.8, 5.3, 6.0, 6.9, 7.0, 10.4, 14.6, 21.3, 27.3, 37.4, 39.4, 44.0, 46.7, 58.3, 68.3, 72.7, 75.7, 75.9, 81.4, 82.1, 84.1, 128.5, 130.2, 130.3, 130.5, 130.8, 133.3, 136.0, 139.2, 164.7, 165.5, 205.8; HRMS (FAB/DCM/NaCl) m/z calcd. for $C_{50}H_{84}O_{10}Si_4H^+$: 957.5220, found: 957.5232 (Δ = 1.3 ppm).

4-Deacetyl-4-acryloyl-10-deacetylbaccatin (3-39):

To a solution of **3-38** (96 mg, 0.1 mmol) in THF (9.6 mL) was added dropwise HF/pyridine (70:30, 1.0 mL) at 0 °C, and the mixture was stirred at room temperature for 10 h. The reaction was quenched with saturated aqueous $NaHCO_3$ solution (30 mL). The mixture was extracted with ethyl ether (30 mL x 3), washed with brine (10 mL), and dried over anhydrous Na_2SO_4. The solvent was removed under reduced pressure and the residue was purified on a silica gel column using chloroform/methanol (20/1) as the eluent to afford **3-39** as a white solid (47 mg, 85%): mp 178-180 °C; ^{1}H NMR (500 MHz, CDCl₃) δ 1.09 (s, 3 H), 1.10 (s, 3 H), 1.25 (s, 2 H), 1.77 (s, 3 H), 1.86 (m, 1 H), 2.09 (s, 3 H), 2.21 (m, 2 H), 2.63 (m, 1 H), 3.41 (s, 1 H), 4.10 (d, *J* = 7.5 Hz, 1 H), 4.18 (s, 1 H), 4.21 (d, *J* = 9.0 Hz, 1 H), 4.35 (m, 2 H), 4.81 (t, *J* = 8.0 Hz, 1 H), 4.98 (dd, *J* = 11.0, 2.0 Hz, 1 H), 5.27 (s, 1 H), 5.66 (d, *J* = 7.0 Hz, 1 H), 6.02 (dd, *J* = 11.5, 1.0 Hz, 1 H), 6.29 (dd, *J* = 17.0, 10.0 Hz, 1 H), 6.52 (dd, *J* = 17.5, 1.0 Hz, 1 H), 7.45 (t, *J* = 7.5 Hz, 2 H), 7.62 (t, *J* = 7.5 Hz, 1 H), 8.11 (dd, *J* = 8.5, 1.0 Hz, 2 H); ^{13}C NMR (100.5 MHz, CDCl₃) δ 9.8, 15.0, 19.7, 26.7, 37.0, 39.3, 42.6, 46.8, 57.8, 68.0, 72.1, 74.8, 75.1, 78.9, 81.2, 84.1, 128.6, 129.6, 130.0, 131.3, 133.7, 142.3, 165.3, 167.0, 211.7.

7-Triethylsilyl-4-deacetyl-4-acryloylbaccatin (3-36):

To a solution of **3-39** (27 mg, 0.048 mmol) in THF (3 mL) was added $CeCl_3.7H_2O$ (1 mg, 0.005 mmol) and acetic anhydride (0.05 mL, 0.48 mmol) then the mixture was stirred for 2 h at room temperature. The reaction was quenched with saterated $NaHCO_3$ (20 mL).

The mixture was then extracted with dichloromethane (30 mL x 3), washed with brine (10 mL), dried over anhydrous $MgSO_4$ and concentrated *in vacuo* to give **3-40** as a white solid (29 mg crude product without purification).

To a solution of **3-40** (29 mg, ~0.048 mmol) and imidazole (13 mg, 0.192 mmol) in dry DMF (0.4 mL) was added chlorotriethylsilane (0.07 mL, 0. 144 mmol) dropwise *via* syringe at 0 °C. The reaction mixture was stirred for 2 h at room temperature and quenched with saturated aqueous $NaHCO_3$ solution (20 mL). The mixture was extracted with EtOAc (20 mL x 3), washed with water (10 mL x 2), brine (10 mL), dried over $MgSO_4$, and concentrated *in vacuo*. The crude product was purified on a silica gel column using Hexanes:EtOAc (4/1 followed by 2/1) as the eluent to give **3-36** as a white solid (25 mg, 73% for 2 steps): mp 67-69 °C; ^{1}H NMR (400 MHz, $CDCl_3$) δ 0.54-0.65 (m, 6 H), 0.89-0.97 (m, 9 H), 1.03 (s, 3 H), 1.20 (s, 3 H), 1.25 (s, 2 H), 1.71 (s, 3 H), 1.90 (m, 1 H), 2.18 (s, 3 H), 2.20 (s, 3 H), 2.23 (m, 2 H), 2.56 (m, 1 H), 3.96 (d, J = 6.8 Hz, 1 H), 4.21 (d, J = 8.0, 1 H), 4.35 (d, J = 8.4, 1 H), 4.55 (dd, J = 10.4, 6.8 Hz, 1 H), 4.77 (t, J = 7.2 Hz, 1 H), 4.95 (d, J = 8.0, 1 H), 5.65 (d, J = 8.5 Hz, 1 H), 6.02 (dd, J = 10.4, 0.8 Hz, 1 H), 6.28 (dd, J = 17.2, 10.4 Hz, 1 H), 6.48 (s, 1 H), 6.53 (dd, J = 17.2, 1.2 Hz, 1 H), 7.48 (t, J = 8.0 Hz, 2 H), 7.61 (t, J = 7.6 Hz, 1 H), 8.11 (dd, J = 8.0, 1.2 Hz, 2 H); ^{13}C NMR (100.5 MHz, $CDCl_3$) δ 5.3, 6.7, 10.0, 14.8, 20.6, 20.9, 27.8, 37.3, 38.9, 42.8, 47.1, 58.8, 68.1, 72.3, 74.7, 75.8, 78.8, 81.3, 84.2, 128.6, 129.5, 129.7, 130.2, 131.1, 132.7, 133.6, 143.9, 165.3, 169.3, 169.3, 202.1. HRMS (FAB/DCM/NaCl) m/z calcd. for $C_{38}H_{52}O_{11}SiH^{+}$: 713.3357, found: 713.3340 (Δ = -2.4 ppm).

(*3R,4S*)-1-(4-Methoxyphenyl)-3-allyloxy-4-phenylazetidin-2-one (3-41):

Method a:[71] To a solution of **1-13** (130 mg, 0.49 mmol) in anhydrous DMF (1 mL) and THF (6 mL) at 0 °C under nitrogen was treated with NaH (30 mg, 0.75 mmol). The reaction mixture was stirred at 0 °C for 30 min and allyl bromide (0.064 mL, 0.75 mmol). The reaction mixture was allowed to stir at 0 °C for 1 h, quenched with saturated aqueous NH_4Cl (20 mL), and was extracted with CH_2Cl_2 (30 mL x 3). The combined organic layers were washed with brine, dried over $MgSO_4$, filtered, and concentrated. The residue was purified on a silica gel column using hexanes/EtOAc (7/1) as the eluent to afford **3-41** (95 mg, 66% for 2 steps) as white solid.

Method b:[54] To a solution of **1-13** (130 mg, 0.49 mmol) in DMF (17 mL) was added 1.0 M NaHMDS in THF (0.74 mL, 0.74 mmol) at -40 °C and the reaction mixture was stirred for 5 min and then allyl iodide (0.087 mL, 0.74 mmol) was added. The reaction was quenched after 1 h with saturated aqueous NH_4Cl solution (20 mL), and extracted with EtOAc (30 mL x 3) and washed with H_2O (10 mL x 2) and brine (10 mL). The organic layer was dried over anhydrous $MgSO_4$, filtered, and the solvent was removed under reduced pressure. The residue was purified on a silica gel column using hexanes/EtOAc (7/1) as the eluent to afford **3-41** as a white solid (138 mg, 94%): mp 103-104 °C; ^{1}H NMR (300 MHz, $CDCl_3$) δ 3.80 (s, 3 H), 3.81 (ddt, J = 12.6, 5.7, 1.5 Hz, 1 H), 3.96 (ddt, J = 12.6, 5.7, 1.5 Hz, 1 H), 5.02 (d, J = 5.1 Hz, 1 H), 5.10 (dt, J = 6.3, 1.5 Hz, 1 H), 5.14 (s, 1 H), 5.22 (d, J = 4.8 Hz, 1 H), 5.64 (m, 1 H), 6.84 (dt, J = 10.2, 3.3 Hz, 1 H), 7.31-7.36 (m, 2H), 7.40-7.47 (m, 5 H); ^{13}C NMR (75.5 MHz, $CDCl_3$) δ 55.4, 62.0, 71.4, 82.7, 114.3, 118.0, 118.7, 128.1, 128.4, 128.5, 128.5, 128.5, 130.6, 133.2, 133.5, 156.3, 163.8; HRMS calcd. for $C_{19}H_{19}NO_3^{+}$: 309.1365, found 309.1362 (Δ= 0.9 ppm).

(*3R,4S*)-3-Allyloxy-4-phenylazetidin-2-one (3-42):[39]
To a solution of β-lactam **3-41**(92 mg) in acetonitrile (8.9 mL) and water (8.8 mL) at -10 °C was slowly added a solution of ceric ammonium nitrate (640 mg) in water (1.75 mL). The mixture was stirred for 15 min at -10 °C and quenched by 20 mL of saturated sodium bisulfate. The aqueous layer was extracted with dichloromethane (20 mL x 3), and the combined organic layer was washed with brine, dried over anhydrous MgSO$_4$, filtered and the solvent was removed under reduced pressure. to give **3-42** (51 mg, 84%) as a white solid: mp 125-127 °C; ^{1}H NMR (300 MHz, CDCl$_3$) δ 3.78 (dd, *J* = 12.6, 6.0 Hz, 1 H), 3.90 (dd, *J* = 12.6, 6.0 Hz, 1 H), 4.89 (d, *J* = 4.8 Hz, 1 H), 4.94 (dd, *J* = 4.5, 3.0 Hz, 1 H), 5.07 (dd, *J* = 6.6, 1.2 Hz, 1 H), 5.12 (s, 1 H), 5.62 (m, 1 H), 6.72 (bs, 1 H), 7.42 (m, 5 H); ^{13}C NMR (75.5 MHz, CDCl$_3$) δ 58.3, 71.2, 84.5, 116.1, 117.9, 127.8, 128.2, 128.2, 128.2, 128.3, 133.2, 135.7, 168.4; HRMS calcd. for C$_{12}$H$_{13}$NO$_2$$^+$: 203.0946, found 203.0947 (Δ= -0.7 ppm).

(*3R,4S*)-1-Benzoyl-3-allyloxyl-4-phenyl-azetidin-2-one (3-37): [39]
To a solution of β-lactam **3-42** (49 mg, 0.24 mmol), triethylamine (0.07 mL, 0.48 mmol) and DMAP (1 mg, 0.001 mmol) in CH$_2$Cl$_2$ (2.6 mL), was added benzoyl chloride (0.03 mL, 0.26 mmol) dropwise at 0 °C. The mixture was stirred overnight at room temperature and the reaction was quenched with saturated aqueous NH$_4$Cl solution (20 mL). The mixture was then extracted with CH$_2$Cl$_2$ (20 mL x 3). The combined extracts were dried over anhydrous MgSO$_4$ and concentrated *in vacuo*. The crude product was purified on a silica gel column using hexanes/EtOAc (5/1) as the eluent to afford **3-37** a white solid (60 mg, 81% yield): mp 57-58 °C; ^{1}H NMR (300 MHz, CDCl$_3$) δ 3.85 (ddt, *J* = 11.4, 7.6, 2.0 Hz, 1 H), 3.96 (ddt, *J* = 11.4, 7.6, 2.0 Hz, 1 H), 4.96 (d, *J* = 6.0 Hz, 1 H), 5.09 (ddd, *J* = 5.4, 2.4, 1.2 Hz, 1 H), 5.14 (t, *J* = 1.8 Hz, 1 H), 5.44 (d, 6.0 Hz, 1 H), 5.63 (ddd, *J* = 22.5, 10.8, 5.7 Hz, 1 H), 7.32-7.52 (m, 7 H), 7.60 (td, *J* = 5.7, 1.2 Hz, 1 H), 8.04 (dd, *J* = 4.2, 2.7 Hz, 1 H); ^{13}C NMR (75.5 MHz, CDCl$_3$) δ 59.8, 71.9, 81.1, 118.6, 127.9, 127.9, 127.9, 127.9, 128.2, 128.2, 128.4, 128.4, 128.4, 128.5, 129.9, 131.8, 132.8, 133.4, 133.5, 163.6, 166.1. HRMS (FAB/DCM/NaCl) m/z calcd. for C$_{19}$H$_{17}$NO$_3$$^+$: 307.1208 found: 307.1204 (Δ = 1.4 ppm).

4-Deacetyl-4-acryloyl-2'*O*-allyl -7-triethylsilylpaclitaxel (3-35):[37]
To a solution of **3-36** (25 mg, 0.035 mmol) and β-lactam **3-37** (35 mg, 0.114 mmol) in THF (3.2 mL) was added 1 M LiHMDS in THF (0.05 mL, 0.05 mmol) at -40 °C. The reaction mixture was warmed up to 0 °C over 4 h, quenched with dilute aqueous NaHCO$_3$ solution, and extracted with EtOAc. The organic layers were combined, washed with brine, dried over anhydrous MgSO$_4$, and the solvent was removed under reduced pressure. The residue was purified by using column chromatography on silica gel (eluent: Hex/EtOAc, 3/1) to afford **3-35** as a white solid (20 mg, 58%): mp 102-104 °C; ^{1}H NMR (500 MHz, CDCl$_3$) δ 0.62 (m, 6 H), 0.90-1.01 (m, 9 H), 1.17 (s, 3 H), 1.20 (s, 3 H), 1.74 (s, 3 H), 1.93 (m, 1 H), 2.05 (s, 3 H), 2.18 (m, 1 H), 2.19 (s, 3 H), 2.42 (m, 1 H), 2.55 (m, 1 H), 3.90 (d, *J* = 7.0 Hz, 1 H), 3.97 (dd, *J* = 13.5, 6.5 Hz, 1 H), 4.25 (m, 2 H), 4.36 (d, *J* = 8.0 Hz, 1 H), 4.47 (d, *J* = 2.0 Hz, 1 H), 4.55 (dd, *J* = 10.5, 6.5 Hz, 1 H), 4.93 (d, *J* = 9.5 Hz, 1 H), 5.30 (m, 2 H), 5.71 (m, 3 H), 5.84 (m, 1 H), 6.21 (t, *J* = 9.0 Hz, 1 H), 6.30 (dd, *J* = 17.0, 10.0 Hz, 1 H), 6.48 (s, 1 H), 6.54 (d, *J* = 17.5 Hz, 1 H), 7.03 (d, *J* = 9.5 Hz, 1 H), 7.15 (m, 1 H), 7.34-7.56 (m, 11 H), 7.77 (d, *J* = 7.0 Hz, 2 H), 8.16 (d, *J* = 7.5 Hz, 2

H); ^{13}C NMR (100.5 MHz, CDCl$_3$) δ 5.3, 6.7, 10.1, 14.4, 20.9, 21.2, 26.6, 35.4, 37.2, 36.5, 43.3, 46.9, 54.1, 58.5, 71.1, 71.7, 72.2, 74.9, 75.1, 76.6, 78.2, 78.8, 81.4, 84.1, 85.1, 119.1, 126.8, 126.9, 127.1, 127.7, 127.9, 128.1, 128.5, 128.6, 128.9, 129.2, 129.4, 129.9, 130.1, 131.7, 132.0, 133.1, 133.6, 133.8, 134.0, 138.7, 140.2, 164.9, 167.1, 169.3, 170.4, 201.6. HRMS calcd. for C$_{57}$H$_{69}$NO$_{14}$SiNa$^+$: 1142.4835, found 1142.4391 (Δ= 0.6 ppm).

SB-TCR-501:[39]
To a solution of **3-35** (18 mg, 0.017 mmol) in CH$_2$Cl$_2$ (7 mL) was added the "first generaion Grubbs catalyst" (5 mg, 0.0052 mmol) in CH$_2$Cl$_2$ (0.2 mL). The reaction was stirred overnight and the solvent was removed under reduced pressure. The residue was passed through a short silica gel column (eluent: hexanes/EtOAc = 5/1) to remove the catalyst to afford **3-43** as a crude yellow solid (*E*-isomer only, 13 mg, 75%).
To a solution of the **3-43** (13 mg) in CH$_3$CN (0.26 mL) and pyridine (0.26 mL) was added HF-pyridine (70:30, 0.13 ml) and the reaction mixture was stirred overnight. The reaction mixture was diluted with EtOAc (50 mL) and washed with saturated aqueous NaHCO$_3$ solution (10 mL x 2), CuSO$_4$ solution (10 mL x 3), water (10 mL x 3) and brine (3 mL). The organic layer was dried over anhydrous MgSO$_4$ and the solvent was removed under reduced pressure. The residue was purified by column chromatography on silica gel using hexanes/EtOAc (1/1) as the eluent to afford **SB-TCR-501** as white solid (9 mg, 80%): mp 182-184 $^{\circ}$C; ^{1}H NMR (400 MHz, CDCl$_3$) δ 1.16 (s, 3 H), 1.24 (s, 3 H), 1.66 (s, 3 H), 1.69 (s, 3 H), 1.88 (m, 1 H), 2.00 (m, 1 H), 2.24 (s, 3 H), 2.42 (m, 2 H), 2.59 (m, 1 H), 3.56 (d, *J* = 7.2 Hz, 1 H), 3.93 (dd, *J* = 14.0, 9.6 Hz, 1 H), 4.17 (d, *J* = 8.4 Hz, 1 H), 4.38 (d, *J* = 8.4 Hz, 1 H), 4.43 (d, *J* = 2.8 Hz, 1 H), 4.49 (t, *J* = 8.4 Hz, 1 H), 4.86 (ddd, *J* = 12.4, 2.4, 1.2 Hz, 1 H), 5.13 (d, *J* =7.6 Hz, 1 H), 5.69 (d, *J* = 7.2 Hz, 1 H), 5.83 (dd, *J* = 9.2, 2.0 Hz, 1 H), 5.93 (t, *J* = 8.0 Hz, 1 H), 6.02 (d, *J* = 16.4 Hz, 1 H), 6.16 (s, 1 H), 7.21 (ddd, *J* = 10.4, 9.6, 3.6 Hz, 1 H), 7.36 (m, 4 H), 7.48 (m, 7 H), 7.61 (t, *J* = 7.6 Hz, 1 H), 7.83 (d, *J* = 7.2 Hz, 2 H), 8.03 (d, *J* = 6.8 Hz, 2 H); ^{13}C NMR (100.5 MHz, CDCl$_3$) δ 9.8, 14.2, 20.8, 22.8, 27.0, 29.7, 35.1, 36.5, 43.1, 45.6, 55.5, 58.0, 71.8, 72.9, 73.3, 75.3, 75.7, 77.3, 80.3, 81.1, 84.1, 85.1, 121.6, 126.9, 127.0, 128.1, 128.6, 128.7, 129.1, 130.0, 131.9, 133.3, 133.8, 138.2, 141.9, 147.8, 165.5, 166.2, 167.0, 170.9, 171.4, 203.6. HRMS calcd. for C$_{47}$H$_{53}$NO$_{14}$Na$^+$: 878.3364, found 878.3375 (Δ= 1.3 ppm).

2-Allyloxybenzaldehyde (3-46):[66]
To the solution of salicylaldehyde (1.03 mL, 10 mmol) and potassium carbonate (2.7 g, 20 mmol) in anhydrous acetone (30 mL) was added allylbromide (1.73 ml, 20 mmol). The reaction mixture was refluxed for 2 h and filtered. Solvent and excess allylbromide were removed under reduced pressure to give colorless oil (1.62g, 100%): ^{1}H NMR (300 MHz, CDCl$_3$) δ 4.66 (m, 2 H), 5.34 (dq, *J* =10.8, 1.5 Hz, 2 H), 6.09 (m, 1 H), 7.00 (m, 2 H), 7.53 (td, *J* =8.4, 2.4 Hz, 1 H), 7.85 (dd, *J* = 7.5, 1.5 Hz, 1 H), 10.54 (s, 1 H). All data are consistant with literature data.[66]

***N-p*-Methoxyphenyl-2-allyloxybenzaldimine (3-47):**
To a mixture of *p*-anisidine (420 mg, 4.3 mmol) and magnesium sulfate (1.63 g, 13.6 mmol) in dichloromethane (7 mL) was added **3-46** (550 mg, 3.4 mmol). The reaction mixture was stirred overnight and filtered. The solvent was removed under reduced

pressure to give yellow oil. The crude product was immediately used for the synthesis of β-lactam without further purification.

(±)-1-(4-Methoxyphenyl)-3-acetoxyl-4-(2-allyloxyphenyl)azetidin-2-one (3-48):
Aldimine **3-47** was dissolved in CH_2Cl_2 (22 mL), and triethylamine (0.94 mL, 6.8 mmol) was added. Then, the solution was cooled to -78 ˚C. To the mixture was added acetoxyacetyl chloride (0.7 g, 5.1 mmol) and the reaction mixture was warmed up to room temperature overnight. The reaction was quenched with CH_2Cl_2 (150 mL). The organic layer was washed with water, brine, dried over anhydrous $MgSO_4$, and concentrated *in vacuo*. Column chromatography of the residue on silica gel (hexanes/ ethyl acetate = 6/1) afforded **3-48** as a colorless oil (1.554 g, 100 % for 2 steps): ^{1}H NMR (400 MHz, CDCl$_3$) δ 1.73 (s, 3 H), 3.76 (s, 3 H), 4.58 (m, 2 H), 5.32 (dd, J = 11.2, 2.8 Hz, 1 H), 5.43 (dd, J = 17.6, 1.2 Hz, 1 H), 5.78 (d, J = 5.2 Hz, 1 H), 6.09 (d, J = 4.8 Hz, 1 H), 6.09 (m, 1 H), 6.81 (d, J = 8.8 Hz, 2 H), 6.90 (t, J = 8.0 Hz, 2 H), 7.19 (dd, J = 8.0, 0.8 Hz, 1 H), 7.30 (m, 3 H); ^{13}C NMR (100.5 MHz, CDCl$_3$) δ 20.0, 55.4, 56.2, 69.3, 75.7, 111.8, 114.4, 117.7, 118.7, 120.5, 120.9, 128.4, 129.6, 130.5, 133.1, 156.5, 156.7, 161.9, 168.8; HRMS (FAB/DCM/NaCl) m/z calcd. for $C_{21}H_{21}NO_5H^+$: 368.1498, found: 368.1485 (Δ = -3.5 ppm).

Enzymatic resolution of β-lactam (3-48):[72]
To racemic β-lactam **3-48** (1.26 g, 3.4 mmol) suspended in 0.2 M sodium phosphate buffer (pH = 7.5, 150 mL) and acetonitrile (20 mL) was added PS-Amano lipase (600 mg), and the mixture was vigorously stirred at 50 ºC. After 6 days, the ^{1}H NMR analysis of the reaction mixture showed that the conversion of the reaction was 50%. The reaction was terminated by adding dichloromethane (150 mL) and the mixture was extracted with ethyl ether (3 x 50 mL). The organic layer was dried over anhydrous $MgSO_4$ and concentrated *in vacuo*. The residue was subjected to flash column chromatography on silica gel (hexane/ethyl acetate = 6/1 and then 1/1) to give **(+)-3-48** (503 mg) in 40% yield and **(-)-3-49** (481 g) in 45% yield.
(-)-3-49: white solid; mp 142-144ºC; ^{1}H NMR (500 MHz, CDCl$_3$) δ 3.76 (s, 3 H), 4.60 (m, 2 H), 5.20 (s, 1H), 5.31 (dd, J = 10.5, 1.5 Hz, 1 H), 5.40 (dd, J = 17.5, 1.0 Hz, 1 H), 5.51 (d, J = 3.5 Hz, 1 H), 6.05 (m, 1 H), 6.81 (m, 2 H), 6.90 (m, 2 H), 7.21 (d, J = 7.5 Hz, 1 H), 7.31 (m, 3 H); ^{13}C NMR (100.5 MHz, CDCl$_3$) δ 55.4, 59.9, 69.4, 77.6, 112.6, 114.3, 118.1, 118.6, 121.4, 121.9, 129.0, 129.8, 130.9, 132.7, 156.2, 156.6, 165.7; HRMS (FAB/DCM/NaCl) m/z calcd. for $C_{19}H_{19}NO_4H^+$: 326.1392, found: 326.1397 (Δ = 1.4 ppm).

(3R,4S)-3-Acetoxyl-4-(2-allyloxyphenyl)azetidin-2-one (3-50):
To a solution of **(+)-3-48** (311 mg, 0.846 mmol) in acetonitrile (25 mL) and water (5 mL) at -10 °C was slowly added an aqueous solution of ceric ammonium nitrate (1.60 g) in water (25 mL). The mixture was stirred for 20 min at -10 °C and quenched with saturated sodium bisulfate (25 mL). The aqueous layer was extracted with ethyl acetate (30 mL x 3), and the combined organic layer was washed with brine, dried over anhydrous $MgSO_4$, and concentrated *in vacuo* to give **3-50** (196 mg, 89%): ^{1}H NMR (500 MHz, CDCl$_3$) δ 1.73 (s, 3 H), 4.52 (m, 2 H), 5.29 (dt, J = 11.5, 1.5 Hz, 1 H), 5.37 (dq, J = 17.5, 1.5 Hz, 1 H), 5.41 (d, J = 5.0 Hz, 1 H), 6.04 (m, 1 H), 6.08 (m, 1 H), 6.10 (s, 1 H), 6.85 (d, J =8.5

Hz, 1 H), 7.00 (t, J = 7.5 Hz, 1 H), 7.29 (td, J = 8.0, 1.5 Hz, 1 H), 7.36 (dd, J = 7.0, 1.0 Hz, 1 H); ^{13}C NMR (100.5 MHz, CDCl$_3$) δ 19.9, 53.0, 68.9, 77.3, 111.2, 117.5, 120.3, 123.4, 127.4, 129.2, 132.9), 156.1, 165.7, 168.6; HRMS (FAB/DCM/NaCl) m/z calcd. for C$_{14}$H$_{15}$NO$_4$H$^+$: 262.1079, found: 262.1089 (Δ = 3.7 ppm).

(*3R*,*4S*)-3-Triethylsilyloxy-4-(2-allyloxyphenyl)azetidin-2-one (3-51):[54]

To a solution of 1 M KOH aqueous solution (10 mL) at 0 °C was added a solution of **3-50** (193 mg, 0.739 mmol) in THF (25 mL). The solution was stirred at 0 °C for 1 h and saturated NH$_4$Cl (20 mL) was added. The mixture was extracted with dichloromethane (20 mL x 3). The combined organic layers were dried over MgSO$_4$ and concentrated to give 3-hydroxy-4-(2-allyloxyphenyl)azetidin-2-one (169 mg, 100%) as a crude solid, and the β-lactam was used for the next step without further purification.

To a solution of 3-hydroxy-4-(2-allyloxyphenyl)azetidin-2-one (169 mg, 0.70 mmol), DMAP (2 mg, 0.02 mmol) and triethylamine (0.22 mL, 1.4 mmol) in dichloromethane (29 mL) was added chlorotriethylsilane (0.123 mL, 0.735 mmol). The solution was stirred at 0 °C for 4 min, quenched with saturated NH$_4$Cl solution (30 mL) and stirred at room temperature for 30 min. The mixture was extracted with CH$_2$Cl$_2$ (20 mL x 3) and the combined organic layers were dried over MgSO$_4$. The solution was concentrated *in vacuo* and the residue was separated using column chromatography on silica gel (hexanes/ethyl acetate = 4/1) to give **3-51** as a white solid 192 mg (78% for 2 steps): mp 73-74 °C; ^{1}H NMR (400 MHz, CDCl$_3$) δ 0.44 (m, 6 H), 0.74 (m, 9 H), 4.50 (d, J = 5.2 Hz, 2 H), 5.06 (m, 1 H), 5.23 (d, J = 4.8 Hz, 1 H), 5.27 (dq, J = 10.8, 1.2 Hz, 1 H), 5.38 (dq, J = 17.6, 1.6 Hz, 1 H), 6.05 (m, 1 H), 6.80 (d, J = 8.0 Hz, 1 H), 6.82 (s, 1 H), 6.95 (t, J = 7.6 Hz, 1 H), 7.21 (td, J = 7.6, 1.6 Hz, 1 H), 7.36 (dd, J = 7.2, 1.2 Hz, 1 H); ^{13}C NMR (100.5 MHz, CDCl$_3$) δ 4.3, 6.1, 54.0, 68.5, 79.1, 110.7, 117.1, 120.2, 125.0, 127.9, 128.4, 133.1, 156.2, 170.3; HRMS (FAB/DCM/NaCl) m/z calcd. for C$_{18}$H$_{27}$NO$_3$SiH$^+$: 334.1838, found: 334.1849 (Δ = 3.1 ppm).

(*3R*,*4S*)-1-Benzoyl-3-triethylsilyloxy-4-(2-allyloxyphenyl)azetidin-2-one (3-52):

To a solution of β-lactam **3-51** (117 mg, 0.315 mmol), triethylamine (0.1 mL, 0.702 mmol) and DMAP (2 mg, 0.03 mmol) in CH$_2$Cl$_2$ (4 mL), was added benzoyl chloride (0.045 mL, 0.386 mmol) dropwise at room temperature. The mixture was stirred overnight at room temperature and the reaction was quenched with saturated aqueous NH$_4$Cl solution (20 mL). The mixture was then extracted with dichloromethane (20 mL x 3). The combined organic layer was dried over anhydrous MgSO$_4$ and concentrated *in vacuo*. The crude product was purified on a silica gel column using hexanes/EtOAc (50/1) as the eluent to afford **3-60** as a white solid (153 mg, 99% yield): mp 66-67 °C; ^{1}H NMR (400 MHz, CDCl$_3$) δ 0.51 (m, 6 H), 0.80 (m, 9 H), 4.57 (m, 2 H), 5.17 (d, J = 6.4 Hz, 1 H), 5.30 (dd, J = 10.8, 1.2 Hz, 1 H), 5.44 (dq, J = 17.2, 1.6 Hz, 1 H), 5.83 (d, J = 6.0 Hz, 1 H), 6.10 (m, 1 H), 6.88 (d, J = 8.0 Hz, 1 H), 6.95 (t, J = 7.2 Hz, 1 H), 7.25 (t, J = 7.6 Hz, 2 H), 7.48 (t, J = 8.0 Hz, 2 H), 7.58 (t, J = 7.6 Hz, 1 H), 8.07 (d, J = 7.2 Hz, 2 H); ^{13}C NMR (100.5 MHz, CDCl$_3$) δ 4.3, 6.2, 56.9, 68.9, 76.2, 111.3, 117.3, 120.4, 122.1, 127.5, 128.0, 128.9, 129.8, 132.6, 133.1, 133.2, 156.4, 165.5, 166.3; HRMS (FAB/DCM/NaCl) m/z calcd. for C$_{25}$H$_{31}$NO$_4$SiH$^+$: 438.2101, found: 438.2107 (Δ = 1.5 ppm).

2-Allylbenzyl alcohol (3-53):[68]
To a solution of acid **3-21** (600 mg, 3.7 mmol) in dry THF (8 mL) at 0 °C under nitrogen was added $LiAlH_4$ (280 mg, 7.4 mmol). The mixture was allowed to warm to room temperature for 30 min and then heated at reflux for overnight. Excess $LiAlH_4$ was quenched by careful addition of aqueous 3 M hydrochloric acid at 0 °C, and the aqueous phase was extracted with Et_2O (30 mL x 3). The combined organic layer was washed with brine (20 mL x 2), dried over $MgSO_4$, and concentrated under reduced pressure. The reside was purified on a silica gel column using hexanes:EtOAc (7:1) as the eluent to afford acid **3-53** as colorless oil (520 mg, 95%): ^1H NMR (300 MHz, $CDCl_3$) δ 3.04 (s, 1 H), 3.54 (dt, J = 6.3, 2.7 Hz, 2 H), 4.73 (s, 2 H), 5.09 (ddd, J = 16.8, 3.6, 1.8 Hz, 1 H), 5.20 (ddd, J = 9.9, 3.0, 1.5 Hz, 1 H), 6.10 (m, 1 H), 7.33 (m, 3 H), 7.47 (dd, J = 9.6, 1.5 Hz, 1 H); ^{13}C NMR (75.5 MHz, $CDCl_3$) δ 36.4, 62.4, 115.6, 126.4, 127.7, 127.9, 129.5, 137.1, 137.5, 138.5.

2-Allylbenzaldehyde (3-54):[69]
Pyridinium chlorochromate (1.16g, 5.4 mmol) was added a solution of 2-allylbenzyl alcohol **3-53** (539 mg, 3.6 mmol) in dichloromethane (10.8 mL). The mixture was stirred at room temperature for 2.5 h and quenched with Et_2O (50 mL). After filtration, the solid residue was washed with Et_2O (50 mL x 2) and the combined organic layer was washed with 5% aqueous citric acid solution (5 mL), saturated aqueous $NaHCO_3$ solution (10 mL) and brine (10 mL). The organic layer was dried over anhydrous $MgSO_4$ and solvent was removed under reduced pressure. The crude product was immediately used for the synthesis of β-lactam without further purification.

N-p-Methoxyphenyl-2-allylbenzaldimine (3-55):
To the solution of **3-54** (~3.6 mmol) and sodium sulfate (2.1 g, 14.4 mmol) in dichloromethane (8 mL) was added *p*-anisidine (440 mg, 3.6 mmol). The reaction mixture was stirred for 2 h and filtered. The solvent was removed under reduced pressure to give yellow oil. The crude product was immediately used for the synthesis of β-lactam without further purification.

(±)-1-(4-Methoxyphenyl)-3-acetoxyl-4-(2-allyloxyphenyl)azetidin-2-one (3-56):[42]
Aldimine **3-55** was dissolved in CH_2Cl_2 (23 mL) and triethylamine (1.0 mL, 5.4 mmol) was added. Then solution was cooled to -78 °C. To the mixture was added acetoxyacetyl chloride (0.6 mL, 4.3 mmol) and the reaction mixture was warmed up to room temperature overnight. The reaction was quenched with CH_2Cl_2 (60 mL). The organic layer was washed with water, brine, dried over anhydrous $MgSO_4$, and concentrated *in vacuo*. Column chromatography of the residue on silica gel (hexanes/ ethyl acetate = 8/1) afforded **3-56** (979 mg, 79 % for 3 steps) as a white solid: mp 110-111 °C; ^1H NMR (400 MHz, $CDCl_3$) δ 1.59 (s, 3 H), 3.33 (dd, J = 16.0, 5.2 Hz, 1 H), 3.56 (dd, J = 16.8, 6.8 Hz, 1 H), 3.67 (s, 3 H), 5.03 (d, J = 17.2 Hz, 1 H), 5.13 (d, J = 10.0 Hz, 1 H), 5.51 (d, J = 4.8 Hz, 1 H), 5.94 (d, J = 4.8 Hz, 1 H), 6.03 (m, 1 H), 6.74 (d, J = 8.8 Hz, 2 H), 7.18 (m, 6 H); ^{13}C NMR (100.5 MHz, $CDCl_3$) δ 19.4, 31.3, 55.1, 57.8, 75.8, 114.1, 116.1, 118.5, 118.6, 126.1, 127.0, 128.4, 129.8, 130.0, 130.0, 136.5, 138.1, 156.2, 161.8, 168.8. HRMS (FAB/DCM/NaCl) m/z calcd. for $C_{21}H_{21}NO_4H^+$: 352.1549, found: 352.1547 (Δ = -0.6 ppm).

Enzymatic resolution of β-lactam (3-56):[73]

To racemic β-lactam **3-56** (1.56 g, 3.4 mmol) suspended in 0.2 M sodium phosphate buffer (pH = 7.5, 140 mL) and acetonitrile (15 mL) was added PS Amano lipase (600 mg), and the mixture was vigorously stirred at 50 °C. After 5 days, the ^{1}H NMR analysis showed that the conversion of the reaction was 55%. The reaction was terminated by adding dichloromethane (100 mL) and the mixture was extracted with dichloromethane (3 x 50 mL). The organic layer was dried over anhydrous MgSO$_4$, and concentrated *in vacuo*. The residue was subjected to flash column chromatography on silica gel (hexanes:EtOAc = 8:1 to 2:1) to give (+)-**3-56** (670 mg) in 43% yield and **(-)-3-57** (626 mg) in 46% yield.

3-57: white solid; ^{1}H NMR (400 MHz, CDCl$_3$) δ 3.51 (m, 2 H), 3.73 (s, 3 H), 4.10 (m, 1 H), 5.17 (m, 3 H), 5.44 (d, *J* = 4.8 Hz,1 H), 6.08 (m, 1 H), 6.80 (d, *J* = 8.8 Hz, 2 H), 7.19 (m, 6 H); ^{13}C NMR (100.5 MHz, CDCl$_3$) δ 37.0, 55.2, 59.7, 76.6, 114.2, 116.2, 118.7, 126.5, 126.8, 128.2, 130.1, 130.4, 131.2, 136.4, 138.0, 156.2, 166.1. HRMS (FAB/DCM/NaCl) m/z calcd. for C$_{19}$H$_{19}$NO$_3$H$^+$: 310.1443, found: 310.1447 (Δ = 1.3 ppm).

(3R,4S)-3-Acetoxyl-4-(2-allylphenyl)azetidin-2-one (3-58):[72]

To a solution of **(+)-3-56** (560 mg, 1.59 mmol) in acetonitrile (45 mL) and water (9 mL) at -10 °C was slowly added a solution of ceric ammonium nitrate in 45 mL of water. The mixture was stirred for 2.5 h at -10 °C and quenched by saturated sodium bisulfate (30 mL). The aqueous layer was extracted with ethyl acetate (40 mL x 3), and the combined organic layer was washed with brine, dried over anhydrous MgSO$_4$, and concentrated *in vacuo*. The residue was subjected to flash column chromatography on silica gel (hexanes:EtOAc = 4:1) to afford **3-58** as a white solid (309 mg, 89%): mp 104-105; ^{1}H NMR (400 MHz, CDCl$_3$) δ 1.60 (s, 3 H), 3.23 (dd, *J* =16.4, 5.6 Hz, 1 H), 3.38 (dd, *J* = 16.4, 5.6 Hz, 1 H), 4.92 (dd, *J* = 17.2, 1.2 Hz, 1 H), 5.03 (dd, *J* = 10.4, 1.2 Hz, 1 H), 5.17 (d, *J* = 4.8 Hz, 1 H), 5.88 (m, 2 H), 6.61 (s, 1 H), 7.12 (m, 1 H), 7.22 (m, 2 H), 7.41 (m, 1 H); ^{13}C NMR (100.5 MHz, CDCl$_3$) δ 19.6, 36.2, 54.4, 77.5, 116.1, 126.1, 126.6, 128.2, 129.6, 132.4, 136.3, 137.8, 166.1, 168.9. HRMS (FAB/DCM/NaCl) m/z calcd. for C$_{14}$H$_{15}$NO$_3$H$^+$: 246.1133, found: 246.1118 (Δ = -4.9 ppm).

(3R,4S)-3-Triethylsilyloxy-4-(2-allylphenyl)azetidin-2-one (3-60):[74]

To an aqueous solution of 1 M KOH (16 mL) at 0 °C was added a solution of **3-58 (**300 mg, 1.22 mmol) in THF (40 mL). The solution was stirred at 0 °C for 30 min and quenched by saturated NH$_4$Cl (30 mL). The mixture was extracted with dichloromethane (40 mL x 3). The combined organic layers were dried over MgSO$_4$ and concentrated to give **3-59** (225 mg, 91%) as a crude solid. The β-lactam **3-59** was used for the next step without further purification.

To a solution of **3-59** (225 mg, 1.1 mmol), DMAP (3 mg, 0.03 mmol) and triethylamine (0.35 mL, 2.2 mmol) in dichloromethane (45 mL) was added chlorotriethylsilane (0.193 mL, 1.2 mmol). The solution was stirred at 0 °C for 25 min, quenched with saturated NH$_4$Cl solution (30 mL) and stirred at room temperature for 30 min. The mixture was extracted with CH$_2$Cl$_2$ (20 mL x 3) and the combined organic layers were dried over MgSO$_4$. The organic layer was concentrated *in vacuo* and the residue was subjected to column chromatography on silica gel (hexanes:EtOAc = 5:1) to give **3-60** as a colorless

oil (226 mg, 65%): ^{1}H NMR (300 MHz, CDCl$_3$) δ 0.52 (m, 6 H), 0.83 (m, 9 H), 3.44 (d, J = 6.0 Hz, 2 H), 5.14 (m, 4 H), 6.01 (m, 1 H), 6.83 (s, 1 H), 7.22 (m, 1 H), 7.30 (m, 2 H), 7.48 (m, 1 H); ^{13}C NMR (100.5 MHz, CDCl$_3$) δ 5.0, 6.3, 37.0, 55.9, 79.1, 116.7, 126.1, 127.1, 127.6, 129.1, 134.4, 136.6, 137.4, 169.8. HRMS (FAB/DCM/NaCl) m/z calcd. for C$_{18}$H$_{27}$NO$_2$SiH$^+$: 318.1889, found: 318.1891 (Δ = 0.6 ppm).

(*3R*,*4S*)-1-Benzoyl-3-triethylsilyloxy-4-(2-allylphenyl)azetidin-2-one (3-61):
To a solution of *β*-lactam **3-60** (125 mg, 0.39 mmol), triethylamine (0.11 mL, 0.78 mmol) and DMAP (2 mg, 0.03 mmol) in CH$_2$Cl$_2$ (4.5 mL), was added benzoyl chloride (0.051 mL, 0.43 mmol) dropwise at room temperature. The mixture was stirred overnight at room temperature and the reaction was quenched with saturated aqueous NH$_4$Cl solution (20 mL). The mixture was then extracted with dichloromethane (20 mL x 3). The combined extracts were dried over anhydrous MgSO$_4$ and concentrated *in vacuo*. The crude product was purified on a silica gel column using hexanes:EtOAc (50:1) as the eluent to afford **3-61** as a colorless oil (152 mg, 92% yield): ^{1}H NMR (400 MHz, CDCl$_3$) δ 0.51 (m, 6 H), 0.78 (m, 9 H), 3.49 (ddt, J = 16.4, 6.0, 1.6 Hz, 1 H), 3.57 (dd, J = 16.0, 6.4 Hz, 1 H), 5.11 (m, 2 H), 5.17 (d, J = 6.4 Hz, 1 H), 5.68 (d, J = 6.0 Hz, 1 H), 6.07 (m, 1 H), 7.22 (m, 3 H), 7.33 (dd, J = 8.8, 2.0 Hz, 1 H), 7.49 (m, 2 H), 7.60 (tt, J = 6.8, 1.2 Hz, 1 H), 8.07 (dd, J = 6.0, 1.2 Hz, 2 H); ^{13}C NMR (100.5 MHz, CDCl$_3$) δ 4.5, 6.2, 37.3, 57.4, 76.0, 116.3, 126.1, 128.0, 128.1, 129.5, 129.9, 131.8, 132.0, 133.3, 136.5, 138.0, 165.2, 166.2. HRMS (FAB/DCM/NaCl) m/z calcd. for C$_{25}$H$_{31}$NO$_3$SiH$^+$: 422.2151, found: 422.2169 (Δ = 4.3 ppm).

K2a:[37]
To a solution of **3-36** (20 mg, 0.028 mmol) and *β*-lactam **3-52** (37 mg, 0.084 mmol) in THF (3 mL) was added 1 M LiHMDS in THF (0.042 ml, 0.042 mmol) at -40 °C. The reaction mixture was warmed up to 0 °C over 3 h and then quenched with dilute aqueous NaHCO$_3$ solution (10 mL) and extracted with EtOAc (20 mL x 3). The organic layers were combined and solvent was removed under reduced pressure. The residue was purified by column chromatography on silica gel (eluent: hexames/EtOAc = 5/1) to afford **3-62** as white solid. (19 mg, 60%).
To a sulotion of **3-62** (10 mg, 0.0096 mmol) in CH$_2$Cl$_2$ (5 mL) was added the "first-generation Grubbs's catalyst" (4 mg, 0.0004 mmol) in CH$_2$Cl$_2$ (0.04 mL). The reaction was stirred overnight and the solvent was removed under reduced pressure. The residue was passed through a short silica gel column (eluent: hexames/EtOAc = 2/1) to remove the catalyst to afford **3-63** as a crude yellow solid.
To a solution of the **3-63** (10 mg) in CH$_3$CN (0.2 mL) and pyridine (0.2 mL) was added HF-pyridine (70:30, 0.1 ml) and the reaction mixture was stirred overnight. The reaction mixture was diluted with EtOAc (60 mL) and washed with saturated aqueous NaHCO$_3$ solution (5 mL x 2), CuSO$_4$ solution (5 mL x 3), water (5 mL x 3) and brine (3 mL). The organic layer was dried over anhydrous MgSO$_4$ and solvent was removed under reduced pressure. The residue was purified by column chromatography on silica gel using hexanes:EtOAc (1/1) as the eluent to afford **K2a** as white solid (5 mg, 60% in 2 steps): ^{1}H NMR (400 MHz, CDCl$_3$) δ 1.13 (s, 3 H), 1.23 (s, 3 H), 1.70 (s, 3 H), 1.87 (s, 3 H), 1.92 (m, 1 H), 2.24 (s, 3 H), 2.48 (m 2 H), 2.59 (m, 1 H), 3.19 (bs, 1 H), 3.74 (d, J = 6.8 Hz, 1 H), 4.28 (d, J = 8.4 Hz, 1 H), 4.46 (m, 2 H), 4.78 (s, 1 H), 4.89 (m, 2 H), 5.10 (dd, J

= 9.6, 2.0 Hz, 1 H), 5.70 (d, J = 7.2, 1 H), 5.99 (d, J = 6.8 Hz, 1 H), 6.16 (t, J = 8.8, 1 H), 6.27 (s, 1 H), 6,78 (d, J = 16.0 Hz, 1 H), 7.10 (m, 3 H), 7.29-7.43 (m, 5 H), 7.48-7.55 (m, 3 H), 7.61 (t, J = 7.8 Hz, 1 H), 7.71 (dd, J = 8.8, 0.8 Hz, 2 H) , 8.11 (dd, J = 8.4, 0.8 Hz, 2 H). ^{13}C NMR (100.5 MHz, CDCl$_3$) δ 9.7, 14.8, 21.0, 22.3, 27.0, 35.0, 35.7, 43.2, 45.9, 58.6, 58.8, 66.1, 70.5, 72.5, 75.1, 75.7, 76.4, 76.7, 77.4, 79.4, 81.5, 84.3, 111.2, 119.3, 122.5, 126.8, 127.3, 128.9, 129.6, 130.1, 131.2, 132.4, 132.6, 133.6, 134.1, 138.4, 142.9, 143.3, 155.7, 163.6, 167.0, 169.3, 171.5, 173.0, 203.7. HRMS calcd. for C$_{49}$H$_{51}$NO$_{15}^+$: 894.3337, found 894.3294 (Δ= 4.8 ppm). All data are consistent with the reported values.[37]

4-Deacetyl-4-acryloyl-3'-dephenyl-3'-(2-allylphenyl)-7,2'-triethylsilylpaclitaxel (3-64):[37]

To a solution of **3-36** (45 mg, 0.063 mmol) and β-lactam **3-61** (80 mg, 0.19 mmol) in THF (6 mL) was added 1.3 M LiHMDS in THF (0.07 ml, 0.094 mmol) at -40 ^{o}C. The reaction mixture was warmed up to -30 ^{o}C over 30 min, quenched with dilute aqueous NH$_4$Cl solution, and extracted with Et$_2$O. The organic layers were combined, washed with brine and solvent was removed under reduced pressure. The residue was purified by column chromatography (eluent: hexanes/EtOAc = 4/1) to afford **3-64** as a white solid (53 mg, 74%): mp 125-127 ^{o}C; ^{1}H NMR (400 MHz, CDCl$_3$) δ 0.59 (m, 12 H), 0.94 (m, 18 H), 1.19 (s, 3 H), 1.23 (s, 3 H), 1.71 (s, 3 H), 1.90 (m 3 H), 2.01 (s, 3 H), 2.16 (s, 3 H), 2.44 (m, 2 H), 2.52 (m, 1 H), 3.53 (dd, J = 15.6, 6.4 Hz, 1 H), 3.67 (dd, J = 15.6, 6.4 Hz, 1 H), 3.91 (d, J = 6.8 Hz, 1 H), 4.26 (d, J = 8.4 Hz, 1 H), 4.34 (d, J = 8.4 Hz, 1 H), 4.53 (dd, J = 10.4 Hz, 6.4 Hz, 1 H), 4.58 (d, J = 1.2 Hz, 1 H), 4.88 (d, J = 3.6 Hz, 1 H), 5.11 (dd, J = 10.4, 1.6 Hz, 1 H), 5.16 (dd, J = 17.2, 1.6 Hz, 1 H), 5.47 (dd, J = 10.0, 1.2 Hz,1 H), 5.74 (d, J = 7.2 Hz, 1 H), 5.77 (dd, J = 17.2, 1.6 Hz, 1 H), 6.05 (m, 2 H), 6.26 (dd, J = 17.6, 10.4 Hz, 1 H), 6.43 (dd, J = 17.2, 1.2 Hz, 1 H), 6.47 (s, 1 H), 6.87 (d, J = 9.2 Hz, 1 H), 7.35 (m, 8 H), 7.54 (d, J = 7.6 Hz, 1 H), 7.60 (t, J = 7.6 Hz, 1 H), 7.68 (d, J = 6.8 Hz, 2 H), 8.11 (d, J = 7.2 Hz, 1 H); ^{13}C NMR (100.5 MHz, CDCl$_3$) δ 5.7, 5.3, 6.6, 6.8, 10.1, 14.1, 20.8, 21.5, 26.5, 35.7, 36.8, 37.2, 43.4, 46.7, 51.7, 58.4, 72.1, 72.4, 73.3, 75.0, 75.1, 76.6, 78.7, 81.5, 84.2, 116.9, 126.5, 126.9, 127.3, 128.3, 128.5, 129.3, 129.6, 130.0, 130.1, 131.5, 133.5, 134.3, 136.3, 136.8, 137.7, 140.6, 164.8, 166.8, 167.0, 169.3, 172.2, 201.7. HRMS calcd. for C$_{63}$H$_{83}$NO$_{14}$Si$_2$H$^+$: 1134.5430, found 1134.5393 (Δ= -3.3 ppm).

K1a:[37]

To a sulotion of **3-64** (35 mg, 0.03 mmol) in CH$_2$Cl$_2$ (7 mL) was added the "first-generation Grubbs catalyst" (8 mg, 0.01 mmol) in CH$_2$Cl$_2$ (0.2 mL). The reaction was stirred overnight, and the solvent was removed under reduced pressure. The residue was passed through a short silica gel column (hexanes/EtOAc = 4/1) to remove the catalyst to afford **3-65** as a crude yellow solid (Z-isomer, 20 mg, 60%).
To a solution of the **3-65** (17 mg) in CH$_3$CN (0.34 mL) and pyridine (0.34 mL) was added HF-pyridine (70:30, 0.17 mL) and the reaction mixture was stirred overnight. The reaction mixture was diluted with EtOAc (50 mL) and washed with saturated aqueous NaHCO$_3$ solution (10 mL x 2), CuSO$_4$ solution (10 mL x 3), water (10 mL x 3) and brine (3 mL). The organic layer was dried over anhydrous MgSO$_4$ and solvent was removed under reduced pressure. The residue was purified by column chromatography on silica gel using hexanes:EtOAc (1/1) as the eluent to afford **K1a** as white solid (11 mg, 84%):

mp 214-216 °C; ^{1}H NMR (400 MHz, CDCl$_3$) δ 1.18 (s, 3 H), 1.30 (s, 3 H), 1.76 (s, 3 H), 1.94 (m, 1 H), 1.95 (s, 3 H), 2.22 (m, 1 H), 2.25 (s, 3 H), 2.47 (m, 2 H), 2.68 (m, 1 H), 3.30 (bs, 1 H), 3.89 (d, J = 6.8 Hz, 1 H), 3.93 (dt, J = 19.6, 2.8 Hz, 1 H), 4.25 (d, J = 8.0 Hz, 1 H), 4.34 (d, J = 8.4 Hz, 1 H), 4.46 (m, 2 H), 4.86 (dd, J = 19.6, 9.2 Hz, 1 H), 5.01 (d, J =7.6 Hz, 1 H), 5.73 (d, J = 6.8 Hz, 1 H), 5.93 (d, J = 8.0 Hz, 1 H), 6.29 (dd, J = 11.2, 5.6 Hz, 1 H), 6.36 (s, 1 H), 6.49 (t, J = 8.4 Hz, 1 H), 6.76 (td, J = 11.2, 1.6 Hz, 1 H), 7.14 (d, J = 8.4 Hz, 1 H), 7.33 (m, 3 H), 7.52 (m, 6 H), 7.60 (t, J = 7.6 Hz, 1 H), 7.77 (d, J = 6.8 Hz, 2 H), 8.15 (d, J = 6.8 Hz, 2 H); ^{13}C NMR (100.5 MHz, CDCl$_3$) δ 9.5, 15.3, 20.8, 21.8, 27.1, 34.9, 35.5, 36.1, 43.4, 46.0, 50.8, 58.9, 72.0, 72.4, 72.7, 74.8, 75.6, 78.9, 81.1, 84.4, 120.4, 126.3, 127.1, 127.7, 128.4, 128.7, 128.8, 129.0, 130.3, 130.8, 131.9, 133.1, 133.7, 133.8, 136.8, 138.4, 142.2, 153.0, 165.4, 166.6, 167.1, 171.2, 173.1, 203.6. HRMS calcd. for C$_{48}$H$_{51}$NO$_{14}$$^+$: 878.3388, found 878.3389 (Δ= 0.1 ppm). All data are consistent with the reported values.[37]

In vitro cell growth inhibition assay:

(a) Tumor cell growth inhibition was examined according to the method established by Skehan et al.[75] Human cancer cells HT-29, LCC6-WT (Pgp-), MCF-7 (Pgp-), LCC6-MDR (Pgp+) and NCI/ADR (Pgp+), were plated at a density of 400-2,000 cells/well in 96-well plates and allowed to attach overnight. These cell lines were maintained in RPMI-1640 medium (Roswell Park Memorial Institute growth medium) supplemented with 5% fetal bovine serum and 5% Nu serum (Collaborative Biomedical Product, MA). Taxoids were dissolved in DMSO and further diluted with RPMI-1640 medium. Triplicate wells were exposed to various treatments. After 72 h incubation, 100 µL of ice-cold 50% trichloroacetic acid (TCA) was added to each well, and the samples were incubated for 1 h at 4 °C. Plates were then washed five times with water to remove TCA and serum proteins, and 0.4% sulforhodamine B (SRB) (50 µL) was added to each well. Following a 5-min incubation, plates were rinsed five times with 0.1% acetic acid and air-dried. The dye was then desolved in 10 mM Tris-base (pH 10.5) for 5 min on a gyratory shaker. Optical density was measured at 570 nm. The IC$_{50}$ values were then calculated by fitting the concentration-effect curve data with the sigmoid-E_{max} model using nonlinear regression, weighted by the reciprocal of the square of the predicted effect.[76]

(b) Human cancer cell lines, HT-29, A2780, LCC6-WT (Pgp-), MCF-7 (Pgp-), LCC6-MDR (Pgp+) and NCI/ADR (Pgp+), were cultured as specified by ATCC (Manassas, Virginia). For cytotoxicity assays the cells were plated at a density of 10,000 cells/well in 96-well plates and allowed to adhere overnight. Then, the media was replaced with media containing taxane derivatives or vehicle control. Taxoids were dissolved in DMSO to 10 mM concentration and were further diluted in appropriate media prior to addition to cells. Each dose of drug or vehicle was tested in triplicate, and the final value was a representative of at least 3 independent trials. After 72 h of treatment, the media was aspirated and the cells were washed with warm PBS. MTT reagent (Sigma) was diluted in RPMI-1640 media without phenol red (Invitrogen), and added to the cells at a concentration of 0.5 mg/mL. After 3 hours of incubation, the reagent was aspirated, the plate was washed with PBS and MTT formazan crystals were dissolved in 50 µL acidified isopropanol (0.04 N hydrochloric acid). Absorbance at 570 nM was measured

on a thermomax plate reader (Molecular Devices). The IC_{50} values were obtained by using the same method as that described for (a).

Tubulin polymerization assay
(Professor Susan B. Horwitz's laboratory at the Albert Einstein College of Medicine):
Assembly and disassembly of calf brain microtubule protein (MTP) was monitored spectrophotometrically (Beckman Coulter DU 640, Fullerton, CA) by recording changes in turbidity at 350 nm at 37 °C.[77, 78] MTP was diluted to 1mg/mL in MES buffer containing 3 M glycerol. The concentration of tubulin in MTP is 85% and that was taken into consideration when the ratios of tubulin to drug were presented in **Figure 3-23** and **Figure 3-24**. Microtubule assembly was carried out with 10 μM new-generation taxoids. Paclitaxel (10 μM) was also used for comparison purpose. Calcium chloride (6 mM) was added to the assembly reaction after 50 min to follow the calcium-induced microtubule depolymerization.

Electron microscopy
(Professor Susan B. Horwitz's laboratory at the Albert Einstein College of Medicine):
Aliquots (50 μL) were taken from *in vitro* polymerization assays at the end of the reaction and placed onto 300-mesh carbon-coated, formavar-treated copper grids. Samples were then stained with 2% uranyl acetate (20 μL) and viewed with a JEOL model 100CX electron microscope.

§ 3.5 References

1. Schiff, P. B.; Fant, J.; Horwitz, S. B. Promotion of Microbubule Assembly *in vitro* by Taxol. *Nature* **1979,** 277, 665-667.
2. Kumar, N. Taxol-Induced Polymerization of Purified Tubulin. *J. Biol. Chem.* **1981,** 256, 10435-10441.
3. Bollag, D. M.; McQueney, P. A.; Zhu, J.; Hensens, O.; Koupal, L.; Liesch, J.; Goetz, M.; Lazarides, E.; Woods, C. M. Epothilones, a New Class of Microtubule-stabilizing Agents with a Taxol-like Mechanism of Action. *Cancer Res.* **1995,** 55, 2325-2333.
4. Lindel, T.; Jensen, P. R.; Fenical, W.; Long, B. H.; Casazza, A. M.; Carboni, J.; Fairchild, C. R. Eleutherobin, a New Cytotoxin that Mimics Paclitaxel (Taxol) by Stabilizing Microtubules. *J. Am. Chem. Soc.* **1997,** 119, 8744-8745.
5. ter Haar, E.; Kowalski, R. J.; Hamel, E.; Lin, C. M.; Longley, R. E.; Gunasekera, S. P.; Rosenkranz, H. S.; Day, B. W. Discodermolide, A Cytotoxic Marine Agent That Stabilizes Microtubules More Potently Than Taxol. *Biochemistry* **1996,** 35, 243-250.
6. Mooberry, S. L.; Tien, G.; Hernandez, A. H.; Plubrukarn, A.; Davidson, B. S. Laulimalide and isolaulimalide, new paclitaxel-like microtubule-stabilizing agents. *Cancer Res* **1999,** 59, 653-60.
7. Sato, B.; Nakajima, H.; Hori, Y.; Hino, M.; Hashimoto, S.; Terano, H. A new antimitotic substance, FR182877. II. The mechanism of action. In *J. Antibiot.*, 2000; Vol. 53, pp 204-206.
8. Kowalski, R. J.; Giannakakou, P.; Hamel, E. Activities of the Microtubule-Stabilizing Agents Epothilones A and B with Purified Tubulin and in Cells Resistant to Paclitaxel. *J. Biol. Chem.* **1997,** 272, 2534-2541.
9. Kowalski, R. J.; Giannakakou, P.; Gunasekera, S. P.; Longley, R. E.; Day, B. W.; Hamel, E. The Microtubule-Stabilizing Agent Discodermolide Competitively Inhibits the Binding of Paclitaxel (Taxol) to Tubulin Polymers, Enhances Tubulin Nucleation Reactions More Potently Than Paclitaxel, and Inhibits the Growth of Paclitaxel-Resistant Cells. *Mol. Pharmacol.* **1997,** 52, 613-622.
10. Giannakakou, P.; Sackett, D. L.; Kang, Y.-K.; Zhan, Z.; Buters, J. T. M.; Fojo, T.; Poruchynsky, M. S. Paclitaxel-resistant human ovarian cancer cells have mutant beta -tubulins that exhibit impaired paclitaxel-driven polymerization. *J. Biol. Chem.* **1997,** 272, 17118-17125.
11. Kowalski, R. J.; ter Haar, E.; Longley, R. E.; Gunasekera, S. P.; Lin, C. M.; Day, B. W.; Hamel, E. Comparison of Novel Microtubule Polymerizing Agents, Discodermolide, and Epothilone A/B with Taxol. *Mol Biol. Cell* **1995,** 6, 368a.
12. Hung, D. T.; Nerenberg, J. B.; Schreiber, S. L. Synthesis of Discodermolides Useful for Investigating Microtubule Binding and Stabilization. *J. Am. Chem. Soc.* **1996,** 118, 11054-11080.
13. Williams, H. J.; Scott, A. I.; Dieden, R. A.; Swindell, C. S.; Chirlian, L. E.; Francl, M. M.; Heerding, J. M.; Krauss, N. E. NMR and Molecular Modeling Study of the Conformations of Taxol and of its Side Chain Methylester in Aqueous and Non-Aqueous Solution. *Tetrahedron* **1993,** 49, 6545-6560.

14. Williams, H. J.; Scott, A. I.; Dieden, R. A.; Swindell, C. S.; Chirlian, L. E.; Franci, M. M.; Heerding, J. M.; Krauss, N. E. NMR and Molecular Modeling Study of Active and Inactive Taxol Analogues in Aqueous and Nonaqueous Solution. *Can. J. Chem.* **1994**, 252-260.

15. Georg, G. I.; Boge, T. C.; Cheruvallath, Z. S.; Clowers, J. S.; Harriman, G. C. B.; Hepperle, M.; Park, H. The medicinal chemistry of taxol. *Taxol: Science and Applications* **1995**, 317-75.

16. Mastropaolo, D.; Camerman, A.; Luo, Y.; Brayer, G. D.; Camerman, N. Crystal and Molecular Structure of Paclitaxel. *Proc. Natl. Acad. Sci. USA* **1995,** 92, 6920-6924.

17. Ojima, I.; Chakravarty, S.; Inoue, T.; Lin, S.; He, L.; Horwitz, S. B.; Kuduk, S. D.; Danishefsky, S. J. A Common Pharmacophore for Cytotoxic Natural Products that Stabilize Microtubules. *Proc. Natl. Acad. Sci. USA* **1999,** 96, 4256-4261.

18. Gueritte-Voegelein, F.; Mangatal, L.; Guénard, D.; Potier, P.; Guilhem, J.; Cesario, M.; Pascard, C. Structure of a Synthetic Taxol Precursor: *N-tert*-Butoxycarbonyl-10-deacetyl-*N*-debenzoyltaxol. *Acta Crstallogr.* **1990,** C46, 781-784.

19. Guéritte-Voegelein, F.; Mangatal, L.; Guénard, D.; Potier, P.; Guilhem, J.; Cesario, M.; Pascard, C. Structure of a Synthetic Taxol Precursor: *N-tert*-Butoxycarbonyl-10-deacetyl-*N*-debenzoyltaxol. *Acta Crstallogr.* **1990,** C46, 781-784.

20. Vander Velde, D. G.; Georg, G. I.; Grunewald, G. L.; Gunn, C. W.; Mitscher, L. A. "Hydrophobic Collapse" of Taxol and Taxotere Solution Conformations in Mixtures of Water and Organic Solvent. *J. Am. Chem. Soc.* **1993,** 115, 11650-11651.

21. Dubois, J.; Guenard, D.; Gueritte-Voegelein, F.; Guedira, N.; Potier, P.; Gillet, B.; Beloeil, J. C. Conformation of Taxotere and analogs determined by NMR spectroscopy and molecular modeling studies. *Tetrahedron* **1993,** 49, 6533-44.

22. Cachau, R. E.; Gussio, R.; Beutler, J. A.; Chmurny, G. N.; Hilton, B. D.; Muschik, G. M.; Erickson, J. W. Solution Structures of Taxol Determined using a Novel Feedback-Scaling Procedure for NOE-restrained Molecular Dynamics. *Int. J. Supercomput. Appl.* **1994,** 8, 24-34.

23. Ojima, I.; Duclos, O.; Zucco, M.; Bissery, M.-C.; Combeau, C.; Vrignaud, P.; Riou, J. F.; Lavelle, F. Synthesis and Structure-Activity Relationships of New Antitumor Taxoids. Effects of Cyclohexyl Substitution at the C-3' and/or C-2 of Taxotère (Docetaxel). *J. Med. Chem.* **1994,** 37, 2602-2608.

24. Ojima, I.; Geney, R.; Ungureanu, I. M.; Li, D. Medicinal chemistry and chemical biology of new generation taxane antitumor agents. *IUBMB Life* **2002,** 53, 269-274.

25. Tyndall, J. D. A.; Fairlie, D. P. Macrocycles mimic the extended peptide conformation recognized by aspartic, serine, cysteine and metallo proteases. *Curr. Med. Chem.* **2001,** 8, 893-907.

26. Grubbs, R. H.; Chang, S. Recent Advances in Olefin Metathesis and Its Application in Organic Synthesis. *Tetrahedron* **1998,** 54, 4413-4450.

27.   Geng, X.; Miller, M. L.; Lin, S.; Ojima, I. Synthesis of Novel C2-C3'N-Linked Macrocyclic Taxoids by Means of Highly Regioselective Heck Macrocyclization. *Org. Lett.* **2003,** 5, 3733-3736.

28.   Querolle, O. D., J.; Thoret, S.; Dupont, C.; Gueritte, F.; Guenard,. Synthesis of novel 2-O,3'-N-linked macrocyclic taxoids with variable ring size. *Eur. J. Org. Chem.* **2003**, 542-550.

29.   Liu, C.; Schilling, J. K.; Ravindra, R.; Bane, S.; Kingston, D. G. I. Syntheses and bioactivities of macrocyclic paclitaxel bis-lactones. *Bioorg. Med. Chem. Lett.* **2004,** 12, 6147-6161.

30.   Larroque, A.-L.; Dubois, J.; Thoret, S.; Aubert, G.; Guenard, D.; Gueritte, F. Novel C2-C3' N-peptide linked macrocyclic taxoids. Part 1: Synthesis and biological activities of docetaxel analogs with a peptide side chain at C3'. *Bioorg. Med. Chem. Lett.* **2005,** 15, 4722-4726.

31.   Larroque, A.-L.; Dubois, J.; Thoret, S.; Aubert, G.; Chiaroni, A.; Gueritte, F.; Guenard, D. Novel C2-C3'N-peptide linked macrocyclic taxoids. Part 2: Synthesis and biological activities of docetaxel analogues with a peptide side chain at C2 and their macrocyclic derivatives. *Bioorg. Med.Chem.* **2007,** 15, 563-574.

32.   Ojima, I.; Lin, S.; Inoue, T.; Miller, M. L.; Borella, C. P.; Geng, X.; Walsh, J. J. Macrocycle Formation by Ring-Closing Metathesis (RCM). Application to the Syntheses of Novel Macrocyclic Taxoids. *J. Am. Chem. Soc.* **2000,** 122, 5343-5353.

33.   Ojima, I.; Geng, X.; Lin, S.; Pera, P.; Bernacki, R. J. Design, synthesis and biological activity of novel C2-C3' N-Linked macrocyclic taxoids. *Bioorg. Med. Chem. Lett.* **2002,** 12, 349-352.

34.   Metaferia, B. B.; Hoch, J.; Glass, T. E.; Bane, S. L.; Chatterjee, S. K.; Snyder, J. P.; Lakdawala, A.; Cornett, B.; Kingston, D. G. I. Synthesis and biological evaluation of novel macrocyclic paclitaxel analogues. *Org. Lett.* **2001,** 3, 2461-2464.

35.   Querolle, O. D., J.; Thoret, S.; Roussi, F.; Montiel-Smith, S.; Gueritte, F.; Guenard, D. Synthesis of Novel Macrocyclic Docetaxel Analogues. Influence of Their Macrocyclic Ring Size on Tubulin Activity. *J. Med. Chem.* **2003,** 46, 3623-3630.

36.   Querolle, O. D., J.; Thoret, S.; Roussi, F.; Gueritte, F.; Gue´nard, D. Synthesis of C2-C3'N-Linked Macrocyclic Taxoids. Novel Docetaxel Analogues with High Tubulin Activity. *J. Med. Chem.* **2004,** 47, 5937-5944.

37.   Ganesh, T.; Guza, R. C.; Bane, S.; Ravindra, R.; Shanker, N.; Lakdawala, A. S.; Snyder, J. P.; Kingston, D. G. I. The bioactive taxol conformation on b-tubulin: Experimental evidence from highly active constrained analogs. *Proc. Natl. Acad. Sci. USA* **2004,** 101, 10006-10011.

38.   Kingston, D. G. I.; Bane, S.; Snyder, J. P. The taxol pharmacophore and the T-taxol bridging principle. *Cell cycle* **2005,** 4, 279-89.

39.   Geney, R.; Chen, J.; Ojima, I. Recent advances in the new generation taxane anticancer agents. *Med. Chem.* **2005,** 1, 125-139.

40.   Ganesh, T.; Yang, C.; Norris, A.; Glass, T.; Bane, S.; Ravindra, R.; Banerjee, A.; Metaferia, B.; Thomas, S. L.; Giannakakou, P.; Alcaraz, A. A.; Lakdawala, A. S.; Snyder, J. P.; Kingston, D. G. I. Evaluation of the Tubulin-Bound Paclitaxel

Conformation: Synthesis, Biology, and SAR Studies of C-4 to C-3' Bridged Paclitaxel Analogues. *J. Med. Chem.* **2007,** 50, 713-725.

41. Ojima, I.; Park, Y. H.; Sun, C.-M.; Fenoglio, I.; Appendino, G.; Pera, P.; Bernacki, R. J. Structure-Activity Relationships of New Taxoids Derived from 14β-Hydroxy-10-deacetylbaccatin III. *J. Med. Chem.* **1994,** 37, 1408-1410.

42. Geng, X. Design, synthesis, and biological evaluations of novel taxane-based and taxane-free anticancer agents. 2002.

43. Nogales, E.; Wolf, S. G.; Downing, K. H. Structure of the αβ Tubulin Dimer by Electron Crystallography. *Nature* **1998,** 391, 199-203.

44. Lowe, J.; Li, H.; Downing, K. H.; Nogales, E. Refined structure of alpha beta-tubulin at 3.5 A resolution. *J. Mol. Bol.* **2001,** 313, 1045-1057.

45. Rao, S.; Krauss, N. E.; Heerding, J. M.; Swindell, C. S.; Ringel, I.; Orr, G. A.; Horwitz, S. B. 3'-(*p*-Azidobenzamido)taxol Photolabels the N-Terminal 31 Amino Acids of β-Tubulin. *J. Biol. Chem.* **1994,** 269, 3132-3134.

46. Rao, S.; Orr, G. A.; Chaudhary, A. G.; Kingston, D. G. I.; Horwitz, S. B. Characterization of the Taxol-Binding Site on the Microtubule: 2-(*m*-Azidobenzoyl)taxol Photolabels a Peptide (amino acids 217-231) of β-Tubulin. *J. Biol. Chem.* **1995,** 270, 20235-20238.

47. Rao, S.; He, L.; Chakravarty, S.; Ojima, I.; Orr, G. A.; Horwitz, S. B. Characterization of the Taxol Binding Site on the Microtubule. *J. Biol. Chem.* **1999,** 274, 37990-37994.

48. Snyder, J. P.; Nettles, J. H.; Cornett, B.; Downing, K. H.; Nogales, E. The binding conformation of Taxol in .beta.-tubulin: a model based on electron crystallographic density. *Proc. Natl. Acad. Sci. USA* **2001,** 98, 5312-5316.

49. Geney, R.; Simmerling, C.; Ojima, I. Computational analysis of the paclitaxel binding site in .alpha.-tubulin. *Abstracts of Papers, 222nd ACS National Meeting, Chicago, IL, United States, August 26-30, 2001* **2001**, MEDI-065.

50. Chen, S.-H.; Kadow, J. F.; Farina, V.; Fairchild, C. R.; Johnston, K. A. First Syntheses of Novel Paclitaxel (Taxol) Analogs Modified at the C-4 Position. *J. Org. Chem.* **1994,** 59, 6156-6158.

51. Holton, R. A.; Zhuming, Z.; Clarke, P. A.; Nadizadeh, H.; Procter, D. J. Selective Protection of the C(7) and C(10) Hydroxyl Groups in 10-Deacetyl Baccatin III. *Tetrahedron Lett.* **1998,** 39, 2883-2886.

52. Ojima, I.; Wang, T.; Delaloge, F. Extremely Stereoselective Alkylation of 3-Siloxy-b-lactams and Its Applications to the Asymmetric Syntheses of Novel 2-Alkylisoserines, Their Dipeptides, and Taxoids. *Tetrahedron Lett.* **1998,** 39, 3663-3666.

53. Sun, L.; Geney, R.; Geng, X.; Ojima, I. Rational design, synthesis and evaluation of conformationally restrained novel paclitaxel analogs. *Abstracts of Papers, 228th ACS National Meeting, Philadelphia, PA, United States, August 22-26, 2004* **2004**, MEDI-097.

54. Geney, R.; Sun, L.; Pera, P.; Bernacki Ralph, J.; Xia, S.; Horwitz Susan, B.; Simmerling Carlos, L.; Ojima, I. Use of the tubulin bound paclitaxel conformation for structure-based rational drug design. *Chem. Biol.* **2005,** 12, 339-48.

55. Li, Y.; Poliks, B.; Cegelski, L.; Poliks, M.; Cryczynski, A.; Piszcek, G.; Jagtap, P. G.; Studelska, D. R.; Kingston, D. G. I.; Schaefer, J.; Bane, S. Conformation of Microtubule-Bound Paclitaxel Determined by Fluorescence Spectroscopy and REDOR NMR. *Biochemistry* **2000,** 39, 281-291.

56. Chang, G.; Guida, W. C.; Still, W. C. An internal-coordinate Monte Carlo method for searching conformational space. *Journal of the American Chemical Society* **1989,** 111, 4379-86.

57. Dorman, G.; Prestwich, G. D. Benzophenone Photophores in Biochemistry. *Biochemistry* **1994,** 33, 5661-5673.

58. Paik, Y.; Yang, C.; Metaferia, B.; Tang, S.; Bane, S.; Ravindra, R.; Shanker, N.; Alcaraz, A. A.; Johnson, S. A.; Schaefer, J.; O'Connor, R. D.; Cegelski, L.; Snyder, J. P.; Kingston, D. G. I. Rotational-Echo Double-Resonance NMR Distance Measurements for the Tubulin-Bound Paclitaxel Conformation. *J. Am. Chem. Soc.* **2007,** 129, 361-370.

59. Ojima, I.; Habus, I.; Zhao, M.; Zucco, M.; Park, Y. H.; Sun, C. M.; Brigaud, T. New and Efficient Approaches to the Semisynthesis of Taxol and Its C-13 Side-Chain Analogs by Means of Beta-Lactam Synthon Method. *Tetrahedron* **1992,** 48, 6985-7012.

60. Reich, S. H.; Melnick, M.; Pino, M. J.; Fuhry, M. A. M.; Trippe, A. J.; Appelt, K.; Davies, J. F.; Wu, B. W.; Musick, L. Structure-based design and synthesis of substituted 2-butanols as nonpeptidic inhibitors of HIV protease: Secondary amide series. *J. Med. Chem.* **1996,** 39, 2781-2794.

61. Kim, B. M., Park, J.K. A Short Synthesis of a Chiral Alcohol as a New Chiral Auxiliary for Asymmetric Reactions. *Bull. Korean Chem. Soc.* **1999,** 20, 744-746.

62. Ford, J. M.; Hait, W. N. Pharmacology of drugs that alter multidrug resistance in cancer. *Pharmacological Rev.* **1990,** 42, 155-99.

63. Gottesman, M. M.; Pastan, I. Biochemistry of Multidrug Resistance Mediated by the Multidrug Transporter. *Annu. Biochem.* **1993,** 62, 385-427.

64. Kant, J.; Huang, S.; Wong, H.; Fairchild, C.; Vyas, D.; Farina, V. Studies Toward Structure-Activity Relationships of Taxol: Synthesis and Cytotoxicity of Taxol Analogues with C-2' Modified Phenylisoserine Side Chains. *Bioorg. Med. Chem. Lett.* **1993,** 3, 2471-2474.

65. Appendino, G.; Gariboldi, P.; Gabetta, B.; Pace, R.; Bombardelli, E.; Viterbo, D. 14β-Hydroxy-10-deacetylbaccatin III, a New Taxane from Himalayan Yew (*Taxus Wallichiana Zucc.*). *J. Chem. Soc., Perkins Trans 1* **1992**, 2925-2929.

66. Chang, S.; Grubbs, R. H. A Highly Efficient and Practical Synthesis of Chromene Derivatives Using Ring-Closing Olefin Metathesis. *J. Org. Chem.* **1998,** 63, 864-866.

67. Annunziata, R.; Benaglia, M.; Cinquini, M.; Cozzi, F.; Poletti, L.; Raimondi, L.; Perboni, A. A novel approach to the synthesis of precursors of tricyclic b-lactam antibiotics. *Eur. J. Org. Chem.* **1999**, 3067-3072.

68. Shanks, D.; Amorati, R.; Fumo Maria, G.; Pedulli Gian, F.; Valgimigli, L.; Engman, L. Synthesis and antioxidant profile of all-rac-alpha-selenotocopherol. *J. Org. Chem.* **2006,** 71, 1033-8.

69. Semmelhack, M. F.; Zask, A. Synthesis of racemic frenolicin via organochromium and organopalladium intermediates. *J. Am. Chem. Soc.* **1983,** 105, 2034-43.

70. Vichai, V.; Kirtikara, K. Sulforhodamine B colorimetric assay for cytotoxicity screening. *Nature Protocols* **2006,** 1, 1112-1116.

71. Boger, D. L.; Kim, S. H.; Mori, Y.; Weng, J. H.; Rogel, O.; Castle, S. L.; McAtee, J. J. First and second generation total synthesis of the teicoplanin aglycon. *J. Am. Chem. Soc.* **2001,** 123, 1862-71.

72. Brieva, R.; Crich, J. Z.; Sih, C. J. Chemoenzymic synthesis of the C-13 side chain of taxol: optically active 3-hydroxy-4-phenyl b-lactam derivatives. *J. Org. Chem.* **1993,** 58, 1068-75.

73. Gueritte-Voegelein, F.; Senilh, V.; David, B.; Guénard, D.; Potier, P. Chemical Studies of 10-deacetyl Baccatin III. Hemisynthesis of Taxol Derivatives. *Tetrahedron* **1986,** 42, 4451-4460.

74. Denis, J.-N.; Greene, A. E.; Guénard, D.; Guéritte-Voegelein, F.; Mangatal, L.; Potier, P. A. Highly Efficient, Practical Approach to Natural Taxol. *J. Am. Chem. Soc.* **1988,** 110, 5917-5919.

75. Skehan, P.; Storeng, R.; Scudiero, D.; Monks, A.; McMahon, J.; Vistica, D.; Warren, J. T.; Bokesch, H.; Kenney, S.; Boyd, M. R. New colorimetric cytotoxicity assay for anticancer-drug screening. *J. Natl. Cancer Inst.* **1990,** 82, 1107-12.

76. Motulsky, H. J.; Ransnas, L. A. Fitting curves to data using nonlinear regression: a practical and nonmathematical review. *Faseb J* **1987,** 1, 365-74.

77. Weisenberg, R. C. Microtubule formation in vitro in solutions containing low calcium concentrations. *Science* **1972,** 177, 1104-5.

78. Shelanski, M. L.; Gaskin, F.; Cantor, C. R. Microtubule assembly in the absence of added nucleotides. *Proc. Natl. Acad. Sci. USA* **1973,** 70, 765-8.

Chapter IV

Computational Study of the Binding Conformation of Paclitaxel in Tubulin

§ 4.1 Introduction

The investigation of possible bioactive conformations of paclitaxel in microtubules could lead to the development of novel microtubule-stabilizing drugs with much simpler structures than paclitaxel. However, the polar conformation and the nonpolar conformation (**Figure 4-1**) of paclitaxel found in solution and in solid state (by NMR and X-ray crystallography) are not the binding conformation in tubulin/microtubule.[1-5]
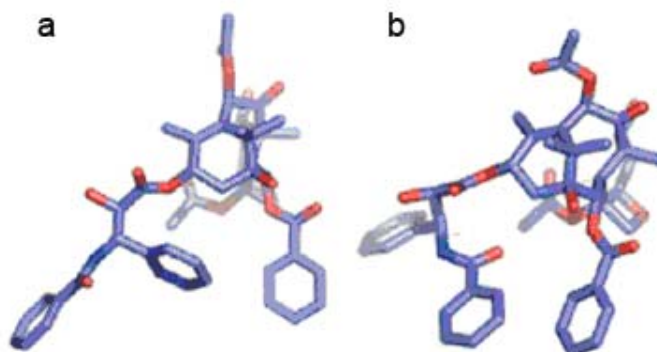
Figure 4-1. Polar conformation (a) and nonpolar conformation (b)

The structural biology study of paclitaxel did not start until the first cryo-electron microscopy (cryo-EM) (or "electron crystallograpy") structure of a microtubule model, i.e., Zn^{2+}-stablized α,β-tubulin dimer, with a paclitaxel molecule was reported in 1998 with 3.7 Å resolution (1TUB structure, **Figure 4-2**).[6] In the 1TUB structure, the binding site of the drug was identified, which was consistent with the photolabeling studies,[7-9] but due to the very low resolution, a docetaxel molecule taking nonpolar conformation[1], instead of a paclitaxel molecule, was placed to show the binding site.
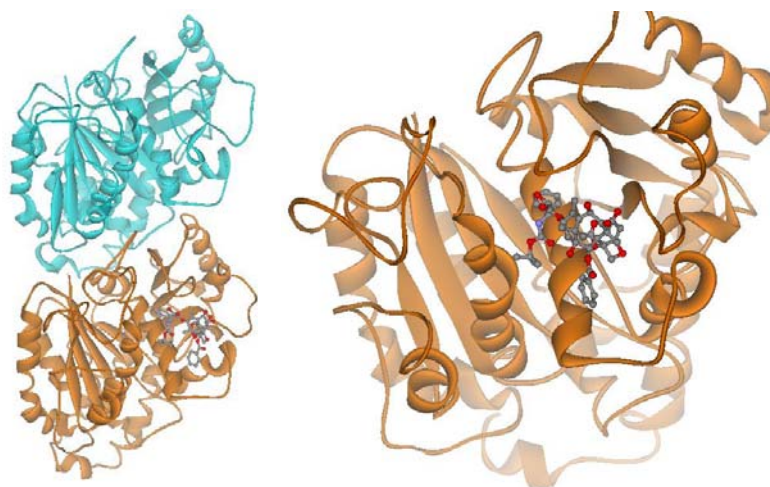
Figure 4-2. Structure of 1TUB with a docetaxel molecule[6]

This rather fuzzy crystal structure was refined to 3.5 Å resolution (1JFF structure, **Figure 4-3**) in 2001.[10] In the 1JFF structure, a paclitaxel molecule was actually placed in the binding site. However, the structure of the crucial *N*-benzoylphenylisoserine moiety

at C13, especially the C2-phenyl and C3'*N*-phenyl groups, was still difficult to determine with confidence due to the low diffraction level in the electron density map for this moiety.[10]
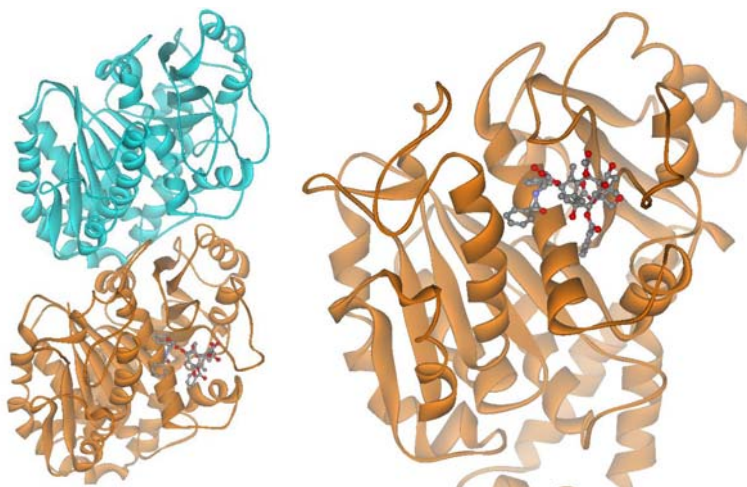
Figure 4-3. Structure of 1JFF with a paclitaxel molecule[10]

Based on further computational analysis of the solution structures of paclitaxel, and docking study on the 1TUB structure, the "T-Taxol" structure was proposed in 2001.[11] Unlike the polar and nonpolar conformations of the drug, which experience intramolecular hydrophobic collapse, T-Taxol opens up to permit intermolecular hydrophobic association as seen for the irregularly stacked C-3' benzamido, His229, and C-2 benzoyl moieties. The new model is in complete harmony with three photoaffinity-labeling studies focused on β-tubulin.[7-9] Using the same density map, the T-Taxol structure is very similar to the 1JFF structure, except for torsional rotations of the side-chain phenyl rings.[10]
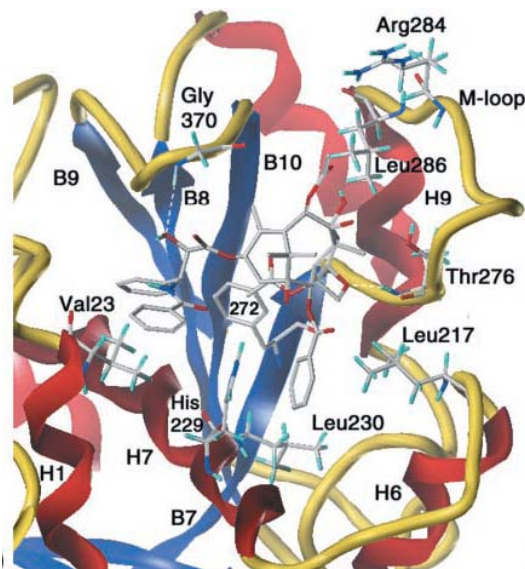
Figure 4-4. The T-Taxol structure (*PNAS*, 2001)
[Adapted from ref. 11]

The critical C2'-OH,[12, 13] which forms an intramolecular H-bond with C1'-O in the polar or nonpolar structure, was claimed to form a H-bond with the backbone carbonyl of Arg369. However, in the figure of the T-Taxol article (**Figure 4-4**),[11] the H-bond was seen between the H-N of Gly-370 and C2'-O, which was confirmed in the later papers.[14, 15] The change in the H-bond was probably caused by the change in the protein backbone from 1TUB to 1JFF. The new H-bond is not only weaker than the first one, but is not consistent with the well-known SAR that the C2'-OH acts as a H-bond donor,[16] instead of an accepter.

To prove the validity of the T-Taxol structure, rigidified paclitaxel congeners were designed, synthesized and assayed for their tubulin polymerization ability and cytotoxicity.[17-22] The first rigidified taxoid appeared in 2004 with higher activity than paclitaxel.[20]

In the mean time, another breakthrough in the investigation on the structure of the tubulin-bound paclitaxel was achieved by the application of the REDOR (rotational-echo double-resonance) NMR spectroscopy to the $^{19}F/^{13}C/^{15}N$-labeled paclitaxel-microtubule complex in the solid state in 2000.[23] The REDOR NMR data provided two ^{13}C-^{19}F intramolecular distances in the microtubule-bound 2-(4-fluorobenzoyl)paclitaxel (**2-FB-PT**) (**Figure 4-5**). Since real microtubules, not the Zn^{2+}-stabilized tubulin dimer model, were used in this experiment, the results were critically important to probe the relevance of the cryo-EM structure (1TUB, 1JFF).
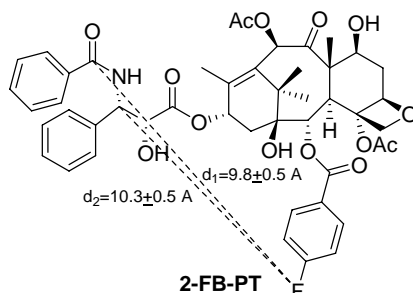
Figure 4-5. Intramoleculer distances

On the basis of the REDOR distances[23], MD analysis of paclitaxel conformers, the photoaffinity labeling[9] and molecular modeling using the 1TUB coordinate,[6] we proposed the "REDOR-Taxol" structure as the most plausible microtubule-bound paclitaxel structure in 2005.[24] The REDOR-Taxol structure was also successfully used for the design of a highly active rigidified macrocyclic taxoids, **SB-T-2053**.[24]

The locations of the C3' phenyl rings in the REDOR-Taxol and T-Taxol structures are close to each other. Essentially all SAR, photoaffinity labeling and REDOR-NMR results support both structures. The critical difference between these two structures is the orientation of the C2'-OH group. In the REDOR-Taxol structure, the C2'-OH group interacts with His227 as the hydrogen-donor (**Figure 4-6**),[24] while the original H-bonding is between the C2'-OH and the backbone carbonyl oxygen of Arg369 in the T-Taxol structure.[11] (The revised H-bonding in the T-Taxol structure is between the H-N of Gly-370 and C2'-O.[14, 15])
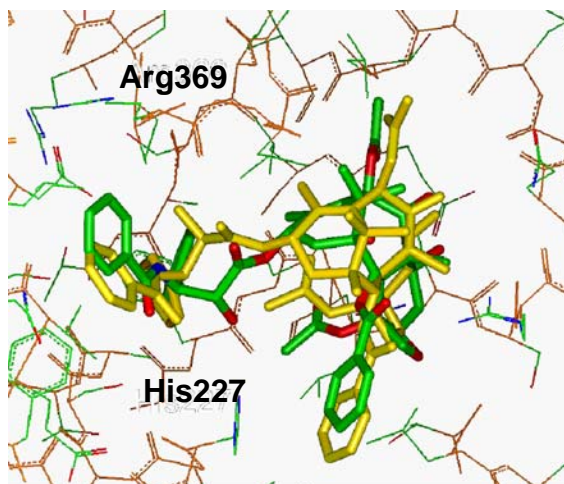
Figure 4-6. Overlay of REDOR-Taxol and T-Taxol in 1TUB

To compare the REDOR-Taxol structure with the "real" T-Taxol structure, we obtained the T-taxol structure with 1JFF protein from the Emory University group.[15] Because the 1JFF structure has higher resolution than 1TUB, we decided to prepare the REDOR-Taxol-1JFF complex to check reliability of the conformation, and to compare with the T-Taxol structure farely.

§ 4.2 The REDOR-Taxol-1JFF and T-Taxol-1JFF Complexes

The REDOR-Taxol structure in the 1TUB protein was manually docked into the β-tubulin of the 1JFF protein, wherein the "1JFF-Taxol" molecule had been removed from the protein prior to the docking. The resulting drug-protein complex structure (REDOR-Taxol-1JFF) was minimized by using the Insight II 2000 (CVFF force field) program. The H-bond between the C2'-OH and His227 was very stable during the process, converged to the H--N distance of 2.2 Å. (**Figure 4-7**).
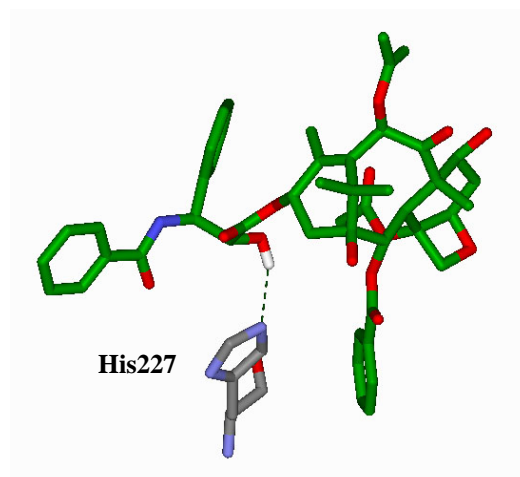
Figure 4-7. The REDOR-Taxol-1JFF complex

The coordinates of the T-Taxol-1JFF complex structure was obtained directly from the Emory University group for fair comparison purpose.[14, 15] There was no H-bond between the C2'-O-H and the O=C of Arg369 in the given coordinates although this particular H-bond had been reported to be crucial for bioactivity in the original T-Taxol paper.[11] Unexpectedly, we found that there was no H-bond between the C2'-OH and Gly370 either, because the C2'-OH was pointed to the H-N of Gly370 in the given coordinates (**Figure 4-8a**). After energy-minimization (InsightII 2000, CVFF), a H-bond (3.4 Å) was formed between the C2'-O and H-N of Gly370.[15] The energy-minimization caused a slight change in the T-Taxol structure in the 1JFF protein.
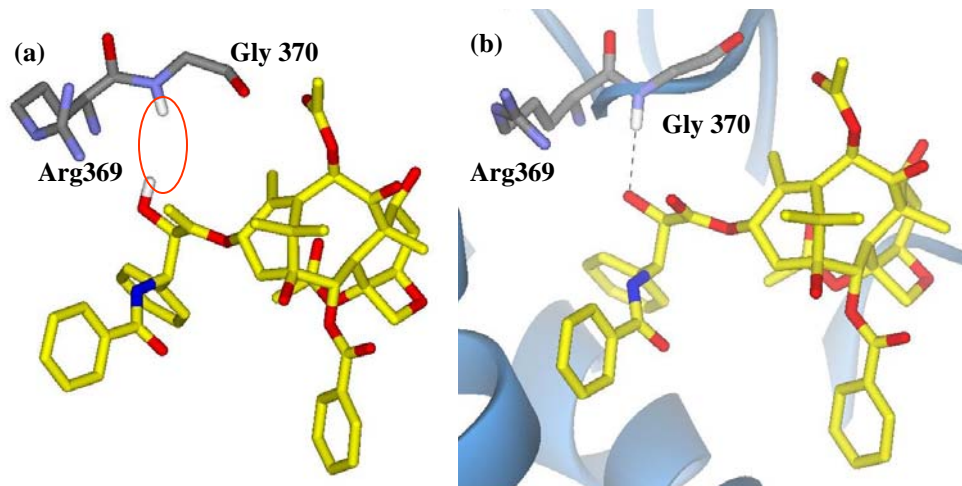
Figure 4-8. The T-Taxol-1JFF complex: (a) before minimization and (b) after minimization.

Very recently, three additional intramolecular distances of the key atoms in the microtubule-bound $^{19}F/^2H$-labeled paclitaxel were determined by means of the solid state REDOR NMR spectroscopy.[25] Accordingly, we measured the total 5 distances in the energy-minimized REDOR-Taxol-1JFF structure and compared with the experimental REDOR distances. As **Table 4-1** shows, the distances obtained from the REDOR-Taxol-1JFF are in very good agreement with the experimental data. Also, the values from the original REDOR-Taxol-1TUB are very close to those from the REDOR-Taxol-1JFF.

Table 4-1. Intramolecular atom distances of paclitaxel using $^{19}F/^{13}C/^{15}N/^{2}H$-labeled paclitaxels[25]
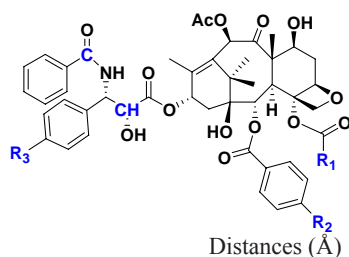
		Distances (Å)	
Separations	REDOR-NMR distances	REDOR-Taxol (2005/ Minimized in 1JFF)	T-Taxol (2001/ Minimized in 1JFF)
R_1-R_2	7.8	7.3/7.6	7.9/8.2
R_1-R_3	6.3	6.4/6.1	6.6/5.9
R_2-R_3	> 8	13.1/13.1	12.2/11.5
R_2-CH	10.3	9.4/9.5	9.9/9.9
R_2-C	9.8	10.0/9.9	9.1/8.9

The 5 key intramolecular atom-atom distances in the energy-minimized T-Taxol were also measured. The corresponding distances reported for the original T-Taxol structure are shown for comparison. On the basis of the comparison of the 5 key atom-atom distances in the REDOR-Taxol, T-Taxol and the experimental data, it can be safely concluded that both REDOR-Taxol and T-Taxol structures are consistent with the REDOR-NMR data.[25]

The overlay of the energy-minimized T-Taxol-1JFF and the REDOR-Taxol-1JFF is shown in **Figure 4-9**, wherein the critical H-bonds that distinguish these two structures are highlighted.
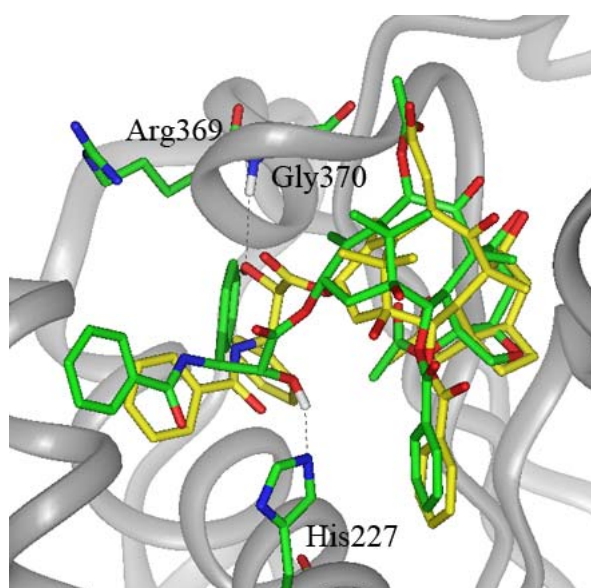
Figure 4-9. Overlay of the minimized REDOR-Taxol-1JFF (green, H-bond with His227) and T-Taxol-1JFF (yellow, H-bond with Gly370) structures

To further examine the validity of the minimized REDOR-Taxol-1JFF structure, a 50-ps MD simulation was performed to the complex in the 10 Å diameter sphere around the

binding site using the Macromodel program (MMFF94 force field[26]). The stability of the C2'-OH--N(His227) H-bond was monitored during the whole simulation. The overlay of 100 snapshots (sampled every 0.5 ps) of the Taxol conformations is shown in **Figure 4-10**. As the overlay clearly shows, the MD simulation of the REDOR-Taxol structure is very stable and does not cause any substantial structural change. The C2'-OH--N(His227) H-bond is also very stable throughout the MD simulation process, maintaining an average distance of 2.0 ± 0.2 Å. The simulation confirms that the REDOR-Taxol conformation is a stable local minimum in the tubulin binding site.
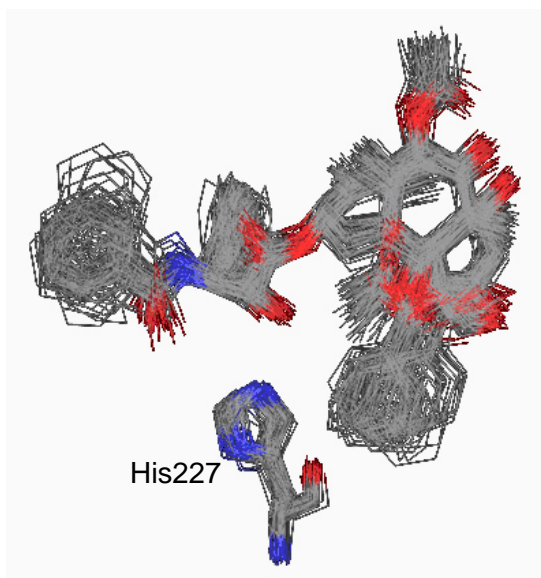
Figure 4-10. MD simulation of REDOR-Taxol in 1JFF
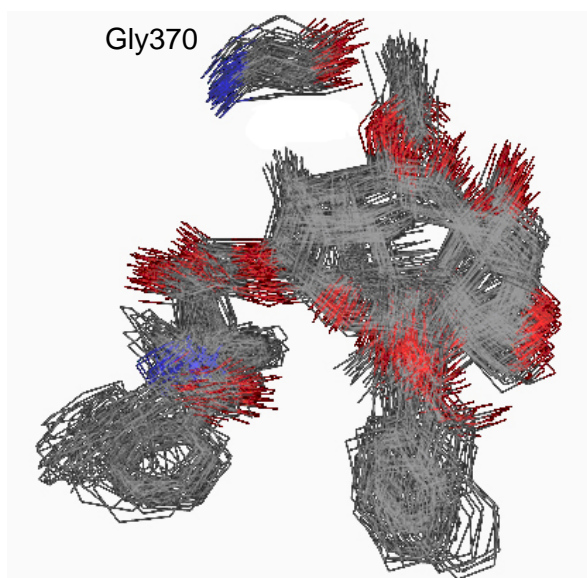
Figure 4-11. MD simulation of T-Taxol in 1JFF

The same MD-simulation was performed to the T-Taxol-1JFF complex in the 10 Å diameter sphere around the binding site using the Macromodel program (MMFF94 force

field). The stability of the C2'-O--HN(Gly370) H-bond was monitored during the whole simulation. The C2'-O--HN(Gly370) H-bond was not recognized by the MMFF94 force field. Nevertheless, the structure was stable throughout the simulation, maintaining the C2'-O--HN(Gly370) distance of 5.0 ± 0.8 Å in average.

§4.3 The Macrocyclic Taxoids and the Binding Conformations

§ 4.3.1 Kingston's C4-C3'-Linked Macrocyclic Taxoids

Kingston and his coworkers reported a series of macrocyclic paclitaxel analogs designed based on the T-Taxol structure and some of these analogs exhibited higher cytotoxicity than paclitaxel.[20, 21] Some energy-minimization and short MD simulations of the "created REDOR-Taxol" * claimed that "REDOR-Taxol" could not predict the highly active taxoids.[14, 15] In order for us to claim that the REDOR-Taxol structure is a valid model for bioactive paclitaxel conformation, it is necessary to examine whether those analogs can be predicted by the REDOR-Taxol structure in the 1JFF protein. Thus, we selected two of those highly active macrocyclic analogs, **K1** and **K2** (**Figure 4-12**), by directly introducing the linkers to the paclitaxel molecule in the REDOR-Taxol-1JFF complex and these structures were energy-minimized (InsightII 2000, CVFF).
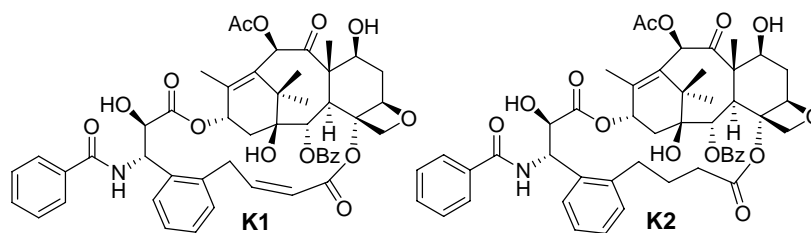
Figure 4-12. Structure of K1 and K2

As **Figure 4-13** shows, **K1** and **K2** can readily take the REDOR-Taxol structure, keeping the critical H-bond between the C2'-OH and His227. Next, a 20-ps MD simulation of the "REDOR-**K2**-1JFF" structure was performed to examine the stability of this complex (Macromodel, MMFF94). As Figure **4-14** shows, the "REDOR-**K2**" structure was very stable and the C2'-O-H--N(His227) H-bond distance was kept at 2.0 ± 0.3 Å during the whole MD simulation.[27]

---

* Johnson, Alcaraz, and Snyder (Emory University) unfairly and erroneously criticized the validity of the REDOR-Taxol structure in their paper in 2005 (Ref. 14) without asking us to provide them with the coordinates. They inappropriatetly "reconstructed" the REDOR-Taxol structure by themselves and misled the conclusion. Therefore, we made sure to do fair comparison by obtaining the T-Taxol in 1JFF cooordinates directly from them.
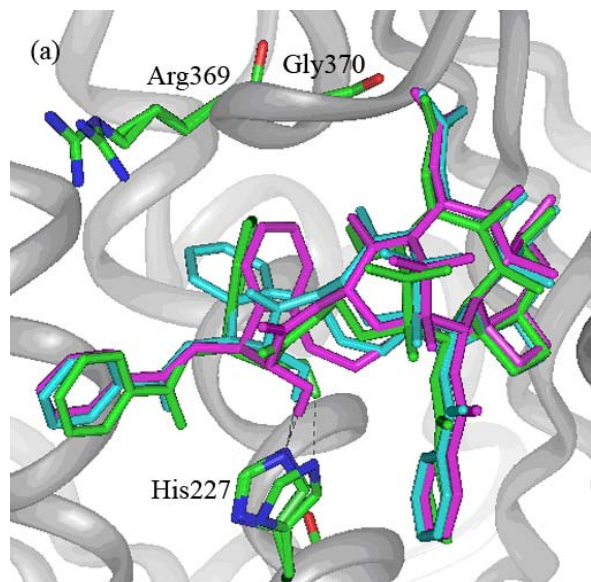
Figure 4-13. Overlay of the REDOR-Taxol (green) with "REDOR-K1" (cyan) and "REDOR-K2" (magenta) structures
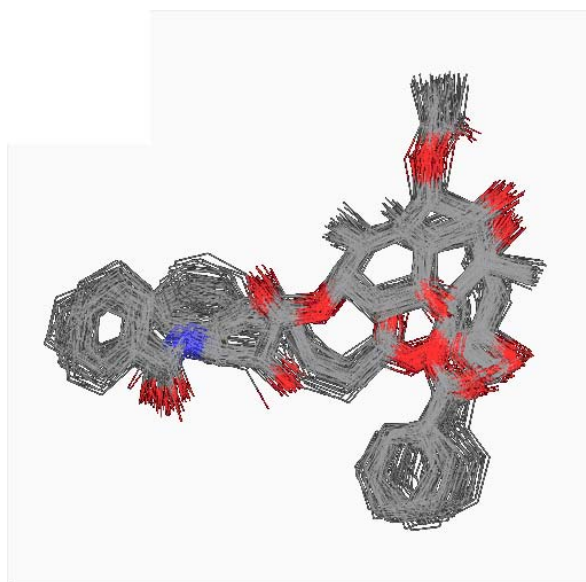
Figure 4-14. MD simulation (MMFF94) of the "REDOR-K2" in 1JFF

In the same manner, the "T-**K2**" structure was created by directly introducing the linker to the paclitaxel molecule in the T-Taxol-1JFF structure, followed by energy-minimization (InsightII 2000, CVFF) (**Figure 4-15**). The MD simulation of the "T-**K2**-1JFF" was also performed in the same manner as that for the "REDOR-**K2**-1JFF". The simulation showed a stable structure, but the C2'-O--HN(Gly370) H-bonding was not recognized by the MMFF94 force field. The distance between the C2'-O and N(Gly370) was 5.1 ± 0.5 Å (**Figure 4-16**).
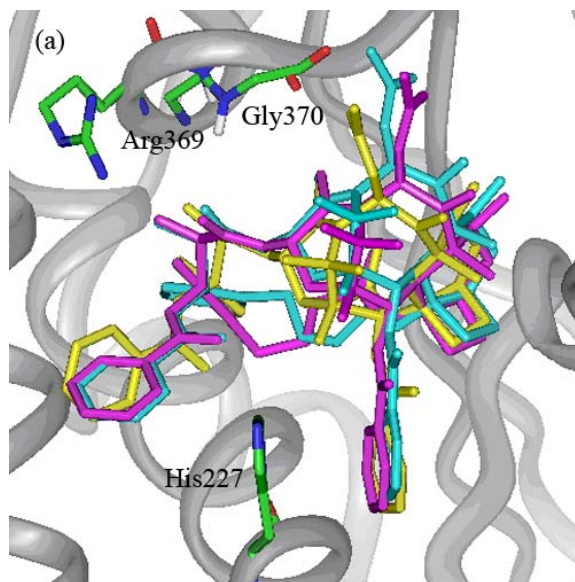
Figure 4-15. Overlay of the T-Taxol structure (yellow) with "T-K1" (cyan) and "T-K2" (magenta) structures
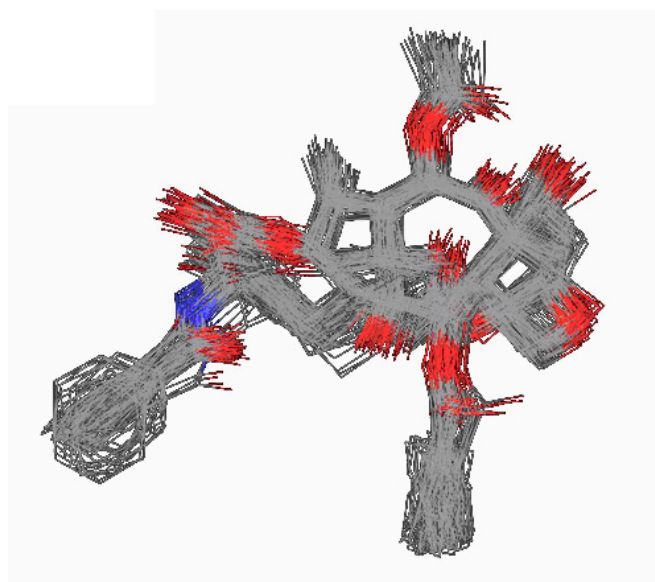
Figure 4-16. MD simulation (MMFF94) of the "T-K2" in 1JFF

Although, the "T-**K2**" is 10.3 kcal/mol more stable than the "REDOR-**K2**" in vacuum (InsightII, CVFF), the "REDOR-**K2**" is more favorable than the "T-**K2**" in the binding pocket, because of the strong and stable C2'-OH--N(His227) H-bonding that is critical for paclitaxel's binding to microtubule, especially based on the fact that the C2'-OH is a H-bond donor from SAR studies.[28]

In order to measure the level of conformational restriction imposed, we conducted a Monte Carlo conformational search on **K1** and **K2** in a simulated aqueous environment. Our attention was focused on the C13 side-chain dihedral angles since they should be the ones most affected by the introduction of the constraint. **Figure 4-17** shows that the

dihedral angle distributions for the three macrocyclic taxoids and compares those to the reference values of REDOR-Taxol and T-Taxol.
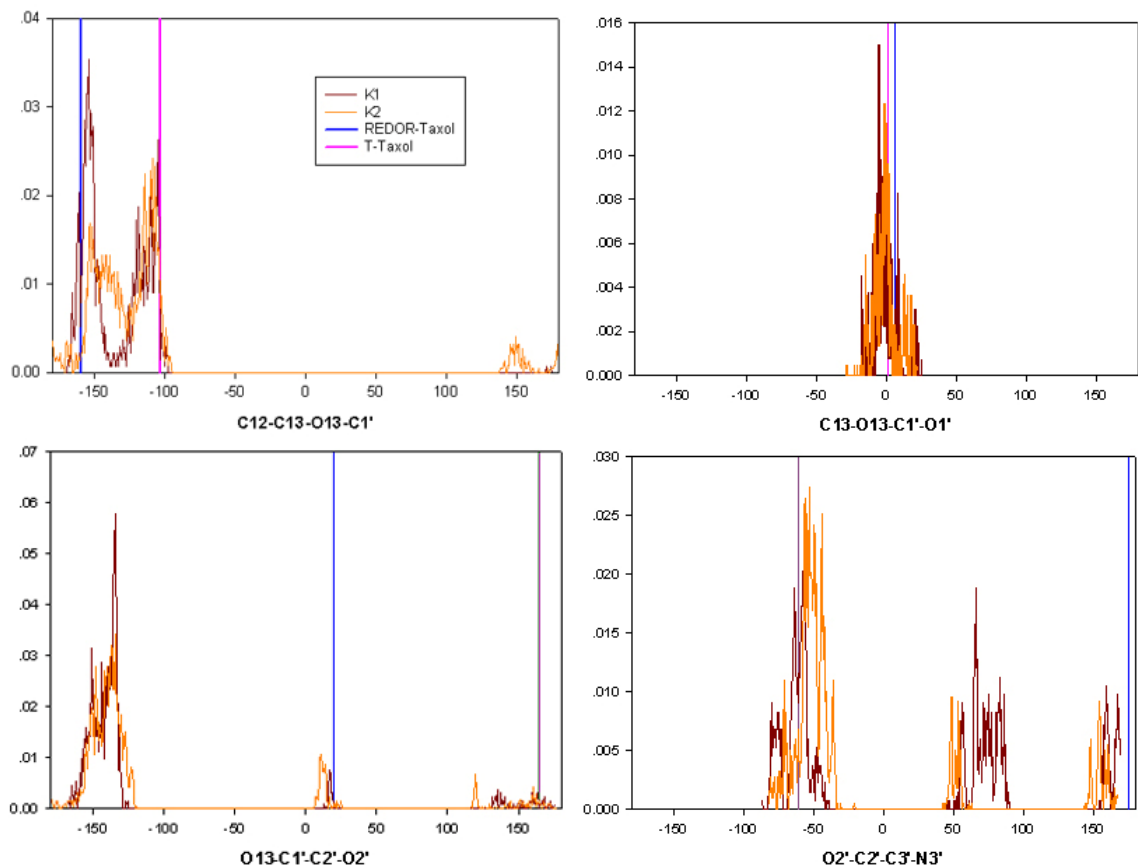
Figure 4-17. Conformational diversity in macrocyclic taxoids (K1, brown; K2, orange) (The reference value for REDOR-Taxol (blue) and T-Taxol (magenta) are indicated by vertical lines.)

K2 has very similar dihedral angle distributions to **K1**. Both taxoids shared the same range between -100° and -150° for the C13-O13 torsion angle. For the C13-C1'-C2'-C2' dihedral angle, however, neither REDOR-Taxol nor T-Taxol is in the major dihedral angle distributions, while the two structures are consistent with the distributions of the last torsion angle (O2'-C2'-C3'-N3'). The results indicate that both the REDOR-Taxol structure and T-Taxol structure could equally predict the tubulin-binding structure of the macrocyclic taxoids.

§ 4.3.2 Ojima's C14-C3'*N*-Linked Macrocyclic Taxoids

SB-T-2053 was designed based on the REDOR-Taxol structure.[24] Its analogues, **SB-T-2054**, **SB-T-2055*E*** and **SB-T-2055*Z*** were synthesized and their biological activities tested. **SB-T-2054** and **SB-T-2053** showed at least the same activity in the tubulin polymerization assay, and **SB-T-2054** showed similar or slightly higher potency in the *in vitro* cytotoxicity assay, while **SB-T-2055*E*** and **SB-T-2055*Z*** showed much lower activities. The relative activities could be explained by the flexibility of the C13 side-

chains: **SB-T-2054** has the most rigid structure and **SB-T-2055***E* has the most flexible structure. The overlay of the macrocyclic taxoids with REDOR-Taxol structure in the 1JFF tubulin is shown in **Figure 4-19**.

SB-T-2053: linker = -CH$_2$CH=CH-
SB-T-2054: linker = -CH=CHCH$_2$-
SB-T-2055: linker = -OCH$_2$CH=CH-
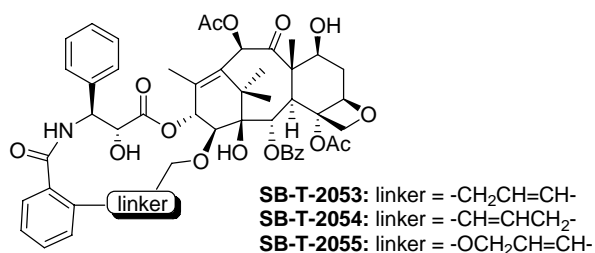
Figure 4-18. Structure of C14-C3'*N*-linked macrocyclic taxoids
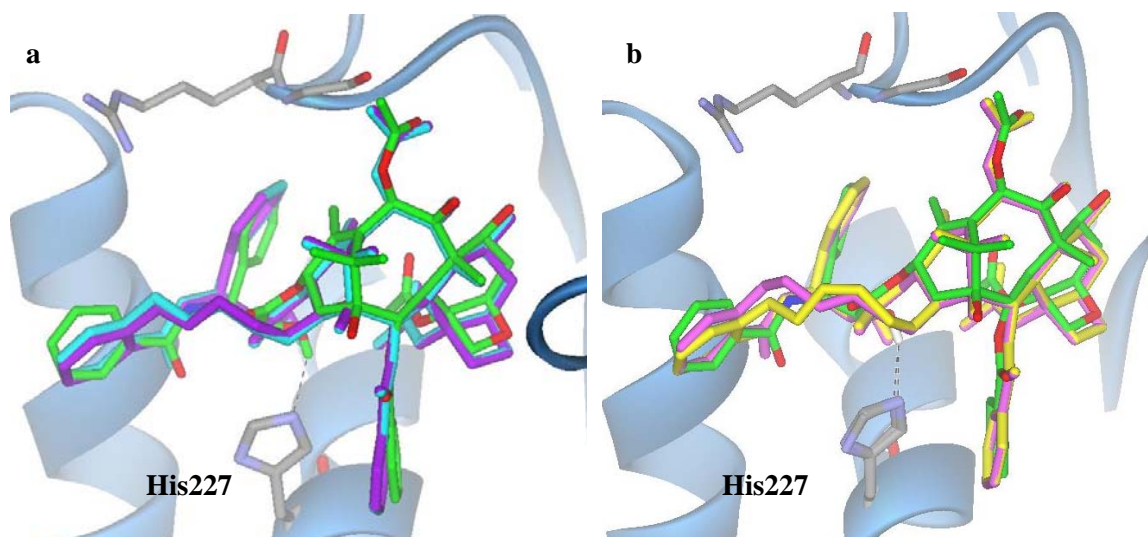
Figure 4-19. Overlay of REDOR-Taxol (green), SB-T-2053 (cyan), SB-T-2054 (purple), SB-T-2055E (magenta) and SB-T-2055Z (yellow)

The MD simulation of the "REDOR-**SB-T-2054**-1JFF" was performed in the same manner as that for the Kingston's compounds. The simulation showed a stable structure, and the average distance of the C2'-OH--N(His227) H-bonding was 2.6 ± 0.5 Å (**Figure 4-20**).
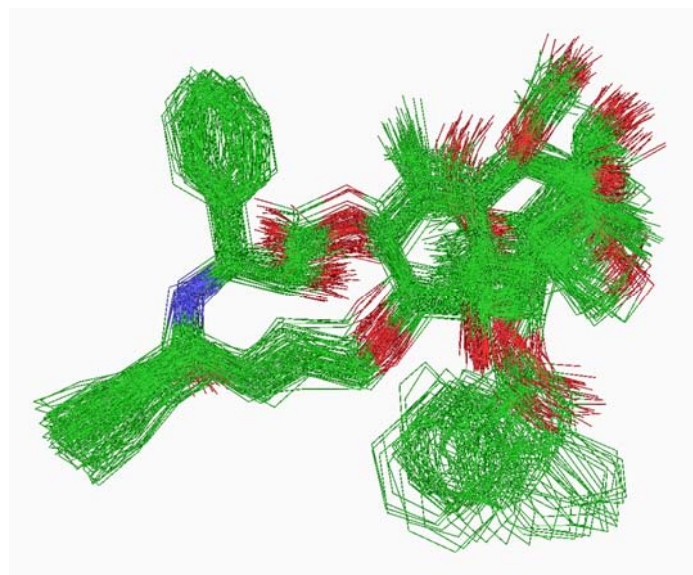
Figure 4-20. MD simulation (MMFF94) of the SB-T-2054 in 1JFF

The results of the Monte Carlo conformational search for the C14-C3'*N*-linked macrocyclic taxoids in a simulated aqueous environment are shown in **Figure 4-21**.
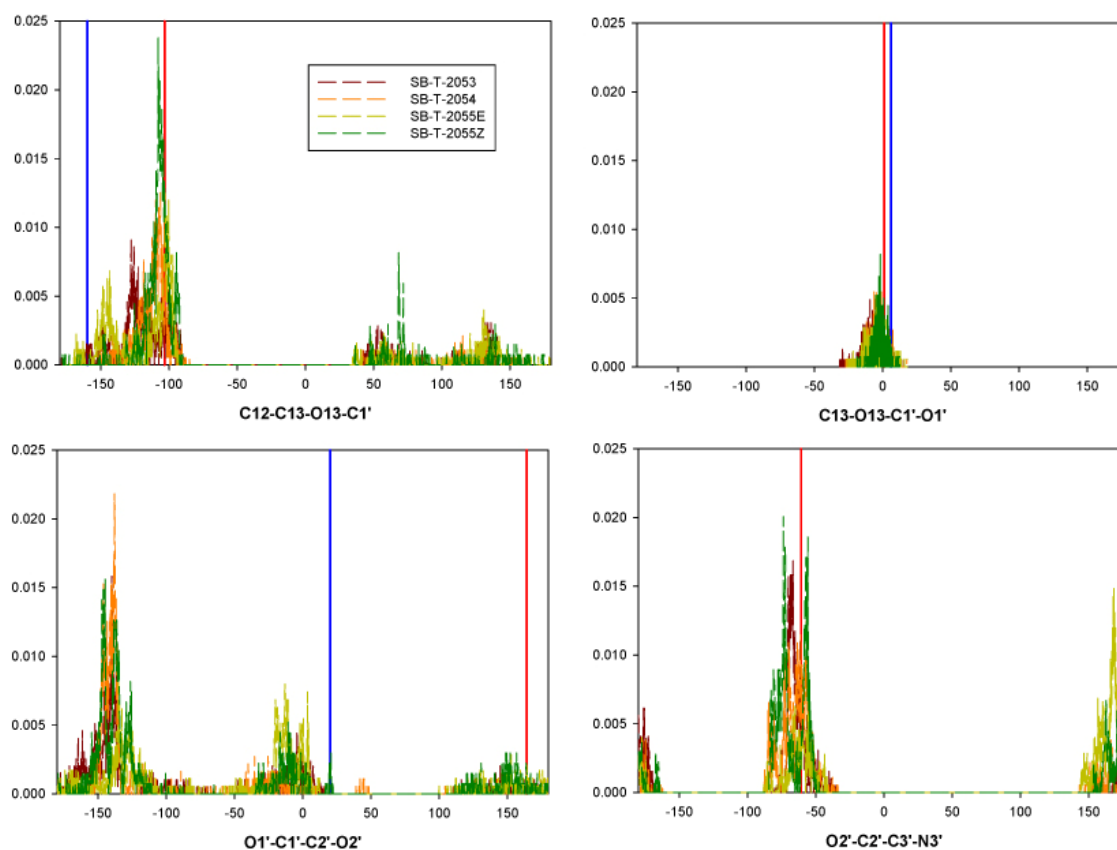
Figure 4-21. Conformational diversity in macrocyclic taxoids (SB-T-2053, brown; SB-T-2054, orange; SB-T-2055*E*, yellow and SB-T-2055*Z*, green) (The reference value for REDOR-Taxol (blue) and T-Taxol (red) are indicated by vertical lines.)

All macrocyclic taxoids show similar dihedral angle distributions and the flexibility of the C13 side-chain increases in the following order: **SB-T-2054** < **SB-T-2053** < **SB-T-2055Z** < **SB-T-2055E**, which is parallel to the order of cytotoxicities. The dihedral angle distributions were also compared to the reference values of the REDOR-Taxol structure and the T-Taxol structure. Except for the O13-C1'-C2'-O2' value, the dihedral angle distributions are consistent with both T-Taxol and REDOR-Taxol structures, indicating that both structures could equally predict the tubulin-bound structures of the macrocyclic taxoids.

§ **4.3.3 Dubois's C2-C3'*N*-Linked Macrocyclic Taxoids**

A series of C2-C3'*N*-linked macrocyclic taxoids were reported to mimic the T-Taxol structure, one of which (**QT, Figure 4-20**) showed the same activity as paclitaxel in the microtubule depolymerization inhibitory experiment, while it was ~10 times less active in the *in vitro* cytotoxicity assay.[19] To investigate the tubulin-bound structure of **QT**, the eight-atom linker was introduced between the C3'*N* and C2 *meta*-position to the paclitaxel molecule in the REDOR-Taxol-1JFF and T-Taxol-1JFF complexes and these structures energy-minimized. There are two possibilities for the orientation of the linker in **QT**,[19] i.e., in front of the taxoid or behind the taxoid. Since we hope to keep the C3'-phenyl group in a similar place to that in the paclitaxel molecule, the linker was placed in front of the taxoid. The overlay of "REDOR-**QT**" with the REDOR-Taxol and that of "T-**QT**" with the T-Taxol after minimization are shown in **Figure 4-23** and **Figure 4-24**, respectively.
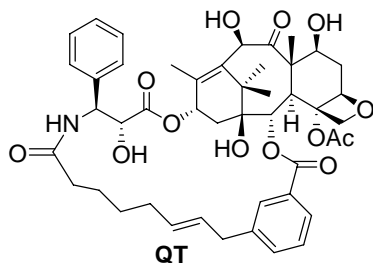
Figure 4-22. Structure of QT
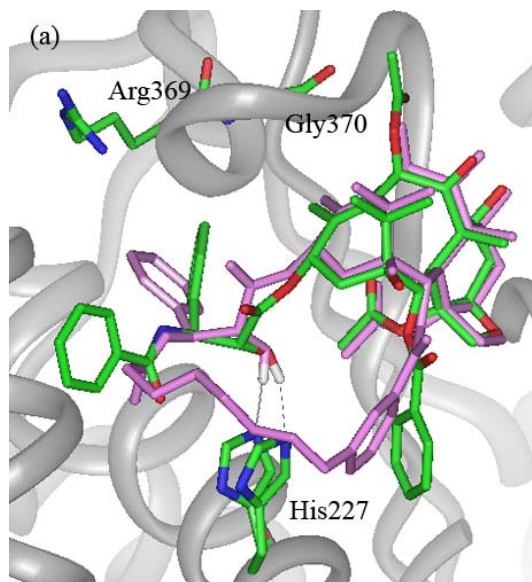
Figure 4-23. Overlay of the REDOR-Taxol structure (green) with "REDOR-QT" (magenta)
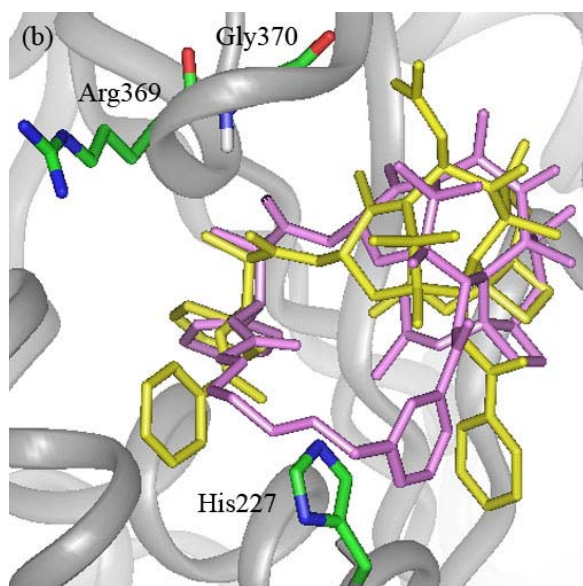
Figure 4-24. Overlay of the T-Taxol structure (yellow) with "T-QT" (magenta)

After energy-minimization (InsightII 2000, CVFF), the distance between C2'-OH and N(His227) was 1.8 Å in "REDOR-**QT-**1JFF" (**Figure 4-23**), while the distance between C2'-O and HN(Gly370) was 3.7 Å in "T-**QT-**1JFF", (**Figure 4-24**). In both overlays, the C2-benzoyl group moves substantially due to the linker, but the linker is long and flexible enough to avoid the collision with His227, which has been recognized in some inactive C2-C3'-linked taxoids with short linkers.[11]

Since the macrocyclic taxoid shows some bent bonds caused by the short linker, we hope to check the level of conformational restriction imposed, by conducting a Monte Carlo conformational search in a simulated aqueous environment. The results are shown in **Figure 4-25**.

182
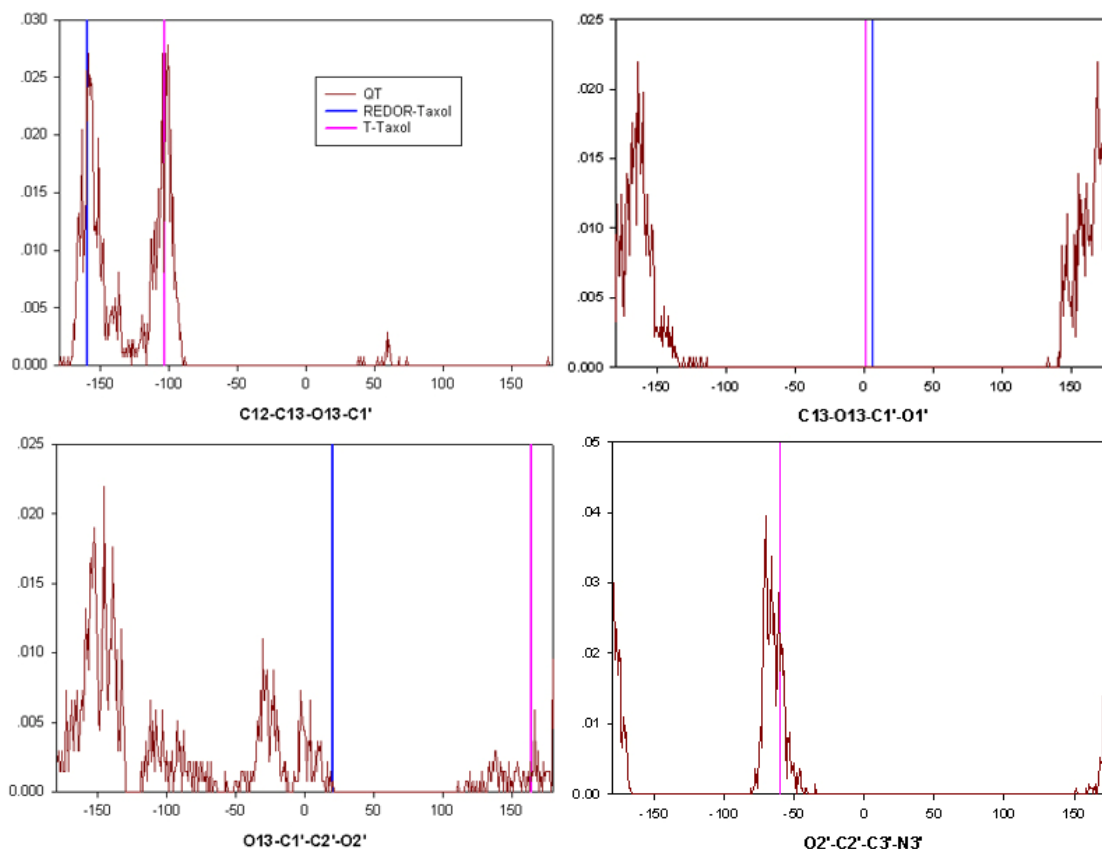
Figure 4-25. Conformational diversity in macrocyclic taxoid QT (The reference value for REDOR-Taxol (blue) and T-Taxol (magenta) are indicated by vertical lines.)

The C12-C13-O13C1' and the O2'-C2'-C3'-N3' dihedral angles have similar distribution to the one of the REDOR-Taxol or the T-Taxol structure, while the C13-O13-C1'-O1' and the O13-C1'-C2'-O2' dihedral angle distributions are very different from the ones in the REDOR-Taxol and the T-taxol structures, as well as other macrocyclic taxoids (**Figure 4-17** and **Figure 4-21**). The abnormal dihedral angle distributions, which may be caused by the linker, could account for the bad overlay with the two structures and poor activity in *in vitro* cytotoxicity assay.

§ 4.3.4 Ojima's C4-C2'-Linked Macrocyclic Taxoids

After checking the REDOR-Taxol, we found that the C4 acetyl was close to C2'O, instead of C2'H. In **SB-TCR-102**, the C13 side-chain was forced to point to the other direction by the linker, which made it similar to the T-Taxol conformation. The low activity was claimed by the Emory University group to be ascribed to the interaction between the linker and Phe270,[15] but in our minimized structure, it had a very good overlay with the T-Taxol structure (**Figure 4-27**).
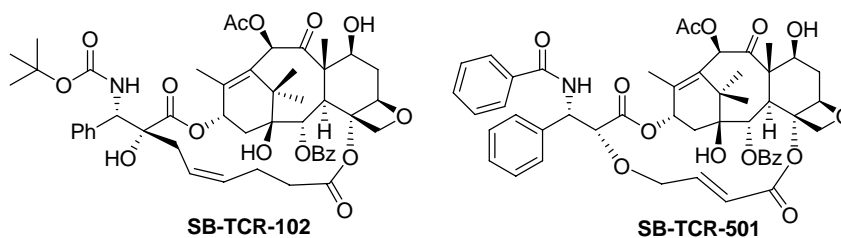
Figure 4-26. Structure of C4-C2' linked macrocyclic taxoids
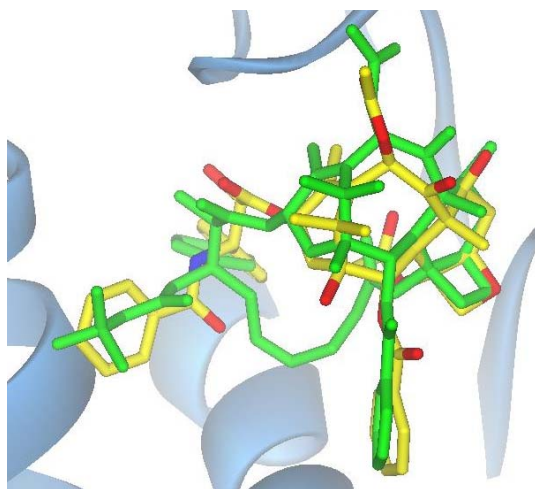
Figure 4-27. Overlay of T-Taxol (yellow) and SB-TCR-102 (green) in tubulin

The distance between C4 acetyl and C2'O was measured in the REDOR-Taxol structure as well as the T-Taxol structure. As shown in **Figure 4-28**, the distance is 3.1 Å in the REDOR-Taxol structure and 5.5 Å in the T-Taxol structure with C2'O pointed to the opposite direction. Therefore, **SB-TCR-501** is designed by linking C4 acetyl and C2'O with a two-atom bridge. Although the critical H-bond is sacrificed, the macrocyclic taxoid has a very good overlay with the REDOR-Taxol structure in the binding site (**Figure 4-29**). Moreover, if the compound has some activity, we could conclude that the REDOR-Taxol structure, instead of the T-Taxol structure, is the real binding conformation in tubulin/microtbule. Unfortunately, since the C2'-OH is extremely important, **SB-TCR-501** was found to possess very low activity in the cytotoxicity assay.
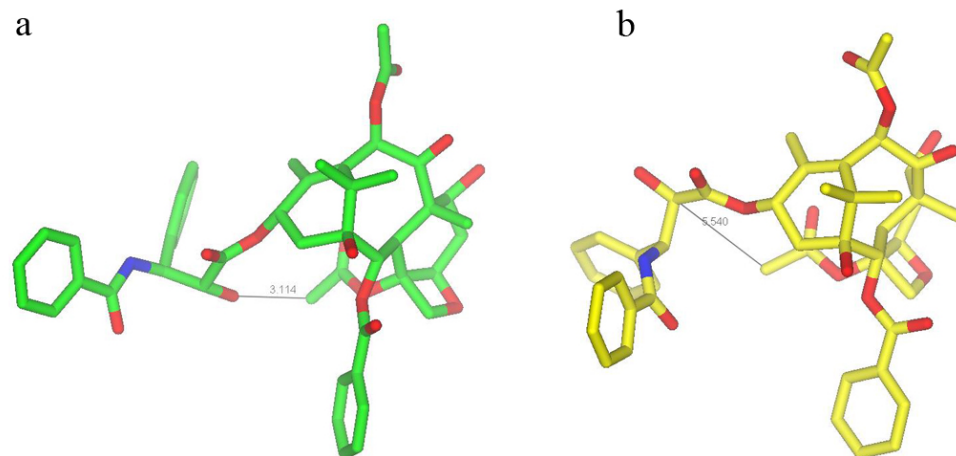
Figure 4-28. The intramolecular distances in REDOR-Taxol (a) and T-Taxol (b)
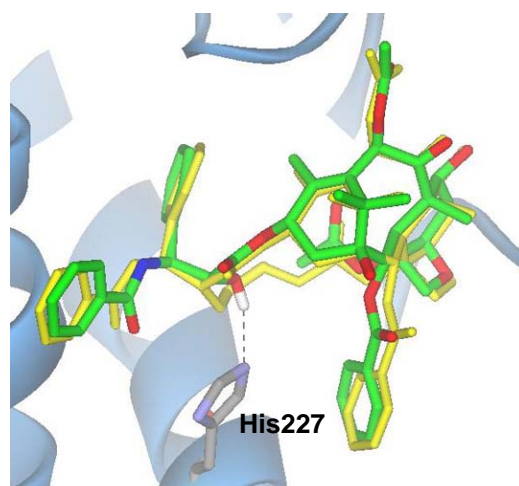
Figure 4-29. Overlay of REDOR-Taxol (green) and SB-TCR-501 (yellow) in tubulin

The Monte Carlo conformational search on the C4-C2'-linked macrocyclic taxoids was conducted in a simulated aqueous environment. The four dihedral angles involved in the C13 side-chain were monitored (see **Figure 4-30**), since those should be the angles most affected by the introduction of the constraint. **SB-TCR-102** shows similar dihedral angle distribution to both REDOR-Taxol and T-Taxol, except for the O13-C1'-C2'-O2' dihedral angle. The weak biological activity may be caused by the unfavorable interaction between the long linker and the binding site.[15] **SB-TCR-501** showed perfect dihedral angle distribution to the REDOR-Taxol structure as designed, but it is inactive in cytotoxicity assay.
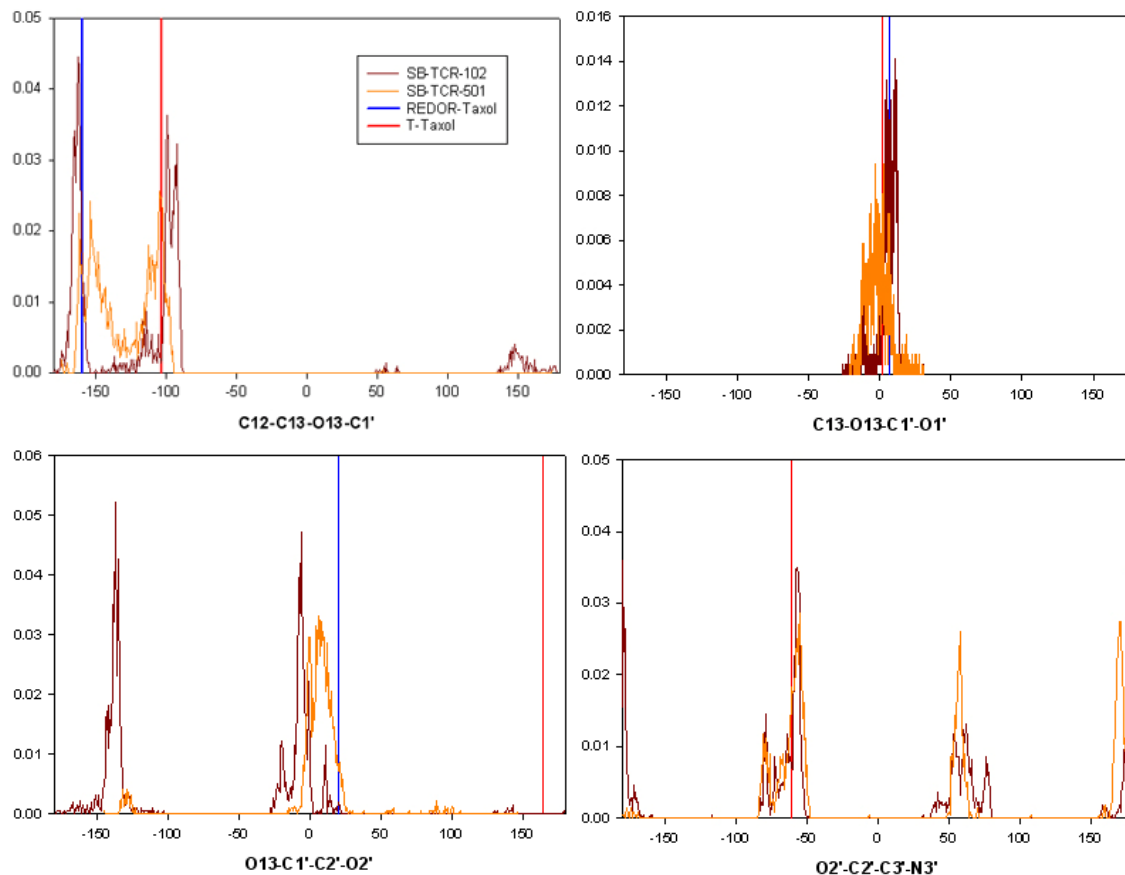
Figure 4-30. Conformational diversity in macrocyclic Taxoids: SB-TCR-102, brown; SB-TCR-501, orange (The reference value for REDOR-Taxol (blue) and T-Taxol (red) are indicated by vertical lines.)

§ 4.4 The MD Simulations of REDOR-Taxol and T-Taxol-1JFF Complexes by AMBER9 Package

§ 4.4.1 Introduction

Although short MD simulations (50 ps) were performed on both REDOR-Taxol-1JFF and T-Taxol-1JFF complexes within 10-Å sphere around the binding site, we hope to check the stability and compare the energy of the complexes during a longer-time simulation. However, the Macromodel® is not an ideal program for long-time simulation. Accordingly, the MD simulations of REDOR-Taxol-1JFF and T-Taxol-1JFF complexes were performed with AMBER9® package, in collaboration with Professor Carlos Simmerling.

AMBER (**A**ssisted **M**odel **B**uilding with **E**nergy **R**efinement), a package evolved from a program that was constructed in the late 1970s, contains a group of programs embodying a number of powerful tools of modern computational chemistry, focused on

molecular dynamics and free energy calculations of proteins, nucleic acids, and carbohydrates.[29]

The principal flow of information is shown in **Figure 4-31**. There are three main steps, shown top to bottom in the figure: system preparation, simulation, and trajectory analysis: (1) The main preparation programs are *antechamber* (which assembles force fields for residues or organic molecules that are not part of the standard libraries) and *LEaP* (which constructs biopolymers from the component residues, solvates the system, and prepares lists of force field terms and their associated parameters). The result of this preparation phase is contained in two text files: a coordinate (*rst*) file that contains just the Cartesian coordinates of all atoms in the system, and a parameter-topology (*parm*) file that contains all other information needed to compute energies and forces; this includes atom names and masses, force field parameters, lists of bonds, angles, and dihedrals, and additional bookkeeping information. (2) The main molecular dynamics program is called *sander*, a parallel program, using the MPI programing interface to communicate among processors. (3) The *ptraj* analysis program was designed to process AMBER trajectories, parsing the *parm* files to atom and residue names and connectivity, and can assemble trajectories from partial ones, often stripping out parts (such as solvent) that might not be needed for a particular analysis. After this, a variety of common analysis tasks may be carried out.
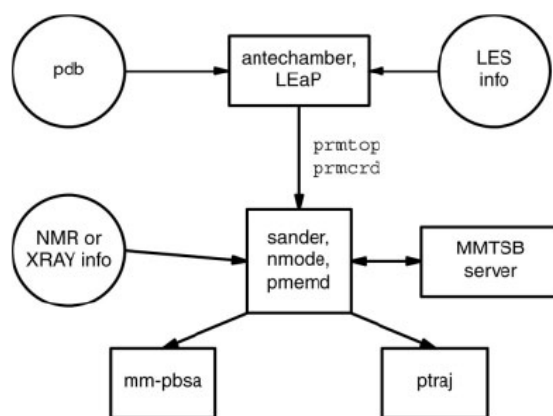
Figure 4-31. Information flow in the Amber program suite[29]

The AMBER-related force fields are among the most widely used for biomolecular simulation.[30, 31] AMBER also supports a more generic force field for organic molecules, called GAFF (the general Amber force field).[32] The *antechamber* program takes a three-dimensional structure as input, and automatically assigns charges, atom types, and force field parameters.

§ 4.4.2 System Preparation, Simulation and Analysis

The minimized REDOR-Taxol-1JFF and T-Taxol-1JFF complexes were used for the simulations. *Antechamber* program was used to assign charges, atom types and force field (GAFF) to the paclitaxel molecule. The complexes were soaked in a truncated octahedral water box, which is ~ 8 Å around the protein and contains 5754 water molecules, by *tLeap* program (ff99sb). Both complexes contain the same number of water molecules to

compare the total energies later. A long-time MD simulation (~ 40 ns) was performed to both REDOR-Taxol/T-Taxol-1JFF-water complexes by Professor Simmerling using CPU time from the Silicon Graphics, Inc (SGI). The system temperature was raised from 0 K to 300 K in 50 ps and the equilibrium was reached after simulation with 5.0 and 1.0 kcal/(mol*Å) on protein backbone for 100 ps each. The simulations with a weak restraint of 0.1 kcal/(mol*Å) on protein backbone, at a constant pressure of 1 atm, periodic boundary conditions, and particle mesh Ewald treatment of electrostatics, were performed with a time step of 1 fs. Snapshots were saved every 10 ps. The trajectories were analyzed by *ptraj* program. The results are shown below.

§ 4.4.2.1 Conformations

The snapshots of the MD simulations (500 ps and 39,000 ps) are shown in **Figure 4-32** and **Figure 4-33**. The REDOR-Taxol forms a H-bond between C2'-OH and His227, which is very stable in the whole simulation (**Figure 4-32**), but there is some substantial movement of the C3'-benzoylamido group (**Figure 4-32b**), which is not shown in the short-time simulation.
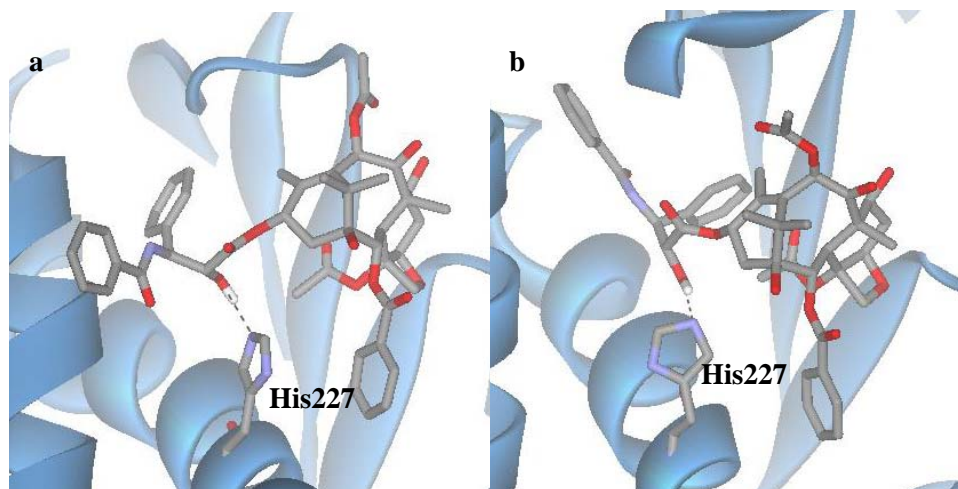
Figure 4-32. Snapshots of the REDOR-Taxol-1JFF simulation

In the T-Taxol-1JFF simulation, the H-bond between C2-O and Gly370 is not stable (**Figure 4-33a**), similar to the short-time simulation, but the whole structure is more stable than the REDOR-Taxol during the simulation. Another H-bond between C2'-OH and Arg369 (**Figure 4-33b**) forms during the simulation and these two H-bonds were switching from time to time.
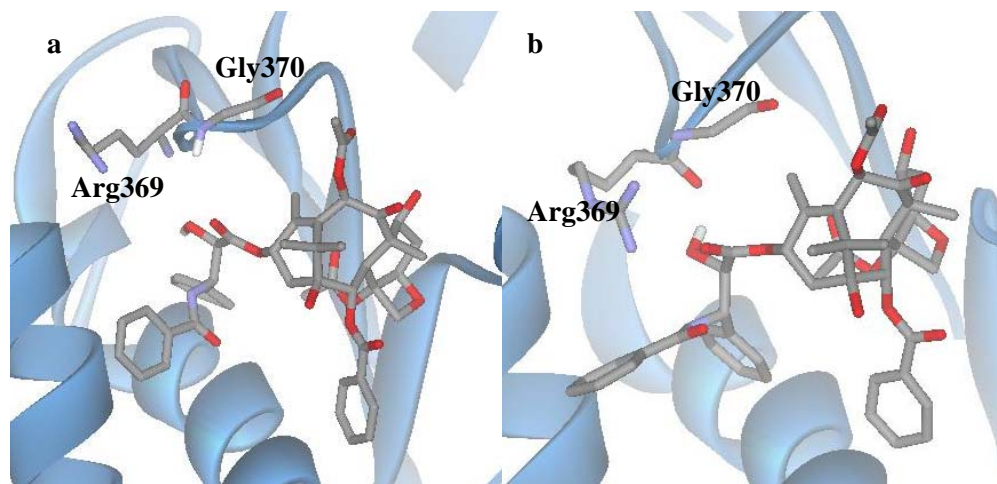
Figure 4-33. Snapshots of the T-Taxol-1JFF simulation

§4.4.2.2 Energy

The total energy of the two simulations is shown in **Figure 4-34**. The energies increase in the beginning as the system temperature increases from 0 K to 300 K and quickly decrease until the equilibrium is reached in ~ 500 ps. The total energies fluctuate around -10400 Kcal/mol and are very stable. But the two systems have similar total energies and the detailed difference between different conformations could not be accurately compared, because the system is too big. This is confirmed later by *MM-PBSA* method, the tiny energy difference between the two complexes is less than the errors of the total system energy (**Figure 4-35**).
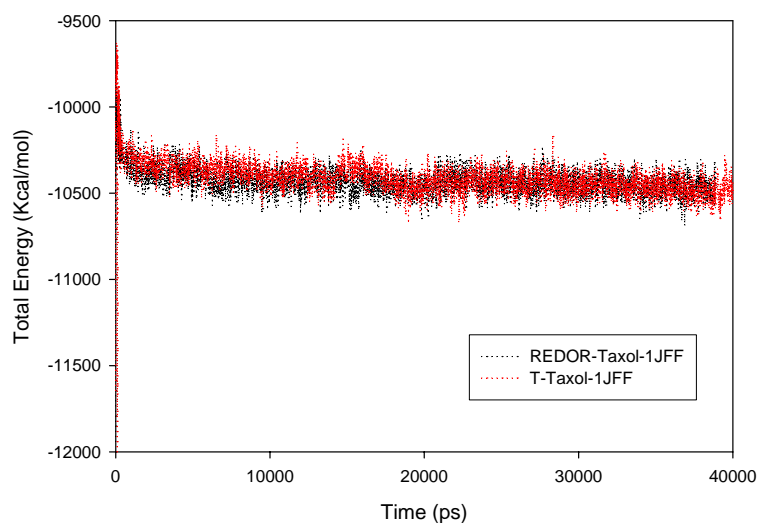
Figure 4-34. The total energy of the simulation of REDOR-Taxol (black) and T-Taxol (red) in 1JFF
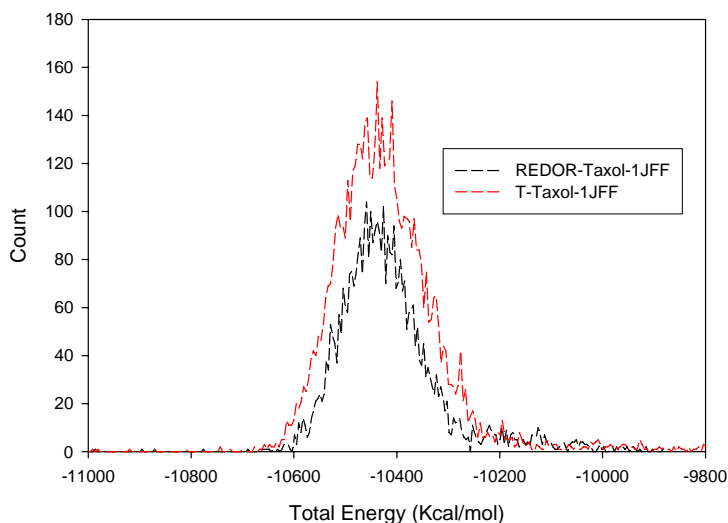
Figure 4-35. The histogram of the total energy in the simulation of REDOR-Taxol (black) and T-Taxol (red) in 1JFF

§4.4.2.3 rmsd

The rmsd (root mean square deviation) of the protein backbone and paclitaxel molecule were monitored. As shown in **Figure 4-36** and **Figure 4-37**, the rmsd of protein backbone in both complexes is ~ 1 Å, which means the backbones do not move much, probably due to the stability of the starting conformation and the small constraint on the protein backbones. Although the C3'-benzoyl group in REDOR-Taxol molecule has some substantial movement, the rmsd of the paclitaxel molecule is ~ 2 Å, i.e., still very small (**Figure 4-36**). The T-Taxol molecule is more stable with a rmsd ~ 1 Å, except for the last 7-ns simulation (~1.3 Å) (**Figure 4-37**).
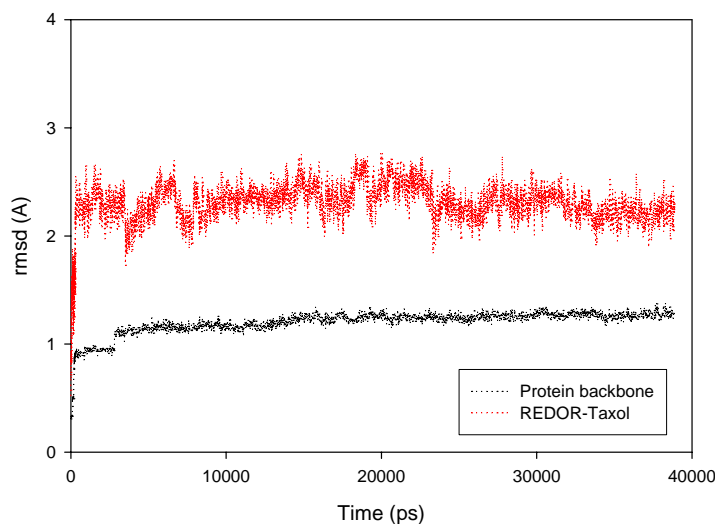
Figure 4-36. rmsd of protein backbone (black) and paclitaxel molecule (red) in REDOR -Taxol- 1JFF simulation
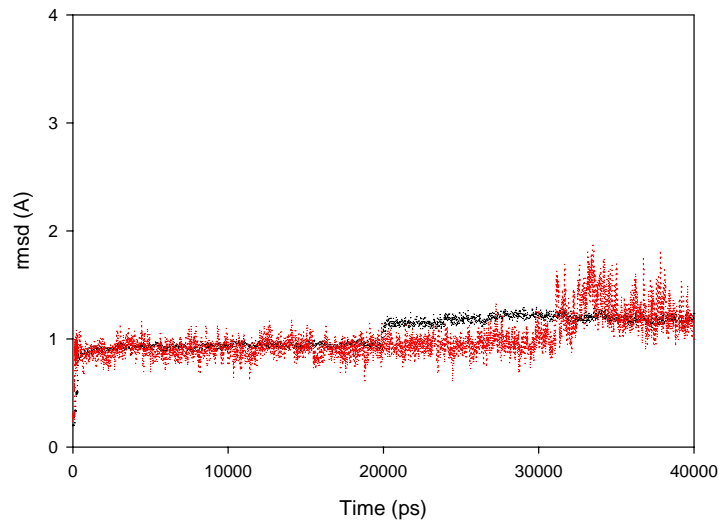
Figure 4-37. rmsd of protein backbone (black) and paclitaxel molecule (red) in T-Taxol- 1JFF simulation

The movement of the M-loop (residue 279 – residue 287), which is very important for the lateral interaction between two β-tubulins, was also monitored in both simulations. As shown in **Figure 4-38**, there is no big change for the M-loops in both complexes (rmsd < 1.5 Å).
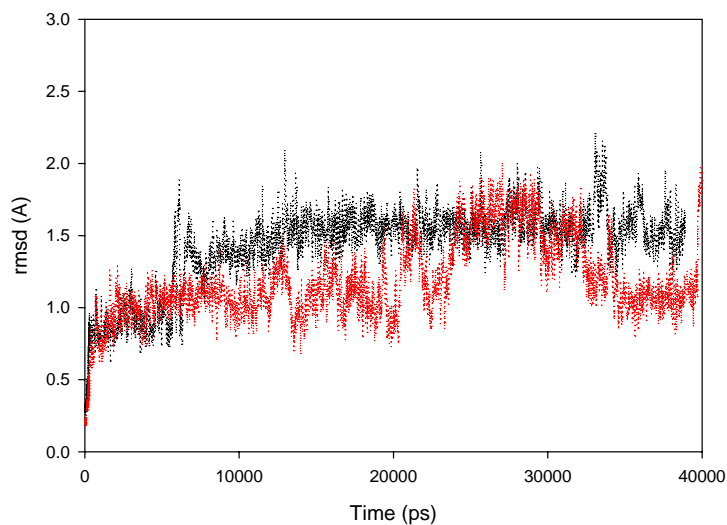
Figure 4-38. rmsd of M-loop in REDOR-Taxol-1JFF (black) and T-Taxol-1JFF (red) simulations

§ 4.4.2.4 Hydrogen Bonds

Since the major difference between the two conformations lies in the hydrogen bonds formed between the C2'-OH and different residues, the H-bond between C2'-OH and His227 in the REDOR-Taxol complex and H-bond between C2'O and Gly370 in the T-Taxol complex were monitored.

The H-bond in the REDOR-Taxol complex is very stable with the average distance around 3 Å from the beginning (**Figure 4-39**). The H-bond between C2'O and Gly370 in the T-Taxol complex interchange with another H-bond between C2'-OH and Arg369 (**Figure 4-39**), and both H-bonds are not as stable as the one in the REDOR-Taxol complex. The movement of the protein backbone makes the interchange between H-bonds happen, which is not observed in the short–time simulation by Macromodel program.
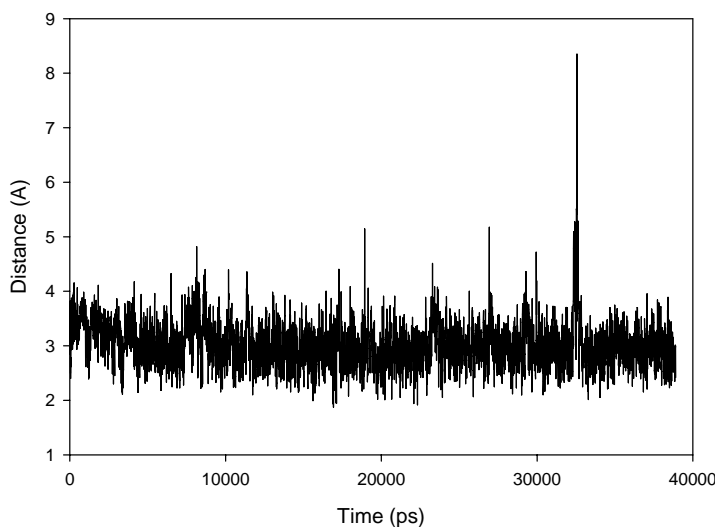
Figure 4-39. Distances of H-bond in REDOR-Taxol-1JFF complex
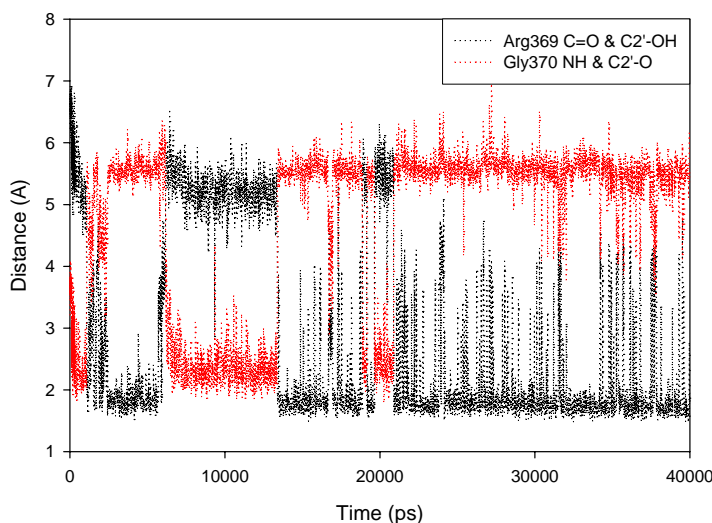
Figure 4-40. Distances of H-bonds in T-Taxol-1JFF complex

§ 4.4.2.5 Intramolecular Distances

The five intramolecular distances were also monitored in **Figure 4-41**, although there is no fluorine atom in the paclitaxel molecules. For T-Taxol, the distances fit with the experimental data well in the beginning, but three of them changed substantially after 30 ns. For REDOR-Taxol, however, only two distances fit with the experimental data well, because of the movement of the C3'*N*-benzoyl group.
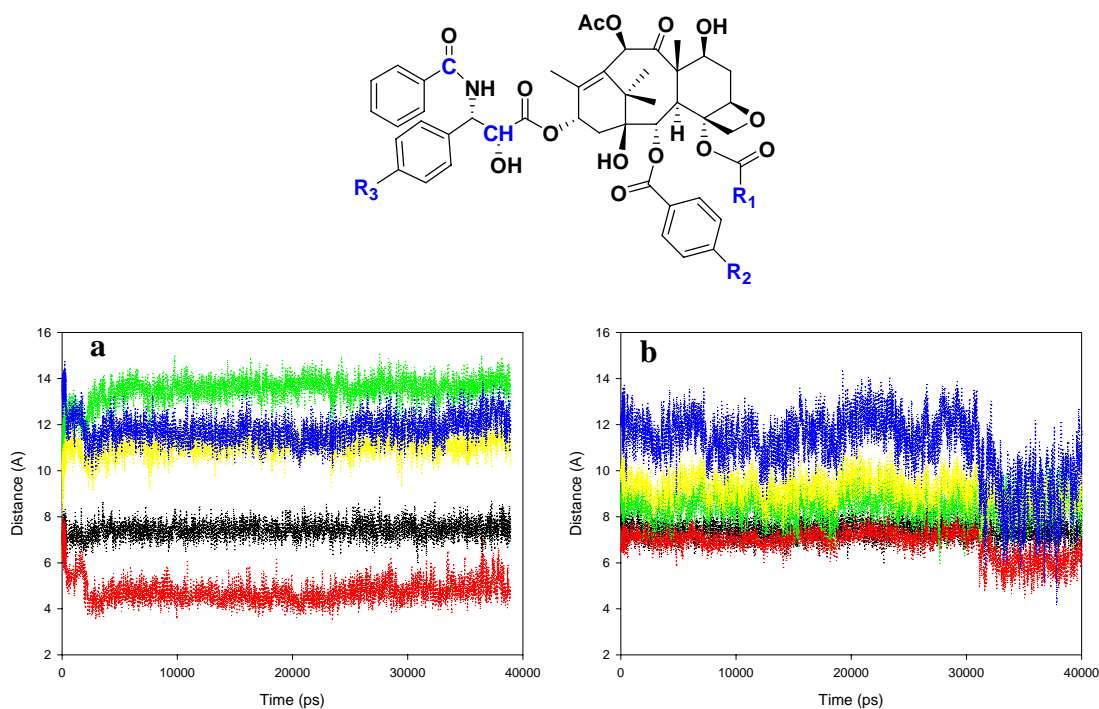
Figure 4-41. Intramolecular distances (R_1-R_2, black; R_1-R_3, red; R_2-R_3, blue; R_2-C, green; R_2-CH, yellow) in the REDOR-Taxol (a) and T-Taxol (b) simulations

Long-time MD simulations of the REDOR-Taxol structure and the T-Taxol structure in 1JFF were studied, but the two structures could not be distinguished. Several factors may cause the simulations inaccurate: (1) The alignment of tubulins in Zn-stabilized sheet and microtubule is different, so the M-loop conformation in 1JFF, which interact with paclitaxel, may be different from the one in microtubule. (2) The binding between paclitaxel and free β-tubulin is very weak, so the modeling studies with paclitaxel in β-tubulin alone may not provide the true binding conformation in microtubule. (3) The simulations were performed with weak constraint on protein backbones, which may not be accurate, but the simulation without any constraint may not be accurate either. (4) The C-terminal has 18 amino acid residues that are missing in the 1JFF structure, so the protein structure may be slightly different in their presence. (5) The GAFF/ff99sb force field may not be suitable for paclitaxel, so the accuracy of the simulation may not be good. It is also very difficult to check the accuracy of the force field, because the paclitaxel molecule is too big for quantum mechanics (QM) studies.

The best way to solve the problems is to perform a MD simulation for microtubule model with correct force field. With the coordinates of microtubule fragment obtained from Dr. Downing's group (Lawrence Berkerly National Laboratory), Professor Simmerling built a fragment model with REDOR/T-Taxol. The simulation of the microtubule fragment will be performed after the confirmation of the force field we used.

§ 4.4.3 The Quantum Mechanics (QM) and Molecular Mechanics (MM) Studies of Paclitaxel Conformations

Since the molecular parameters of the paclitaxel molecule was determined by *Antechamber* using semi-empirical method, we need to examine whether the energies of T-Taxol and REDOR-Taxol are consistent using GAFF force field and quantum mechanics (QM) studies. Otherwise, the energies of the conformations could not be compared accurately from results of the MD simulations. Thus, the QM energies of the REDOR-Taxol and T-Taxol were calculated. Paclitaxel is a very large molecule for QM calculation. The two conformations were first optimized at the Hartree-Fork (6-31g*) level and the single-point energies were calculated at the MP2 (6-31g*) level using the Gaussian03w program. MM energies were calculated using GAFF force field (sander, AMBER9) and the MMFFs force field (Macromodel). The results are listed in **Table 4-2**.

Table 4-2. The energy difference between REDOR-Taxol and T-Taxol by QM and MM studies ($E_{\text{T-Taxol}} - E_{\text{REDOR-Taxol}}$)

Method	ΔE (kcal/mol)
MP2 (Guassian)	-0.695
GAFF (AMBER)	7.08
MMFFs (Macromodel)	-6.49

The T-Taxol is 0.695 kcal/mol more stable than REDOR-Taxol by QM calculation, while REDOR-Taxol is 7.1 kcal/mol more stable than T-Taxol by GAFF force field and 6.5 kcal/mol less stable than T-Taxol by MMFFs force field. The results of MM calculations are not fully consistent with the one by QM calculation. Therefore, the AMBER force field needs to be modified to get accurate MD simulation.

§4.4.4 Progress in Modifying the GAFF Force Field

Similar to the AMBER force field, the GAFF also applies a simple harmonic function form as follows:

$$E_{\text{pair}} = \sum_{\text{bonds}} K_r(r-r_{eq})^2 + \sum_{\text{angles}} K_\theta(\theta-\theta_{eq})^2 +$$

$$\sum_{\text{dihedrals}} \frac{V_n}{2}[1+\cos(n\phi-\gamma)] + \sum_{i<j}\left[\frac{A_{ij}}{R_{ij}^{12}} - \frac{B_{ij}}{R_{ij}^6} + \frac{q_i q_j}{\varepsilon R_{ij}}\right]$$

(r_{eq} and θ_{eq} are equilibration structural parameters; K_r, K_θ, V_n are force constants; n is multiplicity and γ is phase angle for torsional angle parameters). We can modify the dihedral term using the following formula:[33]

$$E_{\text{tors}} = V_1 \times (1 + \cos(\phi - \gamma_1)) + V_2 \times (1 + \cos(2\phi - \gamma_2))$$

The paclitaxel molecule is too large for QM calculation, so we decided to focus on the C13 side-chain (**4-1**) to minimize the calculation. Three dihedral angles were checked (**Figure 4-42**) by the reported procedure:[33] (1) the fragment **4-1** was optimized at the Hartree-Fork (6-31g*) level and the optimized structure was used as the starting conformation; (2) The dihedral angle O1-C2-C3-O4 was fixed at 0°, followed by another optimization (HF 6-31g*) and the single-point energy was calculated (MP2, 6-31g*); (3) The MM energy of the optimized structure was calculated using the standard GAFF force field and GAFF without explicit dihedral term; (4) The procedure was repeated to the same dihedral angle, i.e., O1-C2-C3-O4, by changing every 10° ($-180^o \sim 180\ ^oC$); (5) the same procedure was repeated to another two dihedral angles (C2-C3-O5-C6 and C3-O5-C6-H7).
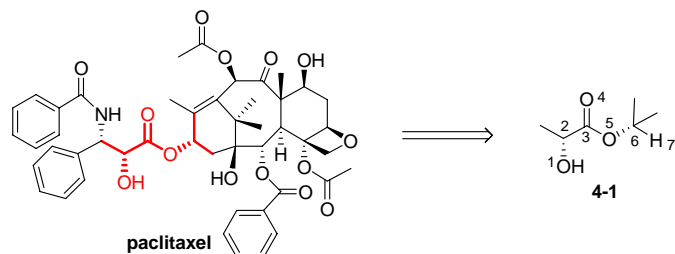
Figure 4-42. Fragment 4-1 of C13 side-chain (paclitaxel)

The energies of the three dihedral angles are shown in **Figure 4-43**. There is some difference in the first two QM-MM energies, while the difference in the third one is very small.
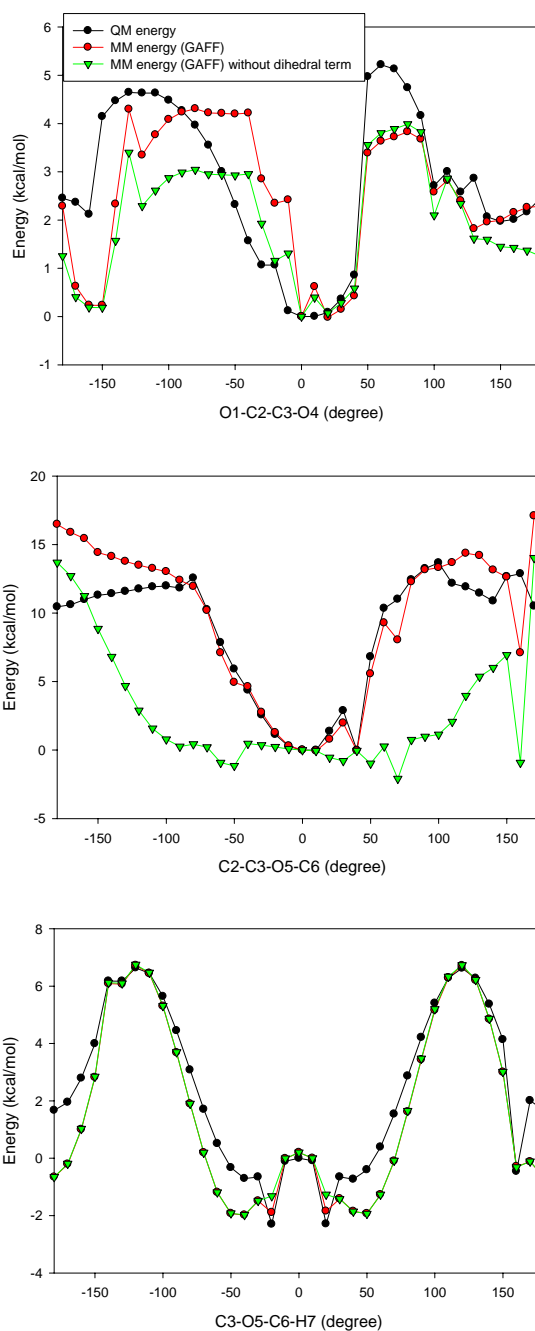
Figure 4-43. Energies of the fragment 4-1 by QM and MM calculation

The difference between the QM energy and the MM energy (without explicit dihedral term) was calculated and a nonlinear least-squares fit was used to obtain parameters that minimize this difference (V_1, V_2, γ_1 and γ_2) in the formula "$E_{\text{tors}} = V_1*(1+\cos(\phi - \gamma_1)) + V_2*(1+\cos(2\phi - \gamma_2))$". The results of the MM calculation of two dihedral angles are shown in **Figure 4-44**. Unfortunately, the fit is not very good and this work is still in progress.
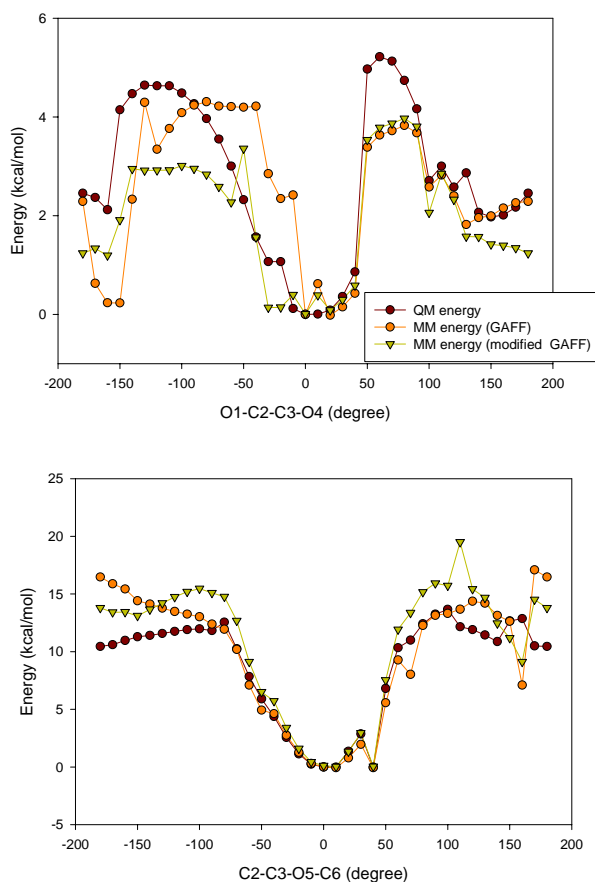
Figure 4-44. Energies of the fragment by QM and MM calculation

§ 4.5 Summary

The REDOR-Taxol structure, first proposed using 1TUB coordinate, was compared with the T-Taxol structure in the higher-resolution 1JFF coordinate using molecular mechanics (MM) and molecular dynamics (MD) simulation methods. The REDOR-Taxol structure has a stable H-bond between C2'-OH and His227, while the H-bond between C2'-O and Gly370 in the T-Taxol structure is not stable in MD simulation. The REDOR-Taxol structure is not only consistent with the REDOR-NMR, but also can predict the tubulin-bound structures of a series of active macrocyclic taxoids. The long-time MD simulations by AMBER program confirm the stability of the H-bond in REDOR-Taxol-1JFF complex, but the AMBER force field need to be modified for accurate simulations of taxoids.

§ 4.6 Experimental Section

The REDOR-Taxol structure[24], obtained in the 1TUB[6], was manually docked into the paclitaxel binding site of the deposited β-tubulin EC structure (1JFF)[10] using the InsightII 2000 program (CVFF force field) by overlaying the baccatin skeleton (carbon atoms of the A, B, and C rings) with those of the paclitaxel molecule present in the 1JFF. The molecular complex was energy-minimized in 5000 steps or till the maximum derivative being < 0.001 kcal/A by means of the conjugate gradients method using the CVFF force field and the distance-dependent dielectric. The backbone of the protein was fixed during the energy minimization. Since there are differences in the protein structure between 1TUB and 1JFF, the paclitaxel structure underwent small changes, but the H-bond between the C2'-OH and His227 was very stable during the energy minimization. The five key distances in the REDOR-Taxol-1TUB structure as well as REDOR-Taxol-1JFF structure, bearing a fluorine substituent at proper positions in accordance with the structures of the fluoro-taxoids used in the REDOR-NMR experiments,[23, 25] were measured.

The T-Taxol structure in the 1JFF was obtained from the Emory University group[11], in which no H-bond with the C2'-OH or C2'-O was found by the InsightII program (CVFF). This structure was energy-minimized by the InsightII program in the same manner as that described above to give the energy-minimized T-Taxol structure. After the energy minimization, a H-bond was identified between the C2'-O and HN of Gly370 (3.4 Å). The five key distances in the original T-Taxol structure and the energy-minimized T-Taxol structure were measured in the same manner as that for the REDOR-taxol structure.

To examine the stability of the REDOR-Taxol and T-Taxol structures, molecular dynamics (MD) simulation was performed using the Macromodel program (MMFF94 force field).[34] The complexes, after 1000-step energy minimization (MMFF94), were used for the MD simulations with a 10 Å sphere around the binding site at 300 K with the time step of 0.5 fs and the constant dielectric constant of 1.0 for 50 ps in a generalized born with surface area term (GBSA) continuum solvent description of water solvation.[35] Within the 10 Å sphere, the ligand and the protein were allowed to move, and all atoms outside the sphere were frozen in order to maintain the overall integrity of the protein. The structures were sampled every 0.5 ps and overlaid with the backbones of the protein.[15] Both REDOR-Taxol and T-Taxol structures gave good overlays without major structural changes.

The structures of macrocyclic paclitaxel analogs,[20] **K1**, **K2**, **SB-T-2053**, **SB-T-2054**, **SB-T-2055Z&E**, **SB-TCR-501**, **SB-TCR-102** and **QT** in the 1JFF were produced by directly introducing the linker into the REDOR-Taxol and the T-Taxol in the 1JFF complexes using the Builder module in the InsightII 2000 program (CVFF). Then, these structures were energy-minimized in 5000 steps or till the maximum derivative being < 0.001 kcal/A by means of the conjugate gradients method using the CVFF force field and the distance-dependent dielectric. The backbone of the protein was fixed throughout the energy minimization.

The energy-minimized REDOR-**K2**-1JFF, REDOR-**SB-T-2054**-1JFF and T-**K2**-1JFF complexes were used for the MD simulations. The MD simulations of these complexes were carried out in the same manner as those described for the REDOR-Taxol-1JFF and

T-Taxol-1JFF, i.e., 20-ps simulation, within 10 Å sphere around the binding site at 300 K using the MMFF94 force field. The structures were sampled every 0.2 ps and overlaid by the backbones of the protein.

Monte Carlo conformational searches on the macrocyclic taxoids (**K1**, **K2**, **SB-T-2053**, **SB-T-2054**, **SB-T-2055Z&E**, **SB-TCR-501**, **SB-TCR-102** and **QT**) were performed with energy minimization (5000 MC steps, minimization for 1000 steps with Polak-Ribiere conjugated gradients) using the Macromodel program by employing a generalized born with surface area term (GBSA) continuum solvent description of water solvation[35]. The dihedral angles were measured directly from the REDOR-Taxol structure and the T-Taxol structure (the Emory University group structure given by Dr. Snyder).

§ 4.7 References

1. Dubois, J.; Guenard, D.; Gueritte-Voegelein, F.; Guedira, N.; Potier, P.; Gillet, B.; Beloeil, J. C. Conformation of Taxotere and analogs determined by NMR spectroscopy and molecular modeling studies. *Tetrahedron* **1993,** 49, 6533-44.
2. Williams, H. J.; Scott, A. I.; Dieden, R. A.; Swindell, C. S.; Chirlian, L. E.; Francl, M. M.; Heerding, J. M.; Krauss, N. E. NMR and Molecular Modeling Study of the Conformations of Taxol and of its Side Chain Methylester in Aqueous and Non-Aqueous Solution. *Tetrahedron* **1993,** 49, 6545-6560.
3. Vander Velde, D. G.; Georg, G. I.; Grunewald, G. L.; Gunn, C. W.; Mitscher, L. A. "Hydrophobic Collapse" of Taxol and Taxotere Solution Conformations in Mixtures of Water and Organic Solvent. *J. Am. Chem. Soc.* **1993,** 115, 11650-11651.
4. Mastropaolo, D.; Camerman, A.; Luo, Y.; Brayer, G. D.; Camerman, N. Crystal and Molecular Structure of Paclitaxel. *Proc. Natl. Acad. Sci. USA* **1995,** 92, 6920-6924.
5. Ojima, I.; Slater, J. S.; Kuduk, S. D.; Takeuchi, C. S.; Gimi, R. H.; Sun, C.-M.; Park, Y. H.; Pera, P.; Veith, J. M.; Bernacki, R. J. Syntheses and Structure-Activity Relationships of Taxoids Derived from 14β-Hydroxy-10-deacetylbaccatin III. *J. Med. Chem.* **1997,** 40, 267-278.
6. Nogales, E.; Wolf, S. G.; Downing, K. H. Structure of the αβ Tubulin Dimer by Electron Crystallography. *Nature* **1998,** 391, 199-203.
7. Rao, S.; Krauss, N. E.; Heerding, J. M.; Swindell, C. S.; Ringel, I.; Orr, G. A.; Horwitz, S. B. 3'-(*p*-Azidobenzamido)taxol Photolabels the N-Terminal 31 Amino Acids of β-Tubulin. *J. Biol. Chem.* **1994,** 269, 3132-3134.
8. Rao, S.; Orr, G. A.; Chaudhary, A. G.; Kingston, D. G. I.; Horwitz, S. B. Characterization of the Taxol-Binding Site on the Microtubule: 2-(*m*-Azidobenzoyl)taxol Photolabels a Peptide (amino acids 217-231) of β-Tubulin. *J. Biol. Chem.* **1995,** 270, 20235-20238.
9. Rao, S.; He, L.; Chakravarty, S.; Ojima, I.; Orr, G. A.; Horwitz, S. B. Characterization of the Taxol Binding Site on the Microtubule. . *J. Biol. Chem.* **1999,** 274, 37990-37994.
10. Lowe, J.; Li, H.; Downing, K. H.; Nogales, E. Refined structure of alpha beta-tubulin at 3.5 A resolution. *J. Mol. Bol.* **2001,** 313, 1045-1057.
11. Snyder, J. P.; Nettles, J. H.; Cornett, B.; Downing, K. H.; Nogales, E. The binding conformation of Taxol in .beta.-tubulin: a model based on electron crystallographic density. *Proc. Natl. Acad. Sci. USA* **2001,** 98, 5312-5316.
12. Guéritte-Voegelein, F.; Guénard, D.; Lavelle, F.; Le Goff, M. T.; Mangatal, L.; Potier, P. Relationships Between the Structure of Taxol Analogues and Their Antimitotic Activity. *J. Med. Chem.* **1991,** 34, 992-998.
13. Swindell, C. S.; Krauss, N. E.; Horwitz, S. B.; Ringel, I. Biologically Active Taxol Analogues with Deleted A-Ring Side Chain Substituents and Variable C-2' Configurations. *J. Med. Chem.* **1991,** 34, 1176-1184.
14. Johnson, S. A.; Alcaraz, A. A.; Snyder, J. P. T-Taxol and the Electron Crystallographic Density in b-Tubulin. *Org. Lett.* **2005,** 7, 5549-5552.

15.   Alcaraz, A. A.; Mehta, A. K.; Johnson, S. A.; Snyder, J. P. The T-Taxol Conformation. *J. Med. Chem.* **2006,** 49, 2478-2488.

16.   Williams, H. J.; Moyna, G.; Scott, A. I.; Swindell, C. S.; Chirlian, L. E.; Heerding, J. M.; Williams, D. K. NMR and Molecular Modeling Study of the Conformations of Taxol 2'-Acetate in Chloroform and Aqueous Dimethyl Sulfoxide Solutions. *J. Med. Chem.* **1996,** 39, 1555-9.

17.   Kingston, D. G. I.; Bane, S.; Snyder, J. P. The taxol pharmacophore and the T-taxol bridging principle. *Cell cycle* **2005,** 4, 279-89.

18.   Metaferia, B. B.; Hoch, J.; Glass, T. E.; Bane, S. L.; Chatterjee, S. K.; Snyder, J. P.; Lakdawala, A.; Cornett, B.; Kingston, D. G. I. Synthesis and biological evaluation of novel macrocyclic paclitaxel analogues. *Org. Lett.* **2001,** 3, 2461-2464.

19.   Querolle, O. D., J.; Thoret, S.; Roussi, F.; Gueritte, F.; Gue´nard, D. Synthesis of C2-C3'N-Linked Macrocyclic Taxoids. Novel Docetaxel Analogues with High Tubulin Activity. *J. Med. Chem.* **2004,** 47, 5937-5944.

20.   Ganesh, T.; Guza, R. C.; Bane, S.; Ravindra, R.; Shanker, N.; Lakdawala, A. S.; Snyder, J. P.; Kingston, D. G. I. The bioactive taxol conformation on b-tubulin: Experimental evidence from highly active constrained analogs. *Proc. Natl. Acad. Sci. USA* **2004,** 101, 10006-10011.

21.   Ganesh, T.; Yang, C.; Norris, A.; Glass, T.; Bane, S.; Ravindra, R.; Banerjee, A.; Metaferia, B.; Thomas, S. L.; Giannakakou, P.; Alcaraz, A. A.; Lakdawala, A. S.; Snyder, J. P.; Kingston, D. G. I. Evaluation of the Tubulin-Bound Paclitaxel Conformation: Synthesis, Biology, and SAR Studies of C-4 to C-3' Bridged Paclitaxel Analogues. *J. Med. Chem.* **2007,** 50, 713-725.

22.   Larroque, A.-L.; Dubois, J.; Thoret, S.; Aubert, G.; Chiaroni, A.; Gueritte, F.; Guenard, D. Novel C2-C3'N-peptide linked macrocyclic taxoids. Part 2: Synthesis and biological activities of docetaxel analogues with a peptide side chain at C2 and their macrocyclic derivatives. *Bioorg. Med.Chem.* **2007,** 15, 563-574.

23.   Li, Y.; Poliks, B.; Cegelski, L.; Poliks, M.; Cryczynski, A.; Piszcek, G.; Jagtap, P. G.; Studelska, D. R.; Kingston, D. G. I.; Schaefer, J.; Bane, S. Conformation of Microtubule-Bound Paclitaxel Determined by Fluorescence Spectroscopy and REDOR NMR. *Biochemistry* **2000,** 39, 281-291.

24.   Geney, R.; Sun, L.; Pera, P.; Bernacki Ralph, J.; Xia, S.; Horwitz Susan, B.; Simmerling Carlos, L.; Ojima, I. Use of the tubulin bound paclitaxel conformation for structure-based rational drug design. *Chem. Biol.* **2005,** 12, 339-48.

25.   Paik, Y.; Yang, C.; Metaferia, B.; Tang, S.; Bane, S.; Ravindra, R.; Shanker, N.; Alcaraz, A. A.; Johnson, S. A.; Schaefer, J.; O'Connor, R. D.; Cegelski, L.; Snyder, J. P.; Kingston, D. G. I. Rotational-Echo Double-Resonance NMR Distance Measurements for the Tubulin-Bound Paclitaxel Conformation. *J. Am. Chem. Soc.* **2007,** 129, 361-370.

26.   Halgren, T. A. Merck molecular force field. I. Basis, form, scope, parameterization, and performance of MMFF94. *J. Comput. Chem.* **1996,** 17, 490-519.

27.   Discover. Accelrys Software Inc.

28. Kant, J.; Huang, S.; Wong, H.; Fairchild, C.; Vyas, D.; Farina, V. Studies Toward Structure-Activity Relationships of Taxol: Synthesis and Cytotoxicity of Taxol Analogues with C-2' Modified Phenylisoserine Side Chains. *Bioorg. Med. Chem. Lett.* **1993,** 3, 2471-2474.

29. Case, D. A.; Cheatham, T. E., III; Darden, T.; Gohlke, H.; Luo, R.; Merz, K. M., Jr.; Onufriev, A.; Simmerling, C.; Wang, B.; Woods, R. J. The amber biomolecular simulation programs. *J. Comput. Chem.* **2005,** 26, 1668-1688.

30. Weiner, S. J.; Kollman, P. A.; Case, D. A.; Singh, U. C.; Ghio, C.; Alagona, G.; Profeta, S., Jr.; Weiner, P. A new force field for molecular mechanical simulation of nucleic acids and proteins. *J. Am. Chem. Soc.* **1984,** 106, 765-84.

31. Cornell, W. D.; Cieplak, P.; Bayly, C. I.; Gould, I. R.; Merz, K. M., Jr.; Ferguson, D. M.; Spellmeyer, D. C.; Fox, T.; Caldwell, J. W.; Kollman, P. A. A Second Generation Force Field for the Simulation of Proteins, Nucleic Acids, and Organic Molecules. *J. Am. Chem. Soc.* **1995,** 117, 5179-97.

32. Wang, J.; Wolf, R. M.; Caldwell, J. W.; Kollman, P. A.; Case, D. A. Development and testing of a general amber force field. *J. Comput. Chem.* **2004,** 26, 114.

33. Song, K.; Hornak, V.; de los Santos, C.; Grollman Arthur, P.; Simmerling, C. Molecular mechanics parameters for the FapydG DNA lesion. *J. Comput. Chem.* **2008,** 29, 17-23.

34. Halgren, T. A. Merck molecular force field. I. Basis, form, scope, parameterization, and performance of MMFF94. *J. Computat. Chem.* **1996,** 17, 490-519.

35. Still, W. C.; Tempczyk, A.; Hawley, R. C.; Hendrickson, T. Semianalytical treatment of solvation for molecular mechanics and dynamics. *J. Am. Chem. Soc.* **1990,** 112, 6127-9.

Chapter V

Design and Synthesis of *De Novo* Taxol-Mimicking Anticancer Agents

§ 5.1 Introduction

The mechanism of action of paclitaxel was found to be shared by several other natural products. Epothilones A and B,[1, 2] eleutherobin,[3] discodermolide,[4] laulimalide[5] and FR181277[6] showed activities comparable to those of paclitaxel in cytotoxicity assays and inhibition of microtubules disassembly in purified tubulin assembly assays (**Figure 5-1**).[2, 7, 8] The recognition of a pharmacophore common to all these microtubule-stabilizing agents (MSA) could provide rationale and guidance for the design of the next-generation microtubule-stabilizing anticancer agents.

In the SAR studies of paclitaxel and the investigation into its bioactive conformation, Ojima *et al.* proposed a plausible common pharmacophore for several microtubule-stabilizing agents based on molecular modeling studies as well as 2-D NMR experiments using a second-generation taxoid, nonataxel, as the template **(Figure 5-1)**.[9] This common pharmacophore model successfully accommodated existing SAR data for these microtubule-stabilizing agents and identified the key structural requirement for biological activity of paclitaxel: the properly oriented C2-benzoate, the C3'-phenyl and C3'*N*-benzoyl moieties.
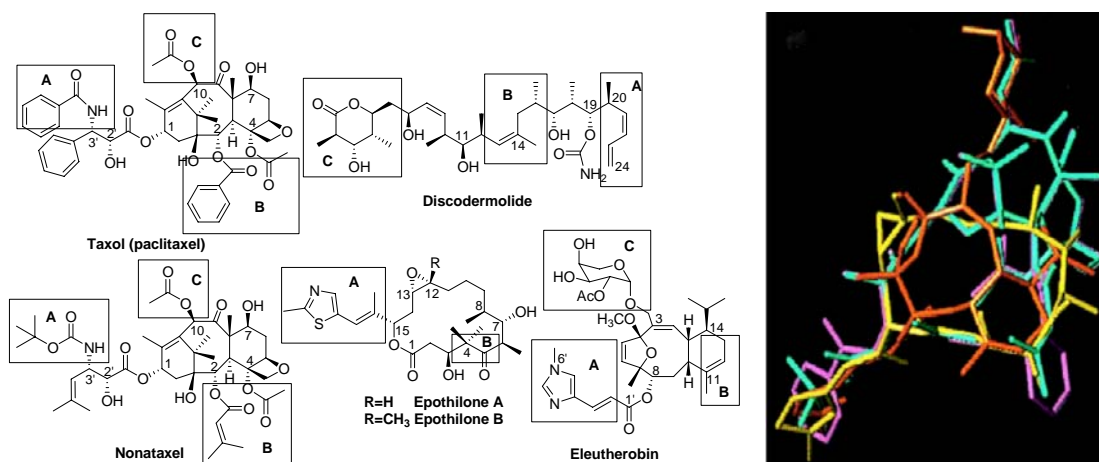
**Figure 5-1: Overlay of paclitaxel (magenta), nonataxel (cyan), epothilone B (yellow),
and eleutherobin (orange) using molecular modeling
(Labeled boxed regions are areas of common overlap)
[Adapted from ref. 9]**

Two other common pharmacophore models were also proposed. Based on microtubule mutation and molecular modeling studies, Giannakakou *et al.* proposed a common pharmacophore for paclitaxel and epothilone, in which the C2-benzoate of paclitaxel was overlaid with the C15 side chain of epothilone as well as the oxetane oxygen of paclitaxel with the epoxide oxygen of epothilone,[10] as shown in **Figure 5-2**.
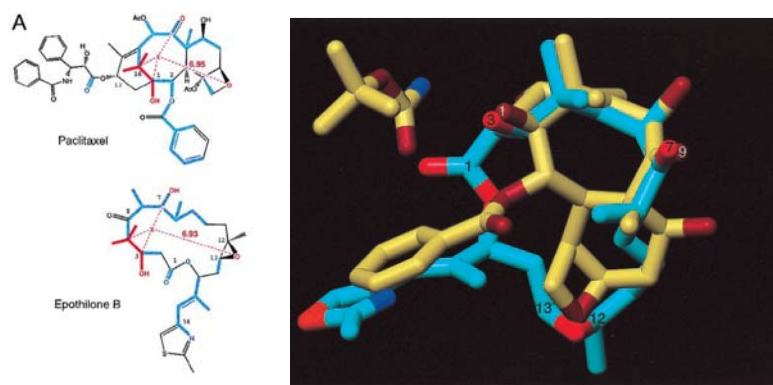
Figure 5-2. A proposed common pharmacophore by Giannakakou *et al.*
[Adapted from ref. 10]

Horwitz *et al.* proposed a similar pharmacophore based on a taxane analog 2-(3-azidonezoyl)baccatin III **(Figure 5-3)**.[11] This compound was found to possess cytotoxicity 15-40 times less potent than that of paclitaxel but it indeed promotes the polymerization of tubulins to form microtubules. In their proposal, the C2 *m*-azidobenzoyl moiety was overlaid with the thiazole moiety of epothilone.
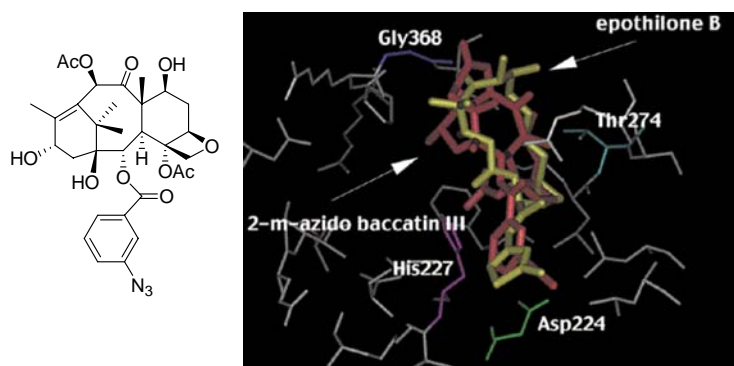
Figure 5-3. A proposed common pharmacophore by Horwitz *et al.*
[Adapted from ref. 11]

The two similar models described above failed to include the crucial C13 side-chain of paclitaxel as part of the common pharmacophore, thereby could not explain the vast amount of SAR studies on the C13 side-chain. Also, those two models identified the oxetane oxygen of paclitaxel and epoxide oxygen as important parts of the pharmacophore. However, SAR studies revealed that the 12,13-dexoyepothilone analog exhibited a far more promising profile for *in vivo* activity than that of either paclitaxel or epothilone.[12, 13] In addition, the 12,13-cyclopropane analog of epothilone was also synthesized and found to be equally active as epothilone B in tubulin binding assay as well as cytotoxicity assay.[14] Moreover, a docetaxel analog in which the oxetane ring was replaced by a cyclopropane ring was synthesized and found to possess biological activities as potent as paclitaxel and docetaxel.[15] These results provide further evidence that the role of the 12,13-epoxide of epothilones as well as the oxetane ring in paclitaxel is largely conformational, which is unfavorable to these two pharmacophore illustrated above, and in favor of the pharmacophore model proposed by Ojima *et al.*[9]

The Ojima pharmacophore model (**Figure 5-4**)[9] suggests that the role of the baccatin core (including the oxetane ring) is to serve as a "scaffold" which helps maintain the proper orientation of the C2, the C3' as well as the C3'*N* moieties. Accordingly, in theory the baccatin core could be replaced by much simpler scaffolds that retain most of the three-dimensional features but without the structural complexity of baccatin. The common pharmacophore model paves the way for designing the *new-generation taxoids* that could be essentially baccatin-free, or "hydrids" integrating the structural features of paclitaxel as well as other microtubule-stabilizing agents.
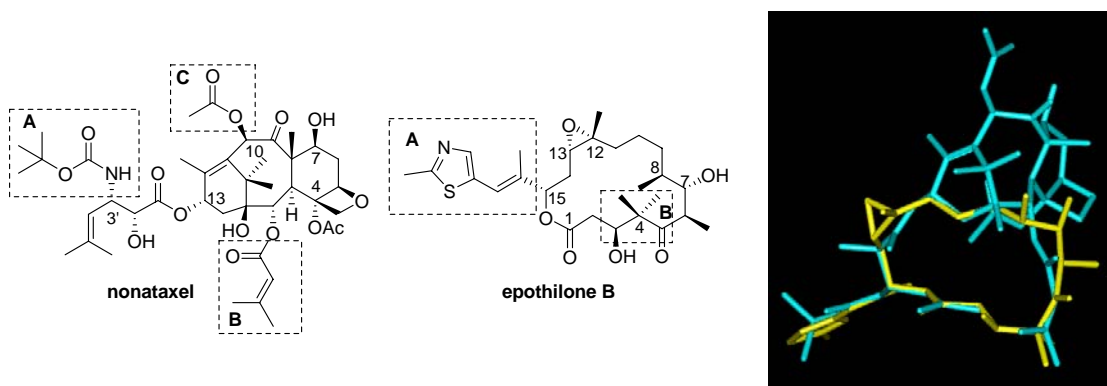
Figure 5-4. Overlay of nonataxel (cyan) with epothilone B (yellow)

Thus, in the Ojima's laboratory, *de novo* paclitaxel-mimicking anticancer agents was designed based on the proposed common pharmacophore.[9] Through extensive molecular modeling studies, we investigated various bicyclic structures bearing two hydroxy groups which could closely mimic the two hydroxyl groups at the C2 and the C13 positions of paclitaxel or baccatin III. Indeed, modeling studies identified bicyclic structure **5-1** bearing two hydroxy groups with a dihedral angle of -50°, which is similar to that of paclitaxel and docetaxel. The presence of the olefin moiety in the molecule also provided additional opportunities for modifications such as epoxidation and hydroxylation, etc.
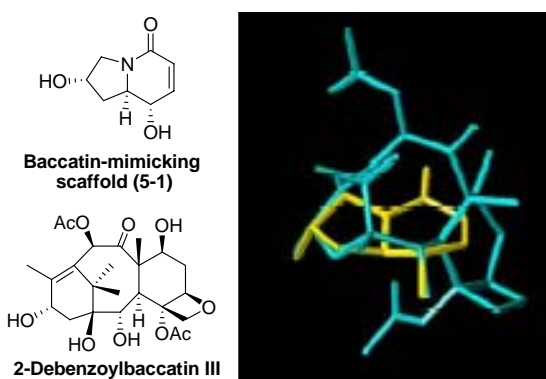
Figure 5-5. Overlay of scaffold (5-1, yellow) with 2-debenzoylbaccatin III (cyan) using molecular modeling [Adapted from ref. 16]

The third-generation paclitaxel-mimicking anticancer agents based on the scaffold designed above will provide not only additional data for the evaluation of our common

pharmacophore but also provide valuable information regarding the three-dimensional structural requirements of the microtubule-stabilizing agents.

Based on scaffold **5-1**, two types of paclitaxel-mimicking anticancer agents were designed as shown in **Figure 5-6**. Since epothilones possess a 16-membered lactone ring, an additional macrocycle was introduced to the paclitaxel-mimicking anticancer agents. The presence of such a large ring system may also serves as additional conformational constraint to retain the proper conformation of the side chains. Accordingly, **SB-H-1010** and **SB-H-1020** were designed with paclitaxel-like side-chains attached to the bicyclic system bearing a 19-membered macrocyclic tether linking the C5 and the C3'*N* positions. The novel paclitaxel-mimicking anticancer agents without the macrocycle were also synthesized. Based on the fact that **SB-T-121303**, a third-generation taxoid developed in Ojima's laboratory, possesses extremely potent cytotoxicities against drug-sensitive as well as drug-resistant cancer cell line, the same side chain of **SB-T-121303** was attached onto the designed scaffold **5-1** to construct novel compounds **SB-H-101** and **SB-H-201**.[16]
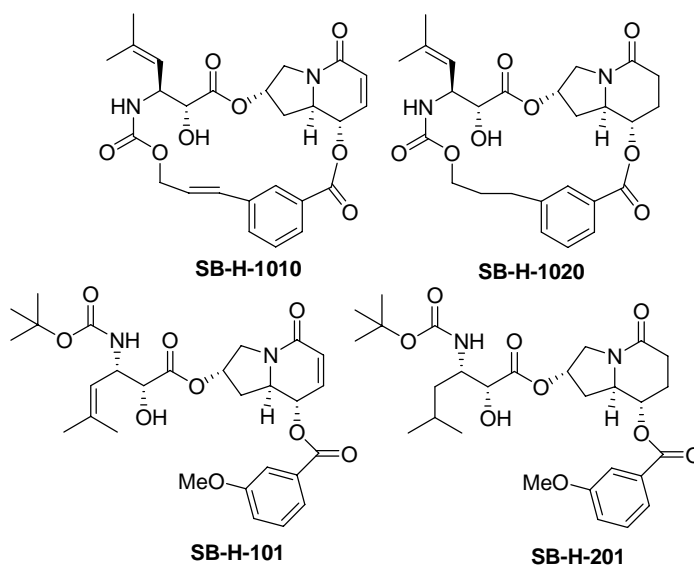
Figure 5-6. Paclitaxel-mimicking anticancer agents based on scaffold 5-1

The four 'taxoid-mimics' were evaluated for their *in vitro* cytotoxicities against drug-sensitive and drug-resistant cancer cell lines. The results are summarized in **Table 5-1**. **SB-H-101** and **SB-H-1010** exhibit micromolar level IC_{50} values against LCC6-WT and MCF7 human breast cancer cell lines in spite of their simplified structures. The hydrogenated congeners, **SB-H-201** and **SB-H-1020**, showed much lower cytotoxicities. It should be noted that these two compounds are not affected by P-glycoprotein-based multi-drug resistance. **SB-H-101** was found to possess cytotoxic activities comparable to cisplatin against the human breast carcinoma cell line MCF7 (wild type and MDR phenotype).

Table 5-1. *In vitro* cytotoxicities (IC$_{50}$, μM[a]) of the Taxol-mimics

Taxoids	LCC6-WT[b]	LCC6-MDR	MCF7[d]	NCI/ADR[e]
Paclitaxel	0.004±0.00015	0.379±0.007	0.0022±0.00018	1.185±0.04
SB-H-101	8.9±0.22	10±0.56	5.7±0.26	8.7±0.1
SB-H-201	>10	>10	14±3.4	>10
SB-H-1010	14±1.0	>10	8.1±0.22	13±0.6
SB-H-1020	>10	>10	>10	>10

[a]The concentration of compound which inhibits 50% of the growth of human tumor cell line;
[b]LCC6-WT: human breast carcinoma; [c]LCC6-MDR: MDR1 transduced line;
[d]MCF7: human breast carcinoma; [e]NCI/ADR: MDR phenotype human ovarian carcinoma.

The fact that the hydrogenated congeners **SB-H-201** and **SB-H-1020** are much less active may suggest that a certain rigidity of the scaffold is crucial for biological activity. On the other hand, the result that the open-chain 'taxoid-mimic' **SB-H-101** is a little more potent than the macrocyclic 'taxoid-mimic' **SB-H-1010** may imply an advantage of having rather flexible side chains to accommodate favorable conformation(s) for bioactivity.

However, none of the 'taxoid-mimics' showed appreciable activity in promoting the formation of microtubules in the standard *in vitro* tubulin polymerization assay. Nevertheless, **SB-H-101** and **SB-H-1010** could certainly serve as leads for the development of *de novo* anticancer agents, considering the numerous functionalization possibilities of their simple structure.

Recently, the Kingston group also reported C3'-C4 bridged paclitaxel mimics based on the T-taxol model, which showed micromolar level of IC$_{50}$ value against A2780 cell line in the cytotoxicity assays.[17] The three hydroxyl groups of the bicyclic compound were designed to mimic the C2-, C4- and C13- hydroxyl groups of baccatin. The macrocyclic paclitaxel mimics used the same "C4-C3' linked bridge as in the active macrocyclic taxoids.

X= CH$_2$, OCH$_2$

R= Ph, O*t*Bu
X'=O, bond, OCH$_2$, OCH$_2$CH$_2$
Ar= Ph, 3-MeO-Ph, 3-Azido-Ph
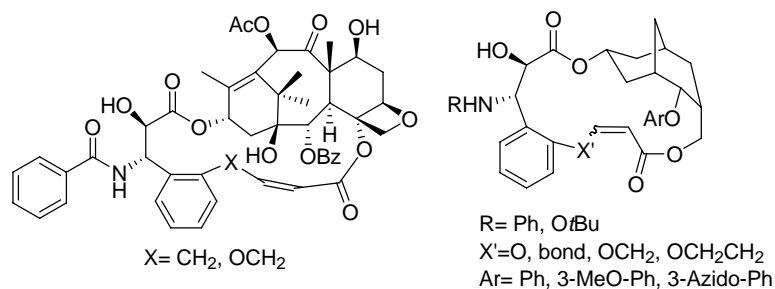
Figure 5-7. Kingston's macrocyclic taxoids and paclitaxel mimics

Table 5-2. *In vitro* cytotoxicities and tubulin-polymerization (TP) assays of the Kingston's macrocyclic taxoids[18]

Compound with Bridge	IC$_{50}$ µg/ml	TP µg/ml
	A2780	
Taxol	0.006-0.02	
X= OCH$_2$	7.25	weak
X= OCH$_2$	9.6	weak
X= OCH$_2$CH$_2$	15	ND
X= OCH$_2$CH$_2$	16	ND
X= CH$_2$	5	weak
X= CH$_2$	6	weak
CH$_2$ with C-2-*m*-MeOBz & *N*-Boc	5.6	ND

§ 5.2 Results and Discussion

§ 5.2.1 Synthesis and Evaluation of SB-H-102

Based on the bicyclic scaffold **5-1**, a paclitaxel mimic **5-2** was designed, which has the same C13 side-chain as paclitaxel. The overlay of the minimized structure in vacuum is shown in **Figure 5-8** by overlaying the two hydroxyl groups.

Designed novel paclitaxel mimic (5-2)
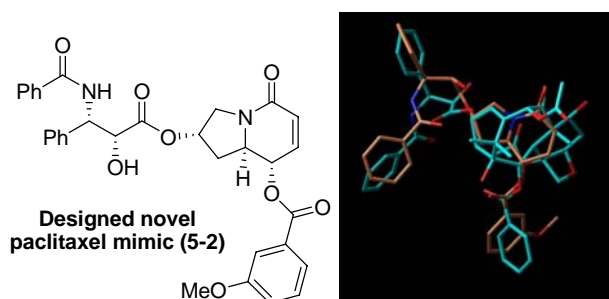
Figure 5-8. Overlay of SB-H-102 (orange) with paclitaxel (cyan)

The designed scaffold could be synthesized by a ring-closing metathesis reaction from readily available hydroxyproline derivatives. As shown in **Scheme 5-1**, bicyclic system **5-5** could be obtained by modification of commercially available *trans*-4-hydroxy-L-proline **5-6**. The isoserine side chain could be synthesized from enantiopure *β*-lactam (**1-16**).
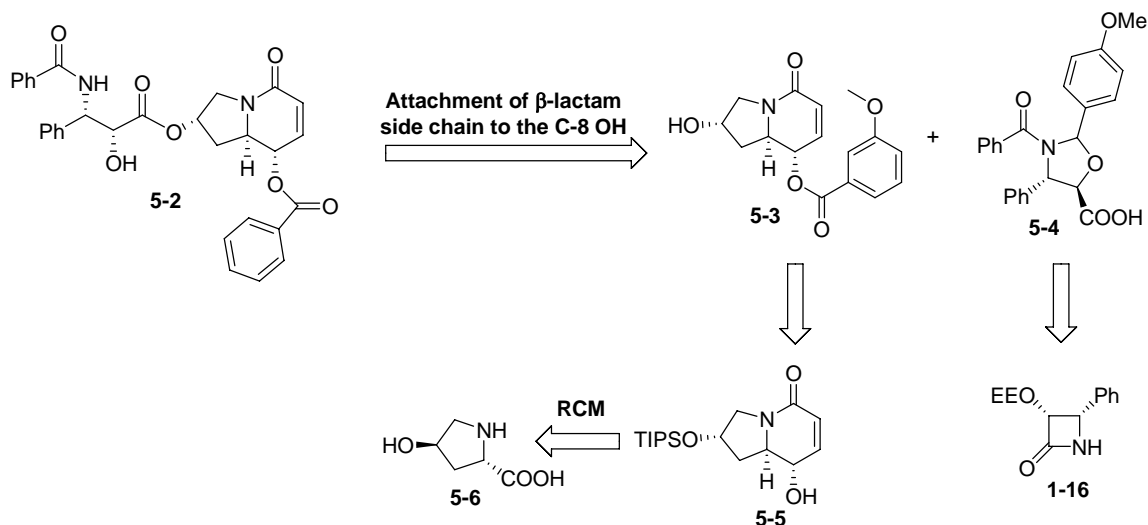
Scheme 5-1. Retro-synthesis of Taxol mimic 5-2

The synthesis of intermediate **5-14** is shown in **Scheme 5-2**. The unnatural hydroxy-D-proline was prepared from commercially available *trans*-4-hydroxy-L-proline (**5-6**) following a published procedure.[19-21] Then, **5-6** was refluxed in a mixture of acetic acid and acetic anhydride for 5 h, followed by additional reflux in 2 *N* HCl for another 2 h to give **5-7**. Crude **5-7** was refluxed in methanol in the presence of hydrochloric acid (*in situ* generated upon the addition of AcCl) to give methyl ester hydrochloric salt **5-8**, which was then reacted with Boc anhydride to afford *N*-Boc-4-*β*-hydroxy-D-proline methyl ester (**5-9**) in excellent yield (75% in 3 steps). The inversion of the configuration of the C4 hydroxy group was achieved by the Mitsunobu reaction[22] using standard conditions. Thus, **5-9** was treated with triphenylphosphine, benzoic acid and diisopropyl azodicarboxylate (DIAD) in THF to afford *N*-Boc-4-α-hydroxy-D-proline methyl ester (**5-10**) in high yield.

In order to construct the six member ring in the scaffold, various reactions needed to be performed, including reduction, oxidation as well as acylation. Accordingly, the 4-α-hydroxy group needed to be protected as a TIPS ether. Thus, the benzoyl group was cleaved by hydrolysis using potassium hydroxide in methanol to give the *trans*-hydroxy-D-proline derivative **5-11**, which was then protected with TIPSCl in the presence of imidazole to give **5-12** in excellent yield. Then, the methyl ester moiety of **5-12** was reduced using lithium borohydride to afford alcohol **5-13** in high yield. The oxidation utilizing sulfur trioxide pyridine complex in the presence of triethylamine and dimethyl sulfoxide (DMSO) afforded the desired aldehyde **5-14** in excellent yield.
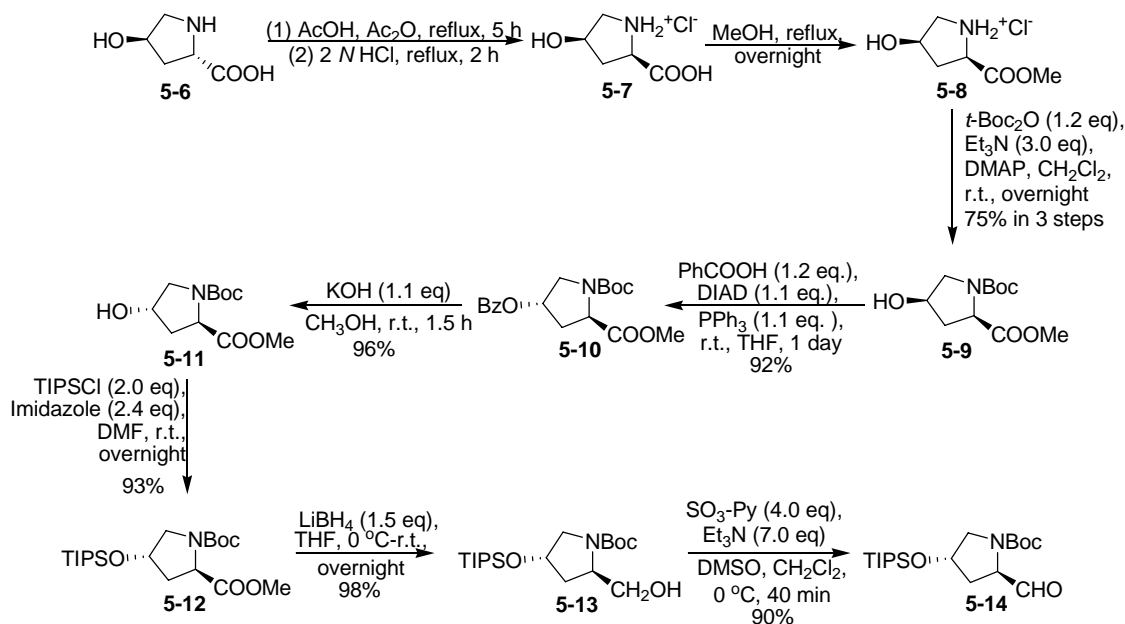
Scheme 5-2. Synthesis of intermediate 5-14

Aldehyde **5-14** was treated with vinylmagnesium chloride to afford a ~5/1 diastereomeric mixture of alcohol **5-15,** favoring the desired isomer (stereochemistry of the products were determined after the formation of the six-membered ring by NOE analysis). Then alcohol **5-15** was treated with acetic anhydride in the presence of DMAP and triethylamine to afford acetate **5-16** in 80% yield (**Scheme 5-2**).

The Boc protecting group was cleaved by using trifluoroacetic acid (TFA) at 0 $^{\circ}$C and after the removal of solvent and excess amount of TFA, the residue was treated with triethylamine and acryloyl chloride to afford diene **5-18** in 27% yield for two steps. Next, diene **5-18** was subjected to ring closing metathesis using the "first-generation Grubbs catalyst"[23] to afford scaffold **5-19** in 83% yield (~5:1 ratio). The two isomers could not be separated by silica gel column chromatography. Fortunately, after hydrolysis of the acetyl group using potassium carbonate, the two resulting alcohols were easily separated by column chromatography to afford pure scaffold **5-5** in 80% yield. The scaffold **5-5** was first subjected to esterification reaction with 3-methoxybenzoic acid in the presence of DIC and DMAP to afford ester **5-21**. The TIPS group was then removed using HF-pyridine conditions to give **5-3** in 94% yield for two steps. **(Scheme 5-3)**
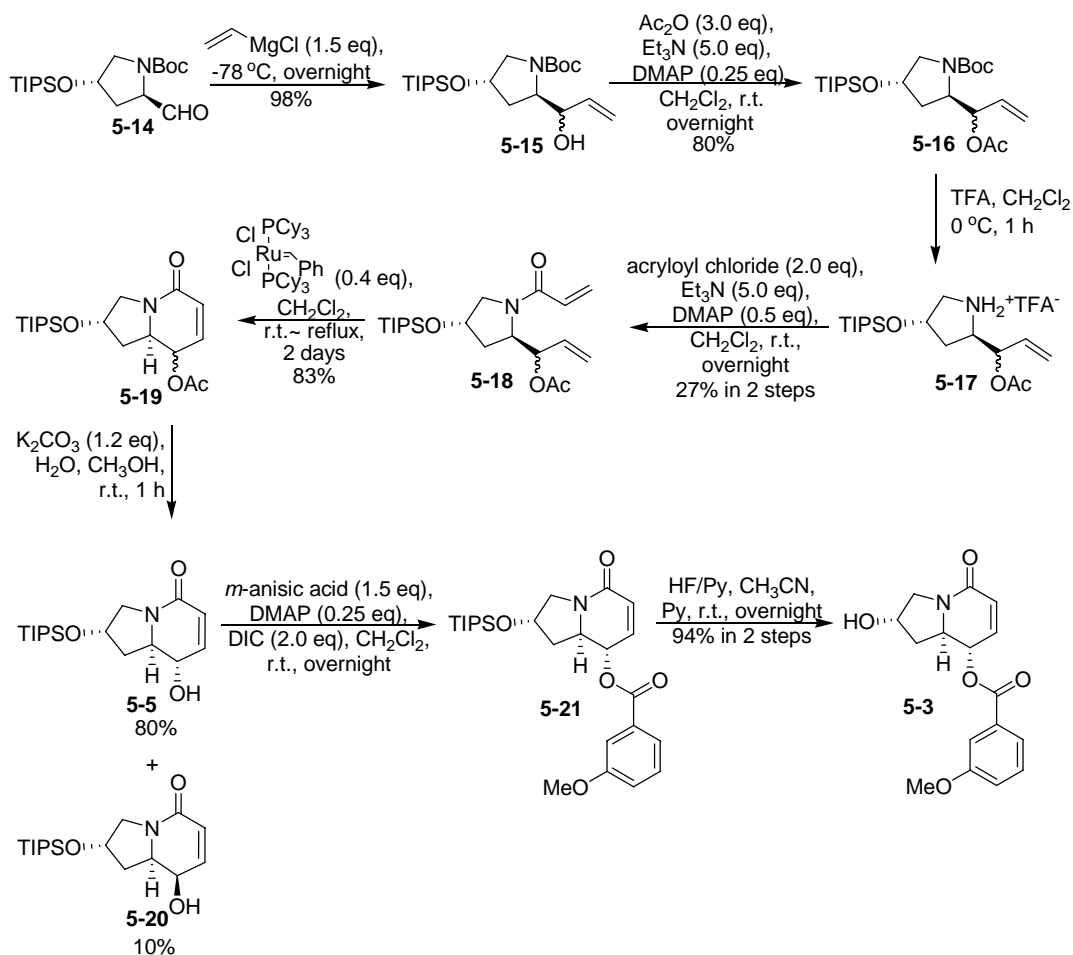
Scheme 5-3. Synthesis of intermediate 5-3

Although the stereoselectivity of the addition of vinyl Grignard reagent to aldehyde **5-14** could be predicted by Felkin-Anh model, the real chirality of C5 needed to be determined to make sure the desired compound was obtained. Due to the free rotation of the side chain, the chiral center (C5) could not be determined by NMR before RCM reaction. After RCM reaction, six-membered ring was formed and the peaks of the diastereomers were clearly seen by NMR. The C5 stereochemistry was only determined by the coupling constant between H5 and H6 (11.7 Hz) previously.[16] The relative chirality was confirmed by NOE study and the ^{1}H & ^{13}C NMR of **5-5** and **5-20** were fully assigned using COSY and HMQC (**Table 5-5** in **Experimental Section**).

The C13 side chain was synthesized from β-lactam **1-16**. Due to the concern that the α-position of the carbonyl group might epimerize during esterification, the OH and the NH groups were protected as oxazolidine. EE protected β-lactam was first reacted with DMAP, TEA, and benzoyl chloride to produce **5-22**. Ethanol and hydrochloric acid were then used to remove the 1-ethoxyethoxy (EE) protecting group. The resulting compound **5-23** was reacted with DMAP and TEA in methanol to open the lactam ring to produce **5-24** in good yield. Then, **5-24** was treated with *p*-anisaldehyde dimethyl acetal in the presence of a catalystic amount of pyridinium *p*-toluenesulfanate (PPTS) to generate

oxazolidine **5-25**. The purified compound **5-25** was then hydrolyzed with lithium hydroxide to afford the protected side chain **5-4**.
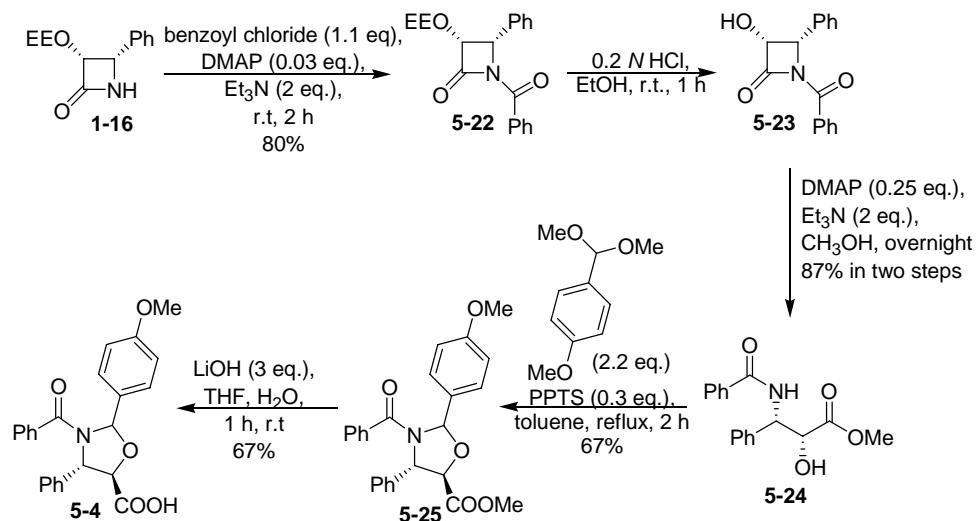
Scheme 5-4. Synthesis of intermediate 5-4

Acid **5-4** was then coupled to the scaffold **5-3** in the presence of DMAP and 1-ethyl-3-(3-dimethylaminopropyl)carbodiimide hydrochloride (EDC·HCl) to produce **5-26**. The protecting group was then removed using *para*-toluenesulfonic acid (*p*-TSA) to afford the desired compound **5-2** (**SB-H-102**) in good yield.
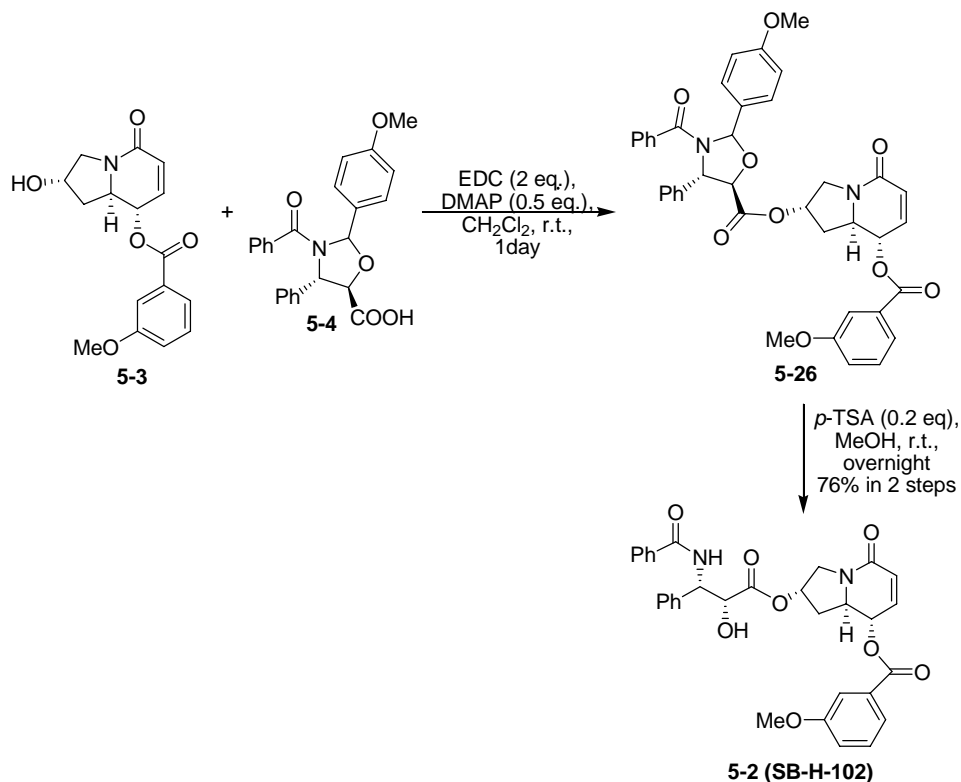
Scheme 5-5. Synthesis of SB-H-102

As shown in **Table 5-3**, **SB-H-102** possesses only modest cytotoxicity against all the cell lines assayed.

Table 5-3. *In vitro* cytotoxicities (IC$_{50}$, μM^a) of newly synthesized taxol-mimicking anticancer agents

Taxoids	LCC6-WT^b	LCC6-MDR^c	H460^d	HT-29^e	MCF7^f	NCI/ADR^g
Paclitaxel	0.0045	0.323	0.0047	0.0042	0.003	0.518
SB-H-102	29	>30	17	>30	26	27±2.5

^{a}The concentration of compound which inhibits 50% of the growth of human tumor cell line; ^{b}LCC6-WT: human breast carcinoma; ^{c}LCC6-MDR: MDR transduced line; ^{d}H460: NSCLC; ^{e}HT-29: human colon carcinoma; ^{f}MCF7: human breast carcinoma; ^{g}NCI/ADR: human ovarian carcinoma with MDR phenotype.

The weak activities in cytotoxicity assay and tubulin polymerization assay of the paclitaxel mimics based on structure **5-1** indicated that these compounds are over-simplified and could not effectively mimic the three-dimentional structure of paclitaxel bound to tubulin.

Recently, Downing *et al* determined the structure of epothilone A, bound to α,β-tubulin in zinc-stabilized sheets, by a combination of electron crystallography at 2.89 angstrom resolution and nuclear magnetic resonance–based conformational analysis.[24] The overlay of epothilone A and paclitaxel (T-Taxol structure) demonstrated that the binding pocket in a unique and qualitatively independent manner, although they overlapped in their occupation of a rather expansive common binding site on tubulin (**Figure 5-9**). The result indicated that none of the three common pharmacophore models was accurate.
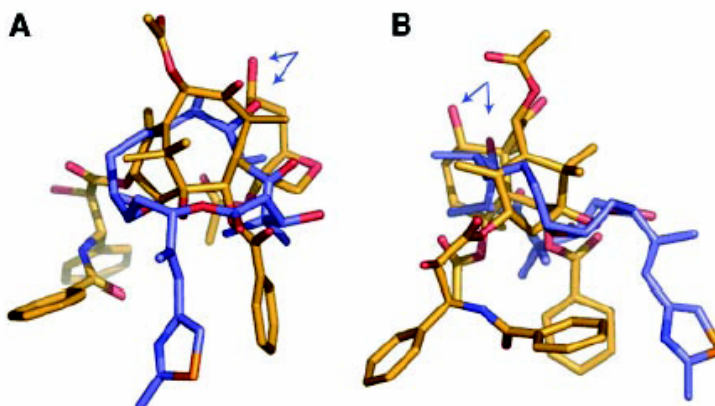
Figure 5-9. Superposition of EpoA (blue) and T-Taxol (gold) in β-tubulin as determined by electron crystallography[24]

Ojima's model common pharmacophore model used the polar conformation of paclitaxel, which is proven not to be the binding conformation, but the complex baccatin skeleton indeed served as a scaffold and active paclitaxel mimics could be designed based on the binding conformation of paclitaxel in tubulin. Therefore, the accomodadtion of the bioactive conformation of paclitaxel to the molecular design is necessary.

§ 5.2.2 Design of Novel Paclitaxel Mimics Based on the REDOR-Taxol Conformation

The new design of the paclitaxel mimics was based on the search of structure-simplified compounds keeping the binding conformation of paclitaxel in β-tubulin. The structure search began with the modification of the indolizidine scaffold to mimic REDOR-Taxol conformation. The two-step minimization procedure (described in **Chapter III**)[25] was modified and a series of compounds were examined by MM energy-minimization in β-tubulin.

To mimic **SB-T-2053**, compound **5-27** was first designed, which contained the macrocycle moiety of **SB-T-2053** and the scaffold **5-1**. However, because the dihedral angle of the *trans*-diol in the indolizidine was different from the dihedral angle in 14-OH-10-DAB, the overlay was very poor. The analogues of compound **5-27** with different chirality in the bicycle system (**5-28**), or the [4,4,0] bicyclic system (**5-29**) were also tried, but the results were still not satisfactory.
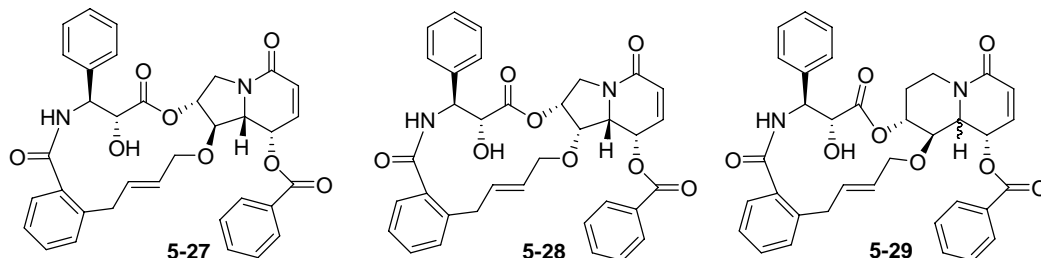
Figure 5-10. Designed macrocyclic paclitaxel mimics based on 5-1 and SB-T-2053

Inspired by the C4-C3'-linked macrocyclic taxoids, macrocyclic paclitaxel mimics with tricyclic scaffolds (**5-30** - **5-33**) were designed, which gave good overlays with the REDOR-Taxol structure in β-tubulin.

215
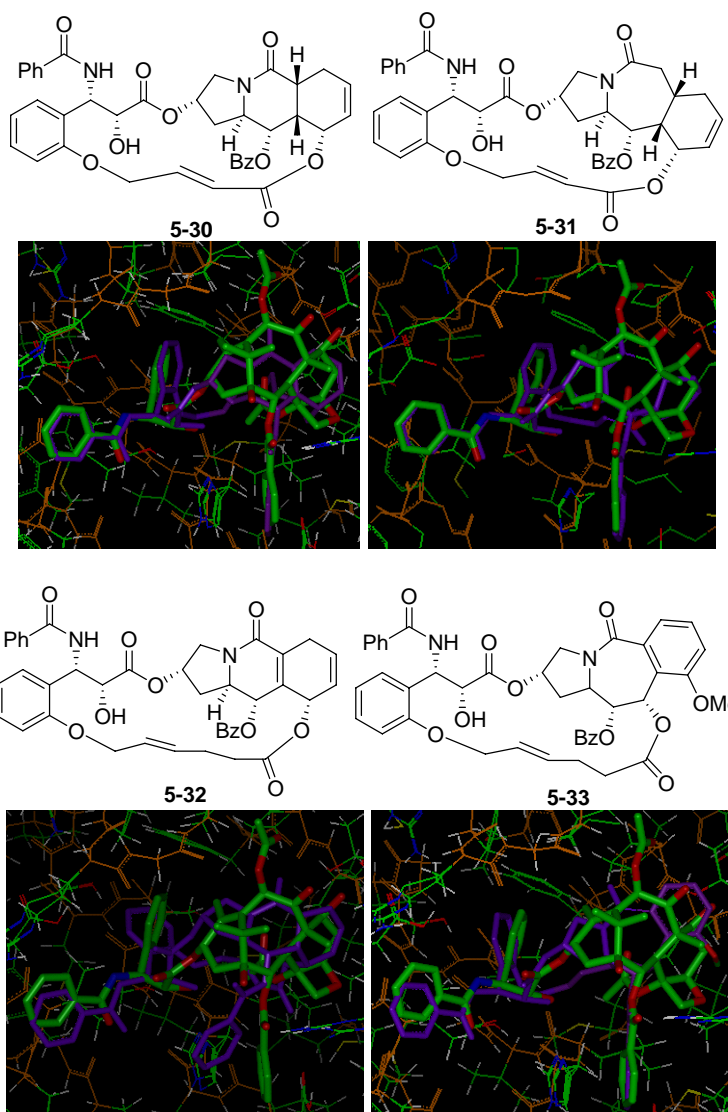
Figure 5-11. Overlays of 5-30, 5-31, 5-32, 5-33 (blue) and REDOR-Taxol (green)

However, these compounds contain too many chiral centers and are not easy to synthesize. when the structures were simplified to bicyclic systems, such as **5-34** and **5-35**, the overlays became poor, which indicated that the third ring is necessary to keep the position even if it was benzene ring.
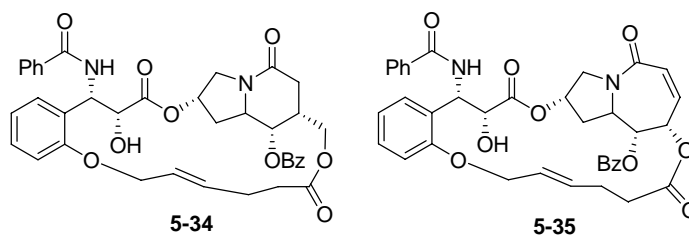
Figure 5-12. Structures of 5-34 and 5-35

Compound **5-36,** with a benzene ring as the third ring, was designed, which showed a very good overlay with the REDOR-Taxol. Its open-chain analogues **5-37** and **5-38** (with 5-7-6 ring system) also show a good overlay. The structures of these compounds are simple, since the third ring is a benzene ring. Thus, they were selected as our designed paclitaxel mimics.
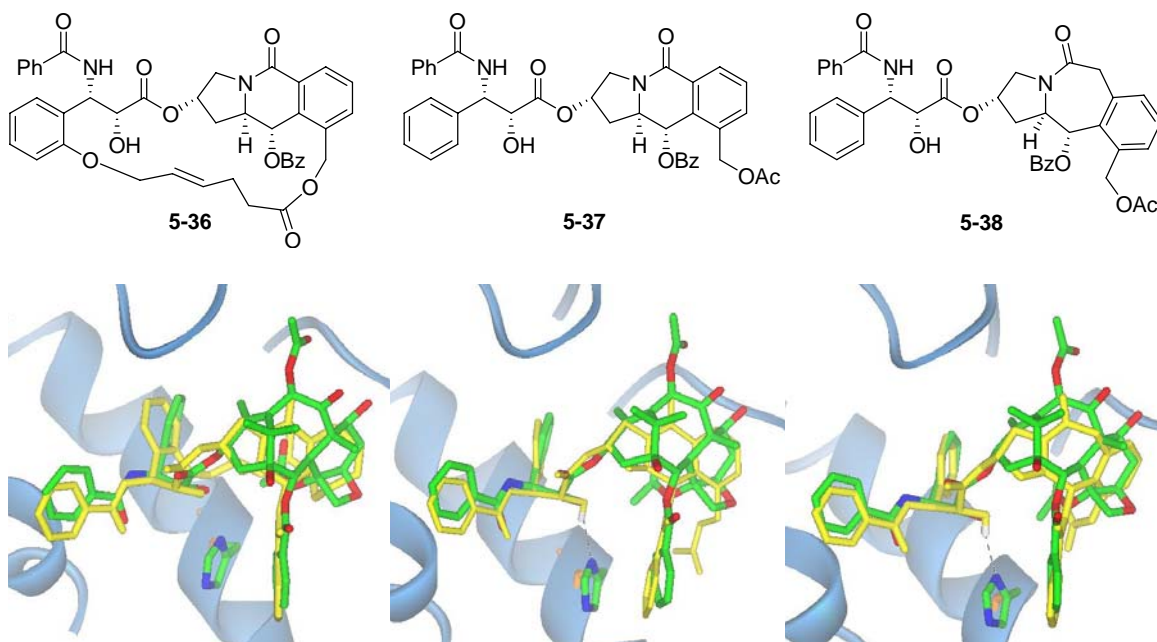
Figure 5-13. Overlays of 5-36, 5-37, 5-38 (yellow) and REDOR-Taxol (green)

§ 5.2.3 Preliminary studies

The original synthetic plan is shown in **Scheme 5-6**. The syntheses of **5-36** and **5-37** began with 1,6-dimethylbromobenzene. Dibromination, hydrolysis and protection with different group would afford **5-41**. The lithium reagent or Grignard reagent **5-40** would couple with aldehyde **5-14** and ring closure would give **5-39**. Macrocylic compound **5-36** and open-chain compound **5-37** could be obtained after side chain attachment.
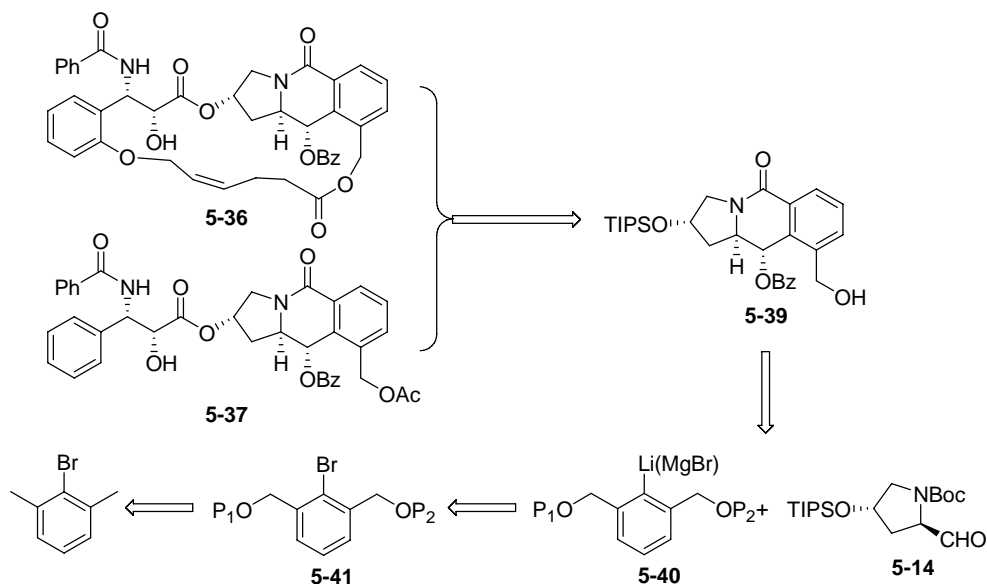
Scheme 5-6. Retro-synthesis of 5-36 and 5-37

As shown in **Scheme 5-7**, the reaction of 1,6-dimethylbromobenzene with 2.3 equiv of NBS in the presence of AIBN in CCl$_4$ [26] followed by hydrolysis in water and dioxane with calcium carbonate[27] afforded the desired diol **5-43** in 49% yield for two steps, accompanied by **5-42** and **5-44**. By using 1.3 or 4.0 equivalent of NBS, **5-42** or **5-44** was obtained in good yields with better selectivity.
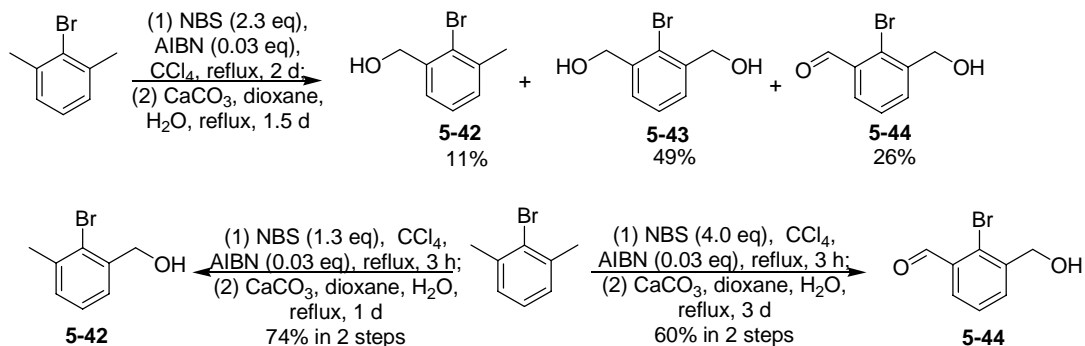
Scheme 5-7. Preparation of 5-42, 5-43 and 5-44

Alcohol **5-42** was protected with TMS group to afford **5-45** in 92% yield. Diol **5-43** was mono-protected with benzyl group using Boger's procedure to give **5-46** in 52% yield[28] and the di-protected product **5-47** in 29% yield. Protection of **5-46** with TES group or TMS group afforded **5-48** or **5-49** in good yield.
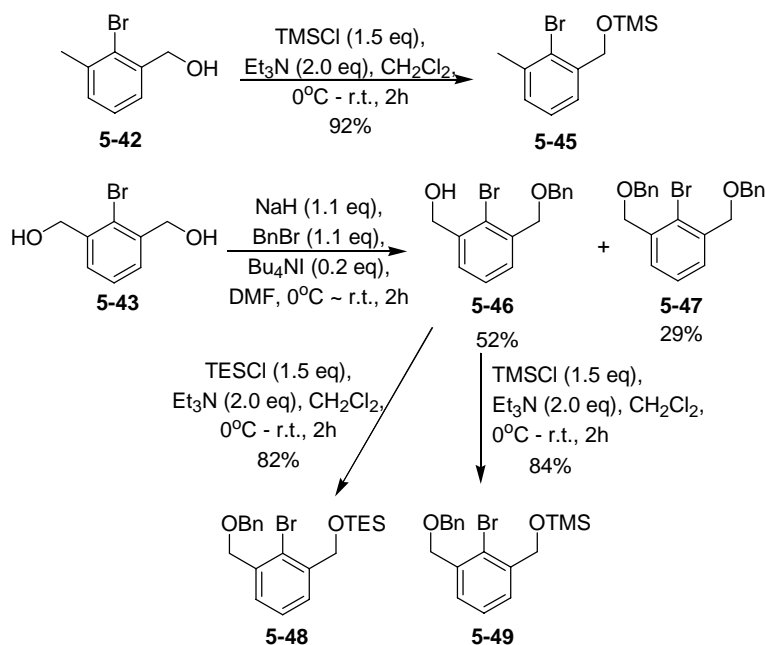
Scheme 5-8. Preparation of 5-45, 5-48 and 5-49

The Grignard reagents and the lithium regents were successfully obtained from **5-45**, **5-48** and **5-49** using standard methods.[29, 30] However, the coupling reaction with aldehyde **5-14** was not successful, probably due to the steric hindrance of the substrates.

5-45: R_1 = H, R_2 = TMS;
5-48: R_1 = OBn, R_2 = TES;
5-49: R_1 = OBn, R_2 = TMS
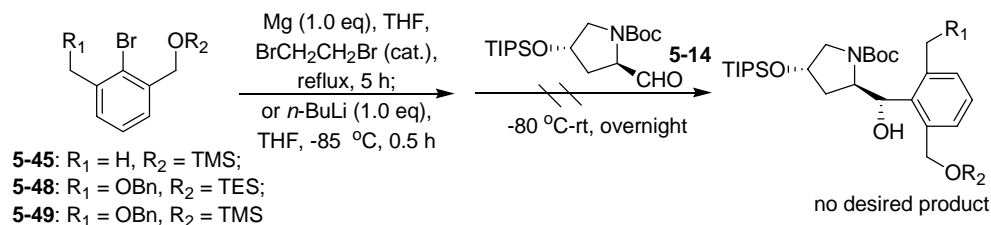
Scheme 5-9. The coupling reaction with 5-14

In 2005, Akiba *et al.* reported similar reactions with diphenyl ketone using a lithium reagent, indicating that a similar substrate with small protecting groups might afford the desired product, while the silyl protecting groups were too bulky for this reaction.[31] Because a methyl ether group would need very harsh conditions to remove, MOM group was selected as the protecting group.
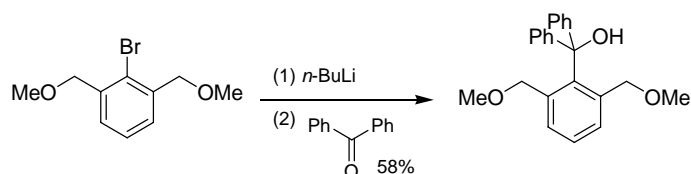
Scheme 5-10. Similar coupling reaction[31]

As shown in **Scheme 5-11**, diol **5-43** was first reacted with MOMCl in the presence of *N,N'*-diisopropylethylamine to afford **5-50** in quantative yield. To further minimize

the steric hindrance, a mono-protected substrate **5-52** was also prepared using a two-step procedure from **5-44**.
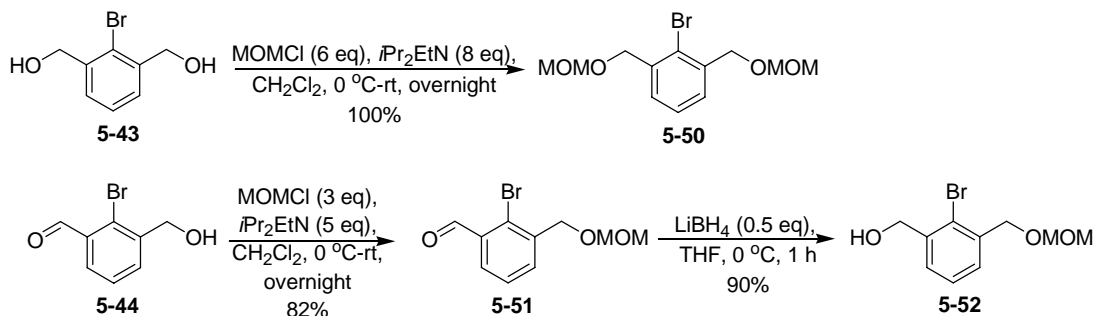
Scheme 5-11. Preparation of 5-50 and 5-52

As shown in **Scheme 5-12**, the corresponding Li-reagent was generated by treating **5-50** with *n*-BuLi and then reacted with **5-14** to give the desired product **5-53** in 35% yield. The two MOM groups were still too bulky and the conversion was not complete (only 37% conversion in the coupling step). The alcohol **5-53** was protected by Ac group to afford **5-54** in good yield. Thus, **5-52** was converted to the dilithium reagent by using 2.1 equivalents of *n*-BuLi and reacted with **5-14** to gibe the coupling product **5-55** in 45% yield. The yield of **5-55** was improved to 83% when HMPA was used. The product **5-55** was protected by Ac group to give **5-56** in 100% yield.
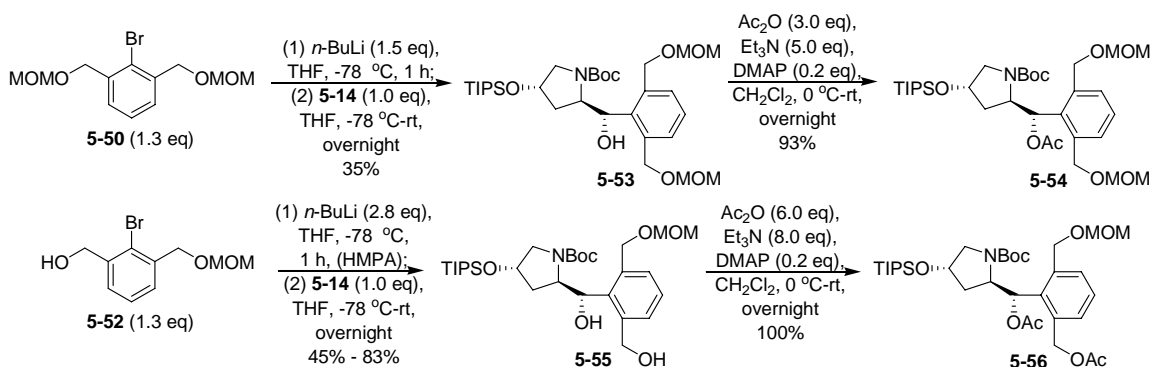
Scheme 5-12. The coupling reactions of 5-50 and 5-52 with 5-14

However, it needed too many steps to convert **5-56** or **5-58** to the desired tricyclic product **5-39**, which is due to the fact that MOM group could not be removed under very mild conditions. Thus, two other substrates, **5-59** and **5-60**, were prepared, but the coupling reactions did not afford the desired products.

Scheme 5-13. Preparation of 5-59 and 5-60

In 2000, Yamamoto *et al.* reported Pd-catalyzed intramolecular nucleophilic addition of aryl bromides to ketones with excellent diastereoselectivity,[32] which could be used for our system (**Scheme 5-14**).

Scheme 5-14. New method to prepare 5-62[33]

As shown in **Scheme 5-15**, acetic ester **5-63** was obtained by acetylation of alcohol **5-13**. After deprotection using TFA conditions, the resulting amine **5-64** was reacted with acid chloride **5-65** to afford the desired amide in moderate yield. However, an undesired product **5-68**, instead of **5-67**, was obtained after the deprotection under basic conditions. The strange reaction may be caused by the steric conflict between the groups on benzene ring and the proline moiety. The relatively unstable amide, instead of the ester, was hydrolyzed and the resulting amino ester underwent intramolecular acetyl transfer to afford more stable hydroxyl amide alcohol **5-68**.

Scheme 5-15. Preparation of 5-67

As shown in **Scheme 5-16**, the Boc group in **5-13** was removed by the standard procedure and the direct coupling of amino alcohol **5-69** and acid chloride **5-65** afforded **5-67** in 56% yield. The moderate yield was probably due to the impurity in **5-69**, which could not be purified by column chromatography, because of its extremely high polarity. Since the 5-6-6 scaffold was successfully obtained by another method, this route was abandoned.

Scheme 5-16. Preparation of 5-67

§ 5.2.4 Synthesis of Novel Paclitaxel Mimics SB-H-301 and SB-H-2001

After unsuccessful screening of substrates, bromide **5-70** with a small vinyl group serving as a protecting group was selected. Wittig reaction of the formyl alcohol **5-44** with methyltriphenylphosphonium ylide afforded vinylbenzyl alcohol **5-70** in good yield.[34] As shown in **Scheme 5-17**, the Li-reagent was generated by treating **5-70** with 2.2 equivalents of *n*-BuLi. The coupling reaction of **5-71** with **5-14** in the presence of HMPA afforded the desired product **5-72** in 81% yield. The subsequent protection of hydroxyl groups by acetyl groups gave **5-73** in 97% yield.

Scheme 5-17. Synthesis of 5-73

As shown in **Scheme 5-18**, the vinyl compound **5-73** was subjected to ozonolysis oxidization, esterification, deprotection and cyclization to afford the desired 5-6-6 scafold in 50% yield for 5 steps. The diastereomers, **5-77** and **5-78**, were separated by column chromatography. However, the diastereoselectivity was not high (d.r. ~2:1) with the undesired diastereomer **5-78** as the major product.

Scheme 5-18. Synthesis of 5-77 and 5-78

The relative chirality in **5-77** and **5-78** was confirmed by NOE measurements and analysis. The ^{1}H NMR and ^{13}C NMR of **5-77** and **5-78** were fully assigned based on 2D NMR studies (see **Table 5-6** in **Experimental Section**).

The side-chain modification began with the undesired diastereomer **5-78** to check whether it could be converted to the desired diastereomer by the Mitsunobu reaction. As shown in **Scheme 5-19**, deprotection of **5-78** under basic condition afforded diol **5-79** in good yield. The selective esterification of the primary alcohol did not have good selectivity, which indicated that the acetyl group was not bulky enough to distinguish the two hydroxyl groups. Thus, the bulkier TBDMS group was used to protect the primary alcohol, affording **5-80** in excellent yield.[35] However, the Mitsunobu reaction of **5-80** or **5-81** was not successful under standard conditions.[36] Harsh conditions could not be used, because elimination reaction could occur to produce very stable product **5-83**.
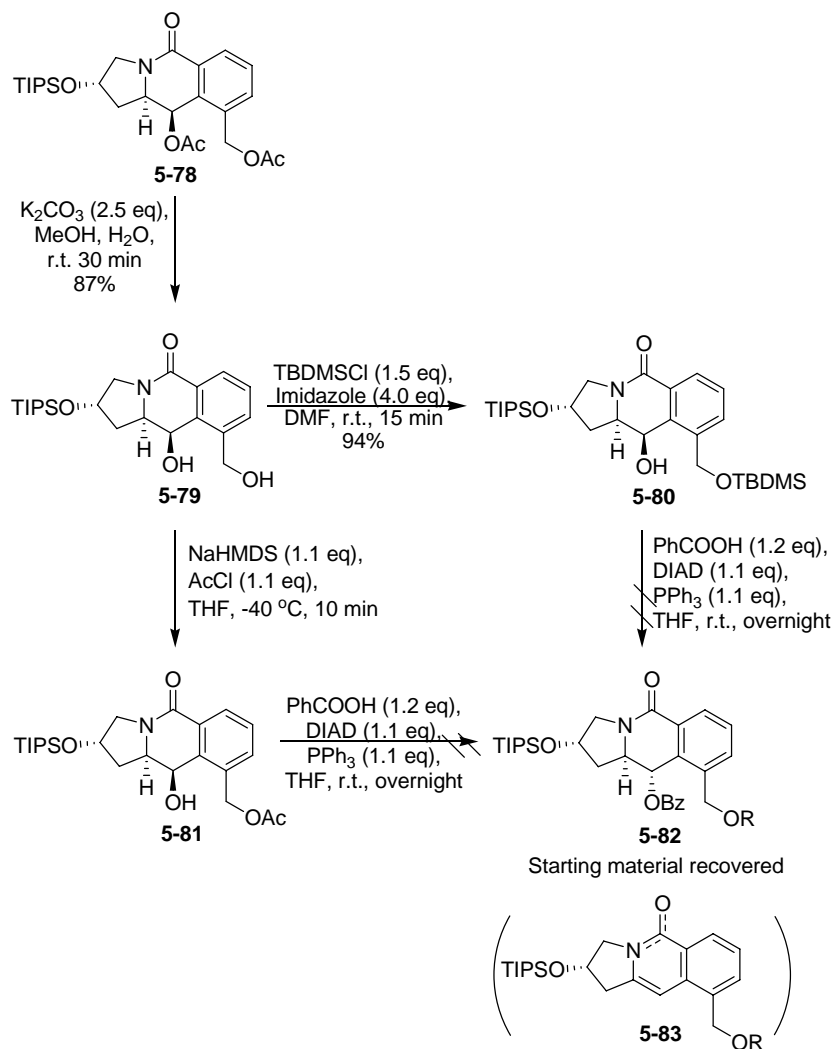
Scheme 5-19. Synthesis of 5-80 from 5-81

The modification of **5-77** proceeded in a straightforward manner (**Scheme 5-20**). Deprotection of **5-77** under basic conditions gave **5-84** in good yield. The protection of the primary alcohol moiety of **5-84** by TBDMSCl in the presence of imidazole showed very high selectivity, affording **5-85** in 99% yield.[35] Benzoylation of the secondary alcohol moiety of **5-85** gave **5-86** in quantitative yield. Using less amout of benzoyl chloride resulted in low conversion, probably due to the steric hinderance caused by the TBDMS group. Acidic deprotection of TBDMS group followed by esterification with Ac₂O gave **5-88** in excellent overall yield.[37]

Scheme 5-20. Synthesis of 5-88

Scheme 5-21. Synthesis of 5-37 (SB-H-301)

The synthesis of **5-37 (SB-H-301)** was completed in **Scheme 5-21**. After removal of TIPS, **5-89** was coupled with oxazolidine acid **5-4** in the presence of EDC and DMAP in dichloromethane to give **5-90** in 82% yield. The final deprotection of **5-90** afforded **5-37** (**SB-H-301**) in good yield.

The synthesis of **5-36** started from the preparartion of oxazolidine acid **5-98**, as shown in **Scheme 5-22**. Compound **5-94** was obtained in high overall yield from enantiopure β-lactam **3-54** through standard modifications. The TIPS group of **5-94** was removed by HF/Py, followed by ring opening under basic conditions, affording **5-96** in 82% yield for two steps.[32] Then, **5-96** was treated with *p*-anisaldehyde dimethyl acetal in the presence of catalytic amount of pyridinium *p*-toluenesulfanate (PPTS) to afford oxazolidine **5-97** in good yield. The hydrolysis with lithium hydroxide provided the carboxylic acid **5-98** in 88% yield.[38]
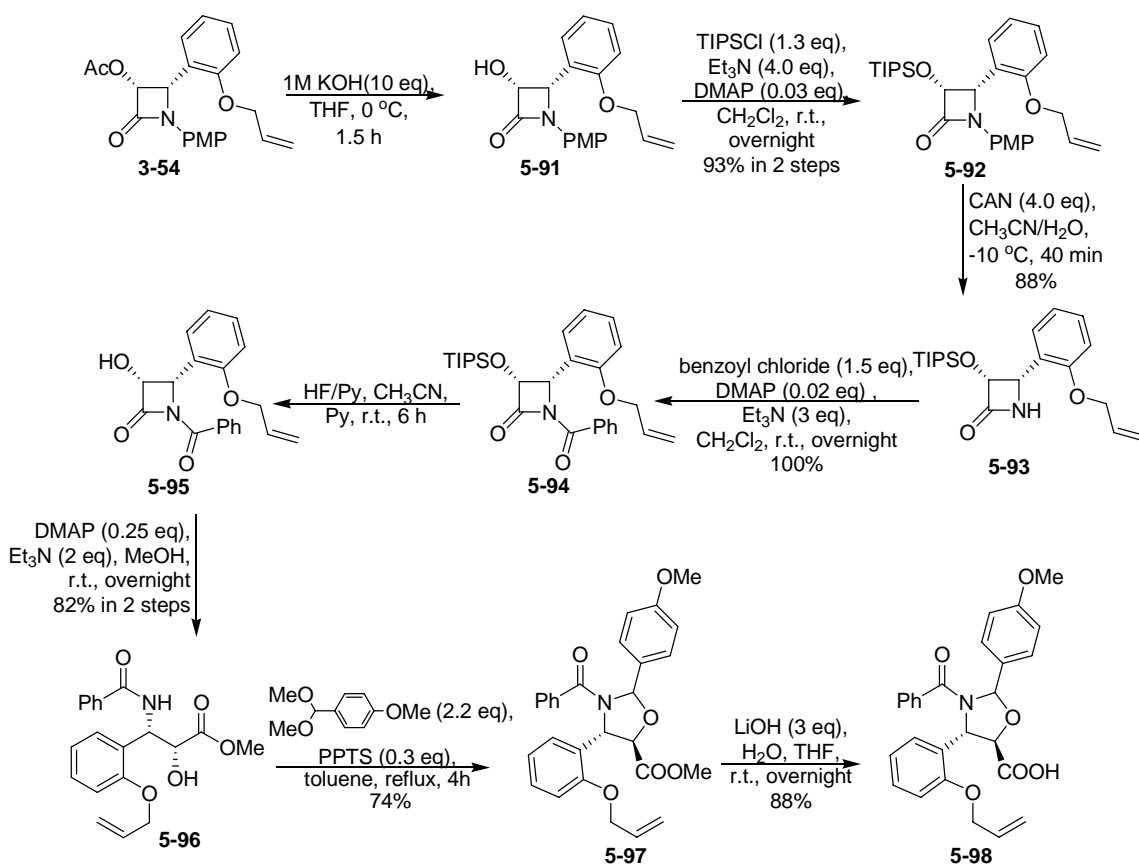
Scheme 5-22. Prepapration of 5-98

The synthesis of intermediate **5-100** is shown in **Scheme 5-23**. Modification of the primary alcohol moiety of **5-85** with 4-pentenoyl chloride followed by TIPS deprotection under standard HF/pyridine conditions afforded **5-100** in 97% yield for two steps.
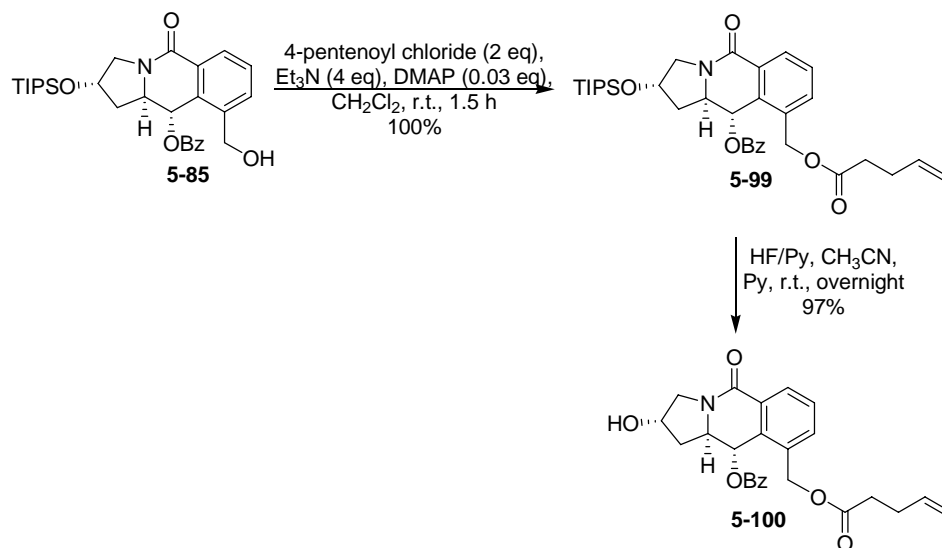
Scheme 5-23. Synthesis of 5-100

The coupling reaction of **5-100** with oxazolidine acid **5-98** gave **5-101** in high yield and the subsequent acidic deprotection afforded **5-102** in good yield. The RCM reaction was very slow and not complete after 3 days at room temperature and 2 days at reflux. The final product **5-36** (**SB-H-2001**) was obtained in moderate yield. The same reaction at room temperature for 2 days gave almost no product.
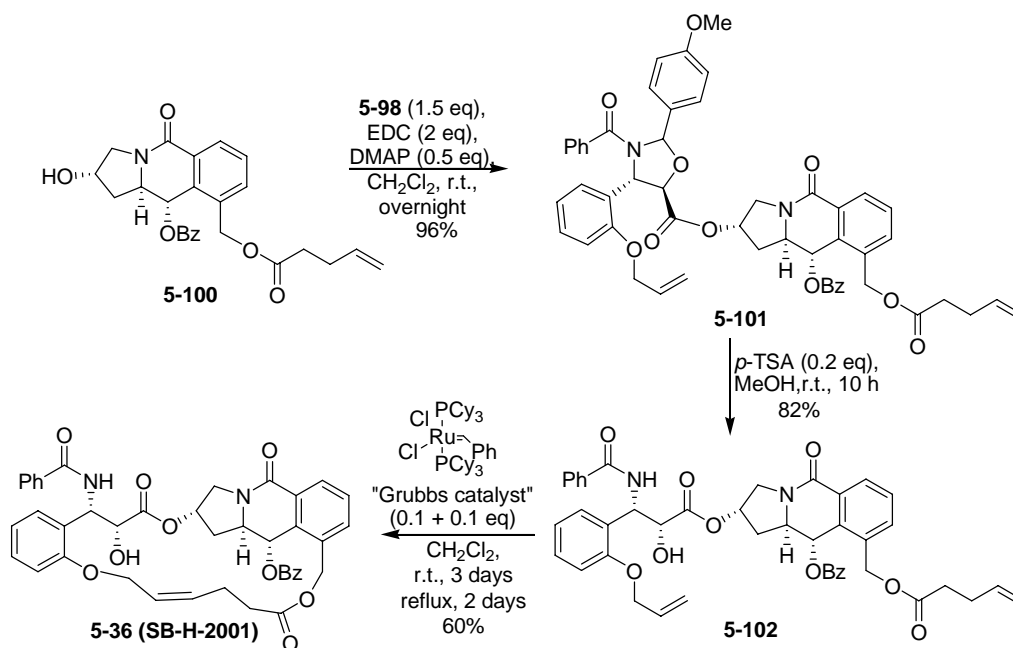
Scheme 5-24. Synthesis of 5-36 (SB-H-2001)

§ 5.2.5 The Diastereoselectivity of the Coupling Reaction

The ratio of **5-77** to **5-78** was about 1:2, in favor of the undesired diastereomer. This selectivity was different from previous bicyclic indolizidine synthesis. By using Grignard reagent, a 5:1 d.r was obtained in favor of the desired diastereomer, while 1:1 d.r. was obtained by using more active lithium reagent (**Scheme 5-25**).[39]
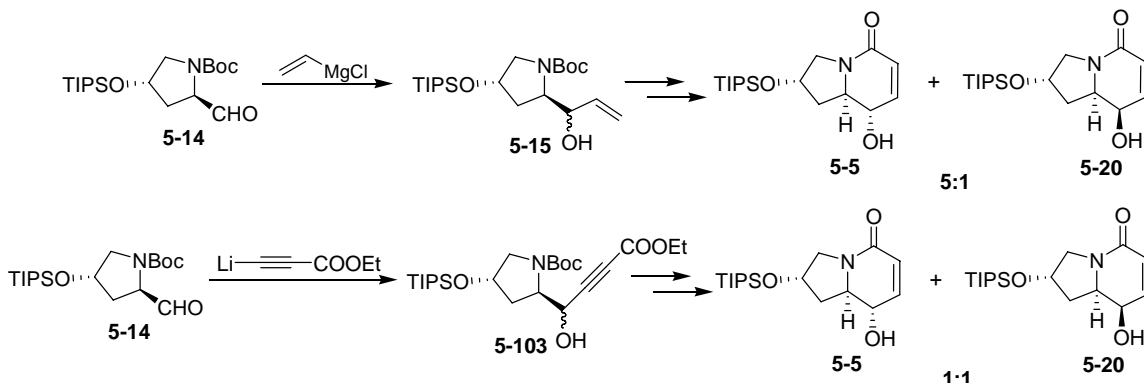
Scheme 5-25. Diastereoselectivity in the indolizidine synthesis

The reversed diastereoselectivity was probably caused by chelation between the carbonate carbonyl of the Boc group with the benzylic *O*-Li, forcing the aldehyde to take a chelated conformation (**Scheme 5-26**).[40] If the chelation is blocked and less active Grignard reagent could be used, satisfactory diastereoselectivity should be obtained.
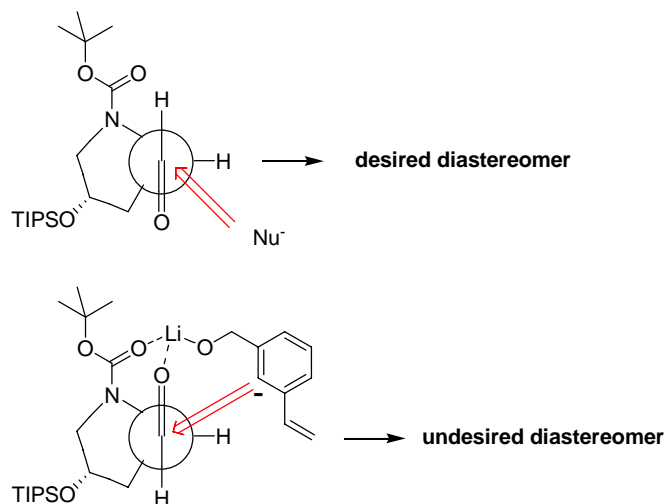
Scheme 5-26. Possible mechanism in the two nucleophilic reactions

Thus, two other bromides, **5-104** and **5-106**, were prepared to check the diastereoselectivity as shown in **Scheme 5-27**. Wittig reaction of aldehyde **5-51** with a ylide afforded vinylbenzene **5-104** in 97% yield.[34] The diol **5-43** was oxidized and the resulting carbonyl groups were converted to vinyl groups with a Wittig reagent to give **5-106** in good yield.

229
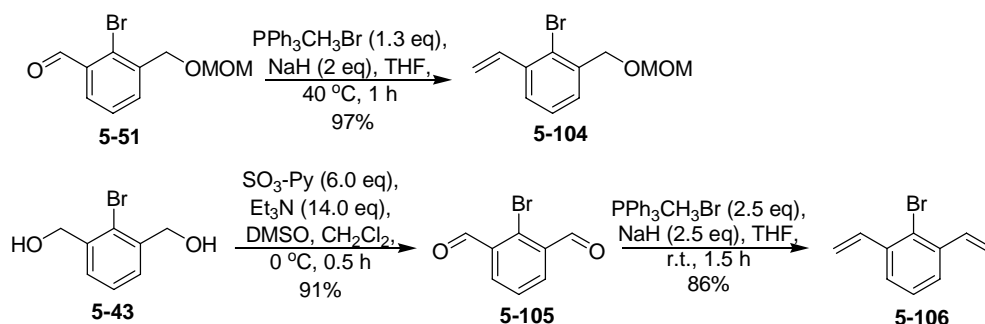
Scheme 5-27. Preparation of 5-104 and 5-106

The Li-reagent **5-107** was generated by treating **5-104** with 1.1 equivalents of *n*-BuLi and the coupling reaction afforded the desired product **5-108** in good yield. The subsequent protection of the hydroxyl group gave **5-109** in 70% yield for 2 steps. A diastereomer mixture **5-108** was subjected to a straightforward five-step transformations to give the desired product **5-113** and **5-114** without purification of any intermediate in 50% overall yield for five steps.[39, 41] However, the diastereoselectivity was found to be 3:4, still in favor of the undesired diastereomer (**Scheme 5-28**).
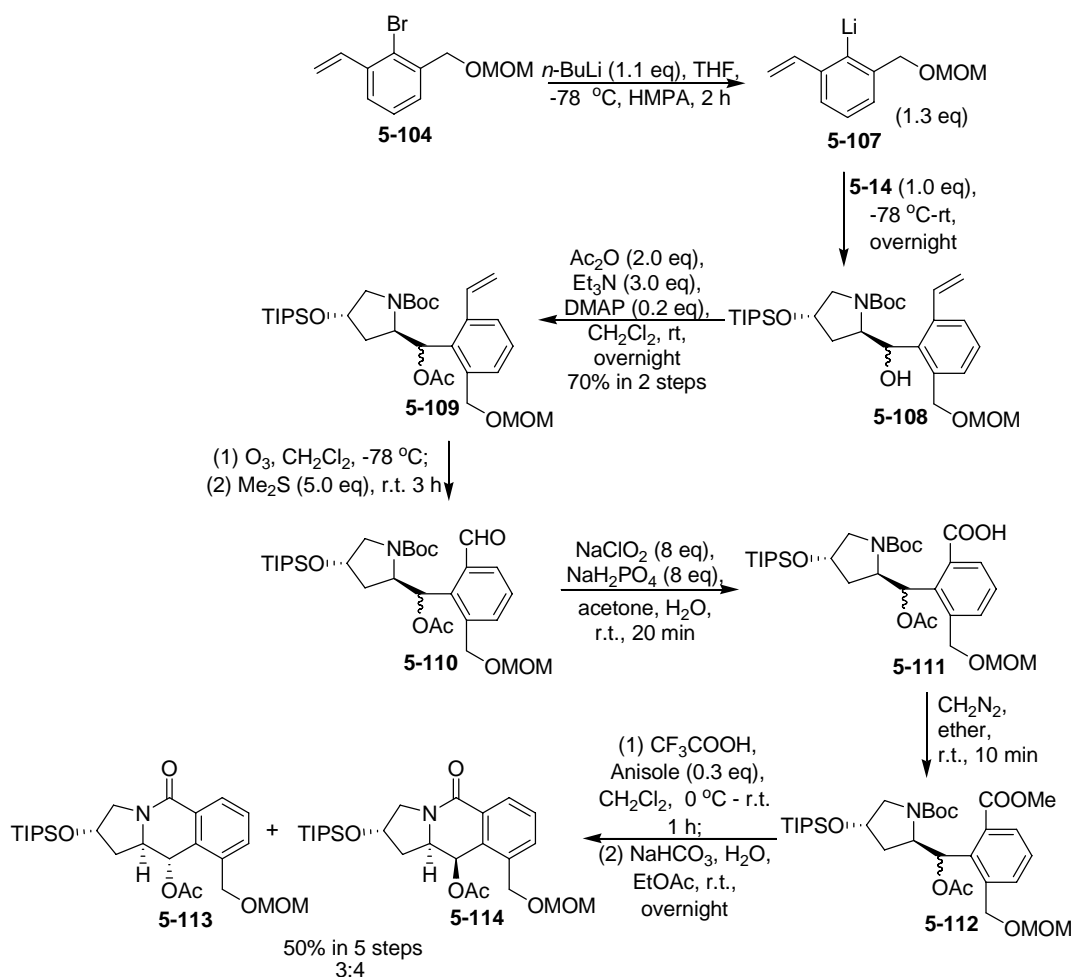
Scheme 5-28. Synthesis of 5-113 and 5-114

Because lithium reagents are very reactive with low selectivity, the weaker but more selective reagents, such as Grignard reagents and zinc reagents, were examined.[42] As shown in **Scheme 5-29**, bromobenzene **5-102** was successfully converted to Grignard reagent **5-115** by standard procedure,[29] but the coupling reaction only afforded the desired product in only very low yield. The conversion was very low even when the temperature was raised to room temperature. Thus, the zinc reagent **5-116** was generated by metal-exchange method.[43] As anticipated, this weak nucleophile **5-116** did not afford any desired product.
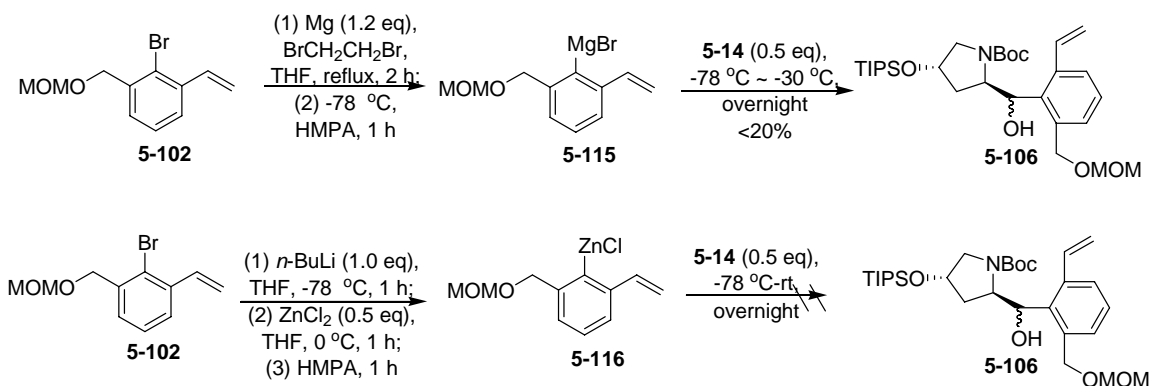
Scheme 5-29. Coupling reaction with Grignard reagent and zinc reagent

Next, divinylbromobenzene **5-106** was selected, because it has no oxygen to chelate and the size of vinyl group is smaller than the protected hydroxyl groups. As shown in **Scheme 5-30**, bromide **5-106** was converted to the corresponding lithium reagent[30] and the subsequent coupling reaction with **5-14** afforded the product 5-117 in 70% yield. After acetylation, ozonolysis,[44] oxidation,[41] esterification, deprotection and cyclization,[39] the desired product **5-121** was obtained in good yield in 5 steps and the diastereoselectivity was 1:1.
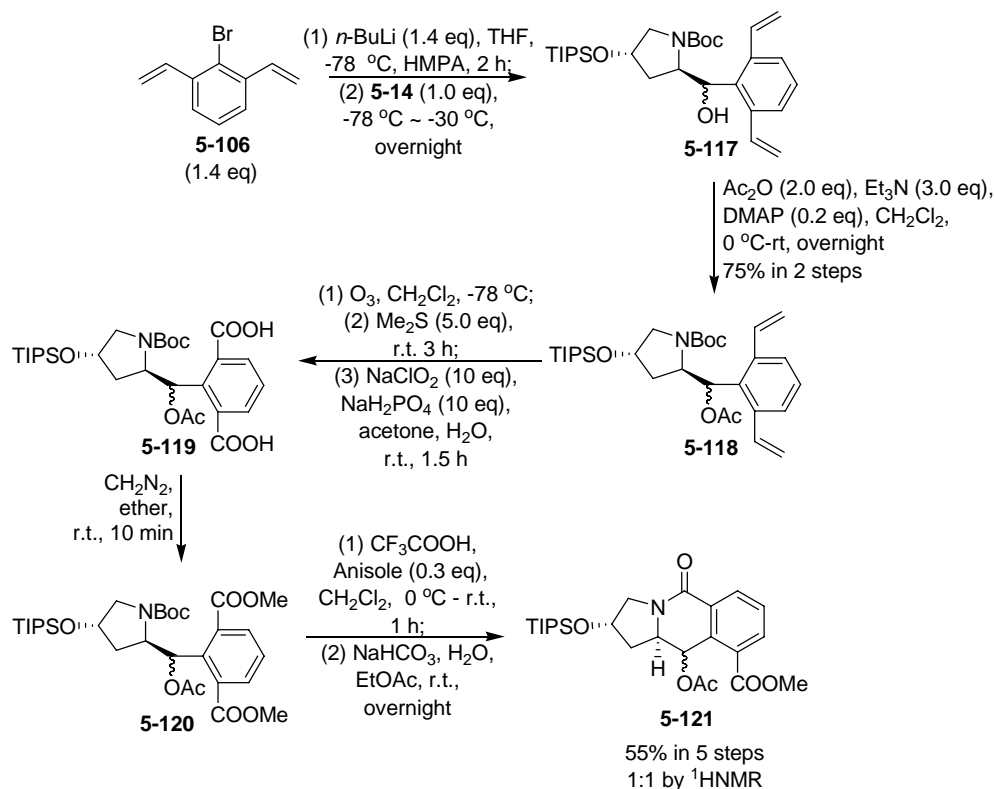
Scheme 5-30. Synthesis of 5-121

As shown in **Scheme 5-31**, by using two equivalents of the Grignard reagent generated from **5-106**, the desired product **5-117** was obtained in good yield. Using the same protocol as shown in **Scheme 5-31**, the same cyclized product **5-121** was obtained in good yield with a 1.5:1 ratio in favor of the desired diastereomer, which is so far the best result.[45] The ester **5-121** was converted to diols **5-83** and **5-79** by using 2 equivalents of lithium borohydride.
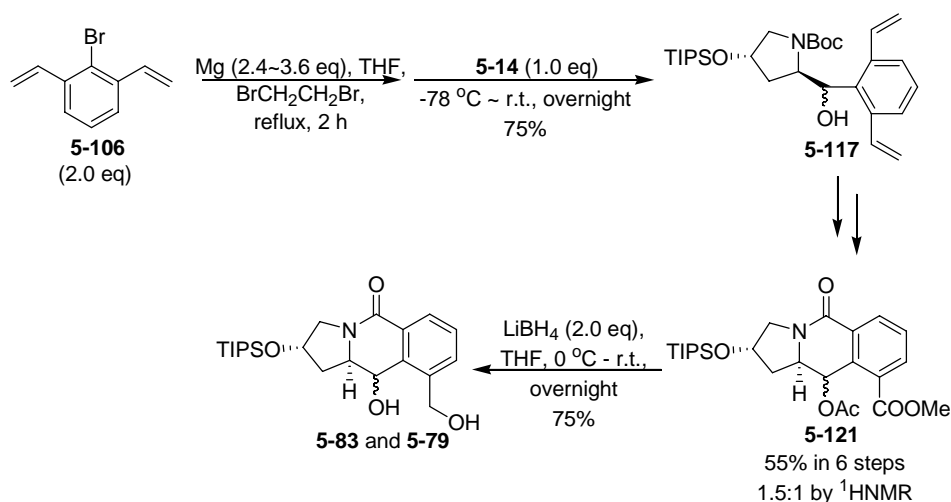
Scheme 5-31. Synthesis of 5-83 and 5-79

§ 5.2.6 Synthesis of SB-H-401

Wittig homologation of aldehyde **5-44** in the presence of NaHMDS, followed by hydrolysis afforded aldehyde **5-123** in good yield.[46] The second Wittig reaction afforded the allylbromobenzene **5-124** in moderate yield, due to polymerization of the aldehyde. The protection of the hydroxyl moiety of **5-124** by MOM group gave **5-125** in good yield.
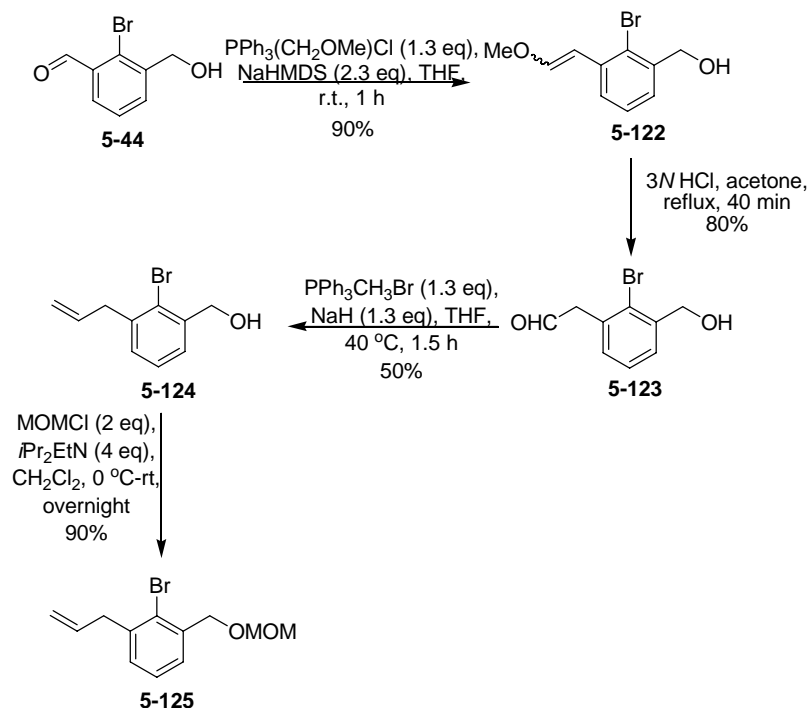
Scheme 5-32. Preparation of 5-125

With **5-125** in hand, a synthetic route similar to that described above was used to afford the coupling product **5-126**. The subsequent acetylation of **5-126** gave **5-127** in 70% yield for 2 steps.[45] After the same five-step protocol, the 5-7-6 scaffolds, **5-128** and **5-129**, were obtained in good overall yields, but the diastereoselectivity was 10:1 in favor of the undesired diastereomer **5-129**.[39, 41, 44]
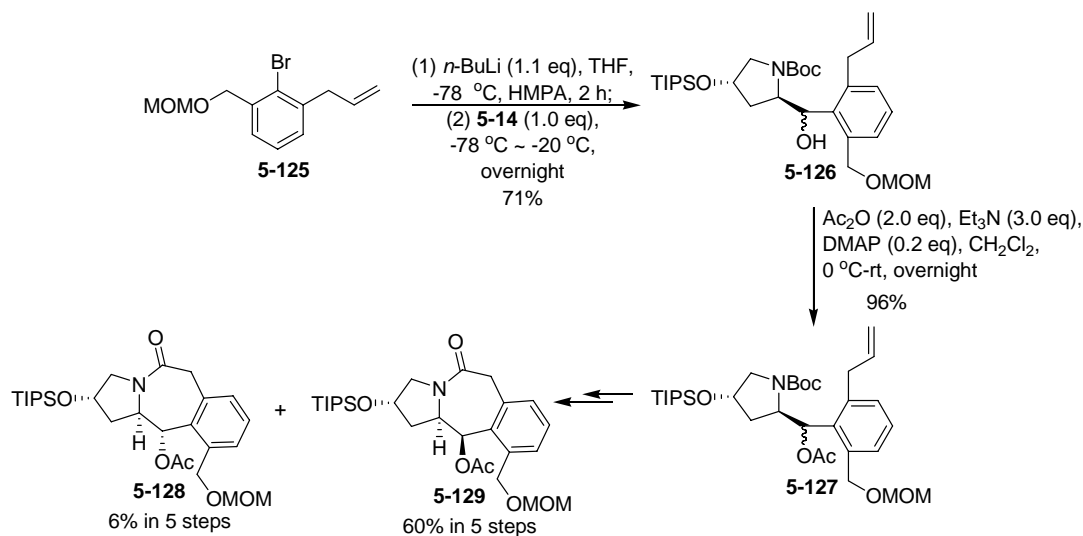
Scheme 5-33. Synthesis of 5-128 and 5-129

Compounds **5-128** and **5-129** were hydrolyzed to afford **5-130** and **5-132**, respectively, in good yields. However, the direct benzoylation of **5-130** did not proceed well, unlike the same reaction for the 5-6-6 scaffold **5-85**. Although a large excess amount of reagents were used, the reaction was still incomplete and the formation of an elimination product was observed. The same reaction was tried for **5-132** in a larger scale. In the presence of 12 equiv. of benzoyl chloride and 16 equiv. of triethylamine, the reaction was still not complete after 2 days. The desired product **5-133** was obtained only in 50% yield, accompanied by the elimination product as the major side-product. After deprotection of MOM group, **5-134** was obtained in excellent yield.
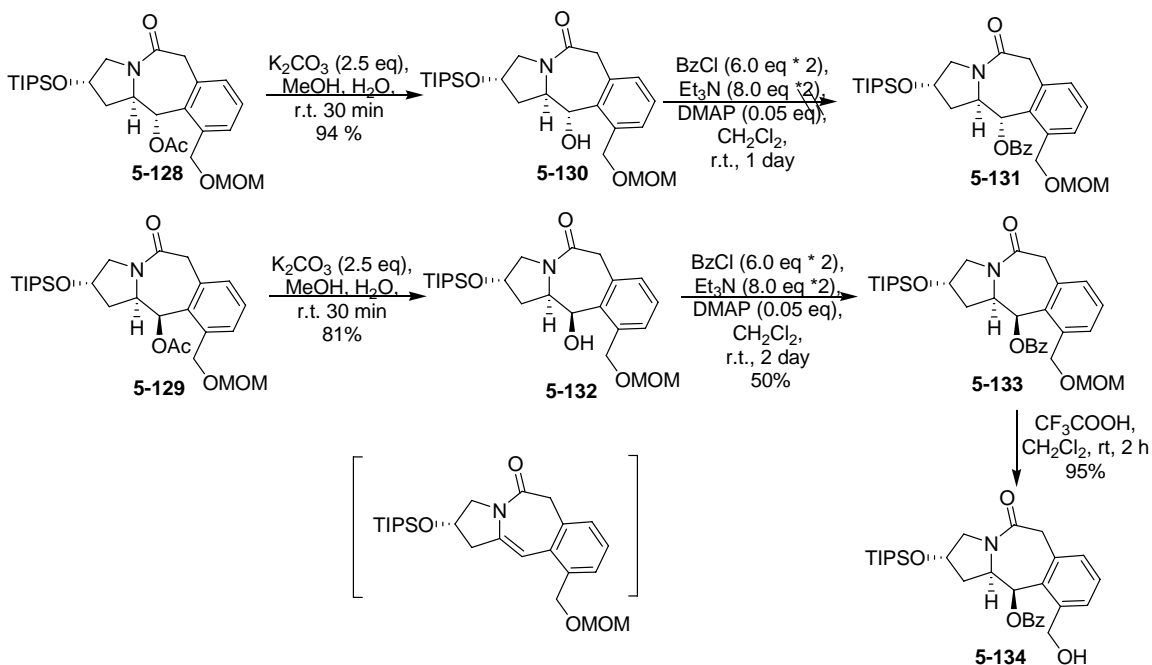
Scheme 5-34. Modification of 5-128 and 5-129

The Mitsunobu reaction was performed on **5-132** to invert the chiral center under very harsh conditions. The conversion was low, but the desired product **5-135** was obtained, albeit mixed with impurities. The removal of MOM group afforded pure **5-135** in 63% yield for 2 steps. The hydroxyl group was converted to an acetyl group, followed by standard deprotection with HF/py to afford **5-137** in high yield.
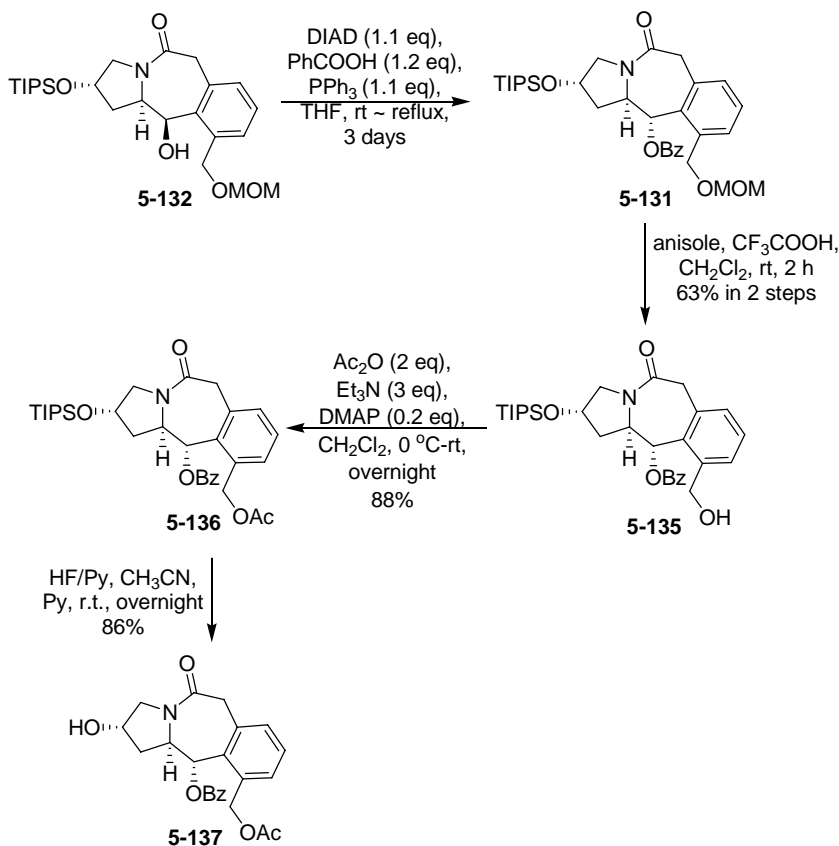
Scheme 5-34. Synthesis of 5-137

Unlike the 5-6-6 tricyclic scaffold, the 5-7-6 scaffold **5-128** can not aromatize if the hydroxyl group is oxidized. As shown in **Scheme 5-35**, **5-128** was oxidized with PCC to afford **5-133** in good yield, albeit with low conversion (40%). However, the reduction using sodium borohydride did not show any selectivity, which could be explained by molecular modeling study. As shown in **Figure 5-14**, compound **5-133** was built and minimized by Macromodel® program. There is no obvious difference between the *Re* face and *Si* face for the carbonyl group.

Scheme 5-35. Synthesis of 5-134

Figure 5-14. Energy-minimized structure of 5-133

The synthesis of **5-38** (**SB-H-401**) was completed as shown in **Scheme 5-36**. Alcohol **5-137** was coupled with oxazolidine acid **5-4** in the presence of EDC and DMAP in dichloromethane. The final deprotection afforded **5-38 (SB-H-401)** in good yield.

Scheme 5-36. Synthesis of 5-38 (SB-H-401)
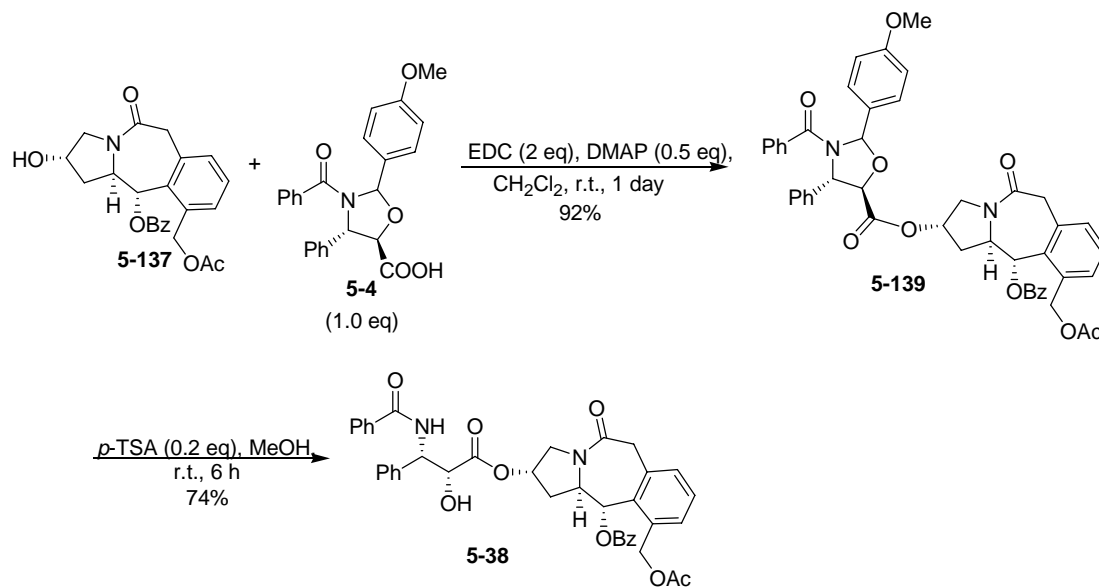
§ 5.2.7 Preliminary Cytotoxicity Assay of the Paclitaxel Mimics

SB-H-301 and **SB-H-2001** were assayed against the drug-resistent pancreatic cancer cell lines (PANC-1 and CFPAC) and the preliminary results are shown in **Table 5-4**.

Table 5-4. Preliminary Cytotoxicity Assay of the Paclitaxel Mimics

Coumpounds	IC_{50} (µM) (CFPAC)	IC_{50} (µM) (PANC-1)
Paclitaxel	0.013	0.06
SB-H-102	174.6	85.6
SB-H-301	1.86	70.2
SB-H-2001	/	94.8

The paclitaxel mimic **SB-H-301** with 5-6-6 scaffold shows 100 times higher potency than the bicyclic mimic **SB-H-102**, but still 100 times less potent than paclitaxel, against the CFPAC pancreatic cancer cell line. In the assay against PANC-1 pancreatic cancer cell line, these two mimics as well as the macrocyclic mimic **SB-H-2001** show similar activity, ~ 1000 times less activtive than paclitaxel. The results are not consistent with the result against CFPAC cell line and previous studies, which may caused by the low solubility of the mimics in cell culture media. Further cytotoxicity assay is still in progress in our laboratories.

§ 5.3 Summary

Paclitaxel mimics with simpler structures and similar or higher activity could be designed based on the binding conformation of paclitaxel. Accordingly, **SB-H-102** with the scaffold **5-1**, was synthesized and evaluated, which showed only modest cytotoxicity. Three new paclitaxel mimics were designed based on the REDOR-Taxol structure in β-tubulin. **SB-H-301** and **SB-H-2001** with a 5-6-6 core and **5-38** with a 5-7-6 core were synthesized. The coupling reaction of the lithium reagent or the Grignard reagent with the aldehyde produced the undesired diastereomer as the major product, due to the chelation of the substrates with lithium or magnesium. The diastereoselectivity was improved by modifying the substrates and a d.r. of 1.5:1 in favor of the desired diastereomer was obtained. New methods to improve the diastereoselectivity and further cytotoxicity assay are still in progress in our laboratories.

§ 5.4 Experimental Section

General Methods: ^{1}H and ^{13}C NMR spectra were measured on a Varian 300, 400, 500 or 600 NMR spectrometer. Melting points were measured on a Thomas Hoover Capillary melting point apparatus and are uncorrected. Optical rotations were measured on a Perkin-Elmer Model 241 polarimeter. IR spectra were recorded on a Perkin-Elmer Model 1600 FT-IR spectrophotometer. TLC was performed on Merck DC-alufolien with Kieselgel 60F-254 and column chromatography was carried out on silica gel 60 (Merck; 230-400 mesh ASTM). Purity was determined with a Waters HPLC assembly consisting of dual Waters 515 HPLC pumps, a PC workstation running Millennium 32, and a Waters 996 PDA detector, using a Phenomenex Curosil-B column, employing CH_3CN/water (2/3) as the solvent system with a flow rate of 1 mL/min. High-resolution mass spectra were obtained from Mass Spectrometry Laboratory, University of Illinois at Urbana-Champaign, Urbana, IL.

Materials: The chemicals were purchased from Aldrich Co. and Sigma and purified before use by standard methods. Tetrahydrofuran was freshly distilled from sodium metal and benzophenone. Dichloromethane was also distilled immediately prior to use under nitrogen from calcium hydride.

cis-4-Hydroxy-D-proline hydrochloride salt (5-7):[21]
To a mixture of acetic acid (12 mL) and acetic anhydride (12 mL) was added *trans*-hydroxy-L-proline **5-6** (1.0 g, 7.6 mmol). The mixture was refluxed for 5.5 h and then the solvent was removed to give a brown sticky oil. The oil was dissolved in 2 *N* hydrochloric acid (12 mL) and refluxed for 2 h. The brown solution was treated with activated carbon while hot and cooled down to room temperature. The mixture was filtered through celite and concentrated under reduced pressure. This solid obtained was used in the next step without any further purification.

N-(*tert*-Butoxycarbonyl)-*cis*-4-hydroxy-D-proline methyl ester (5-9):[36]
In a suspension of **5-7** (1.554 g, 7.6 mmol) in MeOH (6 mL) was added AcCl (0.25 mL, 3.8 mmol). The reaction mixture became homogeneous after the temperature reached 70 ℃. The reaction mixture was refluxed overnight before being poured into ether to precipitate out the methyl ester as a white solid. The reaction mixture was filtered and the solid collected was dried under vacuum to afford **5-8** as a white solid, which was used in the next step without any further purification. HRMS calcd. for $C_6H_{11}NO_3H^+$ 146.0817, found 146.0815 (Δ= -1.5 ppm).
To a solution of the white solid, thus obtained, in CH_2Cl_2 (35 mL) was added triethylamine (4.3 mL, 22.8 mmol), DMAP (0.232 g, 9.1 mmol) and *t*-Boc anhydride (1.98 g, 9.1 mmol). The reaction mixture was stirred overnight, quenched with saturated aqueous NH_4Cl solution and extracted with EtOAc (50 mL x 3). The organic layers were combined and dried over anhydrous $MgSO_4$ and the solvent was concentrated under reduced pressure. The residue was purified by column chromatography on silica gel using 1% MeOH in CH_2Cl_2 as the eluent to afford **5-9** as a white solid (1.38 g, 75% in 3 steps): ^{1}H NMR (300 MHz, $CDCl_3$) δ 1.38 (s, 4.5 H), 1.42 (s, 4.5 H), 2.02-2.07 (m, 1 H), 2.22-2.36 (m, 1 H), 3.38 (m, 1 H), 3.45-3.62 (m, 2 H), 3.73 (s, 1.5 H), 3.74 (s, 1.5 H), 4.23-

4.44 (m, 2 H); ^{13}C NMR (62.9 MHz, CDCl$_3$) δ 27.3, 28.2, 28.3, 37.6, 38.5, 52.3, 52.6, 55.1, 55.7, 57.6, 57.8, 70.0, 71.0, 80.3, 153.6, 154.4, 175.1, 175.4. HRMS calcd. for C$_{11}$H$_{19}$NO$_5$H$^+$ 246.1341, found 246.1333 (Δ= -3.4 ppm). All data are in agreement with literature values.[47]

N-(tert-Butoxycarbonyl)-trans-4-benzoxy-D-proline methyl ester (5-10):[36]
To a solution of **5-9** (1.38 g, 5.6 mmol), benzoic acid (0.83 g, 6.8 mmol) and triphenylphosphine (1.62 g, 6.2 mmol) in THF (23 mL) was added diisopropyl azodicarboxylate (1.22 mL, 6.2 mmol). The mixture was stirred for 1 day and solvent was removed under reduced pressure. The residue was purified by column chromatography on silica gel using hexanes:EtOAc (8:1) as eluent to give **5-10** as a white solid (1.80 g, 92%): mp 91-92 °C; [α]$_D^{20}$ +42.8° (c 0.5, CHCl$_3$); ^{1}H NMR (300 MHz, CDCl$_3$) δ 1.43 (s, 4.5 H), 1.45 (s, 4.5 H), 2.32 (m, 1 H), 2.50 (m, 1 H), 3.75 (m, 4 H), 4.41 (m, 0.5 H), 4.52 (m, 0.5 H), 5.52 (br s, 1 H), 7.47 (m, 2 H), 7.57 (m, 1 H), 8.00 (d, J = 7.2 Hz, 2 H); ^{13}C NMR (62.9 MHz, CDCl$_3$) δ 28.2, 28.3, 35.6, 36.6, 52.0, 52.1, 52.3, 52.4, 57.6, 58.0, 72.5, 73.2, 80.4, 153.5, 154.2, 165.7, 172.7, 173.0. HRMS calcd. for C$_{18}$H$_{23}$NO$_6$H$^+$ 350.1604, found 350.1607 (Δ= 1.0 ppm). All data are in agreement with literature values.[39]

N-(tert-Butoxycarbonyl)-trans-4-triisopropylsiloxy-D-proline methyl ester (5-12):
To a solution of **5-10** (1.74 g, 5.0 mmol) in methanol (20 mL) was added potassium hydroxide (0.31 g, 5.5 mmol). The mixture was stirred for 1 h and being quenched with EtOAc and washed with saturated aqueous NH$_4$Cl solution, water and brine. The organic layer was dried over anhydrous MgSO$_4$ and then the solvent was removed under reduced pressure to give **5-11** as a white solid (1.17 g, 96%). This solid was used directly in the next step without any further purification. HRMS calcd. for C$_{11}$H$_{19}$NO$_5$H$^+$ 246.1341, found 246.1340 (Δ= -0.6 ppm).

The solid, thus obtained, was dissolved in DMF (6 mL). Then, imidazole (0.77 g, 11.3 mmol) and triisopropylsilyl chloride (2.08 mL, 9.7 mmol) were added to the reaction mixture. The mixture was stirred overnight before being quenched with EtOAc and washed with saturated aqueous NH$_4$Cl solution, water and brine. The organic layer was dried over anhydrous MgSO$_4$ and then solvent was removed under reduced pressure. The residue was purified by column chromatography on silica gel using hexanes:EtOAc (17:1 ~ 8:1) as the eluent to afford **5-12** as a colorless oil (1.57g, 93%): ^{1}H NMR (300 MHz, CDCl$_3$) δ 0.90 (s, 21 H), 1.26 (s, 4.5 H), 1.30 (s, 4.5 H), 1.84-1.92 (m, 1 H), 2.08 (m, 1 H), 3.25-3.47 (m, 2 H), 3.56 (s, 3 H), 4.17-4.29 (m, 1 H), 4.38 (br s, 1 H); ^{13}C NMR (62.9 MHz, CDCl$_3$) δ 11.8, 12.4, 17.3, 17.7, 28.0, 28.2, 39.1, 40.0, 51.7, 51.9, 54.7, 55.1, 57.5, 58.0, 69.8, 70.6, 79.7. HRMS calcd. for C$_{20}$H$_{39}$NO$_5$SiH$^+$ 402.2676, found 402.2681 (Δ= 1.3 ppm). All data are in agreement with literature values.[39]

(2R,4S)-2-Hydroxymethyl-4-triisopropylsiloxypyrrolidine-1-carboxylic acid tert-butyl ester (5-13):
To a solution of **5-12** (1.76 g, 4.3 mmol) in THF (35 mL) at 0 °C was added 2 M lithium borohydide in THF (3.3 mL, 6.5 mmol). The mixture was stirred overnight and quenched with ice water. The water layer was extracted with EtOAc and the organic layers were combined and washed with 5% aqueous phosphoric acid (5 mL x 3) and dried over anhydrous MgSO$_4$. The solvent was removed under reduced pressure. The residue was

purified by column chromatography on silica gel using hexanes:EtOAc (6:1) as the eluent to afford **5-13** as a colorless oil (1.57 g, 98%): ^{1}H NMR (300 MHz, CDCl$_3$) δ 0.87 (s, 21 H), 1.27 (s, 9 H), 1.52 (br s, 1 H), 1.83 (br s, 1 H), 3.15-3.50 (m, 4 H), 3.93 (br s, 1 H), 4.23 (br s, 1 H), 4.76 (br s, 1 H); ^{13}C NMR (62.9 MHz, CDCl$_3$) δ 11.8, 12.4, 13.5, 16.9, 17.4, 17.7, 18.5, 28.2, 37.9, 56.0, 58.7, 66.2, 70.0, 79.8, 156.9. HRMS calcd. for C$_{19}$H$_{39}$NO$_4$SiH$^+$ 374.2727, found 374.2731 (Δ= 1.2 ppm). All data are in agreement with literature values.[39]

(*2R,4S*)-2-Formyl-4-triisopropylsiloxypyrrolidine-1-carboxylic acid *tert*-butyl ester (5-14):

Sulfurtrioxide-pyridine (2.02 g, 12.6 mmol) was added to a solution of **5-13** (1.57 g, 4.2 mmol) and triethylamine (4.1 mL, 29.4 mmol) in dimethyl sulfoxide (8 mL) and CH$_2$Cl$_2$ (8 mL) at 0 ^{o}C. The reaction mixture was stirred for 1 h and quenched with ice water, and diluted with EtOAc (100 mL). The organic layer was washed with 5% citric acid aqueous solution (5 mL), water (5 mL), saturated aqueous NaHCO$_3$ solution (15 mL) and brine (15 mL). The organic layer was dried over anhydrous MgSO$_4$ and solvent was removed under reduced pressure. The residue was purified on a silica gel column using hexanes:EtOAc (18:1) as the eluent to afford **5-14** as a colorless oil (1.39 g, 90%): ^{1}H NMR (300 MHz, CDCl$_3$) δ 1.00 (m, 21 H), 1.43 (m, 9 H), 1.86-2.00 (m, 2 H), 3.53 (m, 2 H), 4.46 (m, 2 H), 9.42 (d, *J* = 3.3 Hz, 0.66 H), 9.54 (br s, 0.34 H). HRMS calcd. for C$_{19}$H$_{37}$NO$_4$SiH$^+$ 372.2570, found 372.2579 (Δ= 2.4 ppm). All data are in agreement with literature values.[39]

(*2R,4S*)-2-(1-Hydroxy-allyl)-4-triisopropylsilanyloxy-pyrrolidine-1-carboxylic acid *tert*-butyl ester (5-15):

Aldehyde **5-14** (2.73 g, 7.3 mmol) was dissolved in THF (68 mL) and cooled down to -78 ^{o}C. Vinylmagnesium chloride (1.6 M in THF, 6.7 mL, 10.7 mmol) was added and the reaction mixture was stirred overnight, quenched with saturated aqueous NH$_4$Cl solution (30 mL), and extracted with dichloromethane (50 mL x 3). The organic layer was dried over anhydrous MgSO$_4$ and solvent was removed under reduced pressure. The residue was purified by column chromatography on silica gel using hexanes:EtOAc (12:1) to afford **5-15** as colorless oil (2.85 g, 98%): ^{1}H NMR (250 MHz, CDCl$_3$) δ 1.00 (m, 21 H), 1.43 (m, 9 H), 1.68-2.04 (m, 2 H), 3.20-3.29 (m, 1 H), 3.54-3.61 (m, 1 H), 3.98-4.07 (m, 1 H), 4.35-4.45 (m, 2 H), 5.14 (d, *J* = 10.4 Hz, 1 H), 5.21-5.31 (m, 1 H), 5.68-5.81 (m, 1 H); ^{13}C NMR (62.9 MHz, CDCl$_3$) δ 11.9, 12.5, 17.4, 17.8, 28.0, 28.2, 35.9, 36.0, 37.2, 53.3, 55.4, 56.5, 61.4, 69.8, 69.9, 70.1, 80.1, 105.1, 116.6, 136.3, 170.3. HRMS calcd. for C$_{21}$H$_{41}$NO$_4$SiH$^+$ 400.2883, found 400.2884 (Δ= 0.2 ppm). All data are in agreement with literature values.[39]

(*2R,4S*)-2-(1-Acetoxyallyl)-4-triisopropylsiloxypyrrolidine-1-carboxylic acid *tert*-butyl ester (5-16):

To a solution of **5-15** (2.85 g, 7.1 mmol) and DMAP (216 mg, 1.77 mmol) in CH$_2$Cl$_2$ (22 mL) was added triethylamine (5.4 mL, 35.5 mmol) and acetic anhydride (3.38 mL, 21.3 mmol) at 0 ^{o}C. The reaction mixture was stirred overnight, quenched with saturated aqueous NH$_4$Cl solution (40 mL), and extracted with dichloromethane (50 mL x 3). The organic layer was dried over anhydrous MgSO$_4$ and solvent was removed under reduced

pressure. The residue was purified by column chromatography on silica gel using hexanes:EtOAc (13:1) as eluent to afford **5-16** as colorless oil (2.00 g, 80%): ^{1}H NMR (250 MHz, CDCl$_3$) δ 1.20 (s, 21 H), 1.44 (s, 9 H), 1.70-1.90 (m, 2 H), 2.06 (s, 3 H), 3.34 (br s, 2 H), 3.93-4.10 (m, 2 H), 4.48 (br s, 1 H), 5.13-5.25 (m, 2 H), 5.65 (br s, 1 H), 5.73 (br s, 1 H). HRMS calcd. for C$_{23}$H$_{43}$NO$_5$SiH$^+$ 442.2989, found 400.3000 (Δ= 2.5 ppm). All data are in agreement with literature values.[39]

(2R,4S)-1-Acryloyl-2-(1-acetoxypro-2-enyl)-4-triisopropylsiloxypyrrolidin (5-18):

To a solution of **5-16** (1.00 g, 2.5 mmol) in CH$_2$Cl$_2$ (10 mL) was added triflouroacetic acid (6 mL) at 0 °C. The mixture was stirred for 1 h at 0 °C and toluene (10 mL) was added to the system. The solvent was removed under reduced pressure and dried under high vacuum.

The residue was dissolved in CH$_2$Cl$_2$ (15 mL) together with a catalytic amount of DMAP and triethylamine (3.5 mL, 12.5 mmol). Acryloyl chloride (0.40 mL, 5.0 mmol) was added to the mixture, stirred for 1 day and quenched with saturated aqueous NH$_4$Cl solution. The mixture was then diluted with EtOAc and washed with saturated aqueous NaHCO$_3$ solution, water and brine. The organic layer was dried over anhydrous magnesium sulfate and solvent was removed under reduced pressure. The residue was purified by column chromatography on silica using hexanes:EtOAc (5:1) to afford **5-18** as colorless oil (0.27 g, 27%): ^{1}H NMR (250 MHz, CDCl$_3$) δ 1.14 (s, 21 H), 1.81-2.20 (m, 2 H), 2.14 (s, 3 H), 3.32 –3.72 (m, 2 H), 4.46 (br s, 1 H), 4.63-4.67 (m, 1 H), 5.18-5.28 (m, 2 H), 5.63-5.78 (m, 2 H), 5.86 (m, 1 H), 5.33-5.43 (m, 2 H). HRMS calcd. for C$_{21}$H$_{37}$NO$_4$SiNa$^+$ 418.2390, found 418.2388 (Δ= -0.4 ppm). All data are in agreement with literature values.[39]

(2S,8aR)-8-Acetoxy-2-triisopropylsiloxy-6,7-didehydroindolizidin-5-one (5-19):

A solution of **5-18** (260 mg, 0.66 mmol) and the "first-generation Grubbs's catalyst" (162 mg, 0.198 mmol) in CH$_2$Cl$_2$ (14 mL) was stirred at room temperature overnight. Then, the solvent was removed under reduced pressure and the residue was purified on a silica gel column using hexanes:EtOAc (3:1) as the eluent to afford **5-19** (202 mg, 83%). Major isomer **5-19**: ^{1}H NMR (250 MHz, CDCl$_3$) δ 0.93 (s, 21 H), 1.72-1.81 (m, 2 H), 1.93 (s, 3 H), 3.49-3.63 (m, 2 H), 3.94-4.09 (m, 1 H), 4.52 (br s, 1 H), 5.40 (d, *J* = 12.0 Hz, 1 H), 5.88 (dd, *J* = 10.0, 1.2 Hz, 1 H), 6.29 (d, *J* = 10.0 Hz, 1 H); ^{13}C NMR (62.9 MHz, CDCl$_3$) δ 12.2, 18.2, 26.5, 27.1, 35.0, 42.0, 54.6, 58.3, 69.4, 126.2, 140.0, 162.5, 170.4. HRMS calcd. for C$_{19}$H$_{33}$NO$_4$SiH$^+$ 368.2257, found 368.2244 (Δ= -3.6 ppm). All data are in agreement with literature values.[39]
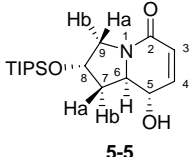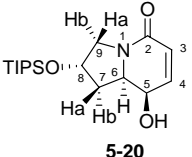
(2S,8aR)-8-Hydroxy-2-triisopropylsiloxy-6,7-didehydroindolizidin-5-one (5-5):

To a solution of **5-18** (200 mg, 0.54 mmol) in methanol (6 mL) and water (3 mL) was added potassium carbonate (128 mg, 0.80 mmol). The reaction mixture was stirred at room temperature for 1 h. Then, the mixture was quenched with saturated aqueous NH$_4$Cl solution and extracted with dichlorormethane (30 mL x 3). The organic layer was washed with brine (10 mL), dried over anhydrous MgSO$_4$, and the solvent was removed under reduced pressure. The residue was purified by column chromatography on silica gel using hexanes:EtOAc (2:3) to afford **5-5** as a white solid (140 mg, 80%) and **5-20** as a white solid (16 mg, 10%).

5-5: ^{1}H NMR (400 MHz, CDCl$_3$) δ 1.09 (m, 21 H), 1.79 (ddd, J = 12.0, 4.0, 1.6 Hz, 1 H), 2.37 (dd, J = 12.4, 2.4 Hz, 1 H), 3.59 (d, J = 12.8 Hz, 1 H), 3.68 (dd, J = 13.2, 4.8 Hz, 1 H), 3.93 (td, J = 13.2, 5.6 Hz, 1 H), 4.36 (d, J = 13.2 Hz, 1 H), 4.61 (t, J = 4.4 Hz, 1 H), 5.91 (dd, J = 10.0, 2.4 Hz, 1 H), 6.45 (dd, J = 10.0, 2.4 Hz, 1 H); ^{13}C NMR (100.5 MHz, CDCl$_3$) δ 11.9, 17.9, 41.8, 54.5, 60.8, 69.4, 71.5, 124.4, 144.8, 162.9. HRMS calcd. for C$_{17}$H$_{31}$NO$_3$SiH$^+$ 326.2151, found 326.2140 (Δ= -3.5 ppm).

5-20: ^{1}H NMR (600 MHz, CDCl$_3$) δ 1.05 (m, 21 H), 1.94 (td, J = 12.4, 7.8 Hz, 1H), 2.11 (bs, 1 H), 2.52 (q, J = 6.6 Hz, 1 H)**,** 3.48 (dd, J = 12.6, 3.6 Hz, 1 H), 3.66 (ddd, J = 10.8, 7.2, 3.0 Hz, 1 H), 3.71 (dd, J = 12.6, 6.6 Hz, 1 H), 4.52 (m, 2 H), 5.87 (dd, J = 9.6, 1.8 Hz, 1 H), 6.43 (d, J = 10.2 Hz, 1 H); ^{13}C NMR (100.5 MHz, CDCl$_3$) δ 11.9, 17.9, 40.3, 52.3, 60.9, 69.7, 71.4, 124.7, 144.2, 162.4. HRMS calcd. for C$_{17}$H$_{31}$NO$_3$SiH$^+$ 326.2151, found 326.2136 (Δ= -4.6 ppm). All data are in agreement with literature values.[39]

Table 5-5. Fully assigned ^{1}H & ^{13}C NMR of diastereomers 5-5 and 5-20

	5-5			5-20		
	^{1}H NMR, ppm a	^{1}H NMR, ppm b	^{13}C NMR, ppm	^{1}H NMR, ppm a	^{1}H NMR, ppm b	^{13}C NMR, ppm
2	------------------	------------------	162.9	------------------	------------------	162.4
3	5.91 (dd, J = 10.0, 2.4 Hz)	------------------	124.4	5.87 (dd, J = 9.6, 1.8 Hz)	------------------	124.7
4	6.45 (dd, J = 10.0, 2.4 Hz)	------------------	144.8	6.43 (d, J = 10.2 Hz)	------------------	144.2
5	4.36 (d, J = 13.2 Hz)	------------------	71.5	------------------	4.52 mixed with H5	71.4
6	------------------	3.93 (td, J = 13.2, 5.6 Hz)	60.8	------------------	3.66 (ddd, J = 10.8, 7.2, 3.0 Hz)	60.9
7	1.79 (ddd, J = 12.0, 4.0, 1.6 Hz)	2.37 (dd, J = 12.4, 2.4 Hz)	41.9	1.94 (td, J = 12.4, 7.8 Hz)	2.52 (q, J = 6.6 Hz)	40.3
8	4.61 (t, J = 4.4 Hz)	------------------	69.4	4.52 mixed with H5	------------------	69.7
9	3.59 (d, J = 12.8 Hz)	3.68 (dd, J = 13.2, 4.8 Hz)	54.5	3.48 (dd, J = 12.6, 3.6 Hz)	3.71 (dd, J = 12.6, 6.6 Hz)	52.3

(2S,8S,8aR)-2-Hydroxy-8-(3-methoxybenzoyl)-6,7-didehydroindolizidin-5-one (5-3): DIC (0.48 mmol) was added to a solution of **5-5** (80 mg, 0.24 mmol), *m*-anisic acid (56 mg, 0.36 mmol) and a catalytic amount of DMAP in CH$_2$Cl$_2$ (1.7 mL) and stirred for 1 day at room temperature. Then, the mixture was quenched with saturated aqueous NH$_4$Cl solution and extracted with dichlorormethane (30 mL x 3). The organic layer was washed by brine (10 mL), dried over anhydrous MgSO$_4$, filtered, and concentrated under reduced pressure. The residue was passed through a short silica gel column using hexanes:EtOAc (4:1) to afford crude **5-21** (150 mg) which was used directly for next step without any further purification. HRMS: *m/e* calcd for C$_{25}$H$_{37}$NO$_5$SiH$^+$: 460.2519 Found: 460.2515 (Δ = -0.9 ppm).

To a solution of **5-21** (110 mg) in pyridine (2.2 mL) and CH$_3$CN (2.2 mL) was added HF/pyridine (70:30, 1.1 mL) at 0 $^{\circ}$C. Then, the mixture was allowed to warm to room temperature and stirred overnight. The reaction mixture was diluted with EtOAc (50 mL) and washed with saturated aqueous NaHCO$_3$ solution (10 mL), saturated aqueous CuSO$_4$ solution (10 mL x 4), water (10 mL x 3) and brine (10 mL). The organic layer was dried

over anhydrous MgSO$_4$, filtered, and concentrated under reduced pressure. The residue was purified by column chromatography on silica gel using hexanes:EtOAc (1:1) to afford **5-3** (68 mg, 94% for two steps) as a white solid: ^{1}H NMR (250 MHz, CDCl$_3$) δ 1.89-2.02 (m, 1 H), 2.25-2.27 (m, 1 H), 2.43 (br s, 1 H), 3.68 (br s, 2 H), 3.85 (s, 1 H), 4.25 (dt, *J* = 11.8 Hz, 5.3 Hz, 1 H), 4.60 (br s, 1 H), 5.73 (d, *J* = 11.8 Hz, 1 H), 5.99 (dd, *J* = 10.0 Hz, 2.4 Hz, 1 H), 6.49 (d, *J* = 10.0 Hz, 1 H), 7.12 (dd, *J* = 8.3 Hz, 2.0 Hz, 1 H), 7.37 (d, *J* = 8.0 Hz, 1 H), 7.55 (s, 1 H), 7.64 (m, 1 H); ^{13}C NMR (62.9 MHz, CDCl$_3$) δ 40.6, 53.7, 55.4, 58.1, 68.2, 73.0, 76.4, 77.0, 77.5, 114.3, 120.0, 122.1, 125.8, 129.5, 130.3, 140.2, 159.6, 162.4, 165.4, 170.3. HRMS: *m/e* calcd for C$_{16}$H$_{17}$NO$_5$H$^+$: 304.1185 Found: 304.1186 (Δ = -0.3 ppm). All data are in agreement with literature values.[39]

(*3R,4S*)-1-Benzoyl-3-(1-ethoxyethoxy)-4-phenyl-2-azetidinone (5-22):[39, 47]

To a solution of *β*-lactam **1-17** (150 mg, 0.636 mmol), triethylamine (0.18 mL, 1.27 mmol), and DMAP (18.2 mg, 0.019 mmol) in CH$_2$Cl$_2$ (6.8 mL) was added benzoyl chloride (0.114 mL, 0.955 mmol) dropwise at 0 ^{o}C. The mixture was then allowed to warm to room temperature and stirred overnight. The reaction was quenched with saturated aqueous NH$_4$Cl solution (30 mL) and extracted with CH$_2$Cl$_2$ (30 mL x 3). The combined extracts were dried over anhydrous MgSO$_4$ and concentrated *in vacuo*. The crude product was purified on a silica gel column using hexanes:EtOAc (10:1) as the eluent to afford **5-22** as a white solid (173 mg, 80% yield): mp 78-80 °C; ^{1}H NMR (400 MHz, CDCl$_3$) δ [0.98 (d, *J* = 5.4 Hz), 1.05 (d, *J* = 5.4 Hz)] (3 H), [1.11 (t, *J* = 7.1 Hz), 1.12 (t, *J* = 7.1 Hz)] (3 H), [3.16-3.26 (m), 3.31-3.42 (m), 3.59-3.69 (m)] (2 H), [4.47 (q, *J* = 5.4 Hz), 4.68 (q, *J* = 5.4 Hz)] (1 H), [4.82 (d, *J* = 4.7 Hz), 4.85 (d, *J* = 4.7 Hz)] (1 H), 5.17-5.21 (m, 1 H), 6.42 (bd, 1 H), 7.35 (m, 5 H). All data are in agreement with literature values.[39, 47]

(*3R,4S*)-1-benzoyl-3-hydroxy-4-phenylazetidin-2-one (5-23):[39]

To a solution of **5-22** (173 mg, 0.510 mmol) in EtOH (3.9 mL) was added 0.2 *N* HCl (4.7 mL) at 0 ^{o}C. The mixture was then allowed to warm to room temperature and stirred for 1 h. The reaction was quenched with water (10 mL), saturated aqueous NaHCO$_3$ solution (10 mL) and extracted with EtOAc (40 mL x 3). The combined extracts were dried over anhydrous MgSO$_4$, filtered, and concentrated *in vacuo*. The product (127 mg, 100%) was used in the next step without further purification.

Methyl (*2R,3S*)-2-hydroxy-3-phenyl-3-(*N*-benzoylamino)propoate (5-24):

To a solution of crude **5-23** (127 mg, 0.510 mmol) and DMAP (9.75 mg, 0.077 mmol) in CH$_3$OH (2.6 mL), was added dropwise triethylamine (0.088 mL, 0.639 mmol) at room temperature. The mixture was stirred overnight at room temperature, the solvent was removed and saturated aqueous NH$_4$Cl solution (20 mL) was added. The mixture was then extracted with CH$_2$Cl$_2$ (30 mL x 3), the combined extracts were dried over anhydrous MgSO$_4$, and concentrated *in vacuo*. The crude product was purified on a silica gel column using hexanes:EtOAc (3:1) to afford **5-24** as a colorless oil (133 mg, 87% yield for two steps): ^{1}H NMR (400 MHz, CDCl$_3$) δ 3.23 (d, *J* = 4.0 Hz, 1 H), 3.85 (s, 1 H), 4.64 (dd, *J* = 3.6, 2.0 Hz, 1 H), 5.74 (dd, *J* = 9.2, 2.0 Hz, 1 H), 6.95 (d, *J* = 9.2 Hz, 1 H), 7.26 (m, 1 H), 7.30-7.54 (m, 7 H), 7.77 (dt, *J* = 8.0, 1.2 Hz, 2 H); ^{13}C NMR (100.5 MHz, CDCl$_3$) δ 53.3, 54.8, 73.2, 126.9, 127.0, 127.9, 128.6, 128.7, 131.8, 134.0, 138.7,

166.9, 173.4. HRMS (FAB/DCM/NaCl) m/z calcd. for $C_{17}H_{17}NO_4H^+$: 300.1236, found: 300.1236 ($\Delta = 0.1$ ppm).

(*4S,5R*)-2-(4-Methoxyphenyl)-*N*-benzoyl-4-phenyl-5-(methoxycarbonyl)oxazolidine (5-25):

To a solution of **5-24** (133 mg, 0.444 mmol) and 4-methoxybenzaldehyde dimethyl acetal (224 mg, 1.22 mmol) in toluene (12.1 mL) was added PPTS (33.63 mg, 0.132 mmol), and the mixture was refluxed for 2 h. The reaction mixture was then extracted with EtOAc (100 mL), washed with saturated aqueous $NaHCO_3$ solution (10 mL x 2) and brine (10 mL), and concentrated *in vacuo*. The crude product was purified on a silica gel column using hexanes:EtOAc (12:1) as the eluent to afford **5-25** as a colorless oil (129 mg, 66% yield): ^{1}H NMR (400 MHz, CDCl$_3$) δ 3.81 (s, 3 H), 3.82 (s, 3 H), 4.87 (s, 1 H), 5.40 (s, 1 H), 6.84 (d, 3 H), 7.20-7.48 (m, 11 H); ^{13}C NMR (100.5 MHz, CDCl$_3$) δ 52.7, 55.2, 73.2, 113.5, 113.7, 114.3, 126.9, 127.0, 127.0, 127.8, 128.0, 128.2, 128.5, 128.6, 128.7, 128.7, 129.8, 130.2, 130.5, 131.7, 135.6, 138.7, 159.9, 170.4, 190.7. HRMS: *m/e* calcd for $C_{25}H_{23}NO_5H^+$: 418.1654 Found: 418.1653 ($\Delta = -0.4$ ppm).

(*4S,5R*)-2-(4-Methoxyphenyl)-*N*-benzyl-4-phenyloxazolidine-5-carboxylic acid (5-4):

To a solution of **5-25** (125 mg, 0.299 mmol) in THF (2.1 mL) and water (2.1 mL) was added lithium hydroxide (37.99 mg, 0.897) and the reaction mixture was stirred for 2 h. The reaction mixture was washed with 1 *N* KOH aqueous solution (5 mL x 3) and then the water layer was collected and acidified using 1 *N* HCl aqueous solution to pH 2. Then, the aqueous layer was extracted with CH_2Cl_2 (20 mL x 3). The organic layers were combined and dried over anhydrous $MgSO_4$ and concentrated *in vacuo*. The crude product was purified on a silica gel column using hexanes:EtOAc (3:1) as the eluent to afford **5-4** as a white solid (81 mg, 67% yield): ^{1}H NMR (400 MHz, CDCl$_3$) δ 3.82 (s, 3 H), 4.41 (s, 1 H), 4.90 (s, 1 H), 5.48 (s, 1 H), 6.85 (d, *J* = 8.4 Hz, 2 H), 6.90 (m, 1 H), 7.21-7.39 (m, 11 H); ^{13}C NMR (100.5 MHz, CDCl$_3$) δ 55.0, 55.6, 72.5, 114.3, 127.0, 127.1, 127.3, 128.1, 128.3, 128.3, 128.7, 128.8, 130.0, 132.0, 132.3, 133.2, 138.1, 164.6, 174.0, 190.9. HRMS: *m/e* calcd for $C_{24}H_{22}NO_5H^+$: 404.1498 Found: 404.1495 ($\Delta = -0.7$ ppm).

(*2S,8S,8aR*)-8-(3-Methoxybenzoyloxy6,7-didehydroindolizidin-5-one-2-yl (*2R,3S*)-2-hydroxy-3-phenyl-3-benzylaminopropionate (5-2):

To a solution of **5-3** (20 mg, 0.066 mmol) acid **5-4** (61 mg, 0.132 mmol) and DMAP (10 mg) in CH_2Cl_2 (0.5 mL) was added EDC (30 mg, 0.16 mmol). The reaction mixture was stirred for 1 day. The mixture was then quenched with EtOAc and washed with water and brine. The organic layer was dried over anhydrous $MgSO_4$, filtered, and concentrated under reduced pressure. The residue was purified by column chromatography on silica gel using hexanes:EtOAc (1:2) as the eluent to afford **5-26** as a white solid, which was used directly in the next step without any further purification. HRMS: *m/e* calcd for $C_{40}H_{36}N_2O_9H^+$: 689.2499 Found: 689.2480 ($\Delta = -2.8$ ppm).

To a solution of **5-26** (37 mg, 0.05 mmol) in methanol (3 mL) was added *p*-TSA (2.4 mg, 0.01 mmol). After stirring overnight, the solvent was removed and the residue was purified by column chromatography on silica gel using hexanes:EtOAc (1:2) as the eluent to afford **5-2** as a white solid (27 mg, 76% in 2 steps): mp 78-80 ^{o}C; ^{1}H NMR (400 MHz,

CDCl$_3$) δ 2.09 (td, J = 10.8, 4.4 Hz, 1 H), 2.47 (dd, J = 14.0, 5.6 Hz, 1 H), 3.54 (br s, 1 H), 3.82 (s, 3 H), 3.83 (m, 2 H), 4.33 (td, J = 11.2, 5.3, Hz, 1 H), 4.64 (d, J = 2.0 Hz, 1 H), 5.11 (d, J = 3.6 Hz, 1 H), 5.75 (m, 2 H), 6.01 (dd, J = 10.4, 2.8 Hz, 1 H), 6.53 (dd, J = 10.0, 1.6 Hz, 1 H), 7.13 (dd, J = 8.0, 2.0 Hz, 1 H), 7.19-7.41 (m, 6 H), 7.45 (d, J = 7.6 Hz, 2 H), 7.55 (d, J = 7.2 Hz, 1 H), 7.59 (t, J = 2.0 Hz, 1 H), 7.71 (d, J = 7.6 Hz, 1 H); ^{13}C NMR (100.5 MHz, CDCl$_3$) δ 31.5, 38.2, 50.8, 54.5, 55.4, 55.4, 58.3, 73.0, 114.4, 120.2, 122.5, 125.7, 126.9, 126.9, 128.0, 128.5, 128.8, 129.6, 130.3, 131.6, 133.8, 140.6, 159.6, 162.4, 165.7, 166.8, 172.2. HRMS: m/e calcd for C$_{32}$H$_{30}$N$_2$O$_8$Na$^+$: 593.1900 Found: 593.1893 (Δ = -1.2 ppm).

1-Bromo-2,6-bis(hydroxymethyl)benzene (5-43):[26]

To a stirred solution of 2-bromometaxylene (1.0 g, 5.4 mmol) and a catalytic amount of 2,2'-azobis(2-methylpropionitrile) (AIBN) (62 mg, 0.324 mmol) in CCl$_4$ (6 mL) was added 2.3 equiv. of N-bromosuccinimide (NBS) (1.9 g, 10.8 mmol). The reaction mixture was refluxed for 2 day. The succinimide formed was then filtered off and the orange filtrate was evaporated to afford 2.285 g crude product.

Dibromide (2.28 g, ~5.4 mmol) was stirred in dioxane (40 mL). A slurry of CaCO$_3$ (6.2 g, 6.2 mmol) in water (20 mL) was added and the mixture refluxed for 36 h. The dioxane was removed *in vacuo* and the residue treated with 6 N HCl until it became acidic. The residue was extracted by ethyl acetate (50 mL x 3) and the organic layer was washed with brine (10 mL). The crude product was purified on a silica gel column using dichloromethane/methanol (95/5) to give **5-43** (626 mg, 49% for two steps) as a white solid: ^{1}H NMR (300 MHz, CDCl$_3$) δ 4.87 (s, 4 H), 7.43 (m, 1H), 7.51 (m, 2 H). HRMS calcd. for C$_8$H$_9$BrO$_2$H$^+$: 216.986416, found 216.987084 (Δ= -3.1 ppm).

2-Bromo-3-(hydroxymethyl)benzaldehyde (5-44):[26]

To a stirred solution of 2-bromoxylene (2.5 g, 13.5 mmol) and a catalytic amount of 2,2'-azobis(2-methylpropionitrile) (AIBN) (76 mg, 0.4 mmol) in CCl$_4$ (15 mL) was added N-bromosuccinimide (NBS) (10 g, 54.0 mmol). The reaction mixture was heated to reflux and stirred overnight. The succinimide formed was then filtered off and the orange filtrate evaporated to afford crude product which was used in the next reaction without further purification.

Tetrabromide (~13.5 mmol) was stirred in dioxane (100 mL). A slurry of CaCO$_3$ (10 g, 10 mmol) in water (50 mL) was added and the mixture refluxed for 2 days. The dioxane was removed on a rotary evaporator and the residue acidified with 6 M HCl. The mixture was extracted with ethyl acetate (60 mL x 3) and the organic layer was washed with brine (10 mL). The crude product was purified on a silica gel column using hexanes/EtOAc (6/1) as eluent to give **5-44** 1.70 g (60% in two steps) as a white solid: mp 86-87 ^{o}C; ^{1}H NMR (300 MHz, CDCl$_3$) δ 4.86 (d, J = 6.3 Hz, 2 H), 7.47 (t, J = 7.5 Hz, 1 H), 7.78 (dd, J = 8.8, 3.9 Hz, 1 H), 7.86 (dd, J = 7.8, 2.1 Hz, 1 H), 10.46 (s, 1 H); ^{13}C NMR (100.5 MHz, CDCl$_3$) δ 64.0, 126.6, 127.7, 128.7, 132.6, 133.7, 141.4, 192.0. HRMS calcd. for C$_8$H$_7$BrO$_2$$^+$: 213.962941, found 213.962545 (Δ= 1.8 ppm).

1-Bromo-2-hydroxymethyl-6-methylbenzene (5-42):[26]

To a stirred solution of 2-bromoxylene (500 mg, 2.7 mmol) in CCl$_4$ (3 mL) was added N-bromosuccinimide (NBS) (620 mg, 3.51 mmol) and a catalytic amount of 2,2'-azobis(2-

methylpropionitrile) (AIBN) (20 mg, 0.1 mmol). The reaction mixture was heated to reflux and stirred for 1.5 h. After starting material disappeared (by TLC), the succinimide formed was then filtered off and the orange filtrate concentrated to afford crude product (894 mg).

The dibromide (894 g, ~2.7 mmol) was stirred in dioxane (40 mL). A slurry of $CaCO_3$ (6.2 g, 6.2 mmol) in water (20 mL) was added and the mixture refluxed for 24 h. The dioxane was removed on a rotary evaporator.and the residue acidified with 6 M HCl. The mixture was extracted with ethyl acetate (30 mL x 3) and the organic layer was washed with brine (10 mL). The crude product was purified on a silica gel column using hexanes/EtOAc (8/1) as eluent to give **5-42** (392 mg, 74% in two steps) as a white solid: ^{1}H NMR (400 MHz, $CDCl_3$) δ 2.40 (s, 3 H), 3.24 (s, 1 H), 4.67 (s, 2 H), 7.13-7.27 (m, 3 H); ^{13}C NMR (100.5 MHz, $CDCl_3$) δ 23.1, 65.1, 124.7, 125.8, 126.9, 129.7, 138.1, 139.9. HRMS calcd. for $C_8H_9BrO^+$: 199.983676, found 199.983834 (Δ= -0.8 ppm).

1-Bromo-2-trimethylsilyloxy-6-methylbenzene (5-45):

To a solution of **5-42** (392 mg, 1.95 mmol) in anhydrous dichloromethane (4 mL) at 0 °C under nitrogen was added with triethylamine (0.41 mL, 3.9 mmol), followed by chlorotrimethylsilane (0.38 ml, 2.93 mmol). The reaction mixture was stirred at room temperature overnight. The reaction was quenched with water (20 mL). The layers were separated and the aqueous layer was extracted with dichlorormathane (3 x 20 mL). The combined organic layers were washed with saturated aqueous NaCl, dried over $MgSO_4$, filtered and concentrated. Flash chromatography (100:1) of the residue afforded **5-45** (490 mg, 92%) as colorless oil: ^{1}H NMR (400 MHz, $CDCl_3$) δ 0.19 (s, 9 H), 2.41 (s, 3 H), 4.72 (s, 2 H), 7.15 (d, J = 7.2 Hz, 1 H), 7.22 (t, J = 7.2 Hz, 1 H), 7.36 (d, J =7.6 Hz, 1 H); ^{13}C NMR (100.5 MHz, $CDCl_3$) δ -0.5, 23.1, 64.7, 123.8, 125.2, 126.8, 129.2, 137.8, 140.3.

1-Bromo-2,6-bis(benzyoxymethyl)benzene (5-46):[28]

To a solution of **5-43** (386 mg, 1.79 mmol) in anhydrous DMF (28 mL) at 0 °C under nitrogen was added with Bu_4NI (132 mg, 0.36 mmol), followed by NaH (75 mg, 1.88 mmol). The reaction mixture was stirred at 0 °C for 30 min and $PhCH_2Br$ (0.222 mL, 1.88 mmol) was added. The reaction mixture was allowed to stir at 0 °C for 2 h and the mixture was quenched with a solution of saturated aqueous NH_4Cl (30 mL) and EtOAc (30 mL) at 0 °C. The layers were separated and the aqueous layer was extracted with EtOAc (3 x 20 mL). The combined organic layers were washed with saturated aqueous NaCl, dried over $MgSO_4$, filtered, and concentrated. Flash chromatography (5:1) of the residue afforded **5-46** (287 mg, 52%) as white solid: ^{1}H NMR (300 MHz, $CDCl_3$) δ 2.24 (s, 1 H), 4.73 (s, 4 H), 4.82 (s, 2 H), 7.39-7.57 (m, 8 H); ^{13}C NMR (100.5 MHz, $CDCl_3$) δ 65.2, 71.7, 72.8, 122.8, 127.4, 127.7, 127.8, 128.3, 128.4, 138.0, 140.1; HRMS calcd. for $C_{15}H_{15}BrO_2H^+$: 307.033366, found 307.032948 (Δ= -1.4 ppm).

Flash chromatography (15:1) also afforded **5-47** (225 mg, 32%) as a colorless oil: ^{1}H NMR (400 MHz, $CDCl_3$) δ 4.69 (s, 4 H), 4.71 (s, 4 H), 7.34-7.54 (m, 13 H); ^{13}C NMR (100.5 MHz, $CDCl_3$) δ 72.2, 73.1, 123.3, 127.5, 128.0, 128.0, 128.4, 128.7, 138.3, 138.4.

1-Bromo-2-benzyloxymethyl-6-triethylsiloxybenzene (5-48):
To a solution of **5-46** (120 mg, 0.39 mmol) in anhydrous dichloromethane (8 mL) at 0 °C under nitrogen was added triethylamine (0.08 mL, 0.77 mmol, 2 equiv), followed by chlorotriethylsilane (0.1 mL, 0.58 mmol, 1.5 equiv). The reaction mixture was stirred at room temperature overnight. The reaction was quenched with water (20 mL). The layer were separated and the aqueous layer was extracted with dichlorormathane (3 x 20 mL). The combined organic layers were washed with saturated aqueous NaCl, dried over MgSO$_4$, filtered, and concentrated. Flash chromatography (100:1) of the residue afforded **5-48** (134 mg, 82%) as colorless oil: ^{1}H NMR (400 MHz, CDCl$_3$) δ 0.74 (q, J = 7.6 Hz, 6 H), 1.05 (t, J = 4.8 hz, 9 H), 4.68 (s, 2 H), 4.70 (s, 2 H), 4.82 (s, 2 H), 7.32-7.59 (m, 8 H); ^{13}C NMR (100.5 MHz, CDCl$_3$) δ 4.4, 6.8, 64.5, 71.7, 72.7, 121.4, 126.6, 127.1, 127.5, 127.6, 127.7, 128.4, 137.3, 138.1, 140.6.

1-Bromo-2-benzyloxymethyl-6-trimethylsiloxybenzene (5-49):
To solution of **5-46** (224 mg, 0.72 mmol) in anhydrous dichloromethane (15 mL) at 0 °C under nitrogen was added triethylamine (0.15 mL, 1.44 mmol) and chlorotrimethylsilane (0.14 mL, 1.08 mmol). The reaction mixture was stirred at room temperature overnight. The reaction was quenched with water (20 mL). The layers were separated and the aqueous layer was extracted with dichlorormathane (3 x 20 mL). The combined organic layers were washed with saturated aqueous NaCl, dried over MgSO$_4$, filtered and concentrated. Flash chromatography (100:1) of the residue afforded **5-49** (224 mg, 90%) as colorless oil: ^{1}H NMR (500 MHz, CDCl$_3$) δ 0.22 (s, 9 H), 4.66 (s, 2 H), 4.67 (s, 2 H), 4.76 (s, 2 H), 7.32-7.50 (m, 8 H); ^{13}C NMR (100.5 MHz, CDCl$_3$) δ -0.5, 64.4, 71.7, 72.7, 121.6, 126.9, 127.1, 127.6, 127.7, 128.4, 137.5, 138.1, 140.3; HRMS calcd. for C$_{18}$H$_{23}$BrO$_2$Si$^+$: 378.065070, found 378.064561 (Δ= 1.3 ppm).

2-Bromo-1,3-bis(methoxymethoxymethyl)benzene (5-50):[48]
To a solution of **5-43** (100 mg, 0.46 mmol) in anhydrous dichloromethane (10 mL) at 0 °C under nitrogen was added *N,N'*-diisopropylethylamine (0.92 mL, 5.58 mmol) and chloromethyl methyl ether (0.21 mL, 3.72 mmol). The reaction mixture was stirred at room temperature overnight. The reaction was quenched with water (20 mL). The layers were separated and the aqueous layer was extracted with ethyl ether (3 x 20 mL). The combined organic layers were washed with saturated aqueous NaCl solution, dried over MgSO$_4$, filtered, and concentrated. Flash chromatography (hexanes/EtOAc = 10:1) of the residue afforded **5-50** (142 mg, 100%) as colorless oil: ^{1}H NMR (500 MHz, CDCl$_3$) δ 1.97 (t, J = 6.0 Hz, 1 H), 3.44 (s, 3 H), 4.70 (s, 2 H), 4.77 (s, 2 H), 4.79 (t, J = 4.5 Hz, 2 H), 7.35 (t, J = 7.5 Hz, 1 H), 7.44 (m, 2 H). HRMS calcd. for C$_{12}$H$_{17}$BrO$_4$NH$_4^+$ 322.0654, found 322.0670 (Δ= 5.0 ppm).

2-Bromo-3-(methoxymethoxymethyl)benzaldehyde (5-51):[48]
To a solution of **5-44** (132 mg, 0.62 mmol) in anhydrous dichloromethane (10 mL) at 0 °C under nitrogen was added *N,N'*-diisopropylethylamine (0.92 mL, 5.58 mmol), followed by chloromethyl methyl ether (0.61 mL, 3.7 mmol). The reaction mixture was stirred at room temperature overnight. The reaction was quenched with water (20 mL). The layers were separated and the aqueous layer was extracted with ethyl ether (3 x 20 mL). The combined organic layers were washed with saturated aqueous NaCl solution,

dried over MgSO$_4$, filtered, and concentrated. Flash chromatography (11:1) of the residue afforded **5-51** (132 mg, 82%) as white solid: ^{1}H NMR (400 MHz, CDCl$_3$) δ 3.41 (s, 3 H), 4.71 (s, 2 H), 4.76 (s, 2 H), 7.41 (t, J = 7.6 Hz, 1 H), 7.73 (ddd, J = 8.8, 1.6, 0.4 Hz, 1 H), 7.80 (ddd, J = 7.6, 1.6, 0.4 Hz, 1 H), 10.42 (s, 1 H); ^{13}C NMR (100.5 MHz, CDCl$_3$) δ 55.5, 68.2, 96.2, 127.1, 127.6, 128.9, 133.7, 134.3, 139.0, 191.9.

2-Bromo-1-hydroxymethyl-3-(methoxymethoxymethyl)benzene (5-52):[39]

To a solution of **5-51** (132 mg, 0.51mmol) in THF (12 mL) at 0 ^{o}C was added 2 M lithiumborohydide in THF (0.12 mL, 0.25 mmol). The mixture was stirred for 1.5 h and quenched with ice water (20 mL). The water layer was extracted with CH$_2$Cl$_2$ (30 mL x 3) and the combined organic layers were dried over anhydrous MgSO$_4$. The solvent was removed under reduced pressure. The residue was purified by column chromatography on silica gel using hexanes:EtOAc (4:1) as the eluent to afford **5-52** as a white solid (119 mg, 90%). ^{1}H NMR (400 MHz, CDCl$_3$) δ 1.98 (t, J = 6.4 Hz, 1 H), 3.44 (S, 1 H), 4.70 (s, 2 H), 4.77 (s, 2 H), 4.79 (t, J = 3.6 Hz, 2 H), 7.35 (t, J = 7.6 Hz, 1 H), 7.44 (m, 2 H). HRMS calcd. for C$_{10}$H$_{13}$NO$_3$BrNH$_4^+$ 278.0392, found 278.0405 (Δ= 4.6 ppm).

2-{Acetoxy-[2,6-bis(methoxymethoxymethyl)phenyl]-methyl}-1-(*tert*-butoxycarboyl)-4-triisopropyl-siloxypyrrolidine (5-54):[31, 39]

Bromide **5-50** (142 mg, 0.465 mmol) was dissolved in dry THF (4.0 mL) under N$_2$. At -78 ^{o}C, 2.5 M *n*-BuLi in hexane (0.23 mL, 0.58 mmol) was added, and the resulting solution was stirred for 1 h. A solution of aldehyde **5-14** (171 mg, 0.46 mmol) in dry THF (6 mL) was added dropwise. The resulting solution was allowed to slowly warm up to room temperature while being stirred overnight. After addition of a saturated NH$_4$Cl solution (20 mL), the mixture was extracted with ethyl ether (3 x 20 mL). The combined organic layers were washed with brine and dried over MgSO$_4$. After evaporation of the solvent, the residue was purified by flash chromatography on silica gel (hexanes/EtOAc = 30/1-5/1) to give desired product **5-53** (96 mg, 35% yield) as colorless oil.

To a solution of **5-53** (96 mg, 0.16 mmol) and DMAP (3.2 mg, 0.04 mmol) in CH$_2$Cl$_2$ (0.6 mL) was added triethylamine (0.12 mL, 0.8 mmol) and acetic anhydride (0.08 mL, 0.48 mmol) at 0 ^{o}C. The reaction mixture was stirred overnight, quenched with saturated aqueous NH$_4$Cl solution (20 mL) and extracted with dichloromethane (30 mL x 3). The organic layer was dried over anhydrous MgSO$_4$ and solvent was removed under reduced pressure to afford a liquid residue. The residue was purified by column chromatography on silica gel using hexanes:EtOAc (60:1) to afford **5-54** as a colorless oil. LRMS calcd. for molecular formula: 639.38, MH+ found: 640.3.

2-[Hydroxy(2-hydroxymethyl-6-methoxymethoxymethyl-phenyl)-methyl]-1(*tert*-butxoycarbonyl)-4-triisopropylsiloxypyrrolidine (5-55):[31, 39]

Bromide **5-52** (118 mg, 0.45 mmol) was dissolved in dry THF (4.5 mL) under N$_2$ and cooled to -78 ^{o}C. Then, 2.5 M *n*-BuLi in hexane (0.4 mL, 0.99 mmol) was added, and the resulting solution was stirred for 1 h. HMPA (0.081 mL) was added and the solution was stirred for 1 h. A solution of aldehyde **5-14** (129 mg, 0.35 mmol) in dry THF (3 mL) was added dropwise. The resulting solution was allowed to slowly warm up to room temperature with stirring overnight. After addition of a saturated NH$_4$Cl solution (20 mL), the mixture was extracted with dichloromethane (3 x 20 mL). The combined organic

layers were washed with brine and dried over MgSO$_4$. After evaporation of the solvent, the residue was purified by flash chromatography on silica gel (hexanes/EtOAc = 10/1-4/1) to give the desired product **5-55** (160 mg, 83% yield) as a colorless oil (without HMPA, 45% yield): ^{1}H NMR (400 MHz, CDCl$_3$) δ 1.00 (m, 21 H), 1.28-1.50 (m, 9 H), 1.65 (m, 1 H), 2.04 (m, 1 H), 3.32 (m, 1 H), 3.42 (m, 5 H), 3.65 (m,1 H), 4.70 (m, 7 H), 5.20 (m, 1 H), 7.36 (m, 3 H); HRMS calcd. for C29H51NO7SiH$^+$ 554.3513, found 554.3500 (Δ= -2.3 ppm).

2-[Acetoxy(2-acetoxymethyl-6-methoxymethoxymethylphenyl)methyl]-1-(*tert*-butoxycarbonyl)-4-triisopropylsiloxypyrrolidine (5-56):[39]

To a solution of **5-55** (155 mg, 0.28 mmol) and DMAP (4.8 mg, 0.06 mmol) in CH$_2$Cl$_2$ (1.65 mL) was added triethylamine (0.41 mL, 1.40 mmol) and acetic anhydride (0.27 mL, 0.84 mmol) at 0 ^{o}C. The reaction mixture was stirred overnight, quenched with saturated aqueous NH$_4$Cl solution (20 mL) and extracted with dichloromethane (30 mL x 3). The organic layer was dried over anhydrous MgSO$_4$ and solvent was removed under reduced pressure to afford a liquid residue. The residue was purified by column chromatography on silica gel using hexanes:EtOAc (7/1) as eluant to afford **5-56** as a colorless oil: ^{1}H NMR (400 MHz, CDCl$_3$) δ 1.04 (m, 21 H), 1.28-1.50 (m, 9 H), 1.65 (m, 1 H), 2.04 (m, 7 H), 3.42 (m, 6 H), 3.65 (m,1 H), 4.70 (m, 4 H), 5.41 (m, 2 H), 6.05 (m, 1 H), 7.36 (m, 3 H); HRMS calcd. for C$_{33}$H$_{55}$NO$_9$SiH$^+$ 638.3724, found 638.3742 (Δ= 2.8 ppm).

2-Bromo-3-(methoxymethoxymethyl)benzoic acid (5-60):[41]

Sodium chlorite (488 mg, 5.40 mmol) was added to a solution of **5-51** (175 mg, 0.68 mmol) and sodium phosphate (monobasic) (842 mg, 5.40 mmol) in acetone/water (1:1, 6 mL). The reaction mixture was stirred at room temperature for 20 min and quenched with ethyl acetate (60 mL). The organic layer was washed with aqueous hydrochloric acid (1 *N*, 10 mL), Na$_2$S$_2$O$_3$ (10%, 10 mL x 2), brine (10 mL), dried over MgSO$_4$, filtered, and concentrated. Flash chromatography (1:1) of the residue afforded **5-60** (135 mg, 74%) as a white solid: mp 106-108 ^{o}C, ^{1}H NMR (300 MHz, CDCl$_3$) δ 3.45 (s, 3 H), 4.75 (s, 2 H), 4.81 (s, 2 H), 7.41 (t, *J* = 7.8 Hz, 1 H), 7.69 (d, *J* = 6.6, 1 H), 7.82 (d, *J* = 7.5 Hz, 1 H), 10.5 (bs, 1 H); ^{13}C NMR (75.5 MHz, CDCl$_3$) δ 55.6, 69.0, 96.2, 121.7, 127.1, 130.6, 131.9, 132.1, 139.6, 171.5.

2-Acetoxymethyl-1-(*tert*-butoxycarbonyl)-4-triisopropylsilanyloxypyrrolidine (5-63):

To a solution of **5-13** (455 mg, 1.22 mmol), DMAP (20 mg, 0.24 mmol) and triethylamine (0.732 mL, 6.10 mmol) in dichloromethane (5 mL) at 0 ^{o}C was added acetic anhydride (0.46 mL, 3.66 mmol). The mixture was stirred overnight and quenched with saturated aqueous ammonium chloride (20 mL). The water layer was extracted with dichloromethane (30 mL x 3). The organic layers were combined and washed with brine (20 mL) and dried over anhydrous MgSO$_4$. The solvent was removed under reduced pressure. The residue was purified by column chromatography on silica gel using hexanes:EtOAc (20/1) as the eluent to afford **5-63** as a colorless oil (477 mg, 95%): ^{1}H NMR (400 MHz, CDCl$_3$) δ 1.05 (m, 21 H), 1.46 (s, 9 H), 1.95 (m, 1 H), 2.02 (m, 1 H), 2.04 (s, 3 H), 3.42 (m, 2 H), 4.18 (m, 3 H), 4.05 (t, *J* = 4.8 Hz, 1 H). ^{13}C NMR (100.5 MHz, CDCl$_3$) δ 12.0, 17.7, 20.6, 28.2, 37.8, 38.5, 54.7, 55.2, 65.1, 69.9, 79.4, 154.6, 170.3. HRMS calcd. for C$_{21}$H$_{41}$NO$_5$SiH$^+$ 416.2832, found 416.2828 (Δ= -1.1 ppm).

2-Acetoxymethyl-1-(2-bromo-3-methoxymethoxymethylbenzoyl)-4 triisopropylsiloxy-pyrrolidine (5-66):

To a solution of **5-63** (57 mg, 0.14 mmol) in dichloromethane (0.55 mL) at 0 °C was added trifluoroacetic acid (0.55 mL). The mixture was stirred at 0 °C for 30 min and at room temperature for 30 min. Then, the reaction was quenched with ethyl acetate (40 mL). The organic layer was washed with saturated aqueous sodium bicarbonate (5 mL x 3), brine (5 mL x 2), dried with $MgSO_4$, filtered and concentrated. The crude compound **5-64** was used in the next step without further purification.

To a solution of **5-60** (41 mg, 0.15 mmol) in dichloromethane (0.7 mL) and 1 drop of DMF at 0 °C was added oxalyl chloride (0.03 mL, 0.30 mmol). The mixture was stirred at room temperature for 2 h. The solvent and acid were removed under reduced pressure and the residue was used in next step without further purification.

To a solution of **5-64** (~0.137 mmol), DMAP (3 mg, 0.04 mmol) and triethylamine (0.08 mL, 0.28 mmol) in dichloromethane (1 mL) at 0 °C was added acid chloride **5-65** (~0.15 mmol) in dichloromethane (1 mL). The mixture was stirred overnight, and quenched with saturated aqueous ammonium chloride (20 mL). The water layer was extracted with dichloromethane (30 mL x 3). The organic layers were combined, washed with brine (20 mL) and dried over anhydrous $MgSO_4$. The solvent was removed under reduced pressure. The residue was purified by column chromatography on silica gel using hexanes:EtOAc (2/1) as the eluent to afford **5-66** as a colorless oil (44 mg, 56%). ^{1}H NMR (300 MHz, $CDCl_3$) δ 1.02 (m, 21 H), 2.06 (s, 3 H), 2.10 (m, 2 H), 3.32 (dd, J = 10.5, 4.8 Hz, 1 H), 3.43 (s, 3 H), 3.65 (dd, J = 10.2, 8.7 Hz, 1 H), 4.35 (m, 2 H), 4.62 (m, 2 H), 4.68 (s, 2 H), 4.77 (s, 2 H), 7.37 (m, 1 H), 7.53 (d, J = 10.2 Hz, 1 H), 7.63 (d, J = 10.2 Hz, 1 H). ^{13}C NMR (100.5 MHz, $CDCl_3$) δ 11.9, 17.8, 22.9, 37.4, 54.5, 55.5, 56.3, 65.7, 68.8, 70.3, 96.2, 120.5, 127.2, 129.3, 130.9, 134.1, 139.2, 166.6, 169.9. HRMS calcd. for $C_{26}H_{42}NO_6SiBrH^+$ 572.2043, found 572.2052 (Δ= 1.6 ppm).

1-Acetyl-2-hydroxymethyl-4-triisopropylsiloxypyrrolidine (5-68):

To a solution of **5-66** (44 mg, 0.08 mmol) in methanol (3 mL) and water (1.5 mL) was added potassium carbonate (19 mg, 0.12 mmol). The reaction mixture was stirred at room temperature for 5.5 h. Then, the mixture was quenched with saturated aqueous NH_4Cl solution, water and brine and extracted with dichlorormethane (30 mL x 3). The organic layer was washed with brine (10 mL) and dried over anhydrous $MgSO_4$ and solvent was removed under reduced pressure. The residue was purified by column chromatography using hexanes:EtOAc (2/3) to afford **5-68** as a colorless oil (25 mg, 80%): ^{1}H NMR (400 MHz, $CDCl_3$) δ 1.05 (m, 21 H), 1.66 (sept, J = 4.4 Hz, 1 H), 2.05 (m, 1 H), 2.09 (s, 3 H), 3.43 (d, J = 12.0 Hz, 1 H), 3.56 (ddd, J = 18.0, 10.8, 4.0 Hz, 2 H), 3.69 (dd, J = 11.6, 2.0 Hz, 1 H), 4.33 (dd, J = 16.8, 9.2 Hz, 1 H), 4.47 (m, 1 H). ^{13}C NMR (100.5 MHz, $CDCl_3$) δ 12.0, 17.9, 23.1, 38.0, 57.8, 60.1, 66.9, 69.9, 172.1.

1-(2-Bromo-3-methoxymethoxymethylbenzoyl)-2-hydroxymethyl-4-triisopropyl-siloxypyrrolidine (5-67):

To a solution of **5-69** (~ 0.13 mmol), DMAP (3 mg, 0.04 mmol) and triethylamine (0.08 mL, 0.28 mmol) in dichloromethane (1 mL) at 0 °C was added acid chloride **5-65** (~0.14 mmol) in dichloromethane (1 mL). The mixture was stirred overnight and quenched with saturated aqueous ammonium chloride (20 mL). The water layer was extracted with

dichloromethane (30 mL x 3). The organic layers were combined, washed with brine (20 mL), and dried over anhydrous MgSO$_4$. The solvent was removed under reduced pressure. The residue was purified by column chromatography on silica gel using hexanes:EtOAc (2/1) as the eluent to afford **5-67** as a colorless oil (38 mg, 56%): ^{1}H NMR (400 MHz, CDCl$_3$) δ 1.00 (m, 21 H), 1.78 (t, J = 9.2 Hz, 1 H), 2.16 (dd, J = 13.2, 7.2 Hz, 1 H), 3.13 (m, 1 H), 3.44 (m, 4 H), 3.78 (m, 1 H), 3.88 (m, 1 H), 4.37 (m, 1 H), 4.57 (m, 1 H), 4.69 (s, 2 H), 4.77 (s, 2 H), 7.21 (t, J = 6.8 Hz, 1 H), 7.38 (t, J = 7.6 Hz, 1 H), 7.52 (t, J = 7.6 Hz, 1 H); ^{13}C NMR (100.5 MHz, CDCl$_3$) δ 11.9, 17.9, 38.1, 55.6, 57.9, 60.3, 66.0, 68.7, 70.1, 96.3, 126.1, 126.5, 127.8, 127.9, 128.9, 129.3, 139.5. HRMS calcd. for C$_{24}$H$_{40}$NO$_5$BrSiNa$^+$ 552.1757, found 552.1761 (Δ= 0.8 ppm).

1-Bromo-2-ethenyl-6-hydroxymethylbenzene (5-70):[34]
To a solution of PPh$_3$CH$_3$Br (2.0 g, 5.60 mmol) in THF (30 mL) at 0 °C was added sodium hydride (60% suspension in mineral oil, 340mg, 8.0 mmol). The mixture was stirred at room temperature for 1 h. The suspension was added to a solution of **5-44** (886 mg, 4.12 mmol) and sodium hydride (60% suspension in mineral oil, 170 mg, 4.0 mmol) in THF (10 mL). The mixture was stirred at 40 °C for 40 min and quenched with saturated aqueous ammonium chloride (60 mL). The water layer was extracted with chloroform (60 mL x 3). The organic layers were combined and washed with brine (20 mL x 2) and dried over anhydrous MgSO$_4$. The solvent was removed under reduced pressure. The residue was purified by column chromatography on silica gel using hexanes:EtOAc (8/1) as the eluent to afford **5-70** as a white solid (725 mg, 83%): mp 69-69 °C; ^{1}H NMR (400 MHz, CDCl$_3$) δ 2.24 (bs, 1 H), 4.75 (s, 2 H), 5.38 (d, J = 10.8 Hz, 1 H), 5.68 (d, J = 13.2 Hz, 1 H), 7.10 (dd, J = 17.2, 10.8 Hz, 1 H), 7.29 (t, J = 7.6 Hz, 1 H), 7.38 (d, J = 6.4 Hz, 1 H), 7.47 (d, J = 7.6 Hz, 1 H); ^{13}C NMR (100.5 MHz, CDCl$_3$) δ 65.5, 117.1, 123.6, 126.2, 127.4, 127.9, 136.0, 138.2, 140.3. HRMS calcd. for C$_9$H$_9$OBr$^+$ 211.9837, found 211.9835 (Δ= 0.9 ppm).

1-(*tert*-Butoxycarbonyl)-2-[hydroxy(2-hydroxymethyl-6-ethenylphenyl)-methyl]-4-triisopropylsiloxy-pyrrolidine (5-72):[31]
Bromide **5-70** (94 mg, 0.44 mmol) was desolved in dry THF (4 mL) under N$_2$ and 2.5 M *n*-BuLi in hexane (0.39 mL, 0.97 mmol) was added at -78 °C. The resulting solution was stirred for 1 h. Then HMPA (0.09 mL) was added and the solution was stirred for 1 h. A solution of aldehyde **5-14** (127 mg, 0.34 mmol) in dry THF (2.8 mL) was added dropwise. The resulting solution was allowed to slowly warm up to room temperature with stirring overnight. Then, the reaction was quenched with a saturated NH$_4$Cl solution (20 mL) and the mixture was extracted with dichloromethane (3 x 20 mL). The combined organic layers were washed with brine and dried over MgSO$_4$. The solvent was removed under reduced pressure, and the residue was purified by flash chromatography on silica gel (hexanes/EtOAc = 8/1-4/1) to give the desired product **5-72** (139 mg, 81% yield) as white solid: mp 38-40 °C; ^{1}H NMR (400 MHz, CDCl$_3$) δ 0.96 (m, 21 H), 1.32-1.44 (m, 9H), 1.74 (m, 1 H), 2.19 (m, 1 H), 3.26 (dd, J =11.2, 3.6 Hz, 1 H), 3.34 (dd, J = 10.4, 5.2 Hz, 1 H), 3.67 (d, J = 9.6, 1 H), 3.99 (s, 1 H), 4.31 (m, 1 H), 4.58 (m, 1 H), 4.76 (m, 1 H), 4.96 (m, 1 H), 5.10 (d, J = 10.8 Hz, 1 H), 5.42 (m, 2 H), 7.03 (m, 1 H), 7.28 (m, 3 H); ^{13}C NMR (100.5 MHz, CDCl$_3$) δ 12.8, 18.5, 28.9, 39.4, 56.5, 57.1, 65.5, 70.9, 80.2, 81.3,

116.5, 117.7, 127.4, 127.7, 131.2, 136.5, 136.8, 140.2, 158.7. HRMS calcd. for $C_{28}H_{47}NO_5SiNa^+$ 528.3121, found 528.3116 (Δ= -1.0 ppm).

2-[Acetoxy(2-acetoxymethyl-6-ethenylphenyl)methyl]-2-(*tert*-butoxycarbonyl)-4-triisopropylsiloxy-pyrrolidine (5-73):[39]

To a solution of **5-72** (134 mg, 0.26 mmol) and DMAP (4.8 mg, 0.06 mmol) in CH_2Cl_2 (2.0 mL) was added triethylamine (0.41 mL, 1.4 mmol) and acetic anhydride (0.27 mL, 0.84 mmol) at 0 ^{o}C. The reaction mixture was stirred overnight, quenched with saturated aqueous NH_4Cl solution (20 mL) and extracted with dichloromethane (30 mL x 3). The organic layer was dried over anhydrous $MgSO_4$ and the solvent was removed under reduced pressure to afford a liquid. The residue was purified by silica gel column chromatography on silica gel using hexanes:EtOAc (8:1) to afford **5-73** (150 mg, 97%) as colorless oil: ^{1}H NMR (400 MHz, CDCl$_3$) δ 1.04 (m, 21 H), 1.28-1.43 (m, 9 H), 1.70 (m, 1 H), 2.06-2.10 (m, 7 H), 3.40 (m, 1 H), 3.62 (m,1 H), 4.57 (m, 2 H), 4.79 (m, 1 H), 5.31 (m, 3 H), 5.54 (m, 2 H), 6.03 (m, 1 H), 7.17-7.52 (m, 4 H); ^{13}C NMR (100.5 MHz, CDCl$_3$) δ 12.1, 17.9, 20.9, 28.0, 28.4, 38.3, 55.0, 58.5, 64.3, 71.0, 73.9, 79.5, 116.6, 128.2, 128.7, 129.9, 132.3, 134.2, 136.5, 139.4, 154.6, 170.3, 170.7. HRMS calcd. for $C_{32}H_{51}NO_7SiNa^+$ 612.3333, found 612.3329 (Δ= -0.6 ppm).

10-Acetoxy-9-acetoxymethyl-2-triisopropylsiloxy-1,2,3,5,10,10a-hexahydropyrrolo[1,2-b]isoquinolin-5-one (5-77 and 5-78):[39, 41, 44]

Nitrogen gas was bubbled into a solution of **5-73** (167 mg, 0.28 mmol) in CH_2Cl_2 (15 mL) at -78 $^{\circ}$C for 3 min. Then, O_3 gas was bubbled into the solution till the color of the solution turned blue (8 min), and N_2 was bubbled into the solution for another 3 min until the blue color disappeared. Dimethyl sulfide (0.1 mL, 1.4 mmol) was added to the solution and the reaction mixture was allowed to warm to room temperature. The reaction mixture was stirred at room temperature for 3 h. The solvents were removed *in vacuo* and crude **5-74** was used in the next step without further purification.

Sodium chlorite (200 mg, 2.24 mmol) was added to a solution of **5-74** (~0.28 mmol) and sodium phosphate (monobasic) (350 mg, 2.24 mmol) in acetone/water (1:1, 2.4 mL). The reaction mixture was stirred at room temperature for 1 h and quenched with ethyl acetate (60 mL). The organic layer was washed with hydrochloric acid (1 *N*, 10 mL), $Na_2S_2O_3$ (10%, 10 mL x 2), brine (10 mL), dried over $MgSO_4$, filtered, and concentrated. Crude **5-75** was used in the next step without further purification.

A solution of potassium hydroxide (4 g) in water (8 mL) and ethanol (32 mL) was added to a solution of diazald$^{®}$ (4 g) in ether (60 mL) at 0 ^{o}C. The mixture was stirred for 10 min at 0 ^{o}C and distilled to afford a yellow ether solution. The diazomethane solution in ether was added to the solution of **5-75** (~ 0.28 mmol) in ether (12 mL) until the yellow color did not disappear. The mixture was stirred for 10 min and the reaction was quenched with acetic acid. The solvents were removed *in vacuo* and crude **5-76** was used in the next step without further purification.
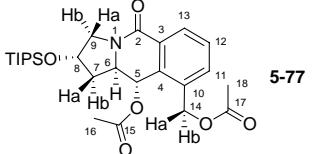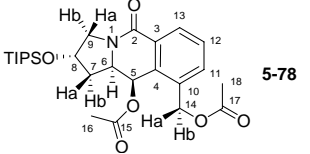
To a solution of **5-76** (~ 0.28 mmol) in dichloromethane (1.5 mL) at 0 ^{o}C was added trifluoroacetic acid (1.5 mL). The mixture was stirred at 0 ^{o}C for 30 min and room temperature for 30 min. The solvent and acid were removed under reduced pressure and the residue was used in next step without further purification.

To a solution of the residue in ethyl acetate (14 mL) was added saturated aqueous sodium bicarbonate (14 mL). The mixture was stirred vigorously overnight and the reaction was quenched with ethyl acetate (50 mL). The reaction mixture was washed with water (10 mL) saturated aqueous ammonium chloride (10 mL), water (10 mL) and brine (10 mL). The organic layer was dried over anhydrous MgSO$_4$ and the solvent was removed under reduced pressure. The residue was purified by column chromatography on silica gel using hexanes:EtOAc (3:1) to afford **5-77** and **5-78** (1:2) in 50% for 5 steps.

5-77: colorless oil; $[\alpha]_D^{22}$ −80.4 (c 1.1, CHCl$_3$); ^{1}H NMR (400 MHz, CDCl$_3$) δ 1.09 (m, 21 H), 2.05 (s, 3 H), 2.06 (m, 2 H), 2.21 (s, 3 H), 3.80 (d, J = 3.2 Hz, 2 H), 4.15 (td, J = 10.8, 5.6 Hz, 1 H), 4.61 (s, 1 H), 5.09 (d, J = 12.8 Hz, 1 H), 5.33 (d, J = 12.8 Hz, 1H), 6.38 (d, J = 12.8, 1 H), 7.43 (t, J = 7.6 Hz, 1 H), 7.50 (d, J = 1.2 Hz, 1 H), 8.15 (dd, J = 7.6, 1.6 Hz, 1 H); ^{13}C NMR (100.5 MHz, CDCl$_3$) δ 12.2, 18.2, 20.8, 21.1, 42.2, 55.3, 58.9, 65.8, 69.5, 73.1, 128.6, 129.2, 130.8, 132.9, 134.2, 135.5, 162.3, 170.4, 171.1. HRMS calcd. for C$_{26}$H$_{39}$NO$_6$SiH$^+$ 490.2625, found 490.2621 (Δ= -0.8 ppm).

5-78: colorless oil; $[\alpha]_D^{22}$ −137 (c 0.9, CHCl$_3$); ^{1}H NMR (400 MHz, CDCl$_3$) δ 1.09 (m, 21 H), 1.83 (td, J = 12.4, 4.0 Hz, 1 H), 2.02 (s, 3 H), 2.07 (s, 3 H), 2.13 (ddd, J = 18.4, 7.2, 4.8 Hz, 1 H), 3.72 (d, J = 13.2 Hz, 1 H), 3.80 (dd, J = 12.8, 4.4, 1 H), 4.31 (ddd, J = 10.8, 5.6, 2.4 Hz, 1 H), 4.66 (t, J = 3.6 Hz, 1 H), 5.17 (d, J = 12.4 Hz, 1 H), 5.28 (d, J = 12.8 Hz, 1 H), 6.40 (d, J = 2.4 Hz, 1 H), 7.55 (m, 2 H), 8.18 (dd, J = 7.2, 1.6 Hz, 1 H); ^{13}C NMR (100.5 MHz, CDCl$_3$) δ 12.0, 17.9, 20.8, 20.9, 37.8, 54.6, 57.5, 63.1, 63.7, 69.5, 128.5, 129.8, 131.5, 133.5, 133.8, 162.0, 170.0, 170.4. HRMS calcd. for C$_{26}$H$_{39}$NO$_6$SiH$^+$ 490.2625, found 490.2618 (Δ= -1.4 ppm).

Table 5-5. Fully assigned ^{1}H NMR and ^{13}C NMR of diastereomers 5-77 and 5-78

	^{1}H NMR, ppm (a)	^{1}H NMR, ppm (b)	^{13}C NMR, ppm	^{1}H NMR, ppm (a)	^{1}H NMR, ppm (b)	^{13}C NMR, ppm
2	------------------	------------------	162.3	------------------	------------------	162.0
3	------------------	------------------	135.5	------------------	------------------	133.8
4	------------------	------------------	134.2	------------------	------------------	133.5
5	6.38 (d, J = 12.8)	------------------	73.1	------------------	6.40 (d, J = 2.4 Hz)	69.5
6	------------------	4.15 (td, J = 10.8, 5.6 Hz)	58.9	------------------	4.31 (ddd, J = 10.8, 5.6, 2.4 Hz)	57.5
7	2.06 (m)	2.06 (m)	42.2	1.83 (td, J = 12.4, 4.0 Hz)	2.13 (ddd, J = 18.4, 7.2, 4.8 Hz)	37.8
8	4.61 (s)	------------------	65.8	4.66 (t, J = 3.6 Hz)	------------------	63.1
9	3.80 (d, J = 3.2 Hz)	3.80 (d, J = 3.2 Hz)	55.3	3.72 (d, J = 13.2 Hz)	3.80 (dd, J = 12.8, 4.4)	54.6
10	------------------	------------------	129.2	------------------	------------------	129.8
11	7.50 (d, J = 1.2 Hz)	------------------	130.8	7.55 (m)	------------------	129.8
12	7.43 (t, J = 7.6 Hz)	------------------	128.6	7.55 (m)	------------------	128.5
13	8.15 (dd, J = 7.6, 1.6 Hz)	------------------	132.9	8.18 (dd, J = 7.2, 1.6 Hz)	------------------	131.5
14	5.09 (d, J = 12.8 Hz)	5.33 (d, J = 12.8 Hz)	69.5	5.28 (d, J = 12.8 Hz)	5.17 (d, J = 12.4 Hz)	63.7
15	------------------	------------------	170.4	------------------	------------------	170.0
16	2.05 (s)	------------------	20.8	2.02 (s)	------------------	20.8
17	------------------	------------------	171.1	------------------	------------------	170.4
18	2.21 (s)	------------------	21.1	2.07 (s)	------------------	20.9

10-Hydroxy-9-hydroxymethyl-2-triisopropylsiloxy-2,3,10,10a-tetrahydro-1H-pyrrolo[1,2-b]isoquinolin-5-one (5-79):[39]

To a solution of **5-78** (140 mg, 0.28 mmol) in methanol (10.9 mL) and water (5.5 mL) was added potassium carbonate (115 mg, 0.70 mmol). The reaction mixture was stirred at room temperature for 35 min. Then, the mixture was quenched with ethyl acetate and the organic layer was washed with saturated aqueous NH_4Cl solution (20 mL), water (10 mL x 2) and brine (10 mL). The organic layer was dried over anhydrous $MgSO_4$ and solvent was removed under reduced pressure. The residue was purified by column chromatography on silica gel using 3% methanol in chloroform as elant to afford **5-79** as a white solid (100 mg, 88%): mp 46-48 ^{o}C; $[\alpha]_D^{22}$ –110 (c 2.0, $CHCl_3$); ^{1}H NMR (400 MHz, $CDCl_3$) δ 1.04 (m, 21 H), 2.06 (dd, J = 12.8, 6.0 Hz, 1 H), 2.48 (td, J = 12.8, 4.0 Hz, 1 H), 3.65 (d, J = 12.8 Hz, 1 H), 3.72 (dd, J = 12.8, 4.0 Hz, 1 H), 4.06 (ddd, J = 10.8, 5.6, 2.8 Hz, 1 H), 4.58 (d, J = 12.8 Hz, 1 H), 4.68 (t, J = 3.6 Hz, 1 H), 4.79 (d, J = 3.2 Hz, 1 H), 4.94 (d, J = 12.8 Hz, 1 H), 7.06 (t, J = 7.6 Hz, 1 H), 7.37 (m, 2 H); ^{13}C NMR (100.5 MHz, $CDCl_3$) δ 12.0, 17.9, 36.7, 55.0, 58.5, 62.6, 63.3, 69.8, 127.0, 128.6, 128.9, 132.3, 137.1, 138.6, 162.9. HRMS: m/e calcd for $C_{22}H_{35}NO_4SiH^+$: 406.2414 Found: 406.2397 (Δ = -4.1 ppm).

9-Acetoxymethyl-10-hydroxy-2-triisopropylsiloxy-1,2,3,5,10,10a-hexahydro-pyrrolo[1,2-b]isoquinolin-5-one (5-81):[39]

To a solution of **5-79 (**42 mg, 0.10 mmol) in THF (1.8 mL) was added 1 M NaHMDS in THF (0.11 mL, 0.11 mmol) at -40 ^{o}C. After the reaction mixture was stirred for 5 min, acetic chloride (7.8 μL, 0.11 mmol) was added dropwise. The reaction was quenched with saturated NH_4Cl (15 mL) after 20 min and extracted with dichloromethane (30 mL x 3). The organic layer was concentrated *in vacuo*. Purification of the crude product by column chromatography on silica gel (2% methanol in chloroform) afforded the **5-81** as a white solid (20 mg, 45%): ^{1}H NMR (400 MHz, $CDCl_3$) δ 1.06 (m, 21 H), 2.11 (s, 3 H), 2.56 (td, J = 12.8, 4.4 Hz, 1 H), 3.67 (d, J = 12.8 Hz, 1 H), 3.79 (dd, J = 12.8, 4.0 Hz, 1 H), 4.08 (ddd, J =10.4, 5.6, 2.4 Hz, 1 H), 4.71 (s, 1 H), 4.84 (d, J = 2.4 Hz, 1 H), 5.24 (d, J = 12.4 Hz, 1 H), 5.35 (d, J = 12.4 Hz, 1 H), 7.09 (t, J = 7.6 Hz, 1 H), 7.39 (d, J = 6.8 Hz, 1 H), 7.58 (d, J = 3.6 Hz, 1 H); ^{13}C NMR (100.5 MHz, $CDCl_3$) δ 12.0, 18.0, 36.8, 55.1, 58.9, 62.6, 63.1, 69.9, 127.8, 128.7, 128.3, 133.0, 133.2, 137.9, 162.5, 170.8. HRMS: m/e calcd for $C_{24}H_{37}NO_5SiH^+$: 448.2519 Found: 448.2523 (Δ = 0.8 ppm).

9-(*tert*-Butyldimethylsiloxymethyl)-10-hydroxy-2-triisopropylsiloxy-2,3,10,10a-tetrahydro-1H-pyrrolo[1,2-b]isoquinolin-5-one (5-80):[35]

To a solution of **5-79** (102 mg, 0.25 mmol) and imidazole (68 mg, 1.00 mmol) in dry DMF (0.3 mL) was added chloro-*t*-butyldimethylsilane (0.38 mmol) in DMF (0.7 mL) dropwise *via* syringe at 0 ^{o}C, and then the reaction mixture was stirred for 15 min at room temperature. The reaction mixture was quenched with saturated aqueous NH_4Cl solution (10 mL). The mixture was extracted with EtOAc (20 mL x 3), then washed with water (10 mL x 2), brine (10 mL), dried over $MgSO_4$, and concentrated *in vacuo*. The crude product was purified on a silica gel column using hexanes:EtOAc (2:1) as the eluent to give **5-80** as a white solid (257 mg, 94%): mp 134-135 ^{o}C; $[\alpha]_D^{22}$ –99 (c 3.7, $CHCl_3$); ^{1}H NMR (400 MHz, $CDCl_3$) δ 0.12 (s, 3 H), 0.14 (s, 3 H), 0.93 (s, 9 H), 1.04 (m, 21 H), 2.06 (dd, J = 12.8, 6.0 Hz, 1 H), 2.55 (td, J = 12.8, 4.0 Hz, 1 H), 3.67 (d, J = 12.8 Hz, 1 H),

3.78 (dd, J = 12.8, 4.4 Hz, 1 H), 4.09 (ddd, J = 11.4, 5.6, 2.8 Hz, 1 H), 4.69 (s, 1 H), 4.82 (d, J = 2.8 Hz, 1 H), 4.84 (d, J = 12.8 Hz, 1 H), 4.96 (d, J = 12.8 Hz, 1 H), 7.09 (t, J = 7.6 Hz, 1 H), 7.40 (d, J = 7.2 Hz, 1 H), 7.59 (d, J = 8.4 Hz, 1 H); ^{13}C NMR (100.5 MHz, CDCl$_3$) δ -5.3, 12.0, 17.9, 18.2, 25.8, 36.8, 55.0, 58.6, 62.4, 63.1, 69.9, 126.7, 128.3, 128.9, 130.9, 137.1, 138.0, 162.7. HRMS: m/e calcd for C$_{28}$H$_{49}$NO$_4$Si$_2$H$^+$: 520.3278 Found: 520.3279 (Δ = 0.1 ppm).

10-Hydroxy-9-hydroxymethyl-2-triisopropylsiloxy-2,3,10,10a-tetrahydro-1H-pyrrolo[1,2-b]isoquinolin-5-one (5-84):[39]

To a solution of **5-77** (133 mg, 0.27 mmol) in methanol (10.9 mL) and water (5.5 mL) was added potassium carbonate (115 mg, 0.70 mmol). The reaction mixture was stirred at room temperature for 35 min. Then the mixture was quenched with ethyl acetate (50 mL) and the organic layer was washed with saturated aqueous NH$_4$Cl solution (10 mL), water (10 mL x 2) and brine (10 mL). The organic layer was dried over anhydrous MgSO$_4$ and solvent was removed under reduced pressure. The residue was purified by column chromatography on silica gel using 3% methanol in chloroform as elant to afford **5-84** as a white solid (92 mg, 84%): mp 153-155 °C; [α]$_D^{22}$ −86 (c 1.5, CHCl$_3$); ^{1}H NMR (400 MHz, CDCl$_3$) δ 1.06 (m, 21 H), 1.85 (ddd, J = 14.8, 10.8, 4.0 Hz, 1 H), 2.48 (dd, J = 12.8, 5.6 Hz, 1 H), 3.68 (d, J = 13.6 Hz, 1 H), 3.72 (dd, J = 13.2, 4.4 Hz, 1 H), 4.02 (td, J = 16.4, 5.2 Hz, 1 H), 4.61 (t, J = 3.6 Hz, 1 H), 4.71 (t, J = 12.4 Hz, 1 H), 4.83 (m, 2 H), 5.79 (bs, 1 H), 7.22 (m, 2 H), 7.78 (dd, J = 7.6, 3.6 Hz, 1 H); ^{13}C NMR (100.5 MHz, CDCl$_3$) δ 11.9, 17.9, 42.3, 55.3, 59.8, 65.1, 69.4, 73.3 127.5, 127.8, 129.5, 133.8, 137.3, 139.7, 162.9. HRMS: m/e calcd for C$_{22}$H$_{35}$NO$_4$SiH$^+$: 406.2414 Found: 406.2411 (Δ = -0.6 ppm).

9-(*tert*-Butyldimethylsiloxymethyl)-10-hydroxy-2-triisopropylsiloxy-2,3,10,10a-tetrahydro-1H-pyrrolo[1,2-b]isoquinolin-5-one (5-85):[39]

To a solution of **5-84** (90 mg, 0.22 mmol) and imidazole (60 mg, 0.88 mmol) in dry DMF (0.6 mL) was added chloro-*t*-butyldimethylsilane (0.29 mmol in 1.2 mL DMF) dropwise *via* syringe at 0 °C. The reaction mixture was stirred for 35 min at room temperature and quenched with saturated aqueous NH$_4$Cl solution (10 mL). The mixture was extracted with EtOAc (20 mL x 3), washed with water (10 mL x 2), and brine (10 mL), dried over MgSO$_4$ and concentrated *in vacuo*. The crude product was purified on a silica gel column using hexanes:EtOAc (2:1) as the eluent to give **5-85** as a white solid (113 mg, 99%): mp 183-184 °C; [α]$_D^{22}$ −110 (c 2.5, CHCl$_3$); ^{1}H NMR (400 MHz, CDCl$_3$) δ -0.01 (s, 3 H), 0.09 (s, 3 H), 0.87 (s, 9 H), 1.04 (m, 21 H), 1.93 (td, J = 12.8, 4.0 Hz, 1 H), 2.51 (dd, J = 12.8, 5.6 Hz, 1 H), 3.72 (d, J = 12.8 Hz, 1 H), 3.84 (dd, J = 12.8, 4.4 Hz, 1 H), 4.09 (td, J = 10.8, 5.6 Hz, 1 H), 4.64 (s, 1 H), 4.74 (d, J = 12.8 Hz, 1 H), 4.88 (dd, J = 10.8, 3.6, 1 H), 5.18 (d, J = 12.8 Hz, 1 H), 5.61 (d, J = 4.4 Hz, 1 H), 7.28 (m, 2 H), 8.04 (dd, J = 7.2, 2.0 Hz, 1 H); ^{13}C NMR (100.5 MHz, CDCl$_3$) δ -5.4, -5.1, 12.0, 17.9, 18.1, 25.6, 42.5, 55.2, 59.6, 66.2, 69.6, 73.8, 127.3, 128.3, 130.4, 132.7, 136.1, 139.9, 162.5. HRMS: m/e calcd for C$_{28}$H$_{49}$NO$_4$Si$_2$H$^+$: 520.3278 Found: 520.3279 (Δ = 0.1 ppm).

10-Benzoyloxy-9-(*tert*-butyldimethylsiloxymethyl)- 2-triisopropylsiloxy-1,2,3,5,10,10a-hexahydropyrrolo[1,2-b]isoquinolin-5-one (5-86):[39]

To a solution of **5-85** (60 mg, 0.115 mmol) and DMAP (4.8 mg, 0.06 mmol) in CH_2Cl_2 (1.0 mL) was added triethylamine (0.13 mL, 0.92 mmol) and benzoyl chloride (0.1 mL, 0.69 mmol) at 0 °C. The reaction mixture was stirred overnight, quenched with saturated aqueous NH_4Cl solution (20 mL) and extracted with dichloromethane (30 mL x 3). The organic layer was dried over anhydrous $MgSO_4$ and solvent was removed under reduced pressure to afford a liquid. The residue was purified by column chromatography on silica gel using hexanes:EtOAc (6:1) to afford **5-86** (73 mg, 100%) as colorless oil: $[\alpha]_D^{22}$ –110 (c 1.3, $CHCl_3$); ^{1}H NMR (400 MHz, $CDCl_3$) δ -0.22 (s, 3 H), 0.21 (s, 3 H), 0.75 (s, 9 H), 1.02 (m, 21 H), 2.15 (m, 2 H), 3.85 (m, 2 H), 4.30 (td, J = 10.8, 6.0 Hz, 1 H), 4.63 (s, 1 H), 4.67 (d, J = 14.4 Hz, 1 H), 4.76 (d, J = 14.0, 1 H), 6.60 (d, J = 10.8 Hz, 1 H), 7.48 (m, 3 H), 7.64 (m, 2 H), 8.13 (m, 3 H). ^{13}C NMR (100.5 MHz, $CDCl_3$) δ -5.7, -5.8, 12.0, 17.9, 18.2, 25.7, 41.9, 55.1, 58.7, 63.2, 69.3, 73.2, 127.2, 128.3, 128.7, 129.2, 129.7, 129.8, 130.7, 133.7, 133.8, 138.9, 162.8, 165.5. HRMS: *m/e* calcd for $C_{35}H_{53}NO_5Si_2H^+$: 624.3541 Found: 624.3516 (Δ = -3.9 ppm).

10-Benzoyloxy-2-triisopropylsiloxy-1,2,3,5,10,10a-hexahydropyrrolo[1,2-b]isoquinolin-5-one (5-87):[37]

To a solution of **5-86** (134 mg, 0.21 mmol) in ethanol (10 mL) was added 0.5 *N* HCl in ethanol (2 mL). The reaction mixture was stirred at room temperature for 2.5 h. Then, the mixture was quenched with saturated aqueous $NaHCO_3$ solution (20 mL) and extracted with dichloromethane (30 mL x 3). The organic layer was washed with water (10 mL) and brine (10 mL). The organic layer was dried over anhydrous Na_2SO_4 and solvent was removed under reduced pressure. The residue was purified by column chromatography on silica gel using hexanes:EtOAc (2:1) to afford **5-87** as a white solid (102 mg, 95%): mp 95-98 °C; $[\alpha]_D^{22}$ -130 (c 1.3, $CHCl_3$); ^{1}H NMR (400 MHz, $CDCl_3$) δ 0.98 (m, 21 H), 2.17 (m, 2 H), 2.68 (bs, 1 H), 3.75 (d, J = 12.8 Hz, 1 H), 3.88 (dd, J = 12.8, 4.4 Hz, 1 H), 4.30 (td, J = 10.8, 6.0 Hz, 1 H), 4.55 (d, J = 13.6Hz, 1 H), 4.62 (d, J = 13.6, 1 H), 4.66 (s, 1 H), 6.53 (d, J = 10.8 Hz, 1 H), 7.32 (t, J = 8.0 Hz, 1 H), 7.49 (t, J = 8.0 Hz, 2 H), 7.61 (m, 2 H), 7.86 (dd, J = 7.6, 1.2 Hz, 1 H), 8.10 (dd, J = 8.4, 1.2 Hz, 2 H). ^{13}C NMR (100.5 MHz, $CDCl_3$) δ 11.9, 17.9, 42.0, 55.1, 58.8, 63.1, 69.2, 73.0, 127.5, 128.4, 128.7, 129.1, 129.8, 132.1, 133.7, 134.1, 138.9, 162.7, 165.9. HRMS: *m/e* calcd for $C_{29}H_{39}NO_5SiH^+$: 510.2676 Found: 510.2672 (Δ = -0.7 ppm).

9-Acetoxymethyl-10-benzoyloxy-2-triisopropylsiloxy-1,2,3,5,10,10a-hexahydropyrrolo[1,2-b]isoquinolin-5-one (5-88):[39]

To a solution of **4-31** (32 mg, 0.06 mmol) and DMAP (1 mg, 0.005 mmol) in CH_2Cl_2 (0.5 mL) was added triethylamine (0.08 mL, 0.24 mmol) and acetic anhydride (0.05 mL, 0.12 mmol) at 0 °C. The reaction mixture was stirred overnight, quenched with saturated aqueous NH_4Cl solution (20 mL) and extracted with dichloromethane (20 mL x 3). The organic layer was dried over anhydrous $MgSO_4$ and solvent was removed under reduced pressure. The residue was purified by column chromatography on silica gel using hexanes:EtOAc (2:1) as the eluent to afford **5-88** (35 mg, 100%) as a colorless oil: $[\alpha]_D^{22}$ –164 (c 14.1, $CHCl_3$); ^{1}H NMR (400 MHz, $CDCl_3$) δ 1.05 (m, 21 H), 1.89 (s, 3 H), 2.17 (m, 2 H), 3.83 (td, J = 12.8, 3.6 Hz, 1 H), 4.32 (dd, J = 16.4, 9.2 Hz, 1 H), 4.63 (d, J =

257

2.0 Hz, 1 H), 5.02 (d, J = 12.8, 1 H), 5.20 (d, J = 12.4 Hz, 1 H), 6.70 (d, J = 10.8 Hz, 1 H), 7.48 (m, 4 H), 7.64 (ddd, J = 8.8, 2.4, 1.2 Hz, 1 H), 8.10 (dd, J = 8.4, 1.2 Hz, 2 H), 8.20 (dd, J = 6.8, 2.4 Hz, 1 H). ^{13}C NMR (100.5 MHz, CDCl$_3$) δ 11.9, 17.9, 20.4, 41.9, 55.1, 58.8, 65.3, 69.3, 73.1, 128.5, 128.7, 129.0, 129.1, 129.7, 130.6, 133.0, 133.8, 134.3, 135.7, 162.2, 165.7, 170.3. HRMS: m/e calcd for C$_{31}$H$_{41}$NO$_6$SiH$^+$: 552.2781 Found: 552.2781 (Δ = -0.1 ppm).

9-Acetoxymethyl-10-benzoyloxy-2-hydroxyl-1,2,3,5,10,10a-hexahydropyrrolo[1,2-b]isoquinolin-5-one (5-89):[25]

To a solution of **5-88** (31 mg, 0.056 mmol) in CH$_3$CN (0.6 mL) and pyridine (0.6 mL) was added HF-pyridine (70:30, 0.31 ml) and the reaction mixture was stirred overnight. The reaction mixture was diluted with EtOAc (40 mL) and washed with saturated aqueous NaHCO$_3$ solution (10 mL x 2), CuSO$_4$ solution (10 mL x 3), water (10 mL x 3) and brine (3 mL). The organic layer was dried over anhydrous MgSO$_4$ and solvent was removed under reduced pressure. The residue was purified by column chromatography using hexanes:EtOAc (1:4) as the eluent to afford **5-89** as white solid (23 mg, 100%): mp 76-77 $^{\circ}$C; [α]$_D$^{22} –239 (c 10.3, CHCl$_3$); ^{1}H NMR (400 MHz, CDCl$_3$) δ 1.90 (s, 3 H), 2.24 (m, 2 H), 3.83 (d, J = 11.2 Hz, 2 H), 4.32 (td, J = 8.4, 4.4 Hz, 1 H), 4.64 (t, J = 3.2 Hz, 1 H), 5.04 (d, J = 10.0, 1 H), 5.21 (d, J = 10.4 Hz, 1 H), 6.70 (d, J = 8.4 Hz, 1 H), 7.48 (m, 4 H), 7.64 (t, J = 6.0 Hz, 1 H), 8.10 (d, J = 6.0 Hz, 2 H), 8.18 (dd, J = 6.0, 1.2 Hz, 1 H). ^{13}C NMR (100.5 MHz, CDCl$_3$) δ 20.6, 41.2, 54.8, 58.9, 65.6, 68.8, 73.4, 128.8, 129.0, 129.1, 129.2, 130.0, 130.7, 133.4, 134.1, 134.6, 135.9, 162.6, 165.9, 170.6. HRMS: m/e calcd for C$_{22}$H$_{21}$NO$_6$H$^+$: 396.1447 Found: 396.1436 (Δ = -2.8 ppm).

9-Acetoxymethyl-10-benzoyloxy-5-oxo-1,2,3,5,10,10a-hexahydro-pyrrolo[1,2-b]isoquinolin-2-yl-3-benzoyl-2-(4-methoxy-phenyl)-4-phenyl-oxazolidine-5-carboxylate (5-90):[39]

To a solution of **5-89** (20 mg, 0.053 mmol) acid **5-4** (21 mg, 0.053 mmol) and DMAP (3.5 mg, 0.026 mmol) in CH$_2$Cl$_2$ (0.5 mL) was added EDC (22 mg, 0.11 mmol) and the reaction mixture was stirred overnight. The mixture was then quenched with EtOAc (50 mL) and washed with water (10 mL x 2) and brine (10 mL). The organic layer was dried over anhydrous MgSO$_4$, filtered, and solvent was removed under reduced pressure. The residue was purified by column chromatography on silica gel using hexanes:EtOAc (1/2) as the eluent to afford **5-90** as a white solid (27 mg, 82% based on 85% conversion): mp 109-111 $^{\circ}$C; ^{1}H NMR (400 MHz, CDCl$_3$) δ 1.90 (s, 3 H), 2.32 (dd, J = 14.0, 5.2 Hz, 1 H), 2.42 (td, J = 10.8, 4.4 Hz, 1 H), 3.80 (s, 3 H), 3.89 (d, J = 14.8 Hz, 1 H), 4.05 (d, J = 14.4, 4.8, 1 H), 4.17 (td, J = 10.8, 5.6 Hz, 1H), 4.81 (d, J = 2.0 Hz, 1 H), 5.05 (d, J = 11.6 Hz, 1 H), 5.22 (d, J = 12.8 Hz, 1 H), 5.36 (bs, 1 H), 5.55 (t, J = 4.0 Hz, 1 H), 6.71 (d, J = 10.8 Hz, 1 H), 6.81 (d, J = 8.4 Hz, 2 H), 7.25 (m, 11 H), 7.47 (m, 4), 7.63 (t, J = 7.6 Hz, 1 H), 8.12 (d, J = 7.2 Hz, 2 H), 8.21 (dd, J = 7.2, 2.0 Hz, 1 H). ^{13}C NMR (100.5 MHz, CDCl$_3$) δ 20.4, 38.3, 51.8, 55.3, 58.8, 65.4, 72.9, 73.0, 113.5, 127.0, 127.1, 128.1, 128.2, 128.6, 128.7, 128.7, 128.8, 129.0, 129.8, 129.8, 130.2, 130.7, 133.3, 134.0, 134.6, 135.2, 135.4, 159.9, 162.1, 165.6, 169.3, 170.2. HRMS: m/e calcd for C$_{46}$H$_{40}$N$_2$O$_{10}$H$^+$: 781.2761 Found: 781.2789 (Δ = 3.6 ppm).

9-Acetoxymethyl-10-benzoyloxy-5-oxo-1,2,3,5,10,10a-hexahydropyrrolo[1,2-b]isoquinolin-2-yl (2S,3R)-3-benzoylamino-2-hydroxy-3-phenylpropanoate (5-37):[39]

To a solution of **5-90** (26 mg, 0.03 mmol) in methanol (0.5 mL) was added *p*-TSA (1.5 mg, 0.006 mmol). After stirring overnight, the solvent was removed and the residue purified by a silica gel column chromatography using Hexanes:EtOAc = 1/2 as the eluent) to afford **5-37** as a white solid (16 mg, 75%): mp 116-118 $^{\circ}$C; $[\alpha]_D^{22}$ –135 (c 2.7, CHCl$_3$); ^{1}H NMR (400 MHz, CDCl$_3$) δ 1.90 (s, 3 H), 2.37 (td, *J* = 8.8, 3.2 Hz, 1 H), 2.48 (dd, *J* = 11.2, 4.4 Hz, 1 H), 3.18 (d, *J* = 2.8 Hz, 1 H), 3.99 (dd, *J* = 11.2, 3.6 Hz, 1 H), 4.03 (d, *J* = 12.0 Hz, 1 H), 4.44 (td, *J* = 8.8, 4.4 Hz, 1 H), 4.62 (s, 1 H), 5.05 (d, *J* = 10.0 Hz, 1 H), 5.22 (d, *J* = 10.4 Hz, 1 H), 5.59 (t, *J* = 3.2 Hz, 1 H), 5.69 (d, *J* = 7.6 Hz, 1 H), 6.71 (d, *J* = 9.2 Hz, 1 H), 6.74 (d, *J* = 7.2 Hz, 1 H), 7.17 (t, *J* = 6.0 Hz, 1 H), 7.41 (m, 11 H), 7.61 (t, *J* = 6.0 Hz, 1 H), 8.13 (d, *J* = 6.0 Hz, 2 H), 8.20 (dd, *J* = 5.6, 1.6 Hz, 1 H). ^{13}C NMR (100.5 MHz, CDCl$_3$) δ 20.3, 38.1, 51.5, 54.4, 58.7, 65.5, 73.2, 73.6, 126.8, 126.9, 128.0, 128.4, 128.5, 128.7, 128.7, 128.9, 128.9, 130.0, 130.3, 131.5, 133.2, 133.6, 133.7, 134.5, 136.0, 138.4, 162.5, 165.7, 166.7, 170.2, 172.2. HRMS: *m/e* calcd for C$_{38}$H$_{34}$N$_2$O$_9$H$^+$: 663.2343 Found: 663.2361 (Δ = 2.8 ppm).

(3R,4S)-4-(2-Allyloxyphenyl)-1-(4-methoxyphenyl)-3-triisopropylsiloxyazetidin-2-one (5-92): [39]

1 M KOH aqueous solution (5 mL) was added to a solution of **3-54 (**176 mg, 0.48 mmol) in THF (15 mL) at 0 °C. The solution was stirred at 0 °C for 1.5 h and saturated NH$_4$Cl (20 mL) was added. The mixture was extracted with CH$_2$Cl$_2$ (20 mL x 3). The combined organic layers were dried over MgSO$_4$ and concentrated to give **5-91** (155 mg, 100%) as a white solid, and the *β*-lactam **5-92** was used in the next step without further purification.[39]

Chlorotriisopropylsilane (0.14 mL, 0.66 mmol) was added to a solution of **5-91** (155 mg, ~ 0.48 mmol), DMAP (12 mg**,** 0.1 mmol) and triethylamine (0.29 mL, 2.0 mmol) in CH$_2$Cl$_2$ (2 mL). The reaction mixture was stirred for overnight and quenched with saturated NH$_4$Cl (20 mL). The mixture was extracted with dichloromethane (20 mL x 3), dried over anhydrous MgSO$_4$ and solvent was removed under reduced pressure. The residue was purified by flash column chromatography on silica gel (hexanes/EtOAc = 15/1) to give **5-92** (223 mg, 96% for 2 steps) as a white solid: mp 98-99 $^{\circ}$C; ^{1}H NMR δ (CDCl$_3$, 400 MHz) 1.00 (m, 21 H), 3.73 (s, 3 H), 4.53 (ddt, *J* = 12.8, 2.8, 1.2 Hz, 1 H), 4.59 (ddt, *J* = 12.8, 2.8, 1.2 Hz, 1 H), 5,25 (d, *J* = 5.2 Hz, 1 H), 5.31 (dd, *J* = 10.4, 1.2 Hz, 1 H), 5.44 (ddd, *J* = 17.2, 3.2, 1.6 Hz, 1 H), 5.69 (d, *J* = 4.8 Hz, 1 H), 6.09 (m, 1 H), 6.78 (dt, *J* = 10.4, 3.6 Hz, 2 H), 6.87 (dd, *J* = 8.0, 2.8 Hz, 2 H), 7.22 (m, 2 H), 7.30 (dt, *J* = 10.0, 3.2 Hz, 2 H); ^{13}C NMR (100.5 MHz, CDCl$_3$) δ 11.8, 17.4, 55.3, 57.2, 68.7, 110.9, 114.2, 117.4, 118.6, 120.4, 122.2, 128.8, 128.9, 131.0, 133.2, 156.0, 156.6, 165.9. HRMS: *m/e* calcd for C$_{28}$H$_{39}$NO$_4$SiH$^+$: 482.2727 Found: 482.2715 (Δ = -2.5 ppm).

(3R,4S)-4-(2-Allyloxyphenyl)-3-triisopropylsiloxyazetidin-2-one (5-93):[49]

To a solution of *N*-PMP-*β*-lactam **5-92** (200 mg, 0.41 mmol) in acetonitrile (12 mL) and H$_2$O (2.6 mL), was added dropwise a solution of ceric ammonium nitrate (0.92 g, 1.64 mmol) in water (9.6 mL). The reaction mixture was stirred for 40 min and quenched with saturated Na$_2$SO$_3$ solution (20 mL). After filtration, the aqueous layer was extracted with EtOAc (20 mL x 3), and the combined organic layer was washed with H$_2$O (10 mL x 3),

dried over MgSO$_4$ and concentrated. The product mixture was purified on a silica gel column using hexanes:EtOAc (7:1) to afford the desired β-lactam **5-92** as a white solid (135 mg, 88%): mp 120-121 °C; ^{1}H NMR (CDCl$_3$, 400 MHz): δ 0.91 (m, 21 H), 4.49 (m, 2 H), 5.17 (dd, J = 4.8, 3.6 Hz, 1 H), 5.27 (dd, J = 10.8, 1.2 Hz, 1 H), 5.31 (d, J = 4.4 Hz, 1 H), 5.39 (dd, J = 17.2, 1.2 Hz, 1 H), 6.04 (m, 1 H), 6.53 (s, 1 H), 6.80 (d, J = 8.0 Hz, 1 H), 6.96 (t, J = 7.6 Hz, 1 H), 7.22 (t, J = 7.6, 1 H), 7.40 (d, J = 7.2 Hz, 1 H); ^{13}C NMR (CDCl$_3$, 100 MHz): 11.8, 17.4, 53.7, 68.6, 79.7, 110.7, 117.2, 120.2, 124.9, 128.4, 128.5, 133.2, 156.3, 170.3. HRMS: *m/e* calcd for C$_{21}$H$_{33}$NO$_3$SiH$^+$: 376.2308 Found: 376.2311 (Δ = 0.8 ppm).

(*3R,4S*)-4-(2-Allyloxyphenyl)-1-benzoyl-3-triisopropylsiloxyazetidin-2-one (5-94):[39]

To a solution of **5-93** (132 mg, 0.35 mmol) and DMAP (4.8 mg, 0.06 mmol) in CH$_2$Cl$_2$ (3 mL) was added triethylamine (0.15 mL, 1.05 mmol) and benzoyl chloride (0.08 mL, 0.53 mmol) at 0 °C. The reaction mixture was stirred overnight, quenched with saturated aqueous NH$_4$Cl solution (20 mL) and extracted with dichloromethane (30 mL x 3). The organic layer was dried over anhydrous MgSO$_4$ and solvent was removed under reduced pressure. The residue was purified by column chromatography on silica gel using hexanes:EtOAc (20:1) as the eluent to afford **5-94** (166 mg, 100%) as colorless oil: ^{1}H NMR (400 MHz, CDCl$_3$) δ 0.96 (m, 21 H), 4.55 (m, 2 H), 5.28 (m, 2 H), 5.41 (dd, J = 17.2, 1.2 Hz, 1 H), 5.87 (d, J = 6.0 Hz, 1 H), 6.12 (m, 1 H), 6.87 (d, J = 8.4 Hz, 1 H), 6.95 (t, J = 15.2 Hz, 1 H), 7.29 (m, 2 H), 7.59 (m, 3 H), 8.04 (d, J = 7.2 Hz, 2 H); ^{13}C NMR (100.5 MHz, CDCl$_3$) δ 11.7, 17.4, 56.9, 69.0, 76.5, 111.4, 117.4, 120.3, 122.2, 128.0, 128.1, 128.8, 129.0, 129.8, 130.5, 132.4, 133.3, 134.5, 156.9, 165.7, 166.2. HRMS: *m/e* calcd for C$_{28}$H$_{37}$NO$_4$SiH$^+$: 480.2570 Found: 480.2568 (Δ = -0.4 ppm).

(*2R,3S*)-3-(2-Allyloxyphenyl)-3-benzoylamino-2-hydroxypropionic acid methyl ester (5-96):[34]

To a solution of **5-94** (166 mg, 0.35 mmol) in pyridine/acetonitrile (1:1, 6 mL) was added dropwise HF/pyridine (70:30, 0.75 mL) at 0 °C, and then the mixture was allowed to warm to room temperature and stirred for 6 h. The reaction was quenched with saturated aqueous NaHCO$_3$ solution (10 mL) and the mixture was diluted with EtOAc (60 mL), washed with saturated aqueous CuSO$_4$ solution (10 mL x 2), H$_2$O (10 mL) and brine (10 mL), dried over anhydrous MgSO$_4$ and concentrated *in vacuo* to afford **5-95** as a white solid. The crude product was used directly without further purification:

To a solution of **5-95** (crude) and DMAP (11 mg, 0.09 mmol) in CH$_3$OH (2 mL), was added dropwise triethylamine (0.10 mL, 0.7 mmol) at room temperature. The mixture was stirred for overnight at room temperature, and then the solvent was removed and saturated aqueous NH$_4$Cl solution (10 mL) was added. The mixture was extracted with CH$_2$Cl$_2$ (20 mL x 3), the combined extracts were dried over anhydrous MgSO$_4$, and concentrated *in vacuo*. The crude product was purified on a silica gel column using hexanes:EtOAc (1.5:1) as the eluent to afford **5-96** as a white solid (100 mg, 81% yield on 2 steps): mp 94-95 °C; [α]$_D^{22}$ –52 (c 1.4, CHCl$_3$); ^{1}H NMR (400 MHz, CDCl$_3$) δ 3.74 (s, 3 H), 4.63 (d, J = 4.8 Hz, 2 H), 4.71 (d, J = 3.6 Hz, 1 H), 5.31 (dd, J = 10.4, 1.2 Hz, 1 H), 5.50 (dd, J = 17.6, 1.6 Hz, 1 H), 5.99 (dd, J = 9.2, 3.2 Hz, 1 H), 6.09 (dd, J = 16.2, 10.4, 4.8 Hz, 1 H), 6.92 (dd, J = 15.2, 7.6, Hz, 2 H), 7.26 (m,2 H), 7.46 (m, 3 H), 7.78 (dd, J = 6.8, 1.6 Hz, 2 H); ^{13}C NMR (100.5 MHz, CDCl$_3$) δ 52.5, 52.7, 68.8, 72.6, 111.9,

117.5, 120.9, 126.1, 127.0, 128.0, 128.5, 129.0, 131.6, 132.8, 134.2, 155.6, 166.9, 173.4. HRMS: m/e calcd for $C_{20}H_{21}NO_5H^+$: 356.1498 Found: 356.1502 (Δ = 1.1 ppm).

Methyl (4S,5R)-4-(2-allyloxyphenyl)-3-benzoyl-2-(4-methoxyphenyl) oxazolidine-5-carboxylate (5-97):[31]
To a solution of **5-96** (100 mg, 0.28 mmol) and 4-methoxybenzaldehyde dimethyl acetal (0.13 mL, 0.62 mmol) in toluene (7.7 mL) was added PPTS (21 mg, 0.08 mmol), and the mixture was refluxed for 4 h. The reaction mixture was then diluted with EtOAc (60 mL), and washed with saturated aqueous $NaHCO_3$ solution (10 mL), brine (5 mL) and concentrated *in vacuo*. The crude product was purified on a silica gel column using hexanes:EtOAc (5:1) as the eluent to afford **5-97** as a colorless oil (95 mg, 75% yield): ^{1}H NMR (400 MHz, CDCl₃) δ 3.79 (s, 3 H), 3.82 (s, 3 H), 4.46 (dd, J = 12.4, 5.2 Hz, 1 H), 4.52 (dd, J = 13.2, 5.2 Hz, 1 H), 4.87 (s, 1 H), 5.19 (d, J = 11.2 Hz, 1 H), 5.24 (d, J = 17.6 Hz, 1 H), 5.52 (s, 1 H), 5.91 (m, 1 H), 6.88 (m, 4 H), 6.99 (s, 1 H), 7.26 (m, 4 H), 7.33 (m, 3 H), 7.58 (s, 2 H); ^{13}C NMR (100.5 MHz, CDCl₃) δ 52.4, 55.2, 61.6, 68.8, 81.6, 90.6, 111.5, 113.3, 117.4, 120.4, 126.9, 128.1, 128.5, 128.9, 129.1, 130.2, 130.5, 132.7, 135.8, 154.8, 159.8, 170.5. HRMS: m/e calcd for $C_{28}H_{27}NO_6H^+$: 474.1917 Found: 474.1902 (Δ = -3.2 ppm).

(4S,5R)-4-(2-Allyloxyphenyl)-3-benzoyl-2-(4-methoxyphenyl)oxazolidine-5-carboxylic acid (5-98):[32]
To a solution of **5-97** (95 mg, 0.21 mmol) in THF (1.5 mL) and water (1.5 mL) was added lithium hydroxide (26 mg, 0.62 mmol) and the reaction mixture was stirred for 1 h. The reaction mixture was washed with aqueous NaOH solution (1 *N*, 10 mL x 3) and then the water layer was collected and acidified using aqueous HCl (1 *N*) to pH 2. The water layer was extracted with EtOAc (30 mL x 3), the organic layers were combined, dried over anhydrous $MgSO_4$ and concentrated *in vacuo*. The crude product was purified on a silica gel column using hexanes:EtOAc (1:1) as the eluent to afford **5-98** as a white solid (83 mg, 88% yield): mp 47-49 °C; ^{1}H NMR (400 MHz, CDCl₃) δ 3.83 (s, 3 H), 4.47 (dd, J = 12.8, 3.6 Hz, 1 H), 4.55 (dd, J = 13.2, 5.2 Hz, 1 H), 4.91 (s, 1 H), 5.18 (d, J = 10.8 Hz, 1 H), 5.25 (d, J = 17.2 Hz, 1 H), 5.59 (s, 1 H), 5.92 (m, 1 H), 6.88 (m, 4 H), 7.03 (m, 1 H), 7.20 (m, 3 H), 7.28 (m, 4 H), 7.59 (s, 2 H), 8.71 (bs, 1 H); ^{13}C NMR (100.5 MHz, CDCl₃) δ 55.2, 60.5, 68.9, 81.4, 90.7, 111.6, 113.3, 117.7, 120.4, 127.0, 128.2, 128.6, 129.0, 129.2, 129.9, 130.7, 132.7, 135.5, 154.9, 159.9, 170.4. HRMS: m/e calcd for $C_{27}H_{25}NO_6H^+$: 460.1760 Found: 460.1754 (Δ = -1.3 ppm).

10-Benzoyloxy-9-pent-4-enoyloxymethyl-2-triisopropylsiloxy-1,2,3,5,10,10a-hexahydropyrrolo[1,2-b]isoquinolin-5-one (5-99):[39]
To a solution of **5-85** (34 mg, 0.07 mmol) and DMAP (1 mg, 0.005 mmol) in CH_2Cl_2 (0.6 mL) was added triethylamine (0.09 mL, 0.26 mmol) and 4-pentenoyl chloride (0.015 mL, 0.13 mmol) at 0 °C. The reaction mixture was stirred overnight, quenched with saturated aqueous NH_4Cl solution (20 mL) and extracted with dichloromethane (20 mL x 3). The organic layer was dried over anhydrous $MgSO_4$ and solvent removed under reduced pressure. The residue was purified by column chromatography on silica gel using hexanes:EtOAc (3:1) to afford **5-99** (39 mg, 100%) as a colorless oil: $[\alpha]_D^{22}$ –158 (c 2.0, CHCl₃); ^{1}H NMR (400 MHz, CDCl₃) δ 1.00 (m, 21 H), 2.22 (m, 6 H), 3.83 (m, 2 H), 4.32

(dd, J = 18.0, 8.8 Hz, 1 H), 4.63 (d, J = 2.0 Hz, 1 H), 4.92 (dd, J = 10.4, 1.6 Hz, 1 H), 4.98 (t, J = 5.6 Hz, 1 H), 5.06 (d, J = 12.8, 1 H), 5.22 (d, J = 12.8 Hz, 1 H), 5.72 (m, 1 H), 6.68 (d, J = 10.8 Hz, 1 H), 7.49 (m, 4 H), 7.64 (t, J = 7.6 Hz, 1 H), 8.10 (dd, J = 8.4, 1.2 Hz, 2 H), 8.20 (dd, J = 7.2, 1.6 Hz, 1 H); ^{13}C NMR (100.5 MHz, CDCl$_3$) δ 11.9, 17.9, 28.5, 32.9, 41.9, 55.1, 58.9, 65.1, 69.3, 73.2, 115.4, 128.4, 128.7, 128.9, 129.0, 129.7, 130.6, 133.2, 133.8, 134.3, 135.7, 136.5, 162.2, 165.7, 172.3. HRMS: m/e calcd for C$_{34}$H$_{45}$NO$_6$SiH$^+$: 592.3094 Found: 592.3077 (Δ = -2.9 ppm).

10-Benzoyloxy-2-hydroxy-9-pent-4-enoyloxymethyl-1,2,3,5,10,10a-hexahydro-pyrrolo[1,2-b]isoquinolin-5-one (5-100):[25]

To a solution of **5-99** (38 mg, 0.06 mmol) in CH$_3$CN (0.76 mL) and pyridine (0.76 mL) was added HF-pyridine (70:30, 0.38 ml) and the reaction mixture was stirred overnight. The reaction mixture was diluted with EtOAc (40 mL) and washed with saturated aqueous NaHCO$_3$ solution (10 mL x 2), CuSO$_4$ solution (10 mL x 3), water (10 mL x 3) and brine (3 mL). The organic layer was dried over anhydrous MgSO$_4$ and solvent was removed under reduced pressure. The residue was purified by column chromatography on silica gel using hexanes:EtOAc (1:4) as the eluent to afford **5-100** as white solid (23 mg, 97%): mp 50-52 °C; [α]$_D^{22}$ –227 (c 1.5, CHCl$_3$); ^{1}H NMR (400 MHz, CDCl$_3$) δ 2.22 (m, 6 H), 3.85 (d, J = 2.4 Hz, 2 H), 4.33 (td, J = 10.4, 5.6 Hz, 1 H), 4.61 (t, J = 2.4 Hz, 1 H), 4.92 (dd, J = 10.4, 1.6 Hz, 1 H), 4.95 (dd, J = 13.2, 1.6 Hz, 1 H), 5.06 (d, J = 12.8 Hz, 1 H), 5.21 (d, J = 12.8 Hz, 1 H), 5.70 (m, 1 H), 6.68 (d, J = 10.8 Hz, 1 H), 7.48 (m, 4 H), 7.63 (t, J = 7.3 Hz, 1 H), 8.08 (d, J = 8.4, 1.2 Hz, 2 H), 8.14 (dd, J = 7.2, 1.2 Hz, 1 H); ^{13}C NMR (100.5 MHz, CDCl$_3$) δ 28.5, 32.9, 40.9, 54.5, 58.7, 65.1, 68.4, 73.1, 115.5, 128.5, 128.7, 128.8, 128.9, 129.8, 130.4, 133.3, 133.9, 134.3, 135.7, 136.5, 162.6, 165.6, 172.3. HRMS: m/e calcd for C$_{25}$H$_{25}$NO$_6$H$^+$: 436.1760 Found: 436.1750 (Δ = -2.3 ppm).

10-Benzoyloxy-5-oxo-9-pent-4-enoyloxymethyl-1,2,3,5,10,10a-hexahydropyrrolo [1,2-b]isoquinolin-2-yl-4-(2-allyloxyphenyl)-3-benzoyl-2-(4-methoxyphenyl) oxazolidine-5-carboxylate (5-101):[39]

To a solution of **5-100** (25 mg, 0.06 mmol), acid **5-98** (40 mg, 0.09 mmol) and DMAP (3.5 mg, 0.028 mmol) in CH$_2$Cl$_2$ (0.56 mL) was added EDC (23 mg, 0.12 mmol) and the reaction mixture was stirred overnight. The mixture was then extracted with EtOAc (50 mL) and washed with water (10 mL x 2) and brine (10 mL). The organic layer was dried over anhydrous MgSO$_4$ and filtered and then solvent was removed under reduced pressure. The residue was purified by column chromatography on silica gel using hexanes:EtOAc (1:1) as the eluent to afford **5-101** as a white solid (48 mg, 96%): mp 73-75 °C; [α]$_D^{22}$ -145 (c 2.0, CHCl$_3$); ^{1}H NMR (400 MHz, CDCl$_3$) δ 2.27 (m, 5 H), 2.42 (m, 1 H), 3.81 (s, 3 H), 3.86 (d, J = 14.4 Hz, 1 H), 4.05 (dd, J = 14.4, 4.8, 1 H), 4.25 (td, J = 10.8, 5.6, Hz, 1 H), 4.39 (m, 2 H), 4.80 (s, 1 H), 4.93 (dd, J = 10.0, 0.8 Hz, 1 H), 4.96 (dd, J = 17.6, 1.6 Hz, 1 H), 5.03 (d, J = 10.4 Hz, 1 H), 5.08 (s, 1 H), 5.11 (d, J = 4.8 Hz, 1 H), 5.24 (d, J = 12.8 Hz, 1 H0, 5.43 (s, 1 H), 5.55 (t, J = 4.8 Hz, 1 H), 5.74 (m, 2 H), 6.71 (d, J = 10.4 Hz, 1 H), 6.76 (d, J = 8.4 Hz, 1 H), 6.81 (m, 3 H), 6.94 (s, 1 H), 7.08 (m, 3 H), 7.19 (m, 5 H), 7.50 (m, 6 H), 7.64 (t, J = 7.2 Hz, 1 H), 8.13 (d, J = 7.6 Hz, 2 H), 8.22 (dd, J = 7.6, 1.6 Hz, 1 H); ^{13}C NMR (100.5 MHz, CDCl$_3$) δ 28.5, 32.9, 38.4, 51.9, 55.2, 58.8, 65.2, 68.8, 72.4, 73.0, 111.5, 113.3, 115.5, 117.7, 120.5, 126.9, 128.2, 128.7, 128.7, 128.8, 128.8, 128.9, 129.2, 129.9, 130.2, 132.5, 133.4, 133.9, 134.6, 135.3, 136.5,

154.7, 159.8, 162.0, 165.5, 169.3, 172.3. HRMS: *m/e* calcd for $C_{52}H_{48}N_2O_{11}H^+$: 877.3336 Found: 877.3322 (Δ = -1.6 ppm).

10-Benzoyloxy-5-oxo-9-pent-4-enoyloxymethyl-1,2,3,5,10,10a-hexahydropyrrolo[1,2-b]isoquinolin-2-yl 2-[3-(2-allyloxyphenyl)-3-benzoylamino-2-hydroxypropanoate] (5-102):[39]

To a solution of **5-101** (47 mg, 0.05 mmol) in methanol (0.9 mL) was added *p*-TSA (2.1 mg, 0.01 mmol). After stirring overnight, the solvent was removed and the residue purified by silica gel column chromatography using Hexanes:EtOAc = 1/2 as the eluent to afford **5-102** as a white solid (33 mg, 82%): mp 110-112 ^{o}C; $[\alpha]_D^{22}$ −139 (c 1.6, CHCl$_3$); ^{1}H NMR (400 MHz, CDCl$_3$) δ 2.27 (m, 6 H), 3.34 (bs, 1 H), 3.95 (m, 2 H), 4.29 (d, *J* = 8.0 Hz, 1 H), 4.33 (d, *J* = 8.0 Hz, 1 H), 4.51 (d, *J* = 4.8 Hz, 2 H), 4.65 (d, *J* = 3.2 Hz, 1 H), 4.92 (dd, *J* = 9.2, 1.6 Hz, 1 H), 4.96 (dd, *J* = 17.2, 1.6 Hz, 1 H), 5.09 (d, *J* = 12.8 Hz, 1 H), 5.21 (dd, *J* = 12.0, 1.2 Hz, 1 H), 5.23 (dd, *J* = 19.6, 12.8 Hz, 1 H), 5.48 (dd, *J* = 25.2, 1.6 Hz, 1 H), 5.66 (d, *J* = 6.0 Hz, 1 H), 5.73 (m 1 H), 5.98 (m, 2 H0, 6.67 (d, *J* = 10.8 Hz, 1 H), 6.78 (d, *J* = 8.0 Hz, 1 H), 6.87 (t, *J* = 7.2 Hz, 1 H), 7.19 (m, 5 H), 7.38 (t, *J* = 11.6 Hz, 1 H), 7.45 (m, 6 H), 7.62 (t, *J* = 7.2 Hz, 1 H), 8.13 (d, *J* = 7.2 Hz, 2 H), 8.18 (dd, *J* = 7.6, 1.6 Hz, 1 H); ^{13}C NMR (100.5 MHz, CDCl$_3$) δ 28.5, 32.9, 38.2, 51.6, 52.0, 58.8, 65.3, 68.7, 72.9, 73.2, 111.8, 115.5, 117.7, 120.9, 126.1, 126.8, 127.8, 128.4, 128.5, 128.7, 128.8, 128.9, 129.2, 130.0, 130.3, 131.4, 132.5, 133.3, 133.7, 133.9, 134.5, 135.9, 136.5, 155.5, 162.3, 165.6, 166.7, 172.1, 172.2. HRMS: *m/e* calcd for $C_{44}H_{42}N_2O_{10}H^+$: 759.2918 Found: 759.2893 (Δ = -3.3 ppm).

5-36 (SB-H-2001):[25]

To a solution of **5-102** (17 mg, 0.02 mmol) in CH$_2$Cl$_2$ (12 mL) was added the "first-generation Grubbs catalyst" (3 mg, 0.004 mmol) in CH$_2$Cl$_2$ (0.2 mL). The reaction was stirred at room temperature for 3 days and reflux for 2 days. The solvent was removed under reduced pressure. The residue was passed through a short silica gel column (hexanes:EtOAc = 1:1.5) to remove the catalyst to afford **SB-H-301** as a white solid (*Z*-isomer only, 8 mg, and 5 mg starting marterial was recovered): ^{1}H NMR (400 MHz, CDCl$_3$) δ 2.30 (m, 5 H), 2.78 (dd, *J* = 10.4, 3.6 Hz, 1 H), 3.32 (d, *J* = 2.8 Hz, 1 H), 3.82 (dd, *J* = 10.0, 1.2 Hz, 1 H), 3.96 (m, 2 H), 4.36 (dd, *J* = 11.2, 2.4 Hz, 1 H), 4.52 (s, 1 H), 4.59 (m, 1 H), 4.77 (d, *J* = 9.2 Hz, 1 H), 5.44 (d, *J* = 9.2 Hz, 1 H), 5.56 (s, 2 H), 6.14 (dd, *J* = 7.2, 1.6 Hz, 1 H), 6.72 (d, *J* = 7.6 Hz, 1 H), 6.75 (d, *J* = 9.6 Hz, 1 H), 6.78 (d, *J* = 6.4 Hz,1 H), 6.96 (t, *J* = 6.4 Hz, 1 H), 7.24 (m, 1 H), 7.42 (m, 3 H), 7.46 (m, 4 H), 7.59 (m, 3 H), 7.74 (dd, *J* = 6.0, 1.2 Hz, 1 H), 8.21 (dd, *J* = 6.4, 1.2 Hz, 1 H), 8.36 (dd, *J* = 6.0, 0.4 Hz, 2 H); ^{13}C NMR (100.5 MHz, CDCl$_3$) δ 28.2, 33.6, 36.9, 49.2, 51.9, 59.1, 64.1, 68.4, 72.9, 73.0, 73.3, 112.4, 121.0, 125.8, 127.0, 127.5, 128.1, 128.4, 128.5, 128.6, 128.6, 129.2, 129.2, 129.6, 130.5, 130.6, 130.7, 131.6, 131.8, 133.8, 134.0, 137.0, 138.8, 154.8, 162.2, 166.7, 171.8, 172.6. HRMS: *m/e* calcd for $C_{42}H_{38}N_2O_{10}H^+$: 731.2605 Found: 731.2597 (Δ = -1.1 ppm).

2-Bromo-1-methoxymethoxymethyl-3-ethenylbenzene (5-104):[34]

To a solution of PPh$_3$CH$_3$Br (890 mg, 2.50 mmol) in THF (12 mL) at 0 ^{o}C was added sodium hydride (60% suspension in mineral oil, 120mg, 2.9 mmol). The mixture was stirred at room temperature for 1 h. The suspension was added to a solution of **5-51** (500

mg, 1.90 mmol) in THF (6 mL). The mixture was stirred at 40 °C for 75 min and the reaction was quenched with saturated aqueous ammonium chloride (30 mL). The water layer was extracted with chloroform (30 mL x 3). The organic layers were combined and washed with brine (20 mL x 2), and dried over anhydrous $MgSO_4$. The solvent was removed under reduced pressure. The residue was purified by column chromatography on silica gel using hexanes:EtOAc (50:1) as the eluent to afford **5-104** as a colorless oil (471 mg, 97%): ^{1}H NMR (400 MHz, $CDCl_3$) δ 3.44 (s, 3 H), 4.70 (s, 2 H), 4.78 (s, 2 H), 5.36 (d, J = 10.8 Hz, 1 H), 5.67 (d, J = 17.2 Hz, 1 H), 7.13 (dd, J = 17.6, 13.2 Hz, 1 H), 7.29 (t, J = 8.0 Hz, 1 H), 7.42 (d, J = 7.6 Hz, 1 H), 7.47 (d, J = 8.0 Hz, 1 H). ^{13}C NMR (100.5 MHz, $CDCl_3$) δ 55.4, 69.2, 96.0, 116.7, 123.7, 125.9, 127.1, 128.1, 136.1, 137.9, 138.1.

2-Bromobenzene-1,3-dicarbaldehyde (5-105):[16]

To a solution of **5-43** (619 mg, 2.80 mmol) in dimethyl sulfoxide (8.4 mL) and CH_2Cl_2 (8.4 mL) was added triethylamine (5.6 mL, 40.0 mmol) and sulfurtrioxide-pyridine (2.8 g, 16.8 mmol) at 0 °C. The reaction mixture was stirred for 0.5 h, quenched with ice water and extracted with EtOAc (100 mL). The organic layer was washed with 5% citric acid aqueous solution (5 mL), water (5 mL), saturated aqueous $NaHCO_3$ solution (15 mL) and brine. The organic layer was dried over anhydrous $MgSO_4$ and the solvent was removed under reduced pressure. The residue was purified on silica gel column using Hexanes:EtOAc = 10:1 as the eluent to afford **5-105** as a white solid (539 mg, 91%): mp. 135-136 °C; ^{1}H NMR (400 MHz, $CDCl_3$) δ 7.49 (t, J = 7.6 Hz, 1 H), 8.04 (d, J = 7.6 Hz, 2 H), 10.41 (s, 2 H). ^{13}C NMR (100.5 MHz, $CDCl_3$) δ 128.0, 130.4, 134.2, 134.9, 190.3. HRMS calcd. for $C_8H_5BrO_2^+$ 211.9473, found 211.9471 (Δ= -0.9 ppm).

2-Bromo-1,3-diethenylbenzene (5-106):[34]

To a solution of PPh_3CH_3Br (2.30 g, 6.25 mmol) in THF (16 mL) at 0 °C was added sodium hydride (60% suspension in mineral oil, 260mg, 6.25 mmol). The mixture was stirred at room temperature for 1 h. The suspension was added to a solution of **5-105** (537 mg, 2.5 mmol) in THF (9 mL). The mixture was stirred at room temperature for 80 min and quenched with saturated aqueous ammonium chloride (30 mL). The water layer was extracted with ethyl ether (40 mL x 3). The organic layers were combined and washed with brine (10 mL x 2) and dried over anhydrous $MgSO_4$. The solvent was removed under reduced pressure. The residue was purified by column chromatography on silica gel using Hexanes as the eluent to afford **5-106** as colorless oil (443 mg, 86%): ^{1}H NMR (400 MHz, $CDCl_3$) δ 5.01 (dd, J = 10.8, 1.2 Hz, 2 H), 5.39 (dd, J = 17.6, 1.2 Hz, 2 H), 6.84 (dd, J = 8.0, 7.2 Hz, 1 H), 7.18 (m, 6 H). ^{13}C NMR (100.5 MHz, $CDCl_3$) δ 116.7, 116.9, 126.3, 127.3, 136.7, 138.6. HRMS calcd. for $C_{10}H_9Br^+$ 207.9888, found 207.9886 (Δ= -1.0 ppm).

1-*tert*-Butoxycarbonyl-2-[hydroxy-(2-methoxymethoxymethyl-6-ethenylphenyl)methyl]-4-triisopropylsiloxy-pyrrolidine (5-108):[31, 39]

Bromide **5-104** (254 mg, 0.98 mmol) was dissolved in dry THF (9.2 mL) under N_2 and 2.5 M *n*-BuLi in hexane (0.44 mL, 1.1 mmol) was added at -78 °C. The resulting solution was stirred for 1 h. Then HMPA (0.18 mL) was added and the solution was stirred for 1 h. A solution of aldehyde **5-14** (276 mg, 0.75 mmol) in dry THF (5.2 mL) was added dropwise. The resulting solution was allowed to slowly warm up to room temperature

with stirring overnight. After addition of saturated NH$_4$Cl solution (20 mL), the mixture was extracted with dichloromethane (3 x 20 mL). The combined organic layers were washed with brine and dried over MgSO$_4$. After evaporation of the solvent, the residue was purified by flash chromatography on silica gel using hexanes:EtOAc (50:1) as the eluent to afford desired product **5-107**.

To a solution of **5-107** (274 mg, 0.49 mmol) and DMAP (5 mg, 0.06 mmol) in CH$_2$Cl$_2$ (3.8 mL) was added triethylamine (0.46 mL, 1.5 mmol) and acetic anhydride (0.33 mL, 1.0 mmol) at 0 ^{o}C. The reaction mixture was stirred overnight, quenched with saturated aqueous NH$_4$Cl solution (20 mL) and extracted with dichloromethane (30 mL x 3). The organic layer was dried over anhydrous MgSO$_4$ and the solvent was removed under reduced pressure. The residue was purified by column chromatography on silica gel using hexanes:EtOAc (11:1-8:1) to afford **5-108** (172 mg, 70% in 2 steps) as colorless oil: ^{1}H NMR (400 MHz, CDCl$_3$) δ 1.02 (m, 21 H), 1.28-1.43 (m, 9 H), 2.06-2.10 (m, 5 H), 3.40 (m, 4 H), 3.59 (m, 1 H), 4.57 (m, 2 H), 4.79 (m, 5 H), 5.28 (d, J = 10.8 Hz, 1 H), 5.51 (d, J = 17.6, 1 H), 6.02-6.22 (m, 1 H), 7.17-7.52 (m, 4 H). ^{13}C NMR (100.5 MHz, CDCl$_3$) δ 12.1, 17.9, 20.9, 28.0, 28.4, 38.3, 54.7, 55.0, 58.6, 66.6, 70.2, 72.7, 79.7, 95.4, 116.0, 127.2, 127.5, 128.9, 129.1, 133.5, 136.4, 136.8, 137.0, 138.6, 154.4, 169.5. HRMS calcd. for C$_{32}$H$_{53}$NO$_7$SiH$^+$ 592.3670, found 592.3663 (Δ= -1.2 ppm).

10-Acetoxy-9-methoxymethoxymethyl-2-triisopropylsiloxy-1,2,3,5,10,10a-hexahydropyrrolo[1,2-b]isoquinolin-5-one (5-113 and 5-114): [39, 44]

Nitrogen gas was bubbled into a solution of **5-109** (167 mg, 0.28 mmol) in CH$_2$Cl$_2$ (15 mL) at -78 $^{\circ}$C for 3 min. Then, O$_3$ gas was bubbled into the solution till the color of the solution turned blue (8 min), and N$_2$ was bubbled into the solution for another 3 min until the blue color disappeared. Dimethyl sulfide (0.1 mL, 1.4 mmol) was added to the solution and the reaction mixture was allowed to warm to room temperature. The reaction mixture was stirred at room temperature for 3 h. The solvents were removed *in vacuo* and crude **5-110** was used in the next step without further purification.

Sodium chlorite (200 mg, 2.24 mmol) was added to a solution of **5-111** (~0.28 mmol) and sodium phosphate (monobasic) (350 mg, 2.24 mmol) in acetone/water (1:1, 2.4 mL). The reaction mixture was stirred at room temperature for 1 h and was quenched with ethyl acetate (60 mL). The organic layer was washed with hydrochloric acid (1 N, 10 mL), Na$_2$S$_2$O$_3$ (10%, 10 mL x 2), and brine (10 mL), dried with MgSO$_4$, filtered, and concentrated. Crude **5-111** was used in the next step without further purification.

A solution of potassium hydroxide (4 g) in water (8 mL) and ethanol (32 mL) was added to a solution of diazald® (4 g) in ether (60 mL) at 0 ^{o}C. The mixture was stirred for 10 min at 0 ^{o}C and distilled to afford a yellow ether solution. The diazomethane solution in ether was added to the solution of **5-111** (~ 0.28 mmol) in ether (12 mL) until the yellow color persisted. The mixture was stirred for 10 min and the reaction was quenched with acetic acid. The solvents were removed *in vacuo* and crude **5-112** was used in the next step without further purification.

To a solution of **5-112** (~ 0.28 mmol) in dichloromethane (1.5 mL) at 0 ^{o}C was added trifluoroacetic acid (1.5 mL). The mixture was stirred at 0 ^{o}C for 30 min and room temperature for 30 min. The solvent and acid were removed under reduced pressure to give a crude product, which was used in the next step without further purification.

To a solution of the crude product in ethyl acetate (14 mL) was added saturated aqueous sodium bicarbonate (14 mL). The mixture was stirred vigorously overnight and the reaction was quenched with ethyl acetate (50 mL). The mixture was washed with saturated aqueous ammonium chloride (10 mL), water (10 mL) and brine (10 mL). The organic layer was dried over anhydrous MgSO$_4$ and the solvent was removed under reduced pressure. The residue was purified by column chromatography on silica gel using hexanes:EtOAc (3:4) to afford **5-113** and **5-114** (3:4 by ^{1}HNMR) as a colorless oil in 50% for 5 steps. **5-113**: ^{1}H NMR (400 MHz, CDCl$_3$) δ 1.06 (m, 21 H), 2.11 (m, 2 H), 2.21 (s, 3 H), 3.31 (s, 3 H), 3.79 (m, 2 H), 4.14 (td, J = 10.8, 5.6 Hz, 1 H), 4.61 (m, 6 H), 4.80 (d, J = 12.8 Hz, 1 H), 6.32 (d, J = 10.4, 1 H), 7.40 (t, J = 7.6 Hz, 1 H), 7.53 (d, J = 7.6 Hz, 1 H), 8.10 (dd, J = 8.0, 1.6 Hz, 1 H). HRMS calcd. for C$_{26}$H$_{41}$NO$_6$SiH$^+$ 492.2781, found 492.2775 (Δ= -1.2 ppm).

1-(*tert*-Butoxycarbonyl)-2-[(2,6-diethenylphenyl)hydroxymethyl]-4-triisopropylsiloxypyrrolidine (5-117):[16, 30, 39]

A mixture of aryl bromide **5-106** (257 mg, 1.22 mmol) and Mg turnings (35 mg, 1.47 mmol) in THF (12 mL) was added 1 drop of 1,2-dibromoethane and the mixture was heated at reflux. After 2 h, the reaction mixture was cooled to room temperature. Aldehyde **5-14** (226 mg, 0.61 mmol) was dissolved in THF (7 mL) and cooled down to -78 °C. The Grignard reagent generated above (1.22 mmol, 2.0 equiv) was added to the aldehyde solution by canula and the reaction mixture was stirred overnight. The rection was quenched with saturated aqueous NH$_4$Cl solution (20 mL) and extracted with dichloromethane (20 mL x 3). The organic layer was dried over anhydrous MgSO$_4$ and solvent was removed under reduced pressure. The residue was purified by column chromatography on silica gel using hexanes:EtOAc (17:1) to afford **5-117** (227 mg, 74%) as colorless oil: ^{1}H NMR (400 MHz, CDCl$_3$) δ 0.96 (m, 21 H), 1.32-1.44 (m, 9H), 1.74 (m, 1 H), 2.19 (m, 1 H), 3.31 (m, 1 H), 3.57 (m, 1 H), 3.85 (m, 1 H), 4.51 (m, 1 H), 4.98 (m, 1 H), 5.12 (dd, J =10.8, 1.6 Hz, 2 H), 5.41 (dd, J = 17.6, 2.0 Hz, 2 H), 6.96-7.74 (m, 5 H). ^{13}C NMR (100.5 MHz, CDCl$_3$) δ 12.0, 18.0, 28.2, 36.8, 39.6, 55.6, 63.8, 70.0, 74.1, 81.0, 114.9, 127.4, 127.9, 128.1, 136.5, 136.4, 137.9, 158.8. HRMS calcd. for C$_{29}$H$_{46}$NO$_4$SiH$^+$ 502.3353, found 502.3373 (Δ= 4.0 ppm).

2-[Acetoxy(2,6-diethenylphenyl)methyl]-1-(*tert*-butoxycarbonyl)-4-triisopropylsiloxypyrrolidine (5-118):

To a solution of **5-117** (227 mg, 0.45 mmol) and DMAP (3 mg, 0.01 mmol) in CH$_2$Cl$_2$ (3.0 mL) was added triethylamine (0.33 mL, 1.05 mmol) and acetic anhydride (0.24 mL, 0.90 mmol) at 0 °C. The reaction mixture was stirred overnight, quenched with saturated aqueous NH$_4$Cl solution (20 mL) and extracted with dichloromethane (30 mL x 3). The organic layer was dried over anhydrous MgSO$_4$ and the solvent was concentrated under reduced pressure. The residue was purified by column chromatography on silica gel using hexanes:EtOAc (15:1) to afford **5-118** (239 mg, 98%) as colorless oil. ^{1}H NMR (400 MHz, CDCl$_3$) δ 1.09 (m, 21 H), 1.28-1.47 (m, 9 H), 1.66 (m, 1 H), 1.71 (m, 4 H), 3.48 (m, 2 H), 4.43 (m, 1 H), 4.79 (m, 1 H), 5.23 (m, 2 H), 5.47 (m, 2 H), 6.43 (m, 1 H), 7.04 (m, 1 H), 7.27-7.74 (m, 4 H). ^{13}C NMR (100.5 MHz, CDCl$_3$) δ 12.7, 18.5, 21.1, 28.7, 37.5, 55.5, 59.4, 71.5, 73.9, 79.4, 116.6, 128.2, 128.7, 129.5, 132.8, 137.4, 139.4, 155.8, 169.4. HRMS calcd. for C$_{31}$H$_{48}$NO$_5$SiH$^+$ 544.3458, found 544.3472 (Δ= 2.6 ppm).

10-Acetoxy-9-methoxycarbonyl-2-triisopropylsiloxy-1,2,3,5,10,10a-hexahydropyrrolo[1,2-b]isoquinolin-5-one (5-121):[45]

Nitrogen gas was bubbled into a solution of **5-118** (239 mg, 0.44 mmol) in CH_2Cl_2 (24 mL) at -78 °C for 3 min. Then, O_3 gas was bubbled into the solution till the color of the solution turned blue (15 min), and N_2 was bubbled into the solution for another 3 min until the blue color disappeared. Dimethyl sulfide (0.16 mL, 1.08 mmol) was added to the solution and the reaction mixture was allowed to warm to room temperature. The reaction mixture was stirred at room temperature for 3 h. The solvent was removed *in vacuo* and crude product was used in the next step without further purification.

Sodium chlorite (407 mg, 4.4 mmol) was added to a solution of the crude product and sodium phosphate (monobasic) (712 mg, 4.4 mmol) in acetone/water (1:1, 5 mL). The reaction mixture was stirred at room temperature for 1 h and quenched with ethyl acetate (60 mL). The organic layer was washed with aqueous hydrochloric acid (1 *N*, 10 mL), $Na_2S_2O_3$ (10%, 10 mL x 2), and brine (10 mL), dried with $MgSO_4$, filtered, and concentrated. Crude **5-119** was used in the next step without further purification.

A solution of potassium hydroxide (4 g) in water (8 mL) and ethanol (32 mL) was added to a solution of diazald® (4 g) in ether (60 mL) at 0 °C. The mixture was stirred for 10 min at 0 °C and distilled to afford a yellow ether solution. The diazomethane solution in ether was added to the solution of **5-119** (~ 0.44 mmol) in ether (20 mL) until the yellow color persisted. The mixture reaction was stirred for 10 min and quenched with acetic acid. The solvent was removed *in vacuo* to give crude **5-120**, which was used in the next step without further purification.

To a solution of **5-120** (~ 0.44 mmol) in dichloromethane (4 mL) at 0 °C was added trifluoroacetic acid (4 mL). The reaction mixture was stirred at 0 °C for 30 min and room temperature for 30 min. The solvent and acid were removed under reduced pressure and the residue was used in the next step without further purification.

To a solution of the residue in ethyl acetate (20 mL) was added saturated aqueous sodium bicarbonate (20 mL). The reaction mixture was stirred vigorously overnight before being quenched with ethyl acetate (50 mL). The mixture was washed with saturated aqueous ammonium chloride (10 mL), water (10 mL) and brine (10 mL). The organic layer was dried over anhydrous $MgSO_4$ and the solvent was removed under reduced pressure. The residue was purified by column chromatography on silica gel using hexanes:EtOAc (3:1) to afford **5-121** (1:1 by ^{1}HNMR) as a colorless oil (131 mg) in 63% for 5 steps: ^{1}H NMR (400 MHz, $CDCl_3$) δ 1.04 (m, 21 H), 1.89 (td, *J* = 12.8, 4.0, 0.5 H), 1.98 (s, 1.5 H), 2.16 (m, 2 H), 3.77 (m, 2 H), 3.84 (s, 1.5 H), 3.92 (s, 1.5 H), 4.07 (m, 0.5 H), 4.30 (ddd, *J* = 11.2, 5.6, 2.4 Hz, 0.5 H), 4.64 (m, 1 H), 6.40 (d, *J* = 10.8, 0.5 H), 6.74 (d, *J* = 2.4 Hz, 0.5 H), 7.49 (t, *J* = 8.4 Hz, 0.5 H), 7.58 (t, *J* = 7.6 Hz, 0.5 H), 7.77 (dd, *J* = 8.0, 1.6 Hz, 0.5 H), 8.04 (dd, *J* = 8.0, 1.6 Hz, 0.5 Hz), 8.24 (dd, *J* = 8.0, 1.6 Hz, 0.5 H), 8.36 (dd, *J* = 7.6, 1.2 Hz, 0.5 H). HRMS calcd. for $C_{26}H_{41}NO_6SiH^+$ 492.2781, found 492.2775 (Δ= -1.2 ppm).

10α-Hydroxy-9-hydroxymethyl-2-triisopropylsiloxy-2,3,10,10a-tetrahydro-1H-pyrrolo[1,2-b]isoquinolin-5-one (5-83) and 10β-Hydroxy-9-hydroxymethyl-2-tri-isopropylsiloxy-2,3,10,10a-tetrahydro-1H-pyrrolo[1,2-b]isoquinolin-5-one (5-79):[16]
To a solution of **5-121** (50 mg, 1:1 ratio, 0.10 mmol) in THF (2.0 mL) was added 2 M lithium borohydide in THF (0.1 mL, 0.2 mmol). The reaction mixture was stirred overnight and quenched with ice water. The water layer was extracted with EtOAc. The organic layers were combined, washed with 5% aqueous phosphoric acid (5 mL x 3), and dried over anhydrous $MgSO_4$. The solvent was removed under reduced pressure. The residue was purified by column chromatography on silica gel using 2% methanol in dichloromethane as the eluent to afford **5-83** as a white solid (15 mg, 38%): mp 153-155 ^oC; $[\alpha]_D^{22}$ −86 (c 1.5, $CHCl_3$); ^1H NMR (400 MHz, $CDCl_3$) δ 1.06 (m, 21 H), 1.85 (ddd, J = 14.8, 10.8, 4.0 Hz, 1 H), 2.48 (dd, J = 12.8, 5.6 Hz, 1 H), 3.68 (d, J = 13.6 Hz, 1 H), 3.72 (dd, J = 13.2, 4.4 Hz, 1 H), 4.02 (td, J = 16.4, 5.2 Hz, 1 H), 4.61 (t, J = 3.6 Hz, 1 H), 4.71 (t, J = 12.4 Hz, 1 H), 4.83 (m, 2 H), 5.79 (bs, 1 H), 7.22 (m, 2 H), 7.78 (dd, J = 7.6, 3.6 Hz, 1 H). ^{13}C NMR (100.5 MHz, $CDCl_3$) δ 11.9, 17.9, 42.3, 55.3, 59.8, 65.1, 69.4, 73.3 127.5, 127.8, 129.5, 133.8, 137.3, 139.7, 162.9. HRMS: *m/e* calcd for $C_{22}H_{35}NO_4SiH^+$: 406.2414 Found: 406.2411 (Δ = -0.6 ppm).

5-79 was eluted using 3% methanol in dichloromethane as a white solid (15 mg, 38%): mp 46-48 ^oC; $[\alpha]_D^{22}$ −110 (c 2.0, $CHCl_3$); ^1H NMR (400 MHz, $CDCl_3$) δ 1.04 (m, 21 H), 2.06 (dd, J = 12.8, 6.0 Hz, 1 H), 2.48 (td, J = 12.8, 4.0 Hz, 1 H), 3.65 (d, J = 12.8 Hz, 1 H), 3.72 (dd, J = 12.8, 4.0 Hz, 1 H), 4.06 (ddd, J = 10.8, 5.6, 2.8 Hz, 1 H), 4.58 (d, J = 12.8 Hz, 1 H), 4.68 (t, J = 3.6 Hz, 1 H), 4.79 (d, J = 3.2 Hz, 1 H), 4.94 (d, J = 12.8 Hz, 1 H), 7.06 (t, J = 7.6 Hz, 1 H), 7.37 (m, 2 H). ^{13}C NMR (100.5 MHz, $CDCl_3$) δ 12.0, 17.9, 36.7, 55.0, 58.5, 62.6, 63.3, 69.8, 127.0, 128.6, 128.9, 132.3, 137.1, 138.6, 162.9. HRMS: *m/e* calcd for $C_{22}H_{35}NO_4SiH^+$: 406.2414 Found: 406.2397 (Δ = -4.1 ppm).

2-Bromo-1-hydroxymethyl-3-(2-methoxyethenyl)benzene (5-122):[46]
To a solution of $PPh_3(CH_2OMe)Cl$ (2.6 g, 4.6 mmol) in THF (30 mL) at 0 ^oC was added 1.0 M NaHMDS in THF (7.0 mL, 7.0 mmol) at 0 ^oC. The mixture was stirred at room temperature for 1 hour. The suspension was added to a solution of **5-44** (750 mg, 3.5 mmol) in THF (15 mL). The mixture was stirred at room temperature for 1 hour and then quenched with saturated aqueous ammonium chloride (30 mL). The water layer was extracted with ethyl ether (40 mL x 3). The organic layers were combined and washed with brine (10 mL x 2) and dried over anhydrous $MgSO_4$. The solvent was removed under reduced pressure to afford **5-122** as yellow waxy solid (761 mg, 90%) with ~ 1:1 ratio of Z/E isomers: ^1H NMR (400 MHz, $CDCl_3$) δ 2.84 (bs, 1 H), 3.72 (s, 1.65 H), 3.75 (s, 1.35 H), 4.69 (s, 2 H), 5.64 (d, J = 7.2 Hz, 0.45 H), 6.13 (d, J = 12.8 Hz, 0.55 H), 6.23 (d, J = 7.2 Hz, 0.45 H), 6.93 (d, J = 12.8 Hz, 0.55 H), 7.24 (m, 2.55 H), 7.94 (t, J = 4.8 Hz, 0.45 H). HRMS calcd. for $C_{10}H_{11}BrO_2Na^+$: 264.9840, found 264.9839 (Δ= 0.4 ppm).

(2-Bromo-3-hydroxymethyl)phenylacetaldehyde (5-123):[46]
To the solution of **5-122** (760 mg, 3.10 mmol) in acetone (25 mL) was added 3 *N* HCl solution (15 mL) and the mixture was refluxed for 40 min and the reaction was quenched with saturated aqueous sodium bicarbonate (20 mL). The water layer was extracted with ethyl ether (30 mL x 3). The organic layers were combined and washed with brine (10 mL x 2) and dried over anhydrous $MgSO_4$. The solvent was removed under reduced

pressure. The crude product was purified on a silica gel column using dichloromethane as eluent to give **5-123** 568 mg (80%) as colorless oil: ^{1}H NMR (400 MHz, CDCl$_3$) δ 2.53 (s, 1 H), 3.88 (s, 2 H), 4.73 (s, 2 H), 7.14 (d, J = 1.2 Hz, 1 H), 7.29 (t, J = 3.6 Hz, 1 H), 7.44 (dd, J = 7.6, 0.8 Hz, 1 H), 9.73 (t, J = 1.6 Hz, 1 H). ^{13}C NMR (100.5 MHz, CDCl$_3$) δ 50.7, 65.2, 124.8, 127.7, 127.8, 130.7, 133.0, 141.0, 198.5. HRMS calcd. for C$_9$H$_9$BrO$_2$$^+$: 227.9786, found 227.9790 (Δ= 1.7 ppm).

1-Allyl-2-bromo-3-hydroxymethylbenzene (5-124):[34]

To a solution of PPh$_3$CH$_3$Br (1.1 g, 3.25 mmol) in THF (30 mL) at 0 ^{o}C was added sodium hydride (60% suspension in mineral oil, 235 mg, 5.75 mmol). The mixture was stirred at room temperature for 1 h. The resulting suspension was added to a solution of **5-123** (568 mg, 2.5 mmol) in THF (10 mL). The reaction mixture was stirred at 40 ^{o}C for 1 h and quenched with saturated aqueous NH$_4$Cl solution (30 mL). The water layer was extracted with dichloromethane (30 mL x 3). The organic layers were combined, washed with brine (10 mL x 2), and dried by anhydrous MgSO$_4$. The solvent was removed under reduced pressure. The residue was purified by column chromatography on silica gel using Hexanes:EtOAc = 20:1 as the eluent to afford **5-124** as a white solid (369 mg, 50%): mp 34-35 ^{o}C, ^{1}H NMR (300 MHz, CDCl$_3$) δ 2.03 (s, 1 H), 3.55 (d, J = 5.2 Hz, 2 H), 4.77 (s, 2 H), 5.08 (dt, J = 13.6, 2.8 Hz, 1 H), 5.12 (dd, J = 8.0, 1.2 Hz, 1 H), 5.97 (m, 1 H), 7.19 (d, J = 6.0 Hz, 1 H), 7.27 (t, J = 6.0 Hz, 1 H), 7.34 (d, J = 6.4 Hz, 1 H). ^{13}C NMR (100.5 MHz, CDCl$_3$) δ 40.2, 65.3, 116.5, 124.4, 126.4, 127.2, 129.3, 135.4, 139.7, 140.2. HRMS calcd. for C$_{10}$H$_{11}$BrONa$^+$ 248.9891, found 248.9897 (Δ= 2.4 ppm).

1-Allyl-2-bromo-3-methoxymethoxymethylbenzene (5-125):[34]

To a solution of **5-124** (369 mg, 1.63 mmol) in anhydrous dichloromethane (27 mL) at 0 ^{o}C under nitrogen was added N,N'-diisopropylethylamine (0.64 mL, 6.6 mmol), followed by chloromethyl methyl ether (0.27 ml, 3.3 mmol). The reaction mixture was stirred at room temperature overnight. The reaction was quenched with saturated aqueous ammonium chloride (30 mL). The water layer was extracted with dichloromethane (30 mL x 3). The organic layers were combined and washed with brine (10 mL x 2) and dried over anhydrous MgSO$_4$. The solvent was removed under reduced pressure. The residue was purified by column chromatography on silica gel using hexanes:EtOAc (50:1) as the eluent to afford **5-125** as a colorless oil (400 mg, 90%): ^{1}H NMR (300 MHz, CDCl$_3$) δ 3.52 (s, 3 H), 3.64 (dd, J = 6.3, 1.2 Hz, 2 H), 4.78 (s, 2 H), 4.85 (s, 2 H), 5.20 (m, 2 H), 6.05 (d, J = 17.2 Hz, 1 H), 7.13 (dd, J = 17.6, 13.2 Hz, 1 H), 7.29 (t, J = 8.0 Hz, 1 H), 7.42 (m, 1 H), 7.25 (dt, J = 7.5, 1.5 Hz, 1 H), 7.34 (t, J = 7.5 Hz, 1 H), 7.45 (d, J = 7.5 Hz, 1 H). ^{13}C NMR (100.5 MHz, CDCl$_3$) δ 40.5, 55.5, 69.5, 96.1, 116.5, 124.9, 127.1, 129.4, 135.5, 137.9, 139.9. HRMS calcd. for C$_{12}$H$_{15}$BrO$_2$$^+$ 270.0255, found 270.0259 (Δ= 1.5 ppm).

2-[(2-Allyl-6-methoxymethoxymethylphenyl)hydroxymethyl]-1-(*tert*-butoxycarbonyl)-4-triisopropylsiloxypyrrolidine (5-126):[31]

Aryl bromide **5-125** (230 mg, 0.835 mmol) was dissolved in dry THF (8 mL) under N$_2$ and 1.6 M n-BuLi in THF (0.58 mL, 0.92 mmol) was added at -78 ^{o}C. The resulting solution was stirred for 1 h. Then, HMPA (0.15 mL) was added and the solution was stirred for 1 h. A solution of aldehyde **5-14** (311 mg, 0.835 mmol) in dry THF (5 mL)

was added dropwise. The resulting solution was allowed to slowly warm up to -20 ^{o}C with stirring overnight. After addition of saturated NH_4Cl solution (20 mL), the mixture was extracted with dichloromethane (3 x 20 mL). The combined organic layers were washed with brine and dried over $MgSO_4$. After evaporation of the solvent, the residue was purified by flash chromatography on silica gel using Hexanes:EtOAc (10:1) as the eluent to afford desired product **5-126** (333 mg, 71% yield) as colorless oil: ^{1}H NMR (500 MHz, $CDCl_3$) δ 1.04 (m, 21 H), 1.32-1.44 (m, 9H), 1.74 (m, 1 H), 2.19 (m, 1 H), 3.40 (s, 3 H), 3.57 (m, 4 H), 4.45 (m, 2 H), 4.70 (m, 4 H), 5.07 (m, 3 H), 5.97 (m, 1 H), 7.15 (d, J = 7.0 Hz, 1 H), 7.21 (m, 1 H), 7.27 (d, J = 6.0 Hz, 1 H). HRMS calcd. for $C_{31}H_{53}NO_6SiH^+$ 564.3720, found 564.3725 (Δ= 0.9 ppm).

2-[Acetoxy(2-allyl-6-methoxymethoxymethylphenyl)-methyl]-1-(*tert*-butoxycarbonyl)-4-triisopropylsiloxy-pyrrolidine (5-127):[31]

To a solution of **5-126** (332 mg, 0.59 mmol) and DMAP (4 mg, 0.03 mmol) in CH_2Cl_2 (5.0 mL) was added triethylamine (0.7 mL, 2.3 mmol) and acetic anhydride (0.4 mL, 1.2 mmol) at 0 ^{o}C. The reaction mixture was stirred overnight, quenched with saturated aqueous NH_4Cl solution (20 mL) and extracted with dichloromethane (30 mL x 3). The organic layer was dried over anhydrous $MgSO_4$ and solvent was removed under reduced pressure. The residue was purified by column chromatography on silica gel using hexanes:EtOAc (12:1) to afford **4-95** (337 mg, 96%) as colorless oil: ^{1}H NMR (400 MHz, $CDCl_3$) δ 1.03 (m, 21 H), 1.28-1.43 (m, 9 H), 1.66 (m, 1 H), 2.05 (m, 4 H), 3.42 (s, 3 H), 3.65 (m, 4 H), 4.70 (m, 6 H), 5.05 (m, 2 H), 5.97 (m, 1 H), 6.10 (m, 1 H), 7.11-7.31 (m, 3 H); ^{13}C NMR (100.5 MHz, $CDCl_3$) δ 11.9, 17.8, 21.0, 27.7, 37.6, 38.4, 55.2, 58.6, 66.9, 70.7, 72.5, 73.4, 79.7, 95.4, 115.9, 127.7, 128.1, 130.3, 133.5, 134.1, 137.1, 139.2, 154.5, 169.6. ^{1}HRMS calcd. for $C_{33}H_{55}NO_7SiH^+$ 606.3826, found 606.3832 (Δ= 1.0 ppm).

5-128 and 5-129:[39]

Nitrogen gas was bubbled into a solution of **5-127** (335 mg, 0.55 mmol) in CH_2Cl_2 (15 mL) at -78 $^{\circ}$C for 3 min. Then, O_3 gas was bubbled into the solution till the color of the solution turned blue (8 min), and N_2 was bubbled into the solution for another 3 min until the blue color disappeared. Dimethyl sulfide (0.1 mL, 1.4 mmol) was added to the solution and the reaction mixture was allowed to warm to room temperature. The reaction mixture was stirred at room temperature for 3 h. The solvents were removed *in vacuo* and crude product was used in the next step without further purification.

Sodium chlorite (200 mg, 2.24 mmol) was added to a solution of the crude product (~0.55 mmol) and sodium phosphate (monobasic) (350 mg, 2.24 mmol) in acetone/water (1:1, 2.4 mL). The reaction mixture was stirred at room temperature for 1 h and was quenched by ethyl acetate (60 mL). The organic layer was washed with hydrochloric acid (1 N, 10 mL), $Na_2S_2O_3$ (10%, 10 mL x 2), and brine (10 mL), dried with $MgSO_4$, filtered, and concentrated. Crude product was used in the next step without further purification.

A solution of potassium hydroxide (4 g) in water (8 mL) and ethanol (32 mL) was added to a solution of diazald$^{®}$ (4 g) in ether (60 mL) at 0 ^{o}C. The reaction mixture was stirred for 10 min at 0 ^{o}C and distilled to afford a yellow ether solution. The diazomethane solution in ether was added to the solution of the crude product (~ 0.28 mmol) in ether (12 mL) until the yellow color did not disappear. The reaction mixture was stirred for 10

min and quenched by acetic acid. The solvents were removed *in vacuo* and crude product was used in the next step without further purification.

To a solution of the crude product (~ 0.55 mmol) in dichloromethane (1.5 mL) at 0 °C was added trifluoroacetic acid (1.5 mL). The mixture was stirred at 0 °C for 30 min and room temperature for 30 min. The solvent and acid were removed under reduced pressure to give a crude product, which was used in the next step without further purification.

To a solution of the crude product in ethyl acetate (14 mL) was added saturated aqueous sodium bicarbonate (14 mL). The reaction mixture was stirred vigorously for overnight and quenched with ethyl acetate (50 mL). The mixture was washed by saturated aqueous ammonium chloride (10 mL), water (10 mL) and brine (10 mL). The organic layer was dried by anhydrous $MgSO_4$ and the solvent was removed by reduced pressure. The residue was purified by column chromatography on silica gel using hexanes:EtOAc (3:1) to afford **5-128** and **5-129** (1:10) as a colorless oil in 66% over 5 steps.

5-128: colorless oil; $[\alpha]_D^{22}$ -26 (c 1.8, CHCl$_3$); ^{1}H NMR (400 MHz, CDCl$_3$) δ 1.01 (m, 21 H), 1.99 (m, 2 H), 2.07 (s, 3 H), 3.36 (s, 3 H), 3.46 (d, *J* = 13.2 Hz, 1 H), 3.75 (d, *J* = 17.2 Hz, 1 H), 3.98 (dd, *J* = 12.8, 5.6 Hz, 1 H), 4.18 (dd, *J* = 10.8, 6.0 Hz, 1 H), 4.38 (d, *J* = 17.2 Hz, 1 H), 4.45 (t, *J* = 3.6 Hz, 1 H), 4.50 (d, *J* = 11.6 Hz, 1 H), 4.61 (dd, *J* = 12.8, 6.4 Hz, 2 H), 5.05 (d, *J* = 11.6 Hz, 1 H), 6.43 (s, 1 H), 7.14 (dd, *J* = 6.0, 2.4 Hz, 1 H), 7.25 (m, 2 H); ^{13}C NMR (100.5 MHz, CDCl$_3$) δ 11.9, 17.9, 20.9, 40.9, 43.8, 55.4, 57.9, 59.8, 67.5, 68.9, 95.3, 128.9, 129.4, 131.2, 134.6, 135.6, 135.7, 167.5, 170.2. HRMS calcd. for $C_{27}H_{43}NO_6SiH^+$ 506.2938, found 506.2928 (Δ= -2.0 ppm).

5-129: colorless oil; $[\alpha]_D^{22}$ +62 (c 0.2, CHCl$_3$); ^{1}H NMR (400 MHz, CDCl$_3$) δ 1.05 (m, 21 H), 2.02 (dt, *J* = 13.6, 2.8 Hz, 1 H), 2.06 (s, 3 H), 2.26 (dd, *J* = 10.0, 4.0 Hz, 1 H), 3.38 (s, 3 H), 3.38 (d, *J* = 11.2 Hz, 1 H), 3.47 (dd, *J* = 10.4, 3.6 Hz, 1 H), 3.52 (d, *J* = 10.0 Hz, 1 H), 4.36 (m, 2 H), 4.46 (d, *J* = 10.0 Hz, 1 H), 4.52 (d, *J* = 9.6 Hz, 1 H), 4.65 (dd, *J* = 10.8, 5.2 Hz, 2 H), 4.84 (d, *J* = 9.6 Hz, 1 H), 6.41 (d, *J* = 2.4 Hz, 1 H), 7.26 (m, 3 H); ^{13}C NMR (100.5 MHz, CDCl$_3$) δ 11.9, 17.8, 21.1, 41.9, 42.7, 55.4, 55.9, 61.6, 67.3, 67.9 70.9, 95.6, 129.2, 129.3, 129.9, 131.9, 137.5, 137.6, 169.9, 170.6. HRMS calcd. for $C_{27}H_{43}NO_6SiH^+$ 506.2938, found 506.2928 (Δ= -2.0 ppm).

5-130:[39]

To a solution of **5-128** (20 mg, 0.04 mmol) in methanol (2 mL) and water (1 mL) was added potassium carbonate (13 mg, 0.08 mmol). The reaction mixture was stirred at room temperature for 35 min. Then the mixture was quenched by ethyl acetate and the organic layer was washed by saturated aqueous NH$_4$Cl solution (20 mL), water (10 mL x 2) and brine (10 mL). The organic layer was dried over anhydrous $MgSO_4$ and solvent was removed under reduced pressure vacuum. The residue was purified by column chromatography on silica gel using hexanes:EtOAc (3:1) to afford **5-130** as a white solid (17 mg, 94%): mp 91-92 °C; $[\alpha]_D^{22}$ –48 (c 1.3, CHCl$_3$); ^{1}H NMR (400 MHz, CDCl$_3$) δ 1.03 (m, 21 H), 2.28 (m, 1 H), 2.55 (m, 1 H), 3.24 (d, *J* = 6.0 Hz, 1 H), 3.40 (s, 3 H), 3.62 (d, *J* = 15.6 Hz, 1 H), 3.63 (d, *J* = 12.0 Hz, 1 H), 3.72 (d, *J* = 10.8 Hz, 1 H), 4.16 (d, *J* = 15.6 Hz, 1 H), 4.51 (d, *J* = 6.4 Hz, 1 H), 4.69 (s, 2 H), 4.72 (s, 2 H), 4.80 (d, *J* = 11.6 Hz, 1 H), 4.89 (d, *J* = 5.6 Hz, 1 H), 7.14 (d, *J* = 7.6 Hz, 1 H), 7.23 (t, *J* = 7.6 Hz, 1 H), 7.31 (d, *J* = 7.6 Hz, 1 H). ^{13}C NMR (100.5 MHz, CDCl$_3$) δ 12.0, 17.9, 39.8, 44.5, 55.7, 58.6, 67.7, 69.3, 69.4, 70.2, 95.6, 128.3, 130.2, 131.8, 132.1, 137.5, 138.9, 169.8. HRMS: *m/e* calcd for $C_{25}H_{41}NO_5SiH^+$: 464.2832 Found: 464.2820 (Δ = -2.6 ppm).

5-132:[39]

To a solution of **5-129** (260 mg, 0.51 mmol) in methanol (20 mL) and water (10 mL) was added potassium carbonate (180 mg, 1.02 mmol). The reaction mixture was stirred at room temperature for 30 min. Then, the reaction mixture was quenched with ethyl acetate and the organic layer was washed with saturated aqueous NH_4Cl solution (20 mL), water (10 mL x 2) and brine (10 mL). The organic layer was dried over anhydrous $MgSO_4$ and solvent was removed under reduced pressure. The residue was purified by column chromatography on silica gel using hexanes:EtOAc (3:1) to afford **5-132** as a white solid (189 mg, 81%): mp 104-105 ^{o}C; ^{1}H NMR (400 MHz, $CDCl_3$) δ 1.05 (m, 21 H), 2.20 (m, 1 H), 2.54 (m, 1 H), 3.35 (d, J = 14.0 Hz, 1 H), 3.40 (s, 3 H), 3.42 (d, J = 5.2 Hz, 1 H), 3.64 (dd, J = 11.6, 3.6 Hz, 1 H), 4.36 (d, J = 14.0 Hz, 1 H), 4.42 (dd, J = 15.6, 6.4 Hz, 1 H), 4.52 (d, J = 4.4 Hz, 1 H), 4.56 (d, J = 11.2 Hz, 1 H), 4.71 (dd, J = 11.6, 6.4 Hz, 2 H), 4.82 (d, J = 2.8 Hz, 1 H), 4.85 (s, 1 H), 7.26 (m, 3 H). ^{13}C NMR (100.5 MHz, $CDCl_3$) δ 12.0, 17.9, 43.0, 43.7, 53.9, 55.8, 60.5, 68.5, 69.4, 73.1, 95.6, 128.2, 130.9, 131.9, 133.7, 136.9, 138.6, 172.2. HRMS: m/e calcd for $C_{25}H_{41}NO_5SiH^+$: 464.2832 Found: 464.2837 (Δ = 1.1 ppm).

5-134:[39]

To a solution of **5-132** (45 mg, 0.10 mmol) and DMAP (4 mg, 0.05 mmol) in CH_2Cl_2 (2.0 mL) was added triethylamine (0.24 mL, 1.60 mmol) and benzoyl chloride (0.12 mL, 1.20 mmol) at 0 ^{o}C. The reaction mixture was stirred overnight, quenched with saturated aqueous NH_4Cl solution (20 mL) and extracted with dichloromethane (30 mL x 3). The organic layer was dried over anhydrous $MgSO_4$ and solvent was removed under reduced pressure to afford a liquid residue. The residue was purified by column chromatography on silica gel using hexanes:EtOAc (3:1) to afford **5-133** (28 mg, 50%) as colorless oil: ^{1}H NMR (500 MHz, $CDCl_3$) δ 1.07 (m, 21 H), 2.15 (td, J = 11.5, 4.0 Hz, 1 H), 2.35 (dd, J = 13.5, 6.0 Hz, 1 H), 3.42 (s, 3 H), 3.55 (d, J = 13.5 Hz, 1 H), 3.59 (s, 2 H), 4.42 (d, J = 2.5 Hz, 1 H), 4.55 (ddd, J = 11.0, 6.0, 2.5 Hz, 1 H), 4.60 (d, J = 11.5 Hz, 1 H), 4.64 (d, J = 13.5 Hz, 1 H), 4.69 (dd, J = 15.0, 6.5 Hz, 2 H), 5.02 (d, J = 11.5 Hz, 1 H), 6.70 (d, J = 1.5 Hz, 1 H), 7.26 (m, 3 H), 7.49 (t, J = 8.0 Hz, 2 H), 7.58 (t, J = 8.0 Hz, 1 H), 8.02 (d, J = 8.0 Hz, 2 H).

To a solution of **5-133** (28 mg, 0.05 mmol) and anisole (0.1 mL) in CH_2Cl_2 (1.0 mL) was added trifluoroacetic acid (1.0 mL) at 0 ^{o}C. The reaction mixture was stirred 2 h at room temperature and quenched by ethyl acetate (50 mL). The organic layer was washed with saturated $NaHCO_3$ solution (10 mL x 2) and NaCl (10 mL), and dried over anhydrous $MgSO_4$ and solvent was removed under reduced pressure to afford a liquid residue. The residue was purified by column chromatography (silica gel) using hexanes:EtOAc (2:1) to afford **5-134** (25 mg, 95%) as colorless oil: ^{1}H NMR (600 MHz, $CDCl_3$) δ 1.06 (m, 21 H), 2.03 (td, J = 16.2, 4.2 Hz, 1 H), 2.30 (dd, J = 12.6, 4.8 Hz, 1 H), 2.88 (bs, 1 H), 3.45 (d, J = 13.8, 1 H), 3.54 (d, J = 13.2 Hz, 1 H), 3.61 (dd, J = 13.2, 4.8 Hz, 1 H), 4.40 (s, 1 H), 5.57 (dd, J = 12.0, 5.4 Hz, 1 H), 4.66 (d, J = 14.4 Hz, 1 H), 4.84 (dd, J = 18.6, 12.0 Hz, 2 H), 6.68 (s, 1 H), 7.30 (m, 3 H), 7.45 (t, J = 7.2 Hz, 2 H), 7.58 (t, J = 7.2 Hz, 1 H), 8.02 (d, J = 9.0 Hz, 2 H). ^{13}C NMR (125.7 MHz, $CDCl_3$) δ 12.0, 17.9, 41.7, 42.8, 56.9, 61.4, 63.2, 67.7, 71.7, 128.6, 129.0, 129.2, 129.4, 129.7, 129.9, 130.1, 130.9, 133.6, 137.5, 140.4, 165.8, 170.2. HRMS: m/e calcd for $C_{30}H_{41}NO_5SiH^+$: 524.2832 Found: 524.2838 (Δ = 1.1 ppm).

5-136:[36]

To a solution of **5-132** (125 mg, 0.27 mmol), benzoic acid (40 mg, 0.32 mmol) and triphenylphosphine (78 mg, 0.30 mmol) in THF (1 mL) was added diisopropyl azodicarboxylate (0.060 mL, 0.30 mmol). The mixture was stirred overnight and refluxed for 3 days. Solvent was removed under reduced pressure and the residue was purified by column chromatography on silica gel using hexanes:EtOAc (5:1) to afford **5-131** (147 mg) accompanied by impurity and the starting material **5-132** (80 mg, conversion 36%).

To a solution of **5-131** and anisole (0.2 mL) in CH_2Cl_2 (2.0 mL) was added trifluoroacetic acid (2.0 mL) at 0 °C. The reaction mixture was stirred 2 h at room temperature and diluted by ethyl acetate (50 mL). The organic layer was washed by saturated $NaHCO_3$ solution (10 mL x 2) and NaCl (10 ml), dried over anhydrous $MgSO_4$, and solvent was removed under reduced pressure to afford a liquid. The residue was purified by column chromatography on silica gel using hexanes:EtOAc (2:1) to afford **5-135** (32 mg, 63% in 2 steps) as colorless oil.

To a solution of **5-136** (22 mg, 0.042 mmol) and DMAP (1 mg, 0.005 mmol) in CH_2Cl_2 (0.5 mL) was added triethylamine (0.04 mL, 0.12 mmol) and acetic anhydride (0.03 mL, 0.08 mmol) at 0 °C. The reaction mixture was stirred overnight, quenched with saturated aqueous NH_4Cl solution (20 mL) and extracted with dichloromethane (20 mL x 3). The organic layer was dried over anhydrous $MgSO_4$ and solvent was removed under reduced pressure to afford a liquid. The residue was purified by column chromatography on silica gel using hexanes:EtOAc (2:1) to afford **5-136** (21 mg, 80%) as colorless oil: $[\alpha]_D^{22}$ +5.5 (c 0.5, $CHCl_3$); ^1H NMR (600 MHz, $CDCl_3$) δ 1.02 (m, 21 H), 1.95 (s, 3 H), 2.18 (m, 2 H), 3.55 (d, J = 13.2 Hz, 1 H), 3.92 (d, J = 17.8 Hz, 1 H), 4.04 (d, J = 13.2, 5.4 Hz, 1 H), 4.35 (dd, J = 10.2, 6.0 Hz, 1 H), 4.39 (d, J = 18.0 Hz, 1 H), 4.46 (s, 1 H), 4.25 (d, J = 12.6 Hz, 1 H), 5.57 (d, J = 12.0 Hz, 1 H), 5.59 (s, 1 H), 7.19 (d, J = 7.2 Hz, 1 H), 7.29 (t, J = 7.2 Hz, 1 H), 7.33 (d, J = 7.2 Hz, 1 H), 7.43 (t, J = 7.2 Hz, 2 H), 7.57 (t, J = 7.8 Hz, 1 H), 7.99 (d, J = 7.8 Hz, 2 H). ^{13}C NMR (125.7 MHz, $CDCl_3$) δ 11.9, 17.9, 20.8, 40.9, 44.1, 57.6, 59.8, 64.5, 67.7, 69.7, 128.7, 129.2, 129.8, 130.3, 131.9, 133.7, 134.5, 134.6, 135.3, 165.6, 167.8, 170.2. HRMS: *m/e* calcd for $C_{32}H_{43}NO_6SiH^+$: 566.2938 Found: 566.2955 (Δ = 3.0 ppm).

5-137:[25]

To a solution of **5-136** (21 mg, 0.037 mmol) in CH_3CN (0.4 mL) and pyridine (0.4 mL) was added HF-pyridine (70:30, 0.2 ml) and the reaction mixture was stirred overnight. The reaction mixture was quenched with EtOAc (40 mL) and washed with saturated aqueous $NaHCO_3$ solution (10 mL x 2), $CuSO_4$ solution (10 mL x 3), water (10 mL x 3) and brine (3 mL). The organic layer was dried over anhydrous $MgSO_4$ and solvent was removed under reduced pressure. The residue was purified by column chromatography on silica gel using 5% MeOH in chloroform as the eluent to afford **5-137** as white solid (13 mg, 86%): ^1H NMR (500 MHz, $CDCl_3$) δ 2.00 (s, 3 H), 2.20 (m, 2 H), 3.64 (d, J = 13.5 Hz, 1 H), 3.93 (d, J = 17.5 Hz, 1 H), 3.98 (m, 1 H), 4.40 (m, 2 H), 4.48 (s, 1 H), 5.26 (d, J = 12.5, 1 H), 5.58 (d, J = 12.5 Hz, 1 H), 6.61 (s, 1 H), 7.18 (d, J = 7.0 Hz, 1 H), 7.29 (t, J = 8.0 Hz, 1 H), 7.34 (d, J = 7.5 Hz ,1 H), 7.45 (t, J = 8.0 Hz, 2 H), 7.59 (d, J = 7.5 Hz, 1 H), 7.99 (d, J = 7.5 Hz, 2 H). ^{13}C NMR (125.7 MHz, $CDCl_3$) δ 20.8, 39.8, 44.0, 57.1, 59.5, 64.5, 67.0, 69.5, 128.7, 129.1, 129.3, 129.7, 129.8, 130.0, 131.8, 133.7, 134.3, 134.5, 135.2, 165.6, 167.9, 170.3. HRMS: *m/e* calcd for $C_{23}H_{23}NO_6H^+$: 410.1604 Found:

410.1594 (Δ = -2.4 ppm).

5-138:[50]
Pyridinium chlorochromate (102 mg, 0.48 mmol) was added to the solution of **5-132** (75 mg, 0.16 mmol) in dichloromethane (3.0 mL). The mixture was stirred at room temperature for 2.5 h and the reaction was quenched with Et_2O (50 mL). After filtration, the solid residue was washed with Et_2O (50 mL x 2) and the combined organic layer was washed with 5% aqueous citric acid solution (5 mL), saturated aqueous $NaHCO_3$ solution (10 mL) and brine (10 mL). The organic layer was dried over anhydrous $MgSO_4$ and solvent was removed by reduced pressure. The residue was purified by column chromatography on silica gel using hexanes:EtOAc (4:1) as the eluent to afford **5-138** as colorless oil (28 mg, 93% based on 40% conversion): $[\alpha]_D^{22}$ +43 (c 0.8, $CHCl_3$); ^{1}H NMR (600 MHz, $CDCl_3$) δ 1.07 (m, 21 H), 2.23 (td, J = 10.8, 4.2 Hz, 1 H), 2.49 (ddt, J = 13.2, 6.6, 1.8 Hz, 1 H), 3.34 (s, 3 H), 3.40 (dd, J = 12.0, 4.2 Hz, 1 H), 3.48 (d, J = 13.8 Hz, 1 H), 3.75 (d, J = 12.6 Hz, 1 H), 4.00 (d, J = 13.8 Hz, 1 H), 4.46 (s, 1 H), 4.63 (s, 2 H), 4.65 (d, J = 13.2 Hz, 1 H), 4.80 (d, J = 13.2 Hz, 1 H), 4.82 (dd, J = 11.4, 6.6 Hz, 1 H), 7.26 (d, J = 7.2 Hz, 1 H), 7.42 (t, J = 7.8 Hz, 1 H), 7.48 (d, J = 7.8 Hz, 1 H). ^{13}C NMR (125.7 MHz, $CDCl_3$) δ 12.0, 17.9, 40.7, 43.1, 55.4, 55.7, 66.7, 67.3, 68.7, 96.3, 128.4, 128.9, 132.2, 133.5, 136.5, 139.8, 170.1, 202.6. HRMS: m/e calcd for $C_{29}H_{35}NO_5H^+$: 462.2312 Found: 462.2330 (Δ = 3.9 ppm).

5-130 and 5-132:
Sodium borohydride (40 mg, 0.24 mmol) was added to a solution of **5-138** (28 mg, 0.06 mmol) in methanol (2.5 mL) at room temperature. The reaction mixture was stirred for 5 min, quenched with saturated aqueous NH_4Cl solution (20 mL), and extracted with dichloromethane (20 mL x 3). The organic layer was dried over anhydrous $MgSO_4$ and solvent was removed under reduced pressure. The residue was purified by column chromatography on silica gel using hexanes:EtOAc (2:1) to afford **5-130** (13 mg, 47%) and **5-132** (13 mg, 47%).

5-37:[39]
To a solution of **5-137** (11 mg, 0.027 mmol), acid **5-4** (12 mg, 0.03 mmol) and DMAP (3.2 mg, 0.027 mmol) in CH_2Cl_2 (0.5 mL) was added EDC (22 mg, 0.11 mmol) and the reaction mixture was stirred for 1 day. The mixture was then quenched with EtOAc (50 mL) and washed with water (10 mL x 2) and brine (10 mL). The organic layer was dried over anhydrous $MgSO_4$, filtered, and then solvent was removed under reduced pressure. The residue was purified by column chromatography on silica gel using hexanes:EtOAc (1:1) as the eluent to afford **5-139** as a white solid (11 mg, 92% based on 50% conversion).
To a solution of **5-139** (11 mg, 0.014 mmol) in methanol (0.5 mL) was added p-TSA (0.5 mg, 0.003 mmol). After stirring overnight, the solvent was removed and the residue purified by column chromatography on silica gel using hexanes:EtOAc (1/2) as the eluent to afford **5-37** as a white solid (7 mg, 74%): mp 130-132 °C; ^{1}H NMR (500 MHz, $CDCl_3$) δ 1.95 (s, 1 H), 2.27 (td, J = 11.0, 5.0 Hz, 1 H), 2.40 (dd, J = 13.5, 6.0 Hz, 1 H), 3.27 (d, J = 4.0 Hz, 1 H), 3.79 (d, J = 14.0 Hz, 1 H), 4.02 (d, J = 17.0, 1 H), 4. 04 (dd, J =14.5, 5.0 Hz, 1 H), 4.40 (dd, J = 17.0 Hz, 1 H), 4.50 (dd, J = 11.0, 5.5 Hz, 1 H), 4.65 (dd, J =

4.2, 1.2 Hz, 1 H), 5.39 (d, *J* = 9.0 Hz, 1 H), 5.41 (d, *J* = 12.5 Hz, 1 H), 5.49 (d, *J* = 12.5 Hz, 1 H), 5.74 (d, *J* = 7.5 Hz, 1 H), 6.64 (s, 1 H), 6.86 (d, *J* = 9.0 Hz, 1 H), 7.21 (d, *J* = 8.0 Hz, 1 H), 7.26 (m, 4 H), 7.43 (m, 6 H), 7.55 (m, 3 H), 7.75 (d, *J* = 9.0 Hz, 2 H), 7.98 (d, *J* = 7.5 Hz, 2 H). HRMS: *m/e* calcd for $C_{39}H_{36}N_2O_9H^+$: 677.2499 Found: 677.2502 (Δ = 0.4 ppm).

§ 5.5 References

1.   Bollag, D. M.; McQueney, P. A.; Zhu, J.; Hensens, O.; Koupal, L.; Liesch, J.; Goetz, M.; Lazarides, E.; Woods, C. M. Epothilones, a New Class of Microtubule-stabilizing Agents with a Taxol-like Mechanism of Action. *Cancer Res.* **1995,** 55, 2325-2333.

2.   Kowalski, R. J.; Giannakakou, P.; Hamel, E. Activities of the Microtubule-Stabilizing Agents Epothilones A and B with Purified Tubulin and in Cells Resistant to Paclitaxel. *J. Biol. Chem.* **1997,** 272, 2534-2541.

3.   Lindel, T.; Jensen, P. R.; Fenical, W.; Long, B. H.; Casazza, A. M.; Carboni, J.; Fairchild, C. R. Eleutherobin, a New Cytotoxin that Mimics Paclitaxel (Taxol) by Stabilizing Microtubules. *J. Am. Chem. Soc.* **1997,** 119, 8744-8745.

4.   ter Haar, E.; Kowalski, R. J.; Hamel, E.; Lin, C. M.; Longley, R. E.; Gunasekera, S. P.; Rosenkranz, H. S.; Day, B. W. Discodermolide, A Cytotoxic Marine Agent That Stabilizes Microtubules More Potently Than Taxol. *Biochemistry* **1996,** 35, 243-250.

5.   Mooberry, S. L.; Tien, G.; Hernandez, A. H.; Plubrukarn, A.; Davidson, B. S. Laulimalide and isolaulimalide, new paclitaxel-like microtubule-stabilizing agents. *Cancer Res.* **1999,** 59, 653-60.

6.   Sato, B.; Nakajima, H.; Hori, Y.; Hino, M.; Hashimoto, S.; Terano, H. A new antimitotic substance, FR182877. II. The mechanism of action. In *J. Antibiot.*, 2000; Vol. 53, pp 204-206.

7.   Kowalski, R. J.; Giannakakou, P.; Gunasekera, S. P.; Longley, R. E.; Day, B. W.; Hamel, E. The Microtubule-Stabilizing Agent Discodermolide Competitively Inhibits the Binding of Paclitaxel (Taxol) to Tubulin Polymers, Enhances Tubulin Nucleation Reactions More Potently Than Paclitaxel, and Inhibits the Growth of Paclitaxel-Resistant Cells. *Mol. Pharmacol.* **1997,** 52, 613-622.

8.   Giannakakou, P.; Sackett, D. L.; Kang, Y.-K.; Zhan, Z.; Buters, J. T. M.; Fojo, T.; Poruchynsky, M. S. Paclitaxel-resistant human ovarian cancer cells have mutant beta -tubulins that exhibit impaired paclitaxel-driven polymerization. *J. Biol. Chem.* **1997,** 272, 17118-17125.

9.   Ojima, I.; Chakravarty, S.; Inoue, T.; Lin, S.; He, L.; Horwitz, S. B.; Kuduk, S. D.; Danishefsky, S. J. A Common Pharmacophore for Cytotoxic Natural Products that Stabilize Microtubules. *Proc. Natl. Acad. Sci. USA* **1999,** 96, 4256-4261.

10.   Giannakakou, P.; Gussio, R.; NOgales, E.; Downing, K. H.; Zaharevitz, D.; Bollbuck, B.; Poy, G.; Sackett, D.; Nicolaou, K. C.; Fojo, T. A Common Pharmacophore for Epothilone and Taxanes: Molecular Basis for Drug Resistance Conferred by Tubulin Mutations in Human Cancer Cells. *Proc. Natl. Acad. Sci. USA* **2000**, 2904-2909.

11.   He, L.; Jagtap, P. G.; Kingston, D. G. I.; Shen, H.-J.; Orr, G.; Horwitz, S. B. A Common Pharmacophore for Taxol and the Epothilones Based on the Biological Activity of a Taxane Molecule Lacking a C-13 Side Chain. *Biochemistry* **2000,** 39, 3972-3978.

12.   Chou, T.-C.; Zhang, X.-G.; Balog, A.; Su, D.-S.; Meng, D.; Savin, K.; Bertino, J. R.; Danishefsky, S. J. Desoxyepothilone B: An Efficacious Microtubule-Targeted

Antitumor Agent With a Promising *in Vivo* Profile Relative to Epothilone B. *Proc. Natl. Acad. Sci. USA* **1998,** 95, 9642.

13. Chou, T. C.; Zhang, X. G.; Harris, C. R.; Kuduk, S. D.; Balog, A.; Savin, K.; Danishefsky, S. J. Desoxyepothilone B is Curative Against Human Tumor Xenografts that are Refractory to Paclitaxel. *Proc. Natl. Acad. Sci. USA* **1998,** 95, 15798.

14. Johnson, J.; Kim, S.-H.; Bifano, M.; Dimarco, J.; Fairchild, C.; Gougoutas, J.; Lee, F.; Long, B.; Tokarski, J.; Vite, G. Synthesis, Structure Proof, and Biological Activity of Epothilone Cyclopropanes. *Org. Lett.* **2000,** 2, 1537-1540.

15. Dubois, J.; Thoret, S.; Guéritte, F.; Guénard, D. Synthesis of 5(20)deoxydocetaxel, a new active docetaxel analogue. *Tetrahedron Lett.* **2000,** 41, 3331-3334.

16. Geng, X.; Geney, R.; Pera, P.; Bernacki, R. J.; Ojima, I. Design and synthesis of de novo cytotoxic alkaloids through mimicking taxoid skeleton. *Bioorg. Med. Chem. Lett.* **2004,** 14, 3491-3494.

17. Ganesh, T.; Norris, A.; Sharma, S.; Bane, S.; Alcaraz, A. A.; Snyder, J. P.; Kingston, D. G. I. Design, synthesis, and bioactivity of simplified paclitaxel analogs based on the T-Taxol bioactive conformation. *Bioorg. Med. Chem.* **2006,** 14, 3447-3454.

18. Ganesh, T.; Bane, S.; Ravindra, R.; Shanker, N.; Lakdawala, A. S.; Snyder, J. P.; Norris, A.; Kingston, D. G. I. Evaluation of the bioactive tubulin-binding paclitaxel conformation: Synthesis and biological evaluation of C4 to C3'-phenyl bridged paclitaxel analogs. *Abstracts of Papers, 229th ACS National Meeting, San Diego, CA, United States, March 13-17, 2005* **2005**, MEDI-471.

19. Greenstein, J. P.; Winitz, M. *Chemistry of the Amino Acids. 3 Vols*. 1961; p 2872 pp.

20. Robinson, D. S.; Greenstein, J. P. Stereoisomers of Hydroxyproline. *J. Biol. Chem.* **1952,** 195, 383-388.

21. Baker, G. L.; Fritschel, S. J.; Stille, J. R.; Stille, J. K. Transition-Metal-Catalyzed Asymmetric Organic-Synthesis Via Polymer-Attached Optically-Active Phosphine-Ligands .5. Preparation of Amino-Acids in High Optical Yield Via Catalytic- Hydrogenation. *J. Org. Chem.* **1981,** 46, 2954-2960.

22. Mitsunobu, O. The Use of Diethyl Azodicarboxylate and Triphenylphosphine in Synthesis and Transformation of Natural-Products. *Synthesis-Stuttgart* **1981**, 1-28.

23. Grubbs, R. H.; Chang, S. Recent Advances in Olefin Metathesis and Its Application in Organic Synthesis. *Tetrahedron* **1998,** 54, 4413-4450.

24. Nettles, J. H.; Li, H.; Cornett, B.; Krahn, J. M.; Snyder, J. P.; Downing, K. H. The Binding Mode of Epothilone A on a,b-Tubulin by Electron Crystallography. *Science* **2004,** 305, 866-869.

25. Geney, R.; Sun, L.; Pera, P.; Bernacki Ralph, J.; Xia, S.; Horwitz Susan, B.; Simmerling Carlos, L.; Ojima, I. Use of the tubulin bound paclitaxel conformation for structure-based rational drug design. *Chem. Biol.* **2005,** 12, 339-48.

26. Bibal, C.; Mazieres, S.; Gornitzka, H.; Couret, C. New arylchlorogermylenes stabilized by two ortho side-chain donor ligands. *Polyhedron* **2002,** 21, 2827-2834.

27. Thibault, M. E.; Closson, T. L. L.; Manning, S. C.; Dibble, P. W. Naphtho[1,2-c:5,6-c]difuran: a reactive linker and cyclophane precursor. *J. Org. Chem.* **2003,** 68, 8373-8.

28. Boger, D. L.; Kim, S. H.; Mori, Y.; Weng, J. H.; Rogel, O.; Castle, S. L.; McAtee, J. J. First and second generation total synthesis of the teicoplanin aglycon. *J. Am. Chem. Soc.* **2001,** 123, 1862-71.

29. Kaiser, F.; Schwink, L.; Velder, J.; Schmalz, H.-G. Studies towards the total synthesis of mumbaistatin: synthesis of highly substituted benzophenone and anthraquinone building blocks. *Tetrahedron* **2003,** 59, 3201-3217.

30. Kaiser, F.; Schmalz, H.-G. Synthetic analogues of the antibiotic pestalone. *Tetrahedron* **2003,** 59, 7345-7355.

31. Akiba, K.; Moriyama, Y.; Mizozoe, M.; Inohara, H.; Nishii, T.; Yamamoto, Y.; Minoura, M.; Hashizume, D.; Iwasaki, F.; Takagi, N.; Ishimura, K.; Nagase, S. Synthesis and Characterization of Stable Hypervalent Carbon Compounds (10-C-5) Bearing a 2,6-Bis(p-substituted phenyloxymethyl)benzene Ligand. *J. Am. Chem. Soc.* **2005,** 127, 5893-5901.

32. Quan, L. G.; Lamrani, M.; Yamamoto, Y. Intramolecular nucleophilic addition of aryl bromides to ketones catalyzed by palladium. *J. Am. Chem. Soc.* **2000,** 122, 4827-4828.

33. Quan, L. G.; Lamrani, M.; Yamamoto, Y. Intramolecular nucleophilic addition of aryl bromides to ketones catalyzed by palladium. *Journal of the American Chemical Society* **2000,** 122, 4827-4828.

34. Kim, B. M., Park, J.K. A Short Synthesis of a Chiral Alcohol as a New Chiral Auxiliary for Asymmetric Reactions. *Bull. Korean Chem. Soc.* **1999,** 20, 744-746.

35. Park, H.; Hepperle, M.; Boge, T. C.; Himes, R. H.; Georg, G. I. Preparation of Phenolic Paclitaxel Metabolites. *J. Med. Chem.* **1996,** 39, 2705-2709.

36. Bellier, B.; McCort-Tranchepain, I.; Ducos, B.; Danascimento, S.; Meudal, H.; Noble, F.; Garbay, C.; Roques, B. P. Synthesis and Biological Properties of New Constrained CCK-B Antagonists: Discrimination of Two Affinity States of the CCK-B Receptor on Transfected CHO Cells. *J. Med. Chem.* **1997,** 40, 3947-3956.

37. Cunico, R. F.; Bedell, L. The triisopropylsilyl group as a hydroxyl-protecting function. *J. Org. Chem.* **1980,** 45, 4797-8.

38. Lin, S. Design, synthesis and medicinal chemistry of novel taxane-based anticancer agents. 1999.

39. Geng, X. Design, synthesis, and biological evaluations of novel taxane-based and taxane-free anticancer agents. 2002.

40. Garner, P.; Ramakanth, S. Stereodivergent synthesis of threo and erythro 6-amino-6-deoxyheptosulose derivatives via an optically active oxazolidine aldehyde. *J. Org. Chem.* **1986,** 51, 2609-12.

41. Hosoya, T.; Takashiro, E.; Matsumoto, T.; Suzuki, K. Total Synthesis of the Gilvocarcins. *J. Am. Chem. Soc.* **1994,** 116, 1004-15.

42. Krasovskiy, A.; Malakhov, V.; Gavryushin, A.; Knochel, P. Efficient synthesis of functionalized organozinc compounds by the direct insertion of zinc into organic iodides and bromides. *Angew. Chem. Int. Ed.* **2006,** 45, 6040-6044.

43. Kim, J. G.; Walsh, P. J. From aryl bromides to enantioenriched benzylic alcohols in a single flask: catalytic asymmetric arylation of aldehydes. *Angew. Chem. Int. Ed.* **2006,** 45, 4175-4178.

44. Ojima, I.; Inoue, T.; Chakravarty, S. Enantiopure fluorine-containing taxoids: potent anticancer agents and versatile probes for biomedical problems. *J. Fluorine Chem.* **1999,** 97, 3-10.

45. Sun, L.; Ojima, I. Design and synthesis of de novo paclitaxel mimics. *Abstracts of Papers, 232nd ACS National Meeting,* **2006**, ORGN-851.

46. Clive, D. L. J.; Wang, J. Synthesis of (+-)-Hamigeran B, (-)-Hamigeran B, and (+-)-1-epi-Hamigeran B: Use of Bulky Silyl Groups to Protect a Benzylic Carbon-Oxygen Bond from Hydrogenolysis. *J. Org. Chem.* **2004,** 69, 2773-2784.

47. Geng, X. Design, Synthesis, and Biological Evaluations of Novel Taxane-Based and Taxane-Free Anticancer Agents. Ph.D. Dissertation, State University of New York, Stony Brook, 2002.

48. Stork, G.; Takahashi, T. Chiral synthesis of prostaglandins (PGE1) from D-glyceraldehyde. *J. Am. Chem. Soc.* **1977,** 99, 1275-6.

49. Ojima, I.; Slater, J. S.; Kuduk, S. D.; Takeuchi, C. S.; Gimi, R. H.; Sun, C.-M.; Park, Y. H.; Pera, P.; Veith, J. M.; Bernacki, R. J. Syntheses and Structure-Activity Relationships of Taxoids Derived from 14β-Hydroxy-10-deacetylbaccatin III. *J. Med. Chem.* **1997,** 40, 267-278.

50. Semmelhack, M. F.; Zask, A. Synthesis of racemic frenolicin via organochromium and organopalladium intermediates. *J. Am. Chem. Soc.* **1983,** 105, 2034-43.

Chapter VI

Synthesis and Molecular Modeling
Studies of C-seco-Taxoids

§ 6.1 Introduction

Although paclitaxel and docetaxel exhibit excellent anti-tumor activity against various cancer cell lines, it has been shown that treatments with the drugs often result in multi-drug resistance (MDR).[1, 2] Among a variety of mechanisms proposed to explain paclitaxel's resistance, one of the most prominent mechanisms seems to be the overexpression of specific tubulin isotypes.[3] β-Tubulin is encoded by at least seven different genes with small differences in the C-terminal region and seven isotypes have been classified (**Table 1**).[4, 5] β-Tubulin isotypes vary in their degree of sensitivity to paclitaxel. Class III β-tubulin exhibited less sensitivity to paclitaxel than the other isotypes. The microtubules composed of purified class III β-tubulin were 7.4-fold less sensitive to the effects of bound paclitaxel and the microtubules immuno-depleted of class III β-tubulin were significantly more sensitive to paclitaxel than microtubules assembled from unfractioned tubulin.[6, 7]

Table 6-1. Tissue distribution of β-tubulin isotypes in normal cells[5]

Isotype	Organ expression	Cellular expression
βI	Constitutive	All cells
βIIa/b	Brain, nerves, muscle, rare elsewhere	Restricted to particular cell types
	Brain	Neurons only
βIII	Testis	Sertoli cells
	Colon	Epithelial cells only
βIVa	Brain	Neurons and glia
βIVb	Most organs	High in ciliated cells, lower in others
βV	Unknown	Unknown
βVI	Blood, bone marrow, spleen	Erythroid cells, platelets
βVII	Brain	Unknown

Through structure-activity relationship (SAR) studies, a series of highly active new-generation taxoids were discovered.[8-10] Most of these taxoids exhibited 1 order of magnitude higher potency than that of paclitaxel against drug-sensitive cancer cell lines, and 2-3 orders of magnitude higher potencies than that of paclitaxel against drug-resistant cell lines. Very recently, we found that second-generation taxoid **SB-T-1214** and third-generation taxoid **SB-T-121303** and **SB-T-11033** exhibited excellent activity against paclitaxel-resistant ovarian cancer cell lines (1A9PTX10 and 1A9PTX22), wherein the drug resistance was mediated by β-tubulin mutation (See **Chapter I**).[11]

One of the new-generation taxoids, IDN5390, in which the six-membered C ring of the baccatin structure is opened, was developed in Indena, SpA.[12]
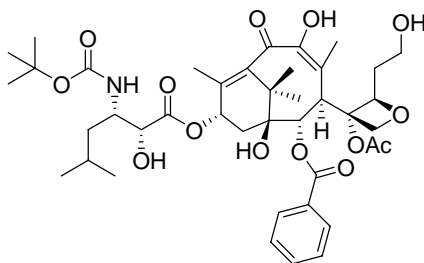
Figure 6-1. IDN-5390

IDN-5390 acted effectively against paclitaxel-resistant cell lines overexpressing class III β-tubulin.[13] Ferlini *et al* assayed **IDN-5390** against human ovarian adenocarcinoma cell line (A2780wt) and the corresponding mutants, A2780CIS, A2780TOP, A2780TAX, and A2780ADR cell lines, resistant to cisplatin, topotecan, paclitaxel and adriamicin, respectively. Multi-drug resistance was also evaluated in the case of A2780TC1 and A2780TC3 cell lines, resistant to both paclitaxel and cyclosporine A. As an example of inherent resistance, OVCAR-3, human ovarian carcinoma was assayed. The IC_{50} values are shown in **Table 6-2**, where the activity of **IDN-5390** is compared to paclitaxel and other chemotherapeutic agents. **IDN-5390** is 4~10 times less active than paclitaxel against A2780TOP, A2780CIS, and A2780wt cells. In the case of cell lines overexpressing P-glycoprotein (P-gp), A2780ADR and A2780TAX (generated upon continuous exposure to doxorubicin and paclitaxel, respectively, without P-gp blockers), **IDN-5390** shows a similar trend i.e., about two times less active than paclitaxel. The results are completely different in case of A2780TC1 and A2780TC3, two drug-resistant cells derived from A2780wt with chronic exposure to paclitaxel in the presence of cyclosporine as P-gp blocker. Although **IDN-5390** is slightly less active than paclitaxel against drug-sensitive cell lines, against drug-resistant cell lines not overexpressing P-gp, **IDN-5390** is more active (up to 8-fold) than paclitaxel. An explanation for this result based on the structural analysis of the cell lines, A2780TC1 and A2780TC3, in comparison with the wild type. Taxol-resistance has been shown to be associated with a consistent overexpression of class III β-tubulin mRNA level for A2780TC1, A2780TC3 and OVCAR-3 without significant changes at the level of class I, IVa and IVb β-tubulin isotypes.[13] This result is in accordance with the previous publications which reported changes in the composition and mutations in β-tubulin isotypes in cells resistant to paclitaxel.[14, 15] The overexpression observed at the level of mRNA was actually translated into parallel changes at the protein level.

Table 6-2. Growth inhibition effect (μM) of anticancer drugs on drug-resistant ovarian cancer cell lines[16]

Drug	A2780wt	A2780CIS	A2780TOP	A2780TAX	A2780ADR	A2780TC1	A2780TC3	OVCAR-3
Paclitaxel	2.7	3.6	7.2	1,824	1,239	10,027	17,800	26.7
IDN 5390	27.45	27.3	27.5	2,300	2,617	2,060	2,237	55.9
Cisplatin	614	7,896	606	3,005	2,057	2,618	2,628	2,146
Topotecan	8.5	20.6	423	75.5	22.7	63.3	98	87.5
Doxorubicin	25.9	164	36.3	1,563	2,012	8,519	5,576	199

The weaker binding ability of paclitaxel to class III β-tubulin can be explained by the mutation of Ser277 to Ala277, which causes the disruption of the H-bond between Ser277 and C7-OH and reorganization of the M-loop region.[13, 17] However, paclitaxel molecule is too flexible for direct docking studies. As shown in **Figure 6-2b**, the docking of paclitaxel in 1JFF protein generated a totally different conformation from the 1JFF structure (**Figure 6-2a**). Therefore, the docking result of more flexible **IDN-5390** in 1JFF (**Figure 6-2c**) is not reliable.
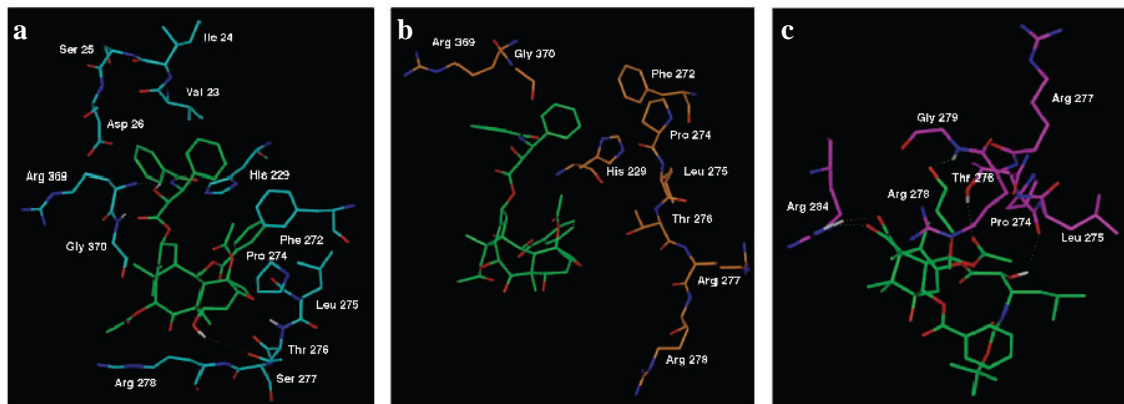
Figure 6-2. Binding conformation of paclitaxel and IDN-5390 in 1JFF (a: 1JFF; b: docking result of paclitaxel; c: docking result of IDN-5390) [Adapted from ref. 12]

Very recently, a combination of molecular modeling and molecular dynamics (MD) techniques have been applied to investigate the binding modes of paclitaxel and **IDN-5390** in the class I and class III human β-tubulins.[17] A 2-ns simulation was performed by Macromodel® for the paclitaxel and **IDN-5390** in the class I/III β-tubulin complexes. A restraint (23.9 kcal/(mol*Å)) was applied to the protein backbones in the simulations and the binding energies were calculated by the thermodynamic module of the MOLINE program.[18] According to the study, IDN-5390 can bind to β-tubulins in a very similar way as paclitaxel (**Figure 6-3**). The result indicates that there is no direct interaction between Ser277 (or Ala277) with paclitaxel or **IDN-5390**. Also, paclitaxel can bind to the class I β-tubulin better than the class III derivative, while **IDN-5390** could bind to the class III β-tubulin better than the class I β-tubulin (**Table 6-3**).[17]
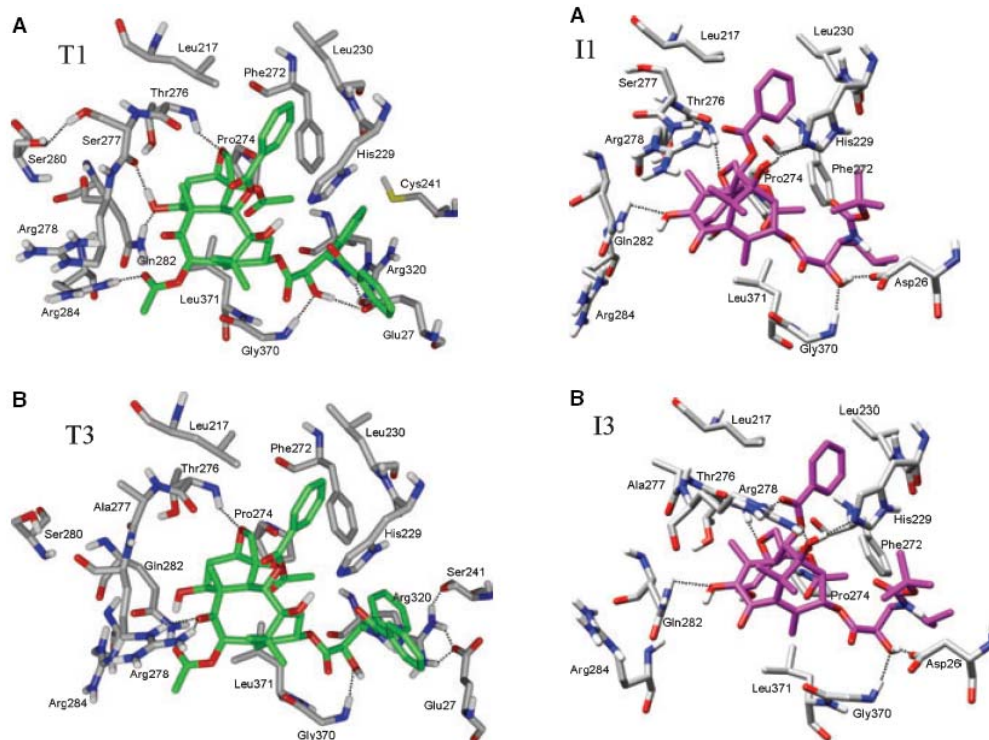
Figure 6-3. The binding conformation of paclitaxel (green) and IDN-5390 (magenta) after MD simulation [Adapted from ref 17]

Table 6-3. Free energy, enthalpy and entropy for taxoid-tubulin complexes[17]

Complex	ΔG (kcal/mol)	ΔH (kcal/mol)	ΔS (cal/mol)
Paclitaxel-class I β-tubulin	-64.47	-64.16	1.01
Paclitaxel-class III β-tubulin	-54.67	-54.64	0.11
IDN-5390- class I β-tubulin	-55.89	-55.49	1.32
IDN-5390- class III β-tubulin	-67.52	-67.12	1.33

In this chapter, the synthesis of one of the C2 modified C-seco taxoids, **SB-CST-10204** (**IDN-5868**) will be reported. The binding energies of paclitaxel, **IDN-5390** and the novel C-seco taxoids with class I and class III human β-tubulins will be investigated by docking and molecular dynamics simulation (AMBER9®).

§ 6.2 Synthesis and Evaluation of Novel C-seco-Taxoids

§ 6.2.1 Synthesis of SB-CST-10204 (IDN-5868)

In order to further investigate the activity of C-seco-taxoids against cell lines overexpressing class III β-tubulin, six novel seco-taxoids with different functional groups at the C2 and C3' were synthesized in the Ojima group and evaluated, in collaborating with Indena, SpA. Five the C-seco-taxoids were synthesized by Dr. Antonella Pepe and I synthesized one compound (**SB-CST-10204**).

R = MeO, **SB-CST-10201**;
Cl, **SB-CST-10202**;
F, **SB-CST-10204**.

R = MeO, **SB-CST-10101**;
Cl, **SB-CST-10102**;
F, **SB-CST-10104**.
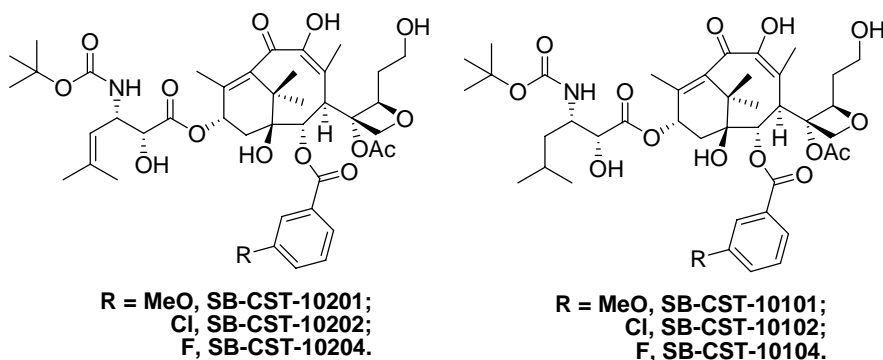
Figure 6-4. The novel C-seco-taxoids

The synthesis of these C-seco-taxoids began with the modification of the C2' position of 10-DAB. The C2-*meta*-F-10-DAB analog was obtained from 7,10,13-tri-TES-baccatin diol **1-29** by the method shown in **Chapter I**. **1-29** was mixed with a large excess of *m*-fluorobenzoic acid, 1,3-diisopropylcarbodiimide (DIC) and *N,N*-dimethyl-aminopyridine (DMAP) and the mixture was refluxed in a concentrated dichloromethane solution (~8 M) overnight to give the desired C2-modified tri-TES-baccatin **6-1** in 90% yield. A global removal of the TES groups using HF-pyridine gave baccatin **6-2** in high yield.

The C2-modified baccatin **6-2** was oxidized to **6-3** by air in the presence of Cu(OAc)$_2$ as catalyst. The diastereomers of **6-3** was treated with L-Selectride at -65 $^{\circ}$C for 40 min to afford **6-4** in 74% yield as a single product. The C7-OH and C9-OH were selectively protected by reacting with TESCl and 1-methylimidazole in a diluted DMF solution at 0 $^{\circ}$C to give di-TES baccatin **6-5** in 60% yield. Protected baccatin **6-5** was coupled with β-lactam **1-10** under the standard conditions to afford the desired product **6-6** in 78 % yield. The desilylation of **6-6** with HF-pyridine gave the *meta*-F-C-seco-taxoid **6-7** in 73% yield.
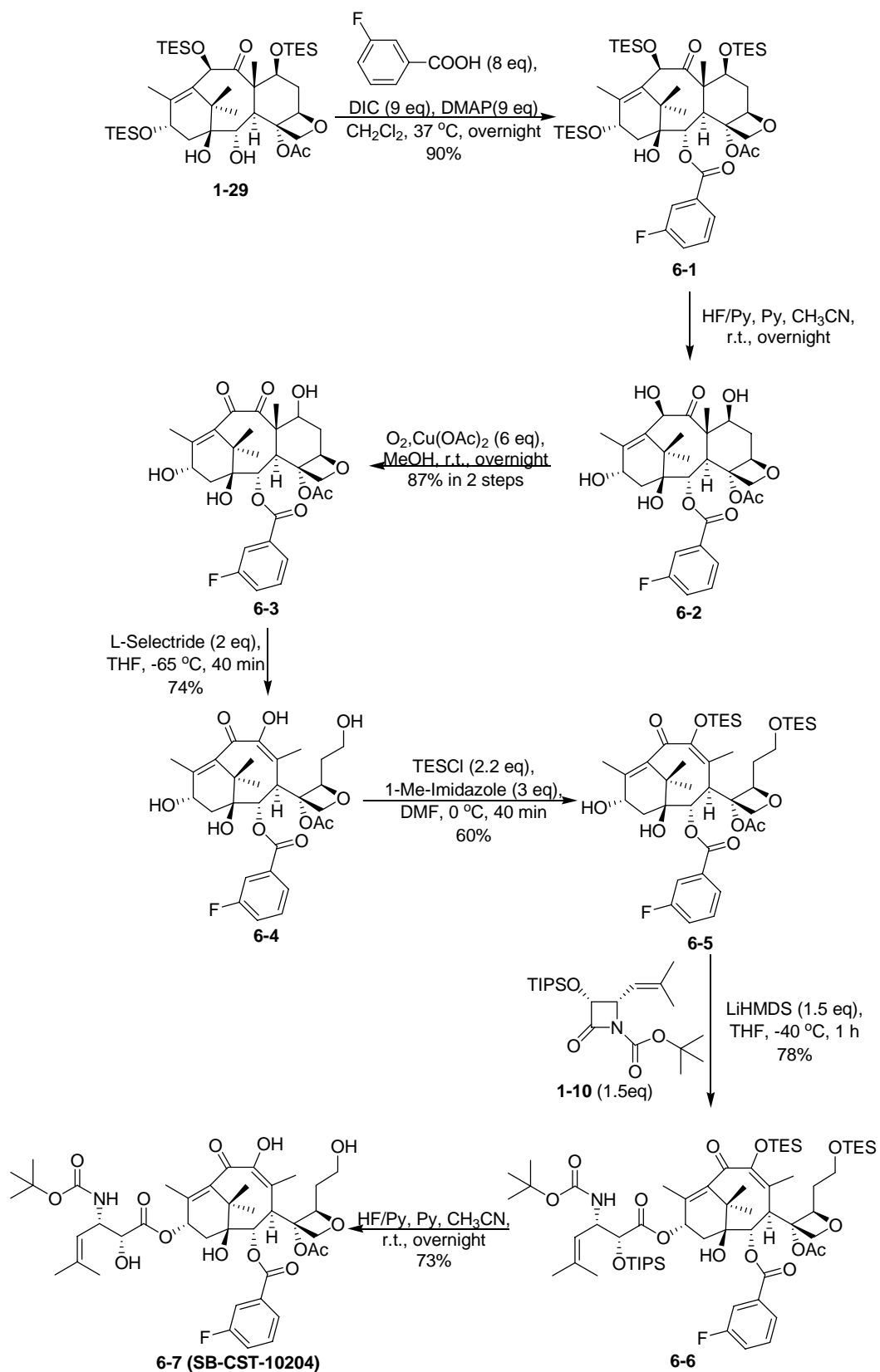
Scheme 6-1. Synthesis of *meta*-F-C-seco-Taxoid

§ 6.2.2 Biological Evaluation of Novel C-seco-Taxoids

The novel C-seco-taxoids, thus synthesized, were sent to Dr. Ferlini, University of Sacred Heart in Rome for biological evaluation. As shown in **Table 6-4**, the growth inhibition effects of **IDN-5390** and six new C-seco-taxoids were evaluated against a panel of drug-resistant cells of A2780wt human ovarian adenocarcinoma cells: A2780CIS, A2780TOP and A2780ADR, resistant to cisplatin, topotecan, and doxorubicin, respectively; two clones from A2780 cells whose paclitaxel resistance were obtained with the concomitant exposure to paclitaxel and cyclosporin A (A2780TC1 and A2780TC3) and OVCAR-3 human ovarian cancer cells inherent of paclitaxel resistance.

Table 6-4 IC$_{50}$ (nM)^a of Taxol and seco-taxoids$^{13, 19}$

Taxoid	A2780wt^b	A2780CIS^c	A2780TOP^d	A2780ADR^e	A2780TC1^f	A2780TC3^g	Ovcar-3
Paclitaxel	2.7	3.6	7.2	1239	10027	17800	26.7
IDN-5390	17.4	16.8	27.5	3434	2543	7030	15.4
SB-CST-10101	6.8	4.3	4.6	467	1384	663.5	9.5
SB-CST-10201	4.6	5.7	3.4	506	1305	1540	22.3
SB-CST-10102	5.5	4.1	6.1	792	2223	1209	11.9
SB-CST-10202	**4.6**	**4**	**2.2**	**593**	**927**	**1122**	**5.5**
SB-CST-10104	11.1	11.8	12.8	4889	1848	1445	5.9
SB-CST-10204	6.1	4.9	6.9	2910	5498	2340	7.3

^{a}The concentration of compound which inhibits 50% (IC$_{50}$, nM) of the growth of a human tumor cell line after 72 h drug exposure; ^{b}human ovarian carcinoma wild type; ^{c}cisplatin-resistant A2780; ^{d}topotecanresistant A2780; ^{e}adriamycin-resistant A2780; ^{f,g}clones derived from chronic exposition of A2780 to paclitaxel and cyclosporine.

The C2-modified C-seco-taxoids are in average three times more active than **IDN-5390** against wild type ovarian cancer cell line A2780wt. A similar pattern is observed in the other cell lines. **SB-CST-10202** shows the highest activity among all the C-seco-taxoids against all the cell lines tested, which indicates that the C2 position plays an important role in the binding of C-seco-taxoids to β-tubulins, including class III β-tubulin.[19]

§ 6.3 Molecular Modeling Studies of the Taxoid-Class I/III β-Tubulin Complexes

§ 6.3.1 Docking Studies of the Taxoid-Class I/III β-Tubulin Complexes

Paclitaxel, **IDN-5390** and the C2-modified seco-taxoids were docked into β-tubulin by Dock6$^®$ program to examine their binding conformations and grid scores (binding affinity) in β-tubulins. The class I and class III β-tubulins were created by modifying the sidechains of the bovine brain tubulin (1JFF) by the InsigntII2000 program.[17] The paclitaxel binding site was the only possible binding site for C-seco-taxoids in the β-tubulins. However, strange binding conformations were obtained, because paclitaxel and C-seco-taxoids were very flexible. Therefore, the results (binding conformation and binding affinity) of the docking studies were not reliable.

Table 6-5. Flexible docking results for taxol/seco-taxoids-ClassI/III β-tubulin complexes (kcal/mol)

Compound	Protein	Grid Score	vdw	Electronic	Cluster Size
Paclitaxel	TBB1	-100.9	-100.4	-0.5	9
Paclitaxel	TBB3	-103.2	-99.5	-3.6	17
IDN-5390	TBB1	-98.6	-97.7	-1	6
IDN-5390	TBB3	-102.3	-100.3	-2	7
SB-CST-10201	TBB1	-107.1	-105.4	-1.7	30
SB-CST-10201	TBB3	-104.5	-102.4	-2.1	9
SB-CST-10202	TBB1	-102.9	-101	-1.9	8
SB-CST-10202	TBB3	-102.2	-102.7	-0.5	8
SB-CST-10204	TBB1	-102.4	-99.8	-2.6	13
SB-CST-10204	TBB3	-102.3	-100.7	-1.6	11

§ 6.3.2 Molecular Dynamics (MD) Simulations of the Taxoids-Class I/III β-Tubulin Complexes

Molecular dynamics (MD) simulation[20] was used to find the binding conformation of C-seco-taxoids in class I and class III β-tubulins. Since the X-ray diffraction structures of the class I and class III β-tubulin were not available, the electron crystallographic structure of the bovine brain tubulin (1JFF)[21] was used as a template to create the class I and class III β-tubulins (**Figure 6-5**). The protein sequences were obtained from Swissprot and aligned by using CLUSTALX.[22] A standard comparative modeling procedure was used by replacing the sidechains of the template by Leap program of AMBER9 package.[20] The modified templates were optimized using 1000 cycles of the steepest descent energy-minimization to remove the unfavorable interactions between side-chains by AMBER9 with the backbone of the protein fixed (ff99 force field), affording the created class I and class III β-tubulins, TBB1 and TBB3, respectively.
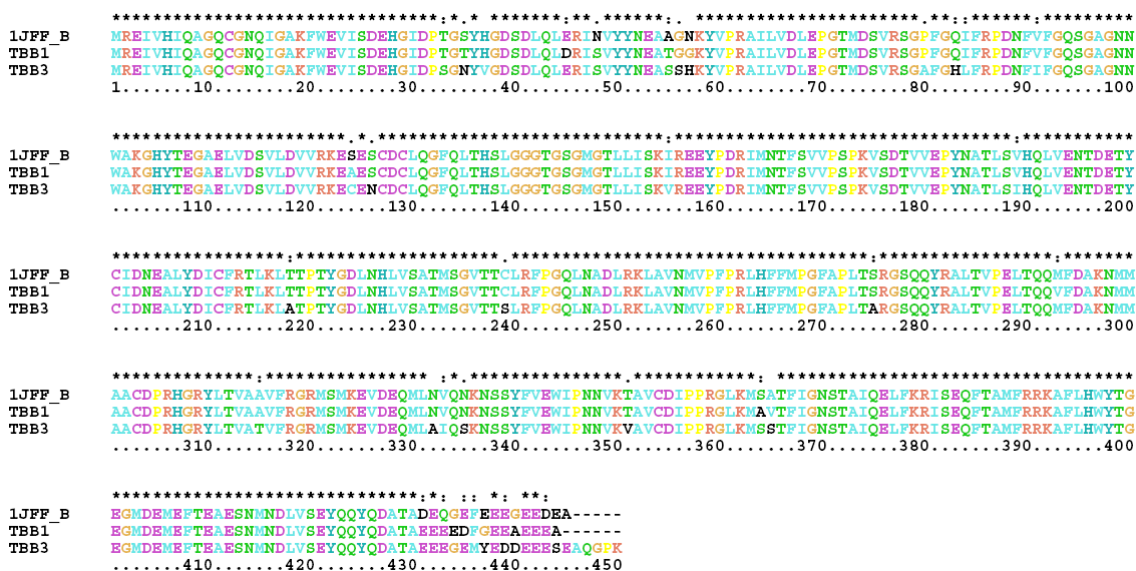
Figure 6-5. Sequence alignment of 1JFF and class I&III β-tubulins by CLUSTALX

Since C-seco taxoids are very flexible, direct docking by DOCK6® program failed to provide the reasonable binding conformation.[23] Accordingly, based on the paclitaxel conformation in 1JFF, the ligands were manually docked into the proteins by the InsightII® 2000 program.[21] The complexes were solvated in a 8-Å truncated octahedron of TIP3P explicit water (~ 7950 water molecules). The *parm7* and *rst7* file pairs of the receptors, ligands, complexes and the solvated complexes were saved. The solvated complexes were equilibrated by carrying out a short minimization, 50 ps of heating from 0 K to 300 K, 50 ps of density equilibration, 200 ps of constant volume equilibration at 300 K with weak restraints of 0.1 kcal/(mol*Å) on the heave atoms of the protein backbones. All simulations were performed with shake on hydrogen atoms, a 2 fs time step and langevin dynamics for temperature control. The temperature, density, total energy and rmsd were monitored.

Then a total of 5 ns (500 ps x 10) production recording the coordinates every 10 ps, was performed for each complexes using the same conditions with no restraints on the protein backbones. Again the temperature, density, total energy and rmsd were monitored.

§ 6.3.3 Results of MD Simulations

The overlay of TBB1 and TBB3 after 5.3-ns simulations are shown in **Figure 6-10** by superimposing the backbone, indicating the high similarity between TBB1 and TBB3 (rmsd = 2.1 Å).
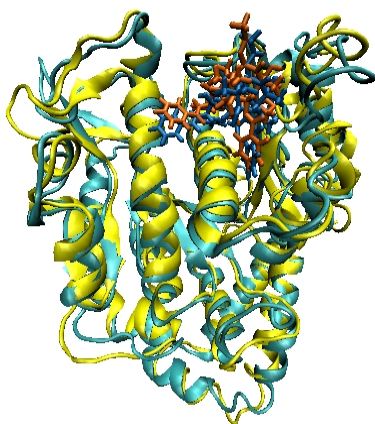
Figure 6-6. Overlay of TBB1 (yellow)-paclitaxel (orange) and TBB3 (cyan)-paclitaxle (blue) complexes

The binding conformations of taxoids in TBB1/TBB3 are shown in **Figure 6-7, Figure 6-8** and **Figure 6-9** (one snapshot at 5.3 ns). The results indicate that the taxoids take similar conformation in the class I and class III β-tubulins. Also, the seco-taxoids can take the binding conformation similar to that of paclitaxel in β-tubulins, although their structures are far more flexible than that of paclitaxel. Similar to the simulations reported by the Italian group,[17] there is no direct interaction between Ser277 (or Ala277) with paclitaxel and C-seco-taxoids.
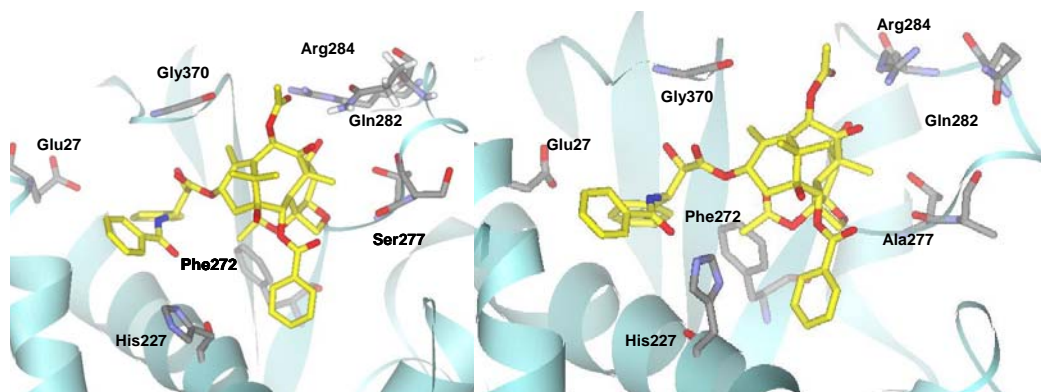
Figure 6-7. Paclitaxel in TBB1 and TBB3
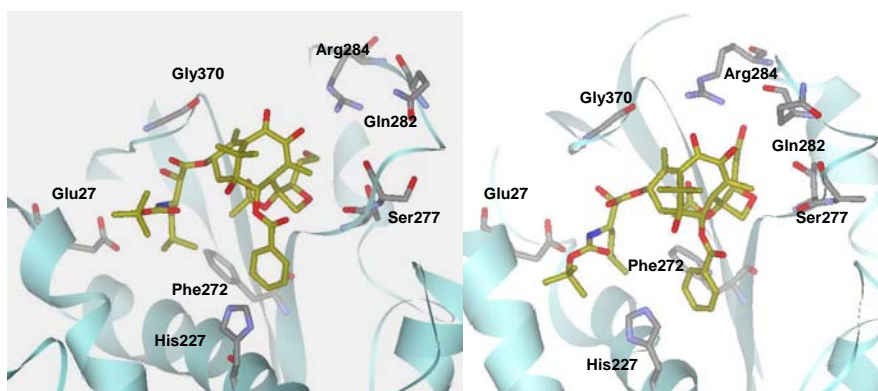
Figure 6-8. IDN-5390 in TBB1 and TBB3
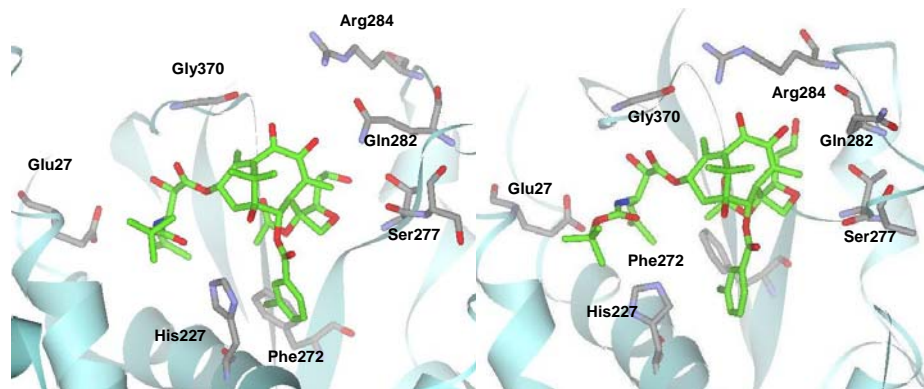
Figure 6-9. SB-CST-10202 in TBB1 and TBB3

The temperature, density, total energy and rmsd and the H-bond distance between C2'O and H-N of Gly370 of the 5.3-ns MD simulations are shown in **Figure 6-10**, **Figure 6-11** and **Figure 6-12**. The total energy, density and temperature become stable very quickly, indicating the MD simulations are stable. The rmsds of the tubulin backbones (heavy atoms: C, O and N) increase gradually, until reaching the equilibrium after ~ 3000 ps. The highest rmsds of the backbones are less than 2 Å, indicating that there is no big change in the protein structures, even without any restraint. Because the C-seco-taxoids have higher flexibility than paclitaxel, the rmsds of **IDN-5390** and **SB-CST-10202** (~1.5 Å) are higher than that of paclitaxel (~1.0 Å). One major H-bond between

290

C2'O and H-N of Gly370 is monitored. The distances of the H-bond are long at the beginning, but go into the H-bond range after equilibrium. The H-bond is not very stable when other H-bonds (between Glu27 and C2'OH or C3'NH) form. The H-bond between C2'O—H-N (Gly370) and C2'OH—OOC (Glu27) could not form at the same time as shown in **Figure 6-3**.[17] Also, the direct interactions between taxoids and Ser277 (or Ala277) are not found.
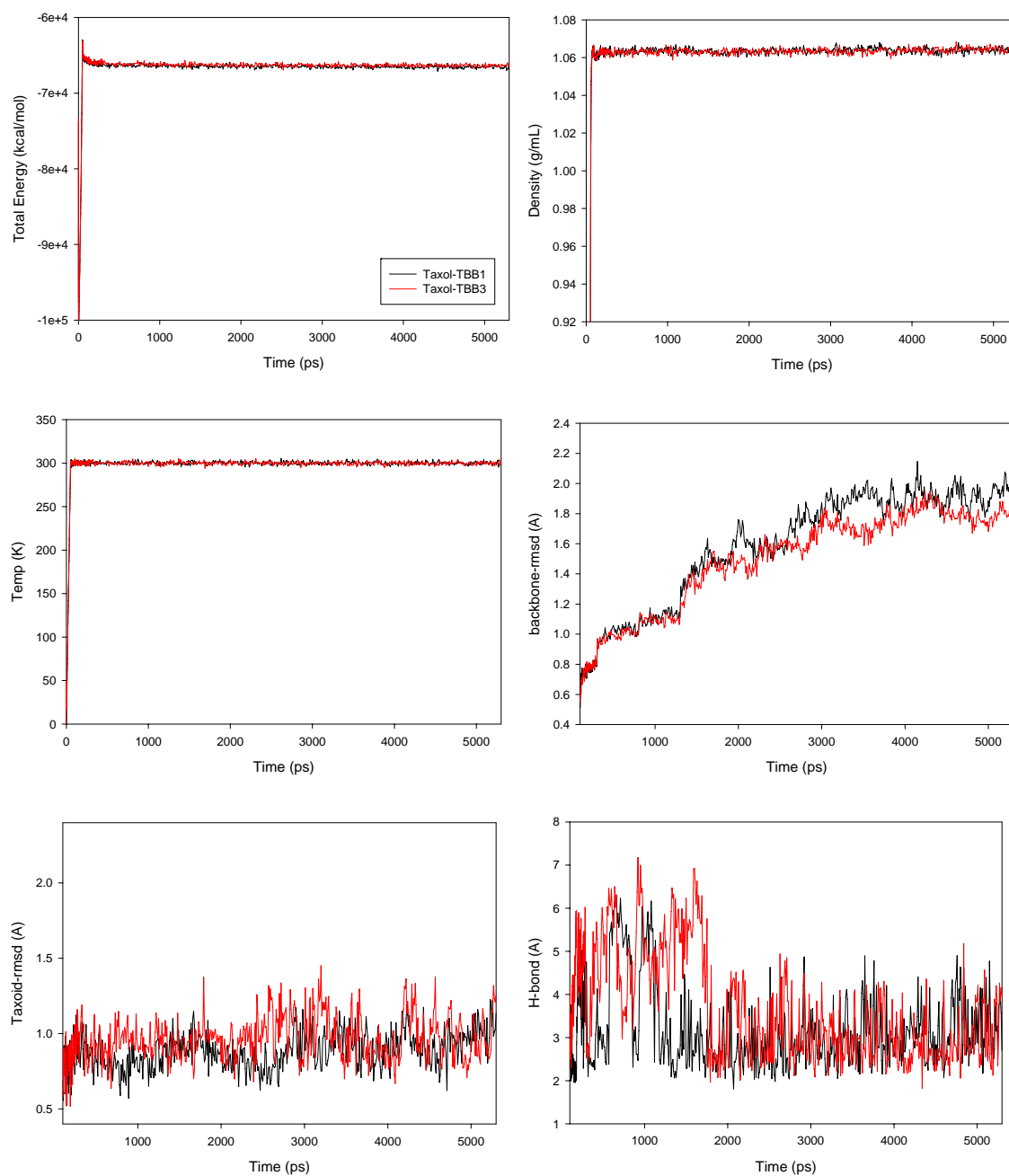
Figure 6-10. MD simulation results of paclitaxel in TBB1(black) and TBB3 (red)
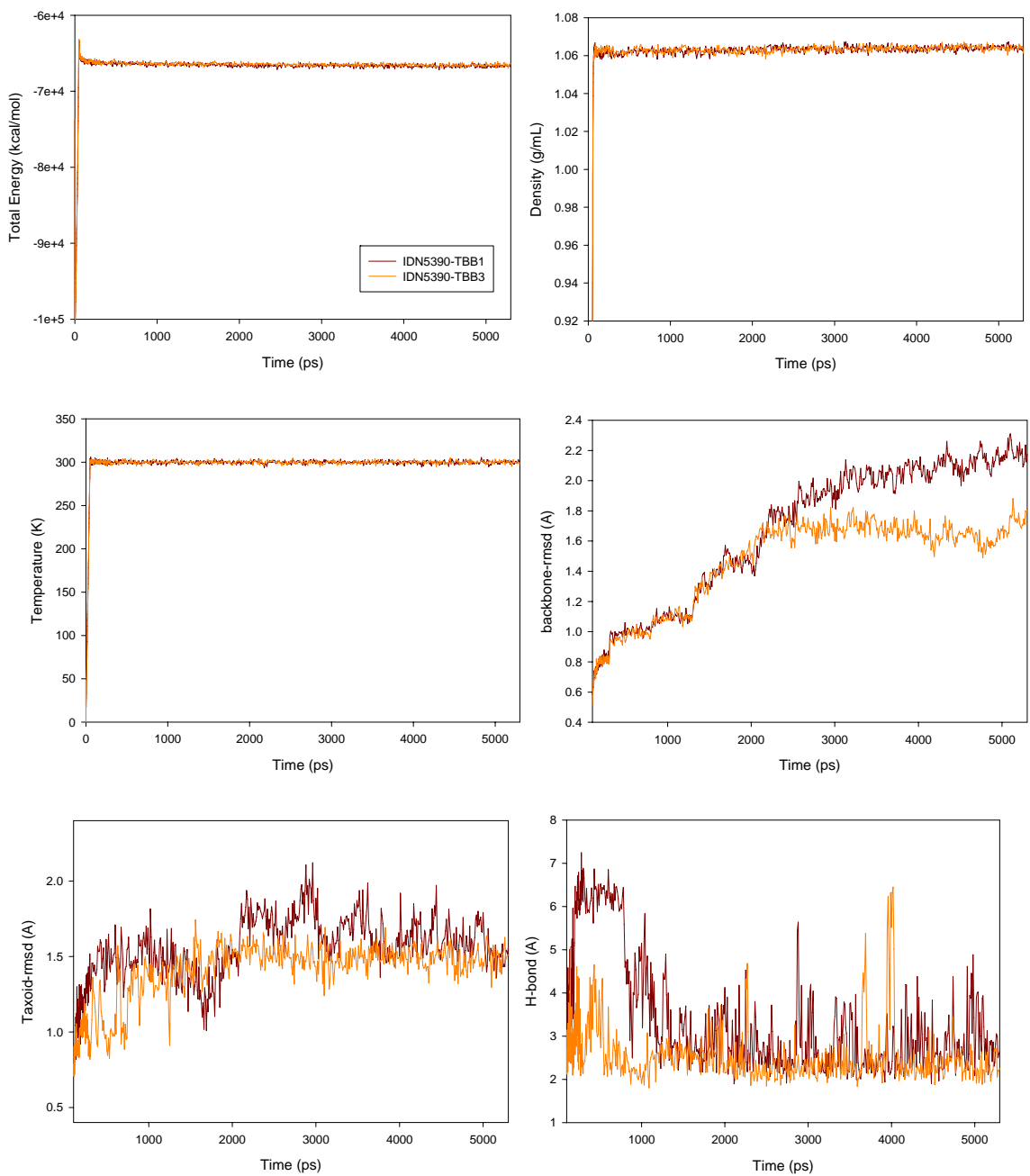
Figure 6-11. MD simulation results of IDN-5390 in TBB1(brown) and TBB3 (orange)
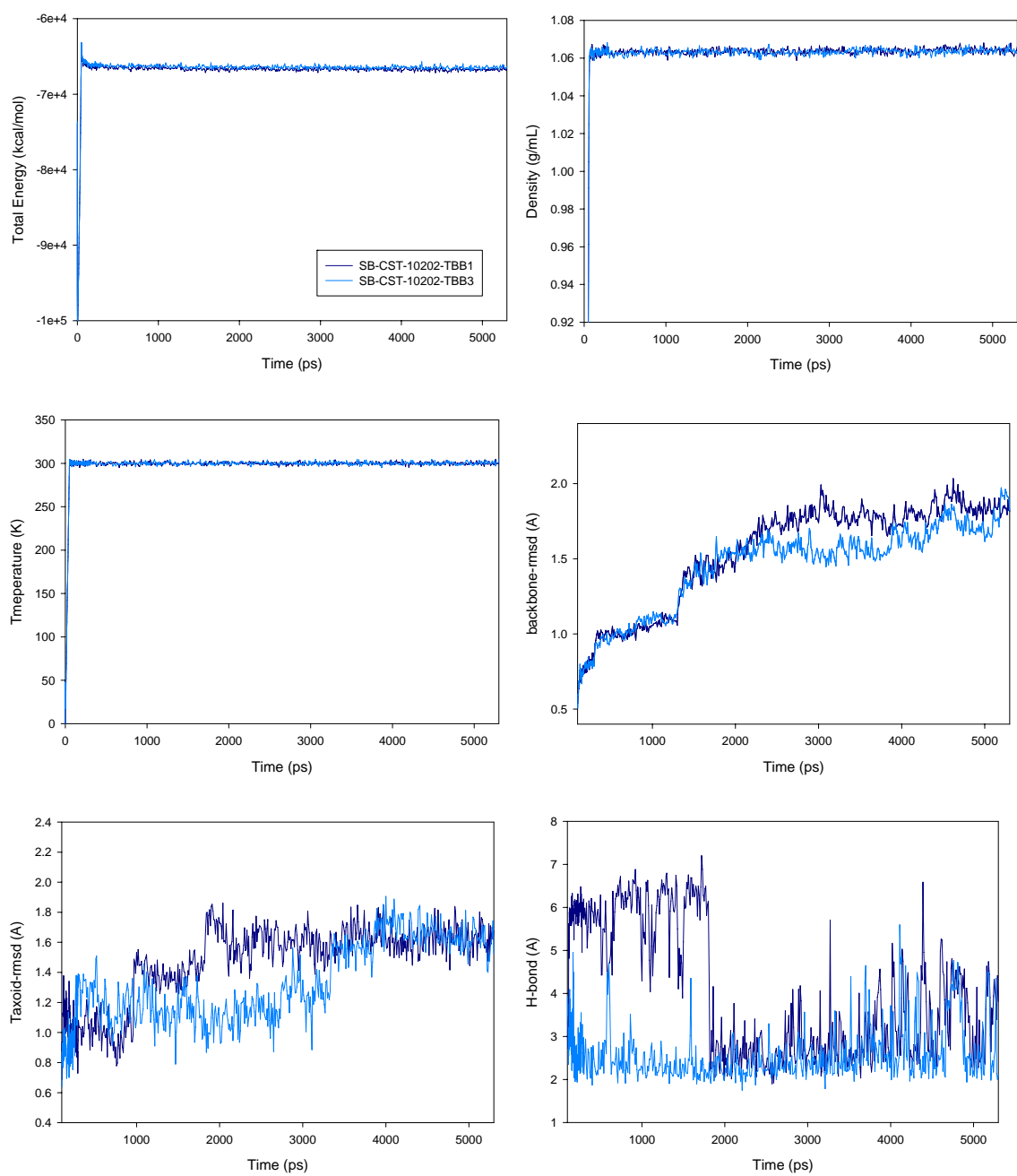
Figure 6-12. MD simulation results of SB-CST-10202 in TBB1 (dark blue) and TBB3 (blue)

§ 6.3.4 The Binding-Energy Calculation by MM-PBSA Method

The overall objective of the MM-PBSA method and MM-GBSA method is to calculate the free energy difference between the bound and unbound state of two solvated molecules to compare the free energy of two different solvated conformations of the same molecule.

$$[A]_{aq} + [B]_{aq} \Longleftrightarrow [A^*B^*]_{aq^*}$$
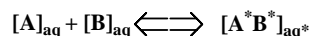
A more effective method is to divide up the calculation according to the following thermodynamic cycle:

$$[A]_{aq} + [B]_{aq} \xrightarrow{\Delta G_{bind,aq}} [A^*B^*]_{aq^*}$$

$$\Delta G_{aq,\,lig} \Updownarrow \qquad \Updownarrow \Delta G_{aq,\,rec} \qquad \Updownarrow \Delta G_{aq,\,com}$$

$$[A]_{va} + [B]_{va} \xrightarrow{\Delta G_{bind,va}} [A^*B^*]_{va^*}$$
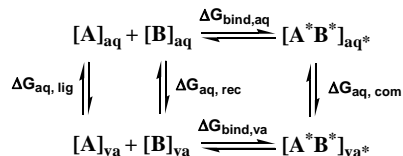
From this diagram the binding free energy $\Delta G_{bind,aq}$ can be calculated by:

$$\Delta G_{bind,aq} = \Delta G_{bind,va} + \Delta G_{aq,\,com} - (\Delta G_{aq,\,lig} + \Delta G_{aq,\,rec})$$

The average interaction energies of receptor and ligand are usually obtained by performing calculations on an ensemble of uncorrelated snapshots collected from an equilibrated molecular dynamics (MD) simulation.

The mm_pbsa.pl script from AMBER 9 package can automatically perform all the necessary steps to calculate the binding free energy of the taxoids and β-tubulin. In principle the calculation of the binding free energy described above would need three independent MD simulations of the complex, ligand and acceptor. However, if the approximation is made that no significant conformational changes occur upon binding, the snapshots for all three species can be obtained from a single trajectory.

From the analysis of the rmsd and H-bond, we found that the real equilibrium was not obtained until ~ 3000 ps. The binding energies were calculated using MM-PBSA method based on 150 snapshots (every 10 ps) taken from the 3.8-5.3 ps simulation. The results are listed in **Table 6-6**.
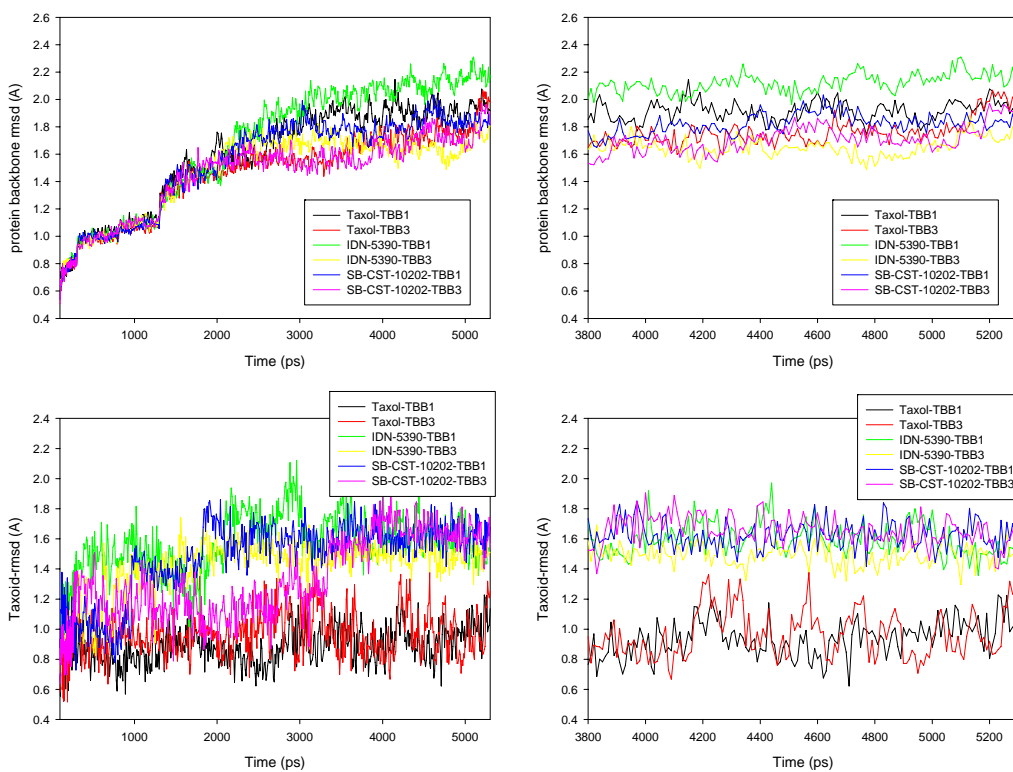
Figure 6-11. rmsd of TBB1/3 and taxoids

As shown in **Table 6-6**, the results are not similar to the one reported by the Italian group[17]. The binding energies of each taxoid with TBB1 and TBB3 are very similar, because there is difference in only two amino acid residues between TBB1 and TBB3 around binding site (Cys241Ser and Ser277Ala) and they do not interact with taxoids diectly. The binding energies increased in the following order: paclitaxel < **IDN-5390** < **SB-CST-10202**. The C7-OH of the C-seco-taxoids can form an extra H-bond with Gln282, while the one of paclitaxel can not. The higher binding energy of C-seco-taxoids with tubulins than that of paclitaxel with tubulins is not consistent with the experimental data.[6, 7] There are three possible reasons for the difference: (1) the AMBER force field may not be accurate for taxoids; (2) the binding of taxoid with β-tubulin may be different from the one with microtubule; (3) the 1JFF structure does not include the C-terminal residues (~20 amino acid residues), which are very important to the microtubular dynamics.

Table 6-6. The binding energy of the taxoid-TBB1/3 complexes (kcal/mol)

Taxoids	TBB1	TBB3
Paclitaxel	-32.92	-32.53
IDN-5390	-34.45	-35.57
SB-CST-10202	-39.29	-40.67

Although the previous study by the Italian group showed good agreement with biological results[6, 7], there are several flaws in the study: (1) the AMBER force field used

is very old (proposed in 1984)[24] and is not as accurate as the one we used; (2) the backbones were fixed with a very high restraint and the TBB1 and TBB3 proteins were not optimized without restraints after homology modeling from 1JFF; (3) the difference in binding energies with TBB1 and TBB3 is very large (~ 12 kcal/mol), although the taxoids form very similar interaction with them. Thus, the Italian study is not reliable. Further studies are still in progress in our laboratories.

§ 6.4 Summary

The overexpression of specific tubulin isotypes has been reported to cause paclitaxel's resistance. **IDN-5390** acts effectively against paclitaxel-resistant cell lines overexpressing class III β-tubulin. Six seco-taxoids with modification at the C2 and C3' positions were synthesized and evaluated, which showed substantially higher potency than **IDN-5390** against drug-sensitive and drug-resistant cell lines. Molecular dynamics simulation of the taxoids-class-I/III β-tubulin complexes showed that the structure of class III β-tubulin was very similar to that of class I β-tubulin, but the binding energies calculated by MM-PBSA method were not consistent with experimental data and previous studies.

§ 6.5 Experimental Section

General Methods: ^{1}H and ^{13}C NMR spectra were measured on a Varian 300, 400 or 500 NMR spectrometer. Melting points were measured on a Thomas Hoover Capillary melting point apparatus and are uncorrected. Optical rotations were measured on a Perkin-Elmer Model 241 polarimeter. IR spectra were recorded on a Perkin-Elmer Model 1600 FT-IR spectrophotometer. TLC was performed on Merck DC-alufolien with Kieselgel 60F-254 and column chromatography was carried out on silica gel 60 (Merck; 230-400 mesh ASTM). Purity was determined with a Waters HPLC assembly consisting of dual Waters 515 HPLC pumps, a PC workstation running Millennium 32, and a Waters 996 PDA detector, using a Phenomenex Curosil-B column, employing CH_3CN/water (2/3) as the solvent system with a flow rate of 1 mL/min. High-resolution mass spectra were obtained from Mass Spectrometry Laboratory, University of Illinois at Urbana-Champaign, Urbana, IL.

Materials: The chemicals were purchased from Aldrich Co. and Sigma and purified before use by standard methods. Tetrahydrofuran was freshly distilled from sodium metal and benzophenone. Dichloromethane was also distilled immediately prior to use under nitrogen from calcium hydride. 10-Deacetyl baccatin III (DAB) was obtained from Indena, SpA, Italy.

7,10,13-Tri(triethylsilyl)-2-debenzoyl-2-(3-fluorobenzoyl)-10-deacetylbaccatin III (6-1):[9]

To a solution of **1-29** (1.115 g, 1.423 mmol), *m*-fluorobenzoic acid (1.593 g, 11.38 mmol) and DMAP (1.549 g, 12.8 mmol) in CH_2Cl_2 (8.92 mL) was added DIC (1.98 mL, 12.8 mmol) and the reaction mixture was refluxed overnight. The reaction mixture was quenched with ethyl acetate (150 mL) and washed with saturated aqueous $NaHCO_3$ solution (30 mL), H_2O (30 mL) and brine (30 mL). The organic lawyer was dried over anhydrous $MgSO_4$. The solvent was removed under reduced pressure and the residue was purified on a silica gel column (hexanes/ ethyl acetate = 10/1) to afford **2-8** as a white solid (1.161 g, 90%): mp 93-95 ˚C; ^{1}H NMR (400 MHz, CDCl$_3$) δ 0.60 (m, 18 H), 0.98 (m, 27 H), 1.13 (s, 3 H), 1.19 (s, 3 H), 1.53 (bs, 1 H), 1.65 (s, 3 H), 1.89 (m, 1 H), 1.98 (s, 3 H), 2.14 (m, 2 H), 2.29 (s, 3 H), 2.50 (m, 1 H), 3.86 (d, *J* = 7.2 Hz, 1 H), 4.13 (d, *J* = 8.0 Hz, 1 H), 4.27 (d, *J* = 8.0 Hz, 1 H), 4.10 (dd, *J* = 10.4 Hz, 6.9 Hz, 1 H), 4.94 (m, 2 H), 5.17 (s, 1 H), 5.59 (d, *J* = 6.9 Hz, 1 H), 7.28 (m, 1 H), 7.44 (m, 1 H), 7.81 (dt, *J* = 9.2 Hz, 2.0 Hz, 1 H), 7.88 (d, *J* = 8.0 Hz, 2 H); ^{13}C NMR (CDCl$_3$) δ 4.8, 5.2, 5.9, 6.9, 10.4, 14.6, 20.6, 22.3, 26.3, 37.2, 39.8, 42.9, 46.9, 58.2, 68.2, 72.6, 75.7, 75.9, 76.5, 79.6, 80.7, 84.0, 116.6, 117.0, 120.3, 120.7, 125.6, 130.1, 130.3, 131.7, 131.9, 132.4, 135.6, 139.5, 160.6, 164.5, 165.6, 169.9, 205.6. HRMS (FAB, DCM/NBA) *m/z* calcd for $C_{47}H_{77}O_{10}Si_3F \cdot H^+$: 905.4887. Found: 905.4869 (Δ = 2.0 ppm). All data are in agreement with literature values.[9]

2-Debenzoyl-2-(3-fluorobenzoyl)-10-deacetylbaccatin III (6-2):[8]
To a solution of **1-1** (1.157 g, 1.28 mmol) in pyridine/acetonitrile (1:1, 46.3 mL) was added dropwise HF/pyridine (70:30, 11.6 mL) at 0 °C, and the mixture was stirred overnight at room temperature. The reaction mixture was diluted with ethyl acetate (300 mL), and quenched with saturated aqueous $NaHCO_3$ solution (150 mL). The organic layer was washed with saturated aqueous $CuSO_4$ solution (100 mL x 2) and H_2O (50 mL x 2), dried over anhydrous $MgSO_4$ and concentrated *in vacuo* to afford 2-debenzoyl-2-(3-methoxy-benzoyl)-10-deacetylbaccatin III (**6-2**) as a white solid. The crude compound was used in the next step without further purification.

2-Debenzoyl-2-(3-fluorobenzoyl)-10-oxo-10-deacetylbaccatin III (6-3):
To a solution of **6-2** (647 mg, 1.199 mmol) in MeOH (25 mL) was added $Cu(OAc)_2$ (1.44 g, 7.2 mmol). The mixture was stirred for 16 h in an open flask. The solvent was removed under reduced pressure and the residue was purified on a silica gel column ($CHCl_3$ to 2% MeOH in $CHCl_3$) to afford **6-3** as a off-white solid (585 mg, 87% in 2 steps): ^{1}H NMR (500 MHz, $CDCl_3$) δ 1.09 (d, *J* =7.0 Hz, 4 H), 1.15 (s, 2 H), 1.22 (s, 2 H), 1.27 (m, 1 H), 1.65 (m, 2 H), 1.71 (d, *J* = 6.0, 4 H), 1.84 (m, 1 H), 1.97 (s, 2 H), 2.15 (s, 3 H), 2.28 (m, 4 H), 2.38 (m, 3 H), 2.60 (m, 1 H), 3.67 (d, *J* = 6.6 Hz, 1 H), 3.86 (dt, *J* = 11.5 Hz, 3.0 Hz, 1 H), 4.12 (m, 2 H), 4.32 (t, *J* = 8.5 Hz, 1 H), 4.42 (d, *J* = 8.5 Hz, 1 H), 4.54 (d, *J* = 11.0 Hz), 4.96 (m, 3 H), 5.74 (d, *J* = 7.0 Hz, 1 H), 5.80 (d, *J* = 7.0 Hz, 1 H), 7.35 (m, 1 H), 7.49 (m, 1 H), 7.81 (t, *J* = 9.0 Hz, 1 H), 7.92 (t, *J* = 8.5 Hz, 1 H); ^{13}C NMR (75 MHz $CDCl_3$) δ 14.8, 15.2, 22.3, 22.7, 26.6, 35.6, 39.1, 39.9, 40.0, 57.6, 67.7, 75.7, 76.9, 77.3, 79.4, 81.5, 82.8, 117.3, 121.4, 126.2, 130.7, 131.7, 140.7, 147.0, 163.0, 166.1, 172.7, 196.4, 208.6.

2-Debenzoyl-2-(3-fluorobenzoyl)-C-secobaccatin III (6-4):
To a solution of **6-3** (563 mg, 1.00 mmol) in THF (10 mL) was added 1.0 M L-Selectride in THF (2.0 mL, 2.0 mmol) at -78 °C. The solution was gradually warmed up to -65 °C over 40 min and stirred for additional 10 min. The reaction was quenched with 2N H_2SO_4 (0.8 mL). Hexanes (10 mL) were added to the mixture and left overnight. The solution was diluted with H_2O and extracted with EtOAc (50 mL x 3). The combined organic layers were dried over anhydrous $MgSO_4$, and concentrated *in vacuo*. Column chromatography of the residue on silica gel (2% MeOH in chloroform) afforded **6-4** as a white solid (415 mg, 74%): ^{1}H NMR (400 MHz $CDCl_3$) δ 1.04 (s, 3 H), 1.10 (s, 3 H), 1.80-2.80 (m, 14 H), 3.70 (m, 2 H), 4.29 (m, 2 H), 4.90 (m, 1 H), 5.10 (bs, 2 H), 5.54 (d, *J* = 9.0 Hz, 1 H), 6.52 (s, 1 H), 7.30 (m, 1 H), 7.40 (m, 1 H), 7.60 (m, 1 H), 7.80 (m, 1 H); ^{13}C NMR (100 MHz $CDCl_3$) δ 11.1, 14.5, 21.1, 22.4, 25.3, 39.7, 39.8, 42.8, 44.5, 59.2, 67.1, 75.4, 76.9, 80.6, 86.5, 87.0, 116.7, 121.2, 123.4, 125.4, 130.8, 131.9, 140.0, 141.1, 149.0, 163.0, 166.0, 169.2, 192.1.

7,9-Triethylsilyl-2-debenzoyl-2-(3-fluorobenzoyl)-C-secobaccatin III (6-5):
To a solution of **6-4** (370 mg, 0.66 mmol) in DMF (4.5 mL) was added 1-methylimidazole (0.16 mL, 2 mmol) and TESCl (0.24 mL, 1.45 mmol) at 0 °C and the mixture was stirred for 40 min. The reaction mixture was diluted with saturated NH_4Cl (20 mL) and extracted with EtOAc (30 mL x 3). The organic layer was washed with H_2O (10 mL x 2) and brine (10 mL). It was dried over anhydrous $MgSO_4$, and concentrated *in*

vacuo. Column chromatography of the residue on silica gel (hexanes/EtOAc= 8/1 to 2/1) afforded **6-5** as a white solid (313 mg, 60%): ^{1}H NMR (400 MHz, CDCl$_3$) δ 0.60 (m, 6 H), 0.80 (m, 6 H), 0.95 (m, 18 H), 1.10 (s, 3 H), 1.15 (s, 3 H), 1.70-2.60 (m, 14 H), 3.60 (m, 1 H), 3.80 (m, 1 H), 4.20 (m, 2 H), 4.90 (m, 2 H), 5.20 (bs, 1 H), 5.58 (d, J = 9.0 Hz, 1 H), 7.35 (m, 1 H), 7.50 (m, 1 H), 7.70 (m, 1 H), 7.80 (m, 1 H).

7,9-Triethylsilyl-13-(2'-triisopropylsilyl-3'-isobutenyl-*N-tert*-butoxycarbonylisoserinyl)-2-debenzoyl-2-(3-fluorobenzoyl)-C-secobaccatin III (6-6):

To a solution of **6-5** (355 mg, 0.45 mmol) and *β*-lactam (270 mg, 0.68 mmol) in THF was added LiHMDS (1.0 M in THF, 0.68 mL, 0.68 mmol) at -40 ^{o}C. The reaction was quenched with aqueous NH$_4$Cl solution (30 mL) after 1 h. The reaction mixture was diluted with water and extracted with EtOAc for 3 times. The combined organic layers were dried over anhydrous MgSO$_4$, and concentrated *in vacuo*. Column chromatography of the residue on silica gel (hexanes/EtOAc= 15/1 to 5/1) afforded **6-6** as a white solid (417 mg, 78%): ^{1}H NMR (400 MHz, CDCl$_3$) δ 0.57 (m, 6 H), 0.75 (m, 6 H), 0.89 (m, 9 H), 0.95 (m, 9 H), 1.04 (m, 4 H), 1.13 (s, 2 H), 1.21 (s, 2 H), 1.26 (m, 2 H), 1.32 (s, 9 H), 1.73 (s, 2 H), 1.79 (m, 6 H), 3.71 (m, 2 H), 4.15 (m, 1 H), 4.39 (s, 1 H), 4.82 (m, 1 H), 4.88 (m, 1 H), 5.31 (d, J = 8.4 Hz, 1 H), 5.59 (d, J = 9.2 Hz, 1 H), 6.02 (m, 1 H), 7.23 (m, 1 H), 7.39 (m, 1 H), 7.75 (m, 1 H), 7.86 (m, 1 H).

13-(3'-*iso*-Butenyl-*N-tert*-butoxycarbonylisoserinyl)-2-debenzoyl-2-(3-fluorobenzoyl)-C-secobaccatin III (6-7, SB-CST-10204):

The protected coupling product **6-6** (417 mg, 0.35 mmol) was dissolved in acetonitrile/pyridine (1/1, 17 mL) and cooled to 0 ^{o}C, and HF/pyridine (70/30) was added dropwise (4.2 mL). The mixture was stirred at 0 ^{o}C for 1 h and then at room temperature overnight. After 10 h, the reaction mixture was extracted with EtOAc, washed with saturated NaHCO$_3$ (2 × 35 mL), CuSO$_4$ (2 × 40 mL) and brine (20 mL) and dried over anhydrous MgSO$_4$. Evaporation of the solvent followed by purification of the crude product by flash chromatography on silica gel (hexane/EtOAc = 3/1 to 1/1) afforded C-seco taxoid **SB-CST-10204** (204 mg, 73% yield) as a white solid: mp 148-150 ^{o}C; ^{1}H NMR (400 MHz, CDCl$_3$) δ 1.08 (s, 4 H), 1.21 (s, 4 H), 1.25 (s, 3 H), 1.34 (s, 9 H), 1.44 (m, 1 H), 1.73 (m, 8 H), 1.85 (m, 8 H), 2.09 (m, 3 H), 2.45 (m, 2 H), 2.80 (m, 1 H), 3.67 (m, 1 H), 3.88 (s, 1 H), 4.24 (d, J = 4.0 Hz, 1 H), 4.28 (d, J = 7.6 Hz, 1 H), 4.76 (m, 1 H), 4.98 (s, 1 H), 5.18 (m, 2 H), 5.26 (d, J = 9.0 Hz, 1 H), 5.59 (d, J = 7.0 Hz, 1 H), 6.14 (m, 1 H), 6.50 (s, 1 H), 7.31 (dt, J = 10.5 Hz, 3.5 Hz, 1 H), 7.45 (m, 1 H), 7.67 (d, J = 7.2 Hz, 1 H), 7.80 (d, J = 7.2 Hz, 1 H); ^{13}C NMR (100.5 MHz, CDCl3) δ 10.0, 14.1, 14.7, 18.6, 21.1, 22.1, 22.6, 25.7, 28.2, 29.6, 31.5, 36.5, 42.9, 51.4, 59.5, 70.1, 74.5, 75.2, 79.9, 86.1, 116.6, 120.8, 121.0, 124.1 125.2, 130.7, 131.5, 131.6, 142.0, 148.8, 155.7, 157.9, 161.4, 163.9, 166.0, 169.0, 172.4, 191.1, 202.4. HRMS (FAB/DCM/NaCl) m/z calcd. for C$_{41}$H$_{54}$FNO$_4$H$^+$: 804.3607, found: 804.3605 (Δ = -0.2 ppm).

§ 6.5 References

1. Georg, G. I.; Chen, T. T.; Ojima, I.; Vyas, D. M. *Taxane Anticancer Agents: Basic Science and Current Status*. American Chemical Society: Washington D.C., 1995.
2. Guénard, D.; Guéritte-Vogelein, F.; Potier, P. Taxol and Taxotere: Discovery, Chemistry, and Structure-Activity Relationships. *Acc. Chem. Res.* **1993,** 26, 160-167.
3. Kavallaris, M.; Kuo, D. Y. S.; Burkhart, C. A.; Regl, D. L.; Norris, M. D.; Haber, M.; Horwitz, S. B. Taxol-resistant epithelial ovarian tumors are associated with altered expression of specific β-tubulin isotypes. *J. Clin. Invest.* **1997,** 100, 1282-1293.
4. Little, M.; Seehaus, T. Comparative analysis of tubulin sequences. *Comp Biochem Physiol B* **1988,** 90, 655-70.
5. Huzil, J. T.; Luduena, R. F.; Tuszynski, J. Comparative modelling of human b tubulin isotypes and implications for drug binding. *Nanotechnology* **2006,** 17, S90-S100.
6. Kavallaris, M. The role of multidrug resistance-associated protein (MRP) expression in multidrug resistance. *Anti-cancer drugs* **1997,** 8, 17-25.
7. Derry, W. B.; Wilson, L.; Khan, I. A.; Luduena, R. F.; Jordan, M. A. Taxol differentially modulates the dynamics of microtubules assembled from unfractionated and purified β-tubulin isotypes. *Biochemistry* **1997,** 36, 3554-62.
8. Lin, S.; Ojima, I. Recent strategies in the development of taxane anticancer drugs. *Expert Opin. Ther. Pat.* **2000,** 10, 869-889.
9. Dubois, J.; Guenard, D.; Gueritte, F. Recent developments in antitumour taxoids. *Expert Opin. Ther. Pat.* **2003,** 13, 1809-1823.
10. Gueritte, F. General and recent aspects of the chemistry and structure-activity relationships of taxoids. *Curr. Pharm. Des.* **2001,** 7, 1229-1249.
11. Ojima, I.; Chen, J.; Sun, L.; Borella, C. P.; Wang, T.; Miller, M. L.; Lin, S.; Geng, X.; Kuznetsova, L.; Qu, C.; Gallager, D.; Zhao, X.; Zanardi, I.; Xia, S.; Horwitz, S. B.; Clair, J. M.; Guerriero, J. L.; Bar-Sagi, D.; Veith, J. M.; Pera, P.; Bernacki, R. J. Design, Synthesis and Biological Evaluation of New Generation Taxoids. *J. Med. Chem.* **2008**, In press.
12. Appendino, G.; Danieli, B.; Jakupovic, J.; Belloro, E.; Scambia, G.; Bombardelli, E. The chemistry and occurrence of taxane derivatives. XXX. Synthesis and evaluation of C-seco paclitaxel analogs. *Tetrahedron Lett.* **1997,** 38, 4273-4276.
13. Ferlini, C.; Raspaglio, G.; Mozzetti, S.; Cicchillitti, L.; Filippetti, F.; Gallo, D.; Fattorusso, C.; Campiani, G.; Scambia, G. The seco-taxane IDN5390 is able to target class III b-tubulin and to overcome paclitaxel resistance. *Cancer Res.* **2005,** 65, 2397-2405.
14. Haber, M.; Burkhart, C. A.; Regl, D. L.; Madafiglio, J.; Norris, M. D.; Horwitz, S. B. Altered expression of Mbeta 2, the class II beta -tubulin isotype, in a murine J774.2 cell line with a high level of taxol resistance. *J. Biol. Chem.* **1995,** 270, 31269-75.

15. Kavallaris, M.; Burkhart, C. A.; Horwitz, S. B. Antisense oligonucleotides to class III b-tubulin sensitize drug-resistant cells to Taxol. *Br. J. Cancer* **1999,** 80, 1020-1025.

16. Ferlini, C.; Raspaglio, G.; Mozzetti, S.; Cicchillitti, L.; Filippetti, F.; Gallo, D.; Fattorusso, C.; Campiani, G.; Scambia, G. The Seco-Taxane IDN 5390 Is Able to Taeget Class III beta-Tubulin and to Overcome Paclitaxel Resistance. *Cancer Res.* **2005,** 65, 2397-2405.

17. Magnani, M.; Ortuso, F.; Soro, S.; Alcaro, S.; Tramontano, A.; Botta, M. The bI/bIII-tubulin isoforms and their complexes with antimitotic agents. Docking and molecular dynamics studies. *FEBS J.* **2006,** 273, 3301-3310.

18. Alcaro, S.; Gasparrini, F.; Incani, O.; Mecucci, S.; Misiti, D.; Pierini, M.; Villani, C. A \"quasi-flexible\" automatic docking processing for studying stereoselective recognition mechanisms. Part I. Protocol validation. *J. Comput. Chem.* **2000,** 21, 515-530.

19. Pepe, A.; Sun, L.; Ferlini, C.; Fontana, G.; Bombardeli, E.; Ojima, I. Synthesis and biological evalution of novel seco-taxanes with high affinity for class III β-tubulin. *Manuscript in preparation.*

20. Case, D. A.; Cheatham, T. E., III; Darden, T.; Gohlke, H.; Luo, R.; Merz, K. M., Jr.; Onufriev, A.; Simmerling, C.; Wang, B.; Woods, R. J. The amber biomolecular simulation programs. *J. Comput. Chem.* **2005,** 26, 1668-1688.

21. Lowe, J.; Li, H.; Downing, K. H.; Nogales, E. Refined structure of alpha beta-tubulin at 3.5 A resolution. *J. Mol. Bol.* **2001,** 313, 1045-1057.

22. Higgins, D. G.; Thompson, J. D.; Gibson, T. J. Using CLUSTAL for multiple sequence alignments. *Methods Enzymol* **1996,** 266, 383-402.

23. http://dock.compbio.ucsf.edu/DOCK_6/index.htm.

24. Weiner, S. J.; Kollman, P. A.; Case, D. A.; Singh, U. C.; Ghio, C.; Alagona, G.; Profeta, S., Jr.; Weiner, P. A new force field for molecular mechanical simulation of nucleic acids and proteins. *J. Am. Chem. Soc.* **1984,** 106, 765-84.

Appendices

A1. Appendix Chapter I

^{1}H NMR Spectrum of **1-53**
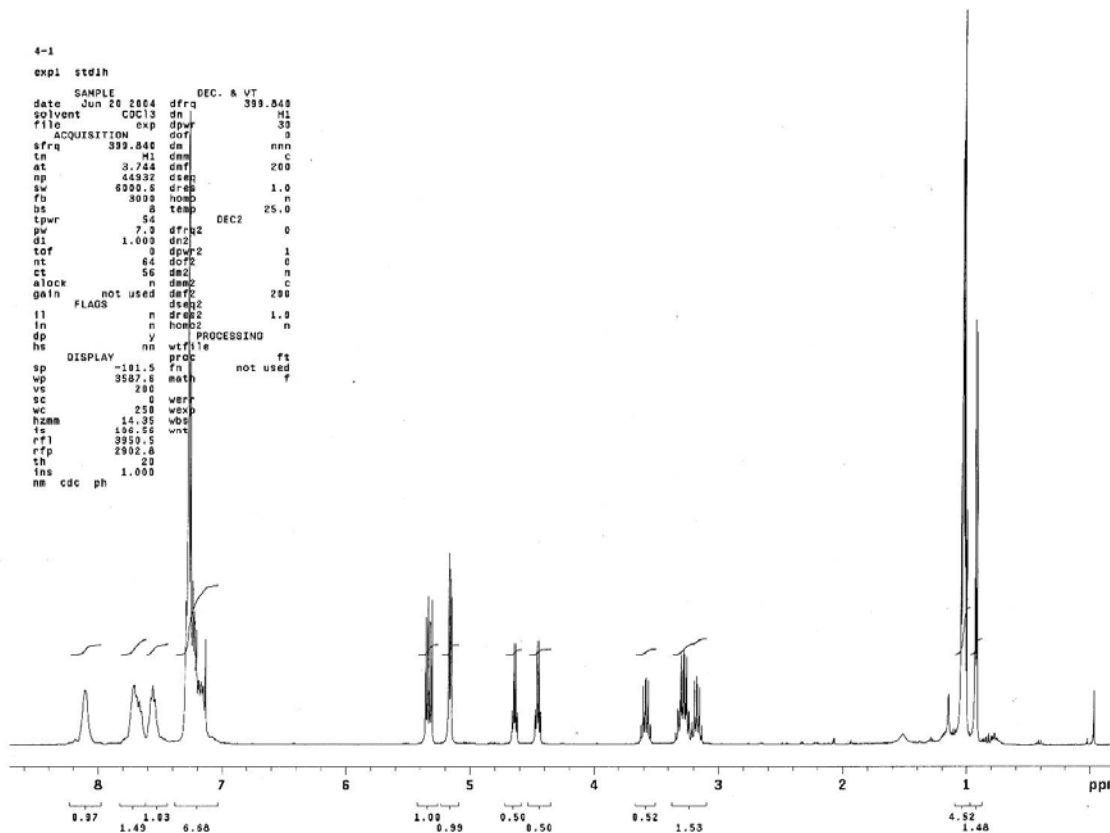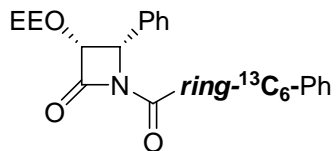
^{13}C NMR Spectrum of **1-53**
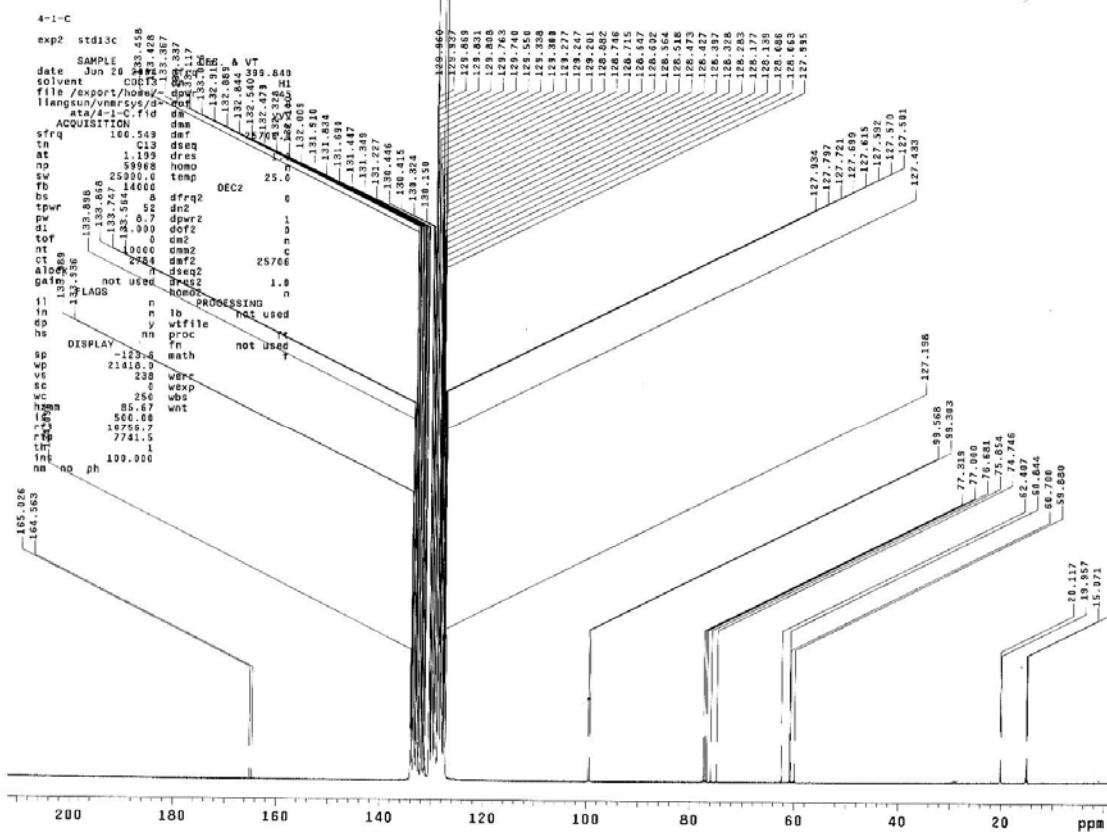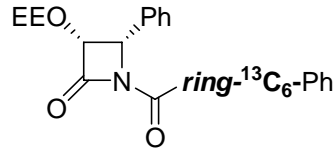
^{1}H NMR Spectrum of **1-55**

^{1}H NMR Spectrum of **1-56**

ring-$^{13}C_6$- Ph
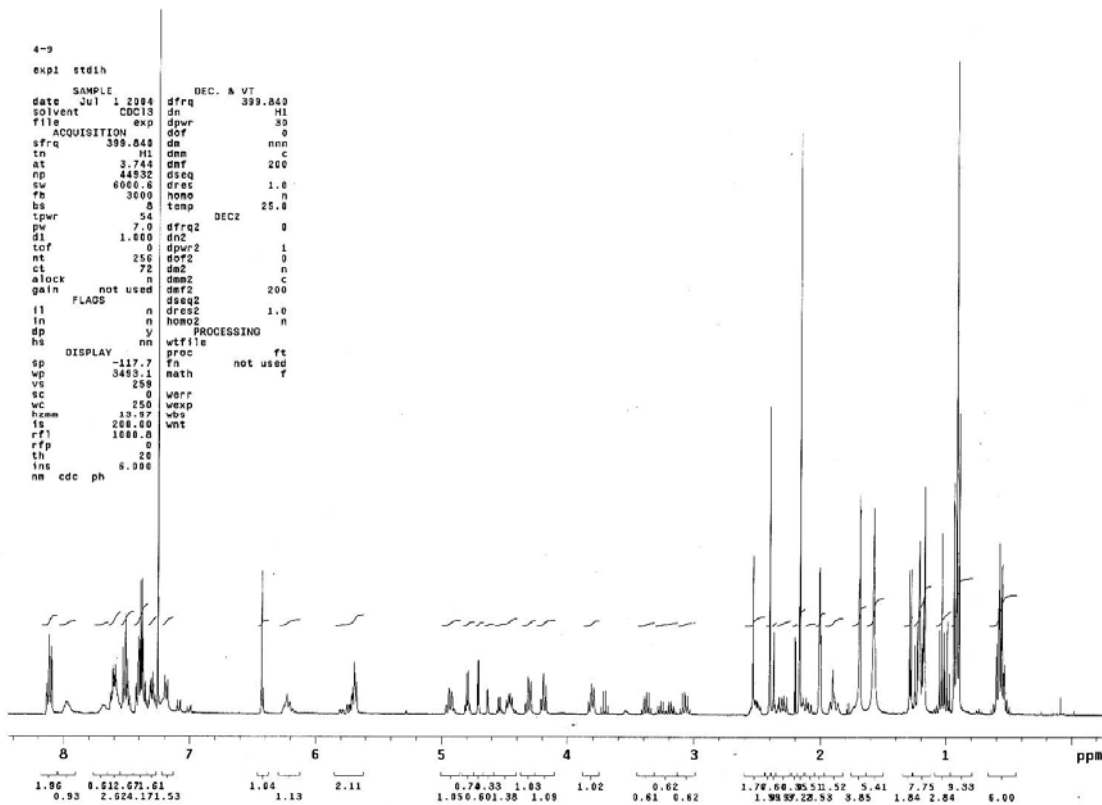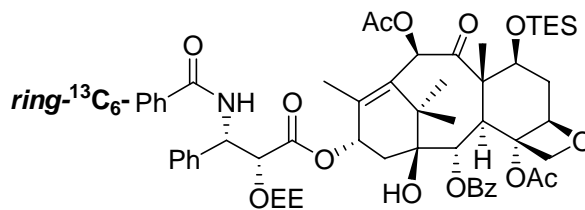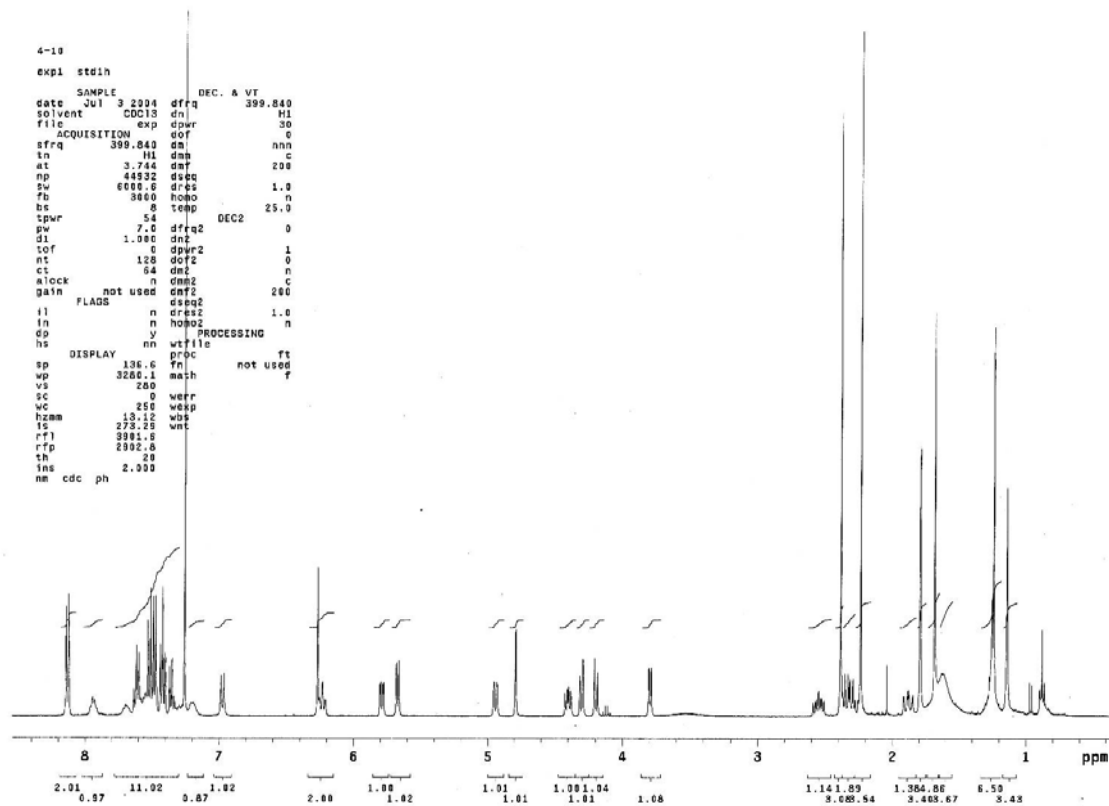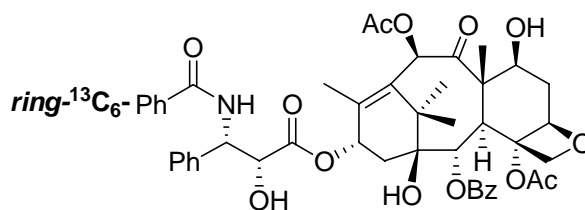
^{13}C NMR Spectrum of **1-56**
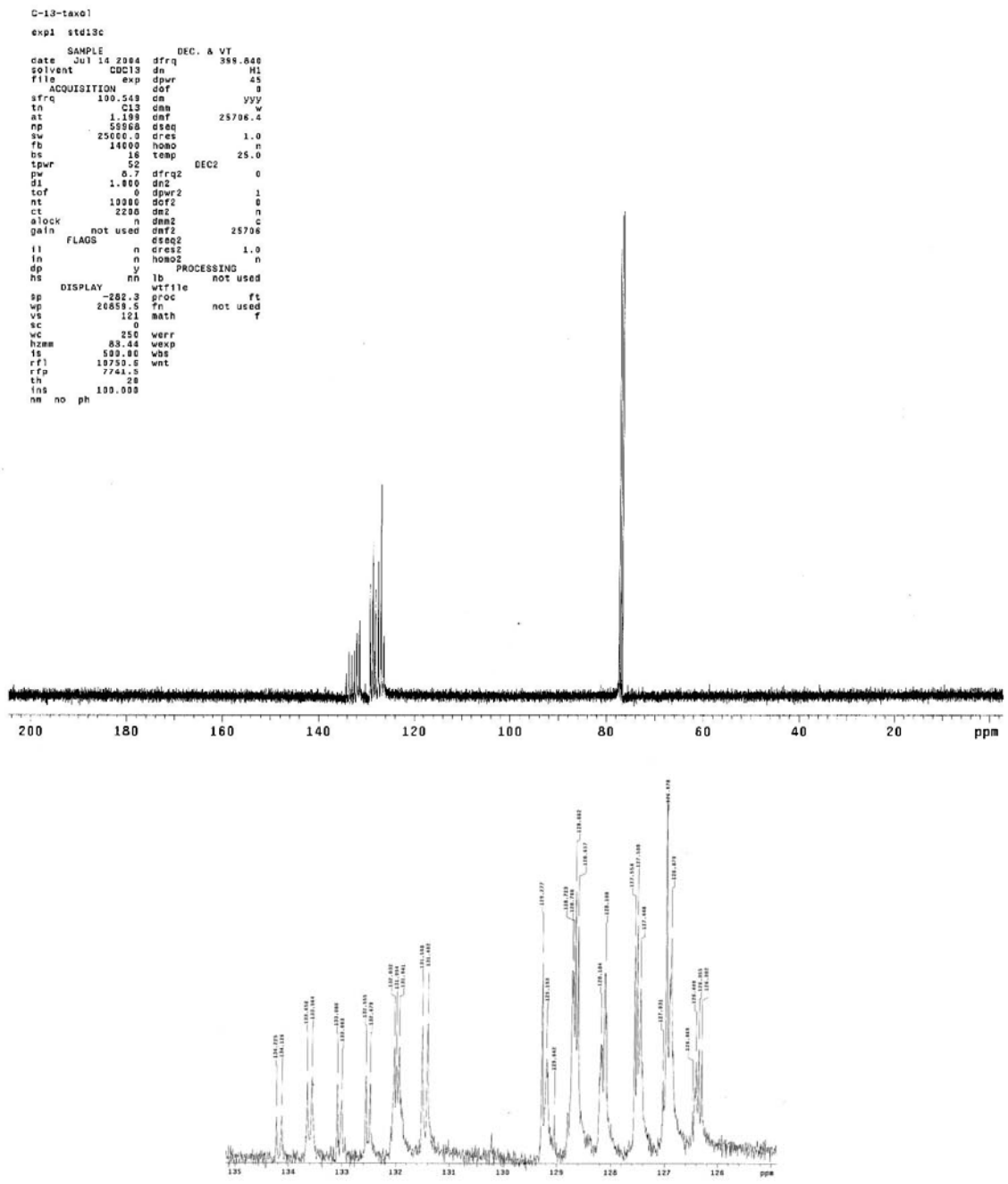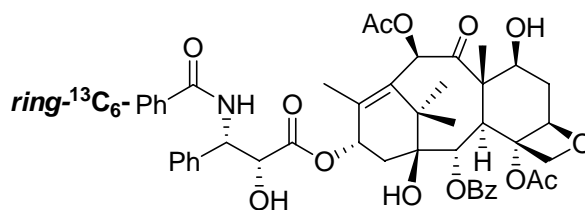
^{1}H NMR Spectrum of **1-57a**

¹³C NMR Spectrum of **1-57a**

TESO O OTES
TESO''
HO H OAc

209.921
170.164
167.478
144.477
138.575
136.076
130.332
129.482
128.951
127.114
84.224
79.762
77.539
77.220
76.909
76.086
75.475
72.895
68.592
58.477
47.155
43.265
40.067
37.533
29.914
26.569
22.569
21.900
20.953
14.782
14.327
10.669
7.173
7.133
7.088
7.004
6.632
6.200
5.471
5.092

200 180 160 140 120 100 80 60 40 20 ppm
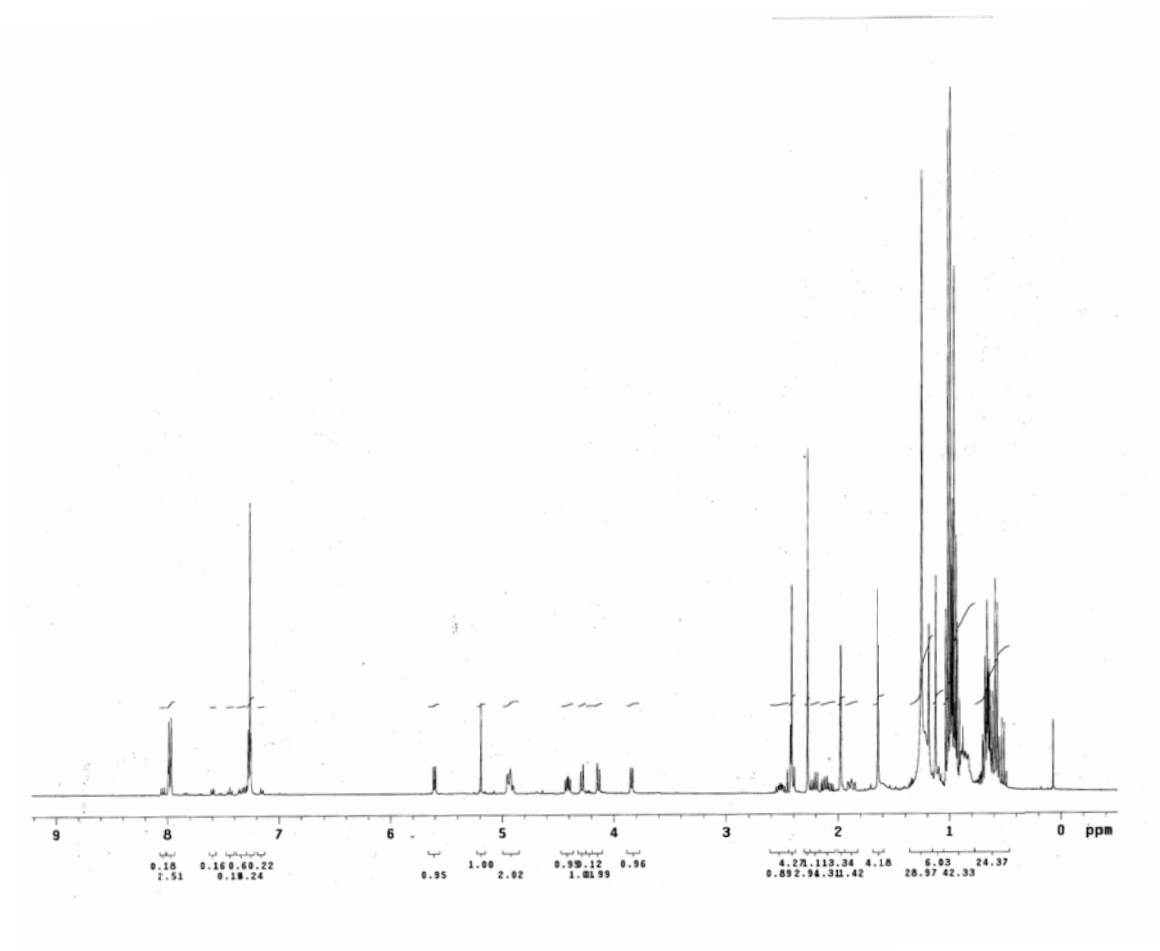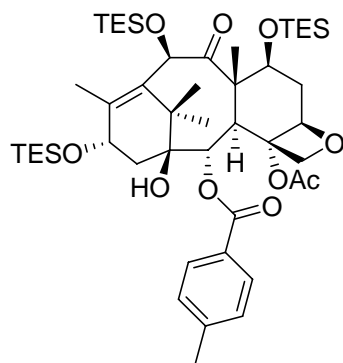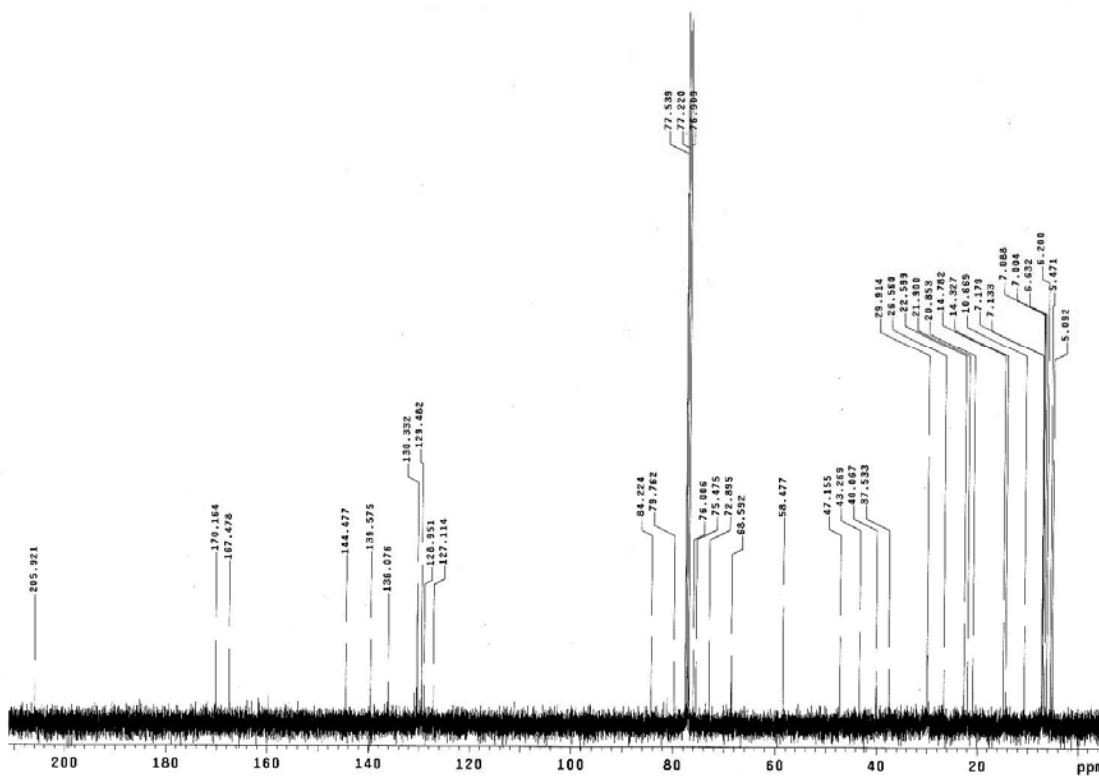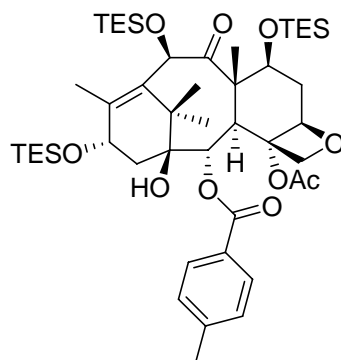
^{1}H NMR Spectrum of **1-57b**

^{1}H NMR Spectrum of **1-57c**

¹H NMR Spectrum of **1-59a**

^{13}C NMR Spectrum of **1-59a**

13C OBSERVE

expl std13c

SAMPLE		DEC. & VT	
date	Aug 26 2003	dfrq	399.848
solvent	CDC13	dn	H1
file	exp	dpwr	45
ACQUISITION		dof	0
sfrq	100.549	dm	yyy
tn	C13	dmm	w
at	1.199	dmf	25706.4
np	59968	dseq	
sw	25000.0	dres	1.0
fb	14000	homo	n
bs	8	temp	25.0
tpwr	52		DEC2
pw	8.7	dfrq2	0
d1	1.000	dn2	
tof	0	dpwr2	1
nt	9000	dof2	0
ct	1192	dm2	n
alock	n	dmm2	c
gain	not used	dmf2	25706
FLAGS		dseq2	
il	n	dres2	1.0
in	n	homo2	n
dp	y	PROCESSING	
hs	nn	lb	not used
DISPLAY		wtfile	
sp	-391.4	proc	ft
wp	21451.6	fn	not used
vs	656	math	f
sc	0		
wc	250	werr	
hzmm	85.81	wexp	
is	500.00	wbs	
rfl	2986.1	wnt	
rfp	0		
th	21		
ins	100.000		
2dm no ph			

Peak labels: 174.884, 170.677, 167.379, 146.336, 144.773, 132.244, 130.362, 129.573, 126.788, 84.687, 81.090, 79.292, 77.547, 77.226, 76.909, 76.697, 76.241, 74.898, 72.553, 68.243, 58.955, 46.366, 42.943, 36.823, 35.833, 29.914, 27.827, 27.197, 22.788, 21.946, 21.126, 15.768, 9.645, 5.250

^{1}H NMR Spectrum of **1-59b**

^{1}H NMR Spectrum of **1-59c**
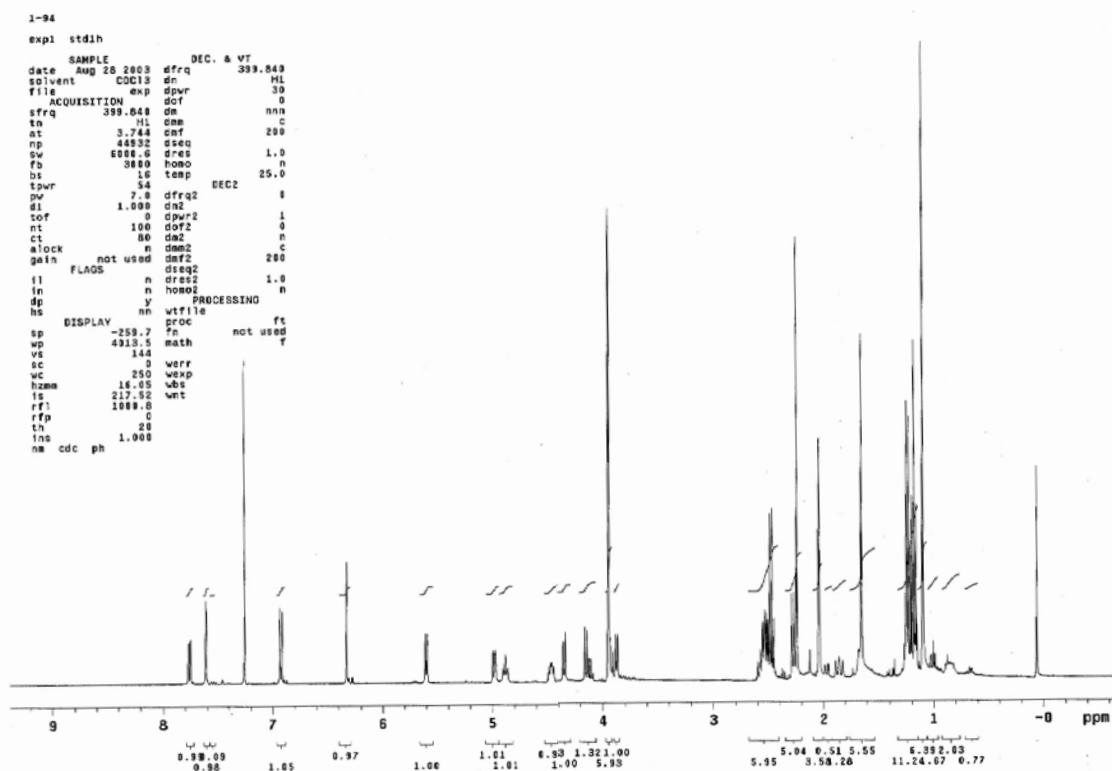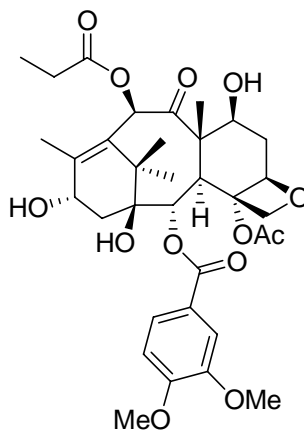
^{1}H NMR Spectrum of **1-60a**
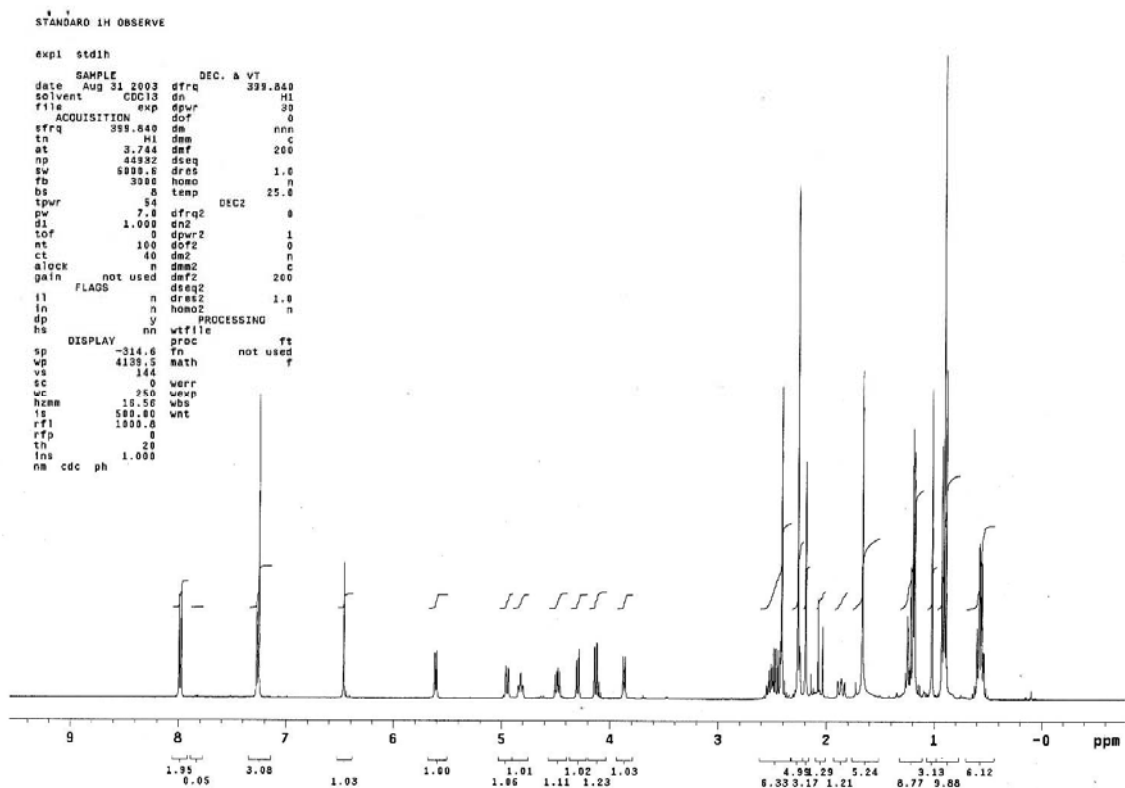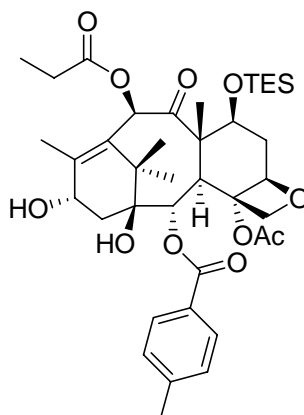
^{13}C NMR Spectrum of **1-60a**
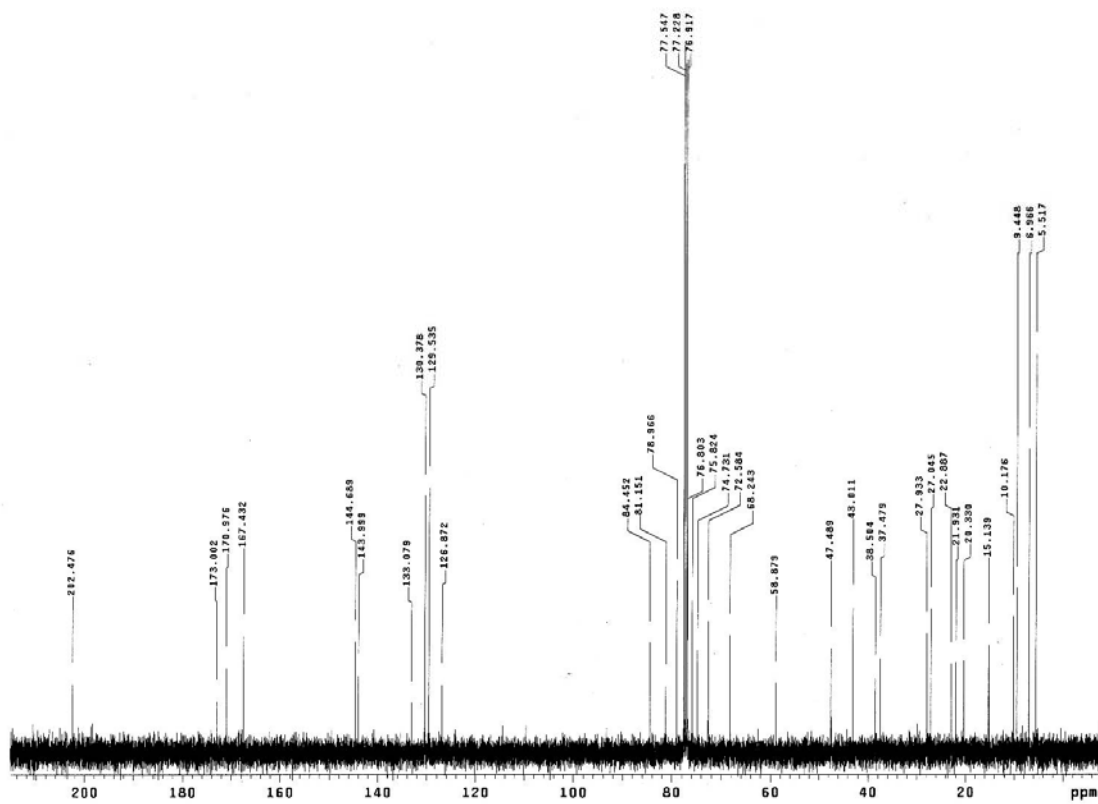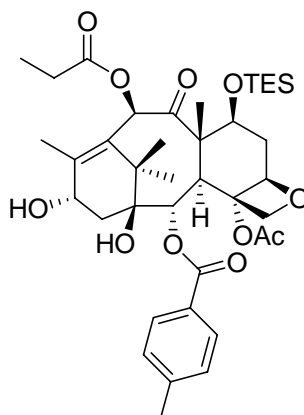
^{1}H NMR Spectrum of **1-60b**
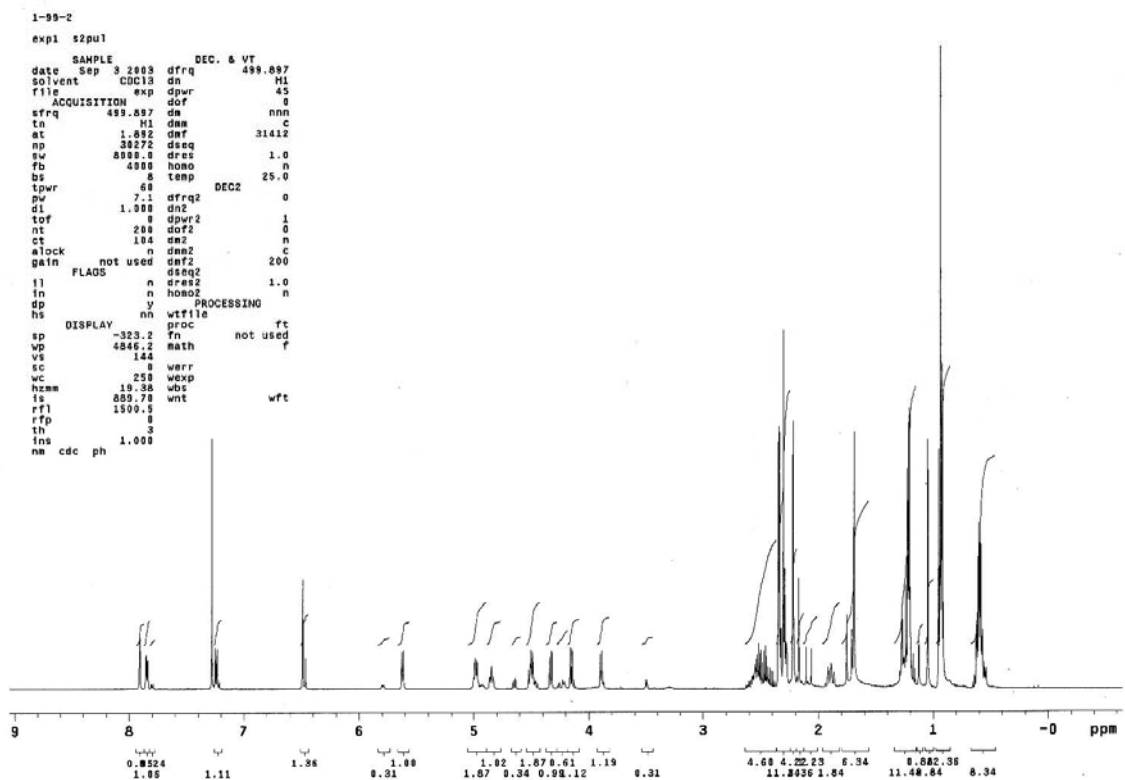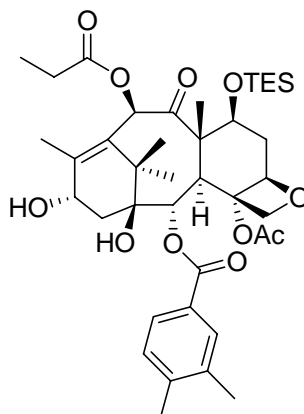
^{1}H NMR Spectrum of **1-60c**
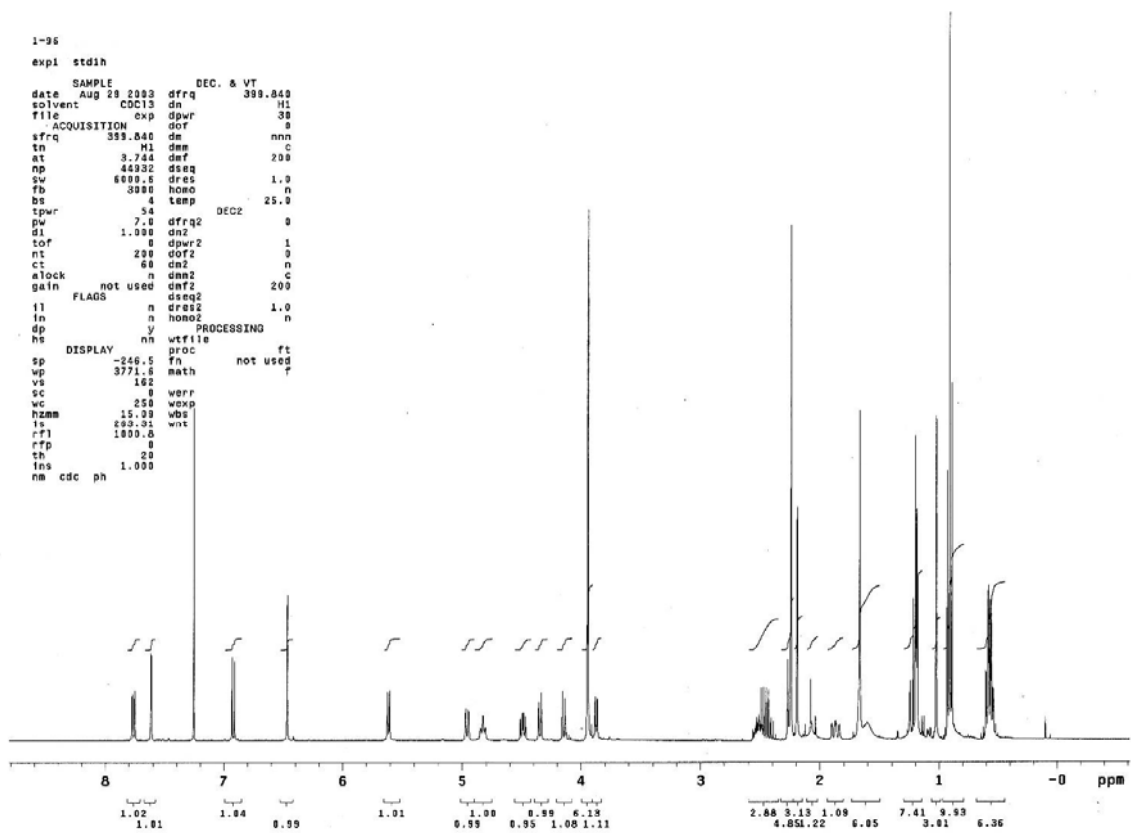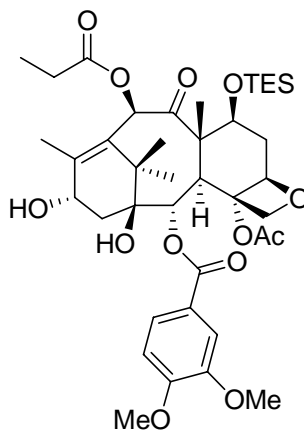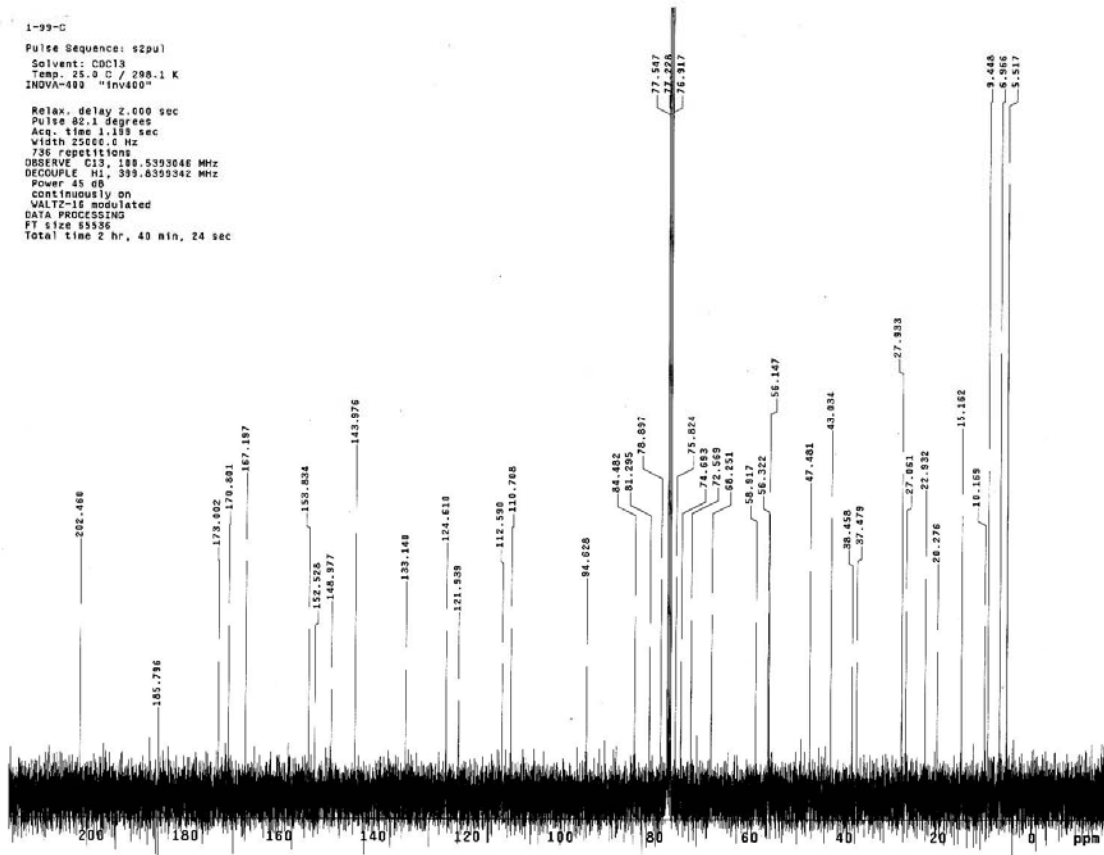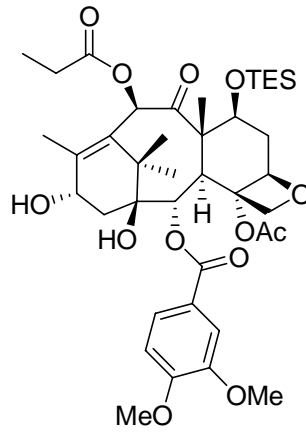
¹³C NMR Spectrum of **1-61a**
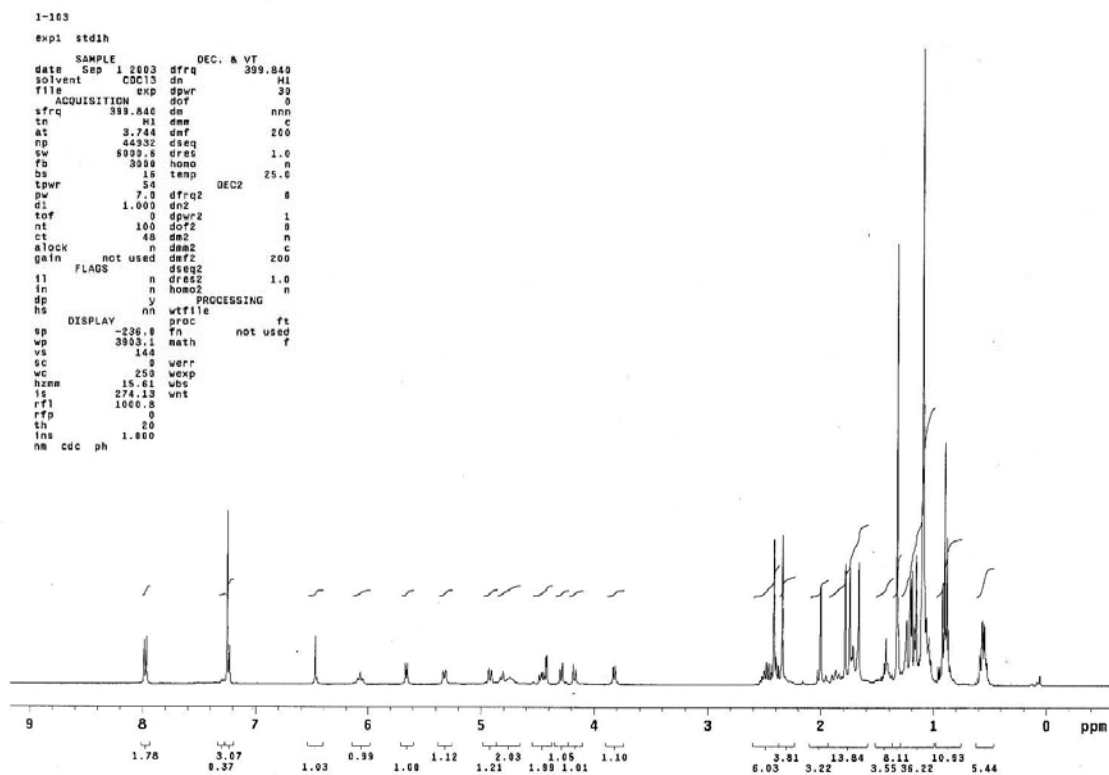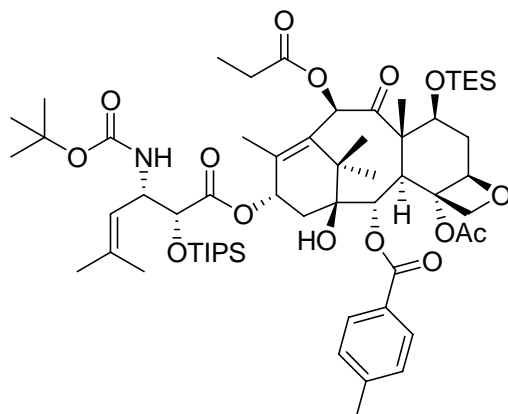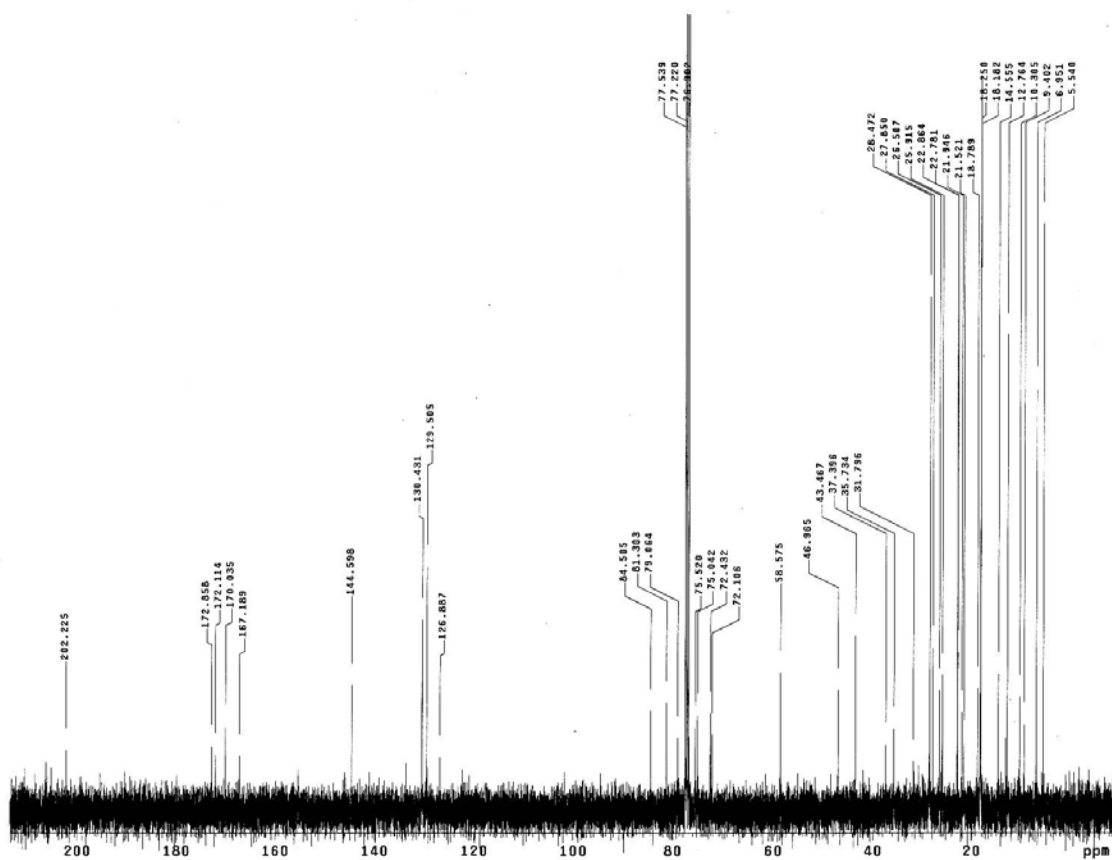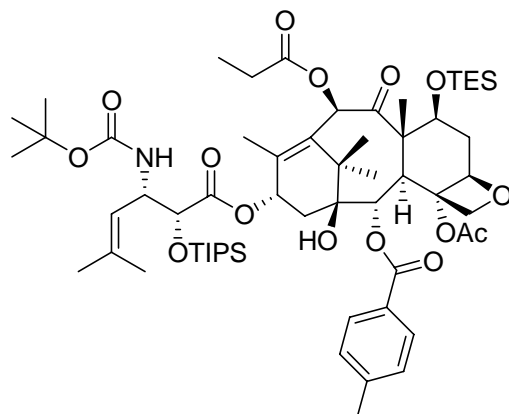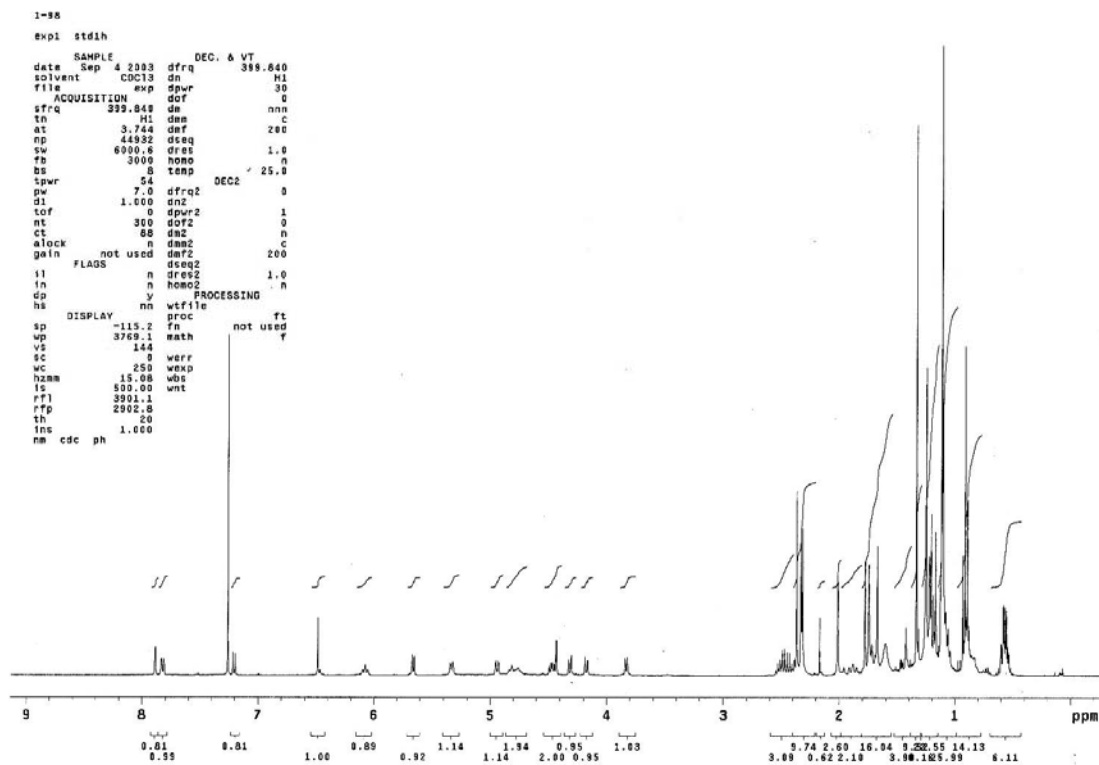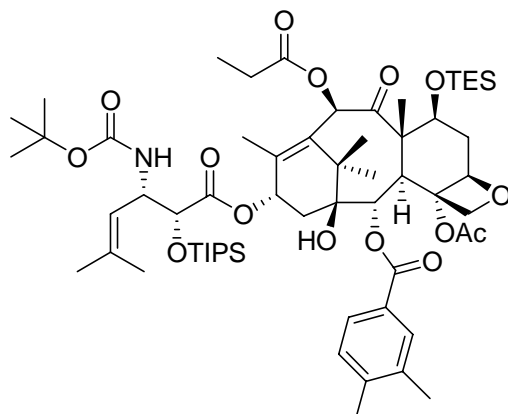
^{1}H NMR Spectrum of **1-61c**
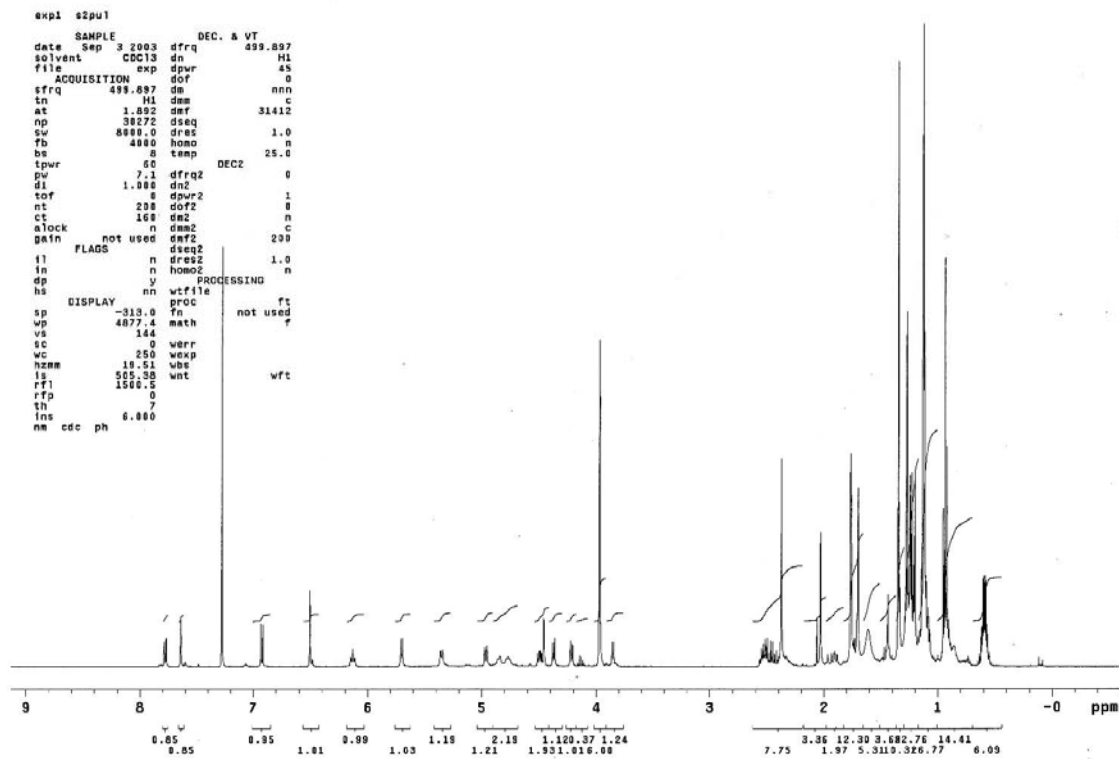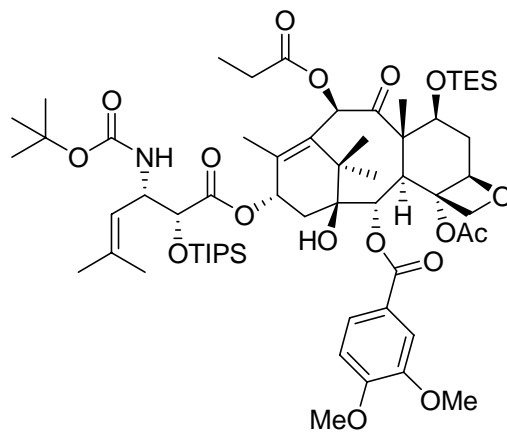
^{1}H NMR Spectrum of **1-62a** (**SB-T-1213P05**)
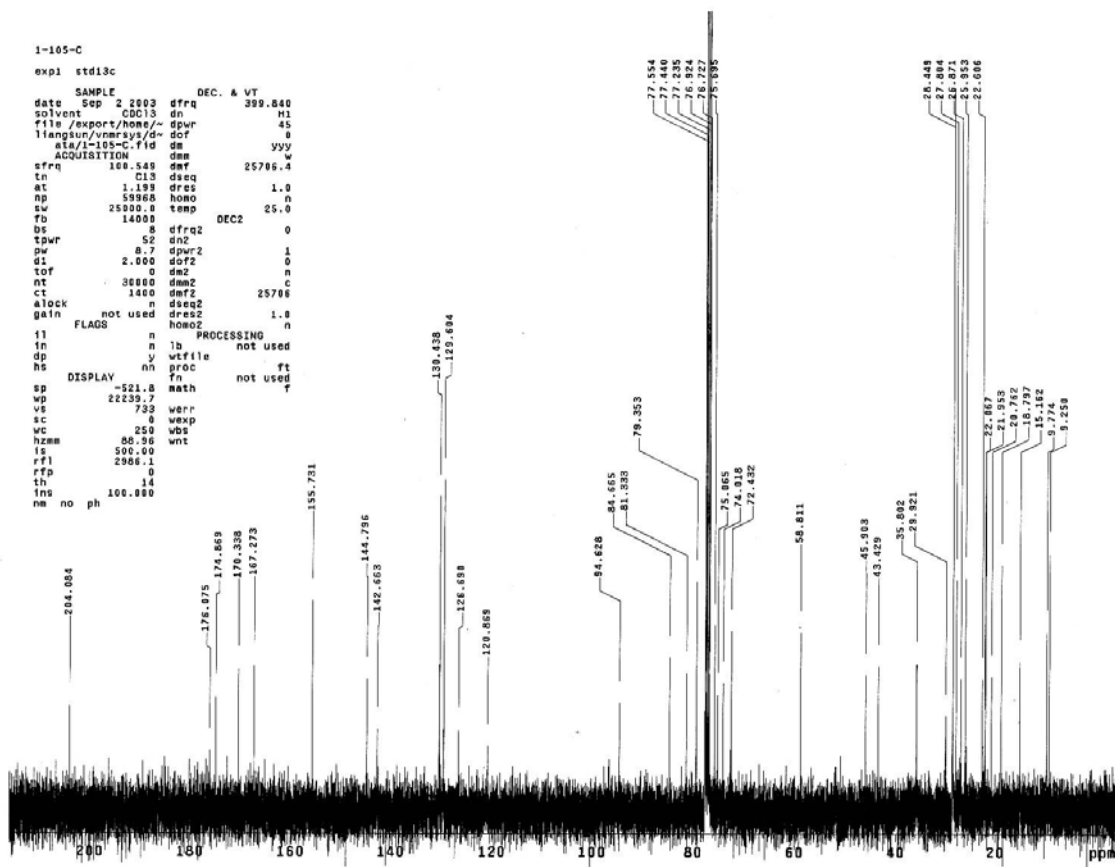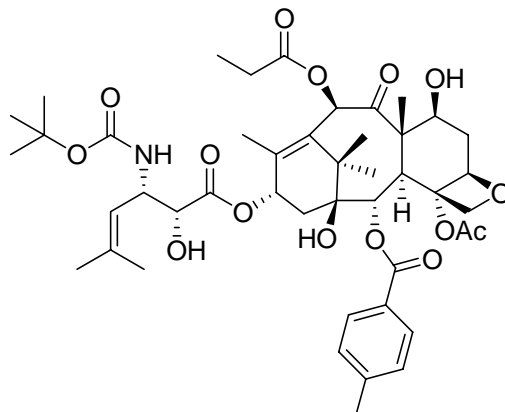
^{1}H NMR Spectrum of **1-62b** (**SB-T-1213P07**)
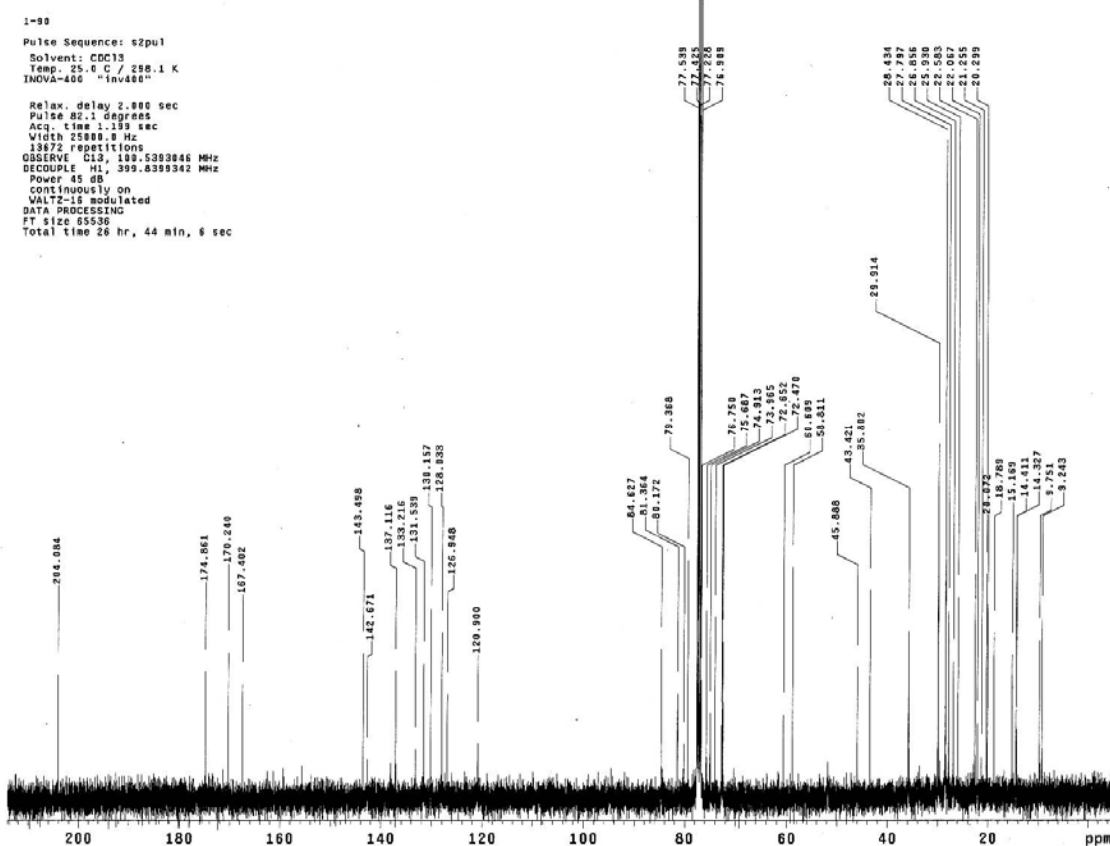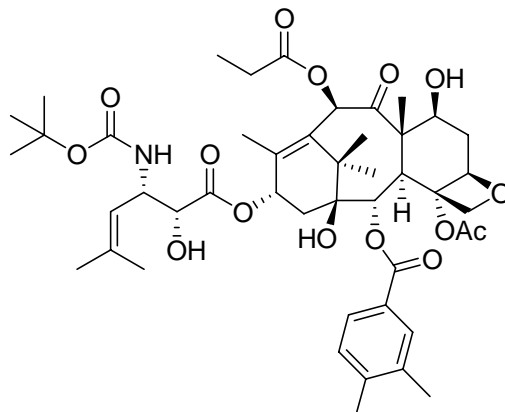
^{13}C NMR Spectrum of **1-62c** (**SB-T-1213P08**)
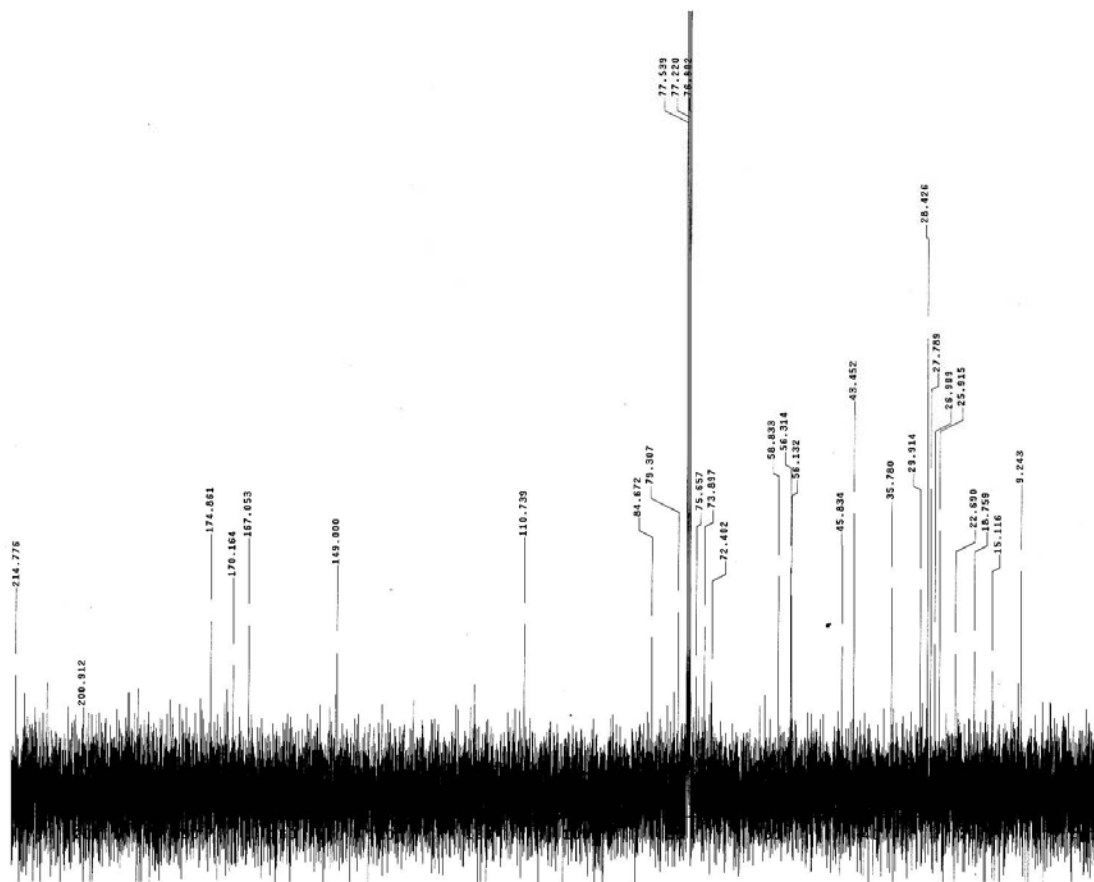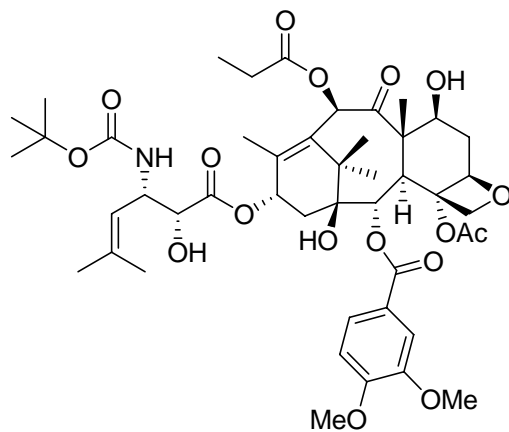
A2. Appendix Chapter II

^{1}H NMR Spectrum of **2-2a** (**LA-SB-T-1213**)
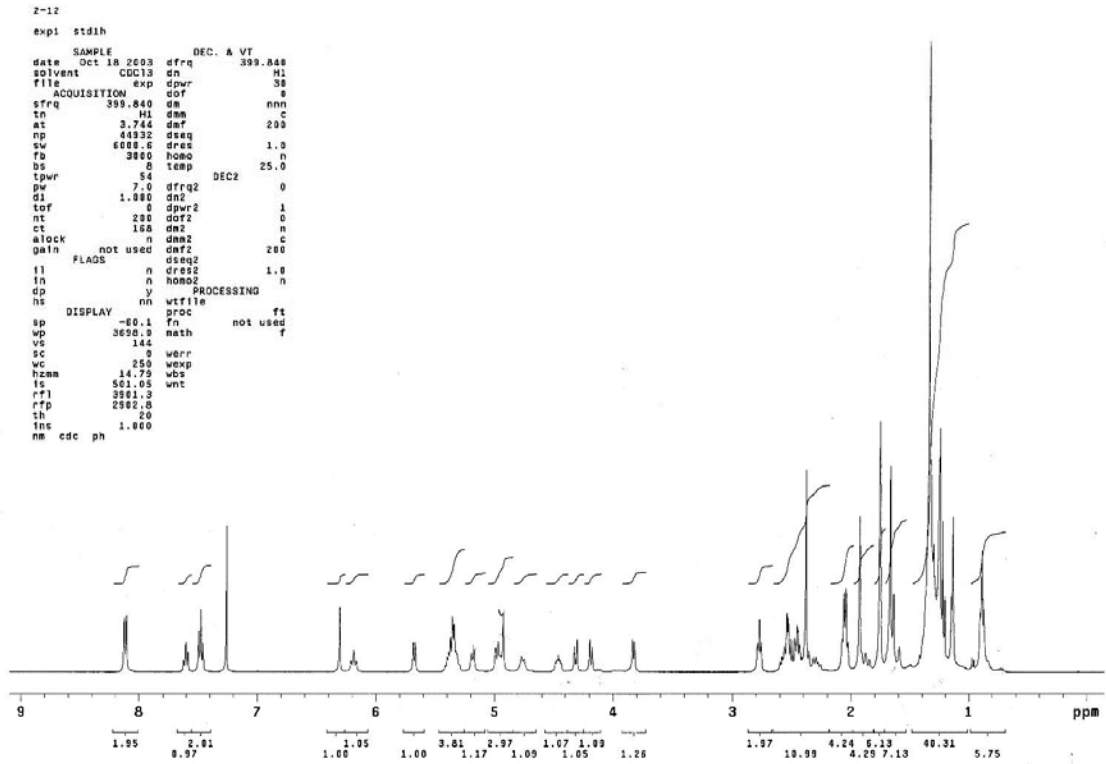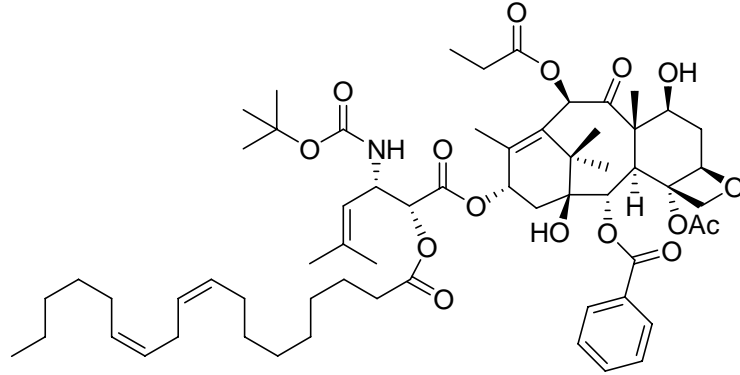
^{13}C NMR Spectrum of **2-2a** (**LA-SB-T-1213**)
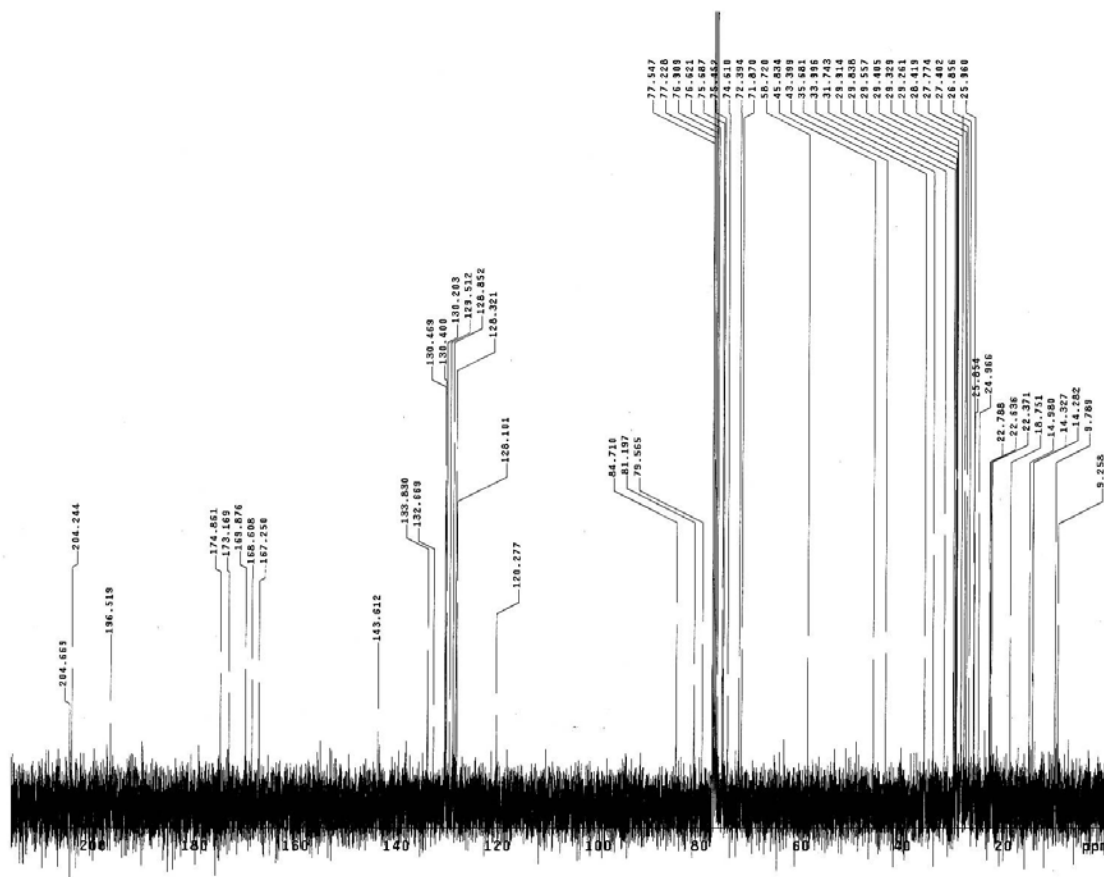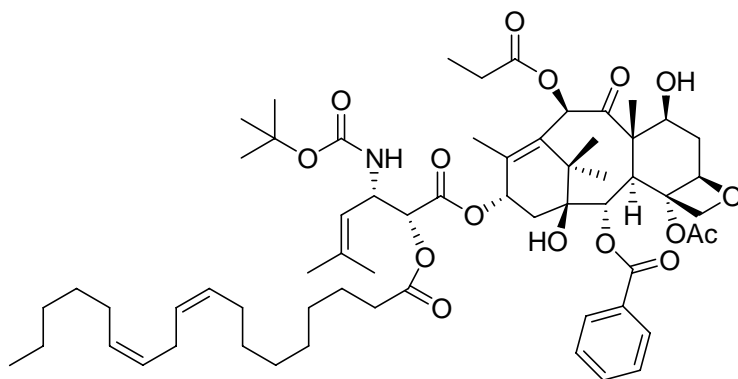
^{1}H NMR Spectrum of **2-2b** (**LNA-SB-T-1213**)

^{13}C NMR Spectrum of **2-2b** (**LNA-SB-T-1213**)

2-27
exp1 stdih

SAMPLE		DEC. & VT	
date	Nov 1 2003	dfrq	399.840
solvent	CDCl3	dn	H1
file	exp	dpwr	30
ACQUISITION		dof	0
sfrq	399.840	dm	nnn
tn	H1	dmm	c
at	3.744	dmf	200
np	44532	dseq	
sw	6000.6	dres	1.0
fb	3000	homo	n
bs	8	temp	25.0
tpwr	54	DEC2	
pw	7.0	dfrq2	0
d1	1.000	dn2	
tof	0	dpwr2	1
nt	108	dof2	0
ct	56	dm2	n
alock	n	dmm2	c
gain	not used	dmf2	200
FLAGS		dseq2	
il	n	dres2	1.0
in	n	homo2	n
dp	y	PROCESSING	
hs	nn	wtfile	
DISPLAY		proc	ft
sp	-172.7	fn	not used
wp	3792.5	math	f
vs	144		
sc	0	werr	
wc	250	wexp	
hzmm	15.17	wbs	
is	136.90	wnt	
rfl	1000.8		
rfp	0		
th	20		
ins	1.000		
nm cdc ph			

^{13}C NMR Spectrum of **2-2c** (**DHA-SB-T-121303**)
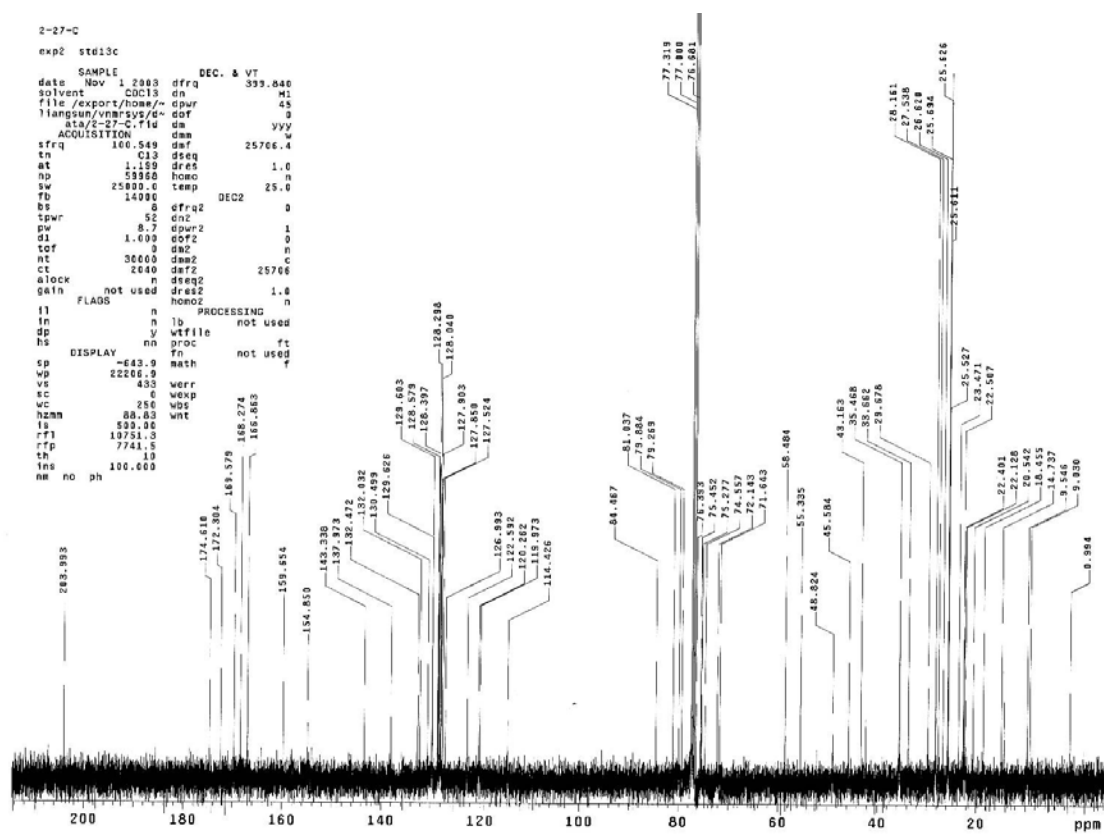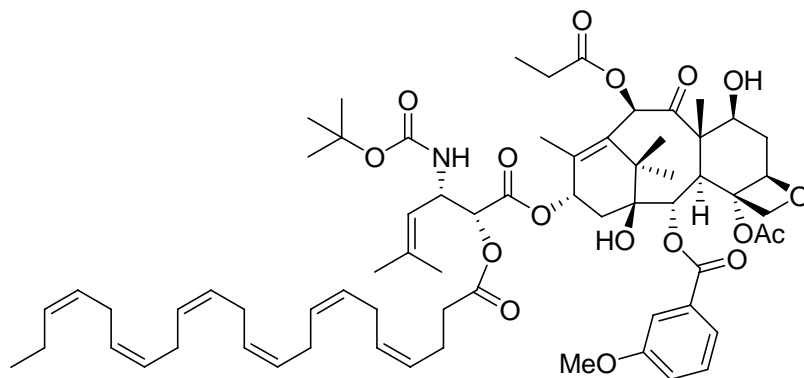
^{13}C NMR Spectrum of **2-2d** (**LNA-SB-T-121303**)
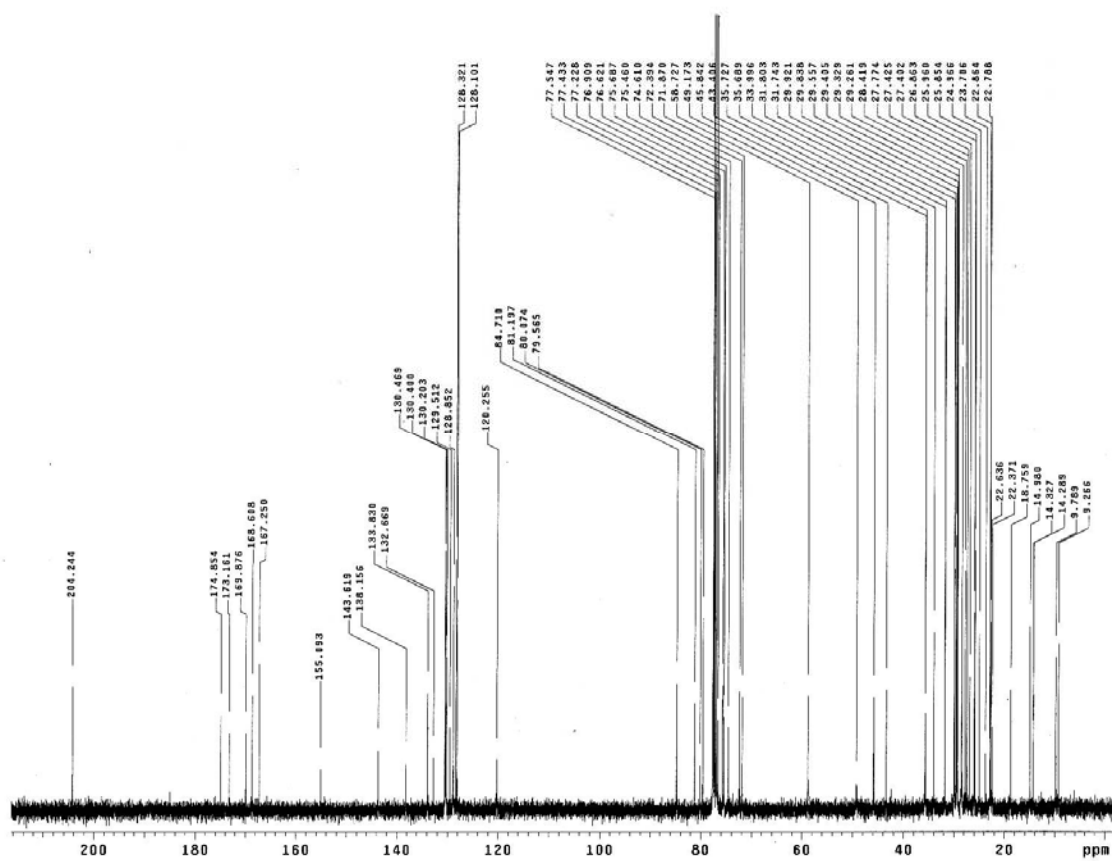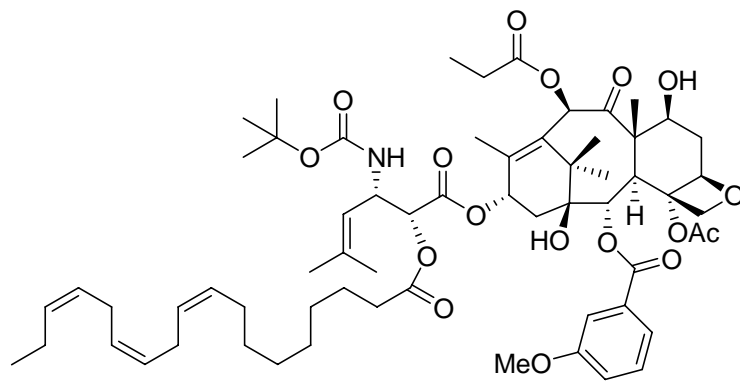
^{1}H NMR Spectrum of **2-2e** (**LA-SB-T-1214**)
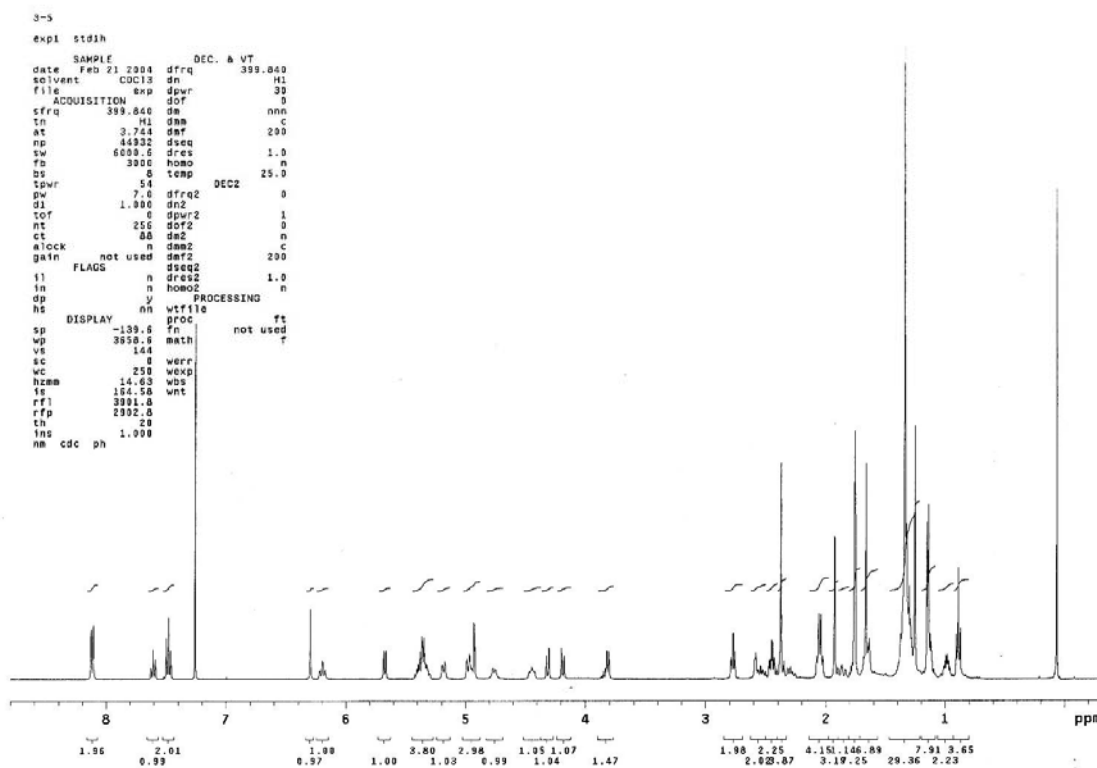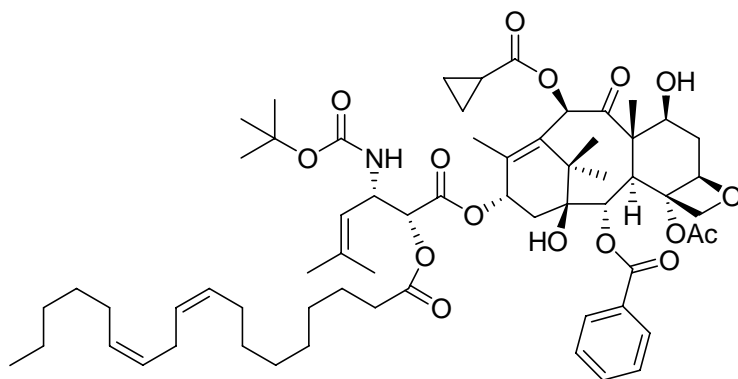
^{13}C NMR Spectrum of **2-2e** (**LA-SB-T-1214**)
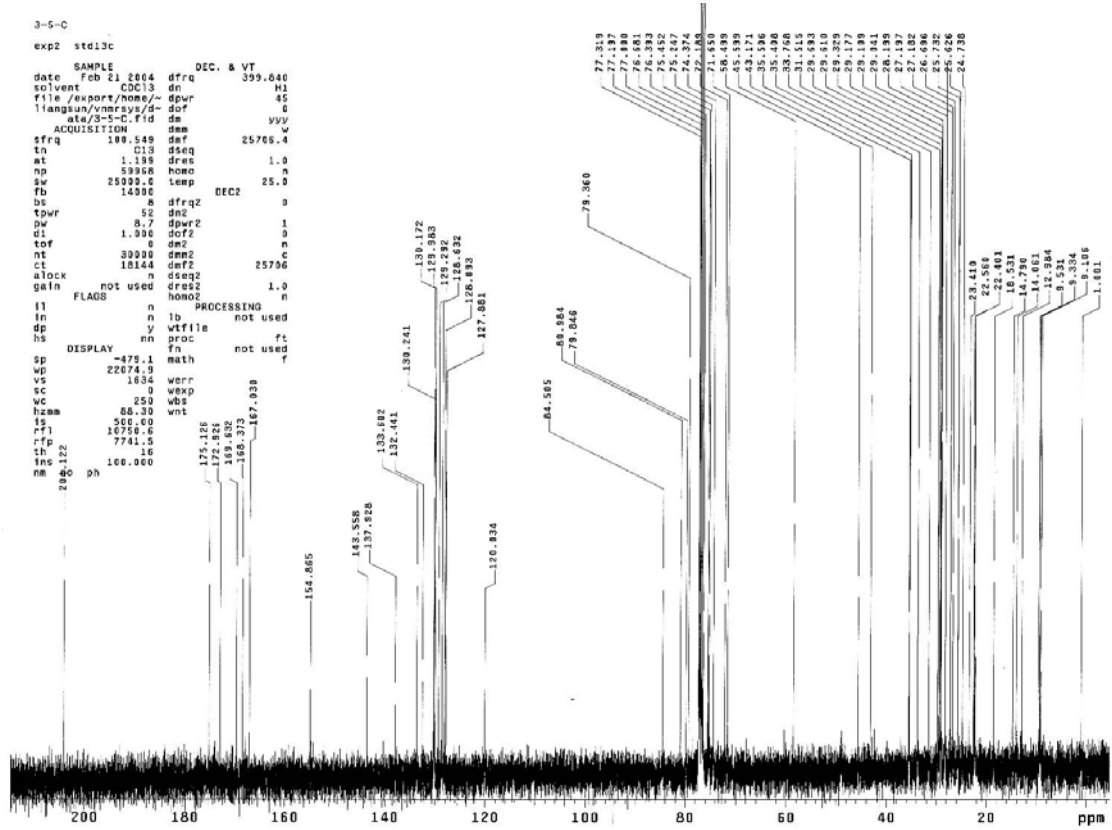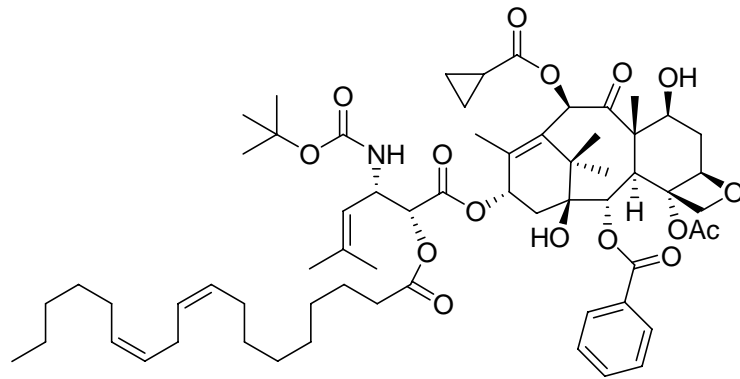
^{1}H NMR Spectrum of **2-2f** (**LNA-SB-T-1214**)
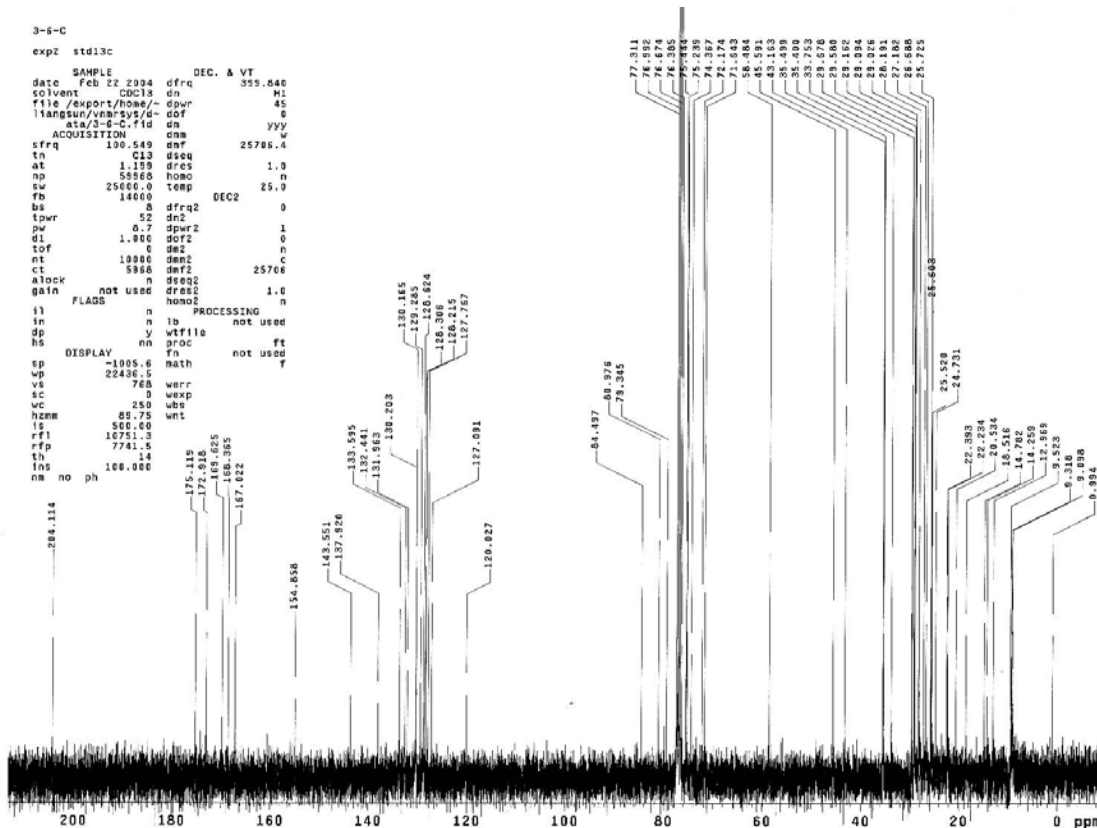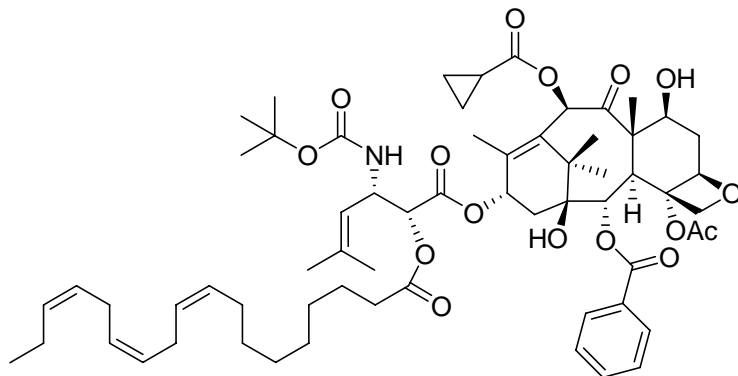
^{1}H NMR Spectrum of **2-2i** (**DHA-SB-T-12853**)
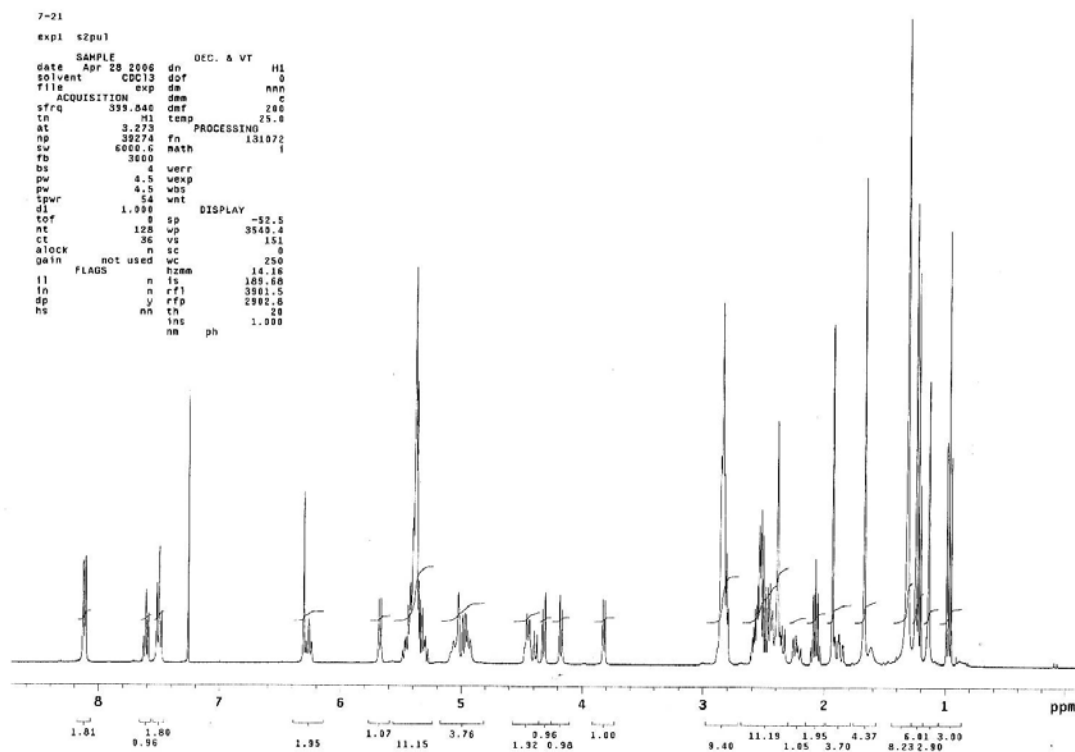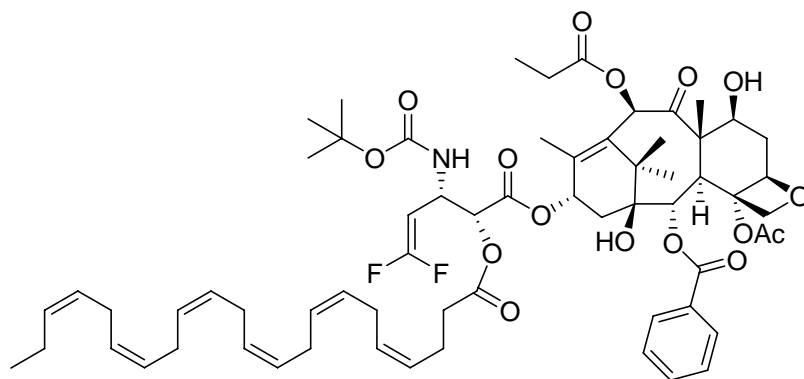
^{19}F NMR Spectrum of **2-2i** (**DHA-SB-T-12853**)
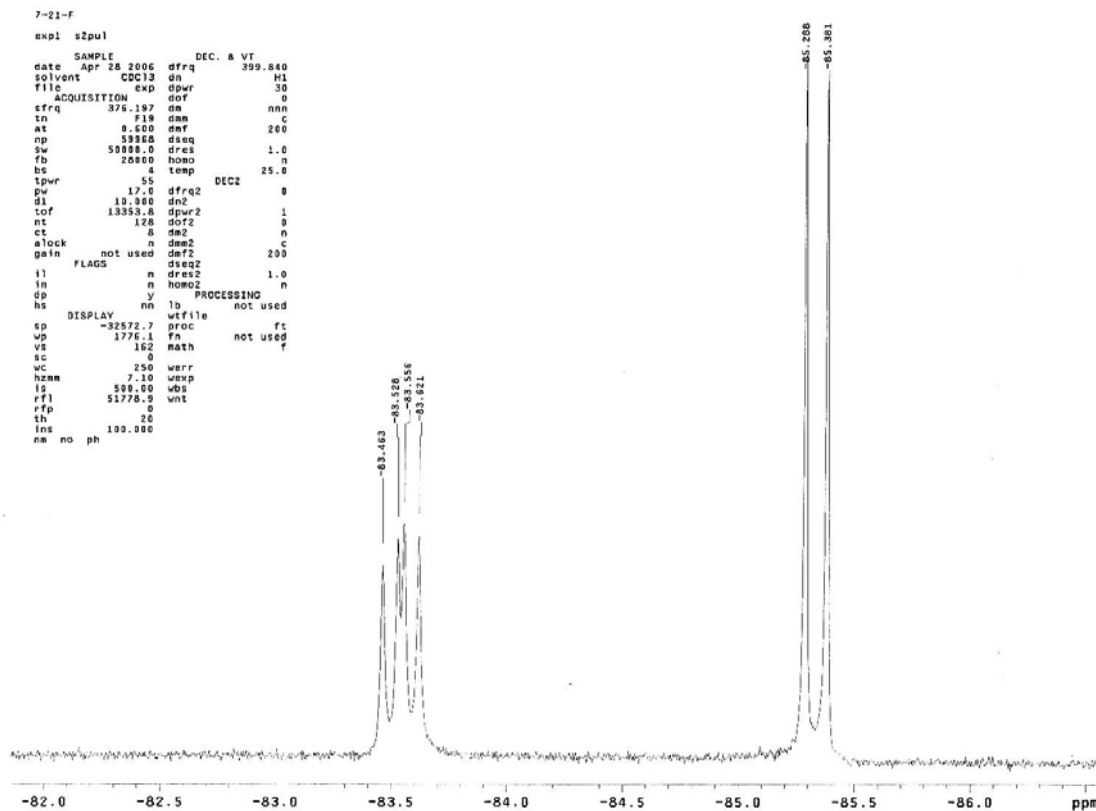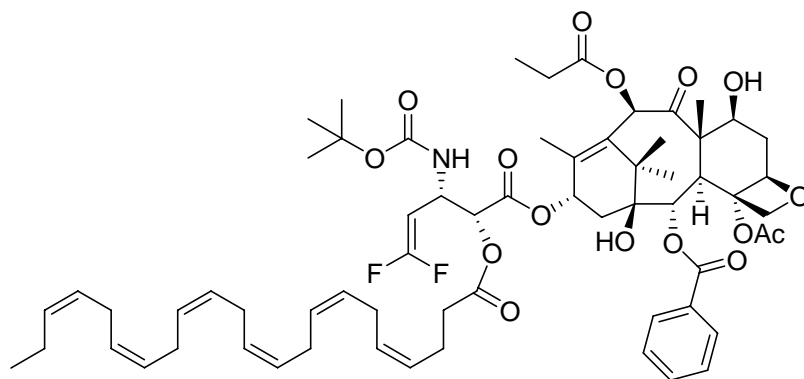
^{1}H NMR Spectrum of **2-2j** (**DHA-SB-T-12854**)
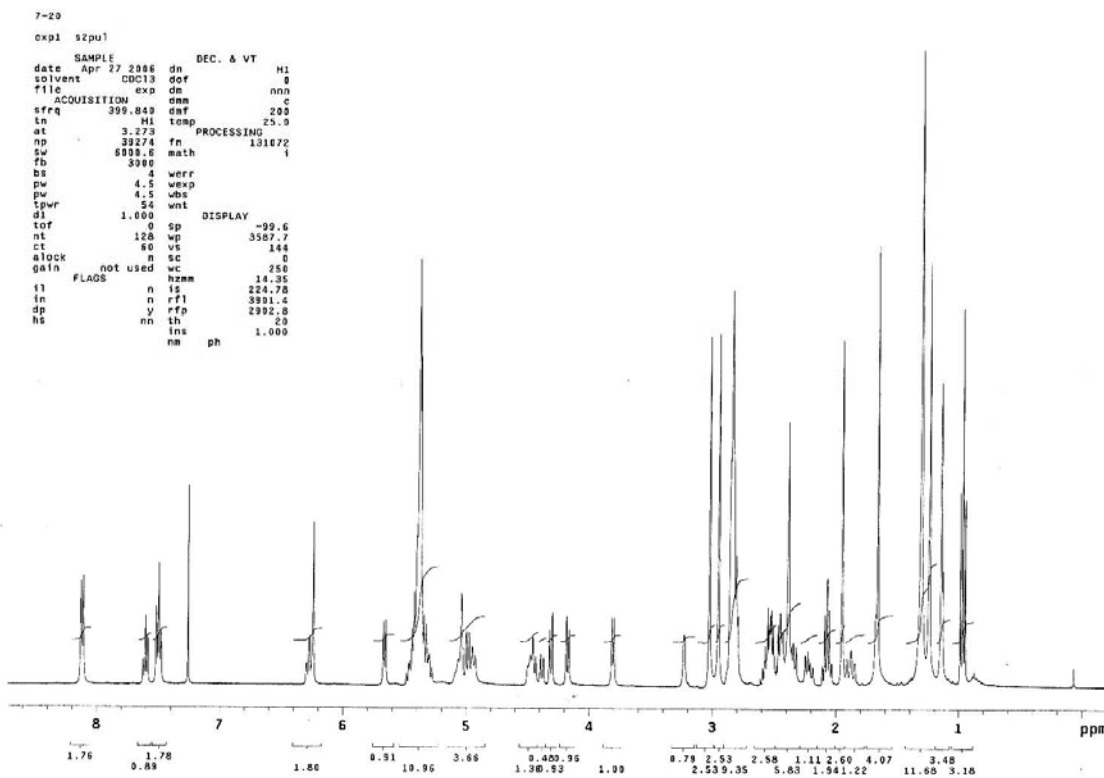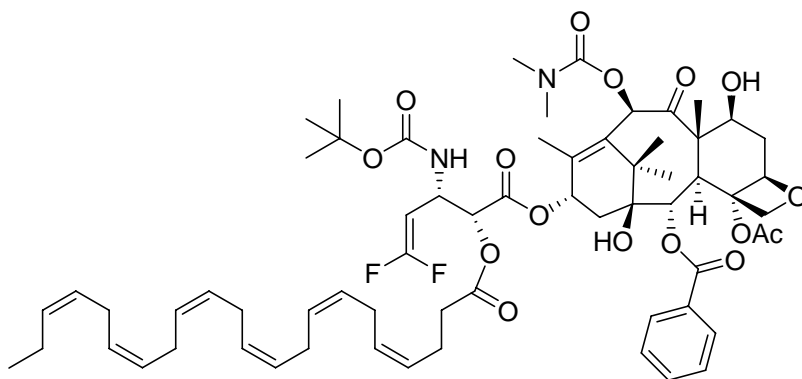
¹³C NMR Spectrum of **2-2j** (**DHA-SB-T-12854**)
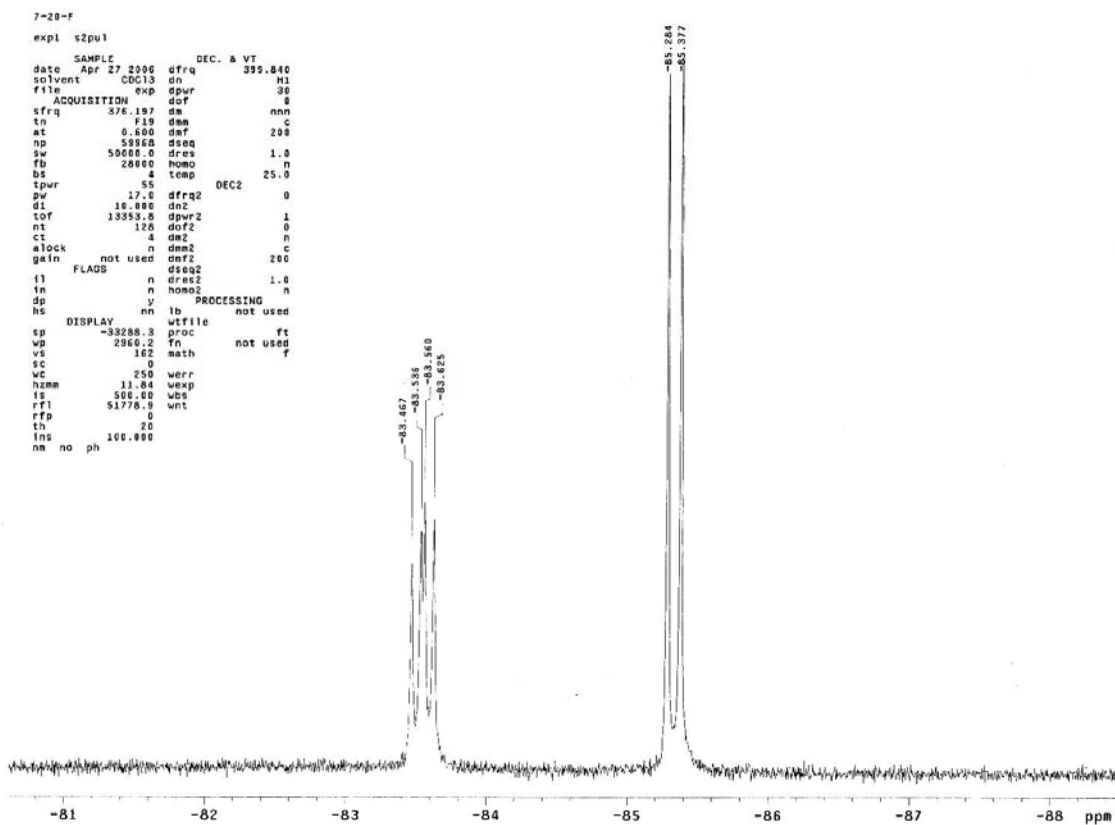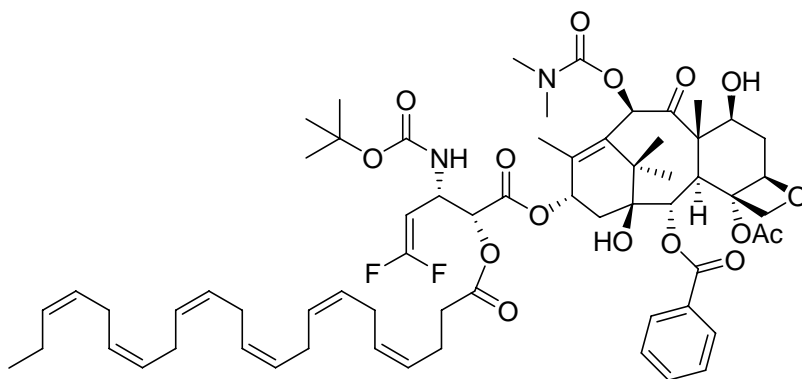
A3. Appendix Chapter III

¹H NMR Spectrum of **3-10**

3-14

exp1 s2pul

SAMPLE		DEC. & VT	
date	Mar 2 2004	dfrq	598.724
solvent	CDCl3	dn	H1
file	exp	dpwr	38
ACQUISITION		dof	0
sfrq	598.724	dm	nnn
tn	H1	dmm	c
at	1.892	dmf	200
np	30272	dseq	
sw	8000.0	dres	1.0
fb	4000	homo	n
bs	8	temp	25.0
tpwr	60	DEC2	
pw	5.5	dfrq2	0
d1	1.000	dn2	
tof	0	dpwr2	1
nt	32	dof2	0
ct	32	dm2	n
alock	not used	dmm2	c
gain	not used	dmf2	200
FLAGS		dseq2	
il	n	dres2	1.0
in	n	homo2	n
dp	y	PROCESSING	
hs	nn	wtfile	
DISPLAY		proc	ft
sp	-149.7	fn	not used
wp	5003.4	math	f
vs	162		
sc	0	werr	
wc	250	wexp	
hzmm	20.01	wbs	
is	147.16	wnt	wft
rfl	1001.2		
rfp	0		
th	7		
ins	5.000		
nm cdc ph			

6.91   2.11   2.13   3.20   8.75 6.00

^{1}H NMR Spectrum of **3-11**

^{13}C NMR Spectrum of **3-11**

NOESY of **3-11**

351
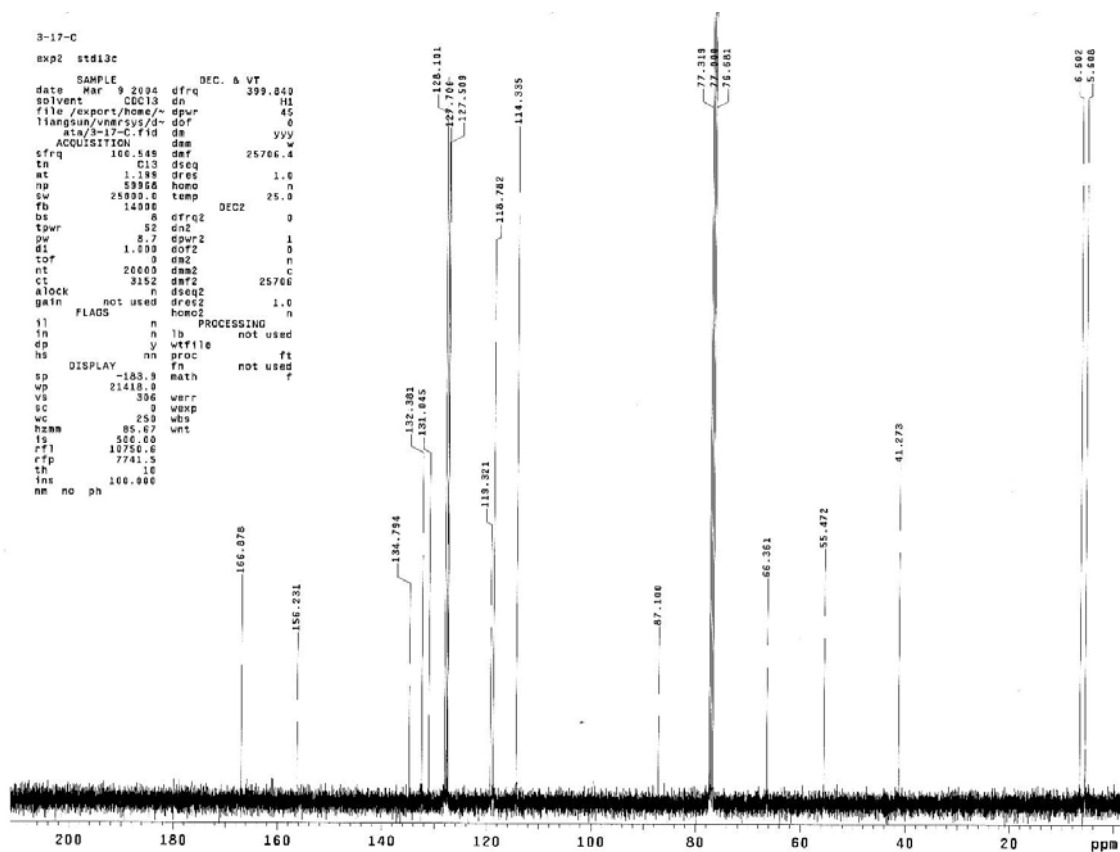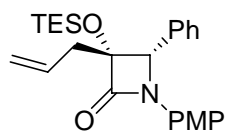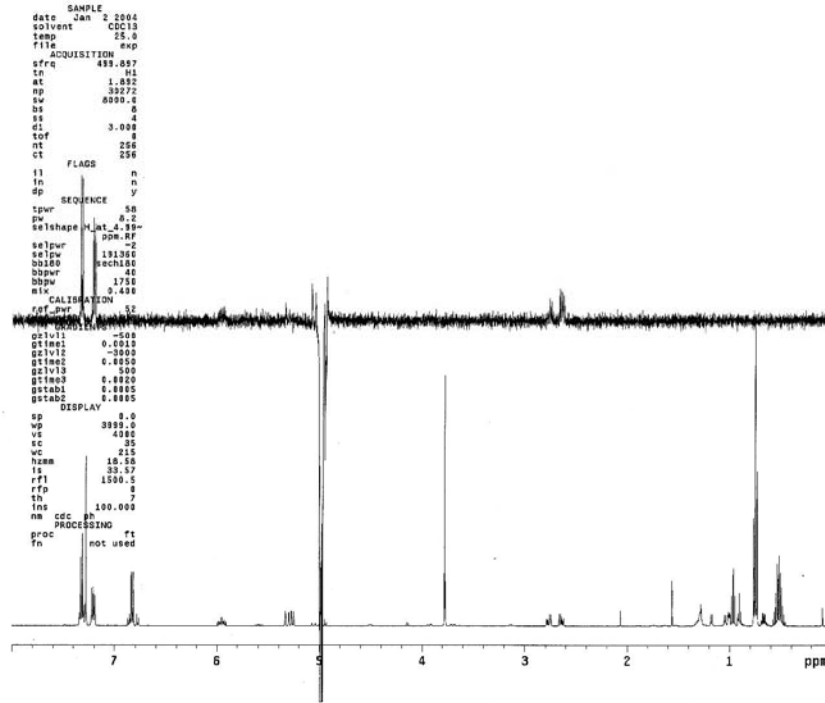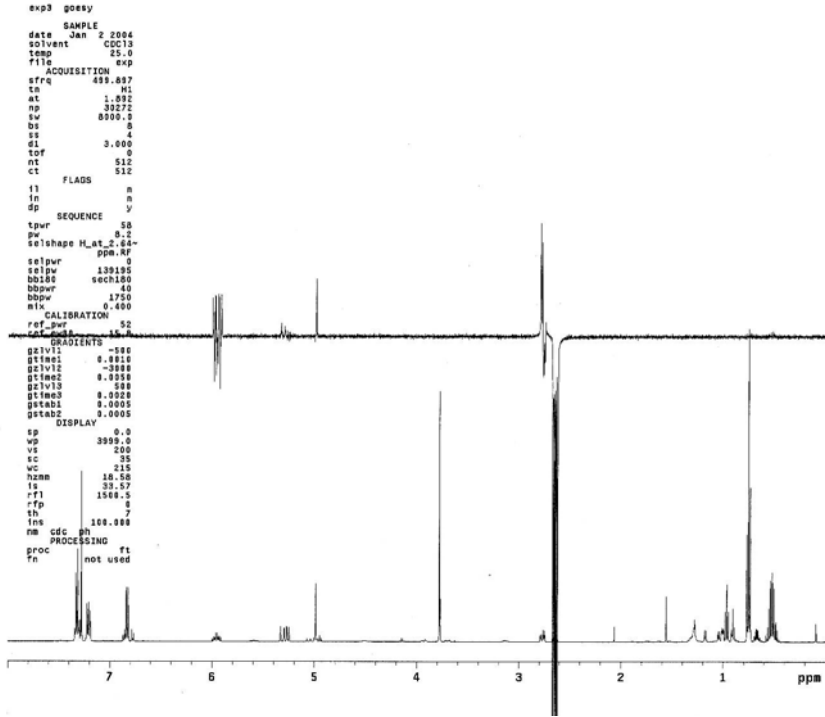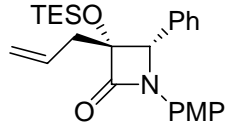
^{1}H NMR Spectrum of **3-12**
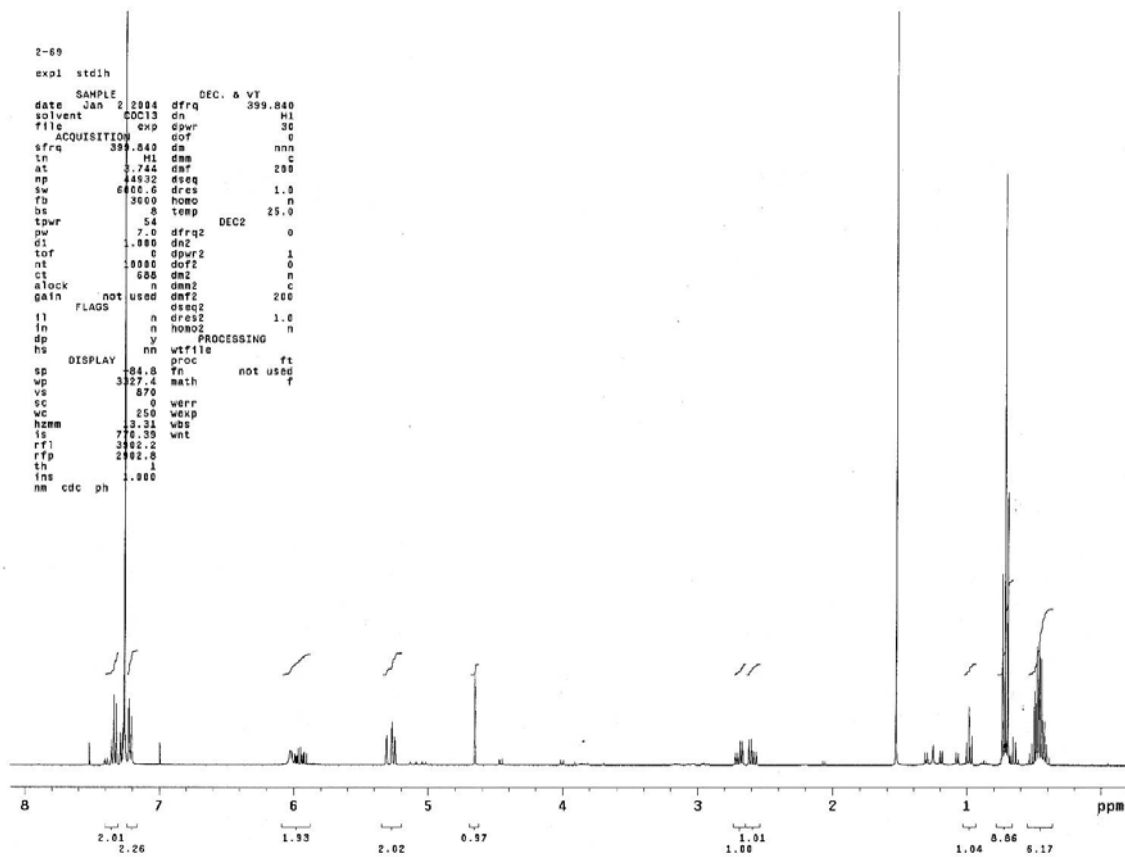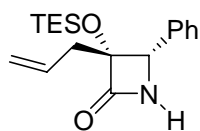
^{13}C NMR Spectrum of **3-12**

^{1}H NMR Spectrum of **3-3**

^{13}C NMR Spectrum of **3-3**

^{13}C NMR Spectrum of **3-1**

357
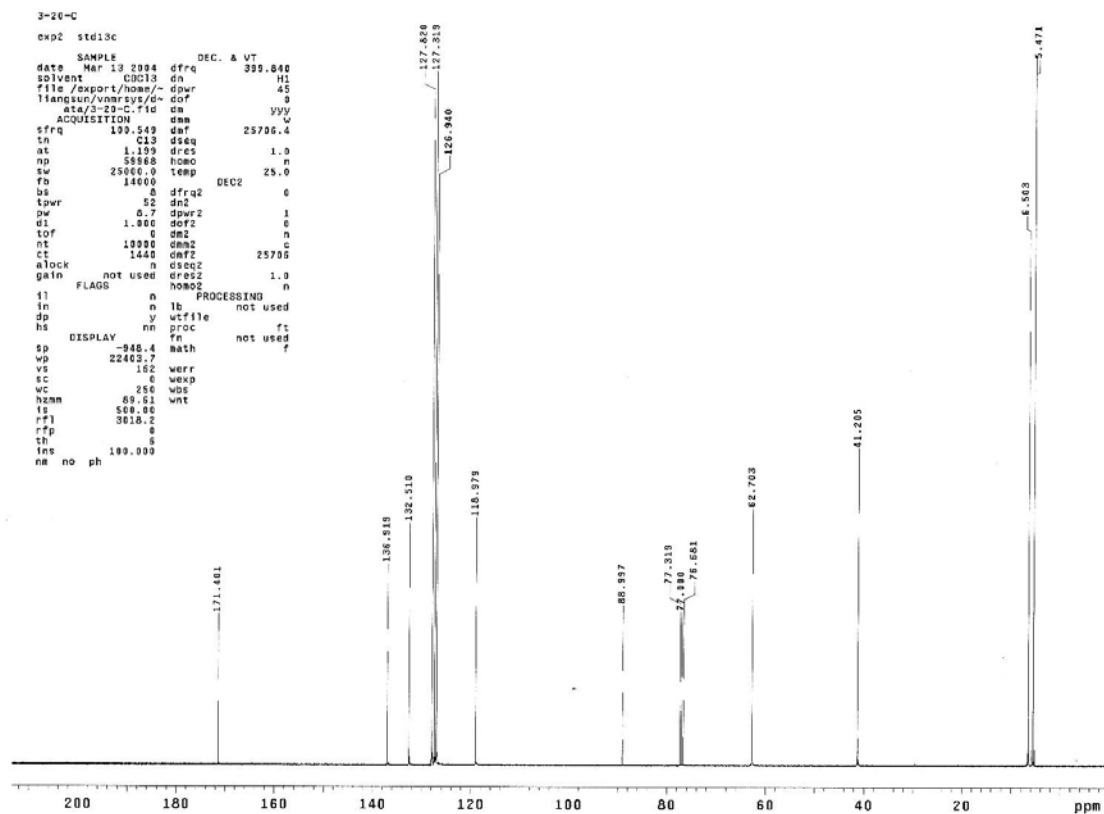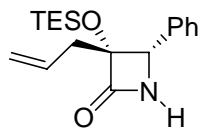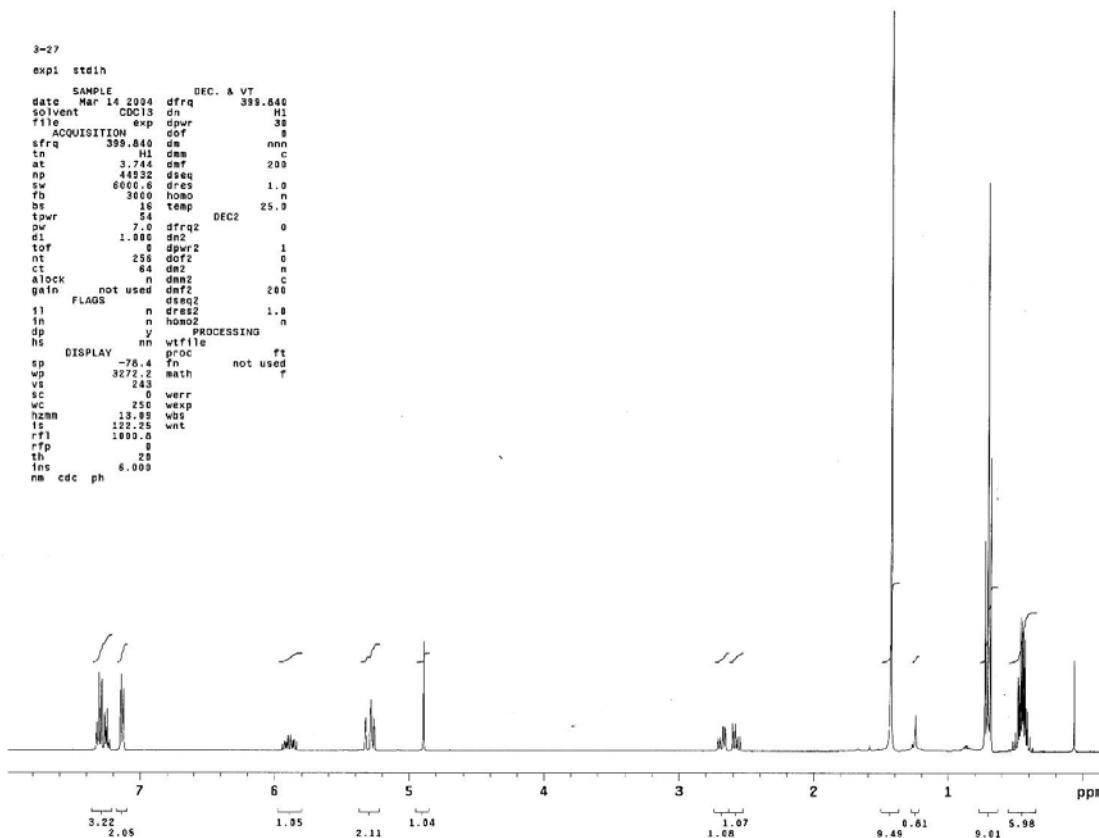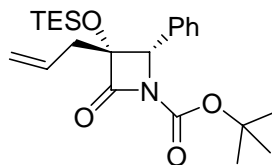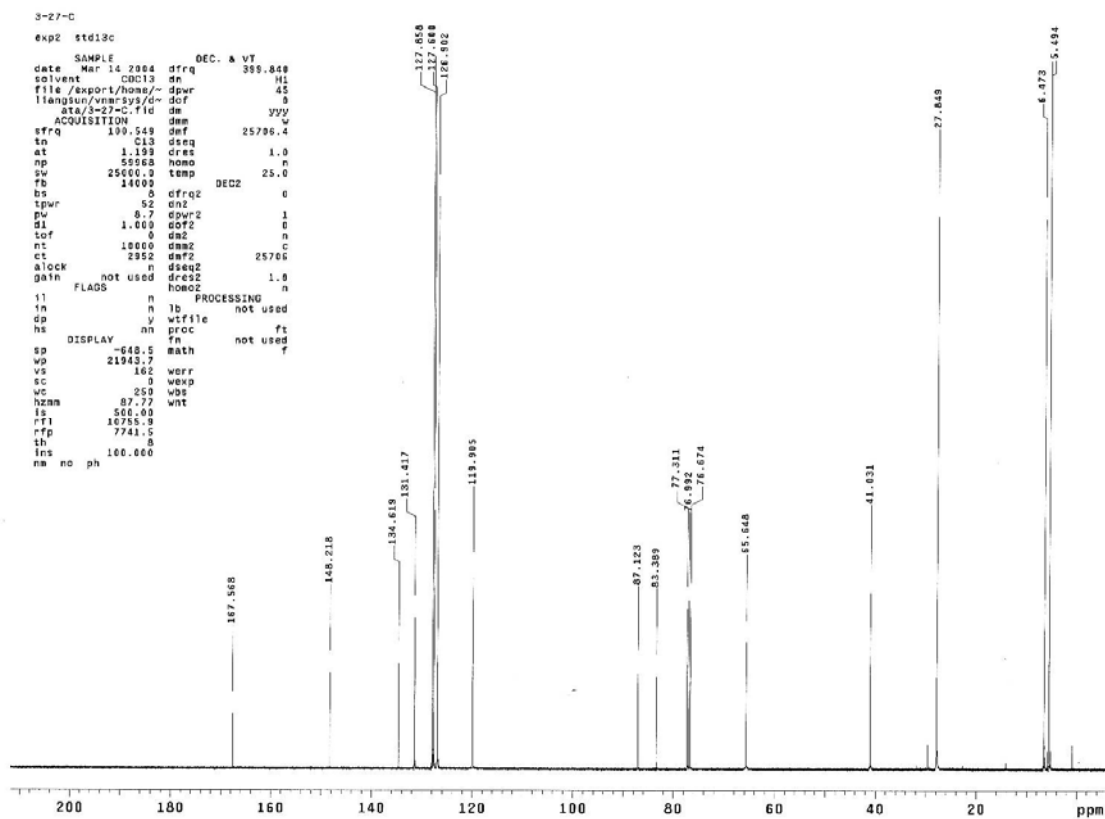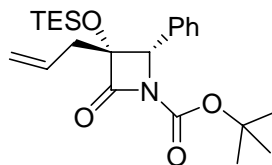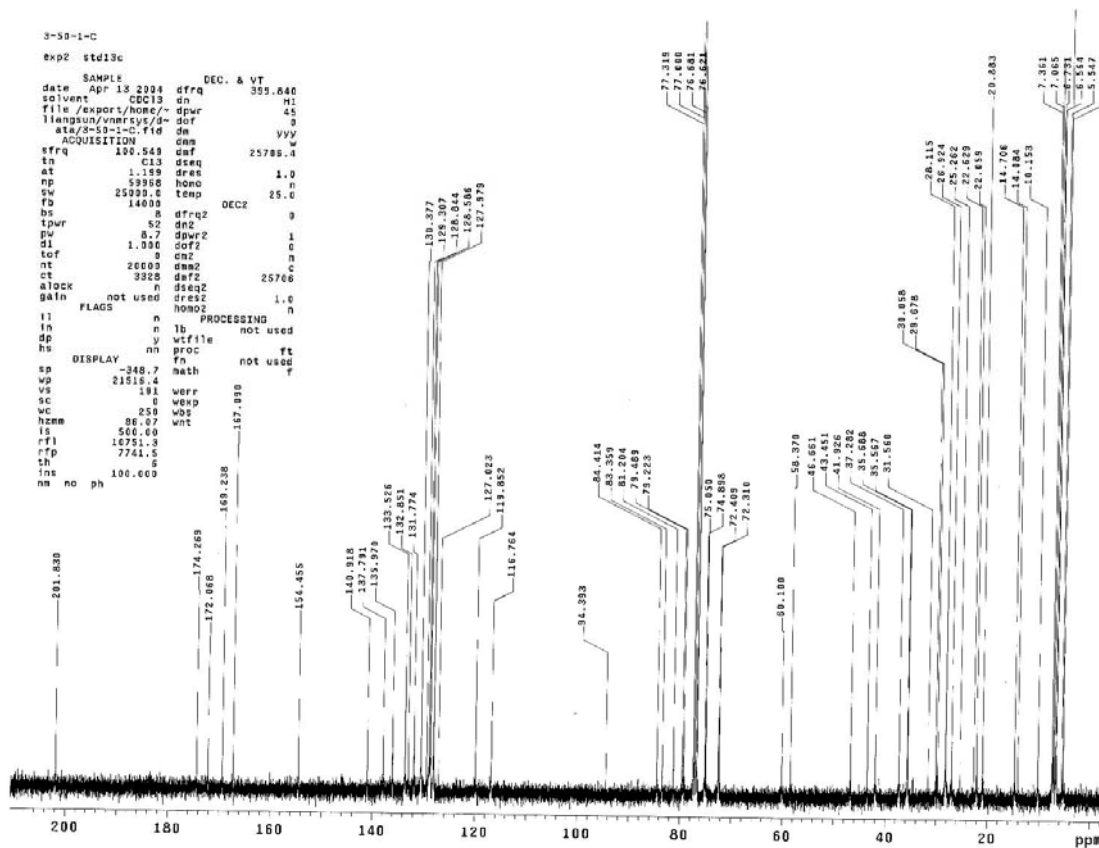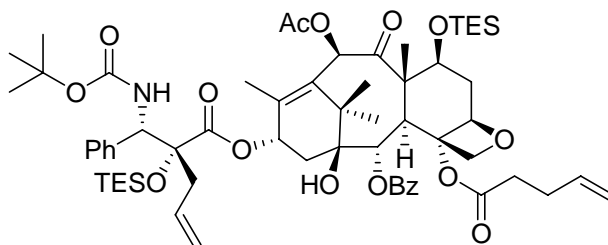
^{1}H NMR Spectrum of **3-13**
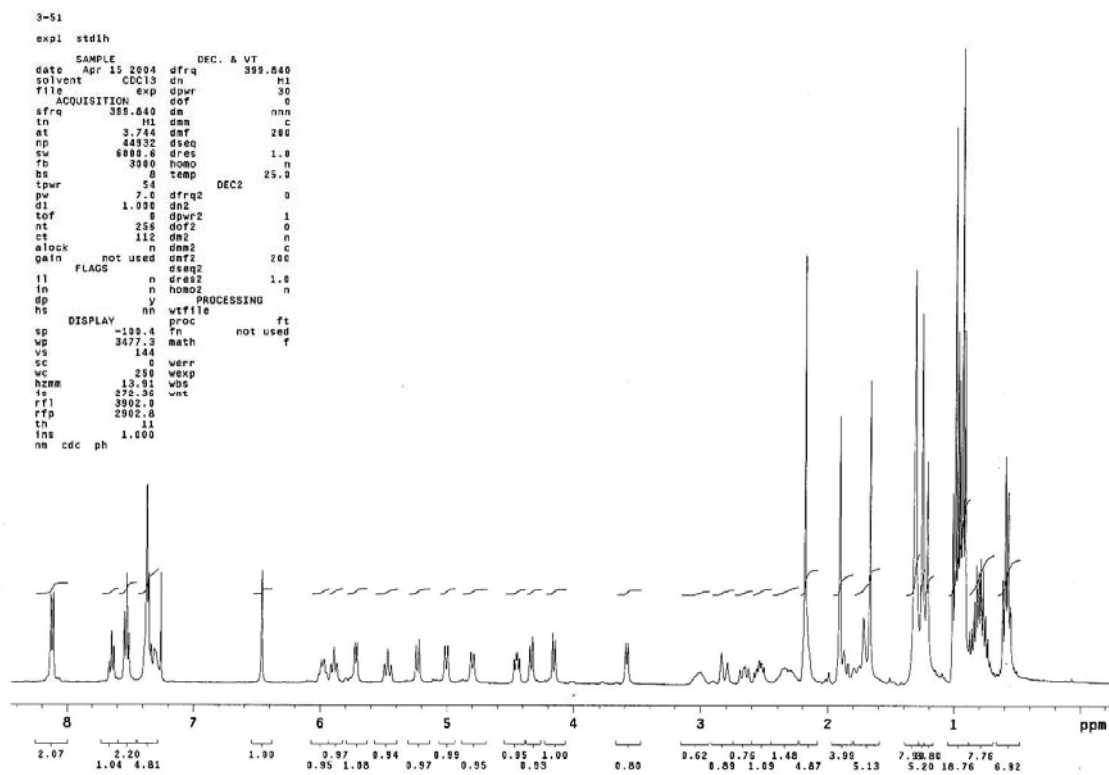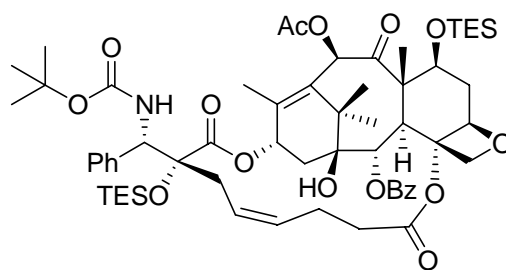
^{13}C NMR Spectrum of **3-13**
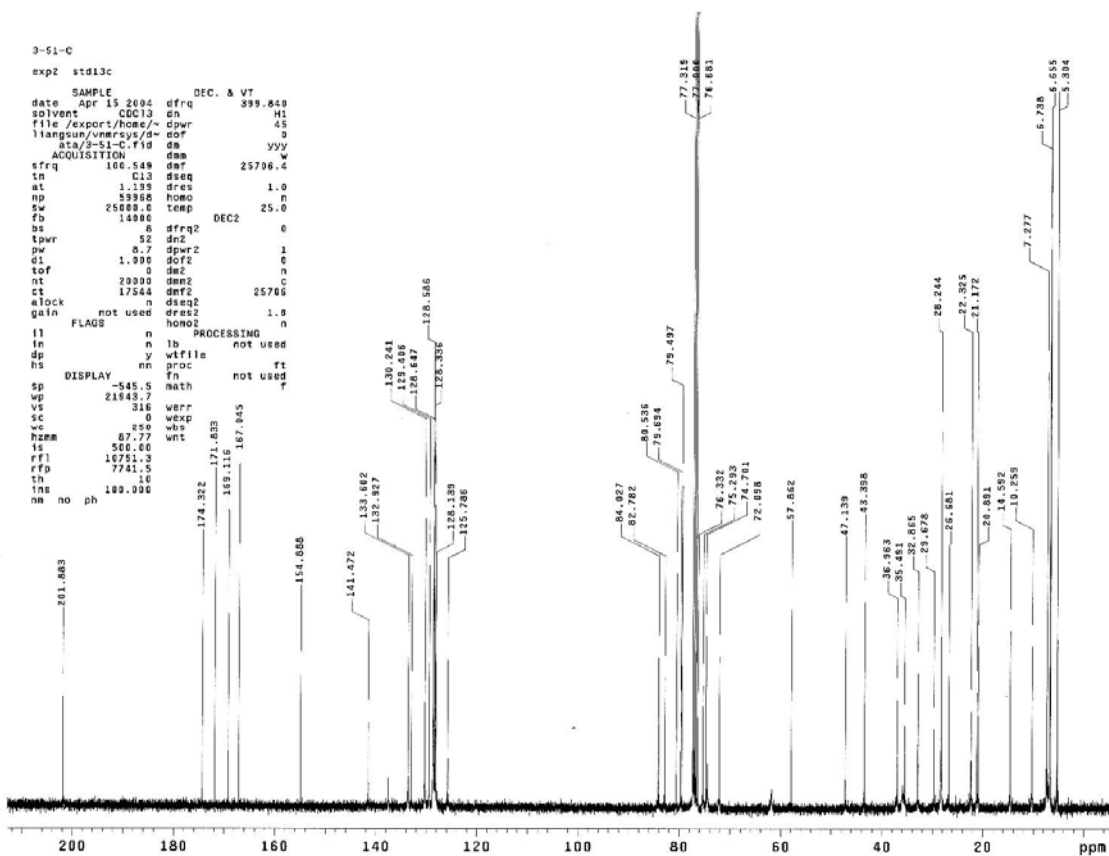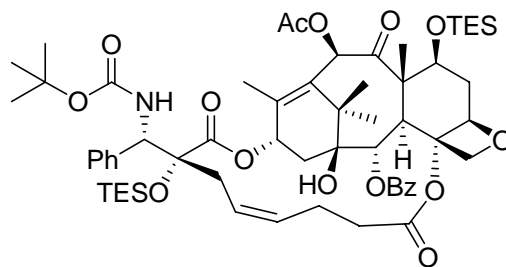
^{1}H NMR Spectrum of **SB-TCR-102**
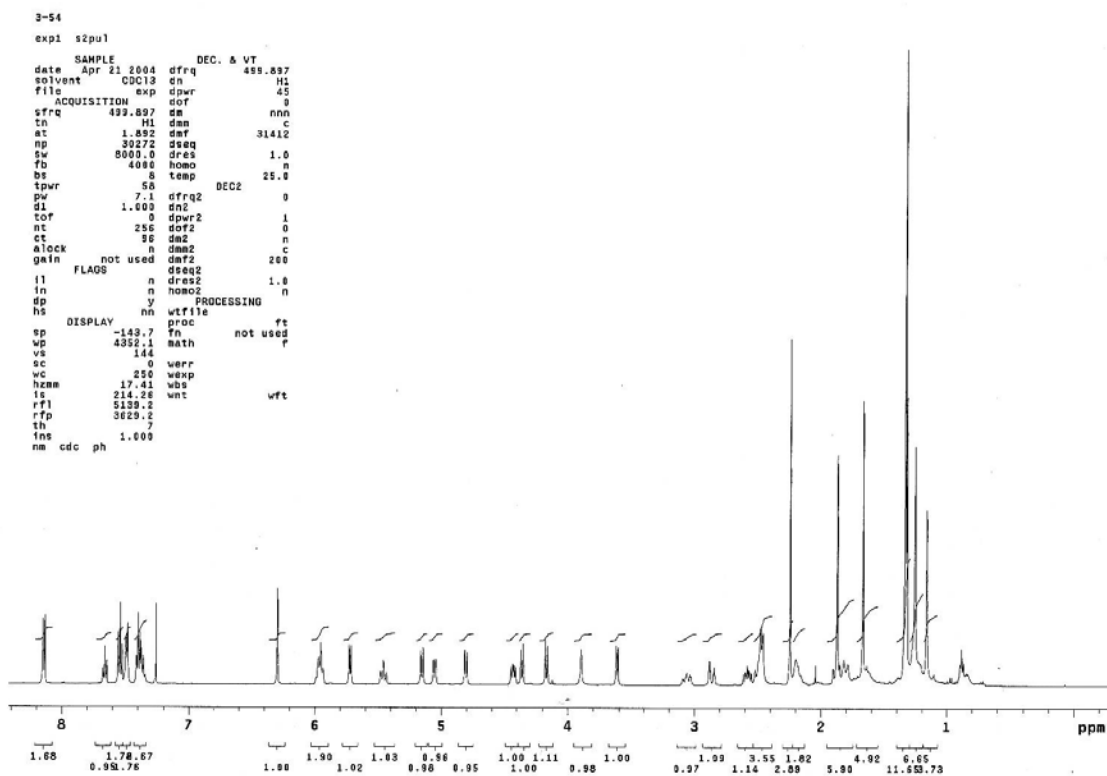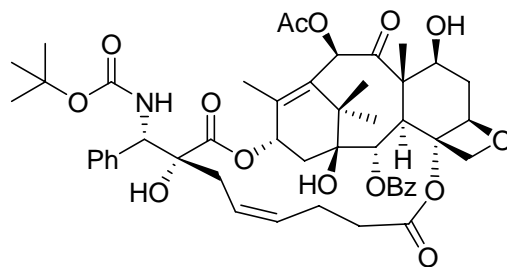
¹³C NMR Spectrum of **SB-TCR-102**
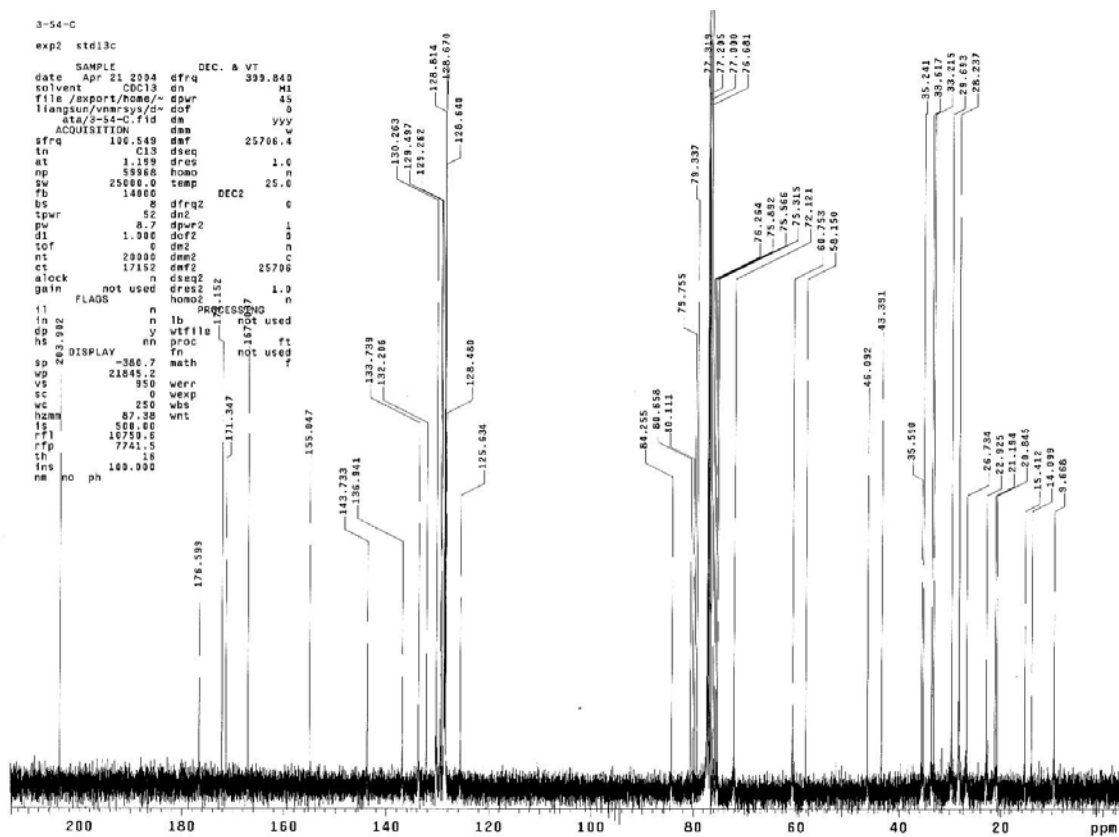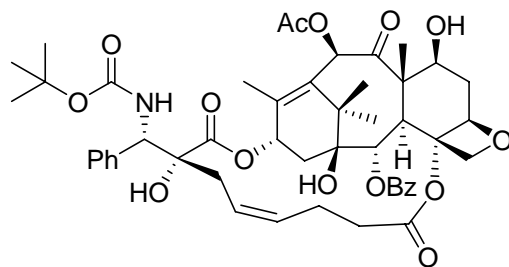
^{1}H NMR Spectrum of **3-19**
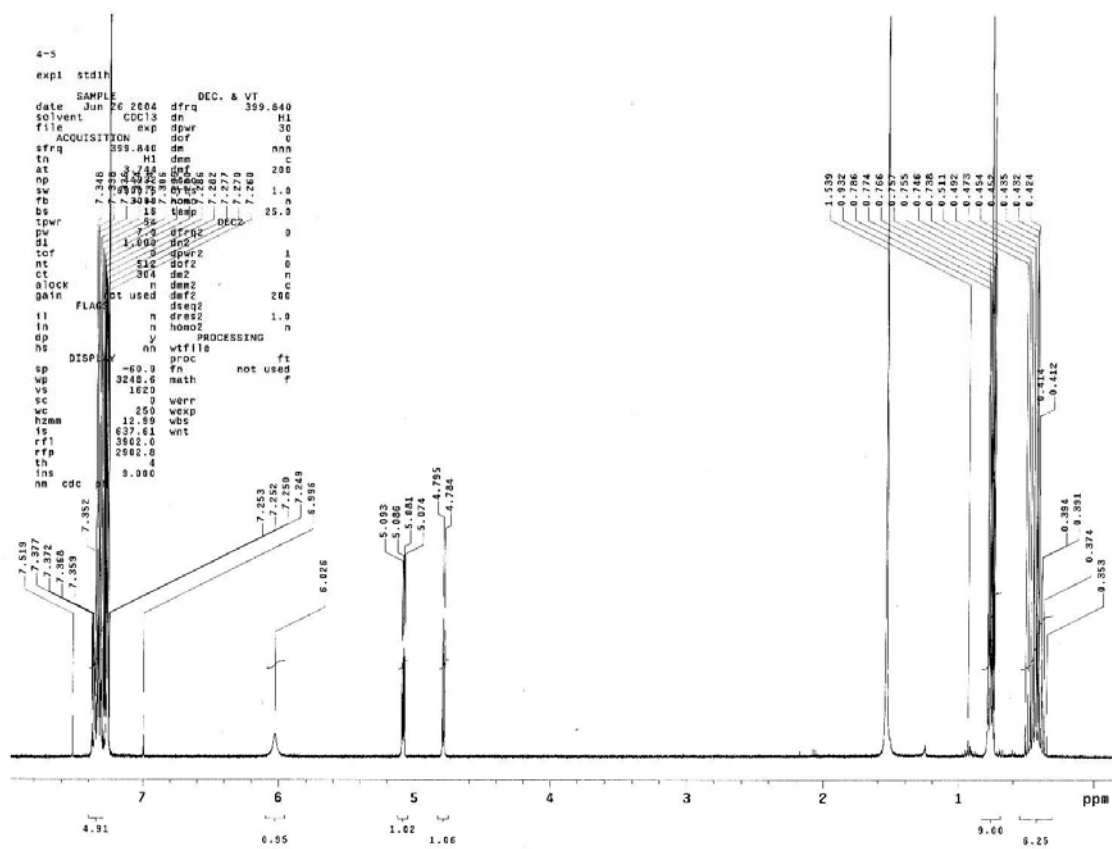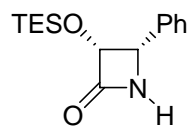
^{13}C NMR Spectrum of **3-19**
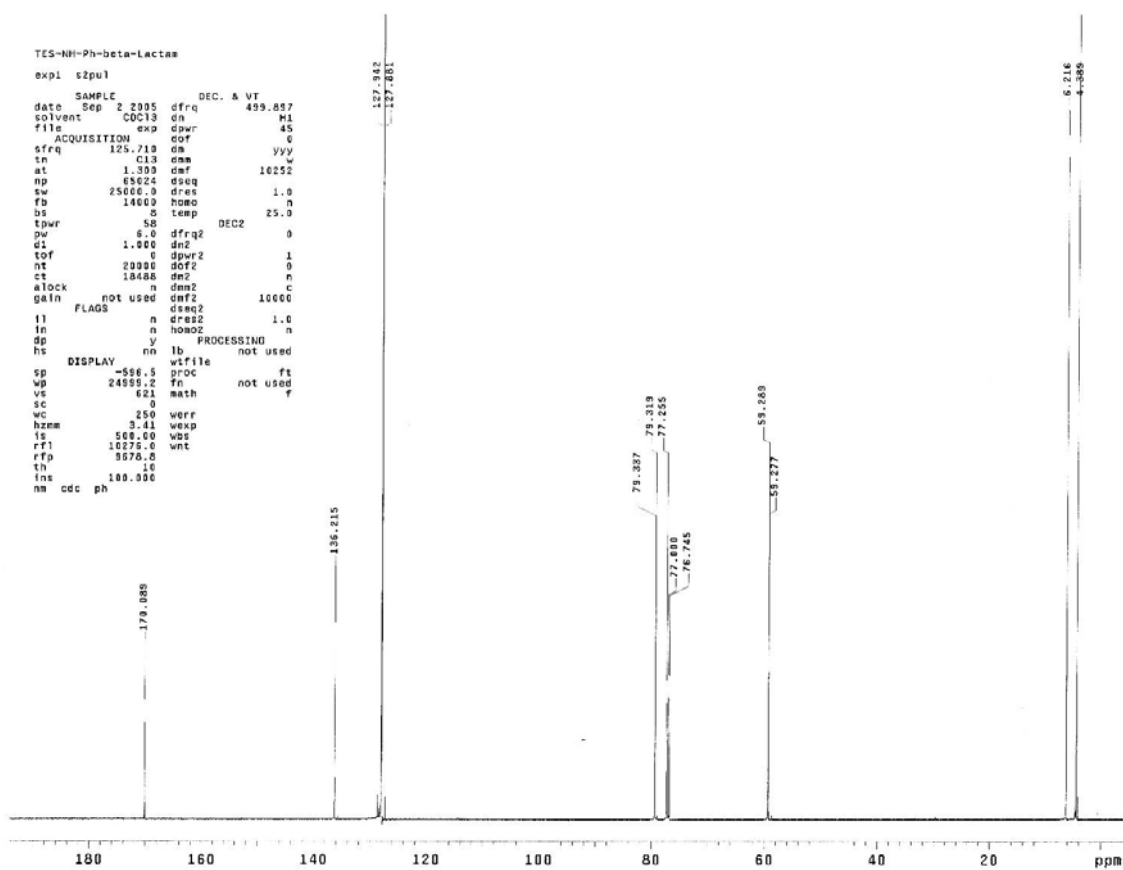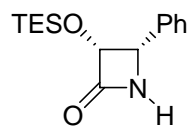
^{1}H NMR Spectrum of **3-23**
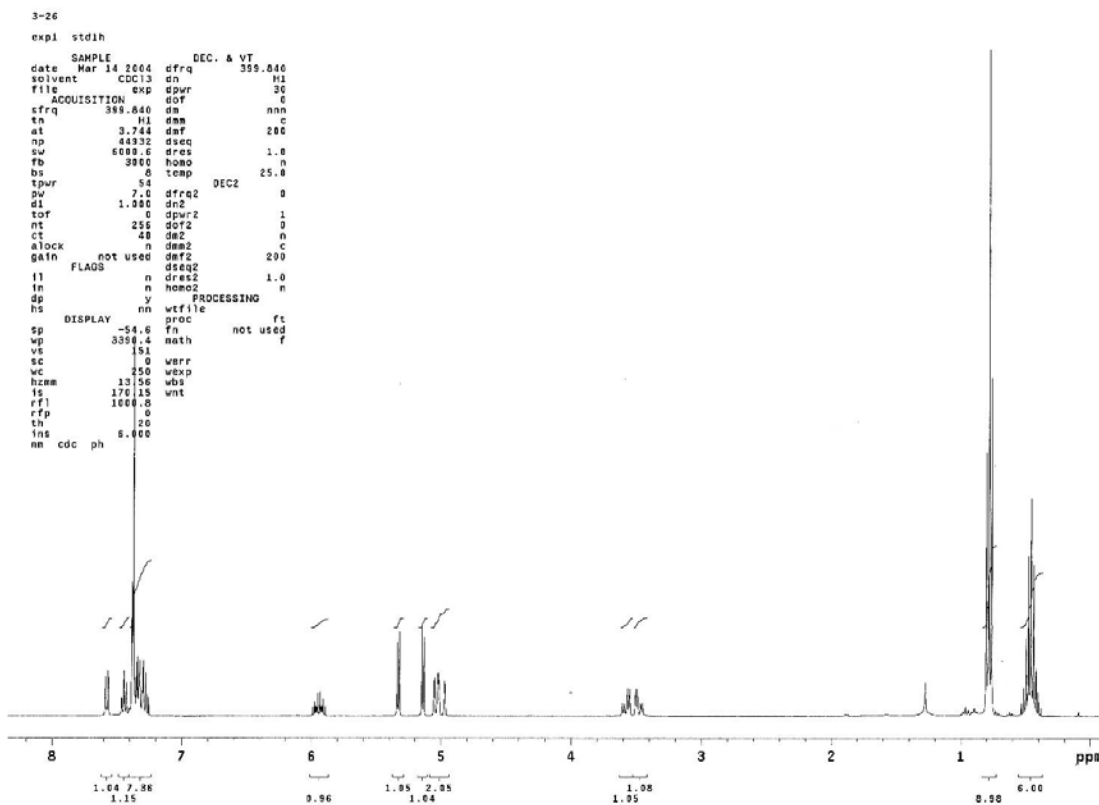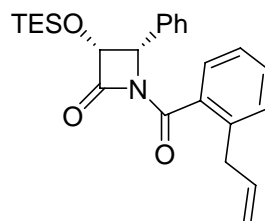
^{13}C NMR Spectrum of **3-23**
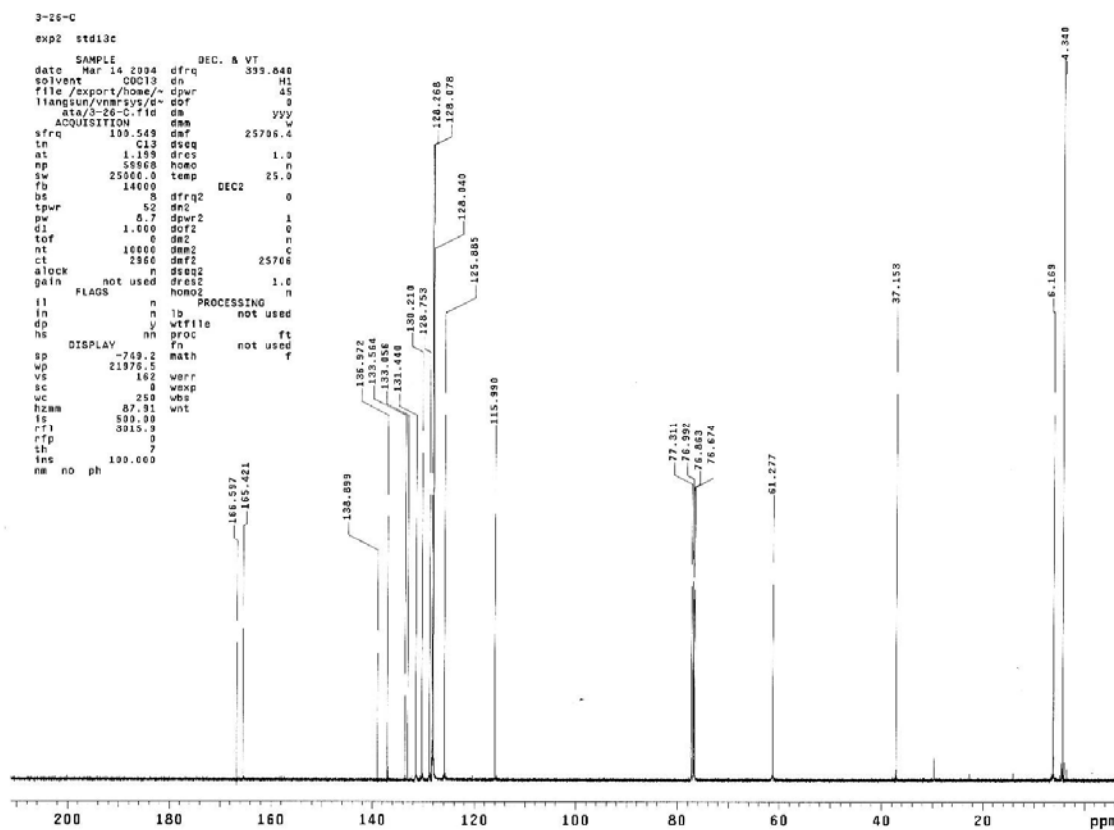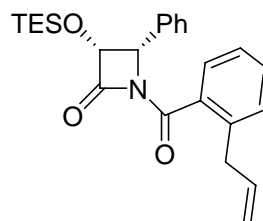
^{1}H NMR Spectrum of **3-24**
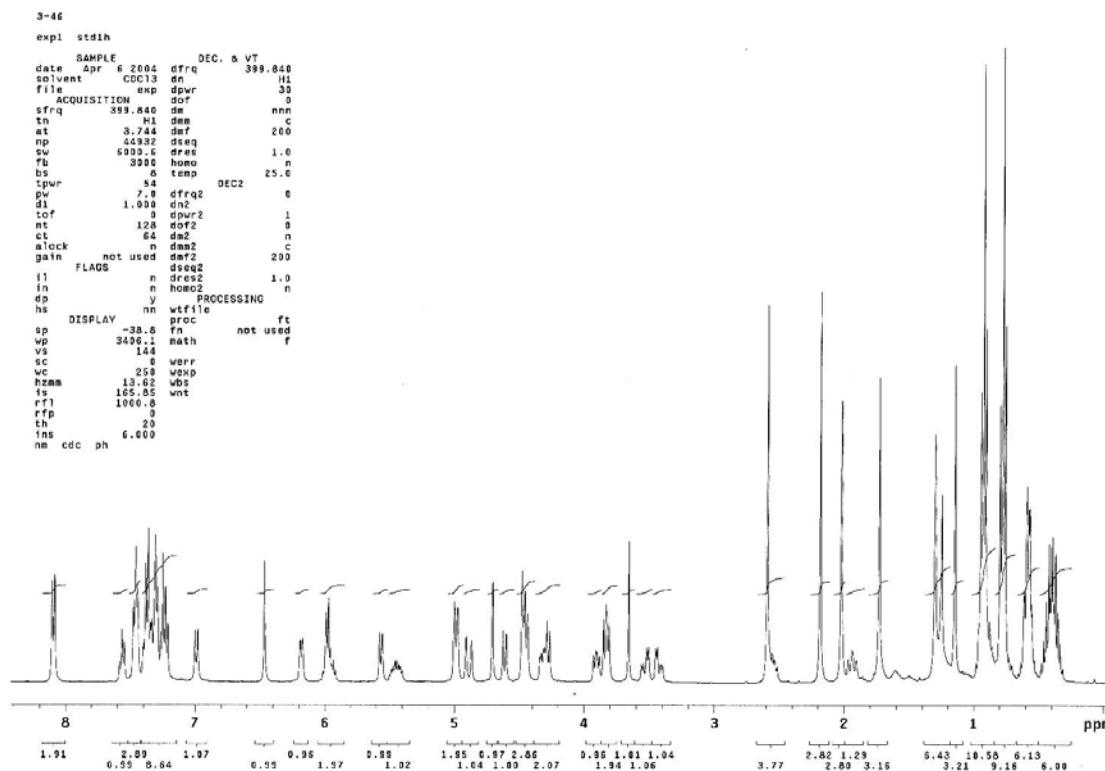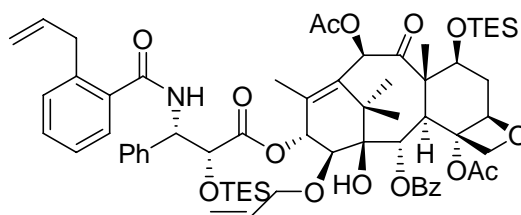
^{13}C NMR Spectrum of **3-24**
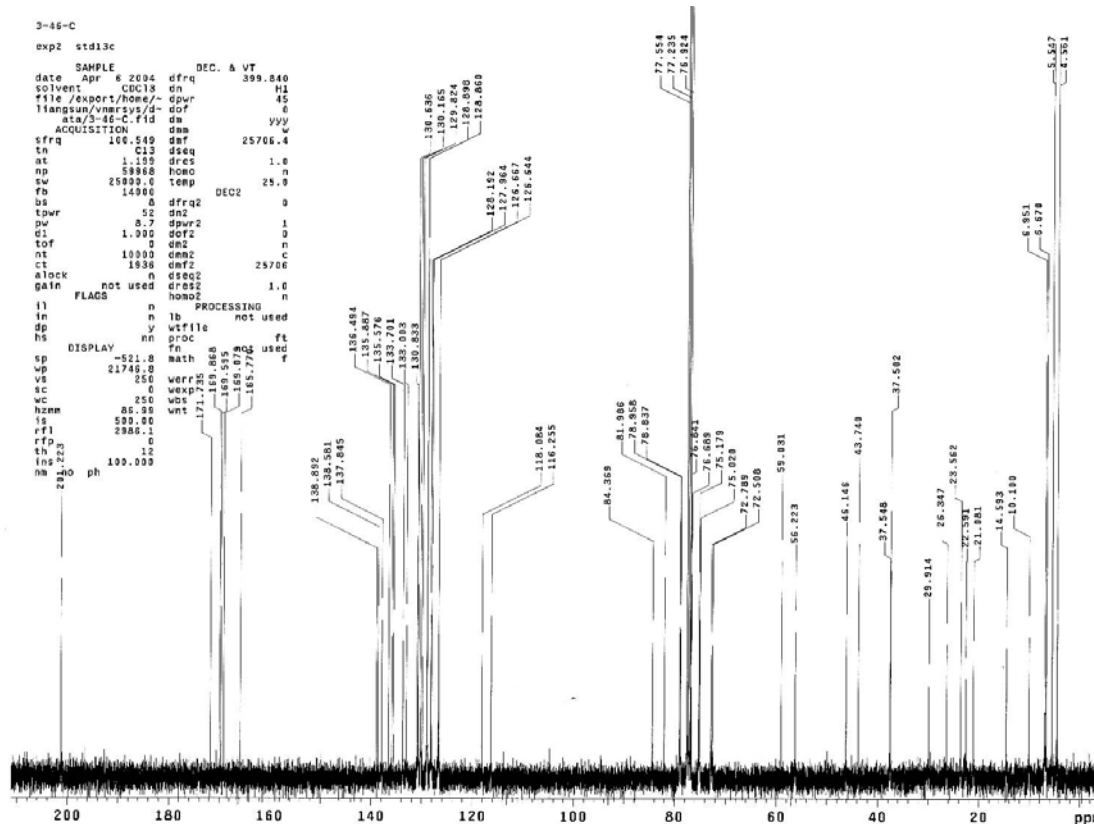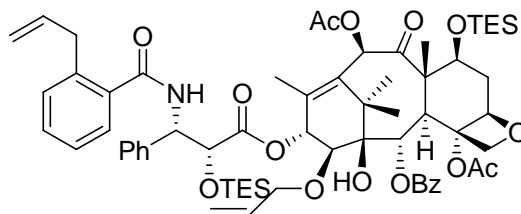
^{1}H NMR Spectrum of **3-25**
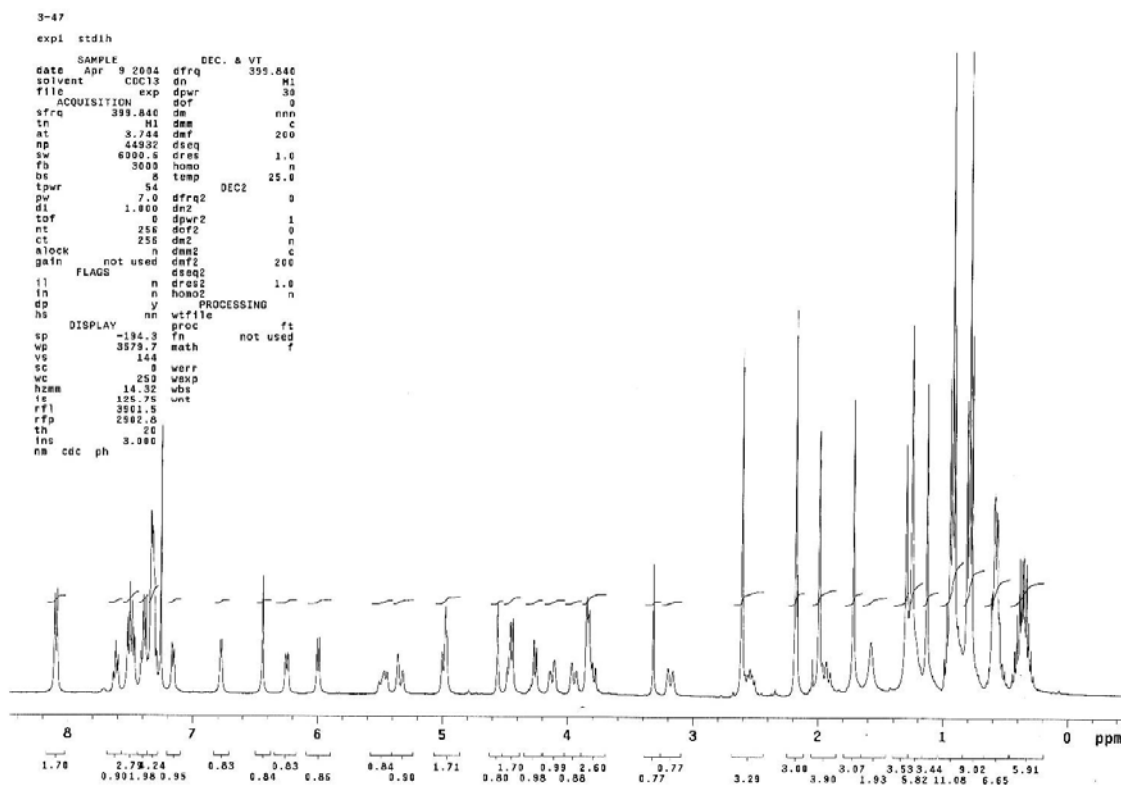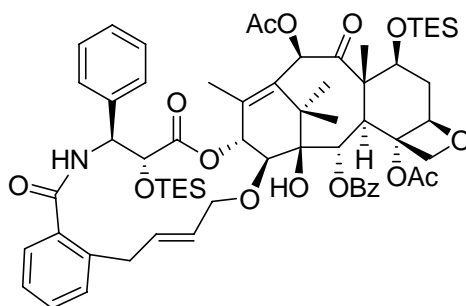
^{13}C NMR Spectrum of **3-25**
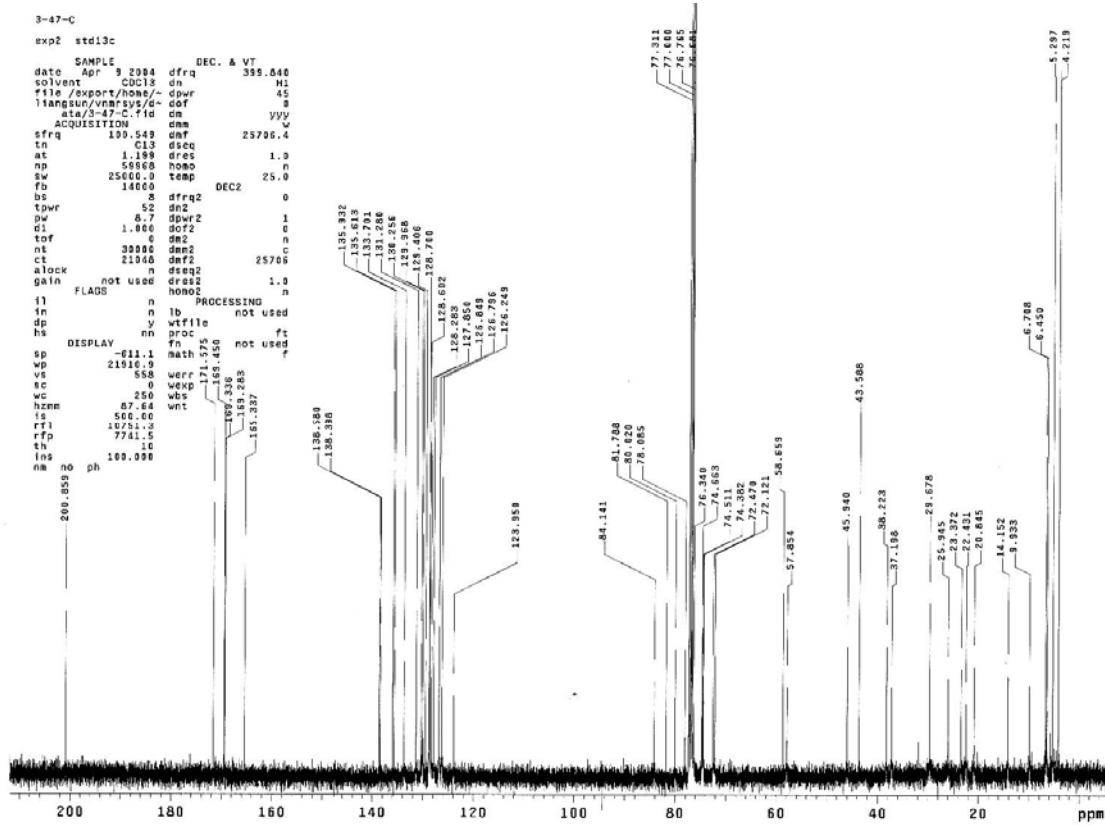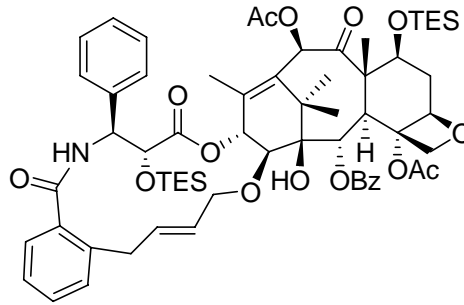
^{1}H NMR Spectrum of **SB-T-2053**
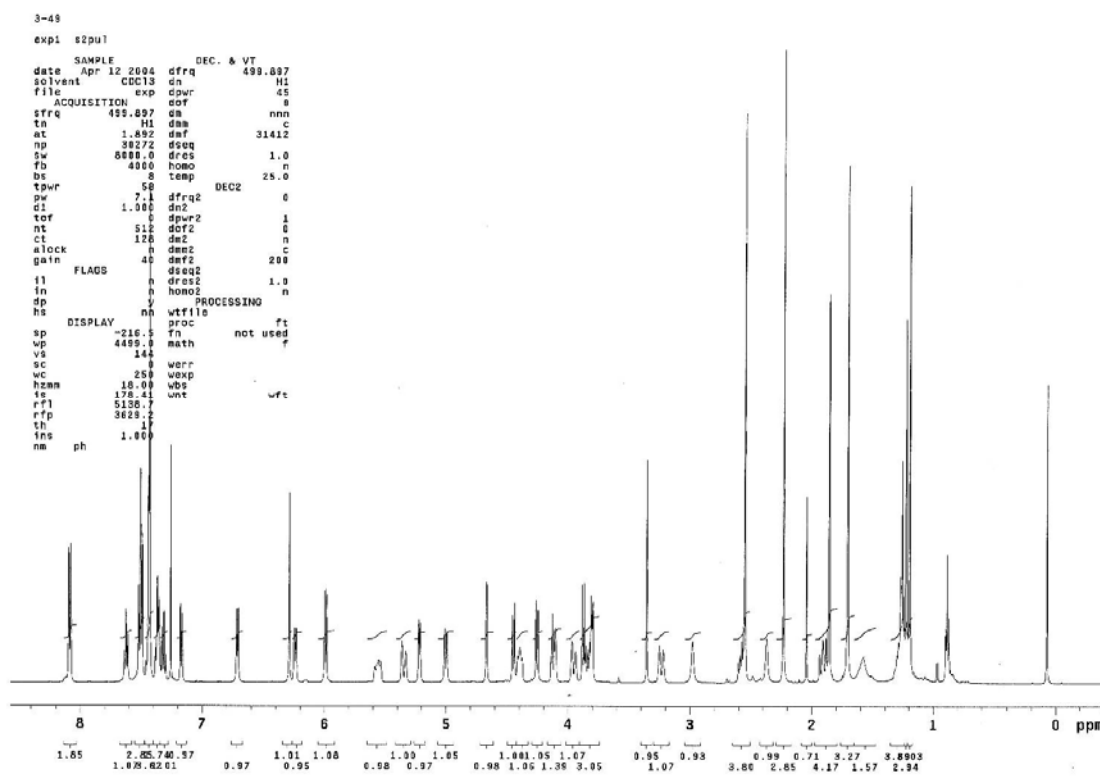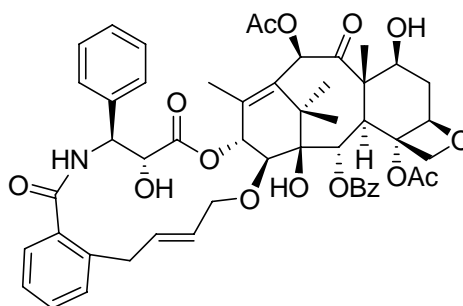
^{13}C NMR Spectrum of **SB-T-2053**
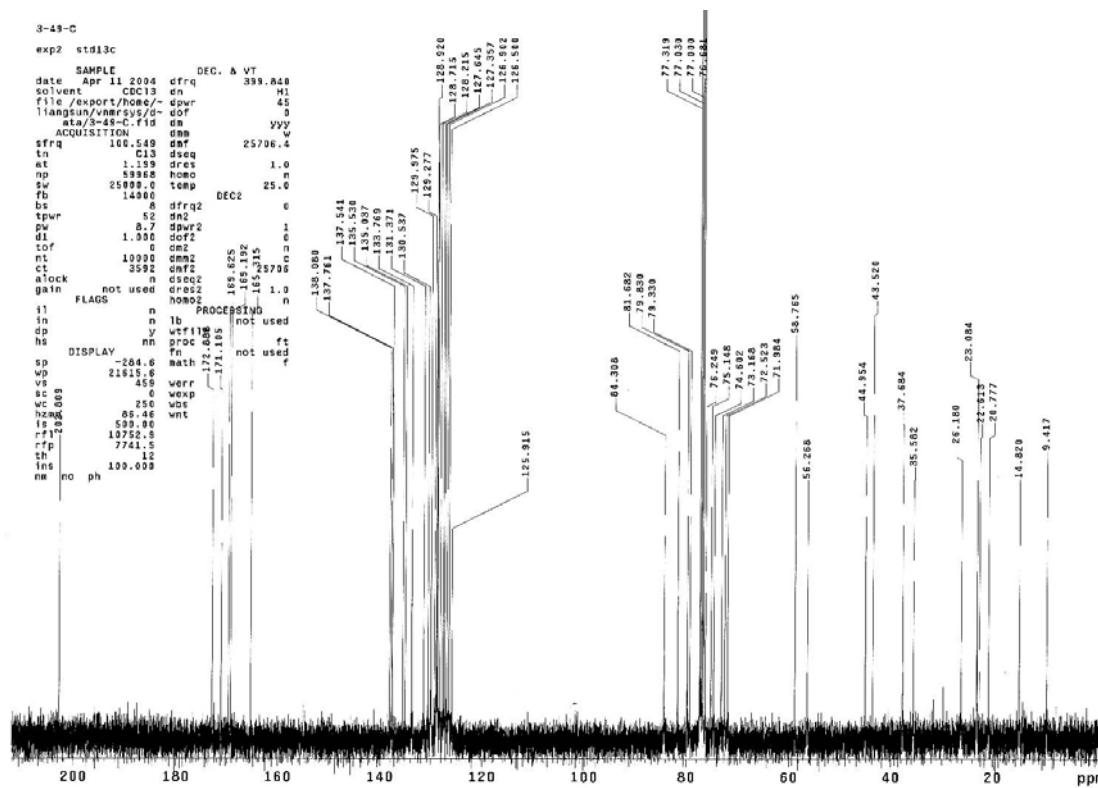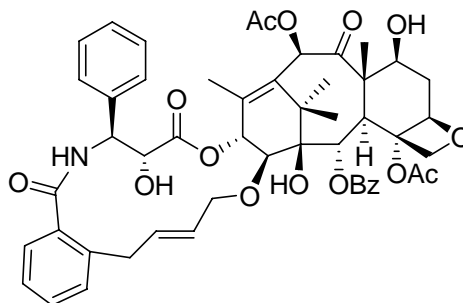
^{1}H NMR Spectrum of **3-26**
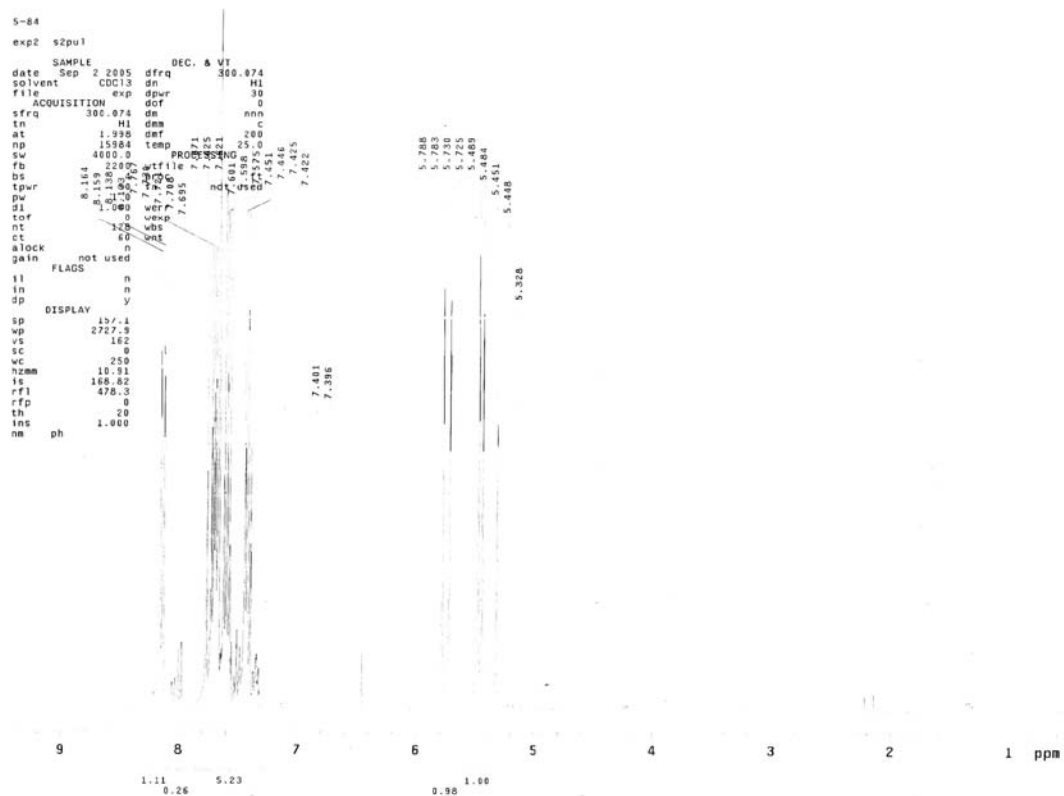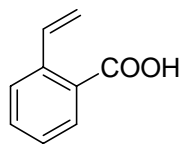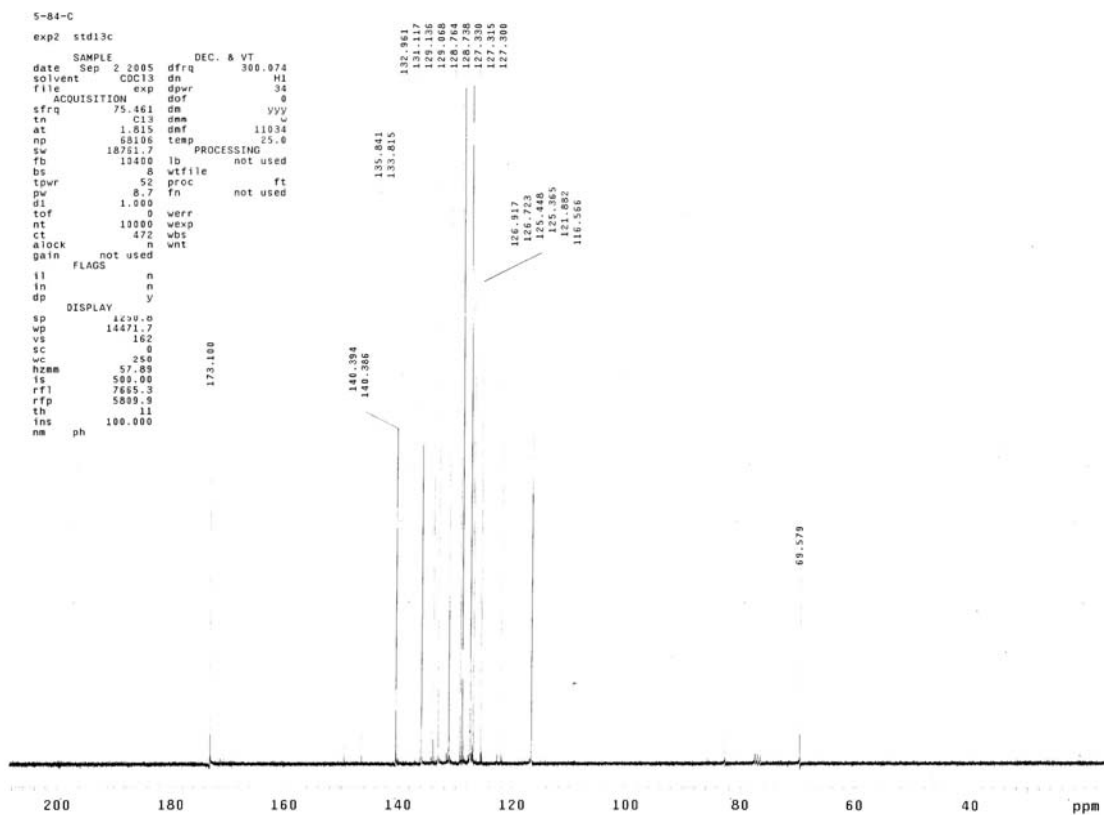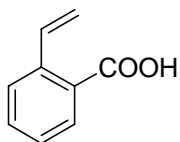
^{1}H NMR Spectrum of **3-27**
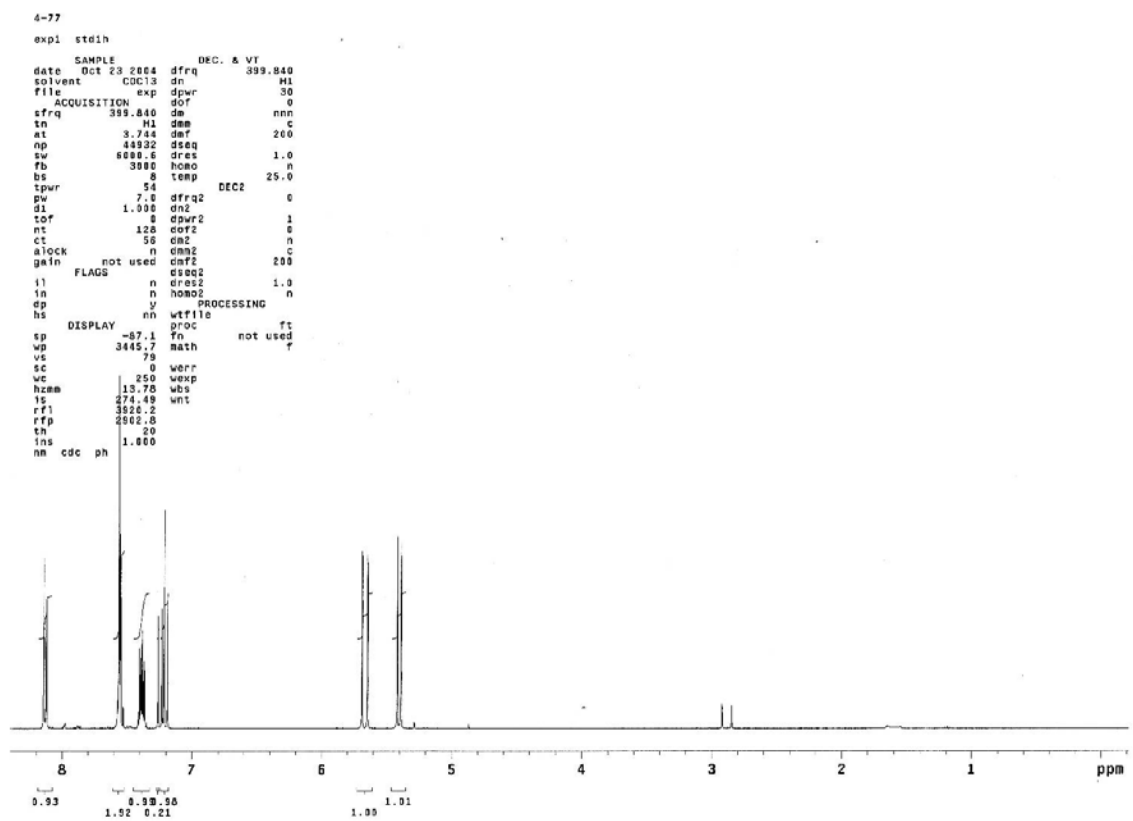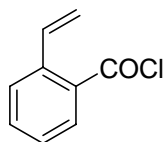
^{13}C NMR Spectrum of **3-27**
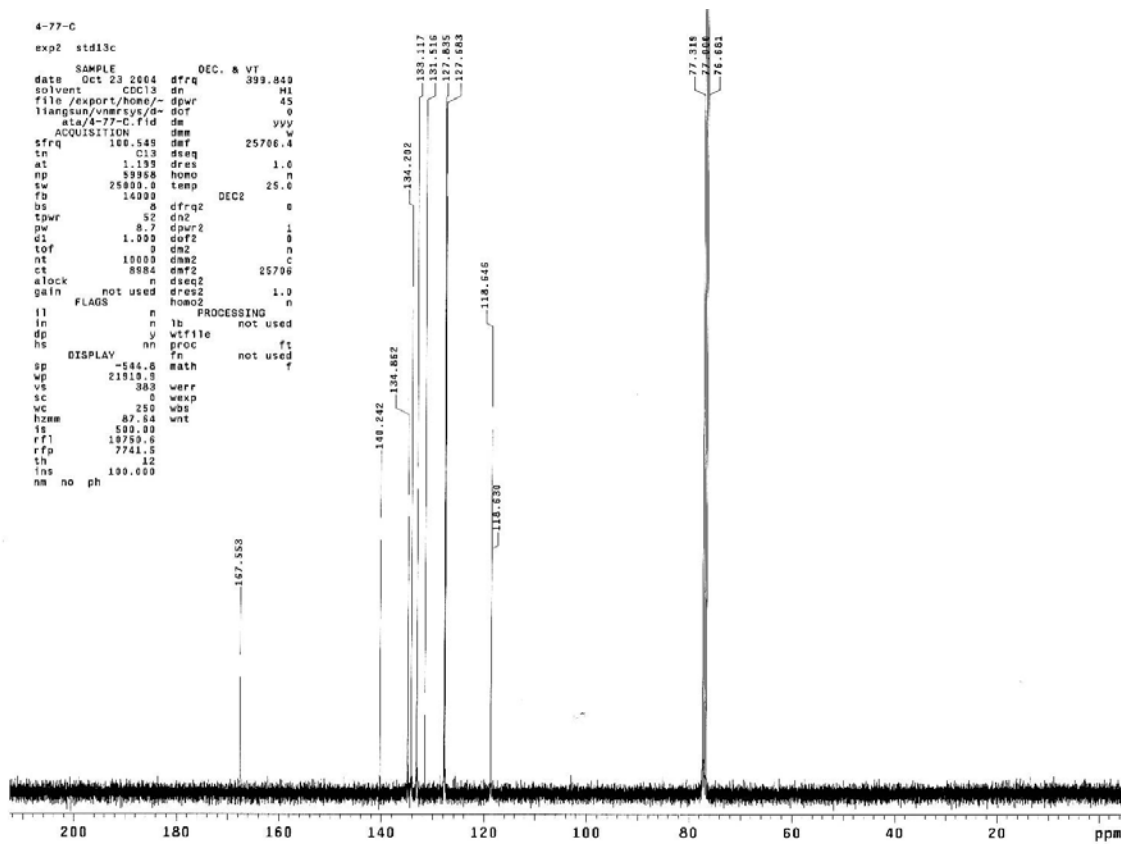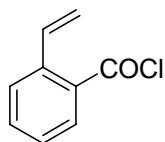
^{13}C NMR Spectrum of **3-28**
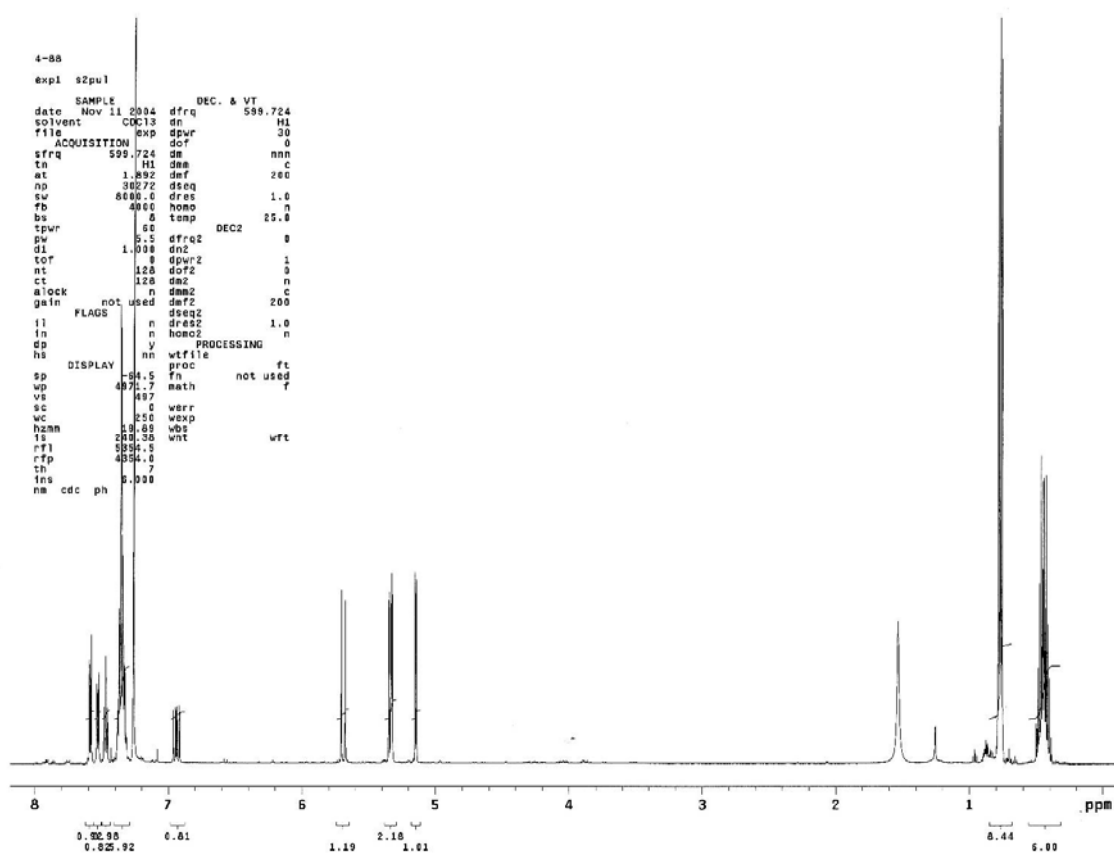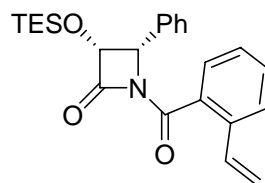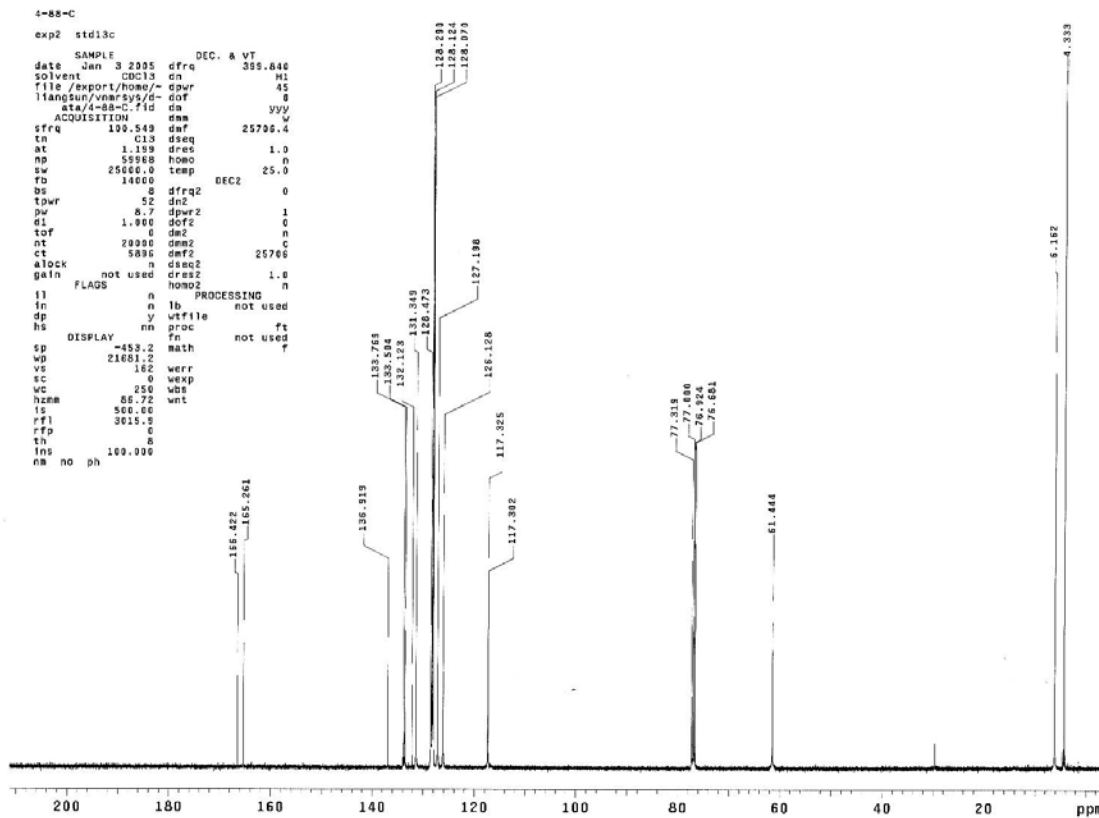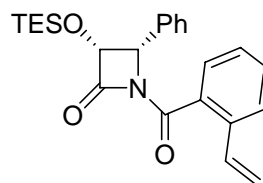
^{1}H NMR Spectrum of **3-29**
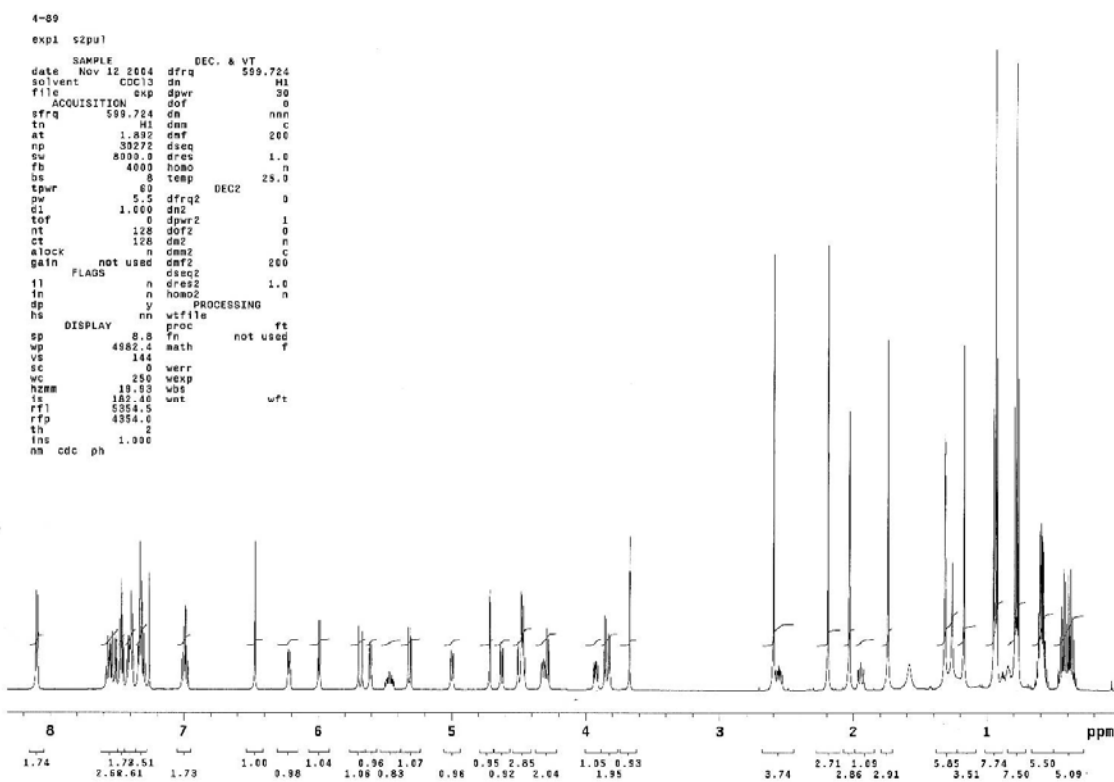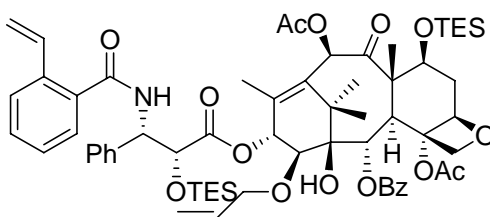
^{13}C NMR Spectrum of **3-29**
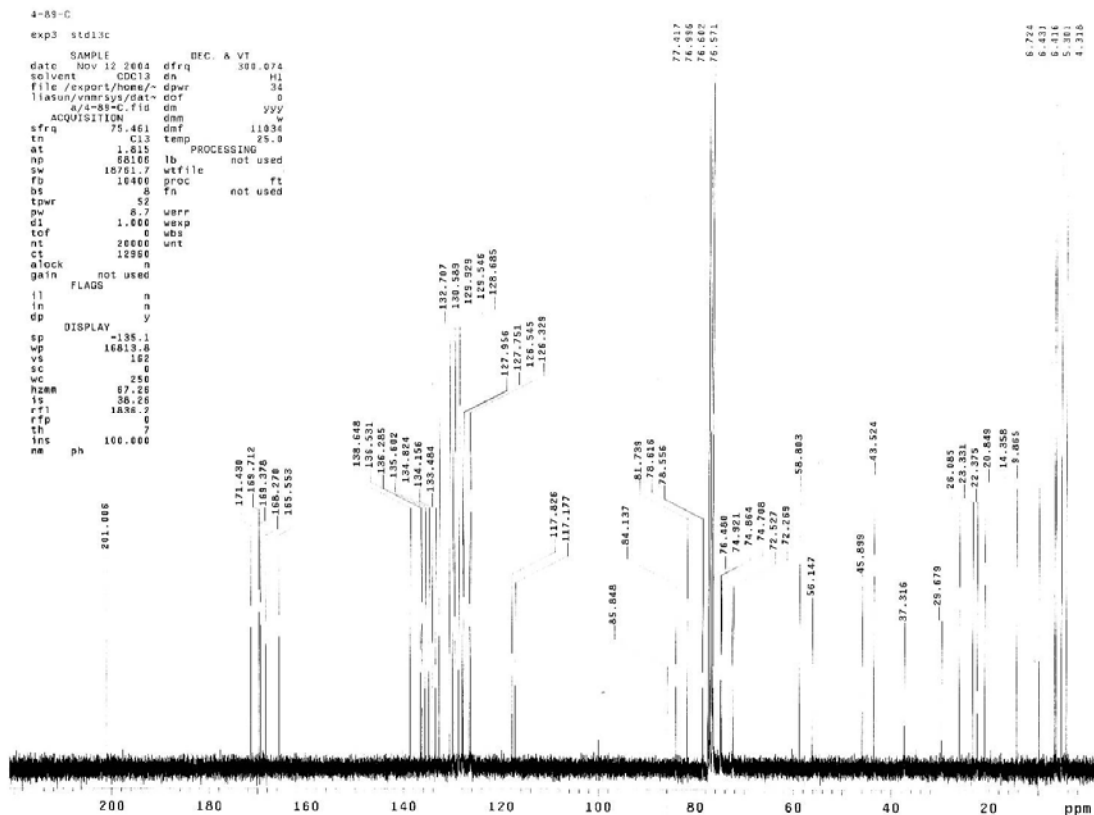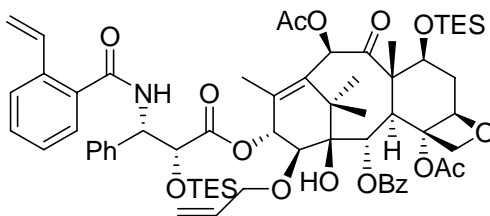
^{1}H NMR Spectrum of **3-30**
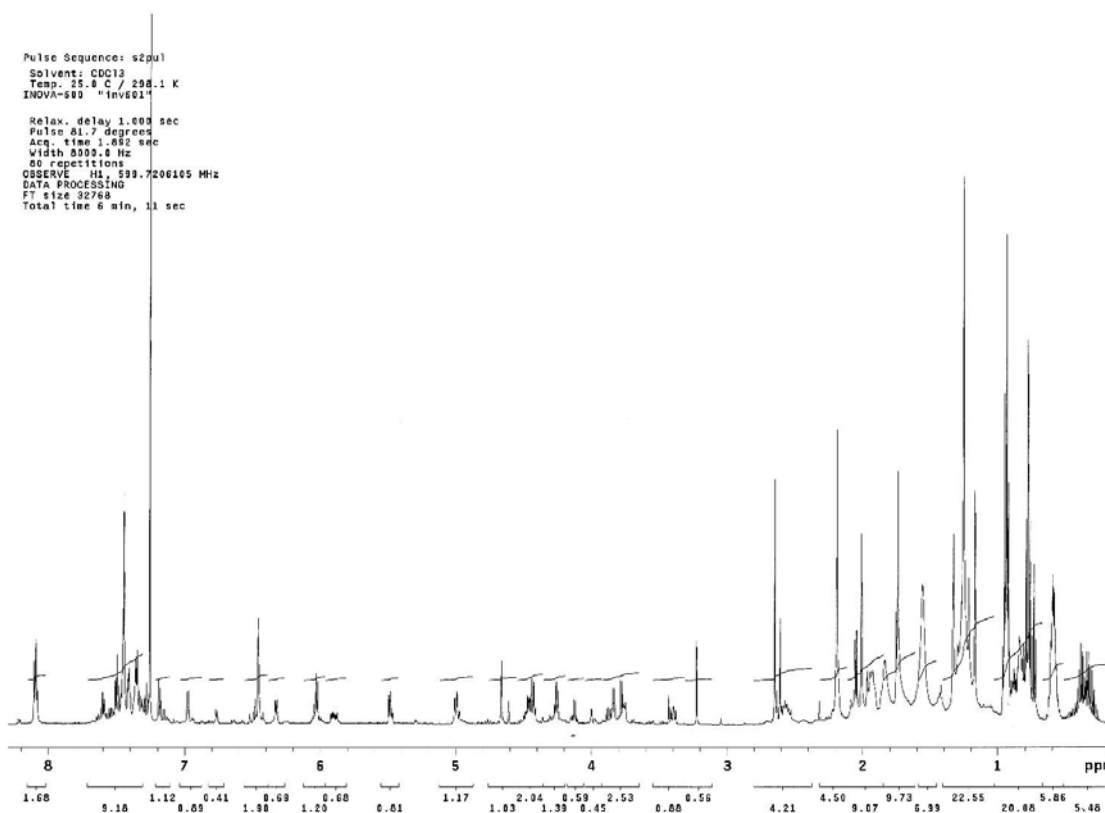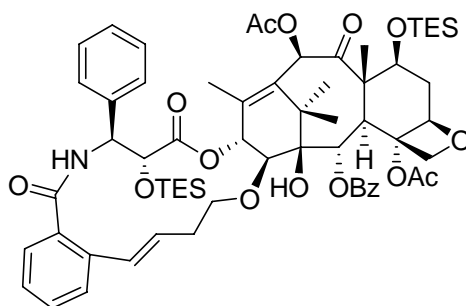
^{1}H NMR Spectrum of **SB-T-2054**
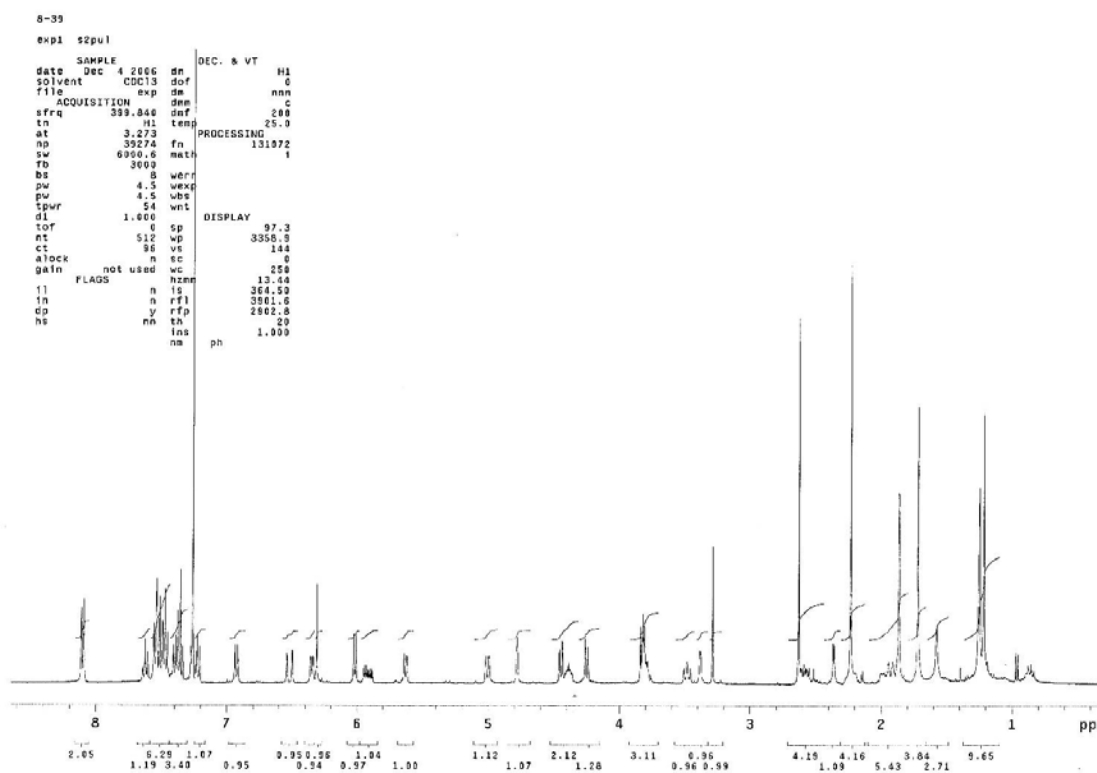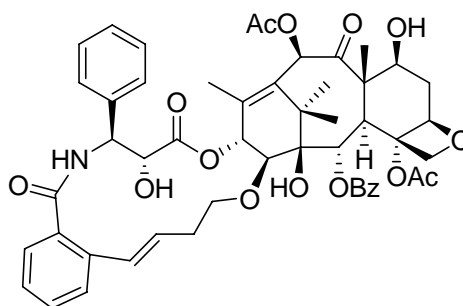
^{13}C NMR Spectrum of **SB-T-2054**

APT Spectrum of **SB-T-2054**
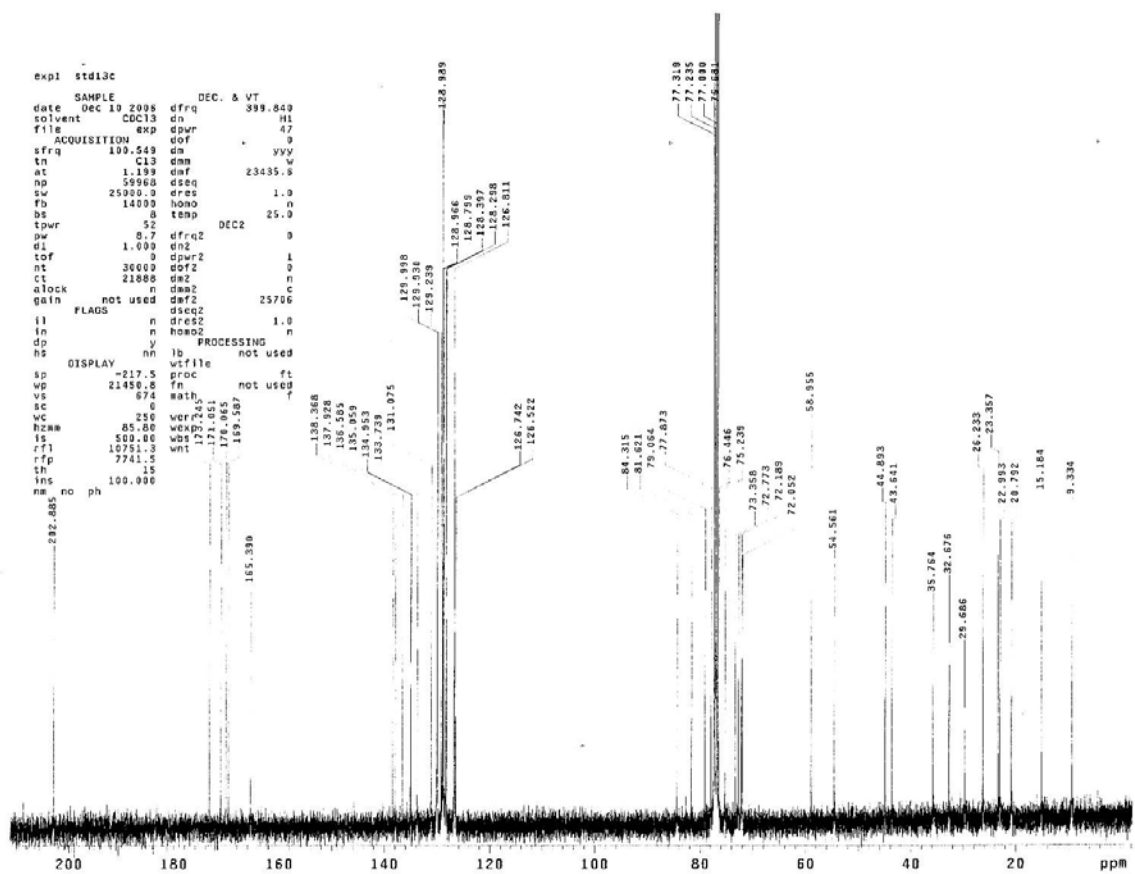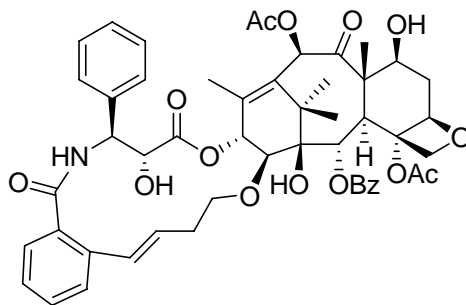
COSY Spectrum of **SB-T-2054**
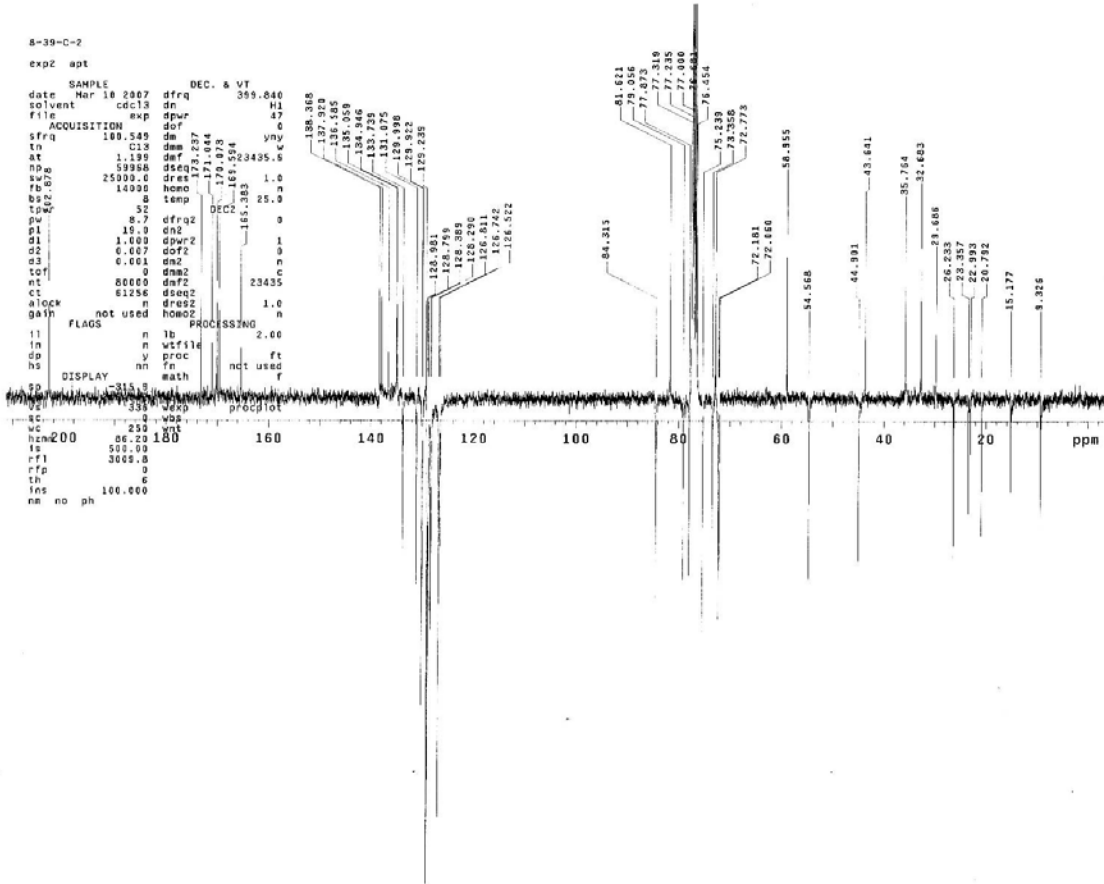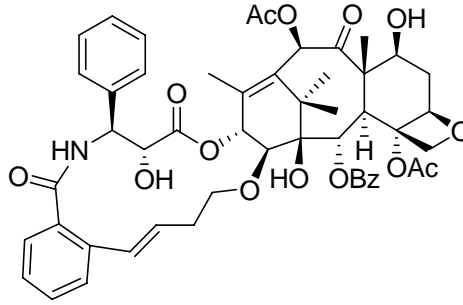
HMQC Spectrum of **SB-T-2054**

HMBC Spectrum of **SB-T-2054**

¹H NMR Spectrum of **3-31**
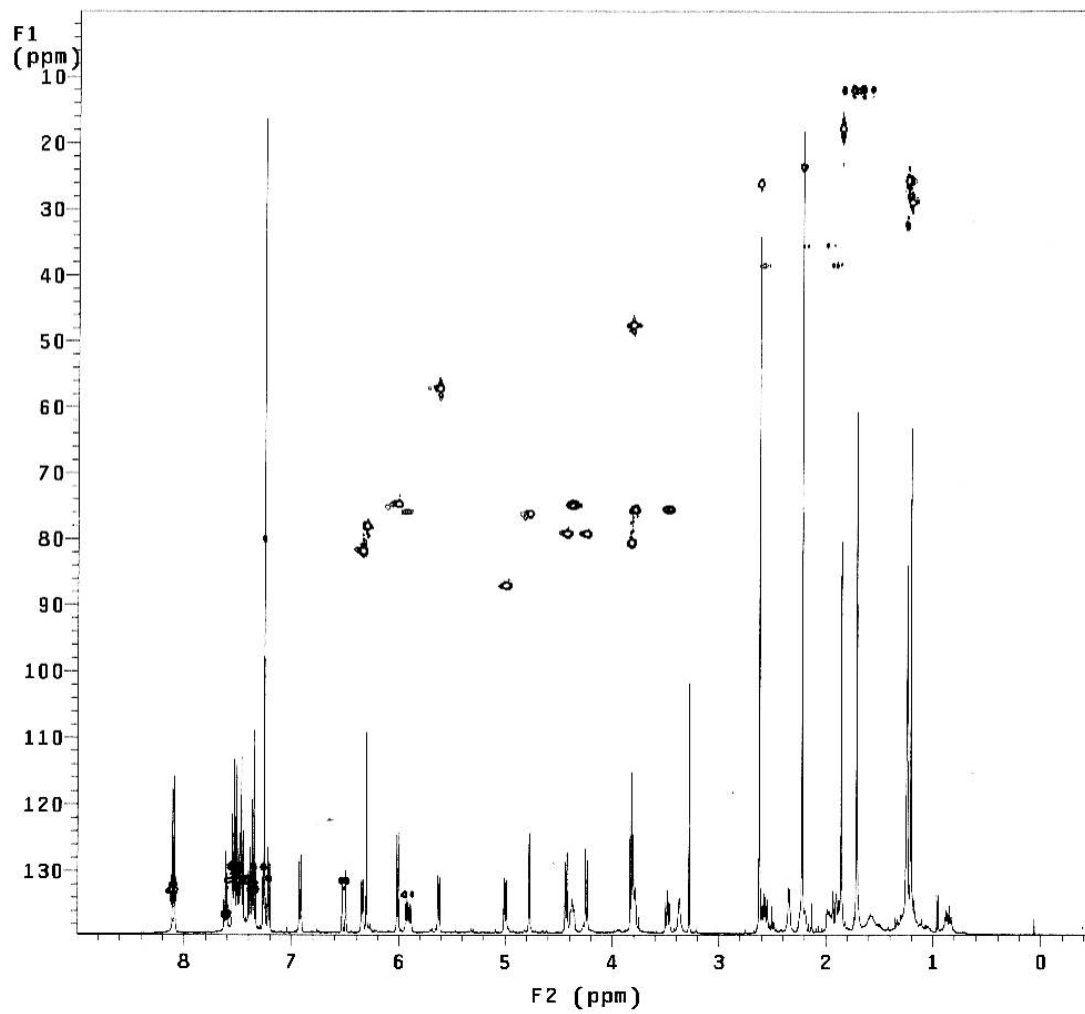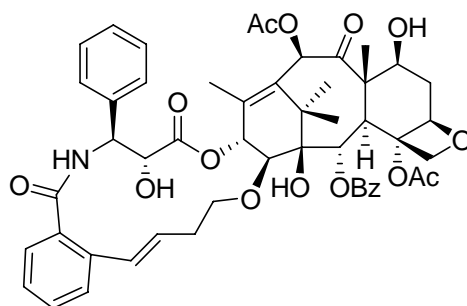
^{13}C NMR Spectrum of **3-31**
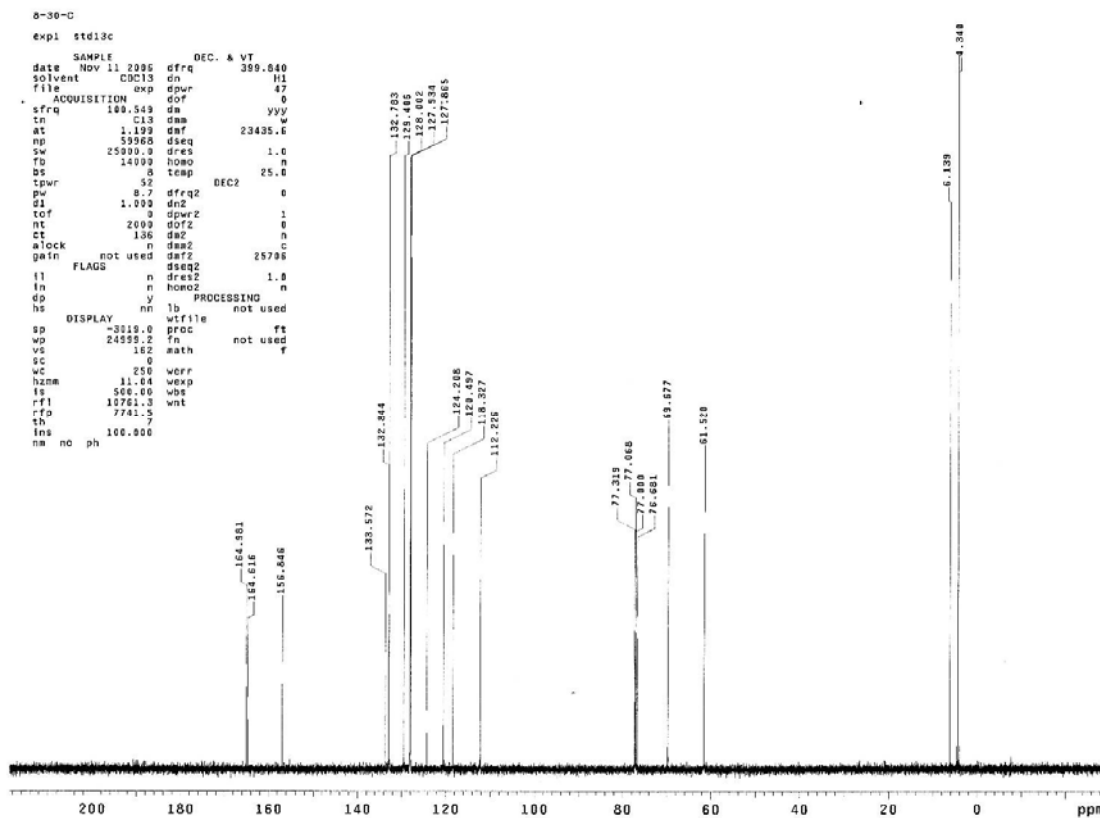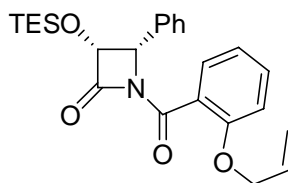
^{1}H NMR Spectrum of **3-32**
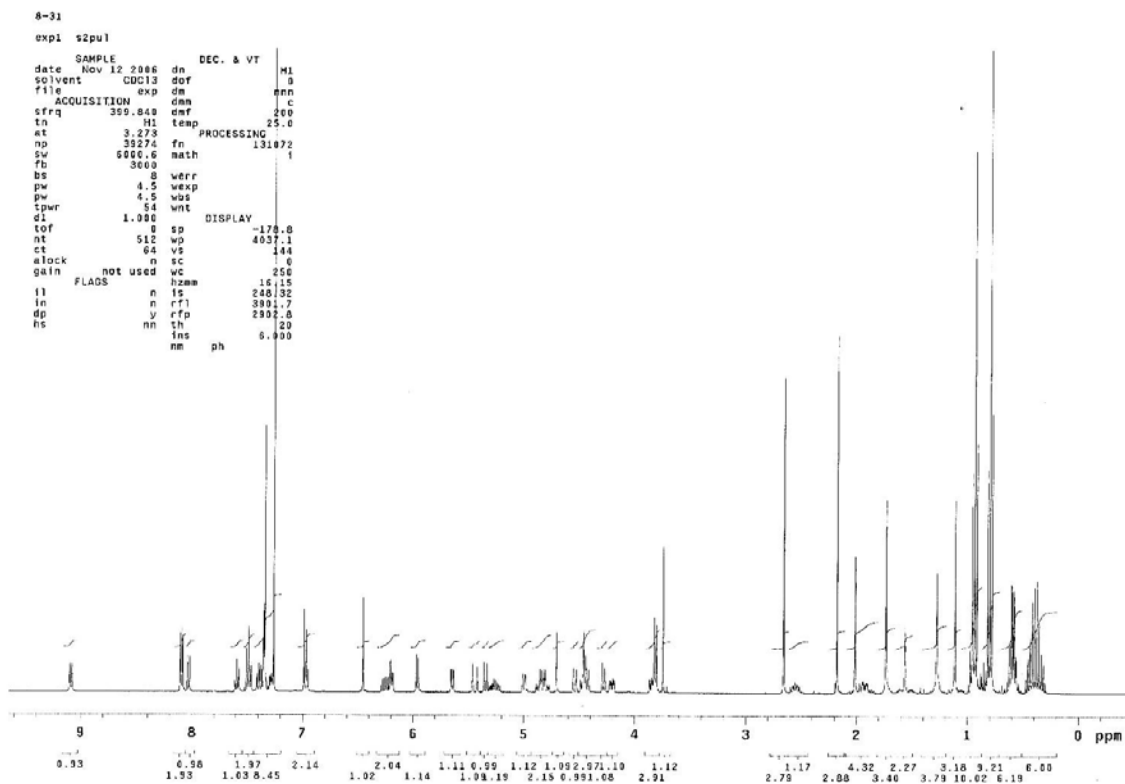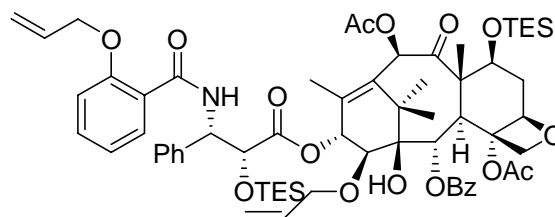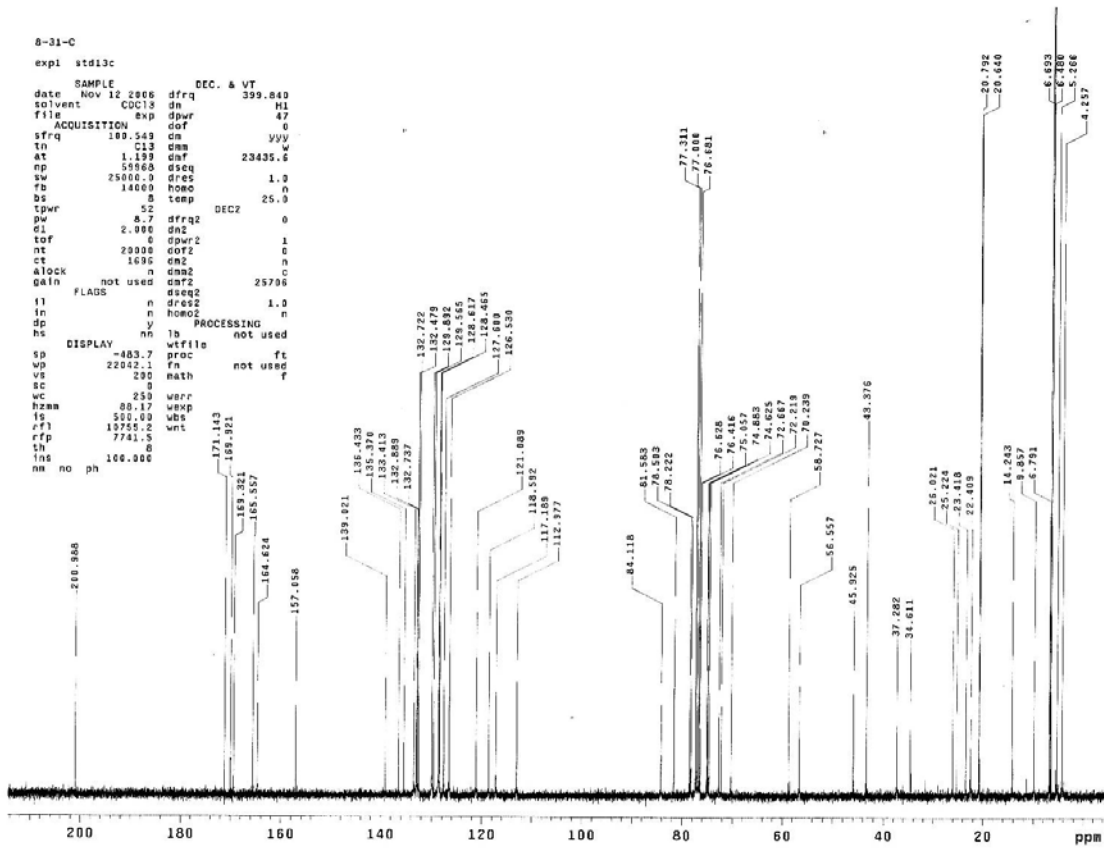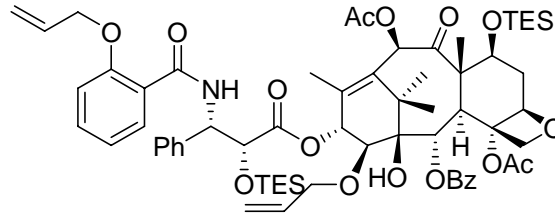
^{1}H NMR Spectrum of **3-33**
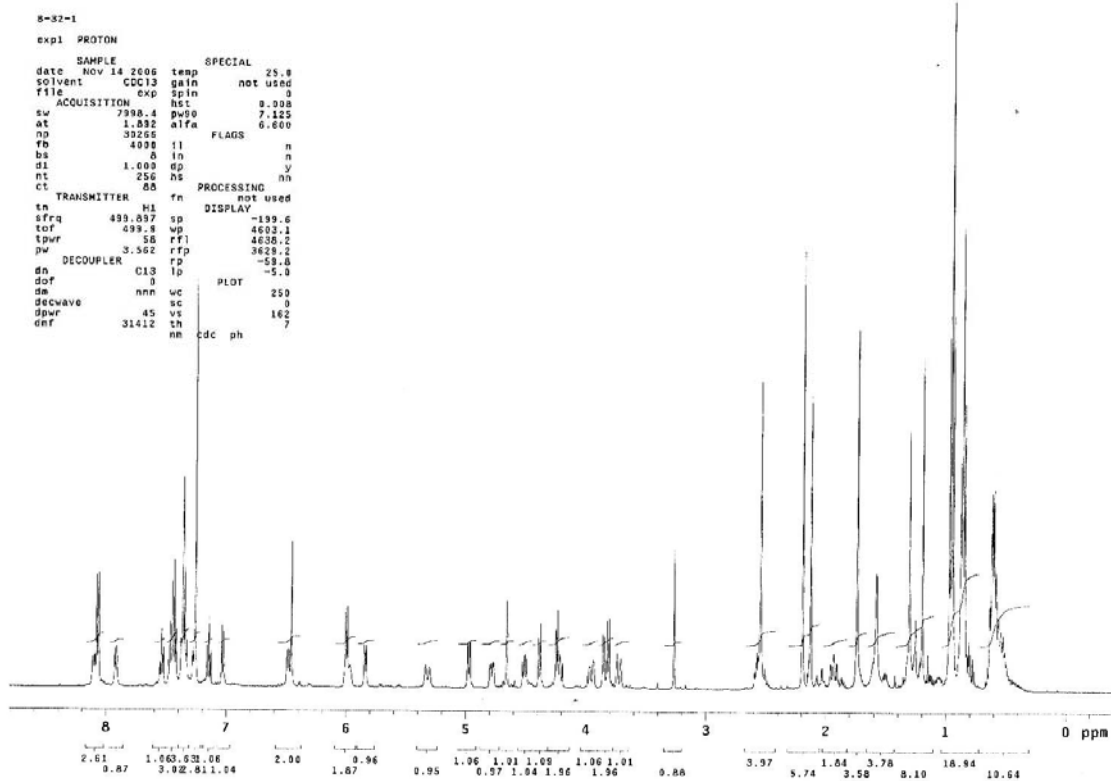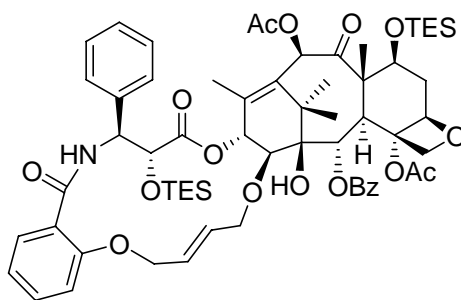
^{1}H NMR Spectrum of **3-34**
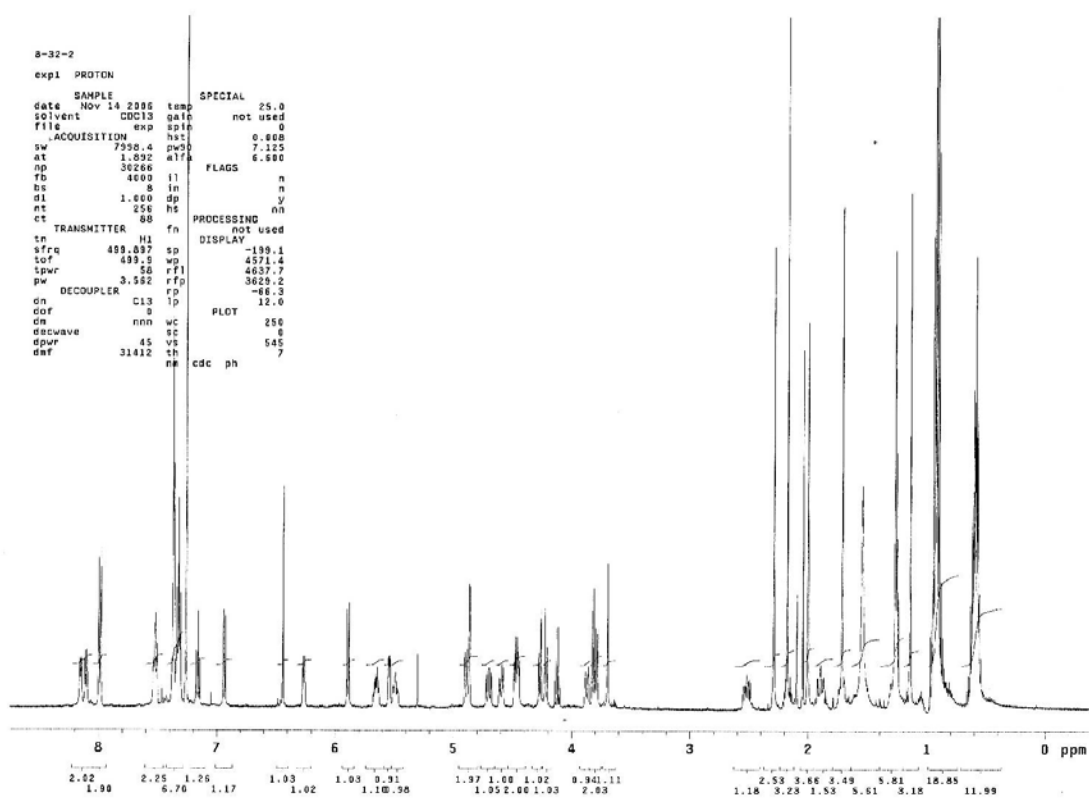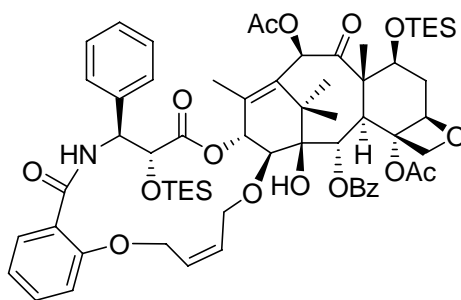
¹H NMR Spectrum of **SB-T-2055Z**
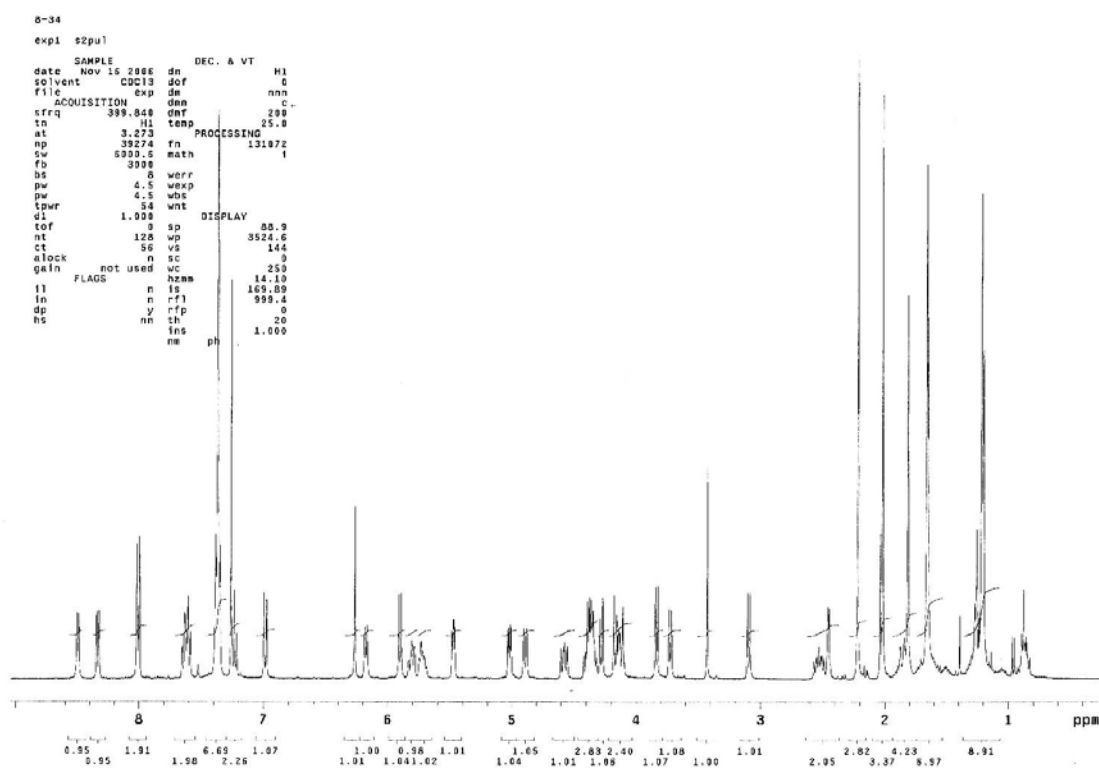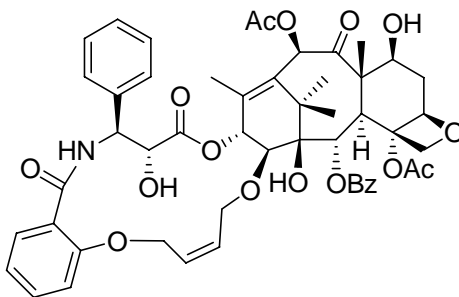
^{13}C NMR Spectrum of **SB-T-2055Z**
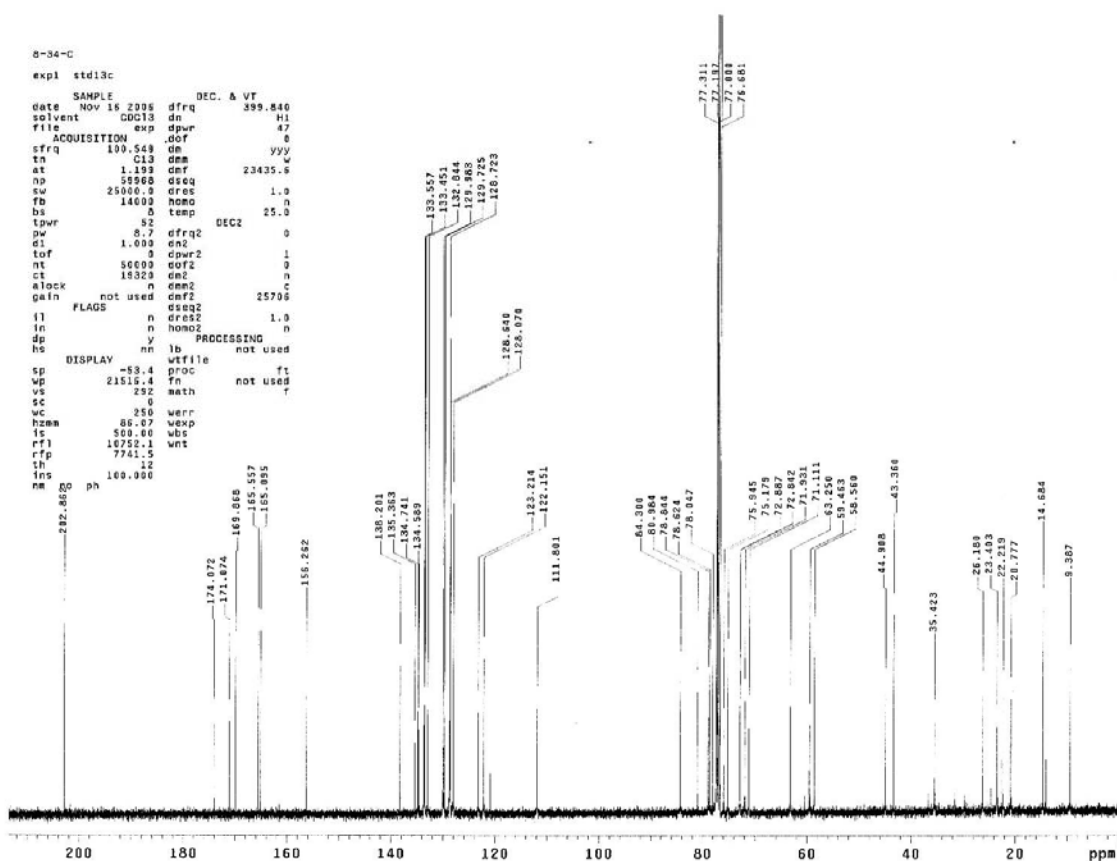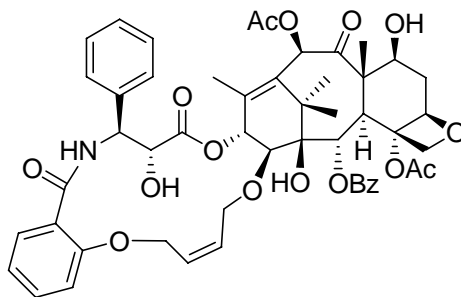
¹H NMR Spectrum of **SB-T-2055*E***
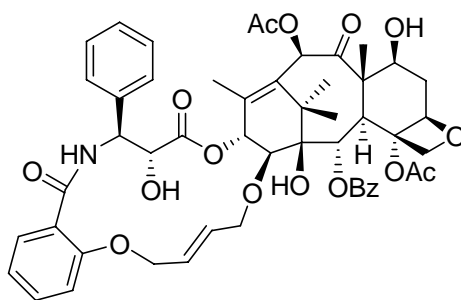

```
Pulse Sequence: s2pul
 Solvent: CDC13
 Temp. 25.0 C / 298.1 K
INOVA-400  "inv400"

 Relax. delay 1.000 sec
 Pulse 47.1 degrees
 Acq. time 3.744 sec
 Width 6009.6 Hz
 40 repetitions
OBSERVE  H1, 399.8379605 MHz
DATA PROCESSING
FT size 65536
Total time 20 min, 16 sec
```
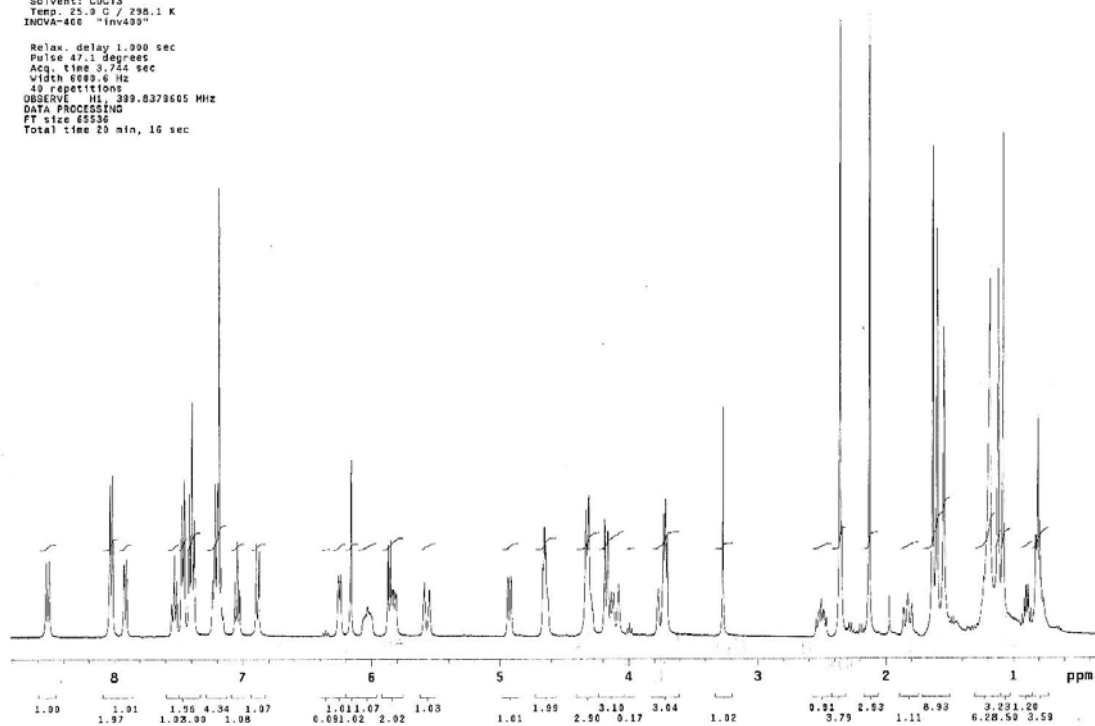
^{13}C NMR Spectrum of **SB-T-2055*E***
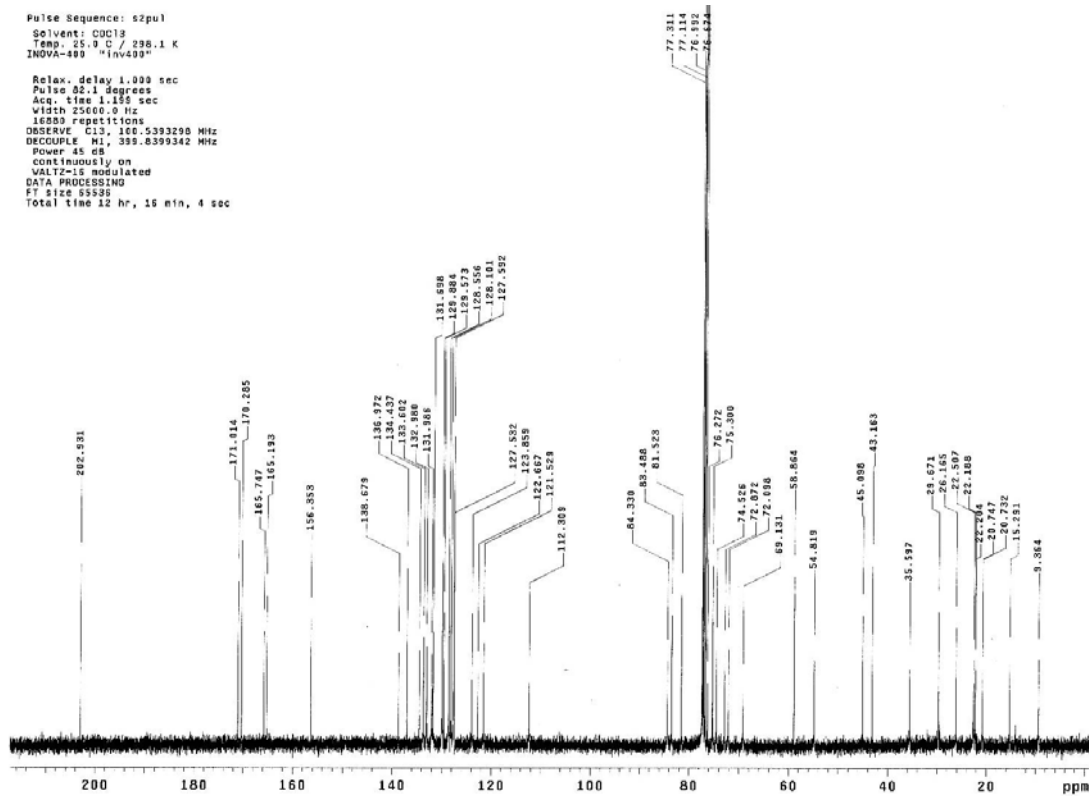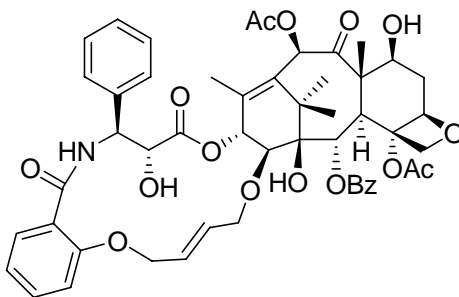
^{1}H NMR Spectrum of **3-38**
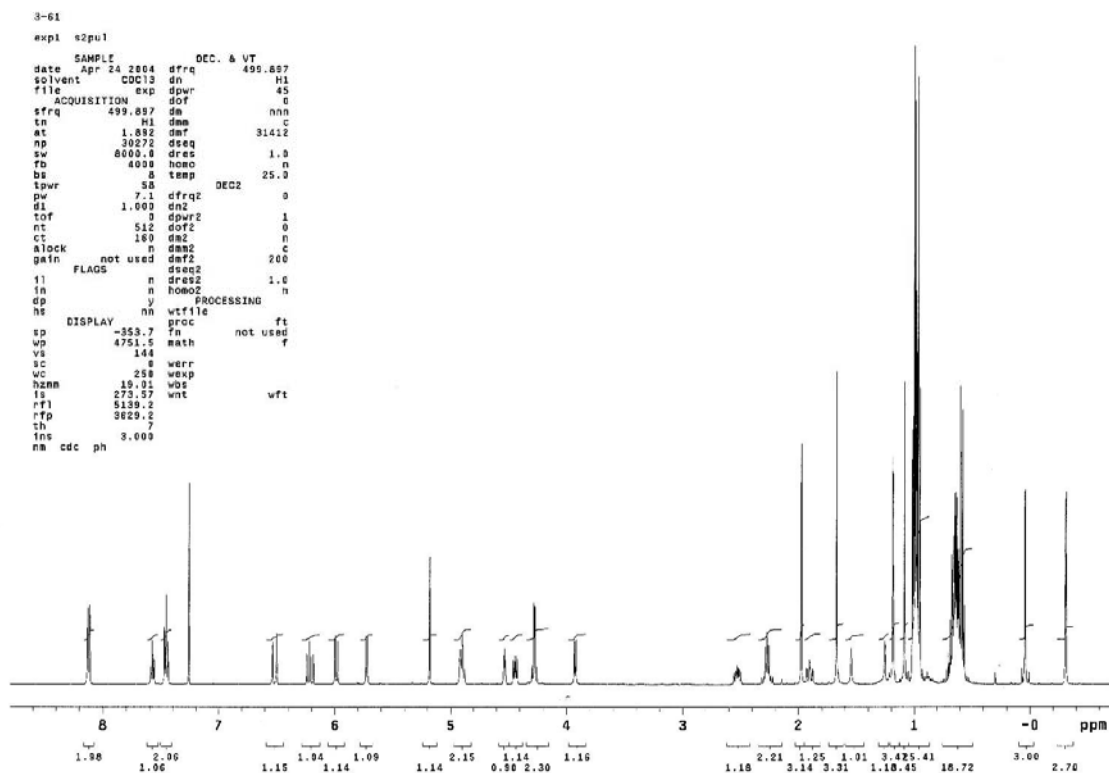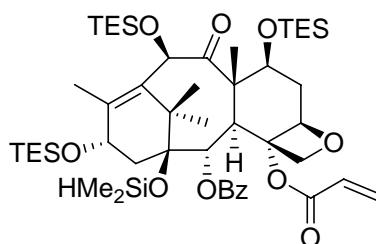
^{13}C NMR Spectrum of **3-38**
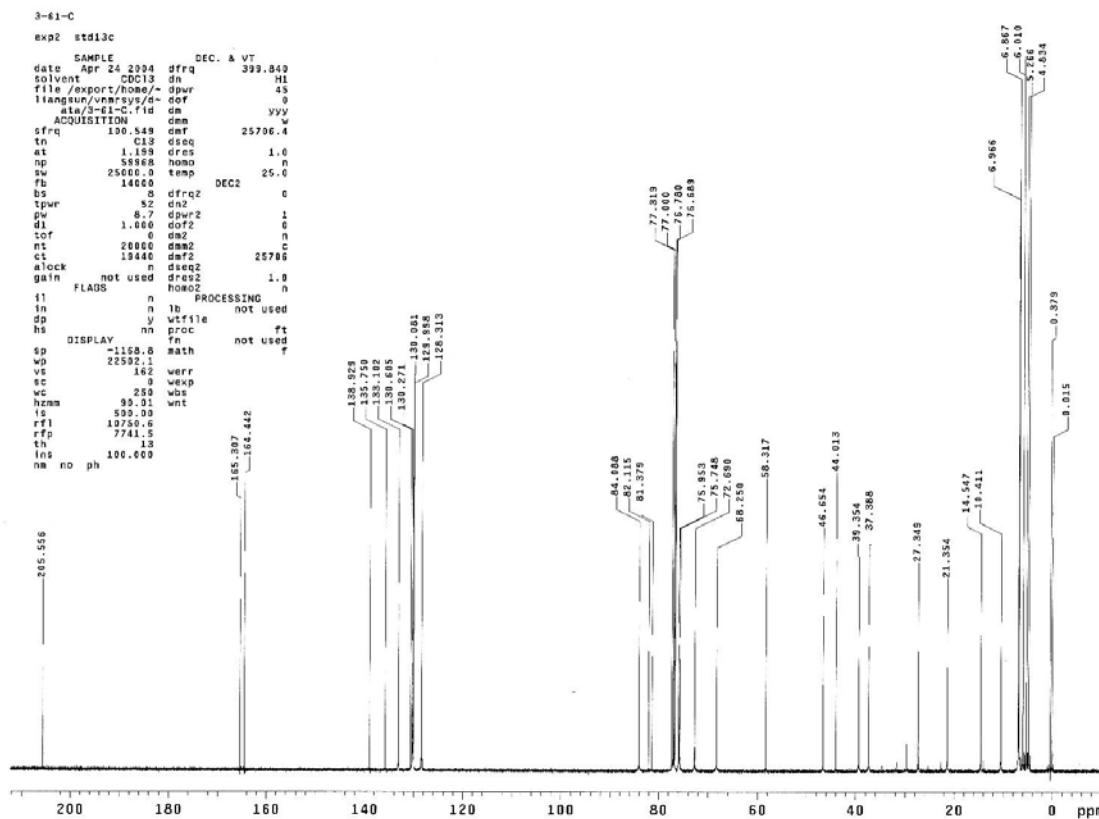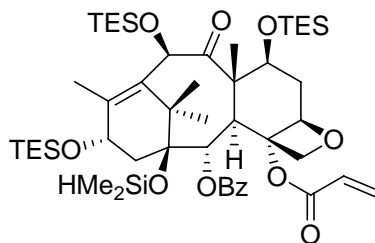
^{1}H NMR Spectrum of **3-39**
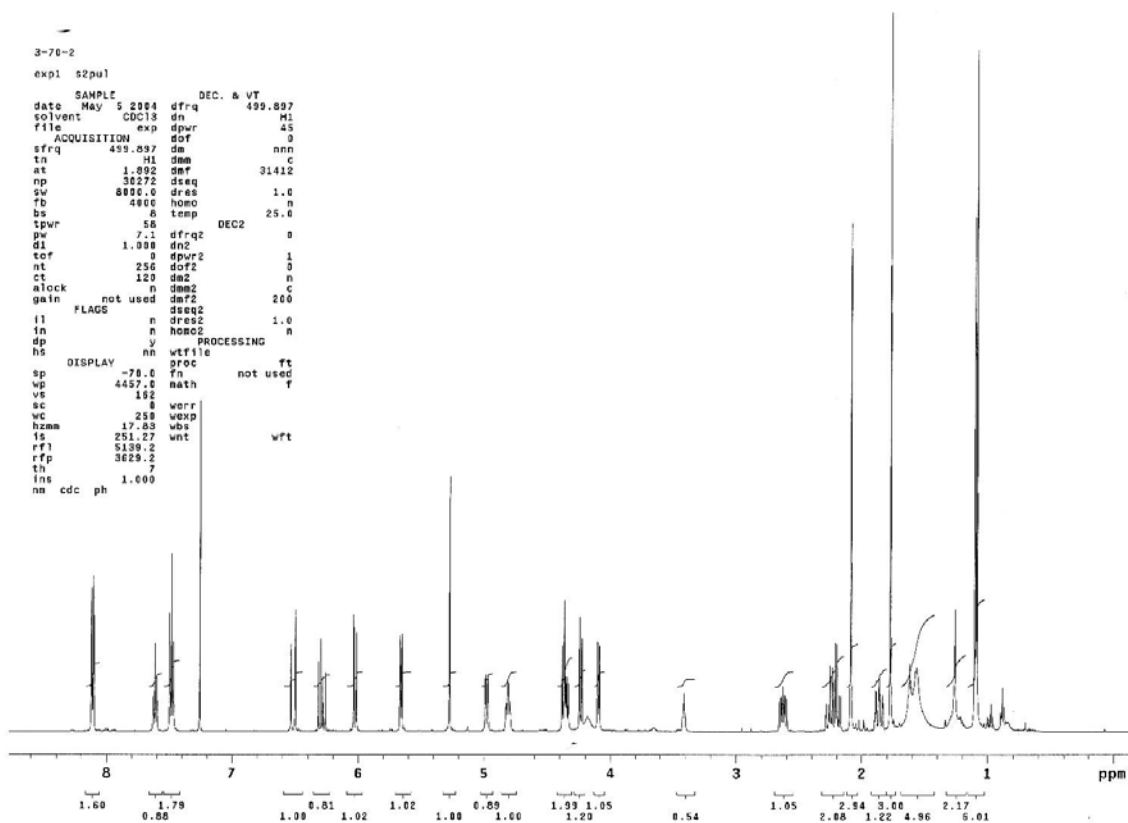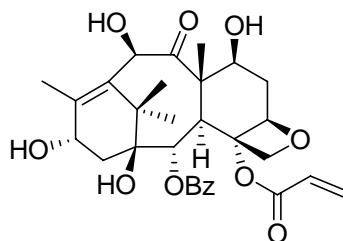
^{13}C NMR Spectrum of **3-39**
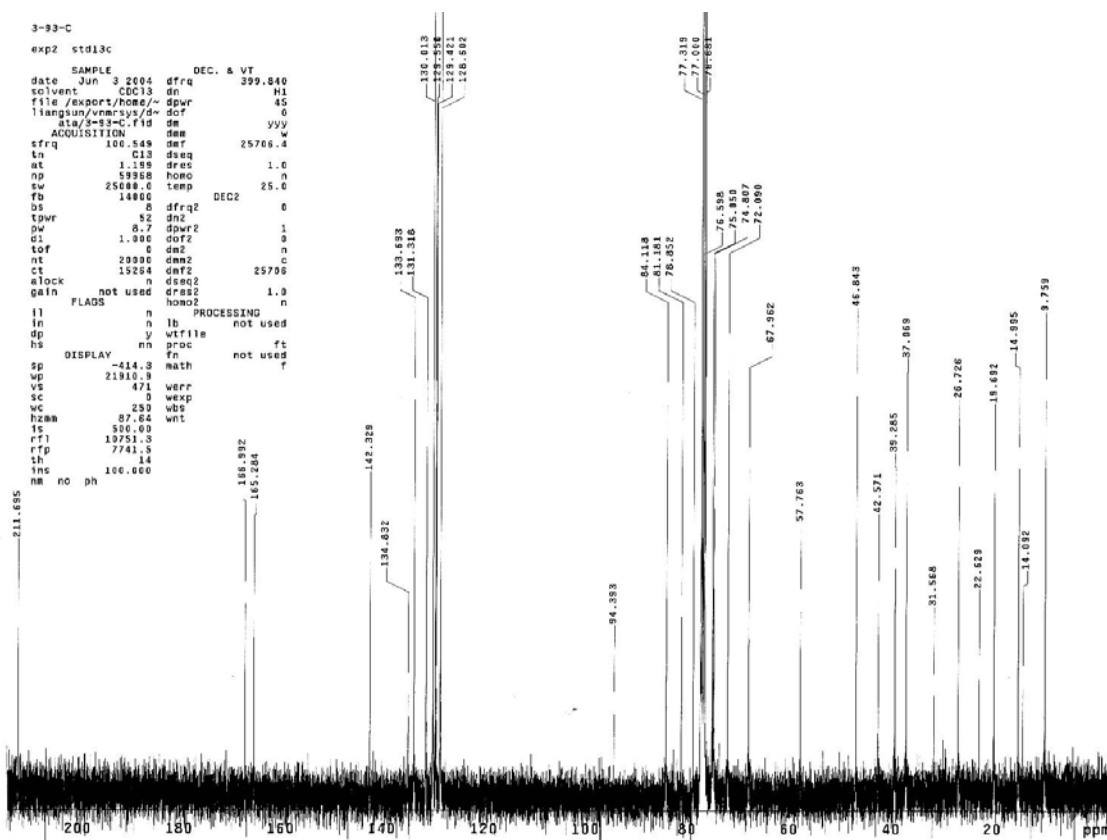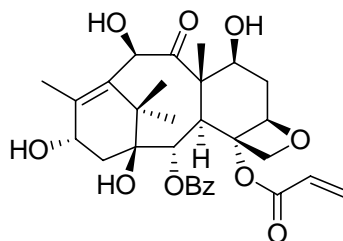
^{1}H NMR Spectrum of **3-40**
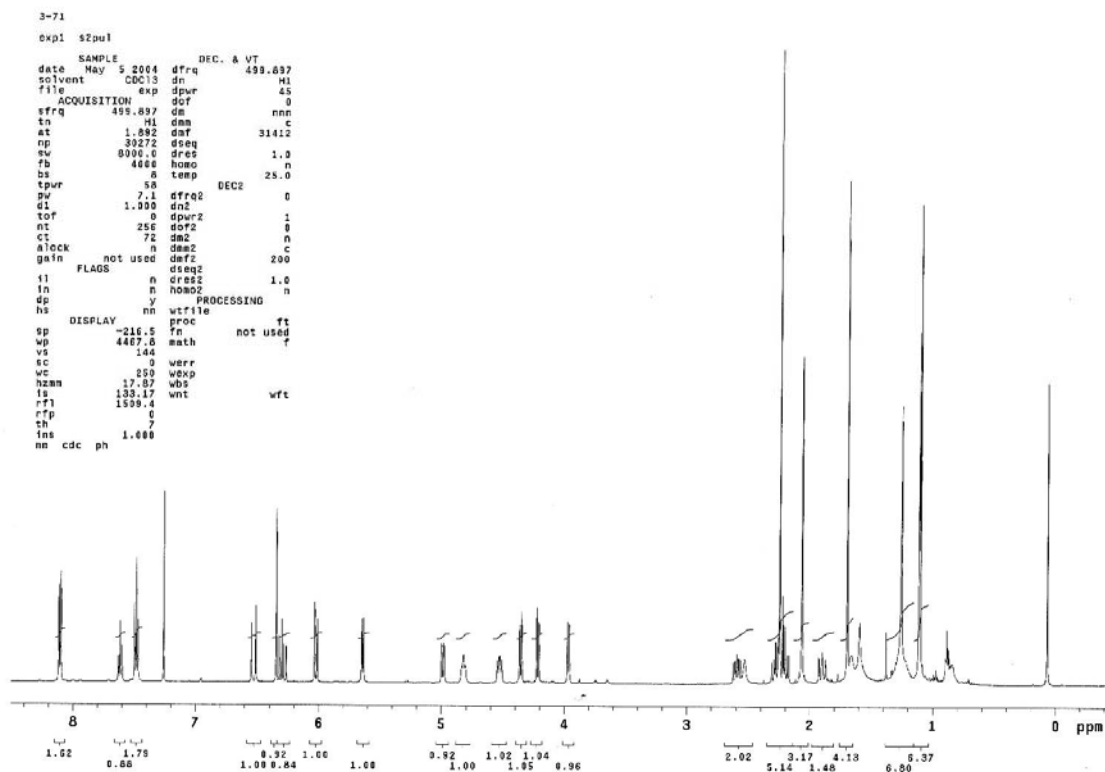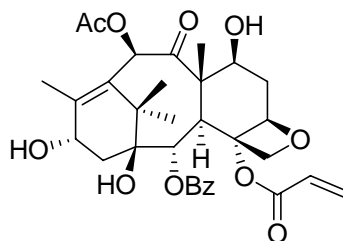
^{1}H NMR Spectrum of **3-36**

^{13}C NMR Spectrum of **3-36**

AcO　O　OTES

HO

HO　OBz　H

3-82-C

exp2　std13c

SAMPLE
date　May 19 2004
solvent　CDC13
file /export/home/~
liangsun/vnmrsys/d~
ata/3-82-C.fid
ACQUISITION
sfrq　100.549
tn　C13
at　1.199
np　59968
sw　25000.0
fb　14000
bs　8
tpwr　52
pw　8.7
d1　1.000
tof　0
nt　20000
ct　16592
alock　not used
gain　not used
FLAGS
il　n
in　n
dp　y
hs　nn
DISPLAY
sp　-512.7
wp　21910.9
vs　697
sc　0
wc　250
hzmm　87.64
is　500.00
rfl　3009.8
rfp　0
th　14
ins　100.000
nm　no　ph

DEC. & VT
dfrq　399.840
dn　H1
dpwr　45
dof　0
dm　yyy
dmm　w
dmf　25706.4
dseq
dres　1.0
homo　n
temp　25.0
DEC2
dfrq2　0
dn2
dpwr2　1
dof2　0
dm2　n
dmm2　c
dmf2　25706
dseq2
dres2　1.0
homo2　n
PROCESSING
lb　not used
wtfile
proc　ft
fn　not used
math　f

werr
wexp
wbs
wnt

202.873

169.314
167.045
165.285

143.930

133.633
132.715
131.121

130.021
129.747
129.451
128.556

84.194
81.318

78.761

77.311
77.130
76.874

76.552
75.771

74.746
72.341
68.068

58.750

47.147

42.753

38.883
37.297

26.833

20.921
20.064

14.828

9.956

8.738

5.269

200　180　160　140　120　100　80　60　40　20　ppm

¹H NMR Spectrum of **3-41**

^{13}C NMR Spectrum of **3-41**

¹H NMR Spectrum of **3-42**

¹³C NMR Spectrum of **3-42**
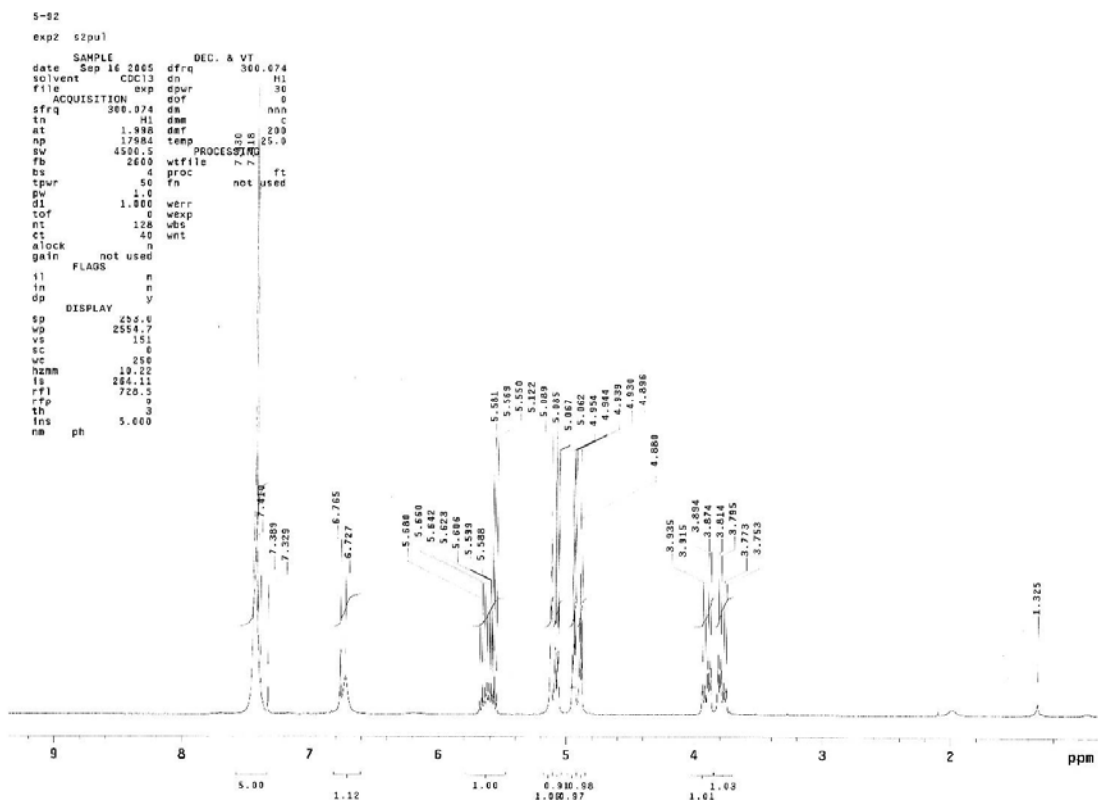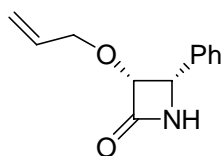
^{13}C NMR Spectrum of **3-42**
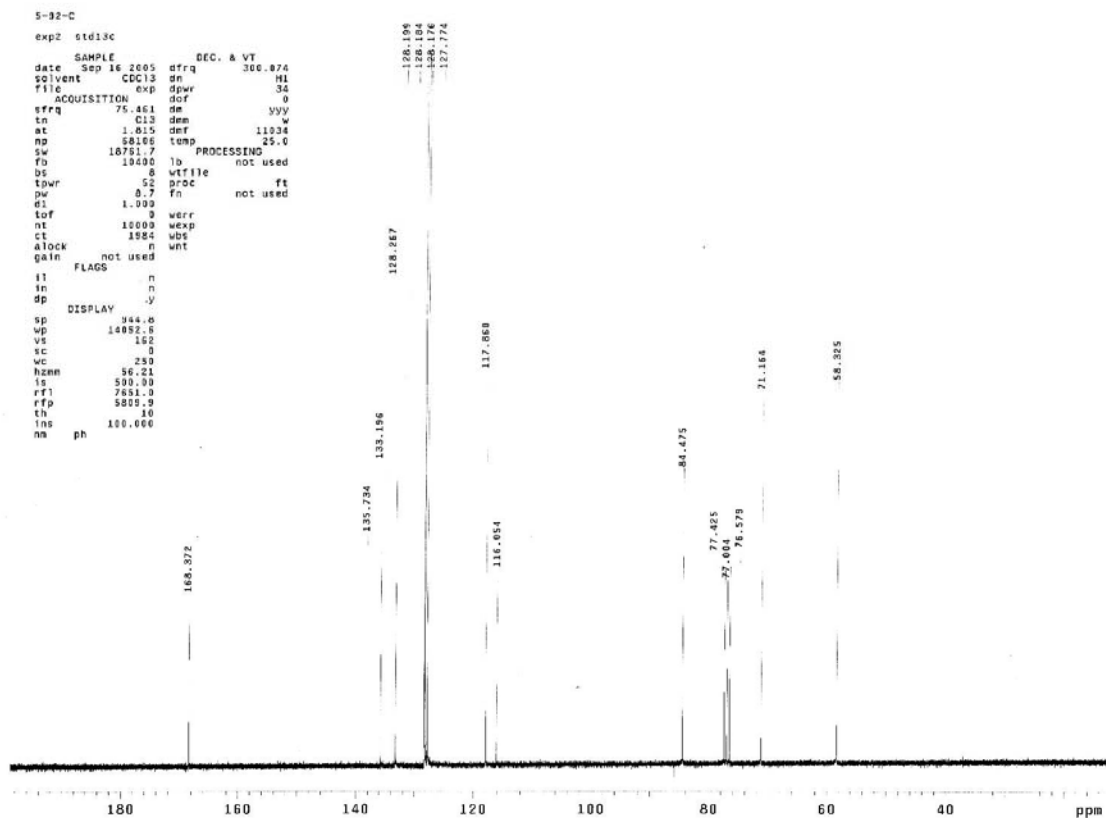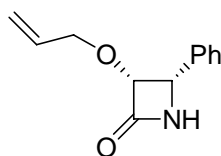
^{1}H NMR Spectrum of **3-37**
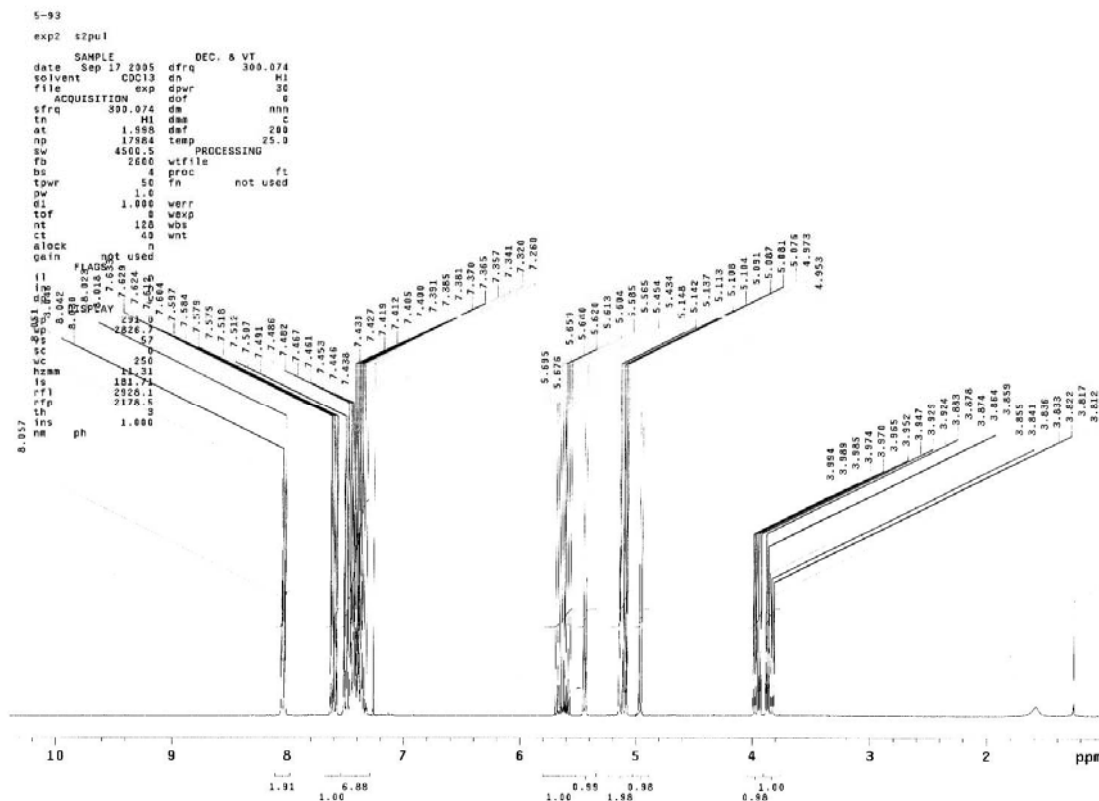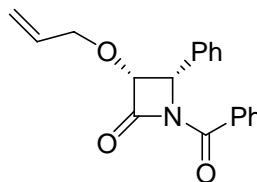
^{13}C NMR Spectrum of **3-37**
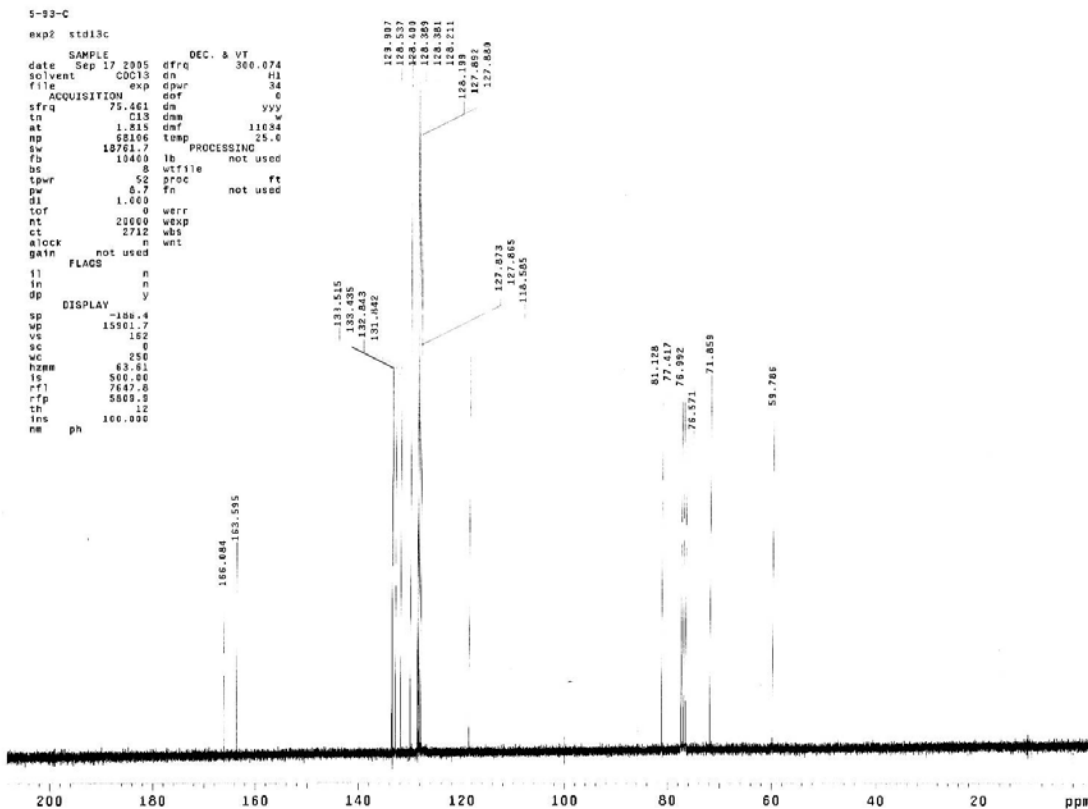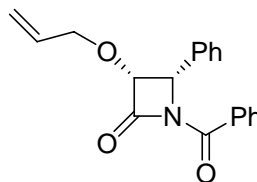
^{1}H NMR Spectrum of **3-35**
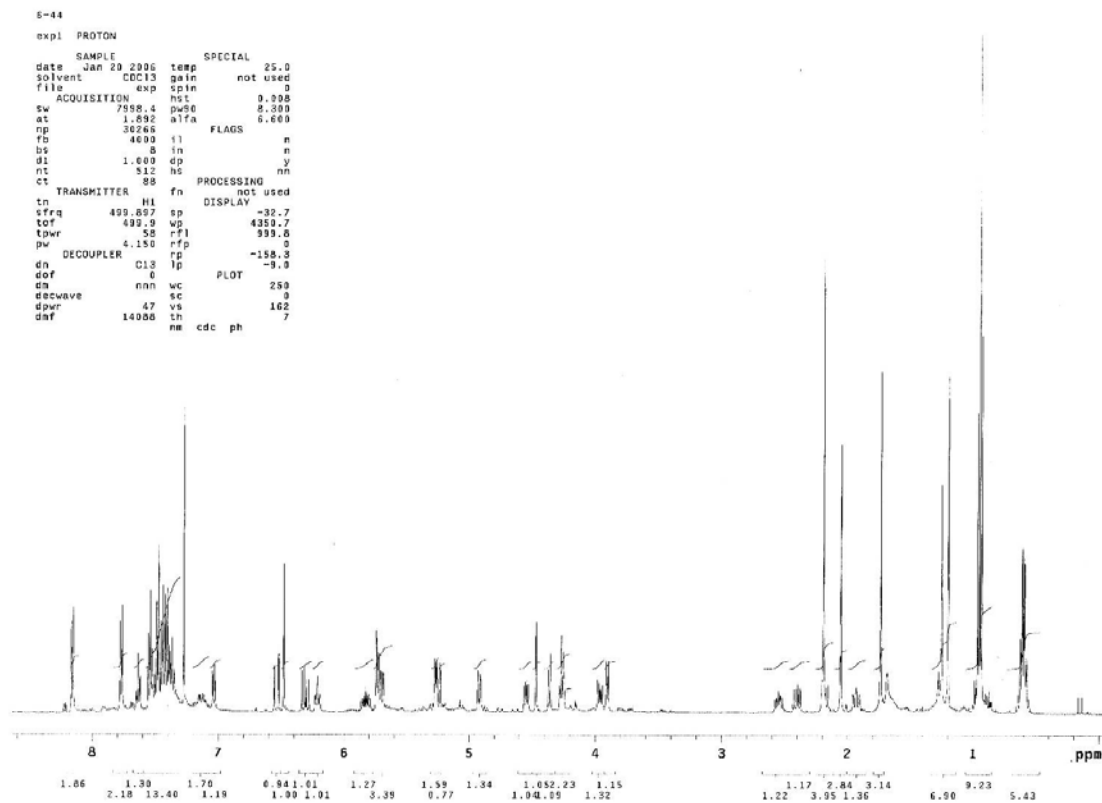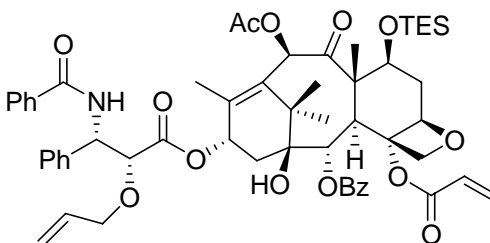
^{13}C NMR Spectrum of **3-35**
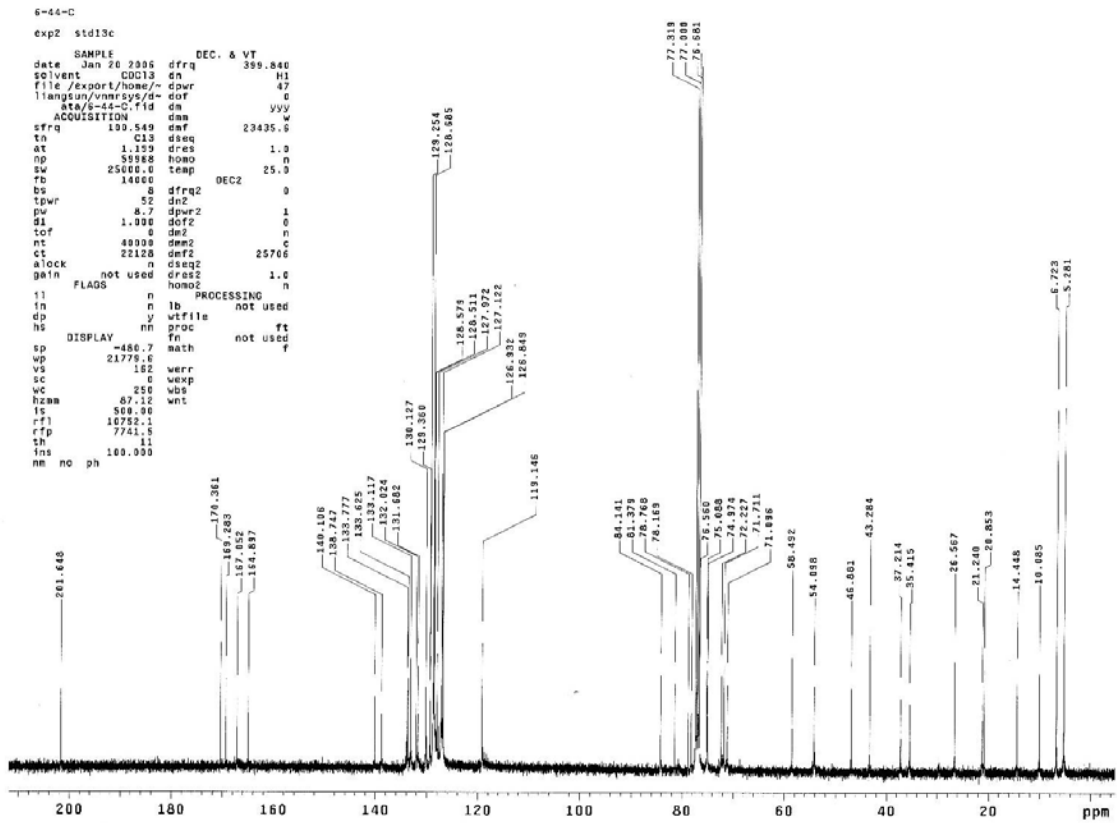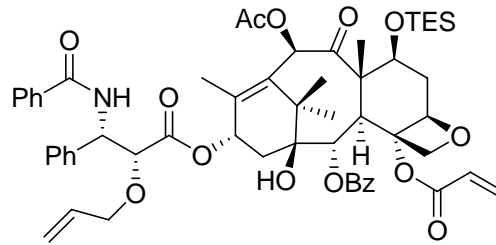
^{1}H NMR Spectrum of **3-43**
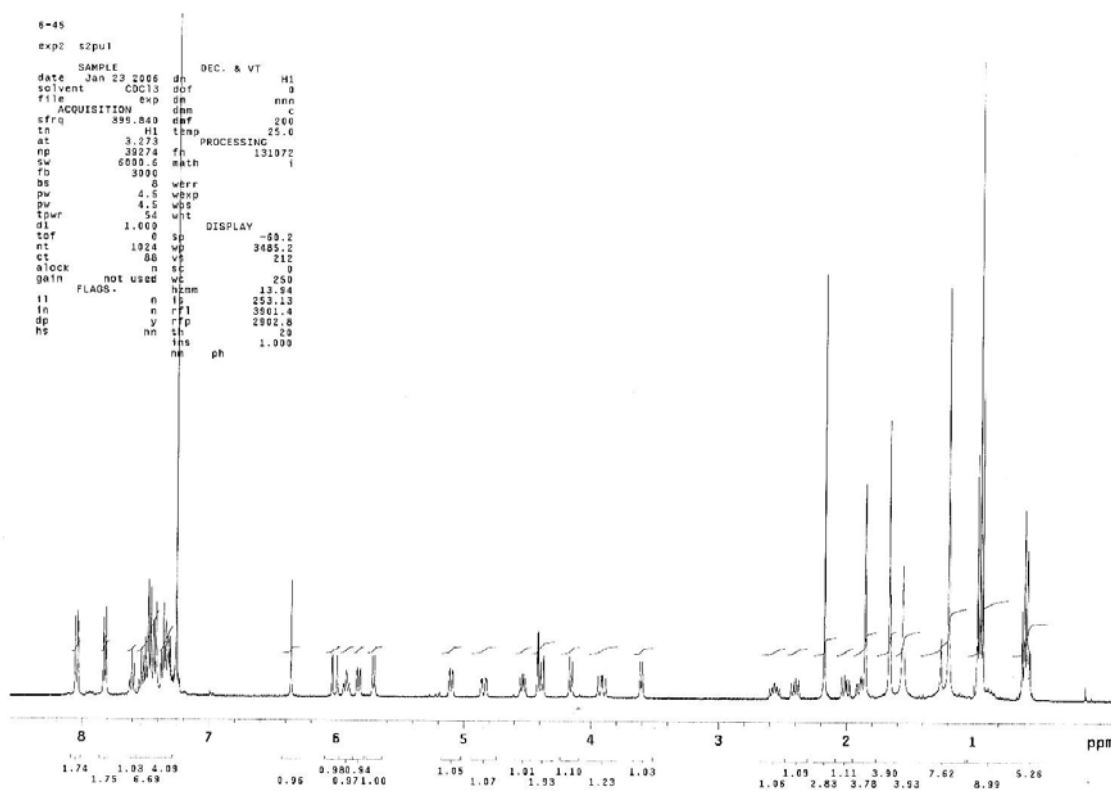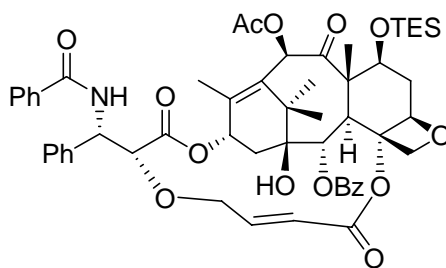
^{1}H NMR Spectrum of **SB-TCR-501**
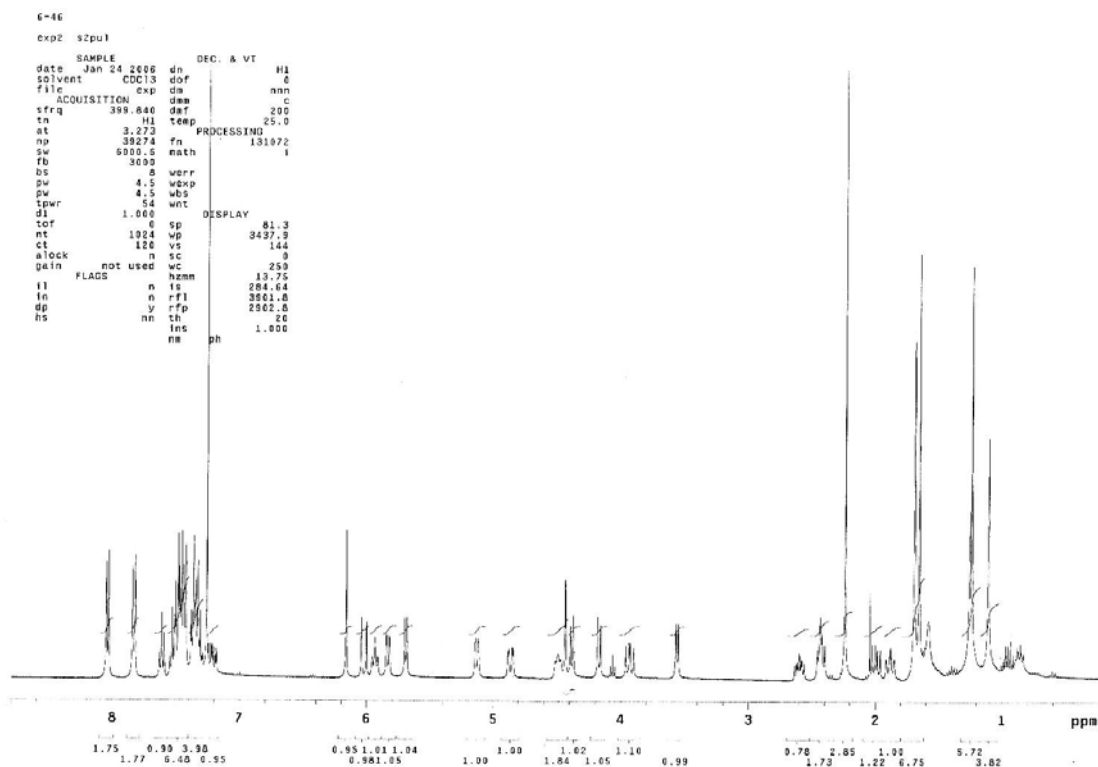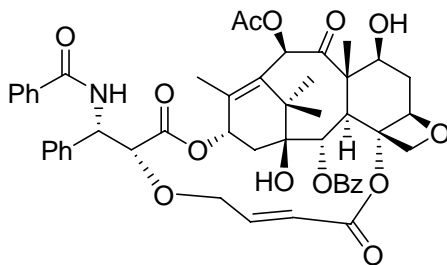
^{13}C NMR Spectrum of **SB-TCR-501**
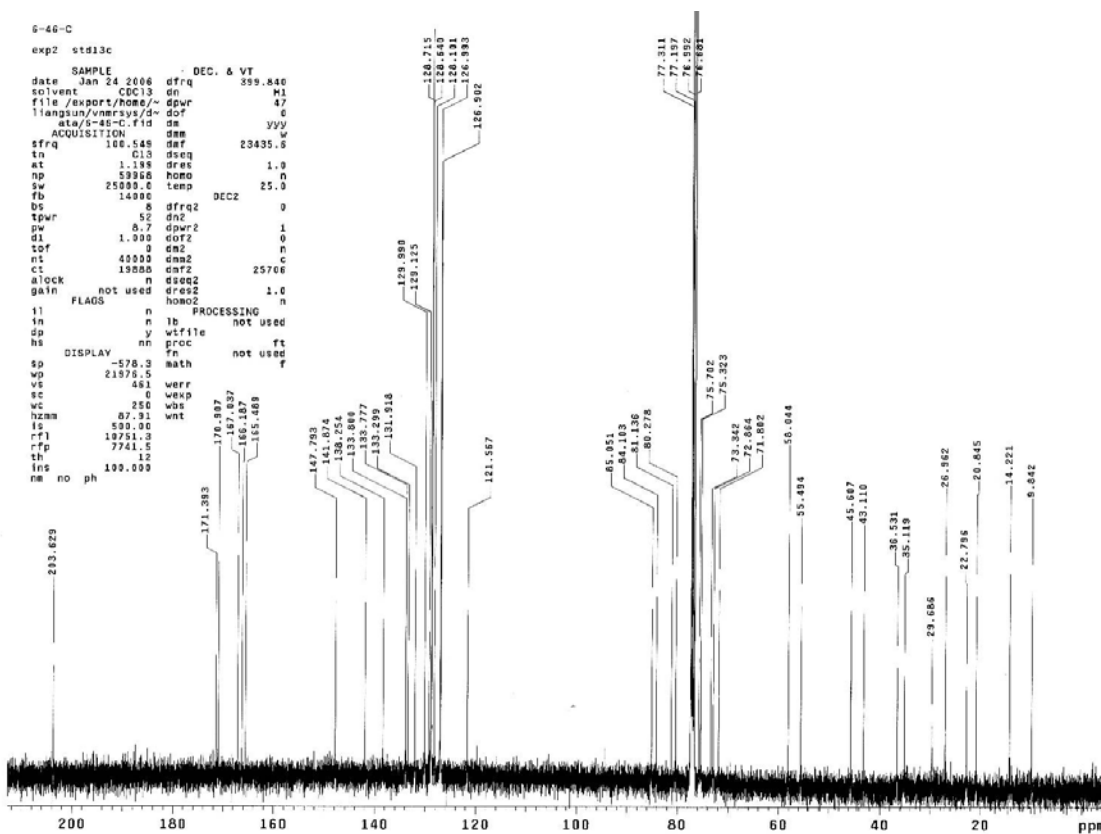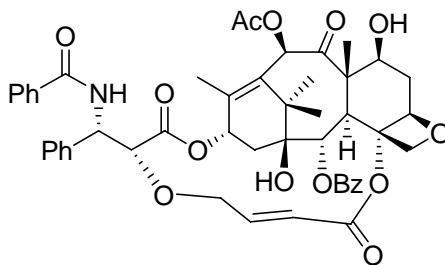
COSY Spectrum of **SB-TCR-501**

HMQC Spectrum of **SB-TCR-501**
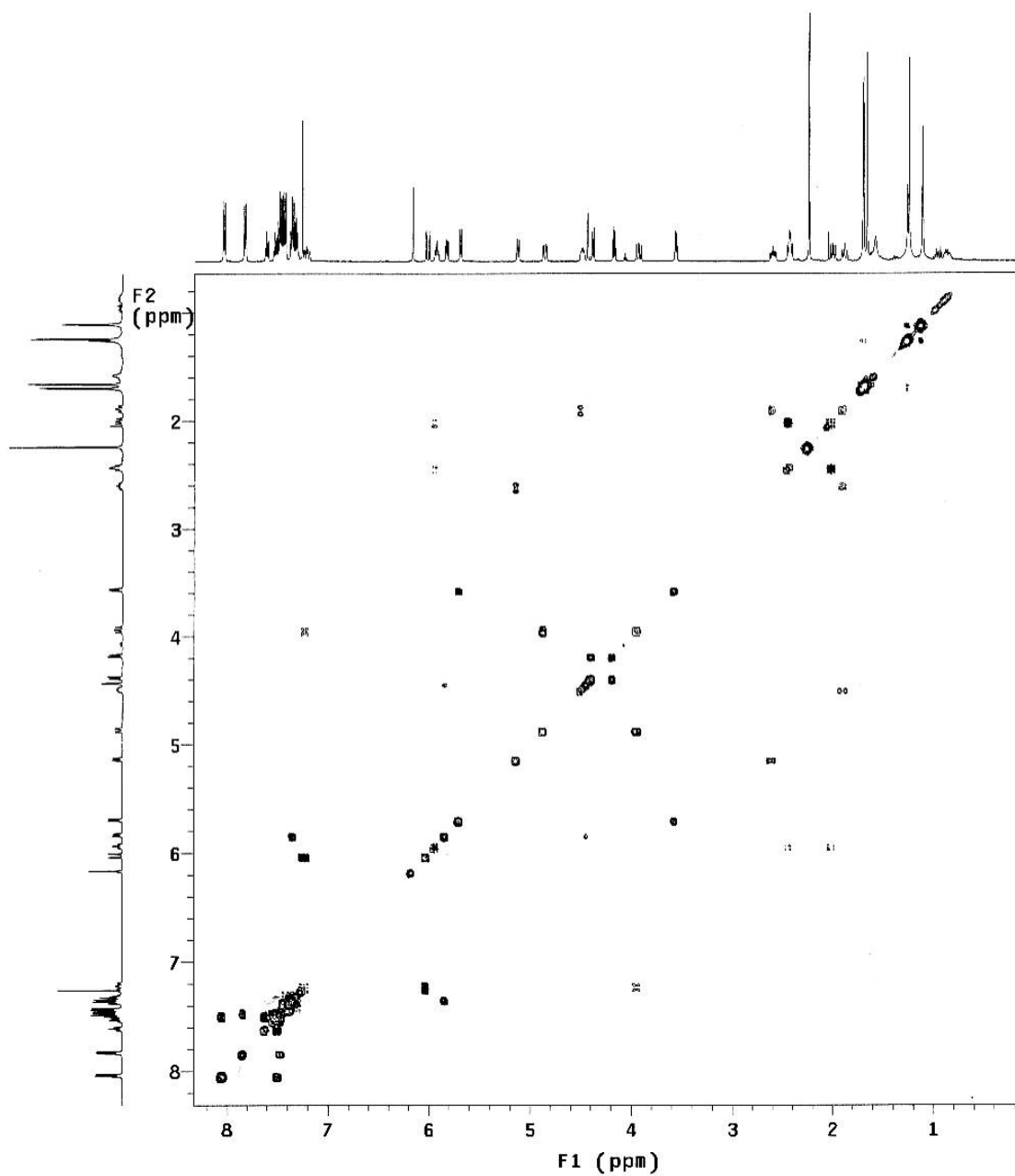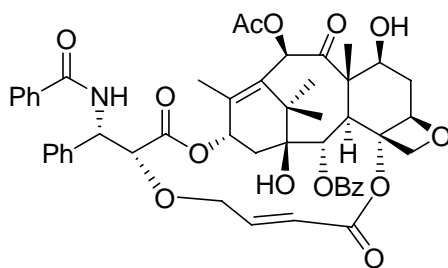
^{1}H NMR Spectrum of **3-46**
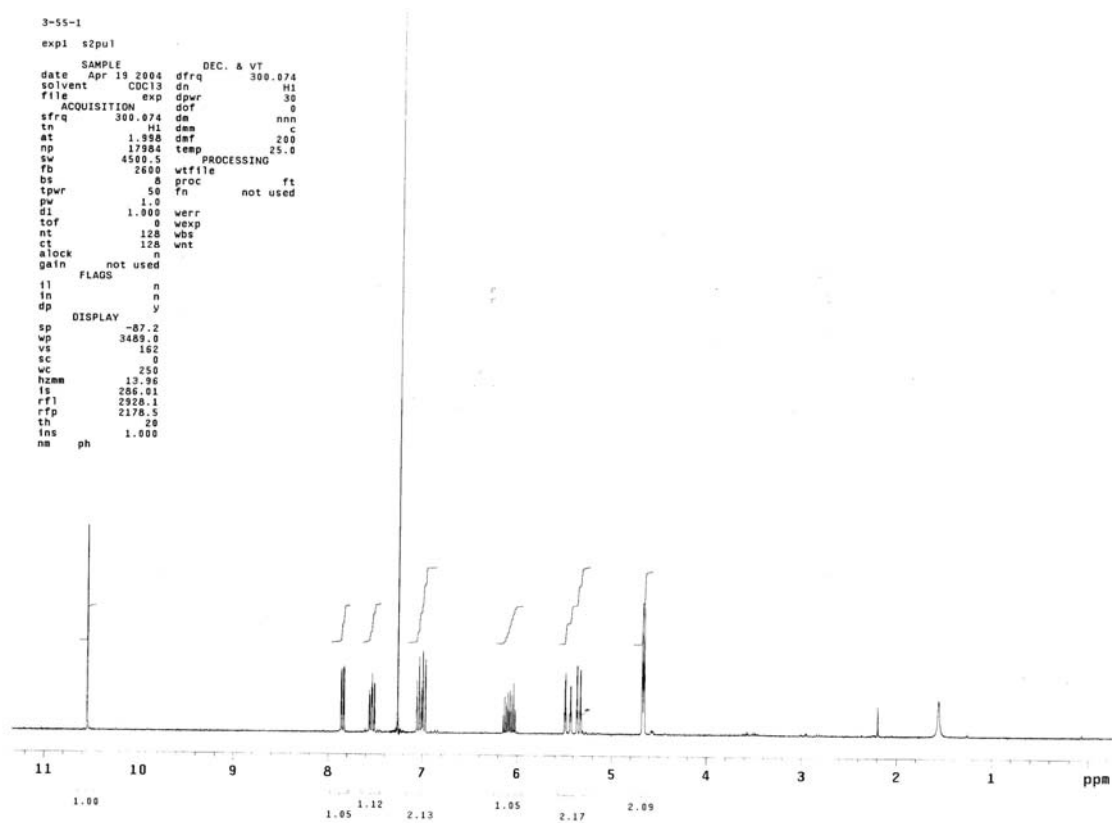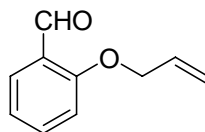
^{1}H NMR Spectrum of **3-48**
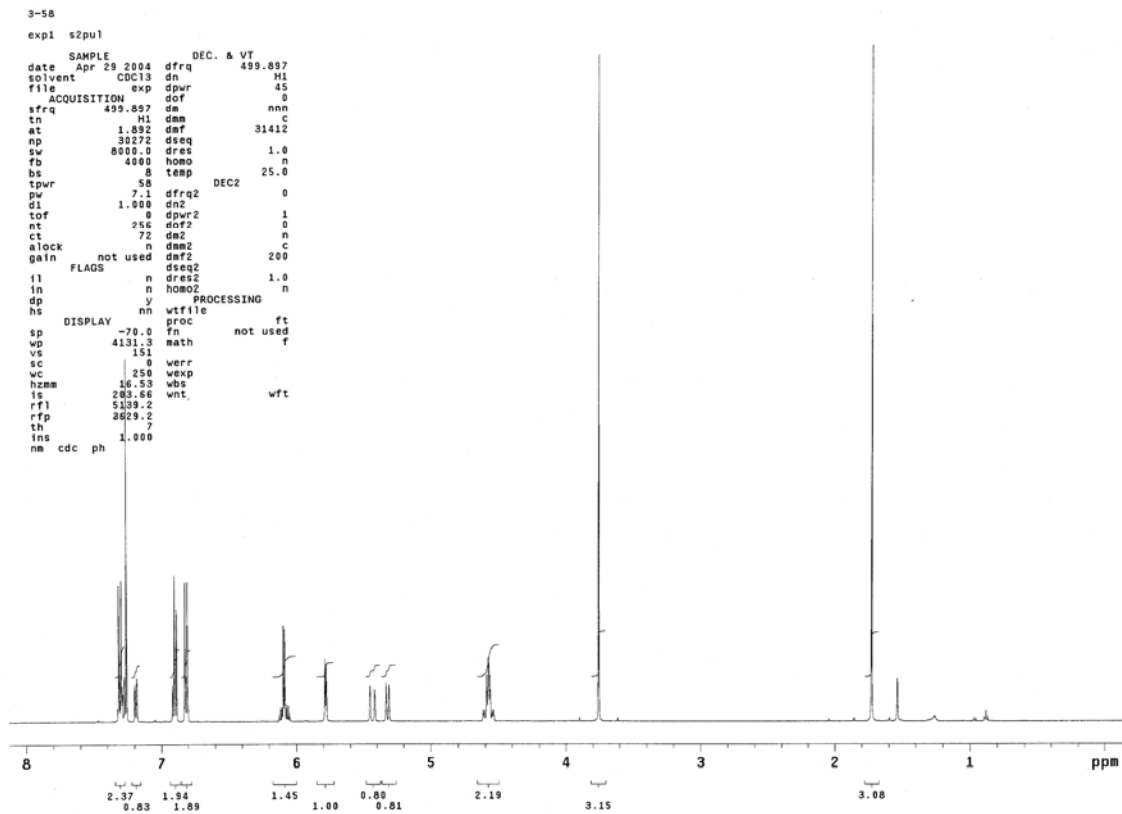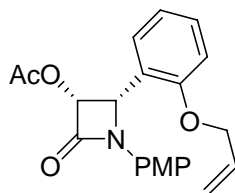
^{13}C NMR Spectrum of **3-48**
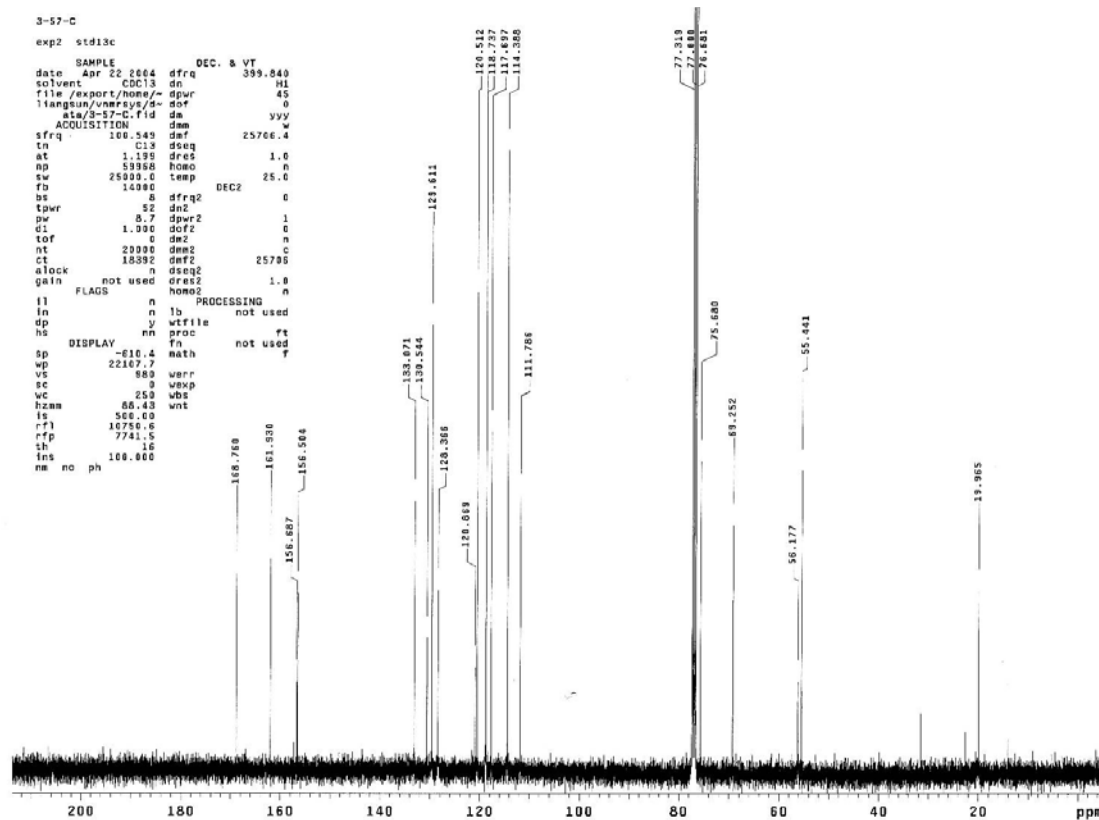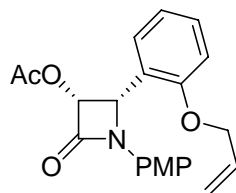
^{1}H NMR Spectrum of **3-49**
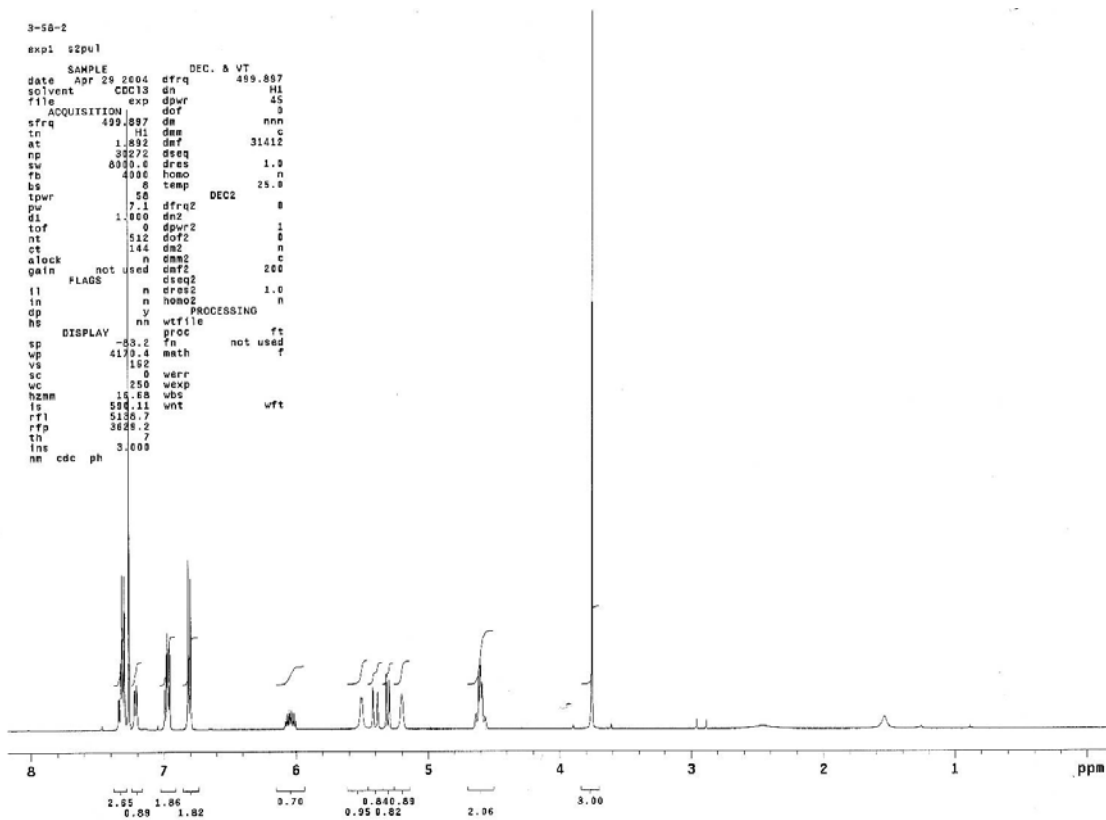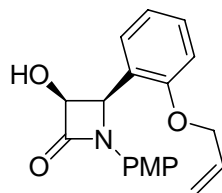
^{13}C NMR Spectrum of **3-49**
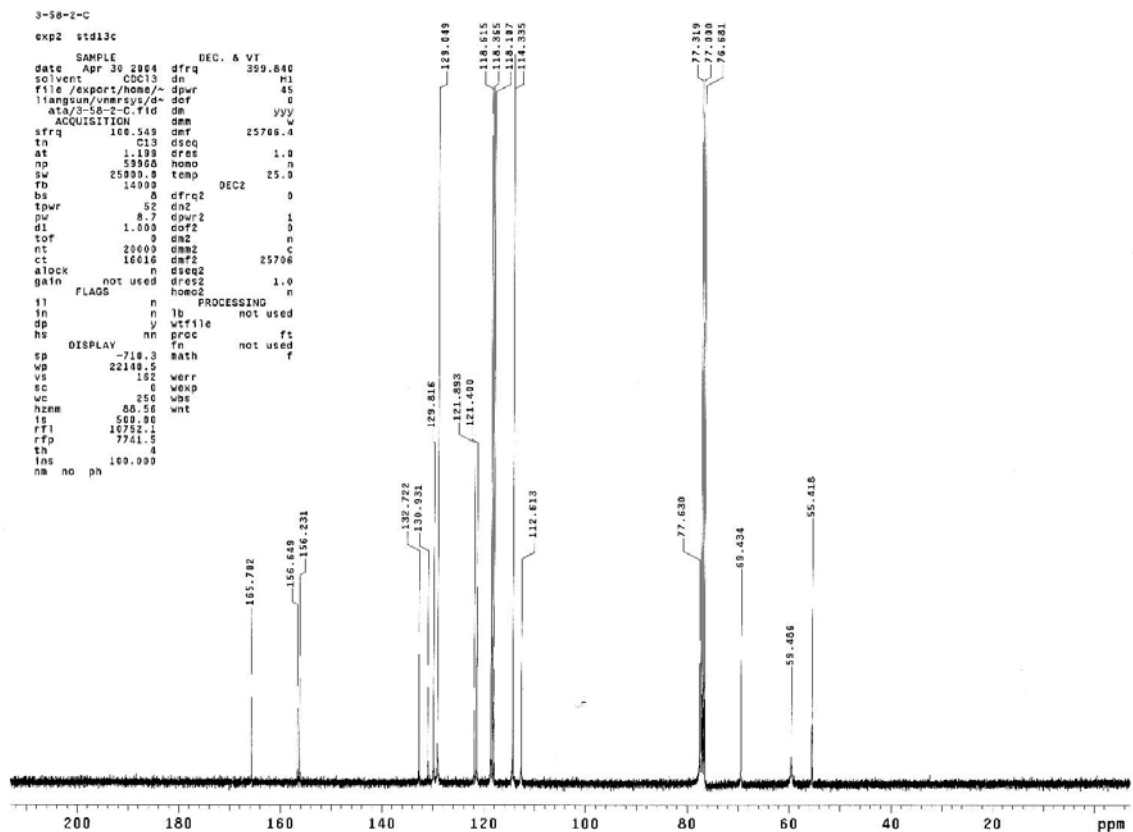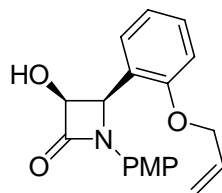
^{1}H NMR Spectrum of **3-50**
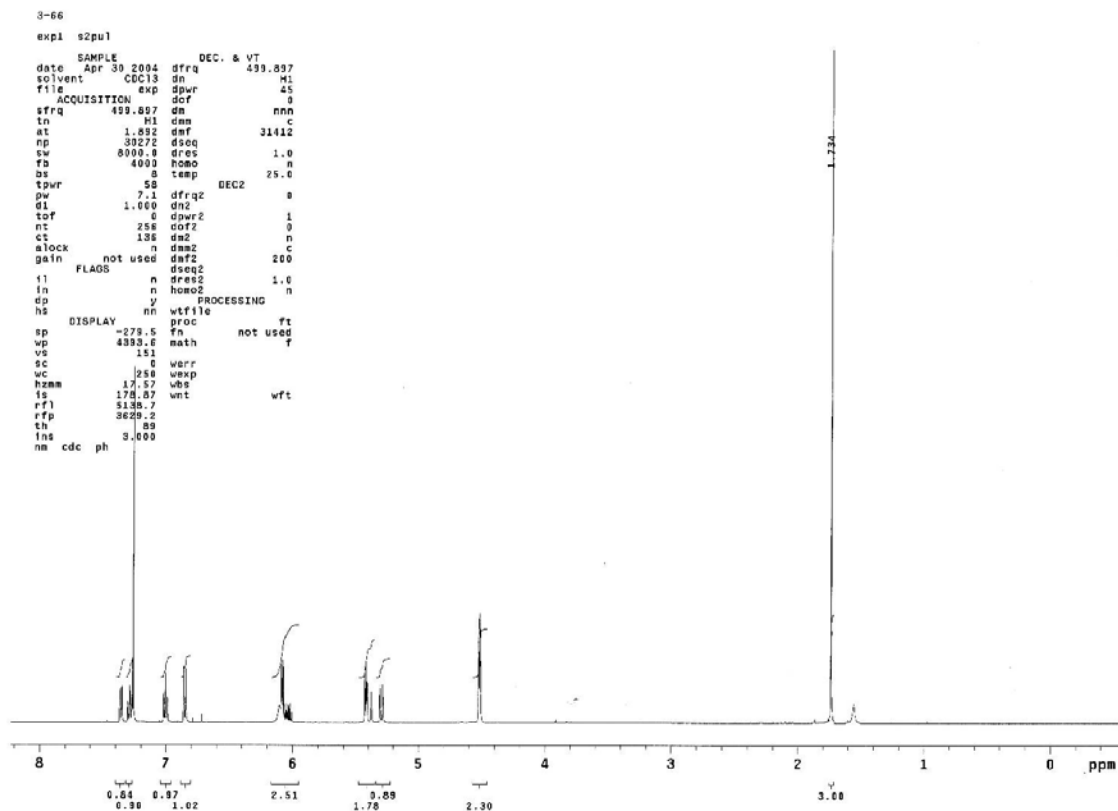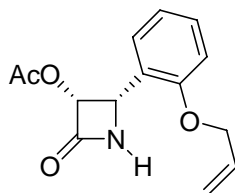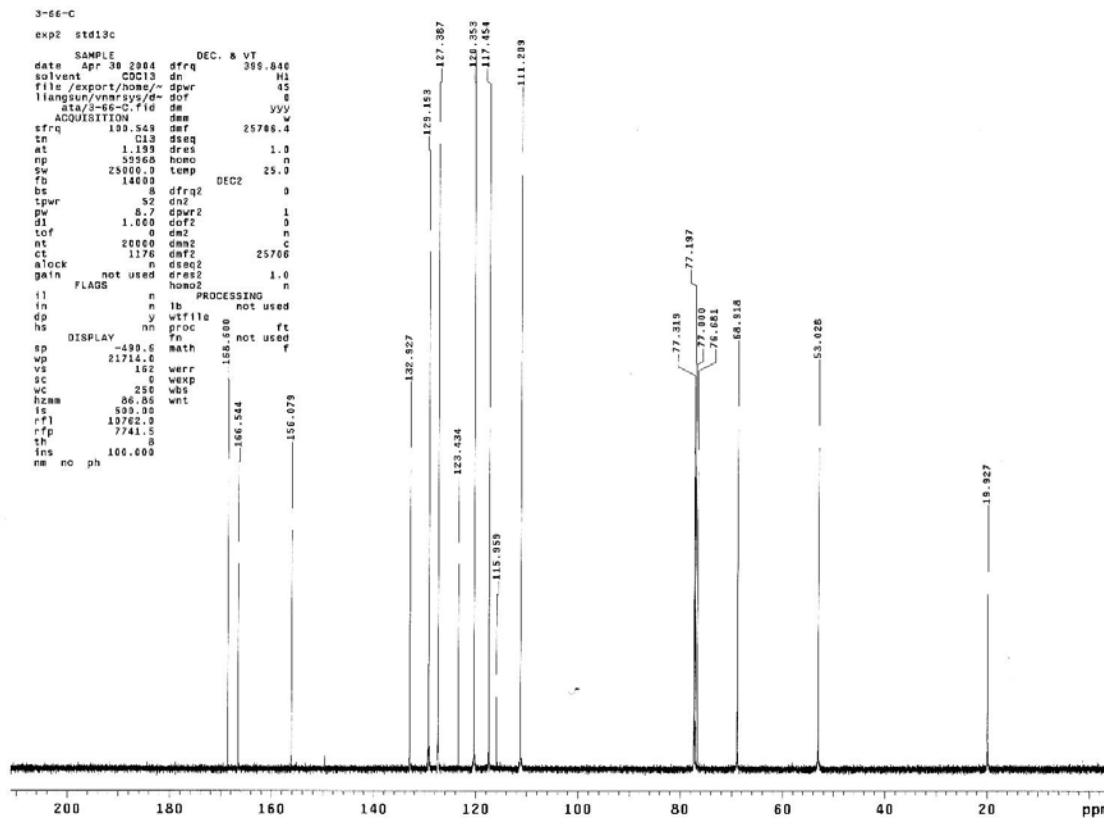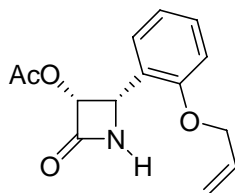
^{13}C NMR Spectrum of **3-51**
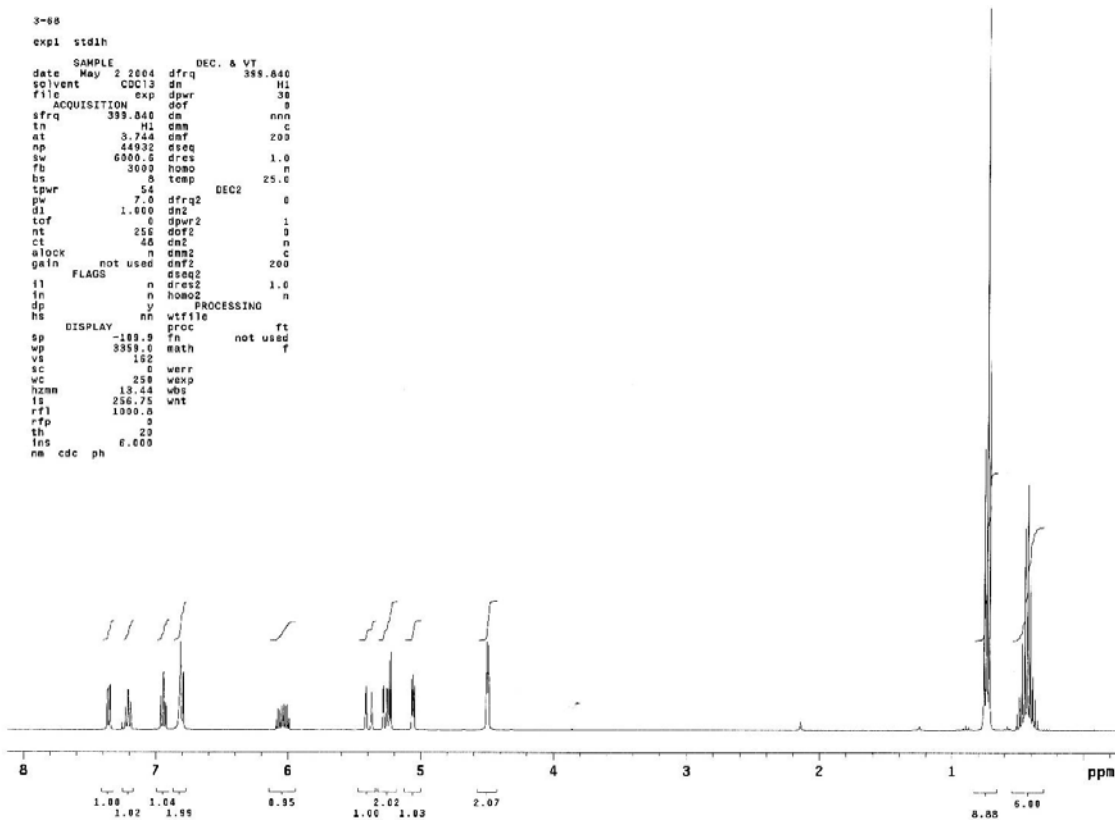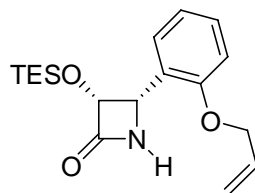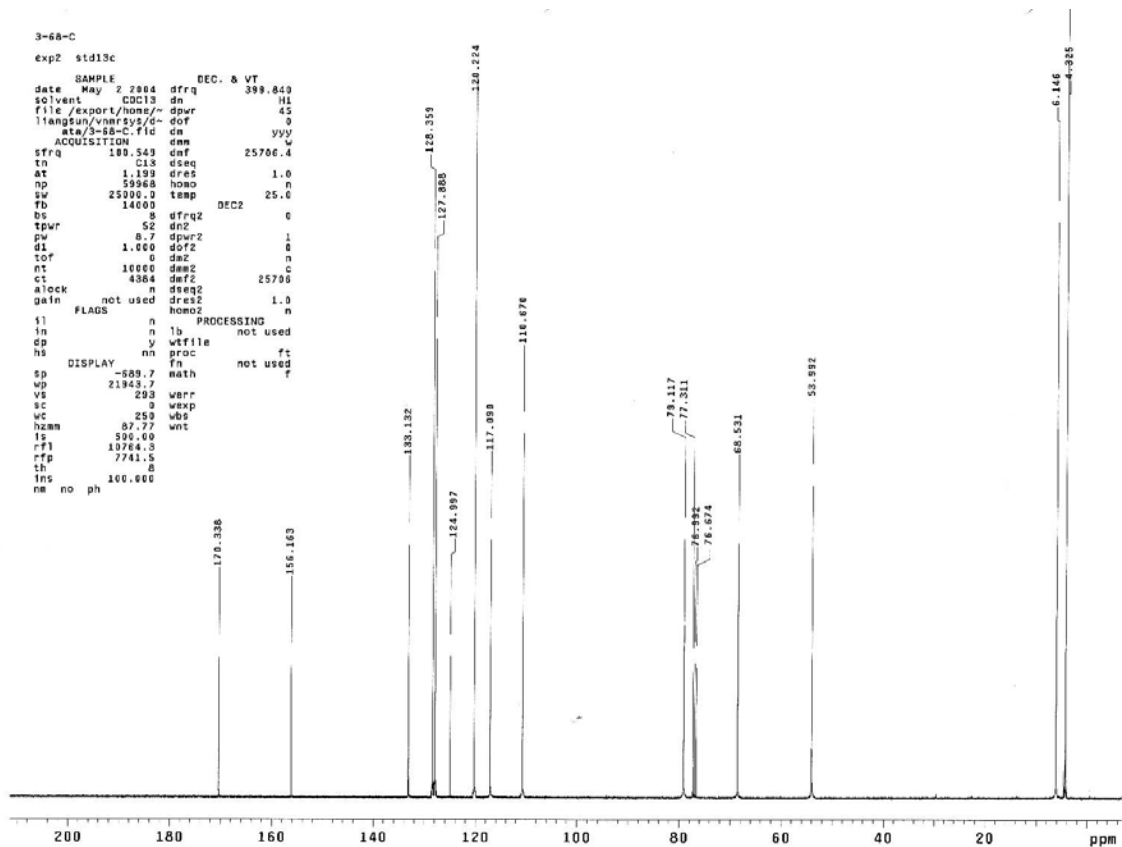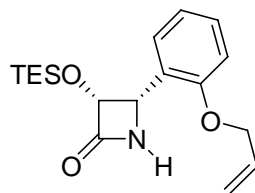
¹H NMR Spectrum of **3-52**
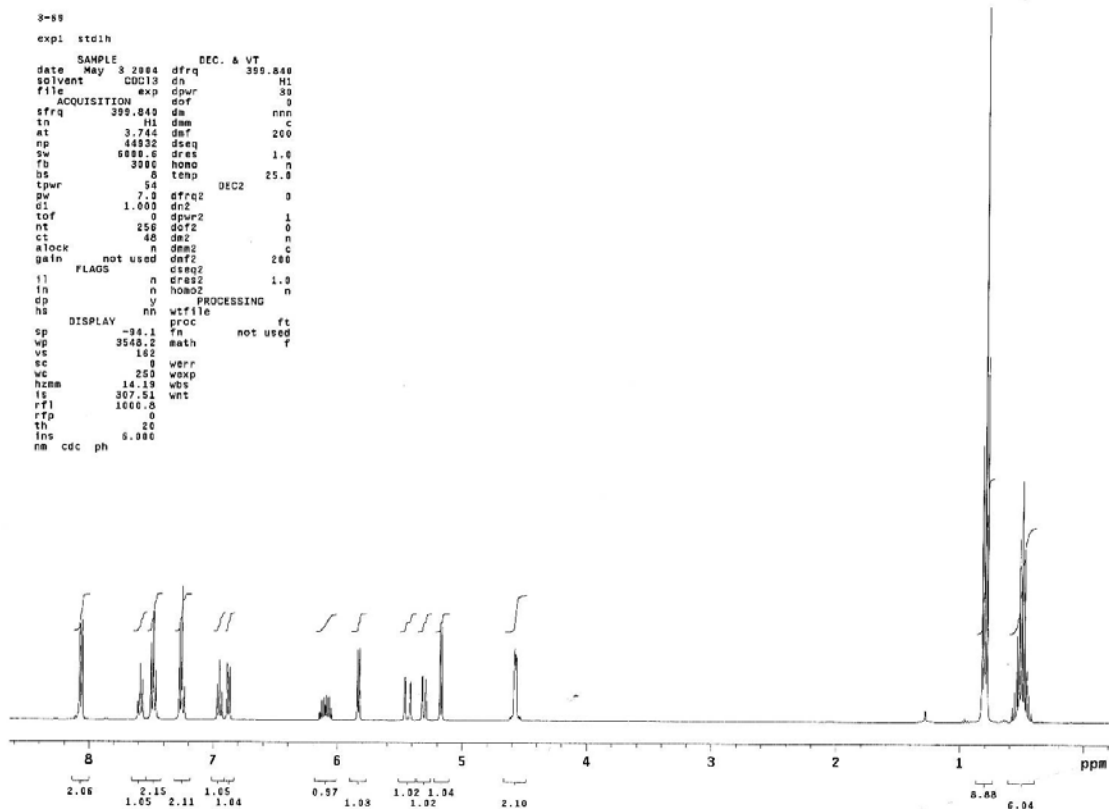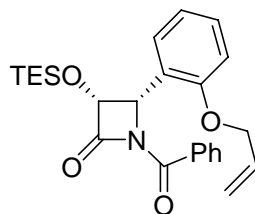
^{1}H NMR Spectrum of **3-53**

CH$_2$OH
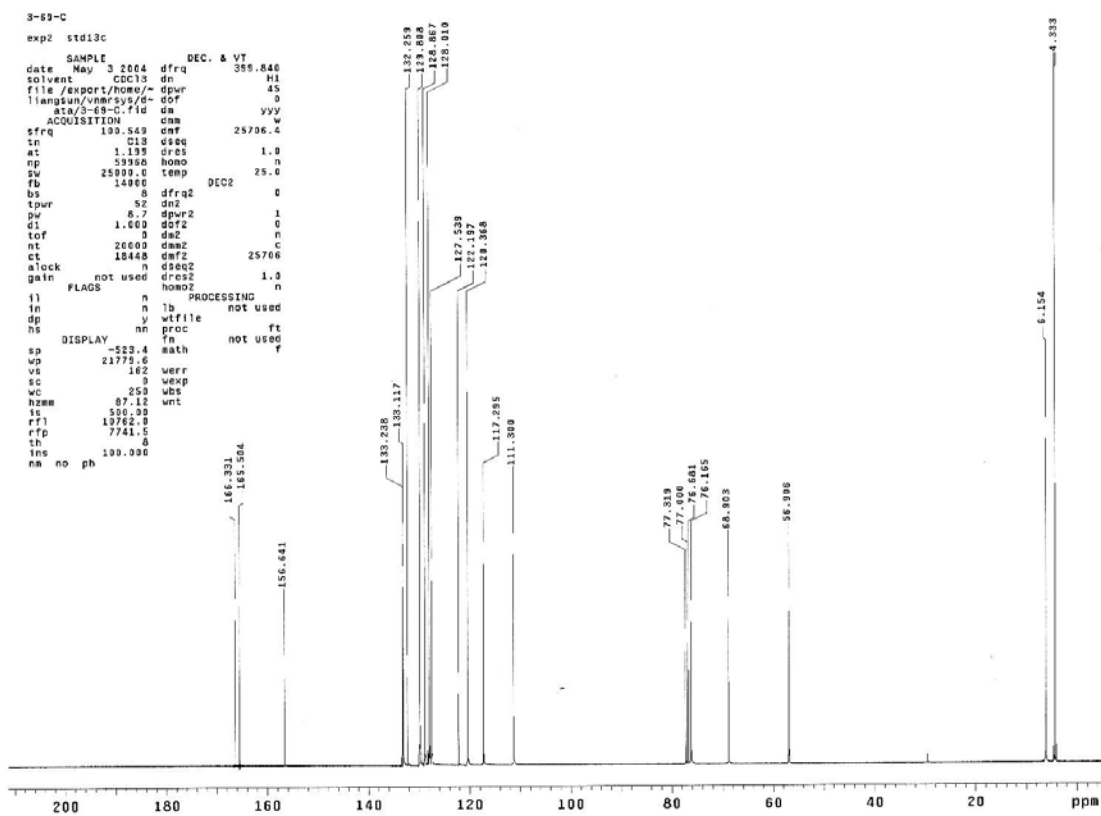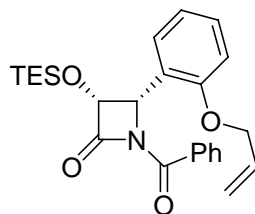
¹³C NMR Spectrum of **3-53**
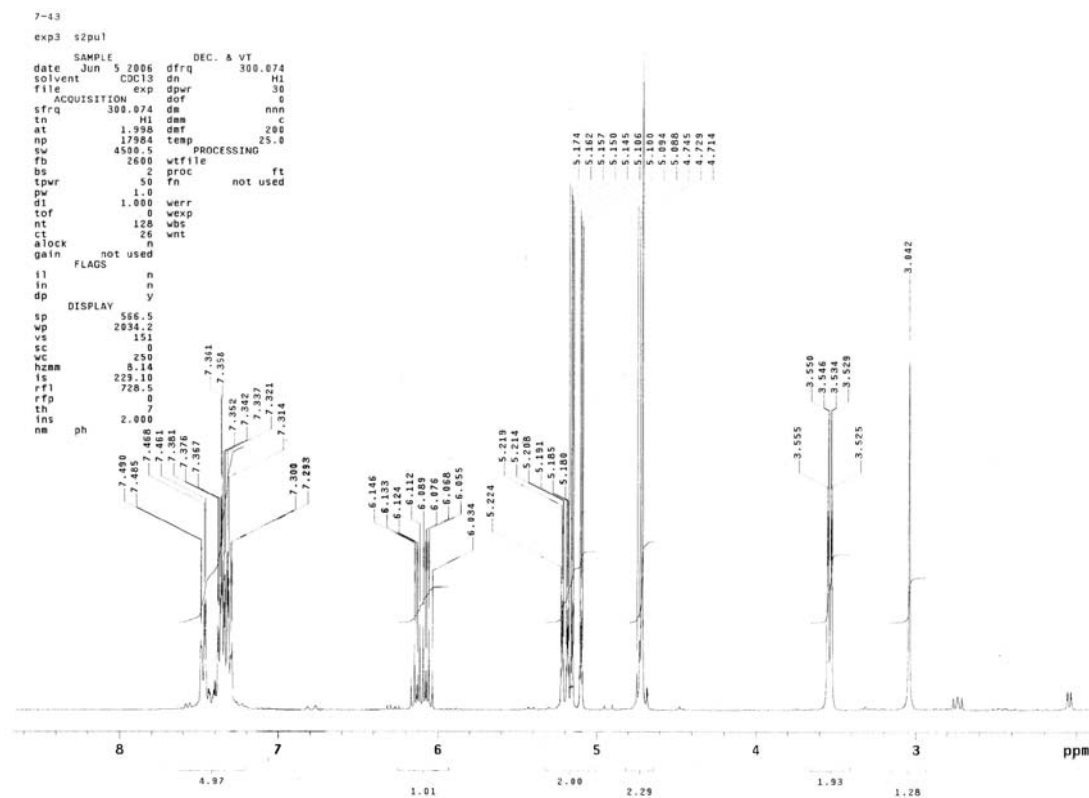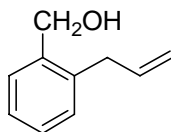
^{13}C NMR Spectrum of **3-53**
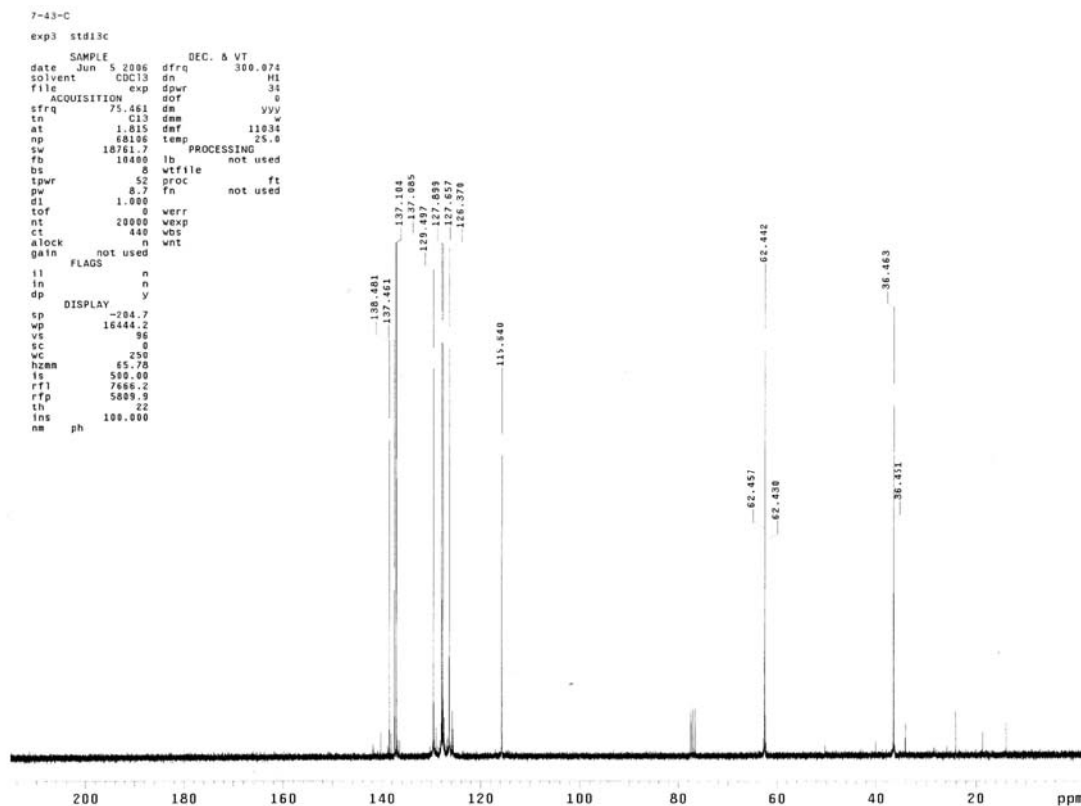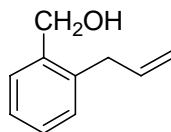
^{1}H NMR Spectrum of **3-56**
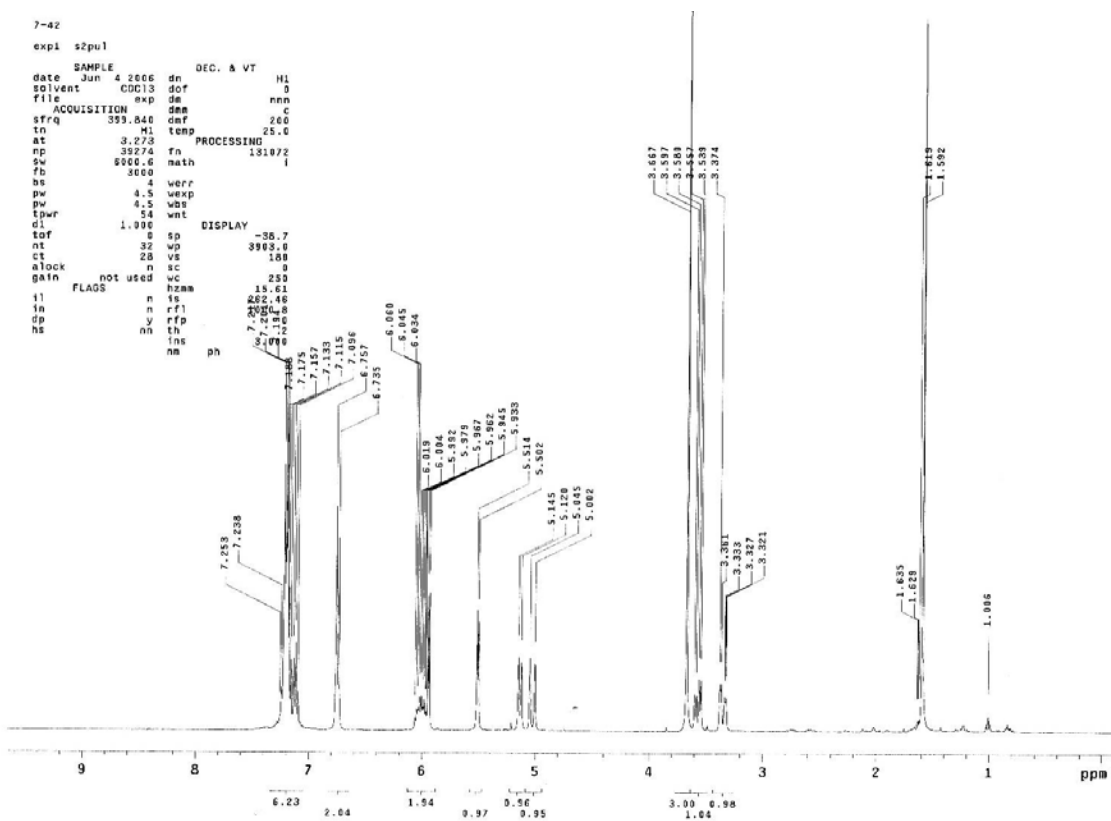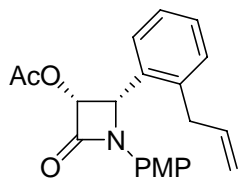
^{13}C NMR Spectrum of 3-56
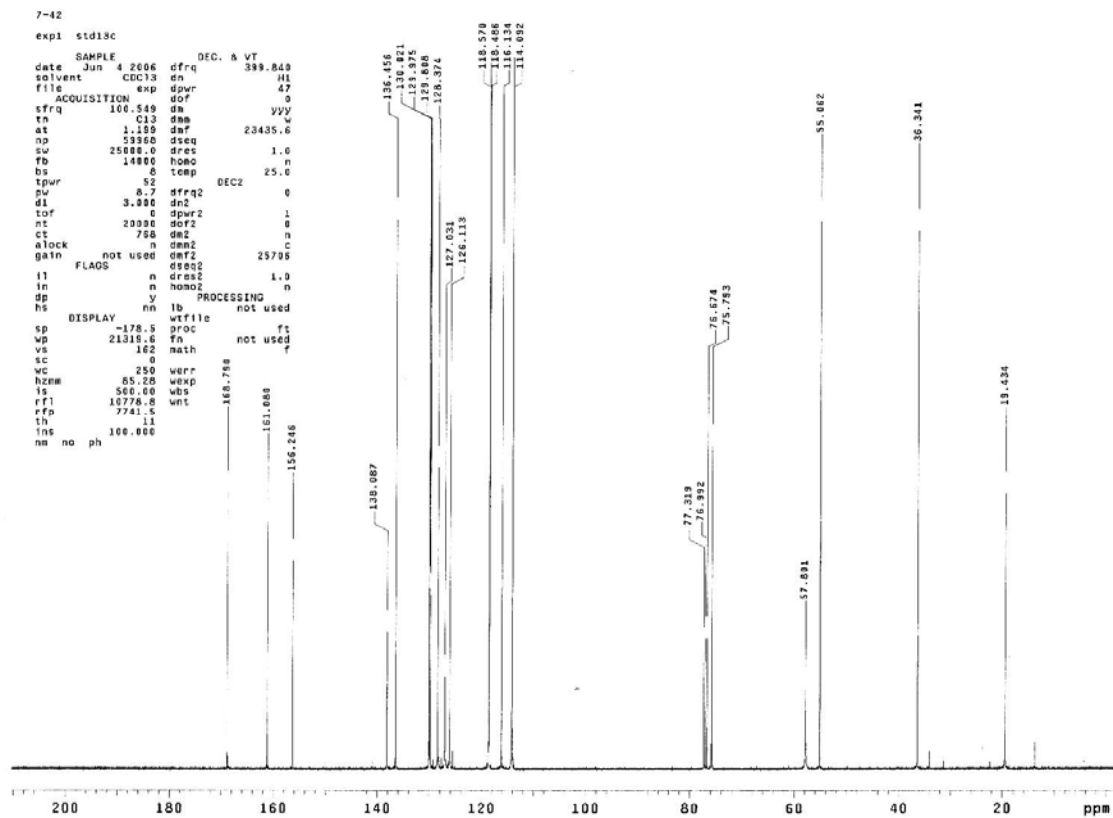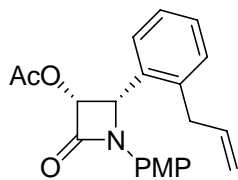
^{1}H NMR Spectrum of **3-57**
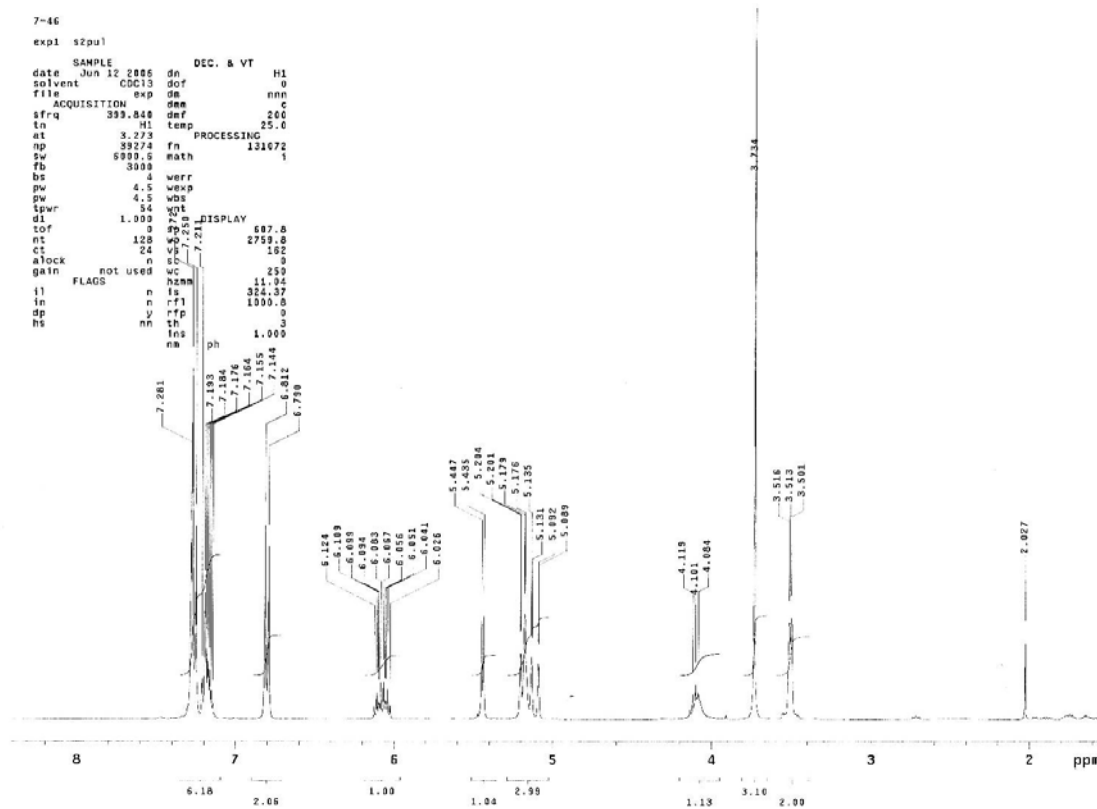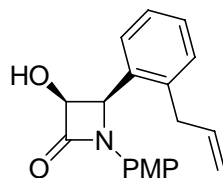
¹³C NMR Spectrum of **3-57**
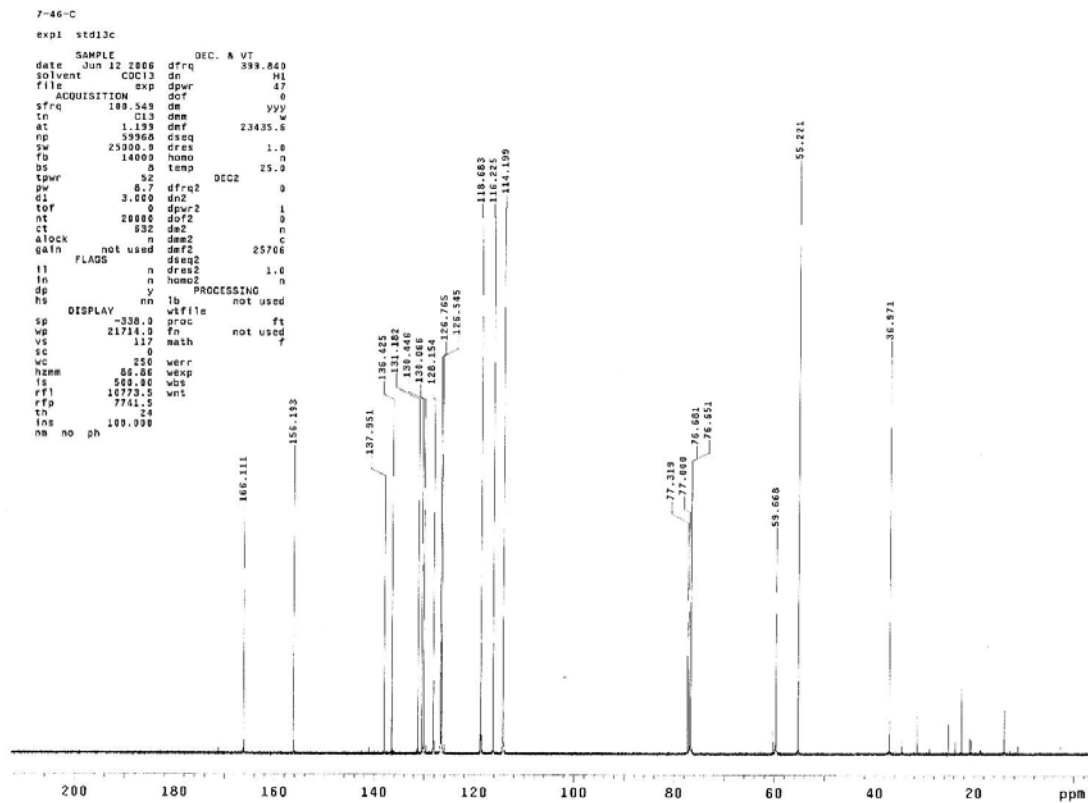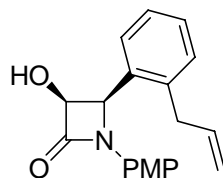
^{1}H NMR Spectrum of **3-58**
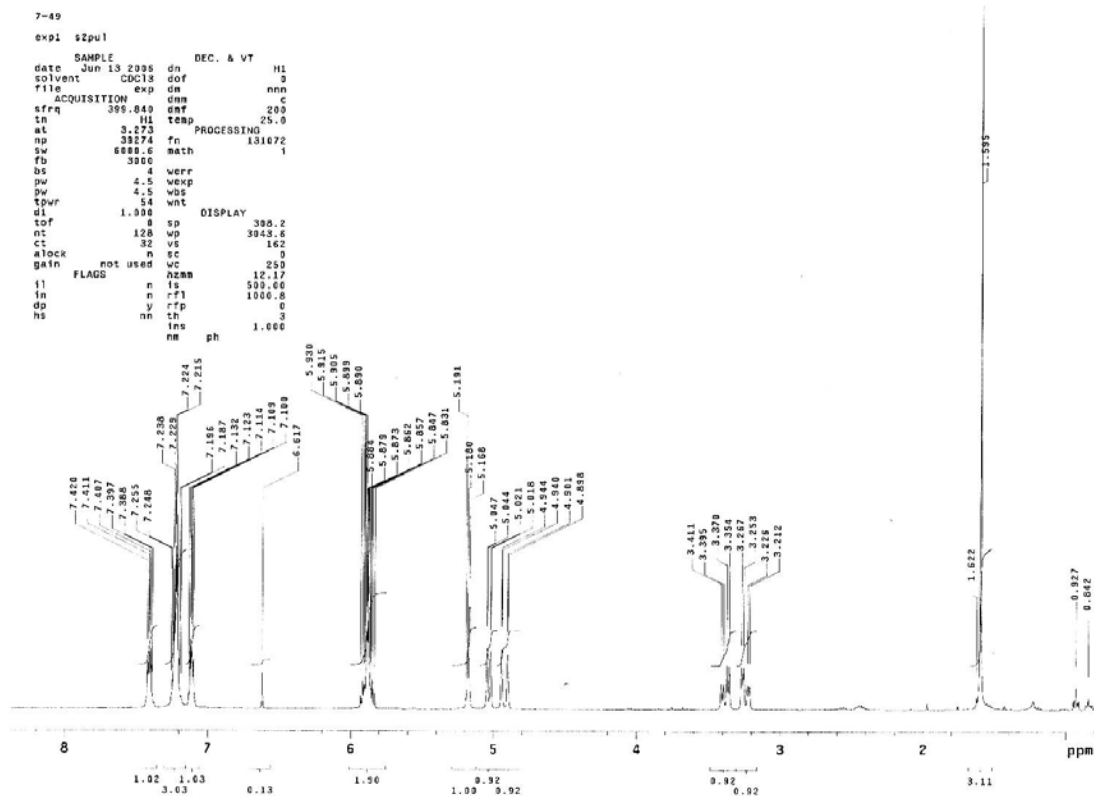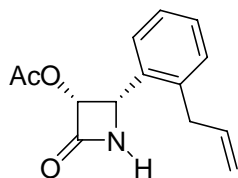
^{13}C NMR Spectrum of **3-58**
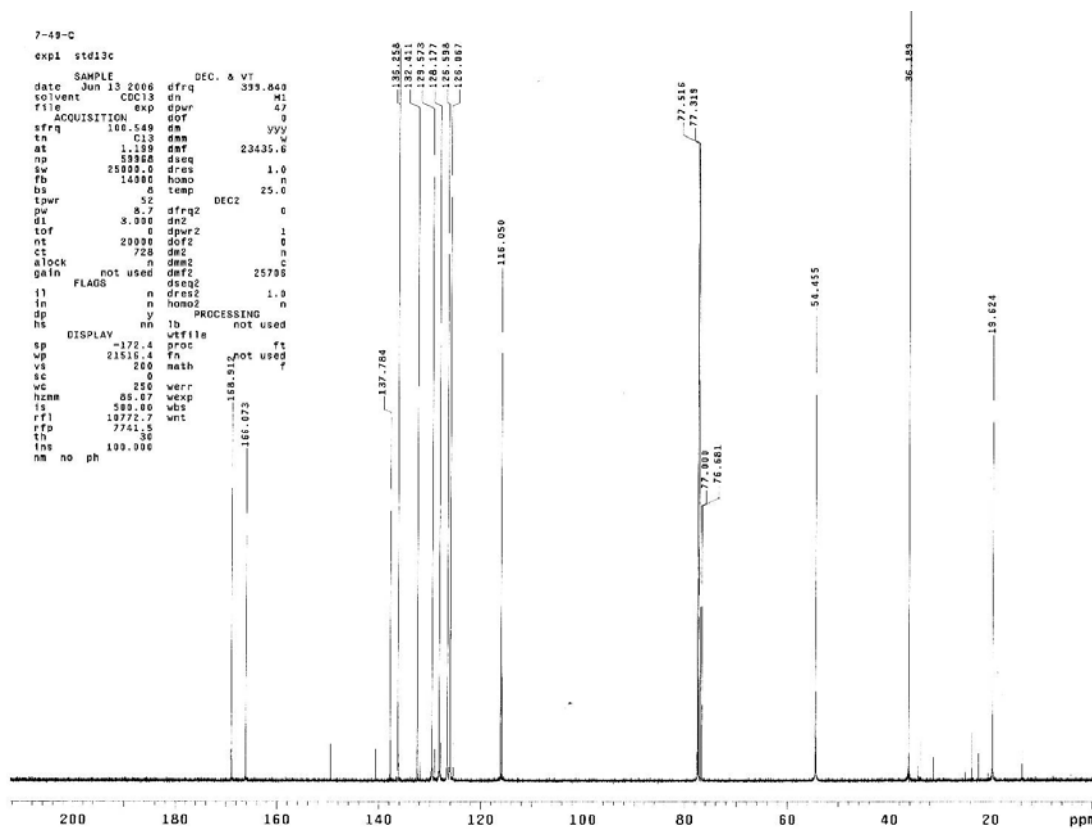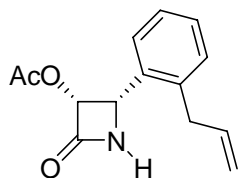
^{1}H NMR Spectrum of **3-60**

^{13}C NMR Spectrum of **3-60**

7-51-C

exp3 std13c

	SAMPLE		DEC. & VT
date	Jun 14 2006	dfrq	300.074
solvent	CDCl3	dn	H1
file	exp	dpwr	34
	ACQUISITION	dof	0
sfrq	75.461	dm	yyy
tn	C13	dmm	w
at	1.815	dmf	11034
np	68106	temp	25.0
sw	18761.7		PROCESSING
fb	10400	lb	not used
bs	8	wtfile	
tpwr	52	proc	ft
pw	8.7	fn	not used
d1	1.000		
tof	0	werr	
nt	20000	wexp	
ct	560	wbs	
alock	n	wnt	
gain	not used		
	FLAGS		
il	n		
in	n		
dp	y		
	DISPLAY		
sp	-485.0		
wp	16444.2		
vs	192		
sc	0		
wc	250		
hzmm	65.78		
is	500.00		
rfl	7650.7		
rfp	5809.9		
th	12		
ins	100.000		
nm	ph		

169.799

137.423
136.550
134.380
129.140
127.596
127.057
126.093

116.973

79.117
77.425
77.000
76.579

55.935

37.001

6.261

4.527
4.496

200   180   160   140   120   100   80   60   40   20   ppm

437

^{13}C NMR Spectrum of **3-61**

^{1}H NMR Spectrum of **3-62**
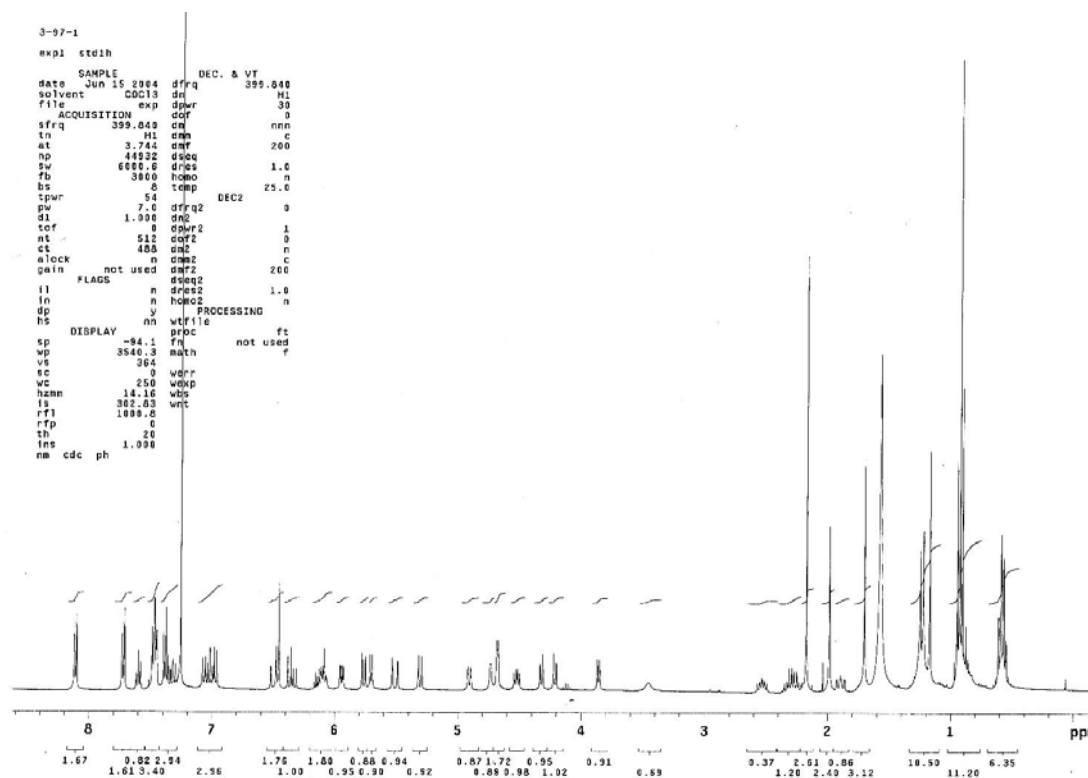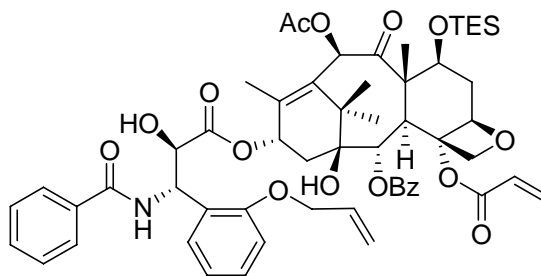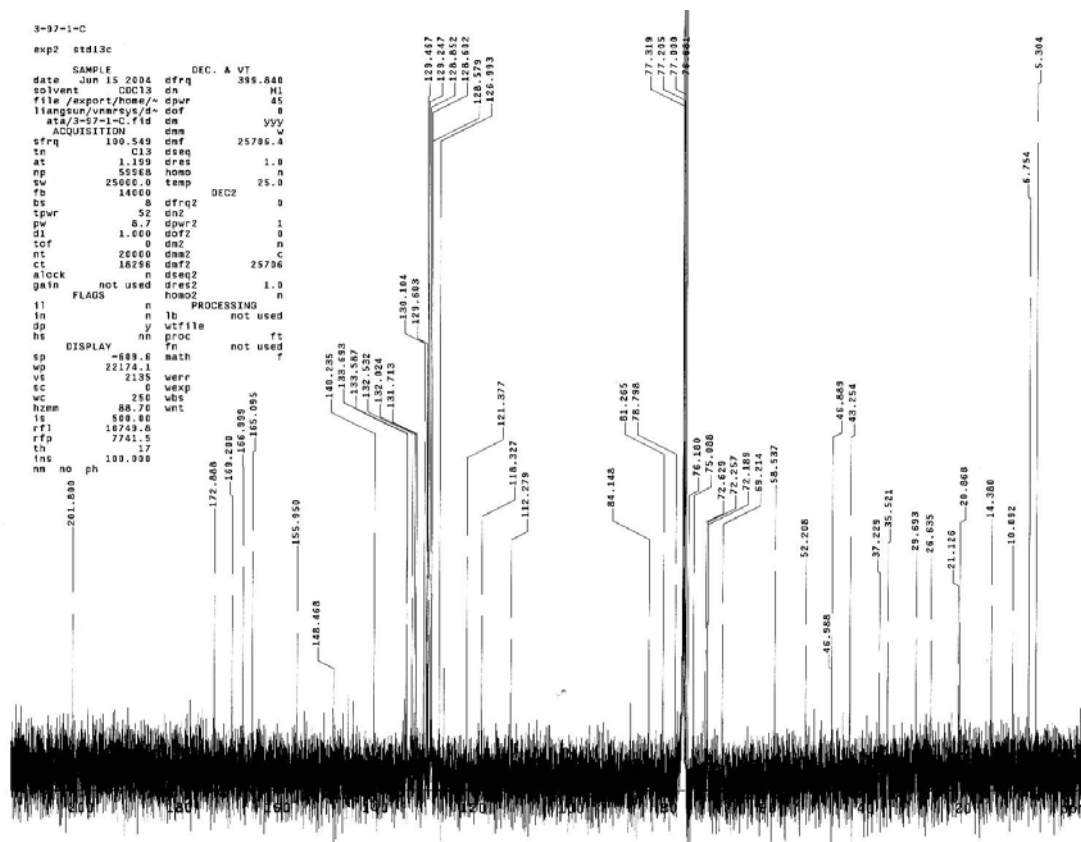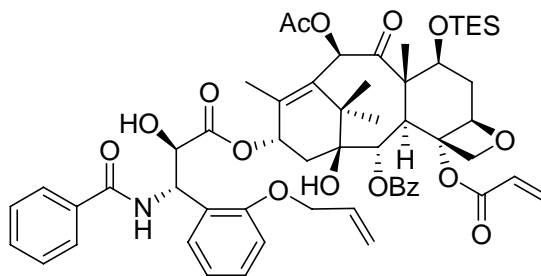
^{1}H NMR Spectrum of **3-63**
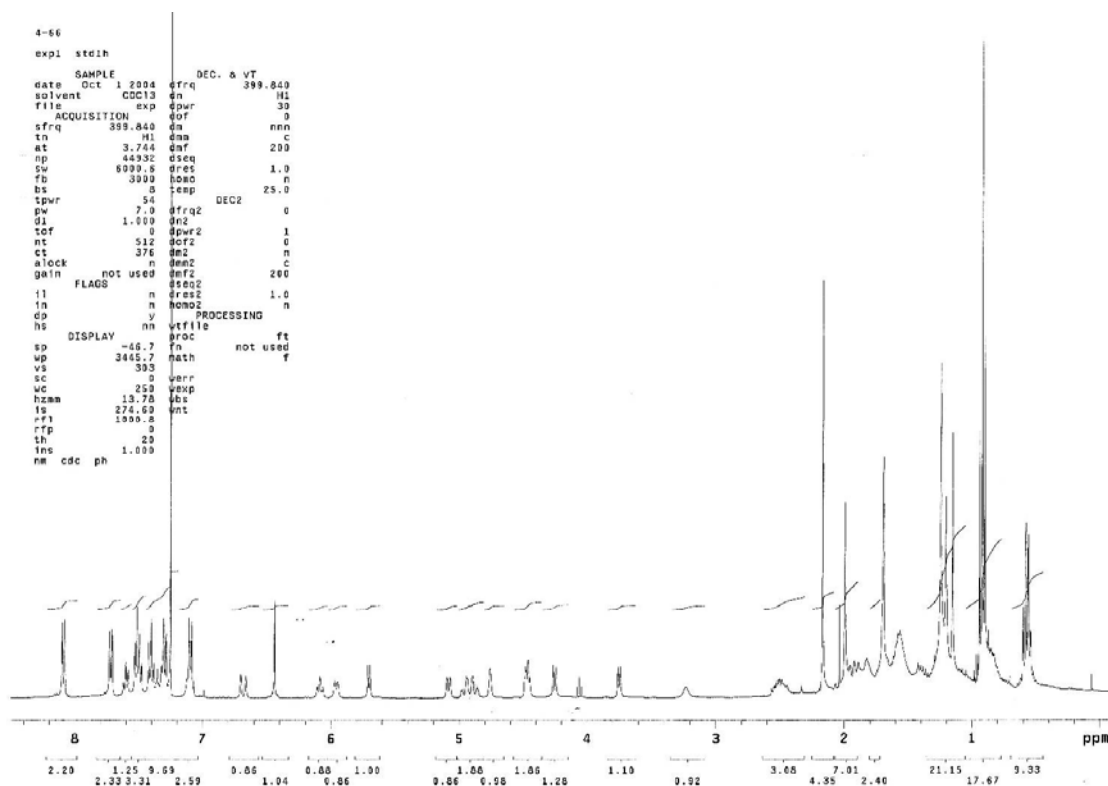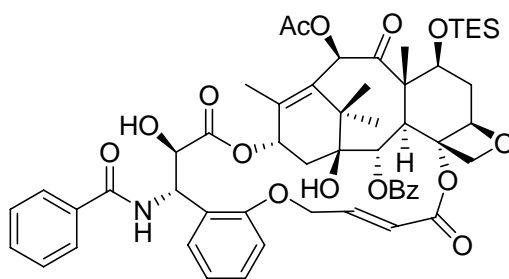
^{1}H NMR Spectrum of **K2a**
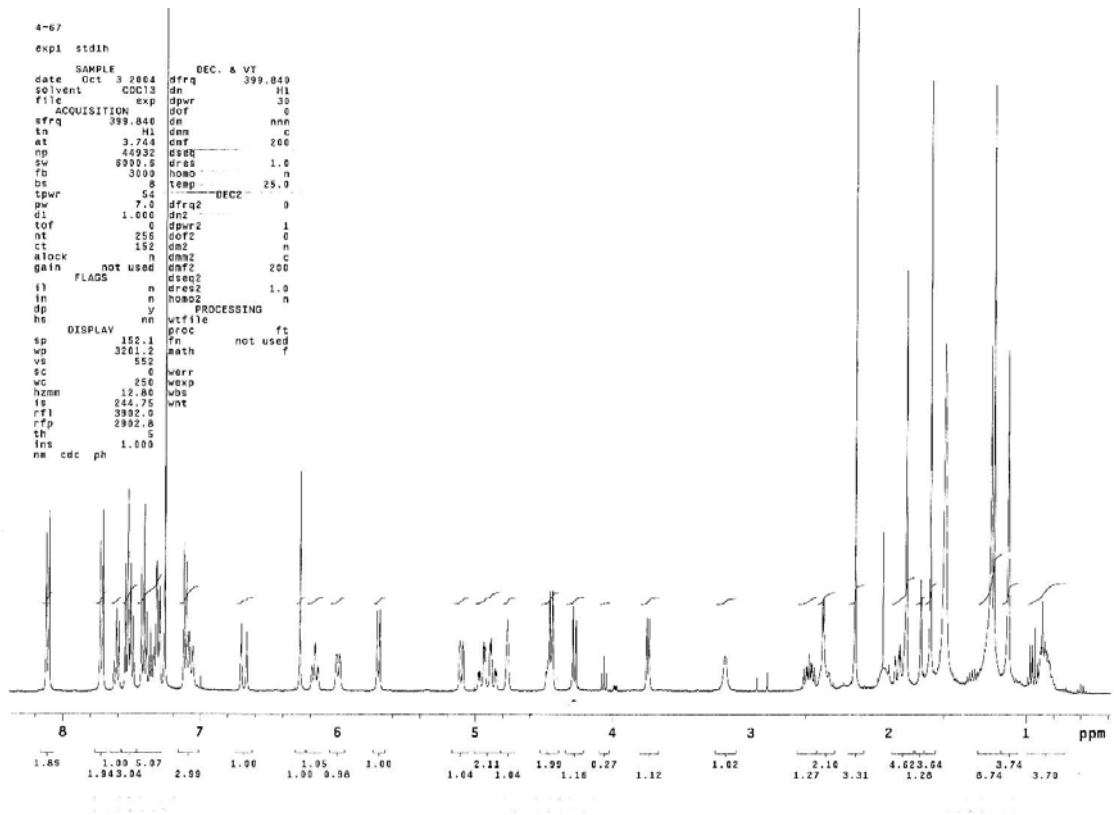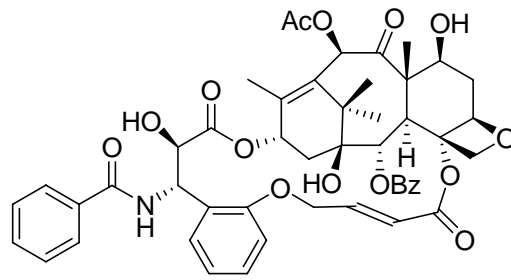
^{13}C NMR Spectrum of **K2a**
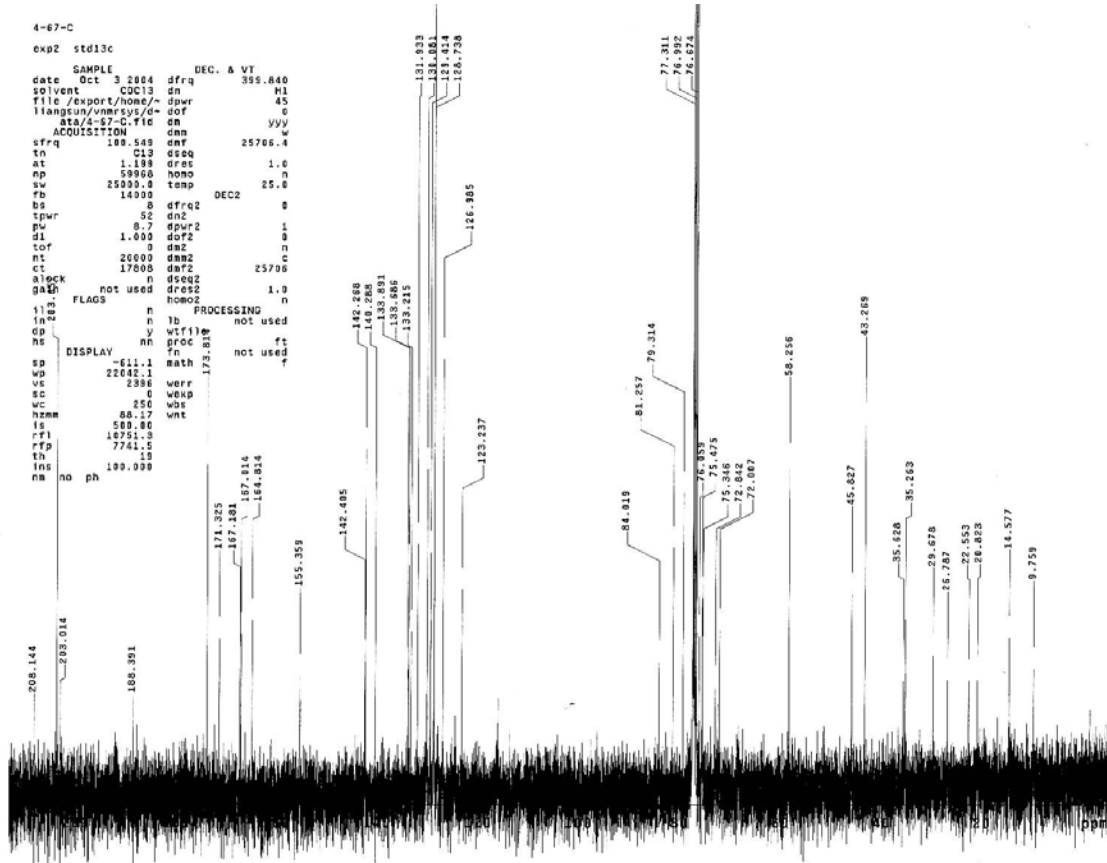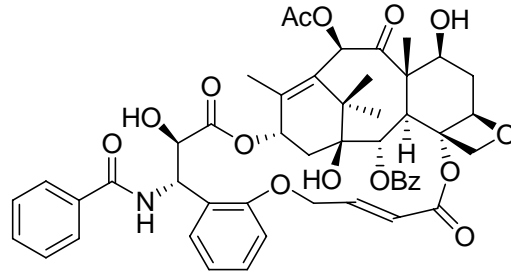
^{1}H NMR Spectrum of **3-64**
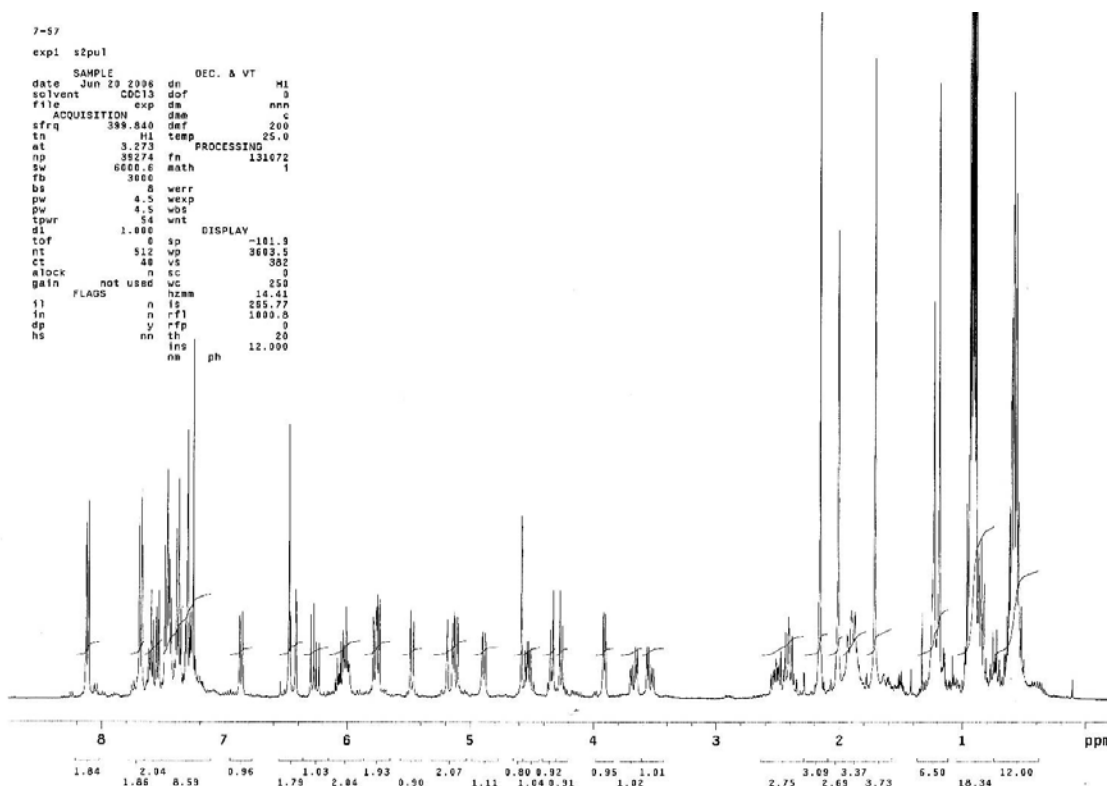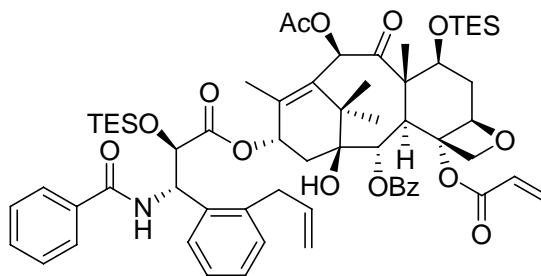
^{13}C NMR Spectrum of **3-64**
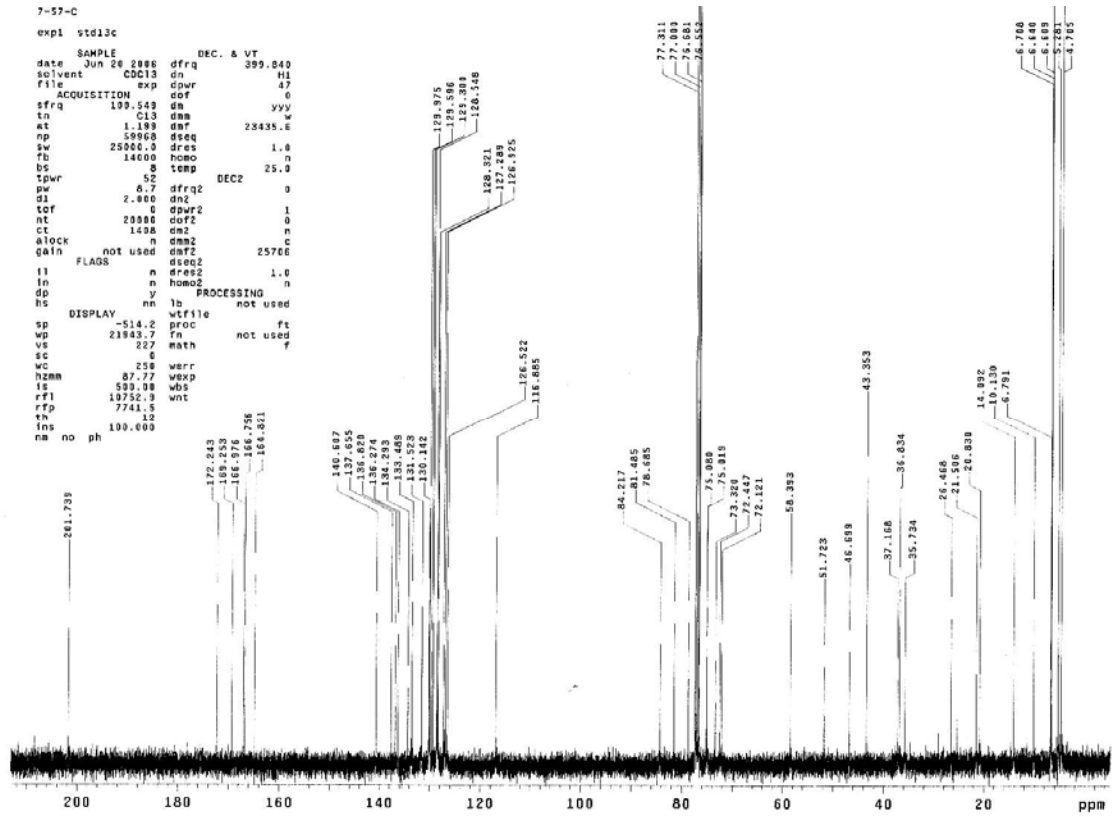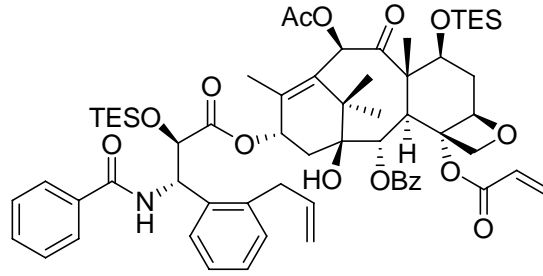
^{1}H NMR Spectrum of **K1a**
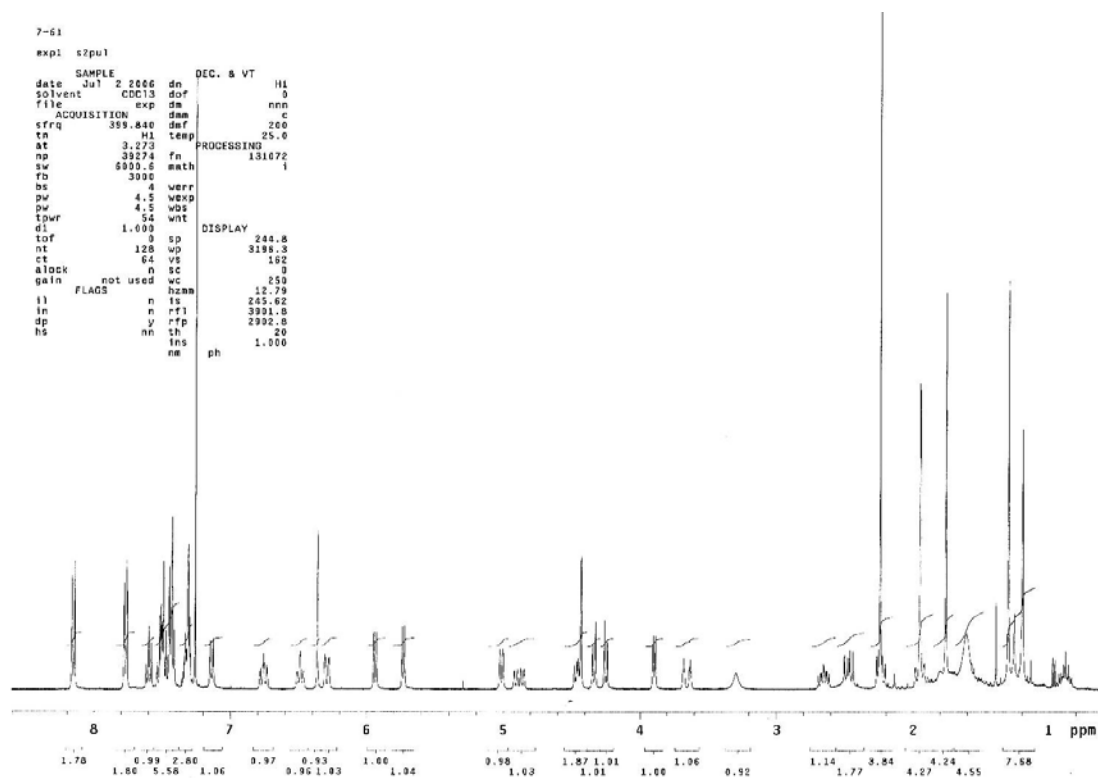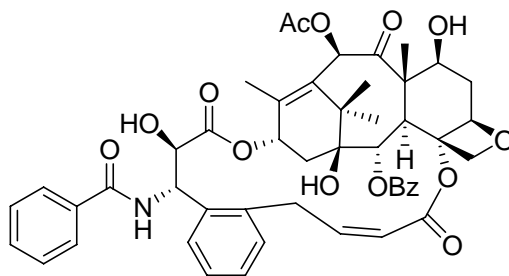
^{13}C NMR Spectrum of **K1a**
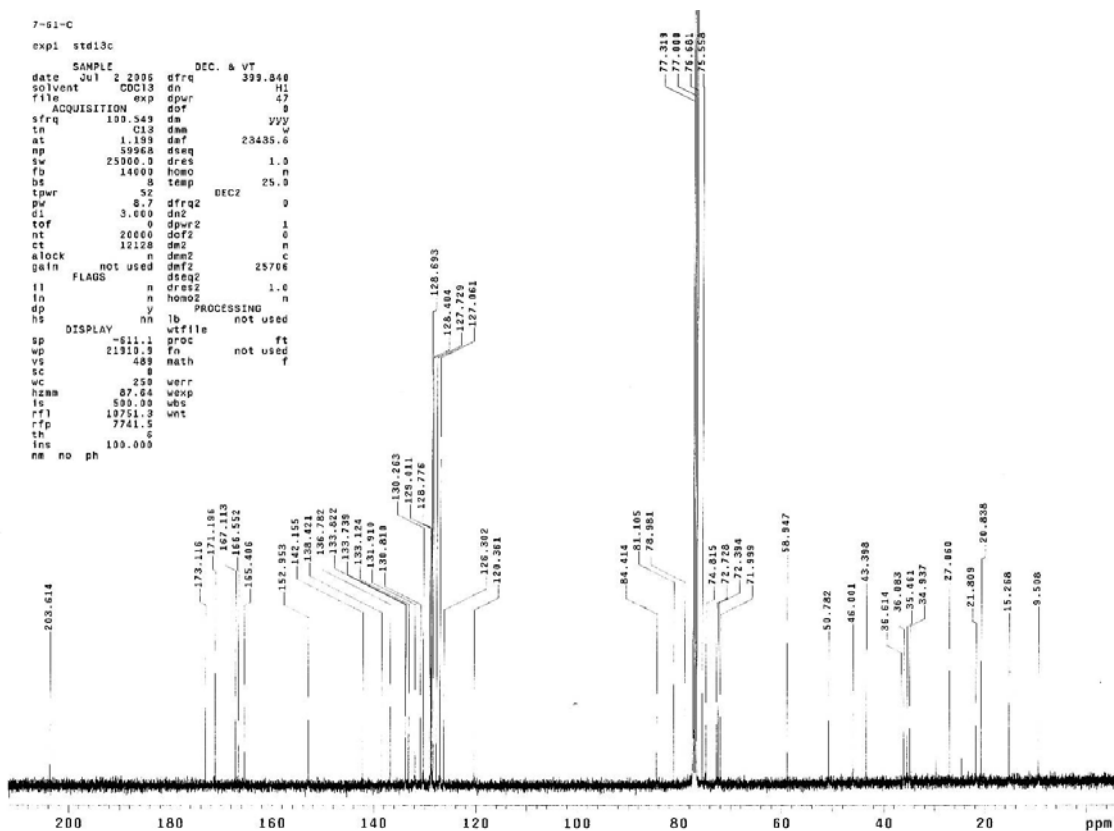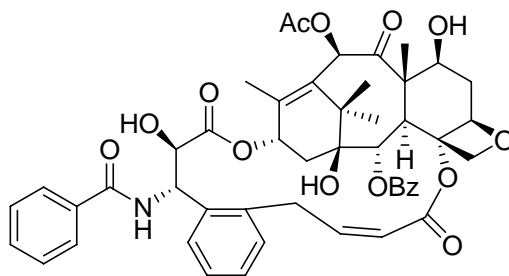
A4. Appendix Chapter V

^{1}H NMR Spectrum of **5-5**
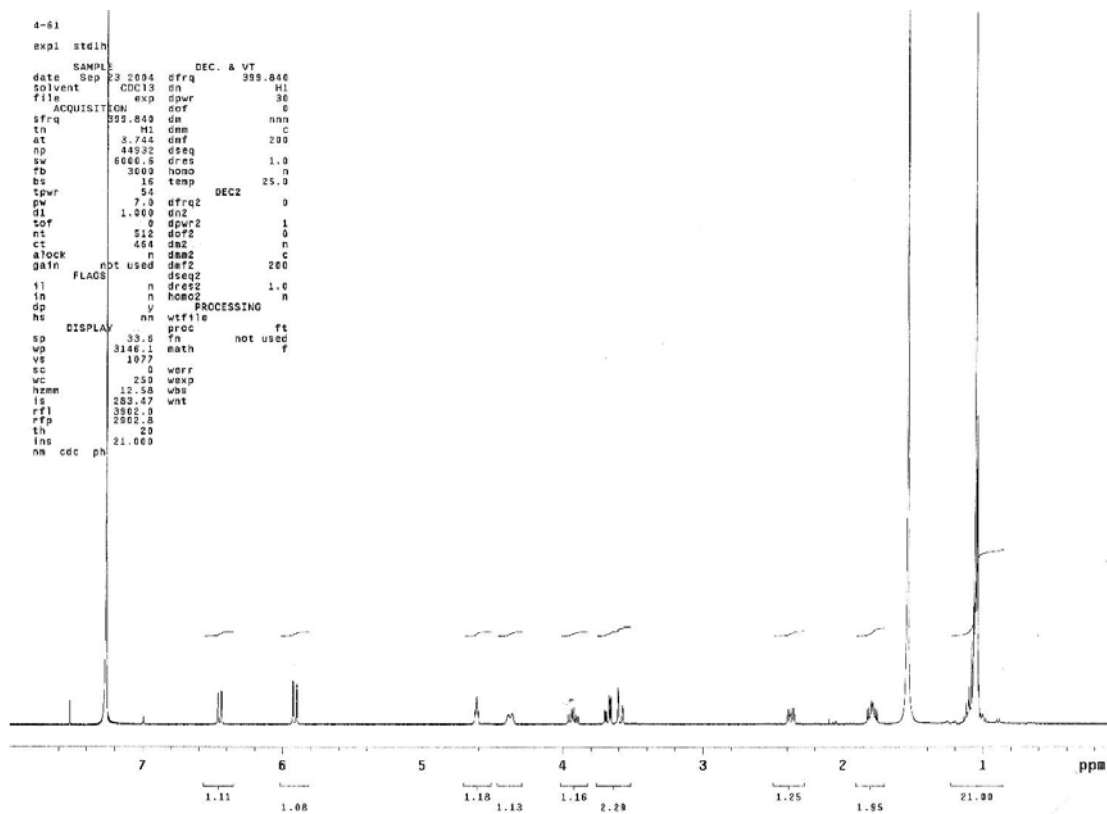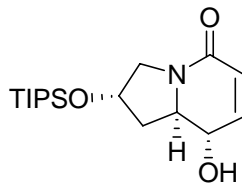
^{13}C NMR Spectrum of **5-5**
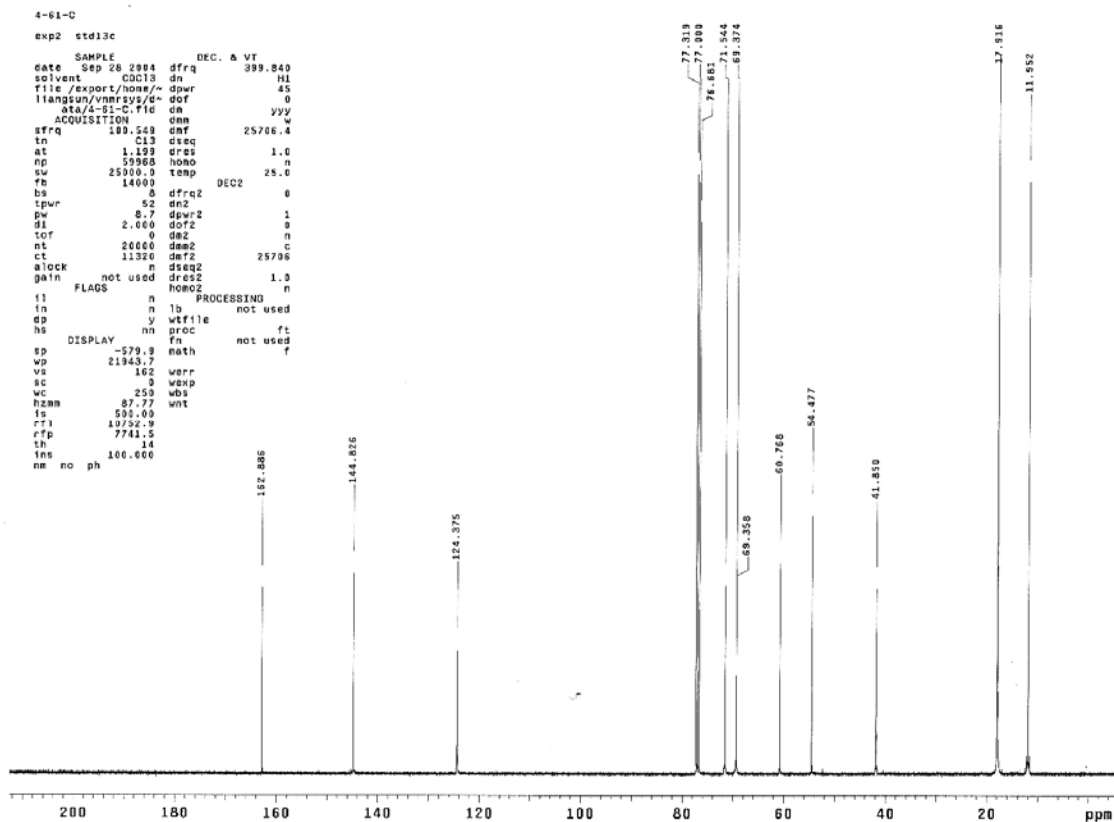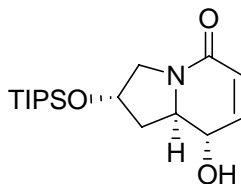
COSY Spectrum of **5-5**

NOESY Spectrum of **5-5**

¹H NMR Spectrum of **5-20**
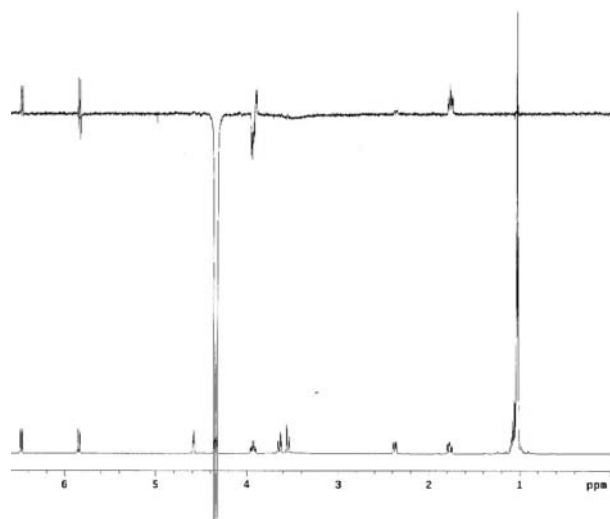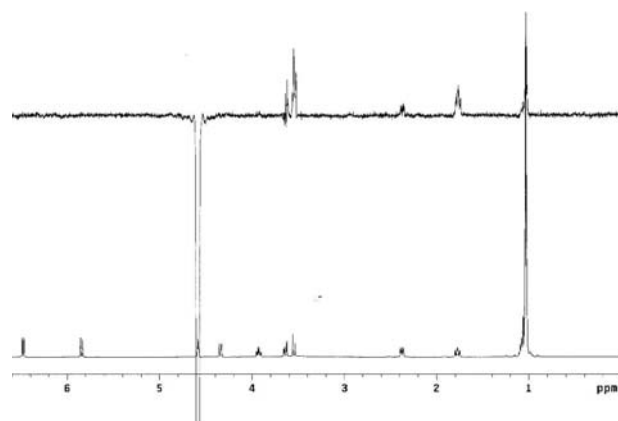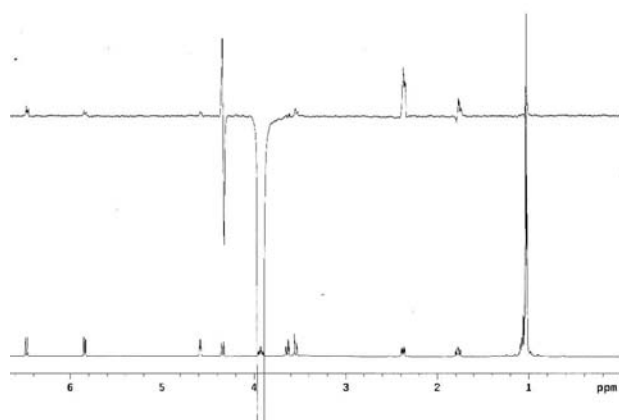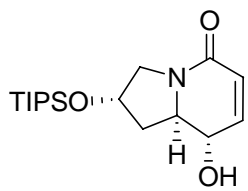
^{1}H NMR Spectrum of **5-20**
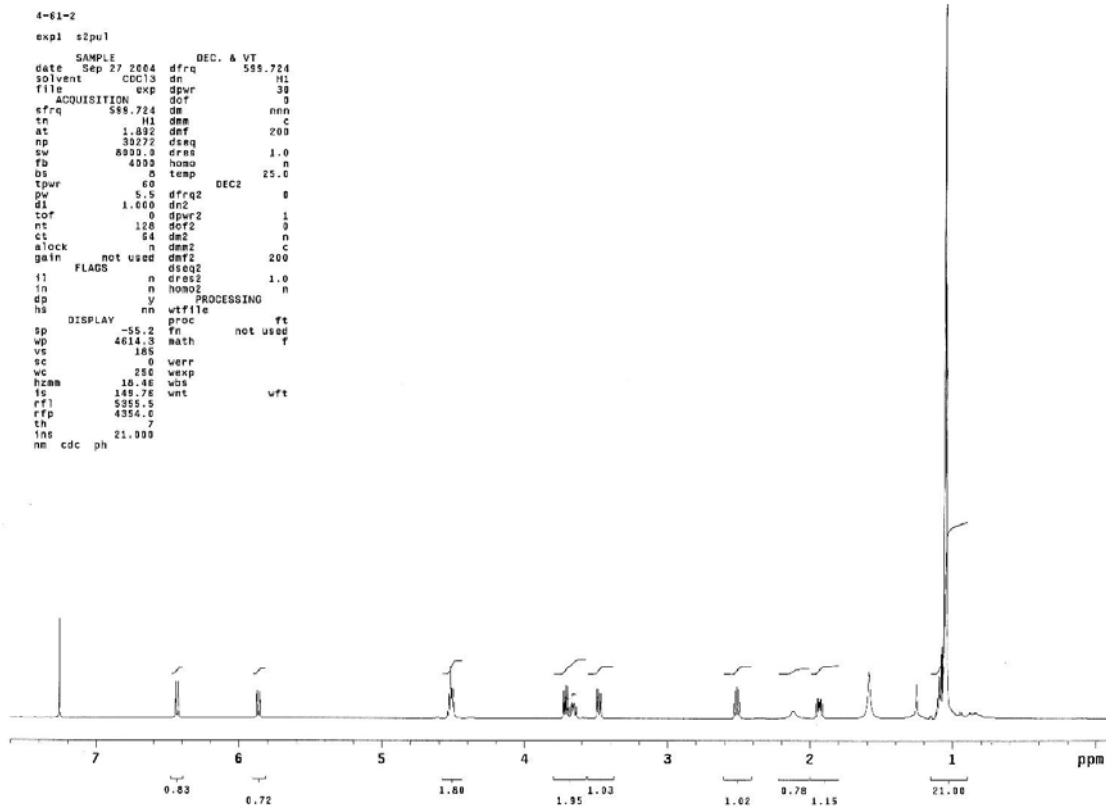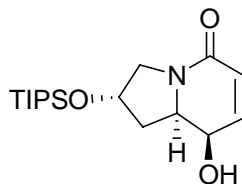
^{1}H NMR Spectrum of 5-23
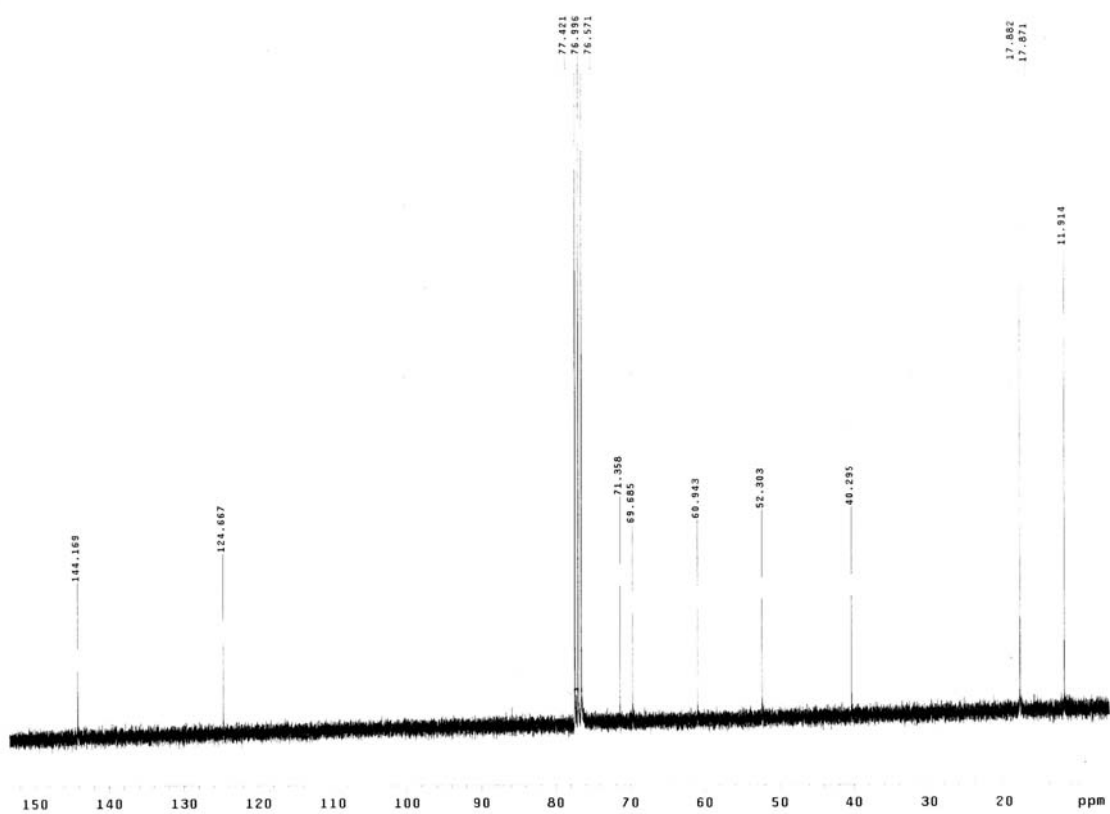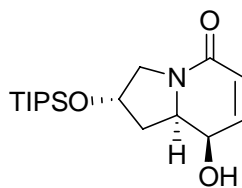
^{13}C NMR Spectrum of **5-23**
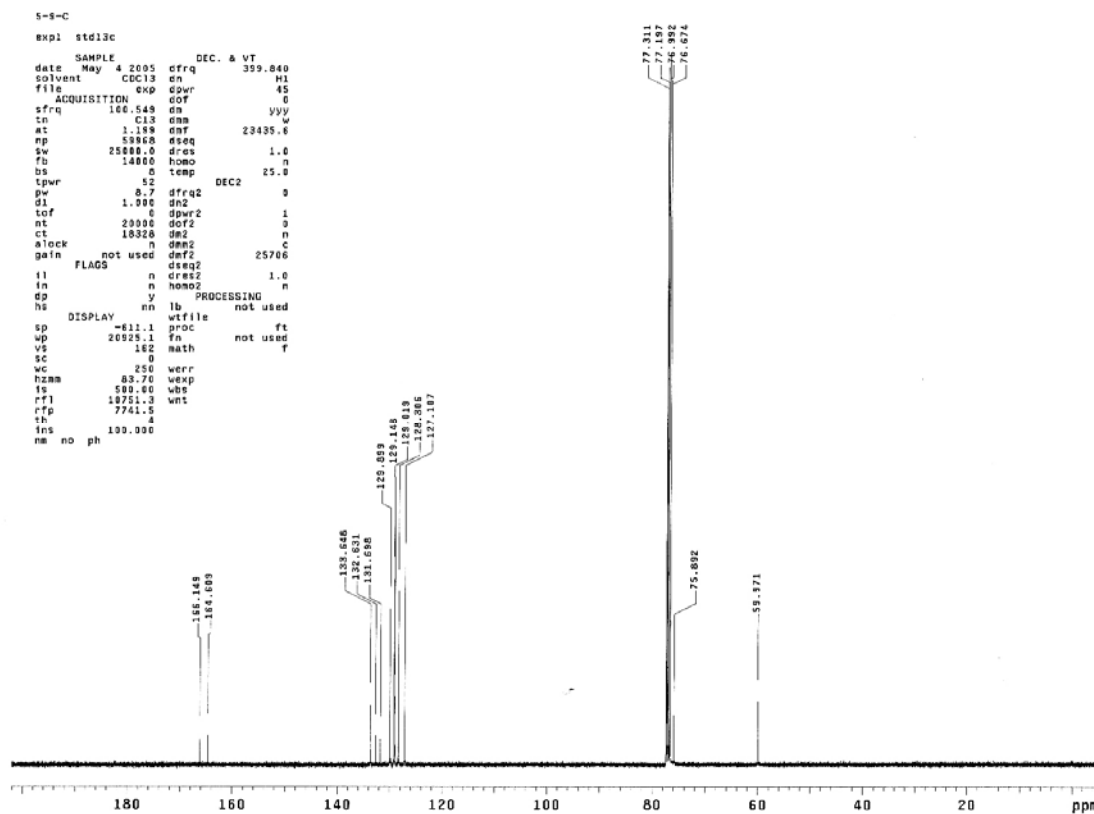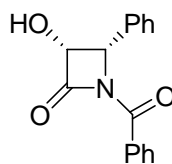
^{1}H NMR Spectrum of **5-24**
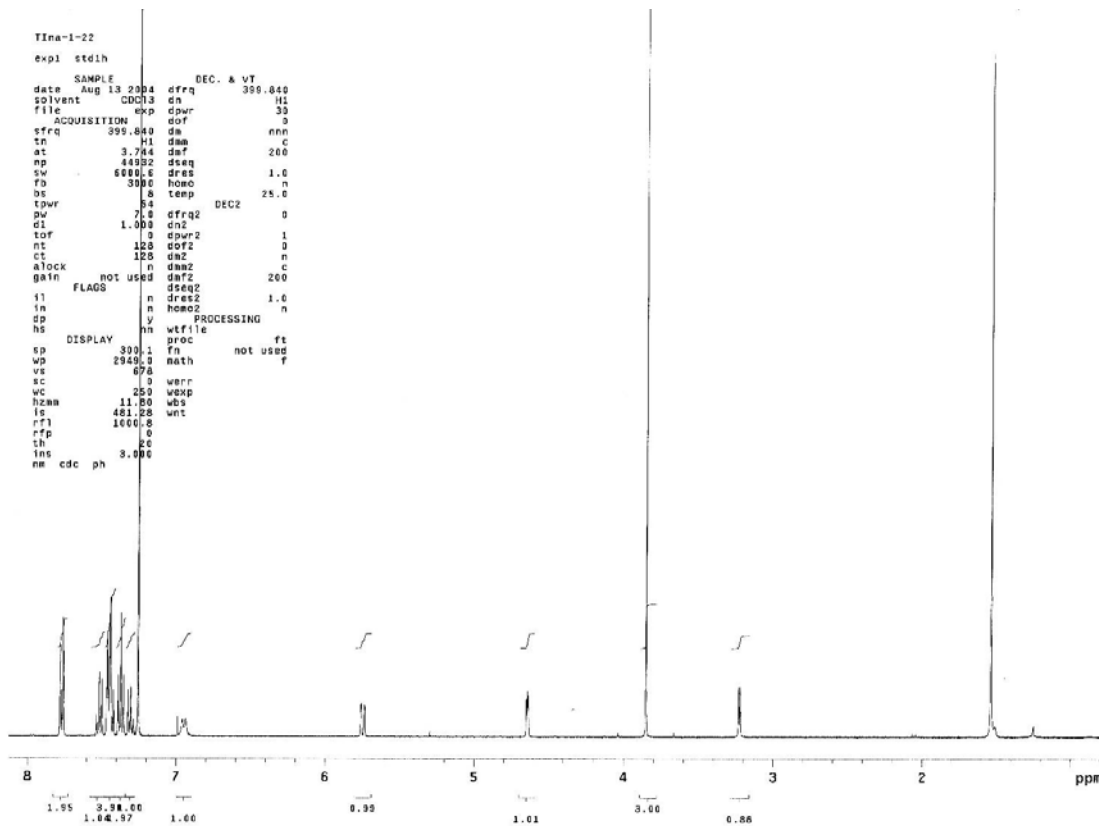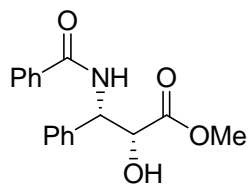
^{13}C NMR Spectrum of **5-24**
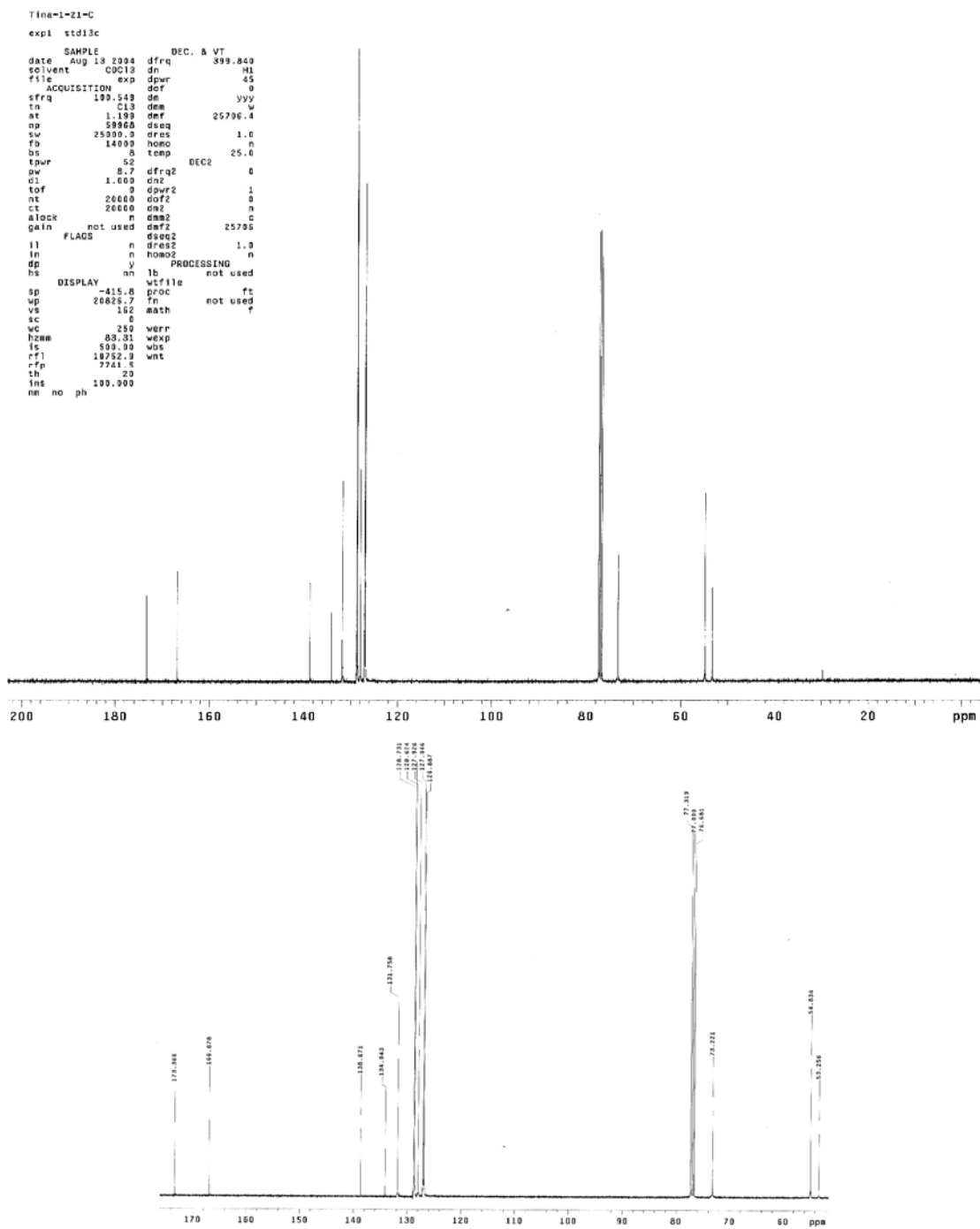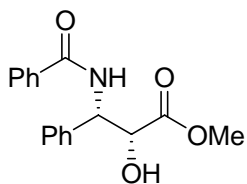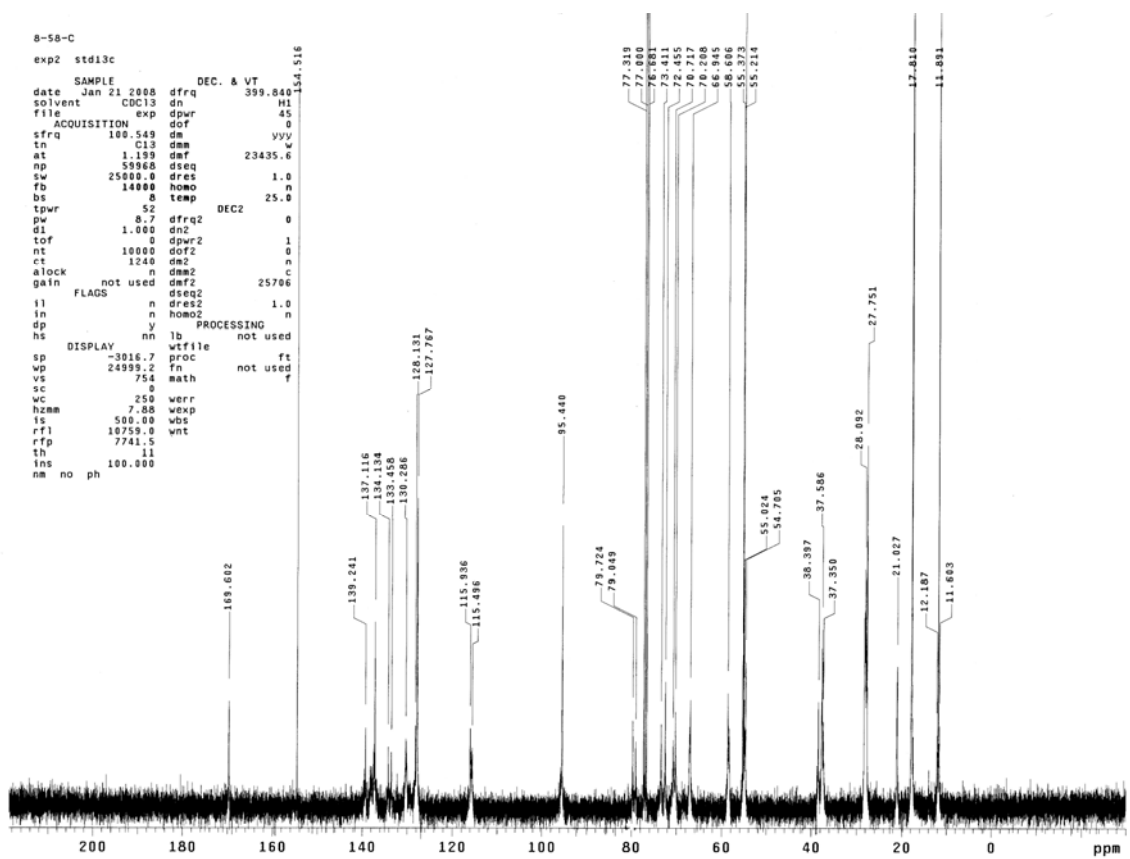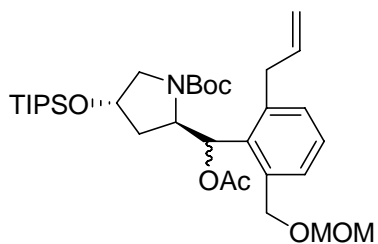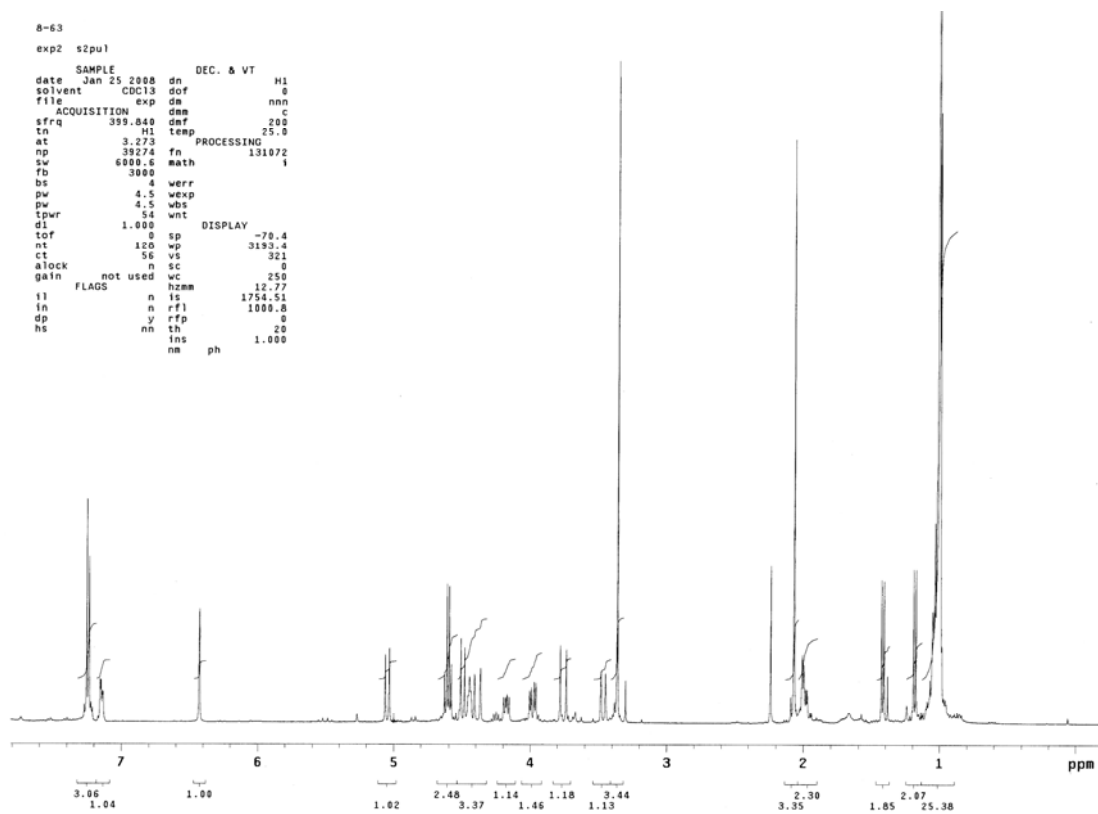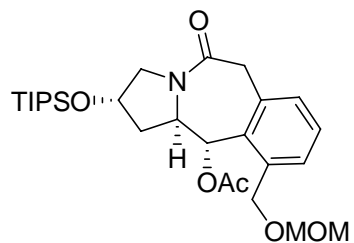
^{1}H NMR Spectrum of **5-25**
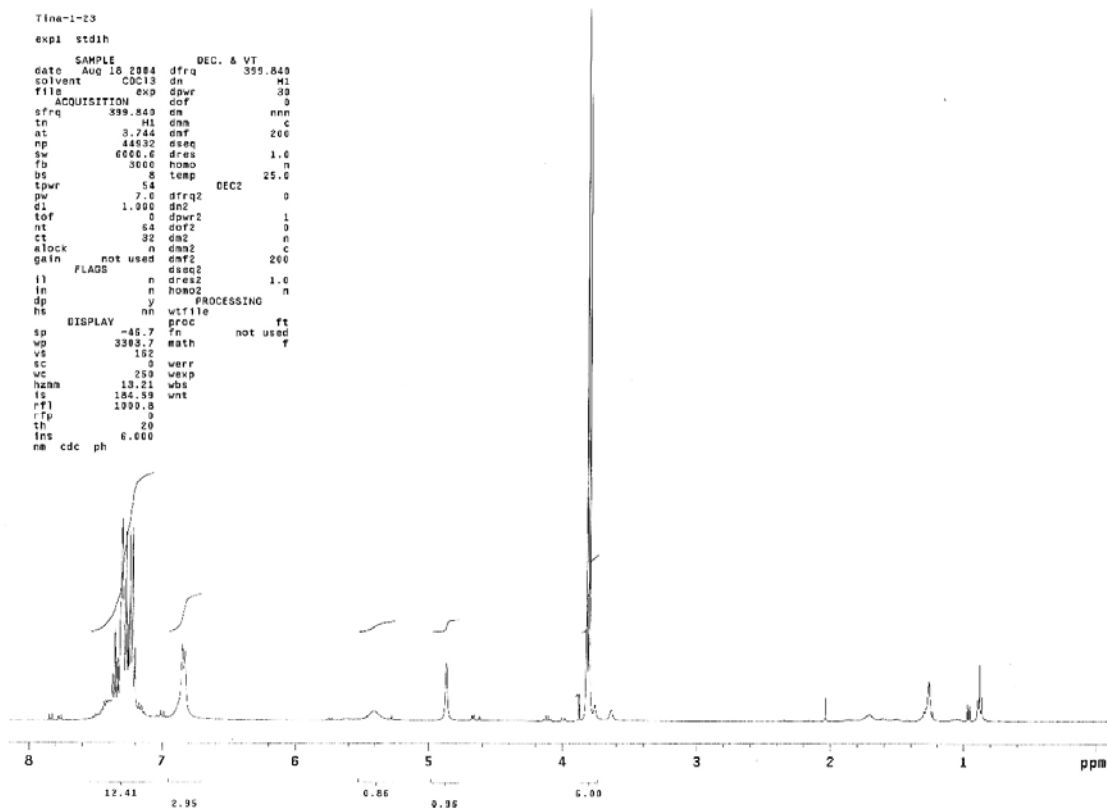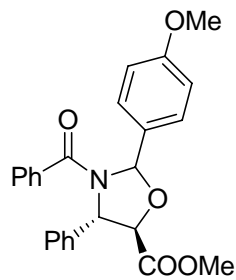
¹³C NMR Spectrum of 5-25
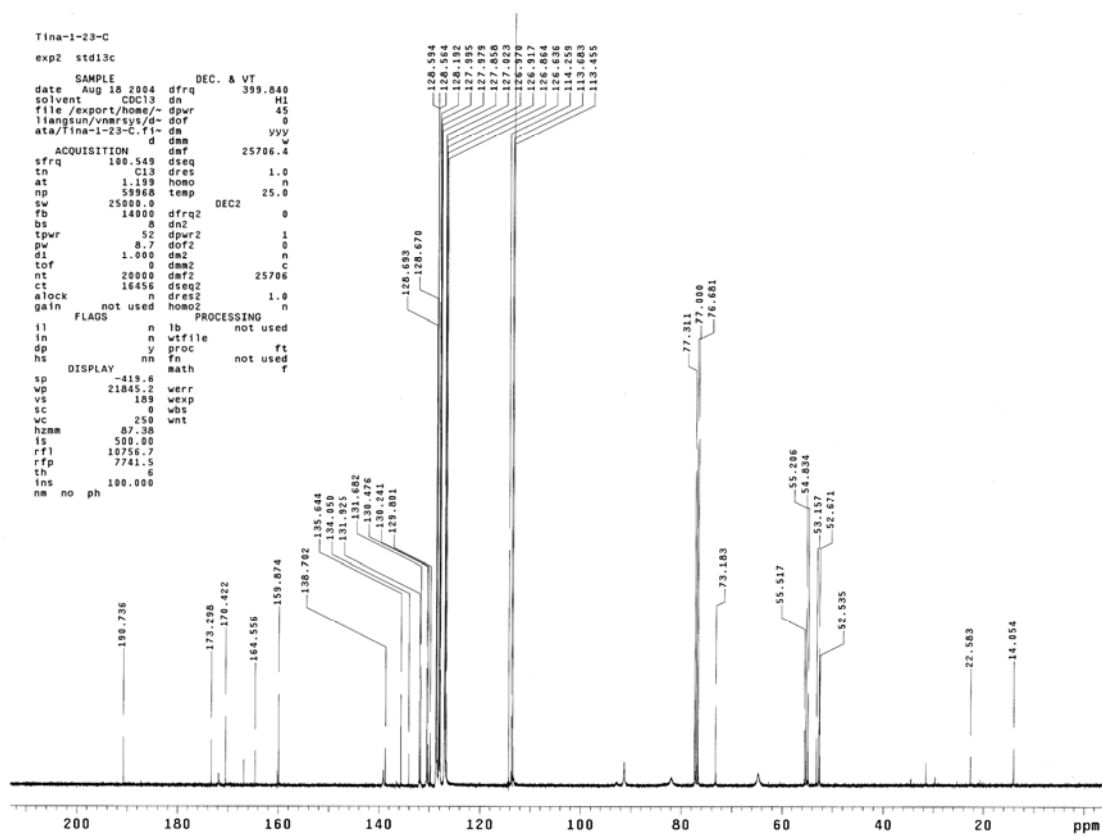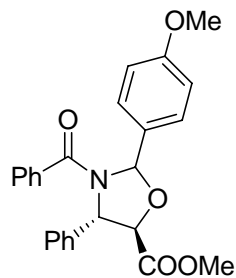
^{1}H NMR Spectrum of **5-4**
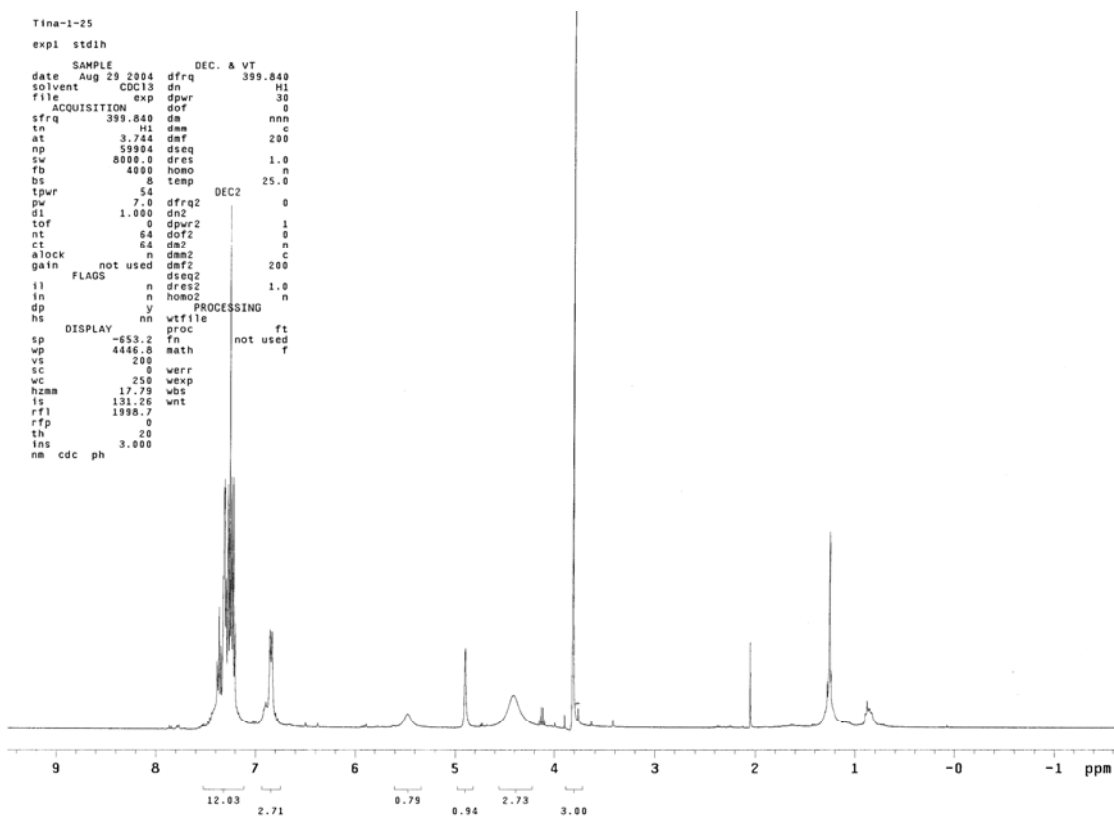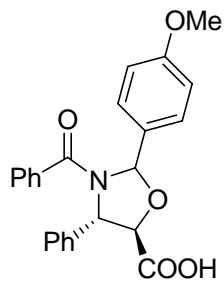
^{13}C NMR Spectrum of **5-4**

^{1}H NMR Spectrum of **5-26**
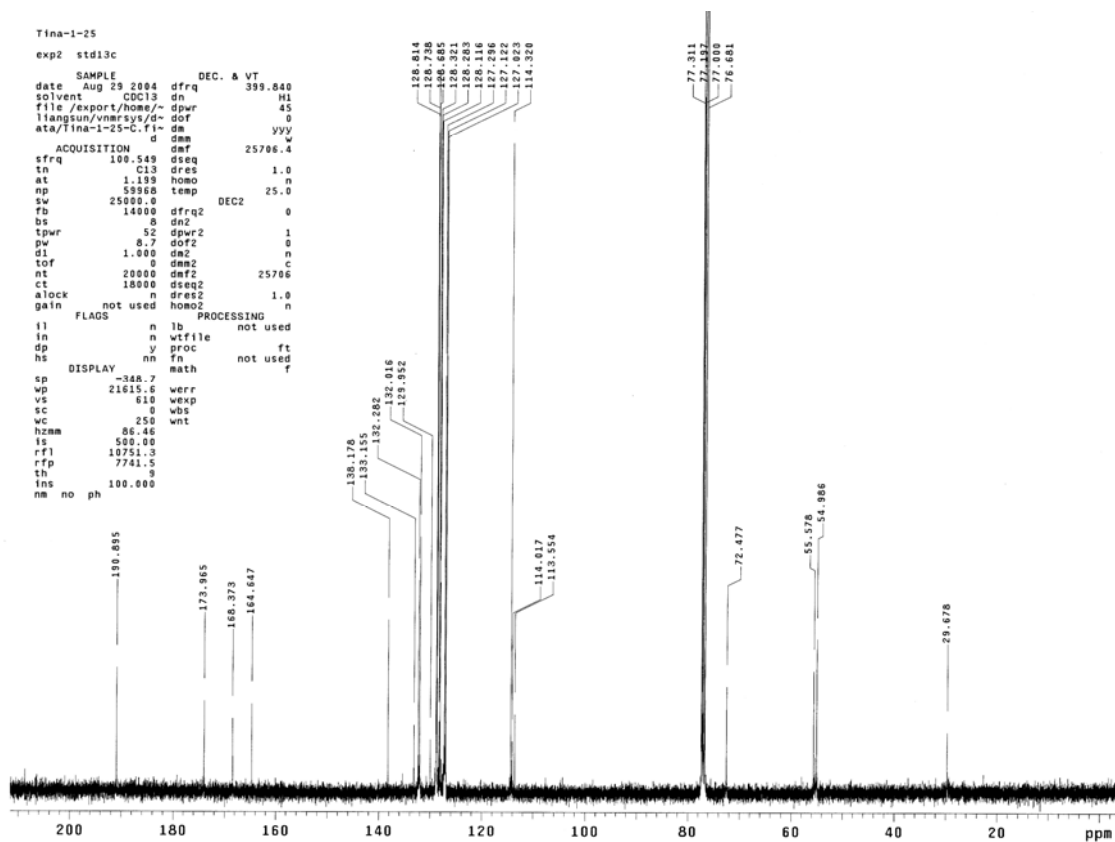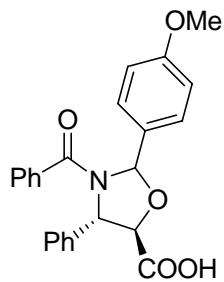
^{13}C NMR Spectrum of **5-26**
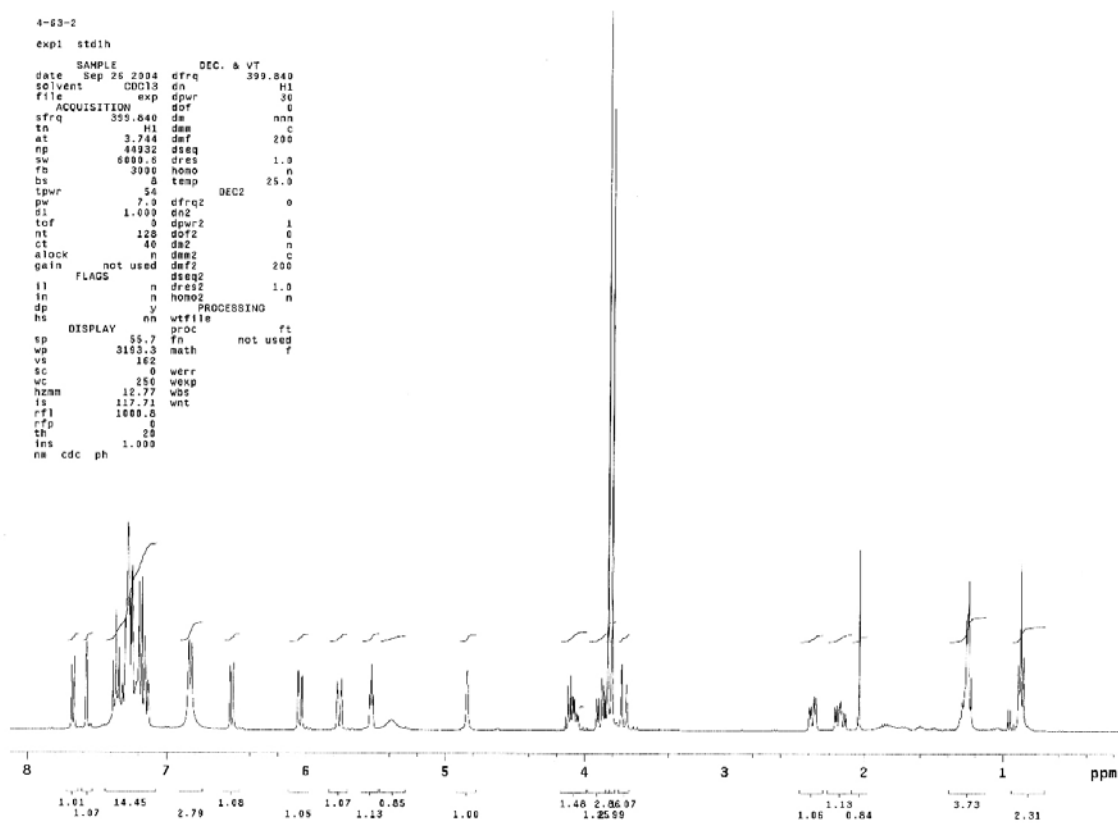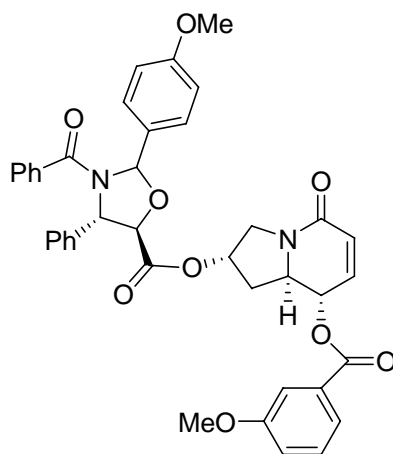
^{1}H NMR Spectrum of 5-2 (SB-H-102)
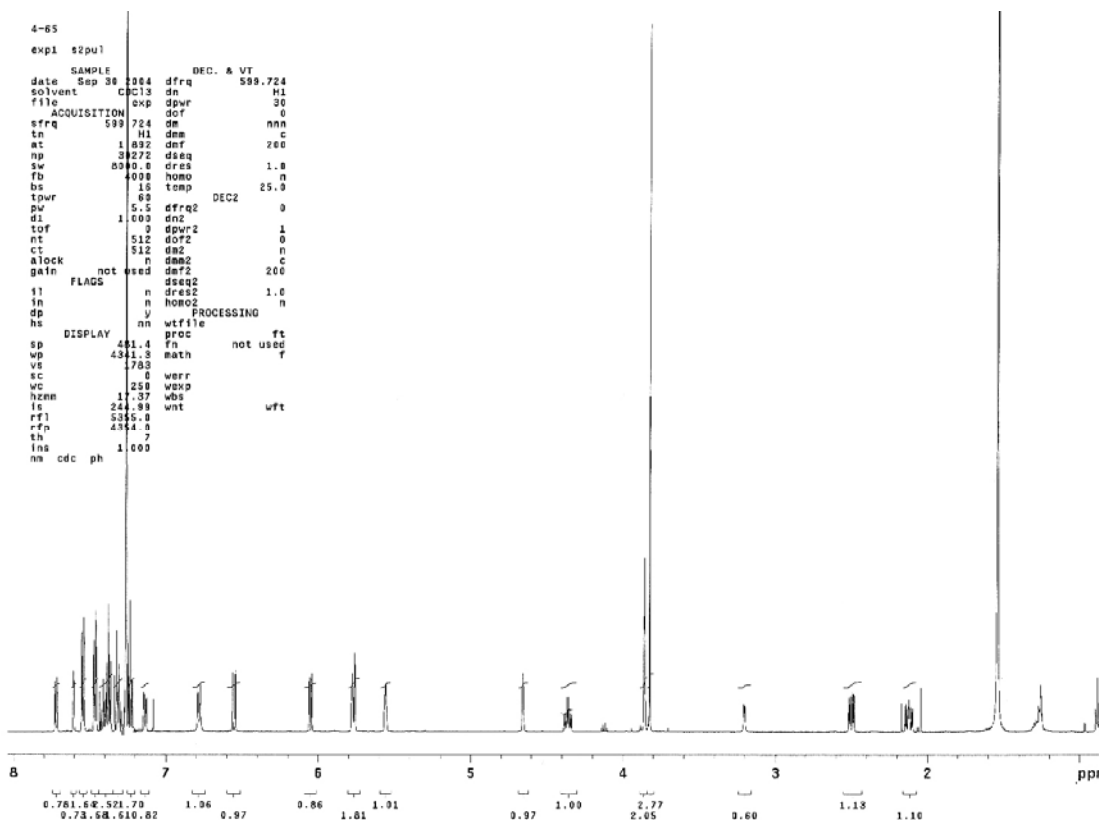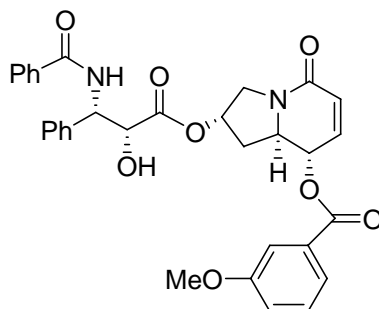
^{13}C NMR Spectrum of 5-2 (SB-H-102)
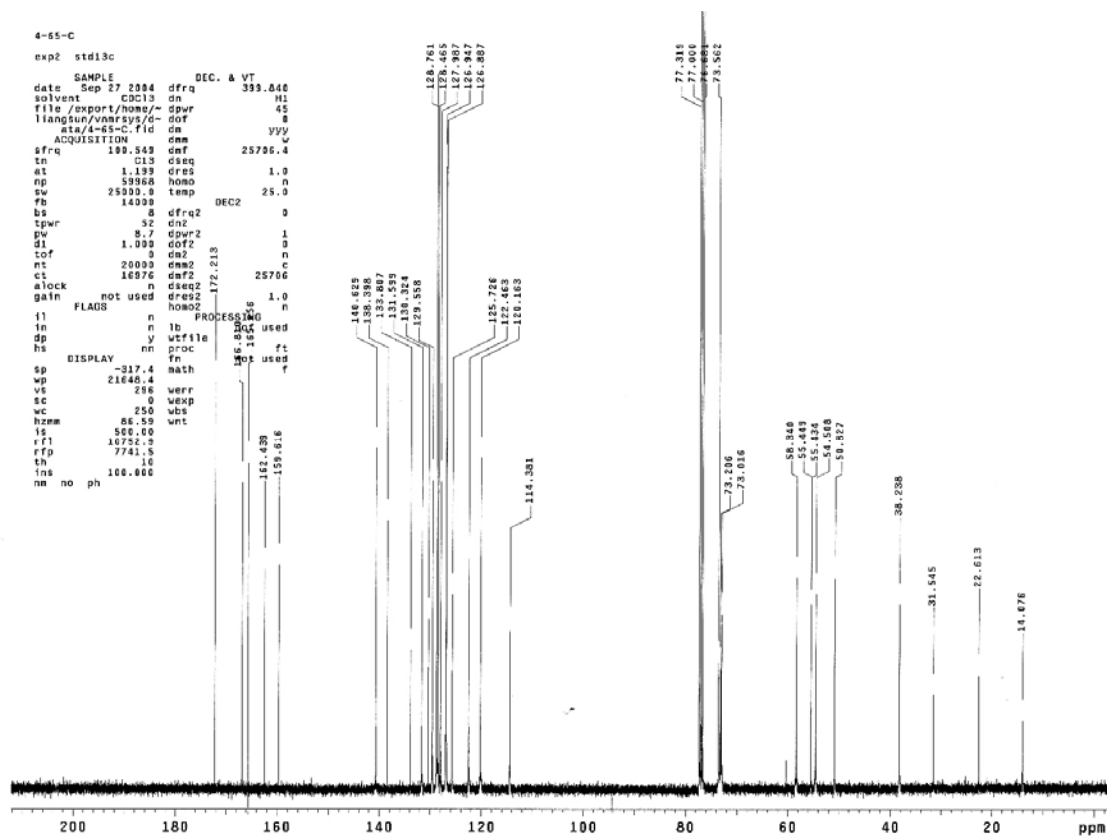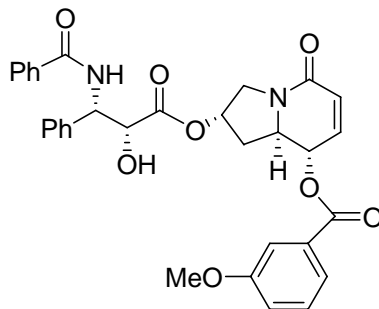
^{1}H NMR Spectrum of **5-42**
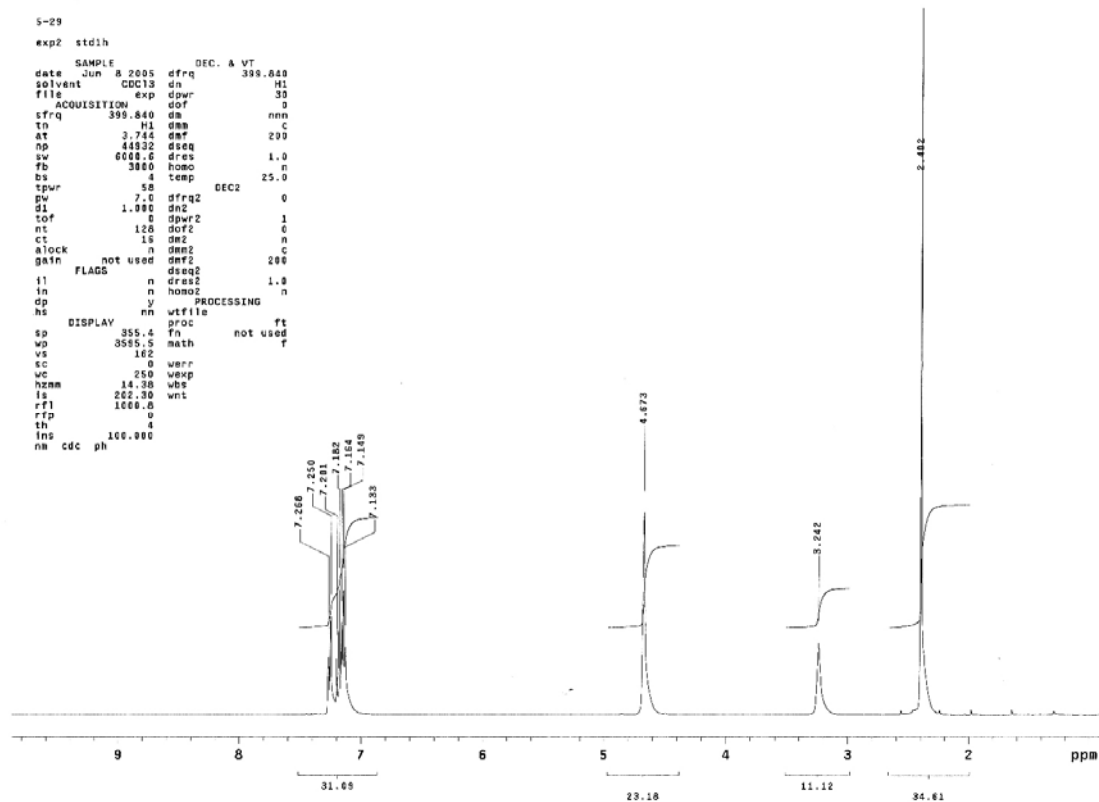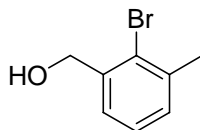
^{1}H NMR Spectrum of **5-43**


```
5-8-2

exp3  s2pul
        SAMPLE              DEC. & VT
date   May  7 2005   dfrq      300.074
solvent      CDC13   dn            H1
file /export/home/~  dpwr          30
liasun/vnmrsys/dat~  dof            0
     a/5-8-2.fid     dm           nnn
    ACQUISITION      dmm            c
sfrq      300.074    dmf          200
tn            H1     temp        25.0
at         1.998        PROCESSING
np         17984    wtfile
sw        4500.5    proc           ft
fb          2600    fn       not used
bs             8
tpwr          50    werr
pw           1.0    wexp
d1         1.000    wbs
tof            0    wnt
nt           512
ct           392
alock          n
gain    not used
        FLAGS
il             n
in             n
dp             y
        DISPLAY
sp         -48.6
wp        2667.1
vs           564
sc             0
wc           250
hzmm       10.67
is        953.67
rfl        728.5
rfp            0
th             2
ins        4.000
nm    ph
```

2.02
1.02

4.00

2.03

8 7 6 5 4 3 2 1 ppm

^{13}C NMR Spectrum of **5-44**

¹H NMR Spectrum of 5-45

^{13}C NMR Spectrum of 5-45
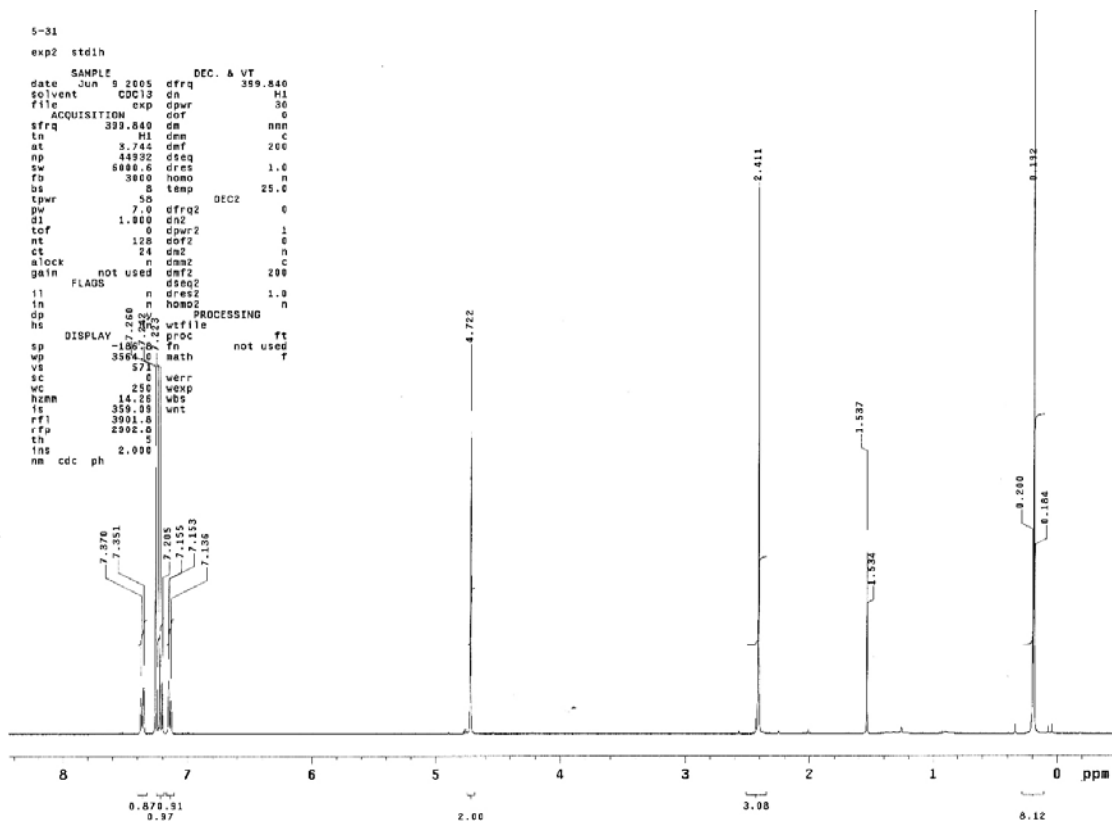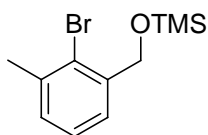
^{1}H NMR Spectrum of **5-46**

^{13}C NMR Spectrum of **5-46**

OH   Br   OBn
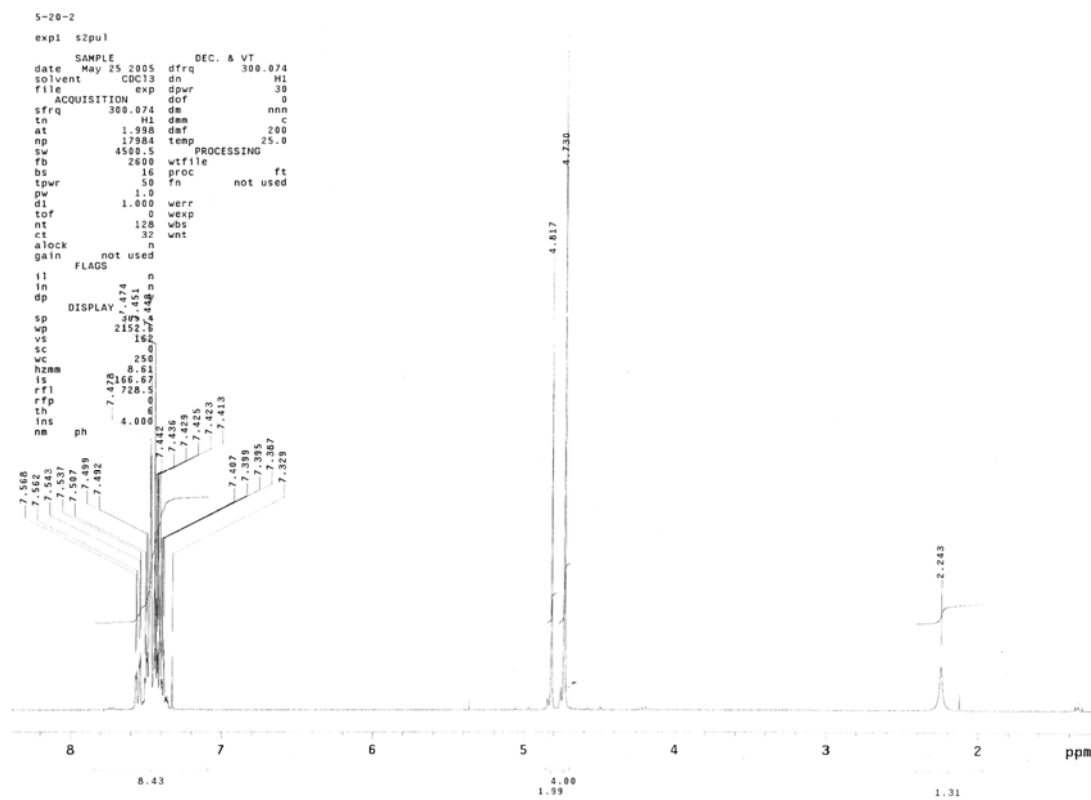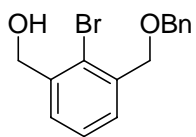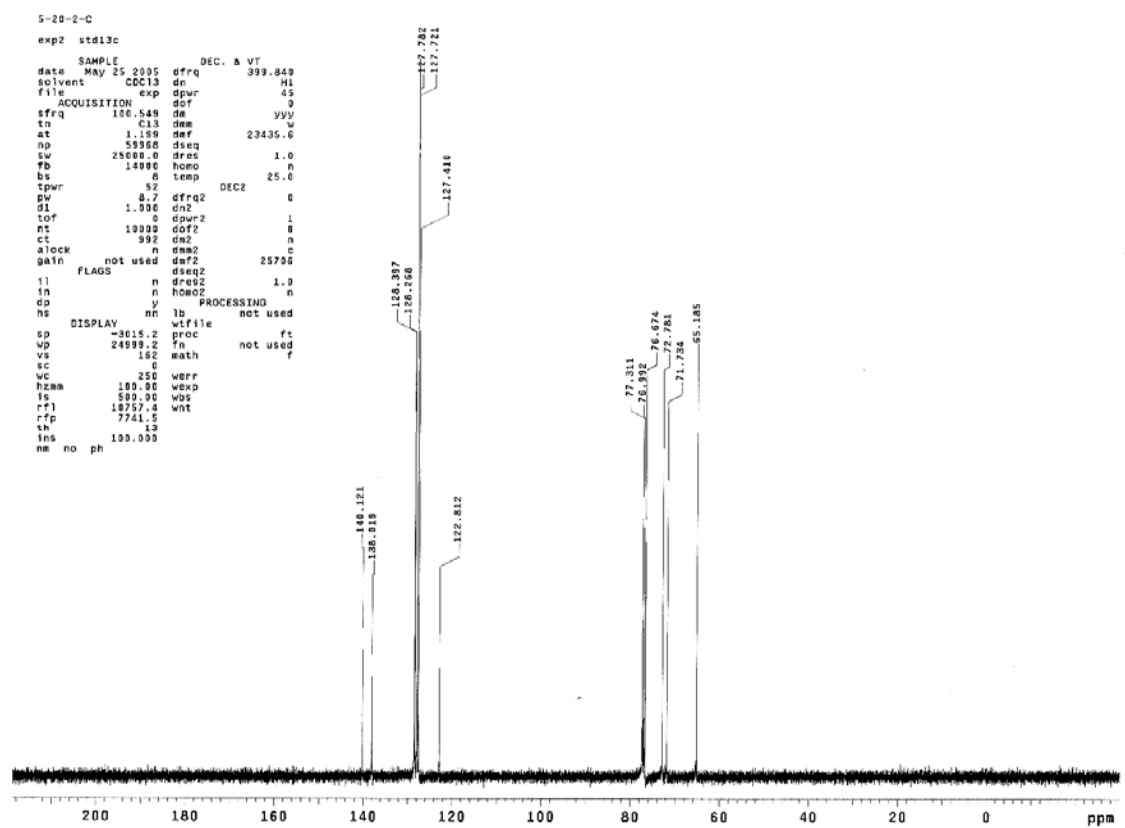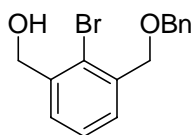
^{1}H NMR Spectrum of **5-47**
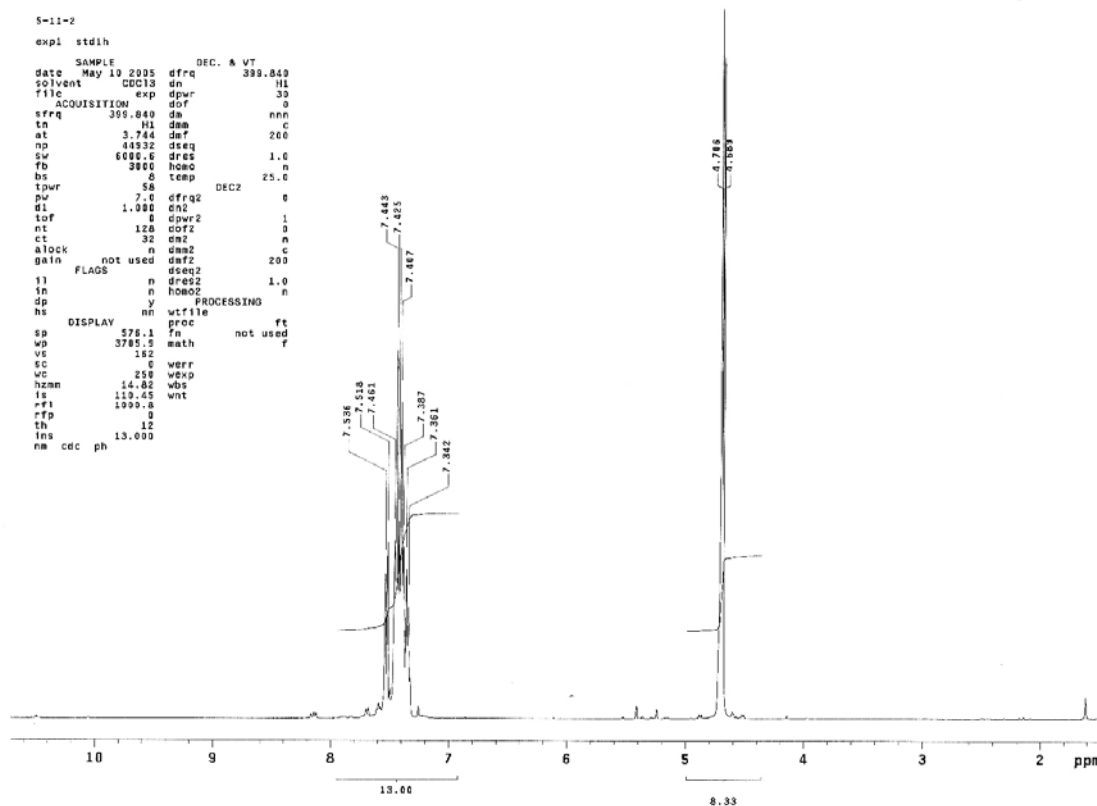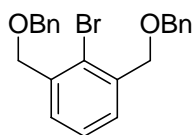
^{13}C NMR Spectrum of **5-47**

^{1}H NMR Spectrum of **5-48**

OBn Br OTES
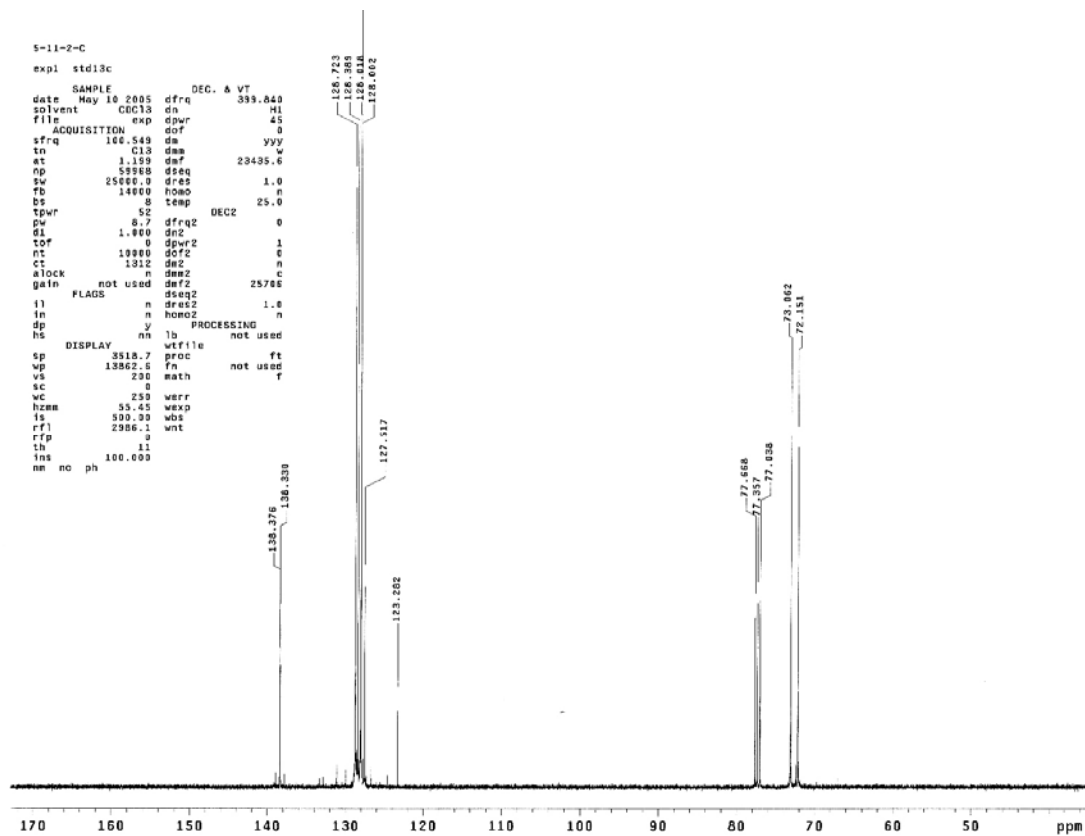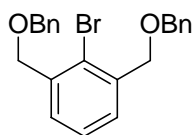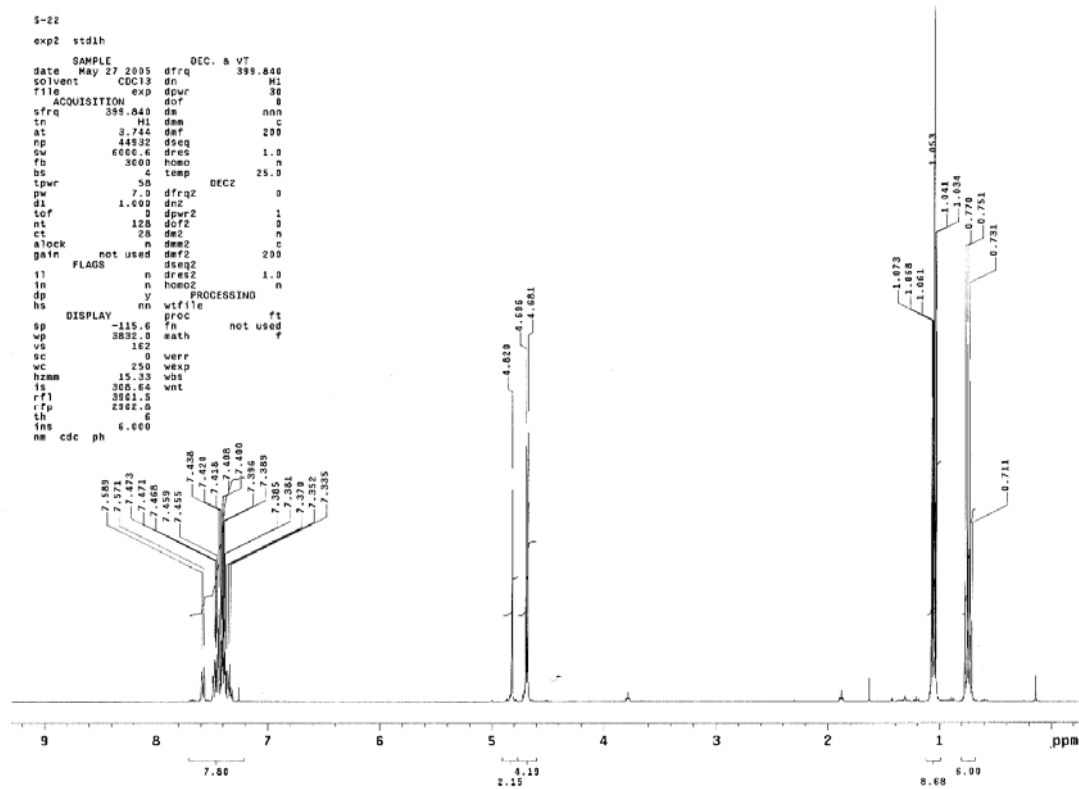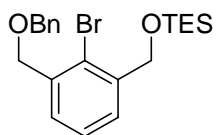
^{13}C NMR Spectrum of **5-48**

^{1}H NMR Spectrum of **5-49**

OBn Br   OTMS

^{13}C NMR Spectrum of **5-49**

OBn Br OTMS
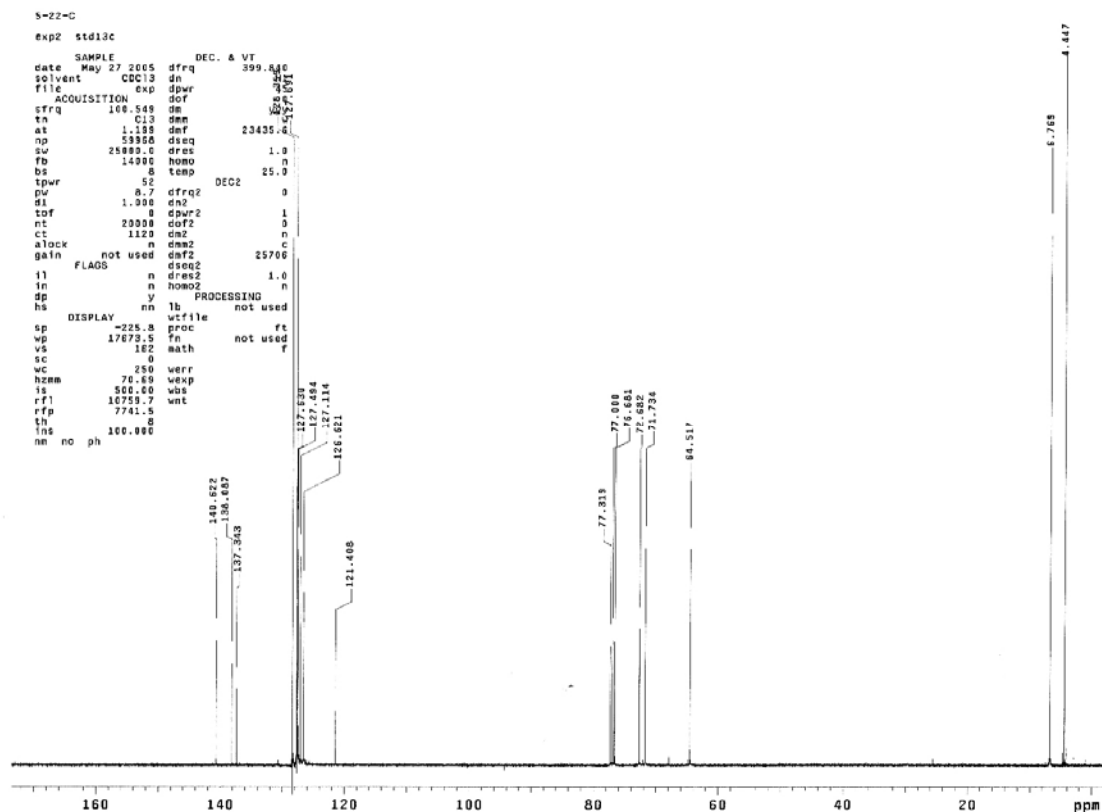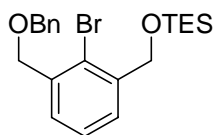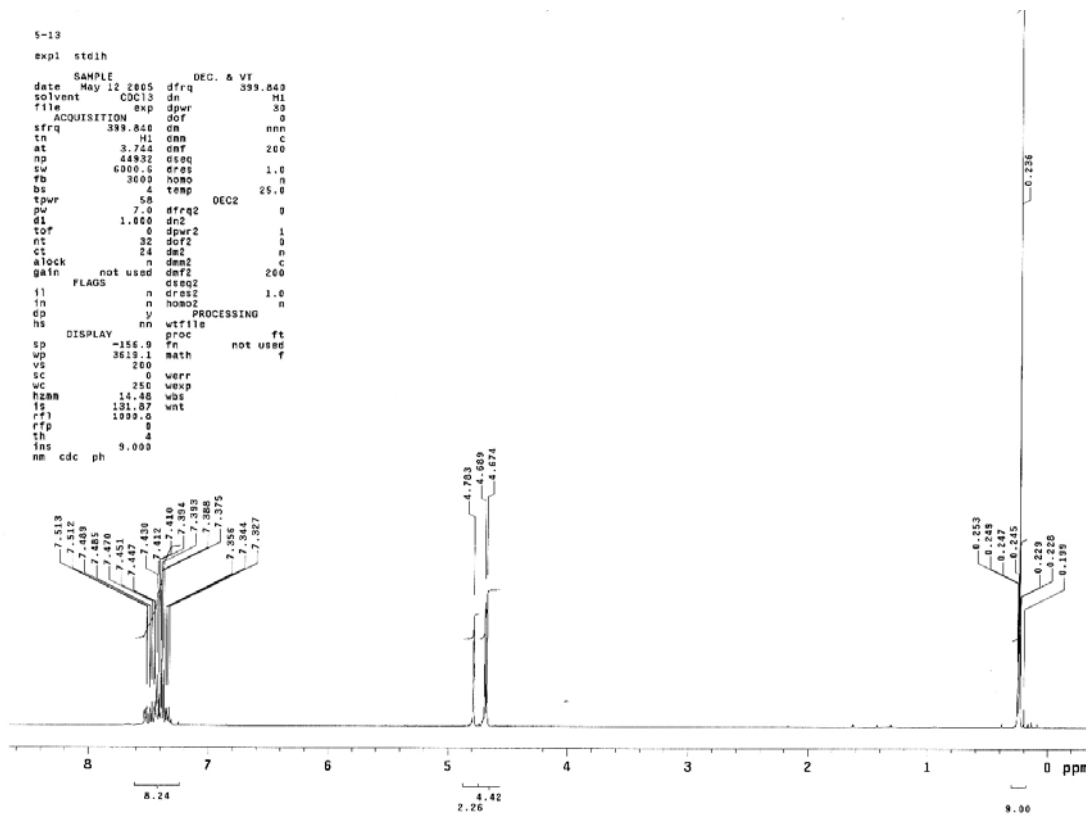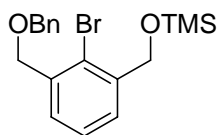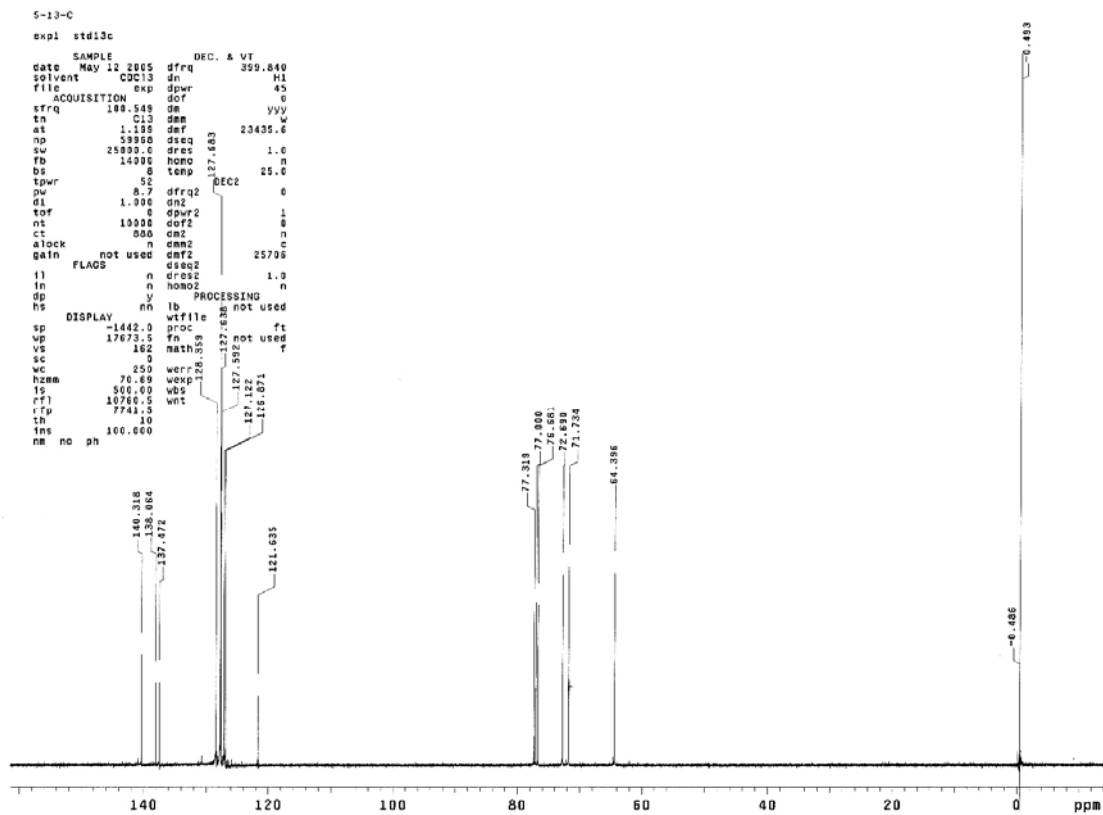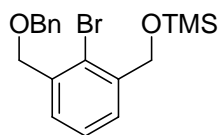
^{1}H NMR Spectrum of **5-50**
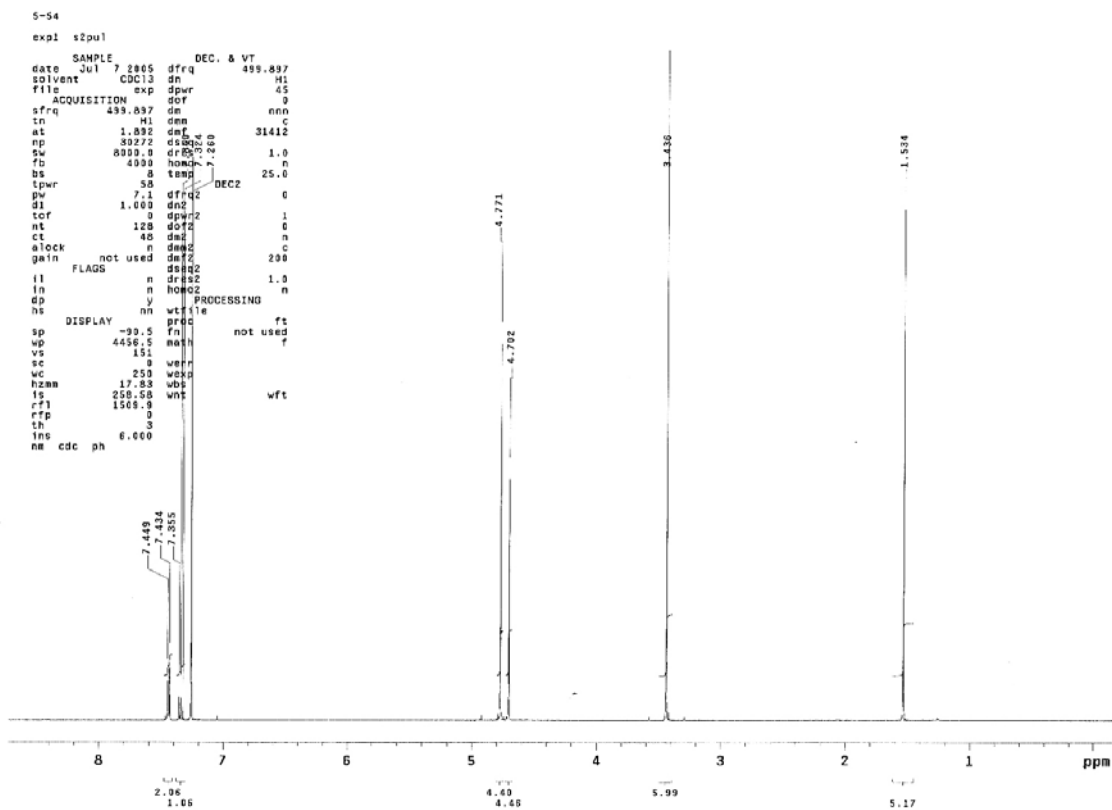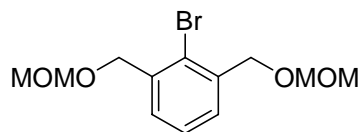
^{1}H NMR Spectrum of **5-51**
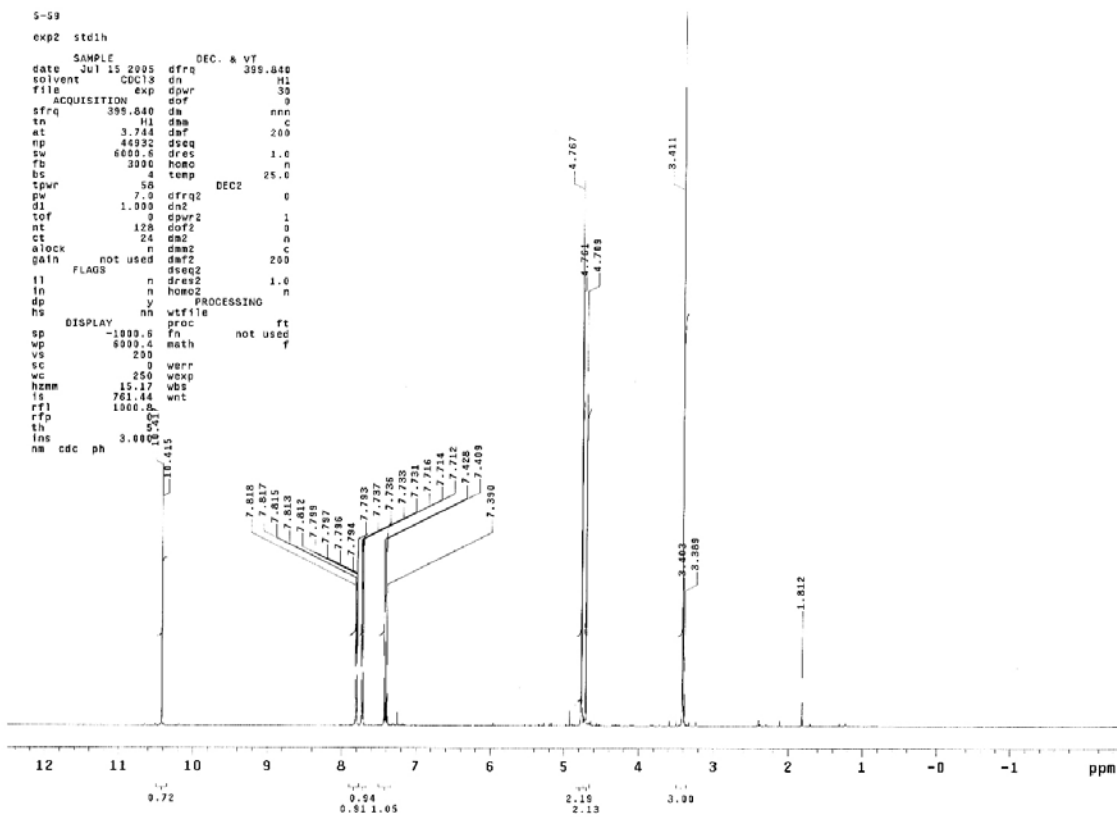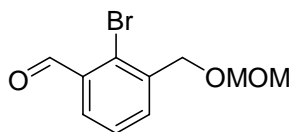
^{13}C NMR Spectrum of **5-51**
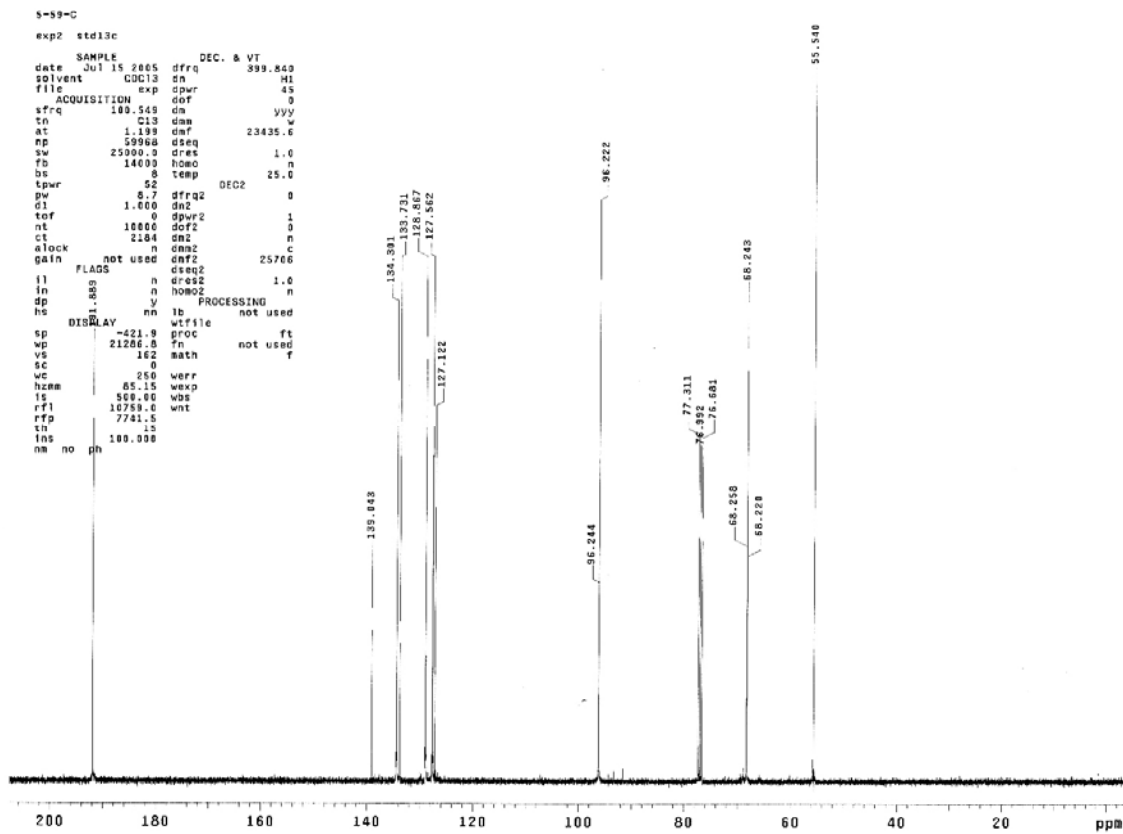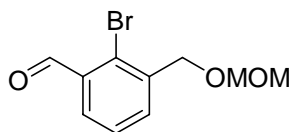
^{1}H NMR Spectrum of **5-52**
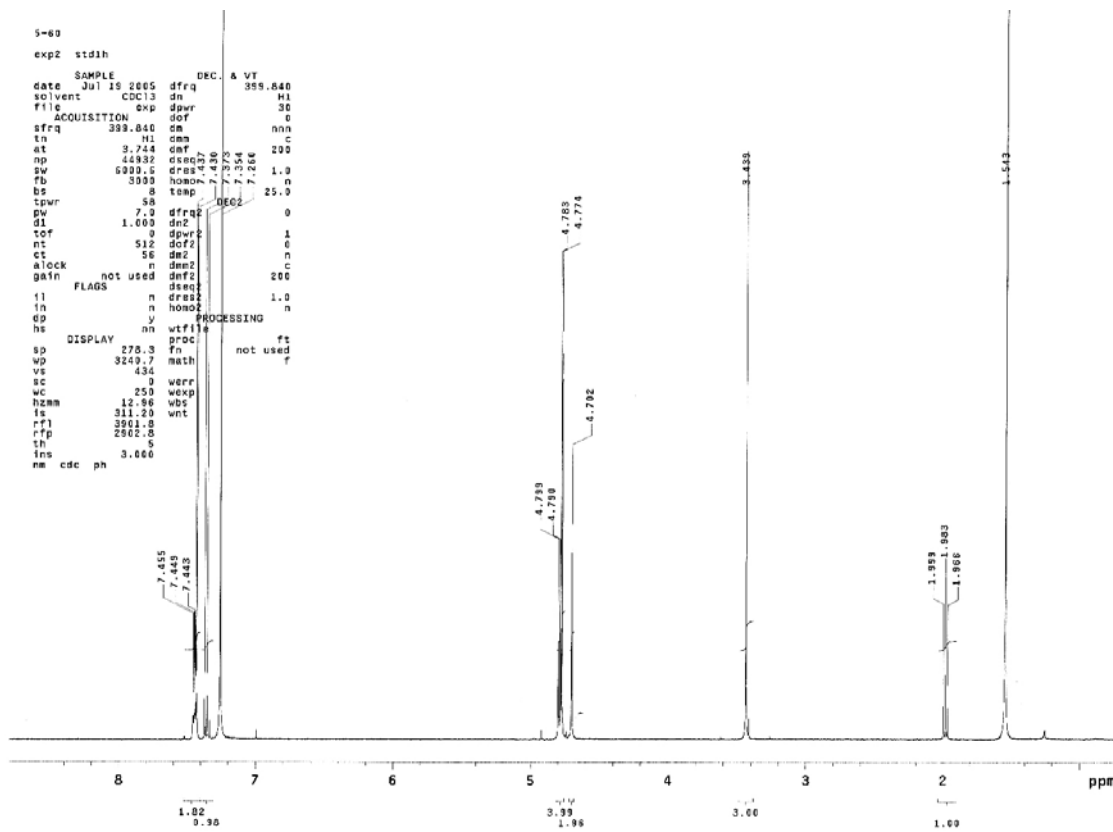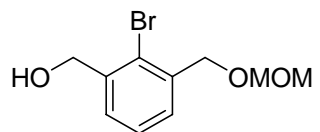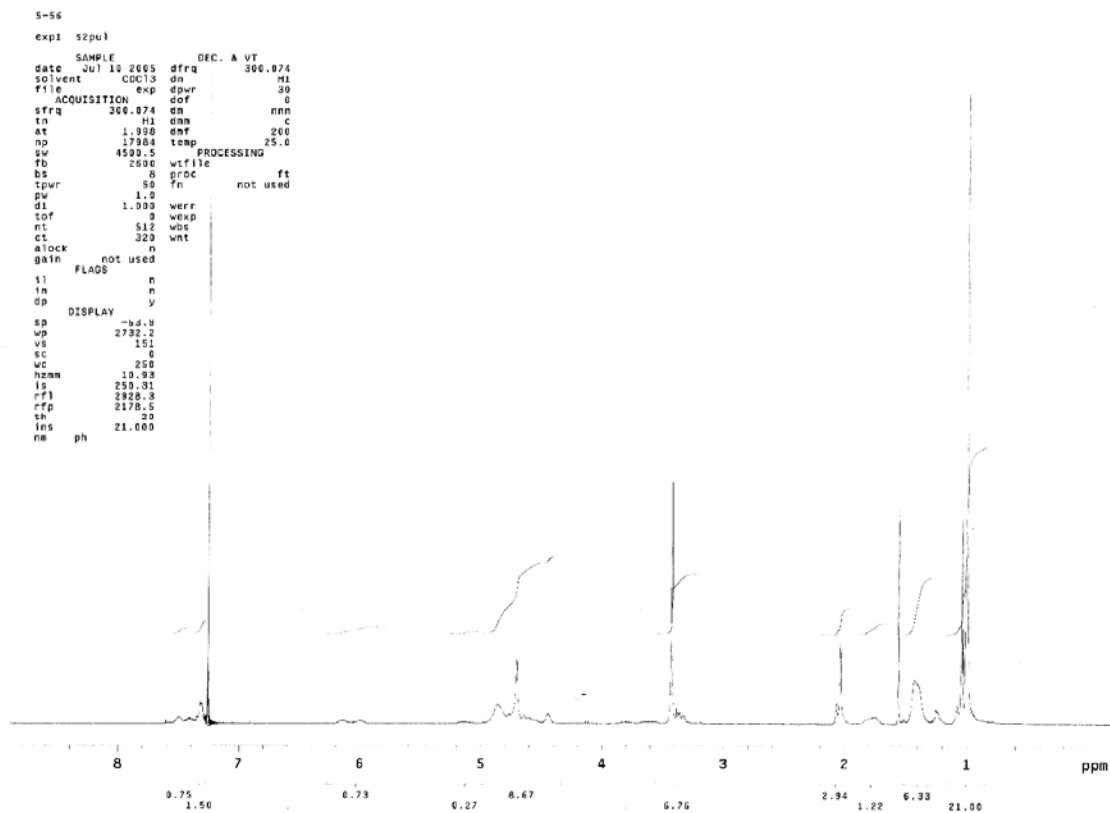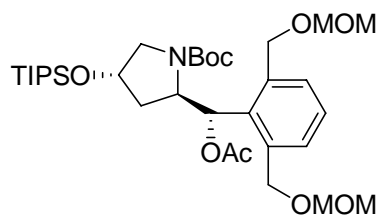
^{1}H NMR Spectrum of **5-55**
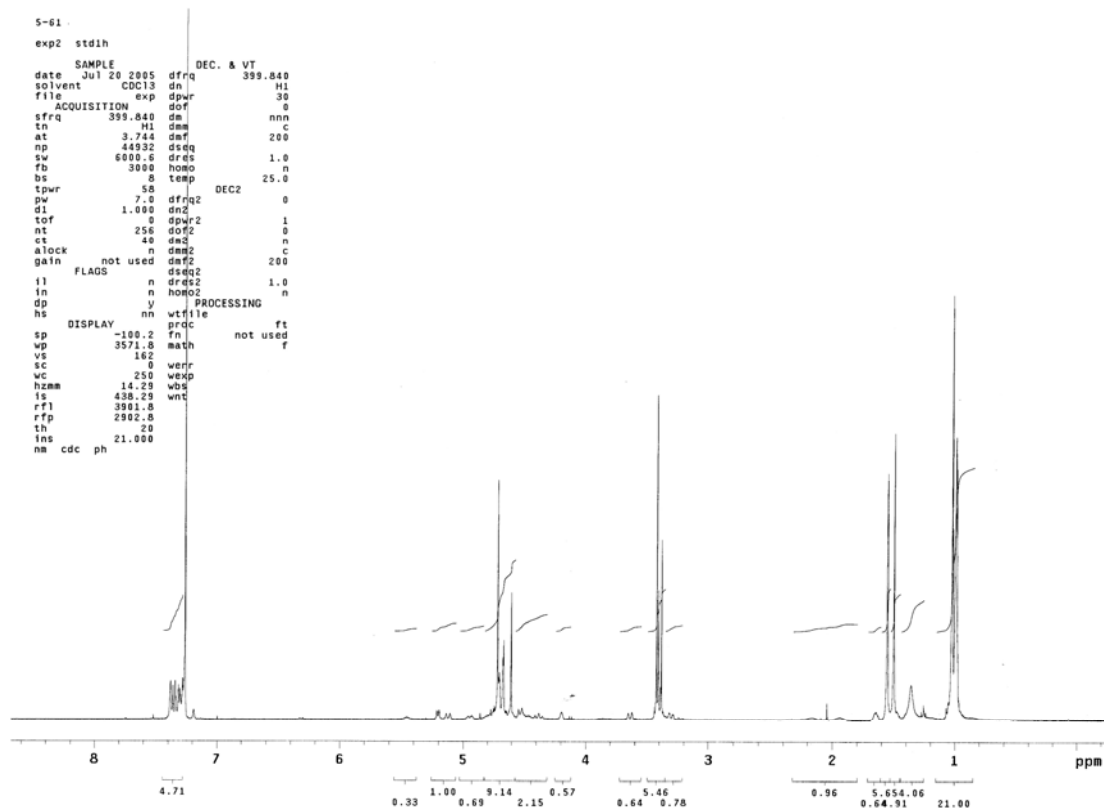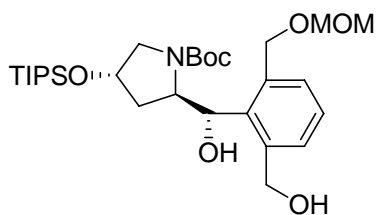
^{1}H NMR Spectrum of **5-56**
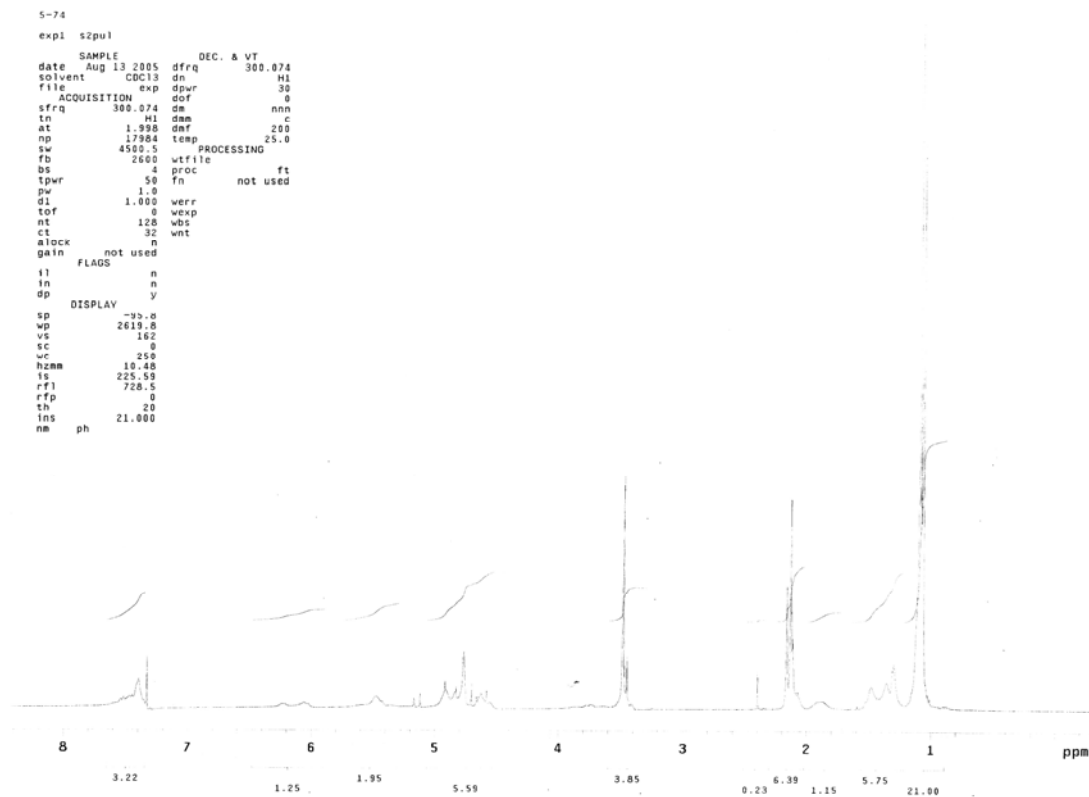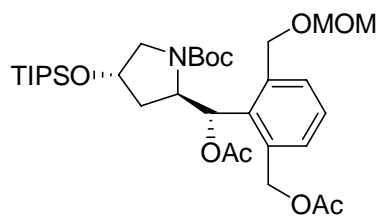
^{13}C NMR Spectrum of **5-56**
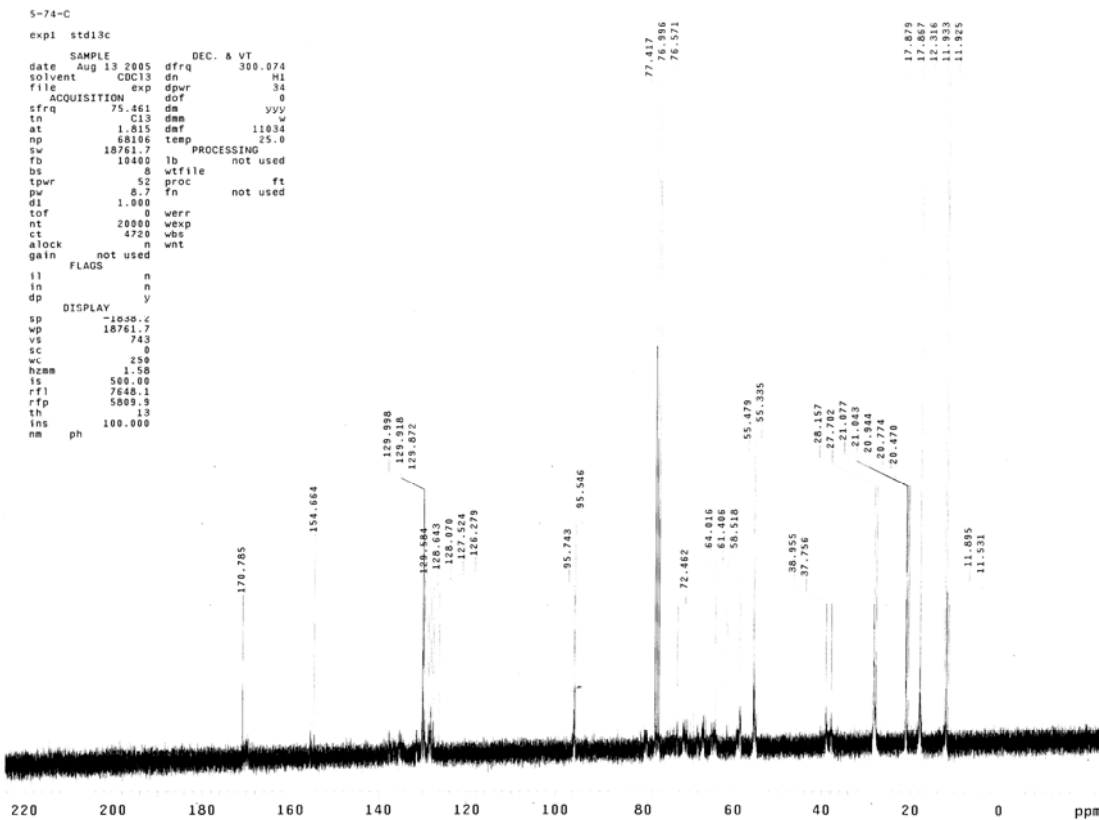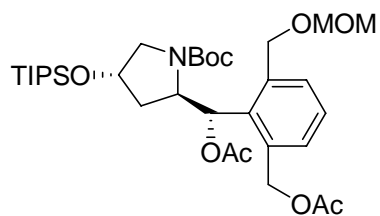
^{1}H NMR Spectrum of **5-59**
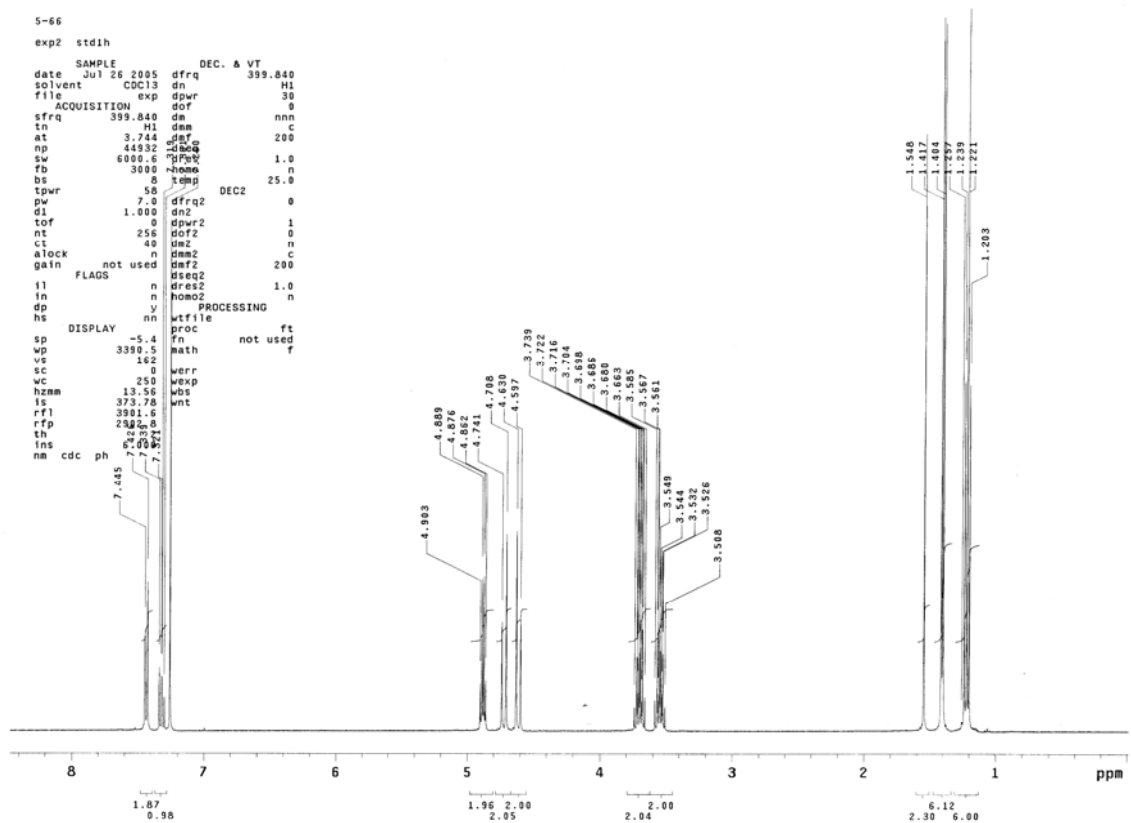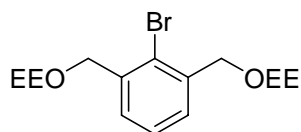
^{1}H NMR Spectrum of **5-60**
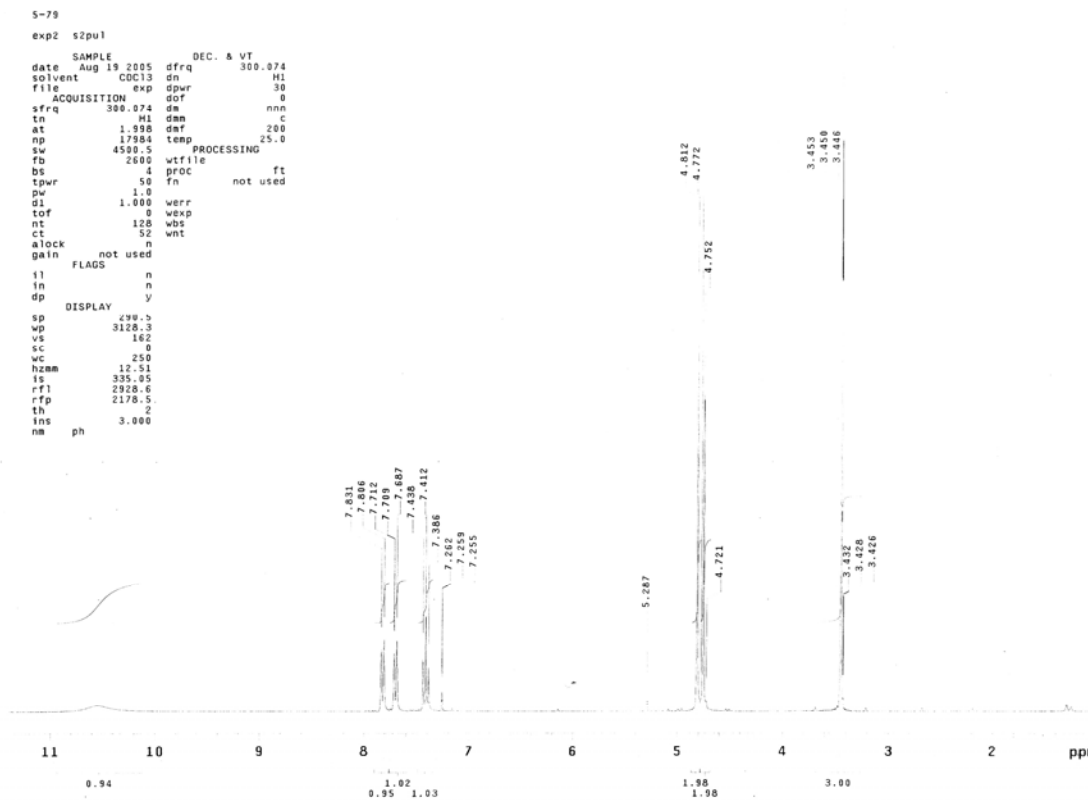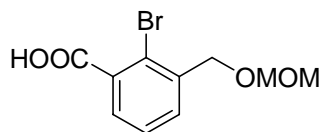
^{13}C NMR Spectrum of **5-60**
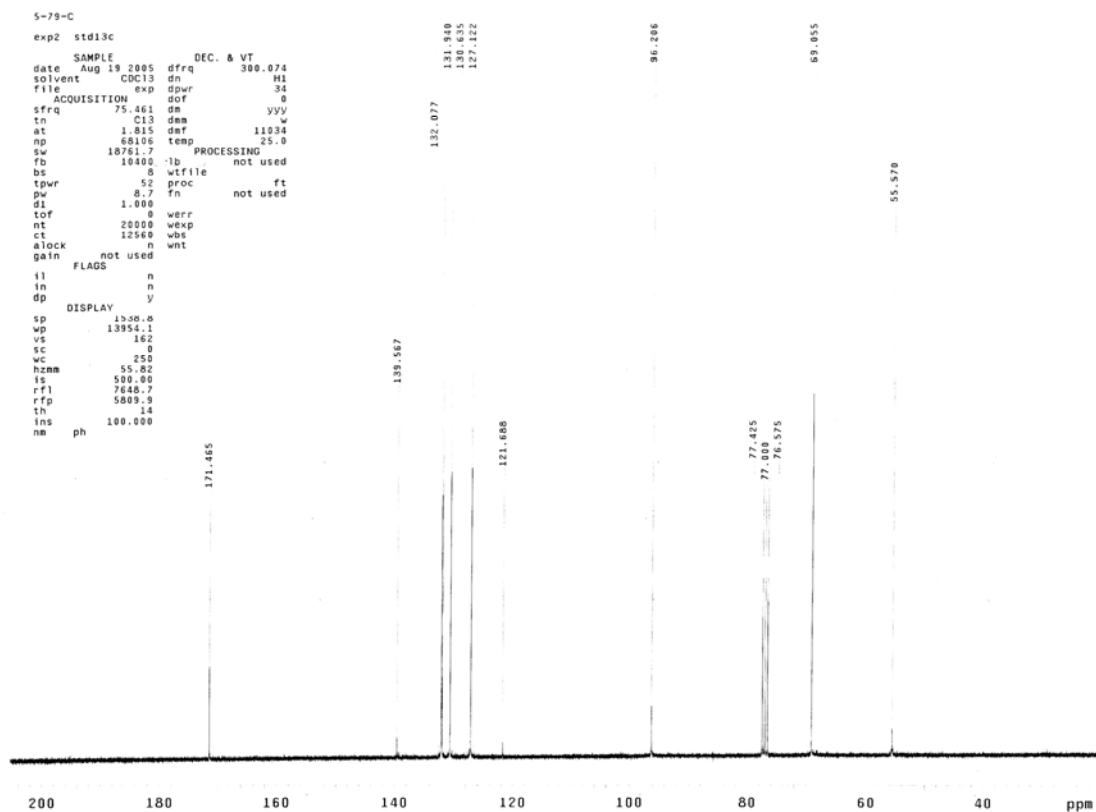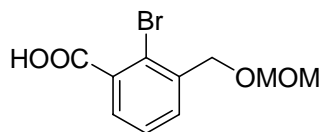
^{13}C NMR Spectrum of **5-63**
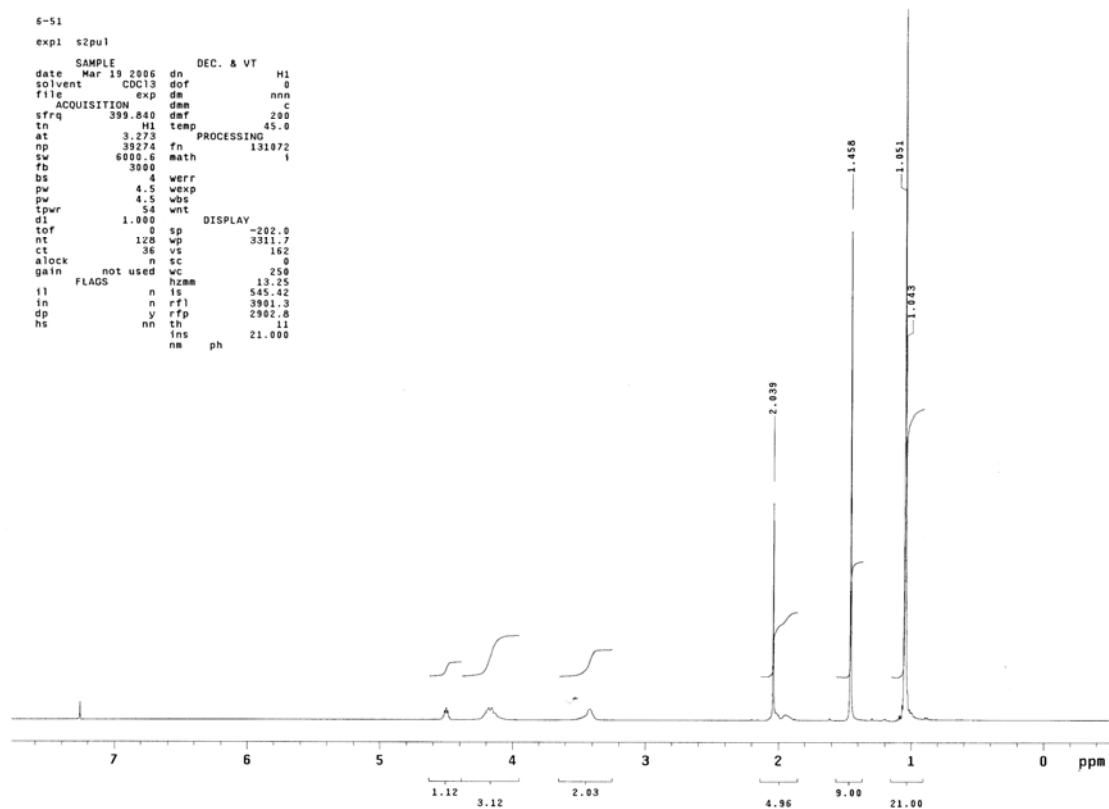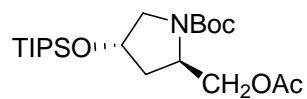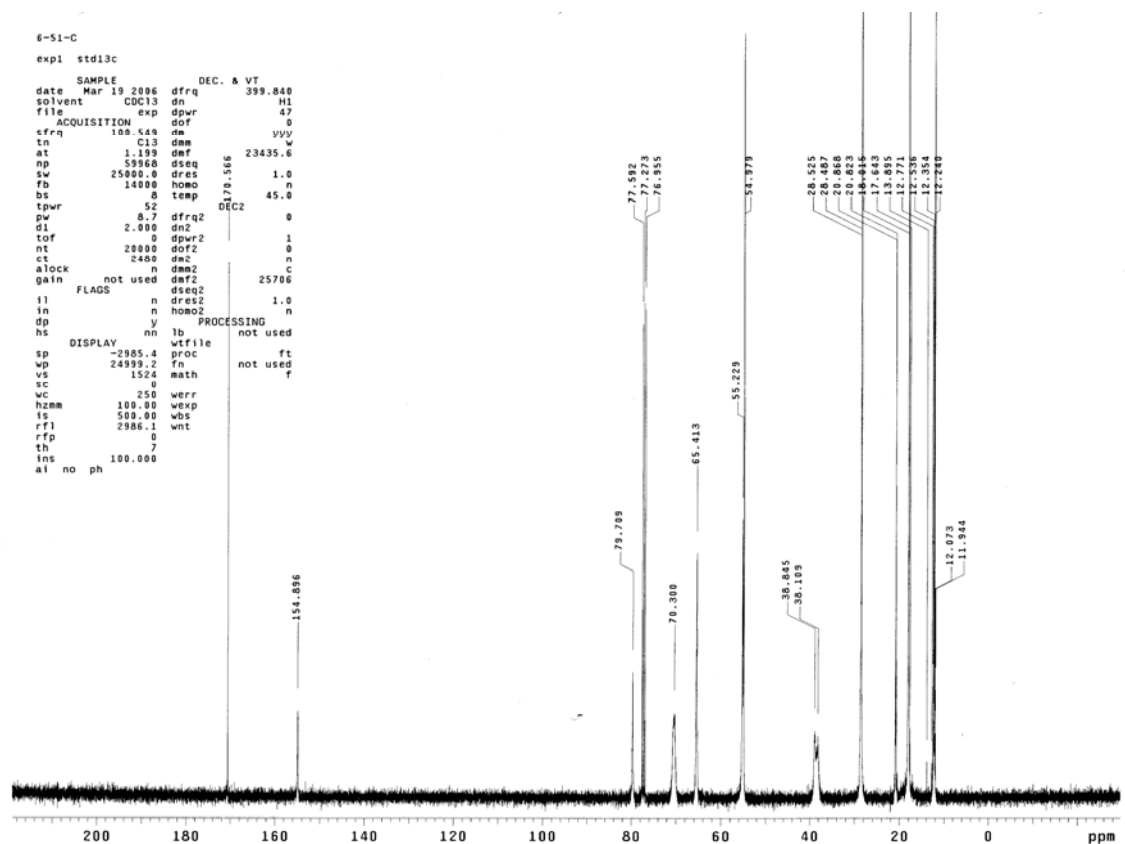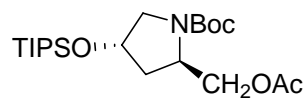
^{1}H NMR Spectrum of **5-66**
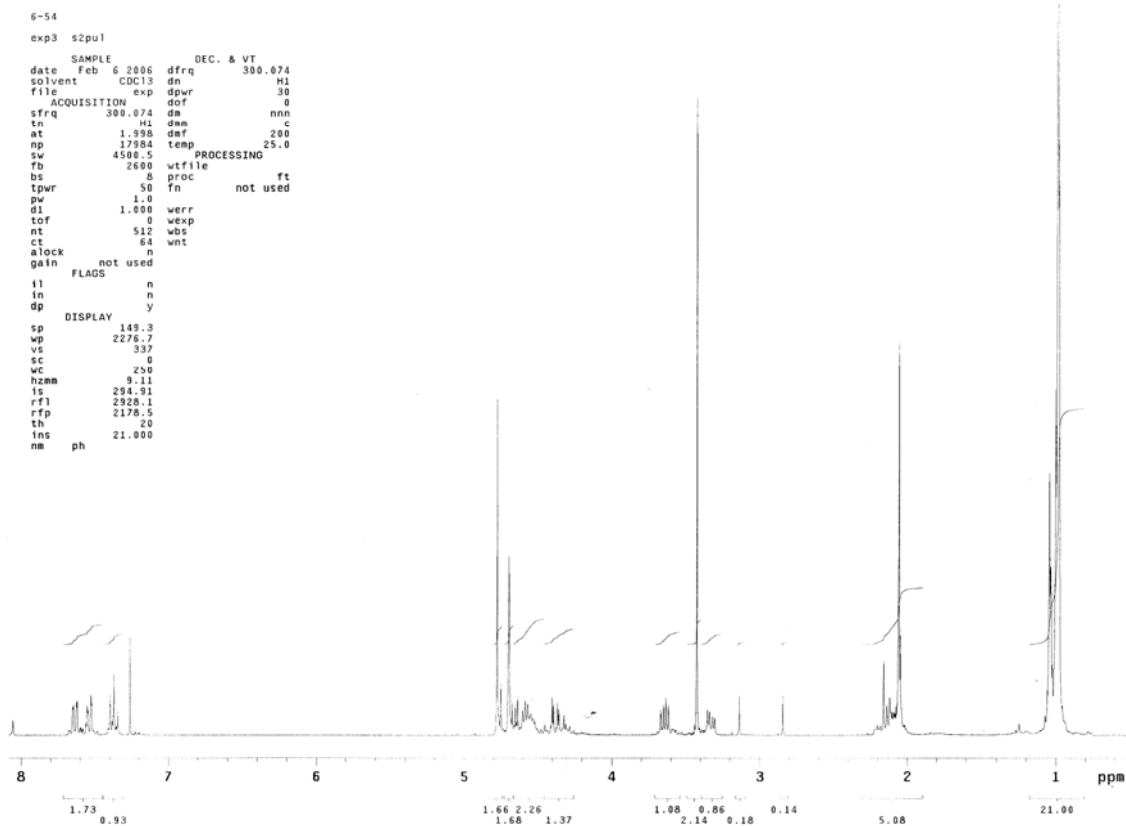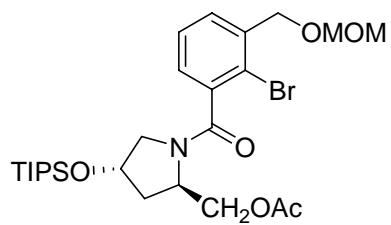
¹H NMR Spectrum of **5-68**
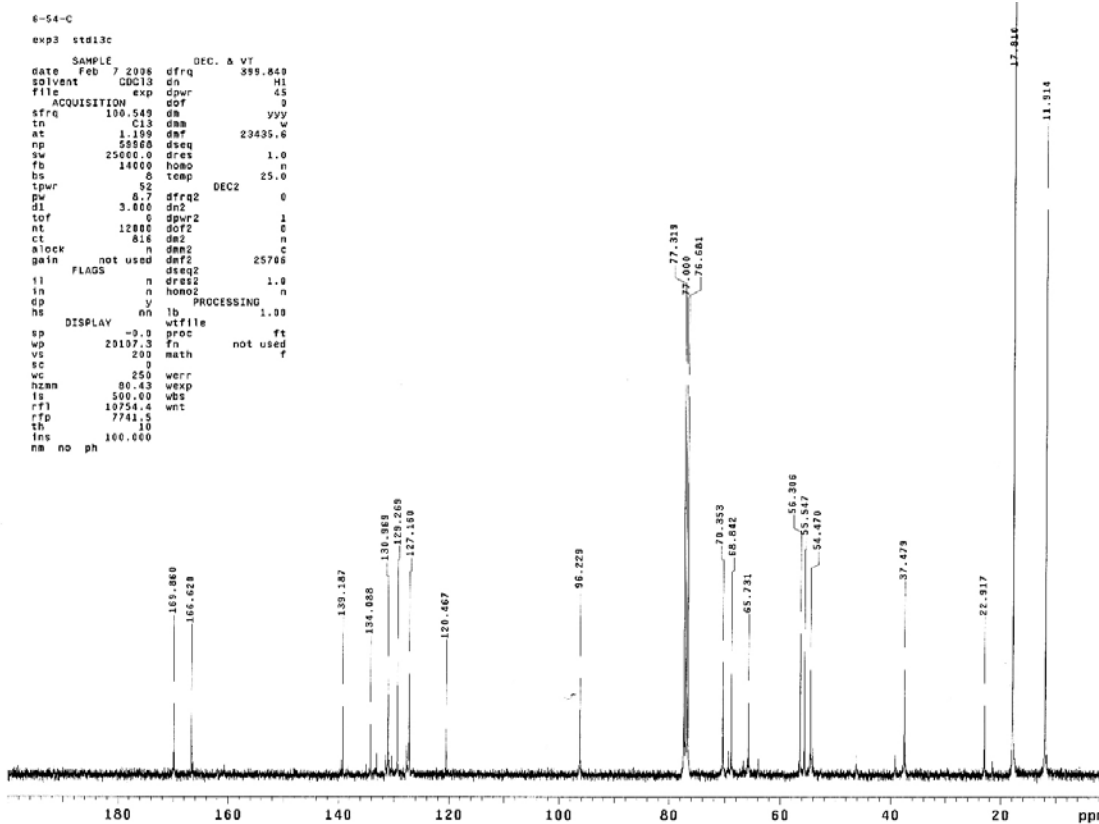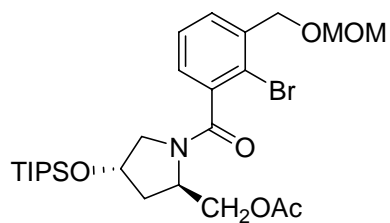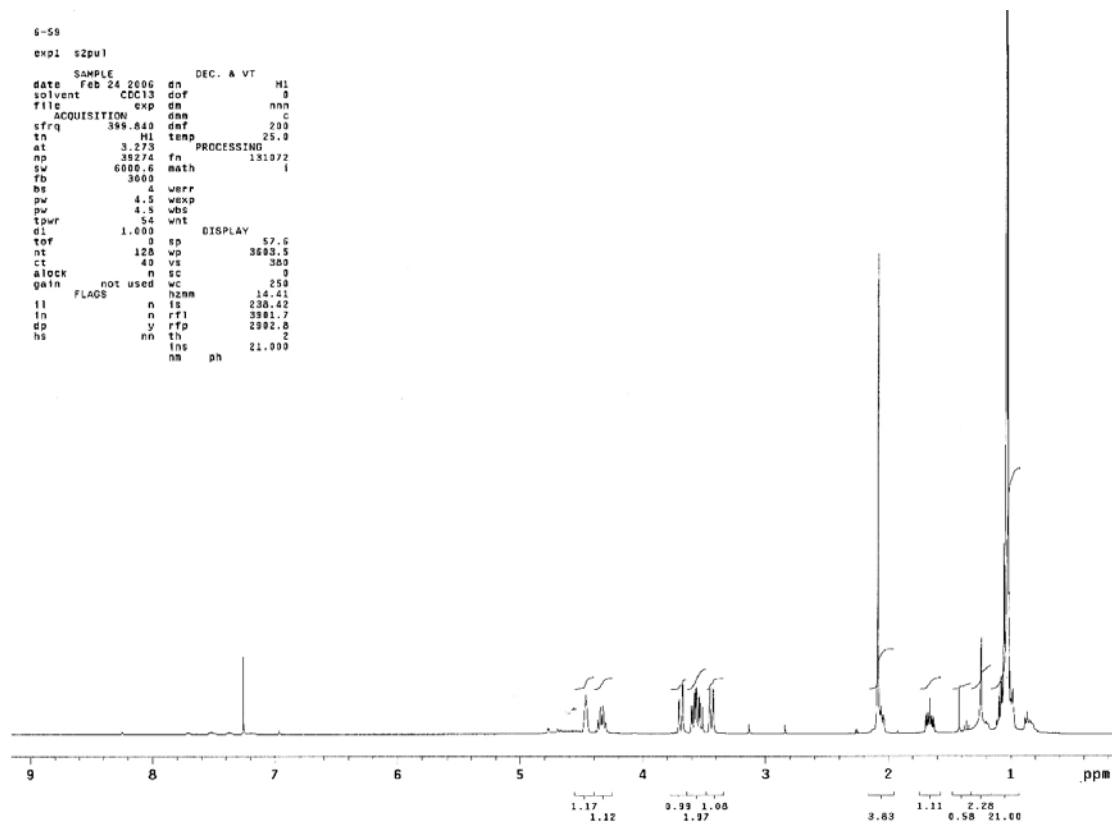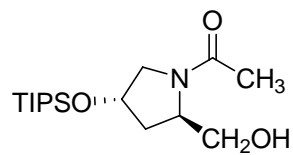
^{1}H NMR Spectrum of **5-68**

^{13}C NMR Spectrum of **5-68**

^{1}H NMR Spectrum of **5-67**
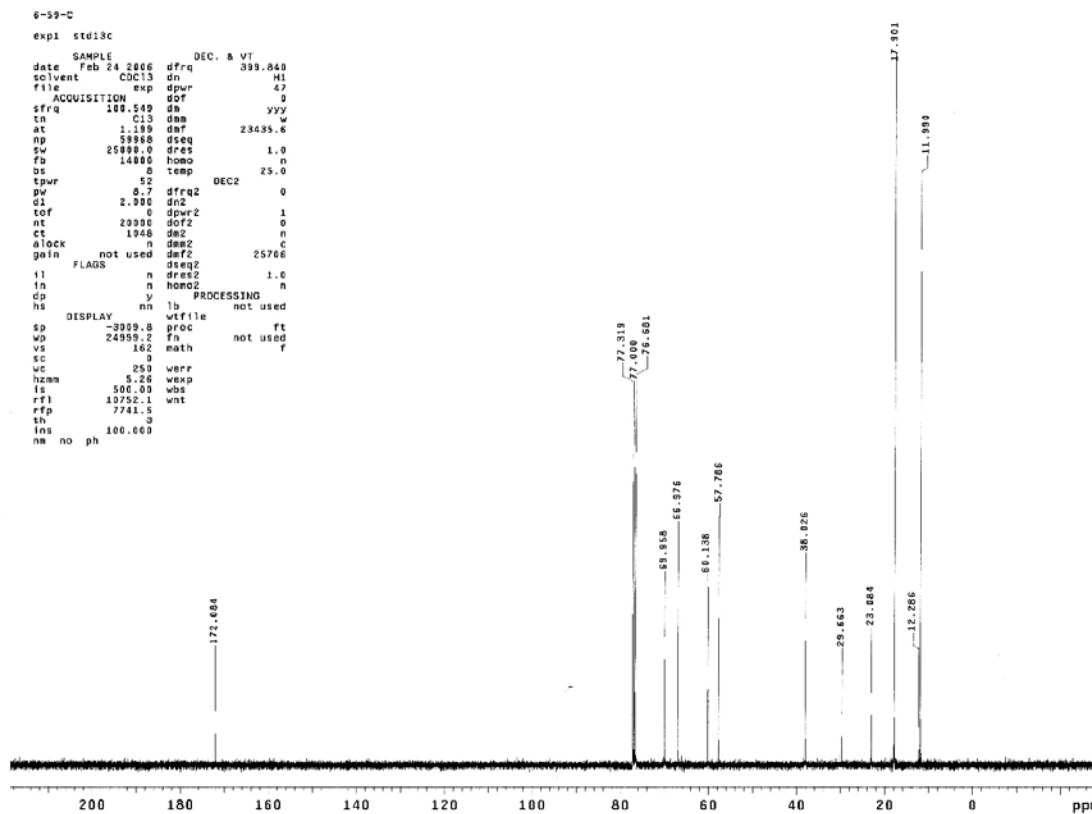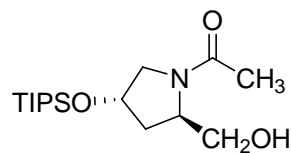
^{13}C NMR Spectrum of **5-67**
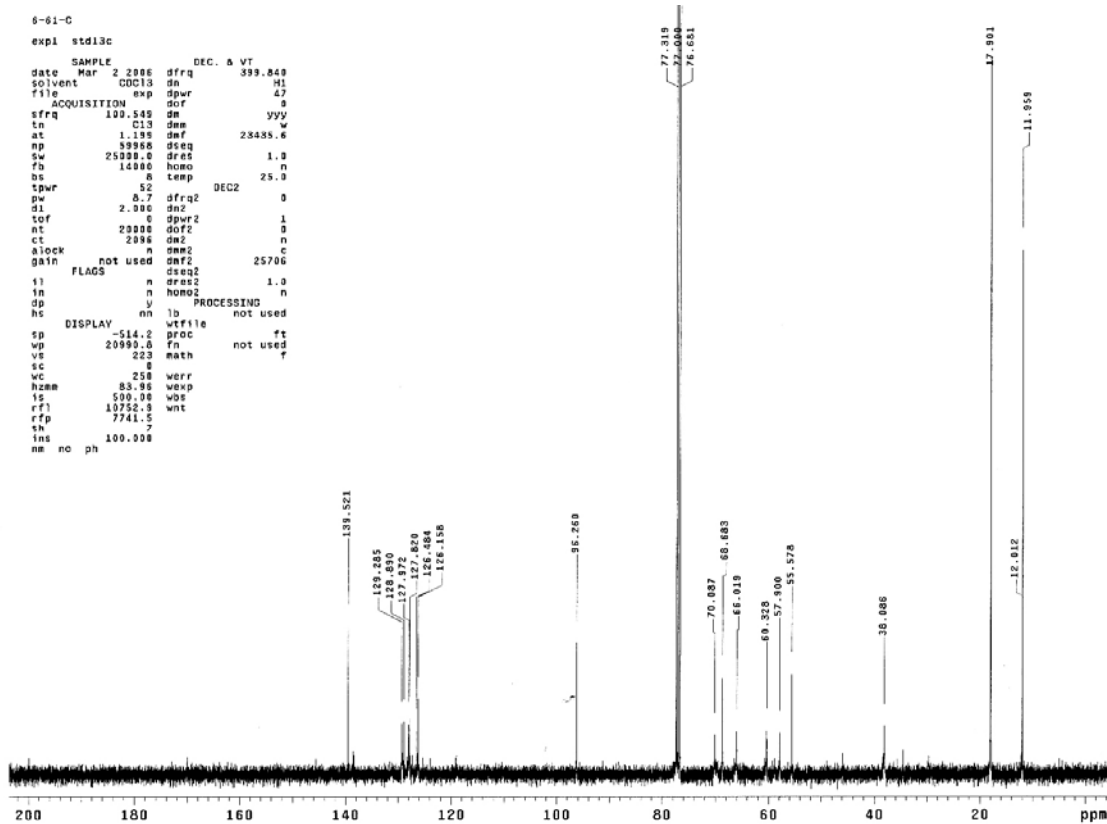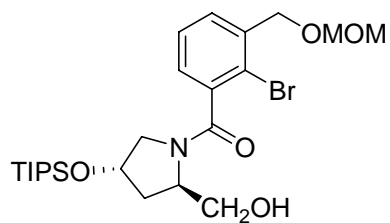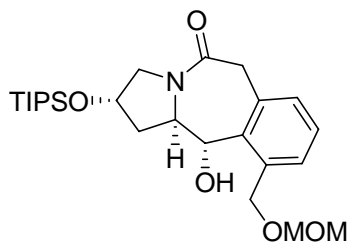
^{1}H NMR Spectrum of **5-70**
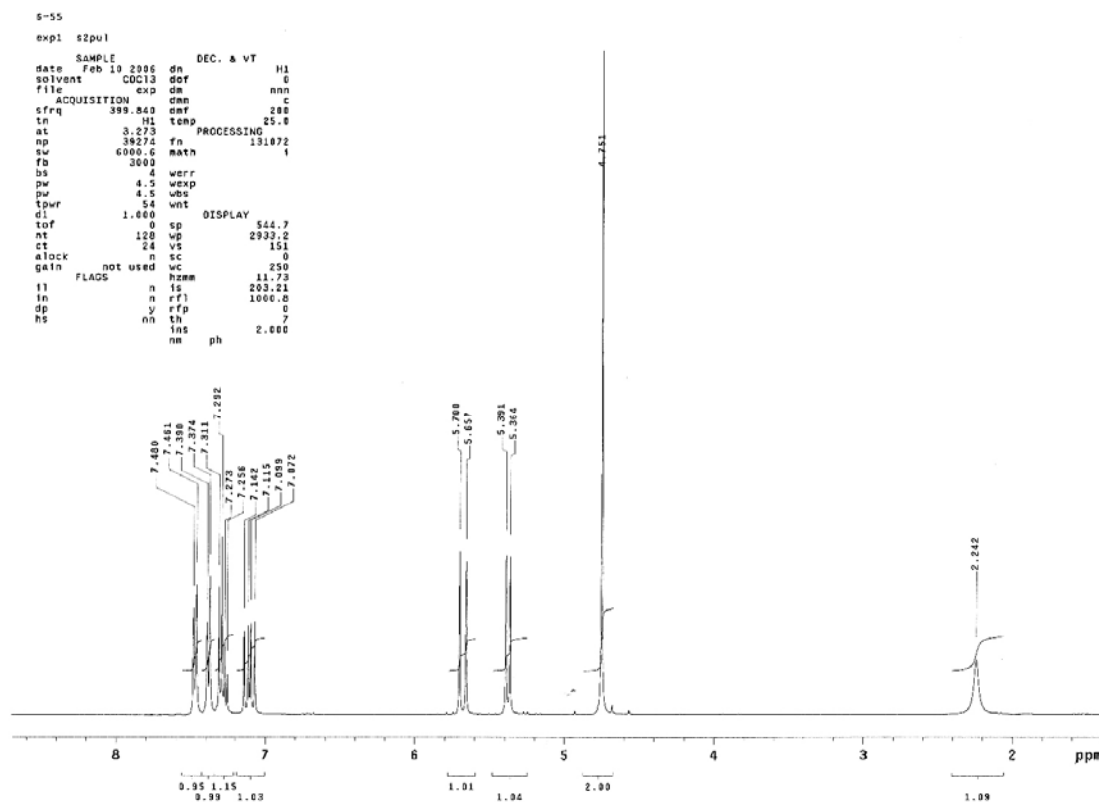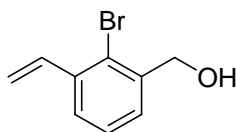
^{13}C NMR Spectrum of 5-70
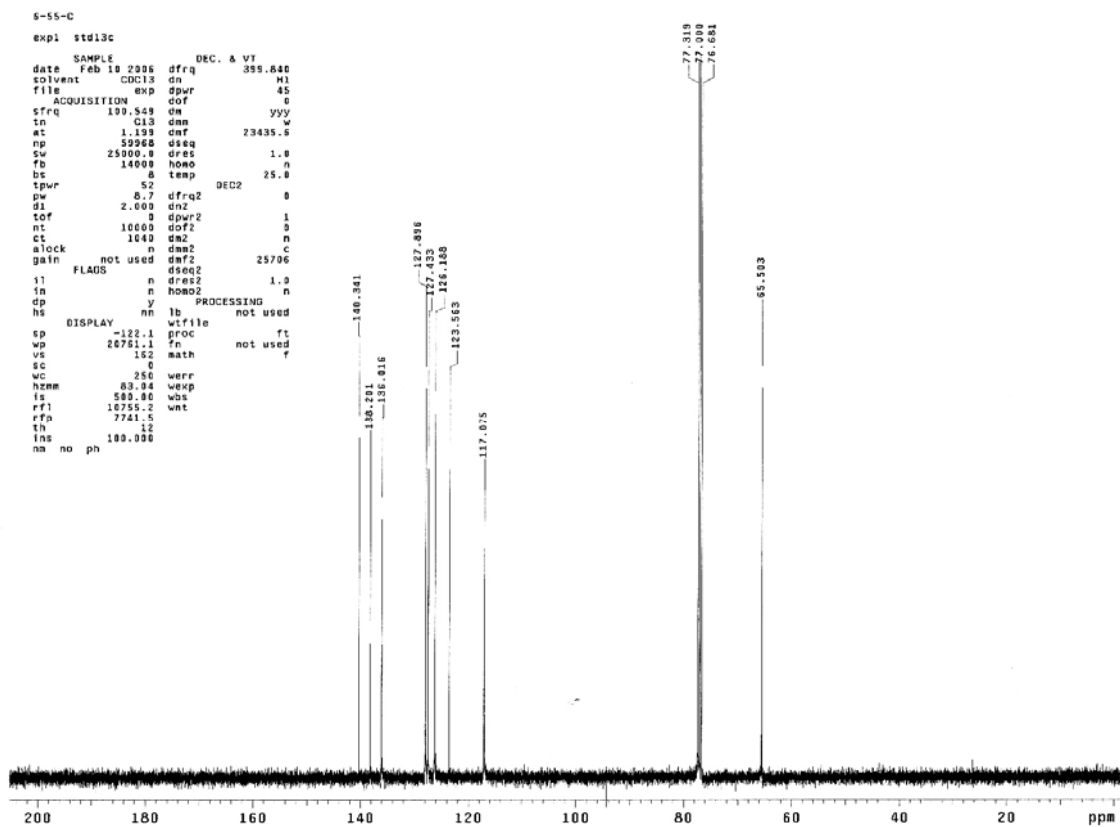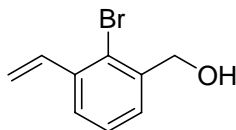
^{1}H NMR Spectrum of **5-72**
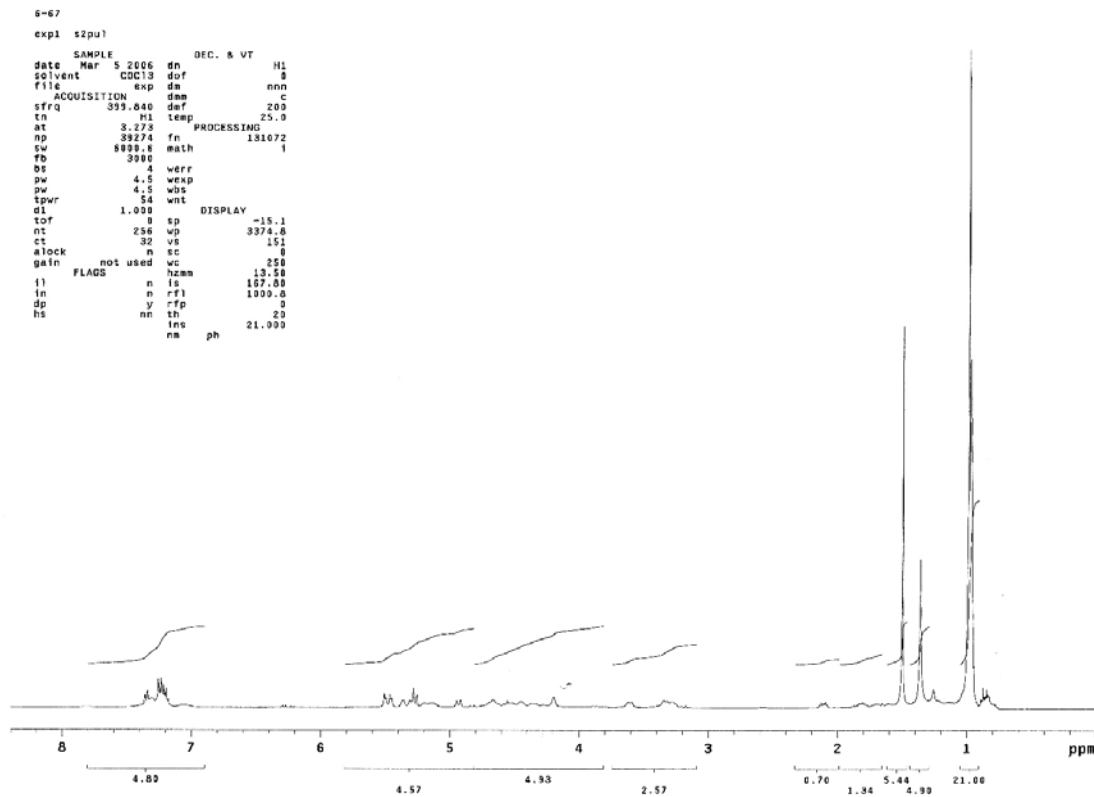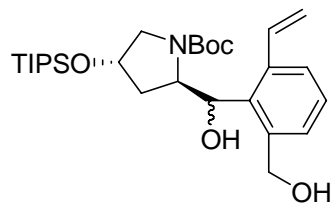
^{13}C NMR Spectrum of **5-72**
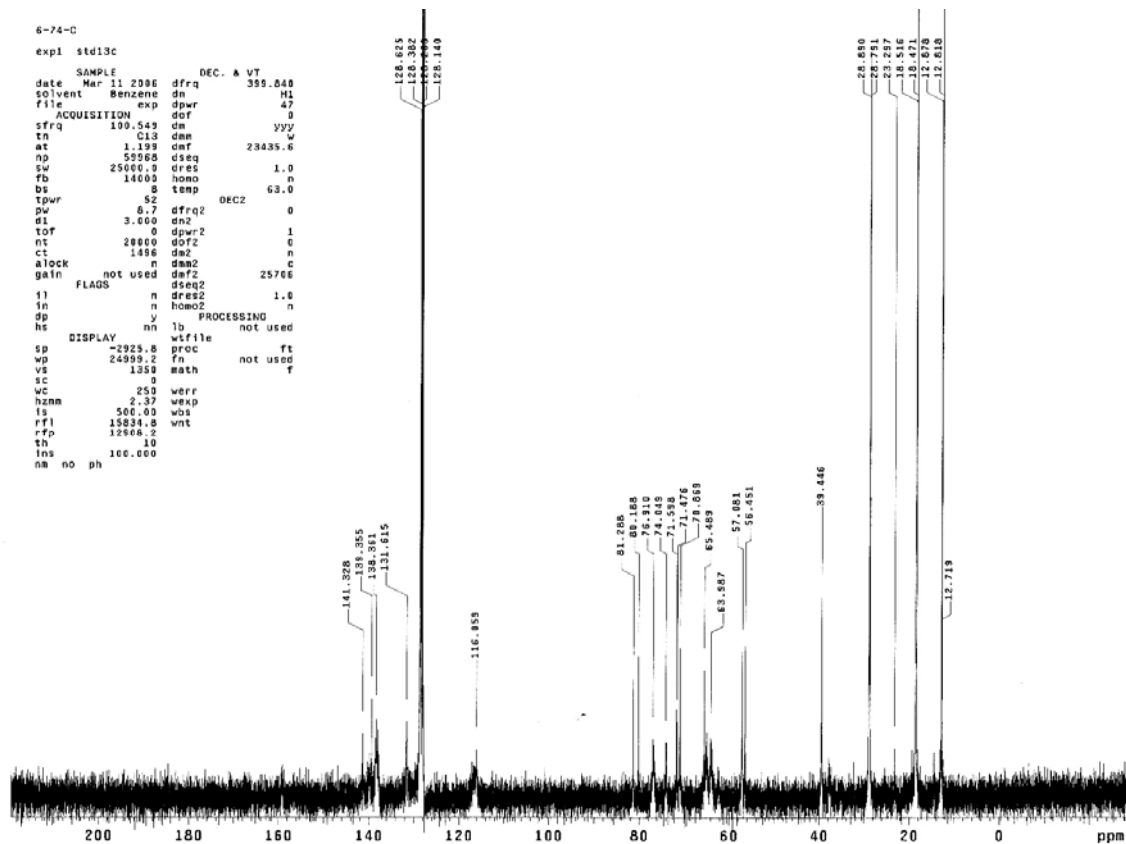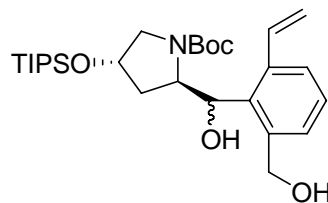
^{1}H NMR Spectrum of **5-73**
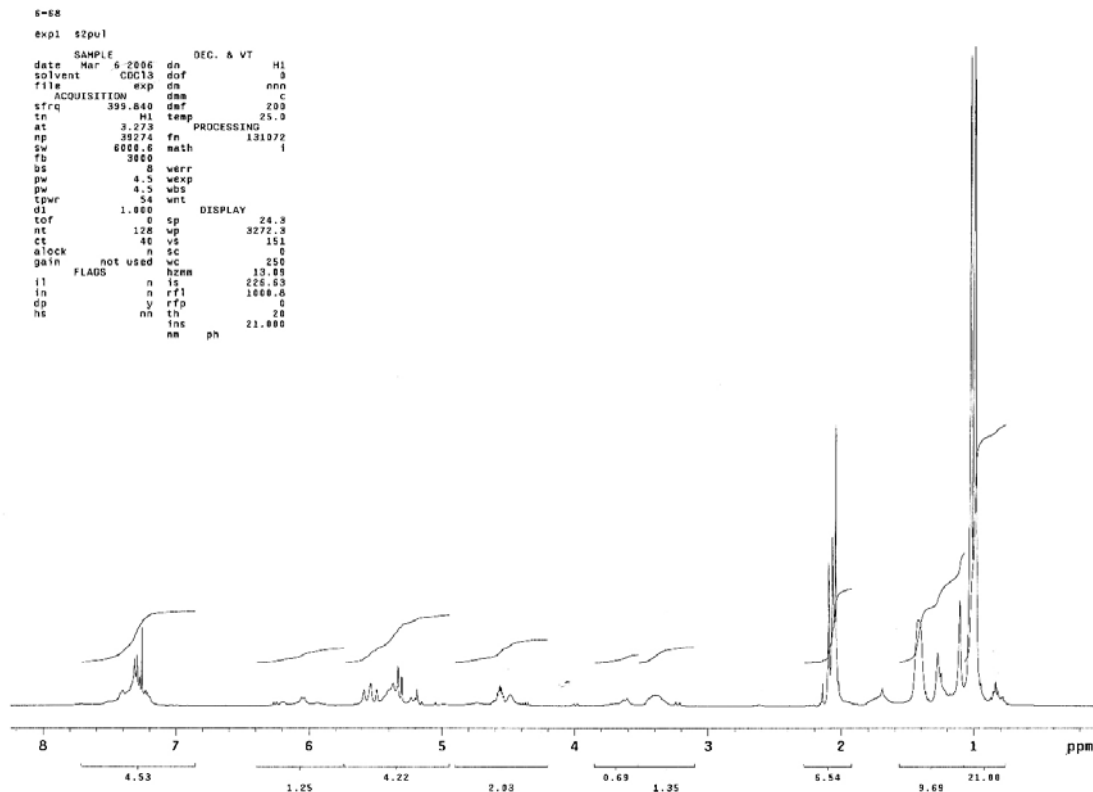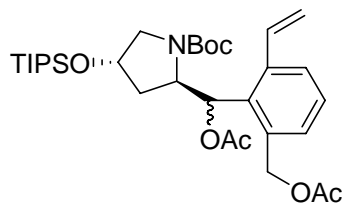
^{13}C NMR Spectrum of **5-73**
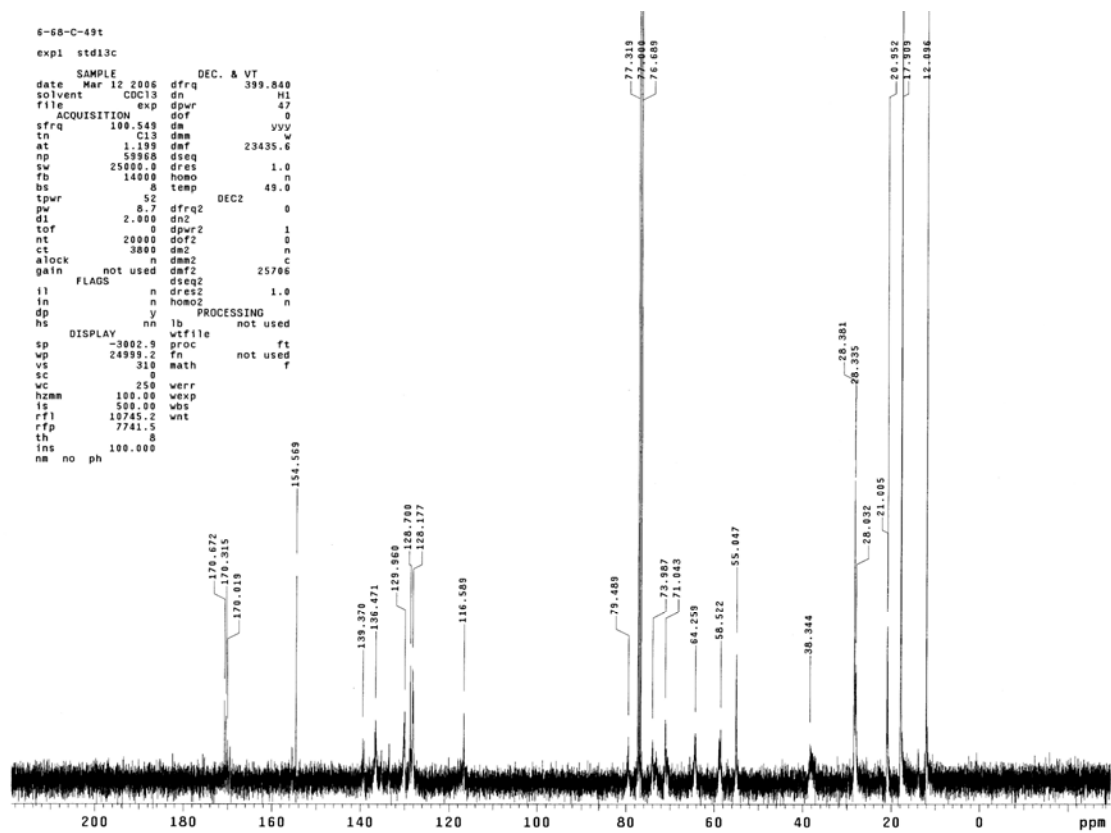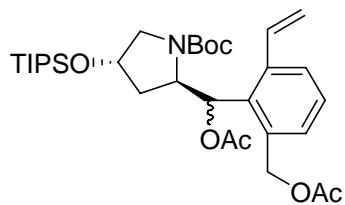
¹³C NMR Spectrum of **5-77**
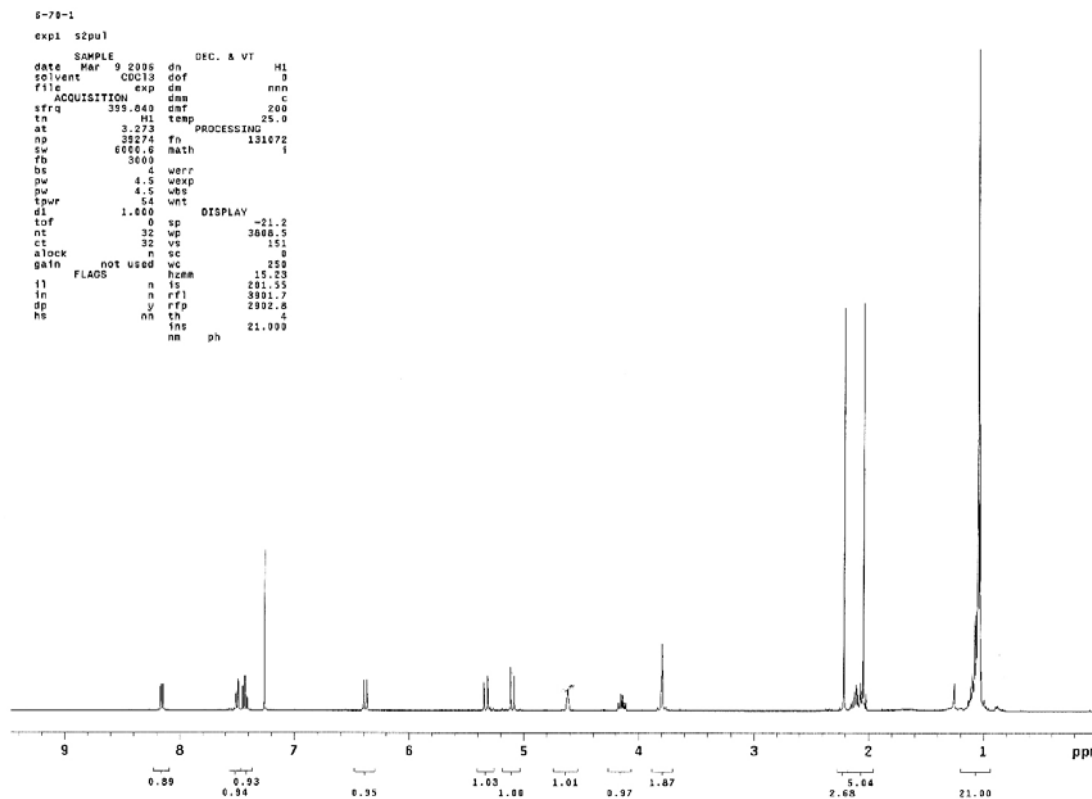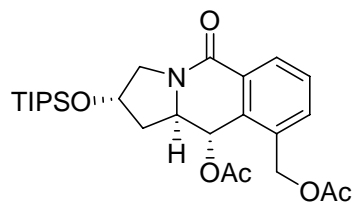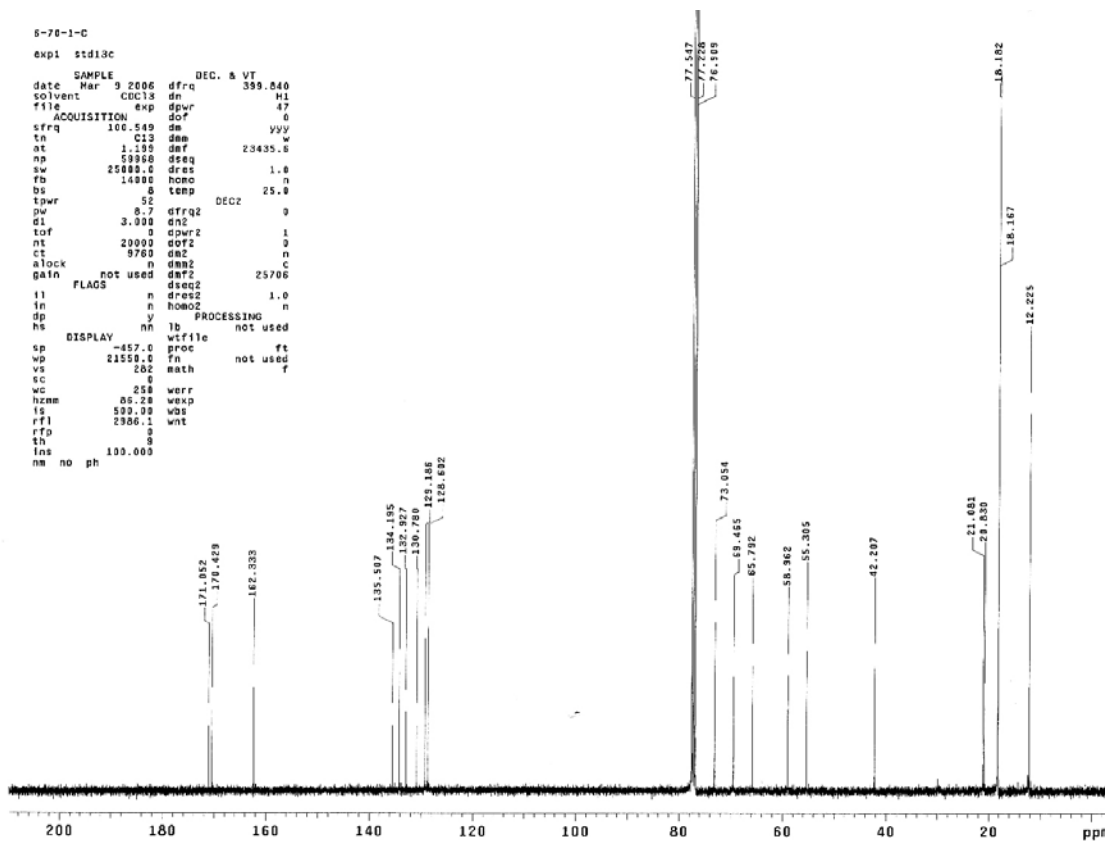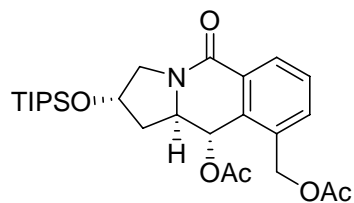
2D NOESY Spectrum of **5-77**
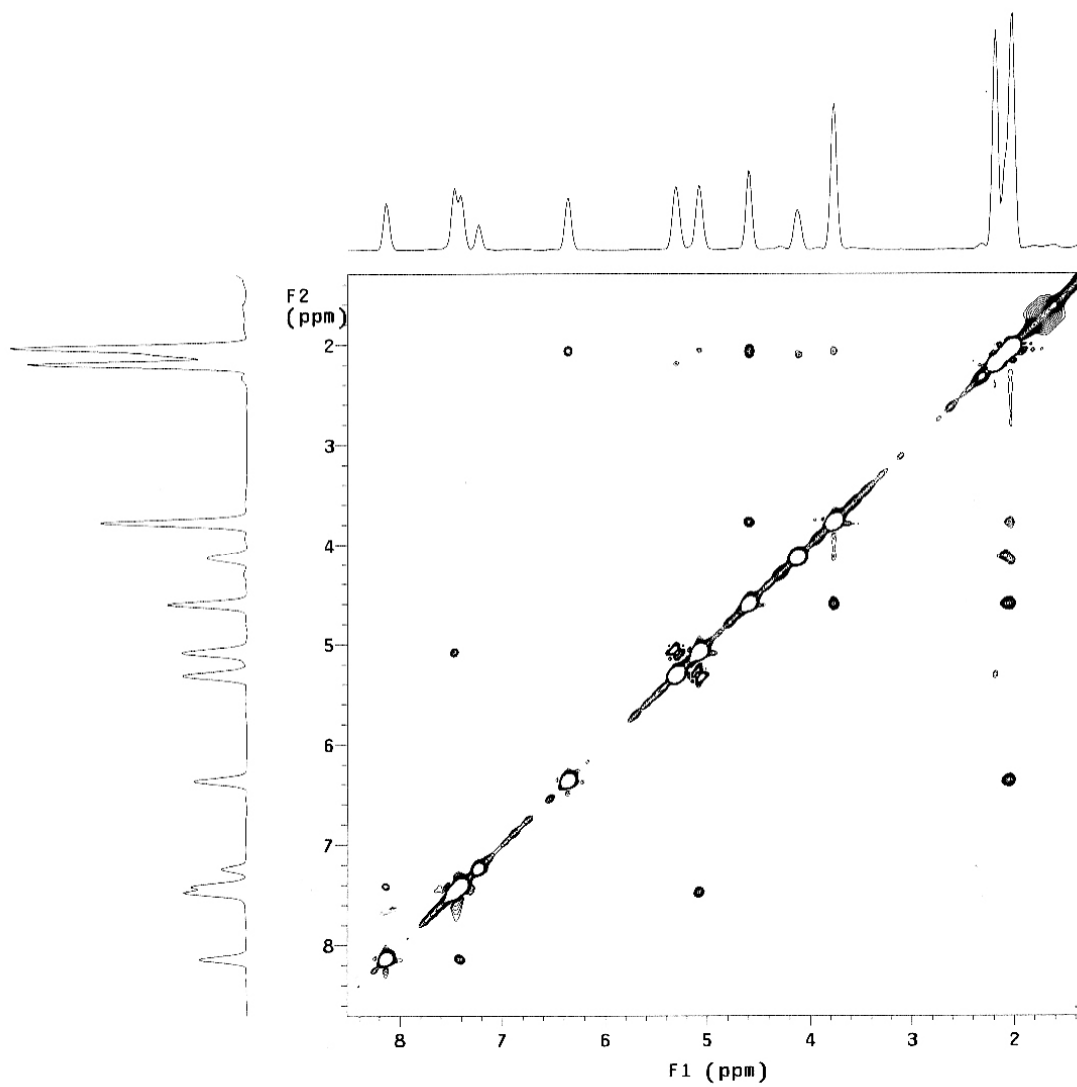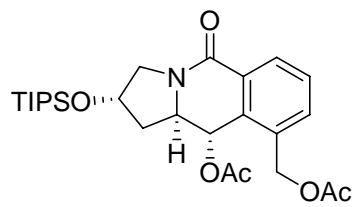
^{1}H NMR Spectrum of **5-78**
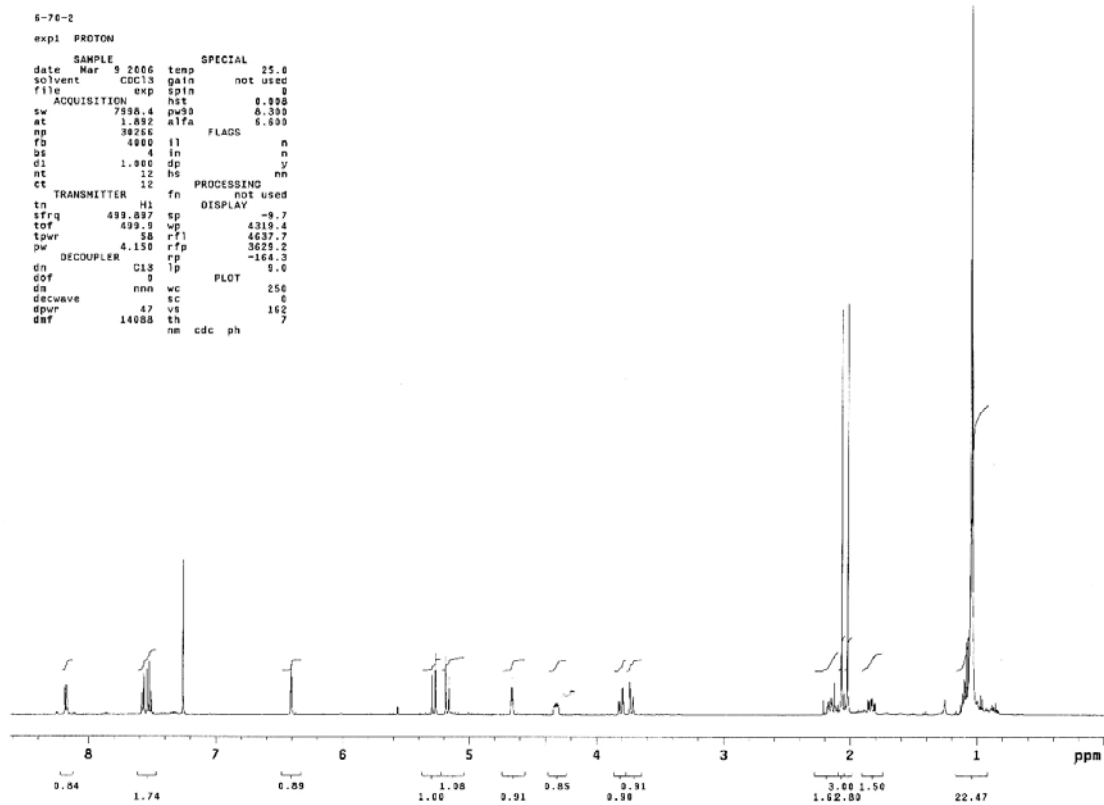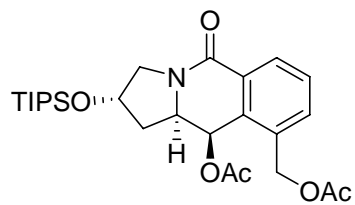
^{13}C NMR Spectrum of **5-78**
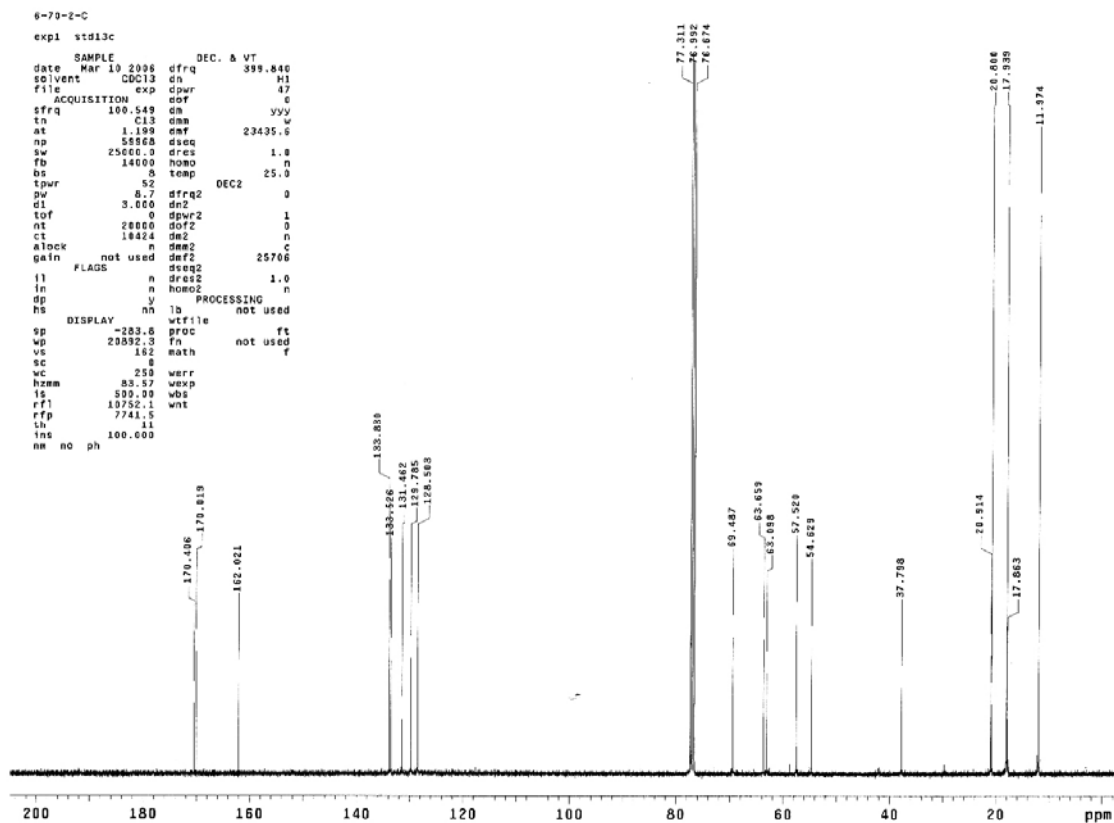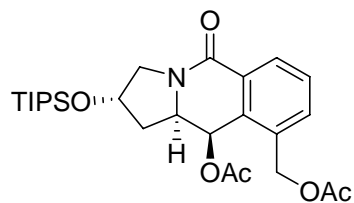
COSY Spectrum of **5-78**
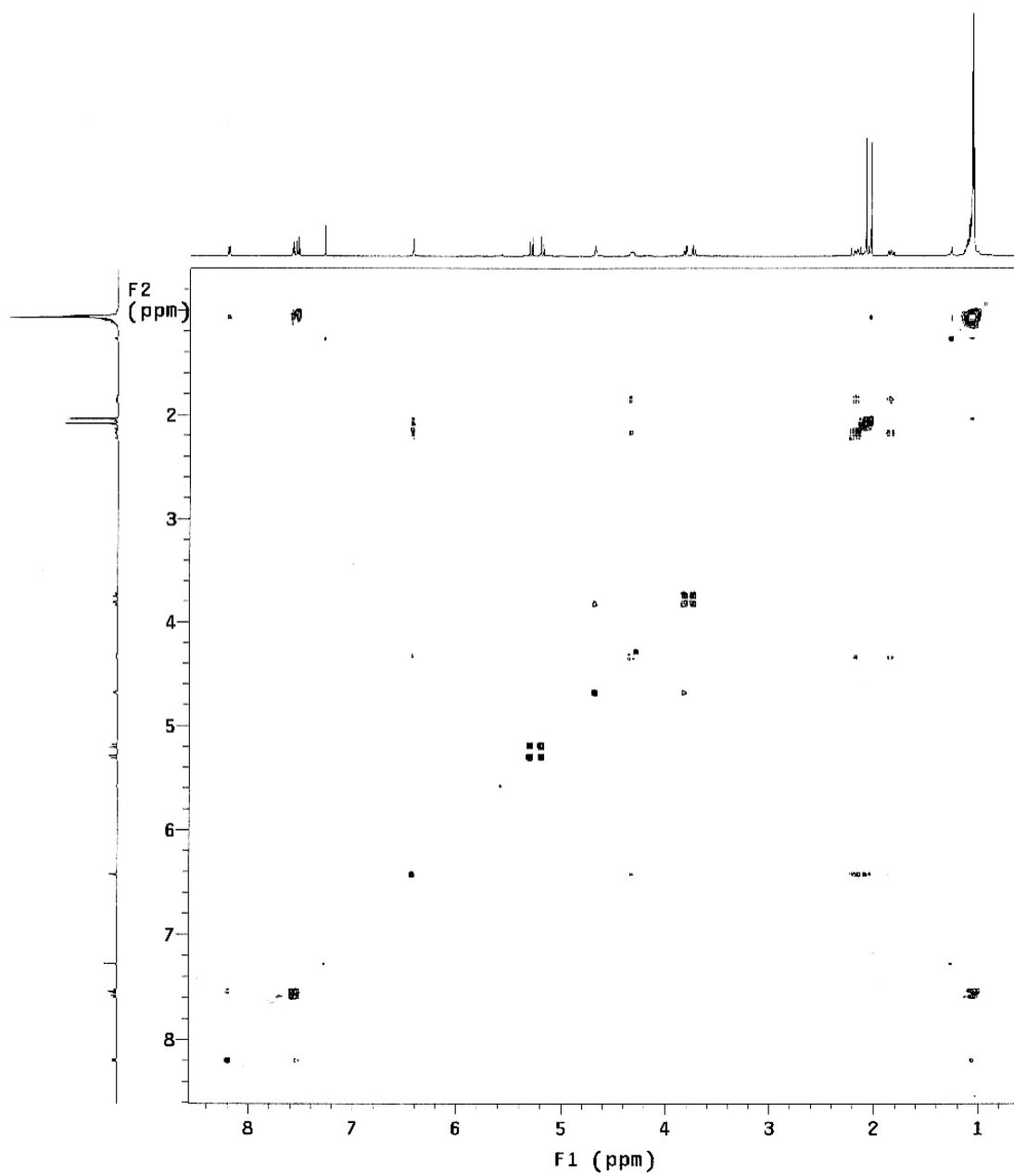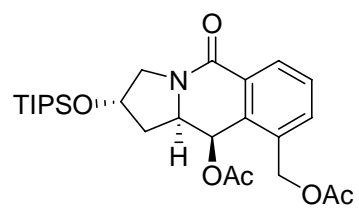
NOESY Spectrum of **5-78**
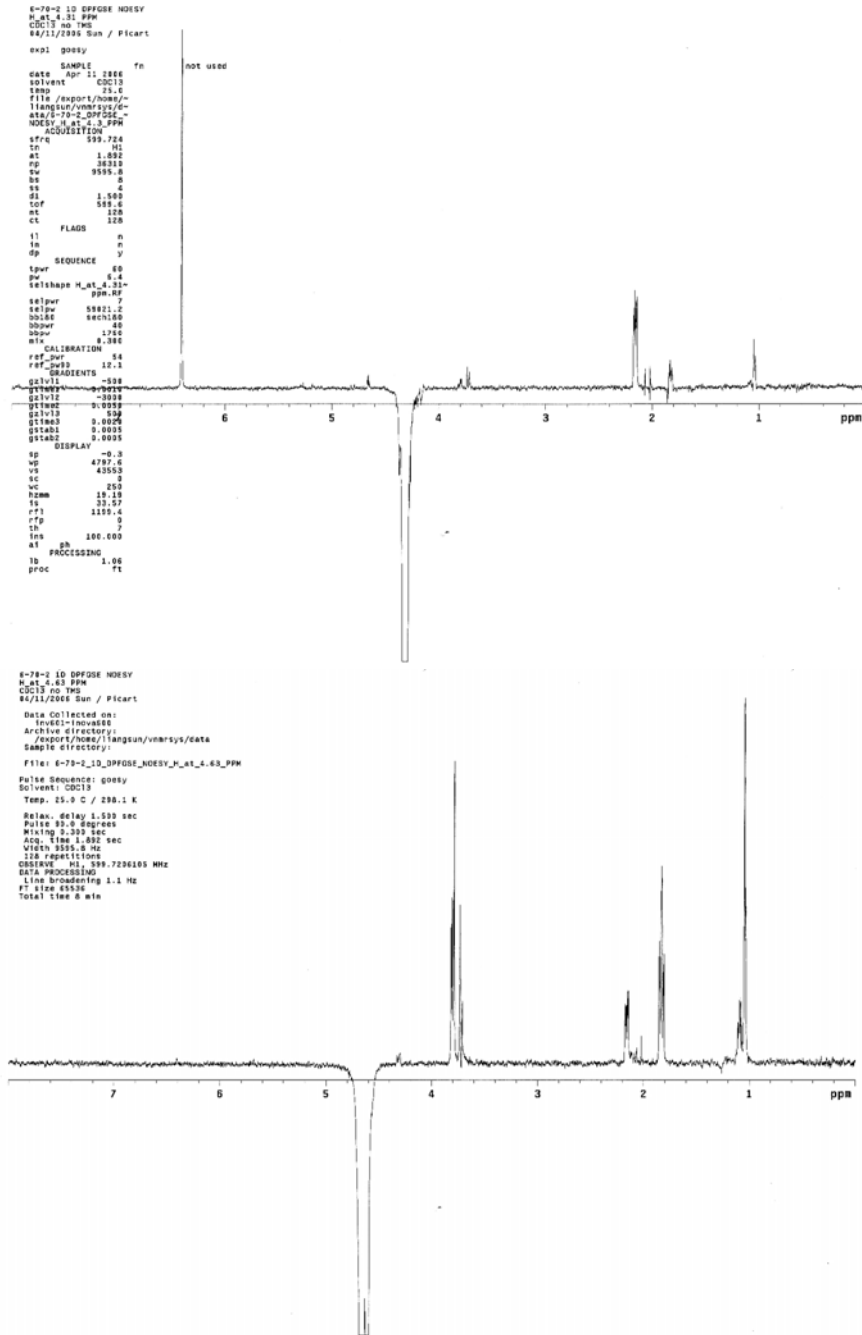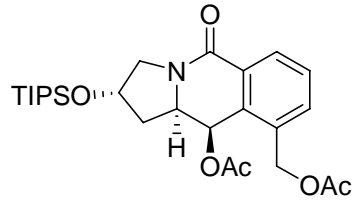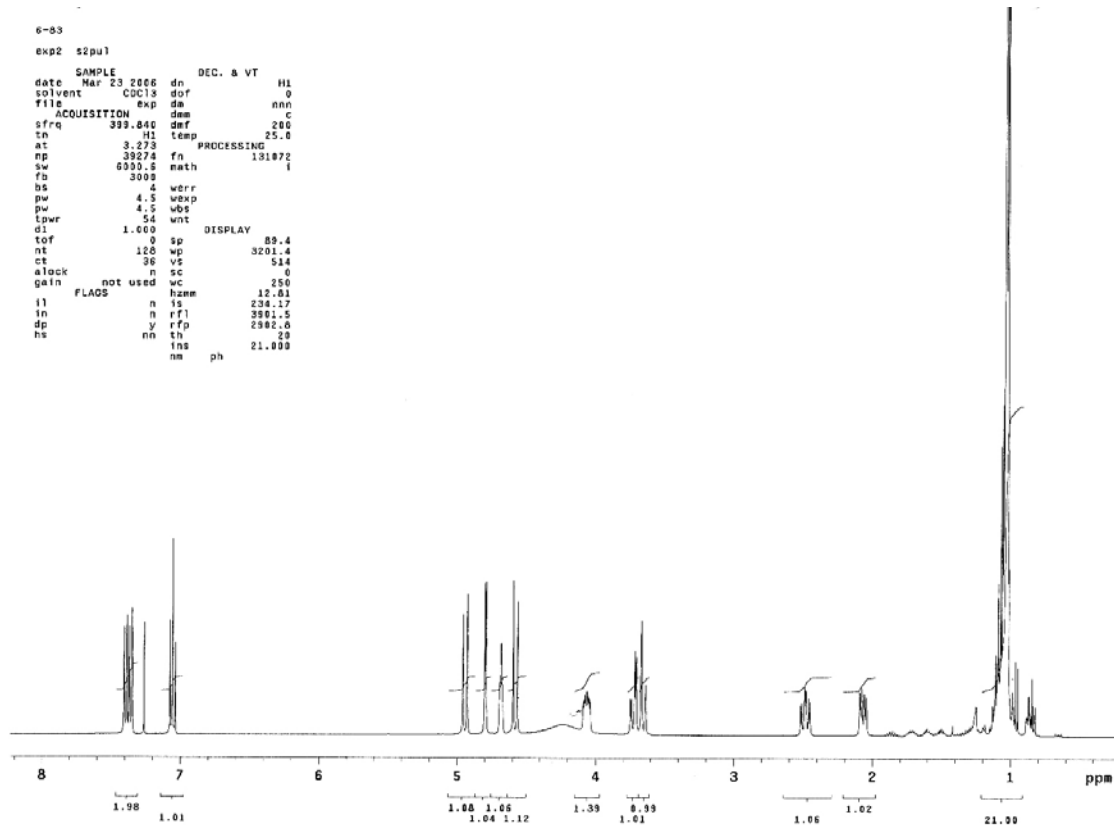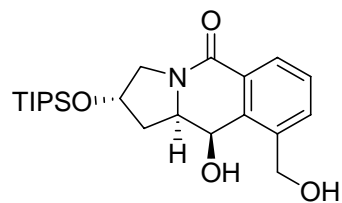
¹³C NMR Spectrum of **5-79**

^{13}C NMR Spectrum of **5-79**

^{1}H NMR Spectrum of **5-80**
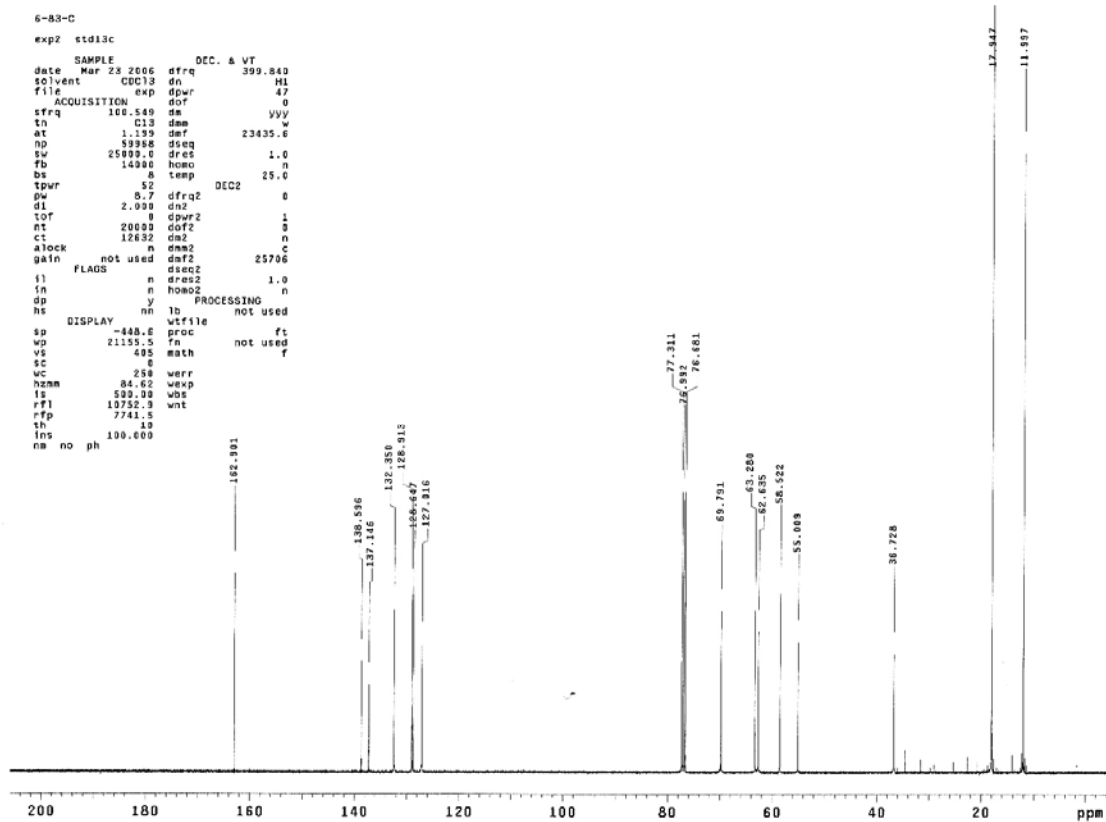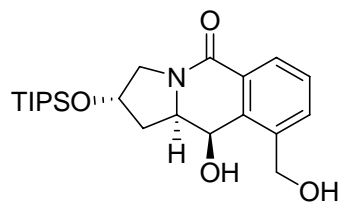
^{13}C NMR Spectrum of **5-80**
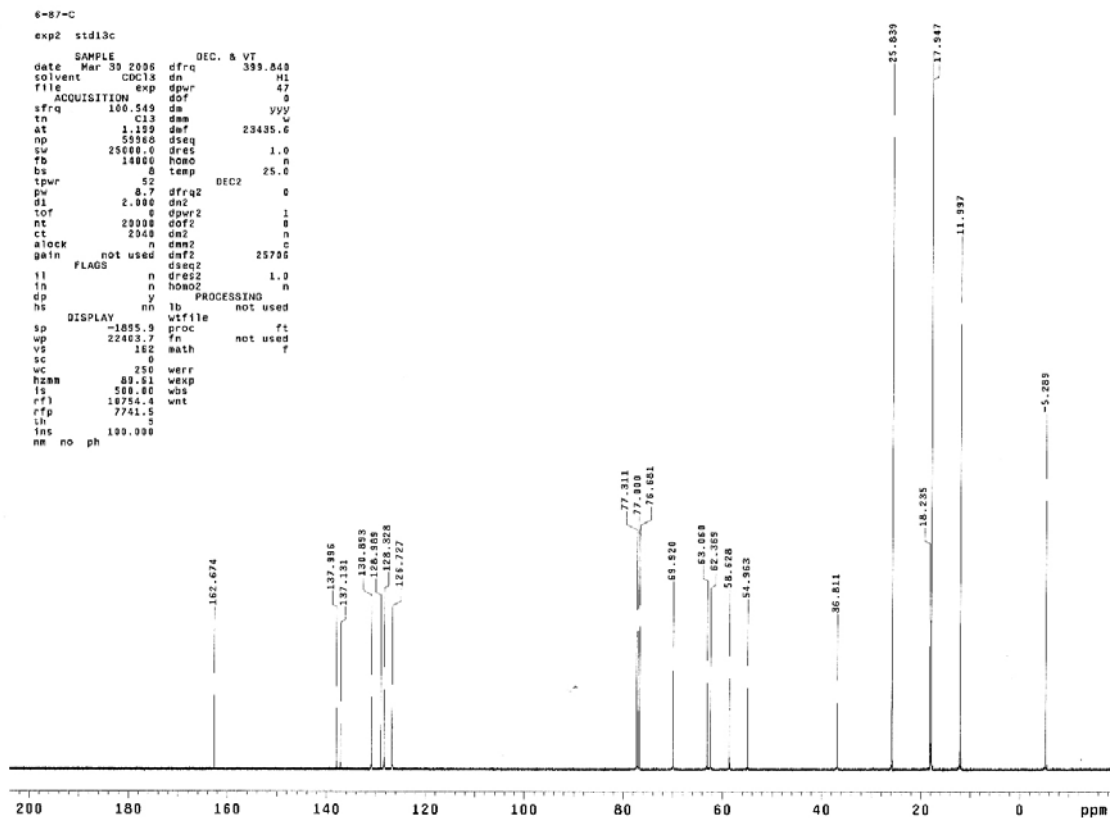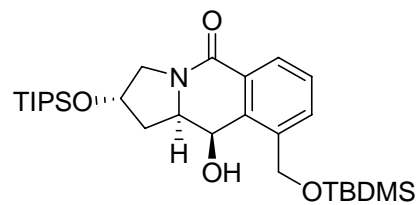
^{1}H NMR Spectrum of **5-81**
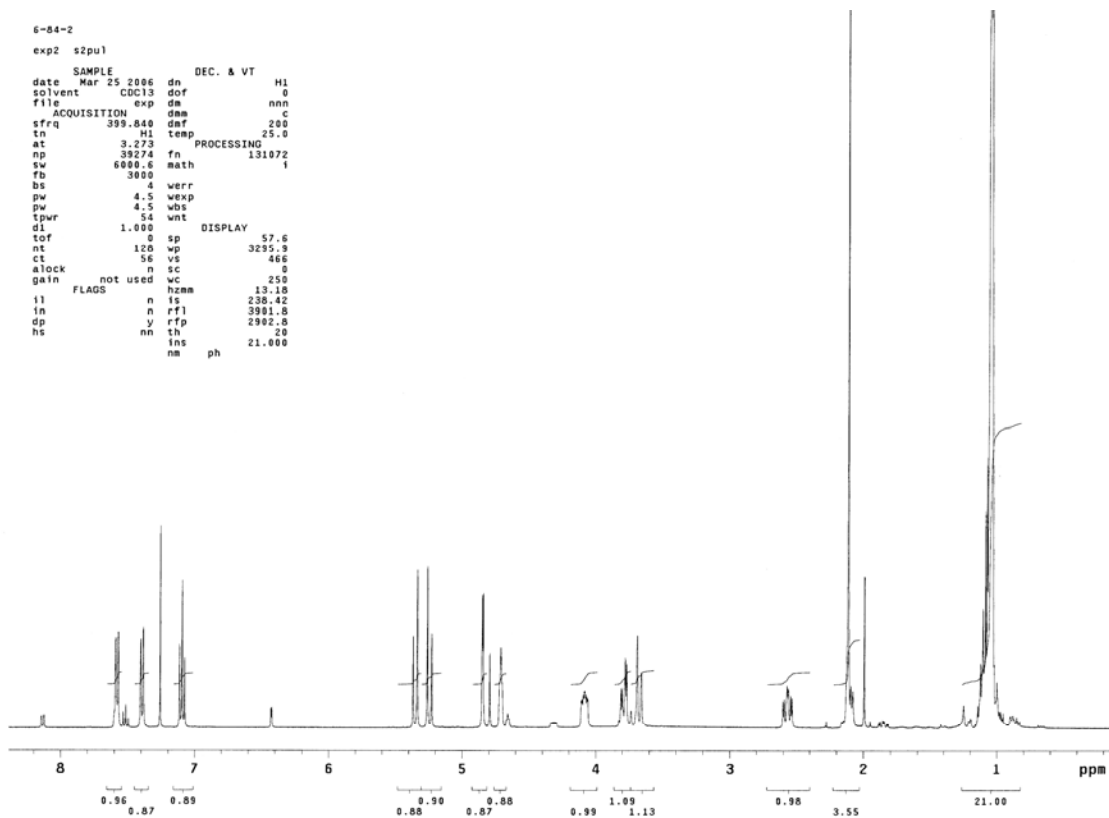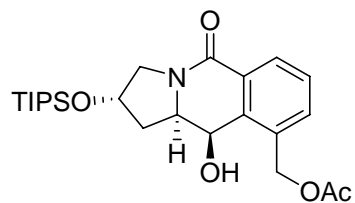
^{13}C NMR Spectrum of **5-81**
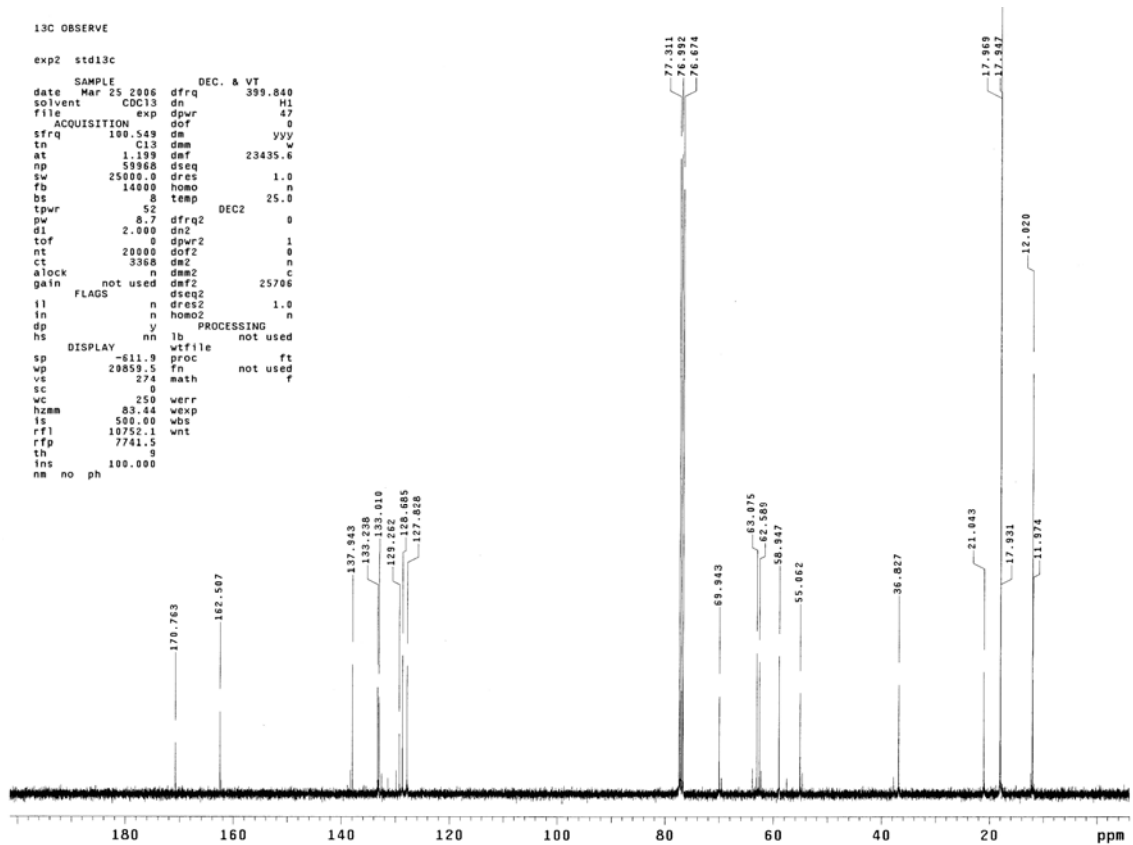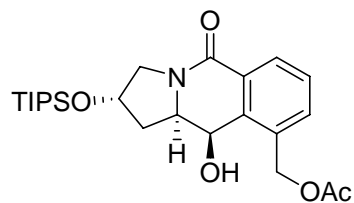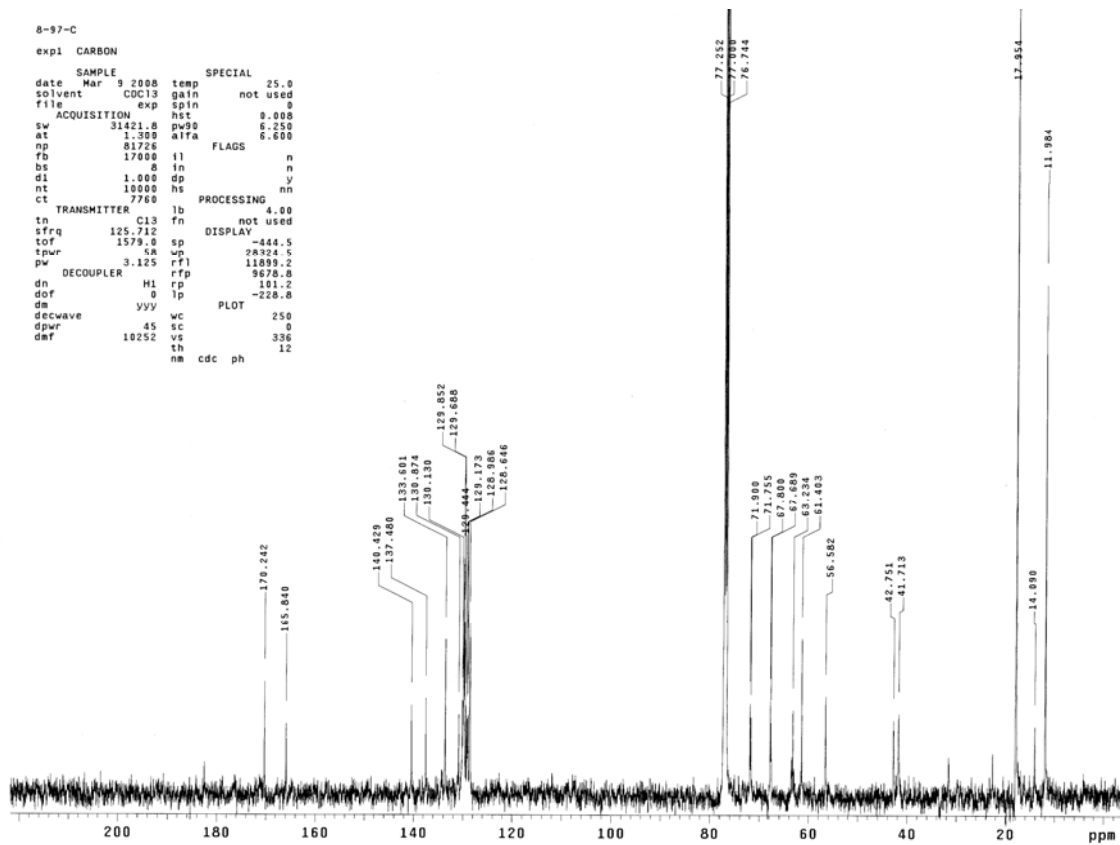
^{1}H NMR Spectrum of **5-84**
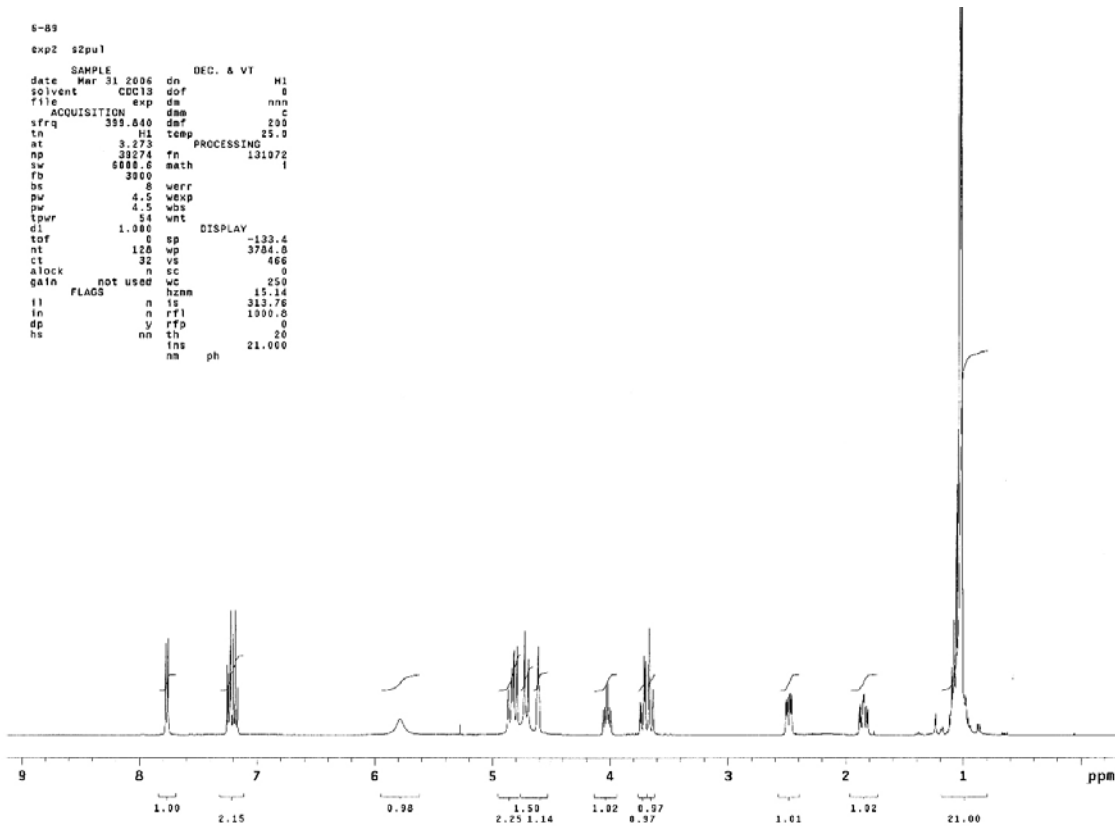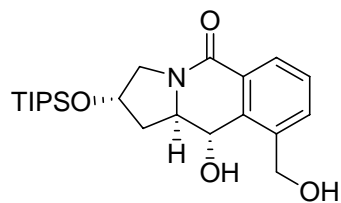
^{13}C NMR Spectrum of **5-84**
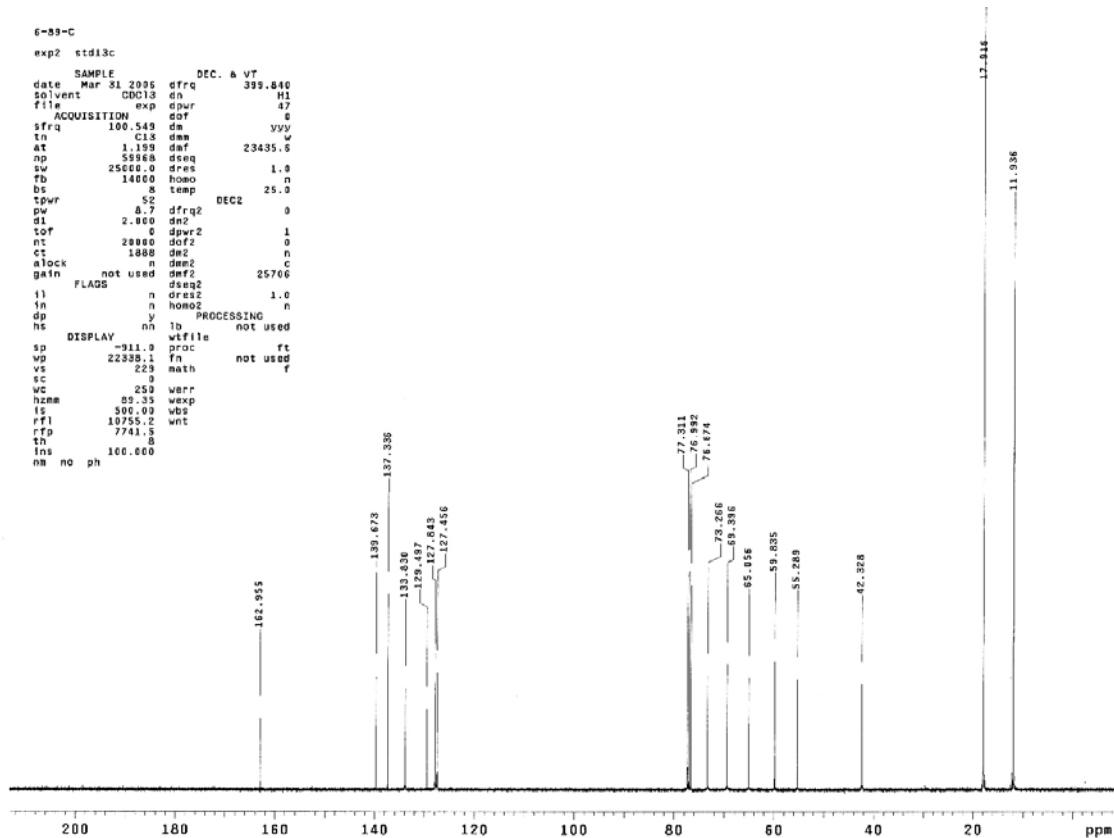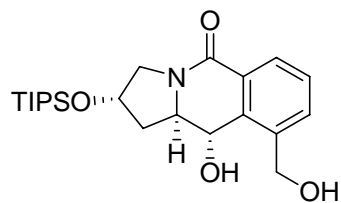
^{1}H NMR Spectrum of **5-85**
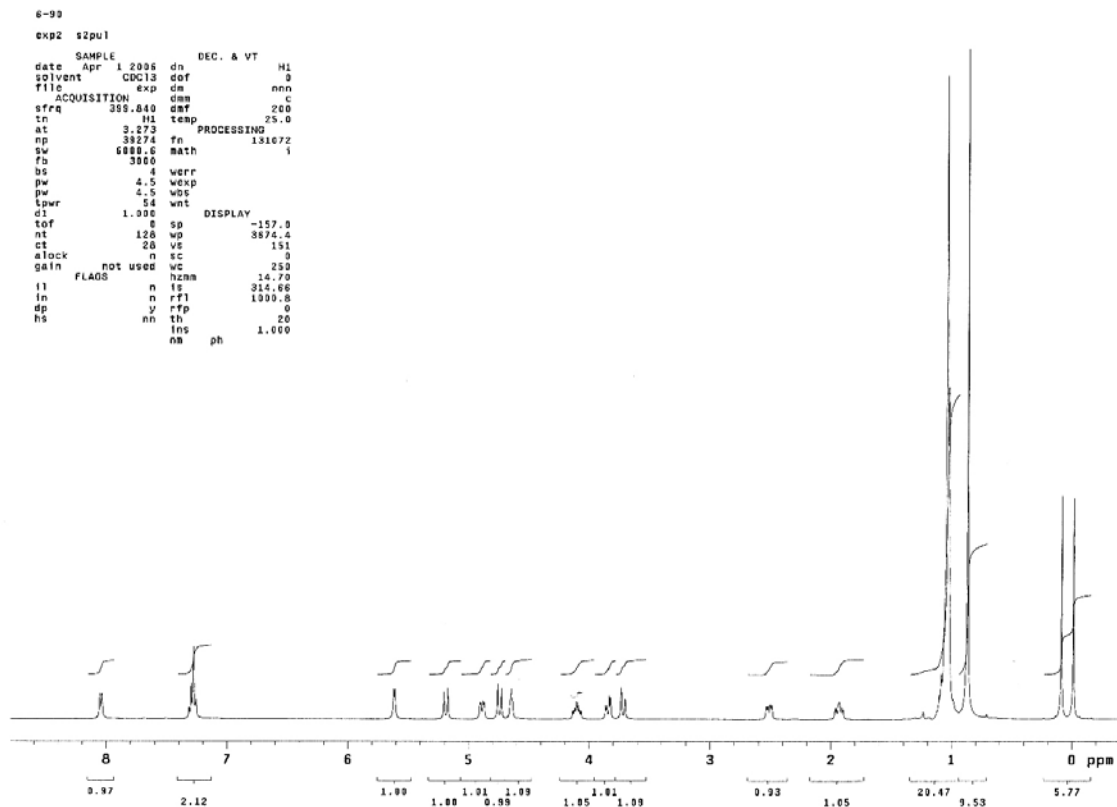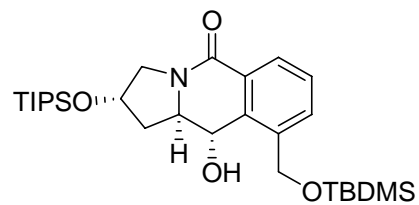
^{13}C NMR Spectrum of **5-85**
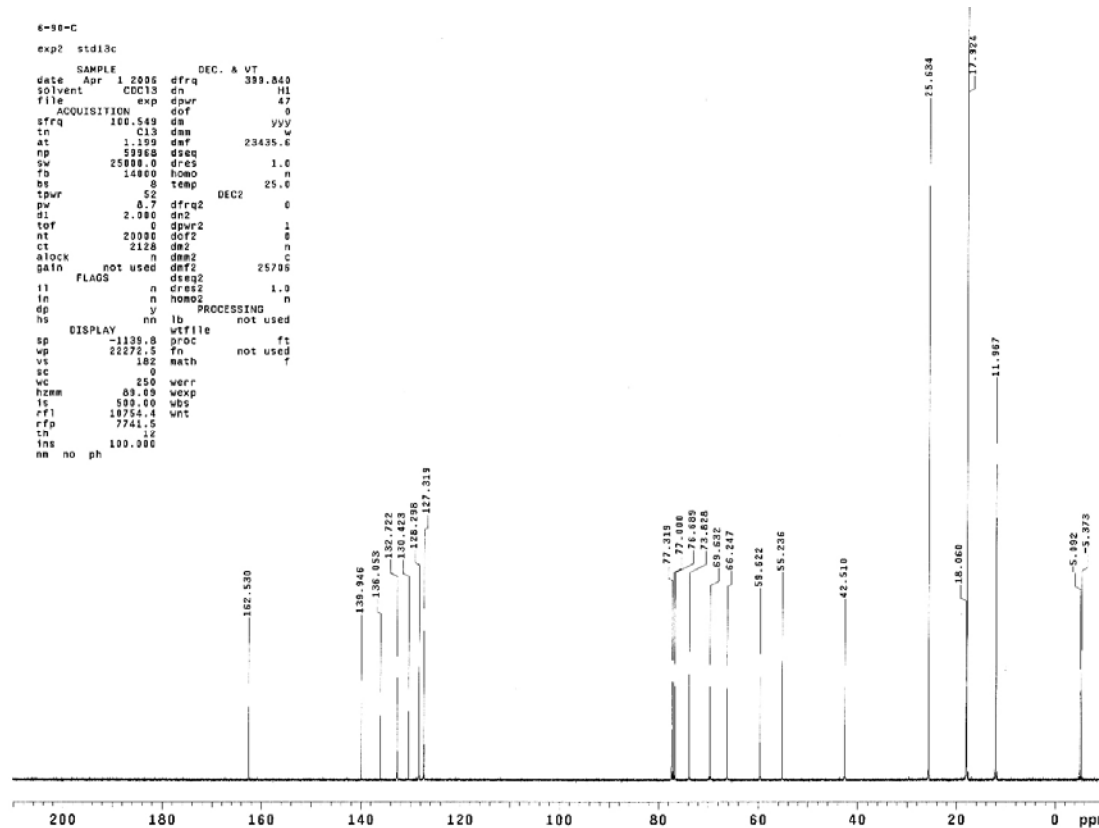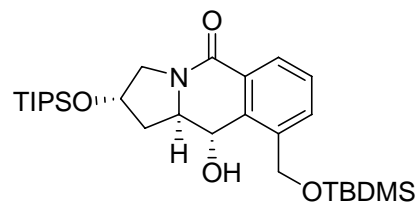
^{1}H NMR Spectrum of **5-86**
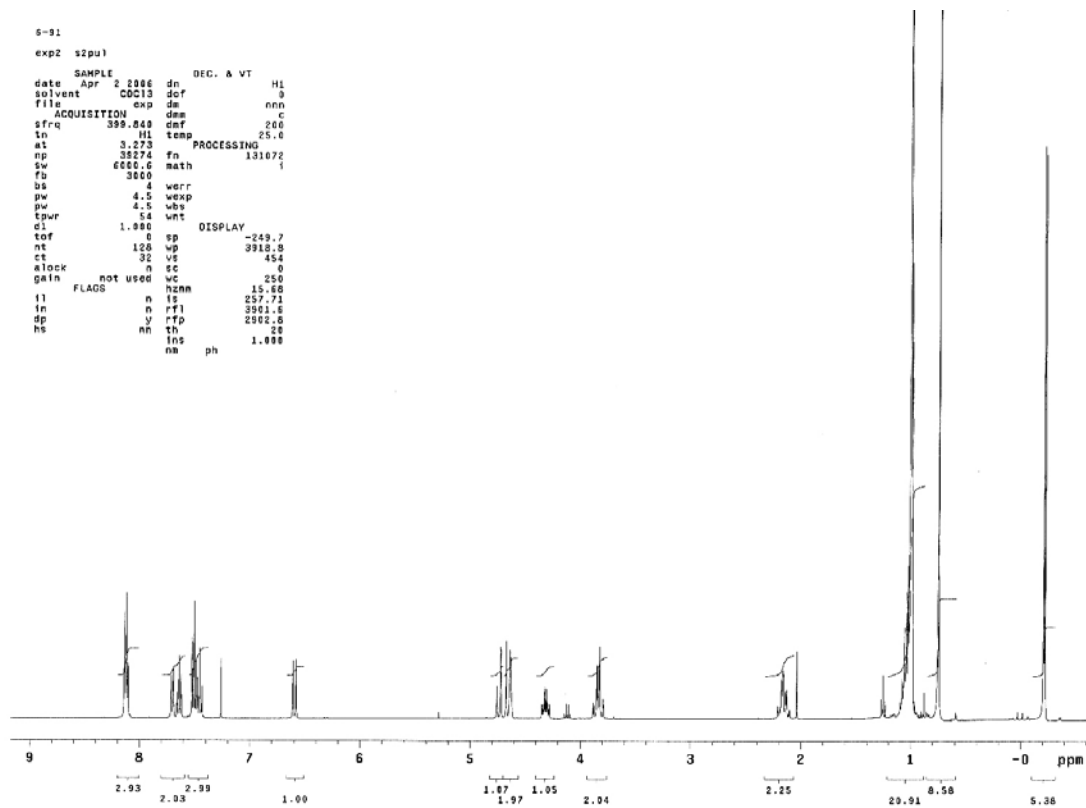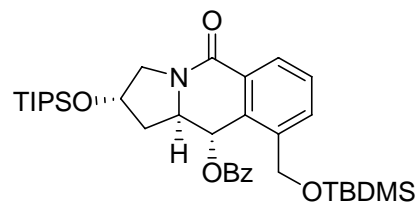
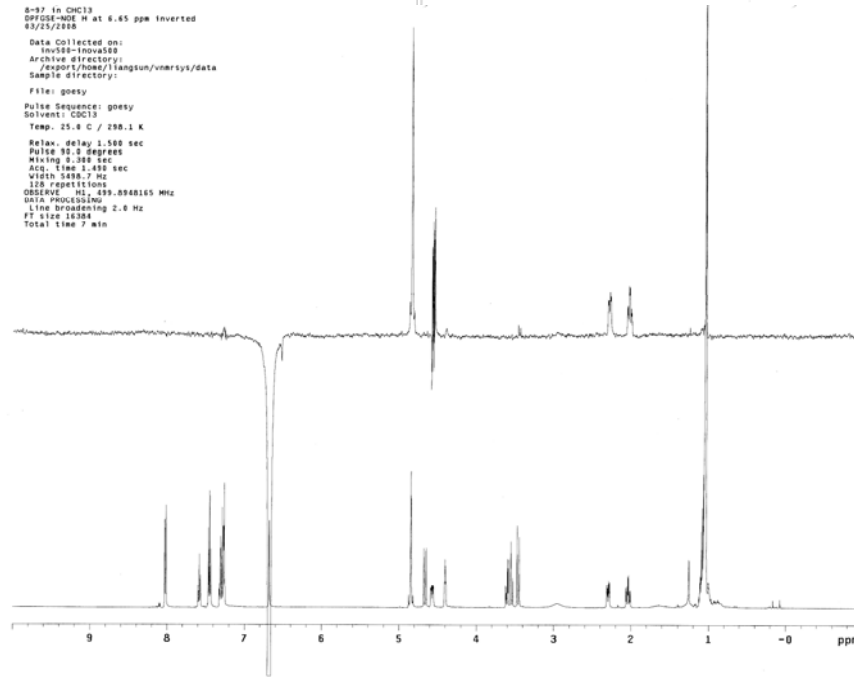# ^{13}C NMR Spectrum of **5-86**
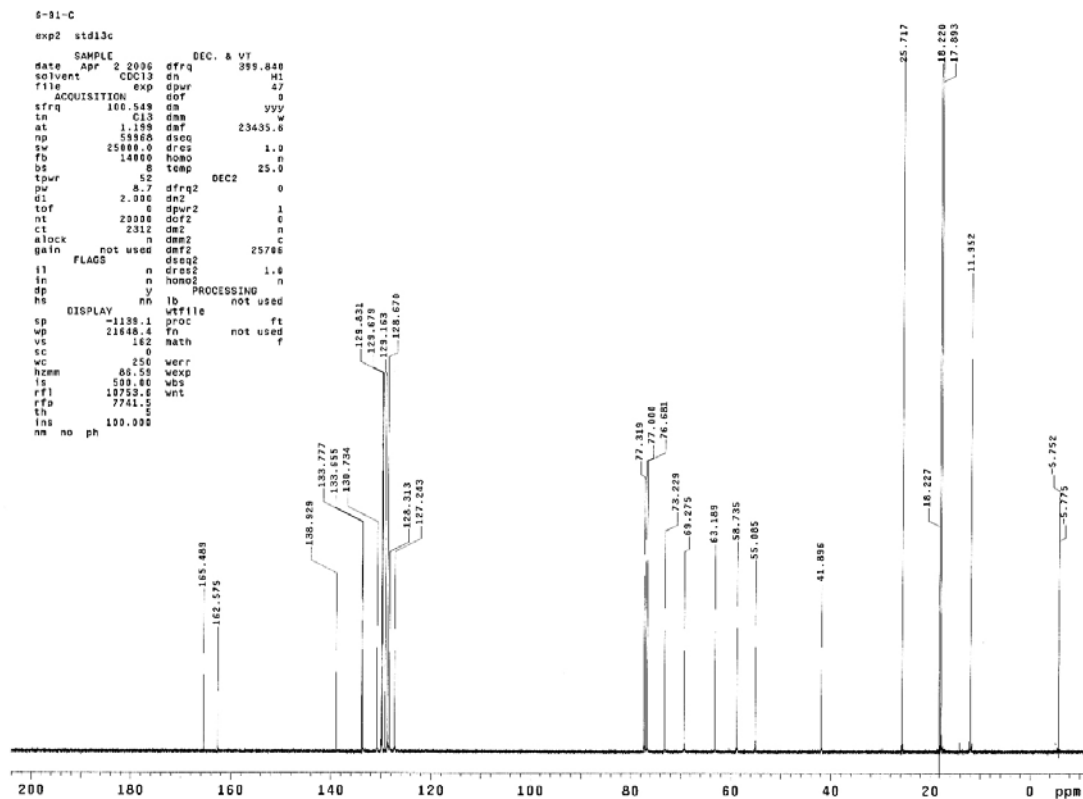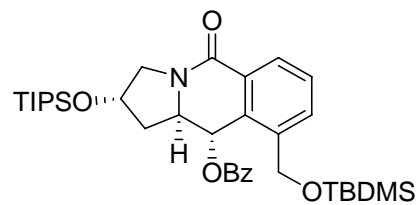
^{1}H NMR Spectrum of **5-87**
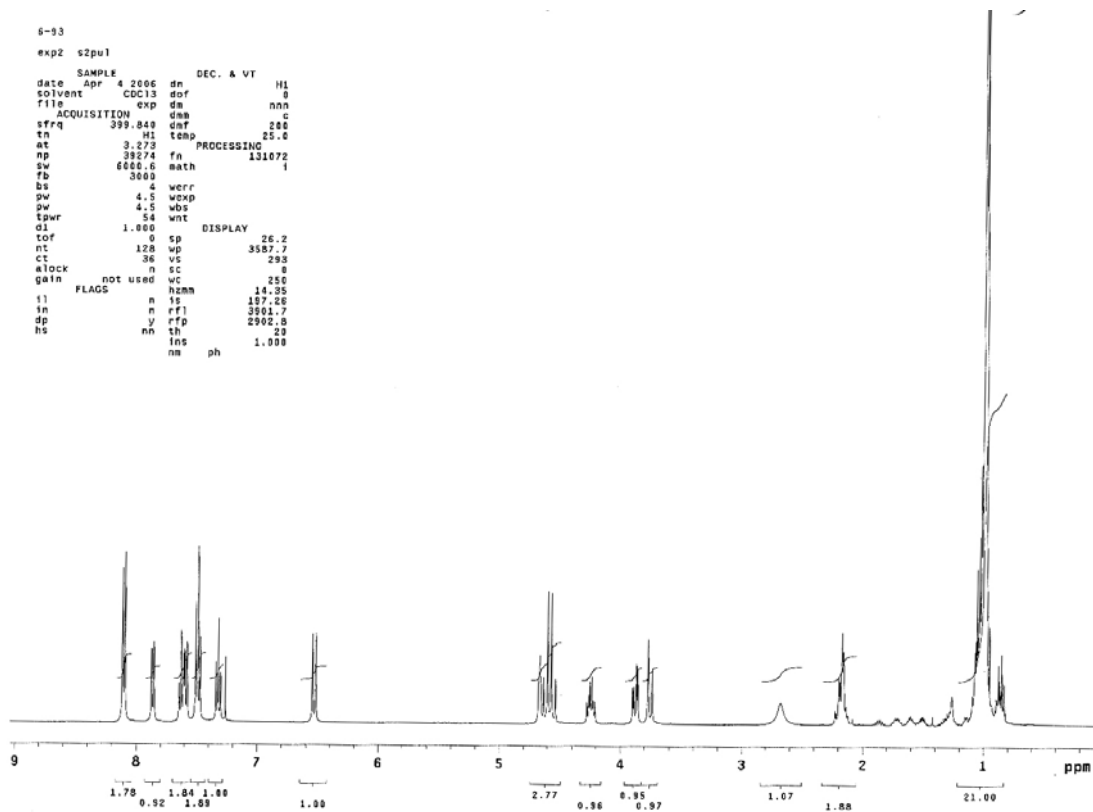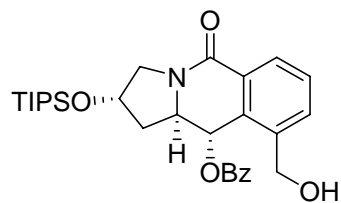
^{13}C NMR Spectrum of **5-87**
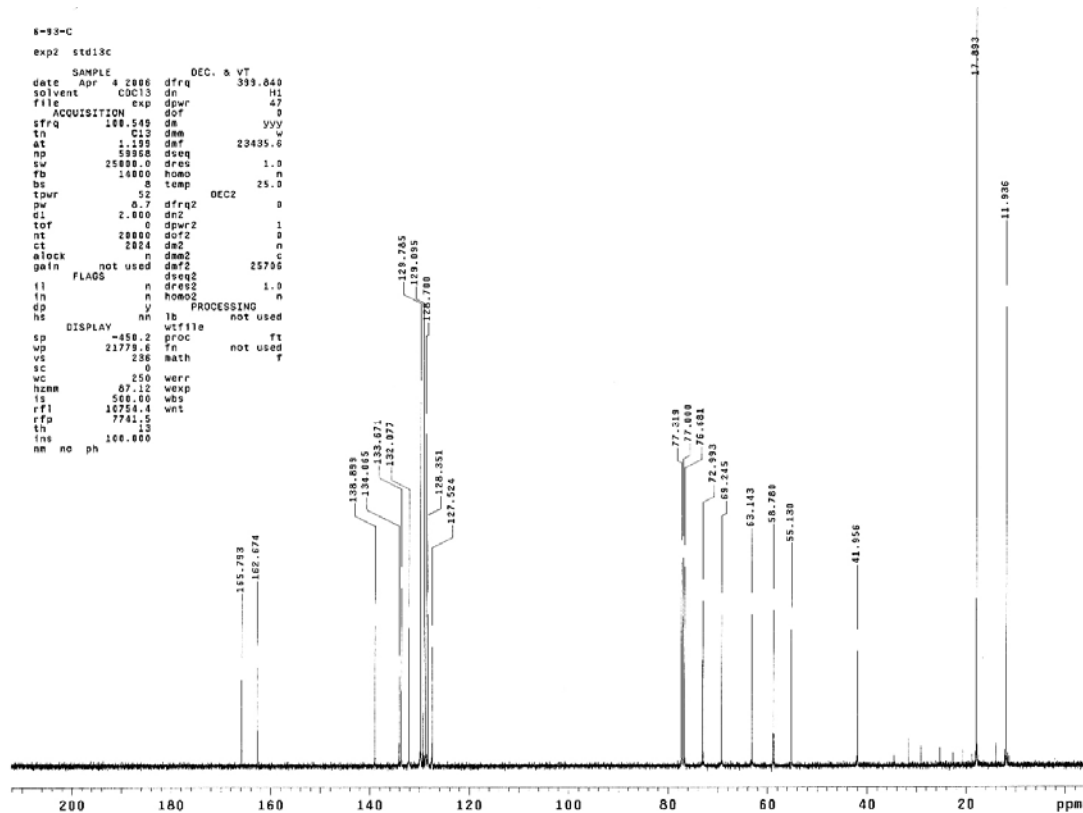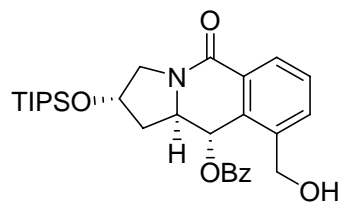
^{1}H NMR Spectrum of **5-88**
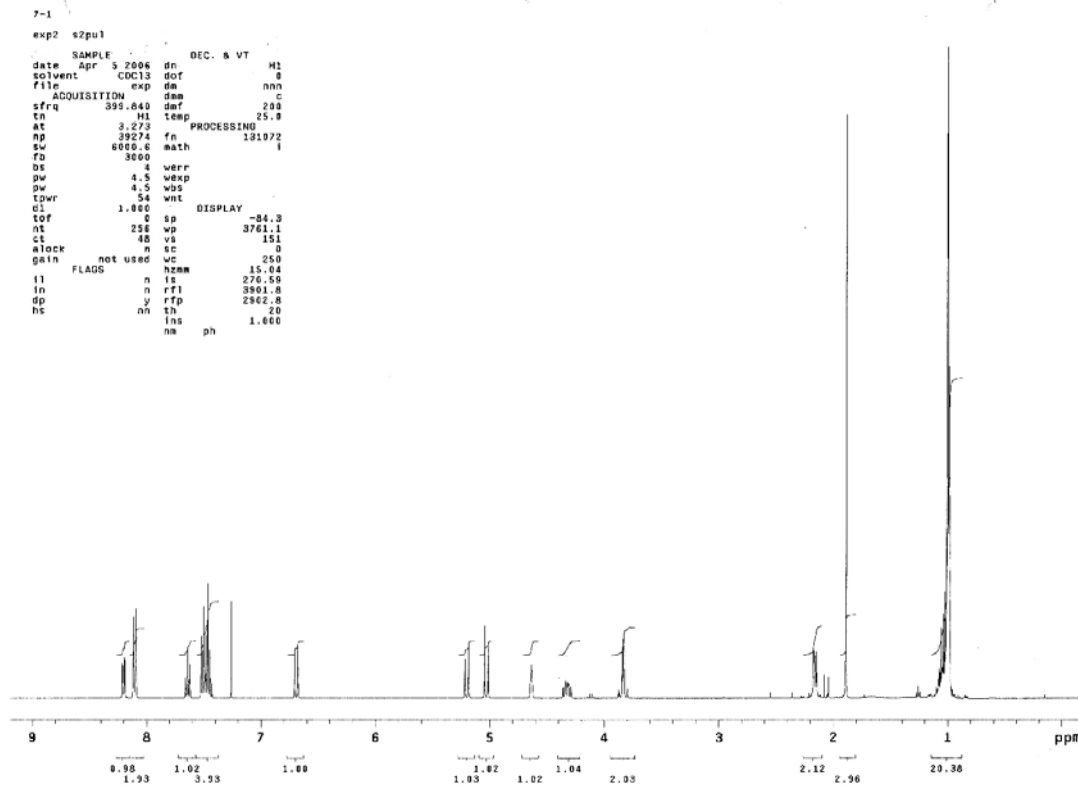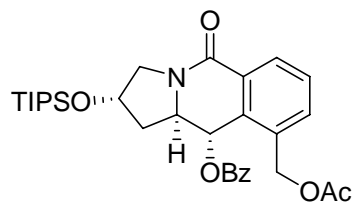
^{13}C NMR Spectrum of **5-88**
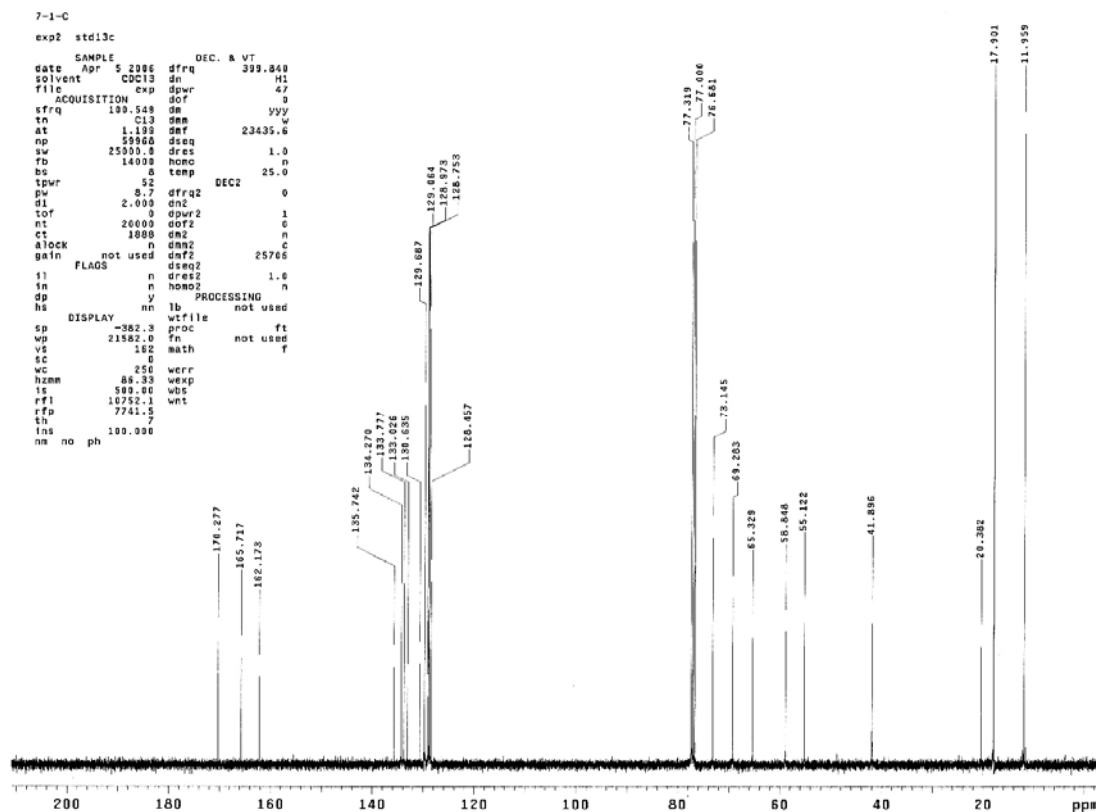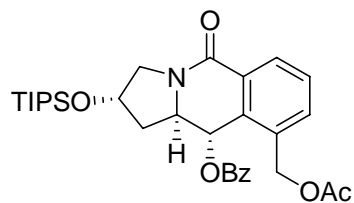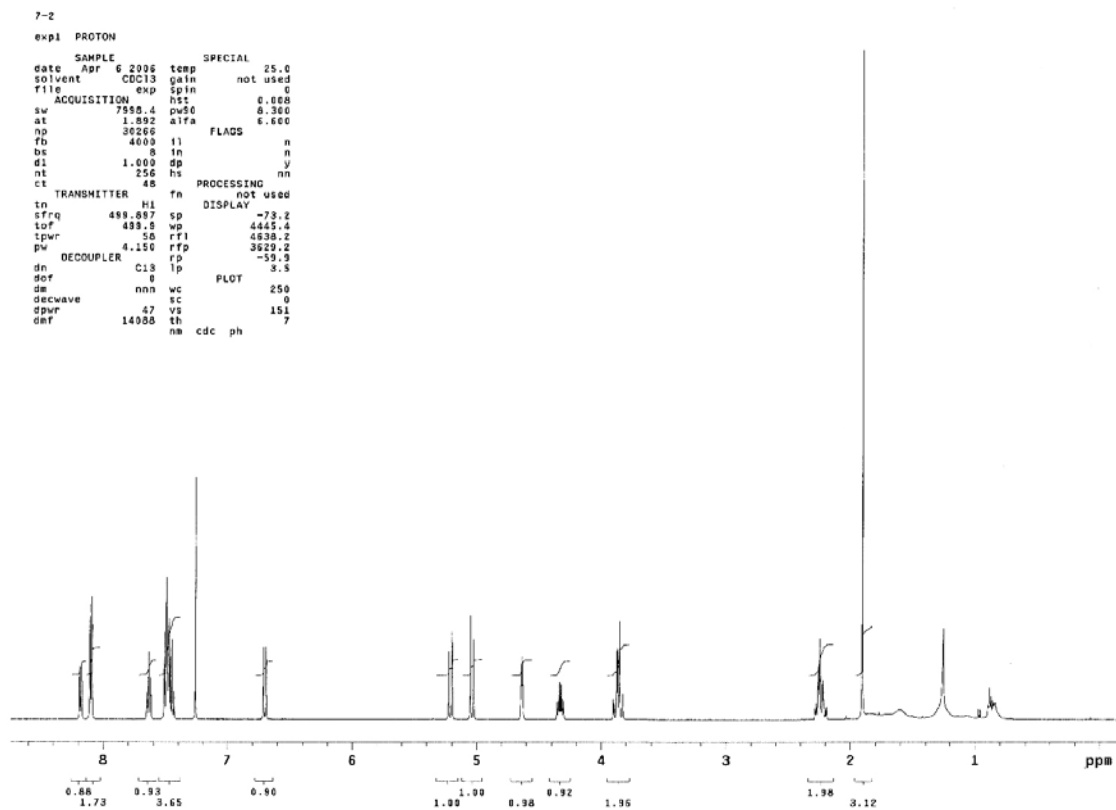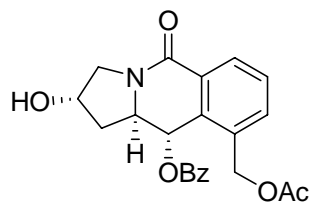
^{1}H NMR Spectrum of **5-89**

^{13}C NMR Spectrum of **5-89**

531
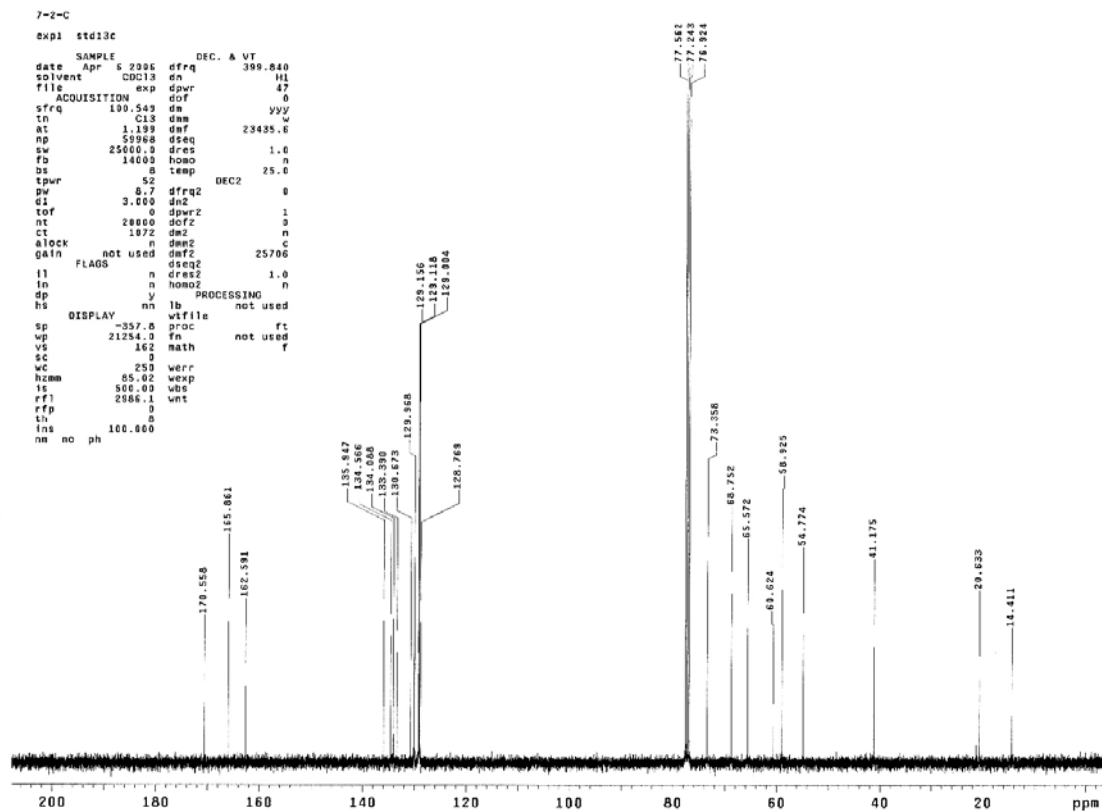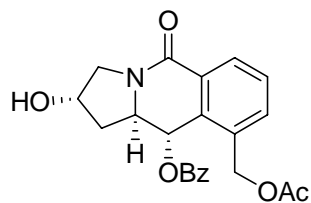
^{1}H NMR Spectrum of **5-90**
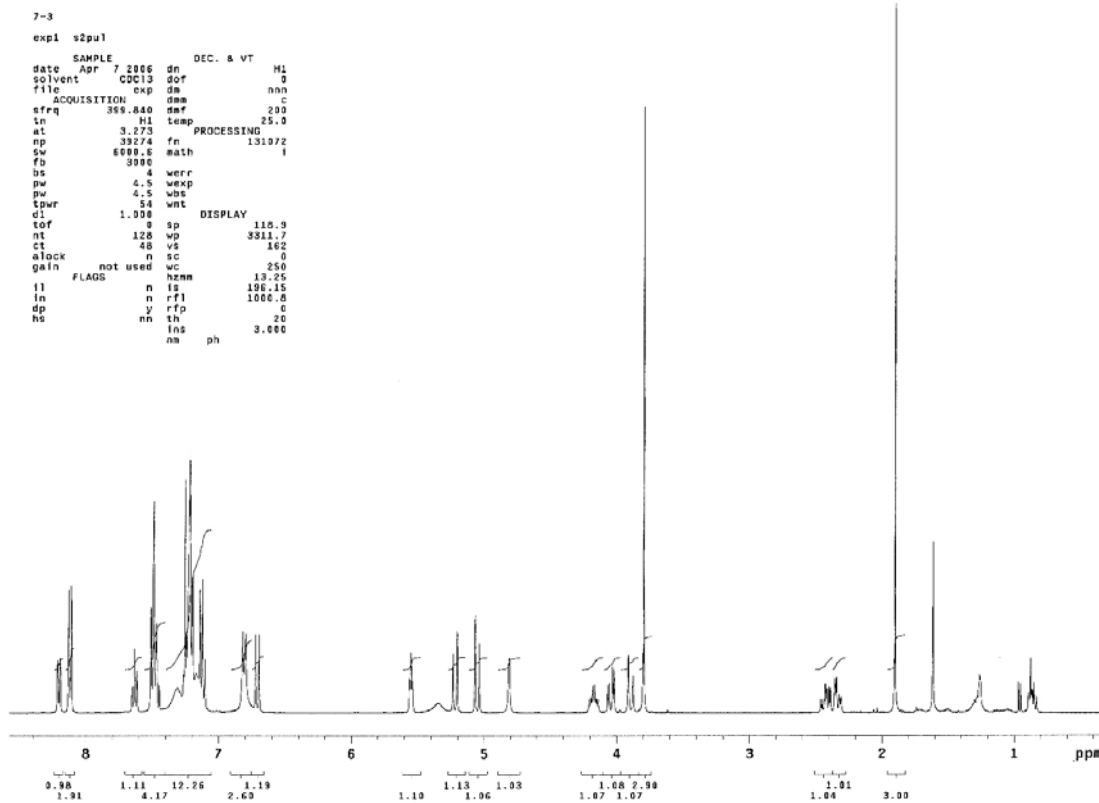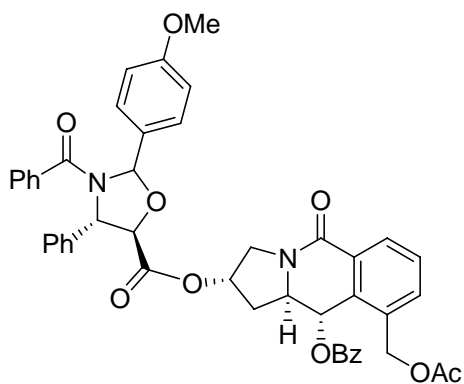
^{13}C NMR Spectrum of **5-90**
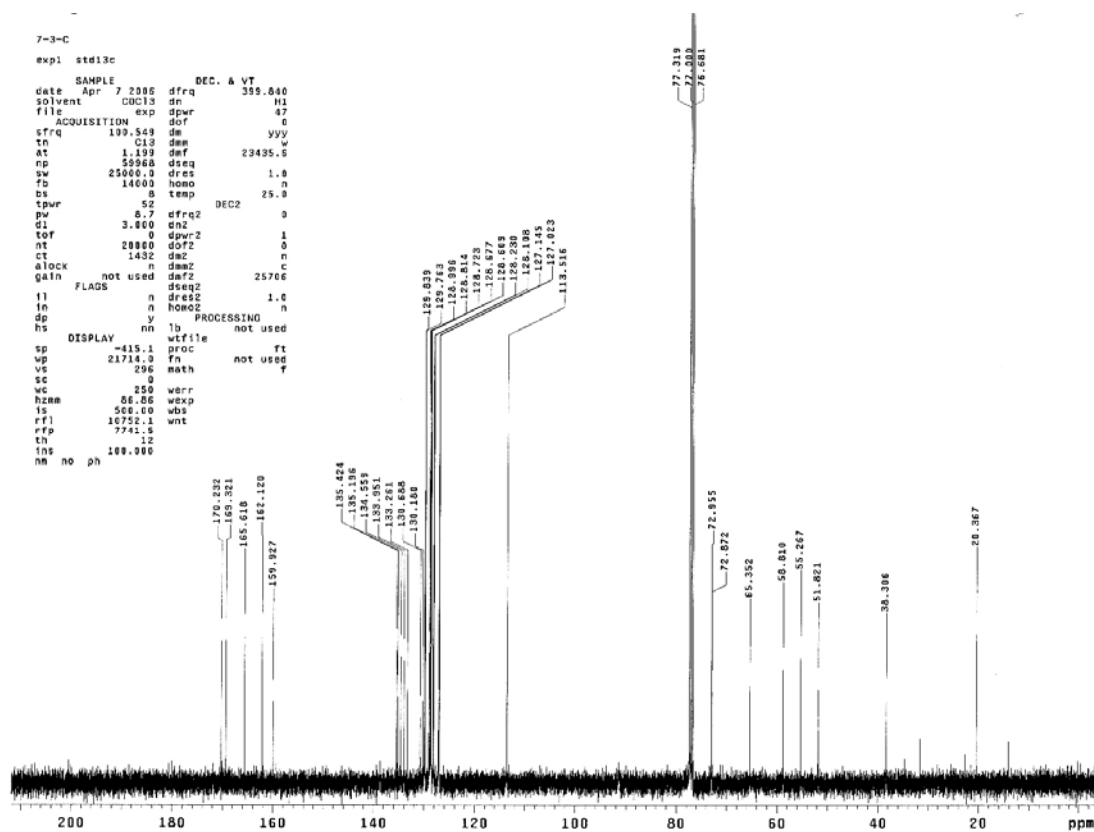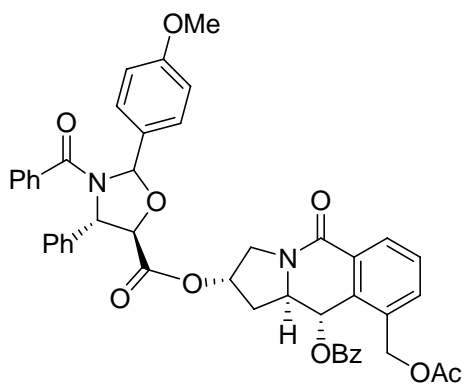
^{1}H NMR Spectrum of **5-37** (**SB-H-301**)
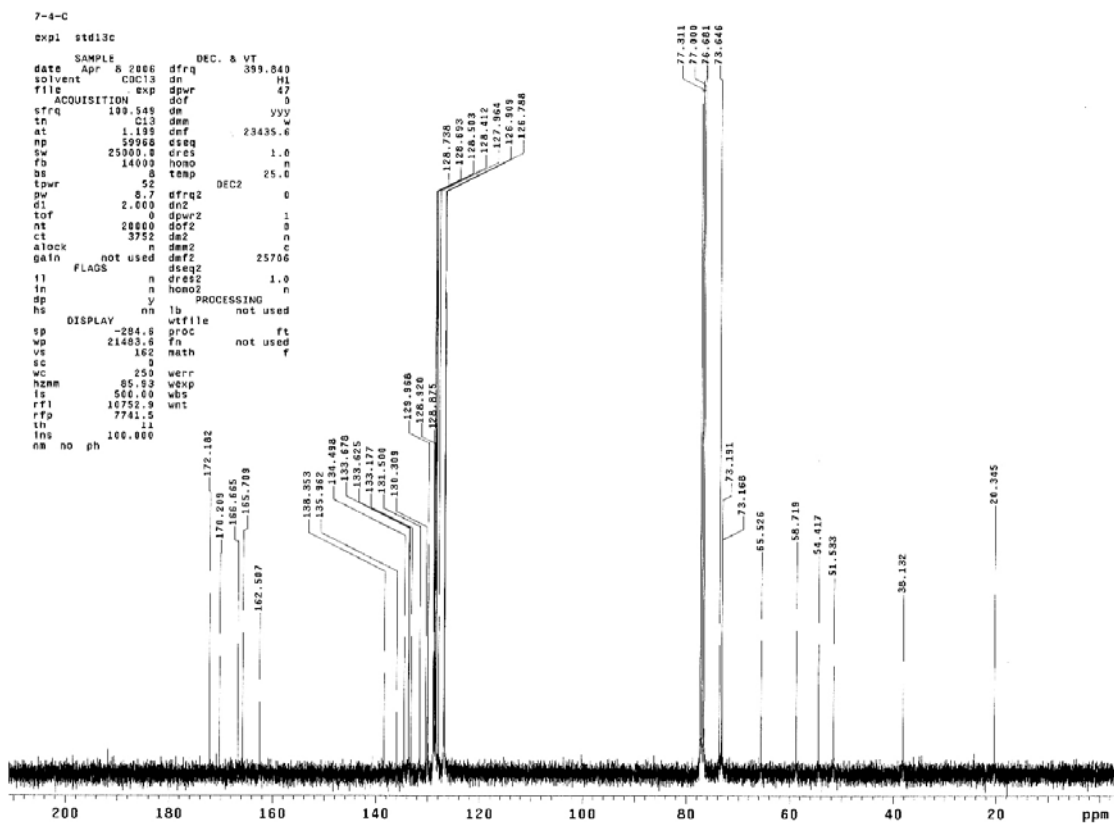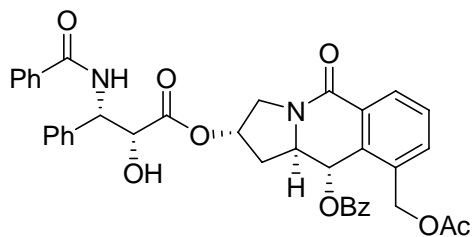
¹³C NMR Spectrum of **5-92**
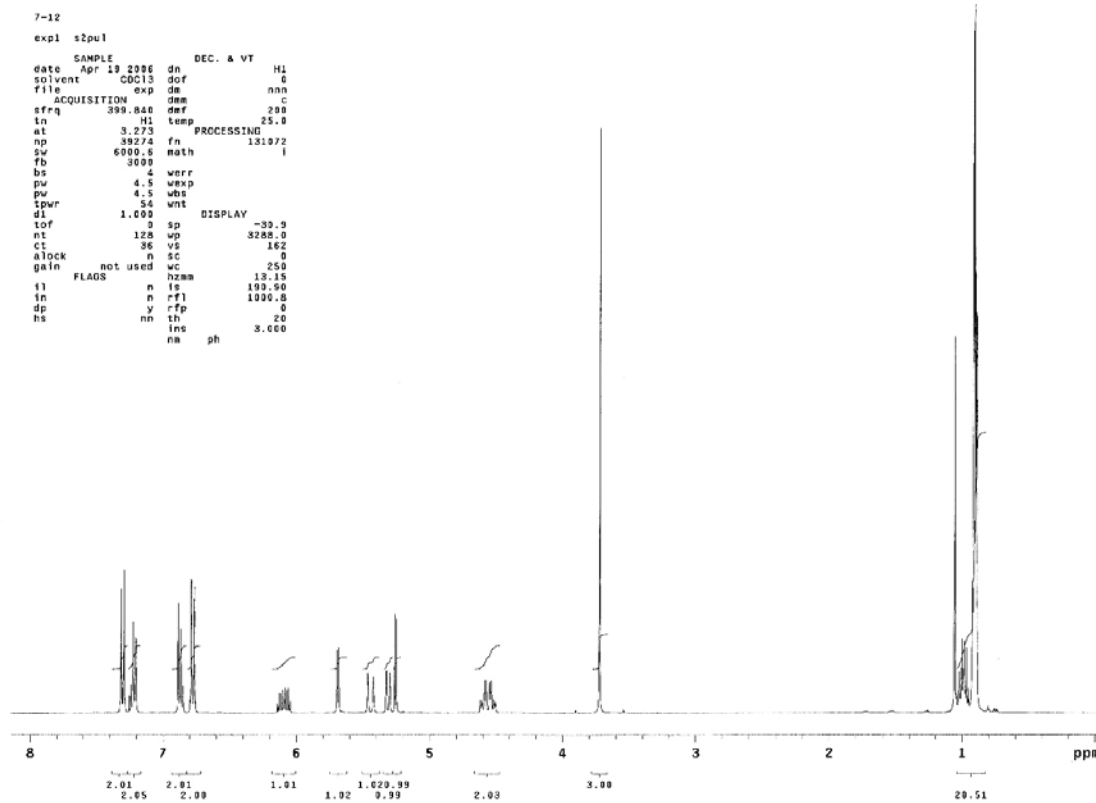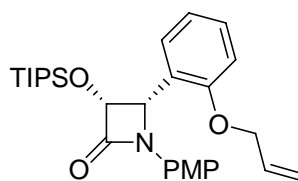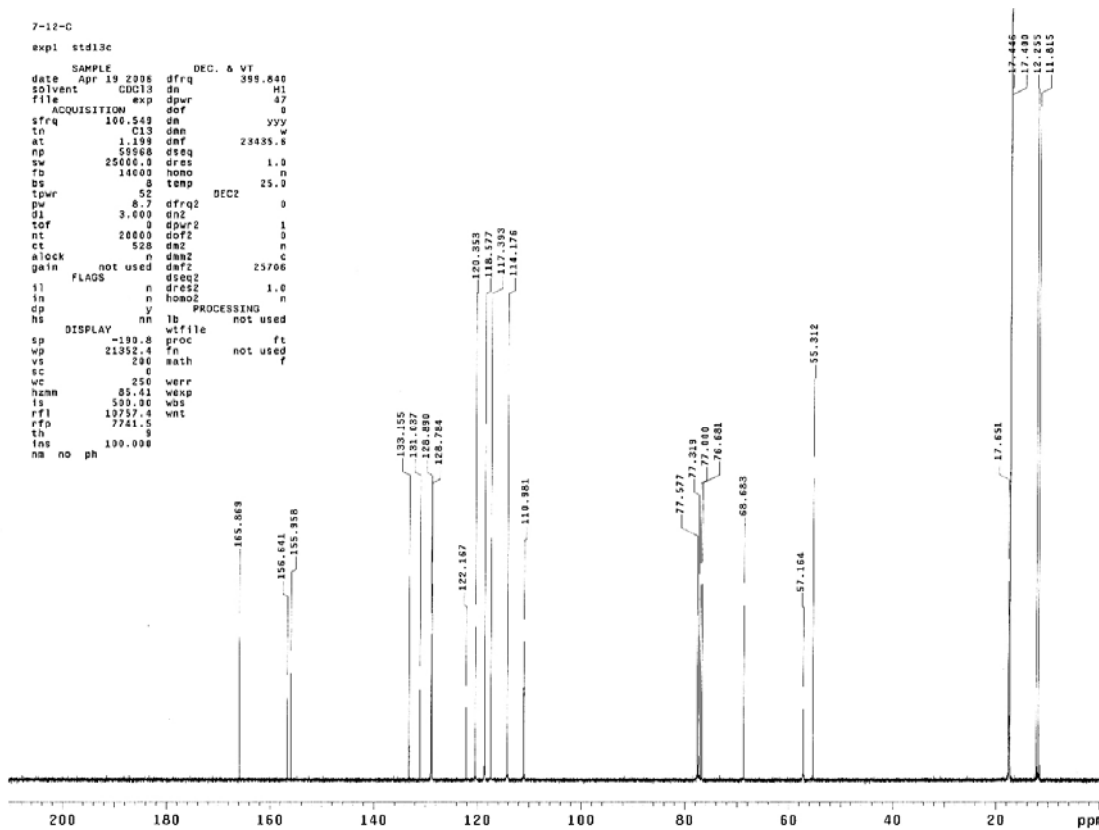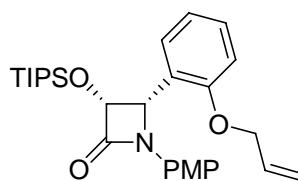
^{1}H NMR Spectrum of **5-93**
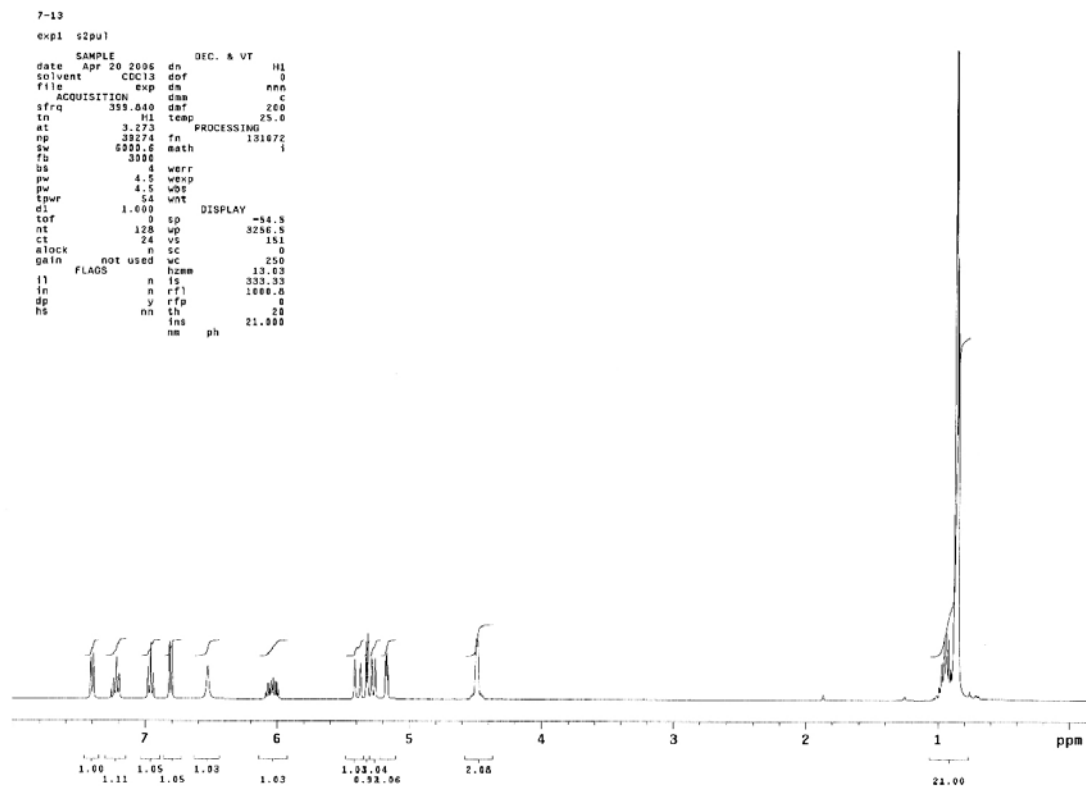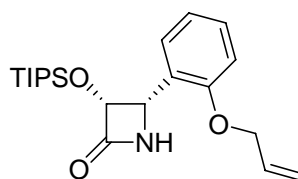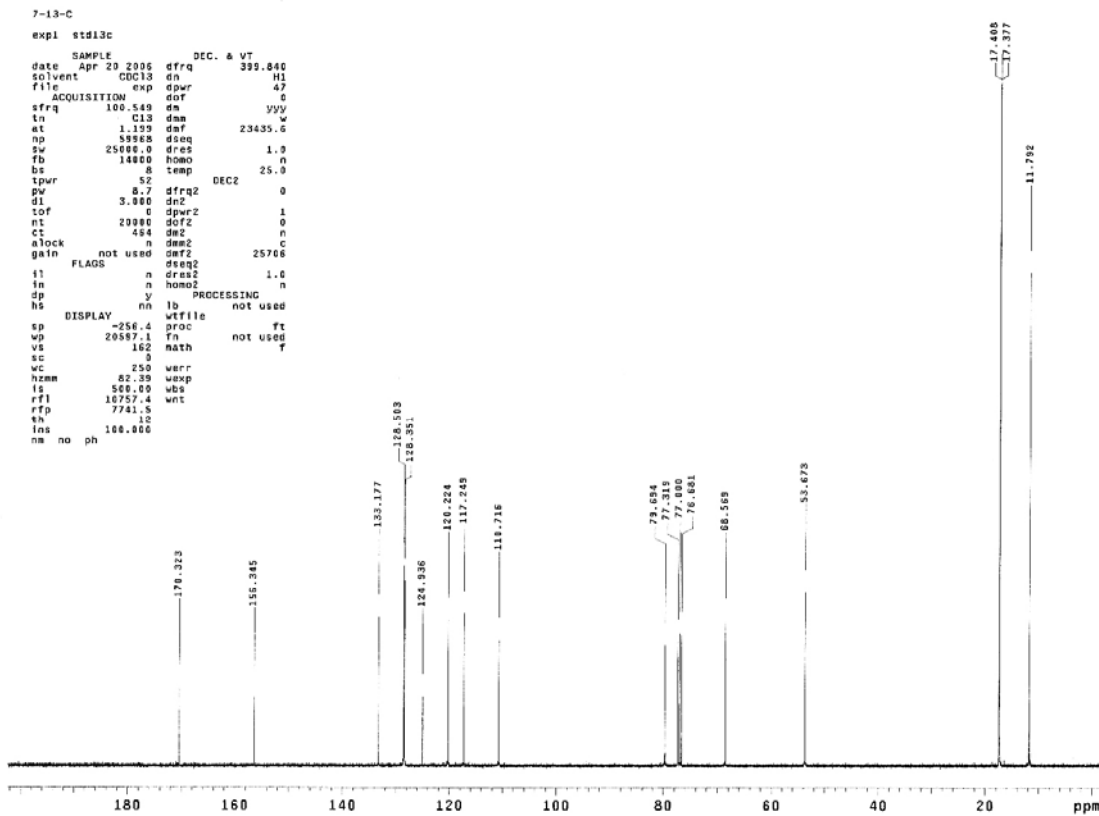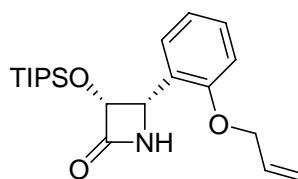
¹H NMR Spectrum of **5-94**
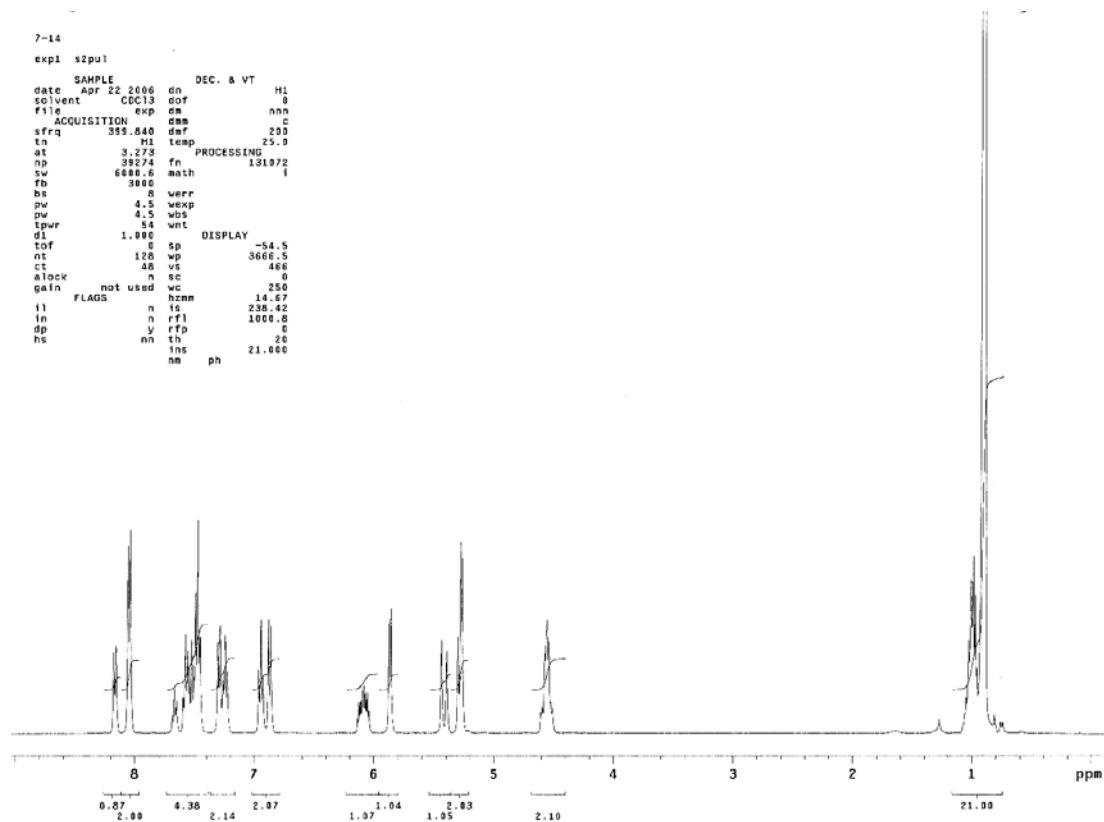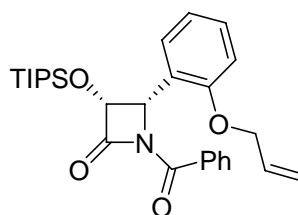
^{13}C NMR Spectrum of **5-94**
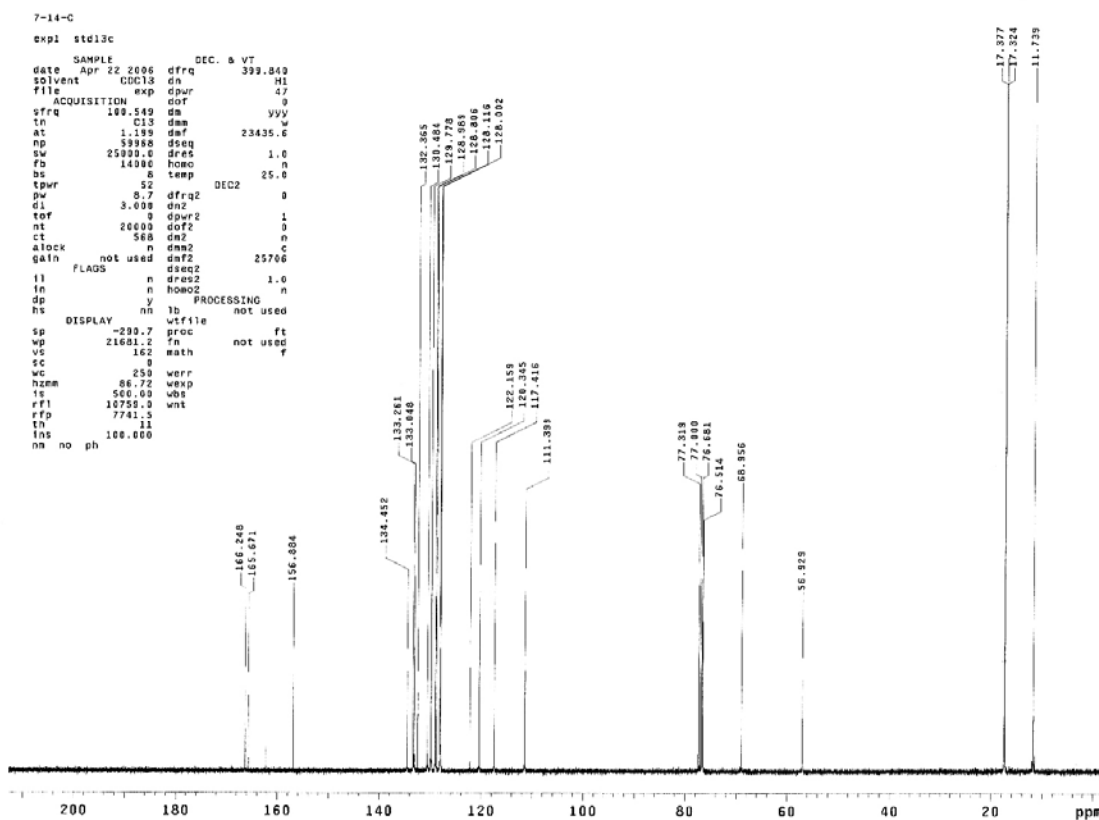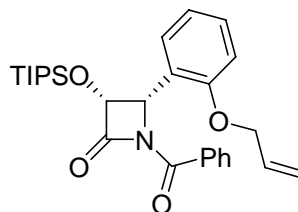
^{1}H NMR Spectrum of **5-96**
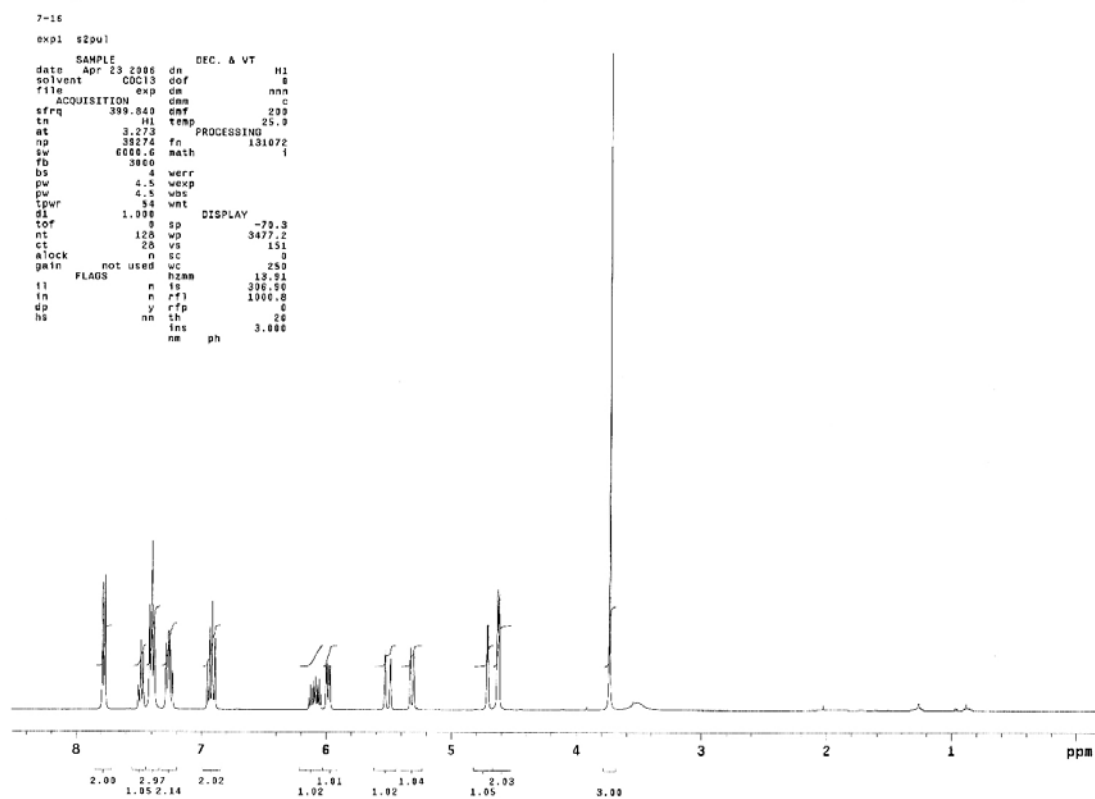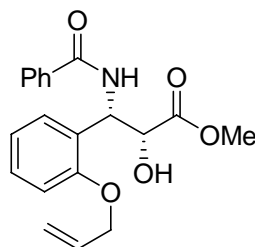
^{13}C NMR Spectrum of **5-96**
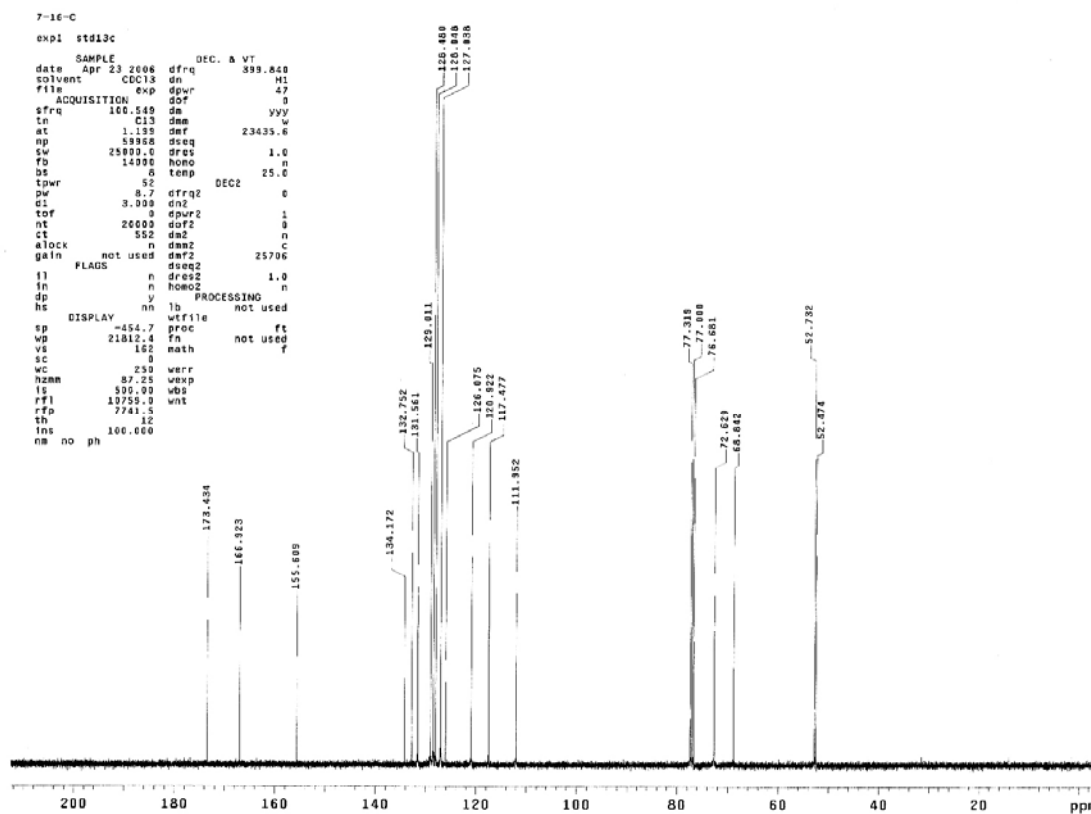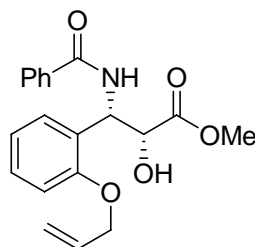
^{1}H NMR Spectrum of **5-97**
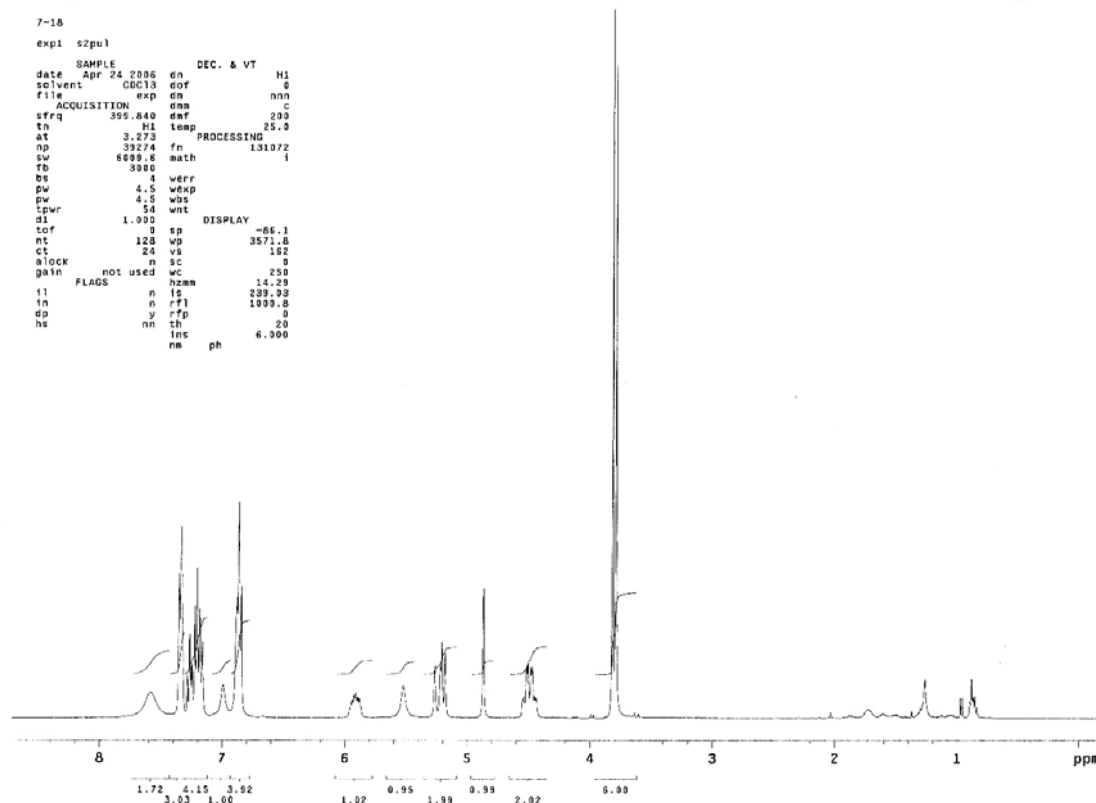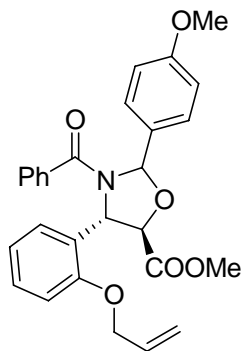
^{13}C NMR Spectrum of 5-97
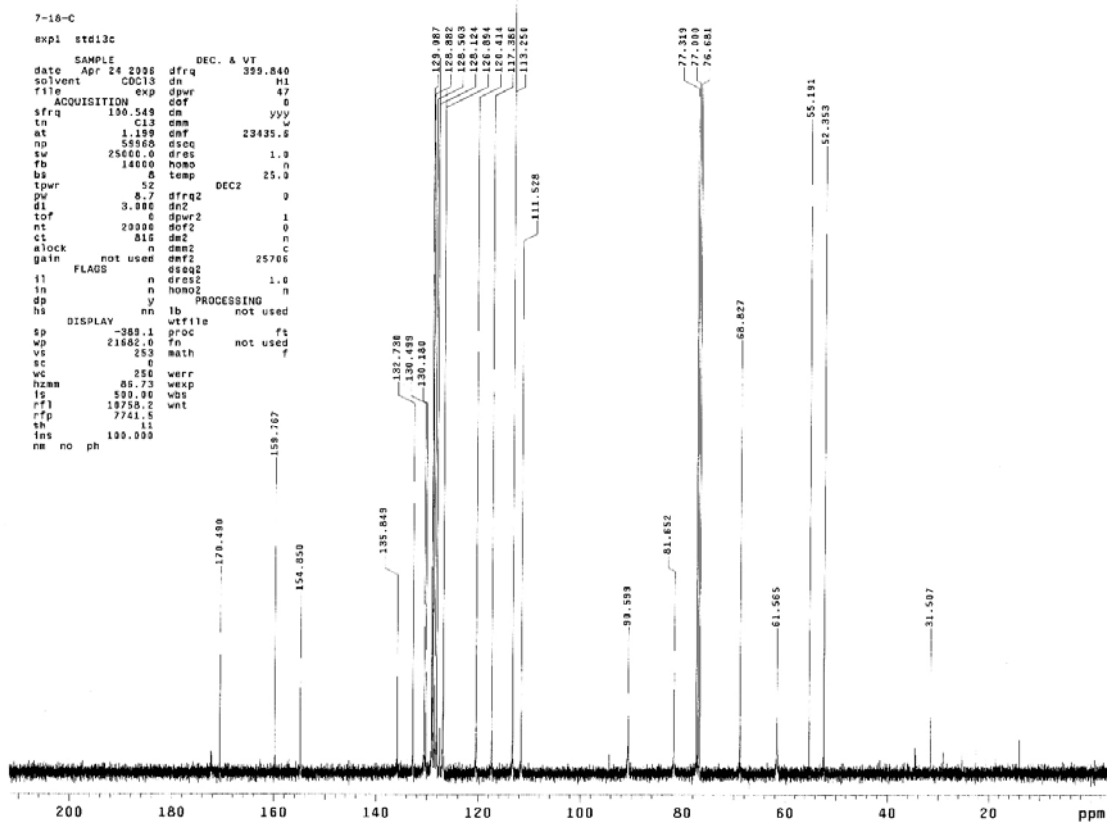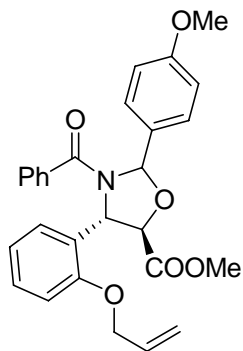
^{1}H NMR Spectrum of **5-98**
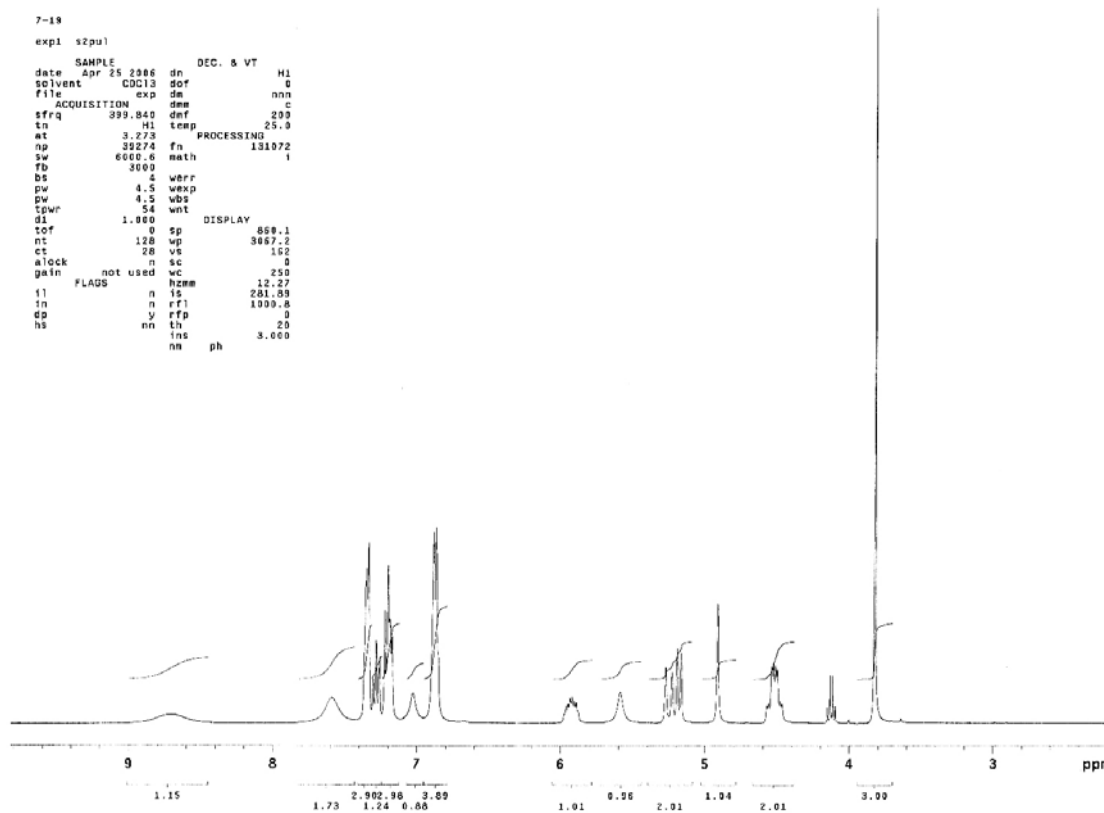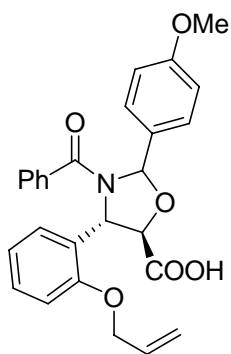
^{13}C NMR Spectrum of **5-98**
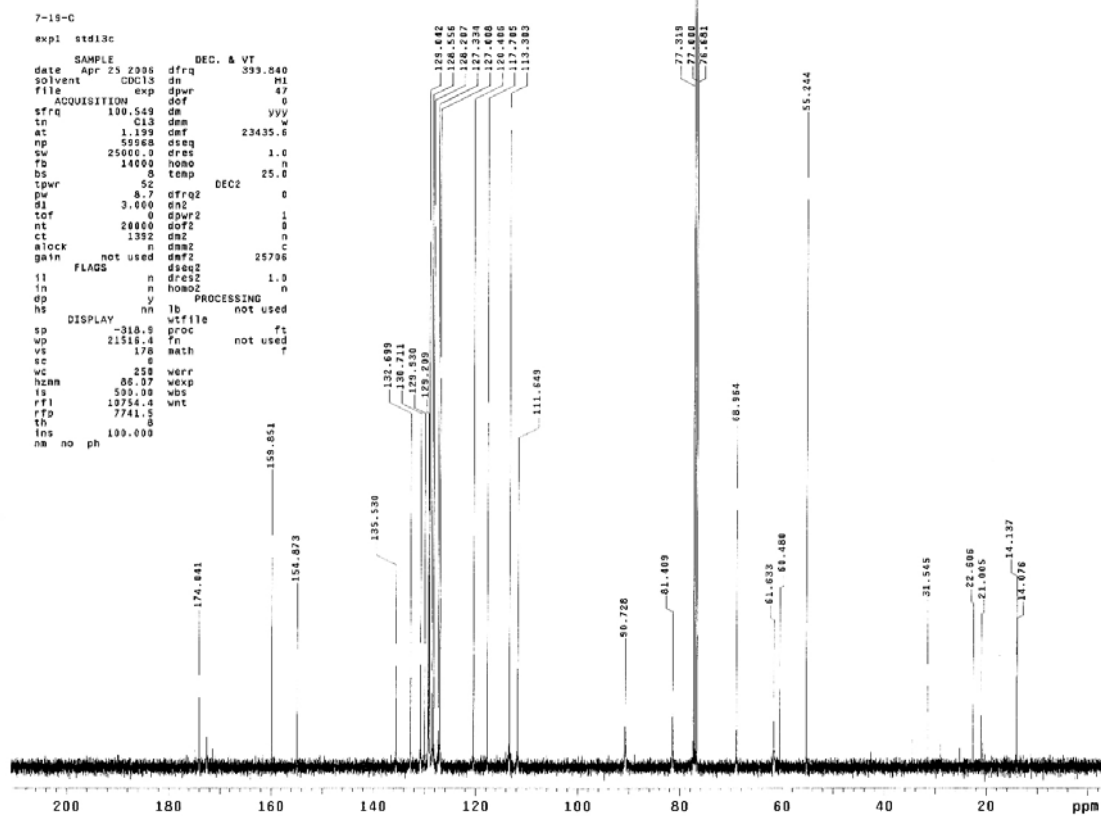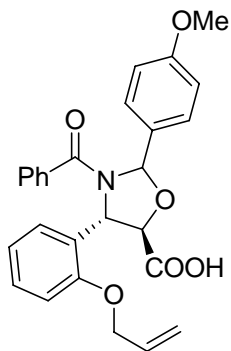
^{1}H NMR Spectrum of **5-99**
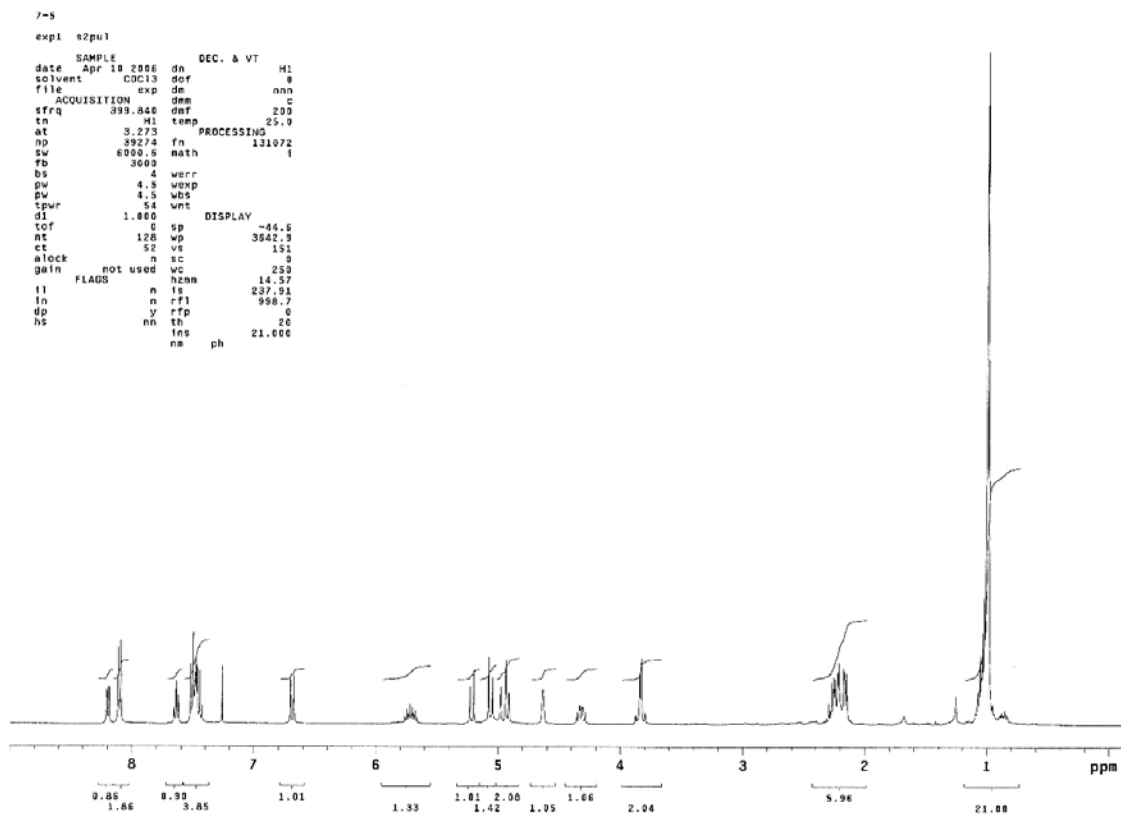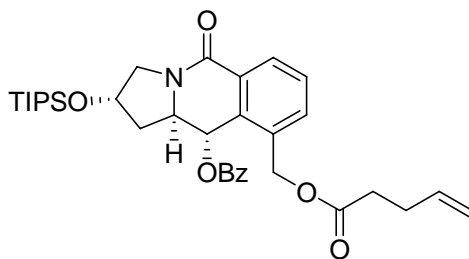
^{13}C NMR Spectrum of **5-99**
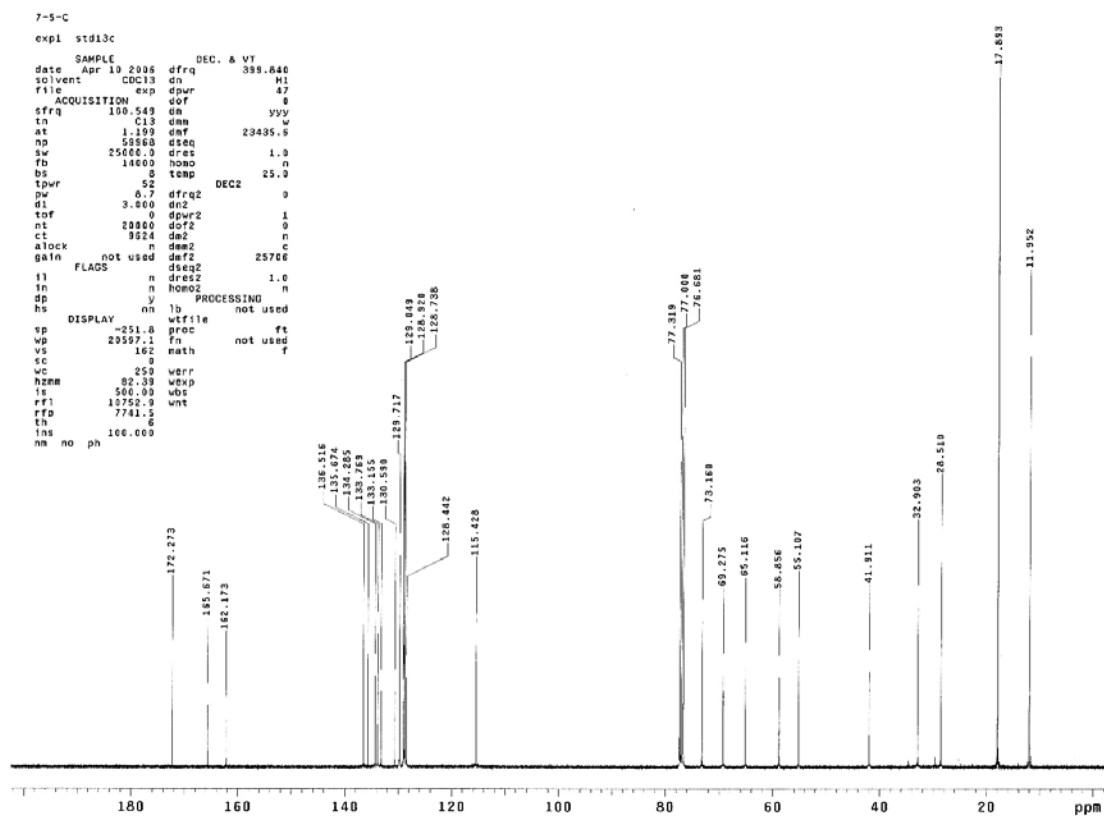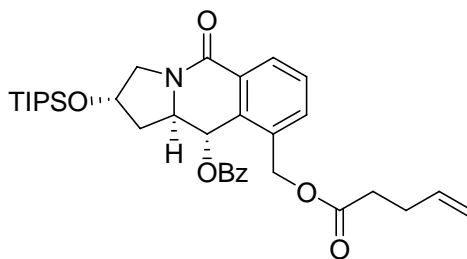
^{1}H NMR Spectrum of **5-100**
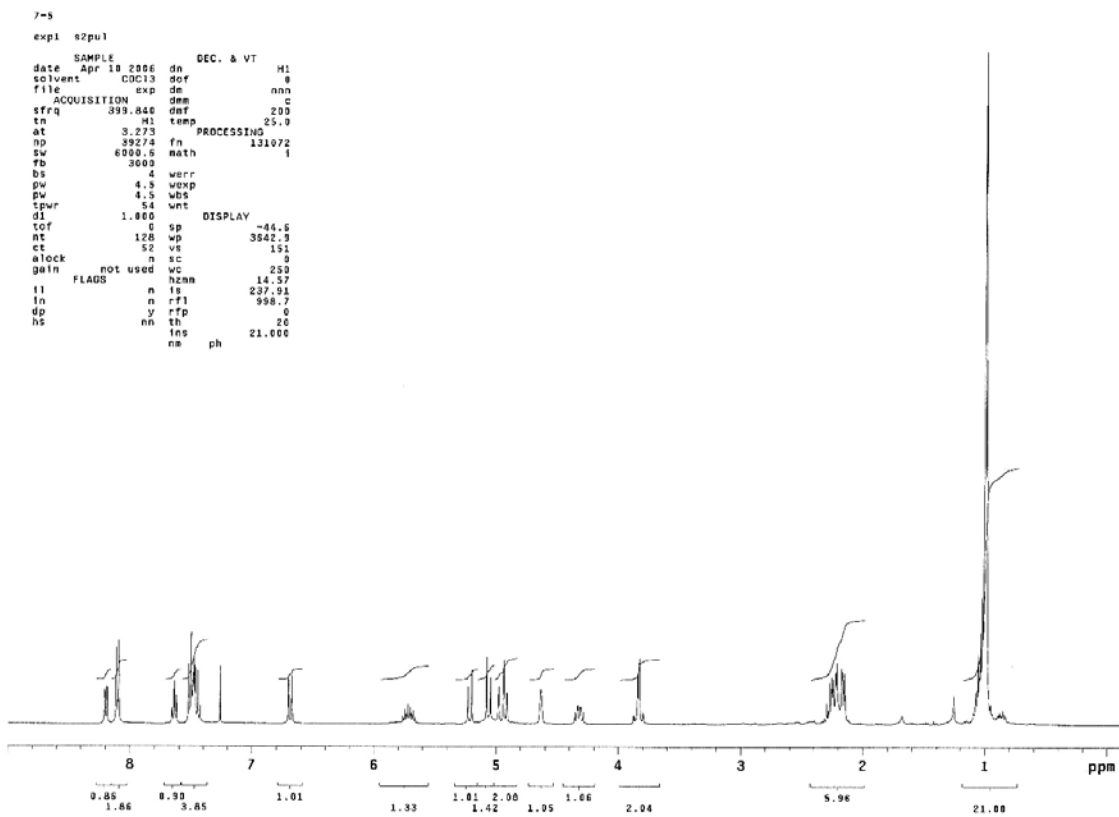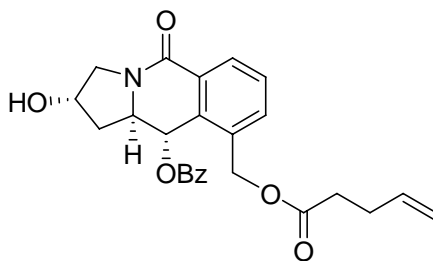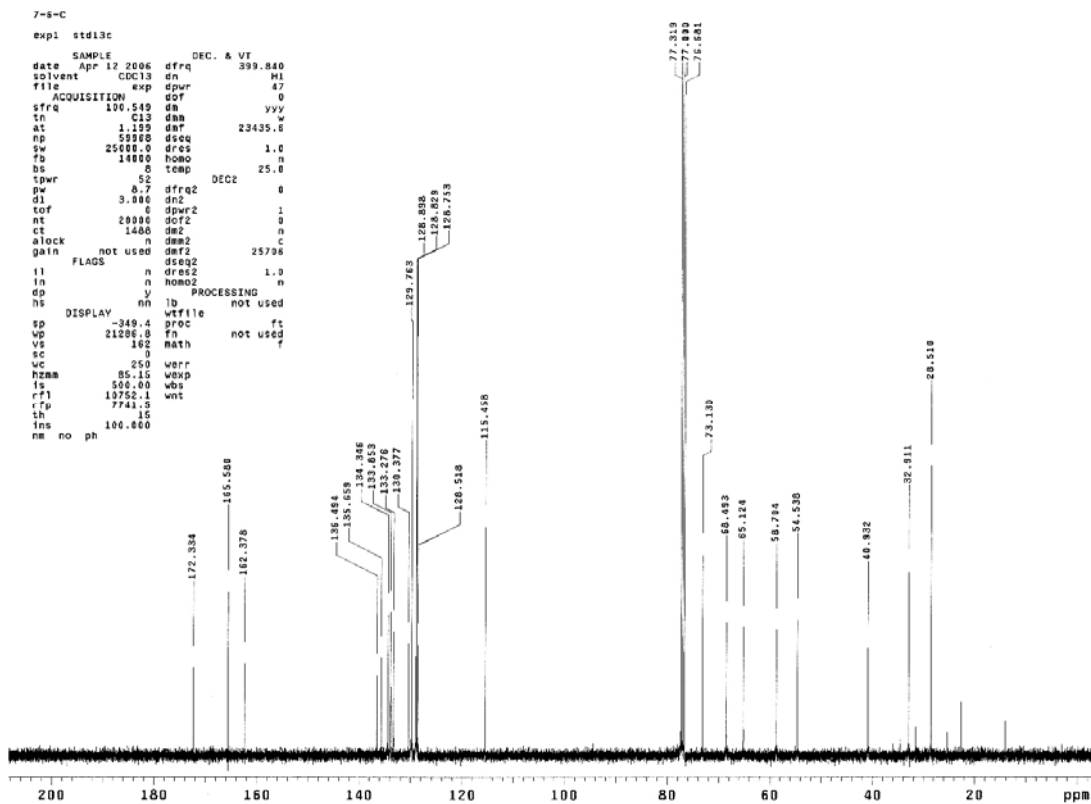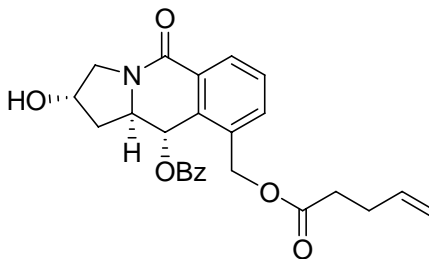
^{1}H NMR Spectrum of **5-101**
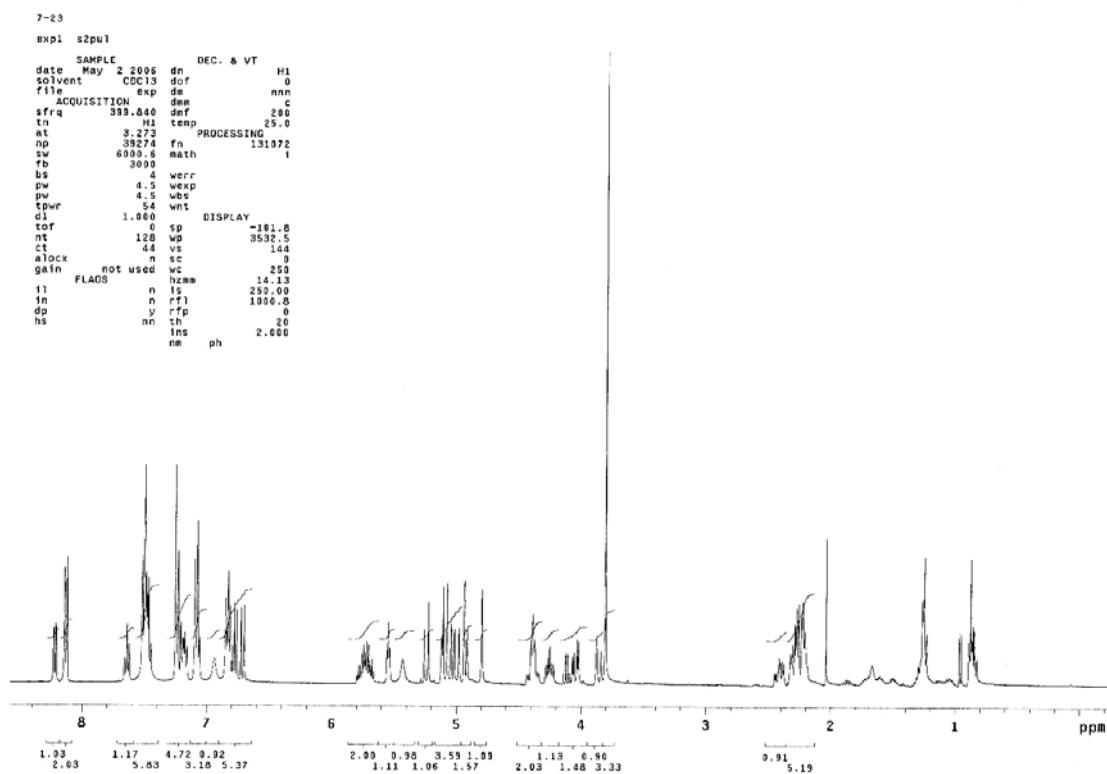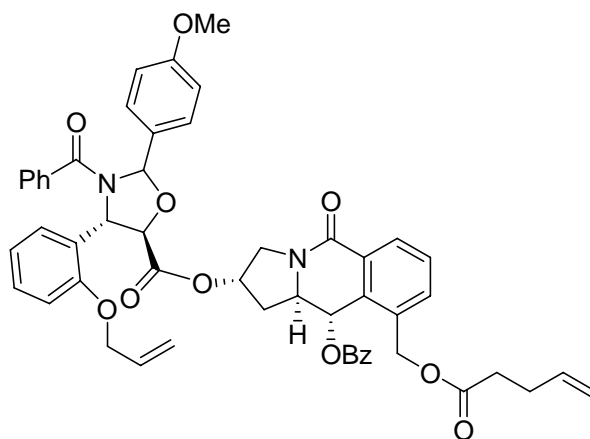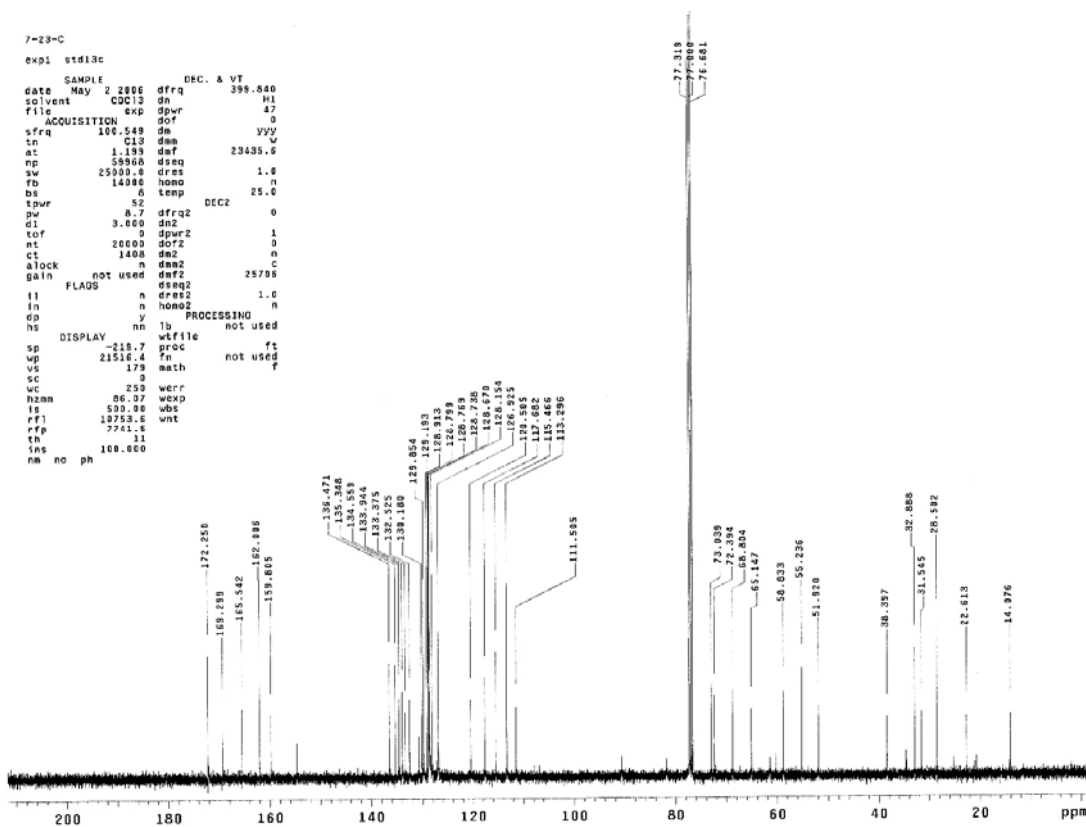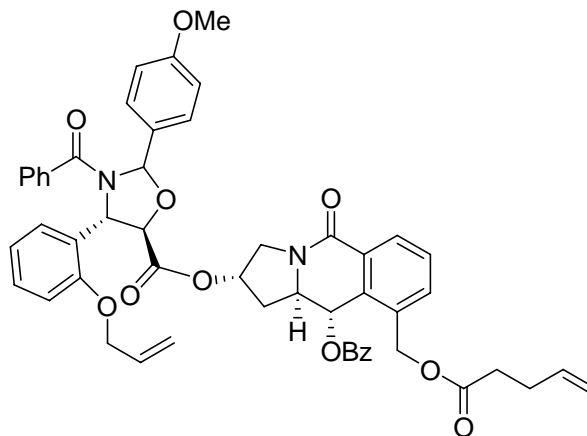
^{1}H NMR Spectrum of **5-102**
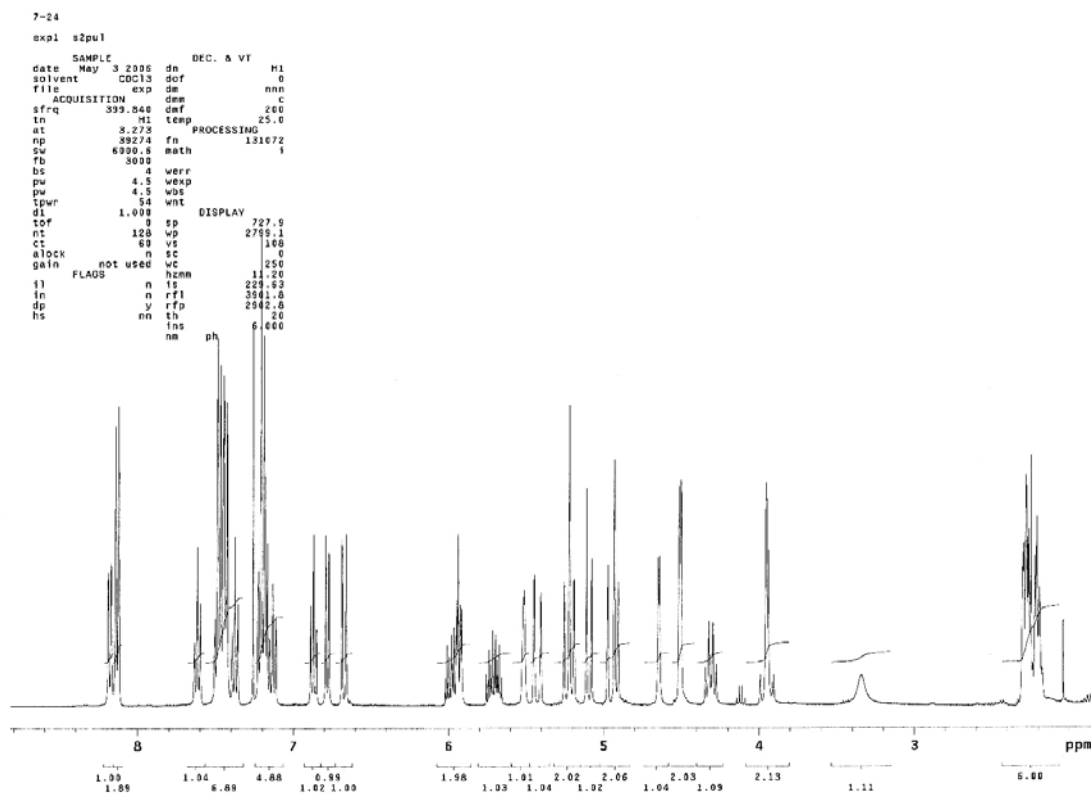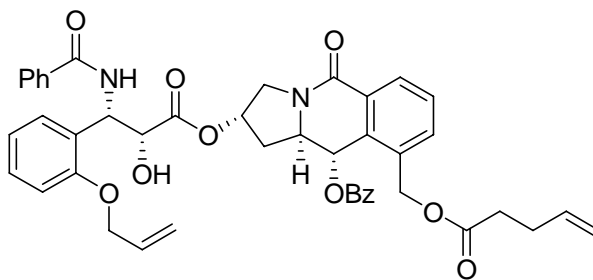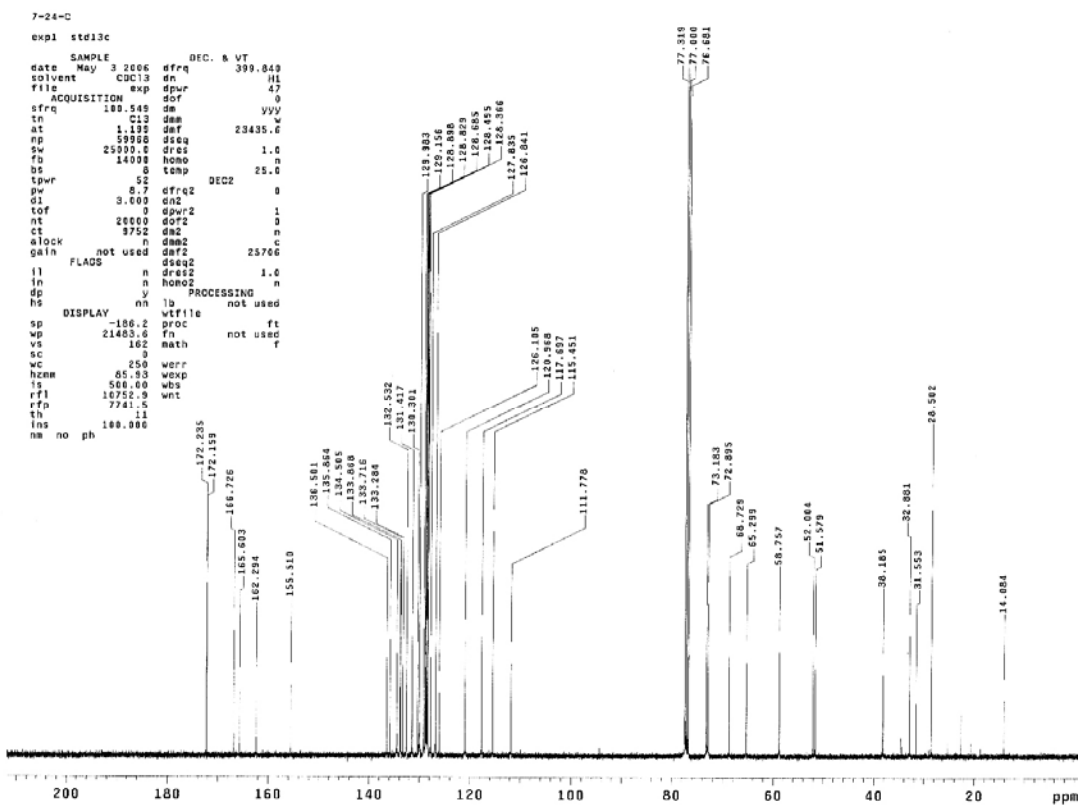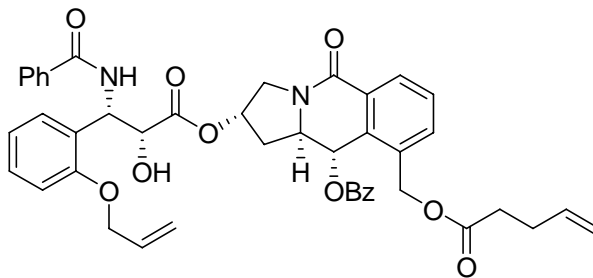
^{1}H NMR Spectrum of **5-36** (**SB-H-2001**)
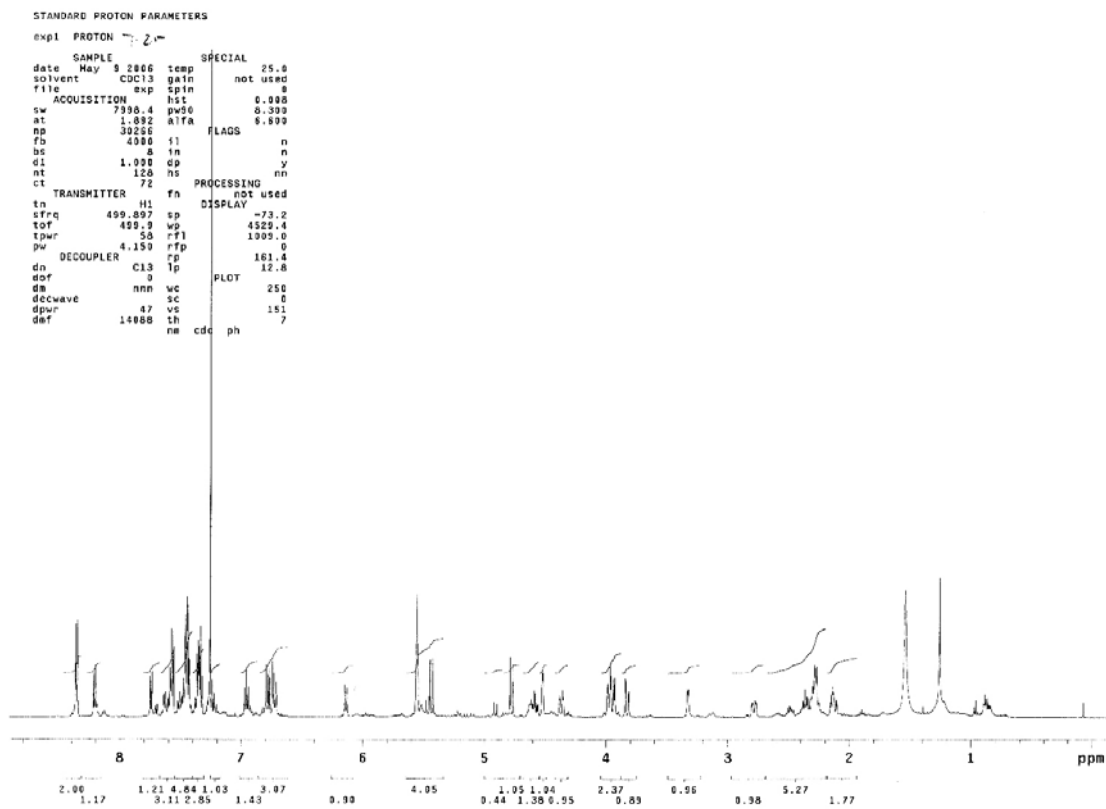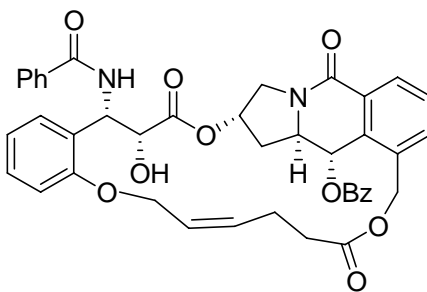
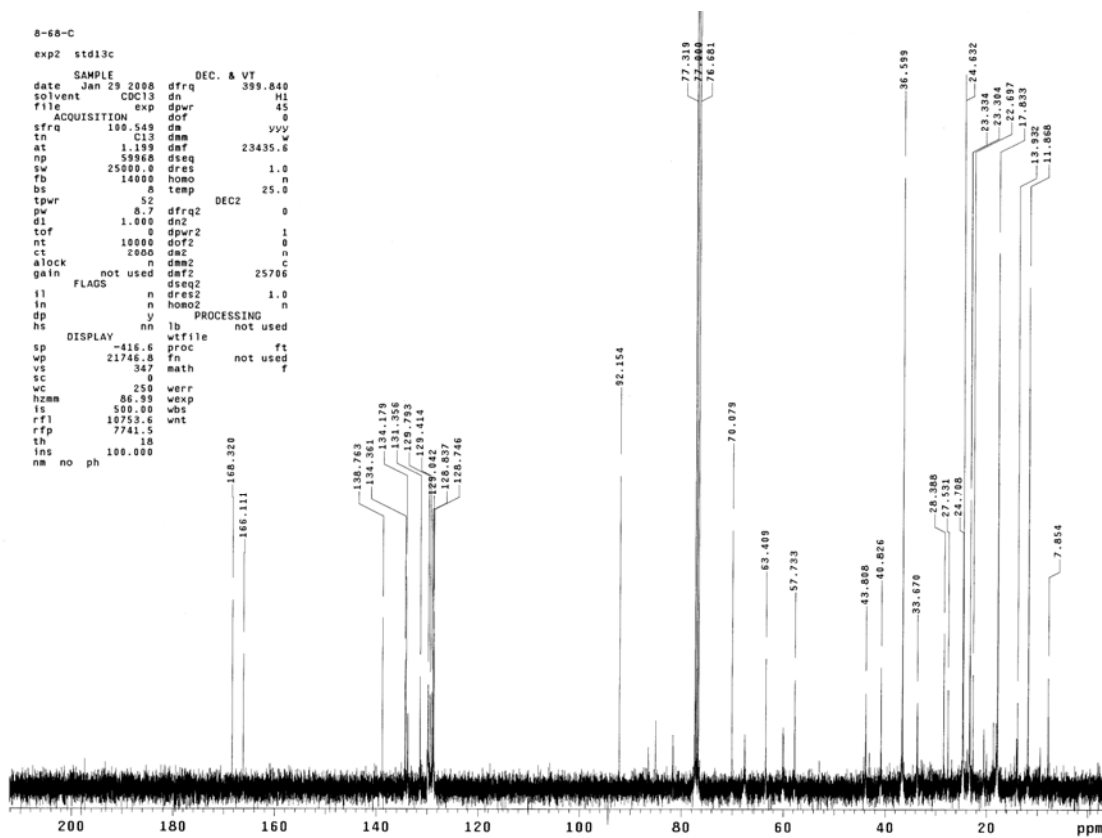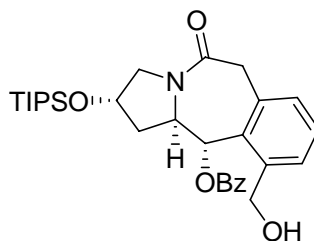# ^{13}C NMR Spectrum of 5-36 (SB-H-2001)
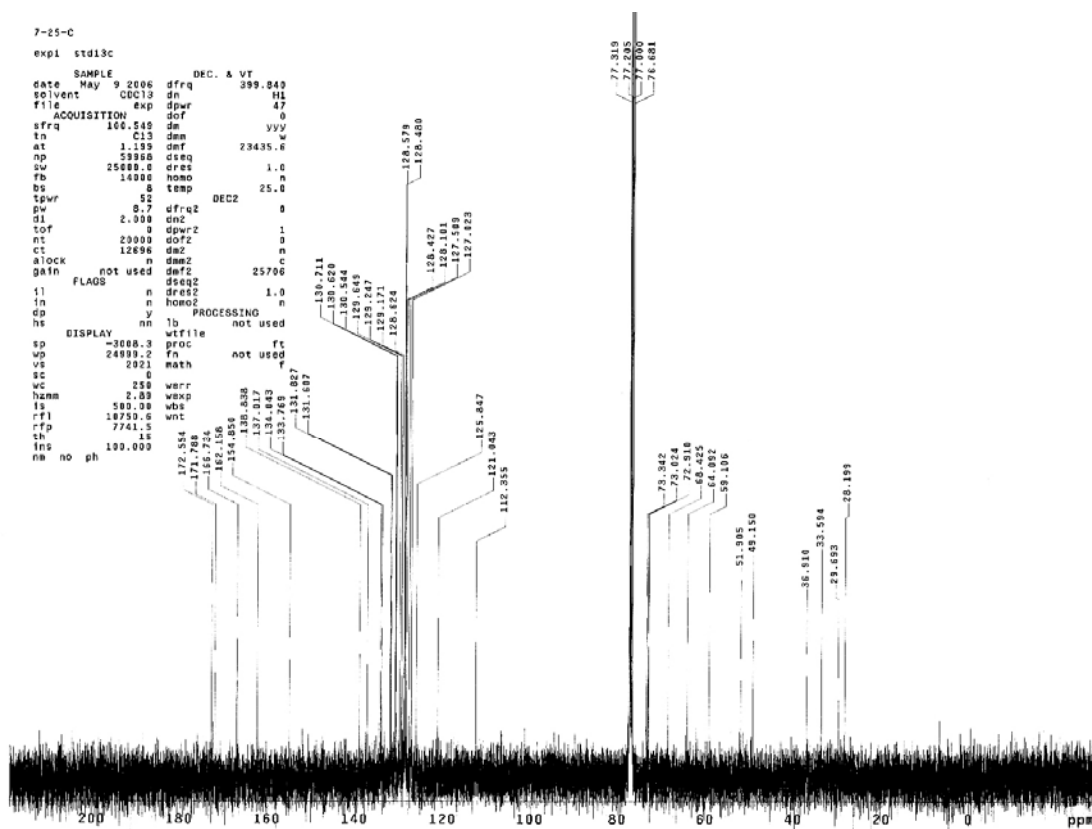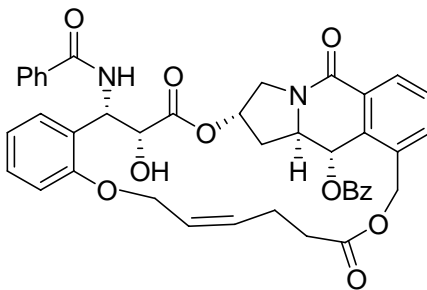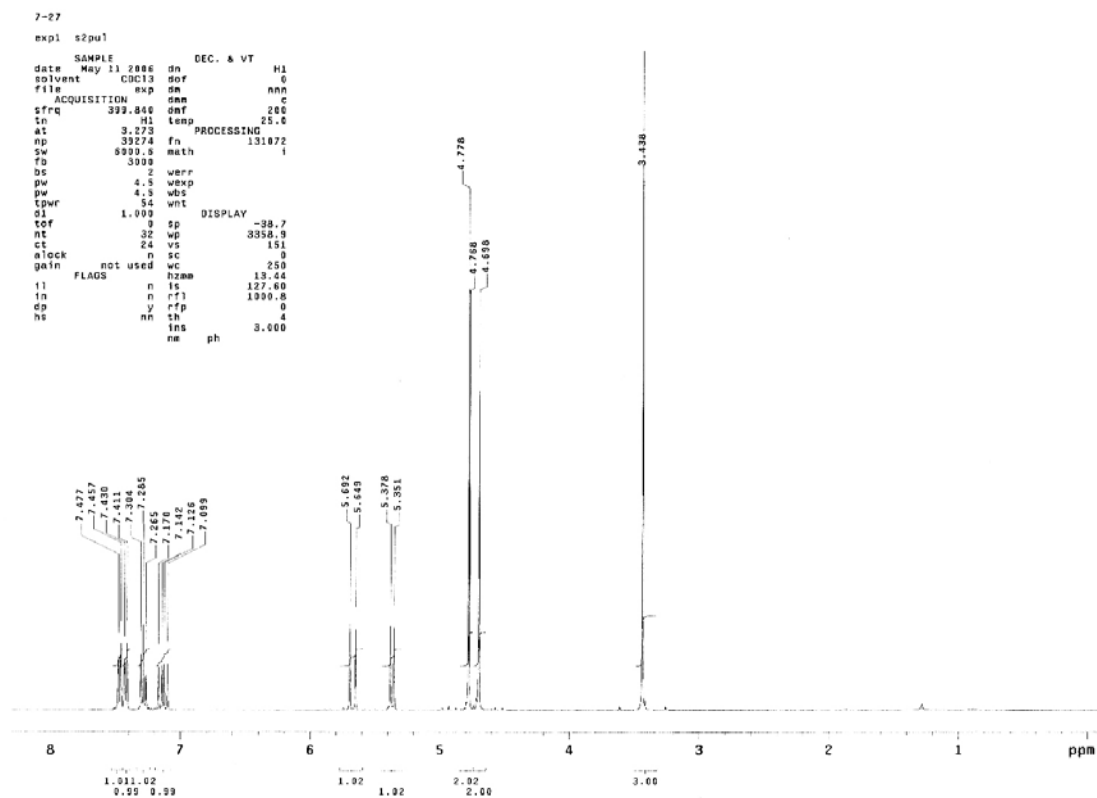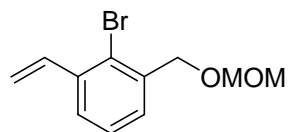
^{1}H NMR Spectrum of **5-104**

^{13}C NMR Spectrum of 5-104

^{1}H NMR Spectrum of **5-105**
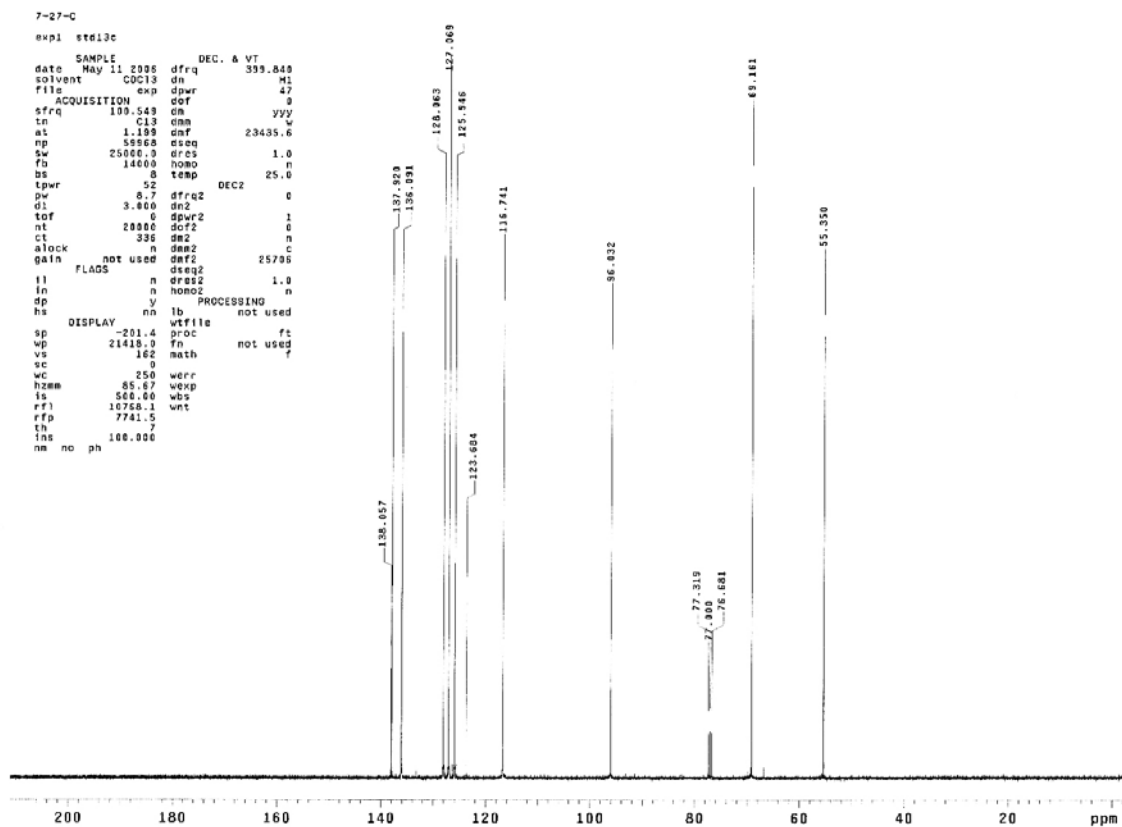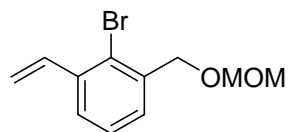
^{13}C NMR Spectrum of **5-105**
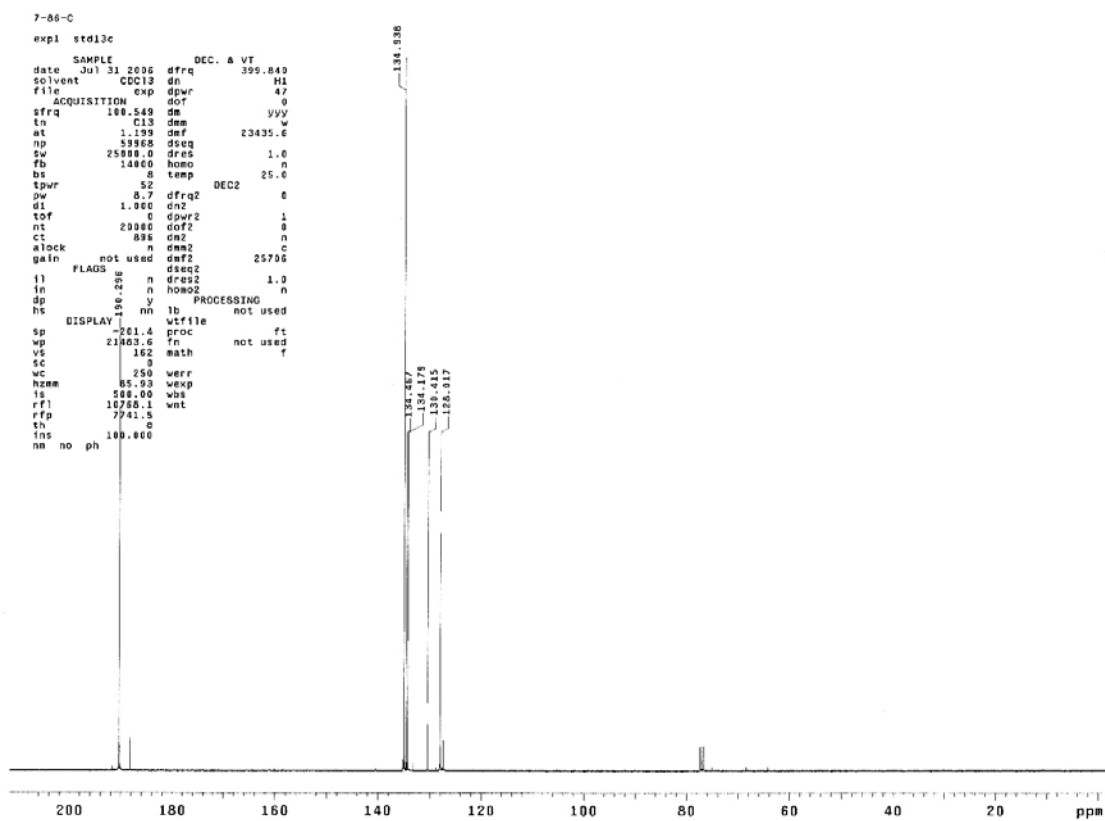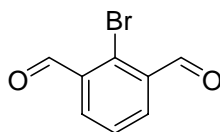
^{1}H NMR Spectrum of **5-106**
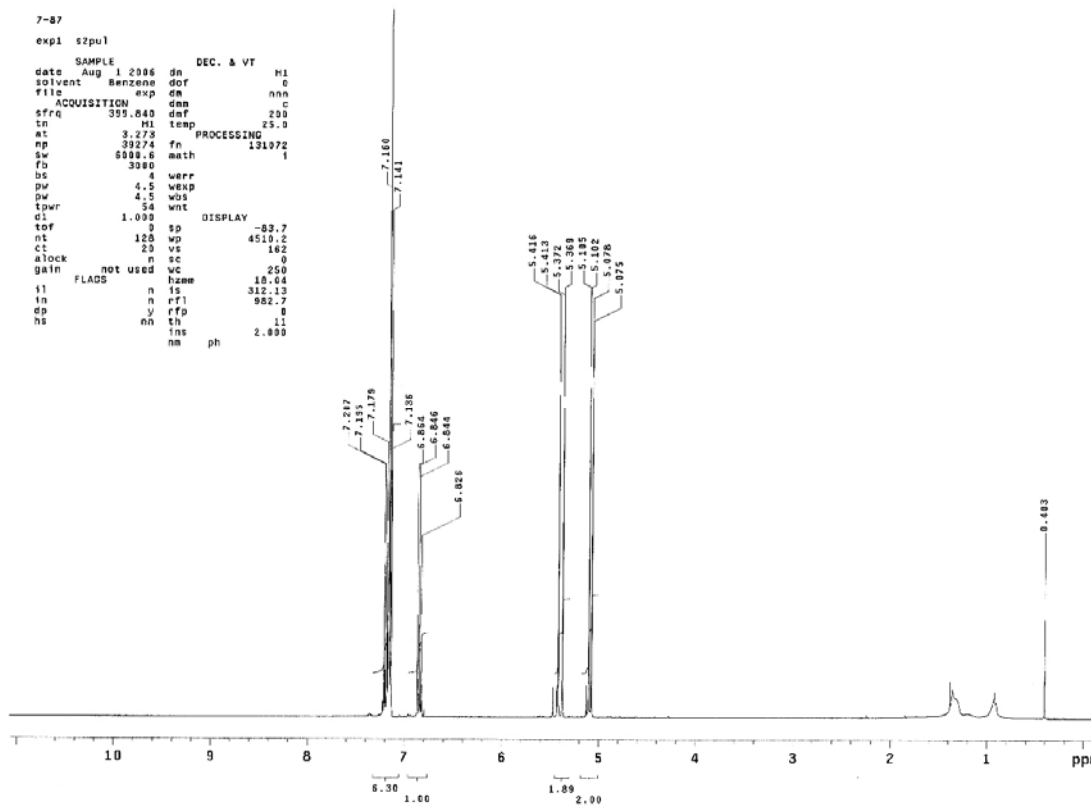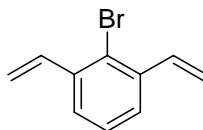
^{13}C NMR Spectrum of **5-106**
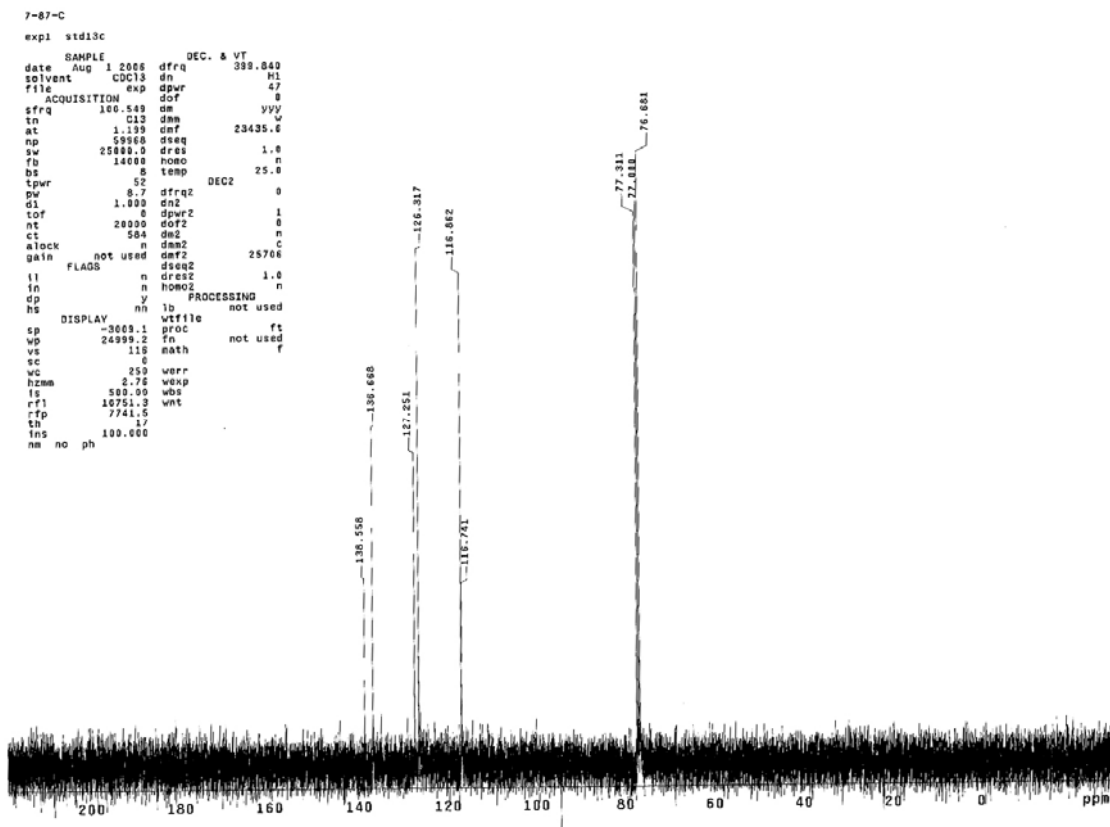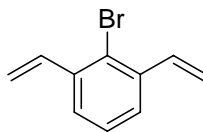
^{1}H NMR Spectrum of **5-108**
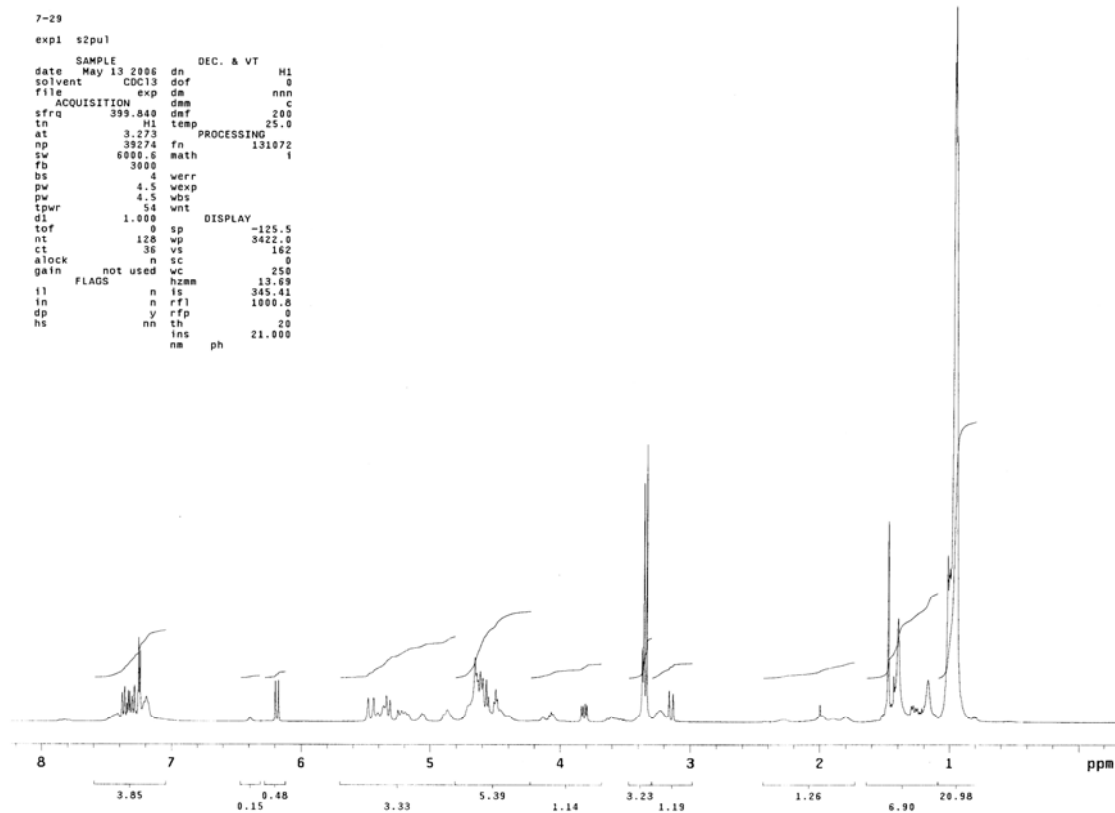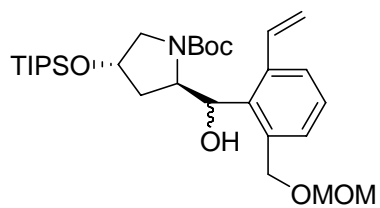
^{13}C NMR Spectrum of **5-108**
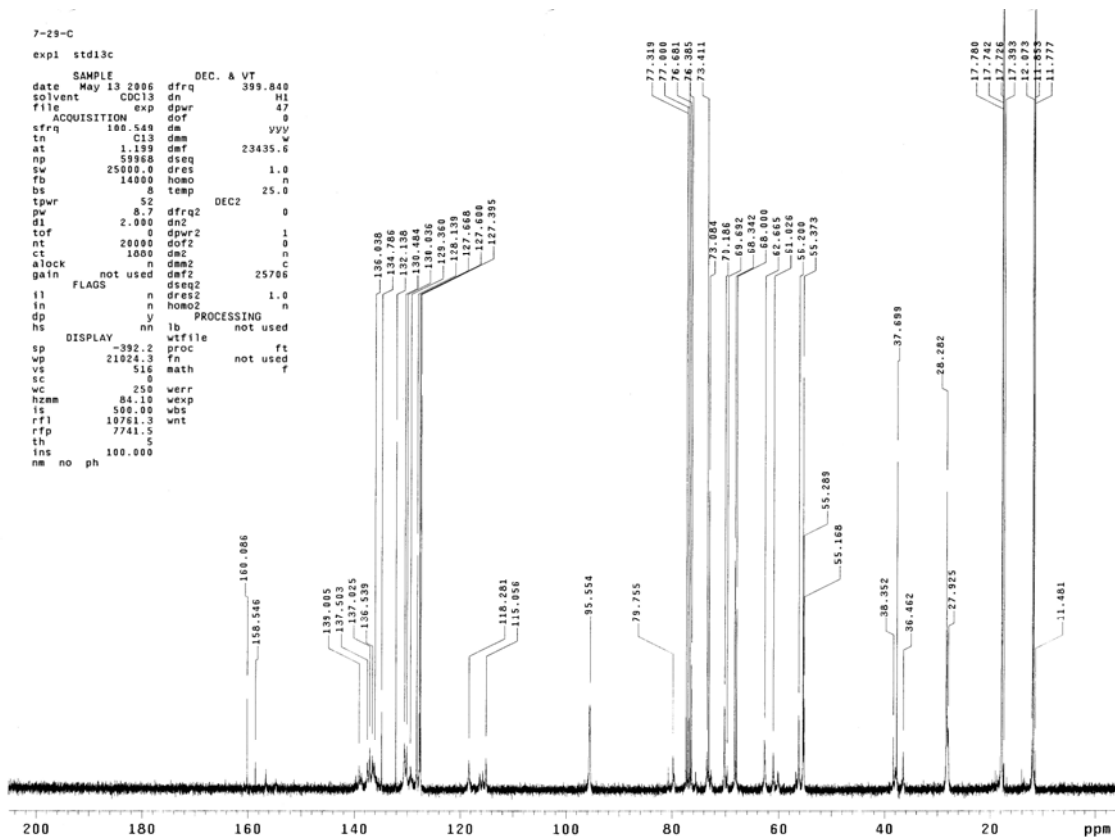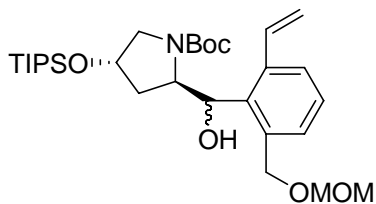
^{1}H NMR Spectrum of **5-109**
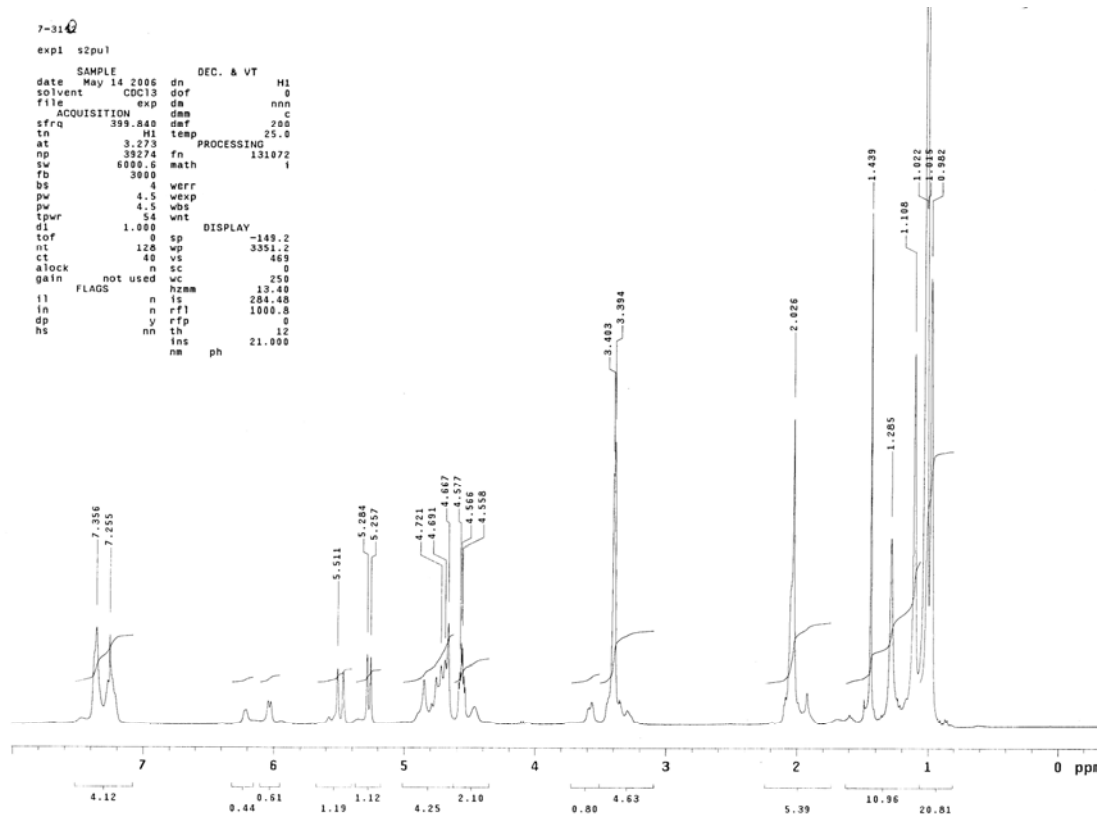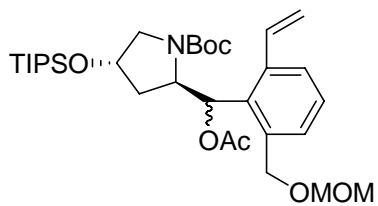
¹³C NMR Spectrum of **5-109**
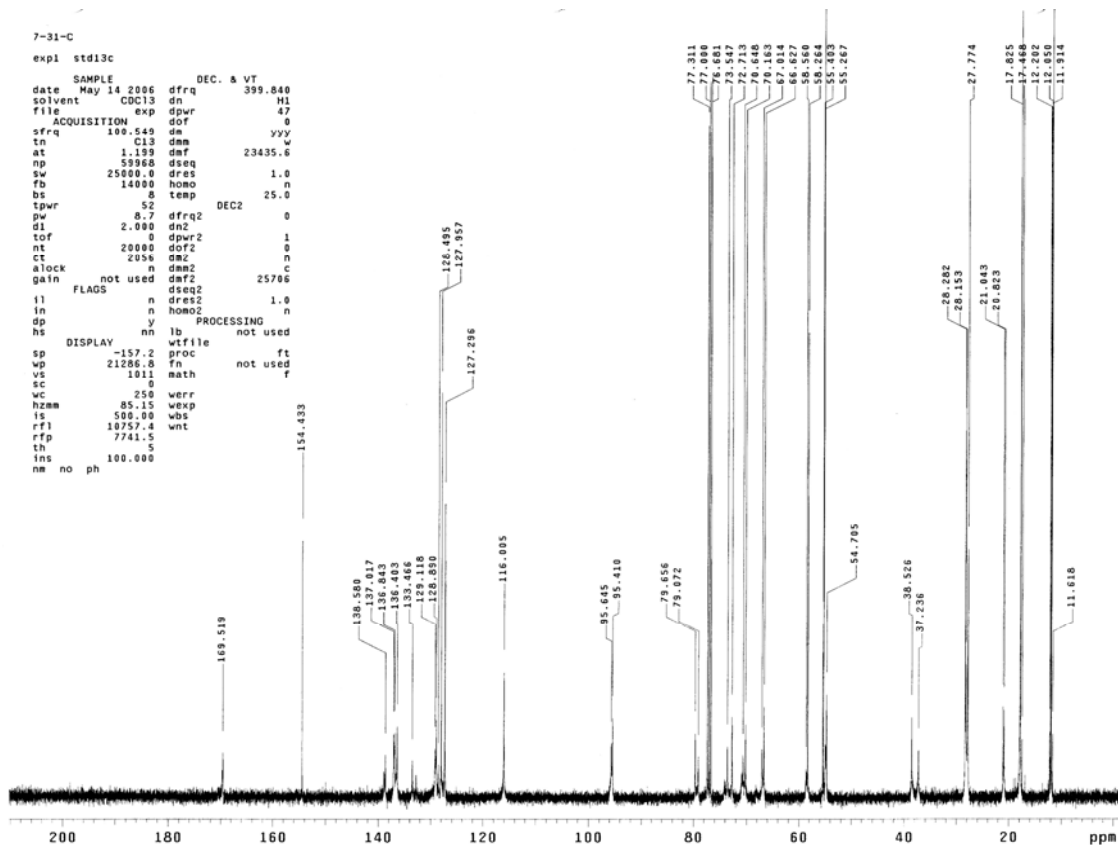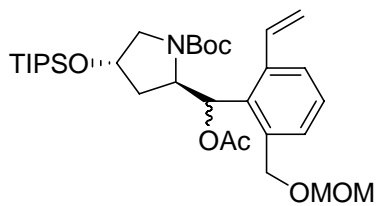
^{13}C NMR Spectrum of **5-117**
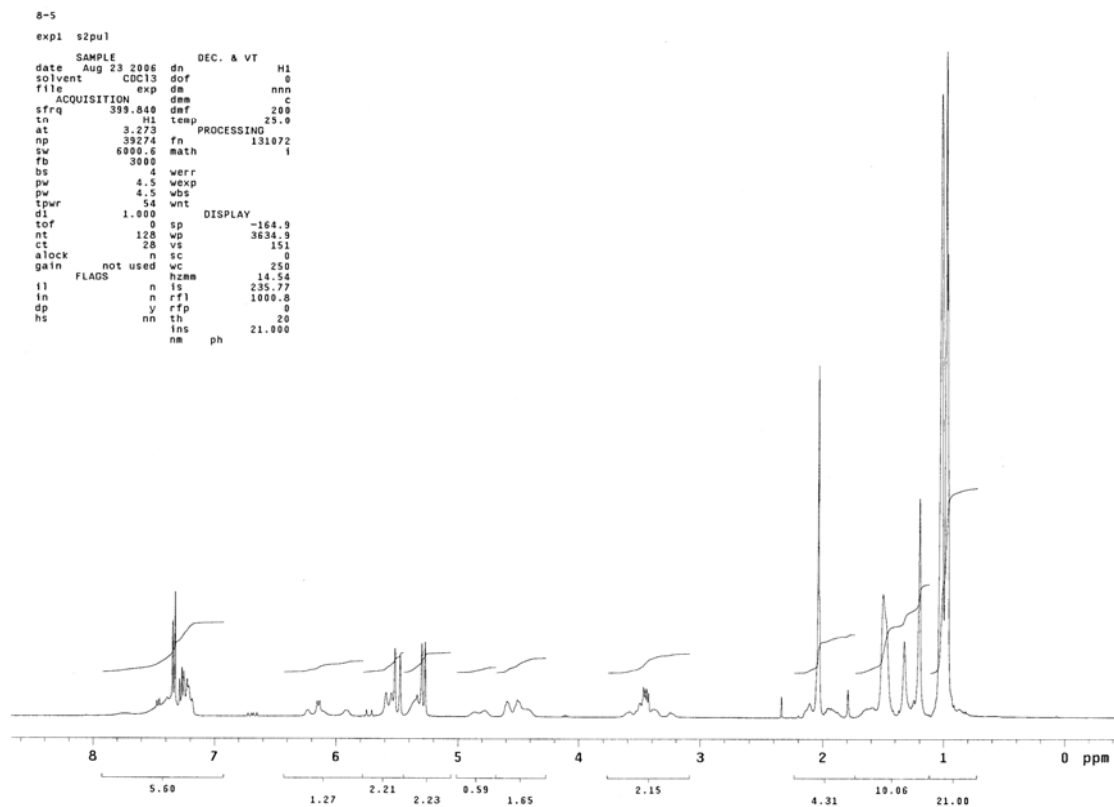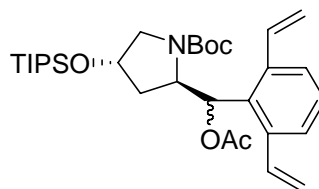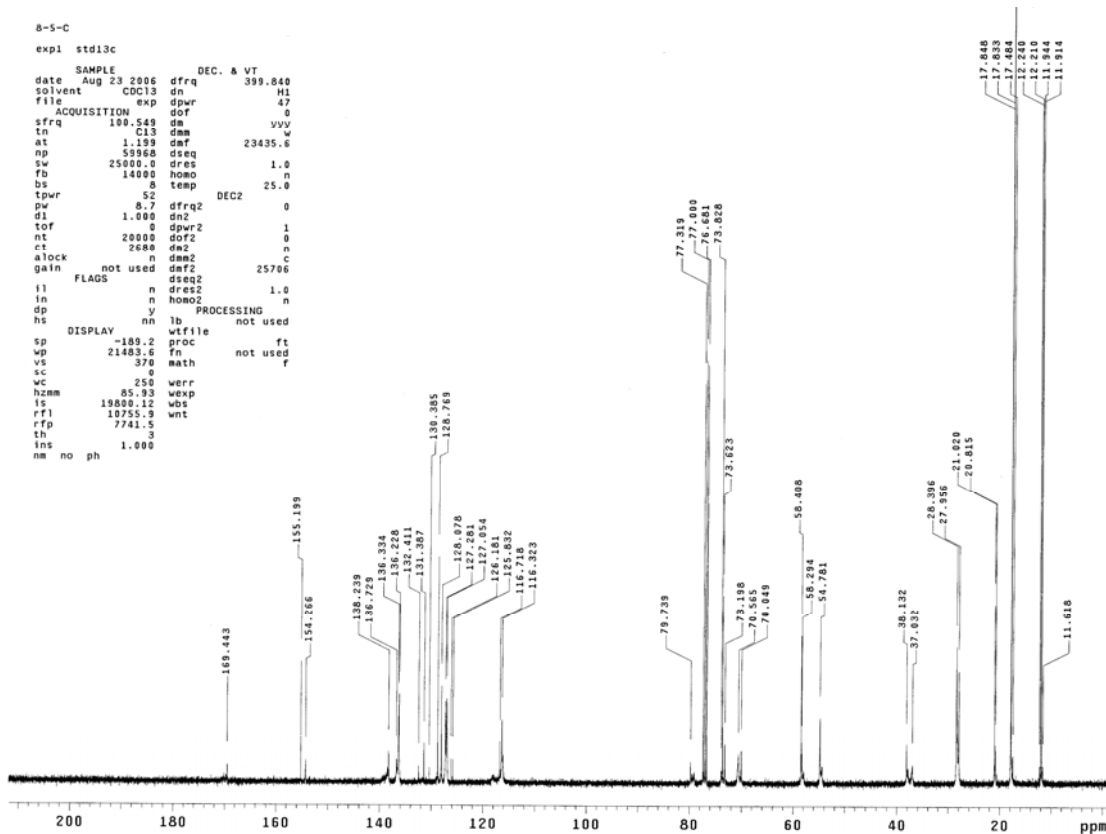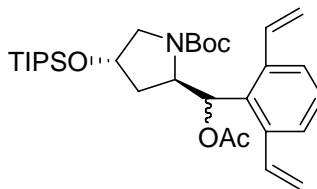
^{1}H NMR Spectrum of **5-121**
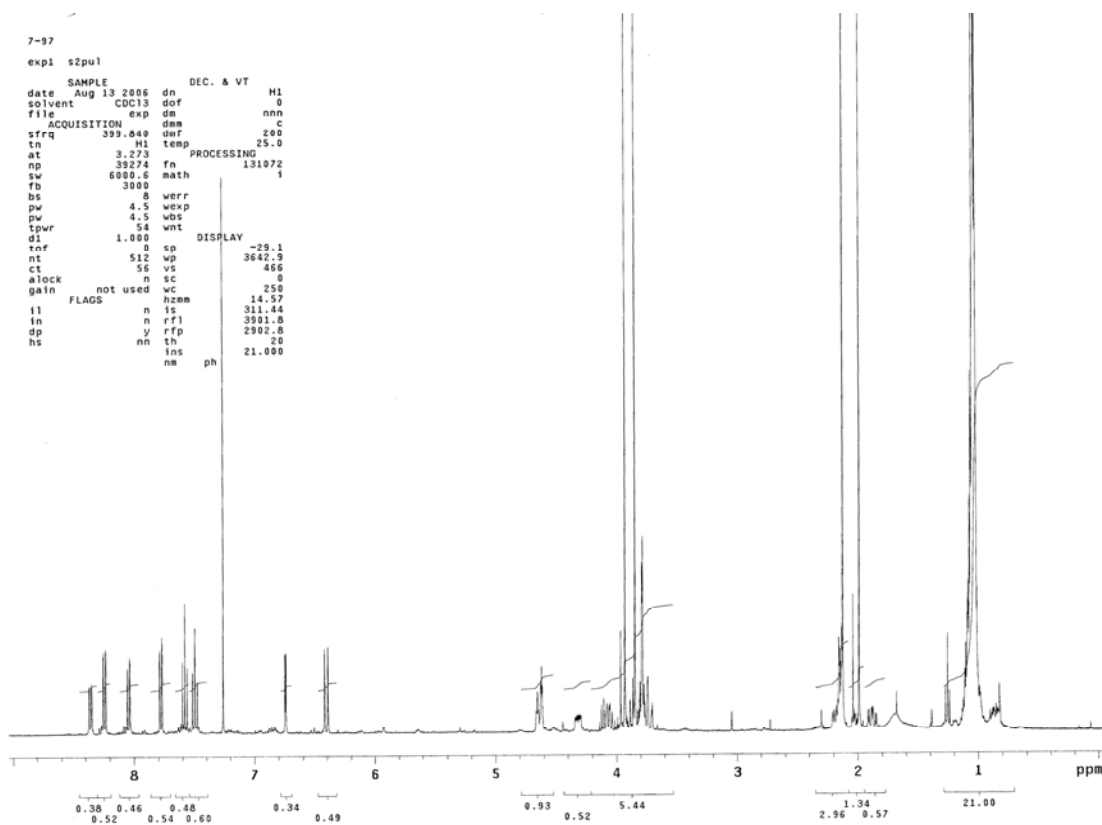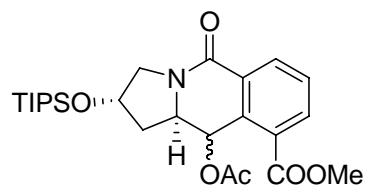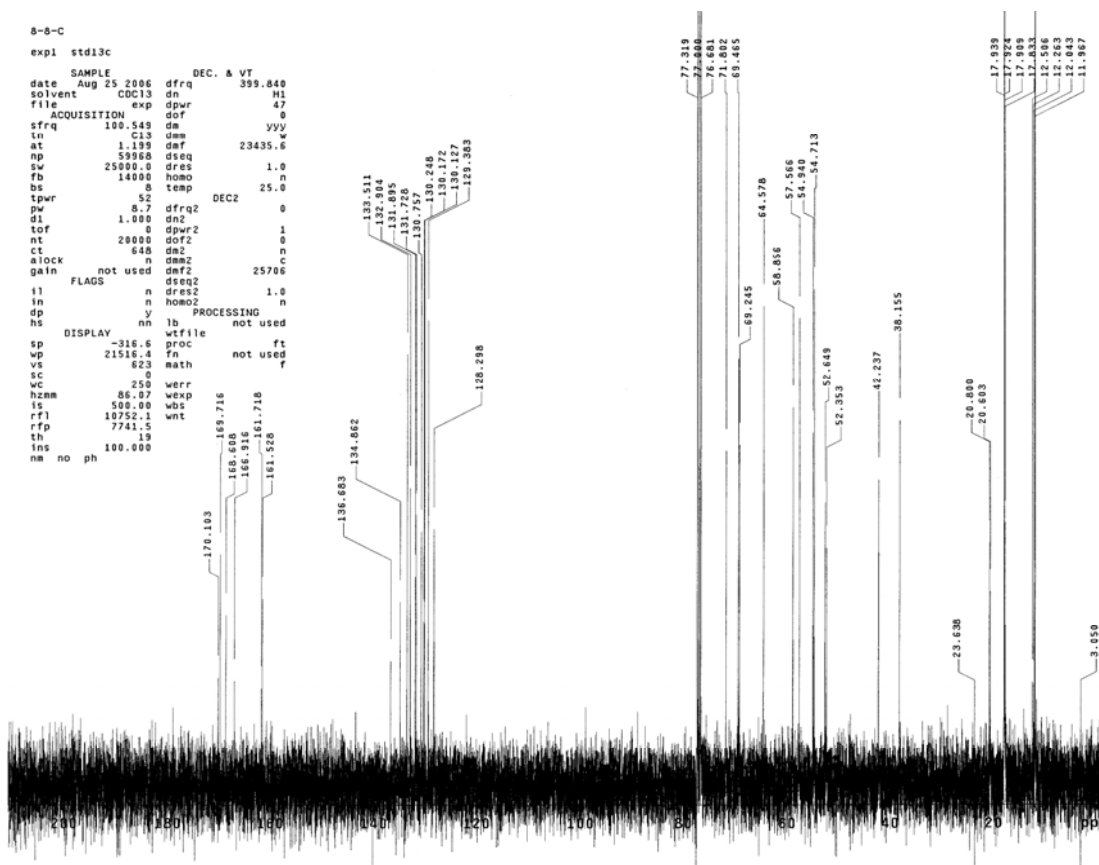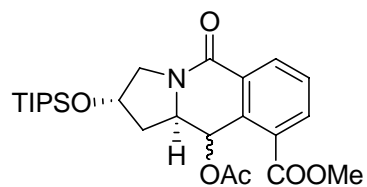
^{1}H NMR Spectrum of **5-122**
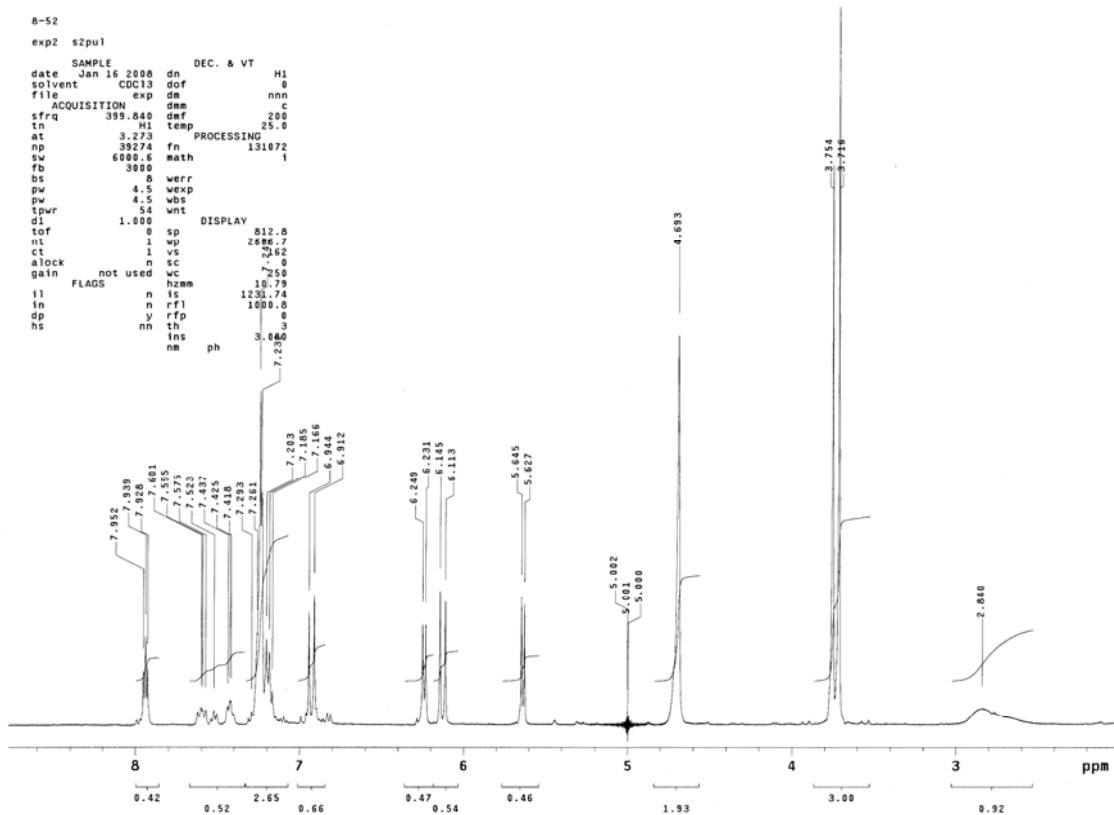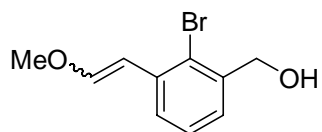
^{13}C NMR Spectrum of **5-122**
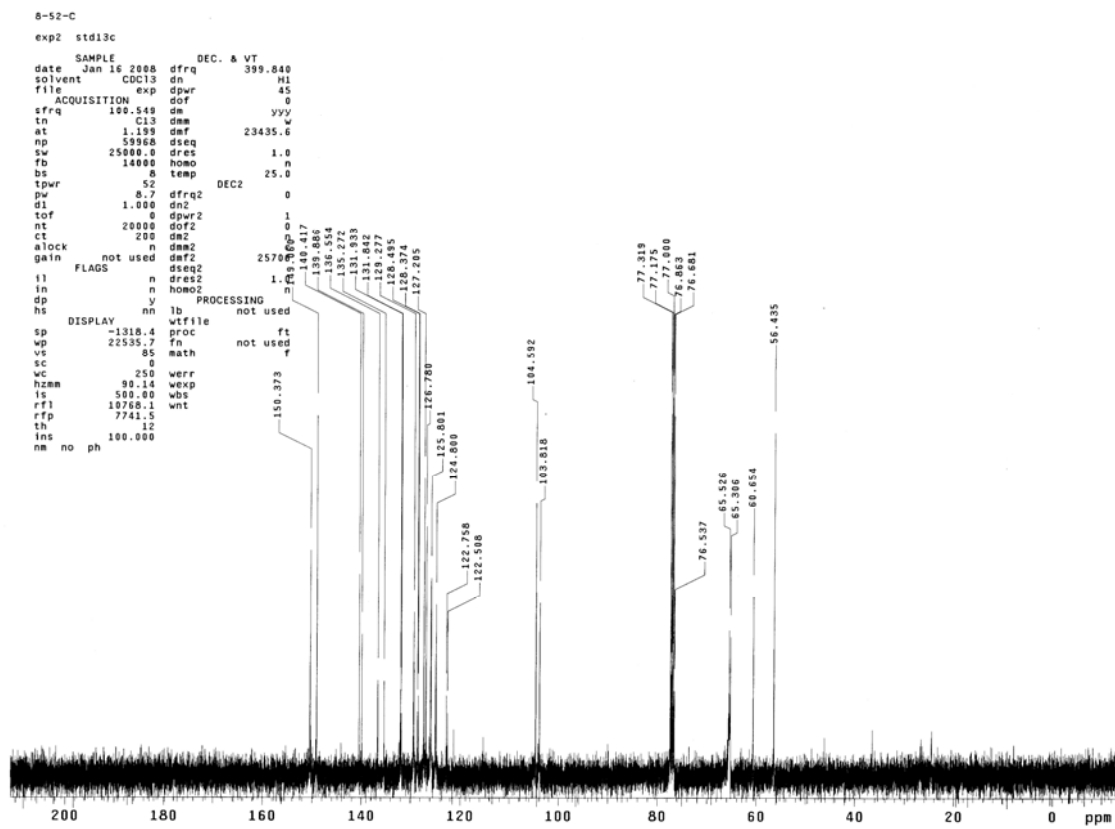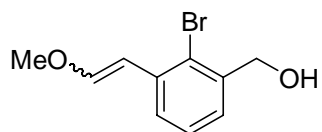
^{1}H NMR Spectrum of **5-123**
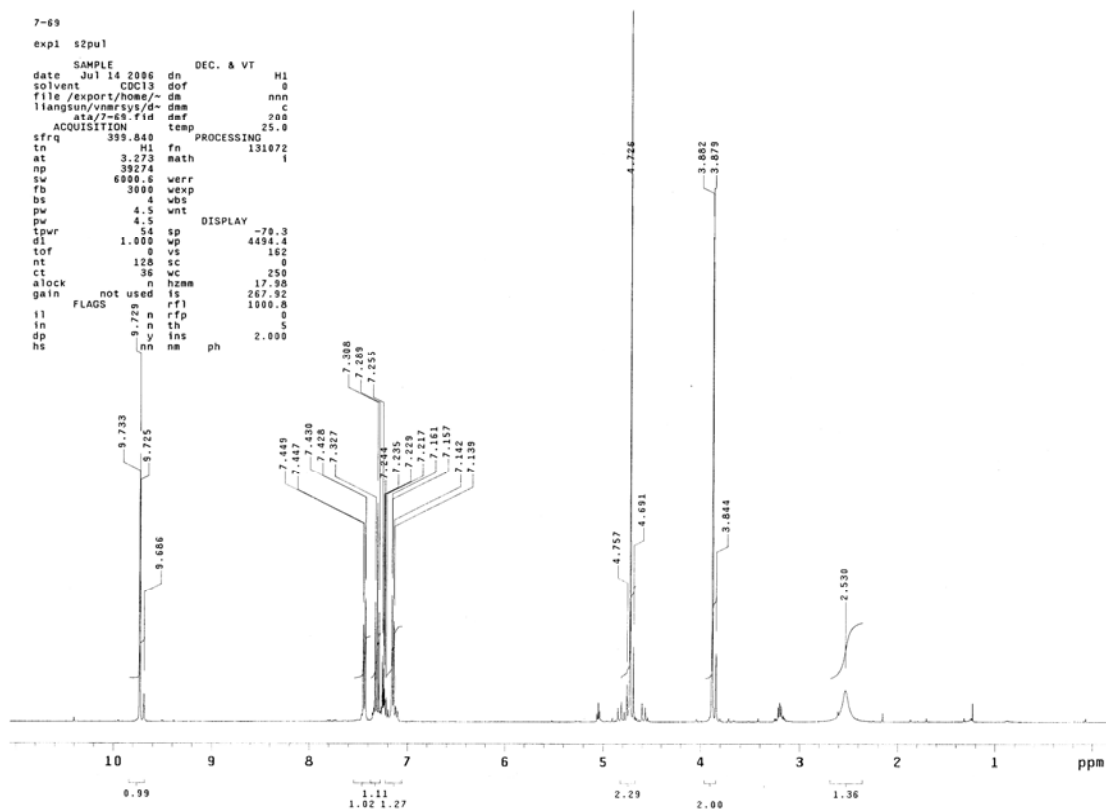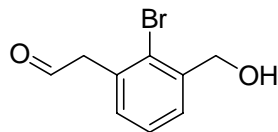
^{13}C NMR Spectrum of **5-123**
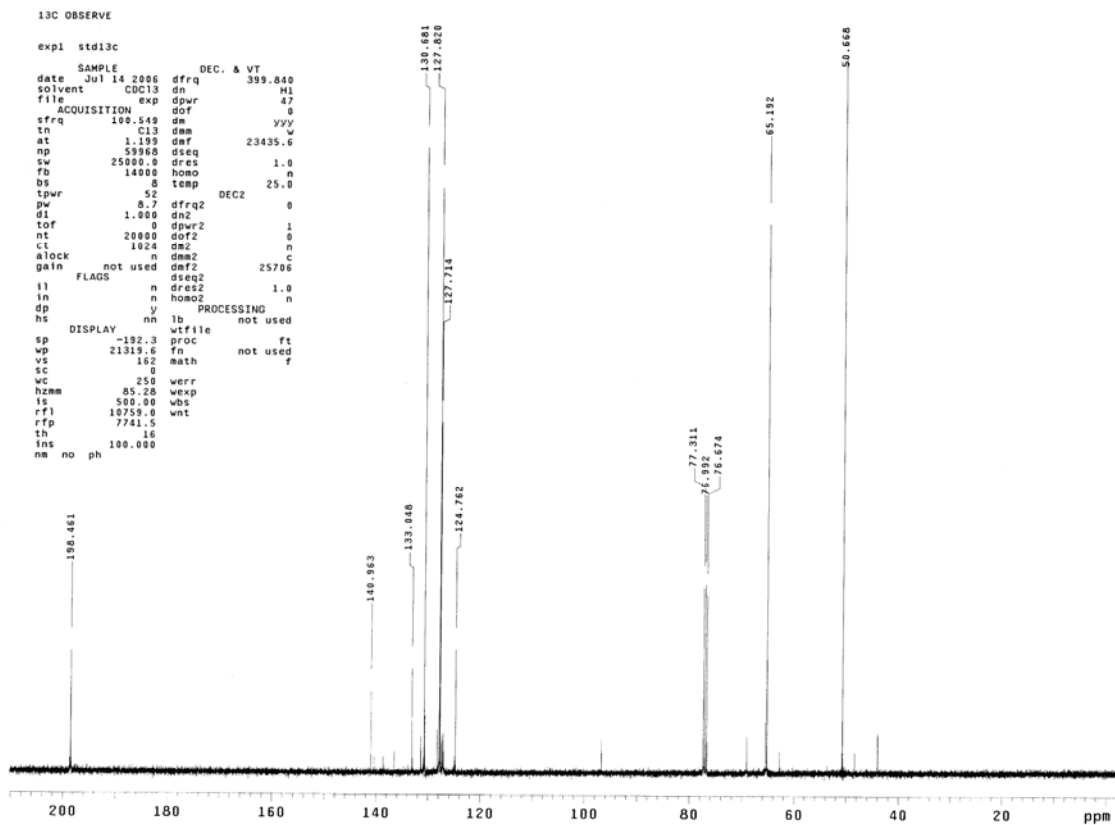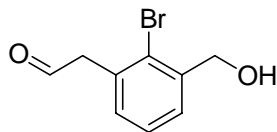
^{1}H NMR Spectrum of **5-124**
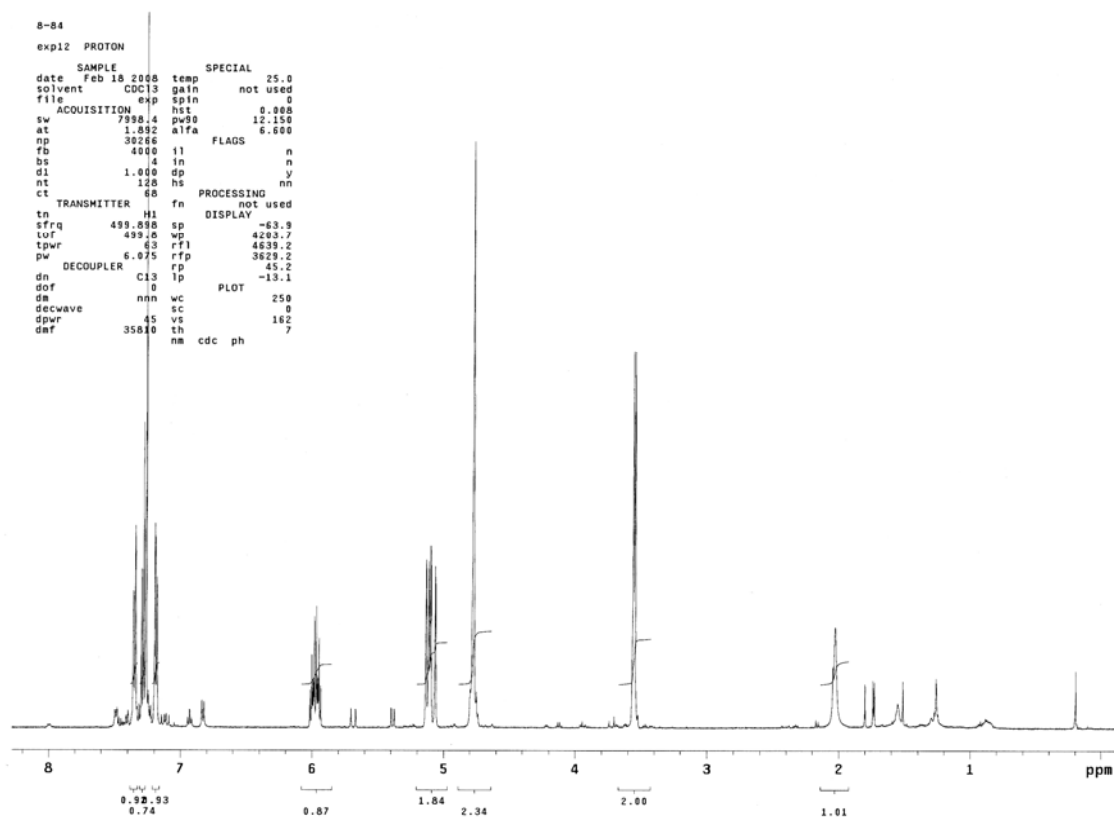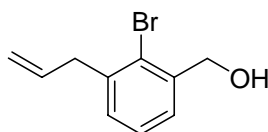
^{13}C NMR Spectrum of **5-124**
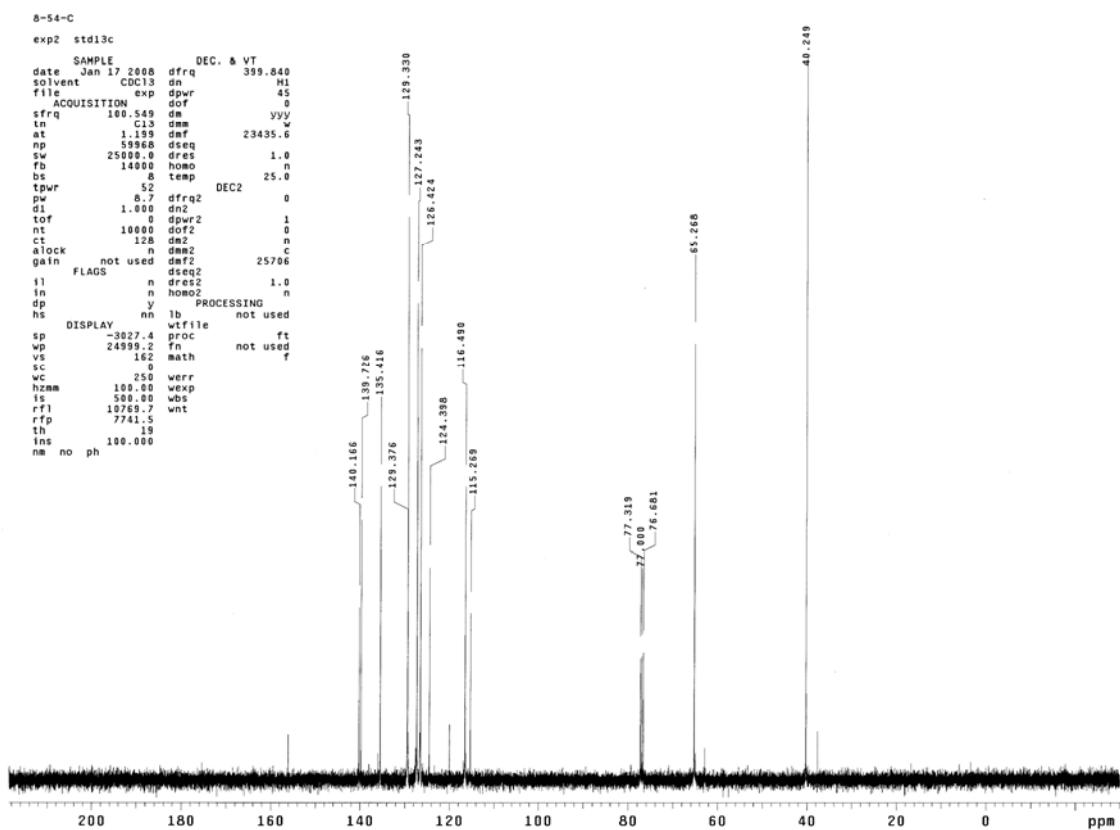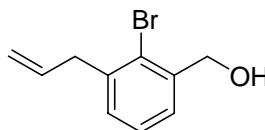
^{1}H NMR Spectrum of **5-125**
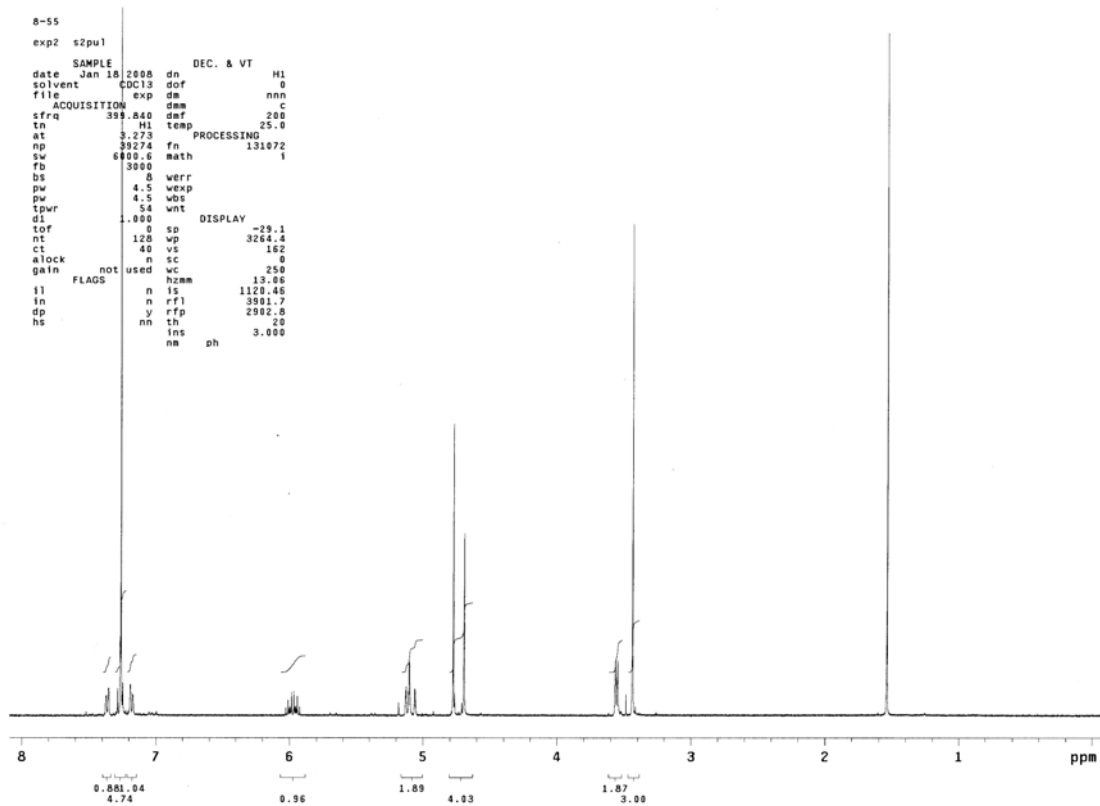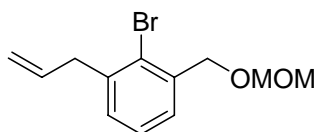
^{13}C NMR Spectrum of **5-125**
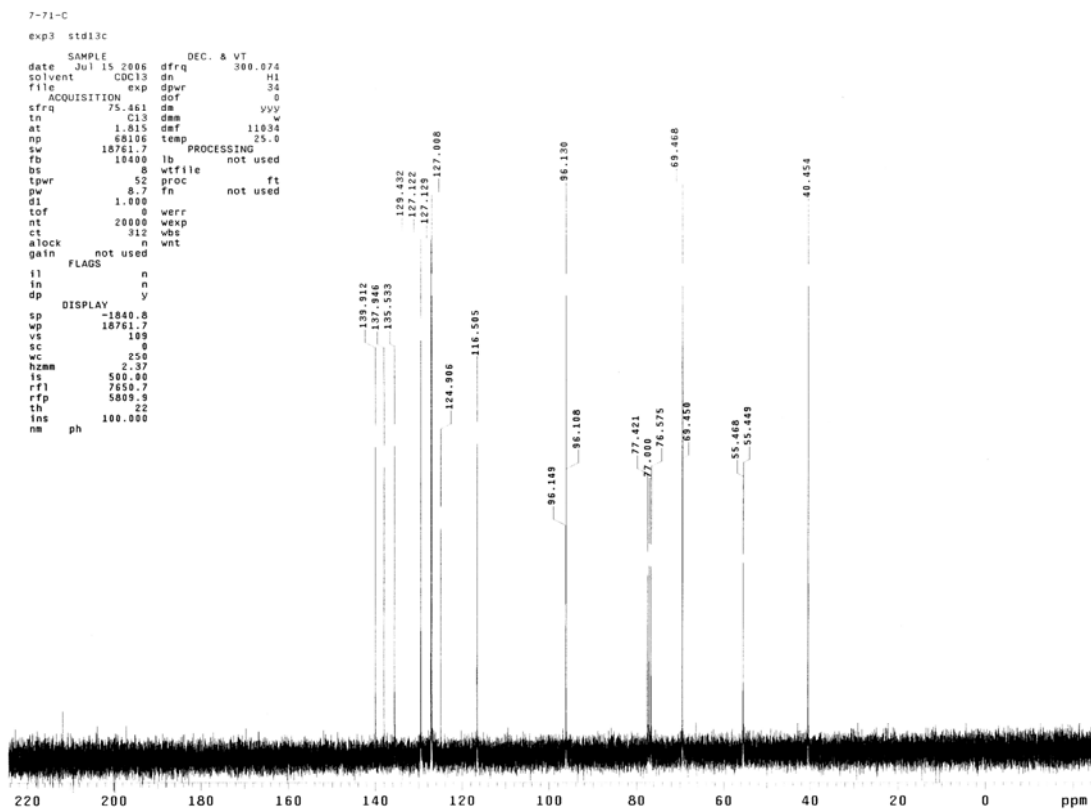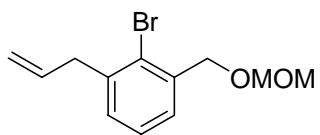
¹H NMR Spectrum of **5-127**
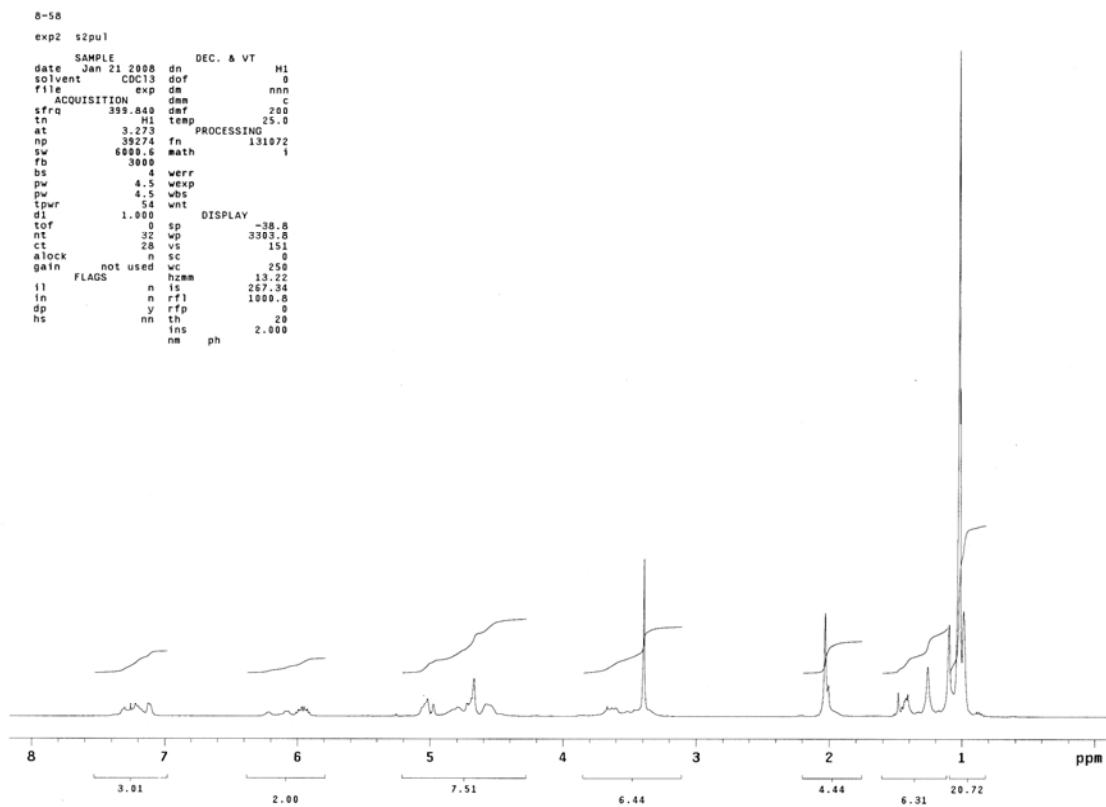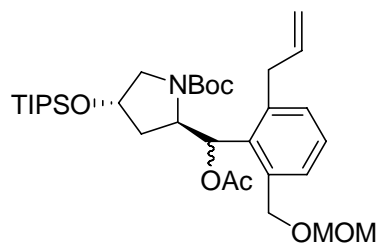
^{13}C NMR Spectrum of 5-127

^{1}H NMR Spectrum of **5-128**

^{13}C NMR Spectrum of 5-128

8-63-C

exp2 std13c

SAMPLE		DEC. & VT	
date	Jan 25 2008	dfrq	399.840
solvent	CDC13	dn	H1
file	exp	dpwr	45
ACQUISITION		dof	0
sfrq	100.549	dm	yyy
tn	C13	dmm	w
at	1.199	dmf	23435.6
np	59968	dseq	
sw	25000.0	dres	1.0
fb	14000	homo	n
bs	8	temp	25.0
tpwr	52	DEC2	
pw	8.7	dfrq2	0
d1	1.000	dn2	
tof	0	dpwr2	1
nt	10000	dof2	0
ct	2832	dm2	n
alock	n	dmm2	c
gain	not used	dmf2	25706
FLAGS		dseq2	
il	n	dres2	1.0
in	n	homo2	n
dp	y	PROCESSING	
hs	nn	lb	not used
DISPLAY		wtfile	
sp	-507.4	proc	ft
wp	21837.6	fn	not used
vs	402	math	f
sc	0		
wc	250	werr	
hzmm	87.35	wexp	
is	500.00	wbs	
rfl	10752.1	wnt	
rfp	7741.5		
th	15		
ins	100.000		
nm no ph			

^{1}H NMR Spectrum of **5-129**

^{13}C NMR Spectrum of **5-129**
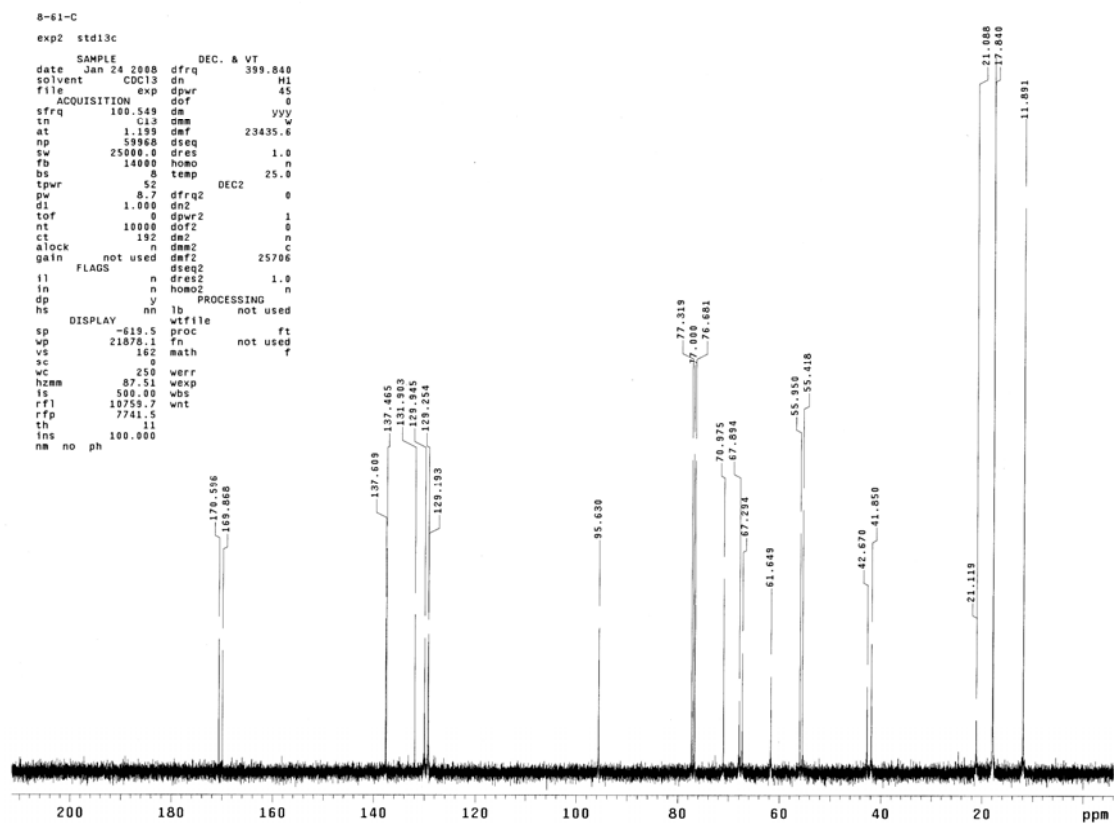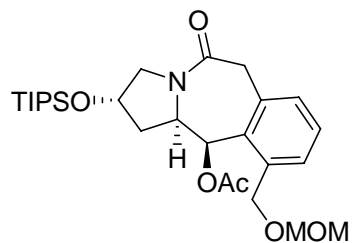
^{1}H NMR Spectrum of **5-130**
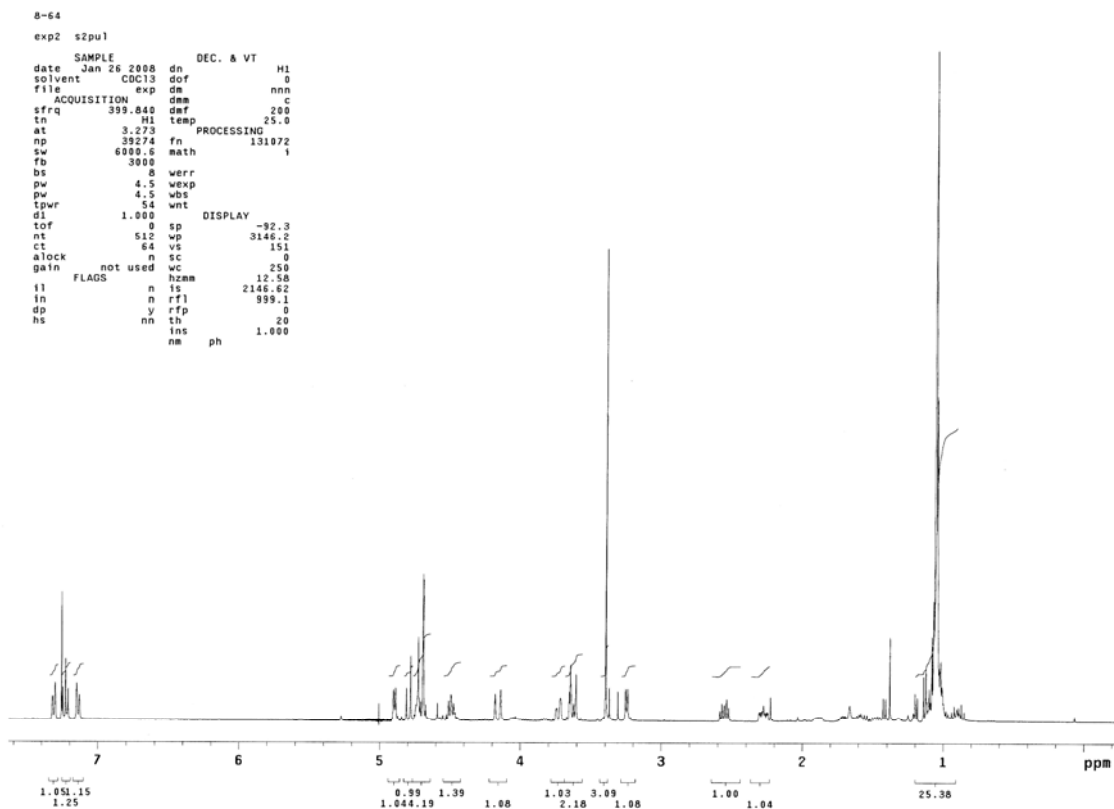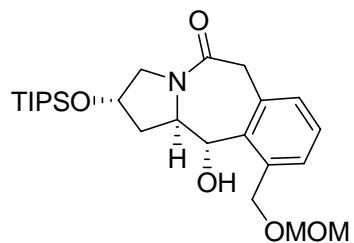
^{13}C NMR Spectrum of **5-130**
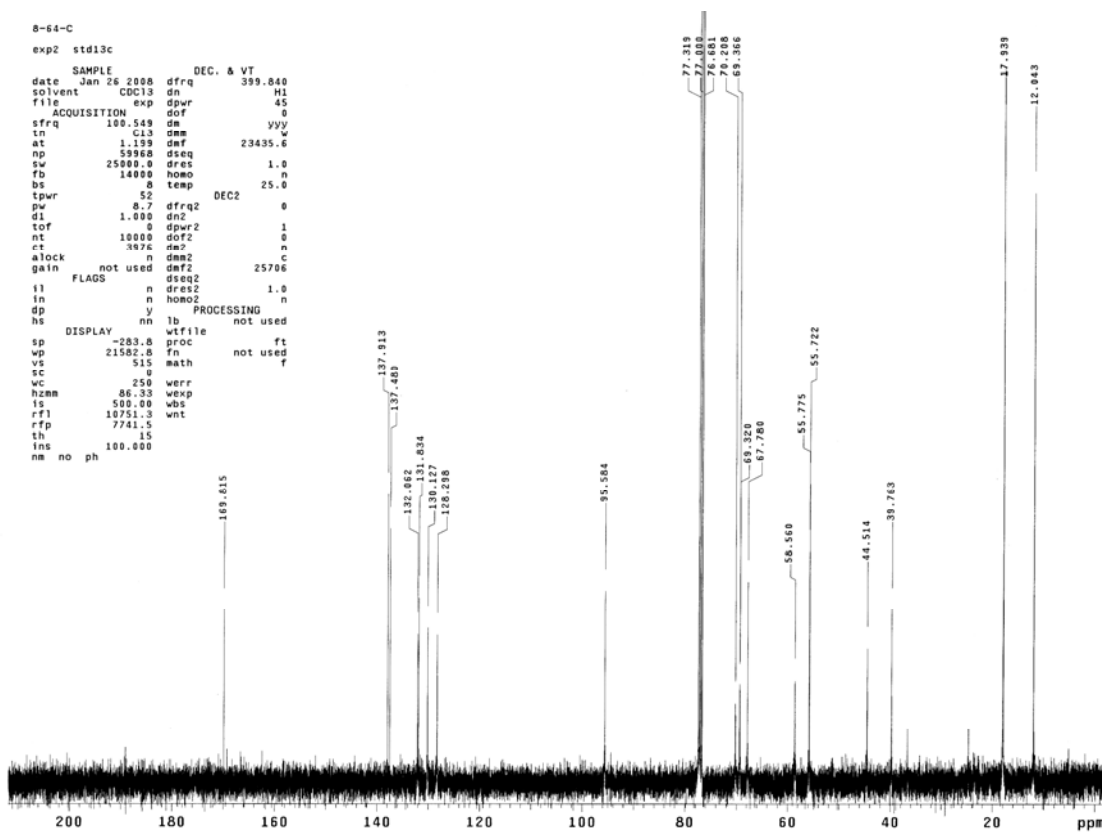
^{1}H NMR Spectrum of **5-132**
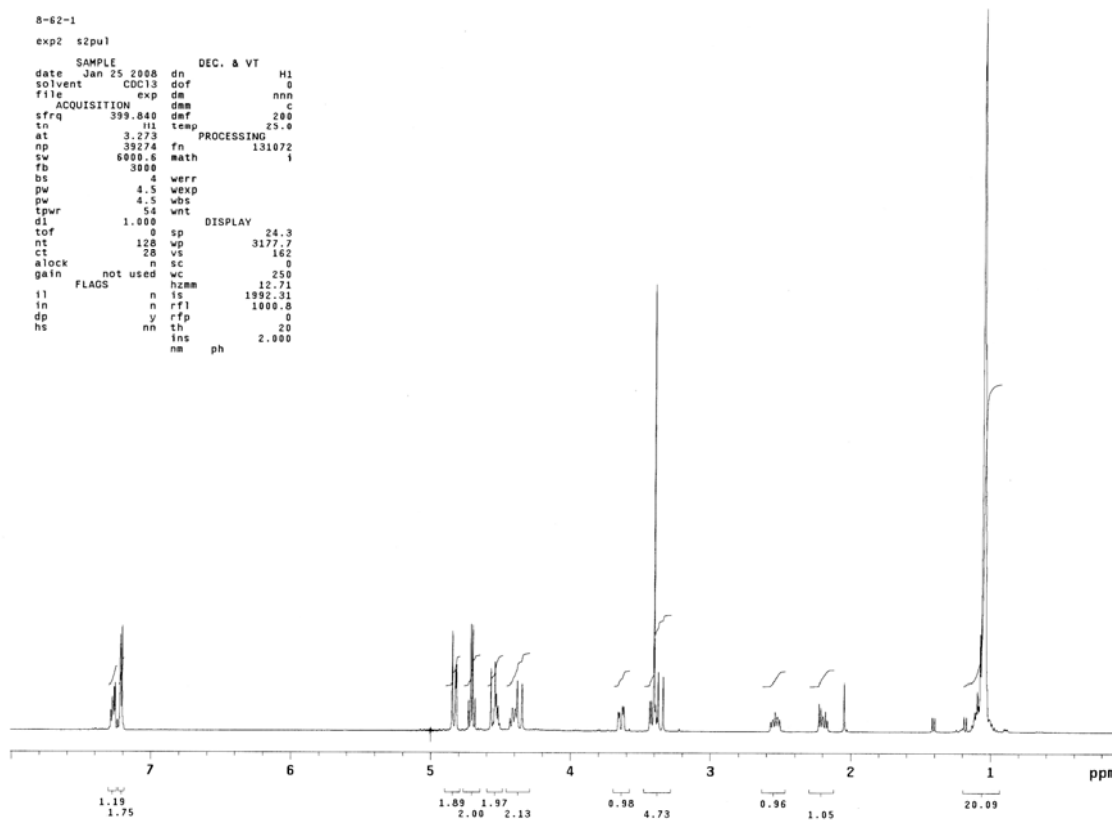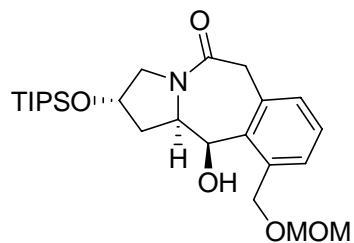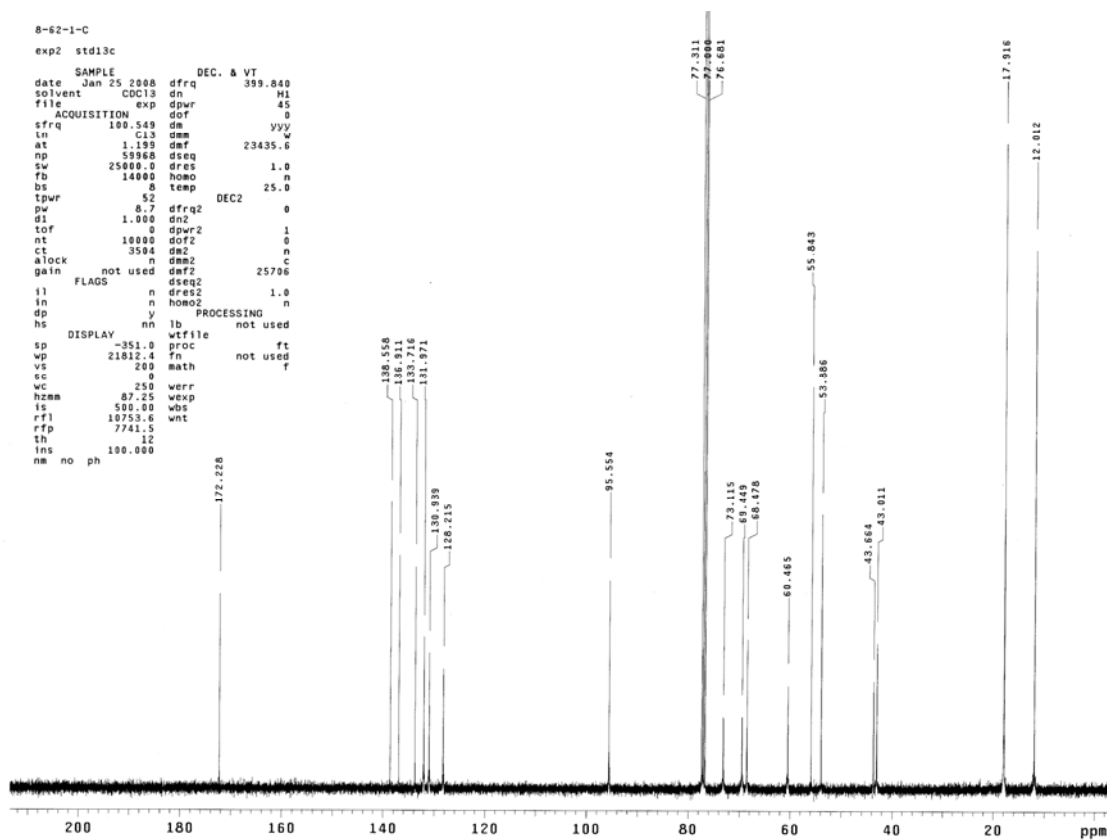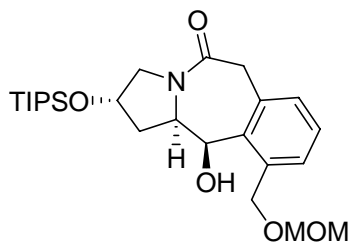
^{1}H NMR Spectrum of **5-134**
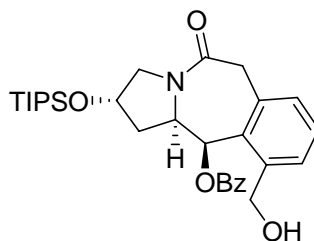
NOESY Spectrum of **5-134**
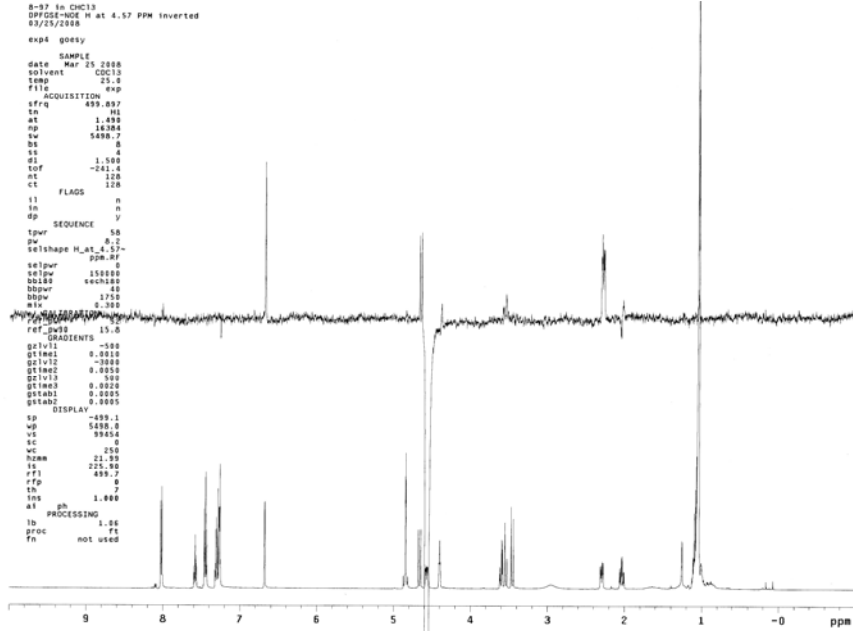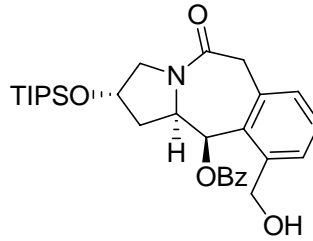
^{1}H NMR Spectrum of **5-135**
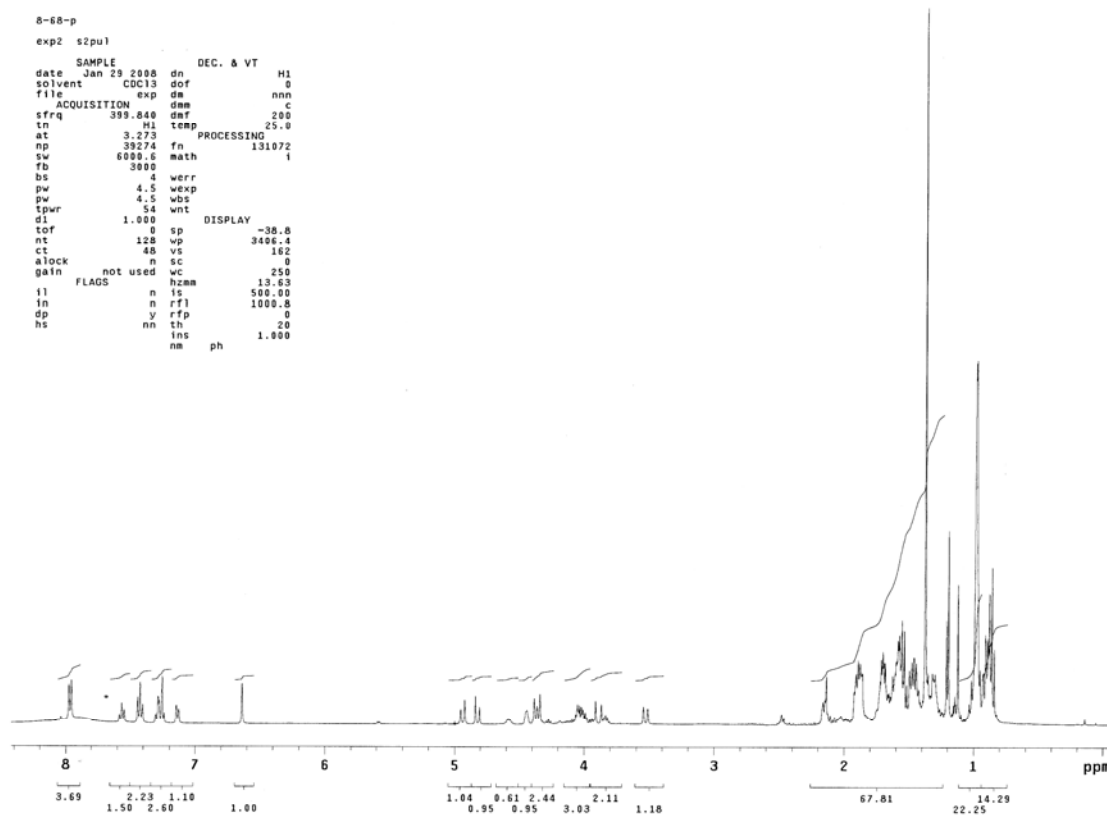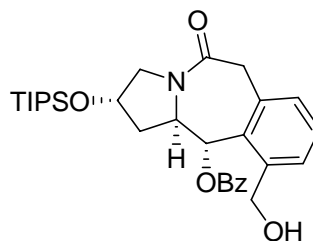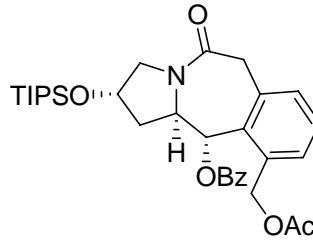
^{13}C NMR Spectrum of **5-135**

^{1}H NMR Spectrum of **5-136**
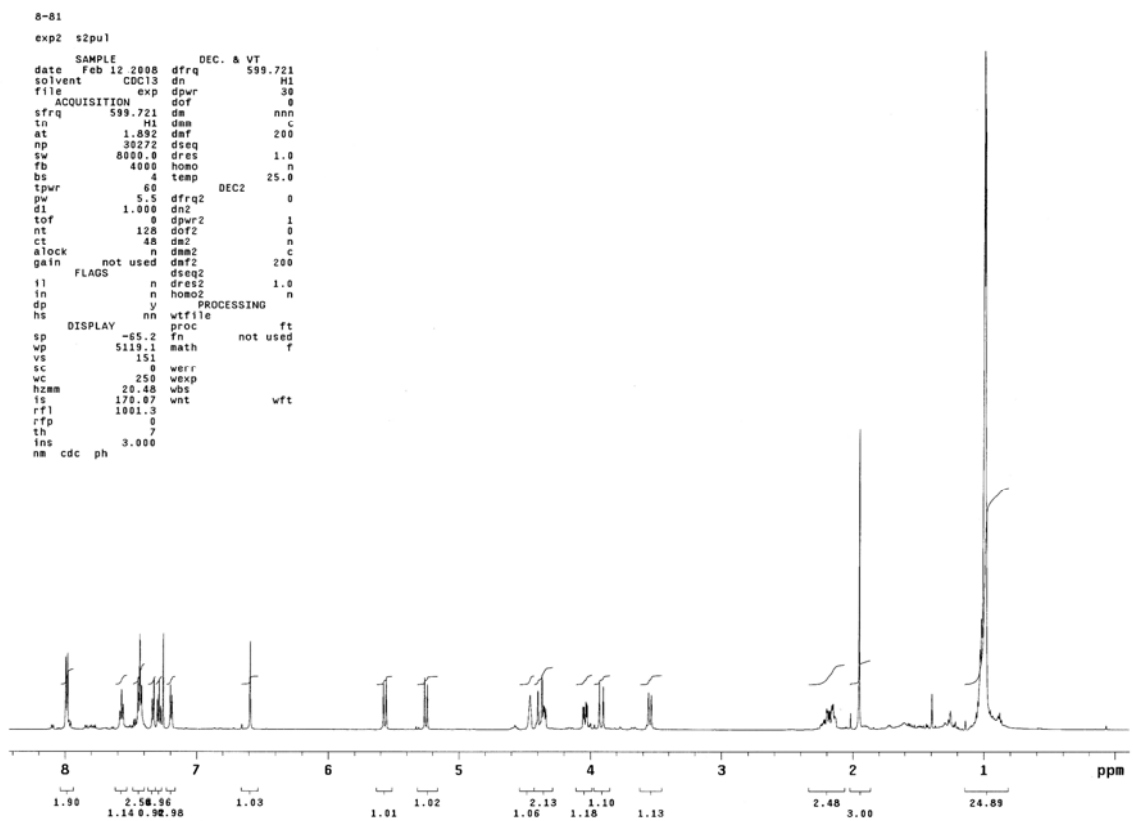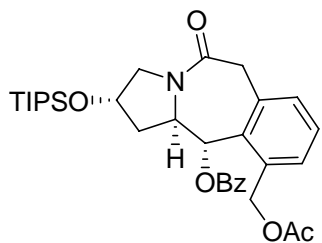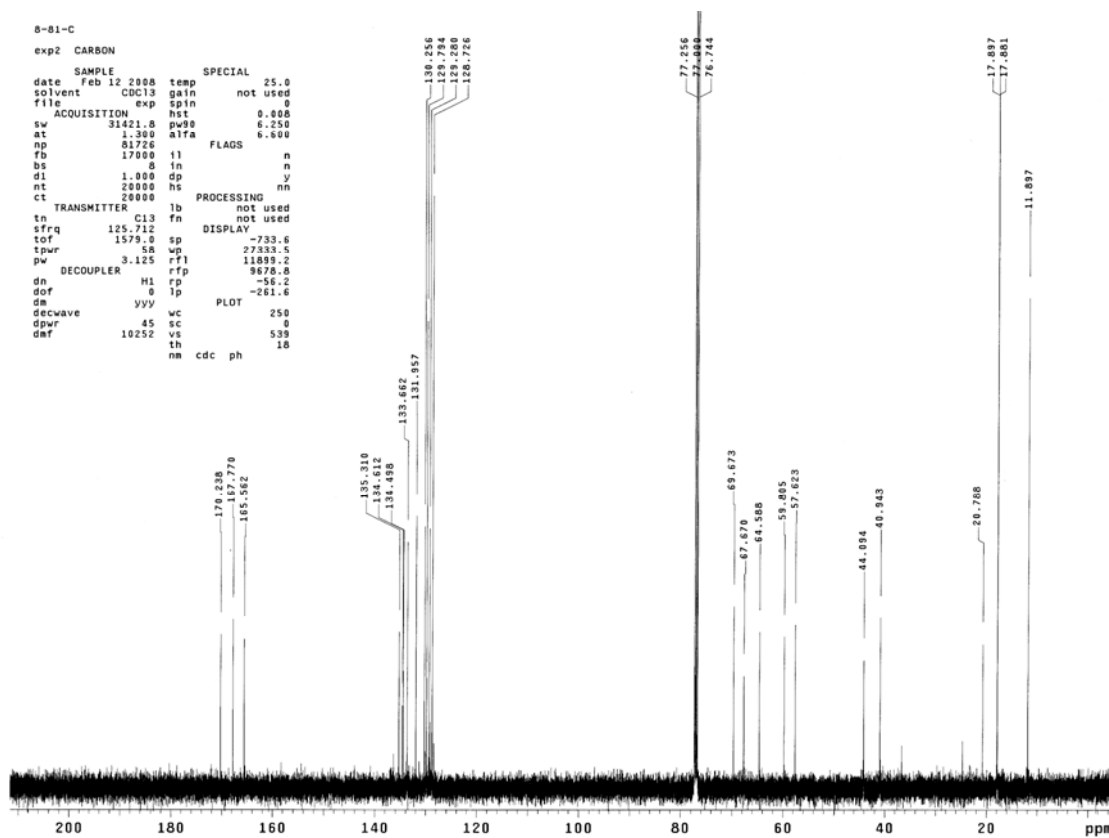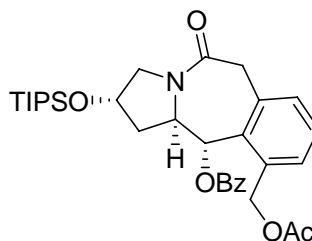
NOESY Spectrum of **5-136**
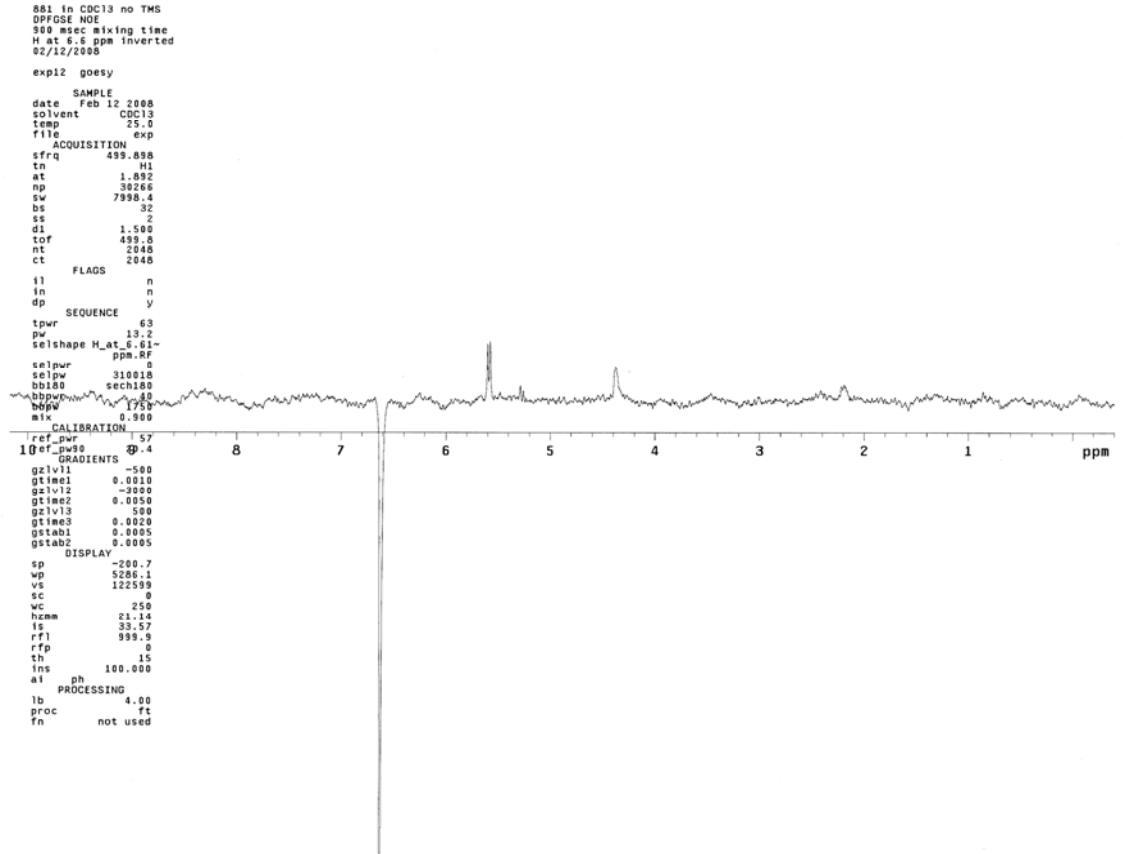
881 in CDC13 no TMS
DPFGSE NOE
900 msec mixing time
H at 4.48 ppm inverted
02/12/2008

exp20 goesy
            SAMPLE
date   feb 12 2008
solvent   CDC13
temp   25.0
file   exp
        ACQUISITION
sfrq   499.898
tn   H1
at   1.892
np   30266
sw   7998.4
bs   32
ss   4
d1   1.500
tof   499.8
nt   1024
ct   1024
        FLAGS
il   n
in   n
dp   y
        SEQUENCE
tpwr   63
pw   13.2
selshape H_at_4.48~
            ppm.RF
selpwr
selpw   133600
bb180   sechl80
bbpwr   40
bbpw   1750
mix   0.900
        CALIBRATION
ref_pwr   57
ref_pw90   20.4
        GRADIENTS
gzlvl1   -500
gtime1   0.0010
gzlvl2   -3000
gtime2   0.0050
gzlvl3   500
gtime3   0.0020
gstab1   0.0005
gstab2   0.0005
        DISPLAY
sp   -127.5
wp   4455.7
vs   81949
sc   0
wc   250
hzmm   17.82
is   33.57
rfl   999.9
rfp   0
th   7
ins   100.000
ai   ph
        PROCESSING
lb   2.00
proc   ft
fn   not used
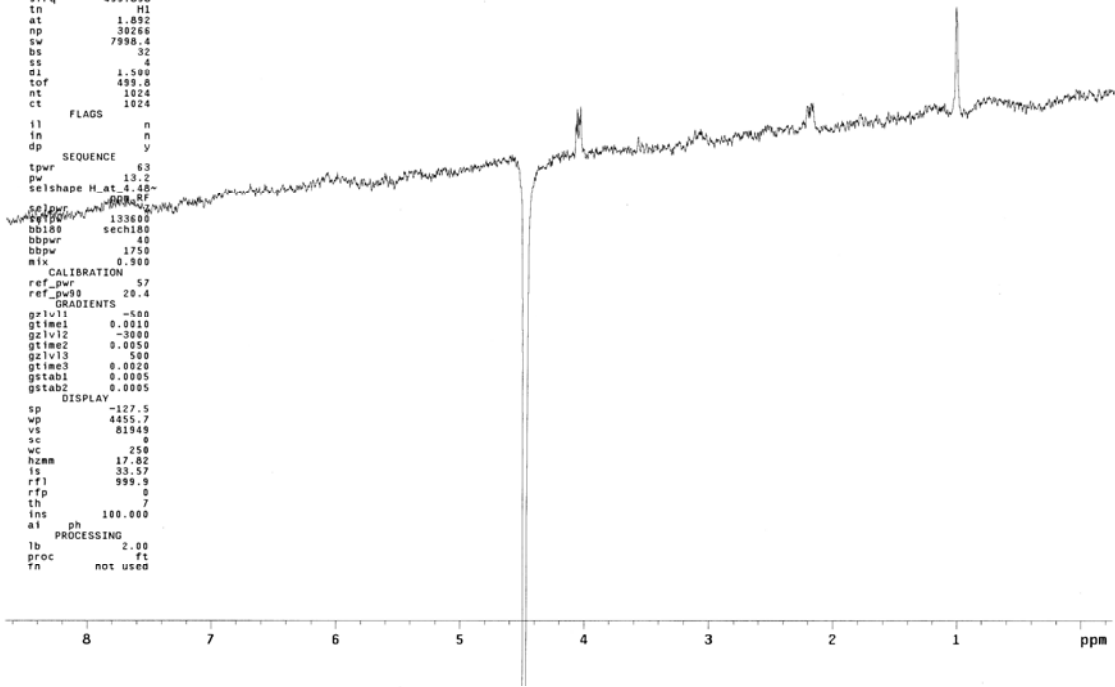
881 in CDC13 no TMS
DPFGSE NOE
900 msec mixing time
H at 3.57 ppm inverted
02/12/2008

exp21 goesy
            SAMPLE
date   Feb 12 2008
solvent   CDC13
temp   25.0
file   exp
        ACQUISITION
sfrq   499.898
tn   H1
at   1.892
np   30266
sw   7998.4
bs   32
ss   4
d1   1.500
tof   499.8
nt   128
ct   128
        FLAGS
il   n
in   n
dp   y
        SEQUENCE
tpwr   63
pw   13.2
selshape H_at_3.57~
            ppm.RF
selpwr   8
selpw   115413
bb180   sechl80
bbpwr   40
bbpw   1750
mix   0.900
        CALIBRATION
ref_pwr   57
ref_pw90   20.4
        GRADIENTS
gzlvl1   -500
gtime1   0.0010
gzlvl2   -3000
gtime2   0.0050
gzlvl3   500
gtime3   0.0020
gstab1   0.0005
gstab2   0.0005
        DISPLAY
sp   -999.4
wp   7997.9
vs   43142
sc   0
wc   250
hzmm   31.99
is   33.57
rfl   999.9
rfp   0
th   7
ins   100.000
ai   ph
        PROCESSING
lb   4.00
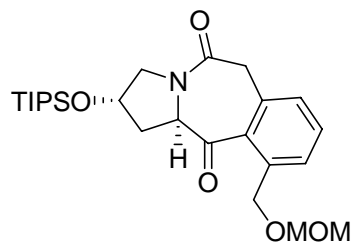proc   ft
fn   not used

600
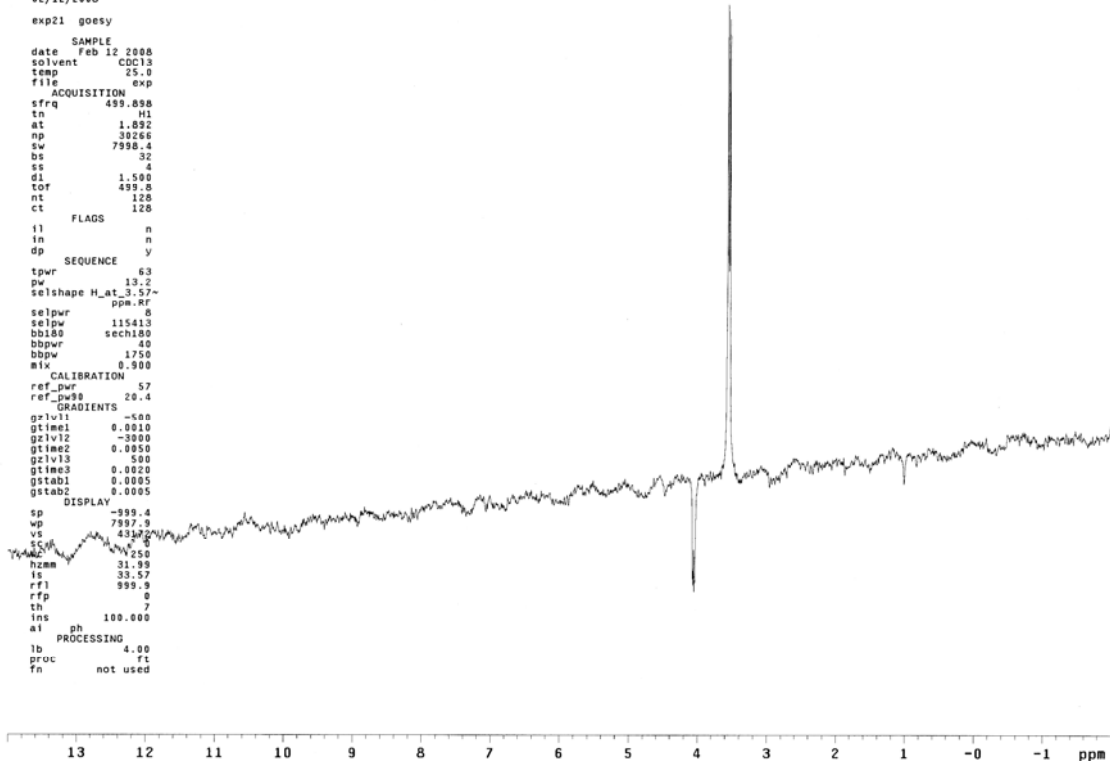
^{1}H NMR Spectrum of **5-137**
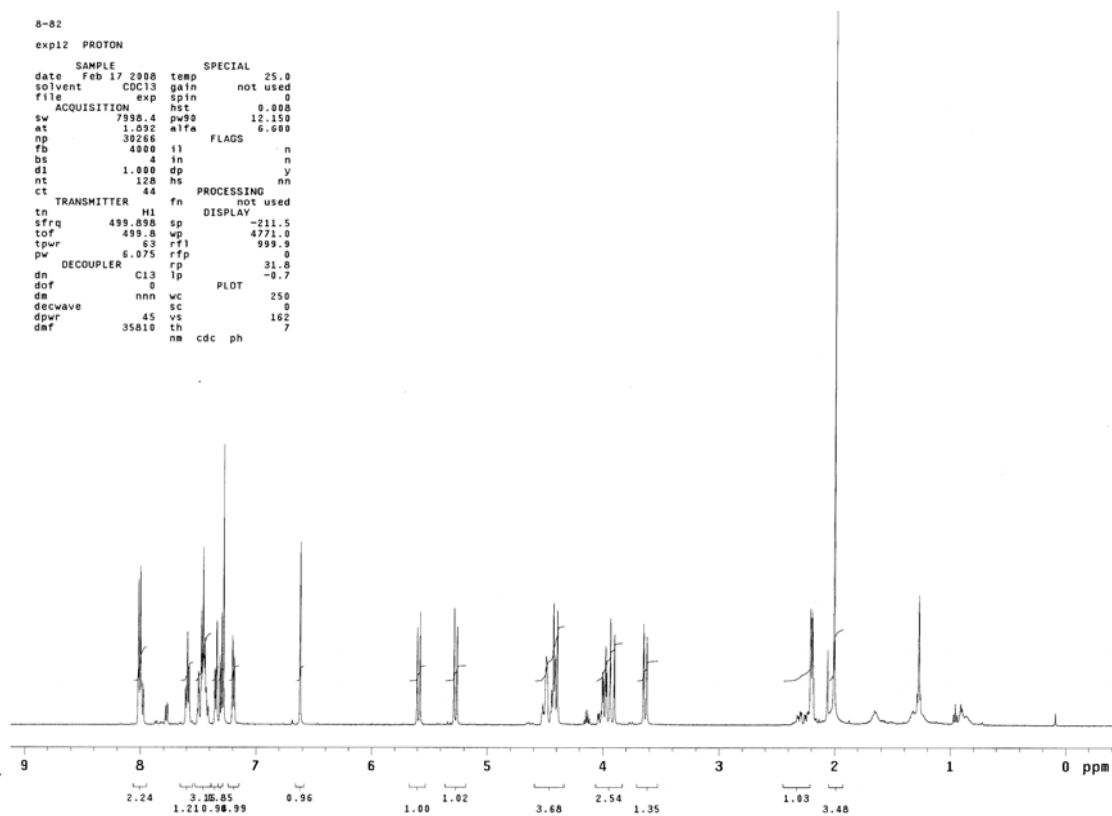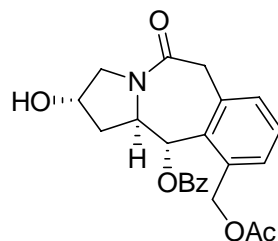
^{13}C NMR Spectrum of **5-137**
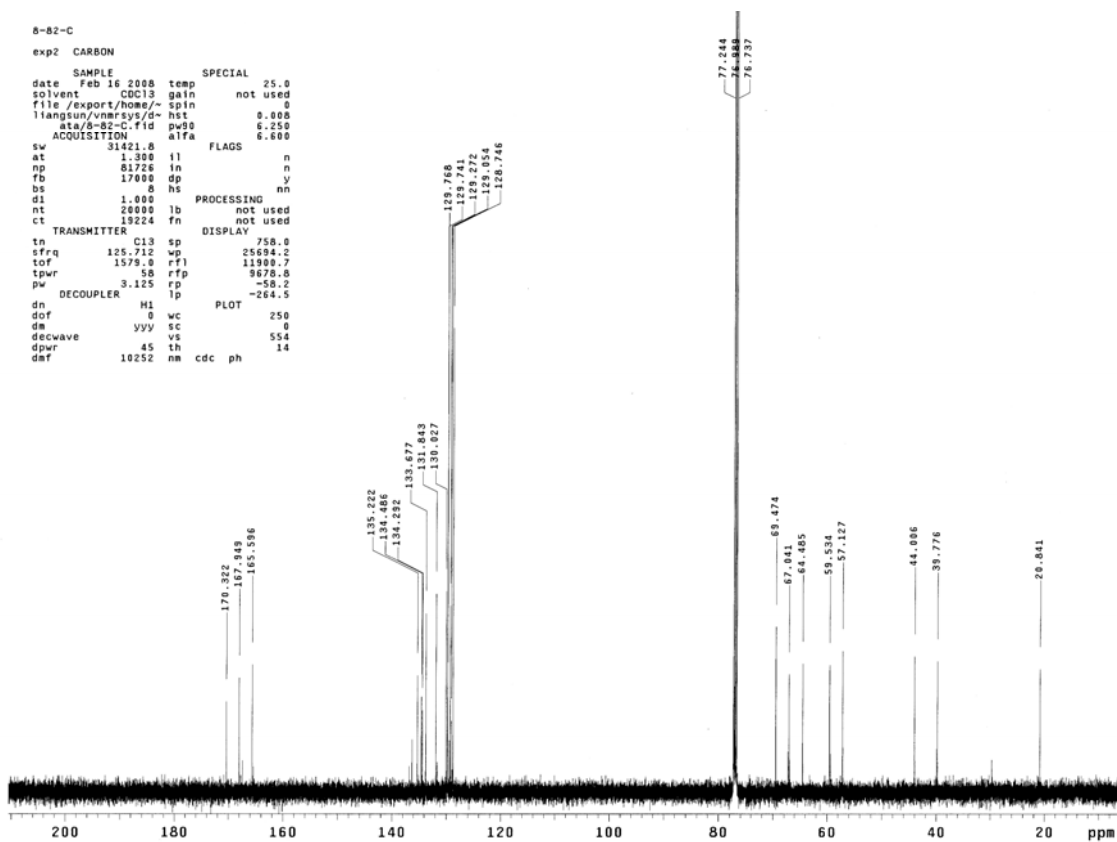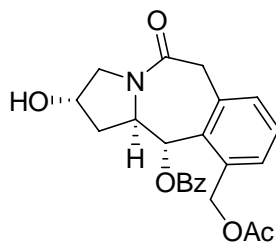
^{1}H NMR Spectrum of **5-138**
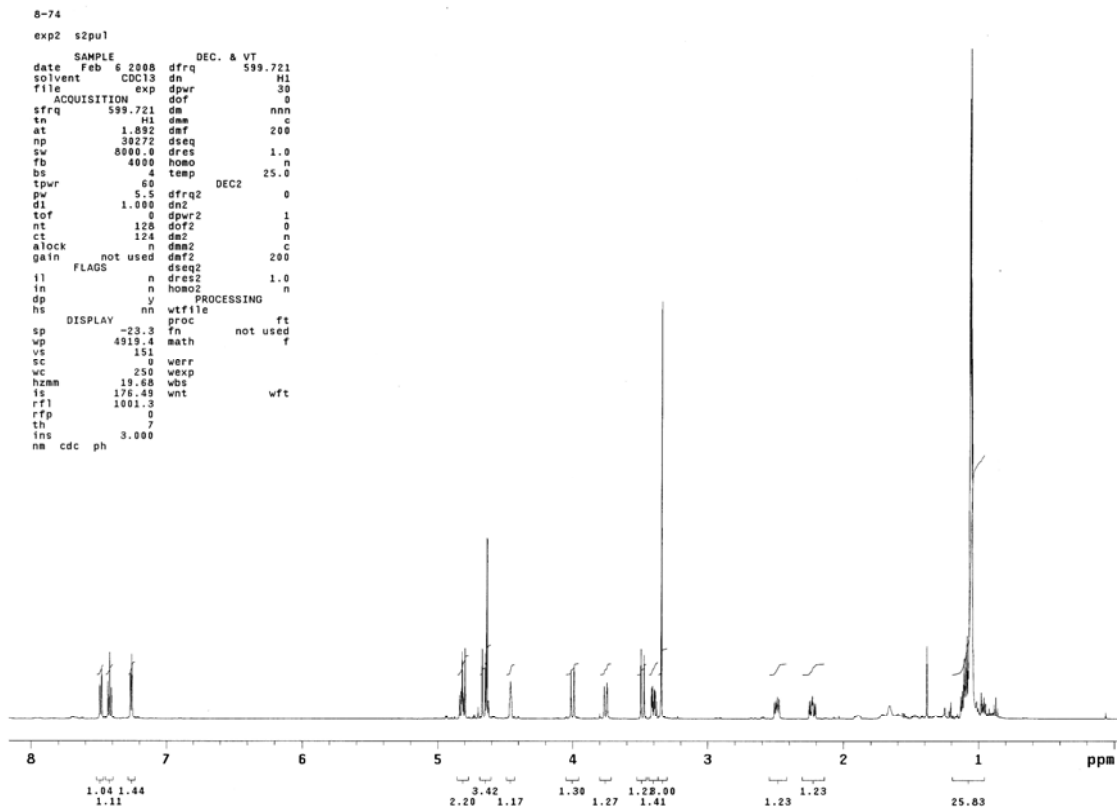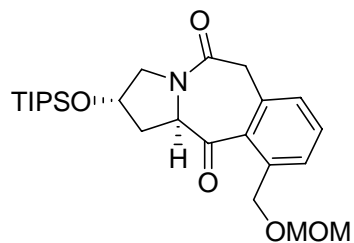
¹³C NMR Spectrum of **5-138**
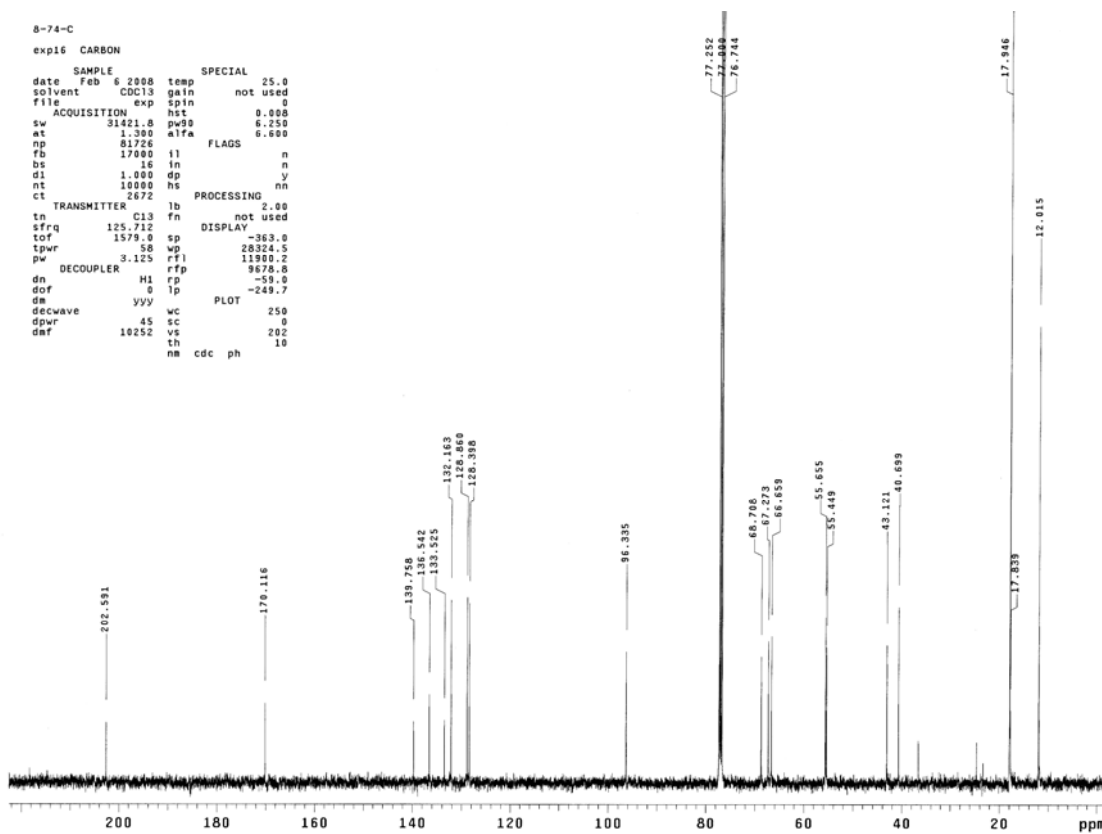
^{1}H NMR Spectrum of **5-139**
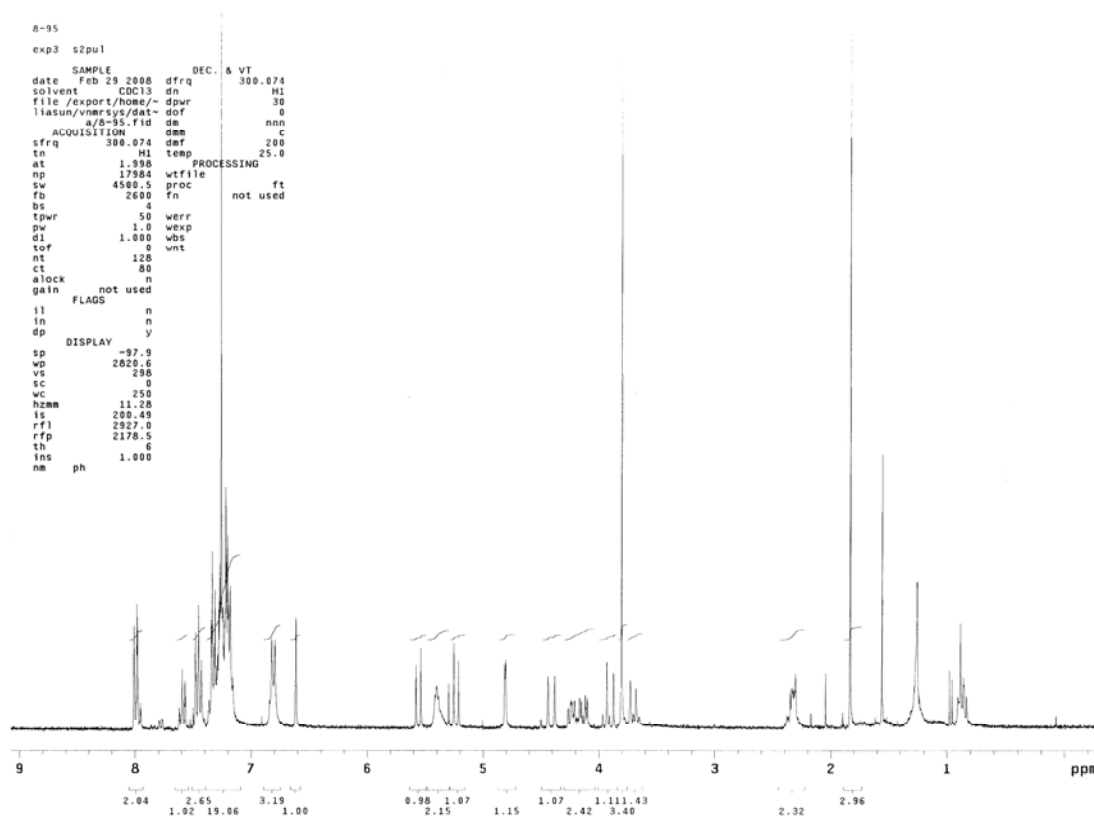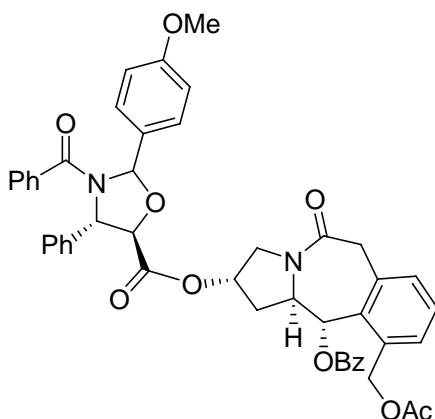
^{1}H NMR Spectrum of **5-38** (**SB-H-401**)
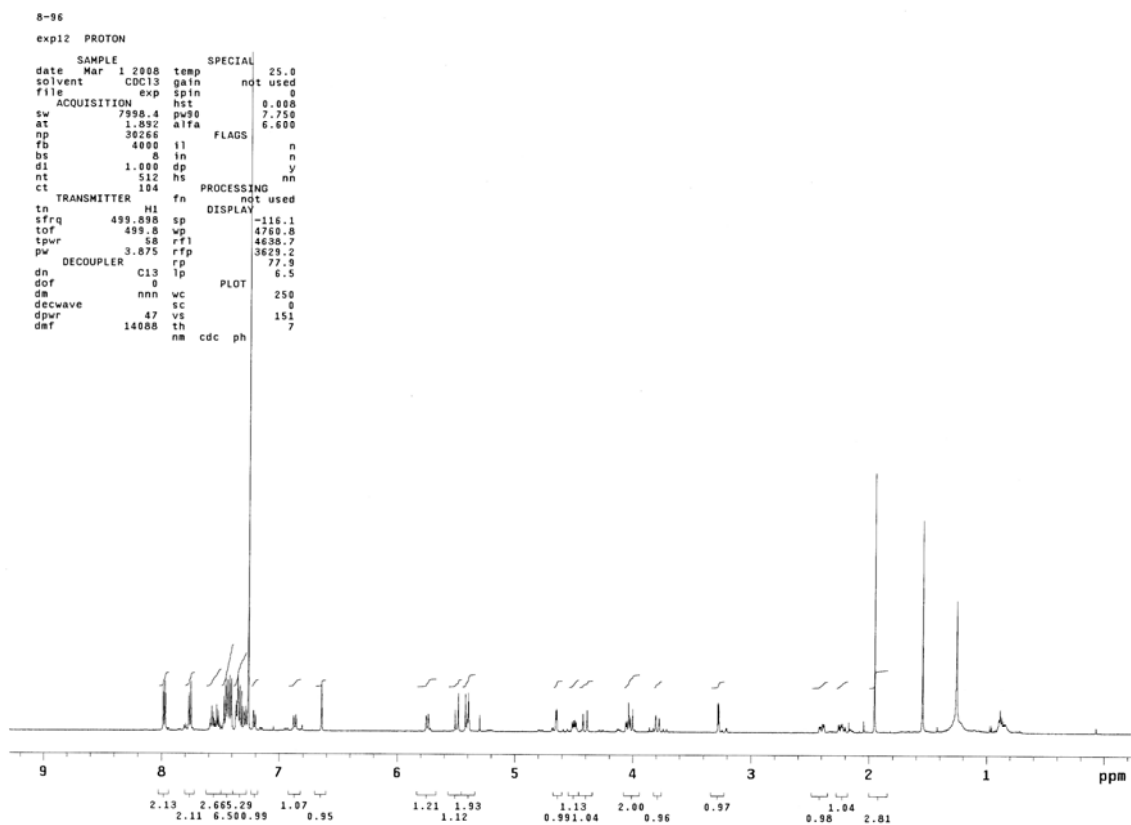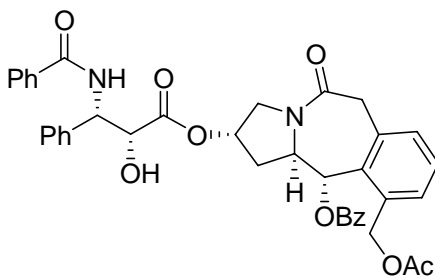
A5. Appendix Chapter VI

^{1}H NMR Spectrum of **6-7** (**SB-CST-10204**)

^{13}C NMR Spectrum of 6-7 (SB-CST-10204)